



## Study on Influence of Thickness and Span Length of Flat Slab for Progressive Collapse

K. Senthil,<sup>\*1</sup> B. Shailja<sup>2</sup>, J.K. Saurabh<sup>3</sup>, R. Abhishek<sup>3</sup> and A. Tanzeem<sup>3</sup>

<sup>1\*</sup> Assistant Professor, Department of Civil Engineering, Dr. BR Ambedkar NIT Jalandhar, Punjab 144011;  
E-mail: urssenthil85@yahoo.co.in; kasilingams@nitj.ac.in, Phone: +91-9458948743 (Corresponding Author)

<sup>2</sup>Assistant Professor, Department of Civil Engineering, Dr. BR Ambedkar NIT Jalandhar, Punjab 144011;

<sup>3</sup>PG Student, Department of Civil Engineering, Dr. BR Ambedkar NIT Jalandhar, Punjab 144011;

### ABSTRACT

In present study attempt has made to study the flat slab through ABAQUS/Explicit finite element program and the result thus obtained through simulation were compared with the experimental results available in the literature. The results were predicted and discussed in terms of reaction force and deflection. The predicted results through numerical simulations of the present study were found to be in good agreement with the experimental results. Further, the simulations were carried out for considering for both corner column failure and penultimate column failure. It is concluded that the percentage variation of 1.25% to 28% occurs in force redistribution. It was observed that the deflection keeps on decreasing as the slab thickness and span increases. It was also noticed that deflection for penultimate column is more than corner column failure case.

**KEYWORDS:** Progressive Collapse Load, Deformation, Finite element analysis, Flat slab thickness and span.

### INTRODUCTION

A progressive collapse of a building is initiated by an unexpected event that causes local damage and subsequently propagates throughout the structural system, leading to a final damage state in large-scale or entire collapse of the building. A progressive collapse can be triggered by accident actions, including fire hazard, gas explosion, terrorist attack, vehicle collision, design and construction errors, and environmental corrosion. Ngo and Scordelis (1967) proposed a discrete crack analysis finite element model for reinforced concrete beams. Abbasi et al. (1992) reviewed the possible failure modes and highlights the differences between flexural and shear failure. Saito et al. (1995) tested concrete slabs under static and dynamic loading. Das and Morley (2005) constructed experimental investigations into compressive membrane action in restrained slabs, which revealed the additional stiffness provided by the geometric nonlinearity. At a displacement of 5% of the double span length, twice the flexural capacity was observed for beam-slab sections. Sasani et al. (2007) explosively removed a column of the University of Arkansas Medical Center dormitory. An interesting observation is that the large axial stiffness of the columns, leads to almost identical vertical movement of different floors. Sasani, (2008) tested on the Hotel San Diego with the sudden failure of two columns demonstrated the frame action, of the beams and columns was the main mechanism for the redistribution of loads, with the hollow clay tile infill walls assisting by providing constraint to the beams. Baker et al. (2008) showed the list of common definitions, from a number of fields, before highlighting that for structural robustness, design codes such as EN 1990 (2002) do not quantify robustness in a manner that is helpful for an engineer considering different options. Sasani and Sagioglu (2010) studied the 20 storey Baptist Memorial Hospital which was scheduled for demolition to explosively remove a column. In this case, the structure did not fail progressively and little damage was observed away from removal area. Iribarren et al. (2011) modelled RC frames numerically under a column loss scenario. They concluded that the reinforcement ratio and the column removal time were very significant in the extent of damage, and potential for progressive failures, as was the inclusion of a strain-rate dependant material model for the steel bars. Fang et al. (2011) observed the fire in multi-storey structures has the potential to start a progressive collapse and this has been especially considered for car parks, and steel structures. Jayasooriya et al. (2011) modelled the effect of explosions on an RC frame structure and concluded that both the details of the local damage to elements and a global analysis are required in evaluating the response of the structure. Kokot et al. (2012) conducted quasi-static experiments, and dynamic modelling, of RC frame structures with slabs. Their investigations demonstrated that no progressive collapse occurred due to the ductile ALPs utilizing additional capacity from plastic hinges in the beams. Choi and Kim (2012) studied the change in bending moment redistribution of flat slabs and concluded that it is directly affected by the ratio of shear and flexural strength. Russell et al. (2015) prevented disproportionate collapse under an

extreme loading event; a sudden column loss scenario is often used to ensure the structure has suitable robustness. Based on the detailed literature survey, it is observed that the response of the building subjected to sudden column collapse has been rarely studied. Response of structural elements such as slab and beam subjected to column failure also rarely been studied. It is clear that not only in progressive collapse of RC flat slab structures a potential issue; there is currently a lack of experimental and numerical information regarding their response after sudden column loss. Objective of present study is to develop a numerical model to simulate a column loss event for an RC flat slab structure, validate the numerical model against the results from the experimental tests, use the results of the parametric study to identify key factors influencing the potential for progressive collapse, Response of the flat slab against absent of the column. to study the response of flat slab against column failure by sudden impact and comparison of deflection under static condition.

## CONSTITUTIVE MODELLING

In finite element modelling, inelastic behaviour of concrete was defined by using concrete damaged plasticity model (CDP) providing a general capability for modelling concrete and other quasi-brittle materials. The concrete damaged plasticity model is a continuum, plasticity-based, damage model for concrete. The stress strain relations under uniaxial compression and tension loading are given by the following equations where  $E_o$  is the initial (undamaged) elastic stiffness of the material:  $\sigma_t = (1-d_t)E_o(\varepsilon_t - \varepsilon_t^{pl})$  and  $\sigma_c = (1-d_c)E_o(\varepsilon_c - \varepsilon_c^{pl})$ , where  $d_t$  and  $d_c$  are tension damage variable and compression damage variable respectively, **Senthil et al., (2017 and 2018c)**.

The flow and fracture behavior of projectile and target material was predicted employing the **Johnson-Cook (1985)** elasto-viscoplastic material model available in ABAQUS finite element code. The material model is based on the von Mises yield criterion and associated flow rule. It includes the effect of linear thermo-elasticity, yielding, plastic flow, isotropic strain hardening, strain rate hardening, softening due to adiabatic heating and damage. The section of the reinforcement is assigned Fe250 steel and the ultimate tensile strength is 250 MPa is approximately equivalent to the ultimate tensile strength proposed by **Iqbal et al., (2015)**.

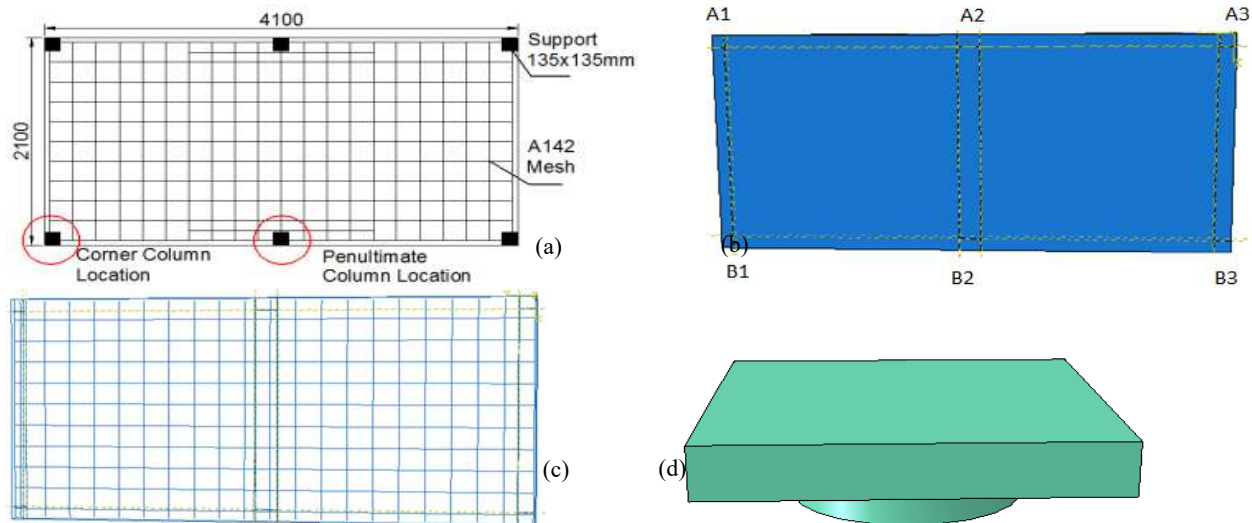


**Fig. 1** Picture showing (a) schematic (Russell et al., 2015) and model of (b) concrete slab (c) reinforcement bar and (d) metal support

## FINITE ELEMENT MODELLING

The finite element model of the reinforced concrete slab was made using ABAQUS/CAE. The length and width of slab was 4.1 and 2.1 m respectively exactly proposed by **Russell et al., (2015)**. The thickness of slab was 80 mm and clear cover is 20 mm on both the side of slab. The top and bottom steel reinforcement of main bar was 6 mm diameter placed at 200 mm center to centre distance. The schematic of slab, reinforcement bar and support are shown in **Fig. 1**. The support was used having the size of 135 x 135 x 20 mm and supported over circular plate of 20 mm thickness. The geometry of the concrete and steel reinforcement was modeled as solid deformable body. The interaction between concrete and steel was modeled using the tie constraint option available in ABAQUS/CAE wherein the concrete was

assumed as host region and the steel as embedded region. The constitutive and fracture behavior of steel and concrete have been predicted using Johnson-Cook and Concrete damaged plasticity model respectively available in ABAQUS.

The load was incorporated using interaction module available in ABAQUS. The plates were modelled as solid elements with elastic material properties. The dimensions were similar to experimental geometry, i.e. 135 x 135 x 20 mm. For both the plate and the circular support, 4 node linear tetrahedron elements (C3D4) were used. To measure reaction forces fixed boundary conditions in the three translational directions were applied to the bases of plates. Interaction between the sections was modelled with a hard contact, i.e. no penetration of the surfaces. For the concrete to steel boundary a coefficient of friction of 0.4 was applied. A schematic representation of the total load and the temporary support load against time is given in **Fig. 2**, showing the linear increase in load under quasi-static conditions up to T<sub>1</sub> and the sudden removal of the support by linearly reducing the support load between T<sub>2</sub> and T<sub>3</sub>.

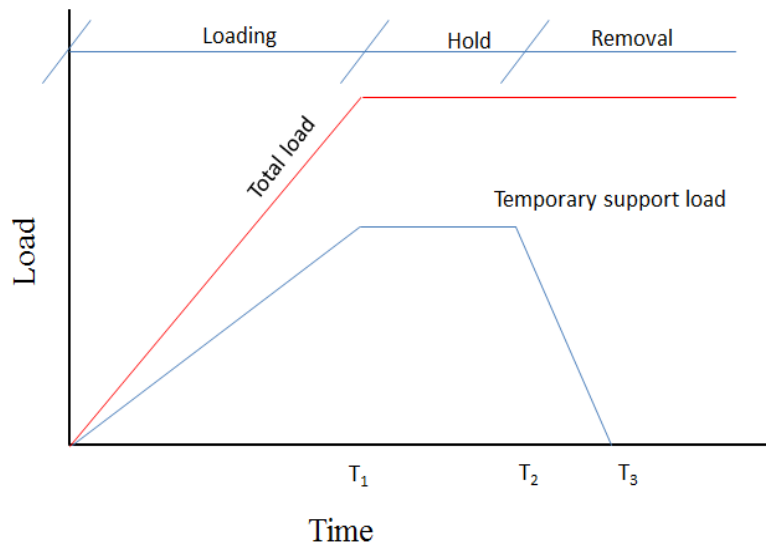


**Fig. 2** A graphic representation of the increase in total load and the failure of a support during dynamic tests

A detailed mesh sensitivity analysis has been carried out to understand the influence of mesh size. The size of element was varied as  $0.07 \times 0.07 \times 0.07$  m,  $0.06 \times 0.06 \times 0.06$  m,  $0.05 \times 0.05 \times 0.05$  m and  $0.04 \times 0.04 \times 0.04$  m. Deformed profile for the corner and penultimate column failure case for 40mm, 50mm, 60mm and 70mm mesh size is shown in **Fig. 3 and 4**, respectively. The deformed profile was shown along with the legend which describes through the colour pattern deflection obtained. The slab displacement was monitored for corner and penultimate column failure case and the graph was plotted between displacement and time and shown in **Fig. 5(a)-(b)**. The displacement for 40, 50, 60 and 70 mm mesh size was 133.8 mm, 115.9 mm, 93.07 mm, and 85.9 mm for corner column failure case is shown in **Fig. 5(a)**. The percentage variation of displacement between 40mm and 50mm mesh size is 15.4%, between 50 mm and 60 mm is 19.6%, between 50mm and 70mm is 25.8%. Here 50mm mesh size is taken as reference for calculating percentage variation of displacement. In case of penultimate column failure case, the displacement for 40 mm, 50 mm, 60 mm, and 70 mm mesh size is 120.1 mm, 119.5 mm, 98.12mm, and 97.09 mm, see **Fig. 5(b)**. The percentage variation of displacement between 40mm and 50mm mesh size is 0.5%, between 50mm and 60mm is 17.8%, between 50mm and 70mm is 18.7%. Here 50mm mesh size is taken as reference for calculating percentage variation of displacement.

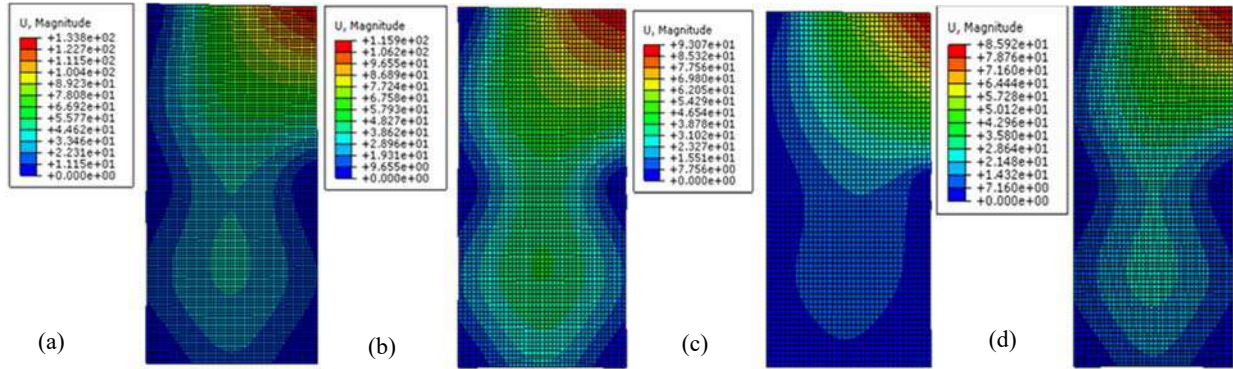


Fig. 3 Deflection (mm) of slab at (a) 40 (b) 50 (c) 60 and (d) 70 mm mesh sizes due to corner column failure

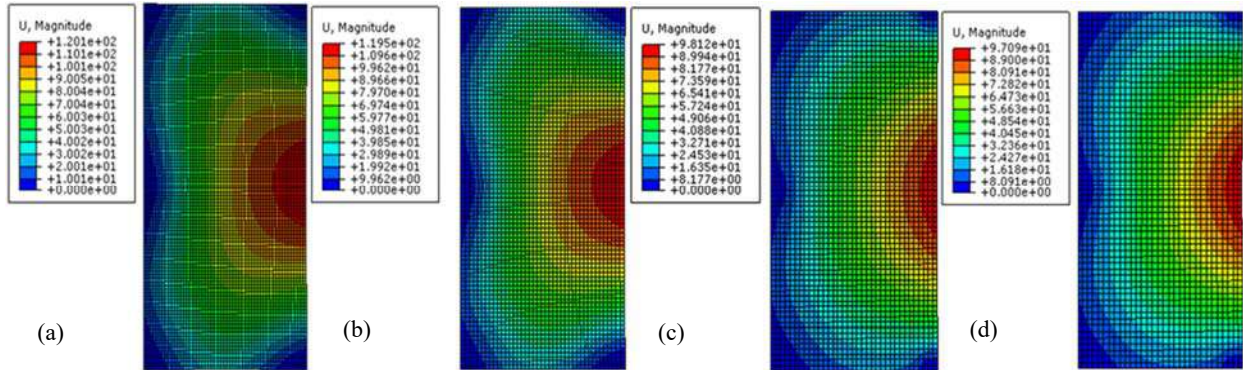


Fig. 4 Deflection (mm) of slab at (a) 40 (b) 50 (c) 60 and (d) 70 mm mesh sizes due to penultimate column failure

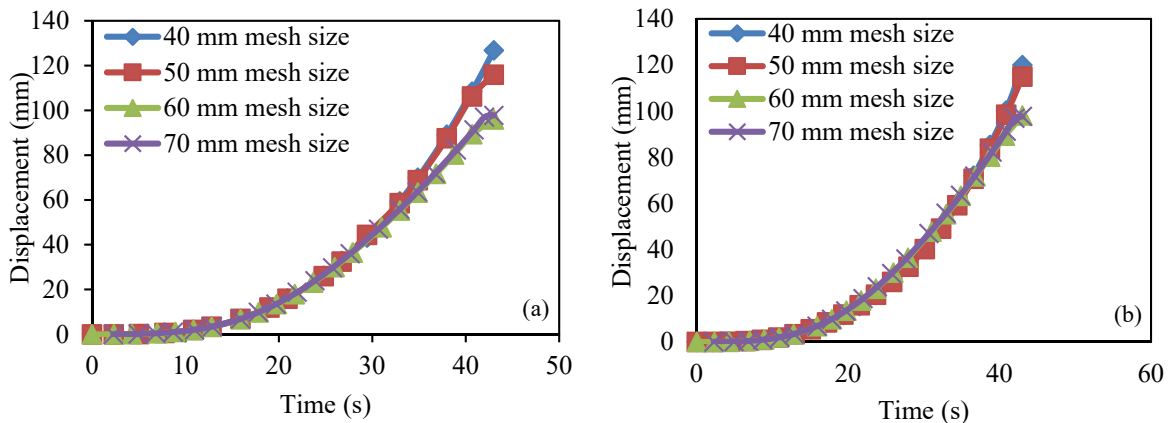
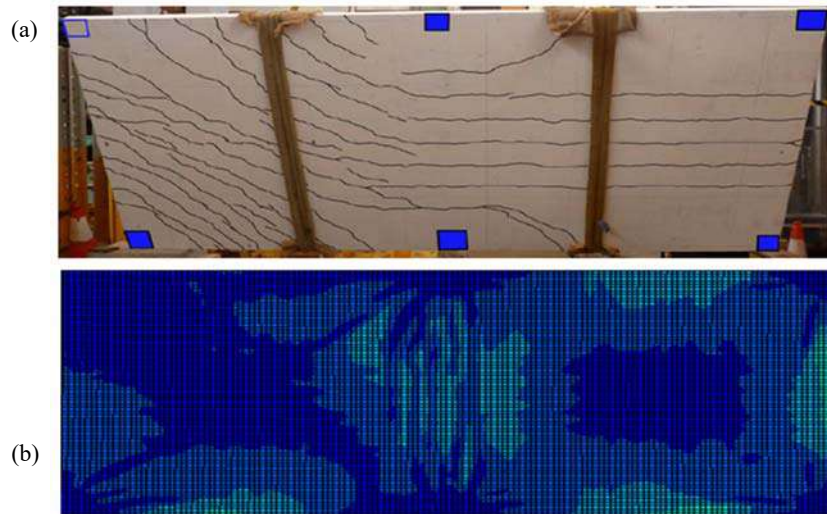


Fig. 5 Displacement against time for mesh size variation subjected to (a) corner (b) penultimate column failure

### COMPARISION OF EXPERIMENT AND SIMULATION

The simulations were carried out on flat slab against progressive collapse loading subjected to corner column failure. The concrete damaged plasticity model has been employed for predicting the material behavior of the concrete, whereas the Johnson-Cook model has been used for predicting the material behavior of steel reinforcement. The simulated results thus obtained have been compared with the experiments carried out by **Russell et al. (2015)** and discussed in this Section. The crack formation was found to be almost similar to that obtained in experimental study is shown in **Fig. 6**. Maximum cracks were observed near the adjacent to the failed column.



**Fig. 6 Comparison of (a) experimental (Russell et al 2015) and (b) numerical results of flexural cracks after corner column failure**

Simulation for static case was carried out and reaction forces at remaining support A2, A3, B1, B2, B3 were monitored and the graph was plotted between support load and total load for each support. For each position support load in model shows similar response to the experiment results, see **Fig. 7**. The **Fig. 7(a)** shows the variation of vertical reaction obtained at A2 support. According to experimental results the vertical reaction increases from 5 kN to 31.5 kN, whereas the same increases for the FEA model is 6.8 kN to 31 kN while increasing the total load from 16 kN to 71 kN. Here the FEA values are nearer to experimental values up to 60 kN load and after that the FEA results converges to experimental values at 60 kN and then it goes down. The difference in support load between FEA and experimental results varies from 1.59% to 15.29%. The graph in **Fig. 7(b)** shows the variation of vertical reaction obtained at A3 support. According to experimental results the vertical reaction increases from 1.5 kN to 6 kN, whereas the same increases for the FEA model is 2 kN to 7.1 kN while increasing the total load from 16 kN to 71 kN. The difference in support load between FEA and experimental results varies from 16.67% to 25%. The graph in **Fig. 7(c)** shows the variation of vertical reaction obtained at B3 support. According to experimental results the vertical reaction increases from 1 kN to 4.8 kN, whereas the same increases for the FEA model is 1.2 kN to 4 kN while increasing the total load from 16 kN to 71 kN. Here the FEA values are nearer to experimental values up to 58 kN load but after that the FEA values converges to experimental values at 58 kN and then it goes down. The difference in support load between FEA and experimental results varies from 7.4% to 23.81%. The graph in **Fig. 7(d)** shows the variation of vertical reaction obtained at B2 support. According to experimental results the vertical reaction increases from 3.8 kN to 16.5 kN, whereas the same increases for the FEA model is 4.5 kN to 15.5 kN while increasing the total load from 16 kN to 71 kN. Here the FEA values are nearer to experimental values up to 65kN load but after that the finite element model results converges to experimental values at 65 kN and then it goes down. The difference in support load between FEA and experimental results varies from 3.02% to 28.21%. The graph in **Fig. 7(e)** shows the variation of vertical reaction obtained at B1 support. According to experimental results the vertical reaction increases from 3 kN to 12.2 kN, whereas the same increases for the FEA model is 3.4 kN to 13 kN while increasing the total load from 16 kN to 71 kN. The difference in support load between FEA and experimental results varies from 7.5% to 22.2%.

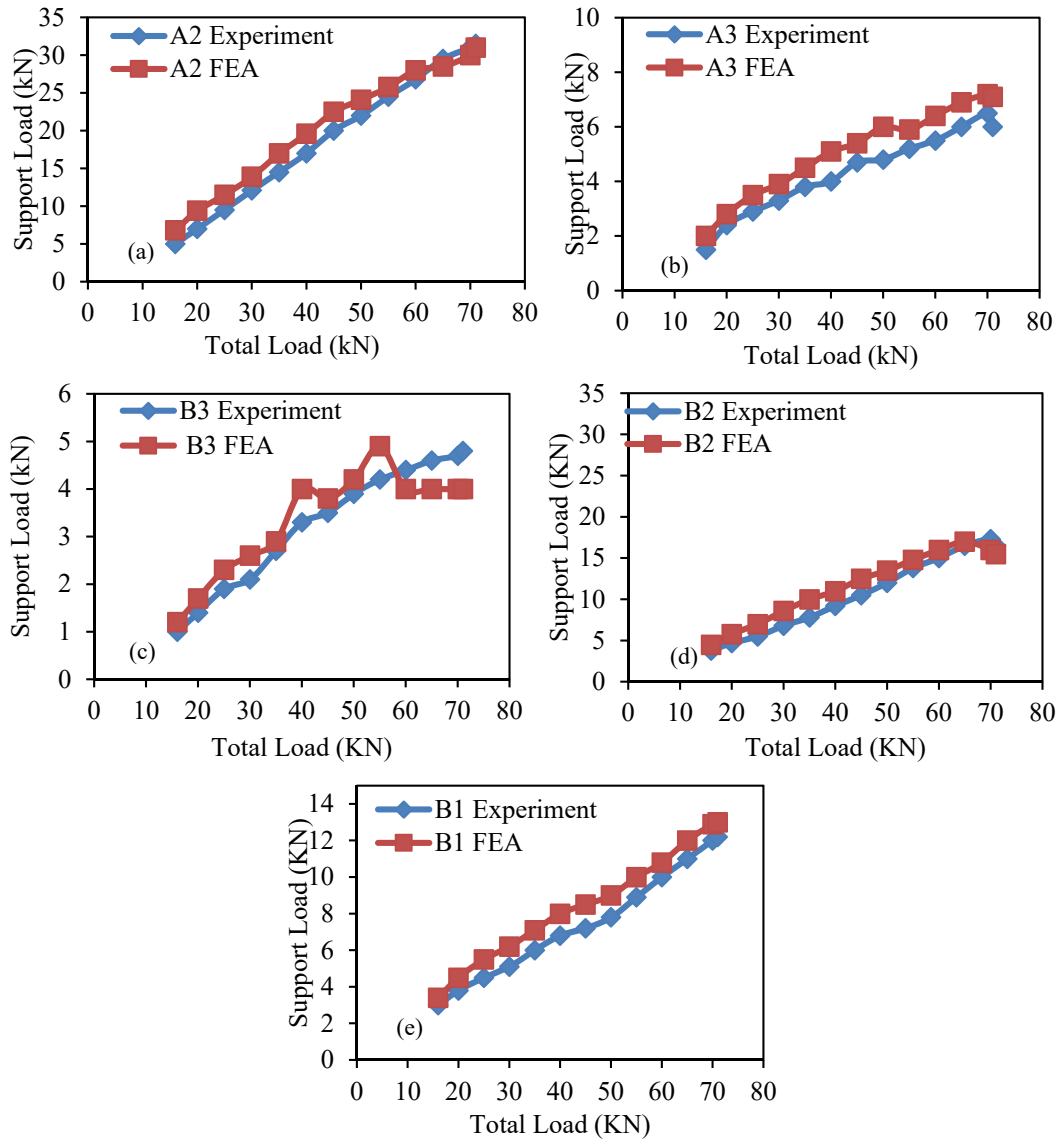


Fig. 7. Reaction forces of support (a) A2 (b) A3 (c) B3 (d) B2 and (e) B1 supports

## INFLUENCE OF THICKNESS AND SPAN LENGTH OF FLAT SLAB AGAINST PROGRESSIVE COLLAPSE

Three-dimensional finite element analysis has been carried out in order to study the response of reinforced concrete slab against progressive collapse using ABAQUS/CAE. The simulations were carried out against varying thickness of slab and span length. The response of structural elements were observed in terms of deflection, therein was presented and discussed.

### *Effect of Varying Thickness of Slab*

Deformed profile for the corner and penultimate column failure case for 70mm, 80mm, 90mm and 100mm slab thickness is shown in Fig. 8 and 9, respectively. The deformed profile is shown along with the legend which describes through the colour pattern the deflection obtained. The slab displacement was monitored for corner column failure case and the graph was plotted between displacement and time is shown in Fig. 10(a). Displacement increases as the time increases for all the slab thickness. The displacement for 70mm, 80mm, 90mm, and 100mm slab thickness is

136.4mm, 115.9mm, 106.8mm, and 98.8mm respectively. The percentage variation of displacement between 70mm and 80mm slab is 17.6%, between 80mm and 90mm is 7.85%, between 80mm and 100mm is 14.75%. Here 80mm slab is taken as reference for calculating percentage variation of displacement.

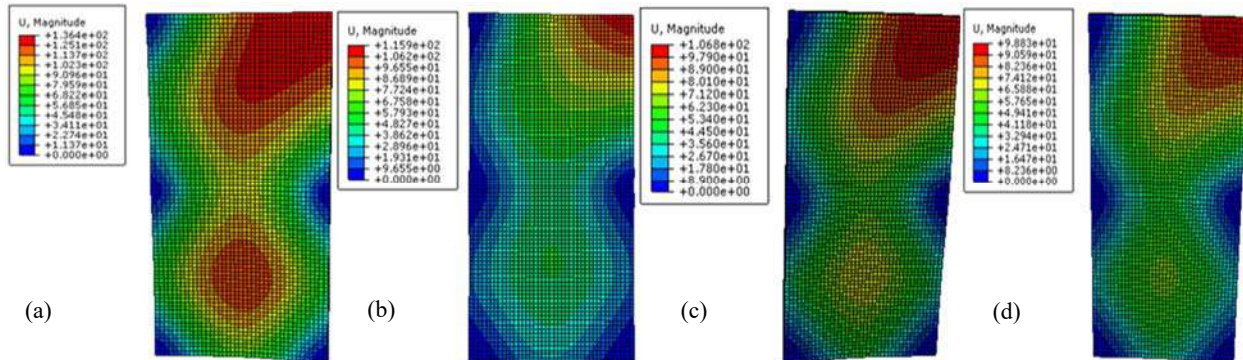


**Fig. 8 Deflection (mm) of (a) 70 mm, (b) 80 mm (c) 90 mm and (d) 100 mm slab thicknesses due to corner column failure**

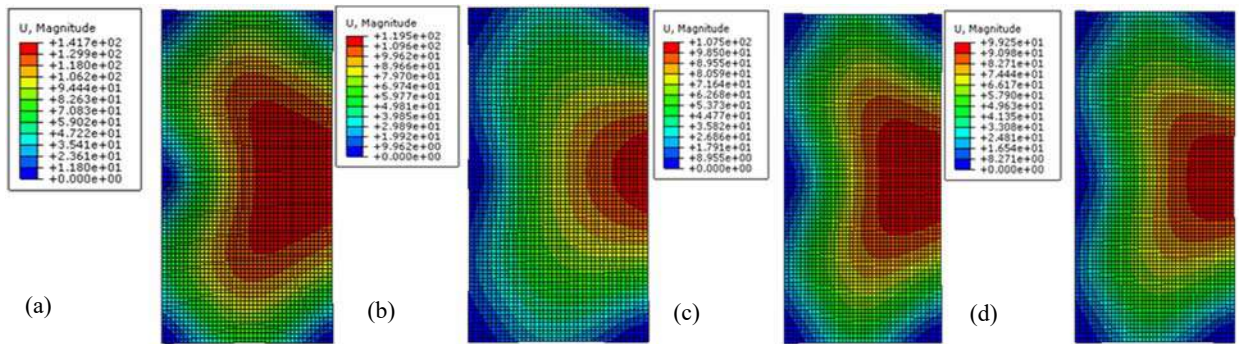


**Fig. 9 Deflection (mm) of (a) 70 mm (b) 80 mm (c) 90 mm and (d) 100 mm slab thickness due to penultimate column failure**

The slab displacement was monitored for penultimate column failure case and the graph was plotted between displacement and time is shown in **Fig. 10(b)**. Displacement increases as the time increases for all the slab thickness. The displacement for 70mm, 80mm, 90mm, and 100 mm slab thickness is 141.7, 119.5, 107.5 and 99.25 mm respectively. The percentage variation of displacement between 70 and 80 mm slab is 18.57%, between 80mm and 90mm is 10.04%, between 80 and 100 mm is 16.94%. In the present study, 80 mm slab is taken as reference for calculating percentage variation of displacement.

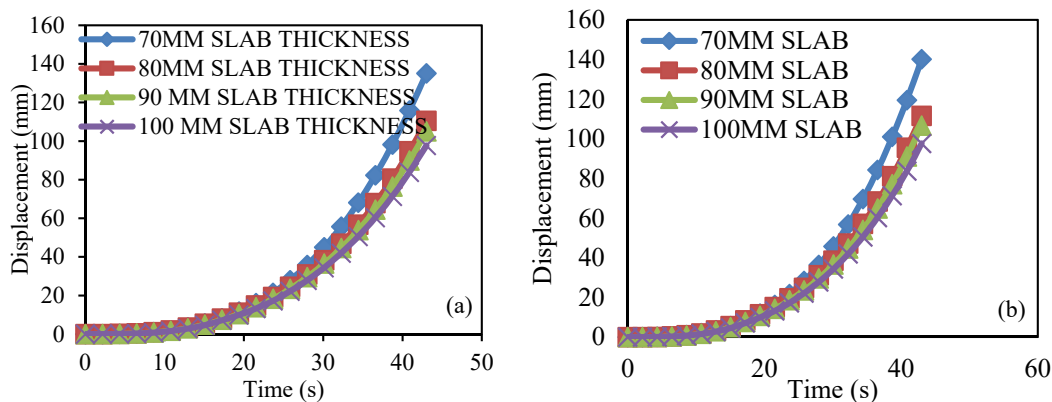


**Fig. 10 Displacement of slab of varying thickness subjected to (a) corner and (b) penultimate column failure**

**Effect of Varying Length of Slab**

Deformed profile for the corner and penultimate column failure case for 3.6 m, 4.1 m, 4.6 m and 5.1 m slab span are shown in **Figs. 11 and 12**, respectively. The deformed profile is shown along with the legend which describes through the colour pattern the deflection obtained.

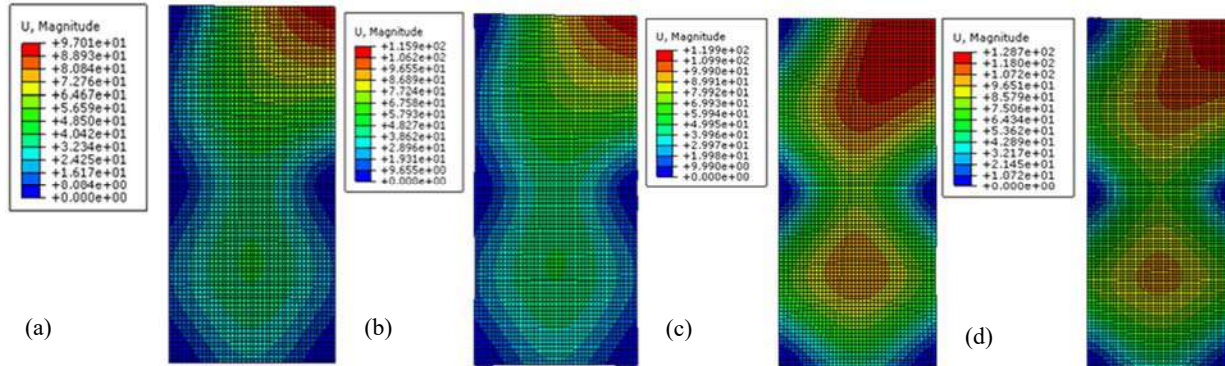


**Fig. 11 Deflection (mm) of (a) 3.6 m (b) 4.1 m (c) 4.6 m and (d) 5.1 m slab span due to corner column failure**

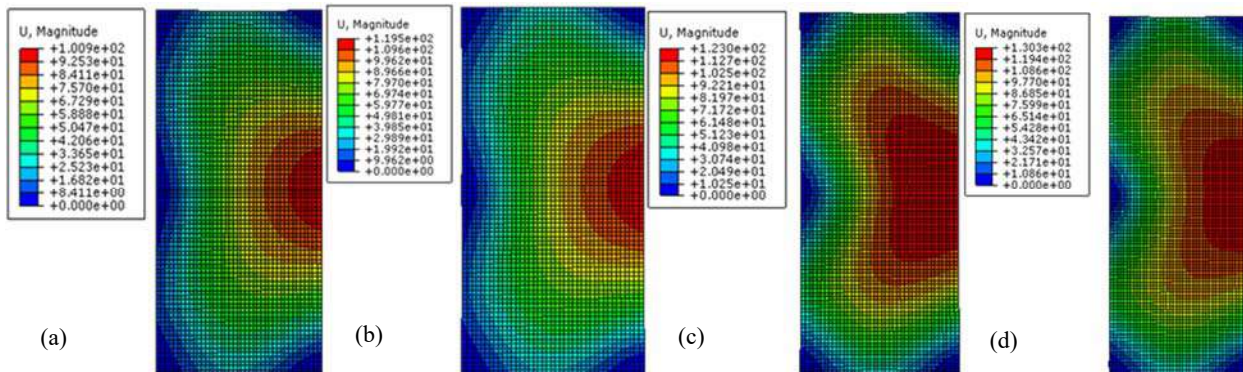


**Fig. 12 Deflection of (a) 3.6 m (b) 4.1 m (c) 4.6 m and (d) 5.1 m slab span due to penultimate column failure**

The simulations were carried out for 3.6m, 4.1 m, 4.6 m, and 5.1 m slab length, see **Fig. 13**. The slab displacement was monitored for penultimate column failure case and the graph was plotted between displacement and time is shown in **Fig. 13(a)**. Displacement increases as the time increases for all the chosen cases. The displacement for 3.6 m, 4.1 m, 4.6 m, and 5.1 m slab length is 97.01 mm, 115.9 mm, 119.9 mm, and 128.7 mm respectively. The percentage variation of displacement between 3.6 m and 4.1 m slab is 16.29%, between 4.1m and 4.6m is 3.45%, between 4.1 m and 5.1 m is 11.04%. Here 4.1m slab is taken as reference for calculating percentage variation of displacement. The slab displacement was monitored for penultimate column failure case and the graph was plotted between displacement and time is shown in **Fig. 13(b)**. Displacement increases as the time increases for all the slab length. The displacement for 3.6 m, 4.1 m, 4.6 m, and 5.1 m slab length is 100.9, 119.5, 123 and 130 mm respectively. The percentage variation of displacement between 3.6 m and 4.1 m slab is 15.56%, between 4.1m and 4.6m is 2.92%, between 4.1 m and 5.1 m is 8.78 %. Here 4.1 m slab is taken as reference for calculating percentage variation of displacement.

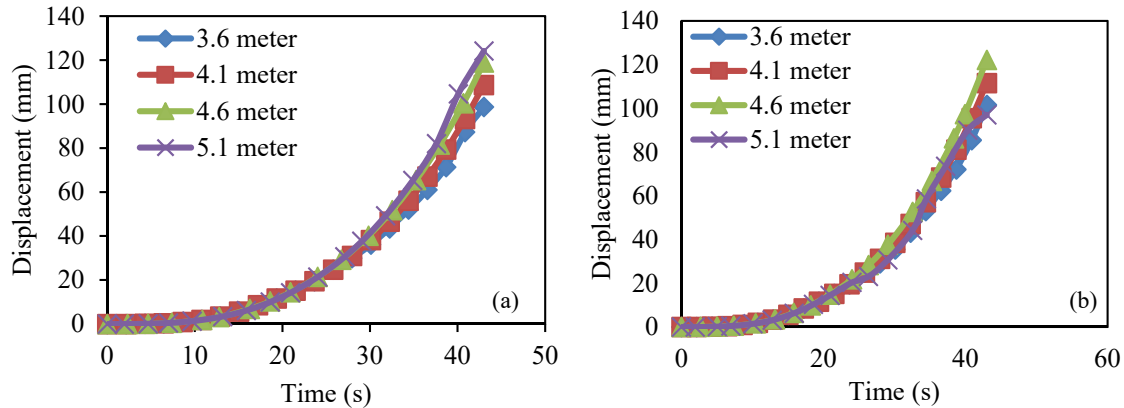


**Fig. 13 Displacement of varying length of span subjected to (a) corner (b) penultimate column failure**

## CONCLUSION

The present study addresses the finite element investigation on the behavior of flat slab for progressive collapse. The numerical simulations were carried out using ABAQUS finite element tool to predict the response of slab and results are compared with the experimental available in literature. The simulations were carried out to study the influence of thickness of slab and span length. The response of reinforced concrete slab was studied in terms of deflection of concrete slab and the following conclusions have been drawn.

- On comparing the result for static case it was found that a good agreement is achieved for force redistribution in other remaining columns with the experiment. The percentage variation of 1.25% to 28% occurs in force redistribution when corner column was removed. It was also observed that when the penultimate column got removed the percentage variation observed is 6.25% to 23%.
- Result showed that the thickness variation of 70mm, 80mm, 90mm, and 100mm for slab as the thickness increases there was decrease in deflection for both corner and penultimate column failure. It was also observed that deflection in corner column failure case is less than penultimate column failure case for the same loading.
- Result also showed that as the length of slab increases from 3.6m to 5.1 m, there was increase in deflection for both corner and penultimate column failure case. It was also observed that deflection in corner column failure case is less than penultimate column failure case for the same loading.

## REFERENCES

- ABAQUS, (2014) 6.14 Documentation. Dassault Systemes Simulia Corporation.
- Abbasi, M. S. A., Baluch M. H., Azad, A. K., and Rahman, H. H. A. (1992) "Nonlinear Finite Element Modelling of Failure Modes in RC Slabs" *Computers & Structures*, 42(5):815– 823.
- Baker, J. W., Schubert M., and Faber M. H. (2008) "On the assessment of robustness" *Structural Safety*, 30(3):253– 267.
- Choi, J. W. and Kim, J. H. J. (2012) "Experimental Investigations on Moment Redistribution and Punching Shear of Flat Plates" *ACI Structural Journal*, 109(3):329–337.
- Das, S. K. and Morley, C. T. (2005) "Compressive membrane action in circular reinforced slabs" *International Journal of Mechanical Sciences*, 47(10):1629–1647.
- Fang, B. A. Izzuddin, A. Y. Elghazouli, and D. A. Nethercot. (2011) "Robustness of steel composite building structures subject to localised fire" *Fire Safety Journal*, 46(6):348– 363.
- Iqbal, M.A., Senthil, K., Bhargava, P. and Gupta, N.K., (2015), "The characterization and ballistic evaluation of mild steel", *Int. J. Impact Eng.*, 78, 98-113.
- Iribarren, B. S., Berke, P., Bouillard, P., Vantomme J., and Massart, T. J. (2011) "Investigation of the influence of design and material parameters in the progressive collapse analysis of RC structures" *Engineering Structures*, 33(10):2805–2820.
- Jayasooriya, R., Thambiratnam, D. P., Perera, N. J., and Kosse, V. (2011) "Blast and residual capacity analysis of reinforced concrete framed buildings" *Engineering Structures*, 33 (12):3483–3495.
- Johnson, G.R. and Cook, W.H. (1985), "Fracture characteristics of three metals subjected to various strains, strain rates, temperatures, and pressures", *Eng. Fracture Mech.*, 21, 31–48.

- Kokot, S., Anthoine, A., Negro, P., and Solomos, G. (2012) “*Static and dynamic analysis of a reinforced concrete flat slab frame building for progressive collapse*” *Engineering Structures*, 40:205–217.
- Saito, H., Imamura A., Takeuchi, M., Okamoto, S., Kasai, Y., Tsubota, H., and Yoshimura, M. (1995) “*Loading Capacities and Failure Modes of Various Reinforced Concrete Slabs Subjected to High-Speed Loading*” *Nuclear Engineering and Design*, 156(1-2):277–286.
- Sasani, Mehrdad, Marlon Bazan, and Serkan Sagiroglu. (2007) “*Experimental and analytical progressive collapse evaluation of actual reinforced concrete structure*” *ACI Structural Journal* 104.6: 731.
- Sasani M. and Sagiroglu S, (2008) “*Progressive collapse resistance of Hotel San Diego*” *Journal of Structural Engineering-ASCE*, 134(3):478–488.
- Sasani M, and Sagiroglu, S, (2010) “*Gravity Load Redistribution and Progressive Collapse Resistance of 20-Story Reinforced Concrete Structure following Loss of Interior Column*” *ACI Structural Journal*, 107(6):636–644.
- Senthil, K., Rupali, S. and Satyanarayanan, K.S. (2017), “Experiments on ductile and non-ductile reinforced concrete frames under static and cyclic loading”, *J. Coupled Sys. Multiscale Dyn.*, 5(1), 38-50.
- Senthil, K., Rupali, S. and Kaur, N. (2018a). “The performance of monolithic reinforced concrete structure includes slab, beam and column against blast load”, *J. Mat. Eng. Struct.* 5(2), 137-151.
- Senthil K., Singhal A., Shailja B. (2018b). “Influence of mass of TNT and standoff distance on the response of reinforced concrete flat slab against blast loading”, *Jordan J. Civil Eng*, Under Review.
- Senthil, K., Gupta A. and Singh, S.P. (2018c) “Computation of stress-deformation of deep beam with openings using finite element method”, *Adv. Concrete Const.* 6(3), 245-268.
- Ngo D. and Scordelis, A. C, (1967) “*Finite Element Analysis of Reinforced Concrete Beams*” *ACI Journal*, Vol. 64, pp. 152-163.
- Russell, J. M., Owen, J. S., Hajirasouliha I, (2015) “*Experimental investigation on the dynamic response of RC flat slabs after a sudden column loss*” *Engineering Structures* 99 28-41.



## Effect of Aspect Ratio Change in Linear Static Analysis of Orthotropic Plates

Safdar Naveed Amini,<sup>1</sup> Manju Dominic<sup>2\*</sup>

<sup>1</sup>M-Tech Scholar, Department of Civil Engineering, FET, Manav Rachna International University, Faridabad  
E-mail id – safdaramini123@gmail.com

<sup>2\*</sup>Associate Professor, Department of Civil Engineering, FET, Manav Rachna International University, Faridabad,  
E-mail id – manjudominic.fet@mriu.edu.in (Corresponding Author)

**Abstract:** - This paper presents a linear static analysis of Glass/Epoxy laminated composite plate. It aims at working on the behavior of laminated composite plates under uniform loading conditions which are transverse in nature. The static analysis includes the maximum deflection analysis on an orthotropic plate when a static load is applied and results are in close agreement with analytical FEM i.e. classical laminated plate theory (CLPT). In FEA, SHELL 181 is being used and orthotropic plate here is selected as composite plate. Analysis is done in ANSYS 14.0. Meshing is done with variation of the finite element and the difference of deflections is calculated. Here, it is seen that as the aspect ratio of the element changes, the deflection also varies. Optimum aspect ratio which gives a close agreement with the analytical value has been found out. Linear static analysis is carried out on a composite laminated plate with dimensions (200x200) mm with 1 to 8 layer and stacking as 45, 0, -45, 90-degree symmetric angle laminated composite plates at simply supported boundary conditions.

**KEYWORDS:** - Laminated Composite plate, Orthotropic plate, Stacking, Orientation FEM, CLPT, ANSYS

### INTRODUCTION

Composite materials are those which have two or more different macroscopical phases. Now-a-days, composite materials enormously used in civil and structural engineering, aerospace, automobile and nuclear engineering. Composite materials combine with each other in such a way that their individual materials can be easily distinguished. They have high specific strength and high specific stiffness as compared with its weight ratio. They have a better ability to change the fiber orientations and volume compositions to meet the design requirements. Laminated composite materials and thin shells structures are foremost need of high rise, modern and advanced buildings.

Matrix when compared with its fiber direction and orientation, limits the strength of laminated composites. Hence, matrix and fiber are prepared artificially with volume fractions of 60% fiber and 40% matrix to achieve the desired strength with no increase in weight (Mechanics of composite materials, by Robert M Jones). Glass fibers are most commonly used as its main advantages are their low cost, high tensile strength, excellent insulating properties and high chemical resistance. Structural components like plates and beam made of composite laminated materials are being increasingly used in engineering applications because of their high strength. Finite element method and classical lamination plate theory is efficient and versatile method for analysis of its complex structural behavior.

### LITERATURE REVIEW

B. Vijay Kumar (2015) titled- “**An Investigation of Ply Behavior in A GFRP Composite Laminated Plate**”, his objective was to characterize effect of composite ply sequences, material properties and type of loading on composite laminated plate. 3 cases extracted. 1) Tension load- when load applied between fiber and matrix occurs and material breaks. 2) Transverse load- When load applied composite plates max. Change occurs to matrix and fails quickly. 3) Shear load- When load applied composite plates delamination occurs, strength to laminate decreases.

Dominic Manju (2015) titled “**Design of non-metallic ship hulls for strength and sustainability**” explained the importance of composite laminates in ship industry.

K.B Ladhane (2014) titled- “**Bending Analysis of Simply Supported and Clamped Circular Plate**”, analyzed static bending of isotropic plate using CPT and FEM ANSYS. The proposed method includes analysis of plate on simply supported with point load, simply supported with U.D.L.

Niral R. Pate (2014) titled, “**A Research Paper on Static Analysis of Laminated Composite Plate**”, the objective of paper was to statically analyze laminated composite plate with various boundary conditions and various load applications. Comparison is then done between results from numerical analysis FEM and FEM ANSYS simulation which shows a close agreement with a little variation in result.

B. Sidda Reddy (2014) titled- “**Bending analysis of laminated composite plates using finite element method**”,

defines the bending analysis for various side-to-thickness ratios, aspect ratios & Modular ratios to study effect of transverse shear deformation on deflection and stress of laminated composite plates subjected to U.D.L.  
 A. Vijayakumar (2013) titled- “**Analytical Study on Various Types of FRP Beams by using ANSYS**”, the objective was to analyze the behavior of Gfrp and Cfrp composite laminates to enhance their properties in terms of their strength, ductility. Comparison in done between numerical FEM and FEA ANSYS.

**SPECIMEN AND METHODOLOGY**

The specimen details are considered in the present study is shown in Fig. 1 and the geometric as well as material properties are discussed in Tables 1 and 2.

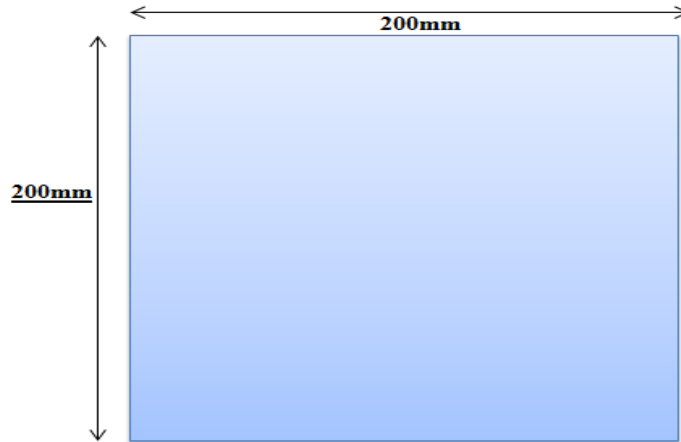


**Fig. 1 (200x200) mm composite plate specimen**

**Table 1  
 Geometric properties**

Nature	E-glass(epoxy/glass)
Length (a)	200 mm
Width (b)	200 mm
Thickness (t)	0.5 mm each
No. of plies	8
Total Thickness	4 mm

**Table 2  
 Material Properties**

Longitudinal stiffness (E1)	44.58 x 10 <sup>3</sup> N/mm <sup>2</sup>
Transverse Stiffness (E2 = E3)	7.94 x 10 <sup>3</sup> N/mm <sup>2</sup>
Major Poisson’s ratio (ν <sub>12</sub> )	0.19
Shear modulus (G <sub>12</sub> =G <sub>23</sub> =G <sub>13</sub> )	2.97 x 10 <sup>3</sup> N/mm <sup>2</sup>
Force applied (p)	0.01 N/mm <sup>2</sup>

**BOUNDARY CONDITIONS**

Here, for the solution of the laminated composite plates we have taken the Simply Supported Edge Conditions, Fig. 1. **Simply Supported Edge Conditions:** - Plate boundaries that is prevented from deflecting but are free to rotate about a line along the boundary edge such as a hinge or a support is defined as a simply supported edge.

**BASIC ASSUMPTIONS**

Following are the assumptions for plate analysis:-

- The laminate deforms according to the Kirchhoff - Love assumptions for bending and stretching of thin plates (as assumed in classical plate theory).
- The plate is initially flat. Therefore, the in-plane deflections in x and y directions at the mid-surface are assumed to be zero.
- The mid-plane is a neutral plane. The middle plane of the plate remains free of in-plane stress/strain. Bending of the plate will cause material above and below this mid-plane to deform in-plane.
- Line elements lying perpendicular to the middle surface of the plate remain perpendicular to the middle surface during deformation this is similar the “plane sections remain plane” assumption of the beam theory
- Line elements lying perpendicular to the mid-surface do not change length during deformation throughout the plate. Again, this is similar to an assumption of the beam theory.
- The individual lamina can be isotropic, orthotropic or transversely isotropic.

### STACKING OF PLATE AND ITS ORIENTATION

Stacking sequence plays a very important role on the deflection and shear resistance of laminates. In a unidirectional laminate, since the reinforcing fibers are all oriented in the same direction, no delamination occurs. Increasing the thickness of each layer will also lead to increased delamination.

Number of plies, thickness of each ply and its stacking sequence are taken as per the ASTM specimen used for the impact testing. Orientation angle as 45/0/-45/90/45/0/-45/90 as also per ASTM standards, Fig. 2. Reason for stacking of plates in different angles is because whenever load is applied to the plate, plate with different angle of orientation gives better rigidity and less deflection.

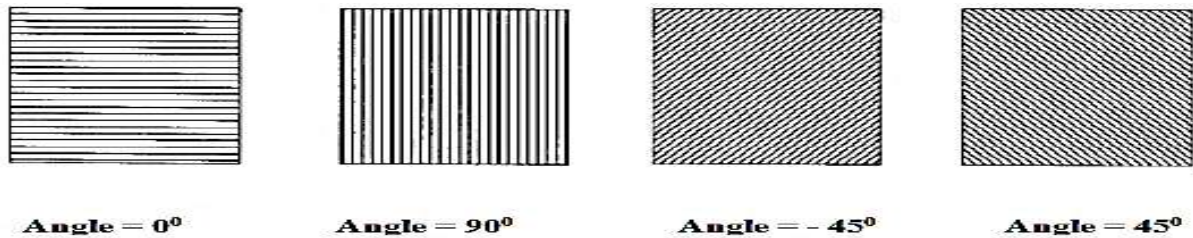


Fig. 2 – Orientation of Laminated Composite plates

### STACKING OF PLATES IN ANSYS

Here, in Fig. 3, we can see 8 number of plates that are placed one above the other in a symmetrical angle formation thus to counteract the deformation and provide strength and shear resistance.

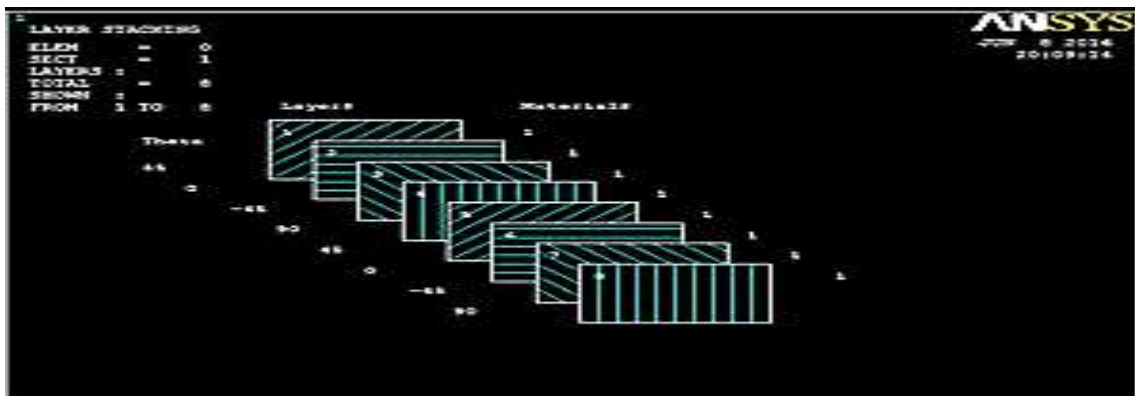


Fig.3 - Stacking descriptions of 8 layers laminated composite plate

### SHELL 181 ELEMENT DESCRIPTION (ANSYS)

SHELL181 element is appropriate for analyzing moderately-thick to thin shell structures. SHELL 181 is a four-node element with six degrees of freedom at each node: The three are translations in the x, y, and z directions, and the other is rotations about the x, y, and z-axes. SHELL181 which thus accounts for load stiffness effects of distributed pressures. SHELL181 may be used for layered and stepwise applications for sandwich construction or for modeling the composite shells. Accuracy in modeling composite shells is described by first-order shear-deformation theory (usually to as known as the Mindlin- Reissner shell theory).

The element solvation and formulation is based on logarithmic strain and true stress measurements. SHELL181 is described in Theory Reference for Mechanical APDL and structural. Following figure shows the node locations, geometry, and element coordinate system for this prescribed element. The element is defined by shell section information and by its four nodes (I, J, K, and L), Fig. 4.

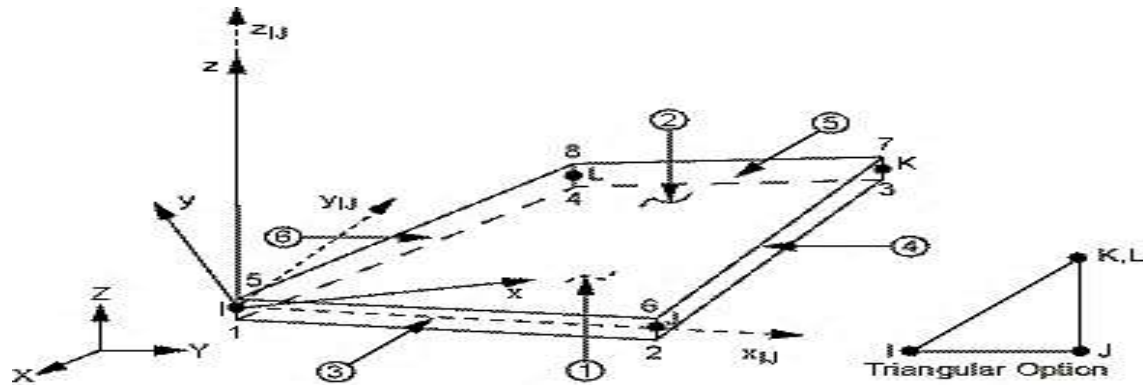


Fig. 4 - SHELL 181 Geometry

### METHODOLOGY

**CLPT:-** The analysis of laminate plates involves the Classical Laminated plate theory which is almost identical to the classical plate theory except for anisotropy. Both require that the laminate be thin where the span of a and b is greater than 10 times the thickness (t). They also require a small displacement in the transverse direction (w), where w is significantly smaller than (t).

#### FORMULAS

$$w_{max} = \frac{16p}{\pi^6 \left[ D_{11} \left(\frac{1}{a}\right)^4 + 2(D_{12} + 2D_{66}) \left(\frac{1}{a}\right)^2 \left(\frac{1}{b}\right)^2 + D_{22} \left(\frac{1}{b}\right)^4 \right]}$$

Where

$$D_{ij} = \frac{1}{3} \sum_{k=1}^N (\bar{Q}_{ij})_k (Z_k^3 - Z_{k-1}^3)$$

$$Q_{11} = \frac{E_1}{1-\nu_{12}\nu_{21}}, \quad Q_{12} = \frac{\nu_{12}E_2}{1-\nu_{12}\nu_{21}}, \quad Q_{22} = \frac{E_2}{1-\nu_{12}\nu_{21}}, \quad Q_{66} = G_{12}$$

where  $E_1$  = Longitudinal stiffness

$E_2$  = Transverse Stiffness

$\nu_{12}/\nu_{21}$  = Major / Minor Poisson's ratio

$$\bar{Q}_{11} = Q_{11} (\cos \theta)^4 + 2(Q_{12} + 2Q_{66})(\sin \theta)^2(\cos \theta)^2 + Q_{22}(\sin \theta)^4$$

$$\bar{Q}_{12} = (Q_{11} + Q_{22} - 4Q_{66})(\sin \theta)^2 (\cos \theta)^2 + Q_{12} ((\sin \theta)^4 + (\cos \theta)^4)$$

$$\bar{Q}_{22} = Q_{11} (\sin \theta)^4 + 2(Q_{12} + 2Q_{66})(\sin \theta)^2(\cos \theta)^2 + Q_{22}(\cos \theta)^4$$

$$\bar{Q}_{66} = (Q_{11} + Q_{22} - 2Q_{12} - 2Q_{66})(\sin \theta)^2(\cos \theta)^2 + Q_{66}((\sin \theta)^4 + (\cos \theta)^4)$$

### DEFLECTION VALUES AND % ERROR WITH INCREASING ASPECT RATIO IN ANSYS

Dx = Number of divisions along x – axis

Ref:- M Jones (1975),  
 Mechanics of composite  
 materials, Page no. 252,  
 section 5.5

Dy = Number of divisions along y- axis

**Table 3**

In Table 3, the no. of divisions on x – axis are Dx = 4 and divisions on y – axis Dy increases by the factor of 2. Thus, Aspect Ratio of the finite element is changed from 1 to 5 changing the deflection values and the no. of elements.

Aspect ratio	1	1.5	2	2.5	3	3.5	4	4.5	5
Deflection (mm)	.596 x 10 <sup>-4</sup>	.597 x 10 <sup>-4</sup>	.597 x 10 <sup>-4</sup>	.597 x 10 <sup>-4</sup>	.598 x 10 <sup>-4</sup>				
% Error	-18.8%	-18.8%	-18.8%	-18.8%	-18.8%	-18.4%	-18.4%	-	-18.1% 18.4%
No. of Elements	16	24	32	40	48	56	64	72	80

**Table 4**

Table 4, the no. of divisions on x – axis are Dx =5 and divisions on y – axis Dy increases by the factor of 2.5. Thus, Aspect Ratio of finite element is changed from 1 to 5 changing the deflection values and no. of elements.

Aspect ratio	1	1.5	2	2.5	3	3.5	4	4.5	5
Deflection in(mm)	0.542 x 10 <sup>-4</sup>	0.562 x 10 <sup>-4</sup>	0.568 x 10 <sup>-4</sup>	0.565 x 10 <sup>-4</sup>	0.566 x 10 <sup>-4</sup>	0.569 x 10 <sup>-4</sup>	0.569 x 10 <sup>-4</sup>	0.570 x 10 <sup>-4</sup>	0.569 x 10 <sup>-4</sup>
% Error	7.35%	3.9%	2.9%	3.4%	3.2%	2.8%	2.8%	2.5%	2.8%
No. of Elements	25	37	50	62	75	87	100	112	125

**Table 5**

Table 5, the no. of divisions on x – axis are Dx =7 and divisions on y – axis Dy increases by the factor of 3.5. Thus, Aspect Ratio of finite element is changed from 1 to 5 changing the deflection values and no. of elements.

Aspect ratio	1	1.5	2	2.5	3	3.5	4	4.5	5
Deflection in(mm)	.0567 x 10 <sup>-4</sup>	.0567 x 10 <sup>-4</sup>	.0581 x 10 <sup>-4</sup>	.0582 x 10 <sup>-4</sup>	.0581 x 10 <sup>-4</sup>	.0582 x 10 <sup>-4</sup>	.0584 x 10 <sup>-4</sup>	.0584 x 10 <sup>-4</sup>	.0584 x 10 <sup>-4</sup>
% Error	3.0%	3.0%	0.68%	0.51%	0.59%	0.51%	0.17%	0.17%	0.17%
No. of Elements	49	74	98	122	147	172	196	220	245

**Table 6**

Table 6, the no. of divisions on x – axis are Dx =8 and divisions on y – axis Dy increases by the factor of 4. Thus, Aspect Ratio of finite element is changed from 1 to 5 changing the deflection values and no. of elements.

Aspect ratio	1	1.5	2	2.5	3	3.5	4	4.5	5
Deflection in(mm)	0.594 x 10 <sup>-4</sup>	0.595 x 10 <sup>-4</sup>	0.596 x 10 <sup>-4</sup>	0.596 x 10 <sup>-4</sup>	0.597 x 10 <sup>-4</sup>	0.597 x 10 <sup>-4</sup>	0.598 x 10 <sup>-4</sup>	0.598 x 10 <sup>-4</sup>	0.598 x 10 <sup>-4</sup>
% Error	-15.3	-16.4	-18.8	-18.8	-18.96	-19.6	-22.2	22.2	-22.2
No. of Elements	64	96	128	160	192	224	256	288	320

**Table 7**

Table 7, number of divisions on x – axis are  $D_x = 10$  and divisions on y – axis  $D_y$  increases by the factor of 5. Thus, Aspect Ratio of finite element is changed from 1 to 5 changing the deflection values and no. of elements.

Aspect ratio	1	1.5	2	2.5	3	3.5	4	4.5	5
Deflection in(mm)	0.594 $\times 10^{-4}$	0.593 $\times 10^{-4}$	0.596 $\times 10^{-4}$	0.596 $\times 10^{-4}$	0.598 $\times 10^{-4}$	0.598 $\times 10^{-4}$	0.598 $\times 10^{-4}$	0.598 $\times 10^{-4}$	0.599 $\times 10^{-4}$
% Error	-15.3	-13.6	-18.8	-18.8%	-22.2%	-22.2%	-22.2%	-22.2%	-24.8%
No. of Elements	100	150	200	250	300	350	400	450	500

**Table 8**

Table 8, the no. of divisions on x – axis are  $D_x = 15$  and divisions on y – axis  $D_y$  increases by the factor of 7.5. Thus, Aspect Ratio of finite element is changed from 1 to 5 changing the deflection values and no. of elements.

Aspect ratio	1	1.5	2	2.5	3	3.5	4
Deflection in(mm)	$0.590 \times 10^{-4}$	$0.593 \times 10^{-4}$	$0.595 \times 10^{-4}$	$0.596 \times 10^{-4}$	$0.596 \times 10^{-4}$	$0.597 \times 10^{-4}$	$0.597 \times 10^{-4}$
% Error	-8.54%	-16.8%	-17%	-18.8%	-18.8%	-19.6%	-19.6%
No. of Elements	225	337	450	562	675	787	900

**Table 9**

Table 9, the no. of divisions on x – axis are  $D_x = 20$  and divisions on y – axis  $D_y$  increases by the factor of 10. Thus, Aspect Ratio of finite element is changed from 1 to 5 changing the deflection values and no. of elements.

Aspect ratio	1	1.5	2	2.5	3	3.5	4	4.5	5
Deflection in(mm)	0.598 $\times 10^{-4}$	0.599 $\times 10^{-4}$	0.600 $\times 10^{-4}$	0.600 $\times 10^{-4}$	0.600 $\times 10^{-4}$	0.601 $\times 10^{-4}$	0.601 $\times 10^{-4}$	0.601 $\times 10^{-4}$	0.601 $\times 10^{-4}$
% Error	-22.2	-23.9	-25.6	-25.6	-25.6	-27.3	-27.3	-27.3	-27.3
No. of Elements	400	600	800	1000	1200	1400	1600	1800	2000

## RESULTS AND DISCUSSIONS

The above graph is a representation of the tabulated values given in above tables and from that it is noticed that the element with aspect ratio 5 when  $D_x = 7$  and  $D_y = 35$ , gives the most close value with the analytical value.

$$\begin{aligned}
 \text{Analytical } W_{\max} &= 0.585 \times 10^{-4} \text{ mm} \\
 \text{ANSYS } W_{\max} &= 0.584 \times 10^{-4} \text{ mm} \\
 \text{\% Error} &= 0.17\%
 \end{aligned}$$

Where  $D_x$  = Number of divisions on x - axis  
 $D_y$  = Number of divisions on y – axis

Analysis was done with varying the aspect ratio by finite element. Here, it is found out that if aspect ratio of the composite plate is changed as described above, the deflection calculations i.e.  $W_{\max}$  also varies, Fig. 5. It is noticed that if we take

the number of divisions along x-axis to 4, 5, 7, 10, 15 and 20 the  $W_{max}$  variations with the analytical value changes with a percentage error difference. In the Finite Element Analysis (FEA) when number of elements are 7 along x-axis, we got a highly close result compared with analytical value i.e. ( $0.585 \times 10^{-4}$  mm).

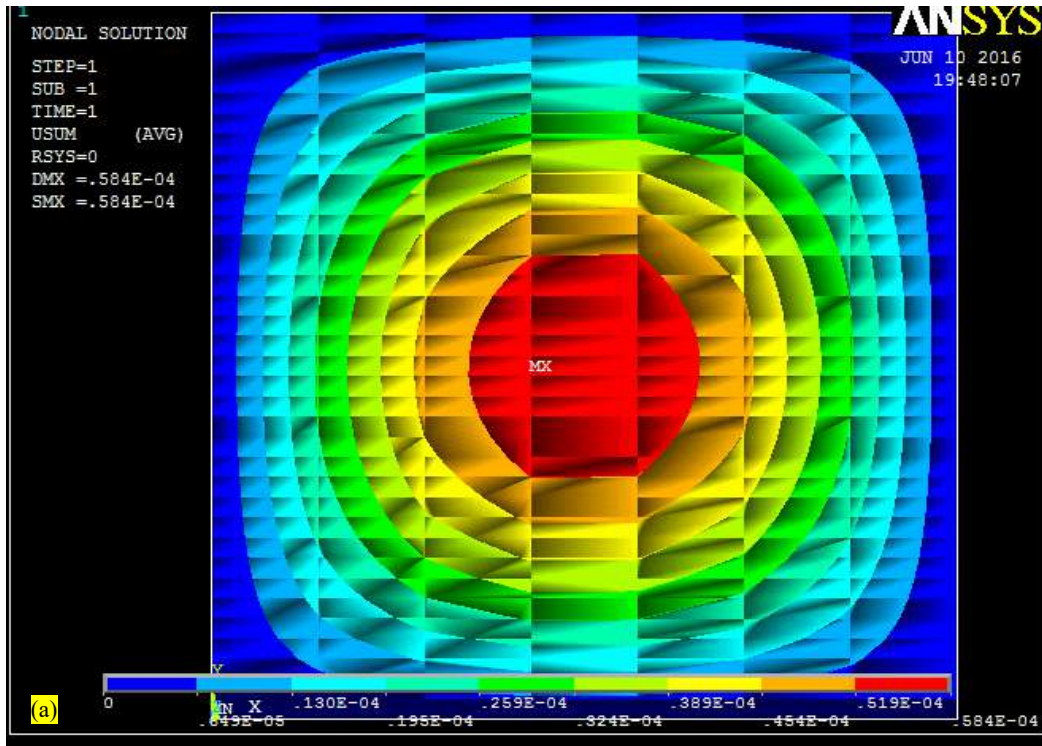
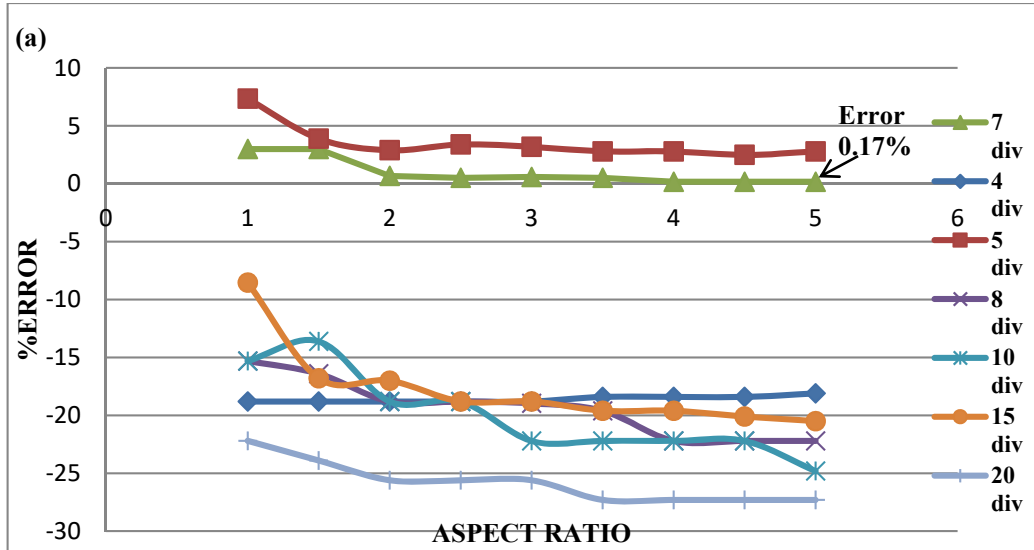


Fig.5 (a) Variation of % Error with Aspect Ratio in Laminated Composite and (b)  $W_{max}$  of Laminated composite plate composite plate

## CONCLUSIONS

- Finer the Mesh, higher the accuracy of result as we can see in above graph where the line having 4, 5, 7, 8, 10, 15 and 20 elements on length side, its value comes closer to the analytical value having aspect ratio 1.
- When no. of elements are 4 on length side we can notice in the above graph that there is no significant change in the deflection value when aspect ratio increased from 1 to 5.
- But, when taking number of elements 5 along x-axis, we find  $W_{max}$  is relatively near to the analytical value giving a less % Error and thus fluctuates from 7.35% to 2.8% as aspect ratio is increasing from 1 to 5.
- The most desirable and highly close result we got with number of elements 7 along x-axis, compared with analytical value giving a % error which fluctuates from 3% to 0.17% as aspect ratio increases from 1 to 5.

Hence, GFRP laminated composite plate modeling in which 8 numbers of layers are made and they are placed one above the other are calculated very effectively and efficiently. Laminated Composite Plates can easily be analysed with ANSYS and can be compared with Classical Laminated Plate Theory (CLPT). Finite element method play a significant role in achieving the appropriate results with less time and cost saving.

## REFERENCES

- Sushil B.Chopade<sup>1</sup>, Prof.K.M.Narkar (2015) “Design and Analysis of E-Glass/Epoxy Composite Monoleaf Spring for Light Vehicle”, International Journal of Innovative Research in Science, Engineering and Technology, (IJRSET), Vol. 4, Issue 1.
- P. S. Gujar<sup>1</sup>, K. B. Ladhane (2015) “Bending Analysis of Simply Supported and Clamped Circular Plate”, SSRG International Journal of Civil Engineering (SSRG-IJCE) Volume 2 Issue 5.
- B.Vijaykumar, Y.VenuBabu (2014) “An Investigation of Ply Behavior in A GFRP Composite Laminated Plate”, (IJRSET), Vol. 3, Issue 11.
- Sunu Mariam Saji<sup>1</sup> & Prabha C (2014), “Free Vibration Analysis Of Laminated Composite Shallow Shells”, Impact: International Journal of Research in Engineering & Technology (IMPACT: IJRET), Vol. 2, Issue 9.
- Mervin Ealiyas Mathews<sup>1</sup>, Shabna M.S (2014) “Thermal-Static Structural Analysis of Isotropic Rectangular Plates”, IOSR Journal of Mechanical and Civil Engineering (IOSR-JMCE).
- Prudhvi Raj Naik, B.Mahasenadhipathi Rao (2013) “Experimental Test on Gfrp-Epoxy Composite Laminate for Mechanical, Chemical & Thermal Properties”, IOSR Journal of Mechanical and Civil Engineering (IOSR-JMCE), Volume 8, Issue 6.
- Puneet Sharma, Vijay Kumar Bhanot (2013) “Research Work on Fiber Glass Wool Reinforced And Epoxy Matrix Composite Material”, (IJMERR), Vol. 2, No. 2..
- Niral R.Patel, A.D.Vadaliya (2013) “A Research Paper on Static Analysis of Laminated Composite Plate”, Indian Journal of Research, Volume: 3, Issue: 5.
- Junaid Kameran Ahmed, V.C. Agarwal (2013) “Static and Dynamic Analysis of Composite Laminated Plate”, International Journal of Innovative Technology and Exploring Engineering (IJITEE), Volume-3, Issue-6.
- Wasim Akram, Sachin Kumar Chaturvedi (2013) “Comparative Study of Mechanical Properties of E-Glass/Epoxy Composite Materials With Al<sub>2</sub>O<sub>3</sub>, CaCo<sub>3</sub>, SiO<sub>2</sub> AND PBO Fillers”, International Journal of Engineering Research & Technology (IJERT), Vol. 2 Issue 7.
- B. Sidda Reddy, A.Ramanjaneya Reddy (2012) “Bending analysis of laminated composite plates using finite element method”, International Journal of Engineering, Science and Technology”, Vol. 4, No. 2.
- Vanam B. C. L. I, Rajyalakshmi M (2012) “Static analysis of an isotropic rectangular plate using finite element analysis (FEA)”, Journal of Mechanical Engineering Research Vol. 4(4), pp. 148-162.
- Dr. Abdulkareem, Al Humdany Dr. Emad Q. Hussein (2012) “Theoretical And Numerical Analysis For Buckling Of Antisymmetric Simply Supported Laminated Plates Under Uniaxial Loads, Journal of Kerbala University, Vol. 10.
- A.Vijayakumar, Dr.D.L.Venkatash babu (2012) “Analytical Study on Various Types of FRP Beams by using ANSYS”, (IJERA), Vol. 2, Issue 5, September.
- M. Khazaei-Poul and F. Nateghi-Alahi (2011) “Theoretical and Numerical Study On The Strengthened Steel Plate Shear Walls By Frp Laminates”, Structural Engineering Research Center. IIEES.



## Enhancing the Characteristics of Structures, Retrofitted with Engineered Cementitious Composites (ECC) – A Review

S. S. Kolhe,<sup>1</sup> M. S. Endait,<sup>\*2</sup> S. K. Wagh<sup>1</sup>

<sup>1</sup> PG Student, Civil Engineering Department, School of Engineering & Technology, Sandip University, Nasik; Email: sskolhe23@gmail.com, Email: suyashwagh15@gmail.com<sup>2</sup>

<sup>2\*</sup> Associate Professor, Civil Engineering Department, School of Engineering & Technology, Sandip University, Nasik; Email: mahesh.endait@sandipuniversity.edu.in (Corresponding Author)

### ABSTRACT

Low tensile capabilities of concrete and the masonry elements can effectively be retrofitted by addition of fibrous components like high tensile fibers, Work herein reviews the endless work carried out in enhancing the characteristics of masonry structures by introducing a composite of such fibers named engineered cementitious composites (ECC). A brief summary of work carried to decide the fiber type, mix design, experimental work, characteristic changes and review of field applications of use of ECC are brought to notice. This paper suggests the low volume addition of tensile fibers of around 2% of total volume of concrete which is effective in terms of economy as well as weight reduction of the entire structure, paper also notifies the increment in load carrying capabilities of masonry structures subjected to out of plane behavior. In terms of applicability, use of hybrid fibrous cementitious composites in strengthening of unreinforced masonry structures as well as the flexural members like masonry beams was noticed. Future direction in development and utilization of ECC in different fields and direct application in retrofitting of masonry structures, use of such composites in enhancing the tensile and load carrying capacity of retaining structures built in masonry is finally suggested.

**KEYWORDS:** ECC; masonry; fibers; strengthening; tensile capabilities; retaining structures.

### INTRODUCTION

Retrofitting is the method to strengthen the structures in order to increase the performance life of the structure. This technique of retrofitting is widely accepted when preserving the structure from historical point of view is very necessary. Retrofitting is also necessary for the structures which starts deteriorating in early ages which may be due to environmental impacts or also because of wrong techniques adopted or variations in the designs and construction materials. There are various methods available in the field of retrofitting, few of which are, use of different types of steel bracings, steel jacketing, use of Carbon fiber reinforced polymers (CFRPs), concrete jacketing, introduction of polypropylene fiber ropes (PPFRs), application of high performance fiber reinforced composites, use of epoxy resins etc. but considering the cost effectiveness and applicability new technique of retrofitting with Engineering cementitious composites (ECC) was introduced.

ECC is the family of material which is regarded with its tensile, higher load carrying and higher deformation capabilities. In recent year's need of introducing different material composites to reduce the overall cost of retrofitting of structures is the main focus and ECC is one of it. Various mix designs are already proposed and widely accepted but cost effectiveness needs to be considered, due to high volume addition of fibers. (Maalej et al., 2012) suggested the use of hybrid fiber composites in enhancing the properties of potential structures. High volume additions can either result in heavy composites or even result in high cost of application due to higher cost of fibers, so cheap fibers and high strength fibers which can result in better performance with minimum additions was needed.

Chemical and physical properties of polyvinyl alcohol (PVA) attracted their utilization in ECCs which almost covers all the shortcomings mentioned above. (Thong, Teo, & Ng, 2016) extracted and reviewed the historical development, production, classes and properties of PVA. According to them PVA fibers can be generated from hydrolysis of acetate groups of PVA and then polymerization of vinyl acetate monomers into polyvinyl acetates. So use of PVA fibers are deeply reviewed in this study.

Application of the composite using PVA fibers have been studied by many researchers but strengthening of unreinforced masonry structures using this composite was to be deeply studied. The objective was laid due to the fact that masonry structures are mainly suitable to damages when loads are applied in out of plane direction, these loads includes seismic

forces, impact loads or wind loads.

Work herein reviewed various retrofitting techniques, different fibers available to be used in ECCs, options to strengthen unreinforced masonry structures and lookover of projects where solution of ECC strengthening was applied. Further it is suggested that the application should be extended to strengthening of earth retaining structures constructed in unreinforced masonry.

## **RETROFITTING TECHNIQUES**

Old age and heritage structures based on their importance & necessity need to be strengthened and preserved for years and years, this can ultimately be done by retrofitting of such structures. Endless research work has been carried out to bring in view new and innovative techniques in retrofitting of such heritage structures. Importance of retrofitting can be observed either in preserving the old structures or to strengthen the damaged buildings. Damages are referred to destruction of few elements of the building or overall collapse of the structure. Earthquake is defined to be a main cause in such destruction of building structures and a huge loss of mankind. So seismic retrofitting is the key which needs to be focused upon to reduce damage during and after the earthquake, an additional reason stating its importance is because of the fact that preliminary and secondary health care centers, daily utility houses & school buildings needs to be started as early as possible after the natural strike of disasters. Same importance of seismic retrofitting and solution proposing retrofitting of RC columns of existing school building using 3D nonlinear time history & dynamic analysis on a finite element based model using ant colony optimization technique (ACO) was brought to view by (Seo, Kim, & Kwon, 2018). Taking into consideration the same aspects, (Almeida, Ferreira, Proença, & Gago, 2017), presented their work in strengthening of old school building by use of steel buckling restrained braces, which in terms of strength increment, deformability, energy dissipation proved to be a better solution. A school building selected was from Portimao city which had highest seismicity level, named “Escola Scundaria, Poeta Antonio Aleixo”. But, both the above mentioned researchers did not take into consideration of design specifications of symmetrical and asymmetrical constructions, (Kim & Jeong, 2016) in their work reviewed different options available in retrofitting of such irregular shaped constructions, and hence considering the structural assembly they proposed to retrofit the structures using steel plate slit dampers. (Rahimi & Maheri, 2018) deeply studied various techniques in retrofitting of RC framed structures, and carried out experimental work on evaluating the performance of RC columns before and after strengthening using X bracings by time history analysis on openSEES software & tried to notify possible side effects of the used system. They also clearly distinguished between external and internal bracing system and stated that external bracing systems can be cheap option but due to architectural aspect and bonding capabilities are proved to be unpopular, whereas on other hand internal bracing systems are widely expected but has higher cost of construction. Researchers finally concluded with the findings that retrofitting system using X bracings can act positively for low rise structures (i.e. 4-6 stories) and not for high rise structures (i.e. 8-12 Stories).

The various different options in retrofitting like steel jacketing, use of Carbon fiber reinforced polymers (CFRPs), concrete jacketing, introduction of polypropylene fiber ropes (PPFRs), application of high performance fiber reinforced composites were discussed by (Truong, Kim, & Choi, 2017), and presented their experimental work with use of steel jacketing, carbon fiber reinforced polymer wrapping, concrete jacketing non shrinkage mortar & amorphous metallic fiber reinforced concrete. Eleven test samples were casted with two categories S series and SF series with high (5.28) & medium (2.03) longitudinal reinforcement ratios respectively. Specimens were partially and completely retrofitted over the column strips and were tested, the test results were compared with modified nonlinear deformation curves, and results concluded that retrofitted specimen's exhibits incremented structural properties.

It is well known that masonry structures has an brittle behavior to applied loads, hence these structures can prove to be a main cause of failure subjected to seismic forces. According to (Bhattacharya, Nayak, & Dutta, 2014), in early 90's constructions in Indian continents, America & Major parts of Asia was mainly focused on unreinforced masonry structures, so importance of retrofitting can majorly be focused. The paper stated above reviewed different techniques viz. construction of steel or polymer meshes, application of shotcrete, grouting, pointing, post tensioning using rubber tires, mesh reinforcements etc. and concluded with grouping those methods into suitable, least suitable and methods in improvement. It was also mentioned that use of plastic bag nets, rubber tires, bamboo reinforcements and fiber reinforced concretes can be an innovative technique for developing countries.

## **ECC AND FIBERS USED**

Going through the literature necessity of strengthening or retrofitting of masonry structures gains a major importance.

Fibers in individual or composites due to their tensile nature can prove to be an effective technique in imparting tensile characteristics to such structures which can resist the out of plane forces due to environmental disasters and seismic activities. Hence development of cementitious composites using such fibers can prove an effective technique in increment of deformability, load carrying capacity, and tensitivity.

There are various methods available to contribute into engineered cementitious composites, one of such composite was proposed by (Coelho Martuscelli et al., 2018) taking into consideration the environmental effect of wastes generated from scrap tires. India as a developing country, everyone now tries to focus upon recycling and reusing and the same view is considered here. One of the example of such recycling is stated in this paper which is use of carbon fiber powder wastes as aggregates for construction. Rubber tiers used herein were produced by using heavy metallic mixtures, these particles were added with epoxy polymers and Portland cement to produce a cementitious mix. 5 samples of each cylindrical samples for compression test, prismatic samples for flexural test and dog bone samples for tensile test were casted and cured for testing. Test results proved that addition of epoxy polymers played main role in imparting flexural, compressive and load carrying capacities whereas rubber particles imparted tensile characteristics to the mortar composite and mortar mix with 10% and 35% addition of rubber particles and epoxy polymers exhibited highest mechanical properties. Discussions also added that these rubber particles due to their low weights can be used in concretes which can ultimately decrease density of the material, application of this material was also seen in rubber reinforced concrete where strength increment of around 15% was observed.

Similar experimental work in accordance to reduce the overall cost of construction, use of blast furnace slag (BFS) and limestone powder was done by (Zhou et al., 2010). They previously studied the characteristics of six coupon specimens of 240\*60\*10mm with composite of Portland cement, BFS and limestone powder and then similar samples with composite replacing Portland cement by BFS cement under four point bending compression testing machine. Mix proportions were decided on the basis of standard mix designs originated from the work proposed by (Qian & Li, 2007). Tensile testing and crack width study to compare the results and to examine the standards norms laid by design codes were carried out and the results obtained were satisfactory and acceptable. The results further stated that flexural deflection capacity and tensile strain capacities of mortar increases from about 50 to 70% when Portland cement was replaced by BFS cement keeping limestone powder content constant, they also added that the properties exhibited by BFS cement were in agreement with use of Portland cement.

Statistics given by (Pakravan, Jamshidi, & Asgharian Jeddi, 2018) shown that rice production gives out about 20% of rice husk i.e. around 80 million tones, taking into consideration the environmental hazardous due to its disposal problem they proposed to use these ground rice husk (GRH) into production of cementitious composites. The generated cementitious composites can prove to be cost effective and high quality composites. Experiments were carried to study the strength gaining behavior and the characteristics increments trend for which specimens were casted, cured and tested with addition of different volumes of GRH in presence of polyvinyl alcohol fibers (PVA) and noted that composite produced by adding GRH increases peak strength substantially but this addition is limited till a point, because addition of more GRH due to stain hardening can reduce strength of mix. it was further added that use GRH due to its tendency of not interrupting with toughness of matrix results in good deformability performance.

(Shanour, Said, Arafa, & Maher, 2018) focused upon studying the performance of RC beams retrofitted with engineering cementitious composites, polyvinyl alcohol and polypropylene fibers were used for the experimentation. 12 RC beam samples with individual and hybrid of mentioned fibers were casted, cured and tested for tensile capacities and compression capacity under four point bending test, results with load deflection response curves and crack behaviors were deeply examined. Laboratory results were then compared with nonlinear finite element analysis NLFEA ANSYS software. These results stated that use of polyvinyl alcohol fibers resulted in better performance than polypropylene fibers, tensile behavior, load carrying capacities and also the load after initial cracking were greatly enhanced.

Similar work to study flexural behavior of RC beams retrofitted with additive fibers was carried by (Ramachandra Murthy, Karihaloo, & Priya, 2018), they proposed a mix of cement and silica fumes, quartz sand, quartz powder and brass coated steel fibers with defined ratios as retrofitting material mix. Beam specimens of size 1500\*100\*200mm were casted cured and then pre damaged for 70, 80 and 90% of their failure load capabilities and then rehabilitated with steel plates and fiber laminates of above mentioned mix. Experimental results in comparison with numerical model based results on ABAQUAS stated that retrofitted beams shows similar failure pattern as well as flexural behavior that of normal beams, they in addition mentioned this technique can prove a best solution in the field of retrofit.

Effect and ability of use of these ECC's and hybrid composites in fire damaged structures was needed to be studied and taking into consideration the same aspects work was carried out by (S. Pourfalah, 2018) which incorporated the use of PVA fibers individually and hybrid of steel fibers and polymeric fibers in studding the performance of mortar subjected to heat. Primary investigation i.e. studying compressive strength, tensile strength, and flexural strengths were carried out

by casting cubes, dog bone samples and prismatic rectangular samples respectively. To study the temperature effect, series of specimens were heated at an incremental temperature rate of 10°C per minute till the required temperature gained and then tested in heating chamber. In addition to heat regime, compression test reveals that at higher temperatures there was reduction in strength and flexural test results up to 100°C increases deflection capacity also load carrying capacity of test samples with proposed composites increases at a great extent, it was further added that presence of steel fibers can effectively limit the crack width.

Solution for rehabilitation of fire damaged structures was given by (Gao et al., 2018) they casted 9 one way slabs which were heated till subsequent damage occurred into heating furnaces and tested after retrofitting. Polymer modified mortar using basalt fibers and cement composites were used in the study. Heating of the samples were carried out according to the norms laid by Indian standards, cracks in the heat damaged slab elements were first filled with epoxy injecting, layer of ECC was then applied, a mesh of fabric impregnation applied and again layered by ECC, these samples were then lifted and kept on constructed walls and applied four point bending load using hydraulic actuator. Study stated that effective use of basalt fabric reinforced shotcrete was an attractive solution in fire damaged structure retrofit due to tendency to enhance flexural performance and peak load capacities by 31.1-127%. But a disadvantage of ductile behavior of the materials was observed.

Shape memory alloys (SMA) is one more option in study of building material to generate a hybrid cementitious composite, these SMA's can comprise of copper zinc aluminates, copper aluminates, nickel, iron manganese silicates or nickel titanium alloys. Use of polyvinyl alcohol fibers and nickel titanium SMA fibers was done in the work to introduce a crack healing composite by (Ali & Nehdi, 2017), in which 2% of PVA and varying percentages of 0, 0.5, 1.0 and 1.5 by weight were added to the concrete mix. 9 cubes and 3 cylindrical samples were tested to study compressive strength and split tensile strength flow table test was carried to check the workability of the mix which reveals that flow reduced by 5.6% compared to that of test specimen. Split tensile test was carried on specimens cured for different days and for addition of different percentage of fibers and the values ranged from 1.5 – 12.1Mpa which was an increasing trend with curing period. It was also observed that addition of SMA fibers does not have any significant role in increasing compressive strength but played a vital role in improving tensile and flexural properties, the increment in flexural strength and strain recovery proved applicability of proposed work in imparting crack healing property.

Comparatively it was observed that the applications of ECC were prominently seen in RCC structures, so need of improvement in retrofitting of unreinforced masonry structures brought to view. (S. Pourfalah, Suryanto, & Cotsovos, 2018) suggested the use of ECC in improving the behavior of masonry wall subjected to wind load loads or seismic vibrations which acts in its out of plane direction, they conducted the experimental work on class B bricks which were encased with mortar bonds to form beam like specimens of size 210\*102\*65mm and tested under uniaxial compression testing machine in accordance to procedure laid by ASTM standards. Cross brick couplets were fabricated tested to know the bond strength of the brick interface bond. 10 bricks and 9 mortar joint prismatic beam like specimens were tested followed by compression testing and tensile testing of dog bone shaped ECC specimens on UTM. ECC utilized in the work comprises of polycarboxylate high-range water-reducing admixture and PVA fibers and the results noted of the retrofitted samples in partially or fully bounded were relatively increased these results were then compared with numerical modelling on NLFEA. Work on ECC for masonry structures was further extended by (S. Pourfalah, Cotsovos, & Suryanto, 2018), they investigated and studied the out plane behavior of URM walls strengthened with layers of ECC which in turn were partially or completely applied, similar work was modelled into nonlinear analyzing software ADINA and results compared thoroughly. Uniaxial compression test of brick specimens used for experimentation, mortar cylinders casted with proposed mix and uniaxial testing of ECC dog legged specimens were carried. Actual work was focused upon 8 beam like specimens of brick mortar interface consisting of 3 bricks and 2 joints. PVA fibers were utilized in the study having 39µm diameter, 12mm length and tensile strength of 1600mpa. Results clearly stated that first cracking load of fully retrofitted samples increased by 9% and that of partially retrofitted samples by 8% and the deflection reduced by 65 and 110% respectively. Hence retrofitting the specimens with partially of fully bonded at tension face can significantly enhance the overall properties. Similar work with same work procedure was experimented by (Saeed Pourfalah, Cotsovos, Suryanto, & Moatamedi, 2018) making a difference in loading pattern where in addition to four point static loading, drop weight impact testing of drop mass 47Kgs was impacted on the test specimen.

Need of strengthening of URM walls due to vulnerability to tensile behavior due to earthquake loading was identified and use of tensile reinforced mortar (TRM) to study the characteristics of URM walls was proposed by (Kouris & Triantafillou, 2018). Authors introduced that these TRM's comprises of high tensile fibers comprising there low weight, high temperature susceptibility and good permeability characterization. These fibers can be prepared by use of glass, carbon, basalt, aramid, polypropylene, polyparaphenyle benzobisoxazole or steel. Modelling and testing of URM samples retrofitted with TRM strips in high stress areas and wrapping to full parameter, on high speed servo hydraulic testing

machine was carried out and results were noted, which says that conflicts of TRM wrapping increases serviceability as well as the load capabilities at a great extent. Analytical modelling was also done for different structures like domes, shell, piers etc. and performances, different failure patterns and also effects of loading was clearly observed.

Cyclic loading testing of old RC beams in controversy were carried out by (Cho, Han, Lim, Morii, & Kim, 2018) which were retrofitted with high performance fiber reinforced concretes with implementation with additional reinforcement. High tensile PVA fibers and high strength Polyethylene fibers were incorporated in the study, individual bending performance of these fiber mixes were done by testing under four point bending tests. Actual implementation was done collected old beam sample of ground level storey, these specimens were first pretreated by forcing water jacket then grooving and concreting and then reinforcing with transverse and additional reinforcement and finally applying with HPFRC spaying. Viscous damping coefficient of the samples were studied in addition to that of bending, tensile and flexural testing which results in considerable increase in bending characteristics as well as axial strains of reinforcements in tension and compression increased greatly. Finally authors added that retrofitted old beams exhibits a similar performance compared to that of newly constructed structures.

Use of polypropylene fibers can be bifurcated into use of fibrillated fibers and use of monofilament fibers, application of this work was done by (Deb, Mitra, Majumder, & Maitra, 2018) they proposed effective use of mentioned fibers in improving properties of concrete in the class of cementitious composites. Amount of fibers for addition was kept low i.e. 2% by volume of the mix wherein the mix contains ordinary Portland cement, fly ash, silica fumes and fine sand. Standard test procedure to know compressive strength on 70.6mm cube specimens, flexural strength on 500100\*30mm prismatic specimen split tensile testing and direct tensile test on servo hydraulic universal testing machine on 6 specimens for each category of individual utilization of fibrillated or monofilament and hybrid with different percentages was conducted and results were plotted. Authors concluded with saying that fibrillated fibers were mainly responsible for imparting flexural and tensile capacities on other hand monofilament fibers play great role in improving ductility. So use of both of these fibers in mortar mix is a proving solution in strengthening.

(Li, 1997) overviewed the properties and applications of various classes of fibers used in fiber reinforced concrete composites. Author used PE fibers to study the compression strength, tensile strength and flexural performance of proposed mortar mix. RC beams with mentioned mortar were casted with very low percentage of fiber mixes i.e. 2% addition by volume results of various tests stated that the structures using the mentioned design aspects are susceptible to high energy absorption structures, high deforming structures as well as heavily loaded structures. It was also added that application can be seen in various fields like repair solutions, permanent formworks etc.

Retrofitting of masonry beams with strain hardening cementitious composites (SHCC) were compared with that of steel fiber reinforced concrete (SFRCC) by (Esmaceli, Manning, & Barros, 2013) and this behavior of SHCC was simulated by simple finite element modelling. Three different fiber mortar composites were designed and tested in accordance to obtain sufficient workability and improved mechanical performance. Tailored rheological properties of composite mix containing sand, cement, fly ash, water, VMA superplasticizer and addition of 2% by weight of PVA fibers were studied in addition to that of tensile behavior of the mix and compression behavior of beam specimens of 55\*105\*205 size under four point bending test. Results stated that maximum load observed was 12.95Kn and deflection at maximum load was 9.70mm while tensile and ultimate strengths observed were 3.57 and 3.87N/mm<sup>2</sup> respectively, which were satisfactorily acceptable.

Mirror work to study the in plane cyclic loading of 6 specimen walls of size 23001250\*240mm grooved with 10mm mortar layers and retrofitted in patches or on full surface with ECC containing 2% PVA fibers was conducted by (Deng & Yang, 2018). Horizontal transducers and load varying deflection transducers were utilized to study the uniaxial testing, compression testing and testing of walls for load capacity and deformability. Testing of walls was done by applying axial load of 280Kn and axial stress to lateral load of 1000Kn where lateral loads and energy dissipation of walls retrofitted with strips and coated wall respectively were increased by 36-45%, 18-27% and 61-99%, 88-96%.

The concept of light weight concrete in ECC was taken into account by (Rana, Lee, Al-Deen, & Zhang, 2018), they studied the flexural performance of steel beams composited with ECC. Three 300Mpa steel encased beams with light weight ECC and one sample specimen of 300\*175\*215mm size were tested for tensile capacity, compressive strength, deformation capacity, load carrying capacity and flexural performance. ECC mix comprises of OPC, fly ash, local sand, HRWR admixture, KURALON PVA fibers, utilization of this mix resulted in about 40% improvement in load carrying & deformability performance and about 13% reduction in weight also 63% strength increment was observed.

Relation between cracking strength and flaw relation using X-ray tomography of ECC retrofitted specimens was studied by (Lu, Li, & Leung, 2018).  $\mu$ CT images were captured for all tests to deeply examine the behavior of specimens during testing. The test samples were divided into various bands and the crack patterns were deeply notified, these crack patterns were the results due variation of crack strengths which were major objectives of the conducted study.

(Kang, Tan, Zhou, & Yang, 2017) studied the shear behavior of ECC by conducting 12 push off tests, they proposed a mix of concrete with ground granulated blast furnace slag and fly ash, nomenclatures of the mix were as ECC-GGBS and ECC-FA respectively, where ECC comprises of PVA fibers with ordinary mortar mix. Similar to that of all previously mentioned authors tensile, compression and four point bending tests were conducted and results were deeply studied. Author concluded that the ECC-GGGBS exhibited better performance in load carrying as well as sustaining to higher deflection. It was noteworthy to say that shear strength of ECC was observed increased due to increase in strain capacity of the mix.

Experimental study of comparing ordinary RC beams with ECC reinforced beams using ultra high performance composites was done by (Ding, Yu, Yu, & Xu, 2018). OPC, granulated furnace slag, limestone powder, silica fumes, HRWR admixtures and PE fibers were utilized for the study. Ordinary test procedures were adopted for testing six beam specimens with steel R/F and two without R/F were tested and noted that stiffness of reinforced and retrofitted beams was much higher than that of non-reinforced retrofitted beams and also the compressive strength observed was much higher.

### PROPERTIES OF POLYVINYL ALCOHOL (PVA)

PVAs are class of polymers classified under vinyl group. It was mentioned by (Thong et al., 2016) with reference that first colloid of polyvinyl was brought into view by Hermann and Haehnel in the year 1924, due to excellent chemical resistance and physical properties of these fibers they have a wide scope of utilization in various fields. It was also observed that application of PVA was majorly seen in construction industries for utilization as,

- Modifiers of mortars
- Aggregated in surface pretreating agent
- Fiber reinforced material

These PVAs were classified under two groups on basis of their extractions viz. a) fully hydrolyzed and b) partially hydrolyzed. It was noteworthy to mention that the properties of PVA depends upon degree of polymerization and hydrolysis during the extraction process. Production outline of PVA from users interface is shown in figure 1.

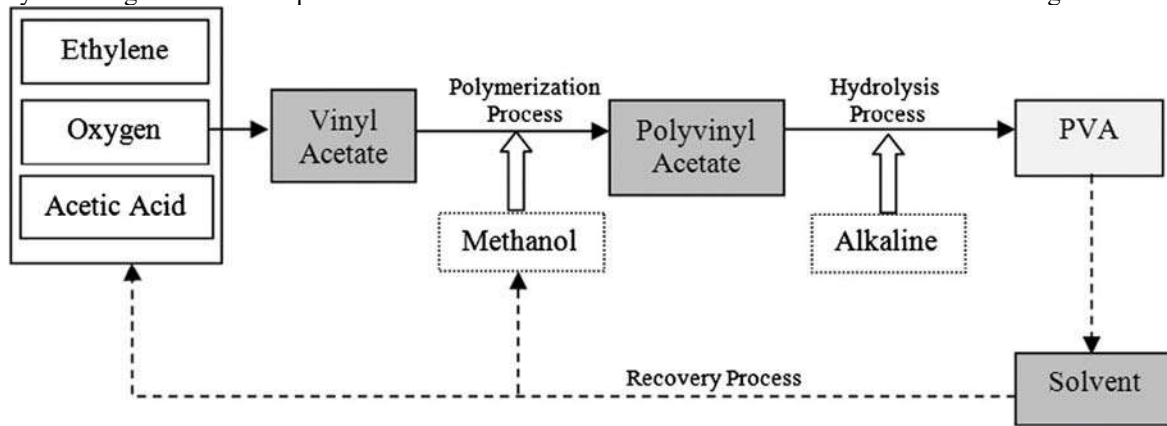


Fig. 1 production outline of PVA

Properties mentioned by authors clearly shows a path in use of these PVA fibers in producing a new cementitious mix i.e. engineered cementitious composite. It will be import to add that the properties of ECC needed by addition of any kind of fibers should be satisfying from the application point of view, those in general acceptable properties were listed by (R, Ramegowda, & Manohara H E, 2015)), the same data from authors review is added and show in table 1.

Table 1. General properties of ECC

Compressive Strength (MPa)	First Crack Strength (MPa)	Ultimate Tensile Strength (MPa)	Ultimate Tensile Strain (%)	Young's Modulus (GPa)	Flexural Strength (MPa)	Density (g/cc)
20 – 95	3 – 7	4 – 12	1 – 8	18 – 34	10 – 30	0.95 – 2.3

## STRENGTHENING OF BRICK MASONRY

Taking into consideration the necessity of retrofitting the brick masonry structures, Application in use of ECC with PVA fibers for strengthening of those structures was proposed by (Arisoy, Ercan, & Demir, 2015). Authors carried out experimental work, which included construction of 42 masonry wall specimens using different brick types and subjecting them to axial tension and diagonal compression testing. Brick types used and the dimensions of the walls were 190\*100\*50mm for solid bricks, 190\*190\*135mm for hollow bricks and 290\*190\*135mm for high strength hollow bricks. Table 2 shows the sample and test specifications directly taken from author's desk.

**Table 2. Types of the samples and applied test description**

Sample definition	Total number of samples	Number of samples for diagonal tension test	Number of samples for compression test
Solid brick wall sample without stucco	2	1	1
Regular hollow brick wall sample without stucco	2	1	1
High strength brick wall sample without stucco	2	1	1
Solid brick wall sample with regular stucco	6	3	3
Solid brick wall sample with fiber reinforced stucco	6	3	3
Regular hollow brick wall sample with regular stucco	6	3	3
Regular hollow brick wall sample with fiber reinforced stucco	6	3	3
High strength brick wall sample with regular stucco	6	3	3
High strength brick wall sample with fiber reinforced stucco	6	3	3

All the tests were performed according to ASTM standards, and results were noted. Results states that compression strength of the walls were related to the strength of brick, retrofitting of these walls by using fibrous plastering can increases the shear strength of wall by 0.5 times and 2.5 times for high strength and regular bricks respectively.

Application of geotextile reinforcement for brick wall was also suggested by (Pinto & Cousens, 1996)). They mentioned that the behavior of retaining walls subjected with geotextile reinforcement facing was carried on sample constructed was which was backfilled and surcharged before observing. They observed that tensile and load carrying capacity of such structures significantly increases by even addition of very small amount of short length grids. They added that cracks were observed at the mid height of the wall which gave clear intimation of degradation before collapse giving sufficient time to make decisions before collapse as compared to that of normal unreinforced wall structures.

(Khan, Nanda, & Das, 2017) in their work experimentally and numerically studied the strength behavior of non-woven geotextile treated masonry structures. Authors previously introduced different failure patterns and reasons of failures, then for the experimentation work 12 masonry panels were constructed using normal bricks and mortar to undergo diagonal compression test, before testing the wall specimens were strengthened in different patterns i.e. parallel, diagonal & cross patterns. Crack patterns, failure modes and strengths of the panels were clearly observed. It was then stated that the performance of strengthened panels was brittle and strengthened panels had deformation capacity in addition they mentioned that, strengthening the panels by cross pattern can give best results in terms of diagonal shear, compressibility, deformability as well as load carrying capacity.

## APPLICATIONS OF ECC

ECC a versatile material in improving characteristic strengths, deflection capabilities and load carrying capacity of structure was proved by (Yildirim, Şahmaran, & Anil, 2018)). Authors highlighted the projects where effective use of ECC was done. According to the authors, applications were seen in,

- Repairing of 60 years old Mitaka Dam in Hiroshima Prefecture, Japan in 2003, where 20mm layer of ECC was sprayed on the upstream side of the dam.
- Repair of concrete gravity retaining wall in Japan which was 18m wide and 5m high strengthened by 80-70mm thick ECC layer (Qian & Li, 2007).
- Repair of concrete bridge deck in United States was suggested by practically comparing ECC repair solution with that of ordinary repairing techniques (Corresponding, Lepech, & Li, 2004).
- Sustaining and incorporating problematic expansion joints of link slab in a two span bridge in United States in 2005. About 32m<sup>3</sup> of ECC was utilized for the work.
- Use of ECC as the shear keys of bridges with adjacent box beams and voided slabs in United States in 2014.
- Retrofitting of earthquake damaged high rise apartment in Tokyo.
- Steel reinforced ECC embedded MIHARA Bridge of about 1 Km in Hokkaido, Japan in 2005 which utilized 800m<sup>3</sup> of ECC.
- Use of ECC in 225mm thick bridge deck in Michigan was done in 2005 to reduce the amount of use of ordinary Portland cement.

## CONCLUSION

Reviewing the necessity of strengthening and retrofitting of structures and different methods available in the field, this study concludes that,

- Use of tensile properties of fibers in individual or hybrids to produce engineered cementitious composites can be utilized effectively in enhancing the structural performance due to capability of ECCs to strain harden by forming of micro cracks.
- Properties of PVA fibers clearly shows its application in strengthening and retrofitting of structures.
- Application of ECC strengthening can not only be seen in RC structures but also be effectively used for unreinforced masonry structures.
- Work has been carried out in application of various methods in strengthening of retaining structures but applicability of ECC with PVA fibers for earth fill masonry walls needs to be studied.

## REFERENCES

- Ali, M. A. E. M., & Nehdi, M. L. (2017). Innovative crack-healing hybrid fiber reinforced engineered cementitious composite. *Construction and Building Materials*, 150, 689–702. <https://doi.org/10.1016/j.conbuildmat.2017.06.023>
- Almeida, A., Ferreira, R., Proença, J. M., & Gago, A. S. (2017). Seismic retrofit of RC building structures with Buckling Restrained Braces. *Engineering Structures*, 130(036), 14–22. <https://doi.org/10.1016/j.engstruct.2016.09.036>
- Arisoy, B., Ercan, E., & Demir, A. (2015). Strengthening of brick masonry with PVA fiber reinforced cement stucco. *Construction and Building Materials*, 79, 255–262. <https://doi.org/10.1016/j.conbuildmat.2014.12.093>
- Bhattacharya, S., Nayak, S., & Dutta, S. C. (2014). A critical review of retrofitting methods for unreinforced masonry structures. *International Journal of Disaster Risk Reduction*, 7(004), 51–67. <https://doi.org/10.1016/j.ijdr.2013.12.004>
- Cho, C. G., Han, B. C., Lim, S. C., Morii, N., & Kim, J. W. (2018). Strengthening of reinforced concrete columns by High-Performance Fiber-Reinforced Cementitious Composite (HPFRC) sprayed mortar with strengthening bars. *Composite Structures*. <https://doi.org/10.1016/j.compstruct.2018.05.045>
- Coelho Martuscelli, C., Cesar dos Santos, J., Resende Oliveira, P., Hallak Panzera, T., Paulino Aguilar, M. T., & Thomas Garcia, C. (2018). Polymer-cementitious composites containing recycled rubber particles. *Construction and Building Materials*, 170(017), 446–454. <https://doi.org/10.1016/j.conbuildmat.2018.03.017>
- Corresponding, V. C. L., Lepech, M., & Li, V. C. (2004). Title Page Title : Crack Resistant Concrete Material for Transportation Construction Authors : Advanced Civil Engineering Materials Research Laboratory Department of Civil and Environmental Engineering The University of Michigan , Ann Arbor Mailing Address. *Advanced Civil Engineering Materials Research Laboratory*, (734).

- Deb, S., Mitra, N., Majumder, S. B., & Maitra, S. (2018). Improvement in tensile and flexural ductility with the addition of different types of polypropylene fibers in cementitious composites. *Construction and Building Materials*, 180, 405–411. <https://doi.org/10.1016/j.conbuildmat.2018.05.280>
- Deng, M., & Yang, S. (2018). Cyclic testing of unreinforced masonry walls retrofitted with engineered cementitious composites. *Construction and Building Materials*, 177, 395–408. <https://doi.org/10.1016/j.conbuildmat.2018.05.132>
- Ding, Y., Yu, K. Q., Yu, J. tao, & Xu, S. lang. (2018). Structural behaviors of ultra-high performance engineered cementitious composites (UHP-ECC) beams subjected to bending-experimental study. *Construction and Building Materials*, 177, 102–115. <https://doi.org/10.1016/j.conbuildmat.2018.05.122>
- Esmaceli, E., Manning, E., & Barros, J. A. O. (2013). Strain hardening fibre reinforced cement composites for the flexural strengthening of masonry elements of ancient structures. *Construction and Building Materials*, 38, 1010–1021. <https://doi.org/10.1016/j.conbuildmat.2012.09.065>
- Gao, W. Y., Hu, K. X., Dai, J. G., Dong, K., Yu, K. Q., & Fang, L. J. (2018). Repair of fire-damaged RC slabs with basalt fabric-reinforced shotcrete. *Construction and Building Materials*, 185, 79–92. <https://doi.org/10.1016/j.conbuildmat.2018.07.043>
- Kang, S. B., Tan, K. H., Zhou, X. H., & Yang, B. (2017). Experimental investigation on shear strength of engineered cementitious composites. *Engineering Structures*, 143, 141–151. <https://doi.org/10.1016/j.engstruct.2017.04.019>
- Khan, H. A., Nanda, R. P., & Das, D. (2017). In-plane strength of masonry panel strengthened with geosynthetic. *Construction and Building Materials*, 156, 351–361. <https://doi.org/10.1016/j.conbuildmat.2017.08.169>
- Kim, J., & Jeong, J. (2016). Seismic retrofit of asymmetric structures using steel plate slit dampers. *Journal of Constructional Steel Research*, 120(001), 232–244. <https://doi.org/10.1016/j.jcsr.2016.02.001>
- Kouris, L. A. S., & Triantafillou, T. C. (2018). State-of-the-art on strengthening of masonry structures with textile reinforced mortar (TRM). *Construction and Building Materials*, 188, 1221–1233. <https://doi.org/10.1016/J.CONBUILDMAT.2018.08.039>
- Li, V. C. (1997). Engineered Cementitious Composites (Ecc) – Tailored Composites through Micromechanical Modeling. *Canadian Society for Civil Engineering*, 1–38.
- Lu, C., Li, V. C., & Leung, C. K. Y. (2018). Flaw characterization and correlation with cracking strength in Engineered Cementitious Composites (ECC). *Cement and Concrete Research*, 107(February), 64–74. <https://doi.org/10.1016/j.cemconres.2018.02.024>
- Maalej, M., Quek, S. T., Ahmed, S. F. U., Zhang, J., Lin, V. W. J., & Leong, K. S. (2012). Review of potential structural applications of hybrid fiber Engineered Cementitious Composites. *Construction and Building Materials*, 36(010), 216–227. <https://doi.org/10.1016/j.conbuildmat.2012.04.010>
- Pakravan, H. R., Jamshidi, M., & Asgharian Jeddi, A. A. (2018). Combination of ground rice husk and polyvinyl alcohol fiber in cementitious composite. *Journal of Environmental Management*, 215(035), 116–122. <https://doi.org/10.1016/j.jenvman.2018.03.035>
- Pinto, M. I. M., & Cousens, T. W. (1996). Geotextile reinforced brick faced retaining walls. *Geotextiles and Geomembranes*, 14(9), 449–464. [https://doi.org/10.1016/S0266-1144\(96\)00037-4](https://doi.org/10.1016/S0266-1144(96)00037-4)
- Pourfalah, S. (2018). Behaviour of engineered cementitious composites and hybrid engineered cementitious composites at high temperatures. *Construction and Building Materials*, 158, 921–937. <https://doi.org/10.1016/j.conbuildmat.2017.10.077>
- Pourfalah, S., Cotsovos, D. M., & Suryanto, B. (2018). Modelling the out-of-plane behaviour of masonry walls retrofitted with engineered cementitious composites. *Computers and Structures*, 201, 58–79. <https://doi.org/10.1016/j.compstruc.2018.02.004>
- Pourfalah, S., Cotsovos, D. M., Suryanto, B., & Moatamedi, M. (2018). Out-of-plane behaviour of masonry specimens strengthened with ECC under impact loading. *Engineering Structures*, 173(January), 1002–1018. <https://doi.org/10.1016/j.engstruct.2018.06.078>
- Pourfalah, S., Suryanto, B., & Cotsovos, D. M. (2018). Enhancing the out-of-plane performance of masonry walls using engineered cementitious composite. *Composites Part B: Engineering*, 140, 108–122. <https://doi.org/10.1016/j.compositesb.2017.12.030>
- Qian, S., & Li, V. C. (2007). Simplified Inverse Method for Determining the Tensile Strain Capacity of Strain Hardening Cementitious Composites. *Journal of Advanced Concrete Technology*, 5(2), 235–246. <https://doi.org/10.3151/jact.5.235>
- R, C. V, Ramegowda, M., & Manohara H E. (2015). Engineered Cementitious Composites-a Review. *International Research Journal of Engineering and Technology*, 2395–56.

- Rahimi, A., & Maheri, M. R. (2018). The effects of retrofitting RC frames by X-bracing on the seismic performance of columns. *Engineering Structures*, 173(March), 813–830. <https://doi.org/10.1016/j.engstruct.2018.07.003>
- Ramachandra Murthy, A., Karihaloo, B. L., & Priya, D. S. (2018). Flexural behavior of RC beams retrofitted with ultra-high strength concrete. *Construction and Building Materials*, 175, 815–824. <https://doi.org/10.1016/j.conbuildmat.2018.04.174>
- Rana, M. M., Lee, C. K., Al-Deen, S., & Zhang, Y. X. (2018). Flexural behaviour of steel composite beams encased by engineered cementitious composites. *Journal of Constructional Steel Research*, 143, 279–290. <https://doi.org/10.1016/j.jcsr.2018.01.004>
- Seo, H., Kim, J., & Kwon, M. (2018). Optimal seismic retrofitted RC column distribution for an existing school building. *Engineering Structures*, 168(April), 399–404. <https://doi.org/10.1016/j.engstruct.2018.04.098>
- Shanour, A. S., Said, M., Arafa, A. I., & Maher, A. (2018). Flexural performance of concrete beams containing engineered cementitious composites. *Construction and Building Materials*, 180, 23–34. <https://doi.org/10.1016/j.conbuildmat.2018.05.238>
- Thong, C. C., Teo, D. C. L., & Ng, C. K. (2016). Application of polyvinyl alcohol (PVA) in cement-based composite materials: A review of its engineering properties and microstructure behavior. *Construction and Building Materials*, 107, 172–180. <https://doi.org/10.1016/j.conbuildmat.2015.12.188>
- Truong, G. T., Kim, J. C., & Choi, K. K. (2017). Seismic performance of reinforced concrete columns retrofitted by various methods. *Engineering Structures*, 134(046), 217–235. <https://doi.org/10.1016/j.engstruct.2016.12.046>
- Yildirim, G., Şahmaran, M., & Anil, Ö. (2018). *Engineered cementitious composites-based concrete. Eco-efficient Repair and Rehabilitation of Concrete Infrastructures*. <https://doi.org/10.1016/B978-0-08-102181-1.00015-0>
- Zhou, J., Qian, S., Beltran, M. G. S., Ye, G., Van Breugel, K., & Li, V. C. (2010). Development of engineered cementitious composites with limestone powder and blast furnace slag. *Materials and Structures/Materiaux et Constructions*, 43(6), 803–814. <https://doi.org/10.1617/s11527-009-9549-0>



## Sustainability of Recycled Aggregates in Construction Industry: An Overview

Chandrika Singh,<sup>1\*</sup> and Gaurav Saini,<sup>1</sup>

<sup>1\*</sup>Department of Civil Engineering, Sharda University, Greater Noida, U.P.; e-mail: chandrikasingh810@gmail.com (\*Corresponding Author)

<sup>1</sup> Department of Civil Engineering, Sharda University, Greater Noida, U.P.; e-mail: gaurav.saini@sharda.ac.in

### ABSTRACT

A rapidly developing economy like, India requires huge investments in infrastructure to sustain its growth. This translates into newer projects, upgradation and/or replacement of existing infrastructure. While the former requires huge quantities of fresh construction material, the latter generates enormous amounts of waste materials. Neither is a very sustainable proposition. An innovative solution is the utilization of aggregates recycled from the construction & demolition waste for developing new infrastructure. This not only reduces the burden of manufacturing new aggregates, but also reduces the responsibility of its disposal, thus leading to economic and environmental sustainability. Recycled aggregates or RA have been extensively studied for potential application in concrete manufacturing for a variety of applications, including (but not limited to) pavements, shoulders, median barriers, sidewalks, curbs and gutters, building and bridge foundations, etc. However, this seemingly sustainable material is not without its own drawbacks. One of the common issues with the use of recycled aggregates in concrete manufacturing is the low-strength of the resulting product, higher water absorption capacity, reduced workability of the concrete, etc. Numerous studies have been conducted to improve the characteristics of recycled aggregate based concrete. In addition, several other applications of the recycled aggregates have also been suggested. This paper presents a state-of-the-art review of the recycled aggregates, their applications in construction industry, advantages and disadvantages of recycled aggregates and other potential applications of this material. Recycled aggregates have shown a great potential in making the construction more sustainable in both economic as well as environmental terms. This work aims to critically evaluate these aspects of recycled aggregates.

**KEYWORDS:** Demolition waste; Recycled Aggregates; Sustainable; Construction Reuse;

### INTRODUCTION

India has been top 2 among the fastest growing economies in the world for last few years. The economic growth requires huge investments in infrastructure such as, roads, high-rise buildings, institutions, commercial development, cities, ports & harbors, airports, etc. Upgradation of existing infrastructure and replacement of aging infrastructure is also needed to sustain a high growth rate for the economy. This has two-pronged effect: While the development of new infrastructure requires fresh building materials, replacement of aging infrastructure results in huge amounts of waste that needs appropriate disposal. The former is not sustainable in the longer run, while the latter creates environmental and economic concerns. A sustainable solution to these twin-pronged problem is needed while still ensuring the sustenance of high growth rate of the country.

One solution is to reuse the wastes generated from the demolition of existing infrastructure. Such waste is typically known as Demolition waste. This includes the waste generated during construction activities as well as demolition activities. This waste includes concrete, bricks, stones, timber, glass, gypsum, ceramics, steel, etc. (Fig. 1). There is no general consensus on the amount of the demolition waste generated in our country. The Ministry of Environment, Forests and Climate Change (GOI) estimated the demolition waste for year 2010 to be 10-12 million tons. In comparison, the Central Pollution Control Board (CPCB) estimated the amount to be 12 million tons for the year 2011. For the year 2017, the estimate of demolition waste has been increased to 25-30 million tons by CPCB. Most recently, two government agencies, the Building Materials and Technology Promotion Council, and the Center for Fly Ash Research and Management estimated an annual amount of 165-175 million tons annually. As a rule of thumb, according to the Technology Information, Forecasting and Assessment Council, a new construction generates 40-60 kg of demolition waste per sq. m. Similarly, the demolition activities generate about 300-500 kg of demolition waste per sq. m. In comparison, the European countries were estimated to have produced approximately 867 million tons of

demolition waste in the year 2010. The major producers in the EU included Belgium (22.29 million tons), Denmark (3.17 million tons), etc. (Faleschini, F., Zanini, M. A., Pellegrino, C., & Pasinato, S. 2016).

Demolition waste is an environmental and public health hazard. Its recycle and reuse offers a sustainable solution to protect the environment. The C & D industry is responsible for the generation of large amount of waste. India is developing faster than the urban planner can handle but hardly any attention is paid to the demolition waste which is generated during infrastructural development activities. Such wastes may include bricks, concrete, stones, topsoil, glass, ceramics, plastics, etc. The abject neglect of this waste results in adverse impacts for public as well as the environment. C & D waste mainly arises from construction and demolition, disaster debris, road planning, and maintenance activities. The estimated amounts of wastes generated from C & D activities has already been mentioned earlier. Use of natural materials is minimized by using demolition waste as it contains reusable, recyclable materials. Due to a lack of knowledge (and/or incentives) regarding the disposal of demolition waste, most of the organizations engaged in construction sector are not compelled enough to reduce/reuse demolition waste during their regular activities and they typically resort to the landfills and/or low-lying areas for its disposal. Even though the constituents of demolition waste may have useful life and role left, there is hardly any incentive for their recovery and reuse. In fact, a lot of time and experience is needed for converting the demolition waste into reliable, skillful, marketable and sustainable product that can be beneficially used in construction.



**Fig. 1 Demolition waste**



**Fig. 2 Recycled Aggregates**

The current paper presents a detailed overview of the production of recycled aggregates (Fig. 2) from demolition waste, the various applications of recycled aggregates and methods to overcome any shortcomings, the economic viability and environmental impacts associated with their application and advantages and disadvantages of using recycled aggregates. This work is expected to provide an overview of recycled aggregates to students and scholars and is expected to enhance their understanding of these materials as a sustainable option in the construction sector.

## PRODUCTION OF RECYCLED AGGREGATES FROM DEMOLITION WASTE

For a really long time, the manual labor coupled with low-quality or poor skills was the method of choice for demolition of the buildings. Such activities were not only poorly regulated but were highly inefficient as well. Recent times, however, have seen a change in the working pattern with more reliance on machines due to difficulties in building design, health, safety, advancement in plant design and legal requirements of various regulatory agencies at the state and the central levels.

For the deconstruction of a building, several steps and equipment are required. Different demolition methods may be required according to the type of concrete structure. With the help of non-destructive and semi-destructive testing, an evaluation of existing materials is done. Different demolition methods may be required according to the type of concrete structure which gives an idea about the quality and condition of the concrete used in the construction.

The demolition and concrete removal techniques are divided into the following methods:

- Manual-labor based demolition- This method is suitable for economically backward regions where the labor is cheaper as compared to the cost of buying or renting the demolition equipment.
- Mechanical demolition method- In this technique, machines are used which are based on the impact, crushing or shear for structural demolition. This method is generally used for heavy demolition.
- Thermal cutting operation- objects are divided into smaller parts by using high temperature, which may be

maintained for a long time. The process is energy-intensive (Silva, R.V., 2015).

- Expansions method- This method is based on the idea that volumetric expansion may cause rupture of components. This technique utilizes explosives, gases and some non-explosives agents like hydro-demolition or water jet-blasting, especially where steel reinforcements are intended for reuse (e.g., Rehabilitation). This method avoids vibration-related damage and minimizes the fire risk, aspects that are characteristics of thermal demolition method.

### **Recycling Plant**

C & D recycling plants are like those plants which produce crushed natural aggregates. The objective of such plant is the manufacturing of granular material by using various crushers, screens, transfer and contaminant-removal equipment. C & D recycling plants can be either mobile or stationary types. The former consists of one crusher and sorting devices, with lower contaminants removal effectiveness, while the latter contains a large primary and a secondary (or tertiary) crusher working in conjunction. They also include various cleaning and sieving devices to produce high quality recycled aggregates (Hansen, 1992).

One such C & D recycling plant is in operation in Delhi. This 500 TPD capacity plant is a joint venture between the Municipal Corporation of Delhi and IL&FS and is situated in Burari, Delhi.

**Recycling procedures:** There are numerous recycling procedures which may vary according to the contamination level of materials. These includes the following stages:

- Crushing Stage- In this stage, demolition waste may enter the processing operation directly or to obtain materials with workable particle size, it may need to be broken down. This is accomplished by a hydraulically mounted on tracked or wheeled excavators. To minimize the contamination, relatively large pieces of steel, wood, plastic and paper may have to be manually sorted out. (Molin et al., 2004).
- Sorting and contamination removal- There are two operations for removal of contaminants from demolition waste. These are pre-crushing separation and post-crushing separation. This initial sorting can help optimize the crushing time, energy spent and quality of the product, e.g. if large quantities of clean debris have accumulated in a stockpile, they can then be crushed in a single, continuous run. (O'Mahony, 1990)

### **Storage of C&D waste before and after processing**

All demolition waste should be stored in a suitable container on site so that it does not get scattered. To preserve the waste characteristics and materials which are to be used at the same site, these must be properly settled into different heaps so that it becomes easy to differentiate the materials which is to be sold or sent to a landfill site. Recycled Aggregate are the most common product obtained from the recycling of demolition waste and needs to be stored separately if they are derived from materials having different quality and different size fraction.

### **APPLICATIONS OF RECYCLED AGGREGATE**

Several different applications of recycled aggregates have been attempted by researchers and field practitioners. The chief among them include applications in concrete manufacturing, road construction, in sound barriers and in embankments. Two important aspects associated with the application of any material are its economic viability and potential environmental impacts. These aspects are discussed after a detailed summary of the various applications of recycled aggregates.

#### **Concrete manufacturing**

The most logical application of recycled aggregates is as a partial (or complete) replacement of fresh aggregates in concrete manufacturing. The resulting concrete is often termed as recycled aggregate concrete (RAC). Although RAC offers the advantages of cost savings and environmental benefits as compared to the conventional concrete, it is not without its own drawbacks. Several studies have reported that the mechanical and durability performance of RAC are generally inferior to conventional concrete and such concrete is typically recommended for low-strength applications. However, one thing is certain. The use of recycled aggregates from demolition waste is a key step towards sustainability in the construction industry (Behera, M et al.. 2014).

Different approaches have been adopted for improving the properties of RAC. The use of superplasticizers is often recommended. Another technique, known as double mixing method, has been shown to deliver 12.6% higher compressive strength, 22% reduction in chloride penetration depth and 12.3% in carbonation depth. Two stages

mixing approach is another method, which has been reported to enhance compressive strength by up to 21.19%. Addition of fly ash or silica fume into concrete has also been recommended as replacement of fine aggregates. Such replacement can potentially improve the pore structure by reducing the pore volume. (Behera, M et al. 2014). Bacterial coating of recycled aggregates is also being studied as a viable approach to ensure adequate characteristics of recycled aggregate concrete.

## **Road construction**

Natural resources, commonly used for road construction, are depleting, thereby requiring increased costs for hauling the good quality stone aggregates from relatively larger distances. Quarrying of fresh material is not without its own share of environmental concerns. The natural resources can be replaced (partially or completely) by recycled aggregates, obtained from demolition waste. Such recycled materials can be used either in an unbound form or in a lightly cemented form. These recycled materials can be used in carrying proportions in the construction of various layers of the road.

## **Sound Barriers**

Several studies have shown that the recycled aggregate can be effectively used in the manufacturing of sound barriers for urban freeways and that they can result in structurally sound recycled aggregate concrete with a good sound absorbing characteristic. (CSIRO, 1998; Krezel, Z. A., & McManus, K. 2002)

## **Embankments**

Waste materials are very commonly used for landfill applications, to raise the level of a given piece of land. Using recycled aggregates for such purposes can reduce the economic and environmental concerns associated with the use of fresh materials. While the fresh materials' excavation, processing and transport are associated with costs and environmental damages (resulting from generation of greenhouse gases and disruption of natural environment & landforms), recycled materials have no such encumbrances. (Soleimanbeigi, 2014).

## **ECONOMIC VIABILITY & ENVIRONMENTAL IMPACTS**

Sustainability is a trend these days, yet it is not without its own economic costs. While the governments adopt the concept of sustainable development by observing and understanding the issues related with the environment, organizations see sustainability as a tool to make them more competitive and more flexible to changing conditions (Bond 2005). Management of demolition waste and/or reuse of recycled aggregates has got their own share of economic and environmental considerations.

In comparison to the fresh aggregates/materials, recycled aggregates (and materials) are often touted to be economical (Braga 2015). However, the economics here is a function of distance between the recycling plant and demolition site and/or place of material usage. In case the distance between the demolition site and recycling plant is large, the transportation cost will negate any economic advantage of not having to excavate and process fresh materials. Similar can be the case if the distance between recycling plant and place of material usage is not optimal. Another barrier to the economic viability of the recycled materials is the lack of credibility in the recycled products. A certified recycling plant has a higher cost and hence lowered economic appeal.

The demolition method itself affects the economic viability of the recycled materials. Several studies have shown the promise of selective demolition over the conventional demolition techniques (ACWMA, 2013; Coelho and de Brito, 2011; Dantata et al., 2005; Guy, 2006; Guy and Gibeau, 2003; Rousset et al., 2009). The main appeal of the former is due to its consideration of labor cost, market prices and tipping fees for recovered materials. Coelho and de Brito (2012) have reported that the use of life-cycle assessment in selective demolition results in a significant reduction in associated environmental impacts as well, apart from the cost advantages. This method is also credited with better

quality control and is encouraged through the application of differential fee calculated as a function of composition, contaminant concentrations and waste origins. (Vyncke and Rousseau, 1993).

Recycling of demolition waste and recovery of useful materials (such as, recycled aggregates) is a step towards mitigating the environmental effects associated with transport and disposal of demolition waste; extraction, processing and transport of fresh materials, etc. The 3 R's of waste management (Reduce, Reuse and Recycle) are very pertinent in the case of demolition wastes. It is to be pointed out that a specialized waste minimization strategy is needed when a large quantity of waste is generated, may have a high salvage value, is toxic or has resulted from valuable materials. Mitigating the environmental impacts of a product and/or process is a big step towards achieving sustainability. (DETR, 2000).

## **ADVANTAGES OF RECYCLED AGGREGATES**

Recycled aggregates offer the following advantages:

1. Reduced use of fresh aggregates (a natural resource).
2. Reduced transportation to/from the extraction site of aggregates.
3. Reduced consumption of energy in excavation and transportation of fresh aggregates.
4. Reduced demolition waste volume sent to landfills.
5. Reduced cost of disposal of demolition waste

## **DISADVANTAGES OF RECYCLED AGGREGATES**

Recycled aggregates have the following disadvantages:

1. A huge amount of water is required to wash the aggregates for removing the contaminants and these contaminants, due to poor disposal, may pollute the ground water or surface water.
2. Due to storage, processing and transportation, dust can be produced which is hazardous to people having breathing-related issues.
3. Due to processing operation and transportation of vehicles, noise, vibration, gas emissions, and odor are produced.
4. Lack of standardized norms for quality and composition of recycled aggregates
5. Typically results in poor mechanical characteristics of concrete when used as a partial/complete replacement of fresh aggregates. The various methods for preventing this have already been mentioned.

## **CONCLUSION**

While the growth engines of a rapidly developing economy like India cannot be stopped, the requisite infrastructure results in millions of tons of waste (demolition waste) that needs management. Currently, such techniques are mostly not in practical application. Deriving a useful product such as the recycled aggregate out of demolition waste has shown promise and is an enviable option from both economic and environmental perspectives. While there are advantages and disadvantages of using RA, it is clear that moving forward, the city planners will need to devise solutions to deal with the huge amounts of demolition waste. The current study described the common and potential applications of recycled aggregates, methods to overcome the shortcomings, the processes involved in demolition and recycling industry and the economic and environmental concerns related to the application of recycled aggregates. One thing, though, is very clear that there is definitely a huge potential of environmental and economic savings by use of recycled aggregates and other useful constituents from demolition waste and that further research is needed to overcome the obstacles found by the studies conducted so far. Recovery and reuse of useful products from demolition waste ensures the sustainability in construction sector and ensures the supply of sustainable construction material thus paving way for ensuring the sustained growth of the country while protecting the environment.

## **REFERENCES**

- ACWMA, (2013). Building 802 deconstruction project - Deconstruction results report: Oakland: Alameda County Waste Manage Authority.
- Braga, A., Welsh, B. C., & Schnell, C., (2015). Can Policing Disorder Reduce Crime? “A Systematic Review and Meta-analysis”. *Journal of Research in Crime and Delinquency*, 52(4), 567–588. doi:10.1177/0022427815576576
- Behera, M., Bhattacharyya, S. K., Minocha, A. K., Deoliya, R., & Maiti, S. (2014). “Recycled aggregate from C&D waste & its use in concrete – A breakthrough towards sustainability in construction sector”: A review. *Construction and Building Materials*, 68, 501–516. doi:10.1016/j.conbuildmat.2014.07.003
- Bond, D., (2005).: Technical and cost benefits of recycled and secondary aggregates: Supply chain case studies (Infrastructure)”, DTI/WRAP Aggregates Research Programme STBF 13/09C, 54 p.
- Coelho, A., de Brito, J., (2012). Influence of construction and demolition waste management on the environmental impact of buildings. *Waste Manage. (Oxford)* 32(3), 532-541.
- CSIRO, “Building, Construction and Engineering (1998), Guide for Specification of Recycled Concrete Aggregate (RCA) for Concrete Production”. EcoRecycle Victoria, East Melbourne, Victoria.pp. 459-469.
- Dantata, N., Touran, A., Wang, J., (2005). An analysis of cost and duration for deconstruction and demolition of residential buildings in Massachusetts. *Resource Conservation Recycling*. 44(1), 1-15
- DETR, (2000). “Controlling the environmental effects of recycled and secondary aggregates production - Good practice guidance”, Rotherham, UK, DETR.
- Faleschini, F., Zanini, M. A., Pellegrino, C., & Pasinato, S., (2016). “Sustainable management and supply of natural and recycled aggregates in a medium-size integrated plant”. *Waste Management*, 49,146-155doi:10.1016/j.wasman.2016.01.013
- Guy, B., Gibeau, E.M., (2003). “A guide to deconstruction. Deconstruction Institute”, Floride, USA, 93 p.
- Hansen, T.C., (1992). *Recycling of Demolished Concrete and Masonry*. E & FN Spon, London UK.
- Krezel, Z. A., & McManus, K. (2000). “Recycled aggregate concrete sound barriers for urban freeways. *Waste Management Series*”, 884–892. doi:10.1016/s0713-2743(00)80097-5
- Molin, C., Larsson, K., Arvidsson, H., (2004). Quality of reused crushed concrete strength, contamination and crushing technique, in: Vázquez, E., Hendriks, C., Janssen, G.M.T. (Eds.), *International RILEM Conference on the Use of Recycled Materials in Buildings and Structures*. RILEM Publications, Barcelona, Spain, pp. 150-155
- O'Mahony, M.M., (1990). “Recycling materials in Civil Engineering”. New College, University of Oxford, Oxford, UK. 233p
- Soleimanbeigi, A., Edil, T. B., & Benson, C. H. (2014). “Engineering Properties of Recycled Materials for Use as Embankment Fil”l. *Geo-Congress 2014 Technical Papers*.
- Silva, R.V., de Brito, J., Dhir, R.K., (2016). “Establishing a relationship between modulus of elasticity and compressive strength of recycled aggregate concrete”. *J. Cleaner Prod.* 112, 2171-2186
- Roussat, N., Dujet, C., Méhu, J., 2009. “Choosing a sustainable demolition waste management strategy using multicriteria decision analysis”. *Waste Management*. 143p.
- Vyncke, J., Rousseau, E., 1993. “Recycling of construction and demolition waste in Belgium: Actual situation and future evolution”, in: Lauritzen, E.K. (Ed.), *Proceedings of the Third International. RILEM Symposium on Demolition and Reuse of Concrete and Masonry*. CRC Press, Odense, Denmark, 60-74.



## Review of Autoclaved Aerated Concrete: - Advantages and Disadvantages

K. Sherin<sup>1\*</sup>, J.K. Saurabh<sup>2</sup>

<sup>1</sup>P.G.scholar, Department of Civil Engineering, Samrat Ashok Technological Institute Vidisha, M.P.464001, India

<sup>2</sup>P.G.scholar, Department of Civil Engineering, National Institute of Technological Jalandhar, Punjab 144011, India

\* Corresponding Author

**ABSTRACT:** As the name suggests light weight concrete blocks are light in weight as compared to our conventional concrete blocks. Lightweight concrete is a concrete which includes an foaming agent in it that increases the volume of the mixture while reducing the dead weight. This concrete has its advantages of higher strength for unit weight, better tensile strain carrying capacity, lower coefficient of thermal expansion, and better heat and sound insulation characteristics due to air voids in the concrete. Autoclaved Aerated Concrete block is a present time green building material in India which is used as a substitute over conventional red clay bricks in residential, commercial and industrial construction activities. AAC block is a light weight precast building material that provides construction economy. It is an eco-friendly product, as it is manufactured using 60-65% of fly ash, which is nothing but just an unavoidable waste from coal based thermal power plants. Being bigger in size than clay brick, AAC wall construction involves less joints. It provides us with minimal wear and tear over prolonged use along with minimum maintenance due to weathering. AAC blocks require substantially less of surface treatment. This paper represents reviews on AAC block and its material.

**KEYWORDS:** Light weight concrete blocks; Autoclaved aerated concrete blocks; Green building material; Ecofriendly; Aluminium powder

### INTRODUCTION

As we know that burnt clay bricks manufacturing require a large amount of energy and release smoke to kilns of brick and spoiling of the top soil in production of brick. So, there is a need of finding an alternative construction material. AAC is considered as eco-friendly building material. It is a mixture of cement, water, fine aggregates (sand, fly ash etc.) and aluminium powder. According to Neville, A.M. (1995), the densities of light weight concrete is varies between 300-1850 kg/cum. Kurama, H.et.al(2009), AAC mix having coal bottom ash(CBA) between 25%-50% help in gaining strength to it but thermal conductivity reduce with increase of CBA. Yiquan, L.et.al(2017), Although aluminium powder as a foaming agent may not be achieve low density, but it does not compromise mechanical properties of AACs. Chen, Y.L.(2017), amount of aluminium powder present in mix as well as water to solid ratio alter the bulk density of AAC. Instead of an increase in the amount of cement, autoclave curing greatly enhanced the compressive strength, and the AAC specimen kept for autoclaving at 12 atm for 16 h had the highest compressive strength of 13.3 MPa. Milos, J.et.al(2013), State as per their research that thermal conductivity of AAC is higher in case of saturated state by 6 times as compared to dry state and also thermal conductivity increase with temperature. They further stated that resistant of AAC against freezing/thawing in case of capillary saturated state found to be satisfactory (25 cycle of freezing /thawing and increase with temperature). Malhotra, H.L.(1968), He stated that fire resistance of AAC block is two times more than that of dense concrete block. Mathey, R.G.(1988), He stated that compressive strength per unit weight of AAC block is better than normal dense concrete/clay block. According to him AAC blocks have compressive strength 5.99Mpa and 1.99Mpa for density 400Kg/m<sup>3</sup> and 704Kg/m<sup>3</sup>. Valore, R.C.(1989), He confirmed same in his research. Autoclaved aerated concrete have desirable characteristics such as low weight, high compressive strength, good heat insulation, fire resistant. It makes productive use of unavoidable waste fly ash. This product helps creation of a sustainable environment by reducing CO<sub>2</sub> emissions, agricultural soil erosion and water pollution. It provides us with non-polluting manufacturing process – the only by-product is steam.

Here sand(Quartz), gypsum(calcined), lime (mineral), water and/or cement are used as a binding agent. Generally aluminium powder is used as an expanding agent at a rate varies between .05%-.08% of volume. Several chemical reactions take place during mixing and casting of AAC mix. These chemical reactions are the reason for light weight of AAC. Aluminium powder reacts with calcium hydroxide(CA(OH)<sub>2</sub>) and water to form hydrogen gas which then foams and doubles the volume of the raw mix creating gas bubbles up to 3mm (1/8 inch) in diameter. At the end of the foaming process, the hydrogen escapes into the atmosphere and is replaced by air and hence resulting in light weight concrete.

The following Table 1 shows the mix proportion for Autoclaved aerated concrete.

**Table 1. Mix proportion of autoclaved aerated concrete**

S. No.	Cement	Fine aggregate	Fly ash	Al <sub>2</sub> O <sub>3</sub> (gm)
1.	1	3	0.5	1
2.	1	2.25	0.75	1
3.	1	1.5	1.5	1
4.	1	0.75	2.25	1
5.	1	0.5	3.0	1

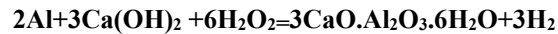
**Composition of Autoclaved Aerated Concrete**

Autoclaved aerated concrete is a mixture of cement, water, fine aggregates (sand and fly ash) and aluminium powder.

- 1). Cement: generally, we used Portland cement of grade 33, 43 or 53 as commercially available. Cement content used for most commonly mixes are 300 - 375 Kg/cum
- 2). Water: The water used in formed concrete is portable water. Mixing water for concrete should free from injurious amount of oils, acids, alkalis, salts, and organic matter.
- 3). Fly ash: The byproduct of thermal power plant is known as fly ash.
- 4). Sand: Fine sand is used for producing higher density of foam concrete.
- 5). Aluminium powder: Aluminum powder is an expansion agent; this material reacts with calcium hydroxide which is the product of reaction between cement and water.

**Chemical Reaction in AAC Mix**

The reaction between aluminum powder and calcium hydroxide causes forming of microscopic air bubbles which results in increasing of pastes volume. Mehta, Choksi and Chohan(2016),they state that the hydrogen bubble which is produced in this process is replaced by bubble of air. Domingo(2008) state that hydrogen, which is a light in weight then that of air, rises up and is replaced by air bubble as the hydrogen bubble come out of the material. Hamad(2014) understand that increase in volume is dependent upon the quantity of aluminum powder that is add in the mix to react with the calcium hydroxide in the mixture. This reaction is shown in following equations.



Or

**Aluminium paste + calcium hydroxide = Tricalcium aluminohydrate + Hydrogen gas**

**Table 2. Properties of AAC**

Dry density (kg/m <sup>3</sup> )	Compressive strength (MPa)	Flexure strength (mpa)	Modulus elasticity(E-value) (Gpa)	Thermal conductivity (3%moisture) (W/mK)
400	0.5-1	0.65	1.6	0.12
600	1-1.5	0.75	2.0	0.14
800	1.5-2	0.85	2.4	0.16
1000	2.5-3	1.00	2.5	0.18
1200	4.5-5.5	1.25	2.7	0.20

Hamad(2014) stated relationship between the expansion induced versus strength of material. according to him expansion introduced is inversely proportional to the strength of material. So for higher strength lesser expansion should be introduced. Autoclave, which is a powerful and steam-heated vessel, is used as a large pressure cooker for curing AAC block thoroughly. Autoclaving is a process in which the concrete is cured at temperature and pressure for a certain time period. A pressure range of (4-15mpa) and duration range of (8-13hr) is used in autoclaving process. Furthermore, it reduces the shrinkage after drying in AAC significantly, and it is necessary if AAC block are required within acceptable range of shrinkage as well as strength. Coarse natural aggregates cannot be used as they will segregate in light weight concrete, but it is possible to use light weight aggregates with a similar density to the Autoclaved aerated concrete. Table 2 specify the various properties of AAC.

**Comparison of AAC Brick with Ordinary Clay Brick:**

Comparison of AAC brick and ordinary clay brick is shown in Table 3.

**Table 3 Comparison of ACC and ordinary Brick**

	<b>AAC Block</b>	<b>Clay Brick</b>
Consumption of soil	No soil consumption as Primary raw material for it is fly ash which is a waste of industry generated by coal-based thermal power plants.	One clay brick consumes more than three kg of upper layer of soil
Consumption of fuel and CO <sub>2</sub> production	1ft <sup>2</sup> of it consumes 1 kg of coal. Less CO <sub>2</sub> gas production.	1ft <sup>2</sup> of clay brick consumes 8 kg of coal. Higher CO <sub>2</sub> gas production.
Density	550-700 kg per cubic meter	Around 1,800 kg per cubic meter
Availability	Available throughout the year.	Since clay brick construct in open, it cannot be manufactured in rainy season.
Facility of Production	Production facilities are good because of less emission of harmful gasses.	Hazardous working condition
Size	Available in custom size to fit individual requirement	Available in fix size only
Production cost break-up	Raw material-55%, Fuel-10%, labour-15% and other.	Fuel-45%, Raw material-15%, labour-30% and other.
Selling price	it had selling price of 2350/cubic in 2015 which is decreasing rapidly with increment of production.	it has selling price of 2050/cubic in 2015 which is increasing rapidly with increment of production

**Advantage of Autoclaved Aerated Concrete**

- Hamad(2014), according to him light weight concrete is very advantageous as it has higher strength-weight ratio, better tensile strain carrying capacity, lower coefficient of thermal expansion, and better heat and sound insulation characteristics due to air voids present in the concrete. By using AAC we can get reduction in the dead load of the construction materials which could result in a decrease in cross-section of concrete structural and Subsequently, reinforcement can be reduce due to the lightweight of the concrete.
- It makes productive use of unavoidable waste - fly ash. Through the use of fly ash, AAC helps in creation of a sustainable environment by reducing CO<sub>2</sub> emissions, agricultural soil erosion and water pollution.
- Zero-pollution manufacturing process as this process have zero emission of gases, the only emission of steam.
- It is lighter than normal clay bricks, therefore, simpler and economical to transport. Lighter weight makes construction easier and faster.

- Being light weight, it reduces the dead load of the structure, resulting in to reduction in reinforcement and concrete on foundation structure work and hence allows construction of taller buildings. AAC's light weight saves on labour cost.
- Being bigger in size than clay brick, AAC wall construction involves fewer joints.
- Energy consumption for producing AAC is less as compared to the production of other building materials. Small air voids and thermal mass of block provide thermal insulation, therefore reducing costs of artificial maintenance of temperature of a building.
- Easy workable.
- Resistant to Pest and moisture.
- No waste produces in this process.
- AAC concrete uses fly ash about 60 to 75%.
- It has resource efficient manufacturing process.
- AAC Blocks uses less power there is a reduction in power consumption by 27%.
- Reduced transportation costs - saves fuel.
- Broken blocks of AAC are also usable.
- Reduction in wastage at site.
- It is durable.
- Minimum deterioration over prolonged use.
- It requires minimum repair and retrofitting work due to resistance to weathering.

#### ***Disadvantage of Autoclaved Aerated Concrete***

- Few contractors are aware with the AAC, and skilled masons must employ for using thin-set mortar as opposed to traditional cement-based mortar, which requires less accuracy in its application. Local government body such as department for building construction, design review department, and planning commissions are also unaware with AAC so they must be educated with respect to the ability of AAC to satisfy local building codes.
- Crack after installation is a disadvantage of AAC, which can be remove by reducing the mortar strength and by assuring that the blocks are dry during installation.
- AAC need much careful handling than clay bricks to avoid any breakage because of their brittleness.
- Fixings: the brittleness of the blocks requires long thin screws for fitting cupboards and panting. also drill bits or hammering in suitable in wood is require for it.
- Requirement of heat Insulation in newer northern European building codes would require very thick walls of AAC when using it alone for the same. Thus many builders decide to come back to the traditional methods of installing an extra layer of insulating material around the building.

#### **CONCLUSION**

In conclusion we can say that autoclaved aerated concrete brick is lightweight, environment friendly, thermal resistant, sound insulator, water conversant, highly workable, fire resistant, moisture resistant and resistant to freezing-thawing. it is a very good replacement of ordinary brick. Apart from these properties it has same strength as ordinary brick in less cost thus it is economical also. due its light weight it is helpful in reducing dead load of structure. also it is helpful in developing heat resistant structure in cold region such as Europe, Russia etc. it is also helpful in making our structure more fire resistant. it also use in highly sound polluted area to make structure sound insulated . it has wide application in future construction such as-smart city, smart transportation, light weight structure etc.

#### **REFERENCES**

Brady, K.C., Watts, G. R. A. and Jones, M.R. (2001) "Specification for Foamed Concrete." UK: Highway Agency.

- Chen, Y.L., Juu-En, C., Yi-Chien, L. and Mei-In, M.C. (2017) "A Comprehensive Study on the Production of Autoclaved Aerated Concrete: Effects of Silica-Lime-Cement Composition and Autoclaving Conditions" *Construction and Building Materials*, 153(2017)622-629.
- Darshan, M., Kavita, C. and Tarjani, C. (2016) "Comparison on Auto Aerated Concrete to Normal Concrete" *GRD Journals*, "Global Research and Development Journal for Engineering" Recent Advances in Civil Engineering for Global Sustainability March e-ISSN: 2455-5703.
- Department of Building and Construction Technology Engineering/Engineering Technical College, Mosul, Iraq.
- Domingo, E.R. (2008) "An introduction to autoclaved aerated concrete including design requirements using strength design," M.S. thesis, Kansas State University, Manhattan, Kansas.
- Hamad, A.J. "Materials, Production, Properties and Application of Aerated Lightweight Concrete: Review",
- Kurama, H., Topcu, I.B. and Karakurt, C. (2007) "Properties of the autoclaved aerated concrete produced from coal bottom ash" *Journal of materials processing technology*, 209 (2009) 767-773.
- Malhotra, H.L. (1968) "The fire resistance of Autoclaved Aerated Concrete". Proceedings of the first international congress on lightweight concrete (pp. 129-131). London: Cement and Concrete Association.
- Mathey, R.G. (1988) "A review of autoclaved aerated concrete products" (Report No. NBSIR 87-3670). Gaithersburg, MD: U.S. Department of Commerce
- Miloš, J., Martin, K., Jaroslav, V. and Robert, C. (2013) "Hygric, thermal and durability properties of autoclaved aerated concrete" *Construction and Building Materials* 41 (2013) 352-359
- Neville, A.M. and Brooks, J. J. (2010) "Concrete Technology." second edition, Prentice Hall, Pearson Education, 2010, pp. 351-352.
- Nambiar, E. K. K. and Ramamurthy, K. (2007) "Air-void characterization of foam concrete." *Cement and Concrete Research*, vol. 37, no. 2, pp. 221-230 .
- Newman, J., Choo, B.S. and Owens, P. (2003) "Advanced Concrete Technology Processes." Elsevier Ltd, part 2, pp. 2/7-2/9.
- Richard, O., Ramli, M. and Al Shareem, K.L. (2013) "Experimental production of sustainable lightweight foamed concrete." *British Journal of Applied Science & Technology*, vol. 3, no. 4, pp. 1-12.
- Rooyen, S. (2013) "Structural lightweight aerated concrete," M.S. thesis, Stellenbosch University.
- Yiquan, L., Bo, S.L., Zhong, T.H. and En-hua, Y. (2017) "Autoclaved Aerated Concrete Incorporated Waste Aluminium Dust as a Foaming Agent" *Construction and Building Materials*, 148(2017)140-147.
- Sulaiman, S.H. (2011) "Water permeability and carbonation on foamed concrete," M.S. thesis, University Tun Hussein Onn Malaysia.
- Yen, L.B. (2006) "Study of water ingress into foamed concrete," M.S. thesis, National University of Singapore.
- Li, Z. (2011) "Advanced Concrete Technology", Hoboken, New Jersey: John Wiley & Sons, pp. 219-220.



## Determination of Most Suitable Position of Shear Wall in an Asymmetrical Multistory Building for Earthquake Zone IV

Ashish Simalti<sup>1\*</sup>, A. P. Singh<sup>1</sup>

<sup>1</sup> Dr B R Ambedkar National Institute of Technology, Jalandhar, Punjab

\*Corresponding Author

### ABSTRACT

Shear walls have high in-plane stiffness and strength. It concurrently withstands high parallel loads and support vertical plane loads. These properties make it valuable in many structural engineering applications. The designing of a shear wall in buildings is complex, specifically when the location of shear wall in asymmetric building need to be decided. And the location of shear wall should in a way that the cost is minimal while still satisfying specific performance objectives when subjected to natural and human-induced loads. This study was conducted to inspect the behavior of multistory building for the different position of shear wall, and elucidate the best possible location of shear wall in terms of quantity of concrete and steel consumption for construction, nodal displacement and storey drift of the building. These parameters were evaluated using the software STAAD PRO in accordance with IS 456:2000, IS 1893:2002 and IS 13920.

**KEYWORDS:** Shear wall, STAAD Pro, Storey drift

### INTRODUCTION

Shear walls are the structural component that provide lateral stability and stiffness to the structure. In several cases, multistory structures are designed as a framed building with shear walls that can efficiently resist parallel forces (Raju 2015). Horizontal loads are generated either due to wind or due to earthquake tend to cracks and sometime break down the structure in shear and thrust it over in bending. These kinds of loads can be defied by using a shear wall element. Over the several other techniques, it is the most effective systems of ensuring the lateral stability of high-rise structures (Masood et.al 2012). Shear wall can be imperative from the economic point of view and to limit the horizontal deflection. When shear wall is positioned in advantageous locations in the structure, they can perform effective during the application of parallel forces (Raju 2015, J Tarigan et.al 2018, Harne 2018). Anshuman S. et al. (2011) studied about the location of shear wall in high rise structure on the basis of both elastic and elastoplastic behaviors. H. Kaplan et al. (2011) found an innovative strengthening alternate for reinforced concrete (RC) structures, namely external shear walls and experimentally investigated under reverse cyclic loading. By this technique, it makes possible without troubling their users or evacuating building throughout the renovation. Post installed external shear walls acted as a monolithic member of the building. It was detected that the usage of external shear walls significantly enhances the capacity and sway stiffness of RC structures. S.J. Sardar et al. (2013) studied that shear wall at outward corners of the building is subjected to a lesser amount of displacement compared to the building with shear wall at Centre. Agrawal and Charkha (2012) reveals that the important effects on deflection in orthogonal direction by the shifting the shear wall location. Placing Shear wall away from center of gravity resulted in increase in most of the members forces.

This study was conducted for performance- based design of asymmetric building by investigating the performance of different position of shear wall (position of wall was decided on the basis of literature reviewed) in asymmetric structure (G+7 Storey). These cases have been further analyzed in terms of Cost analysis by estimating quantity of steel and concrete. Analysis of structure was done by STAAD Pro. 8Vi.

### Problem Statement

In present study the shape of asymmetrical building G+7 storey (Type 1) is shown in fig 1.1 & fig. 1.2, with the following parameters as mentioned in table 1:

**Table-1: Data of Building Elements**

S.No.	Particulars	Units	Parameters
1	Floor to Floor Height of First Storey	Meter	2.20
2	Floor to Floor Height of all other Storeys	Meter	3.66
3	Size of Column	Meter	0.6 X 0.8
4	Size of Beam	Meter	0.305 X 0.535
5	Thickness of Slab	Meter	0.150
6	Thickness of Shear Wall	Meter	0.23
7	Floor Load <b>all slabs (except terrace)</b>	kN/ m <sup>2</sup>	4.0
8	Weight of Floor Finish <b>all slabs (except terrace)</b>	kN/ m <sup>2</sup>	1.5

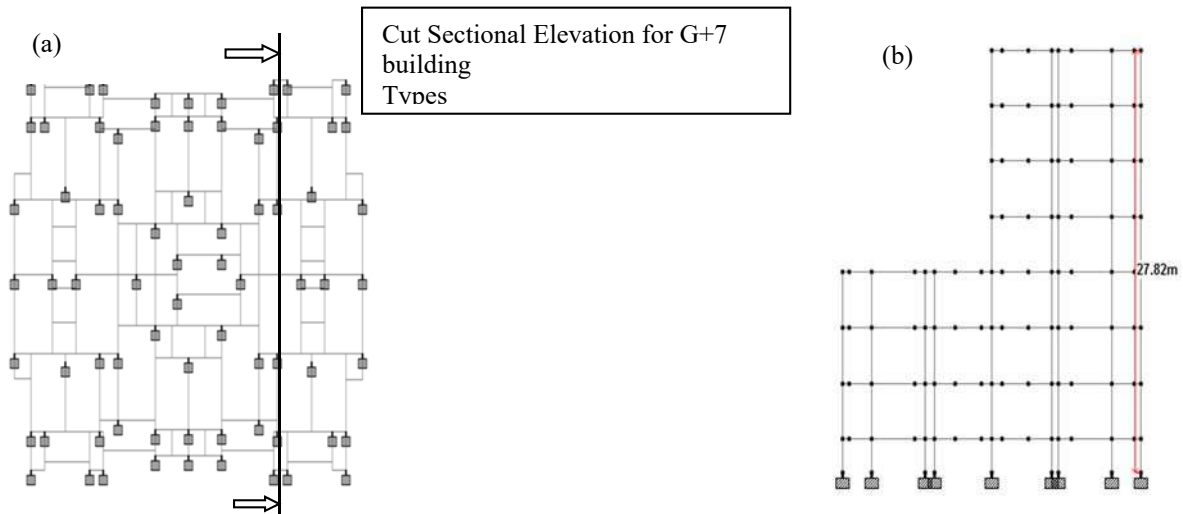


**Fig.-1 (a) Plan for Case-1, (b) Sectional Elevation of G+7 Storey building**

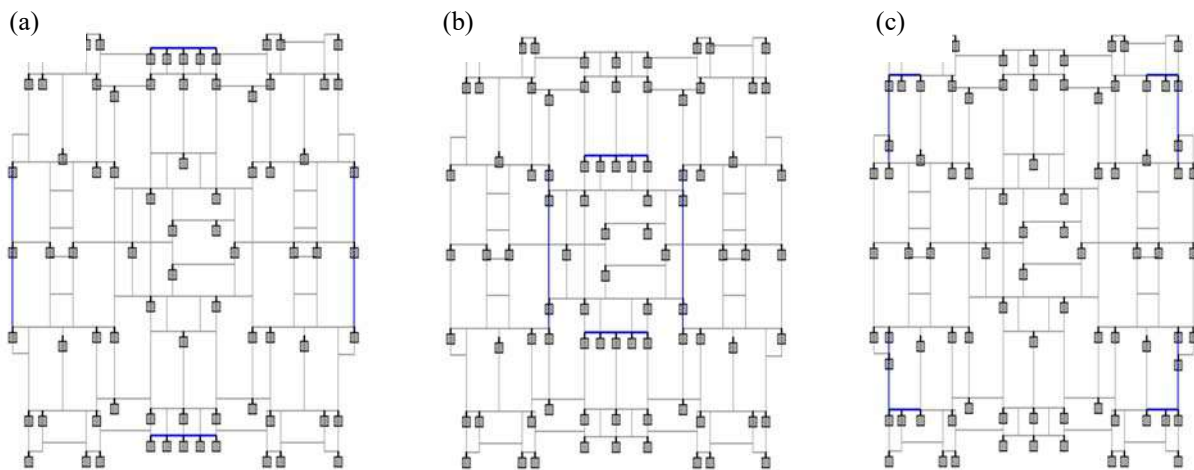


**Fig.-2 (a) Plan for Case-2, (b) Plan for Case-3, (c) Plan for Case-4**

Asymmetrical building (G+7 storey), the plan and elevation of building shown in fig 1 (a) & (b) is considered with following locations:

- CASE -1: Structure having no shear wall.
- CASE- 2: Structure having external shear wall. (fig. 2 (a))
- CASE- 3: Structure having shear wall near core area (fig. 2 (b))
- CASE- 4: Structure having shear wall at corners. (fig. 2(c))

The three amalgamations of loads were considered for analysis of structure as follows:

1. 1.5 DL + 1.5 LL
2. 1.2 ELX + 1.2 DL + 1.2 LL
3. 1.2 ELZ + 1.2 DL + 1.2 LL

## RESULT AND DISCUSSION

### *Comparisons of Node Displacement*

Nodes selected for the comparisons of result are 195, 381, 567, 753, 939, 1125, 1311 & 1497 at a storey height of 2.20 (from foundation), 5.86, 9.52, 13.18, 16.84, 20.50, 24.16 & 27.82 m respectively. For comparative study displacement are checked at these nodes for load combination 1, 2 & 3 as mentioned above in section.

Table-2: Node Displacement (cm) in X- direction in Type 1 Building for load Combination 1 for all four cases.

Type 1						
Storey Level	Node No.	L/C	Case 1	Case 2	Case 3	Case 4
2.20	195	1.5 DL +1.5 LL	0.064	0.081	0.054	0.008
5.86	381	1.5 DL +1.5 LL	0.106	0.174	0.095	0.021
9.52	567	1.5 DL +1.5 LL	0.019	0.12	0.059	0.053
13.18	753	1.5 DL +1.5 LL	0.151	0.014	0.11	0.118
16.84	939	1.5 DL +1.5 LL	0.329	0.039	0.174	0.214
20.50	1125	1.5 DL +1.5 LL	0.555	0.192	0.239	0.332
24.16	1311	1.5 DL +1.5 LL	0.821	0.423	0.353	0.463
27.82	1497	1.5 DL +1.5 LL	1.598	1.259	0.093	0.679

### *Comparison of Node Displacement for Load Combination – 1*

The results of node displacement in X, Y and Z -directions are compared for all cases. And observed that for this particular load case, when earthquake occurs major displacements happened only in X – direction and values of displacement in other directions are very less. Displacements in X –direction for having no shear walls and with all shear walls configurations are compared along the different storey height of the building in Table- 2

From Table- 2, it is concluded that displacement for building without shear walls is maximum as compared to other cases. At top of the building i.e. at height of 27.82 m. maximum node displacement is 1.598 cm. whereas for building with shear walls near core area of the building has maximum node displacement is 0.093 cm at height of 27.82 m. So there is 94.18 % decrease of node displacement for this load combination by providing the shear walls near the core area of building. And the Table-3 clearly demarks that percentage decrease of node displacement is more for top storey. A Figure 3 is plotted between node displacement v/s storey heights for all cases. From figure, it is evident that the node displacements get increased with the increase of height for all cases.

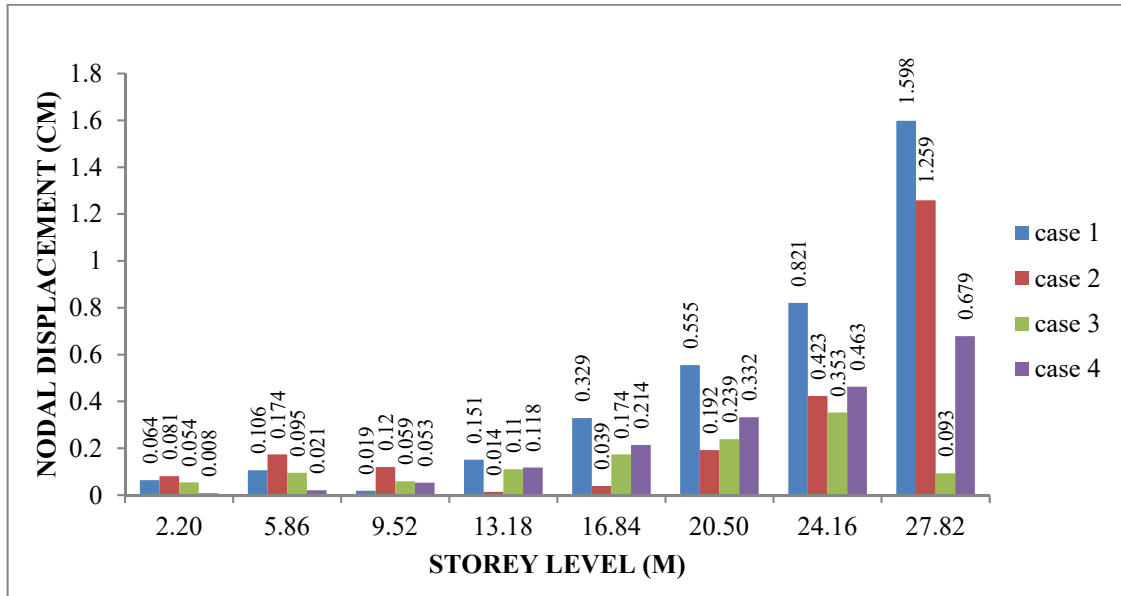


Fig.-3: G+7 Storey Node Displacement V/S Storey Level for Load Combination 1 for Type 1.

Table -3: Comparison of Percentage decrease of Node Displacement in Type 1 Building for load Combination 1.

Type 1					
Storey Level	Node	L/C	Case 1	Case 3	% Decrease
2.20	195	1.5 DL +1.5 LL	0.064	0.054	15.63
5.86	381	1.5 DL +1.5 LL	0.106	0.095	10.38
9.52	567	1.5 DL +1.5 LL	0.019	0.014	26.32
13.18	753	1.5 DL +1.5 LL	0.151	0.11	27.15
16.84	939	1.5 DL +1.5 LL	0.329	0.174	47.11
20.50	1125	1.5 DL +1.5 LL	0.555	0.239	56.94
24.16	1311	1.5 DL +1.5 LL	0.821	0.353	57.00
27.82	1497	1.5 DL +1.5 LL	1.598	0.093	94.18

### Comparison of Node Displacement for Load Combination - 2

The results of node displacement in X, Y and Z -directions are compared for all cases. And observed that for this particular load case, when earthquake occurs major displacements happened only in X – direction and values of displacement in other directions are very less. Displacements in X-direction for without and with all shear walls configurations are compared along the different storey height of the building in Table- 4

From Table- 4, it is concluded that displacement for building without shear walls is maximum as compared to other cases. At top of the building i.e. at height of 27.82 m. maximum node displacement is 2.864 cm. Whereas for building with shear walls near core area of the building has maximum node displacement is 0.805 cm at height of 27.82 m. So there is 71.89 % decrease of node displacement for this load combination by providing the shear walls near the core area of building. And the Table- 5 clearly demarks that percentage decrease of node displacement is more for top storeys.

A Figure 4 is plotted between node displacement v/s storey heights for all cases. From figure, it is evident that the node displacements get increased with the increase of height for all cases.

Table-4: Node Displacement (cm) in X- direction in Type 1 Building for load Combination 2 for all four cases.

Type 1						
Storey Level	Node	L/C	Case 1	Case 2	Case 3	Case 4
2.20	195	1.2 DL +1.2 LL + 1.2EQX	-0.012	-0.042	-0.023	0.034
5.86	381	1.2 DL + 1.2 LL + 1.2EQX	0.133	-0.015	0.036	0.169
9.52	567	1.2 DL + 1.2 LL + 1.2 EQX	0.472	0.167	0.185	0.362
13.18	753	1.2 DL + 1.2 LL + 1.2 EQX	0.84	0.372	0.281	0.603
16.84	939	1.2 DL + 1.2 LL + 1.2 EQX	1.246	0.614	0.373	0.879
20.50	1125	1.2 DL + 1.2 LL + 1.2 EQX	1.671	0.892	0.463	1.164
24.16	1311	1.2 DL + 1.2 LL + 1.2 EQX	2.088	1.21	0.498	1.434
27.82	1497	1.2 DL + 1.2 LL + 1.2 EQX	2.864	1.981	0.805	1.736

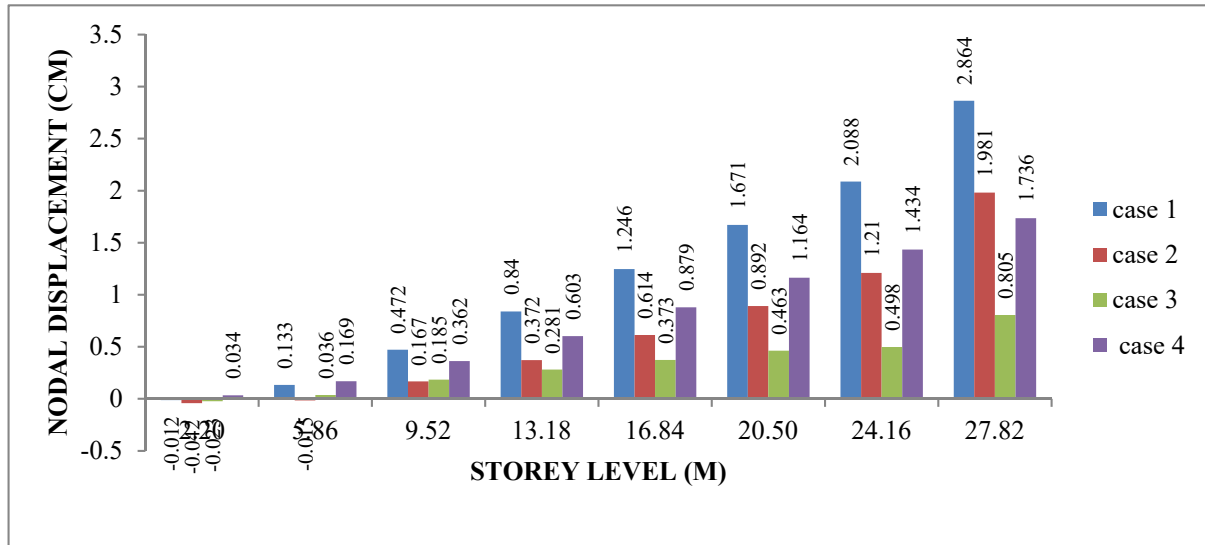


Fig.-4: G+ 7 Storey Node Displacement V/S Storey Level for Load Combination 2.

Table- 5: Storey Node Displacement V/S Storey Level for Load Combination 2 for Type 1.

Type 1					
Storey Level	Node	L/C	Case 1	Case 3	% Decrease
2.20	195	1.2 DL +1.2 LL + 1.2 EQX	-0.012	-0.023	91.67
5.86	381	1.2 DL +1.2 LL + 1.2 EQX	0.133	0.036	72.93
9.52	567	1.2 DL +1.2 LL + 1.2 EQX	0.472	0.185	60.81
13.18	753	1.2 DL +1.2 LL + 1.2 EQX	0.84	0.281	66.55
16.84	939	1.2 DL +1.2 LL + 1.2 EQX	1.246	0.373	70.06
20.50	1125	1.2 DL +1.2 LL + 1.2 EQX	1.671	0.463	72.29
24.16	1311	1.2 DL +1.2 LL + 1.2 EQX	2.088	0.498	76.15
27.82	1497	1.2 DL +1.2 LL + 1.2 EQX	2.864	0.805	71.89

**Comparison of Node Displacement for Load Combination – 3**

The results of node displacement in X, Y and Z -directions are compared for all cases. And observed that for this particular load case, when earthquake occurs major displacements happened only in Z – direction and values of displacement in other directions are very less. Displacements in Z –direction for without shear walls and with all shear walls configurations are compared along the different storey height of the building in Table- 6

From Table- 6, it is concluded that displacement for building without shear walls is maximum as compared to other cases. At top of the building i.e. at height of 27.82 m. maximum node displacement is 1.332 cm. whereas for building with shear walls near core area of the building has maximum node displacement is .037 cm at height of 27.82 m. So there is 97.22 % decrease of node displacement for this load combination by providing the shear walls near the core area of building. And the Table- 7 clearly demarks that percentage decrease of node displacement is more for top storeys.

A Figure 5 is plotted between node displacement v/s storey heights for all cases. From figure, it is evident that the node displacements get increased with the increase of height for all cases.

Table-6: Node Displacement (cm) in X- direction in Type 1 Building for load Combination 3 for all four cases.

Type 1						
Storey Level	Node	L/C	Case 1	Case 2	Case 3	Case 4
2.20	195	1.2 DL + 1.2 LL + 1.2 EQZ	0.051	0.064	0.044	0.006
5.86	381	1.2 DL + 1.2 LL + 1.2 EQZ	0.08	0.137	0.078	0.015
9.52	567	1.2 DL + 1.2 LL + 1.2 EQZ	0.025	0.091	0.049	0.034
13.18	753	1.2 DL + 1.2 LL + 1.2 EQZ	0.139	0.037	0.087	0.078
16.84	939	1.2 DL + 1.2 LL + 1.2 EQZ	0.291	0.047	0.134	0.147
20.50	1125	1.2 DL + 1.2 LL + 1.2 EQZ	0.481	0.175	0.18	0.233
24.16	1311	1.2 DL + 1.2 LL + 1.2 EQZ	0.704	0.365	0.262	0.329
27.82	1497	1.2 DL + 1.2 LL + 1.2 EQZ	1.332	1.034	0.037	0.488

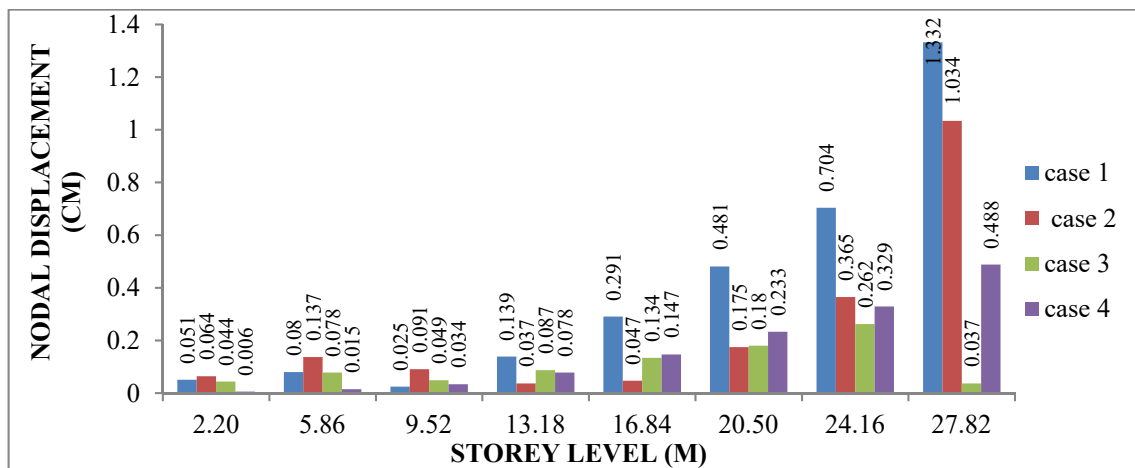


Fig.-5: G+7 Storey Node Displacement V/S Storey Level for Load Combination 3 for Type 1.

Table-7: Comparison of Percentage decrease of Node Displacement in Type 1 Building for load Combination 3.

Type 1					
Storey Level	Node	L/C	Case 1	Case 3	% Decrease
2.20	195	1.2 DL + 1.2 LL + 1.2 EQZ	0.051	0.044	13.73
5.86	381	1.2 DL + 1.2 LL + 1.2 EQZ	0.08	0.078	2.50
9.52	567	1.2 DL + 1.2 LL + 1.2 EQZ	0.025	0.049	-96.00
13.18	753	1.2 DL + 1.2 LL + 1.2 EQZ	0.139	0.087	37.41
16.84	939	1.2 DL + 1.2 LL + 1.2 EQZ	0.291	0.134	53.95
20.50	1125	1.2 DL + 1.2 LL + 1.2 EQZ	0.481	0.18	62.58
24.16	1311	1.2 DL + 1.2 LL + 1.2 EQZ	0.704	0.262	62.78
27.82	1497	1.2 DL + 1.2 LL + 1.2 EQZ	1.332	0.037	97.22

### Comparisons of Storey Drift

The results of storey drift are shown in Table- 2.7 to 2.9 for all the four cases. As per IS 1893-2002 (Clause no. 7.11.1) the storey drift in any storey due to minimum specified design force shall not exceed 0.004 times the storey height (i.e. ratio between storey height and average displacement should not be less than 250). From the results underneath, it is found that the values are within permissible limit.

### Comparison of Storey Drift for Load Combination – 1

From the Table- 8, it is clear that the storey drift is minimum in case-3 as compare to without shear wall building.

Table-8: Comparison of Percentage decrease of Storey Drift in Type 1 Building for load Combination 1.

Type 1						
Storey Level	Node	L/C	Case 1	Case 2	Case 3	Case 4
2.20	195	1.5 DL +1.5 LL	-	-	-	-
5.86	381	1.5 DL +1.5 LL	0.0001	0.0000	0.0001	0.0000
9.52	567	1.5 DL +1.5 LL	-0.0002	0.0001	-0.0001	0.0001
13.18	753	1.5 DL +1.5 LL	0.0004	0.0000	0.0001	0.0002
16.84	939	1.5 DL +1.5 LL	0.0005	0.0000	0.0002	0.0003
20.50	1125	1.5 DL +1.5 LL	0.0006	0.0000	0.0002	0.0003
24.16	1311	1.5 DL +1.5 LL	0.0007	0.0002	0.0003	0.0004
27.82	1497	1.5 DL +1.5 LL	0.0021	0.0015	-0.0007	0.0006

### Comparison of Storey Drift for Load Combination – 2

From the Table- 9, it is clear that the storey drift is minimum in case-3 as compare to without shear wall building.

Table-9: Comparison of Percentage decrease of Storey Drift in Type 1 Building for load Combination 2.

Type 1						
Storey Level	Node	L/C	Case 1	Case 2	Case 3	Case 4
2.20	195	1.2 DL + 1.2 LL + 1.2 EQX	-	-	-	-
5.86	381	1.2 DL + 1.2 LL + 1.2 EQX	0.0003	0.0000	0.0002	0.0004
9.52	567	1.2 DL + 1.2 LL + 1.2 EQX	0.0009	0.0000	0.0004	0.0005
13.18	753	1.2 DL + 1.2 LL + 1.2 EQX	0.0010	0.0002	0.0003	0.0007
16.84	939	1.2 DL + 1.2 LL + 1.2 EQX	0.0011	0.0006	0.0003	0.0008
20.50	1125	1.2 DL + 1.2 LL + 1.2 EQX	0.0012	0.0015	0.0002	0.0008
24.16	1311	1.2 DL + 1.2 LL + 1.2 EQX	0.0011	0.0029	0.0001	0.0007
27.82	1497	1.2 DL + 1.2 LL + 1.2 EQX	0.0021	0.0065	0.0008	0.0008

### Comparison of Storey Drift for Load Combination – 3

From the Table-10, it is clear that the storey drift is minimum in case-2 as compare to without shear wall building.

Table-10: Comparison of Percentage decrease of Storey Drift in Type 1 Building for load Combination 3.

Type 1						
Storey Level	Node	L/C	Case 1	Case 2	Case 3	Case 4
2.20	195	1.2 DL + 1.2 LL + 1.2 EQZ	-	-	-	-
5.86	381	1.2 DL + 1.2 LL + 1.2 EQZ	0.0005	0.0000	0.0002	0.0002
9.52	567	1.2 DL + 1.2 LL + 1.2 EQZ	0.0007	0.0000	0.0003	0.0000
13.18	753	1.2 DL + 1.2 LL + 1.2 EQZ	0.0007	0.0000	0.0003	0.0002
16.84	939	1.2 DL + 1.2 LL + 1.2 EQZ	0.0007	0.0000	0.0003	0.0002
20.50	1125	1.2 DL + 1.2 LL + 1.2 EQZ	0.0006	0.0000	0.0002	0.0002
24.16	1311	1.2 DL + 1.2 LL + 1.2 EQZ	0.0000	0.0000	0.0002	0.0002
27.82	1497	1.2 DL + 1.2 LL + 1.2 EQZ	0.0003	0.0001	0.0001	0.0000

Comparison of quantity of Steel and Concrete for the three load combinations and all the four case for G+7 storey building have been tabulated in table. 11 Which shows that the most economical is case 3.

Table11: Comparison of Steel and Concrete in G+7 storey Building for all Cases.

G+7 Storey Building	Case 1	Case 2	Case 3	Case 4
Total Concrete Required (Cum)	1580.27	1580.99	1583.20	1581.23
Total Steel Required (Tons)	126.26	127.44	116.08	124.23

## CONCLUSIONS

Based upon the limited scope of the work carried out in this investigation, following conclusions are drawn:

- For the G+7 storey building the Nodal Displacements are reduced for the case 3 i.e. building with shear wall near core area.
- For the G+7 storey building the storey drift are reduced for the case 3 i.e. building with shear wall near core area.
- The quantity of steel also reduced for case 3 this conclude that the building with the shear wall near core area is most economical and efficient location for installation.

## References

- Indian Standard IS: 456-2000, Bureau of India Standards, Manak Bhawan, 9 Bahadur Shah Zafar Marg, New Delhi 110002.
- Indian Standard IS: 875, Part 3 Bureau of India Standards, Manak Bhawan, 9 Bahadur Shah Zafar Marg, New Delhi 110002.
- Indian Standard IS: 1893-2002, Bureau of India Standards, Manak Bhawan, 9 Bahadur Shah Zafar Marg, New Delhi 110002.
- Indian Standard IS: 13920-1993, Bureau of India Standards, Manak Bhawan, 9 Bahadur Shah Zafar Marg, New Delhi 110002
- K. Lova Raju and K.V.G.D. Balaji (2015), Effective location of shear wall on performance of building frame subjected to earthquake load, International Advanced Research Journal in Science, Engineering and Technology Vol. 2, Issue 1, January 2015
- J Tarigan, J Manggala and T Sitorus, (2018) The effect of shear wall location in resisting earthquake, IOP Conf. Series: Materials Science and Engineering 309, 012077
- Varsha R. Harne, (2014) Comparative Study of Strength of RC Shear Wall at Different Location on Multi-storied Residential Building, International Journal of Civil Engineering Research, ISSN 2278-3652 Volume 5, Number 4 (2014), pp. 391-400
- Masood M., Ahmed I. and Assas M. (2012), "Behaviour of shear wall with base opening", Jordan Journal of Civil Engineering, Volume 6, No. 2.
- Kaplan H., Yilmaz S., Cetinkaya N. and Atimtay E. (2011), "Seismic strengthening of RC structures with exterior shear walls", Indian Academy of Sciences, Volume 36, Issue 1, pp 17-34.
- Anshuman. S., Bhunia D. and Ramjiyani B. (2011), "Solution of Shear Wall Location in Multi-Storey Building", International Journal of Civil and Structural Engineering, Volume 2 Issue 2.
- Sardar S.J. and Karadi U.N. (2013), "Effect of change in shear wall location on storey drift of multistorey building subjected to lateral loads", IJIRSET, Vol. 2, Issue 9.
- Agrawal A.S. and Charkha S.D. (2012), "Effect of change in shear wall location on storey drift of multistorey building subjected to lateral loads", International Journal of Engineering Research and Applications (IJERA) ISSN: 2248-9622, Vol. 2, Issue 3, pp.1786-1793.

## Response of Reinforced and Prestressed Concrete Slabs Under Drop Weight Impact

Vimal Kumar,<sup>1\*</sup> M. A. Iqbal,<sup>2</sup> Achal Kumar Mittal<sup>3</sup>

<sup>1\*</sup> Research Scholar, Department of Civil Engineering, Indian Institute of Technology Roorkee, Roorkee-247667; e-mail: panchariya.vimal@gmail.com

<sup>2</sup> Associate Professor, Department of Civil Engineering, Indian Institute of Technology Roorkee, Roorkee-247667; e-mail: iqbal\_ashraf@rediffmail.com (Corresponding Author)

<sup>3</sup> Senior Principal Scientist, Structural Engineering Group, Central Building Research Institute, Roorkee-247667; e-mail: akmittal@cbri.res.in

### ABSTRACT

The dynamic response of prestressed and reinforced concrete slabs ( $800 \times 800 \times 100$  mm) has been investigated under falling of a steel mass (243 kg) at the center of slab span. These slabs were subjected to single impact from 1 m height and successive multiple impacts on the same pre-damaged slab from 0.5 m height. The generated response of the slabs such as impact force, reaction and displacement were measured. The response and energy absorption capacity of fresh and damaged slabs were obtained under each impact and compared. The resistance of prestressed concrete found to enhance due to pre-tensioning. Thus, prestressed concrete slabs were subjected to relatively higher impact force, higher reaction and reduced displacement in comparison to reinforced concrete slab. Under repeated impact, the peak impact load and reaction were reduced while displacement was found to increase due to accumulated damage in both of the concrete slabs.

**KEYWORDS:** Drop Impact; Prestressed Concrete; Reinforced Concrete; Slab; Energy Absorption; Dynamic Response.

### INTRODUCTION

Concrete structures may subject medium to high-intensity impacts in their service lifespan. Some commonly seen examples of such impacts are vehicle accidents with structures, falling of heavy mass on the structures, ballistic and blast impacts on military bunkers etc. Studies are available wherein the influence of fiber content on the drop impact performance of the self-compacting concrete (SCC) plates was investigated under drop weight impact (Kantar et al., 2017). It was reported that the energy absorption capacity of these plates (with fiber) increased by 6-14 time that of the SCC plates without fiber content. In another study, the influence of the CFRP strengthening was investigated on the impact performance and also on their residual load carrying capacity under static loading (Radnić et al., 2015). The results showed an increase in the ultimate load carrying capacity under both static and impact loading. However, the performance was reported to be governed by the height of drop of impactor and amount of reinforcement provided (Zineddin and Krauthammer, 2007).

Studies are also available on beam specimens wherein the performance of reinforced concrete beams was studied experimentally and numerically (Tachibana et al., 2010; Chen and May, 2009; Adhikary et al., 2012; Bhatti et al., 2011; Saatci and Vecchio, 2009). The impulse under drop weight impact was found to be proportional to impactor momentum and impact duration; on the other hand, displacement was noticed to be inversely proportional to impact force (Tachibana et al., 2010). Further, impact force was found to be less sensitive to the change in beam support conditions as compared to that of the beam span (Chen and May, 2009). The load carrying capacity of the reinforced concrete beams increased with increase in the loading rate and increase in the shear reinforcement (Adhikary et al., 2012). In another study, the disturbed stress field model with smeared rotating crack approach was accurately predicted the experimental impact load, reaction, displacements and rebar strains (Saatci and Vecchio, 2009). However, no studies have reported in the available articles wherein the behaviour of prestressed concrete slab was studied against drop impact.

This study focuses on the investigation of the dynamic response of prestressed and reinforced concrete slabs subject to single and repeated (multiple) drop weight impact. The impact was applied by dropping a steel weight (242.85 kg) at the

center of the slab span. The impact force, reaction, displacement and acceleration response have been measured for prestressed concrete (PC) slab and compared with that of the reinforced concrete (RC) slab. For a given slab (RC or PC), the magnitude of peak impact and reaction have reduced under repeated impact while displacement has increased.

### MATERIAL AND TEST SPECIMENS

Two types of slabs namely prestressed and reinforced have casted in identical size (800 mm × 800 mm) and thickness 100 mm, see Fig. 1. Both types of the slabs were prepared using same concrete batch mix having 28 days compressive strength 68 N/mm<sup>2</sup>. The compressive strength of the concrete was obtained in a Compression Testing Machine (CTM) at a loading rate 5 kN s<sup>-1</sup>. The curing conditions were also kept identical for 28 days to avoid any variation in the strength of concrete. Similar reinforcement arrangement has been provided in both types of the slabs, also see (Kumar et al., 2018a). The prestressed concrete slab was pre-tensioned to 20% of its characteristic compressive strength of concrete.

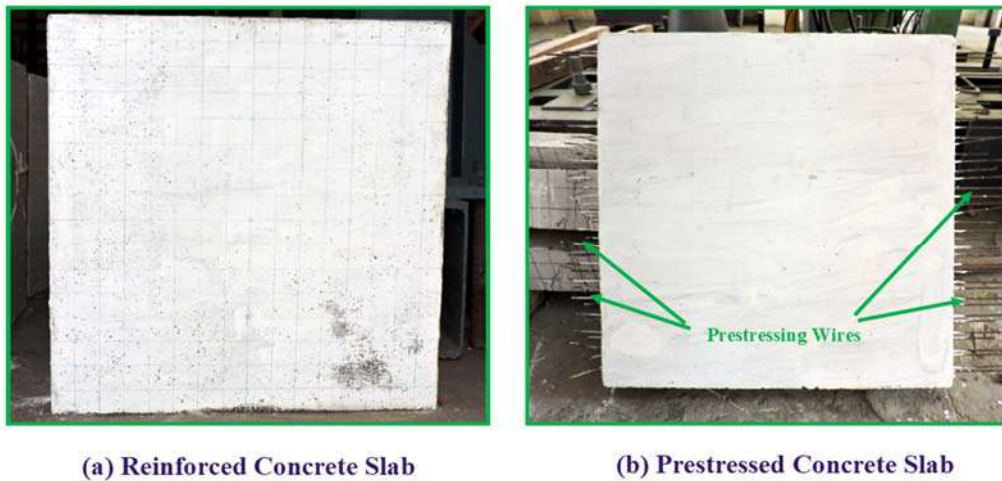


Fig. 1 Target reinforced and prestressed concrete slabs

### EXPERIMENTAL APPROACH

The prestressed and reinforced concrete slabs were tested in an instrumented drop impact setup (Kumar et al., 2018a). A steel weight (242.85 kg) has been dropped freely under gravity from 0.5 and 1.0 m height (H). The slabs were clamped in a steel frame made of steel angles and rested at their corners on the load-cells (Kumar et al., 2018b). The steel mass was then lifted up to the discussed heights and dropped to hit the slabs at the center. The generated dynamic response under impact such as impact force, reaction, displacement and acceleration response were measured for both of the concretes. The data has been recorded in a data-logger at a time interval  $1 \times 10^{-4}$  second, compared and also discussed. The detail of drop impact experiments has shown in Table 1, also see Kumar et al., 2018a and 2018b.

Table 1. Details of drop weight impact experiments

Type of Concrete	28 days Strength of Concrete (N/mm <sup>2</sup> )	Drop Mass, M (kg)		First Impact on Fresh Slab, (H=1.0 m)	First Repeated Impact, (H= 0.5 m)	Second Repeated Impact, (H= 0.5 m)
<i>a</i>	<i>b</i>	<i>c</i>	<i>d</i>	<i>e</i>	<i>f</i>	<i>g</i>
Prestressed Concrete (PC)	68	242.85	Test ID	PC-R0	PC-R1	PC-R2
Reinforced Concrete (RC)	68	242.85	Test ID	RC-R0	RC-R1	RC-R2

### IMPACT FORCE UNDER SINGLE AND REPEATED IMPACTS

The impact force/load response under drop impact experiments was measured using a load-cell of 50 T capacity. The magnitude of impact force increased rapidly up to a peak value as soon as the establishment of contact between the hammer and the target slabs due to high inertia. The magnitude of the obtained peak impact load is presented in Fig. 2. The magnitude of the peak impact force in fresh prestressed concrete slab (PC-R0) observed to be 4.52% higher than that of the fresh reinforced concrete slab (RC-R0), see Table 2. The prestressed concrete slab also reported higher peak impact force under repeated impacts. Under second repeated impact, the peak load in prestressed concrete slab (PC-R2) found to be 57% higher than that of the reinforced concrete slab (RC-R2). However, in a given concrete (RC or PC), the peak impact force has observed to reduce under successive repetition of impact due to accumulated pre-damage in the slab.

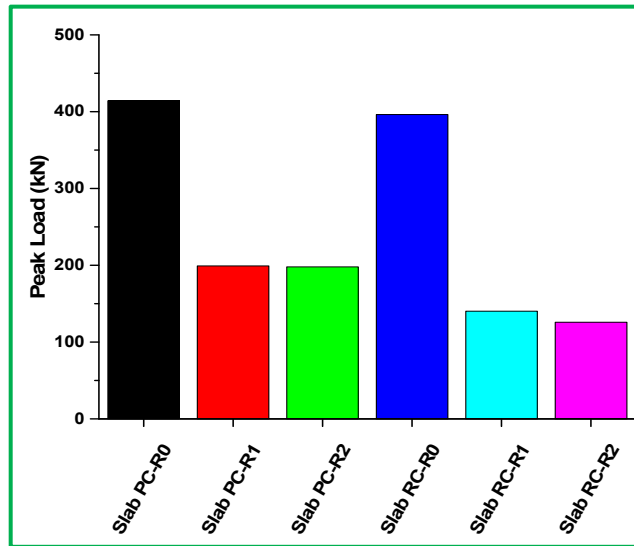


Fig. 2 Peak impact force under single and repeated impact

Table 2. Peak impact force under single and repeated impact

Test ID for RC slab	Peak Impact Force (kN)	Test ID for PC slab	Peak Impact Force (kN)	Increase (%)
<i>a</i>	<i>b</i>	<i>c</i>	<i>d</i>	$e=(d-b)/b$
RC-R0	396.2	PC-R0	414.1	4.52
RC-R1	140.2	PC-R1	199.1	42.01
RC-R2	125.9	PC-R2	198.0	57.27

## REACTION UNDER SINGLE AND REPEATED IMPACTS

The response of support reaction under drop impact was measured using a load-cell of 150 T capacity. The magnitude of peak reaction obtained is presented in Fig. 3. In slab PC-R0, the magnitude of the reaction has noticed to be 38% higher in comparison to slab RC-R0, see Table 3. This increase is due to improvement in the slabs stiffness owing to the pre-tensioning of concrete. The prestressed concrete slab also reported higher support reaction under repeated impacts too. Under first and second repeated impact, the peak reaction in the prestressed concrete slab also found to be 43% and 23% higher, respectively, than that of the reinforced concrete slab. Similar to the impact force, for given type of concrete (RC or PC), the peak reaction also found to reduce under successive multiple impacts.

Table 3. Peak reaction under single and repeated impact

Test ID For RC Slab	Peak Reaction (kN)	Test ID For PC Slab	Peak Reaction (kN)	Increase (%)
<i>a</i>	<i>b</i>	<i>c</i>	<i>d</i>	$e=(d-b)/b$
RC-R0	256.5	PC-R0	353.3	37.74
RC-R1	212.1	PC-R1	303.3	43.00

RC-R2	220.4	PC-R2	271.6	23.23
-------	-------	-------	-------	-------

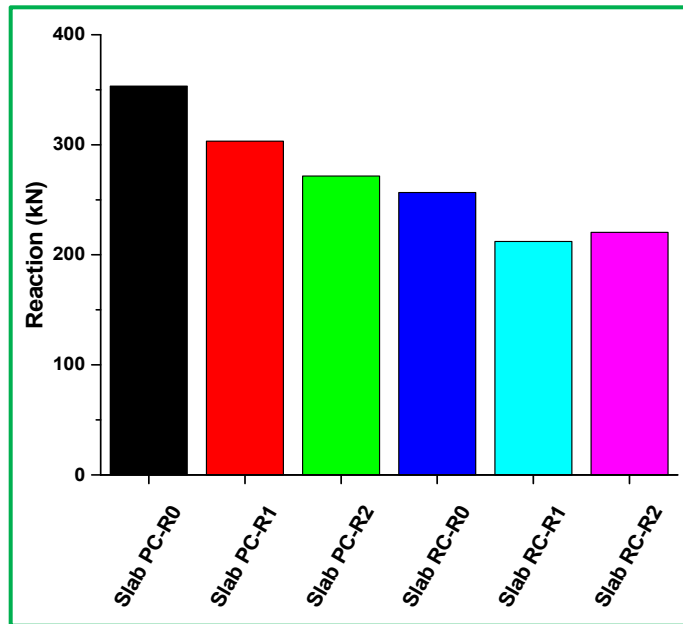


Fig. 3 Peak reaction under single and repeated impact

#### DISPLACEMENT AND ACCELERATION UNDER SINGLE AND REPEATED IMPACTS

The mid-span displacement and acceleration of the slabs were measured using Laser Displacement Sensor (LDS) and accelerometer, respectively. Similar, to impact-load response the displacement also attained a peak just after impact. Subsequently, the displacement reduced after partial recovery and attained some permanent displacement value. The magnitude of peak displacement is presented in Fig. 4. Under first impact on fresh slabs, the peak displacement in prestressed concrete observed to be 28% smaller than reinforced concrete, see Table 4. On the other hand, the acceleration response in prestressed concrete slabs under impact increased due to increase in the stiffness of the slab, see Fig. 5. Under repeated impact, the displacement in prestressed concrete slab also found to be smaller compared to that of the reinforced concrete slab. On the other hand, for a given concrete, the peak displacements increased under repeated impacts.

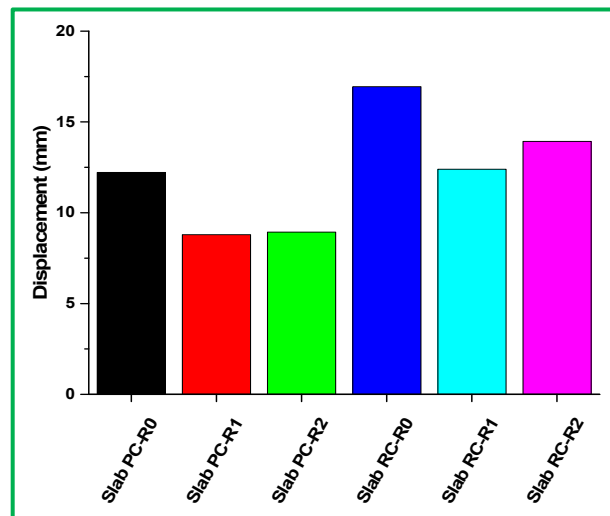


Fig. 4 Peak displacement under single and repeated impact

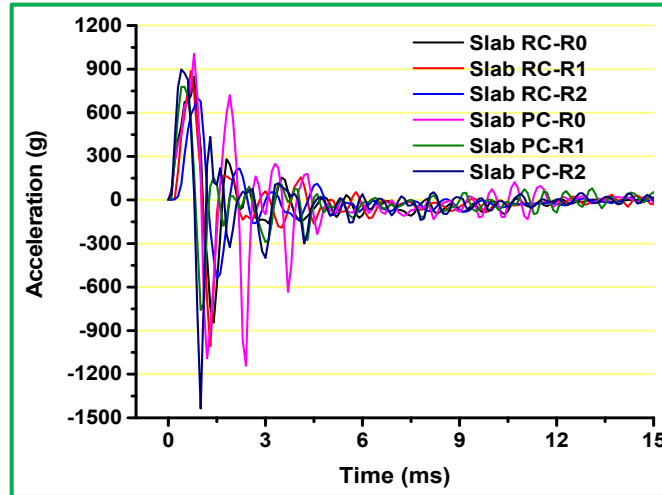


Fig. 5 Acceleration response of PC and RC slabs under repeated impact

Table 4. Peak displacements under single and repeated impact

Test ID For RC Slab	Peak Displacement (mm)	Test ID For PC Slab	Peak Displacement (mm)	Reduction (%)
<i>a</i>	<i>b</i>	<i>c</i>	<i>d</i>	$e=(b-d)/b$
RC-R0	16.95	PC-R0	12.2	28.02
RC-R1	12.4	PC-R1	8.8	29.03
RC-R2	13.9	PC-R2	8.9	35.97

### ENERGY ABSORPTION CAPACITY

The energy absorption capacity is obtained by calculating area under the load-displacement curve for prestressed and reinforced concrete slab, is presented in Fig. 6. Under first impact on fresh slabs, no significant difference in the energy absorbed by prestressed and reinforced concrete slabs has observed. However, the energy absorption capacity of the RC slab has found to be little higher than that of the PC slab. A similar observation could be noticed under successive repeated impacts.

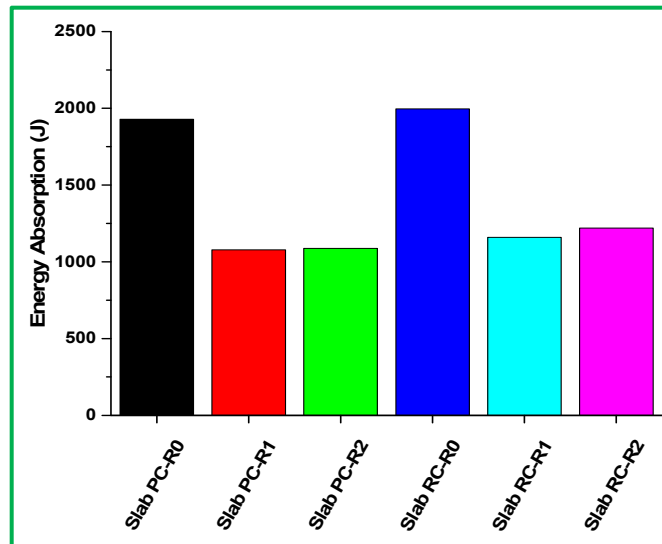


Fig. 6 Energy absorption capacity of prestressed and reinforced concrete slab

## CONCLUSIONS

Drop weight impact experiments have been performed on prestressed and reinforced concrete slabs. Both the slabs were having identical geometry and concrete strength. The prestressed concrete slabs were pre-tensioned to 20% of its characteristic compressive strength and subjected to repeated drop impact at their center. The response of prestressed concrete slabs thus generated has been measured and compared with that of the reinforced concrete slabs. Due to induced prestressing the impact resistance capacity of the prestressed concrete slab has increased. The magnitude of peak impact force in prestressed concrete slab noticed to be 4.5% and 57% higher under single and repeated impact, respectively. Similarly, the peak displacement in the prestressed concrete slab has noticed to be 28% and 35% smaller, respectively, than that of the reinforced concrete slab.

## ACKNOWLEDGEMENTS

Authors gratefully acknowledge the financial support provided by Science and Engineering Research Board, Department of Science and Technology, India through the research Grant No. SB/S3/CEE/0032/2014 for carrying out the present study.

## REFERENCES

- Adhikary, S. D., Li, B. and Fujikake, K. (2012). "Dynamic behavior of reinforced concrete beams under varying rates of concentrated loading." *Int. J. Impact Eng.*, 47, 24–38. Doi:10.1016/j.ijimpeng.2012.02.001.
- Bhatti, A. Q., Kishi, N. and Mikami, H. (2011). "An applicability of dynamic response analysis of shear-failure type RC beams with lightweight aggregate concrete under falling-weight impact loading." *Mater. Struct.*, 44, 221–231. Doi:10.1617/s11527-010-9621-9.
- Chen, Y. and May, I. M. (2009). "Reinforced concrete members under drop-weight impacts." *Proc. ICE - Struct. Build.*, 162, 45–56. Doi:10.1680/stbu.2009.162.1.45.
- Kantar, E., Yuen, T. Y. P., Kobya, V. and Kuang, J. S. (2017). "Impact dynamics and energy dissipation capacity of fibre-reinforced self-compacting concrete plates." *Constr. Build. Mater.*, 138, 383–397. Doi:10.1016/j.conbuildmat.2017.02.011.
- Kumar, V., Iqbal, M. A. and Mittal, A. K. (2018a). "Experimental investigation of prestressed and reinforced concrete plates under falling weight impactor." *Thin-Walled Struct.*, 106–116. Doi:10.1016/j.tws.2017.06.028.
- Kumar, V., Iqbal, M. A. and Mittal, A. K. (2018b). "Study of induced prestress on deformation and energy absorption characteristics of concrete slabs under drop impact loading." *Constr. Build. Mater.*, 188, 656–675. Doi: 10.1016/j.conbuildmat.2018.08.113.
- Radnić, J., Matešan, D., Grgić, N. and Baloević, G. (2015). "Impact testing of RC slabs strengthened with CFRP strips." *Compos. Struct.*, 121, 90–103. Doi:10.1016/j.compstruct.2014.10.033.
- Saatci, S. and Vecchio, F.J. (2009). "Nonlinear finite element modeling of reinforced concrete structures under impact loads." *ACI Struct. J.*, 106, 717–725.
- Tachibana, S., Masuya, H. and Nakamura, S. (2010). "Performance based design of reinforced concrete beams under impact." *Nat. Hazards Earth Syst. Sci.*, 10, 1069–1078. Doi:10.5194/nhess-10-1069-2010.
- Zineddin, M. and Krauthammer, T. (2007). "Dynamic response and behavior of reinforced concrete slabs under impact loading." *Int. J. Impact Eng.*, 34, 1517–1534. Doi:10.1016/j.ijimpeng.2006.10.012.



## Effect of Chemical Admixtures on the Rheological Behaviour of Cementitious Paste

Aishwarya D Sabale,<sup>1</sup> Sunil D. Bauchkar,<sup>2</sup> Hemant S. Chore,<sup>3</sup> Nilesh S. Lende<sup>4</sup>

<sup>1</sup>#P. G. Student, <sup>2</sup>\* Research Scholar and <sup>4</sup>Assistant Professor

Department of Civil Engineering, Datta Meghe College of Engineering; Navi Mumbai-400708 (M.S.) India

Email: aishwarya.sabale@gmail.com; sunil\_bauchkar@rediffmail.com; lendenilesh09@gmail.com

<sup>3</sup> Associate Professor, Deptt. of Civil Engg., Dr. B. R. Ambedkar National Institute of Technology, Jalandhar-144011 (Punjab)

E-mail: chorehs@nitj.ac.in (Corresponding Author)

### ABSTRACT

This is an experimental investigation into the rheological behavior of high strength cement paste (HS-CP) which aims at quantifying the impact of  $\beta$ -Naphthalene Sulphonate (BNS) and Polycarboxylate Ether (PCE) based chemical admixtures in conjunction with a mineral admixture along with, the effect of three varying Water/Binder ratio ( $w/b$ ) (0.3, 0.4, and 0.5) on the rheological properties of High Strength Cement Paste (HS-CP). Rheological properties of HS-CP are measured using Brook-Field Rotational Viscometer DV II+ Pro for an elapsed period of 180 min and at uniform interval of 60 minutes, which detects the systematic changes in rheological properties due to changes in cementitious materials and  $w/b$  ratio successfully. The yield stress and viscosity of HS-CP measured using Brook-field Rotational Viscometer DV II+ Pro, follows the Bingham model. Fly Ash replacement of 25%, showed a higher rate of yield stress and plastic viscosity as compared to the control paste of 100% Ordinary Portland Cement (OPC). Between BNS and PCE, PCE enhances the rheological properties more than BNS. The yield stress and viscosity are found to increase due to decrease in the  $W/B$  ratio.

**KEYWORDS:**  $\beta$ -Naphthalene Sulphonate (BNS); Brook-Field RV DVII+ Pro viscometer; Fly Ash (FA); High Strength Cement Paste (HS-CP); Ordinary Portland Cement (OPC); Polycarboxylate Ether (PCE); Water/Binder ratio ( $w/b$ ).

### INTRODUCTION

Rheology is the study of the flow characteristics of a fluid and in this case, cement paste is the fluid under consideration, which is a Non-Newtonian fluid. Rheology is important because of the scope it offers for characterizing fresh cement paste, grout, mortar and concrete, and for understanding how they perform in practical applications. Rheology is dominated by the structure that exists in the cement paste which in turn affects mortar and concrete systems, as cement paste is the only binding matrix in these systems. The cement paste is that component of concrete which governs its workability, flowability and hardening. With the recent increase in the demand for more workable concrete to be used in different working as well as atmospheric conditions, the concrete quality has to be improved and thereby its flow characteristics have to be studied on a broader scale. The flow properties of the concrete are governed by its cement paste and therefore, it is necessary to study the flow properties of the cement paste. In the recent times, the concrete has gone beyond the typical four component mixture, and has evolved with the conjunction of different mineral and chemical admixtures.

The rheology can be defined in terms of two parameters viz., yield stress and viscosity. The viscosity of a fluid is a measure of its resistance to gradual deformation by shear stress or tensile stress. Viscosity is a property of the fluid which opposes the relative motion between the two surfaces of the fluid that are moving at different velocities. Yield stress represents the shear stress required to initiate flow for cement paste mixes. The cement paste mix should have both high flow ability and high bleeding resistance. Therefore, a high static yield stress is desirable because it improves the resistance to bleeding (Yahia and Khayat, 2001). Therefore, rheology-based studies are important to determine the functionality of the cement paste. The following investigation witnesses the approval of the Bingham model, which can be expressed mathematically as,

$$\tau = \tau_0 + \mu \cdot \dot{\gamma} \quad (\text{Eq. 1})$$

Where,  $\tau$  is the shear stress applied to the material,  $\dot{\gamma}$  is the shear rate (also called strain gradient),  $\tau_0$  is the yield stress and  $\mu$  is the plastic viscosity. While the adaptation of the Bingham model, there are two possibilities likely to occur: 1) the stress applied to paste increases slowly and the shear rate is recorded. When the stress is high enough, the paste will start flowing. The point at which the paste flows is the yield stress and the slope of the curve beyond yield stress is the viscosity; 2) fresh cement paste is sheared at high rate before the rheological test. Then the shear rate is decreased gradually and the stress is measured. These parameters are highly dependent on the  $w/b$  ratio and the dosage of the superplasticizer which is also a high range water reducer.

## REVIEW OF LITERATURE

In 1929, Professor Bingham founded the society of Rheology. Since then rheology has formally become an independent subdiscipline. There have been many research works involving the studies on the rheological behavior of cement paste discussed in a number of studies. But, the potential benefit of using various amounts of SCM in binary combinations with OPC on rheological and thixotropic properties of cement paste is not well documented. Thus, the effects of different blends of SCM, using different chemical admixtures along with varied  $w/b$  ratios on rheological properties as well as flow ability of cement pastes are studied. Wildemuth *et al.* (1984), studied, by both his model and experimental work, that the time-dependent behavior is governed by both thixotropy (combination of coagulation, dispersion and re-coagulation of the cement particles) and structural breakdown (breaking of chemically formed linkages between the particles).

Water to cement ratio actually reflects the volume fraction of dispersion phase in suspension dispersion system. At a higher  $w/b$  the distance between the cement grains and flocculated structures is larger. In the first minutes of cement-water contact, the crosslinking of cement grains and flocculating structures is not obvious. With the progressing cement hydration, more newly formed hydrates are produced to create new links among cement grains. Compared with lower  $w/b$ , more hydration products are required at higher  $w/b$ , in order to achieve a stronger inter-particle crosslinking. Hence, in the premise of constant cement type, the yield stress and plastic viscosity of fresh cement pastes as well as their growing rates are reduced at higher  $w/b$ .

Rheological behavior of cementitious materials highly depends upon availability of water in mix compositions. As water content effects proper flocculation and dispersion of powder material, it is most important aspect when analyze rheological properties. Tregger *et al.* (2015) studied effect of water content on cementitious paste compositions.

Malhotra and Mehta (1996) stated that using cementitious material it was possible to have a favorable influence on many properties of cement paste with presence of very fine particles or physio-chemical effects associated with pozzolanic and cementitious reaction which result in pore-size reduction and grain-size reduction phenomena. Effect of FA replacement for flowability analysis in cement paste were studied by Ferris *et al.* (2001). Kwan *et al.* (2013) reported that in cementitious pastes, replacement with class C fly ash decreases the values of the rheological parameter. Ahari (2015); investigated that class F fly ash has a spherical morphology and a smooth surface texture of grains, leading to a higher ball bearing effect to reduce inter-particle friction. Therefore, it reduces the plastic viscosity and enhances the workability.

Further, some of the researchers (Tattersall and Banfill 1983, Plank 2009) studied the effect of chemical admixtures on the rheology of self-compacting concrete. It was found that the super-plasticizers can significantly improve the workability of concrete, reduce the water demand and enhance the strength of cementitious construction materials. Due to dispersion effect, the fluidity of the paste is increased whereby yield stress and plastic viscosity is reduced. The chemical admixtures can alter the rheological properties of cementitious materials from three perspectives, in the opinion of Cyr *et al.* (2000): (a) changing the rheological models; (b) impacting the initial rheological properties and the development of rheological properties with the elapsed time; (c) affecting the thixotropy of paste. To improve on the workability of grouts without causing bleeding by adding extra water and affecting the strength, its common practice now to add superplasticizer. Their effects of on rheology of cement pastes have been documented by Park (2005). They have also proved, considering the shear thickening effect, that when compared with naphthalene-based superplasticizer, Polycarboxylate ether is said to be more effective. From the rheological point of view, it is absolutely necessary to choose the right type and concentration of Polycarboxylate ether (PCE)-based super plasticizer for the cement and concrete technology according to the application.

## OBJECTIVES OF THE STUDY

The objectives of the present investigation are as under:

- 1) To understand the effects on the rheology of cementitious paste, prepared using different chemical admixtures, viz., BNS and PCE and also to determine their optimum dosages for the cementitious compositions at the given *w/b* ratios.
- 2) To determine the effects of the SCM undertaken viz., the Fly Ash (FA) on the rheological properties of the cementitious paste, and its comparison with the control paste.
- 3) To understand the effects on the rheology of cementitious paste when mixed with different water binder ratios.

## RESEARCH METHODOLOGY

### Materials

#### A. Cement and Supplementary Cementitious Materials.

Cement used was Ordinary Portland Cement (OPC) (ASTM – Type-I) conforming to IS 12269 (OPC53). Physical and chemical properties are indicated in Table 1 and 2. The supplementary cementitious material (SCM) viz., fly ash (FA) meeting the requirement of IS 3812-1981 ASTM C618 (Class F) is used. The physical and chemical compositions of the SCM used in the present study are also shown in Table 1 and 2.

**Table 1. Physical Properties of the materials used in the study**

Properties of binders	OPC	FA
Density (g/cm <sup>3</sup> )	3.15	2.25
Specific Surface (m <sup>2</sup> /kg)	328	386

**Table 2: Chemical composition (wt. %) of cement and SCM**

Materials	SiO <sub>2</sub>	Al <sub>2</sub> O <sub>3</sub>	Fe <sub>2</sub> O <sub>3</sub>	CaO	MgO	SO <sub>3</sub>	Na <sub>2</sub> O
Cement	21.4	4.3	2.4	64.4	2.1	2.3	0.6
FA	68.1	25.8	6.9	8.7	1.39	0.26	0.18

#### B. Superplasticizers

Master Polyheed 8632, an economical admixture based on modified polycarboxylate ether, especially designed to allow considerable reduction of mixing water while maintaining control on extend of set retardation, was used in this study. The physical properties of Master Polyheed 8632 were evaluated using state of art instrumentation available at research and development center of BASF India Ltd. The properties of the PCE are given in the Table 3. Master Rheobuild 1125, the BNS based admixture, composed of synthetic polymers, specially designed to allow considerable reduction of mixing water while maintaining control on extend of set retardation, was used in this study. The physical properties of Master Rheobuild 1125 were evaluated using state of art instrumentation available at research and development center of BASF India Ltd. The properties of BNS are given in the Table 3.

**Table 3: Properties of Superplasticizer**

Type of Super-plasticizer	PCE	BNS
Aspect	Light Brown Liquid	Dark Brown Free Flowing Liquid
Relative density	1.08 ± 0.01 at 25°C	1.24 ± 0.02 at 25°C
pH	≥6	≥6
Chloride ion content	<0.2%	<0.2%

## Methodology

In the present work, two different high strength cement paste combinations were designed using OPC and FA with the use of superplasticizers, at different  $w/b$  ratios of 0.3, 0.4 and 0.5, keeping the volume of the cement paste constant. All the measurements were taken at temperature varying between 25° to 30°C. The additional details on the mix proportions are provided in Table 4.

**Table 4: Mix proportions in weight percentage for laboratory trials.**

Compositions			OPC (%)	FA (%)
$w/b$ 0.3	$w/b$ 0.4	$w/b$ 0.5		
A1	B1	C1	100	-
A2	B2	C2	75	25

The experimental test results are obtained in two different experiments viz., the slump cone test and the rheology test.

### A. Flow Cone Test

The flow cone is a simple device used for measuring viscosity from flow spread. The flow cone is 50 mm in height with inner and outer diameter is 25 and 30mm respectively as shown in Fig. 1. Total of 1500 gm cement paste was mixed in Hobart mixer for 3minutes. Then, the cement paste was poured in the cup and lifted. The flow is made to spread for 30 sec and measured. The optimum dosage was taken at a point where cement paste started bleeding, and if not bleeding, it was measured at the point where the flow stops. The mini slump cone, also known as Wacker cup, follows the guideline of ASTM C150. The flow is expected to be around  $130 \pm 5$  mm, to avoid bleeding. The flow is measured with a Digimatic Vernier Caliper, see Fig. 2.



**Fig 1. Flow Cone**

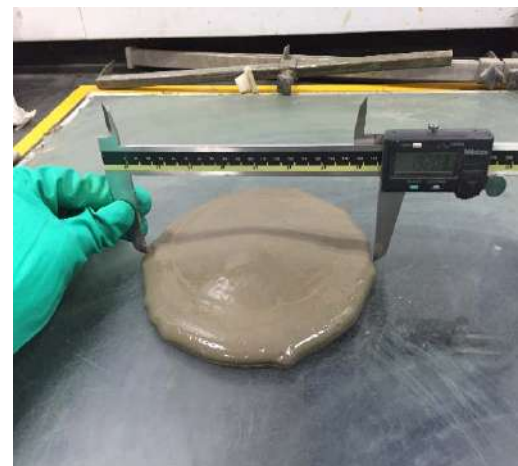


**Fig 2. Measurement of flow with the Digimatic Vernier Caliper**

### B. Rheological Tests

In the rheological study of the cementitious paste, the yield stress and the plastic viscosity are the two rheological parameters. Hence, the rheological properties of cement paste are investigated using Brook-Field RV DV II+ Pro viscometer with disc spindle attachment, where the readings are obtained in Centipoise (cP) which are converted into yield stress and viscosity. The test was performed according to the guidelines given in ASTM C1749-12. The Brook-

Field Rotational Viscometer was used to determine the yield stress and plastic viscosity as defined by the Bingham Model. 5 rotational speeds (100, 50, 20, 10 and 5) were selected from among the speeds mentioned in the Brookfield DV II + Pro Manual, which are also used in the regular lab practices, each step lasting for 2minutes. The rheology test has been carried out in four cycles, each consisting of the mixing of the cement paste, flow measurement and testing at the Brookfield Viscometer. After the initial cycle, the test is repeated at an interval of 60minutes up to 180minutes. The test results were obtained for spindle No. 0.3 and 04, but at many of the positions spindle No. 03 could not give the readings. This might have happened due to the capacity of the spindle being less for that particular cement composition. Also, not all the rpms give readings up to the final test cycle. Hence, to compare the rheology of the different compositions, the readings of the spindle No. 04 taken at 5 rpm are considered for the results, Fig. 3.



Fig 3. Brookfield Viscometer DV II+ Pro

## RESULTS AND DISCUSSION

The results of this investigation are divided into three parameters according to the aforementioned objectives of the study, viz., optimization of PCE and BNS for the two compositions, effects of the SCM on the rheology of the cement paste and their comparison with the controlled sample, i.e., the 100% OPC and effect of the varying  $w/b$  ratio on the rheology of the cement paste.

### A. Optimization of PCE and BNS

The admixture dosages and flows are obtained for the control paste i.e., 100% OPC and OPC75% + FA25% and compared, Table 5 and 6.

Table 5. Admixture dosage and flow measures for PCE

Composition	% Admixture Dosage	Initial flow (mm)
A1	0.3	128
A2	0.35	131
B1	0.16	130
B2	0.2	130
C1	0.07	135
C2	0.12	130

Table 6. Admixture dosage and flow measures for BNS

Composition	% Admixture Dosage	Initial flow (mm)
A1	1.3	132
A2	1.55	128
B1	0.83	130
B2	0.95	130
C1	0.27	130
C2	0.37	125

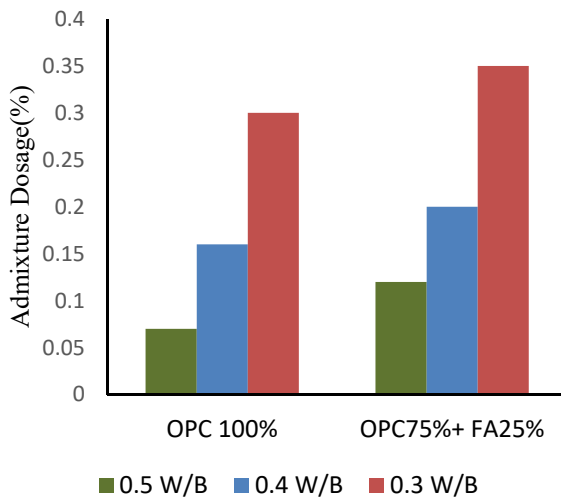


Fig 3: Optimized Admixture dosage in % when PCE is used

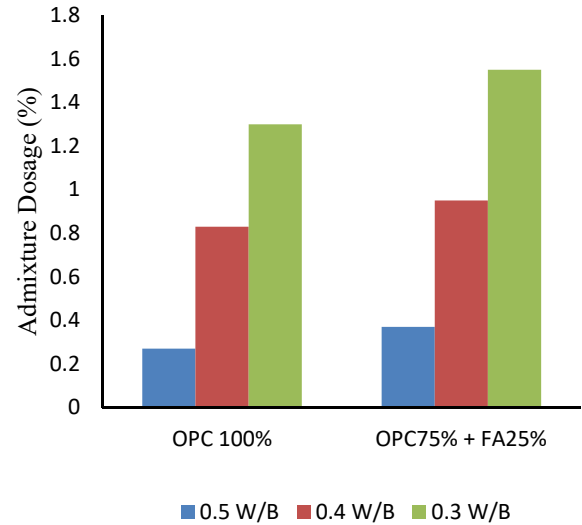


Fig 4: Optimized Admixture dosage in % when BNS is used

Fig. 3 and Table 5 give the variation of PCE admixture dosages and Fig. 4 and Table 6 give the variation of BNS admixture dosages at similar initial flow, for the various cement compositions and  $w/b$  ratio. It is estimated that the increasing variation in the usage of admixture follows an inverse profile with the decrease in the  $w/b$  ratio. The 0.5  $w/b$  ratio requires the lowest amount of admixture and the 0.3  $w/b$  ratio requires the highest amount.

The average flow for the cement paste was estimated to be kept around 130 mm to avoid bleeding of the cement paste. The flow spread variation is not uniform for both the admixtures. The flow obtained almost meets the estimated requirements and here it is also observed that both the admixtures manage to maintain the flow irrespective of the variation in the  $w/b$  ratios. At higher  $w/c$  ratio 0.5 the fluidity is naturally maintained by its higher water content but at lower  $w/c$  ratio 0.3, the flow is managed by the admixtures. Therefore, the admixture dosages for both BNS and PCE are observed to be optimum for the compositions.

The comparison of the amount of dosages for both the admixtures revealed that the dosage for BNS is higher than that for PCE. The BNS is found to be sensitive and required to be used in higher amounts to maintain the stipulated flow, whereas the PCE is used only in minor amounts to maintain the similar flow. The admixture BNS is a plasticizer whereas the admixture PCE is a superplasticizer, which is a chemical admixture used where well-dispersed particle suspension is required. They are used as dispersants to avoid particle segregation and to improve the flow characteristics of suspensions. The admixture PCE is referred to as comb-type plasticizer due to its molecular structure.

When added to the cement paste, the superplasticizer improved the fluidity of the paste. In addition, it maintained the fluidity of the paste much longer than observed with the BNS, and without excessive retardation. Their addition to the paste reduces the water-cement ratio and does not affect the workability of the mixture. This is corroborated by several researchers (Kreppelt *et al.* 2002; Golaszewki *et al.* 2003; Plank *et al.* 2007; Kong *et al.* 2009; Petit *et al.* 2010) in the past or recent past. The BNS is found to be sensitive and requires higher amounts of dosages to give a workable paste. This could be due to the different consumption properties of the cementitious materials, addition time, chemical composition, early hydrates fineness and pH. Similar conclusion was also reported by Marius (2016).

## B. Rheological Parameters

Figure 5-8 indicates the variation of the yield stress and the viscosity for the compositions undertaken in the present investigation. The yield stress and viscosity of the control paste are compared with the other compositions to determine the effect on the rheological properties.

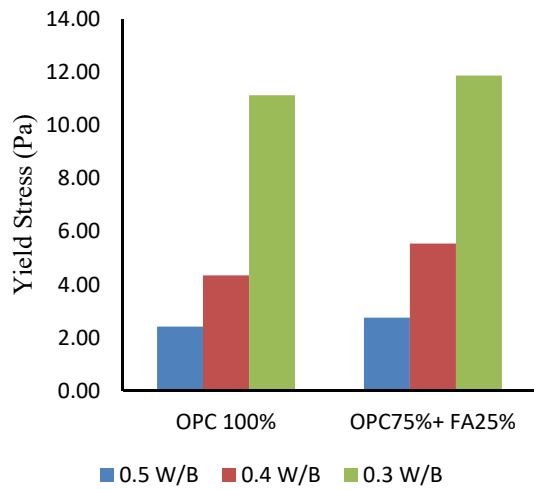


Fig 5. Yield stress variation due to varying w/b ratio using PCE

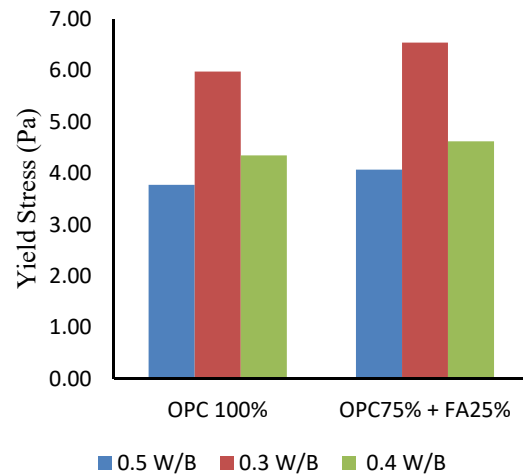


Fig 6. Yield stress variation due to varying w/b ratio using BNS

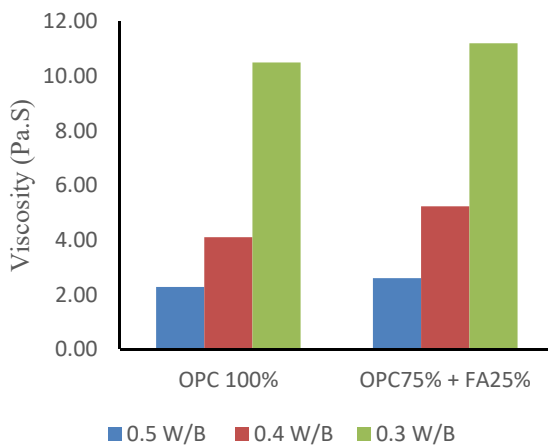


Fig 7. Viscosity variation due to varying w/b ratio using PCE

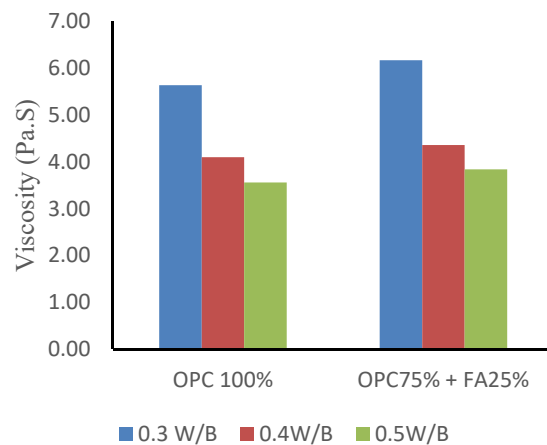


Fig 8. Viscosity variation due to varying w/b ratio using BNS

The measurements of the yield stress and that of viscosity were taken at intervals of 60 minutes after the initial readings on the preparation of the cement paste up to completion of 180 minutes. The basic observation which can be made here is that the yield stress and viscosity increases linearly with time; and hence, the linear relation fits to the Bingham model. Also, it is observed that there is an inverse relation of the w/b ratio with the yield stress and viscosity. At higher water content the values for yield stress and viscosity are minimum whereas for lower water content, the yield stress and viscosity values are maximum.

The replacement of cement by FA slows down the rate of hydration and extends the dormant period. This is likely due to lower surface area of FA, in addition to its spherical shape which reduces frictional forces among angular particles due to a ‘‘ball bearing’’ effect. It is also well known that the spherical particle shape of fly ash particles helps reducing the water demand to obtain a similar fluidity to that of mixture made without any fly ash. The other studies suggested that among all 3D shapes, spheres give the minimum surface area for a given volume resulting in lower water retention and subsequently lower water demand for a particular workability due to a higher particle packing density (Sakai *et al.* 1997 and Yijin *et al.* 2004). The particle size and shape are the key factors for controlling the rheological properties FA based cementitious pastes.

## SUMMARY AND CONCLUSIONS

Based on the experimental investigation of cement paste rheology which comprised of the various  $w/b$  ratios in conjunction with FA as SCM replacement; and the PCE and BNS based chemical admixtures, the results are concluded below:

- PCE and BNS admixture dosages found to be increased due to decrease in  $w/b$  ratio, means admixtures dosages are inversely proportional to  $w/b$  ratio.
- Yield stress and viscosity increases with decrease in  $w/b$  ratio of cement paste
- Addition of SCM like FA, substantially improves the rheology and the flow properties of the cementitious paste.
- $w/b$  ratio 0.5 does not even require the addition of admixture, unless it is the need of the job to get the desired flow and strength for the concrete.
- Rise in water content definitely helps in improving spread flow irrespective of dosage of SCM added in paste system where as detrimental effect is observed as test time elapsed for same.
- The amount of the PCE dosage is less than 1% for all the compositions, which implies that PCE can be an economical admixture than BNS and it is quite a concentrated mixture which gives higher rheology and flow properties.
- The Brook-Field rotational viscometer DV II +Pro employed in the present study found to detect systematic changes in workability, cementitious materials, successfully.

## ACKNOWLEDGEMENTS

The support extended by the management of BASF India Ltd. in carrying out the experimentation at their Research and Development Center at Turbhe, New Mumbai is gratefully acknowledged.

## REFERENCES

- ASTM D 2196 (1986), “Test Methods for Rheological Properties on Non-Newtonian Materials by Rotational (Brookfield) Viscometer”
- ASTM C618-08a (2008), “Standard Specification for Coal Fly Ash and Raw or Calcined Natural Pozzolan for Use in Concrete”, IN INTERNATIONAL, A. (Ed.) West Conshohocken.
- ASTM C 1749 (2012), “Standard guide for measurement of rheological properties of hydraulic cementitious paste using rotational viscometer”.
- Ahari, R. S., Erdem, T. K., and K. Ramyar, (2015), “Effect of various Supplementary Cementitious materials on the rheological properties of self- consolidating Concrete”, *Construction and Building Materials*, (8) pp 43-50.
- Bauchkar S.D and Chore H.S (2014), “Rheological properties of self-consolidating concrete with various mineral admixtures”, *Structural Engineering and Mechanics: An International Journal*, 51 (1), 1-13.
- Brookfield DV II + Pro Viscometer Manual No. M03-165-F0612.
- Cyr, M., C. Legrand, and M. Mouret, (2000), “Study of the shear thickening effect of superplasticizers on the rheological behavior of cement pastes containing or not mineral additives”, *Cem Concr Res* 30(9) pp 1477-1483.
- Ferraris, C.F.; Obla, K.H.; Hill, R., (2001), “The influence of mineral admixtures on the rheology of cement paste and concrete”., *Cem. Concr. Res.*, 31, pp 245–255.
- G. H. Tattersall, P. F. G. Banfill, (1983), “The rheology of fresh concrete”, *Pitman Advanced Publishing Program*, London, pp 118-133.
- Golaszewki J, Szwabowski J, (2003), “Influence of superplasticizer on rheological behavior of fresh cement mortars”, *Cem Concr Res.* 34(2) pp 235-248.
- J. Plank, B. Sachsenhauser, (2009), “Experimental determination of the effective anionic charge density of polycarboxylate superplasticizers in cement pore solution”; *Cement and Concrete Research*, 37(5) pp 767-775.
- Kong XM, Hu B, Hou SS, Liu BY, Hao XY, (2009), “Synthesis and application properties study of polycarboxylate-type superplasticizer”, *J Tsinghua Univ Sci Technol.* (38) pp 195-203.
- Kreppelt F, Weibel M, Zampini D, Romer M, (2002), “Influence of solution chemistry on the hydration of polished clinker surfaces—a study of different types of polycarboxylic acid-based admixtures”, *Cem Concr Res.* 39(1) pp 6-13.
- Kwon, S.H.; Park, C.K.; Jeong, J.H.; Jo, S.D.; Lee, S.H., (2013), “Prediction of Concrete Pumping: Part I—Development of New Tribometer for Analysis of Lubricating Layer”, *ACI Mater. J.* 93(2) pp 111-120.

- Marius E.A, (2016), “Adsorptions Isotherms for Lignosulphonates in Cement with Fly Ash and Blast Furnace Slag”, Norwegian University, Norway, (49) pp 401-424.
- Park, C., M. Noh, and T. Park, (2005), “Rheological properties of cementitious materials containing mineral admixtures”, *Cem. Concr. Res.*, (35) pp 842-849.
- Petit JY, Wirquin E, Khayat KH, (2010), “Effect of temperature on the rheology of flowable mortars”, *Cem Concr Compos.* (35) pp 256-266.
- Plank J, Hirsch C, (2007), “Impact of zeta potential of early cement hydration phases on superplasticizer adsorption”. *Cem Concr Res.* 21(5) pp 431-437.
- Sakai, E., Hoshimo, S., Ohba, Y. and Daimon, M. (1997), “The fluidity of cement paste with various types of inorganic powders”, In: Proceedings of the 10<sup>th</sup> international congress on the chemistry of cement, Sweden, Amarkai AB, Sweden.
- Tregger, N.A.; Pakula, M.E.; Shah, S.P, (2010), “Influence of clays on the rheology of cement pastes”. *Cem. Concr. Res.*, 40, pp 384–391
- V. M. Malhotra, Povinder K. Mehta, (1996), “Pozzolanic and Cementitious materials”, *Advances in Concrete Technology*, (26) pp 283-294.
- Wildemuth, C.R.; Williams, M.C., (1984), “Viscosity of suspensions modelled with a shear-dependent maximum packing fraction”, *Rheol. Acta.*, (41) pp 557-566.
- Yahia, A. and Khayat, K.H. (2001), “Analytical models for estimating yield stress of high-performance pseudoplastic grout”, *Cement Concrete Res.*, 31(5), pp 731-738.
- Yijin, L., Shigiong, Z. and Yingli, G. (2004), “The effect of fly ash on the fluidity of cement paste, mortar and concrete”, In: Proceedings of the international workshop on sustainable development and concrete technology, Beijing;, pp. 339-45.



## Response of Thin Reinforced Concrete Slab under Elevated Temperature against Large Mass Impactor

K. Senthil<sup>1</sup>, A. Thakur<sup>2</sup> and A. P. Singh<sup>3</sup>

<sup>1</sup>\* Assistant Professor, Department of Civil Engineering, Dr. BR Ambedkar NIT Jalandhar, Punjab 144011;

E-mail: urssenthil85@yahoo.co.in; kasilingams@nitj.ac.in, Phone: +91-9458948743 (Corresponding Author)

<sup>2</sup> Research Scholar, Department of Civil Engineering, Dr. BR Ambedkar NIT Jalandhar, Punjab 144011;

<sup>3</sup> Professor, Department of Civil Engineering, Dr. BR Ambedkar NIT Jalandhar, Punjab 144011;

### ABSTRACT

The response of reinforced concrete slab against large mass impact is being attention for the industry as well as commercial applications for a long time. It was observed that many industrial problems require the vulnerability assessment since large mass of hard objects traveling with low velocities on relatively thin concrete slabs. Therefore, this manuscript focuses on the penetration and perforation of thin concrete plates impacted normally by cylindrical impactor with flat nose. The numerical investigations have been carried out on thin reinforced concrete plates using ABAQUS/Explicit finite element program. The thickness of reinforced concrete plate was varied as 20 and 40 mm and the mass of impactor was 4 and 32 kg and impacted by 8.14 m/s velocity. The reinforcement of 6 mm diameter of single layer placed 90 mm spacing at both the directions. The span of the target is 400 mm and their boundaries were clamped tightly. The inelastic behavior of concrete and steel reinforcement bar has been incorporated through Johnson–Holmquist damage (JH2) model and Johnson-cook (JC) models available in ABAQUS, respectively were considered in the present study. The temperatures of target was varied as 293, 500, 900 and 1300 K. The results were predicted and discussed in terms of reaction force, residual velocity and damage intensity on target. The study thus presents a detailed numerical investigations of the material behavior under large masses and leads to some important conclusions pertaining to the mechanics during the interaction of penetrator and target.

**KEYWORDS:** Thin reinforced concrete slab, Deformation and Damages, Impactor mass, Elevated temperature.

### INTRODUCTION

Thin reinforced concrete slabs are being currently used widely in the field of civil engineering such as covering material for industrial flooring, rehabilitation of surfaces of bridge decks, temporary structures etc. The response of such plates against drop impact is being attention for the industry as well as commercial applications for a long time. A considerable amount of studies has been conducted to understand the penetration behaviour of steel plates against low-velocity projectiles impact () however few studies have been focused on the local behaviour of thin plates against large masses passing at low velocity. **Clifton and Knab (1983)** examined the relationship between the compressive strength and the impact resistance of concrete, and it was found that the impact resistance increased with the compressive strength. **Hanchak et al. 1992** observed that compressive strength of concrete is not directly associated with the impact resistance of concrete slab. **Dancygier and Yankelevsky (1996)** found that a reduced brittleness when steel fibers were added into high strength concrete mixes. **Borvik et al. (2002)** concluded that the ballistic limit velocity increases to a maximum of 20% if the compressive strength of the concrete increases. **Tai (2009)** found that addition of steel fibers increases the split tensile strength, flexural strength and reduces brittleness of concrete. It was concluded that addition of 2% and 5% by volume of steel fibers resulting split tensile strengths of 21.9 and 31.6 MPa respectively, and almost equal to the compressive strength of normal concrete, improves the impact resistance significantly. **Li et al. (2016)** found that ultra-high performance concrete displays an improved resistance compared to conventional concrete. **Othman and Marzouk (2016)** concluded that the distribution of the steel reinforcement majorly affects the crack pattern and deformation mode. **Rajput and Iqbal (2017)** was found that the reinforcement minimizes the scabbing and spalling of concrete. Explicitly, experimental investigations are important, however there is always an important need for the implementation of numerical solutions. Few numerical models have been implemented on the impact behavior of reinforced concrete structures (**Ranjan et al (2014), Guo et al. (2017), Oucif and Mauludin (2018), Senthil et al. (2018)**).

Based on the detailed literature survey, it is observed that the response of the thin reinforced concrete against large masses

has been rarely studied. Response of the concrete slab under elevated temperatures also rarely been studied heretofore. Therefore, present manuscript focuses on the impact resistance of thin reinforced concrete targets of 20 and 40 mm against 4 and 32 kg mass cylindrical flat nose impactor speed of 8.14 ms<sup>-1</sup> (assumes drop height of 3.15 m) through numerical simulation using ABAQUS/CAE finite element program. The inelastic behavior of concrete and steel reinforcement bar has been incorporated through JH2 and JC models available in ABAQUS, respectively were used in the present study. The temperatures of target was varied as 293, 500, 900 and 1300 K. The results were predicted and discussed in terms of reaction force, residual velocity and damage intensity on target.

## CONSTITUTIVE MODELLING

The behaviour of steel reinforcement and concrete was predicted using the already defined models in ABAQUS finite element program. For reinforcing steel, damage behaviour has been predicted using J-C model (Johnson-cook model). The parameters for J-C model was used for this study were taken from the literature, see **Iqbal et al 2015**. Inelastic non-linear mechanical behaviour of concrete was defined in the model using JH-2 ceramic model, it provides a general capability for simulating the behaviour of concrete and other quasi-brittle materials such as strain rate effects, dependence on pressure-strength (**Holmquist et al, 1993**). According to JH-2 model, with increase in plastic deformation, the damage variable also increases. Strength is based on the von Mises yield stress given by  $\sigma^* = \sigma_i^* - D(\sigma_i^* - \sigma_f^*)$  where  $\sigma_i^*$ ,  $\sigma_f^*$  are the normalized intact equivalent stress and normalized fractured equivalent stress respectively. D is the damage variables whose value lies in between 0 (undamaged) & 1 (total damage). The material parameters for JH-2 model is shown in **Table 1**, which are proposed by **Holmquist et al, 1993**. The pressure Volume relationship for brittle materials is given by  $K_1\mu + K_2\mu^2 + K_3\mu^3$  if  $\mu \geq 0$  (Compression) and  $K_1\mu$  if  $\mu < 0$  (tension).  $K_1, K_2, K_3$  are the material Parameters and  $\mu$  deals with the density of the material.

**Table 1** Material parameters of the concrete material, **Holmquist et al, 1993**.

$\rho$ (kg/m <sup>3</sup> )	$G$ (GPa)	$A$	$n$	$B$	$m$	$C$
2440	14.86	0.79	0	1.6	0.61	0.007
$\epsilon_0$	$T$ (GPa)	$S_{max}$	$S_{fmax}$	$HEL$ (MPa)	$P_{HEL}$ (MPa)	$\beta$
1.0	0.00354	7	0	80	48	1
$D_1$	$D_2$	$\epsilon_{fmin}^{-pl}$	$\epsilon_{fmax}^{-pl}$	$K_1$ (GPa)	$K_2$ (GPa)	$K_3$ (GPa)
0.04	1	0.01	1.0	85	-171	208

## NUMERICAL MODELLING

The numerical investigation was carried out to determine the behaviour of concrete plate subjected to the normal impact of low-velocity projectile (Impactor) using ABAQUS/CAE. Two targets of varying thickness were modelled i.e. 40 and 20 mm Concrete plate with reinforcement of 6 mm diameter. The behaviour of mild steel reinforcement was simulated using the Johnson-Cook Model whereas, the non-linear behaviour of concrete was modelled using Johnson-Holmquist (JH-2) model readily available in finite element code, **ABAQUS/CAE**. Projectiles(impactors) were impacted on 40 and 20 mm thick target plates of 400 mm diameter including cover concrete at bottom as well as peripheral of target. Impactors were modelled as a three dimensional analytical rigid shell element whereas the concrete plate was modelled as three dimensional deformable body and reinforcements as three dimensional beam element (B31). Both ways reinforcements (longitudinal and transverse) were placed at a distance of 90 mm c/c with a clear cover of 10 mm such that it forms a grid see **Fig 1(a)**. The type of constraints used for bonding between steel and concrete is “Embedded region” readily available in ABAQUS. The reinforcement was considered as an embedded region while concrete was considered to be host region. The mass of impactor was considered 4 kg and 32 kg. The velocity of the impactor(s) was considered to be 8.13 ms<sup>-1</sup> (considering a drop height of 3.36 m with gravitational force). The position of the reinforcement and layout was shown in **Fig. 1(b)**. The diameter of impactors (d) was 12 mm, see **Fig. 2(a)** and the finite element model of impactor is shown in **Fig. 2(b)**. Surface-to-surface (explicit) interaction was used and kinematic contact algorithm was employed for making contact between impactor, concrete target & reinforcement. The coefficient of friction between these bodies is assumed to be zero due to the low velocity of impactor. In all the simulations, the projectile was considered as master surface and target and reinforcement as node-based slave surface. To maintain the fixity at the perimeter of the circular plate “ENCASTRE” option was used, see **Fig 2(c)**. The meshing of the target plate was considered as eight noded linear hexahedron element (C3D8R) of 10 mm at the centre of the plate (primary area). Tertiary

area was meshed with the same type of elements (C3D8R) however the size of element was varied from 10 mm to 15 mm. A six noded tetrahedral element (C3D4) was introduced between primary and secondary area for generating compatibility and reducing the computational time. The hourglass control was kept as enhanced for all the elements and the velocity was incorporated using load module available in ABAQUS.

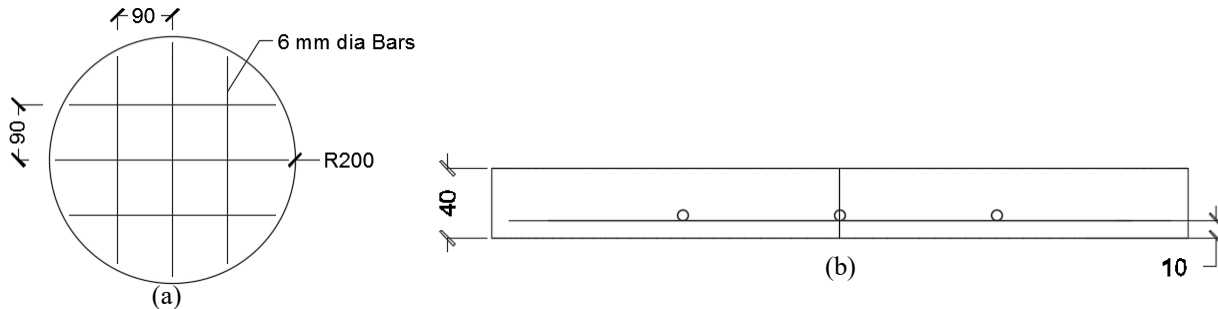


Fig 1. Typical (a) schematic of concrete plate with reinforcement grid and (b) position of reinforcement bar (in mm)

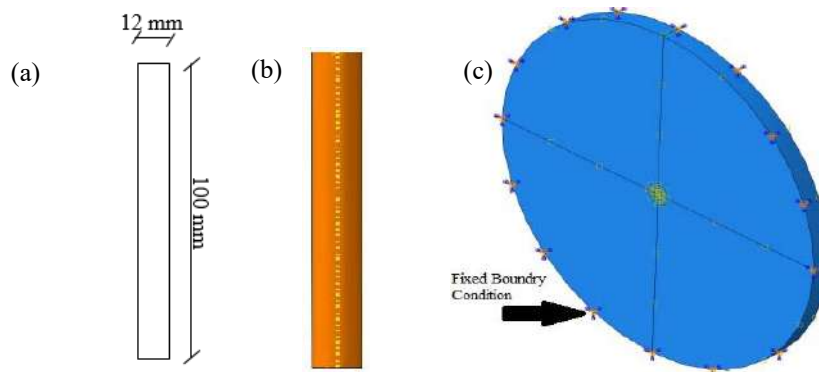


Fig 2. Typical (a) schematic and (b) finite element model of projectile and (c) 20mm thick target with fixed boundary conditions.

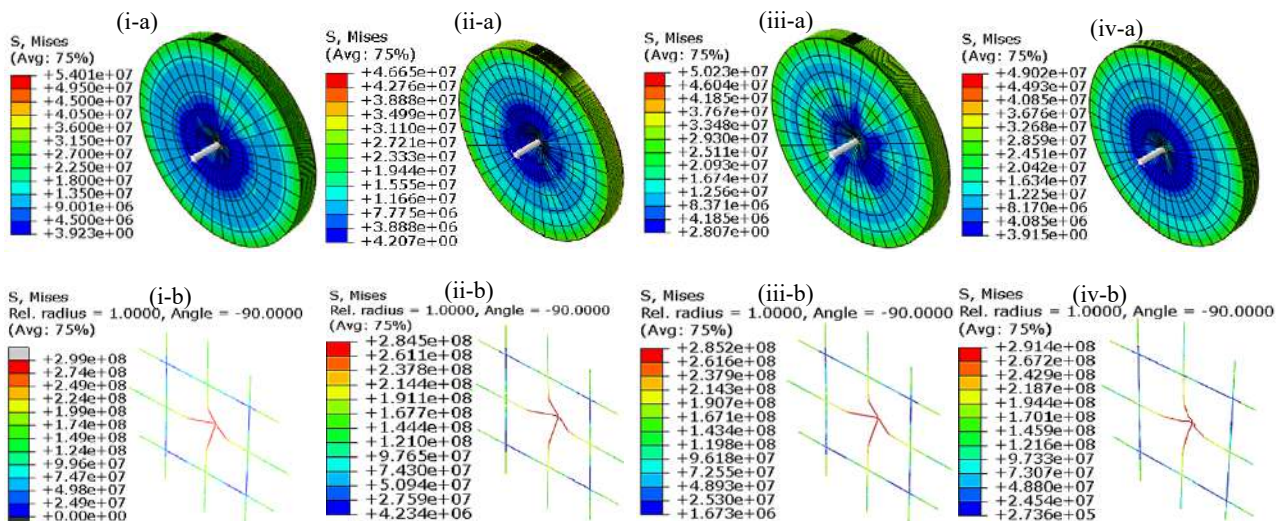


Fig. 3 Von-Mises stresses (MPa) on (a) concrete of 40 mm thickness and (b) steel reinforcement bar at (i) 5 (ii) 10 (iii) 15 and (iv) 20 mm mesh sizes against 32 kg mass

The simulations were carried out on circular thin slab against large mass falling impact loading under elevated temperature. The JH2 model has been employed for predicting the material behavior of the concrete, whereas the Johnson-Cook model was also employed for predicting the behavior of steel reinforcement bar. The simulated results thus obtained have been compared with the conventional method. A detailed mesh convergence has been carried out to study the influence of mesh size in the impact region of target. The size of element was varied as  $0.005 \times 0.005 \times 0.005$  m,  $0.01 \times 0.01 \times 0.01$  m,  $0.015 \times 0.015 \times 0.015$  m and  $0.020 \times 0.020 \times 0.020$  m. Deformed profile (Mises stresses in concrete and steel bar) for the 40 mm thick target against 32 kg mass at 293 K temperature having varying mesh size is shown in **Fig. 3 (a)-(b)**.

The von-Mises stresses in concrete for 5, 10, 15 and 20-mm mesh size was 54, 46.65, 50.23 and 49.02 MPa for chosen case is shown in **Fig. 3(a)**. As 5 mm mesh is closely predicting the behaviour of concrete in terms of stresses, i.e. 54 MPa conventional grade of concrete, hence 5mm mesh was adopted to carry out further simulations. In case of Mises stresses in reinforcement with mesh sizes of 5, 10, 15 and 20 mm was 300, 284.8, 285, and 291 MPa, see **Fig. 3(b)**. The stresses in the reinforcement were found to be almost equal to the yield stress of the steel i.e. 300 MPa and it seems insensitive to the mesh size. Therefore, 5 mm mesh size was considered and used further for conducting simulations and predicted the response of target under elevated temperatures.

### RESULT AND DISCUSSIONS

The simulations were carried out on 20 and 40 mm thick thin slab against large mass falling impact loading under elevated temperature. The JH2 model has been employed for predicting the material behavior of the concrete, whereas the Johnson-Cook model has been used for predicting the material behavior of steel reinforcement. The simulations were carried out to understand the influence of varying mass of impactor and varying temperature. The striking velocity of impactors is chosen as 8.14 m/s and the impact response studied against this velocity. Also, the response of target at elevated temperature has been studied and the temperature was varied from ambient temperature and 500, 900 and 1300 K. The response of structural elements were observed in terms of stresses, damages and reaction forces, therein was presented and discussed in this section.

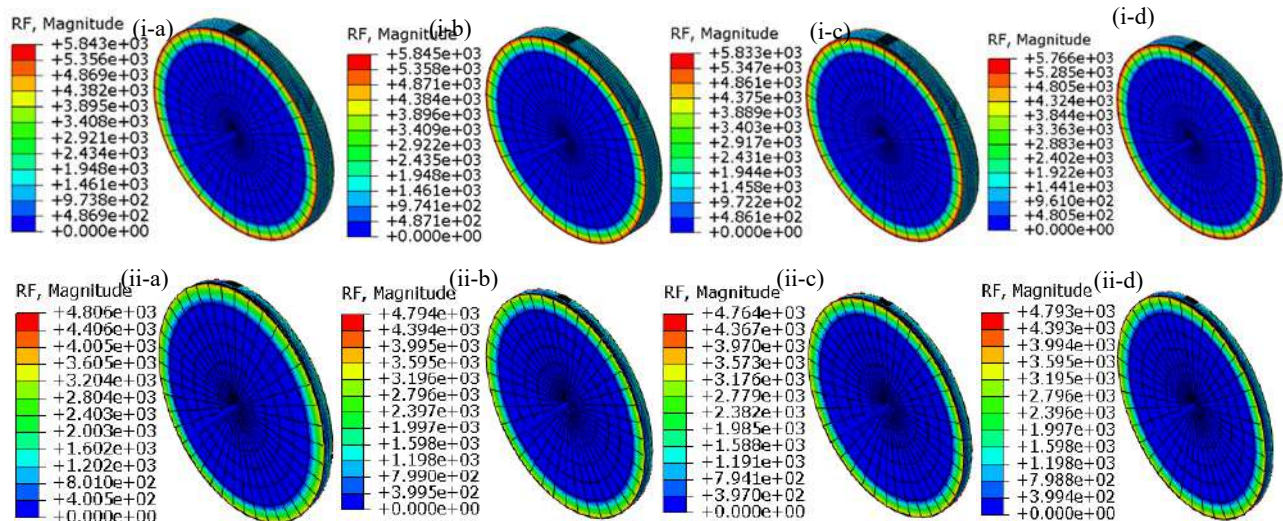


**Fig 4. Forces offered by (i) 40 and (ii) 20 mm thick targets against 4 kg mass impactor at a) 293 b) 500 c) 900 d) 1300 K temperature**

The impact resistance of 20mm and 40 mm thick reinforced concrete targets have been studied through cylindrical flat nose object having masses of 4 and 32 kilograms by finite element simulations and the predicted reaction forces were shown in **Figs. 4 and 5**. The reaction forces offered by the target at ambient as well as elevated temperature against 4 kg mass was found to be insignificant, see **Fig. 4**. However, the resistance offered by 20 and 40 mm thickness of target was found to be 48 and 58 kN respectively. The reaction forces in case of 40 mm thick target against 32 kg mass was found to be insignificant, i.e. 58.43, 58.45, 58.33, 57.66 kN at 293, 500, 900, 1300 K temperature respectively, see **Fig 5 (i)**.

The force offered by the 20 mm thickness target against 32 kg impactor at ambient temperature is 74.4 kN whereas for 500, 900, 1300 K was found to be 69, 62.9, 56.7 kN respectively, see **Fig. 5(ii)**. For both the thickness the reaction force offered by the targets are inversely proportional to the temperature i.e. with an increase in temperature, impact strength decreases. It was observed that the resistance of 40 mm thick target was found to increase by 23% as compared to 20 mm thick target.

The response of thin reinforced concrete slabs against large masses of impactor and their residual velocities at 1.5, 3, 6 and 9 milli second were shown **Figs. 6 and 7**. It was observed that 32 kg mass impactor perforates both the target under ambient as well as elevated temperatures. The numerically predicted lowest residual velocities of impactor were shown in **Table 2**. At elevated temperature, concrete loses its compressive strength hence the ability of concrete to resist the loads decreases significantly. However, at ambient temperature, the resistance of target was found to be significant and the residual velocity of impactor against 40 and 20 mm thick target varies between 3.34 – 4.63 ms<sup>-1</sup> and 2.88 - 6.59 ms<sup>-1</sup> respectively, see **Table 2**. It was observed that 4 kg mass penetrator was not perforated the given target and the penetrator was found struck and bouncing back after striking the concrete slab. The maximum residual velocity was noticed during the penetration and perforation of 20mm thick target at 1300 K temperature, 6.59 m/s. In case of 20 mm thick target, the residual velocity on target under ambient temperature was found to be reduced by 56% as compared to the target at 1300 K. However, the velocity drop on 40 mm thick target under ambient temperature was found to be reduced by 27% as compared to the target at 1300 K. It is concluded that the impact resistance of target under elevated temperature was found to be reduced to 50% if the target thickness increased from 20 to 40 mm. Also, it is noticed that the increase of target thickness from 20 to 40 mm at ambient temperature, the resistance of target increased by 16%.

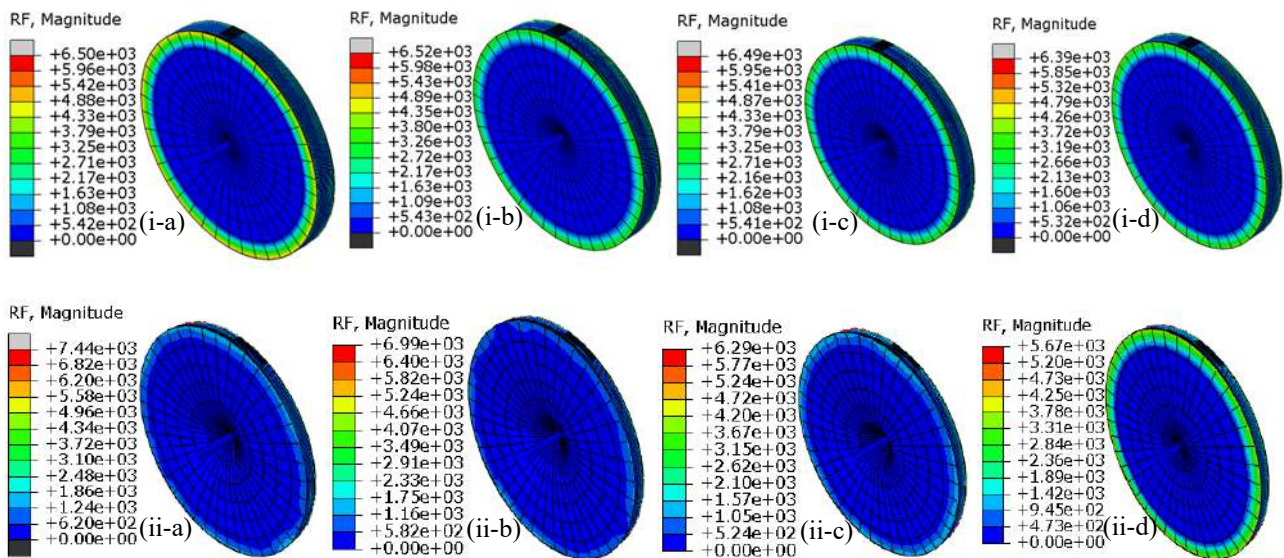


**Fig 5. Forces offered by (i) 40 and (ii) 20 mm thick targets against 32 kg mass impactor at a) 293 b) 500 c) 900 d) 1300 K temperature**

The response of thin slabs against large masses was studied in terms of damage intensity and the typical damage pattern of target (500 K temperature) was shown in **Figs. 8 and 9**. As discussed earlier, the damage was insignificant in case of 4 kg impactor hitting on both the target hence global deformation caused by 32 kg impactor at 500 K temperature were discussed in this section. During perforation, damage contours were plotted at varying time step, i.e. 1, 2.5, 5.2 and 9 milli second. It was observed that significant local damage and crater when the penetrator until touches the reinforcement, see **Fig 8(a)-(c)**, however, the damage start spreading to larger area i.e. global damage when the impactor penetrators further, see **Fig. 8(d)**. Also it was observed that the clear plug and scabbing on the rear side of the target and the reinforcement helps in distributing the stresses to larger portion of the target., see **Fig. 8(d)**. The same phenomenon was noticed in case of 40 mm thick target, see **Fig. 9**. It is concluded that the reinforcement bars helps in distributing the stresses to the larger portion of target and prevents the excessive scabbing at the rear side of the target material.

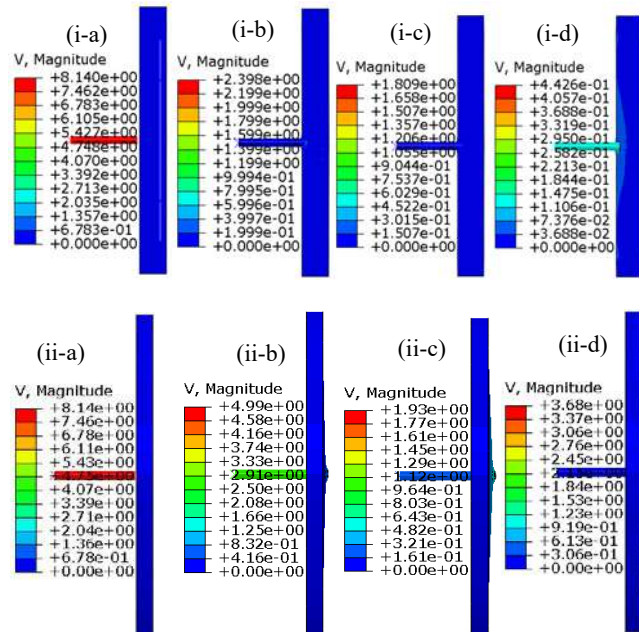


Fig 6. Residual Velocity of 4 kg impactor against (i) 40 and (ii) 20mm targets at ambient temperature on (a) 1.5 (b) 3.0 (c) 6.0 (d) 9.0 milliseconds.

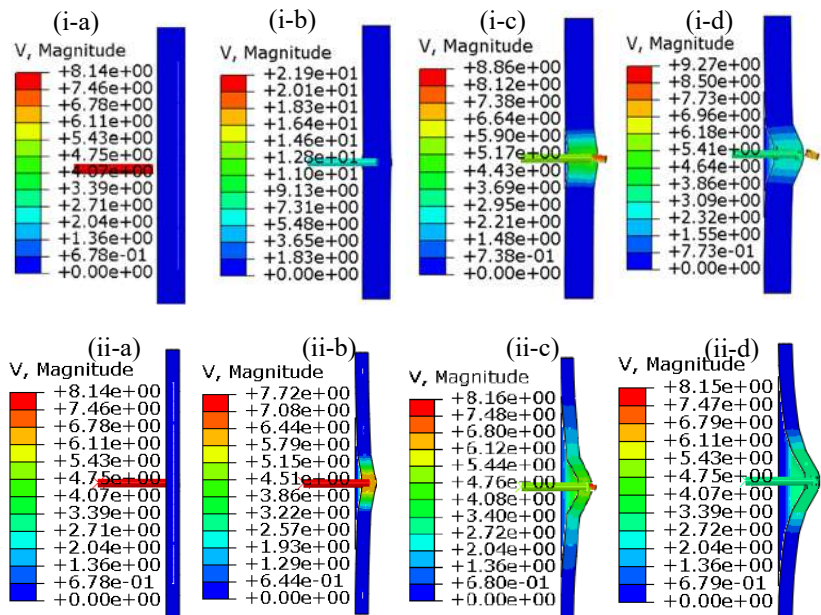
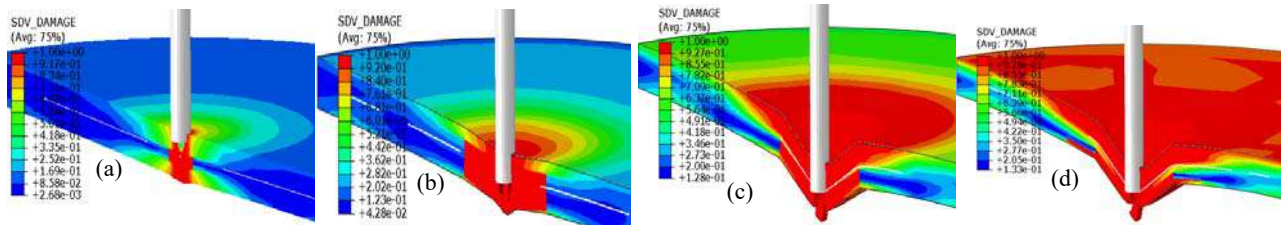


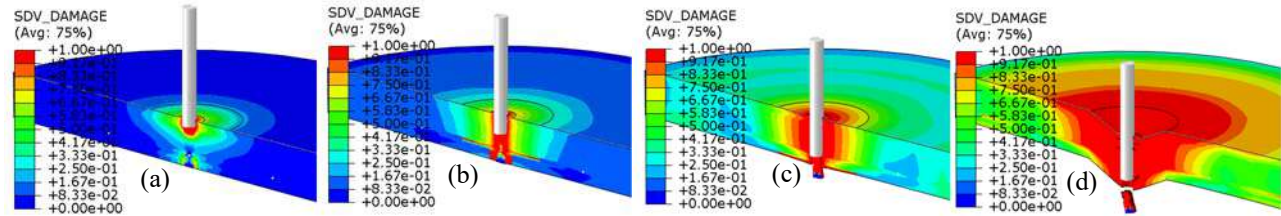
Fig 7. Residual Velocity (m/s) of 32 kg impactor against (i) 40 and (ii) 20mm targets at ambient temperature on a) 0 b) 3.0 c) 6.0 d) 9.0 milliseconds.

Table 2 Influence of residual velocity of 32 kg impactor at varying temperature of target

Thickness of slab (mm)	Temperature (K) and Residual velocity ( $\text{ms}^{-1}$ )			
	293	500	900	1300
20	2.88	3.13	3.87	6.59
40	3.34	3.86	4.11	4.63



**Fig 8. Damage intensity of 20 mm target against 32 kg mass at 500 K temperature at (a) 1 (b) 2.5 (c) 5.2 (d) 9 milli second**



**Fig 9. Damage intensity of 40 mm target against 32 kg mass at 500 K temperature at a) 1 b) 2.5 c) 5.2 d) 9 millisecond**

## CONCLUSION

The present study addresses the finite element investigation on the behavior of thin reinforced concrete slab under elevated temperature against large masses. The impact strength of reinforced concrete target of varying thickness was studied against flat impactor of various masses. The striking velocity of impactors was chosen as 8.14 m/s and the mass of impactor were 4 and 32 kg. Also, the response of target at elevated temperature has been studied and the temperature was varied as 293, 500, 900 and 1300 K. The results thus obtained in terms of reaction forces, residual velocity and damage intensity in concrete were compared and the following conclusions were drawn.

- The reaction forces offered by 40 mm thick target was found to increase by 23% as compared to 20 mm thick target.
- The residual velocity of impactor against the chosen target under elevated temperature was found to be reduced to 50% if the target thickness increased from 20 to 40 mm. Also, it is noticed that the increase of target thickness from 20 to 40 mm at ambient temperature, the residual velocity increased by 16%.
- Based on the damage intensity of target that the reinforcement bars helps significantly in distributing the stresses to the larger portion of target and prevents the excessive scabbing at the rear side of the target material.

## REFERENCES

- ABAQUS, (2014) 6.14 Documentation. Dassault Systemes Simulia Corporation.
- Borvik, T., Langseth, M., Hopperstad, O. S., & Polanco-Loria, M. (2002). "Ballistic perforation resistance of high performance concrete slabs with different unconfined compressive strengths." *WIT Transactions on The Built Environment*, 59.
- Clifton J.R., Knab L.I. (1983). "Impact test of concrete." *Cement Concrete Research* 13 (4): 541–548.
- Dancygier A.N., Yankelevsky D.Z. (1996). "High strength concrete response to hard projectile impact" *Int. J. Impact Eng.* 18 (6): 583–599.
- Hanchak, S. J., Forrestal, M. J., Young, E. R., & Ehrgott, J. Q. (1992). "Perforation of concrete slabs with 48 MPa (7 ksi) and 140 MPa (20 ksi) unconfined compressive strengths." *International Journal of Impact Engineering* (12): 1–7.
- Holmquist, T.J, G.R Johnson, and W.H Cook. (1993). "A Computational Constitutive Model for Concrete Subjected to Large Strains, High Strain Rates, and High Pressures." In *14th International Symposium, Vol 2; Warhead Mechanisms, Terminal Ballistics*, Quebec, Canada: ADPA, 591–600.
- Guo, Y. B., G. F. Gao, L. Jing, and V. P.W. Shim. (2017). "Response of High-Strength Concrete to Dynamic Compressive Loading." *International Journal of Impact Engineering* 108: 114–35.
- Iqbal, M.A., Senthil, K., Bhargava, P. and Gupta, N.K. (2015). "The characterization and ballistic evaluation of mild steel." *International Journal of Impact Engineering* 78: 98-113.

- Johnson, G.R. and Cook, W.H. (1985). "Fracture characteristics of three metals subjected to various strains, strain rates, temperatures, and pressures." *Engineering Fracture Mech.* 21: 31–48.
- Li, J., Wu, C., Hao, H., Wang, Z., & Su, Y. (2016). "Experimental investigation of ultra-high performance concrete slabs under contact explosions." *International Journal of Impact Engineering* 93: 62–75.
- Othman, H., & Marzouk, H. (2016). "An experimental investigation on the effect of steel reinforcement on impact response of reinforced concrete plates." *International Journal of Impact Engineering* 88: 12–21.
- Oucif, C and Mauludin L.M.. (2018). "Numerical Modeling of High Velocity Impact Applied to Reinforced Concrete Panel." *Underground Space* (2): 591–600.
- Rajput, A., & Iqbal, M. A. (2017). Ballistic performance of plain, reinforced and prestressed concrete slabs under normal impact by an ogival-nosed projectile. *International Journal of Impact Engineering* 110: 57–71.
- Ranjan, R, Banerjee S, Singh R. K., and Banerji P. (2014). "Local Impact Effects on Concrete Target Due to Missile: An Empirical and Numerical Approach." *Annals of Nuclear Energy* 68: 262–75.
- Senthil, K., Rupali, S. and Kaur, N. (2018). "The performance of monolithic reinforced concrete structure includes slab, beam and column against blast load." *Journal of Materials and Engineering Structures* 5(2): 137-151.
- Tai, Y. S. (2009). "Flat Ended Projectile Penetrating Ultra-High Strength Concrete Plate Target." *Theoretical and Applied Fracture Mechanics* 51(2): 117–28.



## Effect of Steel Slag as Partial replacement of Fine Aggregate on Mechanical Properties of Concrete

Shailja Bawa\*<sup>1</sup>, Baban Kumar<sup>2</sup> and Asif Basheer<sup>3</sup>

<sup>1</sup>Assistant Professor, Department of Civil Engineering Department at Dr B R Ambedkar National Institute of Technology Jalandhar, India; e-mail: bawas@nitj.ac.in (Corresponding Author)

<sup>2</sup>PG Scholar, Department of Civil Engineering Department at Dr B R Ambedkar National Institute of Technology Jalandhar, India; e-mail: babank690@gmail.com, babank.ce.17@nitj.ac.in

<sup>3</sup>PG Scholar, Department of Civil Engineering Department at Dr B R Ambedkar National Institute of Technology Jalandhar, India;

### ABSTRACT

This study has been conducted to observe the effect of steel slag as partial replacement of fine aggregate on mechanical properties such as compressive strength, split tensile strength and flexural strength. The water/cement (w/c) ratio was kept constant as 0.42 and high range water reducing admixture was used at 1.55% by weight binder. Fine aggregate has been replaced with steel slag as 20%, 30% and 40% by weight. To determine the compressive strength, cubes each of size 100 x 100 x 100 mm were tested at 7, 28, 56 and 90 days of curing. Beam specimens of size 100 x 100 x 500 mm were casted for flexural strength test and cured for 56 and 90 days. Comparisons were made with the normal concrete to show the influence of the additions. The observational results showed that specimen containing 30% steel slag, 20% fly ash and 10% metakaolin performed best among all the proportionated mix.

**KEYWORDS:** Mechanical properties, Cement replacement, Steel slag

### INTRODUCTION

Rising populations and the need for infrastructure development boost the growth of construction industry. It is a major source of pollution, (Li et al 2011) responsible for around 5% of CO<sub>2</sub> emission from cement manufacturing (Warrel et al 2001, Ernst et al 2001). “According to World Commission on Environment and Development, 1987, the sustainable development is the one which meets the needs of the present without compromising the ability of future generations to meet their own needs”. In order to reduce the environmental unsustainability of construction activity worldwide, It is required to find the alternative of natural resource used in construction. Industrial byproduct such as fly ash has been extensively used in concrete input ingredient (**Peng et al 2013**). But there are many other industrial waste such as steel slag and others can also be served as alternative of natural resource. It is required to do research and laboratory trials to find the suitability of another industrial waste as construction material. (**Spence and Mulligan 1995**).

Industrial Solid waste and its management is one of a most critical problem, the gradual accumulation of which results in severe environmental concerns (**Penj et al 2013**). Rather than disposing-off these materials on scarcely available land fill areas, the utilization of waste materials in construction industry can be an attractive alternative (**Ameri et al 2012**). The Indian integrated iron and steel industry poses serious challenges to environment through its inherent complexity (**Pandey et al., 1996**) and may hazardous to environment (**Khan and Shinde, 2013**). Presently, India is the following the China, Japan and the US in the steel manufacturing industry (**Kumar and Naidu, 2013**) following. To meet the present need of the country, steel production will be expected to increase to about 150MT in 2018 (Indian steel).

Among the ingredients of concrete, aggregates play a significant role in concrete occupying the largest volume which is about 60–75% of total concrete volume (**Kosmatka et al. 2002**). Engineering properties of steel slag have shown that, It can be the good alternative of fine aggregate (**Anastasiou and Papayianni 2006**). Although a large number of investigations have been carried out to investigate the properties of concrete made with steel slag as (**Huntzinger and Eatmon 2009**). The primary objective of this research work is to observe the suitability of steel slag as an alternative of fine aggregate by checking the mechanical properties of steel slag blend concrete. Cement is also partially replaced with fly ash and Metakaolin to economize the mix and enhance the strength of mix.

### EXPERIMENTAL PROGRAM

## Materials Used

### *Cement*

Ordinary Portland cement has been used in this work which is conforming to **IS: 8112-1989**. Various physical test has been done in the laboratories to conform the Indian standard code. Result has been compared and tabulated in **Table 1** to check the suitability of cement and consequent adjustment has been made in the mix proportioning.

**Table 1: Properties of OPC 43 Grade Concrete**

Properties	Fineness(m <sup>2</sup> /kg)	Standard Consistency (%)	Initial Setting Time(minutes)	Final Setting Time(minutes)	Specific Gravity
<b>Observed Value</b>	300	32	62	270	3.15
<b>Codal Requirement (IS8112:1989)</b>	225	-----	30 (Min)	600 (Max)	-----

### *Fine and coarse aggregates*

The aggregate has been obtained from Jalandhar (Punjab). Various physical test performed in the laboratory to check the suitability. Sieve analysis has been done and tabulated in **Table 2** which is conforming to **IS-383:1970**. It has been taken as the basis to check the suitability of steel slag as replacement of fine aggregate.

**Table 2: Sieve Analysis of Fine aggregate sample**

Sieve Size(mm)	4.36	2.36	1.18	0.6	0.3	0.15	Pan
<b>Cumulative Retained (%)</b>	3.8	16	36.9	58.1	93.4	98.6	100

### *Steel Slag*

Steel slag has been purchased from nearby steel industry at Jalandhar Punjab. It is black in color and sieve analysis has been done for the gradation **Table 3**. Particle size distribution comparison **Fig. 1** has been made between natural and steel slag for suitability of steel slag as fine aggregate.

**Table 3: Sieve Analysis of Steel Slag**

Sieve Size(mm)	4.36	2.36	1.18	0.6	0.3	0.15	Pan
<b>Cumulative Retained (%)</b>	2	9.8	29.2	82.2	98.2	99.4	100

### *Fly Ash*

Fly ash has been identified as by product of coal combustion. Generally, it has been generated in thermal power plant and boiler plant. Physical characteristics of fly ash support the workability of concrete mix. Fly ash has less heat of hydration due more stable structure. In this work fly ash is taken from PSPCL Ropar (Punjab).

### *Metakaolin*

It is highly pozzolanic material; highly active alumina and silica improves the initial strength due to ettringite formation in higher side and also improves the secondary hydration. In this work, Metakaolin is purchased from locally available.

### *Chemical Admixture*

Water reducing admixture has been used in concrete to adjust the workability of concrete. Super Plasticizer Glenium 51 was used for the required workability (IS: 9103-1999).



Fig 1: Comparison of Natural sand and Steel slag

### Mixing Procedure

Materials have been proportionated according to Indian standard. Drum Mixer has been used to mix all the material. Following steps has been involved for mixing:

1. Dry mixing of coarse and fine aggregate has been done for approx. 30 sec for homogeneity.
2. Binder material has been added to aggregates in the mixer and mixing continued for 30 sec approx.
3. Water has been added in two parts 50 % virgin water added and 50% water has been added with superplasticizer giving 1 minute mixing time each of them.
4. Further, Mixing has been continued for 2 minute approx. and then concrete has been emptied into tray.
5. Concrete has been filled into mold and given vibration to ensure the proper compaction.
6. After 24 hours of air drying, specimen has been unmolded and placed in curing tank.

### Mix Proportion

Many trials executed in laboratory by varying the water cement ratio and aggregate ratio according to IS: 2430- 1986. Based on the trials and observation made on fresh state of concrete and 7 days strength of concrete, Mix proportion is decided which is tabulated in Table 4 which is conforming to IS: 10262-1982. To check the effect of steel slag on mechanical properties of concrete, steel slag along with metakaolin blended in different ratio to get the optimized proportion of concrete ingredients. Various mixes is by varying the ingredient, Mixes are adopted which is tabulated in Table 5.

### Testing Methodology

To observe the effect of steel slag, others variable such as water cement ratio, binder content, curing method are kept constant. Cement is also replaced with fly ash and metakaolin but objectivity has been maintained. Testing sample has been casted in Indian standard conforming mold for mechanical properties. Appropriate no. of cubes and beam has been casted to get the satisfying result. More than one sample has been casted for every test to check the variation of result and average of result has been reported in this paper. Beams have been casted for flexural strength and cubes for compressive and split tensile strength.

Table 4: Quantities of materials finalized for the durable mix

Water(Kg)	Cementitious Material(Kg)	FA (Kg)	CA (Kg)
203	494	775	851

**Table 5: Mixes Adopted**

Mix Name	Portland Cement (%)	Fly Ash (%)	Fine Aggregate (%)	Steel Slag (%)	Metakaolin (%)
Control Mix	70	30	100	0	0
M2	70	30	80	20	0
M3	70	30	70	30	0
M4	70	30	60	40	0
M5	70	20	80	20	10
M6	70	20	70	30	10
M7	70	20	60	40	10

## RESULTS AND DISCUSSIONS

### Compressive Strength

Compressive strength has been tested on universal testing machine according to **IS: 516-1959** at the age of 7, 28, 56 and 90 days are given in **Fig. 2** in tabular graph. The compressive strength first increase by adding steel slag up to 30% but it decreases as steel slag percentage increases to 40%. Also compressive strength further increases on adding metakaolin up to 30% steel slag but it again further decreases due to increase of steel slag in concrete. Addition of 20%, 30% and 40% steel slag in the mix, there is increase of 14.5%, 16.6%, 0.7% after 7 days, 6%, 8.5%, 3.7% increase after 28 days, 5%, 7.7%, 1.1% increase after 56 days and 5.8%, 10.4%, 1.1% increase after 90days respectively as of control mix.

The addition of 10 % Metakaolin increased the compressive strength up to a partial replacement of 30% of steel slag, but then it decreases. 20 % steel slag addition in the mix, increases the strength by 17.9 % after 7 days, 7.9 % increase after 28 days, 5.4 % increase after 56 days and 8.3 % increase after 90 days as compared to the control mix. By adding 30 % steel slag the increase in percentage i.e. 26 % , 15 % , 7.9 % and 12.5 % respectively for 7, 28, 56 and 90 days respectively . Further addition of steel slag to 40 % shown that the compressive strength gut decreased by 2.6 % , 10.4%, 7.5 % and 2.8 % respectively for 7 , 28,56 and 90 days respectively.

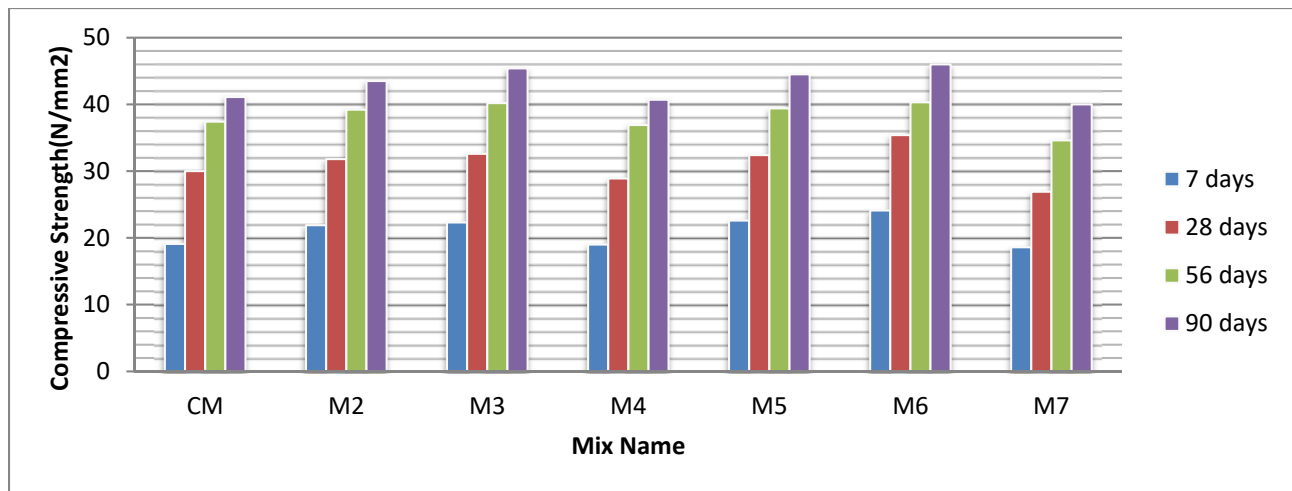


**Fig. 2: Compressive Strength of Concrete**

### Split Tensile Strength

Test has been carried out at the age of 28, 56 and 90 days. Results are incorporated in **Fig. 3** with tabular graph. Strength increment and decrement shows the similar pattern to compressive strength i.e. increases in the percentage of slag till 30% increases the strength and then decreases.. After adding 20%, 30%, 40% steel slag replacement , there has been observed 6.5%, 19.52%, 12.3% increase after 28 days , 7.4%, 16%, 1.94% increase after 56 days and 7.2%, 12.26%,

1.84% increase after 90 days respectively compared to control mix.

The addition of 10 % metakaolin increased the split tensile strength up to a partial replacement of 30 % of steel slag but then it decreases. After adding 20%, 30%, 40% steel slag with 10% metakaolin, there has been observed increase of 10.06 %, 21.91%, 2.36% increase after 28 days , 14.03%, 19.52%, 2.37% increase after 56 days and 7.69%, 13.39%, 5.73% increase after 90 days respectively as compared to the control mix .

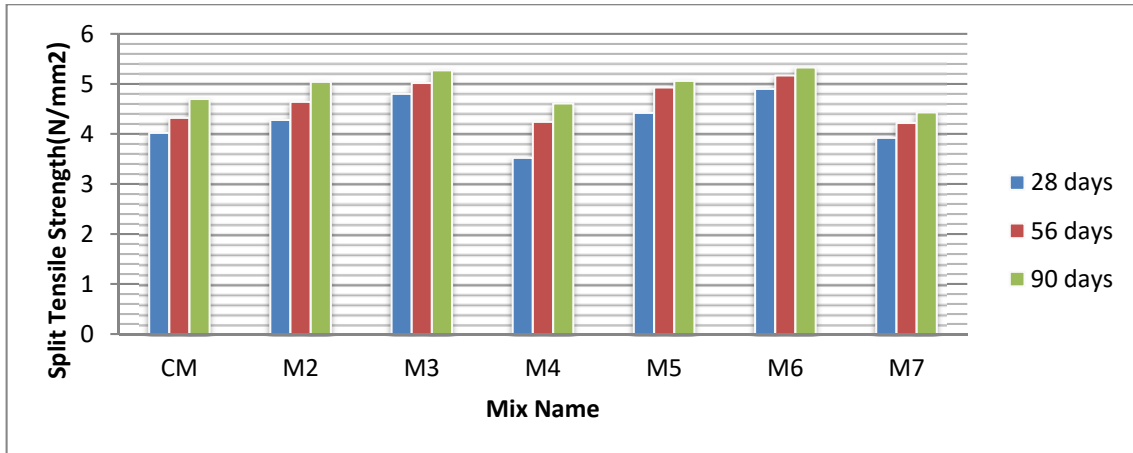


Fig. 3: Split Tensile Strength of Concrete

### Flexural Strength

Flexural strength test shows all mixes performed better with control matrix and results are incorporated in Fig.4. The highest flexural strength has been observed in M6 mix which has 30 % steel slag and 10 % metakaolin. This particular mix have 33 % and 22.9 % increase in flexural strength for 28 and 56 days respectively. These results indicate that there is improvement in the flexural strength, due to addition of steel slag as fine aggregate in every proportion i.e., up to 40 % replacement.

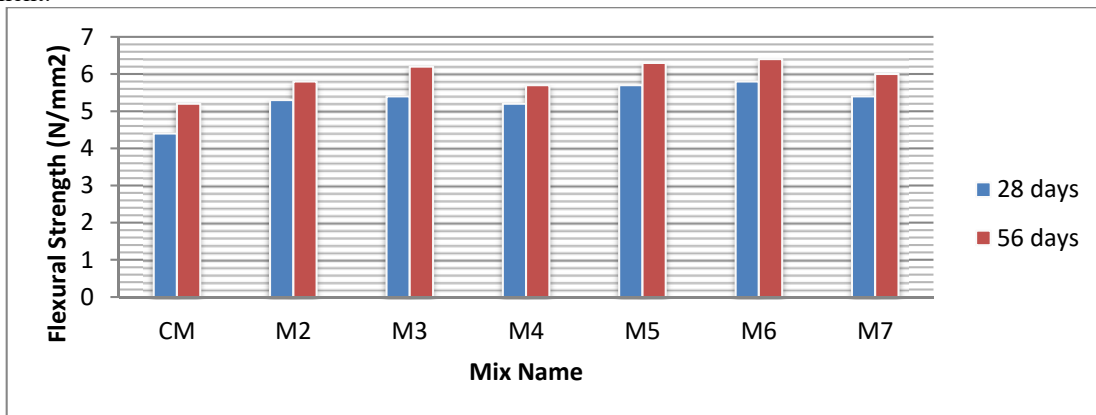


Fig. 4: Flexural Strength of Concrete

### CONCLUSION

The effect on concrete mix have been computed in this work by replacing fine aggregate with steel slag and cement with fly ash and metakaolin. Based upon the scope of the work carried out in this investigation, following conclusion is drawn:

1. The compressive strength increases by replacing sand by Steel slag up to 30 % but it get further reduced when percent increased to 40 % . The increase in compressive strength up to certain amount may be due to the fact that steel slag has stronger strength when compared to natural sand.

2. Further by adding Metakaolin (10%) to mix, strength increases as compared to previous mixes which only steel slag as replacement, Steel slag, fly ash and Metakaolin forms a stronger adhesive bond which increases the strength.
3. Split Tensile Strength and flexural strength also follows the same nature as of Compressive strength and as it increases on adding 30 % steel slag and further reduces when steel slag percentage is increased to 40 %.

This experimental work has been done to check the suitability of steel slag in concrete mix along, with another binder replacing material. This work supports the suitability of steel slag as replacement of fine aggregate and can be good alternative.

## REFERENCES

- Ameri M, and Kazemzadehazad S, (2012). "Evolution of use of steel slag in concrete" *ARRB Conference, 25th, 2012, Perth, Western Australia, Australia, 2012, 9p*
- Anastasiou E, and Papayianni I, (2006). "Criteria for the use of Steel slag aggregate in concrete" *Measuring, Monitoring and Modelling concrete properties*, © 2016 Elsevier Ltd. All rights reserved.
- Ernst Worrell, Lynn Price, Nathan Martin, Chris Hendriks and Leticia Ozawa (2001). "Carbon Dioxide Emissions from the Global Cement Industry" *Annual Review of Energy and the Environment* 26(1):303-29 DOI: 10.1146/annurev.energy.26.1.303
- Huntzinger D. N and Eatmon T.D (2009). "A Life-Cycle Assessment Of Cement Manufacturing: Comparing Traditional Process With Alternative Technologies." *Journal of Cleaner Production* 17(7): 668-675, <https://doi.org/10.1016/j.jclepro.2008.04.007>
- IS: 8112-1989, "Specification for 43 grade ordinary Portland cement", Bureau of Indian standards, New Delhi (India)
- IS: 383-1970, "Indian Standard Specification for Coarse and Fine aggregates from natural sources for concrete." *Bureau of Indian Standard, New Delhi*
- IS: 10262-1982 (Reaffirmed 2004), "Recommended guidelines for concrete mix design", *Bureau of Indian Standard, New Delhi-2004*
- IS: 516-1959, "Methods of Test for Strength of Concrete", *Bureau of Indian Standards*, New Delhi.
- IS: 2430-1986, "Indian Standard Methods For Sampling Of Aggregates For Concrete" *Bureau of Indian Standards, New Delhi*.
- IS: 5816-1999, "Methods of test for Splitting Tensile Strength of Concrete", *Bureau of Indian Standard, New Delhi*
- IS: 9103-1999, "Indian standard concrete admixtures- specification" *Bureau of Indian Standards, New Delhi*.
- Khan, R. and Shinde, S. B. (2013). "Effect Of Unprocessed Steel Slag On The Strength Of Concrete When Used As Fine Aggregate." *International Journal of Civil Engineering & Technology* 4(2): 231–239.
- Kosmatka, S. H., Kerkhoff, B., Panarese, W. C. (2002). "Design And Control Of Concrete Mixtures." *Portland Cement Association, 14th edition., Skokie, Illinois, - 184 - USA, 1-358*
- Kumar, P. S. and Naidu, V. B. (2013). "An Analysis of Indian Steel Industry", *Journal of International Academic Research for Multidisciplinary*, 1(3): 190-196
- Li C, Gong X, Cui S, Wang Z, Zheng Y and Chi B (2011). "CO<sub>2</sub> Emissions Due To Cement Manufacture". *Mater Sci Forum* 2011; 685:181–7.
- Pandey, H.D., Bhattacharya, S., Maheshwari, G. D., Prakash, O. and Mediratta, S. R. (1996). "Research Needs In Environmental and Waste Management in Iron & Steel Industries", *Proceedings: Ns-EWM1996 @NML Jamshedpur, 1-21*
- Peng J, Huang L, Zhao Y, Chen P, Zeng L, Zheng W (2013). "Modeling Of Carbon Dioxide Measurement On Cement Plants" *Adv. Mater Res* 2013;610–613:2120–8.
- Robin Spence and Helen Mulligan (1995). "Sustainable Development and the Construction Industry", *Habitat Intr.* 19(3): 279-292, *Elsevier Science Ltd*.



## Effects of Poly Carboxylate Ether, increase in water content and paste content on rheological properties of smart dynamic concrete

Sunil Bauchkar<sup>1</sup>, Hemant Chore<sup>2\*</sup>

<sup>1</sup>Research Scholar, Deptt. of Civil Engg., Datta Meghe collage of engineering, sunil.bauchkar@basf.com  
<sup>2</sup>\*Professor, Deptt. of Civil Engg., Dr B R Ambedkar National Institute of technology, chorehs@gmail.com

\*Corresponding Author

### ABSTRACT

An experimental investigation into the retention behavior of the rheological properties of Smart Dynamic Concrete (SDC) is presented in this paper. The investigation was aimed at quantifying the impact of two different Polycarboxylate ether (PCE) polymers, increase of water and reduction of cement content on the workability and rheology retention properties of SDC containing two types of Ordinary Portland Cement (OPC) and crushed sand as fine aggregate. Ordinary Portland cement (OPC) in conjunction with the fly ash mineral admixtures was used varying paste volume (44 and 42%) and water binder ratio (0.35-0.33) at controlled laboratory atmospheric temperature (33°C to 35°C). All SDC mixes having a constant initial workability, equal to 650 +/- 25 mm initial slump flow at the end of the mixing procedure. Workability testing methods such as slump-flow and V-funnel are used to assess workability retention properties of SDC. ICAR rheometer deployed in this study for measurement of rheological properties of SDC up to 120 minutes. The results show that the properties of cement, cement content and water to binder ration have a strong influence on the admixture demand for similar initial workability and subsequently it also affects workability retention properties. The rheology retention of SDC over period of 120 minutes also significantly influence by type of cement, cement content, PCE type and water to binder ratio. PAE technology of polymer helps to maintain workability and rheology for longer time, hence it is superior technology amongst existing commercially available PCE for high-rise pumping.

**KEYWORDS:** Smart Dynamic Concrete (SDC); retention; rheology; workability; Polycarboxylate ether, slump-flow, V-funnel, slump-flow loss, paste.

### INTRODUCTION

Smart Dynamic Concrete is designed to upgrade high slump concrete to become self-compacting and robust concrete for day-to-day use at minimum extra cost. Smart Dynamic Concrete adds economical, ecological and ergonomic values to concrete and has the potential to move the market up to the next level of advanced construction practice (Seow et al, 2011 and Bruce et al, 2012). Optimization of normal SCC mixes (25-35 Mpa.) with low cement of fines through the application of SDC concept, and corresponding field test result from experiences in different ready mix and precast plant. (Bryan et al, 2011). It allows the ready-mix industry to reach better construction process economy, higher concrete durability and increased energy efficiency in order to save time and money and reduce CO<sub>2</sub> emissions (Mario et al 2007).

### SMART DYNAMIC CONCRETE (SDC)

Self-compacting concrete (SCC) is undoubtable the major advance of concrete technology in the last two decades. Mainly due to its flowability, SCC differs from conventional vibrated concrete essentially when in fresh state. Currently, a number of guidelines are available for the proportioning, characterization, control and application of SCC (JSCE 1999, PCI 2003, EFNARC 2005, ACI237R 2007, ACHE 2008). The recommendation by the Japanese Society of civil engineers define three types of SCCs according to use of fines (type P), Viscosity modifying agent (type V) or the combined use of both (type C). In type P, self-compatibility is obtained by minimizing the ratio water/fines through the use of superplasticizer to provide appropriate resistance to segregation and bleeding. In case of Type V, the use of viscosity modifying admixture (VMA) provides enough stability to concrete towards bleeding and segregation, since these fix the water providing the appropriate rheology to the cement paste. Type C consist of combination of the other two types. On the other hand, European guidelines define different types of SCCs according to fresh properties, regardless the composition of the concrete. Along this line there are three levels of self-compacting concrete according to the flow value of slump flow, two level of viscosity according to T<sub>500</sub> or the time to pass V-funnel, T<sub>v</sub> and two level of passing ability according to the

passing ratio in the L-box (Table 1)

To classify low grade/low fine concrete in SDC as concept is big challenge, hence BASF Technical experts define SDC in concert with EN 206-9:2010 classification of SCC i.e. SF1.

**Table 1.** Test Value for Different Class of SCC

Class		SF1	SF2	SF3
Slump Flow	mm	550 to 650	660 to 750	760 to 850
T500	sec	≥ 2	≥ 2	< 2
J Ring (12 Bar)	mm	≤ 25	≤ 25	NA
V Funnel	sec	5 to 25	≤ 10	< 9
L Box (2 Bar)	-	see *Note 1	≥ 0.8	NA
For SDC *Note 1 - Preferably not to use this test for SF1, if required use ≥ 0.65				

The lower fines content SCC (SDC) are characterized by a higher yield value and a lower plastic viscosity and are suitable for lightly reinforced structures where the amount of reinforcement is less than 100 kg/m<sup>3</sup> and classified as Rank 3 in the JSCE Recommendations. This type of concrete is typical of structures where concrete of strength class C25 and C40 is used and this forms the major part of the ready mixed concrete produced in European Union. Therefore, if the diffusion of self-compacting concrete is to be increased, it is in this sector where the industry should focus its resources to find an innovative approach (Bruno et al, 2013) without increasing more cement content and cost of concrete. SDC is the innovative solution for making every day concrete better. SDC concept launched in south Asia in 2007, due to its various advantages and cost benefits it is gaining popularity in India day by day.

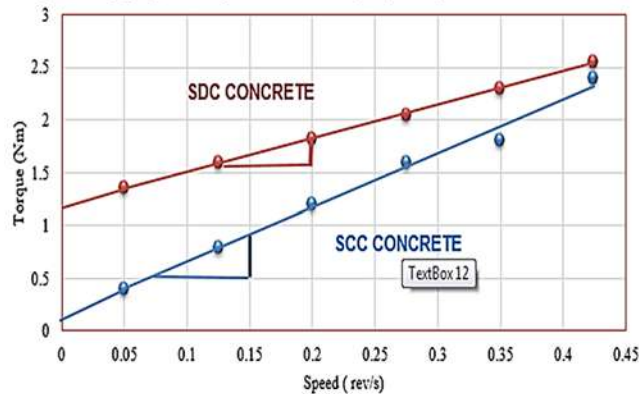


**Fig. 1** SCC and SDC concrete comparison.

Rheology is generally defined as "a science of deformation and flow of matter". It deals with the relationships between stress, strain, rate of strain and time, and it is a broad branch of science. Concrete rheology exhibits a complex behavior, both in fresh and hardened state (Tattersall 1983). flow is so complicated because it is a complex suspension of particles. Particles of coarse aggregate are dispersed in mortar and within mortar, particles of fine aggregate are dispersed in cement paste and within cement paste, cement particles are dispersed in water. Therefore, we cannot describe rheological behavior of fresh concrete with the Newtonian viscosity function. The Bingham model, which is the simplest form of non-Newtonian model, is most frequently used. It is mostly satisfactory for describing the behavior of ordinary concrete. However, some types of concrete, especially the self-compacting concrete, exhibit different kinds of behavior (Feys et al 2008) and so we apply different non-Newtonian models to describe their behavior (Feys et al 2008). The Bingham equation Eq. (1) can be written as (Tattersall 1983):

$$\tau = \tau_0 + \mu \cdot \dot{\gamma} \quad \dots \text{Equation 1}$$

Where:  $\tau$  - Shear stress [Pa]

$\tau_0$  - yield stress [Pa]

$\gamma$  - Shear rate [s<sup>-1</sup>]

$\mu$  - plastic viscosity [Pa·s]

ICAR rheometer uses equation of Bingham parameters for computing fundamental rheological measurements (Tattersall 1983, Wallevik 2009). Different authors and different equipment manufacturers use slightly different computations (Koehler, E.P et al. 2004, Wallevik 2009), but they all use a few assumptions which distinguish them. In this study ICAR rheometer has been deployed to measure rheological parameters of SDC.

## SIGNIFICANCE OF THE PRESENT WORK

Plenty of studies have explored the effect of mineral admixtures, variation of water content, chemical admixtures types, cement types etc. on rheological behaviour of SCC. Study published by S.D. Bauchkar and H.S. Chore (2017) is in line with effect of mineral admixture and PCE admixture on rheological behaviour of Smart Dynamic Concrete, corresponding paste volume 32-35%. Effects of PCE types, water content and cement content on rheological retention behaviour of smart dynamic concrete have not been explored. The research findings revealed rheological behaviour over 120 minutes for SDC due to variation of cement, water and PCE type.

## MATERIALS AND PROPORTIONS OF MIXES

The present work involves the use of International Concrete and Aggregate Research (ICAR) rheometer. A series of SDC mixes covering variation of cement content, cement types, water content and two different types of PCE. Effects of these variations on rheological properties were tested to demonstrate its effect.

The cementitious materials used in the present investigation includes two different brands of ordinary Portland cement (OPC) (53 grade), class- F fly ash (FA). The physical and chemical properties of OPC 1, OPC 2 and PFA as obtained through systematic laboratory investigations carried out at the Research and Development centre of Counto Microfine Products Pvt Ltd.(Goa) are summarized in Table 2. Two aggregate fractions, coarse and natural sand, were used in all the mixes. The particle size distributions of these aggregates are shown in Table 3. A commercially available Polycarboxylate Ether based superplasticisers PCE 1 and PCE 2 was used in the present study for producing SDC. The physical properties of PCE1 and PCE 2, presented in Table 4 were evaluated using state of the art instrumentation available at the Research and Development centre of BASF India Ltd., Navi Mumbai. PCE 2, a new class of chemical admixtures, known as Poly Acrylates Ether (PAE), which has been developed by BASF to provide improved rheological properties in concrete even in demanding mix designs. Although it exhibits similar chemical side chains as other PCE, the presence of new chemical backbone units in combination with a very high density of negative charges is believed to increase the affinity to the cement surface, whereas the presence of side chains adds a steric effect to the electrostatic component of the inter-particle repulsion forces.

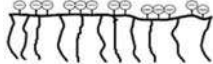
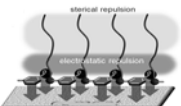
**Table 2.** Chemical compositions of the cementitious materials used in the study.

	Blaine fineness	Lime reactivity	Autoclave expansion	Sp. gravity	Loss on ignition (LOI)	Silica (SiO <sub>2</sub> )	Iron oxide (Fe <sub>2</sub> O <sub>3</sub> )	Alumina (Al <sub>2</sub> O <sub>3</sub> )	SiO <sub>2</sub> + Al <sub>2</sub> O <sub>3</sub> + Fe <sub>2</sub> O <sub>3</sub>	Calcium oxide (CaO)	Magnesium oxide (MgO)	Total sulphur (SO <sub>3</sub> )	Alkalis (Na <sub>2</sub> O + K <sub>2</sub> O)
UoM	(m <sup>2</sup> /kg)	MPa.	(%)	(%)	(%)	(%)	(%)	(%)	(%)	(%)	(%)	(%)	(%)
PFA	345	5.6	0.06	2.3	1.2	60.72	5.32	27.5	93.54	1.42	0.48	0.21	1.71
OPC 1	335	-	0.059	3.14	2.81	20.68	4.76	5.54	30.98	61.39	1.07	2.5	0.38
OPC 2	325	-	0.09	3.15	1.18	20.3	5.31	4.18	29.81	63.22	1.22	2.64	0.062

**Table 3.** Physical properties of coarse and fine aggregates used in the study work.

	IS Sieve Size (mm)	20	10	4.75	2.36	1.18	0.6	0.3	0.15	Silt content (%)	Fineness Modulus	Specific Gravity	Water Absorption
Crushed Sand	% Passing	100	100	93.9	65.2	43	28.9	17.6	10.4	12.50%	3.41	2.72	3%
20 mm		97.4	2.9	1.1	1.1	1.1	1.1	1.1	0	0.50%	6.94	2.82	1.50%
10 mm		100	82.6	3.4	2.8	2.8	2.8	2.8	0	0.50%	5.6	2.8	1.80%

**Table 4.** Physical properties of polycarboxylate ether (PCE)-based superplasticizers used.

Product	PCE 1	PCE 1		PCE 2	PCE 2	
Relative Density @ 25° C	1.05			1.01		
Dry Material content (%)	25			25		
pH	>6			>6		
Chloride-ion content	< 0.2%			< 0.2%		

### SMART DYNAMIC CONCRETE (SDC) MIX DETAILS

Experimental study consists of three main set of mixes (refer Table 5- Table 7), in first set of mixes two different cement OPC1 and OPC2 used in conjunction with two different PCE types. Water content increase by 6% in Second set of SDC mixes and in final set of mixes cement content reduced from 300 to 280 kg/m<sup>3</sup>. All the mixes adjusted with constant flow up to 650 ± 10 mm.

Furthermore, the results obtained using traditional SCC methods in respect of the workability are compared with those obtained using ICAR Rheometer.

#### STUDY 1- EFFECT OF PAE ON RHEOLOGY RETENTION

**Table 5** Mix proportions for effects of different PCE on rheology

Description	Cement (kg/m <sup>3</sup> )	FA (kg/m <sup>3</sup> )	w/b	Water (kg/m <sup>3</sup> )	20 mm (kg/m <sup>3</sup> )	10 mm (kg/m <sup>3</sup> )	CRF(kg/m <sup>3</sup> )	Paste (%)
1C30PCE	320	200	0.33	171	396	484	870	44
1C30PAE	320	200	0.33	171	396	484	870	44
2C30PCE	320	200	0.33	171	396	484	870	44
2C30PAE	320	200	0.33	171	396	484	870	44

#### STUDY 2- EFFECT OF INCREASING 6% WATER ON RHEOLOGY RETENTION

**Table 6** Mix proportions for effects of variation of water content on rheology

Description	Cement Brand	Cement (kg/m <sup>3</sup> )	FA (kg/m <sup>3</sup> )	w/b	Water (kg/m <sup>3</sup> )	20 mm (kg/m <sup>3</sup> )	10 mm (kg/m <sup>3</sup> )	CRF(kg/m <sup>3</sup> )	Paste (%)
1C30PAE	OPC1	320	200	0.33	171	396	484	870	44
1C30PAEWC2	OPC 1	320	200	0.35	182	390	474	865	45
2C30PAE	OPC 2	320	200	0.33	171	396	484	870	44
2C30PAEWC2	OPC 2	320	200	0.35	182	390	474	865	45

#### STUDY 3 – EFFECT OF CEMENT REDUCTION ON RHEOLOGY RETENTION

**Table 7** Mix proportions for effects of variation of cement content on rheology

Description	Cement (kg/m <sup>3</sup> )	FA (kg/m <sup>3</sup> )	w/b	Water (kg/m <sup>3</sup> )	20 mm (kg/m <sup>3</sup> )	10 mm (kg/m <sup>3</sup> )	CRF (kg/m <sup>3</sup> )	Paste (%)
1C30PAE	320	200	0.33	171	396	484	870	44
1C30PAEPC2	280	200	0.33	158	405	498	880	42
2C30PAE	320	200	0.33	171	396	484	870	44
2C30PAEPC2	280	200	0.33	158	405	498	880	42

(1C- OPC1 ,2C – OPC 2, PCE – Poly carboxylate ether PCE 1, PAE- Poly Acrylates Ether PCE 2, WC 2- 0.35 w/b ratio)

## EXPERIMENTAL PROCEDURE

The ICAR Rheometer from German instrument deployed to measure rheology of SDC, it is composed of a container to hold the fresh concrete, a driver head that includes an electric motor and torque meter, a four-blade vane that is held by the chuck on the driver, a frame to attach the driver/vane assembly to the top of the container; and a laptop computer to operate the driver, record the torque during the test and calculate the flow parameters. The container contains a series of vertical rods around the perimeter to prevent slipping of the concrete along the container wall during the test.

The concrete was discharged directly from the ribbon mixer into the ICAR rheometer container. Two types of tests were performed. The first one was a stress growth test in which the vane was rotated at a constant slow speed of 0.025 rev/s. The initial increase of torque was measured as a function of time. The maximum torque measured during the test was used to calculate the static yield stress. The other type of test was a flow- curve test to determine the dynamic yield stress and the plastic viscosity.

In addition, the slump- flow test was performed by filling the concrete into a standard slump cone (ASTM C- 143) that was centered on a level plastic plate. The slump cone was lifted, and three measurements were made- the time for the concrete to spread to a horizontal diameter of 500 mm (T<sub>500</sub>), the final horizontal spread diameter; and the visual stability index (VSI). The VSI ratings, which were determined based on the definition as given by Wallevik (2008), were made on a scale of 0 to 3, with 0 exhibiting excellent stability and 3 exhibiting poor stability. Other than flow L-Box, V-funnel test was performed as per EFNARC (2005) standard.

## RESULTS AND DISCUSSION

To understand the effect of different types of PCE polymers, increase in water content and reduction in cement content on the rheological retention of the SDC, comparative analyses of the obtained values of the Flow, T<sub>500</sub>, V-Funnel, yield stresses and viscosity retention were carried at intervals of 60 minutes over a total duration of 120 minutes and reported in Table 8. The results are reported in section below

**Table 8** Effects of different types of PCE polymers, increase in water content and reduction in cement content on fresh and harden properties of SDC.

Mix ID	Flow in mm.			T500 in sec			V funnel in reading Sec			Yield Stress in Pa.			Viscosity (Pa.s)		
	05 min s	60 min s	120 min s	05 min s	60 min s	120 min s	05 min s	60 mins	120 mins	05 min s	60 mins	120 mins	05 min s	60 mins	120 mins
1C30PCE	640	610	550	3.8	8.3	11.4	17.3	26.4	47.1	79.3	92.8	117.9	47.6	58.5	76.6
1C30PAE	650	600	560	2.6	5.9	8.8	12.4	21.7	36.8	52.2	61.9	94.8	31.3	38.9	61.7
1C30PAEW C2	650	610	530	2.3	5.6	9.1	11.9	20.5	37.4	46.4	58.1	104.6	27.8	36.6	67.9
1C30PAEP C2	650	610	580	3.1	7.9	10.5	16.5	24.9	41.2	59.9	88.9	115.9	35.9	56.1	75.3
2C30PCE	660	620	570	3.6	8.1	12.3	16.6	25.6	49.3	83.1	98.6	143.1	49.9	62.1	93.1
2C30PAE	650	610	550	2.9	6.2	9.1	10.9	20.8	37.2	56.1	67.7	104.4	33.7	42.7	67.9
2C30PAEW C2	650	600	520	2.2	5.5	10.2	10.7	20.1	42.4	48.4	65.8	110.3	29.1	41.5	71.7
2C30PAEP C2	640	600	560	3.2	8	11.9	16.1	24.2	48.9	63.8	94.7	129.5	38.3	59.6	84.2

### STUDY 1- EFFECT OF DIFFERENT TYPES OF POLYCARBOXYLATE ETHERS ON RHEOLOGY RETENTION

Though the paste volume of SDC mixes is constant, the PCE type used influences the rheological properties of concrete.

It has been observed from Fig.2 , Fig. 3 and Fig. 4, different PCE types will give different flow ,  $T_{500}$  and V-funnel retention despite of OPC type used. The slump flow reduction over a period of retention time is observed to be higher for PCE 1 than PCE 2, it is also observed that the flow retention of PCE 2 is superior than PCE 1. Further, the PCE 1 admixtures are found to have low  $T_{500}$  and V-Funnel time retention. At the same time, the PCE 2 admixtures are found to exhibit good  $T_{500}$  and V-Funnel time retention up to 120 minutes.

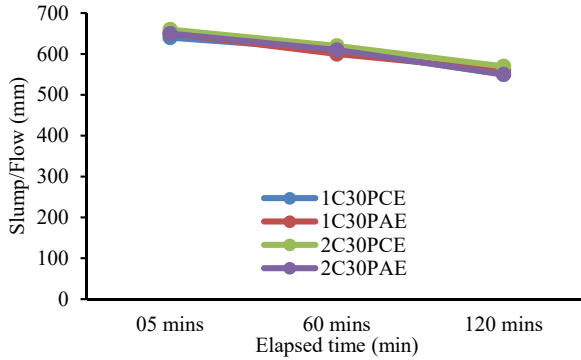


**Fig. 2** Effects of different PCE types on Flow retention

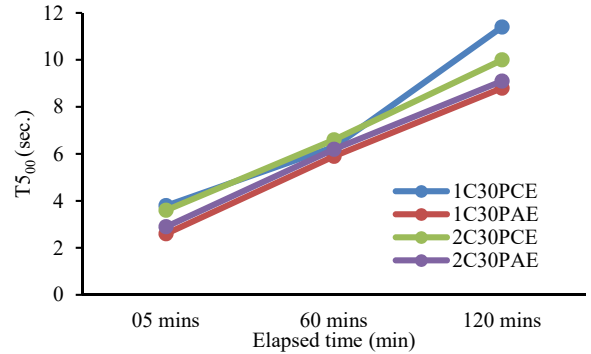


**Fig. 3** Effects of different PCE types on  $T_{500}$  retention

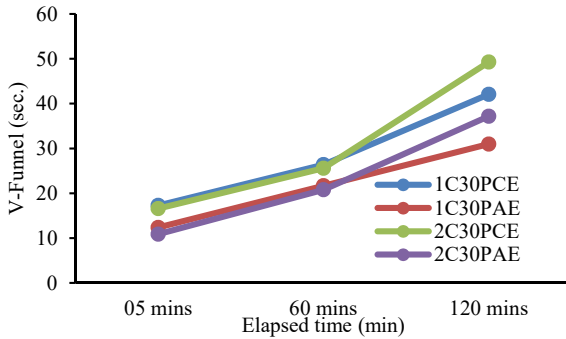


**Fig. 4** Effects of different PCE types on V-Funnel retention

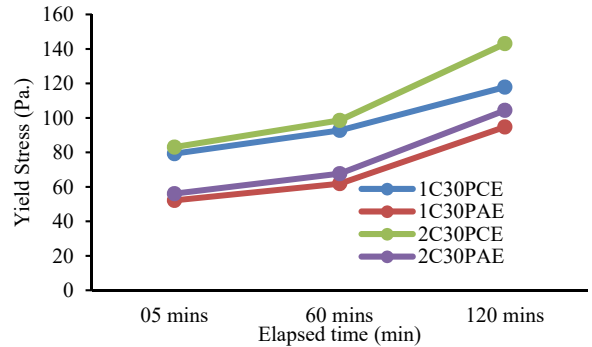


**Fig. 5** Effects of different PCE types on Yield stress retention

The effect of the types of PCEs used in the present investigation in conjunction with two different types of OPCs on yield stress as well as viscosity is also studied over a retention period of 120 minutes. From Fig. 5 and 6, it is observed that the yield stress and plastic viscosity increases with the retention time. It is also observed that the type of PCE and side chain length along with the type of cement also influence the retention of plastic viscosity of SDC. The variation in the viscosity and yield stress of the SDC mixes with PCE 1 type superplasticizers is on a higher side than that of the mixes with 2. The results also indicate that the addition of PCE 2 results in the reduction in yield stress and viscosity retention of the mixes.

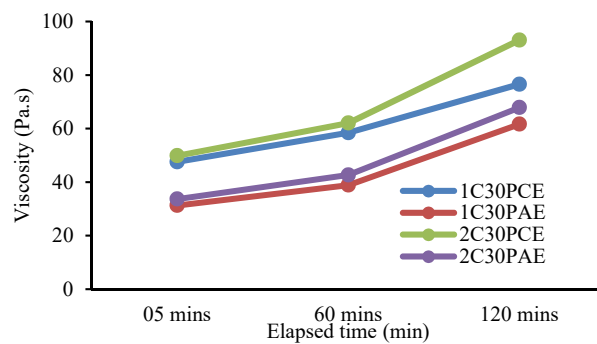


**Fig. 6** Effects of different PCE types on Viscosity retention

**STUDY 2- EFFECT OF INCREASING 6% WATER ON RHEOLOGY RETENTION**

The investigation is aimed at quantifying the effect of the varying amounts of water content on the rheological properties of SDC.

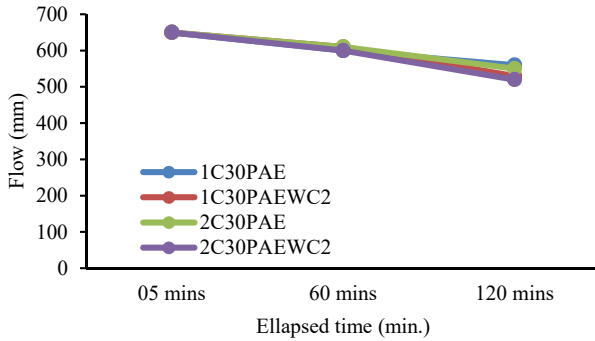


**Fig. 7** Effects of increase in water content on Flow retention

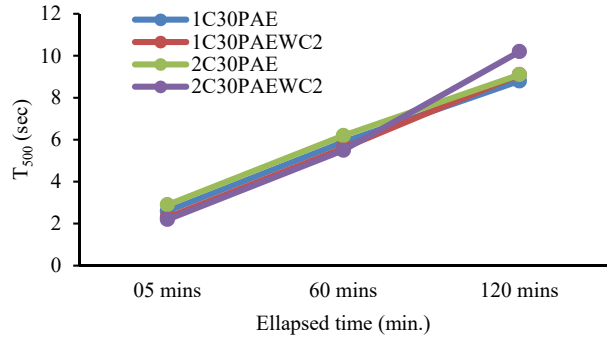


**Fig. 8** Effects of increase in water content on T<sub>500</sub> retention

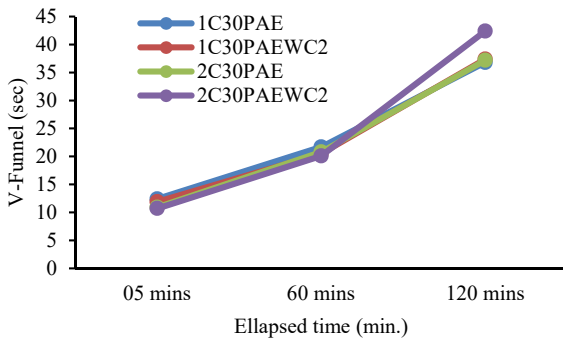


**Fig. 9** Effects of increase water content on V-Funnel

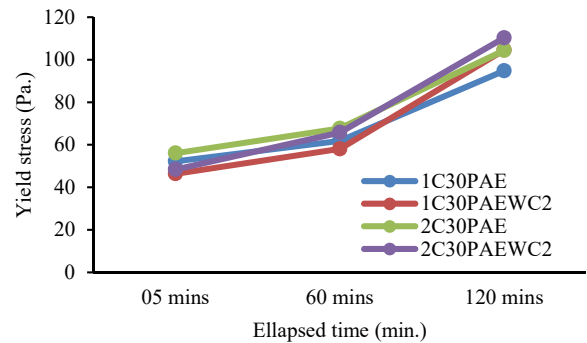


**Fig. 10** Effects of increase water content on Yield stress

The influence of increase water content on Flow, V-funnel and T<sub>500</sub> time for similar workability for different water to binder ratio and paste volume is compared in Fig. 7-11. Increase in water content will improve initial T<sub>500</sub>, V-funnel, Yield stress and Viscosity values despite of PCE type used. Furthermore, it also observed from Fig. 7-11 increase in water content will hamper T<sub>500</sub>, V-funnel, Yield stress and Viscosity values at retention period of 120 min. The dosages of PCE delivered in higher water mix is for same initial flow is lesser and leads to drop in rheology over time. The effect of variation of water content on the flow, V-funnel and T<sub>500</sub> seems to be remarkable in terms of its nature.

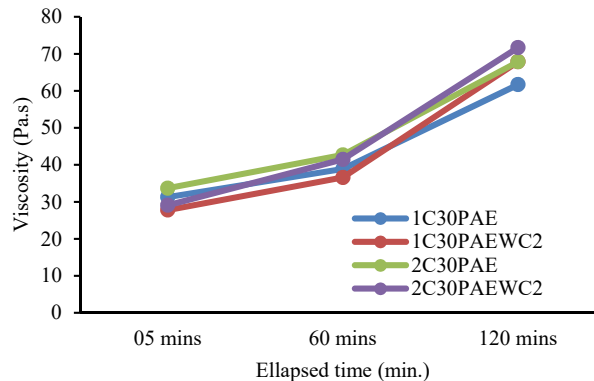


**Fig. 11** Effects of increase water content on Viscosity.

**STUDY 3 – EFFECT OF CEMENT REDUCTION ON RHEOLOGY RETENTION**

The influence of cement content reduction on Slump / Flow, V -funnel and T<sub>500</sub> time retention for similar initial workability SDC mixes for same water to binder ratio and paste volume is compared in Fig. 12- 15.

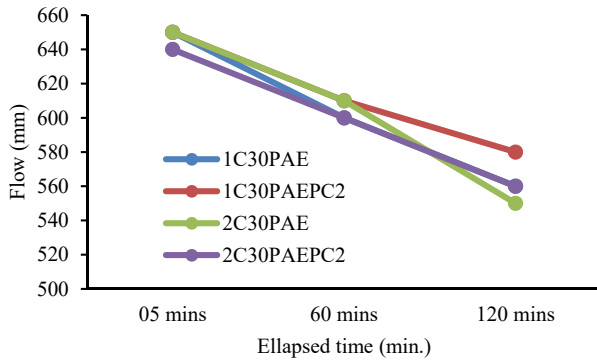


**Fig. 12** Effects of cement content reduction on Flow retention

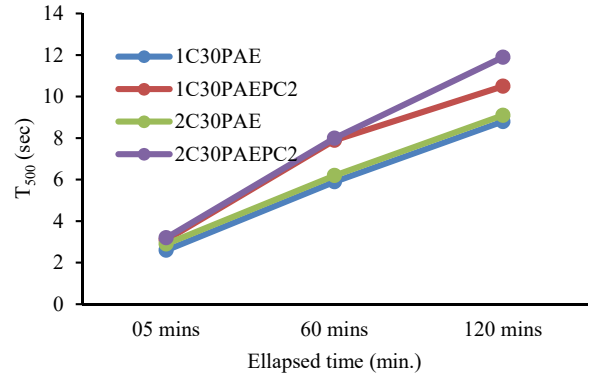


**Fig. 13** Effects of cement content reduction on T<sub>500</sub> retention

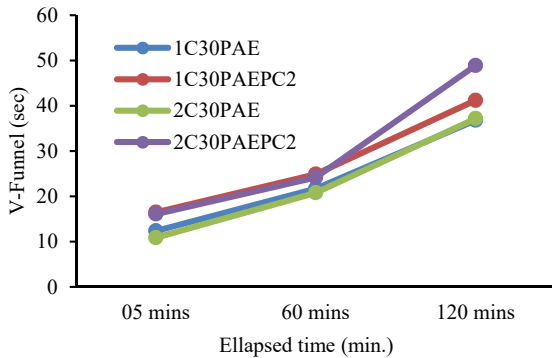


**Fig. 14** Effects of cement content reduction on V-Funnel

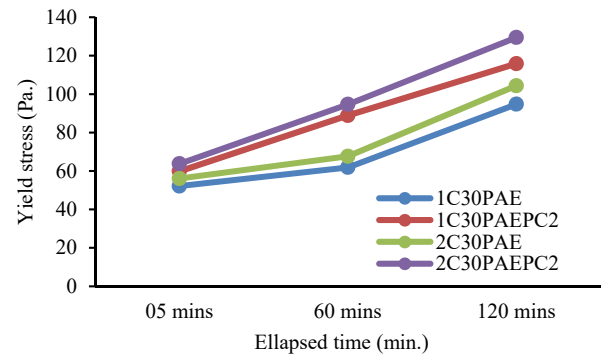


**Fig. 15** Effects of cement content reduction on Yield stress

Decrease in cement content drastically affects the flow, T<sub>500</sub>, V-funnel, Yield stress and Viscosity values despite of PCE and OPC type used. Furthermore, it also observed from Fig. 12-16 increase in cement content will hamper T<sub>500</sub>, V-funnel, Yield stress and Viscosity values at retention period of 120 min. This effect primarily due to reduction of paste content in SDC which increases particle interlocking of aggregates, and translate in to drop in flow, increase in V-Funnel , T<sub>500</sub>, Yield stress and viscosity values over period of 120 minutes.

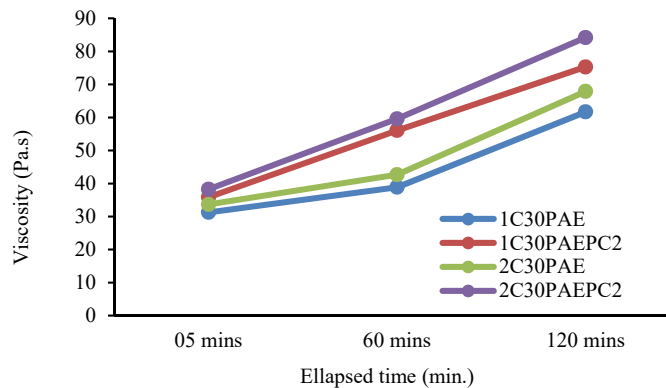


**Fig. 16** Effects of cement content reduction on Viscosity.

**STRENGTH AND DURABILITY**

Effects of different types of PCE polymers, increase in water content and reduction in cement content on the compressive strength is shown in Fig. 17-18. It may be noted that the increase in water content and reduction in cement content affects the strength to a large extent. The mixes with OPC 1 shows higher strength gain whereas that by OPC 2. This means that the type of OPC cement used have significant impact on strength gain properties.

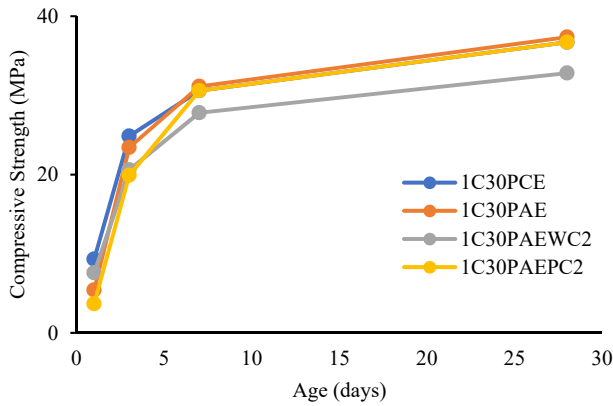


**Fig. 17** Compressive strength with OPC 1 Cement

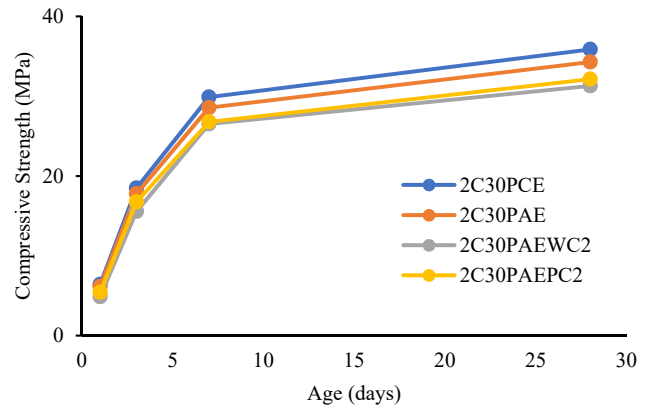


**Fig. 18** Compressive strength with OPC 2 Cement

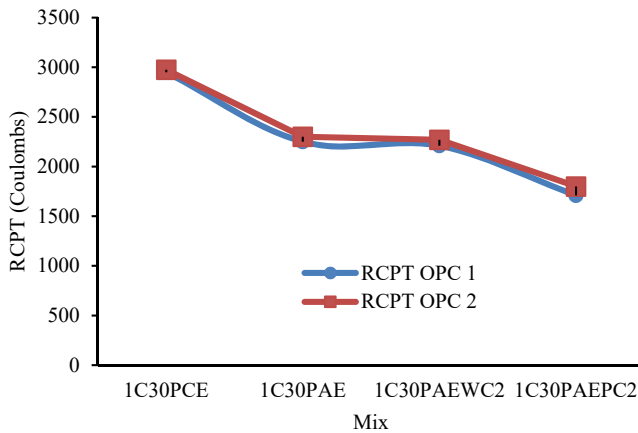


**Fig. 19** Effects of water content, PCE types and cement reduction on rapid chloride penetration value

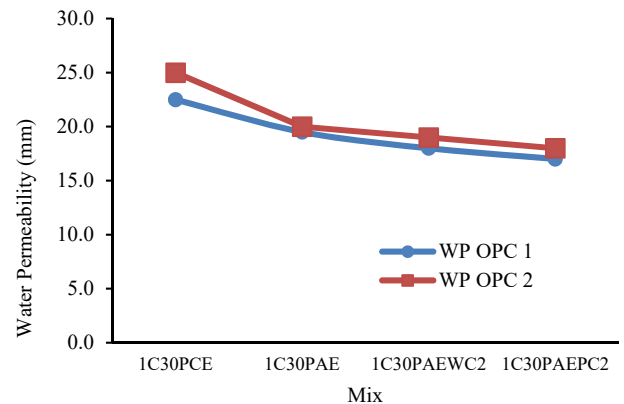


**Fig. 20** Effects of water content, PCE types and cement reduction on water permeability value

Effects of different types of PCE polymers, increase in water content and reduction in cement content on rapid chloride penetration value (RCPT) and water permeability (WP) parameters is indicated in Fig. 19-20. It is seen that the increase in water content and reduction in cement content decreases the durability results. This shows that the water to binder ratio and cement content are crucial parameters for durability point of view.

**CONCLUSIONS**

1. The slump flow for all SDC mixes in study is found to be 650+/-10 mm. This indicates the good deformability of the fresh concrete meeting SF 1 criterion for SCC.
2. The rheological retention property is increasingly becoming important since placement of concrete occurs between 1-3 hours which has different rheology as compared to that in 5-10 min measurement. This property in respect of Smart Dynamic Concrete highly depends upon the selection of polymer type. The structure and chemistry of the PCE governs the ability to hold rheology constant over time. Furthermore, the rheological properties and the demand

of super plasticizer (admixture) in respect of SDC are strongly dependent on the physical and chemical properties of the cement and the PCE structure.

3. The PCE 2 is a new class of chemical admixtures (Poly Acrylates Ether -PAE) which can reduce both, plastic viscosity and yield stress. The conventional water reducing PCE super plasticizers can reduce the yield stress
4. The low cement content mix in conjunction with PCE 2 can be an effective solution for designing an optimum performance based SDC for high rise construction owing to its rheological retention performance.
5. Rheology retention is highly depending on admixture dosages, reduction in PCE dosages for similar flow in higher water content SDC, will result in to poor rheology retention.
6. Reduction in cement content detoriates the rheological retention properties of SDC.
7. Increase in water content and decrease in cement content, reduces the compressive strength and durability of concrete.

## REFERENCES

- ACI 237 R (2007) (American Concrete Institute), "Self-consolidating concrete", Farmington hills, , USA, April 2007.
- ACHE (2008) Spanish Scientific – technical Association for Structural concrete, "Self-compacting concrete – Design and Application", (ACHE 2008), Spain.
- ASTM C 143(2009), (American standard testing methods), "Standard Test Method for Slump of Hydraulic-Cement Concrete". Annual book of ASTM standard, vol.04.02, USA.
- Bruce J. C. and Huebsch, C., (2012), "Solutions to support more sustainable construction practices", Special Publication, 289, 1-12.
- Bruce J. C. and Huebsch, C., (2012), "Solutions to support more sustainable construction practices", Special Publication, 289, 1-12.
- Bruno D'Souza and Hironobu Y., (2013), "Applications of Smart Dynamic Concrete", Third International Conference on Sustainable Construction Materials and Technologies, August 18-21, Kyoto Research Park, Kyoto, Japan.
- Corradi, M., Kluegge, J., Kar, N., Christensen, B. and Yang, J. (2007), "A new viscosity modifying agent (VMA) for low fines self-consolidating concrete.", 5th International RILEM Symposium on Self-Compacting Concrete., 2, 875-880.
- EFNARC (2005), The European guideline for self-compacting concrete (SCC): Specification for Production and Use, 68
- EN206 -9 (2010) (European committee for standardization), "Additional Rules for Self-compacting Concrete (SCC)", Avenue Marnix 17, B-1000 Brussels.
- Feys, D., Verhoeven, R., De Schutter, G. (2008) "Why is fresh self-compacting concrete shear thickening?", Cement and Concrete Research, 39 (6), 510-523.
- JSCE (Japan Society of civil engineers) (1999), "Recommendation for self-compacting Concrete", Tokyo, Japan, August 1999.
- PCI (2003) (Precast/Prestressed Concrete Institute), "Interim Guidelines for the Use of Self consolidating concrete in Precast/Prestressed Concrete Institute Member Plants, Chicago, USA.
- S.D. Bauchkar and H.S. Chore (2017), 'Experimental Studies on Rheological Properties of Smart Dynamic Concrete', Advances in Concrete Construction: An International Journal (Techno Press), 5 (3), 183-199.
- Seow, K.H., Kar, N. and Qiuling, F. (2011), "The Use of low fines self-consolidating concrete (SCC) in everyday applications to improve productivity", SCI Concretus Magazine (Singapore Concrete Institute), 3 (1), 4-6.
- Tattersall G.H., (1983), "Practical user experience with the two-point workability test", Report BS-74, Sheffield University; Department of Building Science.
- Mario Corradi, Jan Kluegge, Nilotpol Kar, Bruce Christensen and Jianying Yang (2007), "A new viscosity modifying agent (VMA) for low fines self-consolidating concrete.", 5th International RILEM Symposium on Self-Compacting Concrete., 2, 875-880.



## RESEARCH AND PRACTICE ON PROGRESSIVE COLLAPSE OF BUILDING STRUCTURES: A CRITICAL REVIEW

Hemkant Yadav,<sup>1</sup> S. M. Gupta,<sup>2\*</sup>

<sup>1</sup> M. Tech Student, Department of Civil Engineering, NIT Kurukshetra, Kurukshetra; hemkant Yadav94@gmail.com:

<sup>2\*</sup> Professor, Department of Civil Engineering, NIT Kurukshetra, Kurukshetra; hemkant Yadav94@gmail.com: (Corresponding Author)

### ABSTRACT

Phenomena of local failure of one or more erect load bearing elements due extreme events like terrorist attacks, explosion etc. pose a consequential threat, causing to the progressive collapse of a huge part or of the entire structure. Risk assessment of extreme events has been becoming a growing interest since early 21st century, particularly after the attacks of Alfred P. Murrah Federal Building (Oklahoma, 1995) following the attack on World Trade Centre (New York, 2001). This paper evaluates the current researches on this issue that have been done from late 20th century. Various aspects of progressive collapse are included with, including: (1) theoretical definitions given by researchers, (2) existing scenario and advancements in codes and design recommendations, (3) assessing the risk of progressive collapse, (4) investigational tests, (5) numerical simulation, and (6) research needs. This paper may come in handy for the professionals and researchers who wish to go in the field of progressive collapse of building structures.

**KEYWORDS:** Aspect Ratio; Progressive Collapse; Standoff Distance; High Performance Concrete; Beam Column Joint.

### INTRODUCTION

All types of building structures may be introduced to extreme events like to natural calamities like hurricanes, tsunamis, earthquakes or to the human activities explosions, vehicle clash or terrorist attacks. These events generally lead to localized failure of the building, which in turn lead to a thorough damage. This is what we say Progressive Collapse. Progressive collapse involves initial local damage causing a disproportionate collapse, but it is tough to give a quantitative expression to the terms 'local' and 'disproportionate'. When looked at progressive collapse as a structural engineer, probability of progressive collapse can be minimized by designing a building in such a way that it is robust, where robustness is termed as a measure of the performance of a structure in damaged state. However, it is difficult to assess progressive collapse quantitatively therefore, it is equally difficult to measure robustness of the building. It was assessed that around 20% of building collapses develop in a progressive mode by Leyendecker & Burnett in 1976. Since the attacks on the "Oklahoma Federal Building" in 1995 and the "World Trade Centre, New York" in 2001 by terrorists, the issue of progressive collapse engaged public consideration which indicates the need of robust building that can withstand the local damage preventing disproportionate failure. There is a great requirement of robust structure that can withstand an extreme event, maintaining functionality. As it is not easy to forecast the possibility of happening of risky events, as discussed above, it is very obvious that we cannot employ outmoded methods for conventional loads to design the structure to resist progressive collapse which will be neither practically sound nor possible. The most critical situation in a building structures is the collapse of erect load bearing member i.e. failure of walls and columns, which results in a consecutive failure of adjoining members as the failure propagates and finally results in the collapse of whole structure. There must be an alternate path for the load propagated to neighboring elements from the damaged element in order to avoid progressive collapse. If sufficient alternate paths are unavailable, progressive collapse will be certain. For framed buildings, to provide alternate load paths to mitigate the risk of progressive collapse, few mechanisms are: (1) sagging of the beam at the failure location of column. (2) "Vierendeel behavior" of the frame (see fig 1a).

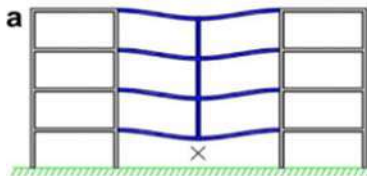
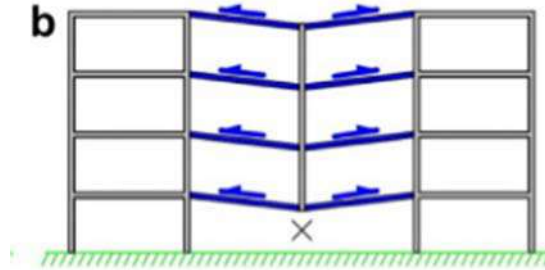


Fig 1a Vierendeel behaviour of frame.

(3) Arch effect of beams at failed column (effective mechanism for slight horizontal displacement of the adjacent columns). (4) Catenary or membrane action of beams and slabs, connecting the damaged column (see fig 1b) through large deformations.



**Fig 1b Catenary action of beams and slabs**

(5) Contribution of infill and partition walls (see fig 1c)

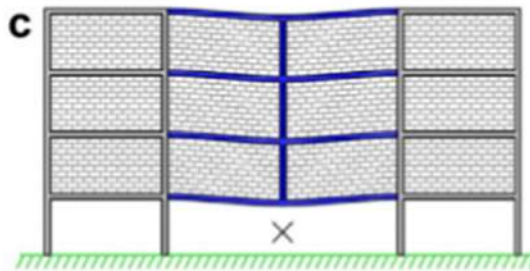


**Fig 1c infill and partition wall contribution**

Out of the above mentioned alternate load paths, most study has been done till date on the mechanism of catenary or membrane behavior of beams, as it is seem to be an vital mode of resistance against progressive collapse of the building.

## LITERATURE REVIEW

**Allen et al. (1972)** presented the need for a new consideration in structural design resistant to progressive collapse due abnormal load that cause a catastrophic failure of a huge part or the whole construction. They referred the phenomena of progressive collapse as the event in which localized failure leads to the collapse of adjoining members which further leads to the collapse of other adjoining members, so that pervasive failure takes place as an outcome of a localized failure. **Gross et al. (1983)** presented research work on the progressive collapse on a RCC precast panel building due to blast loading and gave recommendations for designing progressive collapse resistant buildings. In their research work progressive collapse is regarded as “the loss of load-carrying capacity of a relatively small portion of a structure due to an unusual load which triggers a series of failures affecting a key portion of the building structure.” **Robert et al. (2002)** presents the advancement of analysis of progressive collapse and assessment of damage procedure for incompletely collapsed structures. The resolution of these advancements is improving the safety of occupants in building when subjected to unusual loads. The developed analytical approaches will aid engineers to forecast the nature and range of potential progressive collapse in both the design stage as well as post incidents. **General Services Administration (GSA) (2003)** laid down rules for analysis of progressive collapse and design criteria for renovated and new federal buildings in Washington DC. It is proposed to take a steady level of safety in the design of progressive collapse to Federal facilities and to come up with an alignment with the suite of security standards issued by the “Interagency Security Committee (ISC)” and the “General Services Administration (GSA)”. According to GSA, progressive collapse is an event in which local failure of a major component of structure causes adjoining member collapse which, consecutively, leads to additional failure. **ASCE 7-05 (2005)** defined progressive collapse as a spread of primary localized failure from one element to another element and consequently the failure of whole structure or a huge part. ASCE 7-05 did not intend, at that time, for this standard to establish particular events that to be considered during design to minimize the risk of progressive collapse. **Ellingwood BR (2006)** defines “progressive collapse as a result of localized damage to structure and develops

in a mechanism of chain-reaction, into a failure that is disproportionate to the commencing local damage.” He did work on mitigation and assessment of the risk of progressive collapse. His presentation reviews design and risk-informed decision approaches for minimalizing the probability of progressive collapse, ascertains current research concerns, and recapitulates developments in application of common provisions in national standards such as ASCE Standard 7. **NISTIR 7396 (2007)** proposed to provide the best methods which are to be implemented to mitigate the risk of progressive collapse due to extreme loading. This involves describing threat, control of event and design of structure to withstand postulated event. This also discusses about alternate load path method (allowing alternate paths for progress of loads in case of failure of critical member) and the indirect method. **Krauthammer (2008)** provides a general background on the mechanism that cause them. The work subsequently incorporates the noteworthy dissimilarities between “conventional loads” and “nuclear loads” and between present design techniques and “state-of-the-art” information from current researches This concludes with an organized and balanced protective methodology of design. **Starossek et al. (2010)** presented a variety of terminology and procedures to define structural features and theories in reference of “disproportionate collapse” of buildings, namely “collapse resistance, robustness, and vulnerability as well as redundancy, continuity, ductility, and integrity”. Based upon, a general performance-based framework to resist or reduce the risk of disproportionate collapse is presented and the procedures available for improving the collapse resistance and robustness of a structure are discussed. **Kokot et al. (2012)** conducted a technical literature survey concerning the issues of robustness of building structure. This paper defines the event of progressive collapse as “the situation where local failure of a primary structural component leads to the collapse of adjoining members and to an overall damage which is disproportionate to the initial cause.” **Department of Defense (DoD) (2013)** provides the necessary design requirements to reduce the possibility of progressive collapse for new and existing facilities that experience localized structural damage through normally unforeseeable events. This code of practice recommends all buildings with three or more stories must comply with these standards. **El-Tawil S et al. (2014)** states that Progressive building collapse is a dynamic event with characteristics of inelastic behavior, large strains and contacts or impacts that occurs when failure of a critical member results in the failure and collapse of neighboring members, stimulating additional collapse. Non-linear models can provide more realistic and accurate results as compared to linear one. **Liu et al. (2015)** considered two loading situations- (1) immediate removal of an exterior column and (2) immediate removal of interior column and performed static and dynamic analysis to assess the resistance against progressive collapse of a multistoried reinforced concrete flat plate building deficient in structural integrity reinforcement in the slabs. The analysis shows that the buildings susceptible to the progressive collapse are the older flat-plate buildings; punching resistance increases significantly the combined effects of member action in compression and strain rate; energy-based nonlinear static analysis can estimate the “peak dynamic loading response” specifically for immediate exterior column removal. **ASCE 7-16 (2016)** provides minimum loads, hazard levels, associated criteria, and intended performance objectives for buildings, other structures, and their non-structural elements that are subject to building code requirements. The loads, load-combinations, and associated criteria provided in the code are to be used with design permissible stress-limits contained in the design specifications for conventional structural materials. Used altogether, they are supposed to be capable of providing the targeted performance levels for which the provisions of this standard have been established. **Sagaseta et al. (2017)** defines progressive collapse as the insensitiveness of a structure to local failure. This review paper showed that there are 4 accepted methods to design robust structure in general structures: (1) provision for tying force, (2) alternate load path methods, (3) critical element design and (4) risk-based methods. For low risk structures, it is recommended to use the tying force method. It is also revealed that to review detailing provisions for reliability-reinforcement numerical modelling of post-punching is a capable tool. **Liu-Lian et al. (2018)** conducted a FEM modelling of a steel frame to assess the behaviour of progressive collapse. To quantify the robustness of the frame taking dynamic effect into account, a new index has been introduced a new index has been introduced. The robustness and critical loads with a range of different parameters are investigated.

## EXPERIMENTAL TESTING

**Tests on 2D frames:** To get reliable results, the tests are done on building structure constructed exclusively for testing (called specimen). The results can be used as source for calibrating numerical modelling to simulate the progressive collapse behavior and also the results can be used to propose measures for design code recommendations.

For steel and composite frames, Guo et al. conducted tests on 1/3 scale frames. As a distinctive feature, portion of a concrete slab included in the specimen to analyze the response of composite beams post sudden removal of an intermediate column as shown in (fig 2). Hydraulic jacks were used to stimulate the load on intermediate column. The connections between beam and column were once kept rigid and in another test they were kept semi-rigid. In both the tests, the connections were quite efficient in resisting progressive collapse. The semi-rigid connections had weaker robustness than the rigid beam-column joints, as expected.



**Fig. 2.** View of a test by Guo et al. on a composite frame. Photo by courtesy of Lanhui Guo (Harbin Institute of Technology).

**Test on structures proposed for demolition:** The tests conducted by Song et al., comprising an abrupt failure of column at one of the corner. Song et al. accomplished their experiments on the Ohio Union Building, which was built in 1950 shown in (fig 3). Song et al. conducted their another tests on the three story “Bankers Life and Casualty Company building in Northbrook, Illinois” (built in 1968). The detected damage for both building structures was not much significant, hence it is concluded that those two buildings were sufficiently robust against progressive collapse. The point noted here was that both experiments were performed without the removal of the partition and external walls, which establishes their contribution in establishing alternative load paths.



**Fig. 3.** Testing of Ohio Union Building by Song et al. Photo by courtesy of Halil Sezen (Ohio State University).

## NUMERICAL MODELLING

The advantages of numerical simulation are that with the help of numerical simulation we can make a considerable financial savings. Amongst the modelling tools adopted to mimic the phenomena of progressive collapse, the below mentioned are prominent:

- (a) FEM (Finite Element Method): The most used technique currently at various levels and amount of estimation is FEM. The FEM enables modelling of macro-models (with solid elements), micro-models (with beam/shell elements) and hybrid models.
- (b) DEM (Discrete Element Method): Although very less attention is given to this method for aping the behavior of buildings during progressive collapse, its potentials are irrefutable. One of its predominantly remarkable feature is that it can combine both FEM and DEM techniques to achieve accurate and reliable results.
- (c) AEM (Applied Element Method): This is a recent technique being used increasingly in modelling of sub-assemblages as well as whole building and gives good results in techniques involving progressive collapse of building structure.
- (d) CEM (Cohesive Element Method): The method has been very little used to mimic the progressive failure of structure but proven very efficient for assessment of behavior of building structure in progressive collapse.

## CONCLUSIONS

This paper presents a go-getting assessment of the peak developments in the domain of the disproportionate and progressive collapse of building structures since seventies. Recent years have got significant advancement in this field. In accordance to the current necessity of robust-buildings that are capable of withstanding abnormal loads without getting collapsed, and even resilient buildings which could be functional after an extreme event. New design code recommendations to minimize the risk due to extreme loading have been formulated, while the already prevailing recommendations have been revised in accordance to the latest developments. The engineers are now wholly aware of the inevitable need for robust buildings. Nevertheless, this field still needs much advance to come up with more reliable results and design recommendation. Though, one issue that needs extra attention is the behavior of slabs considered in numerical simulation. Even though the slabs have a key involvement in resistance to progressive collapse, the present software do not have the feature for assignment of plastic-hinges to the shell type elements adopted in modelling, for instance, RC slabs. Although some engineers go for “non-linear shell type elements” in their analysis to approximate the effect which is not sufficient for assessing progressive collapse as there is no allowance to switch from flexural to membrane behavior.

## REFERENCES

- Allen De, Schriever Wr. (1972) “Progressive Collapse, Abnormal Loads and Building Codes. Québec: Division of Building Research Council.”
- Starossek U, Haberland M. (2010). “Disproportionate collapse: terminology and procedures”. *J Perform Construct Facil* 2010; 24(6):519–28
- Gross JL, McGuire W. (1983). “Progressive collapse resistant design.” *J Struct Eng* 1983; 109(1):1–15.
- Robert L. Hall, Stanley C. Woodson, James T. Baylot, John R. Hayes, Young Sohn (2002). “Development of Progressive Collapse Analysis” (2002)
- General Services Administration (GSA) (2003). “Progressive collapse analysis and design guidelines for new federal office buildings and major modernization projects.” Washington, DC: Office of Chief Architects; (2003)
- ASCE (American Society of Civil Engineers) (2005). Minimum design loads for buildings and other structures (ASCE/SEI 7-05). Structural Engineering Institute of the ASCE; 2005.
- ASCE (American Society of Civil Engineers) (2016). Minimum design loads for buildings and other structures (ASCE/SEI 7-16). Structural Engineering Institute of the ASCE; 2016.
- Ellingwood BR. (2006). “Mitigating risk from abnormal loads and progressive collapse.” *J Perform Constr Facil* 2006;20(4):315–23.
- NISTIR 7396 (2007). “Best practices for reducing the potential for progressive collapse in buildings. Gaithersburg.” National Institute of Standards and Technology
- Krauthammer T (2008). “Modern protective structures.” Boca Raton; CRC Press
- Kokot S, Solomos G. (2012). “Progressive collapse risk analysis: literature survey, relevant construction standards and guidelines.” Ispra: Joint Research Centre, European Commission
- DoD (Department of Defence) (2013). “Design of buildings to resist progressive collapse (UFC 4-023-03).” Washington, DC: Unified Facilities Criteria; 2013.

- El-Tawil S, Li H, Kunnath S. (2014). "Computational simulation of gravity-induced progressive collapse of steel-frame buildings: current trends and future needs." *J Struct Eng* 2014; 140(8):1–12.
- Peng Z, Orton SL, Liu J, Tian Y. (2014). "Experimental study of dynamic progressive collapse in flat-plate buildings subjected to exterior column removal." *J Struct Eng* 2017; 143(9):1–13.
- Buitrago M, Sagaseta J, Adam JM. (2018). "Effects of sudden failure of shoring elements in concrete building structures under construction." *Eng Struct* 2018; 172:508–22.
- GSA (General Services Administration) (2013). "Alternative path analysis and design guidelines for progressive collapse resistance." Washington, DC: Office of Chief Architects; 2013
- Sagaseta J, Ulaeto N, Russell J. (2017). "Structural robustness of concrete flat slab structures." *fib Bulletin 81, ACI SP-315*, published by Fédération internationale du béton (fib) and American Concrete Institute (ACI); 2017. p. 273–98.
- National Research Council of Canada. (1995) National building code of Canada. Canadian Commission on Building and Fire Codes
- NYC Department of Buildings. (2014) Building code (Chapter 16–Structural design). NYC Construction Codes.
- Danish Standards Association (DS/INF). (2003) "Robustness – Background and principles – Guidance – 2003". DS/INF 146
- COST (European Cooperation in the field of Scientific and Technical Research) (1995) Theoretical framework on structural robustness. COST Action TU0601
- (European Cooperation in the field of Scientific and Technical Research.) (2008) In: Robustness of structures – proceedings of the 1st workshop, COST Action TU0601. Switzerland: ETH Zurich
- CSA (Canadian Standards Association). (2004) Design of concrete structures (CSA A23. 3–04). CSA, Mississauga
- Chen Y-L, Huang L, Lu Y-Q, Deng L, Tan H-Z. (2016) "Assessment of structural robustness under different events according to vulnerability." *J Perform Constr Facil*
- Adam JM, Parisi F, Delatte NJ, Carper KL. (2017) "Using numerical models for the analysis of structural failures". In: IF CRASC'17. Milan
- BS 5975. (2011) Code of practice for temporary works procedures and the permissible stress design of falsework.
- Guo L, Gao S, Fu F, Wang Y. (2013) "Experimental study and numerical analysis of progressive collapse resistance of composite frames." *J Constr Steel Res* 2013; 89:236–51.
- Guo L, Gao S, Fu F. (2015) "Structural performance of semi-rigid composite frame under columns loss." *Eng Struct* 2015; 95:112–26.
- Song BI, Sezen H. (2013) "Experimental and analytical progressive collapse assessment of a steel frame building." *Eng Struct* 2013; 56:664–72.
- Song BI, Giriunas KA, Sezen H. (2014) "Progressive collapse testing and analysis of a steel frame building". *J Constr Steel Res* 2014; 94:76–83.



## Flexural Capacity of Corroding RC Elements Based on Gaussian Representation of Corrosion loss

S. Muthulingam\*

\*Assistant Professor, Department of Civil Engineering, Indian Institute of Technology Ropar, Rupnagar-140 001, INDIA  
Muthulingam.subramaniyan@iitrpr.ac.in (Corresponding Author)

### ABSTRACT

Chloride-induced steel reinforcing bars corrosion is a problem of worldwide importance because, in addition to massive industrialization, a majority of human population inhabit marine atmosphere zones where salinity is the main source of built infrastructure deterioration. Reinforced concrete structures vulnerable to chloride-induced corrosion potentially experience two stages of damage, namely non-structural and structural. Till date, with regard to non-uniform corrosion, there is very limited information regarding the significant role played by the non- structural stage of damage in influencing the progression of structural damage. The present work examines the process of non-uniform chloride ingress into concrete due to the existence of the steel bars and its influence on the spatial and temporal variations in the depth of corrosion penetration. Mathematical models in the form of Gaussian functions are proposed to represent space-time variation in corrosion initiation, spatial spread of corrosion penetration depth and corroded bar morphologies and are compared with literature data. An assessment of time-variant degradation in the flexural capacity of a corroding RC beam based on non-uniform corrosion is performed.

**KEYWORDS:** Concrete structures; Chlorides; Corrosion; Modelling.

### INTRODUCTION

Reinforced concrete (RC) structures exposed to aggressive chloride environments such as seawater, salt-spray, and de-icing salt are highly vulnerable to premature deterioration, long-or short-term maintenance intervention, and safety failure. This is a matter of concern, especially in the present context of heavy industrialization and increasing human habitation along coastal zones where salinity is the primary source of built infrastructure deterioration. The most widely investigated potential cause is the chloride-induced corrosion of steel bars embedded in concrete. In general, service life models of RC structures represent the corrosion process by two distinct stages, namely a corrosion initiation stage and a corrosion propagation stage (Tuutti, 1982). During the former, RC incurs non-structural damage in the form of depassivation and its length is designated by a single parameter  $T_i$ , time-to-corrosion initiation (years), which is defined as the time for the chloride ions to attain a critical value at the level of the steel bar (Arora, Popov, Haran, Ramasubramanian, Popova and White, 1997). In the latter, RC sustains severe structural damages such as reduction in the sectional area of steel, concrete cover cracking, delamination, and spalling (Bhargava, Mori and Ghosh, 2011).

Owing to the impermeable nature of the steel bars, the chloride ions would display variations, both spatially and temporally, along the circumference of the metal surfaces. That is, the content of chloride ions would be higher on the surface of the bar facing the external chloride environment and progressively decrease as they evolve towards the metal surface facing the interior of concrete. This being the real situation, numerous studies (e.g. Pantazopoulou and Papoulia, 2001; Bhargava, Ghosh, Mori and Ramanujam, 2003) assume uniform corrosion initiation, which implies simultaneous depassivation along the entire metal surface at a single point in time. In recent years, more attention has been paid towards investigating the corrosion propagation stage. However, in most cases, the models assume uniform depth of corrosion penetration along the circumference of the steel bar (e.g. Bhargava, Mori and Ghosh, 2011; Pantazopoulou and Papoulia, 2001; Val, Chemin and Stewart, 2009; Chen and Mahadevan, 2008). Contrary to this assumption, recent investigations reveal non-uniform corrosion pattern as the actual situation (e.g. Zhao, Hu, Yu and Jin, 2011; Zhao, Karimi, Wong, Hu, Buenfeld and Jin, 2011; Liu and Li, 2004). The present work focuses on this point by examining the process of non-uniform chloride ingress into concrete due to the existence of the steel bars and its influence on the spatial and temporal variations in the depth of corrosion penetration. Mathematical models in the form of Gaussian functions are proposed at every stage of the corrosion process and compared with laboratory and field data available in the literature. Further, an assessment of the time-variant degradation in the flexural capacity of a corroding RC beam based on Gaussian representation of corrosion layer is presented.

## CORROSION PROCESS MODELING

Under natural exposure condition, one of the effect ways to model the chloride ingress process is to consider it as an interaction between three physical phenomena, namely heat transfer, moisture diffusion, and chloride ingress (Saetta, Scotta and Vitaliani, 1993; Martin-Perez, Pantazopoulou and Thomas, 2001). Each of these physical phenomena is represented by means of a field equation, and their interaction is considered by solving them simultaneously using a numerical approach—a combination of finite element (FE) and finite difference scheme. The field equations along with the numerical method adopted for solving them are detailed elsewhere (Muthulingam and Rao, 2014; Muthulingam and Rao, 2015) and will not be dealt here. During corrosion propagation, the depth of corrosion penetration,  $p_d$  (in mm), represents the time-variant corrosion loss of the steel bars. Note that, based on Faraday’s law,  $p_d$  can be estimated as follows (Rodriguez, Ortega, Casal and Diez, 1996):

$$p_d(t) = \int_{T_i}^t 0.0116 i_c(t) dt \quad (1)$$

where  $t$  indicates exposure period in years and  $i_c(t)$  represents time-variant nature of the corrosion rate in A/cm<sup>2</sup>. An accurate and realistic model of  $i_c$  is critical for evaluating the extent of structural damage, or in other words, for estimating the service life of RC structures during the corrosion propagation stage. Since,  $i_c$  under natural exposure condition is influenced by various factors such as cover depth, chloride content, water-to-binder ratio, levels of humidity and temperature, etc., various prediction models have been proposed in the literature considering one or more of these factors. In this work,  $i_c$  is evaluated by the following equation (Vu and Stewart, 2000):

$$i_c(t) = \frac{32.13 [1-(w/b)]^{-1.64}}{C_d} (t - T_i)^{-0.29} \quad (2)$$

where  $w/b$  represents water-to-binder ratio and  $C_d$  indicates cover depth (in cm), which measures the distance between the exterior face of the concrete to the surface of the reinforcing bar. By substituting Eq. (2) into Eq. (1),  $p_d$  can be evaluated as a function of time.

The models used to investigate corrosion initiation and propagation stages are cast into an FE framework, which sequentially solves the space-time evolution of the physical variables such as temperature, humidity, and chloride at incremental time steps along with the corrosion loss estimates of steel bars. The important aspects of the FE procedure include discretizing of the chosen computational domain with appropriate FE and enforcing pertinent boundary conditions explicit to the type of physical problem under consideration.

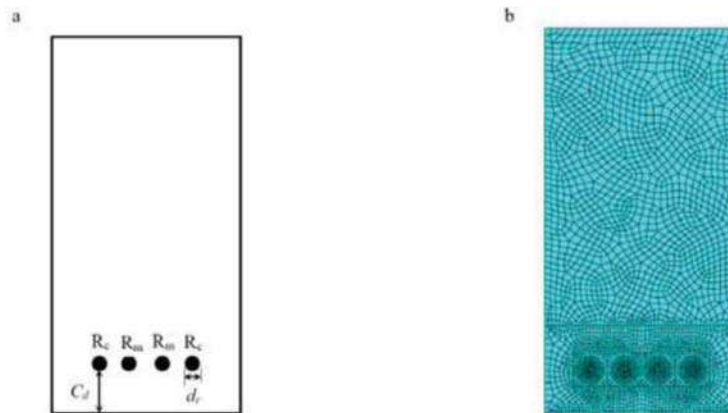


Fig. 1. Geometry of the RC element and finite element discretization

In the current work, a cross-section of an RC beam section of size 350 mm×700 mm is chosen as the domain (see Fig. 1a). This RC beam embeds four reinforcing bars on its tension face and they, based on their positions, can be classified either as a corner bar,  $R_c$  or a middle bar,  $R_m$ . Further in Fig. 1a,  $C_d$  is the cover depth (in mm) and  $d_r$  represents virgin diameter of the reinforcing bar in mm. Moreover, the RC beam as well the reinforcing bars are discretized with a four-

noded quadrilateral element having an edge size of approximately 5 mm (see Fig. 1b). During numerical simulation, cover depths (25–75 mm) and reinforcing bar sizes (12, 16, 20, and 25 mm) are considered as variables. Note that a water-to-binder ratio ( $=0.5$ ) is considered for numerical analyses. The simulation variables corresponding to a particular result sequence, presented in the following sections, are identified as  $R_c/R_m - d_r - C_d$ . For instance, the simulation variable  $R_m-20-50$  corresponds to the numerical analysis pertaining to a middle reinforcing bar  $R_m$ , bar size  $d_r=20$  mm, and cover depth  $C_d=50$  mm. Finally, simulations are conducted over a period of hundred years adopting the numerical procedure detailed in (Muthulingam and Rao, 2015), and the evolution of temperature, humidity, chloride content and depth of corrosion penetration are traced at every incremental time step equal to one day.

## CORROSION INITIATION STAGE

Fig. 2a illustrates the effects of  $C_d$  on space-time propagation of corrosion initiation along the circumferences of  $R_m$  and  $R_c$ . For illustration purposes, the values of  $C_d$  are taken as 25, 35, 45, and 55 mm while  $d_r$  is kept constant equal to 12 mm. As shown in Fig. 2a, on the time scale of 100 years, an increase in  $C_d$  delays space-time propagation of  $T_i$  in both  $R_m$  and  $R_c$ . This is because an increase in cover depth increases the distance between the face of RC beam and the reinforcing bar thereby increasing the time required for chlorides to reach the threshold value at the bar level. Further, Fig. 2b shows that a rise in  $d_r$  size also affects  $T_i$ , specifically for  $R_m$ . An increase in size, especially for  $R_m$ , magnifies the area of obstruction for the chloride ions to pass through; hence, chlorides keep mounting over time in front of the bar leading to quicker corrosion initiation.

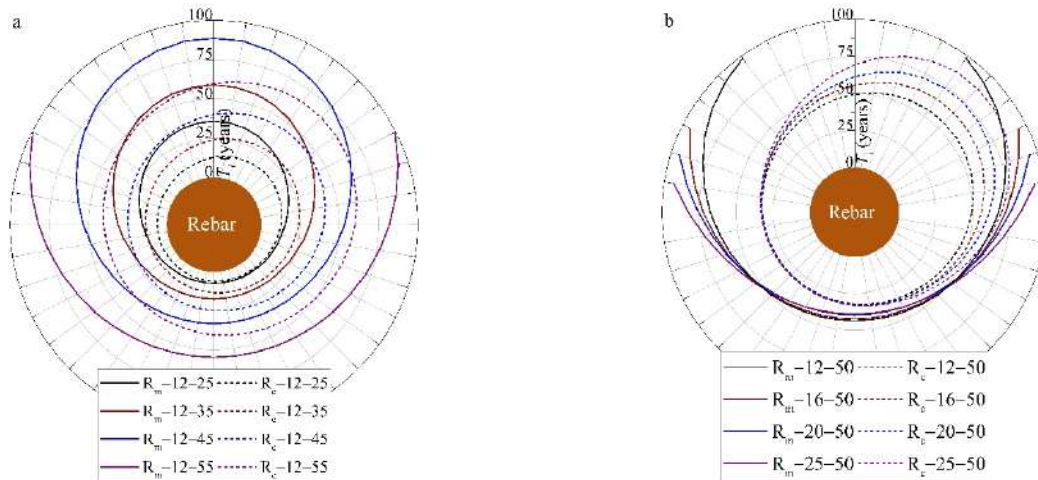


**Fig. 2. Space-time propagation of non-structural damage: (a) Influence of  $C_d$ ; (b) Influence of  $d_r$**

The space-time propagation of  $T_i$  data in Figs. 2a and b were fitted with several forms of mathematical equations such as Gaussian, elliptical, and semi-elliptical, and it was found that an equation based on a Gaussian function is more appropriate to describe  $T_i$  evolutions along steel bar perimeters:

$$T_i = \frac{\vartheta_1}{\vartheta_2 \sqrt{2\pi}} e^{-\frac{(\theta-180)^2}{2\vartheta_2^2}} + T_i^1 \quad (3)$$

where  $\vartheta_1$  and  $\vartheta_2$  represent regression parameters. In Eq. (3), first part describes the nonuniform component of a profile while the second part refers to the uniform component of a  $T_i$  profile. Hence, the proposed Gaussian model could be interpreted as a superposition of uniform and non-uniform components of a value of  $T_i$  evolution.

To illustrate that the Gaussian model can best represent the space-time propagation of  $T_i$ , corrosion initiation profiles shown in Figs. 2a and b each representing either the effects of  $T_i$  on  $C_d$  or  $d_r$  are chosen. Figs. 3a and b show the distribution of selected  $T_i$  profiles data superposed with trend lines drawn through the data points using the proposed model. It can be seen that the regression analysis provided best-fits for all types of  $T_i$  profiles with estimated R-Square values higher than 0.99, which show the presence of a very strong linear relationship between the simulation and

regression data. Hence, it is clear that the proposed Gaussian model can best represent variation of  $T_i$ . Further, Table 1 lists the values of regression parameters  $\vartheta_1$  and  $\vartheta_2$  along with their corresponding  $T_i^1$  and R-Square values for the simulation variables conforming to Figs. 3a and b. Note that an unknown variable X is used in the first column of Table 1 to relate the simulation variable with either  $R_c$  or  $R_m$ .

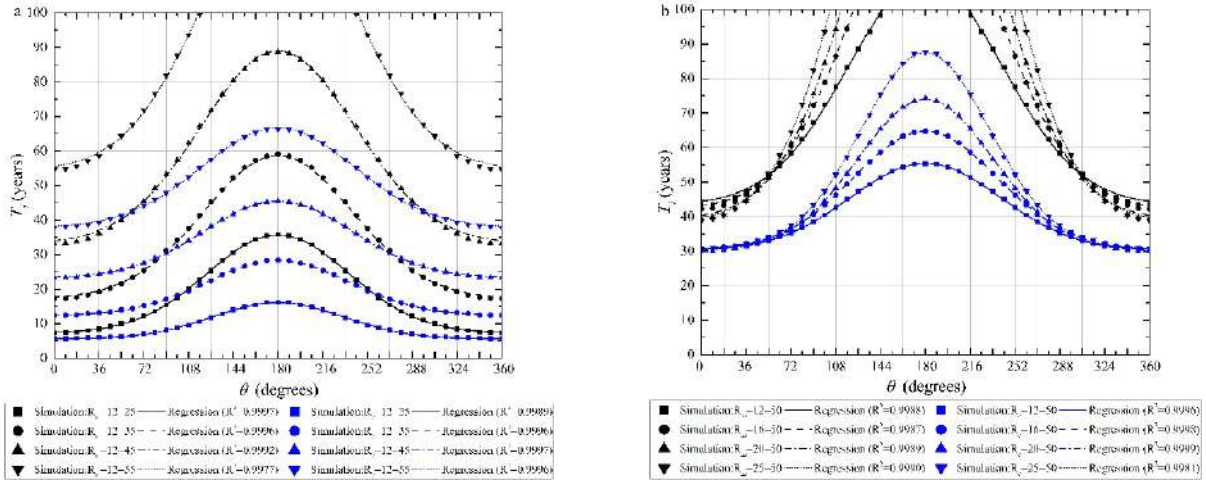


Fig. 3. Regression analysis of the proposed Gaussian model on the data points of  $T_i$

Table 1. Values of  $\vartheta_1$  and  $\vartheta_2$  obtained from regression analysis of  $T_i^1$  data

Variable	$T_i^1$ (years)		$\vartheta_1$		$\vartheta_2$		$R^2$	
	X= $R_c$	X= $R_m$	X= $R_c$	X= $R_m$	X= $R_c$	X= $R_m$	X= $R_c$	X= $R_m$
X-12-25	5.6	7.3	1387.74	4053.65	52.78	56.83	0.9990	0.9998
X-12-35	12.4	17.3	2285.31	6217.32	57.37	59.71	0.9996	0.9996
X-12-45	23.3	33.2	3318.32	8683.87	59.55	61.98	0.9997	0.9993
X-12-55	37.8	54.5	4465.81	11969.65	61.68	61.61	0.9996	0.9978
X-16-50	30.2	43.4	3819.82	10269.65	60.23	62.35	0.9996	0.9988
X-20-50	30.6	42.2	4953.87	13800.39	57.70	59.27	0.9999	0.9987
X-25-50	30.1	39.4	5982.48	17337.68	54.24	58.12	0.9999	0.9989
X-25-50	30.7	38.7	7390.81	21578.86	51.80	57.14	0.9998	0.9990

## CORROSION PROPAGATION STAGE

### Depth of Corrosion Penetration

Figs. 4a and b display the spatial spreads of the depths of corrosion penetration along the circumference of the bars pertaining to the simulation variables listed in Table 1 after the exposure period of 50 years. The following characteristics of the depth of corrosion penetration can be derived from Figs. 4a and b: (1) its spread is spatially non-uniform and is either incomplete or complete along the circumference of the bars; (2) the location of occurrence of its maximum value is influenced by the position of steel bars in an RC beam; (3) the extent of its spread along the surface of  $R_c$  is always larger when compared with that for  $R_m$ , and (4) the sizes of bar also affect its propagation. Depending on the period of exposure after corrosion initiation (i.e.  $t$ ), the value of  $p_d$  is expected to be maximum at the location of  $T_i^1$  (see Fig. 3) and the minimum value of  $p_d$  (i.e. in mm) is likely to fall either at the location of where  $T_i$  is maximum or at any other location on the circumference of the bar having  $t - T_i^1 = 0$ . Under these conditions, a flipped Gaussian form is one of the feasible choices for determining the trends of  $p_d$  data, and thus the following equation is proposed:

$$p_d = \frac{-\chi_1}{\chi_2\sqrt{2\pi}} e^{-\frac{(\theta-180)^2}{2\chi_2^2}} + p_d^{max} \quad (4)$$

where  $\chi_1$  and  $\chi_2$  represent non-linear regression parameters.

Note that Eq. (4) represents only the spatial evolution of  $p_d$  at a single point in time. To estimate the value of regression parameters, standard smooth curve fitting analyses are conducted over the data points of  $p_d$  concerning the simulation variables shown in Figs. 4a and b by employing Eq. (4). Figs. 5a and b display the trend lines based on Eq. (4) superimposed over the data points of  $p_d$ . It could also be noted that the fitting analysis yielded R-Squared values of 0.99 and higher, indicating that the predictions based on Eq. (4) are very close to the values obtained from simulation data.

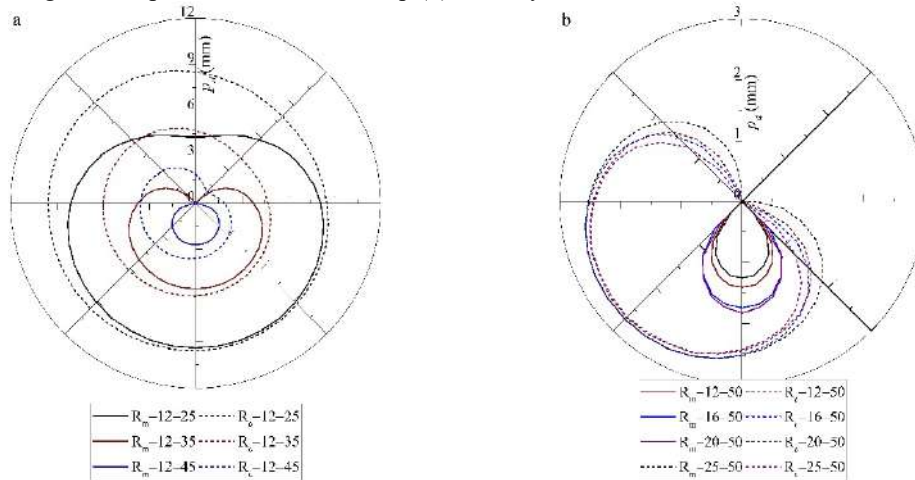


Fig. 4. Spatial spread of  $p_d$  after 50 years of exposure: (a) Effect of  $C_d$ ; (b) Effect of  $d_r$

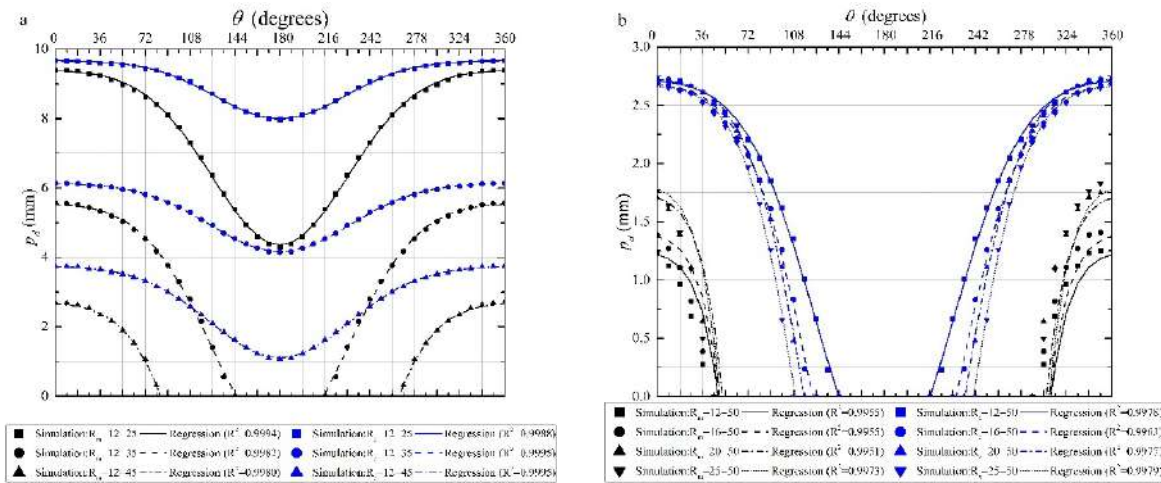


Fig. 5. Best-fits of the proposed Gaussian model on the simulation data points of  $p_d$  after the exposure period of 50 years: (a) Effect of  $C_d$ ; (b) Effect of  $d_r$

### VARIATION IN CORROSION LOSS

From Figs. 6a and b, based on the patterns of the corroded bars, two different types of non-uniform corrosion morphologies of the reinforcing bars can be characterized, namely morphology-I and morphology-II (see Figs. 6a and b). Morphology-I and morphology-II correspond to patterns of corroded bars where the corrosion losses are uneven and are either spread partly or entirely along the circumference of the reinforcing bar, respectively. To determine the trends in spatial variations of corroded rebar diameter ( $d_{cr}$ , mm) along the surface of the bar, once again, a Gaussian form is adopted as follows:

$$d_{cr} = \frac{\chi_1}{\chi_2\sqrt{2\pi}} e^{-\frac{(\theta-180)^2}{2\chi_2^2}} + d_{cr}^{min} \quad (5)$$

To validate that the patterns of corroded bars follow the Gaussian model in Eq. (5), macroscopic specimens reported in (Liu and Li, 2004) are considered. For validation purposes  $d_{cr}$  data of four specimens (L&L 1–4) reported in (Liu and Li, 2004) are subjected to regression analysis based on Eq. (5). Figs. 7a–d show the trend lines drawn over the data points of  $d_{cr}$ , and Table 2 gives the values of regression parameters obtained from the regression analysis. As can be observed from Table 2, all the four macroscopic specimens data are very consistent with the Gaussian form.

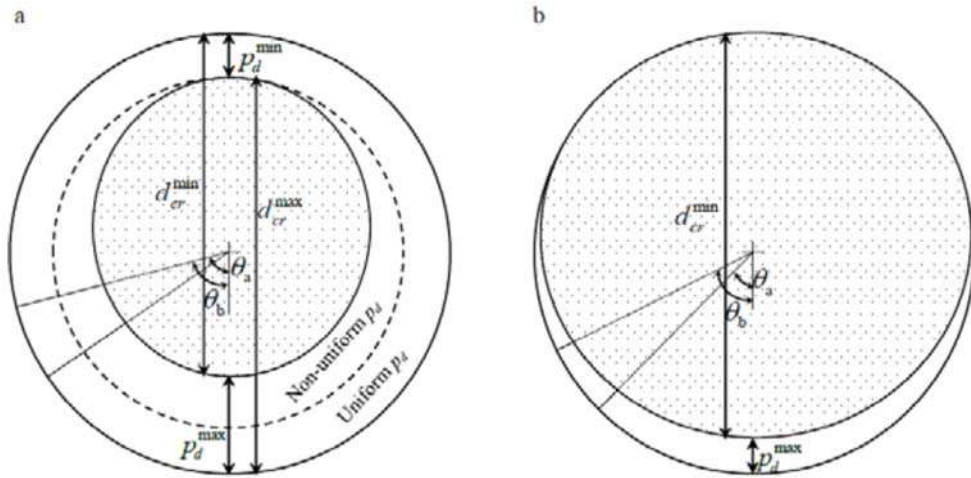


Fig. 6. Classification of corrosion patterns: (a) Morphology-I; (b) Morphology-II

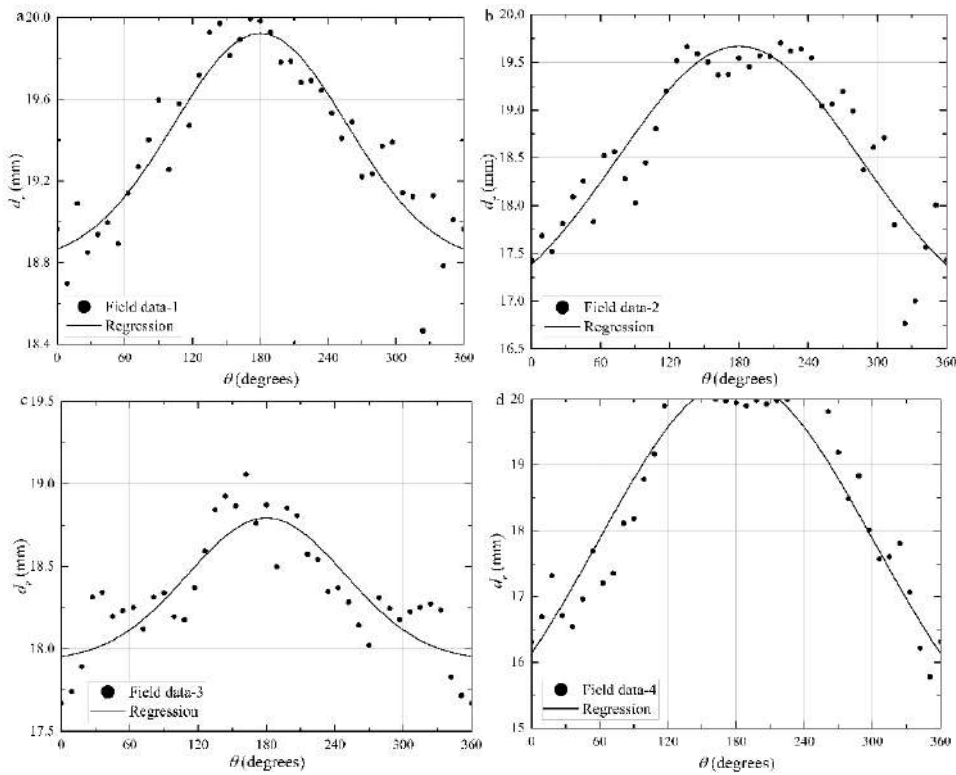


Fig. 7. Regression analysis of the proposed Gaussian model over the experimental data of Liu and Li, 2004

**Table 2. Values of  $\chi_1$  and  $\chi_2$  obtained from regression analysis of field data (Liu and Li, 2004) of  $d_{cr}$**

Specimen	$d_{cr}^{min}$ (mm)	$\chi_1$	$\chi_2$	$R^2$
L&L 1	18.79	215.98	76.42	0.8670
L&L 2	16.69	784.26	105.07	0.8354
L&L 3	17.92	150.60	69.05	0.7168
L&L 4	14.09	1875.45	120.76	0.9089

## FLEXURAL CAPACITY ESTIMATION

The time-variant flexural capacity of the corroding RC beam ( $M_{uR}$ , Nmm) due to the net reduction in the cross-sectional areas of the longitudinal rebars can be given by:

$$M_{uR}(t) = f_s A_s(t) \left( 1 - z_2 \frac{f_s A_s(t)}{z_1 z_3 f_c b d_e} \right) d_e \quad (6)$$

The value of  $z_1$  (conversion factor for compressive stress block of concrete) for a parabolic-rectangular stress block is 0.81. The value of  $z_2$  (ratio of the depth of centroid of the stress block to the depth of neutral axis) for a parabolic-rectangular stress block is 0.42. The value of  $z_3$  (ratio of the compressive strength of concrete in the girder to that of the design cube compressive strength of concrete) was taken as 0.67, which is based on the size factor equal to 0.85 while using cylinder compressive strength, and the conversion of cylinder strength to cube strength.

Eq. (6) relates the time-variant flexural capacity of the corroding RC beam with the time-variant cross-sectional area of the longitudinal rebars. Fig. 8 shows the time-variant flexural capacity of the RC beam, for various combinations of cover thickness (25 and 30 mm) and rebar diameter of 20 mm. The corrosion reaction sets in first around the steel-concrete interfaces of corner bars than the middle bars. The values of  $M_{uR}(t)$  show a clear change in slope, when the middle bars start corroding. This change in slope indicates increased reduction in the values of  $M_{uR}(t)$ .

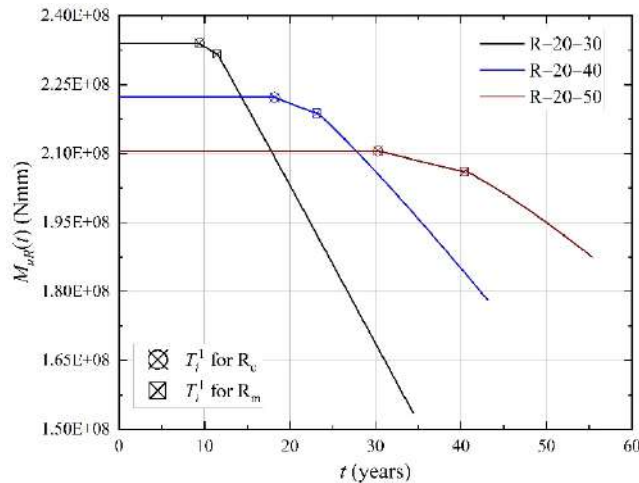


**Fig. 8. Time-variant flexural capacity of the RC beam**

## CONCLUSION

The following conclusions have been drawn from this study:

1. A Gaussian function is found to be more appropriate to describe  $T_i$  evolutions along steel bar perimeters due to non-uniform chloride ingress into concrete.
2. The spatial spread in corrosion loss of steel bars is quantified in terms of corrosion penetration depth considering the space-time propagation in  $T_i$  and observed to have greater affinity for yet another Gaussian model.

3. Based on the patterns of the corroded bars, two different types of non-uniform corrosion morphologies of the reinforcing bars are characterized, namely morphology-I and morphology-II, and are also observed to follow a Gaussian trend.
4. Time-variant reductions in flexural capacity of the RC beam are also estimated. It shows a clear change in slope, when the middle bars start corroding indicating increased reduction in flexural capacity.

## ACKNOWLEDGEMENT

The authors gratefully acknowledge the support provided by Science and Engineering Research Board, Department of Science and Technology, Government of India (No. ECR/2016/001611).

## REFERENCES

- Arora, P., Popov, B. N., Haran, B., Ramasubramanian, M., Popova, S., and White, R. E. (1997). "Corrosion initiation time of steel reinforcement in a chloride environment—A one dimensional solution." *Corrosion Science*, 39(4), 739-759.
- Bhargava, K., Ghosh, A. K., Mori, Y., and Ramanujam, S. (2003). "Analytical model of corrosion-induced cracking of concrete considering the stiffness of reinforcement." *Struct Eng Mech*, 16(6), 749–769.
- Bhargava, K., Mori, Y., and Ghosh, A. K. (2011). "Time-dependent reliability of corrosion-affected RC beams – Part 1: Estimation of time-dependent strengths and associated variability." *Nuclear Engineering and Design*, 241(5), 1371–1384.
- Chen, D., and Mahadevan, S. (2008). "Chloride-induced reinforcement corrosion and concrete cracking simulation." *Cement Concrete Comp*, 30(3), 227–238.
- Liu, Y. D., and Li, Y. H. (2004). "Mechanistic model and numerical analysis for corrosion damage of reinforced concrete structure." *Int J Fracture*, 126(1), 71–78.
- Martin-Perez, B., Pantazopoulou, S. J., and Thomas, M. D. A. (2001). "Numerical solution of mass transport equations in concrete structures." *Comput Struct*, 79(13), 1251–1264.
- Muthulingam, S., and Rao, B. N. (2014). "Non-uniform time-to-corrosion initiation in steel reinforced concrete under chloride environment." *Corrosion Science*, 82(0), 304–315.
- Muthulingam, S., and Rao, B. N. (2015). "Non-uniform corrosion states of rebar in concrete under chloride environment." *Corrosion Science*, 93(0), 267–282.
- Pantazopoulou, S. J., and Papoulia, K. D. (2001). "Modeling cover-cracking due to reinforcement corrosion in RC structures." *J Eng Mech Div-Asce*, 127(4), 342–351.
- Rodriguez, J., Ortega, L. M., Casal, J., and Diez, J. M. "Corrosion of reinforcement and service life of concrete structures." *Proc., Durability of Building Materials and Components 7*, 117–126.
- Saetta, A. V., Scotta, R. V., and Vitaliani, R. V. (1993). "Analysis of chloride diffusion into partially saturated concrete." *ACI Struct. J.*, 90(5), 441–451.
- Tuutti, K. (1982). *Corrosion of steel in concrete*, Swedish Cement and Concrete Research Institute, Stockholm, Sweden.
- Val, D. V., Chemin, L., and Stewart, M. G. (2009). "Experimental and Numerical Investigation of Corrosion-Induced Cover Cracking in Reinforced Concrete Structures." *J Struct Eng-Asce*, 135(4), 376-385.
- Vu, K. A. T., and Stewart, M. G. (2000). "Structural reliability of concrete bridges including improved chloride-induced corrosion models." *Structural Safety*, 22(4), 313–333.
- Zhao, Y. X., Karimi, A. R., Wong, H. S., Hu, B. Y., Buenfeld, N. R., and Jin, W. L. (2011). "Comparison of uniform and non-uniform corrosion induced damage in reinforced concrete based on a Gaussian description of the corrosion layer." *Corrosion Science*, 53(9), 2803–2814.
- Zhao, Y., Hu, B., Yu, J., and Jin, W. (2011). "Non-uniform distribution of rust layer around steel bar in concrete." *Corrosion Science*, 53(12), 4300–4308.



## Seismic Response of R.C.C unsymmetrical buildings with Brick masonry infill wall using “Equivalent diagonal strut method” as per IS 1893:2016

Nitin<sup>1</sup>, S.K.Madan<sup>2\*</sup>

<sup>1</sup>M.Tech Scholar, Department of Civil Engineering, NIT Kurukshetra, Kurukshetra, Haryana, India 136119; e-mail: jindal493@gmail.com

<sup>2\*</sup>Professor, Department of Civil Engineering, NIT Kurukshetra, Kurukshetra, Haryana, India 136119; e-mail: skmadan62@yahoo.co.in (Corresponding Author)

### ABSTRACT

RC frames with infill walls are usually analyzed and designed as bare frame without considering the strength and stiffness contribution of infill. Masonry infilled walls are treated as non-structural elements and these are not considered during the analysis & design of the structure. However, it has been observed that ignoring this element can lead to inaccurate predictions of the system's behavior. For seismic analysis of a framed building with masonry infill walls, it is necessary to model the effect of the walls on the lateral stiffness and strength of the building. In the present study the influence of brick masonry infill wall on the seismic response of RCC unsymmetrical buildings is studied. Equivalent strut methodology given by IS 1893:2016 (part-1) is used to model the infill walls. Linear dynamic Response spectra analysis of building model is performed in ETABS software. Analysis has been carried out for RCC unsymmetrical six storeys and eleven storeys building with, without and partially infill walls in order to access their contribution in seismic response of RCC unsymmetrical buildings during earthquake. The performance of the building is evaluated in the terms of storey drift, lateral deflection, storey stiffness, base shear and overturning moment.

**Keywords:** Equivalent diagonal strut method, lateral force, Masonry infill walls, Stiffness.

### INTRODUCTION

Nowadays, due to the increase in population & industries the development of building in horizontal direction is limited. So it has become important to increase building dimension in vertical direction as multi-storey building for best utilization of land. By increasing the number of floors of building in vertical direction floor area without increase in land area where building is constructed. Generally, infill masonry RC frames are constructed in India, where the probability of occurrence of an earthquake is high. In India multistory buildings are constructed to accommodate parking, shops, gym & reception etc on ground floor which leads to first storey as open storey or soft storey but it is vulnerable to collapse. The IS 1893:2016 (part-1) defines soft storey as one in which the lateral stiffness is less than that in the storey above. Masonry infill panels are constructed in multistory building for aesthetic and architectural purpose and are being considered as non structural member and consider it as the only dead load on supporting beams. But contrary to this past studies has been shown that these characteristics of the infill walls have a significant influence on the global response of the structure due to seismic loads. Moreover, if the masonry infill panels present in all stories of the structure then it contributes to the energy dissipation capacity, decreasing the lateral displacement and increasing the resistance to lateral forces.

Every structural element present at any storey contributes to the lateral stiffness of that storey. Hence the combination of the lateral stiffness of individual structural elements of any storey will give stiffness of that storey. Moreover, Masonry infill possesses significant in-plane stiffness and strength and hence contributes to the overall stiffness and strength of the building. Different Method based upon analytical and experimental research is used to calculate In-plane stiffness and strength of infill panel. According to IS 1893:2016 unreinforced masonry infill panel shall be modeled as an Equivalent diagonal strut. Model suggested by IS code is based on following assumptions a) connection between RC frame and strut is pin-jointed; b) empirical formula is given to calculate the width of diagonal strut; and c) if both the ratio of height to thickness & length to thickness of infill panel are less than 12 then thickness of strut is original thickness of panel and code is silent if the above requirement is not fulfilled. Strength and stiffness of infill panel reduce when openings are present. IS code recommended not to reduce the width of the equivalent diagonal strut if openings are present.

In present study static analysis has been carried out for the bare frame, fully infill frame, infill frame with soft ground storey and infill wall has been modeled by equivalent diagonal strut method. Second stage analysis and design has been carried out by software ETABS 2016 then different parameters has been computed.

## METHODOLOGY

A number of models based on finite element technique have been developed and used to evaluate the response of masonry infill frame. But to use these models in real life is too difficult and time consuming. Therefore based on various factors that govern the response of masonry infill panel an accurate macro model is needed. In present study macro modeling of infilled frame using equivalent diagonal strut has been done by replacing the masonry walls with the diagonal struts (or diagonal compression member) with appropriate mechanical properties. Connection between diagonal strut and frame is considered as pinned jointed. The thickness of the strut is equal to the thickness of the masonry wall and the equivalent width of the strut as per IS-1893:2016 is given by the expression:

$$W_{ds} = 0.175 \alpha_h^{-0.4} L_{ds} \quad \text{----- (Equation no. 1)}$$

$$\alpha_h = h \{ (E_m t \sin 2\theta / 4E_f I_c h)^{1/4} \}$$

$$E_m = 550 f_m$$

$$f_m = 0.433 f_b^{0.64} f_{mo}^{0.36}$$

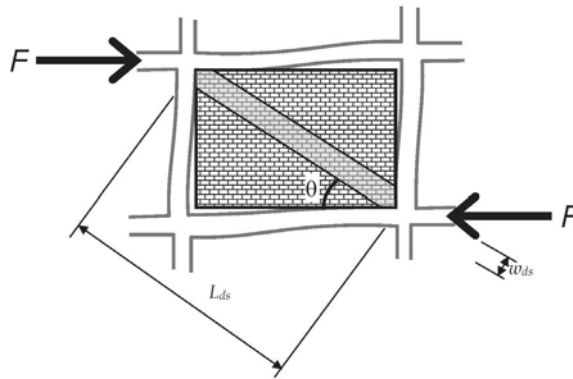


Figure 1: Equivalent diagonal strut model of URM infill wall.

Where,

$W_{ds}$  - width of diagonal strut .

$L_{ds}$  - length of diagonal strut.

$E_m$  - Modulus of elasticity of masonry infill (MPa).

$E_f$  - Modulus of elasticity of frame material (MPa).

$I_c$  - Moment of inertia of column ( $mm^4$ ).

$h$  - Clear height of URM infill wall between top beam and bottom floor slab(mm).

$\theta$  - Slope of diagonal strut to the horizontal (in degrees).

$f_m$  - compressive strength of masonry prism(MPa) obtained as per IS 1905.

$f_b$  - compressive strength of brick, in MPa.

$f_{mo}$  - compressive strength of mortar, in MPa .

$t$  - Thickness of infill wall = Thickness of diagonal strut (mm).

## Modeling

In this study two building frames of six and eleven storey having unsymmetrical plan shown in fig. 2 with storey height of three meters are modeled using different configuration of masonry infill that includes bare frame, frame with fully infilled masonry walls, partially masonry infilled frame (Masonry infill wall is considered alternatively in ground storey)

and frame with soft storey using ETABS software. Dimensional properties are given as shown in table-2 and material properties are defined as shown in table-1. Different models of eleven storey RC frame considered for analysis are shown in Figs. 2 - 5.

**Table 1: Material Properties**

Properties	Materials		
	Concrete	Steel Reinforcement	Brick Masonry Infill
Grade/Compressive Strength (N/mm <sup>2</sup> )	M30	Fe 415	10.5
Density (kN/m <sup>3</sup> )	25	76.82	20
Modulus of elasticity (N/mm <sup>2</sup> )	27386.13	200000	2457.04
Poisson's ratio	0.2		0.2
Coefficient of thermal expansion (°C)	0.0000055	0.0000117	0.0000081

**Table 2: Preliminary data**

Specification of model element	
Total height	18.0 m, for 6 storey 33.0 m, for 11 storey
Column size	500×500mm, For 11 storey 450×450mm, for 6 storey
Beam size	375×500mm, for 11 storey 375×450mm, for 6 storey 5m span length in both direction
Slab thickness	125mm
Masonry wall thickness	230mm
Equivalent width of strut	790mm (calculated as per equation no. 1) 5.83m span length

### Analysis

Modeled frames are assigned the general loading as per IS: 875 (part1, part2) and seismic loading as per IS: 1893 (part1) 2016. The loading data and seismic factors used for analysis are shown in table-3. The linear dynamic response spectra analysis is performed for different models of six and eleven storey unsymmetrical building and the results are obtained using ETABS software.

### Calculation of width of equivalent diagonal strut

Consider First class brick of compressive strength = 10 Mpa.  
& mortar of grade H1 (As per IS 1905:1987) having compressive strength = 10.5 Mpa.

$$f_m = 0.433 \times 10.5^{0.64} \times 10^{0.36} = 4.4673 \text{ Mpa.}$$

$$E_m = 550 \times 4.4673 = 2457.04 \text{ Mpa.}$$

$$\alpha_h = 2500 \left\{ \left( \frac{2457.04 \times 230 \times \sin(2 \times 31)}{4 \times 27386.13 \times 52.08 \times 10^8 \times 2500} \right)^{1/4} \right\} = 1.92$$

$$W_{ds} = 0.175 \times 1.92^{-0.4} \times 5.83 = 0.79 \text{ m}$$

Length of equivalent diagonal strut = 5.83m and;

Ends of equivalent diagonal strut are connected to RCC frame as pinned connection.

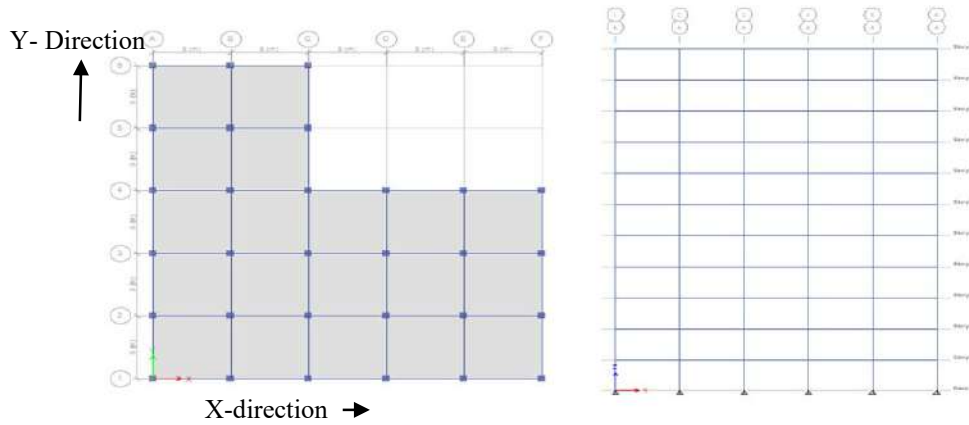


**Figure 2 : Bare frame RC model**

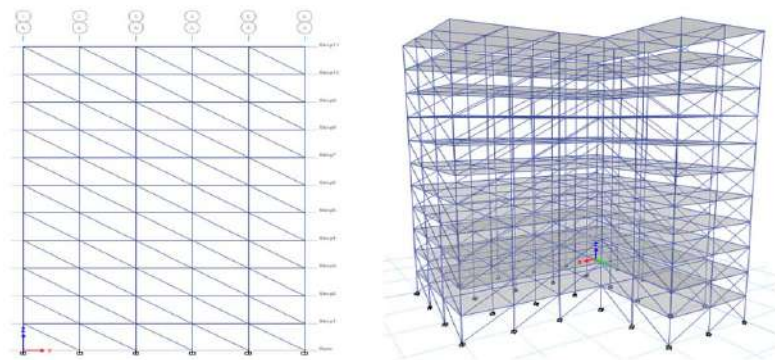


**Figure 3 : fully infill RC frame model**

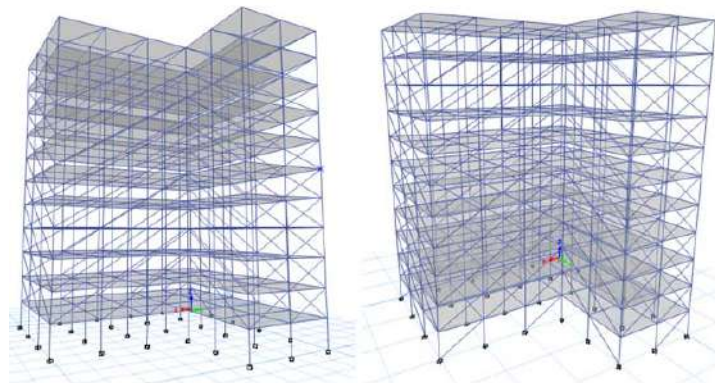


**Fig.4 : RC frame with soft storey model**

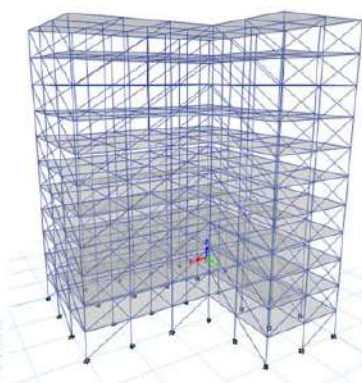


**Fig. 5 : partially infill RC frame model**

## RESULTS AND DISCUSSIONS

The analysis results for six storeys and eleven storey unsymmetrical building with different configuration of masonry brick infill are compared below.

### Comparison results for 6 storey frame

Figure-6 compares the lateral deflection with storey number and figure-7 compares the storey drift with storey number for all four model of RC building. Figure-8 shows storey stiffness for all four different models and figure-9 & 10 show base shear and maximum overturning moment for all four models of RC building.

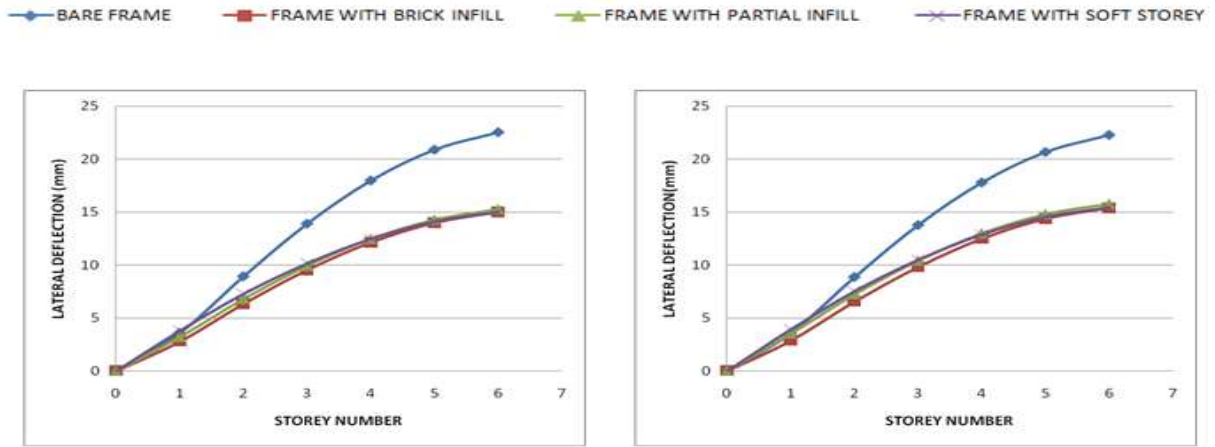


Fig 6: Comparison of lateral deflection in x & y direction respectively.

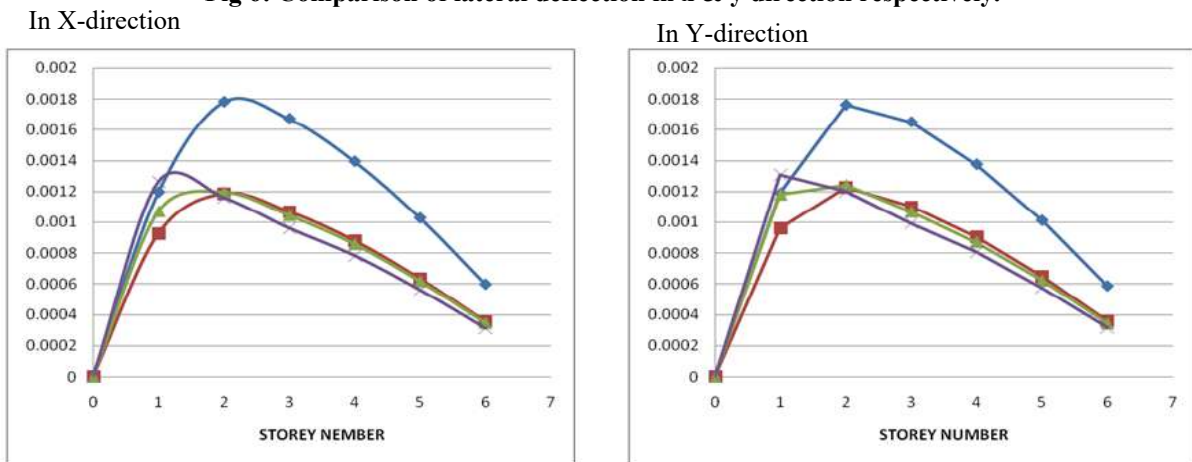


Fig 7: Comparison of Storey drift in x & y direction respectively.

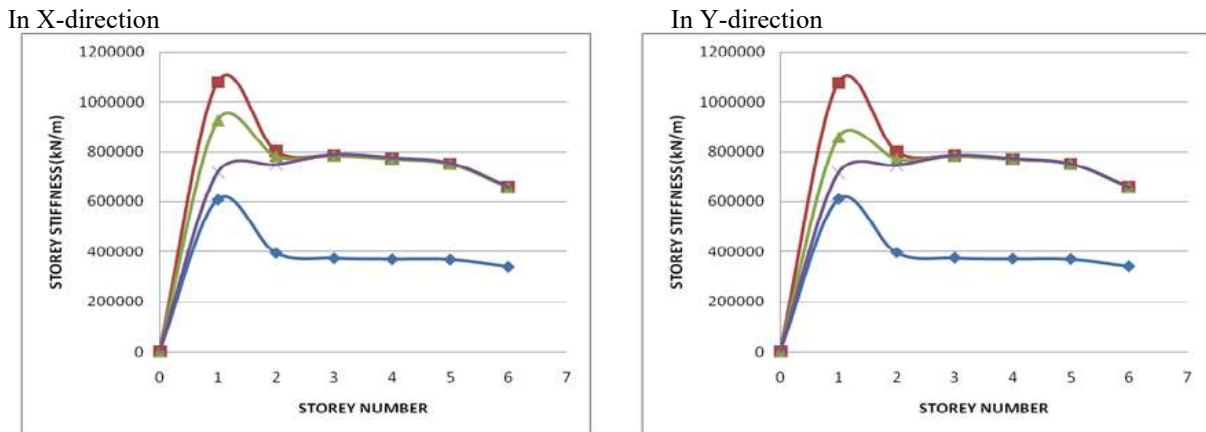
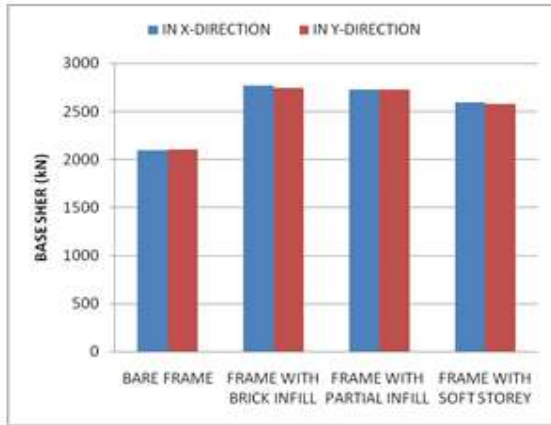
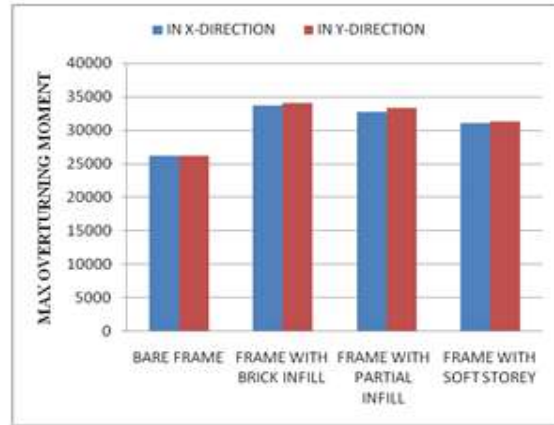


Fig 8: Comparison of Storey stiffness in x & y direction respectively.



**Fig 9: Comparison of base shear in x & y direction respectively.**

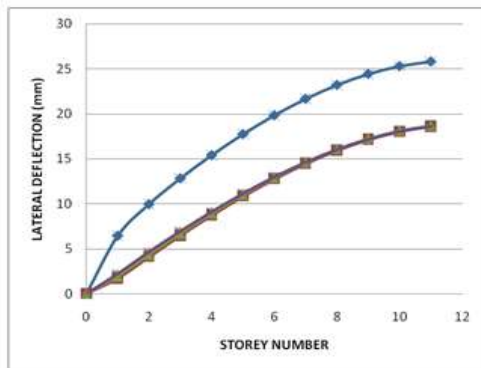


**Fig 10: Comparison of maximum overturning moment in x & y direction respectively.**

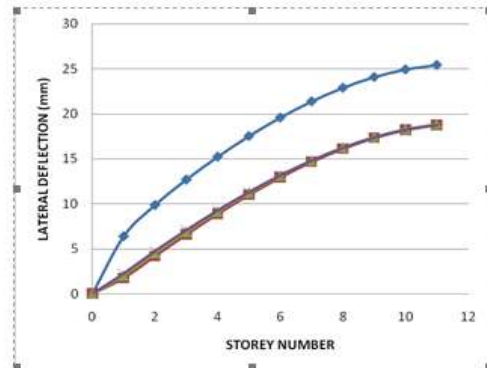
*Comparison results for 11 storey frame*

Figure-11 compares the lateral deflection with storey number and figure-12 compares the storey drift with storey number for all four model of RC building. Figure-13 shows storey stiffness for all four different models and figure-14 & 15 show base shear and maximum overturning moment for all four models of RC building.

—●— BARE FRAME    —■— FRAME WITH BRICK INFILL    —▲— FRAME WITH PARTIAL INFILL    —×— FRAME WITH SOFT STOREY



In X-direction



In Y-direction

**Fig 11: Comparison of lateral deflection in x & y direction respectively.**

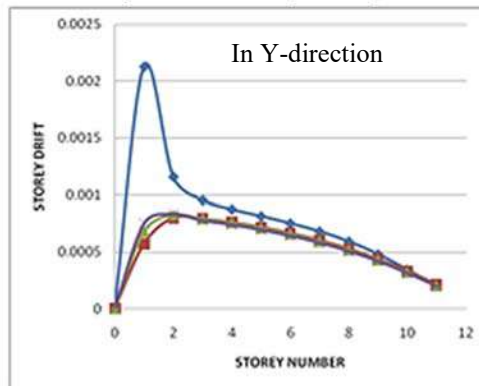
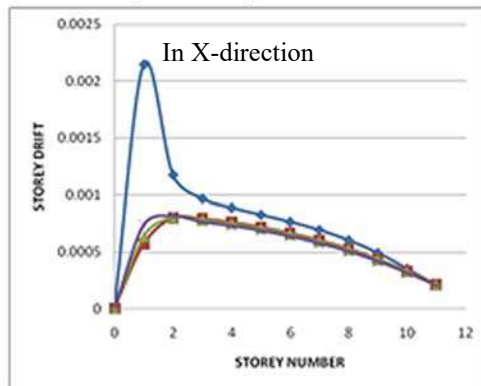


**Fig 12: Comparison of Storey drift in x & y direction respectively.**

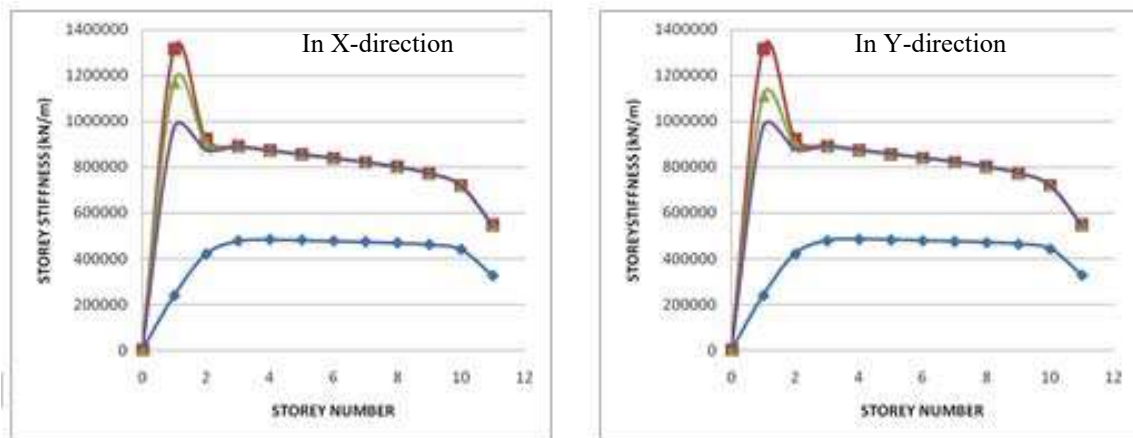


Fig 13: Comparison of Storey stiffness in x & y direction respectively.

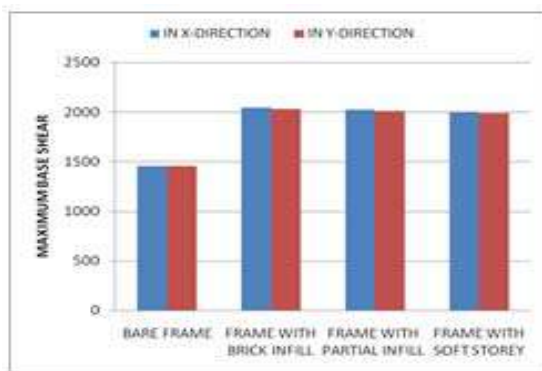


Fig 14: Comparison of base shear in x & y direction respectively.

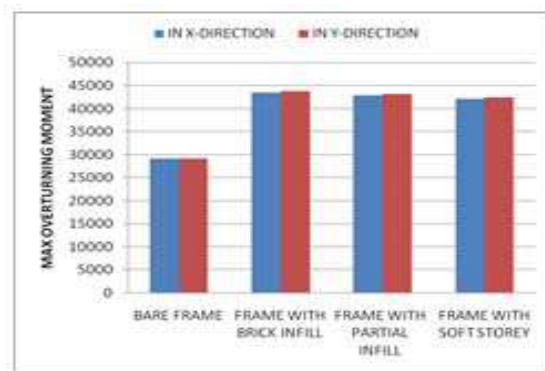


Fig 15: Comparison of maximum overturning moment in x & y direction respectively.

## CONCLUSIONS

This study focused on the structural response of masonry infill reinforced concrete structures under linear dynamic Response spectra analysis. The results clearly indicate the contribution of masonry infill in resisting the in-plane lateral loads irrespective of the interfacial properties. From the observation of the results following conclusions are drawn.

- Lateral deflection in bare frame at top storey is 1.18 times and 1.35 times higher than frame with brick masonry infill for both six storey and eleven storey building in x & y direction respectively.
- Whereas the difference between lateral deflections at the top story for frame with soft storey, without soft storey and for partially infill frame is insignificant for both six and eleven storey buildings.
- In case of bare frame the maximum storey drift (at first storey in eleven storey building and at second storey in six storey building) is very large as compared to the other three models with masonry infill.
- Also, storey drift values for all four storey are less than permissible value i.e. less than 0.004 times the storey height as per IS 1893:2016.
- For a particular storey brick masonry infill wall contribute significantly in stiffness of that storey. Stiffness of brick masonry infill is maximum and minimum for bare frame
- Also above result shows disadvantage of soft ground storey which reduce the stiffness of building.

## REFERENCES

- Arshad k. Hashmi and Alok Madan (2017), Seismic performance of masonry infilled reinforced concrete structures, The Indian Concrete Journal, May 2017, Vol. 91, Issue 5, pp. 24-33.
- Asteris P. G., (2003), Lateral stiffness of brick masonry infilled plane frames, Journal of structural engineering 2003, 129(8): 1071-1079.
- Diptesh Das and C.V.R. Murthy (2004), Brick Masonry Infills in Seismic Design of RC Frame Buildings: part 1- cost implication, Part 2- Behaviour, Indian Concrete Journal, 2004.
- Dhadde Santosh (2014), evaluation and strengthening of soft storey building, International Journal of Ethics in Engineering & Management Education, ISSN: 2348-4748, Volume 1, Issue 5, May 2014.
- Guney D., and Aydin, E. (2012), The Nonlinear Effect of Infill Walls Stiffness to Prevent Soft Story Collapse of RC Structures, The Open Construction and Building Technology Journal, 2012, 6, (Suppl 1-M5) 74-80.
- Hemant B. Kaushik, Durgesh C. Rai and Sudhir K. Jain (2006), Code Approaches to Seismic Design of Masonry-Infilled Reinforced Concrete Frames: A State-of-the-Art Review, Earthquake Spectra, Volume 22, No. 4, pages 961–983.
- IS 1893:2016 (Part 1) Criteria for earthquake resistant design of structure part-1 general provisions & buildings (sixth revision) B.I.S New Delhi.
- IS 1905:1987, Code of practice for structural use of unreinforced masonry, B.I.S New Delhi.
- Madan. A., (2013), seismic vulnerability of masonry infilled reinforced concrete frame structures, Int. J. of Safety and Security Eng., Vol. 3, No. 3 (2013) 174–183.
- Murthy C.V.R. and Sudhir K Jain (2000), Beneficial Influence Of Masonry Infill Walls On Seismic Performance Of RC Frame Buildings, proceedings of twelfth world conference of earthquake engineering, 2000.
- Poonam Patil, Kulkarni D.B. (2015), Effect of different infill material on the seismic behavior of high rise building with soft storey, ijret: International Journal of Research in Engineering and Technology eISSN: 2319-1163 | pISSN: 2321-7308
- Rajashri A. Deshmukh, P. S. Pajgade (2015), a study of effect of infill material on seismic performance of rc buildings, international journal of engineering sciences & research technology, ISSN: 2277-9655.



## Influence of Fiber Hybridization on the Cyclic Behavior of Exterior Beam Column Joint

R. Siva Chidambaram<sup>\*1</sup>, Pankaj Agarwal<sup>2</sup>

<sup>1\*</sup> CSIR-Central Building Research Institute, Roorkee; e-mail:krsinelastic@gmail.com (Corresponding Author)

<sup>2</sup> Professor, Department of Earthquake Engineering, Indian Institute of Tech. Roorkee; e-mail:panagfeq@gmail.com

### ABSTRACT

The concept of fiber hybridization shows promising structural application. The use of multiple fiber in small volume acts as micro and macro level reinforcement and bridges the cracks in micro and macro level also shows better resistance to crack formation and its growth. The type of fiber/profile and its percentage decides the effectiveness of the composites. The fiber hybridization can be with concrete and composites. The ductility enhancement and damage tolerance of the concrete/composites are distinct. This research article presents a comparative study on beam column joint with fiber reinforced composites(FRCC)/ concrete(FRC). The joint region is casted with FRC and FRCC instead of conventional concrete and examined under reverse cyclic loading. The uni-axial compression stress-strain behavior of the matrix used is also examined using standard cylindrical specimens. The mechanical properties as well as the elemental behavior of FRC and FRCC enabled specimen shows improved post peak behaviour interms of stiffness retention, energy dissipation and ductility. The fiber hybridization shows distinguished performance compared to FRC. The ductile response of FRC/FRCC shows its effectiveness in resisting the lateral forces without the need of critical detailing.

**KEYWORDS:** HPRCC; FRC; Beam-column Joint; Energy dissipation; Damage tolerance.

### INTRODUCTION

Beam to column joints of Reinforced Concrete (RC) framed structure are the most susceptible regions during earthquakes. The individual elemental force results joint a shear prone zone. The shear resistance capacity of a joint can be improved by proper design and by employing proper confinement in the potential joint region. This seismic detailing in the joint region creates construction complexity and also a partially successful technique in attaining required ductility. The poor tensile behavior of concrete fails to restricts the crack formation and allows the longitudinal rebar to slip from the anchored joint. This leads to severe distress to joint and collapses the structure.

The use of discontinuous steel fiber in the concrete improves the tensile strain and strength and provides better resistance to crack growth. Previous studies using steel fiber reinforced concrete focused on the improvement of shear resistance capacity of RC joints with optimum amount of confining reinforcement (Filiatrault et al., 1994). Also offers higher energy absorption capability by proving better inelastic rotation. This helps to achieve the required ductility demand with optimum transverse reinforcement in the joint region without compromising the joint shear strength (Liu, 2006). But the absence of even fiber dispersion in FRC fails to bridge the cracks during inelastic deflection and also the volumetric content of fiber (>2%) creates balling problem and segregation. Also the use of coarse aggregate significantly affects the fibers dispersion in FRC. This problem has been addressed well using various strain hardening concrete/composite named as HPRCC. Normally this kind of HPRCC is prepared using higher volume fibers with mineral and chemical admixtures and without coarse aggregates. It provides better fiber dispersion and multiple level crack bridging effect which offers improved tensile strength and strain capacity with strain hardening property. The influence of different HPRCC such as slurry infiltrated fibrous concrete (Naaman et al., 1992; Thirugnanam et al., 2001; Mohammed et al., 2009), Engineered cementitious composites (ECC) (Fang et al., 2013; Shuxin et al., 2007; Shannag et al., 2002) and Hybrid Fibre Reinforced Concrete/Composites (HPFRC/HPFRCC) etc... (Ganesan et al., (2014); Dhaval et al., (2015); Annadurai et al., (2016)) has been studied widely. The presence of higher percentage of steel fiber in SIFCON helps to dissipate higher energy and enhanced damage tolerance capacity compared to the FRC. It also helps to increase the post peak stiffness retention capacity and provides increased ductility to the structural elements. The various issues like improper slurry penetration, fiber profile and its orientation limits the SIFCON application in practice.

The tensile strain capacity of ECC is higher than the FRC and has better crack bridging ability which adds ductility to the RC structural elements (Sudarsana et al., 2008; Gregor et al., 2002; Gregor et al., 2003). The application of HPFRCC in structural components eliminates the need of closely spaced confining reinforcement with better damping property and stiffness retention capability. (Fang et al., 2013; Shuxin et al., 2007; Shannag et al., 2002; Afsin et al., 2004). It is well known that the mono fiber reinforced concrete/composite shows uniform crack growth resistance also the composite fails to control the crack growth upon its widening. In case of fiber hybridization using multiple fibers in different profile and aspect ratio helps to resist both micro and macro level cracks at different level of loading. Few research works is focused on the effect of fiber hybridization in improving the joint shear resistance capacity. This study mainly focused on the influence of hybrid fiber composite on the quasi static performance of beam-column junction using metallic and synthetic fiber combination in different profile and volumes. The performance of different composite enabled beam column joint specimens were compared with conventional specimens.

## MATERIALS AND TESTING PROGRAM

Table 1 shows the materials used in the study. Ordinary Portland Cement as cementitious material, locally available coarse aggregate and river sand as aggregate are used in specimen preparation. Seven joint specimens are used in the experimental study. Fig.1 shows the fibers used in the study. The crimped steel fiber with an aspect ratio of 60 having nominal tensile strength of 1100 MPa is used in FRC/FRCC preparation.



(a) Polypropylene fiber      (b) Crimped steel fiber

Fig. 1 Fibers used in the study

**Table 1 Concrete mix proportions**

Specimen details	Cement	Sand	Coarse aggregate	Water binder ratio	Super Plasticizer	Fibers
Conventional Concrete	1	1.45	2.25	0.45	0.5	-
FRC	1	1.35	2.15	0.45	0.5	Refer Table no 2

## EXPERIMENTAL TEST SETUP AND SPECIMEN DETAILS

Exterior beam - column joint specimens with two different transverse reinforcement details are used as control specimens as shown in Figure 2. The reinforcement detailing of control specimen (BCJ 1) is used for FRC/FRCC specimen. Table 2 presents the configuration of specimens and composite strength. The experimental test setup used is shown in Figure 3. The column portion has been kept horizontal and the beam portion kept in vertical direction as depicted in Figure 3. The column has been subjected to a constant axial load of 20kN. The free end of the beam has been connected with the actuator to apply the reverse cyclic loading. The specimen has been tested under displacement control with an interval of 10mm till failure occurs. The rate of loading was increased gradually from 5 mm to occurrence of failure with an interval of 10 mm under displacement control. Figure 3 shows the loading history and axial load details. The Linear Variable Differential Transducer and the inbuilt load cell has been used to acquire the data during loading.

**Table 2 Compressive and split tensile strength of different composites**

Specimen ID	Description	Volume of fiber			Compressive Strength	Split Tensile Strength	Flexural Strength
		PP*	HSF*	CSF*			
		%			MPa	MPa	MPa
BCJ 1	Control I	×	×	×	30.5	3.4	4.0
BCJ 2	Control II	×	×	×	30.5	3.4	4.0
BCJ 3	Hybrid I(HyFRC)	0.2	×	1	51.6	5.9	6.8
BCJ 4	Hybrid I(HyFRCC)	1	×	2	35.0	5.6	6.7

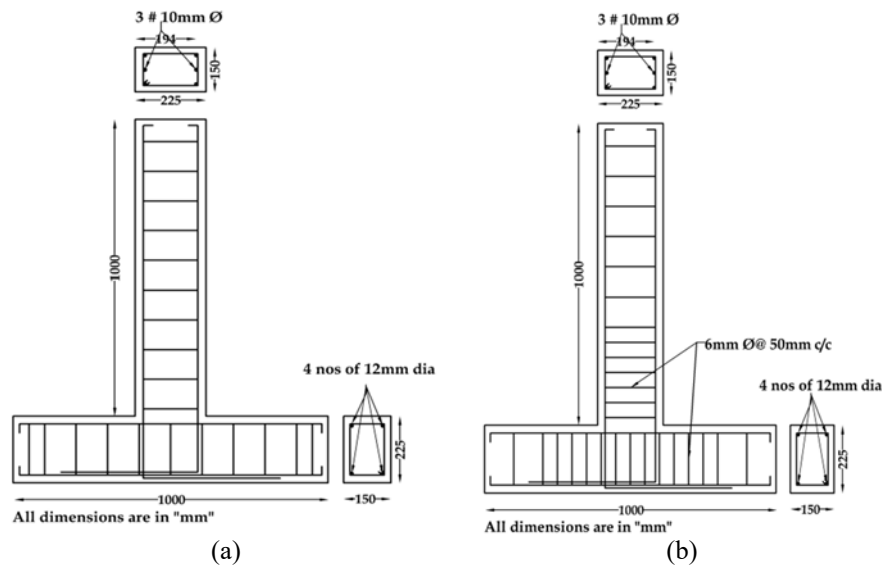


**Fig.2 Detailed configuration of joint specimen (a) BCJ 1 (b) BCJ 2**

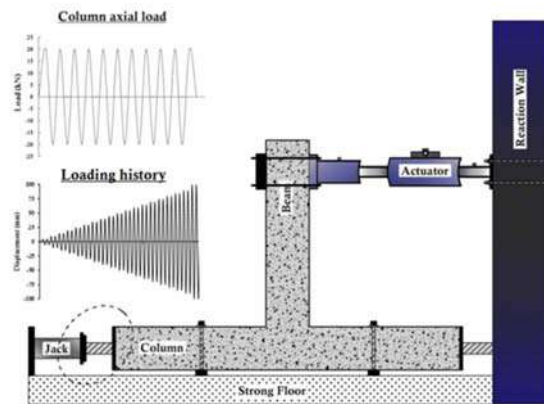


**Fig.3 Experimental test setup and loading sequence**

## RESULTS AND DISCUSSION

### *Hysteresis Behavior*

The closely spaced transverse reinforcement ratio has positive influence on the hysteresis behaviour of joint specimen BCJ 2. The hysteretic curves of specimens BCJ 1 and BCJ 2 are shown in Fig. 4. The absence of seismic detailing in specimen BCJ 1 shows early post peak degradation as a result of the reinforcement buckling. The difference in the post peak degradation of specimen BCJ 1 and BCJ 2 shows the importance of confinement in the joint region. The strength degradation starts after 50mm deflection in specimen BCJ 2 without sudden loss in strength compared to BCJ 1. The seismic detailing confines the core concrete and controls the rebar buckling which enhances the stiffness and strength retention behavior and can be clearly understood from the Figure 4. The post yield strength degradation starts after 0.01 rad in BCJ 1 whereas it is 0.04 rad in BCJ 2. The measured hysteresis loop area of BCJ 2 shows 25% enhanced energy dissipation compared to BCJ 1. Thus the closer confinement significantly improves the inelastic behavior of joint specimen under cyclic loading.

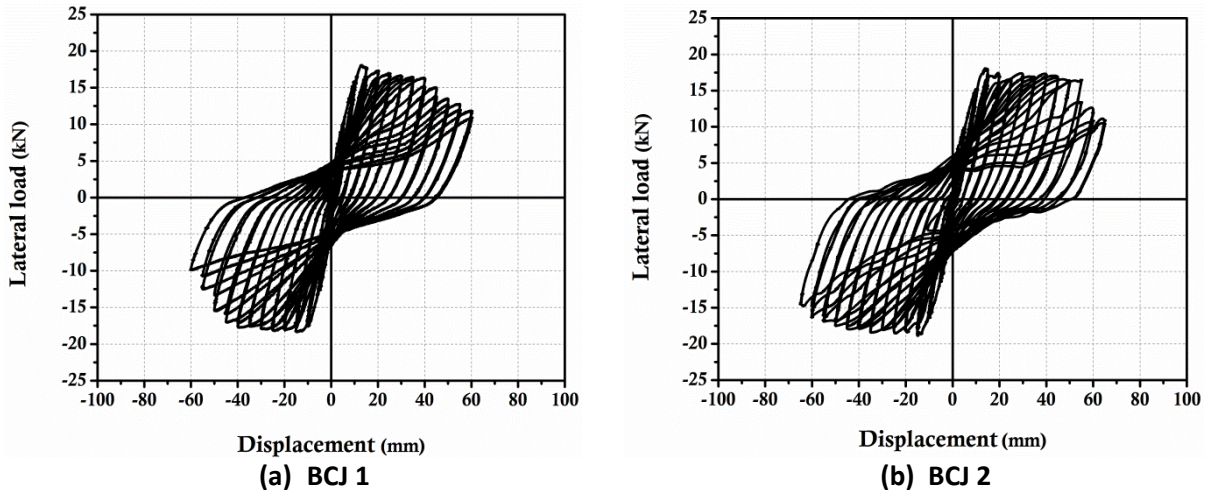


Fig. 4 Hysteresis behavior of Conventional Beam Column Joint Specimens

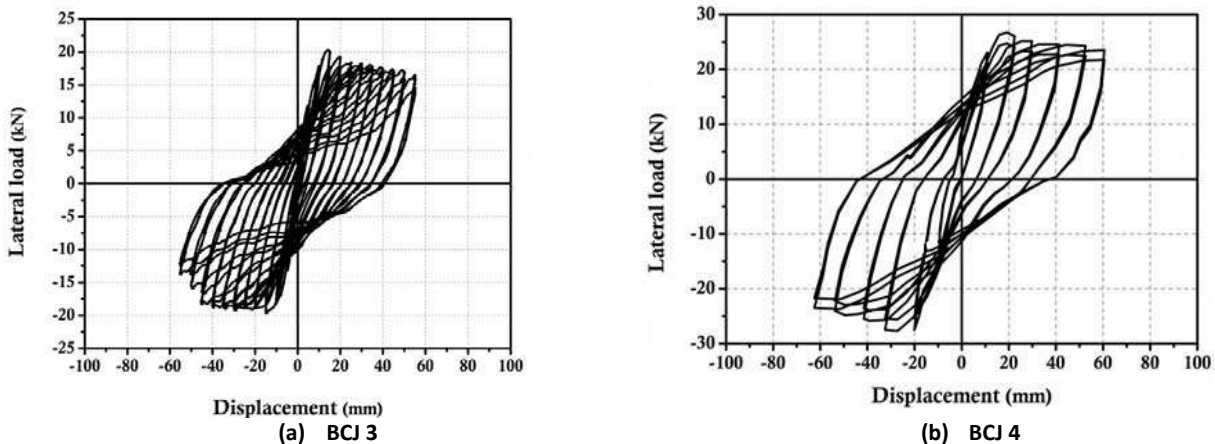


Fig. 5 Hysteresis behavior of Hybrid Fiber Reinforced Beam Column Joint Specimens

Figure 5 shows the hysteresis curve of specimen BCJ3 and BCJ4. The hysteresis curve of BCJ3 and BCJ4 shows different behaviors compared with each other. The peak load of BCJ 3 is comparatively lesser than BCJ 4 irrespective of its compressive strength. The compressive strength of BCJ 4 composite is 30% lesser than the BCJ 3 composite compressive strength. But the joint shear resistance is higher than the BCJ 3. This shows the influence of HPFRCC over HPFRC. The better fiber dispersion and fine mineral admixture improves the resistance to deformation capacity and limits the crack growth effectively compared to HPFRC. The measured energy dissipation and equivalent damping ratio is comparatively higher than the control specimens. The specimens BCJ4 shows enormous amount of energy dissipation compared to the

BCJ 3 due to the enlarged loop area under reverse cyclic loading. It proves that the composites offers better ductility than FRC.

### Crack Pattern

In the beginning stage of loading flexural cracks were noticed in the plastic hinge region of the beams in control specimens BCJ 1 and BCJ 2. Joint connection crack occurred at yield stage and the same started to enlarge after 30mm displacement. The brittle nature of concrete fails to arrest the formation of shear cracks in the joint region. Figure 6 clearly shows the crack pattern of control specimens. In BCJ 1 the connection has been sheared off after 40mm deflection and spalling of concrete occurred. The poor confinement detailing and the absence of cover concrete lead the rebar to buckle in the hinge region as buckle as shown in Figure 6. The critical transverse reinforcement detailing in the joint hinge region limits the rebar buckling and allow the beam to rotate further. The large rotation and the brittle nature concrete leads to concrete crushing failure near the connection region as shown in Figure 6b. The dense flexural cracks in the flexural member are a result of closely spaced confining reinforcement.

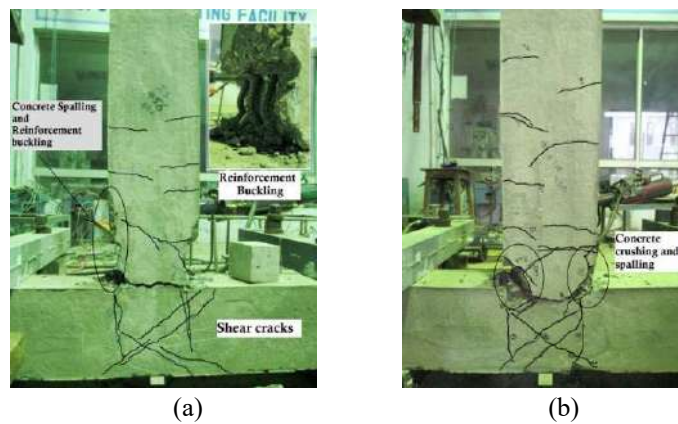


Fig. 6 Failure pattern of BCJ 1 and BCJ 2

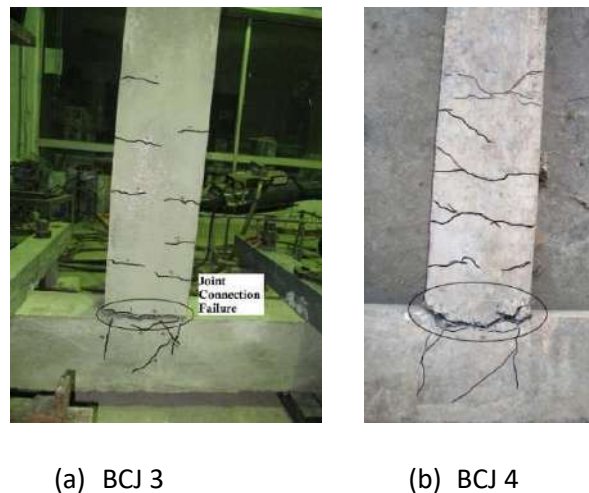


Fig. 7 Failure pattern of BCJ 3 and BCJ 4

The presence of hybrid fibers in the composite/concrete effectively acts as micro and macro level reinforcement in resistance to crack formation and its growth after the occurrence. The hybridization of synthetic and metallic fiber works well in concrete and composites. The absence of coarse aggregate eases the fiber dispersion in composite and provides

perfectly blended mix compared to FRC. The metallic fiber profile further helps to bridge the cracks having higher width and offers better aggregate interlocking capacity. As a result of this BCJ 3 shows fewer cracks in the hinge and joint region and has no sign of shear cracks in the joint. Similar trend has been observed with specimen BCJ 4 but the flexural cracks are little more compare to the BCJ 3. It shows that the high volume content of fiber works in multiple level of crack resistance and restricts the rebar slip. The absence of cover concrete spalling in the hinge region and rebar buckling evidences the importance of fiber in the concrete and composite. The fiber confining effect allows the crack to widen near the joint connection region which results rebar yielding. Thus the FRC and FRCC provides more ductile behavior compared to the control specimens.

### Damage Index

Modified Park and Ang (1987) damage index as per the equation 1 the damage tolerance capacity is calculated.

$$DI = \frac{\delta_M - \delta_y}{\delta_f - \delta_y} + \beta \int \frac{dE}{F_y \delta_f} \quad (1)$$

The damage index [DI] values vary from 0 to 1, whereas “0” indicates no damage and “1” indicates complete damage. In, this study it is assumed the  $0 < DI < 0.20$  represents elastic behavior or no damage in specimens,  $0.20 < DI < 0.40$  represents slight damage,  $0.40 < DI < 0.60$  represents moderate damage and  $0.60 < DI < 0.80$  represents severe damage and  $DI > 0.8$  represents complete damage.

The multiple level crack resistance mechanism due to the fiber hybridization and the effect of crimped steel fiber anchorage capacity the specimens BCJ 3 and BCJ 4 exhibits better damage index level compared to control specimens. In particular the absence of shear cracks allows the specimens to dissipate more energy and offers stable post peak strength retention which intern results better damage tolerant. The HyFRCC enabled specimen shows enhanced damage tolerance capacity compared to HyFRC due to the improved tensile strain capacity of composites and crack bridging effect. It shows that the use of fibers in concrete and in composites with hybridization effectively reduces the damage level even without seismic detailing in the hinge region.

### CONCLUSIONS

In this study the cyclic behavior of different beam column joint specimen with different FRC have been studied and following conclusions are drawn.

- There is an effective enhancement in the post peak response of beam-column joint specimens with FRC/FRCC. The better post peak displacement capacity of HyFRC / HyFRCC with stable post peak strength retention compared to control specimen authenticates the efficiency of the hybrid composites.
- The fiber crack bridging effect arrests the rebar slip and improves the initial and secant stiffness of joint specimens and provides higher ductility which is very difficult to achieve using conventional technique.
- The increased loop area due to the absence of shear cracks and large rotation helps to dissipate 1.5 times more energy compared to control specimens.
- The HyFRC specimens have shows reduced damage level as a result of fiber hybridization. The estimated DI and failure pattern demonstrates the role of HyFRC/HyFRCC in resisting the sudden failure without severe damage to the joint region. Thus the FRC/FRCC enabled joint specimen has undergone two levels lower damage without seismic detailing in the potential hinge region.

### REFERENCES

- Annadurai, A., and Ravichandran.(2016). “Effects of hybrid fiber reinforced high- strength concrete in exterior beam – column joint specimens,” *Asian Jou. of Civil Eng.*, 17(6), 701-712.
- Afsin CB., Gustavo J P., & James K W.(2004) “Behavior of precast high-performance fiber reinforced cement composite coupling beams under large displacement reversals”, 13th World Conference on Earthquake Engineering, Vancouver, B.C., Canada,2004.
- Dhaval, K., Richard, H.S., Deb, S.K., and Anjan, G. (2015). “Ductility enhancement in beam column connection using hybrid fiber reinforced concrete,” *ACI Struct. Jou.*, 112(2), 167-178.
- Fang Y., Jinlong P., Zhun X., & Leung CKY. (2013). “A comparison of engineered cementitious composites versus normal concrete in beam column joints under reverse cyclic loading”, *Mat. and Struct.*,46, 145-159.

- Filiatrault A., Ladicani K., & Massicotte B. (1994). "Seismic Performance of Code- Designed Fiber Reinforced Concrete Joints", *ACI Struct. Journal*, 564-571.
- Gregor F., Hiroshi F., & Victor CL., (2002). "Effect of matrix ductility on the performance of reinforced ecc column under reverse cyclic loading condition" Proceedings of JCI Int. Workshop on Ductile Fiber Reinforced Cementitious Composites-Application and Evaluation, 269-278.
- Gregor F., and Victor C L.(2003). "Intrinsic Response Control of Moment-Resisting Frames Utilizing Advanced Composite Materials and Structural Elements", *ACI Struct. Jou.*,100(2), 166-176.
- Ganesan, N., Indira, P.V. and Sabeena, M.V. (2014). "Behaviour of hybrid fiber reinforced concrete beam-column joints under reverse cyclic loads," *Mat. and. Des.* 54, 686-693.
- Liu, Cong. (2006). "Seismic Behaviour of Beam-Column Joint Subassemblies Reinforced with Steel fibres", M.Tech Dissertation, University of Canterbury, 2006.
- Mohammed AE.,Hamed MS.,Ahmed MF., & Ashraf HE.(2009). "Use of slurry infiltered fiber concrete in reinforced concrete corner connections subjected to opening moments", *Jou. of Adv. Con. Tech.*,7(1), 51-59.
- Naaman AE., Reinhardt HW.,& Fritz C.(1992). "Reinforced concrete beams with SIFCON matrix", *ACI Struct. Journal*, 89(1), 79-88
- Park, Y.J., Ang, A.H.S., and Wen, Y.K. (1987). "Damage limiting aseismic design of buildings," *Earthquake Spectra*, 3, 1-26.
- Sudarsana RH., Gnaneshwar K., & Ramana. (2008). "Behavior of simply supported steel reinforced SIFCON two way slabs in punching shear", *Indian Jou. of Eng. & Mat. Sci.*, 15, 326-333.
- Shuxin W.,&Victor C L.(2007). "Engineered cementitious composites with high volume fly ash", *ACI Mat. Jou.*,104(3), 233-241.
- Shannag M J., Barakat S., & Abdul Kareem M.(2002). "Cyclic behaviour of HPFRC repaired interior beam column joints', *Mat. and Struct.*,35, 348-356.
- Thirugnanam GS.,Govindan P.,Sethurathnam A.(2001). "Ductile behaviour of SIFCON structural members", *Journal..of Struct. Eng.*, 28(1), 27-32.
- Yu FW., Jia FJ., & Kang L. (2010). "Perforated SIFCON blocks-An extraordinarily ductile material ideal for use in compression yielding structural system" *Const. and Build. Mat.*,24, 2454-2465.

## Flexural behavior of hollow slab with plastic void formers - A review

Pankaj Kumar<sup>1</sup>, Babita Saini<sup>2\*</sup>

Department of Civil Engineering, NIT Kurukshetra, Haryana, India 136119;  
e-mail: <sup>1</sup>pankajkish2012@gmail.com, <sup>2\*</sup>babitasaini6@gmail.com (Corresponding Author)

### Abstract

Concrete plays a major role in the construction field. In building construction, slab is one of the largest and important structural member consuming concrete. Concrete slabs use more concrete than required, hence need to be optimized. In order to reduce the volume of concrete and self-weight of slabs, plastic void formers are used. Various shapes of void formers, grade of concrete and size of slab specimen were proposed by researchers. In this paper, an outline is presented on the analysis of voided slab both experimentally and analytically. Various properties such as Load vs Deflection, Flexural strength, Punching shear strength and others were studied and the results of voided slab with various shapes of void formers were compared.

### Introduction

Concrete is easily available and low cost construction material compared to other materials like wood, steel, etc. It gives higher strength and very hard to destroy. Concrete slabs use more concrete than required. The slab is the flexural member which transfer the load to the beams and columns. Slabs are large in size which dominates the complete loading of the structure. Hence, it becomes essential to optimize the dimensions of the members of the structure so that a balance can be maintained between load carrying capacity and economy. The capacity of the structural member (slab) will not be changed if the concrete present in the tension zone of the slab is removed. Therefore, voided slabs are introduced which reduces the material (concrete), self-weight and cost involved in the construction of slabs. This would help in the reduction of self-weight of the slab and the entire structure. Self-weight of the slab reduced about 35% due to voids present inside the slab. Cement production caused nearly 7% of entire greenhouse emissions. Nowadays, industrial waste materials have been used as the limited replacement of cement to take care of the environment. The less quantity of concrete used in the voided slab would aid in green construction.

Though variously shaped void formers have been used in past construction practice, the spherically shaped void former is the most efficient, Some other shapes of void formers like a donut, rectangular blocks, elliptical, etc. are used in voided slabs. Recycled waste plastic is used as the material for the manufacture of void formers. As the plastic is used in the construction of structural members which makes it a green construction. Difficulties in the casting of voided slabs includes movement of void formers, irregular compacting of concrete, irregularity in positioning, uplift of the void formers due to low density, etc. To avoid these problems provide reinforcements at top layer during the casting of the slab. The voided slabs can be designed as the conventional solid slabs according to (IS-456:2000). Many experimental kinds of research have been done over the years to investigate the behavior of these voided slabs. The prime research work was to the ascertained flexural behavior of spherical and modified elliptical voided slabs, punching shear failure of biaxial hollow slabs and shear capacity of spherical voided slabs.

### Literature review

The state of art has been discussed below in detail and also given in Table 1.

(Schnellenbach-et al., 2002) presented the behavior of hollow slabs in punching with plastic balls and nonlinear computation was performed using the finite element method. To find out the punching shear capacity, total of six specimens were considered three of them with a thickness 240mm and rest three of thickness 450mm. It has been reported that failure of these slabs is mostly similar to the solid slabs and to describe punching shear capacity a proposal has been made to modification in the German design code DIN045.

(Chung et al., 2011) presented the hollow slab with special shaped void former look like a donut and checked their capacity in shear. A hollow biaxial slab system is popularly known because it has light weight due to presence of voids. In this study, 4 specimens were used. One test specimen was a conventional solid slab and rest three were hollow slabs. Two different shaped void formers were used, one was donut and other was non donut type. The material of void formers were glass fiber plastic and general plastic. It has been reported that donut type void formers increased the shear capacity of the slab up to 20% compared to the slab with non donut

type void formers.

**(Teja et al, 2012)** presented the structural behavior of bubble deck slab by using high-density polyethylene hollow spheres. This paper has discussed about many characters of bubble deck slab based on the different studies done abroad. The finite element method in SAP2000 was used to verify the results of deflection, moment and stress distribution. It has been reported that bubble deck slab had 6.43% lesser bending stresses than that of a solid conventional slab, 5.88% more deflection in bubble deck slab than a solid slab as the stiffness of slab was decreased due to voids present on the slab and 35% weight of slab decreased compared to solid conventional slab.

**(Hai et al., 2013)** presented an experimental investigation of a bubble deck slab in which modified elliptical balls were used and slab was subjected to static vertical loading. Many factors which influenced the behavior of the bubble deck slab were accounted such as strength of concrete, shape and size of the plastic balls. The behavior of bubble deck slab using traditional hollow spherical balls was investigated experimentally and the results were compared with the finite element program using ANSYS. It was concluded that the slab with hollow elliptical balls had better load bearing capacity than the traditional hollow spherical balls.

Table 1. Experimental Parameters Measured by different Authors on Voided/ Hollow Slab

Sr. No.	Reference	Cost Analysis	Ultimate load carrying capacity	Shear Strength	Compressive Strength	Flexural Strength	Punching Strength	Deflection	Crack pattern
1.	Schnellenbach- et al., 2002	-	✓	✓	-	-	✓	✓	-
2.	Chung et al., 2011	✓	✓	-	✓	✓	-	✓	✓
3.	Teja et al, 2012	-	✓	-	✓	✓	-	✓	✓
4.	Hai et al., 2013	✓	✓	-	✓	✓	-	✓	✓
5.	Subramanian et al, 2017	-	✓	✓	✓	✓	-	✓	✓
6.	Jasna et al., 2017	-	✓	-	✓	✓	-	✓	-
7.	Dheepan et al, 2017	-	✓	✓	-	✓	-	✓	✓
8.	Sarvaiya et al., 2017	-	✓	-	✓	✓	-	✓	✓
9.	Naik et al., 2017	✓	-	✓	✓	-	-	-	✓
10.	Pande et al., 2018	-	✓	-	✓	✓	-	✓	✓

**(Subramanian et al, 2017)** presented an experimental study on spherically voided slabs with varied spacing between void formers. The slab was loaded as area loading as an alternative to five points regular loading. The spacing of the void formers as 20mm, 30mm and 50mm was used. The percentage decrease in the volume of concrete was appeared to be directly proportional to the percentage decrease in the cost of construction. It has been reported that the maximum decrease in volume in concrete was attained by using spherically shaped void formers. It has been found that cracks were formed in the slab and they propagated according to the yield line. As the less concrete was used in the construction of slab, an overall 25% reduction in cost was achieved. **(Jasna et al., 2017)** presented a study on structural behavior of bubble deck slab using spherical shaped and elliptical shaped balls. Two different concrete grades, M25 and M30 were used. The finite element analysis was carried out by using finite element analysis software ANSYS to study and compare the results of bubble deck slab with spherical balls and elliptical balls. It has been reported that bubble deck slab with M30 grade of concrete shows better performance and slab with elliptical balls have better load carrying capacity compare to that of bubble deck slab with spherical balls. Bubble deck slab saved weight up to 33.15% around one spherical ball and 34.9% for one elliptical ball. **(Dheepan et al, 2017)** presented an experimental analysis on bubble deck slab using polypropylene

balls. Two point load test was conducted to determine the flexural strength of the slab. This paper emphasized to find out optimum spacing and diameter of balls to acquire maximum strength. The crack pattern of the slab was also measured by differing the spacing and diameter of plastic balls. It has been concluded that, when the spacing between the balls increased the flexural strength of the slab also increased, irrespective of change in the thickness of the slab. Around 35 – 50 % reduction in self-weight of the slab was observed. It has been reported that due to the voids present in the slab, it had excellent thermal insulation property, lower total cost, decreased construction time and green technology compared to the conventional slab. (Sarvaiya et al., 2017) presented an experimental analysis on a spherical voided slab with plastic hollow spherical balls introduced in the center of the slab. The behavior of voided slabs was affected by the ratio of the diameter of the bubble to the thickness of the slab. Three test specimens were tested, one as a normal solid slab and other two were hollow slabs. These hollow slabs had the void diameter of 37mm and 45 mm. It has been reported that the deflections of voided slab specimens were slightly higher than an equivalent solid slab under service load and the compressive strain of concrete in voided specimens was greater than that of an equivalent solid slab specimen.

(Naik et al., 2017) presented a comparative study on the solid flat slab and voided slab by using finite element analysis in SAP 2000. Manual calculations had been done by design method as per IS 456:2000. This paper emphasized to find out the behavior of bending moment, shear force, deflection and reaction in the slab due to alteration in the span for different load conditions. The analysis was carried out on a G+12 storey structure for grid 6m x 7m, 7m x 8m, 8m x 9m having the thickness of slab 250mm, 280mm, 310mm respectively for the seismic effect on the whole structure due to reduced concrete weight. It has been reported that deflections for all the cases were nearly the same as that of the conventional solid slab under identical loading conditions. The base shear of the structure reduced by 12% to 14% due to reduced concrete weight. The moment of the voided slab decreased from 7% to 10% as compared to a solid flat slab under identical loading condition.

(Pande et al., 2018) presented the structural behavior of voided slab and their structural benefits over a traditional concrete slab. The bubble deck slab was a new type of slab in which concrete present in the middle of the slab was eliminated by some void formers such as plastic balls; because, concrete present below the N.A. did not perform any structural function. Hence, significant structural weight has been reduced. In the construction of slab high-density polyethylene hollow spheres were used to replace the concrete. Thus, self-weight of the slab and finally for entire structure has been reduced. It has been reported that deflection of bubble deck slab was found to be more than the solid slab and weight reduction of 4.7% compared to the solid slab.

## Conclusions

From the previous studies, it has been concluded that voided slabs have more benefits than conventional slabs. Also voided slabs have significant reduction in the weight of slab, saves significant volume of concrete and for larger span slab, reduction in the volume of concrete will be more as the thickness for large span slab will be more. Voided slab shows significant thermal insulation property due to the voids present in the slab. Steps to construct the voided slabs are more than the solid slabs but the construction process is not much complicated. Voided slabs are less costly than the conventional slabs as it uses less volume of concrete. It has been observed that failure pattern of slab similar to yield line pattern. Flexural strength of slab increases when spacing between the balls increases and it is irrespective of change in the thickness of slab.

## References

- Chung J. H, Choi H.K, Lee S. C. and Choi C. S (2011), “Shear Capacity of Biaxial Hollow Slab with Donut Type Hollow Sphere”.
- Dheepan K. R, Saranya S. and Aswini S (2017),,, “Experimental Study on Bubble Deck Slab using Polypropylene Balls”.
- Hai L. V, Hung V. D, Thi T. M, Nguyen-Thoi T and Phoc N. T (2013), “The Experimental Analysis of Bubble Deck Slab using Modified Elliptical Balls”.
- Jasna Jamal , Jiji Jolly (2017), “A Study on Structural Behavior of Bubble Deck Slab using Spherical and Elliptical Balls”.
- Naik Sonal R and Joshi Dinesh (2017), “A Voided Slab and Conventional Flat Slab; A Comparative Study”.
- Pande Abhay M, Anup M. Bhendale and Manish M. Bais (2018), “Voided Slab”.
- Sarvaiya and Jivani (2017), “An Experimental Study on Spherical Voided Slab”,
- Schnellenbach-Held M. and K. Pfeffer (2002), “Punching shear capacity of biaxial hollow slabs”,
- Subramanian K, Buvaneshwari P and Jabez N.A. (2017), “Flexural Behavior of Biaxial Slabs Voided with Spherical HDPP Void Formers”.
- Teja P. Prabhu, Kumar P. Vijay, Anusha S, Mounika CH, Saha Purnachandra (2012), “Structural Behavior of Bubble Deck Slab”.



## Seismic Vulnerability of Single Story Masonry Structures

Pavan Kumar,<sup>1</sup> Sanket Nayak<sup>2\*</sup>

<sup>1</sup>PG Student, Department of Civil Engineering, IIT(ISM), Dhanbad, Dhanbad, Jharkhand

<sup>2\*</sup>Assistant Professor, Department of Civil Engineering, IIT(ISM), Dhanbad, Dhanbad, Jharkhand (Corresponding Author)

### ABSTRACT

In developing countries poor people as well as common people used unreinforced masonry structures because these structures are cost effective and easy in construction. Usually under gravity loading unreinforced structures perform well. But under seismic loading these structures perform very poor. It is observed in the past earthquakes even in low and moderate earthquakes which have low casualties and minor loss of property. In this context, the present paper is an effort in assessing the seismic vulnerability of URM single storey structures using finite element based software (ANSYS). The finite element formulation is validated with the available literature for natural period (the most vital parameter of dynamic analysis) for different cases. A single storey building model is considered for the analysis. Base shear of such building is estimated for six ground motions. Lateral strength of such building is calculated using the formulae available in well accepted literature. Seismic vulnerability is determined by comparing base shear with lateral strength. The building is assumed to be safe at a particular PGA at which the lateral strength is more than the base shear calculated at that PGA.

### INTRODUCTION

Masonry is widely used construction material in India and masonry structures of 1-3 storeys are mostly used. Economically weaker section and common people are mostly used masonry structures due to their fire resistance, thermal capacity and durability properties but at the time of earthquakes these structures are very vulnerable. They badly affected against tensile forces. Masonry structures are found to undergo very severe damage and collapse, leading to a large loss of life, even during low-magnitude earthquakes. If we want to predict the impact of earthquake on the surroundings of anyone part of country then it is most necessary to obtain the seismic vulnerability of that surrounding or environment which is affected. This seismic risk assessment can be estimated in result of earthquake of selected area with parameters like predictable damage, loss from particular given risk to the elements of that risk. In masonry constructions, the walls carry the horizontal and vertical loads. The wall has carried vertical and horizontal loads in masonry structures. Lateral load like wind and earthquake cause out-of-plane and in-plane enforcements into the wall. Moments and shear force are created in masonry structures under that lateral force, due to this, in-plane failure of this structure occurs with effects of the axial forces like tensile/pressure, that moment generated or/and liable gracious stresses which are built by those failure forces. The seismic analysis of masonry structure is very complex by finite element method, but it can be solved in less tedious way using FEM based software (ANSYS). For modeling of masonry specimens, solid 8 node 185 element has used to simulate brick unit and solid 65 has been used to simulate the mortar and PCC layer from ANSYS element library. Several methods of FE modelling are developed for studying the dynamic behavior and static behavior of masonry structure especially walls subjected to out-of-plane in-plane and loading. Earthquake loading can be classified as quasi-static loading of two ways: In first method, a constant horizontal acceleration is applied to the structure; this is equivalent of applied constant horizontal ground motion. This conventionally ignores this fact that real ground motions only take place for a small period, but also rejects the possibility of resonant amplification. So, this method is suitable when we concern stability and elastic resonance is probable to have relatively very small effect. Second method includes applying the horizontal forces which are spread along height of structure, this is meant to estimated (approximate) effects of earthquake and relative magnitudes of those forces have distributed towards top the structures, accounting the amplification which is caused due to dynamic resonance. All horizontal forces can scale to variable magnitude earthquakes and then response of structure is determined.

Normally, maximum countries, masonry construction is very famous in rural populations but in this masonry construction generally damage occurs due to earthquake, so this masonry construction should be reinforced. Assessment of seismic vulnerability of masonry structure is very helpful to minimize or alert against any damage. Seismic analysis by analytical methods is very complex and tedious job. So, computational analysis is easy and very helpful for this purpose. An attempt has been made to analyze the seismic behavior of such kinds of masonry structure.

In previous studies finite element modelling has done using OpenSEES software and other software, but in this

study ANSYS mechanical APDL has used with simple wall and bay model, no complex model has make and due this simplicity of structure calculation is easy approximation is near about real structure.

**MODELLING AND FORMULATION**

Finite element method is considered under numerical method which is used to solving of mathematical physics and engineering problem. The finite element method gives approximate or nearest value of unknowns at different point over that domain. In this method large problem is converted into small parts and that small parts are basically known finite elements and equations which are used to solved these small parts again converted into large system equations of entire problem.

For brick model Solid 8 node 185 (solid185) element is used and for mortar and PCC model concrete 65 (solid65) element is used. Density of materials, elastic modulus and Poisson’s ratio are input parameter. The material model used is elasto-plastic. Only horizontal joints of layer are considered and vertical joints are neglected because vertical mortar layer has no marginal effect (Dutta et al.,2014). Due to brick and mortar masonry is composite material so it is a non-isotropic material but here brick layer and mortar layer has different properties so these two layer model separate layers and has isotropic material. Mesh division number are ignored due to no marginal effect on results. Meshing is done in each layer of PCC, brick and mortar by selecting that material. Material properties are assigned for each material. Size of meshing for both brick layer and mortar layer are considered as 0.15 and meshing taken as hexagonal for calculating base shear. Free tetra meshing is used to calculate natural frequency because number of mesh division has no marginal effect. Linear analysis is carried out for calculating base shear.

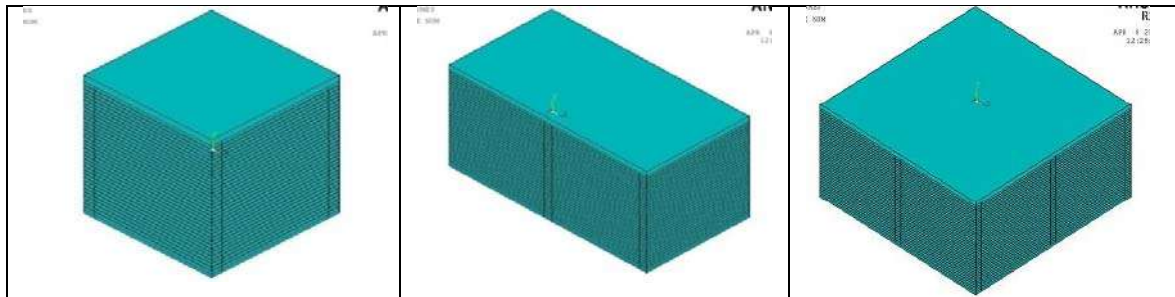
Masonry is considered under complex material, because it is a composition of mortar and bricks. Possibilities of wide range masonry alternatives with structural performance and mechanical behavior increases combining of these elements with different geometry and qualities. It is very clear that masonry gives good performance to resist compressive load and poor performance to resisting tensile loading.

Table1 represents properties of these elements.

**Table 1: Properties of masonry elements**

Elements	Young’s modulus (N/m <sup>2</sup> )	Poisson’s ratio	Material density (kg/m <sup>3</sup> )
PCC	19364.91E6	0.175	2400
Brick	3750E6	0.10	2000
Mortar	545E6	0.19	2200

Using ANSYS, 3-D model of single storey building with different bay combination was built. Different combination are 1 bay × 1 bay, 2 bay × 1 bay and 2 bay × 2 bay for 3 m height shown in Fig. 1.



**Fig.1. 3-D Model of single storey structure**

To obtain more accurate solution, mesh division should be finer. But if mesh division is finer, it increases computation time. At least, three convergences run will be required to show whether convergence is achieved or not and at which point the good refined mesh is within the form of final convergence. Convergence achieved by same result of two different density of meshing and no further convergence curve is required. This is checked on a wall model of size 3m×3m×0.250m with different mesh division using tetrahedral and hexagonal form. This is shown in Table 2.

**Table 2. Natural frequencies of wall with different mesh division for tetrahedral and hexagonal meshing**

Sl. No.	Wall Size	Mesh division	Natural frequency (Hz)	
			Tetrahedral meshing	Hexagonal meshing
1	3m×3.04m×0.250m	5	6.272	4.883
2		10	7.284	4.894
3		15	7.421	4.896

This table shows that finer meshing has no significantly affected the result, it is affected by some range, so that it checked by how much meshing range should be used by using 3-4 number of mesh division.

### NATURAL PERIOD OF MASONRY BUILDING

Natural period of this single storey structure model is calculated using finite element. Using the wall (size, 3m×3m× 0.250 m) model, natural period is calculated for different bay combination of single story with two different heights and this computationally calculated natural period is compared with the period obtained in Dutta et al., (2014) and shown in Table 3.

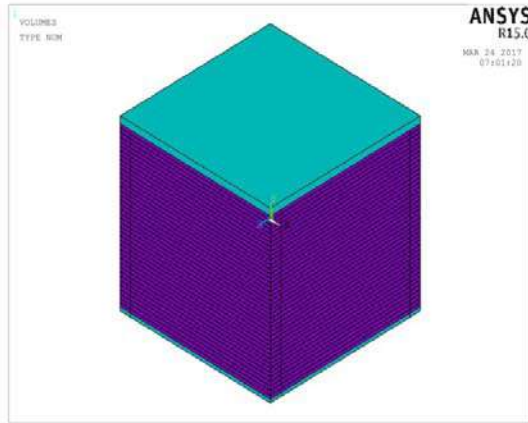
**Table 3. Natural Period of single story structure model**

Model specifications			Natural Period (s)	
Length and thickness	Storey height	No. of storey and no. of bay	FE modelling	Dutta et al., (2014)
3m, 0.250m	3 m	1 storey, 1 bay × 1 bay	0.033	0.035
		1 storey, 2 bay × 1 bay	0.036	0.035
		1 storey, 2 bay × 2 bay	0.034	0.035
		2 storey, 1 bay × 1 bay	0.087	0.086
	3.5 m	1 storey, 1 bay × 1 bay	0.041	0.042
		1 storey, 2 bay × 1 bay	0.043	0.042
		1 storey, 2 bay × 2 bay	0.040	0.042
		2 storey, 1 bay × 1 bay	0.098	0.108

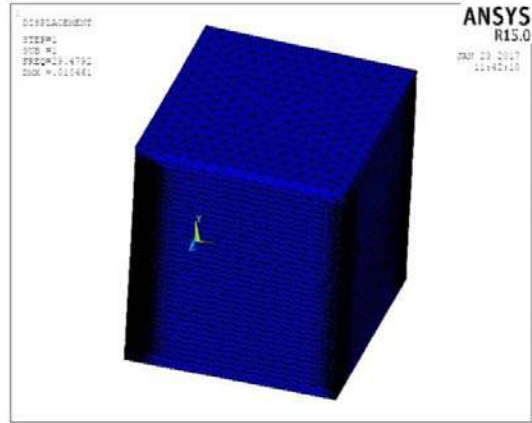
### MODE SHAPE OF MASONRY BUILDING

We can called mode is natural frequency in simple words mode shape shows displacement pattern of the system for that particular mode. If we wants to express mode and mode shape in mathematical expression, mode is expressed by eigen value whereas mode shape is represented by eigen vector. Mode shapes of different configuration of buildings are obtained using ANSYS. Fig. 4.1–Fig. 4.9 shows the five mode shapes of single storey with three bay combinations at different heights. From the mode shapes, this is observed; the mode shape is showing, in-plane, out-of-plane and in most of the cases mixed mode behavior.

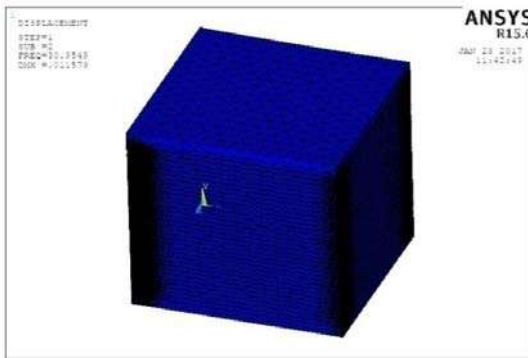
Figure 2 represent single storey model of 1 bay × 1 bay and its five mode shape. Generally, mode shape is representation of out-of-plane and in-plane behavior but in maximum cases it's behavior mixed mode type. In theses mode shapes first three has significant deflection while fourth and fifth mode shape has no significant deflection.



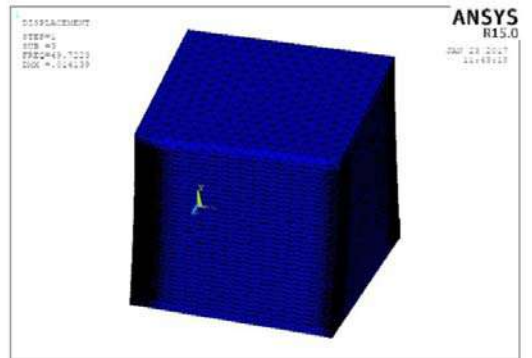
(a) 1 storey, 1 bay x 1 bay, model



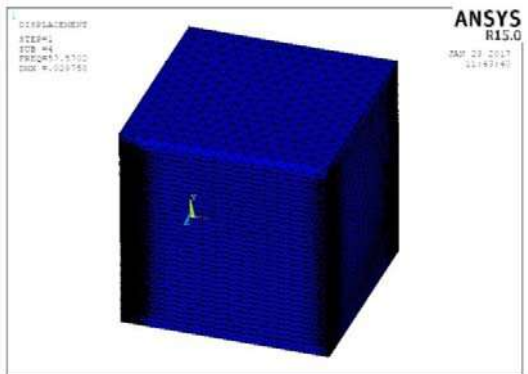
(b) 1<sup>st</sup> mode shape



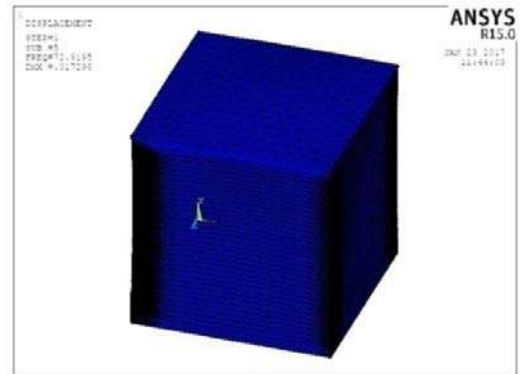
(c) 2<sup>nd</sup> mode shape



(d) 3<sup>rd</sup> mode shape



(e) 4<sup>th</sup> mode shape



(f) 5<sup>th</sup> mode shape

Fig 2. Five mode shapes of 1 storey, 1 bay x 1 bay building of 3 m height

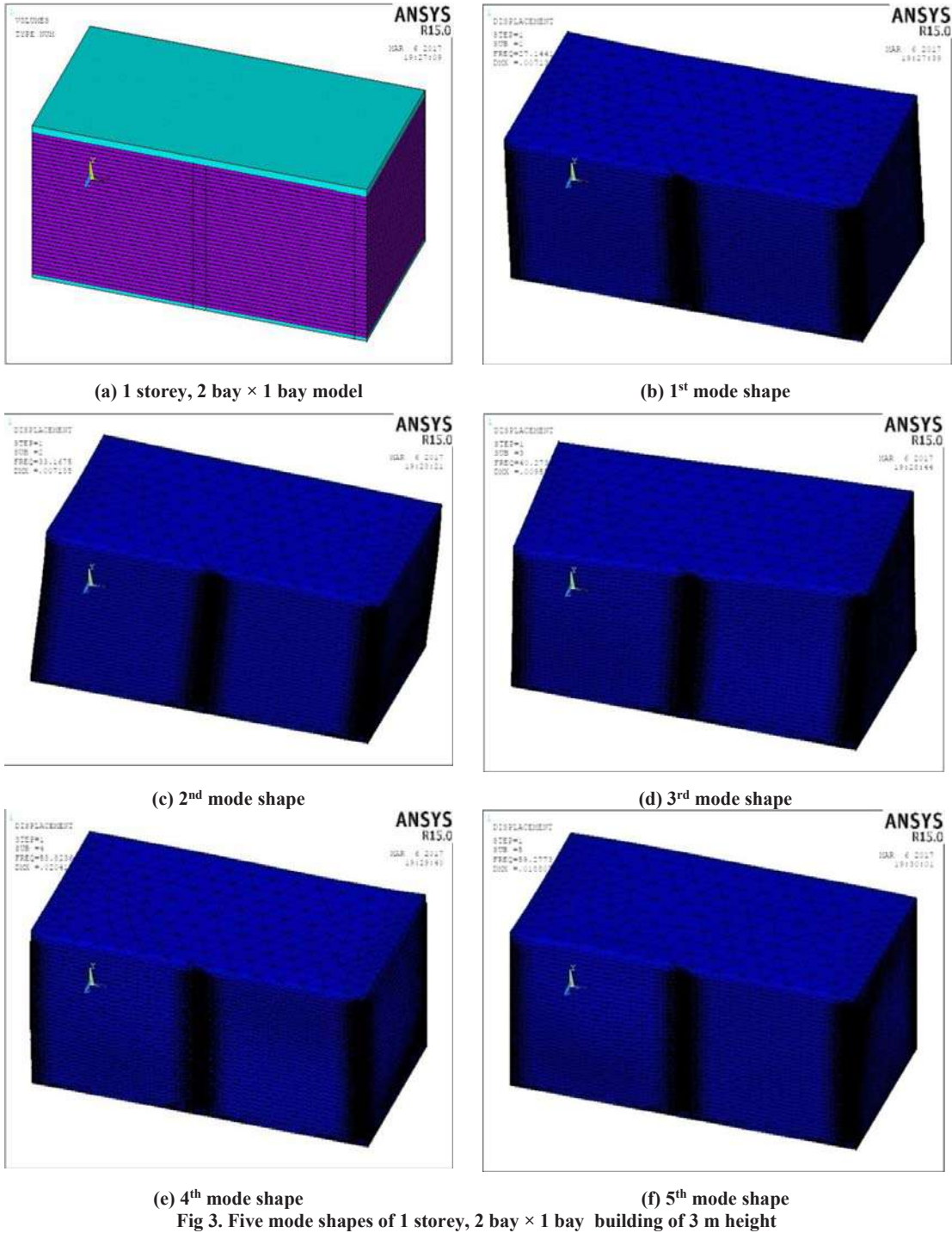


Fig 3. Five mode shapes of 1 storey, 2 bay  $\times$  1 bay building of 3 m height

Figure 3 represent single storey model of 2 bay  $\times$  1 bay and its five mode shape. In this it can be seen that the first three mode shape has significant the damage of structure while last two mode shapes has low effect on structure.

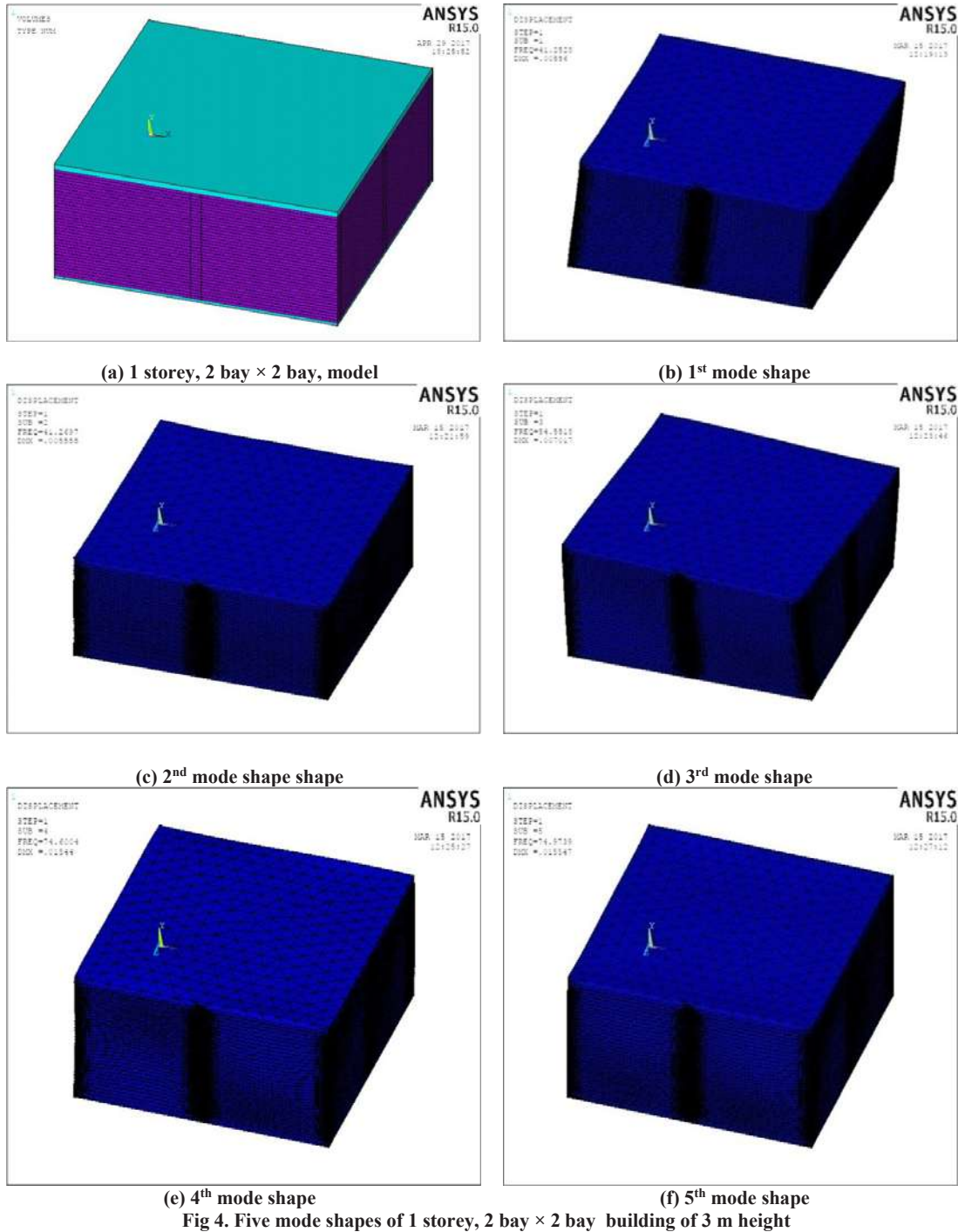


Fig 4. Five mode shapes of 1 storey, 2 bay  $\times$  2 bay building of 3 m height

Figure 4 present single storey model of 2 bay  $\times$  2 bay and its five mode shape. In this it observed that first mode shape can severe damage to structure while second and third can affected significantly and last two has no significant affect.

**ASSESSMENT OF SEISMIC VULNERABILITY**

Single storey 1 bay  $\times$  1 bay model is used to calculate base shear for six ground motions. Total 228 nodes are formed at bottom of the model and reaction forces in X and Z directions are calculated at each node and absolute value is found. This absolute value is checked for different PGA and remarked whether it is safe or not. Five ground motions i.e. El Centro, Kobe, Parkfield, Northridge, Coyote are used to calculate base shear. A model of one storey 1 bay  $\times$  1 bay is shown is presented in Fig 5 and five ground motion data which is used in this research work is presented by Table 4.

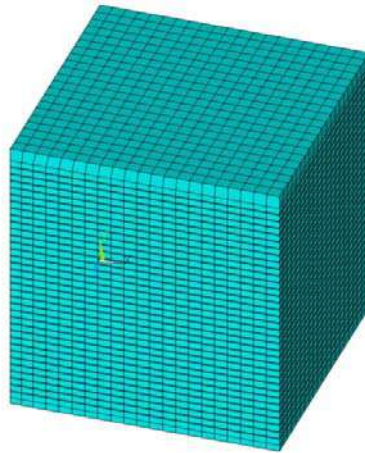


Fig 5. Single storey model of 1 bay × 1 bay with meshing

Table 4. Five ground motions data

Name of the earthquake	Peak ground acceleration (PGA)	Time duration (s)
El Centro	0.32g	31.18
Kobe	0.82g	48
Parkfield	0.36g	30.33
Northridge	0.22g	40
Coyote	0.12g	26.835

Base shear is calculated at different PGA value ranging from 0.05g to 0.5g, to arrive at the limiting PGA value, which the building may safely withstand. The PGA at which the base shear equals to the lateral strength is considered as the optimum value of that PGA, after which the failure of building may be initiated when base shear due to further increase of that PGA value exceeds the value of lateral strength of that building. Linear elastic analysis is adopted for calculating base shear. Table 5 represents the base shear at different PGA with remark.

Table 5. Base shear of 1 storey, 1 bay × 1 bay model with different PGA

Type	Lateral strength (kN) (Dutta et al., 2014)	Station	Base shear at different PGA		Remark
			PGA	Base shear (kN)	
1 Storey, 1 bay × 1 bay	34.018	El Centro	0.05g	10.719	Safe
			0.1g	21.439	Safe
			0.15g	32.159	Safe
			0.2g	42.878	Unsafe
		Kobe	0.05g	10.011	Safe
			0.1g	20.022	Safe
			0.15g	30.033	Safe
			0.2g	40.044	Unsafe
		Parkfield	0.05g	10.085	Safe
			0.1g	20.171	Safe
			0.15g	30.257	Safe
			0.2g	40.343	Unsafe
		Northridge	0.05g	10.226	Safe
			0.1g	20.452	Safe
			0.15g	30.679	Safe
			0.2g	40.905	Unsafe
Coyote	0.05g	13.022	Safe		
	0.1g	26.044	Safe		
	0.15g	39.066	Unsafe		

### TIME-HISTORY OF FORCE

Time history of maximum force acting in X direction at a particular node subjected to six ground motions is presented in Fig. 5.

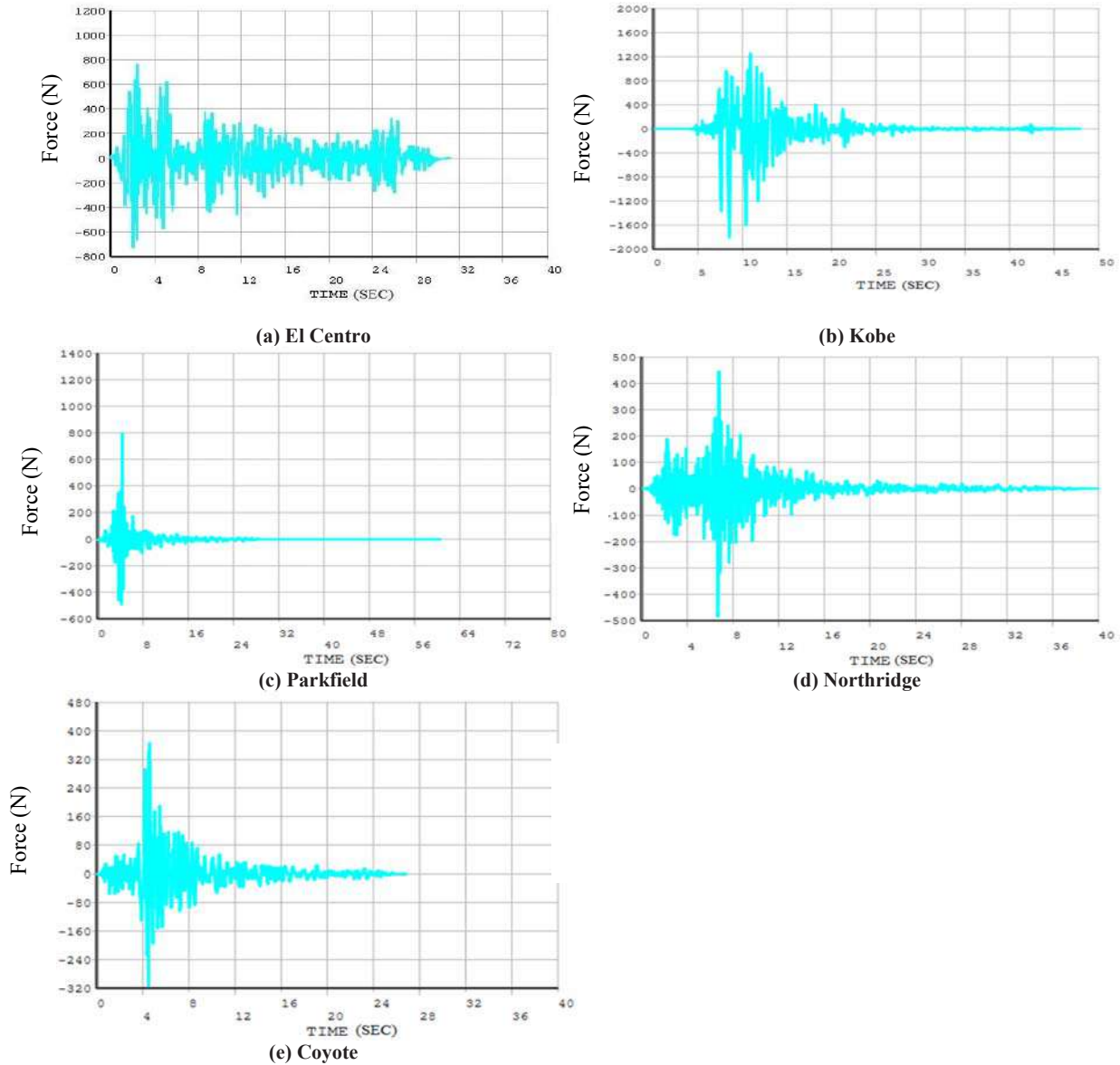


Fig. 5. Time history of maximum force in X direction at a particular node for five ground motions

### CONCLUSION

Seismic vulnerability of single storey structural model (1 bay  $\times$  1 bay) was assessed. Lateral strength of building has calculated as per Dutta et al. (2014). Base shear is calculated for five ground motion data using the above mentioned modelling. Base shear for different PGA value ranging from 0.05g to 0.2g is calculated to arrive at the limiting PGA value, which the building may safely withstand. The PGA at which the base shear equals to the lateral strength is considered as the optimum value of that PGA, after which the failure of building may be initiated when base shear due to further increase of that PGA value exceeds the value of lateral strength of that building. At least five mode shapes are draw using ANSYS and checked their behavior that which mode shape is severe, which one can be neglected and which has significant affect etc. Time history is also calculated and seen maximum force at particular time in x-direction. This study does helpful in analysis of similar earthquakes effects in masonry construction and can be correlated with other similar situations.

## REFERENCES

- Akhavessy A.H. (2012). The DSC Model for the Nonlinear Analysis of In-plane Loaded Masonry Structures. *The Open Civil Engineering Journal*, 2012, 6, (Suppl 1-M8) 200-214.
- Ali S and Page AW (1988) Finite element model masonry subjected to concentrated loads. *Journal of Structural Division Proceedings, ASCE* 114(8): 1761–1784.
- Andreas J. K., Gregory G. P. and Christos G. D (2002). Evaluation of simplified models for lateral load analysis of unreinforced masonry buildings. *Journal of Structural Engineering*, Vol. 128, No. 7, July 1, 2002.. ANSYS. Mechanical APDL.
- Betti M, Galano L, and Vignoli A, (2015), Time-History Seismic Analysis of Masonry Buildings: A Comparison between Two Non-Linear Modelling Approaches *Buildings* 2015, 5, 597-621; doi:10.3390/buildings5020597.
- Cecchi A, Milani G and Tralli A (2005). Validation of analytical multiparameter homogenization models for out-of-plane loaded masonry walls by means of the finite element method. *Journal of Engineering Mechanics, ASCE* 131(2): 185–198.
- Dhanasekar M, Page AW and Kleeman PW (1984). A finite element model for the in-plane behavior of brick masonry. *Proceedings of the 9th Australian Conference of Mechanisms of Structures*, Melbourne, Australia, pp. 262–267.
- Dutta S C, Nayak S, Dinakar P (2014). Lateral period and seismic vulnerability of masonry buildings. *Structures and Buildings*; vol. 167; pages 633-645.
- Gabor A, Bennani A, Jacquelin E, Lebon F (2006). Modelling approaches of the in-plane shear behavior of unreinforced and FRP strengthened masonry panels. *Composite Structures*; 74; 277–288.
- Goel RK and Chopra AK (1998) Period formulas for concrete shear wall buildings. *Journal of Structural Engineering, ASCE* 124(4): 426–433.



## Effect of $w/b$ ratio and Supplementary cementitious material on the rheological behaviour of cement paste

Siddharth S. Tulve,<sup>1</sup> Sunil D. Bauchkar,<sup>2</sup> H.S. Chore<sup>3\*</sup> and Nilesh Lende<sup>4</sup>

<sup>1</sup>\*.P.G. Student, <sup>2</sup>Research Scholar and <sup>4</sup>Assistant Professor

Department of Civil Engineering

Datta Meghe College of Engineering, Airoli, Navi Mumbai-400708 (Maharashtra); India  
e-mail: sid.tulve@gmail.com, sunil\_bauchkar@rediffmail.com and lendenilesh09@gmail.com

<sup>3\*</sup>Associate Professor, Department of Civil Engineering, Dr. B.R. Ambedkar National Institute of Technology, Jalandhar-144011 (Punjab); India (Corresponding Author)

### ABSTRACT

An experimental investigation into the rheological properties of high-strength cement paste is presented in this paper. The study is intended at evaluating the effect of varying water-binder ( $w/b$ ) ratio and supplementary cementitious material (SCM) on the rheology of cement paste. The study emphasizes on determining the yield stress and plastic viscosity (Bingham constants) of the cement paste. In this study Ordinary Portland Cement (OPC) was used as a binder in conjunction with Fly ash (FA), Ground granulated blast furnace slag (GGBS), Micro silica (MS) as SCMs and partial replacement for OPC. The FA, GGBS and MS replacement levels were kept at 40%, 70% and 7.5% respectively (by wt. of cement). The study was carried out with different  $w/b$  ratios (0.35, 0.4 and 0.45). The instrument Brookfield DV II Pro Viscometer was employed in the present study to determine the rheological properties of cement paste prepared with different  $w/b$  ratio and different SCMs. The instrument used in the study is found to detect systematic changes in the rheology of cement paste. It is found that the rheological properties of cement paste are highly dependent on the  $w/b$  ratio and the type and dosage of SCMs used in the study.

**KEYWORDS:** Brookfield DV II Pro Viscometer; fly ash; ground granulated blast furnace slag; micro silica; rheology; plastic viscosity; yield stress

### INTRODUCTION

Rheology is defined by Webster's Dictionary as "the study of the change in form and the flow of matter, embracing elasticity, viscosity, and plasticity". The research on rheology originated in the 19th century. After a large amount of theoretical and experimental work on rheology during the past years, the rheology has become a mature discipline and been widely applied in industry. In 1929, Prof. Bingham founded the Society of Rheology. Since then rheology has formally become an independent sub-discipline. Rheology is the scientific study of the flow and deformation of matter, mostly liquid or solid which responds to paste flow i.e. cement paste in the case of concrete. The cement paste component of concrete is what causes it to harden. With the recent advent of more fluid concrete (pumpable concrete, self-leveling concrete), it was necessary to measure the flow properties of cement paste such as yield stress & plastic viscosity. The complex interaction between cement and chemical/mineral admixtures in concrete mixture with varying  $w/b$  ratio sometimes leads to unpredictable concrete performances in the field, which is generally defined as concrete incompatibilities.

Cement paste rheology measurements, instead of traditional workability tests, can have a great potential to detect those incompatibilities in concrete before the concrete is placed to avoid setting time, workability, and curing-related issues, which sometimes lead to severe early-age cracking, especially in severe weather conditions. Bearing in mind these issues, it is required to recognize these concrete incompatibilities before concrete placement in order to evade the problems in the placing and curing process. The measurement of rheological properties of cement pastes provides crucial information on (i) the evolution of hydrating cementitious systems, (ii) microstructural variations and particle interaction in cement paste (iii) the compatibility of various cement, chemical, and mineral admixtures combinations. Therefore, cement rheological measurements have a great potential to identify those incompatibilities before concrete placement.

The aggregate effects in real concrete can be simulated during cement paste rheology measurements by some suitable means e.g., using a high shear mixing procedure to simulate aggregate shearing effects in concrete and setting a suitable plate gap in rheology test to represent an average gap between aggregate particles in real concrete. Thus, the cement paste rheology results could also be used in predicting the rheological properties of

concrete mixes.

## REVIEW OF LITERATURE

Vom Berg (1979) studied the influence of specific surface area (SSA) and concentration of solids on the flow behavior of cement pastes. It was found that the yield stress and plastic viscosity of cement paste increased as the cement fineness or the solids concentration increased, which reflects the dominance of the water-cement interface in the system. The fineness of cement particles controls the balance of attractive and repulsive force between cement particles, which has a profound impact on the flow of concrete. At a given water content, low cement content tends to produce harsh mixtures with poor workability, while high cement content produces better cohesiveness. Hope and Rose (1990) analyzed the effects of cement composition on the water demand required for the constant slump and stated that the correlation between the composition and water demand varied between different aggregates and mixture proportions. The water demand increased for cement with higher  $Al_2O_3$  or  $C_2S$  contents and decreased for cement with high loss of ignition, high carbonate addition, or high  $C_3S$  content.

Tattersall (1991) stated that the use of a mass replacement of fly ash in cement mixtures resulted in a reduction of yield stress while the plastic viscosity decreased only slightly. Szecsy (1997) found that a 10% fly ash mass replacement level in cement paste mixtures resulted in an increase in yield stress. From 10 to 20%, the use of fly ash reduced the yield stress. Further, the use of 5% fly ash resulted in a reduction of plastic viscosity; however, further replacement of cement with fly ash at rates up to 20% resulted in little additional change in plastic viscosity. Zhang and Han (2000) tested very fine fly ash to study the effect on cement paste rheological properties. It was found that while increasing the quantity of fly ash, yield stress most often was decreased. Koehler and Fowler (2004) observed that the addition of increasing levels of fly ash resulted in a reduction in yield stress in both, the river gravel and crushed limestone mixtures. While the value of the viscosity was reduced with increasing replacement levels of fly ash, the effect of fly ash on the plastic viscosity was variable. Notably, the general trend for plastic viscosity was similar for both, the river gravel and limestone mixtures. The addition of fly ash resulted in an increase in slump. Gao and Ye (2016) observed that the addition of fly ash reduced the initial yield stress and its growth with the rest time. The addition of 10% fly ash increased the apparent viscosity of the SCC mix while a higher addition reduced the apparent viscosity.

Park *et al.* (2005) stated that the ability of the blast furnace slag to fill into the voids between larger cement grains and displace the water in the cement mix helps in improving the rheology i.e. reduces the yield stress and plastic viscosity of the OPC-GGBS paste. However, Skripkiunas *et al.* (2005) ascertained that the addition of GGBS increased the yield stress as well as the plastic viscosity of the paste.

Faroug *et al.* (1999) observed that the replacement of OPC by MS up to 10% increased the yield stress, however, the increase in the MS content after 7.5% replacement level led to a reduction in the plastic viscosity of the cement paste. Zhang and Han (2000) reported that the 10% replacement of OPC by MS reduced the yield stress and plastic viscosity of the OPC-MS paste. The fact that the increase in  $w/b$  ratio reduces the yield stress, as well as the plastic viscosity, has been reported by many researchers (Tattersall and Banfill, 1983; Tattersall, 1991; Banfill, 1994; Domone *et al.*, 1999; Svermova *et al.*, 2003 and Leemann and Winnefeld, 2007). Rosquoet *et al.* (2003) found it difficult to evaluate the effect of  $w/b$  ratio on the rheological properties of concrete due to the limitations in the equipment and, therefore, focused only on the rheology of the paste.

## AIMS AND OBJECTIVES

The investigation aims at evaluating the effect of the  $w/b$  ratio and supplementary cementitious materials on the rheological properties of High-strength cement paste. Some of the objectives emanating from the aim of the present study are outlined as follows.

1. To analyze the effect of time and varying  $w/b$  ratio on the rheology of cement paste.
2. To study the effect of FA on the rheology of cement paste.
3. To determine the influence of GGBS on the rheology of cement paste.
4. To evaluate the impact of MS on the rheology of cement paste.
5. To study the flow spread of the cement pastes.

## RESEARCH METHODOLOGY

### Materials Used

#### a) Cement:

Cement act as a binder material, which sets and hardens and can bind other materials together. Cement used in

the study was ordinary Portland cement (like ASTM – Type-I) conforming to IS 12269 (OPC53). The physical properties and chemical compositions are described in Table 1 and Table 2 respectively.

**b) Supplementary Cementitious Materials**

Supplementary cementitious materials (SCM) such as FA meeting the requirements of IS 3812-2013, ASTM C618 (Class F), GGBS as per IS 12089-1987 and MS as per IS 15388-2003 requirements are used in the study. The physical properties and chemical compositions of the cementitious materials used are also shown in Table 1 and Table 2 respectively.

**Table 3. Physical properties of the materials used**

Properties of binders	OPC	FA	GGBS	MS
Density (g/cm <sup>3</sup> )	3.15	2.25	2.91	2.2
Specific Surface (m <sup>2</sup> /kg)	328	386	421	15000

**Table 4. Chemical compositions of the materials used**

Chemical compound	OPC	FA	GGBS	MS
SiO	21.4	68.1	33.79	88.9
Al <sub>2</sub> O <sub>3</sub>	4.3	25.8	20.73	0.4
Fe <sub>2</sub> O <sub>3</sub>	2.4	6.9	1.12	0.4
CaO	64.4	8.7	31.06	1.6
MgO	2.1	1.39	11.23	-
SO <sub>3</sub>	2.3	0.26	0.10	0.4
Na <sub>2</sub> O	0.60	0.18	0.30	0.5

**c) Water:**

Clean potable water with a temperature of about 25<sup>o</sup>c to 30<sup>o</sup>c is used in the study.

**Design Compositions**

The study is carried out to identify the effect of varying w/b ratio and SCMs on the flow spread and rheology of cement paste. The tests were carried out for the unary system (pure OPC paste) and binary systems (OPC+SCMs paste). For the binary system, the OPC was partially replaced by SCMs at a specified replacement level. Three different w/b ratios (0.35, 0.4 and 0.45) were used in the study keeping the volume of the mix paste constant while testing the samples, Table 3.

**Table 5. Mix proportions in wt. percentage for laboratory trials**

Compositions			% Cementitious material			
w/b ratio			OPC	FA	GGBS	MS
0.35	0.4	0.45				
OPW1	OPW2	OPW3	100	-	-	-
OPFAW1	OPFAW2	OPFAW3	60	40	-	-
OPGBSW1	OPGBSW2	OPGBSW3	30	-	70	-
OPMSW1	OPMSW2	OPMSW3	92.5	-	-	7.5

(\* W1, W2 and W3 represent w/b ratios 0.35, 0.4 and 0.45 respectively; OP-Ordinary Portland Cement; FA-fly ash; GBS- ground granulated blast furnace slag and MS-micro silica)

**Experimental Procedure and Tests**

**High-strength cement paste Mixing Procedure**

The paste compositions were produced by mixing the designed mix proportions of OPC, SCMs, and water in a Hobart mixer. In the unary system (pure OPC paste) the OPC is first added in the specified proportion in the Hobart mixer for mixing at a given speed. In case of binary system (OPC+SCM mix), 3 binary systems were prepared, OPC+FA, OPC+GGBS and OPC+MS. The partial replacement levels of FA, GGBS and MS were kept at 40%, 70% and 7.5 % respectively. Four main mixes were prepared, pure OPC, OPC+FA, OPC+GGBS and OPC+MS and each mix was tested for 3 different w/b ratios (0.35, 0.4 and 0.45). Each sample is first dry mixed and this mixing is continued for a half a minute to one minute. The addition of water is done in three installments in the Hobart mixer. The addition is done at 3 regular intervals, at the end of 1<sup>st</sup>, 2<sup>nd</sup>, and 3<sup>rd</sup> minute. The entire

process of paste mixing lasts for about 5 mins. The paste mix is then taken for flow cone and rheological tests. Special care must be taken during mixing, and the paste mix produced must be a homogeneous one. The whole sample preparation and testing procedures were carried out in a laboratory maintained at a temperature of  $24 \pm 2$  °C. A total of 12 samples were prepared for this study, Table 4.

**Table 6. Detailed description of the mix compositions for laboratory trials**

Compositions		OPC (gm)	FA (gm)	GGBS (gm)	MS (gm)	w/b ratio (gm)
<b>w/b 0.35</b>	OPW1	600	-	-	-	210
	OPFAW1	360	240	-	-	210
	OPGBSW1	180	-	420	-	210
	OPMSW1	555	-	-	45	210
<b>w/b 0.4</b>	OPW2	600	-	-	-	240
	OPFAW2	360	240	-	-	240
	OPGBSW2	180	-	420	-	240
	OPMSW2	555	-	-	45	240
<b>w/b 0.45</b>	OPW3	600	-	-	-	270
	OPFAW3	360	240	-	-	270
	OPGBSW3	180	-	420	-	270
	OPMSW3	555	-	-	45	270

**Flow Cone Test**

The flow cone is a simple device for measuring the viscosity from flow spread. The flow cone (Fig. 1) is 50 mm in height with the inner and outer diameter being 25 and 30 mm, respectively. A certain quantity of cement paste is mixed in Hobart mixer for 5 minutes. The cement paste is then poured into the cup and lifted. The flow is made to spread for 30 sec and measured.

**Rheology Test**

In a rheological study of cementitious paste, the yield stress and the plastic viscosity are the two key factors/rheological parameters. Hence, the rheological properties of cement paste were investigated using Brook-Field RV DV II+ Pro viscometer with disc spindle attachment. The test was performed according to the guidelines given in ASTM C1749-12. The Brook-Field Rotational Viscometer was used to determine the yield stress and the plastic viscosity as defined by modified Bingham model, Fig. 2. 6 rotational speed (100, 50, 20, 10, 5 and 4) were selected each step lasting for 2 minutes. This study was carried out using Spindle no. 3 at a speed of 5 rpm.



**Figure 7. Flow cone**



**Figure 8. Brookfield DV II Pro Viscometer**

**RESULTS AND DISCUSSION**

The results of the effect of w/b ratio and SCMs on the flow and rheological properties are tabulated in Table 5 and are graphically represented in Fig. 3, Fig. 4 and Fig. 5.

**Table 7. Results of flow and rheological properties of High-strength cement paste**

Compositions		Flow			Yield stress			Plastic viscosity		
		mm			Pa			Pa s		
		20 min	70 min	120 min	50 min	100 min	150 min	50 min	100 min	150 min
w/b 0.35	OPW1	164.14	122.29	113.85	6.9	7.12	8.76	1.2	1.82	2.57
	OPFAW1	125.38	111.13	105.41	9.89	11.69	13.78	1.29	1.43	1.65
	OPGBSW1	111.49	106.84	105.53	11.01	12.18	14.28	0.56	0.65	1.23
	OPMSW1	121.04	109.71	106.52	15.75	16.23	18.83	1.55	2.06	2.97
w/b 0.4	OPW2	222.77	186.04	162.57	5.92	6.84	7.72	0.61	0.76	1.14
	OPFAW2	215.68	177.71	154.89	7.2	9.47	11.53	0.55	0.79	0.9
	OPGBSW2	149.91	135.56	121.06	10.51	11.43	12.96	0.6	1.06	1.35
	OPMSW2	160.91	147.48	130.12	12.56	13.55	14.86	1.27	1.62	2.52
w/b 0.45	OPW3	246	221.79	210.52	4.28	5.58	7.03	0.5	0.6	0.74
	OPFAW3	256.5	234.6	217.89	6.04	9.54	10.62	0.48	0.53	0.59
	OPGBSW3	198.42	185.33	166.89	8.36	10.33	11.66	0.4	0.86	0.96
	OPMSW3	204.87	175.89	167.23	10.54	12.57	13.91	0.5	1.17	1.33

### Effect of Time

It can be observed from Fig. 3, Fig. 4 and Fig. 5 that as the time increases the yield stress and plastic viscosity increase for the pure OPC mix as well as for all the OPC+SCMs samples in respect of all the three w/b ratios.

### Effect of w/b ratio W1

Fig. 3 illustrates the effect of w/b W1 on the rheology of cement paste. It can be ascertained that the highest yield stress and plastic viscosity is achieved by the cement paste samples only at w/b ratio W1. The OPC+MS mix attains the highest yield stress followed by OPC+GGBS, OPC+FA and OPC mix. With respect to plastic viscosity, here too, the OPC+MS sample recorded the highest plastic viscosity as compared to the other samples. The OPC+GGBS sample achieved the lowest plastic viscosity throughout the testing period.

### Effect of w/b ratio W2

Fig. 4 demonstrates a reduction in the yield stress and plastic viscosity for all the cement paste samples at w/b W2. The rheological properties are slightly higher for w/b W1. The pure OPC mix recorded the lowest yield stress while the OPC+MS mix recorded the highest yield stress during the testing period. The plastic viscosity of the OPC+MS mix is found to be significantly higher as compared to the other samples. However, not much difference is seen between the plastic viscosity of pure OPC, OPC+FA and OPC+GGBS mix.

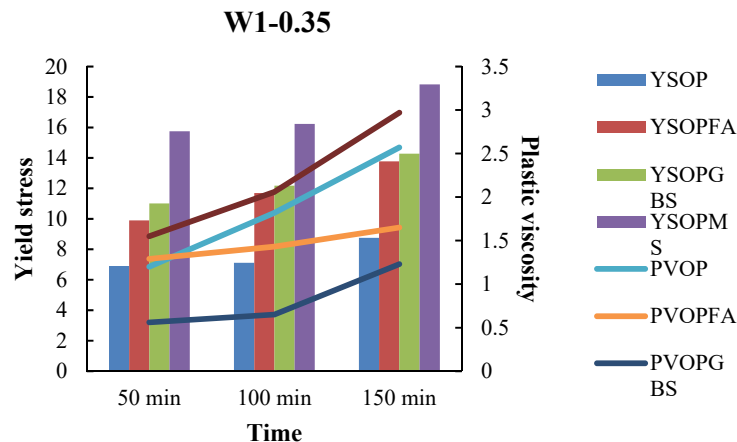


**Fig. 9. Effect of w/b W1 and time on the rheological properties of cement paste**

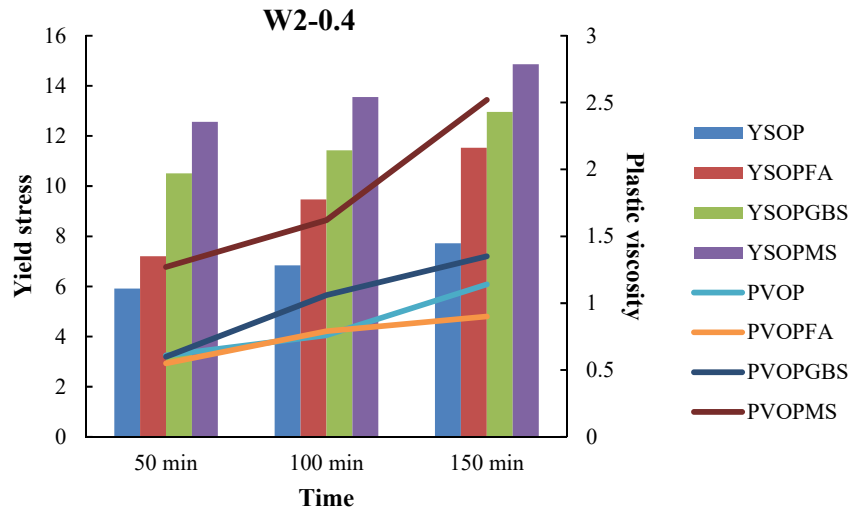


Fig. 10. Effect of *w/b* W2 and time on the rheological properties of cement paste

**Effect of *w/b* ratio W3**

The rheological properties are found to reduce further at the *w/b* ratio W3 as depicted in Fig. 5. The pattern of increase of the yield stress for the *w/b* W3 is similar to the other two *w/b* ratios for all the cement paste samples. The plastic viscosity for the initial testing period for all the cement paste samples is found to be almost similar. However, the plastic viscosity of the OPC+MS sample is found to increase significantly with the progress in testing period. The plastic viscosity of OPC+FA sample at the latter stage of the testing period is less as compared to the pure OPC mix for all the three *w/b* ratios.

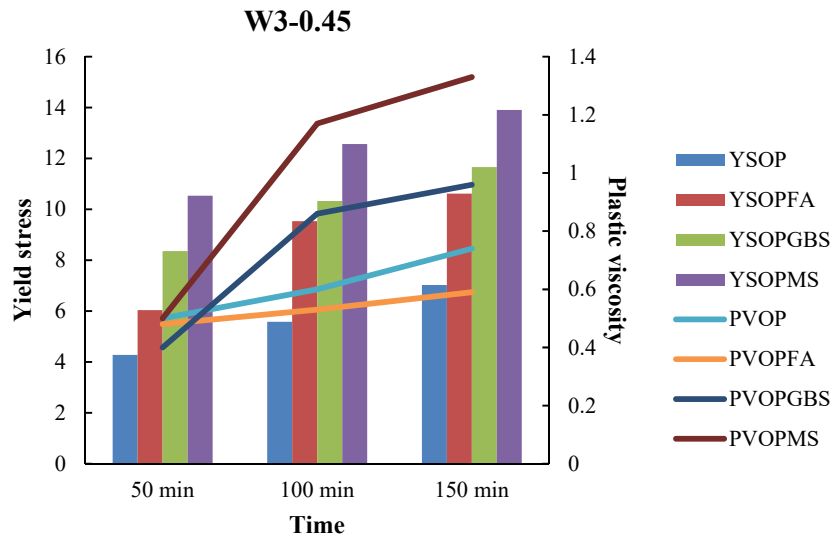


Fig. 11. Effect of *w/b* W3 and time on the rheological properties of cement paste

(\* YS- Yield stress and PV- Plastic viscosity)

## CONCLUSIONS

- The flow spread decreases as time progresses and increases as the w/b ratio increases for all the cement paste mix.
- The increase in time increases the yield stress as well as plastic viscosity for all the cement paste mix.
- The increase in the w/b ratio reduces the yield stress and plastic viscosity for all the cement paste mix.
- The partial replacement of OPC by SCMs increased the yield stress of OPC+SCM mix for all the w/b ratios.
- The OPC+ MS mix achieved the highest yield stress and plastic viscosity for all the w/b ratios.
- The fly ash particles could be attributed for the reduction in the plastic viscosity in the OPC+FA mix as the plastic viscosity of OPC+FA mix was lower for all the w/b ratios as compared to the pure OPC mix.

## ACKNOWLEDGEMENT

The permission accorded by BASF India Ltd., Turbhe, Navi Mumbai (Maharashtra), India for undertaking the experimental work contained in this paper is gratefully acknowledged. The help and assistance provided by the staff of the BASF Laboratory is also acknowledged.

## REFERENCES

- ASTM C 618 (2017) "Standard Specification for Coal Fly Ash and Raw or Calcined Natural Pozzolan for Use in Concrete" ASTM International, West Conshohocken, PA.
- ASTM C 1749 (2012) "Standard Guide for Measurement of the Rheological Properties of Hydraulic Cementitious Paste Using a Rotational Rheometer"; ASTM International; West Conshohocken, PA.
- Banfill P.F.G. (1994) "Rheological methods for assessing the flow properties of mortar and related materials; Construction and Building Materials; 8(1); pp. 43-50.
- BIS 3812 (Part 1) (2013) "Pulverized fuel ash- Specification (For use as Pozzolana in cement, cement mortar and concrete)." Bureau of Indian Standard, New Delhi.
- BIS 12089 (1987) "Specification for granulated slag for the manufacture of Portland slag cement"; Bureau of Indian Standard, New Delhi, India.
- BIS 12269 (2013) "53 grade ordinary Portland cement", Bureau of Indian Standard, New Delhi, India.
- BIS 15388 (2003) "Specification for Silica Fume" Bureau of Indian Standard, New Delhi, India.
- Domone P. L. J., Xu Y. and Banfill, P. F. G. (1999) "Development of the two-point workability test for high-performance concrete" Magazine of Concrete Research; 15(3) June; pp: 171-179.
- Faroug F., Szwabowski, J. and Wild S. (1999) "Influence of superplasticizers on workability of concrete" Journal of Materials in Civil Engineering; 11(2); pp: 151-157.
- Gao X. and Ye H. (2016) "Time-Dependent Evolution of Rheological Performance and Distinct-Layer Casting of Self-consolidating Concrete"; *SCC-2016, 8th International RILEM Symposium on Self-compacted concrete*; pp: 417-427. Washington, USA.
- Hope B.B. and Rose (1990) "Statistical analysis of the influence of different cements on the water demand for constant slump"; H.J. Wierig Editor; Properties of Fresh Concrete; *Proceedings of the Coll. RILEM*; Chapman and Hall; pp: 179-186.
- Koehler E.P. and Fowler D.W. (2004) "Development of A Portable Rheometer for Fresh Portland Cement Concrete", *Research Report ICAR-105-3F*, pp: 56-57 and 274-275.
- Leemann A. and Winnefeld F. (2007) "The effect of viscosity modifying agents on mortar and concrete"; *Cement and Concrete Composites*; 29(5); pp: 341-349.
- Park C.K., Noh. M.H. and Park T.H. (2005) "Rheological properties of cementitious materials containing mineral admixtures"; *Cement Concrete Research*; 35(5); pp: 842-849.
- Rosquoet F., Alexis A., Kjelidj A. and Phelipot A. (2003) "Experimental study of cement grout: Rheological behavior and sedimentation"; *Cement and Concrete Research*; 33(5); pp: 713-722.
- Skripiunas G., Dauksys M., Stuopys A. and Levinskas R. (2005) "The Influence of Cement Particles Shape and Concentration on the Rheological Properties of Cement Slurry" ISSN 1392-1320 *Materials science (MEDZIAGOTYRA)*; 11(2).
- Svermova L., Sonebi M. and Bartos P.J.M., (2003) "Influence of mix proportions on rheology of cement grouts containing limestone powder"; *Cement and Concrete Composites*; 25(7); 737-749.
- Szecszy R.S. (1997) "Concrete Rheology"; PhD Dissertation, University of Illinois at Urbana-Champaign, Urbana, IL.
- Tattersall G. H. (1991) "Workability and Quality-Control of Concrete" London.
- Tattersall G.H. and Banfill P.F.G. (1983) "The rheology of fresh concrete" (No. Monograph). *Pitman Advanced*

*Publication. Program.*

Vom Berg W. (1979) "Influence of specific surface and concentration of solids upon the flow behavior of cement pastes"; *Magazine of concrete research*, 31(109); pp: 211-216.

Zhang X. and Han J. (2000) "The effect of ultrafine admixture on the rheological property of cement paste"  
*Cement and Concrete Research*; 30; pp: 827-830



## Performance of Shear Wall Structure Under Blast Loading

Simranjit singh<sup>1</sup>, Charanjeet Singh<sup>2</sup>, Ankush Thakur,<sup>3</sup> Dushayant singh yadv<sup>4</sup>

<sup>1</sup>Dept. of Civil Engineering, Chandigarh University, SAS Nagar, Punjab, India(\*Corresponding Author)

<sup>2</sup>Dept. of Civil Engineering, Chandigarh University, SAS Nagar, Punjab, India

<sup>3</sup>Dept. of Civil Engineering, National institute of technology, Jalandhar, Punjab, India

<sup>4</sup>Junior engineer, border road organization, India

### ABSTRACT

This paper deal with the comparison of shear wall multistory structure with the bare frame multistory structure under the effect of blast load at varying standoff distance. The result was finally compared in STAAD PRO V8i, where overall maximum displacement value was analyzed and furthermore the maximum displacement value of multiple nodes was also specified. The main aim of the study is to blast the TNT of varying intensities on building and check the displacements. The pitch of energy is examined with a disintegrate assessment of a usual frame structure building. Whereas the result state that more the standoff distance less is the effect on the building and vice versa. Which also shows if higher charge weights, the collapse occurs faster, as is evident from the graphs and result.

**Keywords:** Blast load, shear wall, Bare frame, TNT.

### INTRODUCTION

The volcanic activity issue is though very old, however much of the revision and information on the topic were collected during the last six decades whereas the explosion dilemma is newer. Disasters including the militant bombings at the U.S. embassies of Nairobi, Kenya and Dares Salaam, and at Tanzania in year 1998, military barracks at the Khobar Towers of Dhahran, and in Saudi Arabia in year 1996, at the Murrah Federal Building in Oklahoma City in year 1995, and the W.T.C in New York in 1993 have expressed the requirement for a detailed investigation of the performance of columns impacted by blast loads (Kirk et al. 2005). To ensure enough avoidance adjoining to explosions and blasts, the construction and design of the public buildings have customary transformed attentiveness of architects and civil engineers. Though troubles crop up with these complexities that contain time dependent finite deviations, higher strains, and non-linear non elastic manners of material, have led to various assumptions, approximations that could simplify such models.

Generally during construction work, many unknown factors were overestimate under blast load. However these factors like design methods, construction quality, material used and unpredicted shock wave are different for each type of structure. For making the structure safe during uncertainties conditions it is suggested to the use trinitrotoluene equivalent mass is considered in design formation up to 20 %. The changed increase value in a charged weight is known as the "effective charge weight".

### LITERATURE REVIEW

The essential element is the load that has been produced from a source of explosion, how it interacts with the given structure and how the structure responds to such a load. A source of explosion may include a gas, a highly explosive material, nuclear substances or dirt materials. The common features of an explosion and a blast wave phenomenon have been presented with reference to a discussion of TNT (trinitrotoluene) equivalency, keeping in regard, the blast scaling laws. The characteristic features of an incident that are overpressure-loading due to an atomic weapon, conventionally high explosion and unconfined vapours of a cloud explosion have been addressed that follow a description of other blast loading elements that are associated with the flow of air and the process of reflection. In this case we extensively studied the structures and the computations of the impacts of blast loading on superstructures.

1. **A.K. Pandey (2007)** explore the nuclear containment structure which faces the external explosion on its outer reinforcement concrete shell. He chooses the non-linear material sculpt to make analysis till the final stage. With the help of finite element method DYNAIB the analytical practice for non-linear analysis is adopted the above sculpt is given by (Pandey, Kumar, Paul, & Trikha, 2006) .
2. **Kirk A. Marchand et al. (2005)** had also reviewed the contents of the American Institute of Steel Construction, Inc. for steel buildings that present a generalised scientific study of the effects of blast with the help of a significant number of case studies of different buildings that have been spoilt due to the explosive

pressure i.e. Murrah Building, Oklahoma City, Khobar Towers, Dhahran, Saudi Arabia and others is explained by (Marchand & Alfawakhiri, 2004).

3. **M. V. Dharaneepathy et al. (1995)** has considered the effects of the standoff distances on lofty shells, of varying heights, that were carried out keeping a view of studying the effect of ground-zero distance of allege with the detonation source. An imperative point, while designing blast resistant buildings, kept is to come up with a practical prediction of pressures due to the explosion. The standoff distance of point/source of explosion with respect to geographical coordinates of the structure is very important that governs the magnitude as well as the duration of the blast loads and their relative impacts. The distance, also identified as the critical ground zero distance, is the distance at which the retort of blast becomes the maximum. This distance, due to its significant importance, can be effectively used as a reference distance for designing rather than considering other arbitrary distances.

### PROBLEM DESCRIPTION

Story height of building is 3 meter, Number of stories are five, Number of bays in X and Z direction is eight where length of bay in X and Z direction is 3m, see **Figs. 1 and 2**. Dimension of beam is 0.6 x 0.3m where specification of columns is 0.6 x 0.6m and shear wall having thickness of 0.25m. In material the grade we use is M30 and load indulge on a floor is 5 kN/m<sup>2</sup>. Condition of soil was considered as hard soil which includes damping ratio 5% and quantity of blast which acting on the structure in 100, 200,300,400,500Kg of TNT.

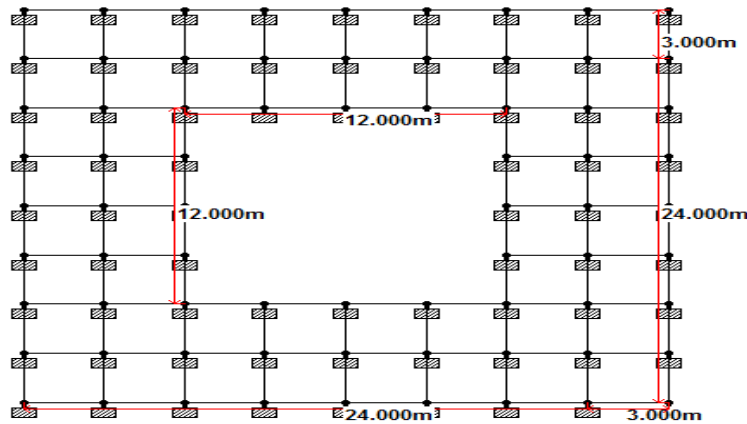


Figure 1: Top View of Open To Space Building

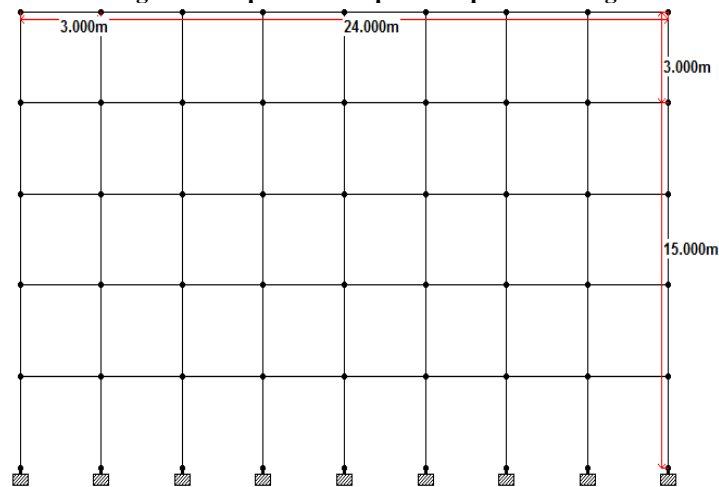


Figure 2: Section view of 5 story building

**RESULT AND DISCUSSION**

Different STAAD models generated were analyzed, the results of analysis have been tabulated below, see **Table 1**. It contains different amount of TNT and varying standoff distance. Each case has its own maximum and minimum displacement which was found by using STAAD Pro V8i. Two different framed structures were used. In one of the cases, we used simple concrete bare frame having only beams and columns, whereas in the other case we used concrete framed structure with shear wall. Maximum overall displacement in the building was chosen to be the main criteria for the comparisons of results all displacement values are in mm.

**Table 1: Maximum value of displacement (in mm) at each blast load category and standoff distance.**

STAND OFF DISTANCE	CASE	TNT kg		
		300	200	100
15m	W/O SW	567.24	67.22	0.957
	SW	378.02	64.72	0.95
20m	W/O SW	33.028	7.85	0.075
	SW	33.25	7.328	0.079
25m	W/O SW	8.97	0.735	0.022
	SW	8.32	0.522	0.031

**CASE ONE:- 15m STAND OFF DISTANCE WITH CHANGING LOAD**

For a displacement of 15m, the trial loads were taken as 300kg, 200kg and 100kg and we checked the displacement or drift occurring in body which is shown in bar graph, see **Fig 3**. There are two cases that were considered first being bare frame structure or without shear wall case and second one with shear wall case. The graph contains two colors, blue and red. Blue represent bare frame and red represent shear wall case.

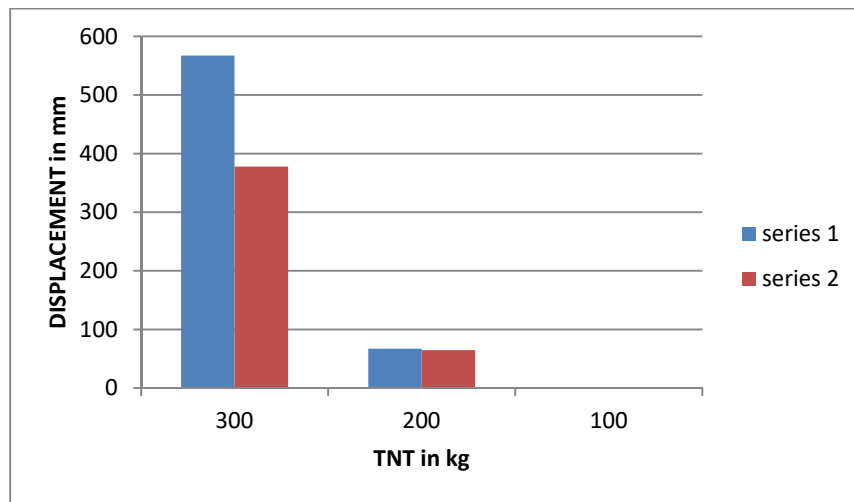


**Figure:3 Bar chart comparison between shear wall and w/o shear wall**

**EFFECT OF SHEAR WALL AT DIFFERENT NODES FOR 300KG LOAD AT STANDOFF 15m.**

In this case node 46 and 486 are identical as the drop in maximum drift due to shear wall in x direction as well as in z direction is 80% where as the drop in resultant maximum drift is also 80%. Nodes 160 and 372 behave identically, see **Fig 4** where the drop in drift in x direction as well as in z direction is 25% and the drop in resultant maximum drift is 30%. For nodes 270 and 482 the drops are 75% and 80% in x and z direction interchangeably where as the drop in maximum resultant drift is 80%, Detailed vaues are tabulated below, see **Table 2**.

**Table 2: comparing result of displacement at 15m standoff distance with 300 kg blast**

Joint number	Displacement w/o shear wall			Displacement with shear wall		
	x direction	z direction	r direction	x direction	z direction	r direction
46	504.404	504.407	713.847	107.153	107.365	154.378
160	523.227	523.225	739.953	375.724	375.693	531.332
270	567.245	502.765	758.137	141.818	97.779	174.725
372	523.226	523.226	739.953	375.706	375.711	531.332
482	502.763	567.242	758.134	97.542	141.227	174.092
486	504.422	504.424	713.862	107.208	107.421	154.373

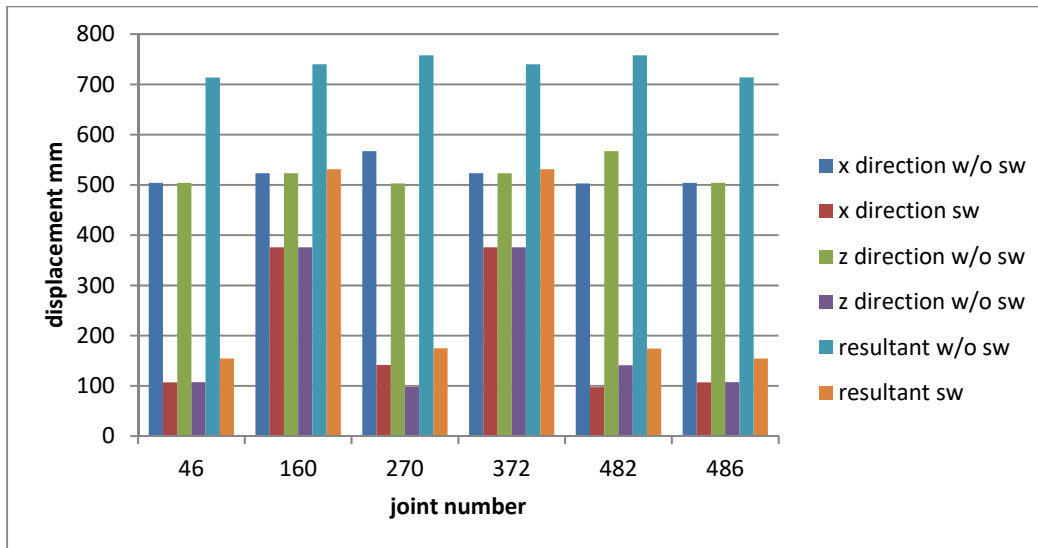


**Figure 4: Comparing result of displacement at 15 m standoff distance with 300 kg blast**

**EFFECT OF SHEAR WALL AT DIFFERENT NODES FOR 200KG LOAD AT STANDOFF 15m.**

For node 160 the drop in drift is negligible for node 216 the drop in drift in x direction is 30%, in z direction is 75% and in resultant maximum drift is 45%. For node 262 the drop in drift is 60% in x direction 70% in z direction and 65% in resultant maximum drift. For node 372 there is slight 2% increase in drift in x direction 20% drop in drift in z direction and 10% drop in resultant maximum direction. For node 374 there is again 2% increase in drift in x direction 70% drop in z direction and 30% drop in resultant maximum drift. For node 486 a 70% drop in drift in x direction as well as in z direction lead to 65% drop in resultant maximum drift, see Fig 5. Detailed Values are tabulated below, see Table 3.

**Table 3: comparing result of displacement at 15m standoff distance with 200 kg blast**

joint number	displacement w/o shear wall			displacement with shear wall		
	x direction	z direction	r direction	x direction	z direction	r direction
160	61.966	61.966	87.633	63.576	64.322	90.44
216	65.473	60.079	88.872	46.031	16.501	48.945
262	67.227	60.088	90.194	24.278	17.036	30.038
372	61.966	61.966	87.633	64.407	47.01	79.744
374	61.905	67.216	91.407	64.565	23.594	68.939
486	60.27	60.27	85.294	19.406	19.012	27.597

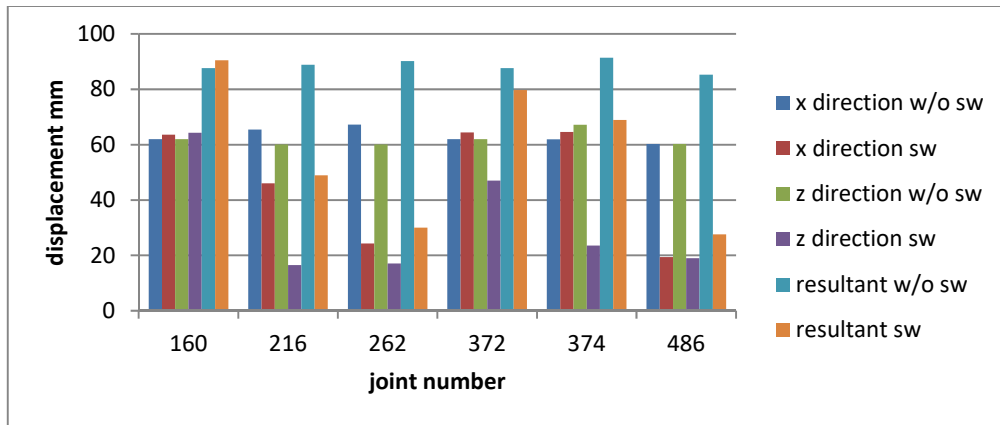


Figure 5: Comparing result of displacement at 15 m standoff distance with 200 kg blast

**EFFECT OF SHEAR WALL AT DIFFERENT NODES FOR 100KG LOAD AT STANDOFF 15m.**

For node 46 the drop in maximum drift in x as well as in z direction is 65% resulting in 55% drop in resultant maximum drift. Almost same behavior is shown by node 50. In node 161 there is 5% increase in drift in x direction 15% drop in drift in z direction resulting into 7% drop in resultant maximum drift. For node 262 there is 65% drop in drift in x direction 70% drop in drift in z direction and 60% drop in resultant maximum drift. For node 263 there is 70% drop in drift in x direction 20% drop in drift in z direction and 40% drop in resultant maximum drift. For node 372 there is 5% increase in drift in x direction 2% increase in drift in z direction leading to 9% increase in resultant maximum drift, see Fig 6. Detailed values are tabulated below, see Table 4.

Table 4: comparing result of displacement at 15m standoff distance with 100 kg blast

joint number	displacement w/o shear wall			displacement with shear wall		
	x direction	z direction	r direction	x direction	z direction	r direction
46	0.848	0.848	1.201	0.306	0.3	0.453
50	0.846	0.957	1.325	0.254	0.338	0.478
161	0.867	0.875	1.331	0.901	0.702	1.245
262	0.957	0.846	1.325	0.341	0.247	0.557
263	0.952	0.864	1.377	0.34	0.676	0.813
372	0.876	0.876	1.239	0.937	0.909	1.383

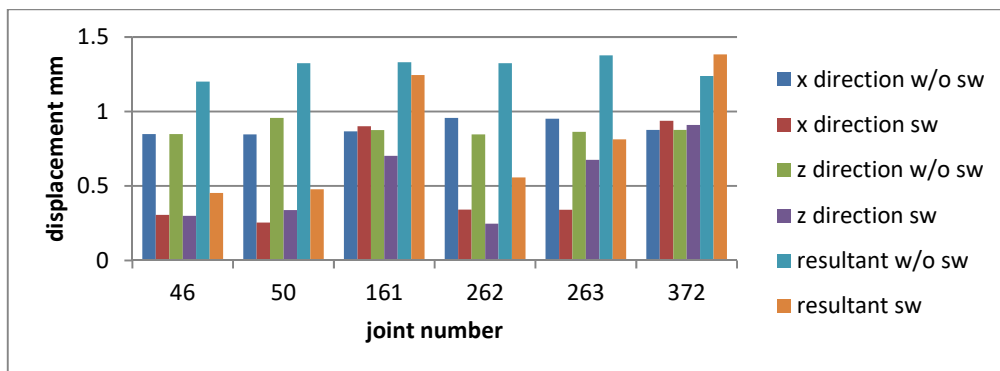


Figure 6: Comparing result of displacement at 15m standoff distance with 100 kg blast

**CASE SECOND: 20m STANDOFF DISTANCE WITH CHANGING LOAD.**

At a displacement of 20m,

**(i) In the framed structure w/o shear wall**

When TNT used is 300 kg the maximum drift obtained is 33.02mm, Furthermore the drift obtained for 200 kg TNT is 7.85 mm and is approximately 25% of the drift obtained for 300 kg TNT and on trial value for 100kg TNT the drift value is decreases to a dismal 0.075mm. it can be inferred from the above discussed result that for the given case the value of drift drops sharply as the value of the TNT decreases and the drops are very sharp as the values of loads tend to become much lower.

**(ii) In the framed structure with shear wall**

When TNT used for 300kg is 33.25mm. At 200kg TNT the drift obtained is 7.32mm which is again equal to drift obtained for 200kg w/o SW and 22% of 300kg with SW. At 100kg the value of drift is 0.079mm. it can be inferred that at 300kg as well as 200 kg,drift remains same. where as at 100kg TNT load the value of drift is such low that the effect of shear wall can be considered to be non obtainable.

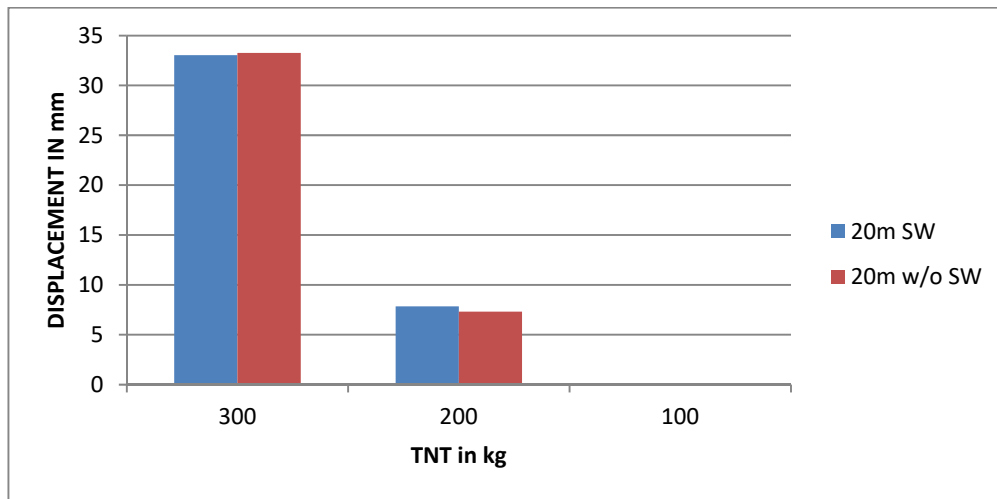


**Figure 7: Comparison B/W Shear Wall And W/O Shear Wall In 20m Standoff Distance**

**EFFECT OF SHEAR WALL AT DIFFERENT NODES FOR 300KG LOAD AT STANDOFF 20m.**

In this case node 46 and 486 are identical as the drop in maximum drift due to shear wall in x direction as well as in z direction is 65% where as the drop in resultant maximum drift is also 65%. For nodes 50 and 262 the drops are 70% and 65% in x and z direction interchangeably where as the drop in maximum resultant drift is 68%. At node 158 the increase in x direction is 7% in z direction the drop is 67% resulting in 25% drop in resultant maximum drift. Similarly, at node 250 a 70% drop in drift in x direction and a 10% increase in drift in z direction result in 20% drop in resultant maximum drift, see Fig 7. Deatiled Values are tabulated below, see Table 5.

**Table 5: comparing result of displacement at 20m standoff distance with 300 kg blast**

joint number	displacement w/o shear wall			displacement with shear wall		
	x direction	z direction	r direction	x direction	z direction	r direction
46	29.863	29.863	42.263	9.912	9.714	14.078
50	29.77	33.028	44.468	9.026	11.777	14.995
158	30.719	33.018	45.116	32.798	11.779	34.957
250	23.078	22.151	31.992	6.612	24.672	25.676
262	33.028	29.77	44.468	12.19	8.805	15.301
486	29.848	29.848	42.252	9.98	9.784	14.261

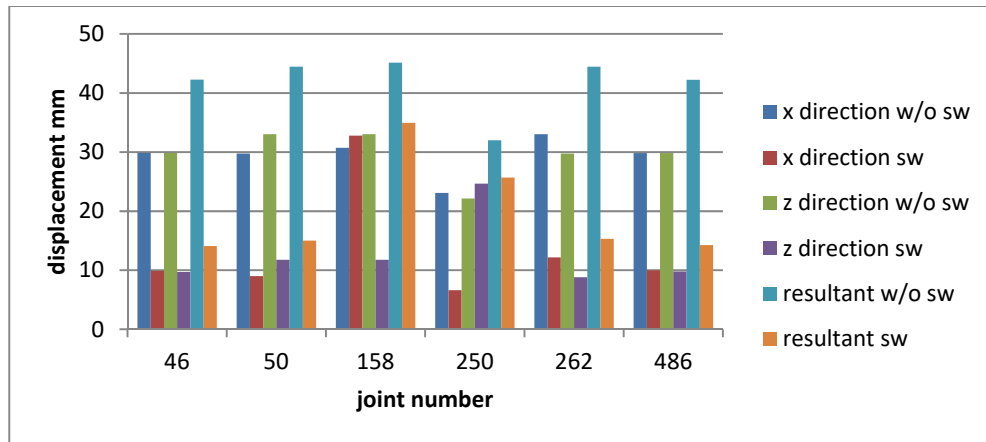


Figure 8: Comparing result of displacement at 20m standoff distance with 300 kg blast

**EFFECT OF SHEAR WALL AT DIFFERENT NODES FOR 200KG LOAD AT STANDOFF 20m.**

In this case node 46 and 486 are identical as the drop in maximum drift due to shear wall in x direction as well as in z direction is 70% resulting in drop in resultant maximum drift is 70%. For nodes 50 and 262 the drops are 70% and 65% in x and z direction interchangeably where as the drop in maximum resultant drift is 68%. At node 23 the drop in maximum drift in x direction is 80% in z direction it is 75% resulting in drop of 78% in resultant maximum drift. Similarly at node 264 a 68% drop in drift in x direction and a negligible drop in drift in z direction result in 30% drop in resultant maximum drift, see Fig 8. Detailed values are tabulated below, see Table 6.

Table 6: comparing result of displacement at 20m standoff distance with 200 kg blast

joint number	displacement w/o shear wall			displacement with shear wall		
	x direction	z direction	r direction	x direction	z direction	r direction
23	3.326	3.495	4.825	0.742	0.814	1.125
46	7.01	7.01	9.92	2.194	2.154	3.094
50	6.987	7.855	10.514	1.978	2.607	3.282
262	7.855	6.987	10.514	2.62	1.933	3.362
264	7.844	7.253	10.7	2.62	7.22	7.685
486	6.994	6.994	9.913	2.166	2.126	3.138

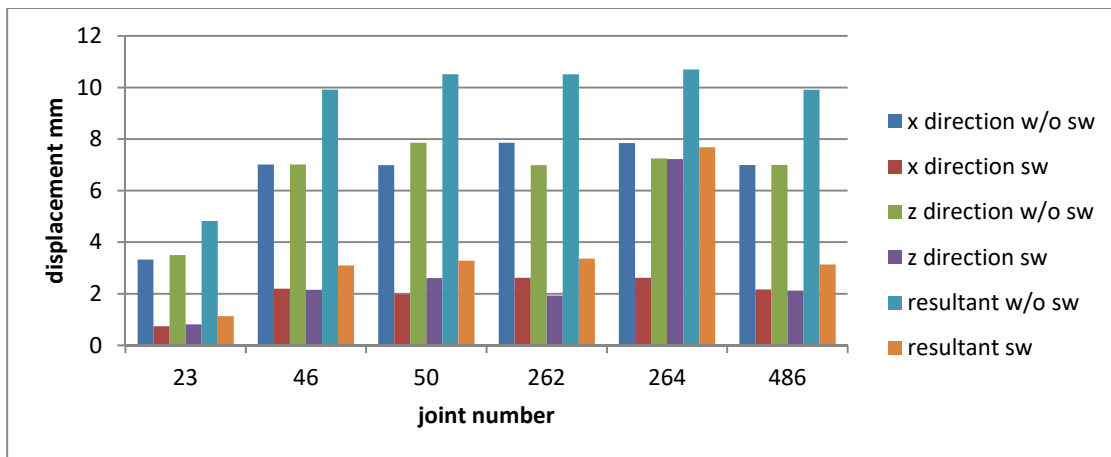


Figure 9: Comparing result of displacement at 20m standoff distance with 200 kg blast

**EFFECT OF SHEAR WALL AT DIFFERENT NODES FOR 100KG LOAD AT STANDOFF 20M.**

Since the load of 100kg TNT is less to create enough maximum drift in any direction the majority of the nodes show minimum changes in the drift value, **Fig. 10**. Except for node 46 where the resultant maximum drift increases to almost 300% which may be attributed to the location of the location of node at the L junction of the shear wall on the outermost exposed position, see **Table 7**.

Table 7: comparing result of displacement at 20m standoff distance with 100 kg blast

joint number	displacement w/o shear wall			displacement with shear wall		
	x direction	z direction	r direction	x direction	z direction	r direction
46	0.053	0.053	0.075	0.044	0.044	0.226
47	0.065	0.075	0.378	0.043	0.07	0.257
100	0.075	0.065	0.378	0.07	0.043	0.257
161	0.044	0.064	0.509	0.036	0.055	0.493
241	0.027	0.026	0.234	0.015	0.027	0.199
347	0.026	0.027	0.234	0.027	0.002	0.192

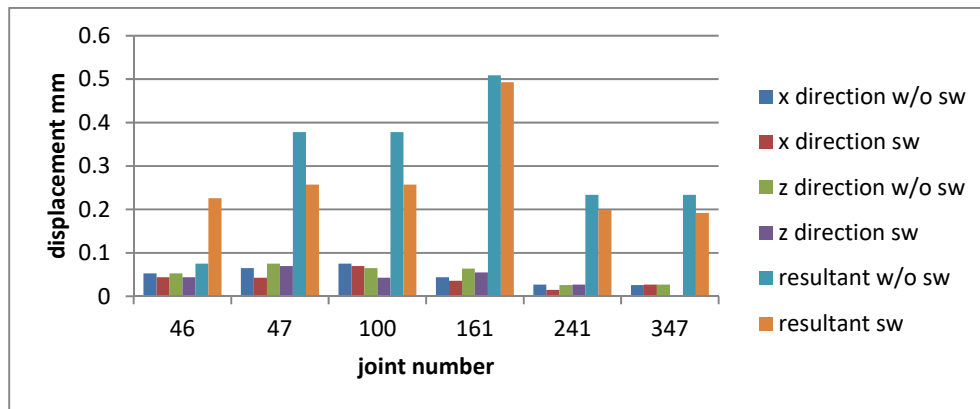


Figure 10: Comparing result of displacement at 20m standoff distance with 100 kg blast

**CASE THIRD: 25m STANDOFF DISTANCE WITH CHANGING LOAD**

At a displacement of 25m,

**(i) In the framed structure w/o shear wall**

When TNT to 300 kg the maximum drift obtained is 8.97mm which approx. of 13% of the first drift obtained TNT, see Fig. 11. Furthermore the drift obtained for 200kg and 100kg TNT tends to attain negligible value even less than 1mm.

**(ii) In the framed structure with shear wall**

When TNT used is 500kg the maximum drift obtained is 8.32mm furthermore the drift obtained for 200kg and 100kg TNT tends to attain negligible value even less than 1mm.

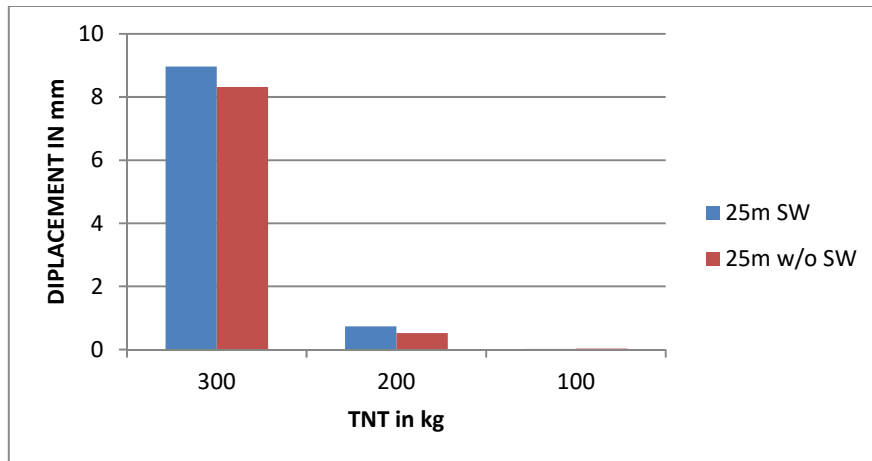


Figure 11: Comparison B/W Shear Wall and W/O Shear Wall In 25m Standoff Distance

**EFFECT OF SHEAR WALL AT DIFFERENT NODES FOR 300KG LOAD AT STANDOFF 25m.**

In this case node 46 and 486 are identical as the drop in maximum drift due to shear wall in x direction as well as in z direction is 70% where as the drop in resultant maximum drift is also 70%. For nodes 50 and 262 the drops are 72% and 67% in x and z direction interchangeably where as the drop in maximum resultant drift is 70%, see Fig. 12. At node 23 the drop in x direction is 70% in z direction the drop is 78% resulting in 78% drop in resultant maximum drift, whereas at node 264 the change in drift due to shear wall is negligible in z direction and 67% drop in x direction resulting in 27% drop in resultant maximum drift, Table 8.

Table 8: comparing result of displacement at 25m standoff distance with 300 kg blast

joint number	displacement w/o shear wall			displacement with shear wall		
	x direction	z direction	r direction	x direction	z direction	r direction
23	3.79	3.992	5.504	0.841	0.926	1.284
46	7.988	7.988	11.304	2.482	2.44	3.506
50	7.961	8.97	11.994	2.24	2.964	3.73
262	8.97	7.961	11.994	2.951	2.193	3.786
264	8.959	8.276	12.213	2.95	8.206	8.726
486	7.972	7.972	11.296	2.458	2.416	3.555

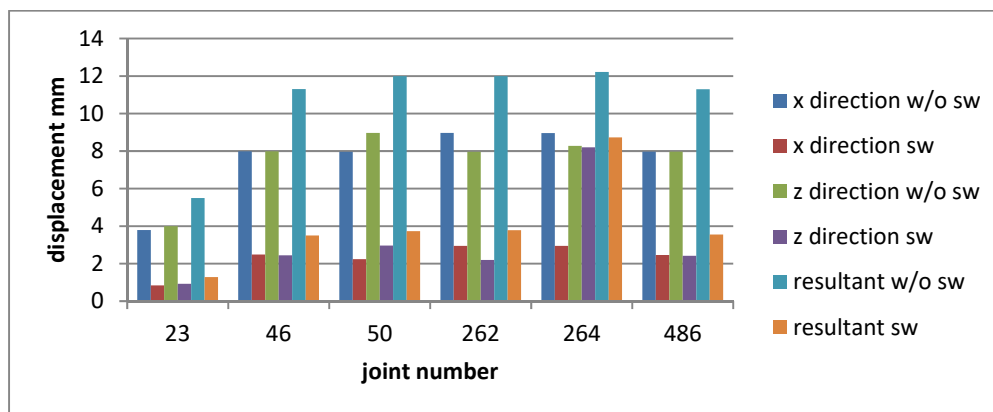


Figure 12: Comparing result of displacement at 25m standoff distance with 300 kg blast

**EFFECT OF SHEAR WALL AT DIFFERENT NODES FOR 200KG LOAD AT STANDOFF 25m.**

In this case at node 46 drop in maximum drift due to shear wall in x direction is 75% where as in z direction it is 75% where as the drop in resultant maximum drift is 67%. For nodes 50 and 262 the drops are 82% and 75% in x and z direction interchangeably where as the drop in maximum resultant drift is 65%, see **Fig. 13**. At node 161 the drop in x direction is 30% in z direction the drop is 45% resulting in 27% drop in resultant maximum drift, whereas at node 23 the drop in drift due to shear wall is 85% in x as well as z direction resulting in 65 % drop in resultant maximum drift. At node 263 the drop in x direction is 75% and in z direction is 45 % resulting in 55% drop in resultant maximum drift, **Table 9**.

**Table 9: comparing result of displacement at 25m standoff distance with 200 kg blast**

joint number	displacement w/o shear wall			displacement with shear wall		
	x direction	z direction	r direction	x direction	z direction	r direction
23	0.307	0.323	0.495	0.048	0.053	0.177
46	0.647	0.647	0.916	0.168	0.168	0.301
50	0.645	0.735	1.041	0.127	0.192	0.342
161	0.66	0.67	1.067	0.477	0.375	0.781
262	0.735	0.645	1.041	0.194	0.128	0.343
263	0.729	0.66	1.101	0.193	0.358	0.504

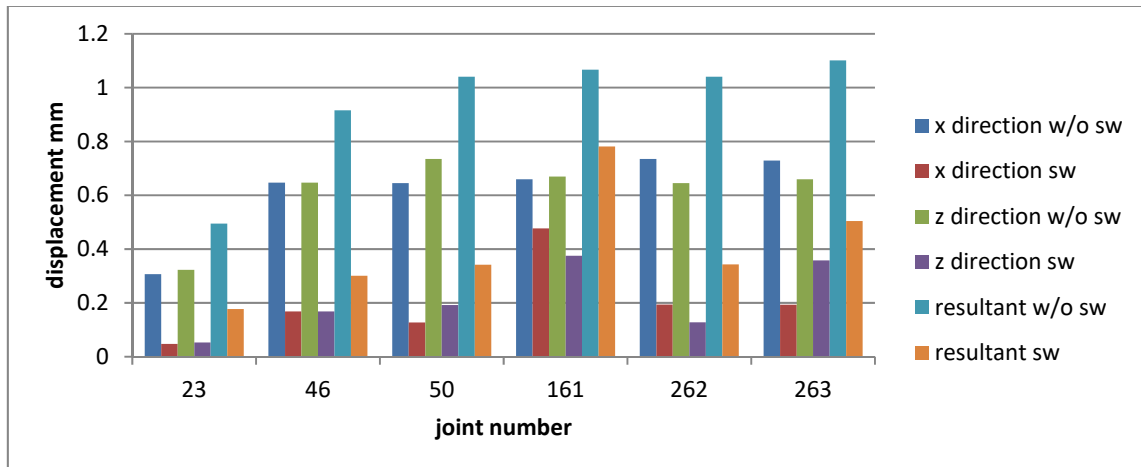


**Figure13: Comparing result of displacement at 25m standoff distance with 200 kg blast**

**EFFECT OF SHEAR WALL AT DIFFERENT NODES FOR 100 kg LOAD AT STANDOFF 25m**

The load of 100kg TNT is less to create enough maximum drift in any direction the majority of the nodes show minimum changes in the drift value for individual direction but the drop in resultant maximum is in the order of 30% except for node 102 where the resultant maximum drift changes negligibly which may be attributed to the location of all other nodes at the L junction of the shear wall on the outermost exposed position except node 102 which is located on inner unexposed, see **Fig. 14**. Detailed Values are tabulated Below, see **Table 10**.

**Table 10: comparing result of displacement at 25m standoff distance with 100 kg blast**

joint number	displacement w/o shear wall			displacement with shear wall		
	x direction	z direction	r direction	x direction	z direction	r direction
47	0.013	0.022	0.367	0.027	0.031	0.248
100	0.022	0.013	0.367	0.027	0.031	0.248
102	0.011	0.011	0.504	0.015	0.018	0.489
108	0.021	0.013	0.367	0.03	0.027	0.248
370	0.016	0.008	0.378	0.025	0.026	0.27
479	0.013	0.021	0.367	0.027	0.03	0.248

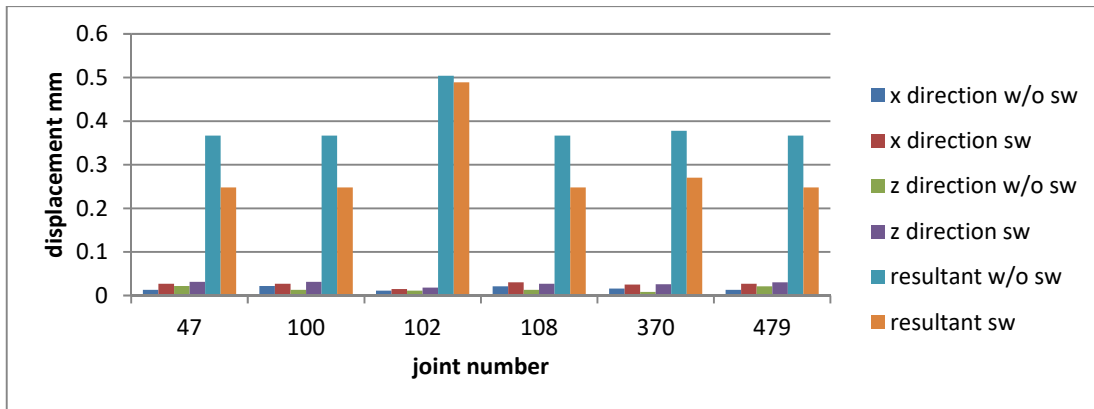


Figure14: Comparing result of displacement at 25m standoff distance with 100 kg blast

This distribution of change in values of maximum drift in x direction z direction and of the resultant maximum drift can be attributed to the position of nodes relative to each other as well as their positions with reference to shear wall, which can be concluded from the values obtained from different nodes under different loading conditions where maximum drift occurs in entirely different nodes for different value of TNT loading. Moreover, it can be observed that the quantum of drop in resultant maximum drift with respect to a certain drop in a particular direction as may be x or z, and its comparison with the effect of increase in individual direction, on the increase in resultant maximum drift is an indicator of the sensitivity of the value of resultant drift to the trends followed by drift in individual direction, see Fig. 15.

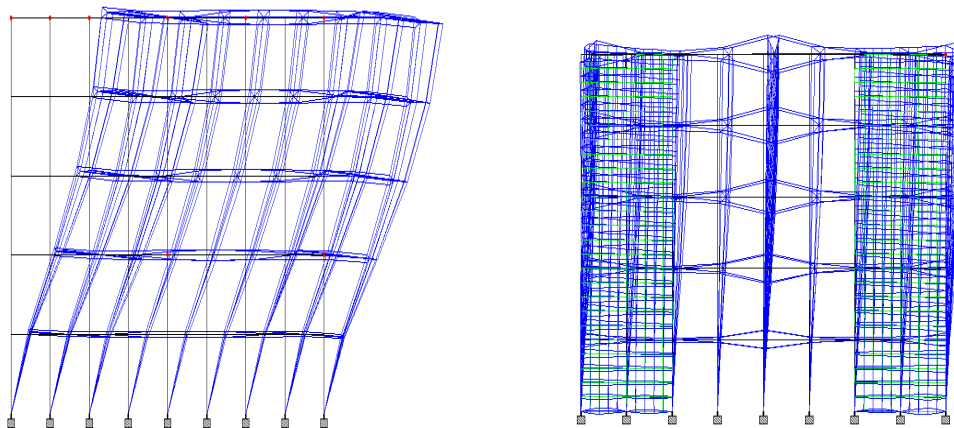


Figure 15: Displacement in w/o shear wall and with shear wall

## CONCLUSION

1. Higher stresses have been observed with higher charge weight than with the lower charge weights as evident from table and graph.
2. For high-risk facilities such as public and commercial tall buildings, design considerations against extreme events (bomb blast, high velocity impact) are required.
3. Pressure contour and time history plots signify that using a steel plate reduces the effect of blast pressure on the concrete wall thus reducing the damage due to pressure created by the 100 kg TNT with standoff distance and height of 3 m and 1 m. Similar observation goes for other plan shapes.
4. For higher charge weights, the collapse occurs faster, as is evident from the graphs. The column fails in half the time for 300 kg TNT than for 200 kg TNT, whereas for 100 kg TNT, it takes about one-fourth the time to fail than 300 kg TNT.

## REFERENCES

- Borvik, T. (2009). "Response of structures to planar blast loads – A finite element engineering approach" *Computers and Structures* 87, 507–520.
- Dharaneepathy M.V. (1995). "Critical distance for blast resistance design" *computer and structure* 54(4): 587-595.
- Kirk A. M., Alfawakhiri, F. (2005), "*Blast and Progressive Collapse*" fact for Steel Buildings, USA.
- Pandya A.K. (2006). "Non-linear response of reinforced concrete containment structure under blast loading" *Nuclear Engineering and design* 236. pp.993-1002.
- Pillai S.U., Menon D. (2003), "*Reinforced Concrete Design*", Tata McGraw-Hill: 121-196.
- Rose, T.A. (2006), "The interaction of oblique blast waves with buildings", Published online: 23 August 06 © *Springer-Verlag* :35-44.
- TM 5-1300(UFC 3-340-02) U.S. Army Corps of Engineers (1990), "Structures to Resist the Effects of Accidental Explosions", *U.S. Army Corps of Engineers, Washington, D.C.*, (also Navy NAVFAC P200-397 or Air Force AFR 88-2).



## Shear Response of SFRC Beams

Mohammad Suhaib<sup>1</sup>, Dr. Harvinder Singh<sup>2</sup> and Sukhwinder Singh<sup>3</sup>

<sup>1</sup>M. Tech Student, Guru Nanak Dev Engg. College, Ludhiana Punjab (Corresponding Author)

<sup>2</sup>Associate Professor, Deptt. of Civil Engg. Guru Nanak Dev Engg. College, Ludhiana, Punjab

<sup>3</sup>Assistant Professor, Deptt. of Civil Engg. Guru Nanak Dev Engg. College, Ludhiana, Punjab

### ABSTRACT

Urban development has changed in the last few decades by a large margin. We see new areas and fields being covered drastically and rapidly. New tech and materials are being used day by day without replacing the original resources. Steel is one of the main components used in construction nowadays but as we see resources are being dwindled by the hour. So an attempt is made to replace the conventional steel through steel fibres. The shear study of beams has always been a primary point of discussion in terms of structural engineering, steps have been taken and improvised along the way to improve flexural as well as shear responses. The use of conventional reinforcement pave the way for further growth and study of shear strengths and with time new development in the field takes place. The replacement of steel bars in terms of volume and economy is highlighted. The comparison between conventional Reinforcement and SFRC is undertaken. Also the contrast of ordinary beams and SFRC, at different percentages of fibre mix with the aspect ratio of 50 and 80 is the main objective of this project. 45 Beams have been cast at respective fibre concentration with the sole purpose of shear response under four point loading.

**KEYWORDS:** Steel; Fibre; Shear; Aspect ratio 80; Aspect ratio 50.

### INTRODUCTION

When discussing the use of convention steel in reinforced concrete, we come across various aspects like workability, economic influence and strength. Conventional steel is obviously a demanding trend in the modern day construction. But with the increase in construction projects resources are being used up at a pacing rate without being replaced. So new methods and materials are being used to increase workability and reduce the economic pressure without reducing the strength of concrete. The influence of Steel Fibres in terms of Shear strength and ductility is investigated. Now there are various types and shapes of steel fibres available. Each fibre type in its individual way improves the characteristics of concrete. This paper is focused on mixing of two steel fibres in selected proportions according to volume.

The steel fibres are of aspect ratio 50 and aspect ratio 80. To see the impact on the shear strength with varying the fibre content of both the fibres individually and together. Optimum fibre content is the perfect amount of fibre by percentage added to concrete that gives us the maximum strength. Now for steel fibres of aspect ratio 50 this optimum mix was calculated at 2% of steel by volume. For steel fibres of aspect ratio 80 this optimum fibre content was calculated at 0.75% of fibre content by volume. Thus upon mixing the two fibres we search for the optimum fibre content. Now we know that concrete as such is brittle in nature and fails miserably in tension, addition of fibre not only improves tensile strength of concrete but also increases resistance to deformation and hinders the propagation of cracks. This phenomenon is known as crack bridging Developing cracks in SFRC requires a debonding (Pulling out) process because the distribution of fibres is random (**Chariolis and Karayannis 2009**). Therefore, a pseudo ductility tension response is demonstrated by the fibrous concrete which further enhances the dissipation of energy, concerning the brittle behavior of plain concrete. When the principle tensile stresses increase above its tensile strength, shear failure is visible through diagonal cracks in the shear span. This way, we understand the behavior of a member under shear by characterizing it in direct tension (**Zararis et al 2006**). This paper also inspired to check for the possibility of at least partially replacing conventional reinforcement like stirrups with steel fibres (**Cucchiara et al 2004**).

So basically this paper discusses the urban sustainability in terms of replacing the conventional steel with steel fibres. The workability is obviously increased along with reduction in the cost of steel and labour without affecting the strength of concrete. When compared to the conventional bars the alignment and orientation of steel fibres is almost next to impossible. The steel bars being relatable in dimensions of the beams are easily oriented while as the steel fibres are quite small in stature and hence to orient each steel fibre in the concrete mix is almost impossible. It is why this paper is merely presented to test the shear parameters of randomly oriented steel fibres.

## EXPERIMENTAL PROGRAM

The experiment included a total of 45 beams to be tested for shear behaviour under four point loading while varying their fibre content. The content of fibres was varied from 1% to 1.5% with 0.25% increment. A series of conventionally reinforced beams are also tested for comparison of results with the SFRC beams.

## SPECIMEN CHARACTERISTICS

The dimensions of all the specimens was uniform with height = 150 mm, width = 150 mm and length = 700 mm. Hooked end steel fibres Dramix ZC of aspect ratio 50 and 80 with length 30 and 60 respectively were used. The fibre was sprinkled throughout the mix thoroughly. No other shear reinforcement was provided. The mix was kept M 25 with coarse aggregates ranging from 12 mm to 16 mm and fine aggregates of grade II.

## TEST RIG AND INSTRUMENTATION

The experimental setup is shown below in Figure 1; simply supported beam on roller supports with cover 100 mm from each side, the separation of supports was kept at 500 mm and the top two points at 200 mm apart. The a/d ratio was kept 1.0 throughout the experiment. Loading was kept constant at a rate of 0.1 mm/min. The testing was performed on Universal Testing Machine of limit 100 kN, loads, displacement and crack widths were recorded and graphs were plotted continuously.

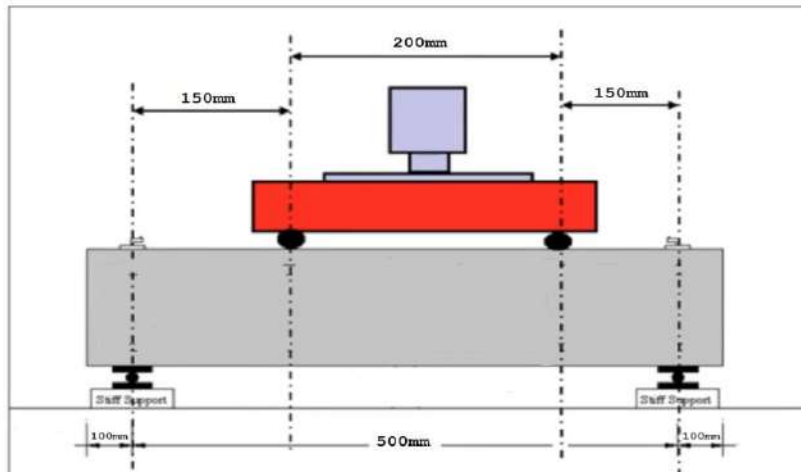


Fig.1 Experimental set up for testing

Table 1: Details of casting of Cubes and Beams

S No	Steel Fibre of Aspect Ratio 80 (%)	Steel Fibre of Aspect Ratio 50 (%)	No of Cubes	Nos. of Beams
1	0	0	3	3
2	1	0	3	3
3	0	1	3	3
4	1.25	0	3	3
5	0	1.25	3	3
6	1.5	0	3	3
7	0	1.5	3	3
8	0.75	0.25	9	9
9	0.50	0.50	9	9
10	0.25	0.75	9	9

**TEST RESULTS AND DISCUSSION**

After the curing period of 28 days finished the beams were carried out of the water tanks for shear testing. 9 batches of varying fibre content with 0.25 increments were tested under four point loading. All the beams underwent slow and gradual loading of rate 0.1 mm/min. The beams showed diagonal cracks with gradually increasing from the bottom to the top. Figure 2 shows diagonal cracks indicating shear failure.



**Fig. 2** Diagonal Cracks depicting shear failure

The shear cracks are depicted by gradually increasing diagonal cracks: all the cracks initiated from the bottom climbing up from the sides towards the centre. This is because the maximum stress is in the middle of the span which is why the beam is fails in bending in the middle. The table 1, shows the values of compressive and shear stress for 1% fibre content evaluated in the experimental study.

**Table 1: Compressive and Shear stress values of 1% Sfrc beams**

S.No.	Aspect Ratio	Fibre Mix (%)	Load (kN)	Compressive Stress (MPa)	Shear Stress (MPa)
1	80	0	31	27.7	1.04
	50				
2	80	0	32	30	1.06
	50	100			
3	80	100	78	36.9	2.61
	50	0			
4	80	75	70	34	2.35
	50	25			
5	80	50	62	33.4	2.06
	50	50			
6	80	25	43	30.46	1.45
	50	75			

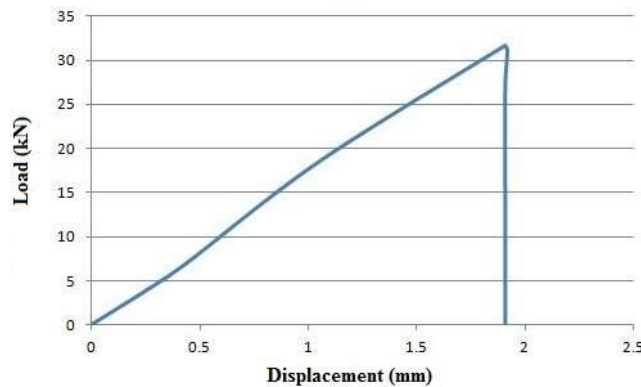


**Fig. 3** Load displacement curve for 0% fibre content

The figure 3 above clearly shows the sudden drop of the curve when the peak value was reached indicating failure in bending. The absence of steel keeps the concrete brittle and vulnerable to failure.

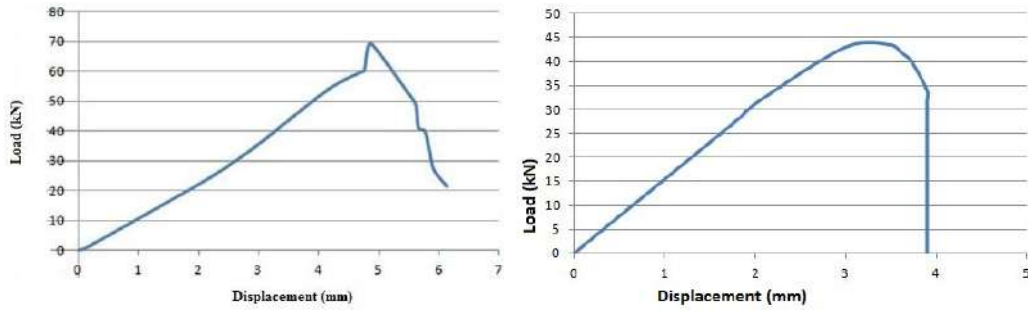


Fig. 4 Load displacement curves for 1% fibre content

The Fig. 4, show clear difference in terms of displacement and modes of failure. The additions of fibre not only made it ductile but also increased its flexural and shear strength. There is a tremendous hike in the peak values. For the same content and concrete mix there is observable increase in compressive and shear strength, see Table 2.

Table 2: Compressive and Shear stress values of 1.25% Sfrc beams

S.No.	Aspect Ratio	Fibre Mix (%)	Load (kN)	Compressive Stress (MPa)	Shear Stress (MPa)
1	80	0	38	30.2	1.28
	50	100			
2	80	100	69	31.6	2.3
	50	0			
3	80	75	84	35.5	2.8
	50	25			
4	80	50	80	33.3	2.67
	50	50			
5	80	25	60	33.7	2.01
	50	75			

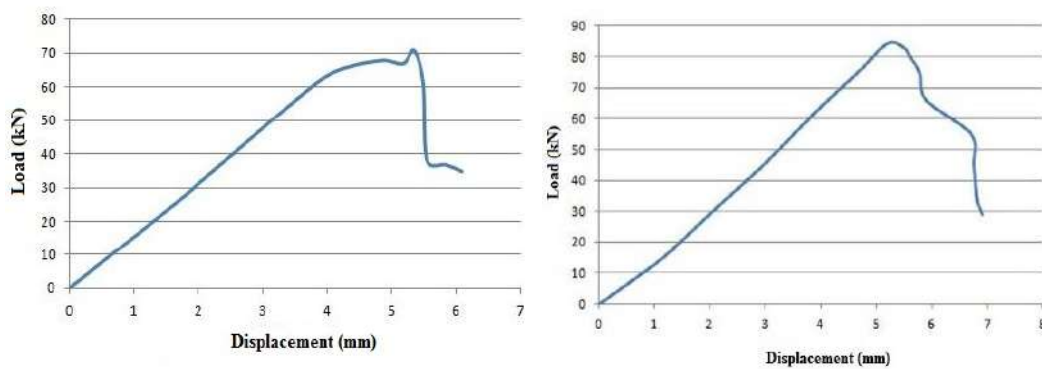


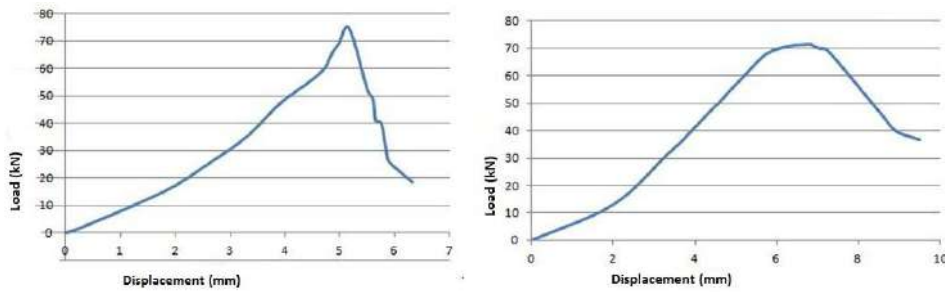
Fig 5 Load displacement curves for 1.25% fibre content

Figure 5 above shows the load displacement curves for the beams with fibre content 1.25%. Here the content of the was mixed with 50% of each fibres in one of the specimen; 3/4 of 80 aspect ratio and 1/4 of 50 aspect ratio in the other. The mix of 3/4 aspect ratio 80 and 1/4 of aspect ratio 50 gave the most high value of shear stress. The two beams are contrasted with respect to their peak values. The beam with 1.25% fibre content 75% of large steel fibres of aspect ratio 80 showed the highest shear strength in all the batches tested.

Conventionally reinforced beams with steel bars were tested at 3 different percentages of steel 1%, 1.25% and 1.5% respectively. They showed very negligible deviation when it came to shear strength. The comparison of steel bars and SFRC proved fruitful in terms of noting the peak value, almost all the peak values lied in the same range according to their steel percentage, see Table 3.

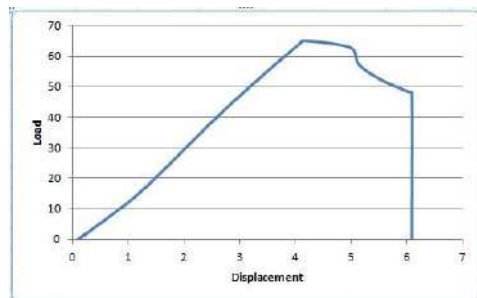
**Table 3: Compressive and Shear stress values of 1.5% Sfrc beams**

S.No.	Aspect Ratio	Fibre Mix (%)	Load (kN)	Compressive Stress (MPa)	Shear Stress (MPa)
1	80	0	73	31	2.43
	50	100			
2	80	100	65	31.2	2.16
	50	0			
3	80	75	70	31.5	2.33
	50	25			
4	80	50	73	34.04	2.44
	50	50			
5	80	25	75	35.02	2.48
	50	75			



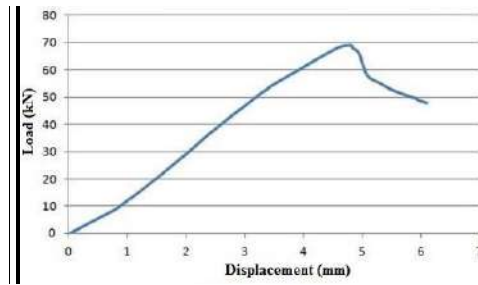
**Fig 6** Load displacement curves for 1.5% fibre content

Fig 6 shows the load displacement curves for 1.5% fibre content. Here two curves are highlighted; one is of beam with 1.5 % content of steel fibre with only small steel fibres of aspect ratio 50 and the other is of beam with fibre content 1.5% with 50% content from both the aspect ratio fibres, Fig. 7 and 8. The values of shear strength are in the same range. The chart below depicts the range of stress values observed with respect to fibre content. The changes in values are noticeable; the highest value is where the optimum mix is approximated.



**Fig 7** Load Displacement Curve for 1% Conventional Reinforcement

We see a particular range of values of peak loading in the steel bars reinforced concrete. The steel bars are provided below the neutral axis and the cracks developed were diagonal in all the cases indicating shear failure.



**Fig 8** Load Displacement Curve for 1.25% Conventional Reinforcement

The value of loading is clearly visible in the range between 60 kN and 70 kN for 1.25% reinforcement, see Fig. 8. The failure is shear with diagonal cracking.

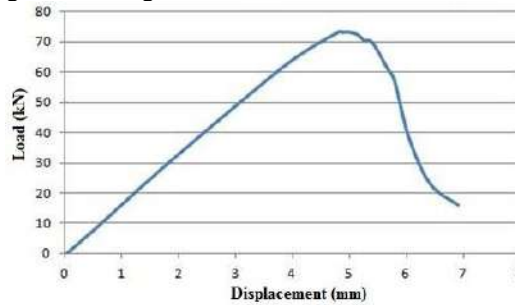


**Fig 9** Load Displacement Curve for 1.5% Conventional Reinforcement

**Note:** The above graphs are plotted for conventional steel denoting shear failure. We see the range of values similar to those of SFRC beams. Hence we can conclude that for shear reinforcement we can definitely use SFRC as a replacement of conventional steel. Although there is still much research to be done in this field but for the time we can still compliment the steel fibres by replacing stirrups and caged mesh by SFRC. Steel fibres prove to be more workable, more economical and provide equivalent strength to conventional steel bars. Here lies the comparison graph of all the beams constructed in the investigation.

#### COMPARISON:

1. When compared to ordinary concrete we find the SFRC is 40% stronger hence we can reduce extra aggregates and decrease the cost.
2. Mostly Steel Fibres are used in order to halt crack propagation; steel bar stirrups fail to provide such control.
3. Designing two beams with same dimensions of  $l = 700\text{mm}$ ,  $b = 150\text{mm}$  and  $w = 150\text{mm}$ ; one with steel stirrups and the other with steel fibres. Comparing the two on the basis of shear strength and cost. According to IS 456 the maximum spacing of stirrups should be  $0.75d$  where  $d$  is the effective depth; in this case  $d = 110\text{mm}$ . So the spacing of stirrups would be  $82.5\text{mm}$  which implies 8 stirrups to be introduced, see Fig. 10 and Table 4.

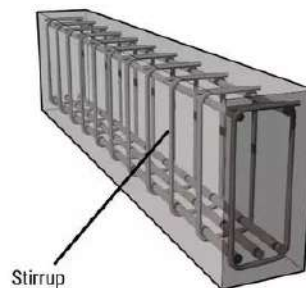


**Fig 10** Stirrups provided in the beam

**Table 4: Cost variation**

S.No	Beam Content	Wt. Of Steel per beam (kg)	Cost of Steel per beam (Rs)
1	Stirrups	1.624	75
2	Fibres	0.549	55

According to IS 456 the area of steel

$$A_{st} = d^2/162.5 \quad \text{Eq.(1)}$$

So the weight of 1 steel stirrup would be  $(A_{st} \times l) / 1000$  where  $l = 330\text{mm}$  is calculated to be 0.203 kg and for 8 stirrups is 1.624kg per beam.

While as when using sfrc only 0.549 kg is used per beam.

The cost of steel stirrup bars is calculated at Rs 75 per beam and that for steel fibres per beam is Rs 55 per beam.

- Steel fibres increase the strength of a structural member hence we can decrease the dimension of the member; be it a slab or an embankment which means we can reduce the extra material.
- It also reduces time and labour work as steel fibres are sprinkled in the mix throughout; while as the steel bars need to be placed below the neutral axis with accuracy.

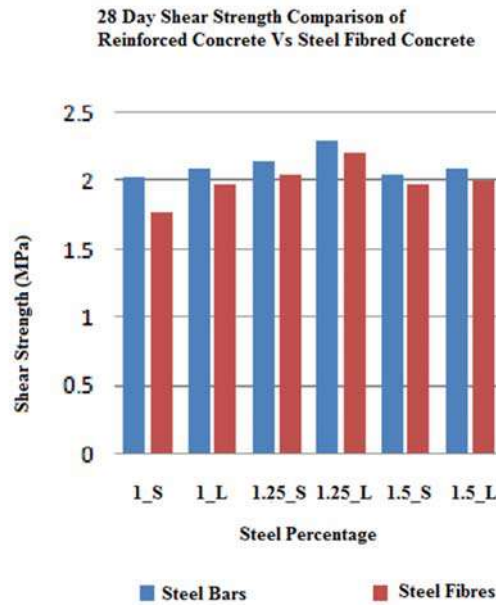


**Fig 11** Chart of Reinforced Concrete and SFRC Shear Strength

Fig 11 shows the comparison chart of Shear strength of reinforced concrete to that of SFRC. There is an equivalent range seen in the strength, which means that SFRC can perfectly replace normal conventional shear reinforcement. Even if there is a hike in the steel bar reinforced concrete but the requirement of strength, stability and economy is fulfilled by SFRC very well. Hence for sustainable urban development SFRC is obviously the better choice as it is cheap, provides sufficient strength and gives better crack control.

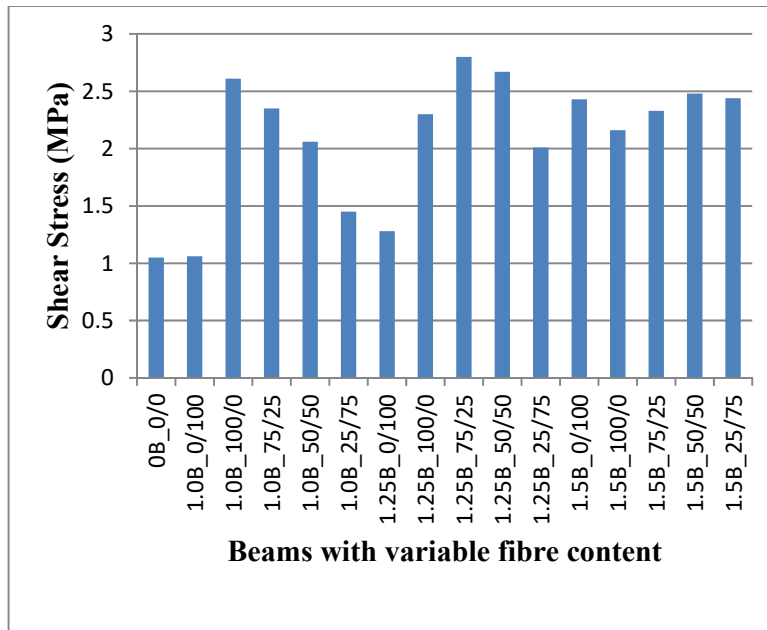


Fig 12 Range of Shear stress with respect to fibre content

Figure 12 depicts the range of values of shear stress achieved with respect to varying fibre content. We see an observable hike in the values starting from the lower fibre content till it reaches the optimum content. Then the values are decreased but not to that extent. The overall conclusion is that addition of fibre up to permissible values increases the shear stress of concrete hence increases the resistance to external forces.

Note: The labeling of the beams is done according to their fibre content. E.g. If the beam is labeled as 1.0B\_75/25, then it means the beam has 1 percent fibre content with 75 percent of large fibres and 25% of small fibres. If the beam is labeled as 1.25B\_25/75, then it means the beam has 1.25 percent fibre content with 25% of large fibres and 75% of small fibres. Large fibres have aspect ratio of 80 and small fibres have aspect ratio of 50.

## CONCLUSION

1. Steel Fibred concrete is almost **40%** stronger than normal concrete; that means we can get the required strength with lesser dimension hence reducing the extra cost of materials.
2. The steel fibres are very well used for replacing conventional steel bars and stirrups and other shear reinforcements reducing the cost and labour work. Hence it can be used a sustainable resource for the upcoming generation.
3. The beams with **0%** fibre content and **1%** content of small fibres of aspect ratio **80** seemed to fail suddenly; this brittle characteristic is of flexural failure. The higher the fibre content went the beams showed ductile nature.
4. The experimental results show that the fibrous concrete exhibit improved behaviour in overall performance such as compressive strength, shear strength and extension in the load carrying capacity at the first crack. With increase in the percentage of fibre from **1%** to **1.5%** we see tremendous improvement in the flexural as well as the shear strength of the specimens.
5. The compressive strength was increased by ample amount and the maximum was seen on 1.5% large fibres. On the other hand shear strength was increased several folds and the maximum value was seen on combining the two aspect ratios.
6. The brittle nature of concrete was improved and ductility was imparted to concrete. There was slower crack propagation. With increased fibre content there was no sudden failure, all the specimens failed in shear with diagonal cracking.
7. The optimum fibre content for aspect ratio 80 fibres was **0.75%** and that for the aspect ratio 50 was **2%**. Upon mixing the two fibres the maximum shear strength was investigated on **1.25%** of fibre content at **3/4** proportion of fibres of **aspect ratio 80** and **1/4** of fibres of **aspect ratio 50**.

8. The deflection also seems to increase with the increase in fibre content. The **crack mouth opening widths** seem to be lesser at 1.25% of the mixed fibre content, above that it increases and below that it also increases. It is due to induced ductility by steel fibres.
9. There are new fields being touched and improved day by day, so the use of steel fibres can be an essential alternative for conventional steel in terms of infrastructure development. It is cheaper, easily available, and more workable and provides equivalent strength.

## References

- A. N. Humnabad, P. B. Autade; " *Experimental Evaluation Shear Strength of Steel Fibre Reinforced Concrete Deep Beam*" International Journal of Engineering Research & Technology (IJERT) ISSN: 2278-0181 Vol. 5 Issue 05, May-2016
- C. E. CHALIORIS, E. F. SFIRI; " *Shear Performance of Steel Fibrous Concrete Beams* "The Twelfth East Asia-Pacific Conference on Structural Engineering and Construction Procedia Engineering 14 (2011) Department of Civil Engineering, Democritus University of Thrace, Greece
- David Carnovale and Frank J. Vecchio; " *Effect of Fiber Material and Loading History on Shear Behavior of Fiber-Reinforced Concrete* " Effect of Fiber Material and Loading History on Shear Behavior of Fiber-Reinforced Concrete ACI Structural Journal/September-October 2014, University of Toronto, Toronto, ON, Canada.
- Miss. Patil Sonali " *Prediction of Shear Strength of Steel Fiber Reinforced Concrete Beams without Web Reinforcement* "P. PG Student ME Civil (Structures) SVERI's C.O.Engg., Pandharpur, Solapur University, India Prof. Pawar Mukund. M. Professor, Department of Civil Engineering, C.O.Engg., Pandharpur, Solapur University, India International Journal of Engineering Research & Technology (IJERT) Vol. 4 Issue 04, April-2015.
- R.S. Londhe " *Experimental investigation on shear strength of sfrc beams reinforced with longitudinal tension steel rebars* " Applied Mechanics, Government College of Engineering., Aurangabad-431 005 (MS) India, ASIAN JOURNAL OF CIVIL ENGINEERING (BUILDING AND HOUSING) VOL. 11, NO. 3 (2010)
- Shunzhi Qian and Victor C. Li " *Influence of Concrete Material Ductility on Shear Response of Stud Connections* " ACI Materials Journal/January-February 2006
- AASHTO, 1998, " *LRFD Bridge Design Specifications,*" 2nd Edition, American Association of State Highway and Transportation Officials, Washington, D.C., 1052 pp.
- An, L., and Cederwall, K., 1996, " *Push-Out Tests on Studs in High Strength and Normal Strength Concrete,*" *Journal of Construction Steel Research*, V. 36, No. 1, pp. 15-29.
- Bursi, O. S., and Gramola, G., 1999, " *Behavior of Headed Stud Shear Connectors under Low-Cycle High Amplitude Displacements,*" *Materials and Structures*, V. 32, pp. 290-297.
- Driscoll, G. C., and Slutter, R. G., 1961, " *Research on Composite Design at Lehigh University,*" *Proceedings, National Engineering Conference, AISC*, pp. 18-24.



## Analysis of beam-column joint of building frame subjected to blast load

Sunil Kumar Meena<sup>1</sup>, Aman Garg<sup>2</sup> and H.D. Chalak<sup>3</sup>

<sup>1</sup> M. Tech Scholar, Department of Civil Engineering, NIT Kurukshetra, Kurukshetra, Haryana, India 136119; e-mail: sunilaicecivil@gmail.com

<sup>2</sup> Ph.D. Scholar, Department of Civil Engineering, NIT Kurukshetra, Kurukshetra, Haryana, India 136119; e-mail: amang321@gmail.com

<sup>3</sup> Assistant Professor, Department of Civil Engineering, NIT Kurukshetra, Kurukshetra, Haryana, India 136119; e-mail: chalakhd@yahoo.co.in (Corresponding Author)

### ABSTRACT

In past years due to rapid development and urbanization conventional structures are being designed for vertical loads and horizontal loads including wind and seismic loadings. But, due to increase in ongoing terrorist activities, accidental explosions etc. the influence of blast load on the behavior of structure is gaining interest among the researchers. The magnitude by which blast load acts upon the structure is many folds along with very small time as compared to wind or earthquake load. The failure of a critical element results in failure of the structure in a progressive manner. The modelling and analysis of 3-D reinforced cement concrete (RCC) frame was done using ABAQUS explicit model and the effect of TNT explosive is investigated. The response of beam-column joints is observed and seen that when blast loading acts upon 3-D building frame the nearest beam-column joints are critically impacted and progressive collapse is observed. For predicting the more accurate behavior, appropriate failure model (such as concrete damage plasticity model for concrete, Johnson-Cook damage model for ductile materials) were incorporated.

**KEYWORDS:** Blast loading, Building frame, ABAQUS, Concrete Damaged plasticity.

### INTRODUCTION

With increase in terrorist activities, the life of people living in the targeted structures is on stake. This highlights the need for the analysis of structures subjected to blast loading. Blast load acting on the structure is transformed in the form of moving pressure waves which introduces dynamics in the structure. Thus, the dynamic response of structure impacted by blast introduces high strain rate change in the constituent materials of the structure. For RCC buildings, this type of analysis should be carried out in nonlinear range, which lies beyond the conventional elastic behaviour of concrete and steel reinforcement. Due to these type of complexities in a single structure using software such as STAAD PRO, E-TABS or SAP cannot be incorporated in design. The advance software such as ANSYS, ABAQUS etc. can be used to carry out the above stated study. Jayashree et al (2013) carried out the dynamic response of 3D framed structure under blast load using SAP 2000 and compared the results of RCC to a new type of concrete termed as Slurry Infiltrated Fiber Reinforced Concrete (SIFCON) under category, Fiber Reinforced Concrete with high fiber content as an alternate to RCC. It was found that the displacement reduction of about 25-30 % achieved using SIFCON as compared to RCC. Amol et al studied the effect of blast on column foundation and at various floor heights using STAAD-PRO, results were compared with real damaged building photographs taken and concluded that building more than 6 floor height have less probability of overturning and crushing but high SF and BM Exists so great care needs to be taken for building height more than 6 floor height. Amy et al (2014) studied the effectiveness of different framing systems subjected to blast load, analysis was done using applied element method. Roof deflection and acceleration was compared and global response analysis was observed and concluded that CBF and EBF had less no of failed members, plastic hinges, roof deflection and accelerations as compared to MRF. Sarita et al (2015) done the analysis of 3D building frame for different amount of blast charge (TNT Pressure) and for different standoff distances and it was found that the blast pressure was maximum for ground story and when TNT amount increases or standoff distance decreases the blast pressure increases Umesh et al (2015) performed the analysis of high-rise building (regular and irregular frame) in ETABS 2015, subjected to blast load. It was found that when building has irregular frame, the storey drift was maximum also the lateral stability of regular building frame was more as compared to irregular building frame. Zubair et al (2016) A comparative study of RCC structures when originally designed earthquake resistant and not designed earthquake resistant was done to establish the minimum standoff distance for a certain blast load, SF & BM values were compared for different blast amount and for different standoff distances in both conditions. It was concluded that less standoff distance required for EQ Resistant frame and building performs better in shorter span direction up to 10kg TNT but for higher TNT behaves identically in short and long span both. Yasser et al (2017) used

ABAQUS to perform the detailed finite element analysis of structure to assess the performance under blast loading. A 4-story RCC model that used the concept of isotropic damaged elasticity along with isotropic compressive and tensile plasticity to model the inelastic behavior of concrete, was modeled. They compared results of RCC frame when used CFST on External columns and when not used CFST and seen that the CFST improved the response of the structure under blast loading though the collapse was not prevented. B.S. SHARMA et al (2013) analyzed and observed the response of containment subjected to missile penetration they have used concrete damaged plasticity model for concrete and Johnson-Cook material properties for steel in Abaqus software to incorporate the realistic behavior of containment and results were carried out for strain rate effect on displacement history of missile, Damage and stresses and concluded that missile penetration depth was reduced up to 40% when strain rate dependent models were used. In this paper we have analyzed a three storey building frame with one bay using ABAQUS/Explicit finite element code to predict the response when subjected to blast loading. The blast explosion can be converted to equivalent blast load in time history mode. Ibrahim et al researched for blast load on building frame and stated that the 1-ton load of TNT blast at the distance of 5 meters from the structure is reasonable. For the present analysis the blast (hemispherical TNT explosion) is simulated at a distance of 5 m from the building with 1 m height from ground are used from the chart developed by UFC 3-340-02.

### MATERIAL PROPERTIES

For the analysis 3 storey 1 bay RCC frame with fixed base was modelled. The concrete damaged plasticity parameters for concrete and Johnson-Cook hardening and dynamic failure parameters are used for steel in present study to predict the more accurate and realistic analysis of building frame. Following finite elements are used for modelling:

1. C3D8R (explicit 8-node linear brick, reduced integration, enhanced hourglass control): For beams, columns.
2. T3D2 (Explicit 2-node linear 3-D truss): for longitudinal reinforcement and shear stirrups.

The material properties, model dimensions and reinforcement detailing used are given in Table 1, Table 2 and Table 3

**Table 1. Concrete damaged plasticity parameters, B.S. Sharma et al.**

Density, $\rho$ (kg/m <sup>3</sup> )	2400	Bulk Modulus, K	0.666
Modulus of elasticity, E (N/m <sup>2</sup> )	2.7386E+10	Viscosity parameter	0
Poisson's ratio, $\nu$	0.17	Fracture energy, $G_f$ (N/m)	720
Dilation angle, $\Psi$	29°	Uniaxial failure stress, $\sigma_{t0}$ (MPa)	10.8
Eccentricity (m)	1.0	Cracking Displacement, $U_{t0}$ (m)	0.0001332
Initial equi-biaxial compressive yield stress to initial uniaxial compressive yield stress, ( $f_{b0}/f_{c0}$ )	1.16	Tensile strength (MPa)	3.86
Compressive Strength (MPa)	25		

**Table 2 : Model properties**

Element	Length (mm)	Cross section (mm × mm)	Main reinforcement	Shear stirrups
Beam	3000	300x300	12 bars of 12 mm $\phi$	14 stirrups of 8 mm $\phi$
Column	3000	300x300	12 bars of 12 mm $\phi$	14 stirrups of 8 mm $\phi$

**Table 3: Johnson-Cook hardening and dynamic failure parameters, B.S. Sharma et al.**

Young's Modulus of elasticity, E (N/mm <sup>2</sup> )	2 x 10 <sup>5</sup>	Reference strain rate (s <sup>-1</sup> )	5x10 <sup>-4</sup>
Poisson's ratio, $\nu$	0.33	C	0.0114
Density, $\rho$ (Kg/m <sup>3</sup> )	7850	T <sub>melt</sub> (K)	1800
Yield stress, A (N/mm <sup>2</sup> )	490	T <sub>0</sub> (K)	293
B (N/mm <sup>2</sup> )	383	Specific Heat Cp (J/Kg K)	452
N	0.45	Inelastic heat fraction, $\alpha$	0.9
M	0.94	D1	0.0705
D2	1.732	D3	-0.54
D4	-0.01	D5	0.0

### FINITE ELEMENT MODELLING

The numerical simulation of RCC building frame subjected to blast loading is carried out using ABAQUS/Explicit 6.14-1 finite element code. A three-dimensional frame of three story with one bay was modelled and the base was assumed to be fix. The geometry and properties considered for modelling are as per Table 1 Table 2 and Table 3. The width and depth of beam and column are considered as 300\*300 mm whereas the length was considered as 3000 mm. The structure is reinforced with 12 bars of 12 mm as main reinforcement for all beam and columns and the shear stirrups considered as 14 stirrups of 8 mm for each beam and column. Fig. 1 shows the 3-story RCC building frame modelled in Abaqus.

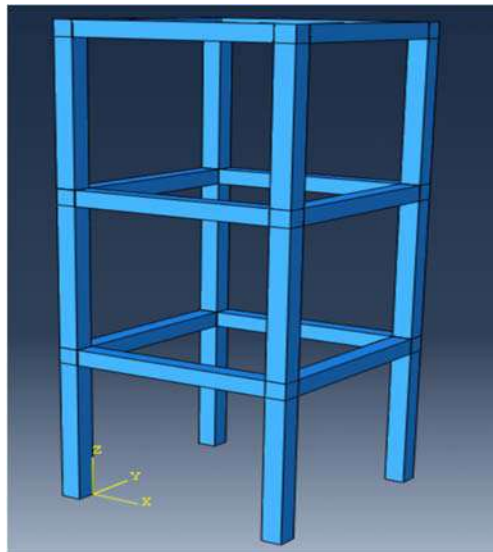


**Fig. 1 3-story reinforced Concrete structure [Abaqus]**

The building frame is meshed with three dimensional C3D8R (explicit 8-node linear brick, reduced integration, enhanced hourglass control): For beams, columns and T3D2 (Explicit 2-node linear 3-D truss): for longitudinal reinforcement and shear stirrups. It was observed when we used fine meshing the results were varying but after a limit when we used more fine mesh the results were almost similar but the finer mesh takes more time for analysis hence we selected the meshing size after which the results shows no variation. The 3-D building frame with meshing is shown below in Fig. 2,

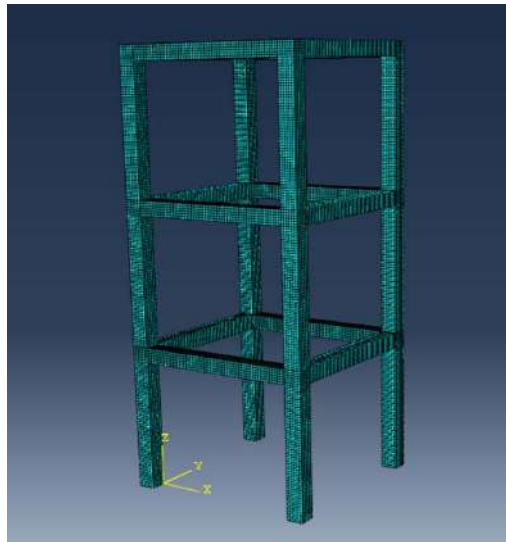


**Fig. 2: Structure mesh [ABAQUS]**

Blast load is applied such that it can purposefully inflict damage to the three-dimensional building frame taken in this paper, the blast (hemispherical TNT explosion) is simulated at a distance of 5 m from the building with 1 m height from ground are used from the chart developed by UFC 3-340-02 and applied at each story. The figure 3 is given below showing the applied blast load on building frame.

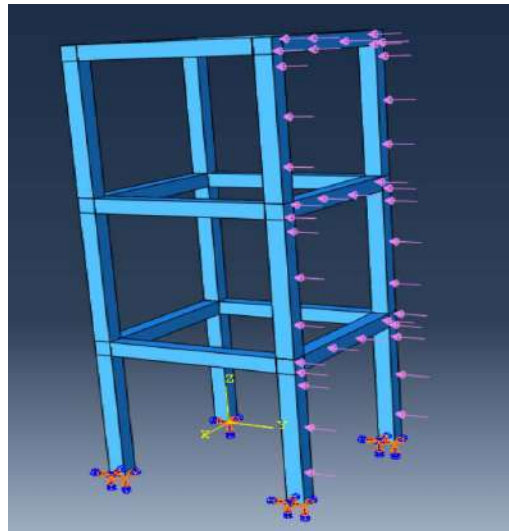


**Fig. 3 Blast load on frame [ABAQUS]**

## RESULTS

After application of blast load, the behaviour of building frame is observed and the stress strain of different point in the face of blast loading is taken. below are the figures and the corresponding graph of strain and stress. Fig. 4(a), Fig. 5(a) and Fig. 6(a) showing the node located at midpoint of ground story column, bottom point of ground story column and beam-column joint of ground story respectively. Fig. 4(b), Fig. 5(b) and Fig. 6(b) showing the graph of stress-strain with respect to time for node located at midpoint of ground story column, bottom point of ground story column and beam-column joint of ground story respectively.

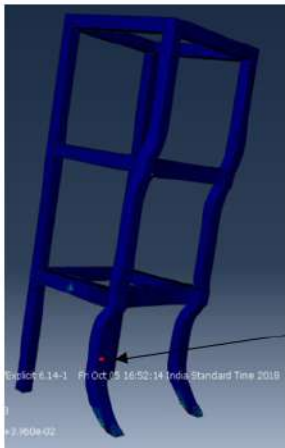


Fig. 4(a) node selected at midpoint of ground story column

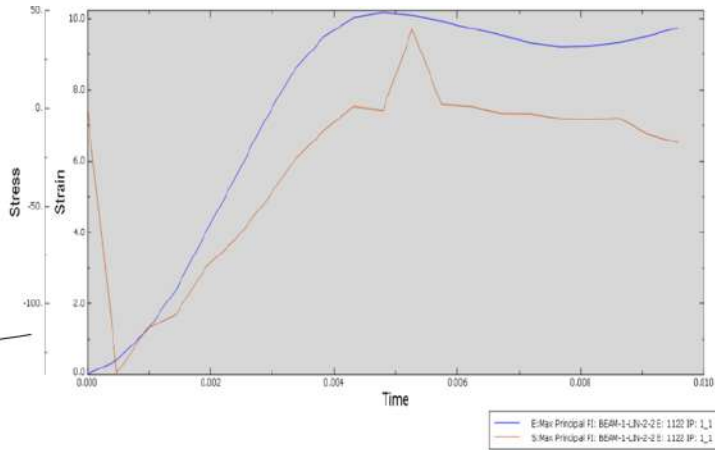


Fig. 4(b) stress-strain graph with respect to time for mid-point on ground story column

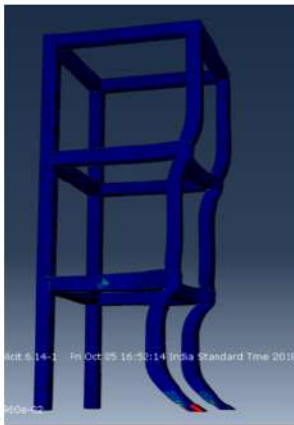


Fig. 5(a) node selected at bottom point of ground story column

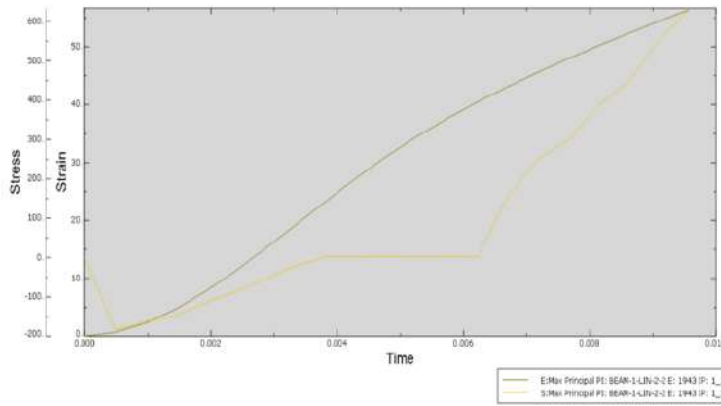


Fig. 5(b) stress-strain graph with respect to time for bottom point of ground story column

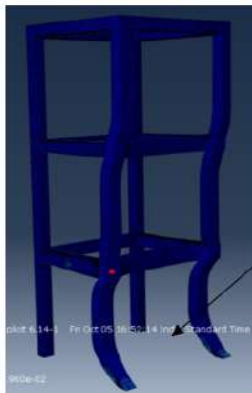


Fig. 6(a) node selected at the beam-column Joint of ground story column

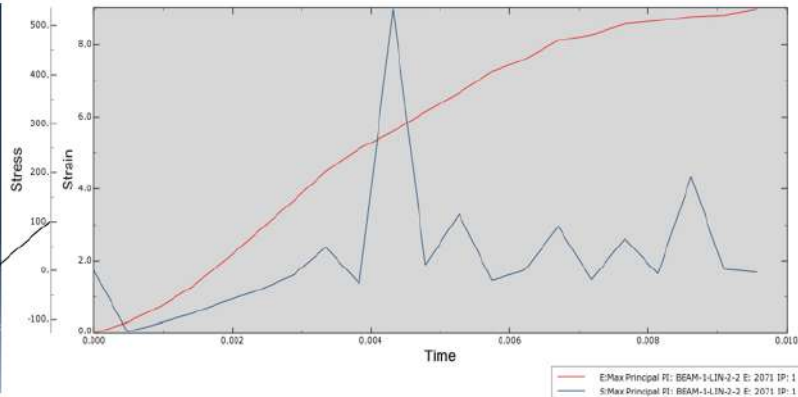
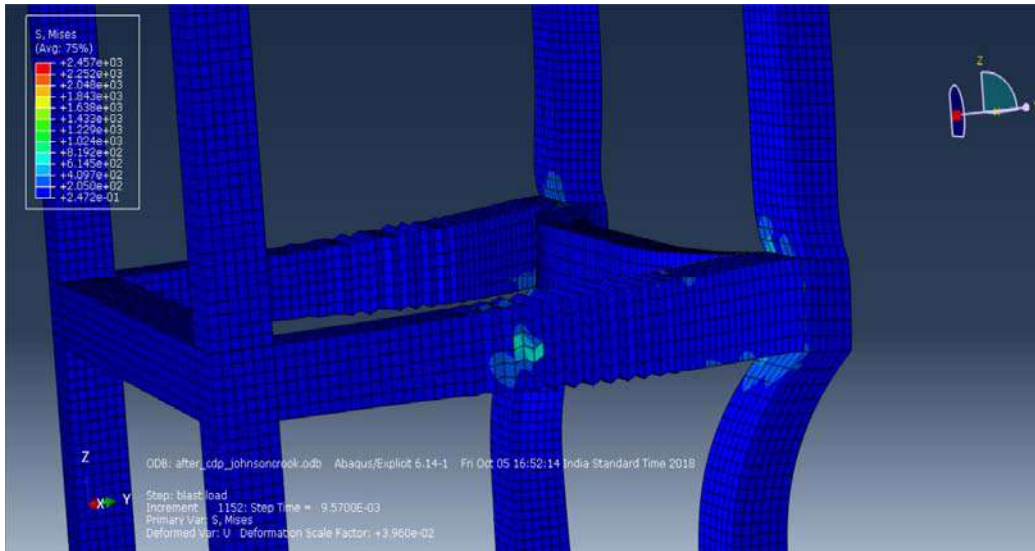


Fig. 6(b) stress-strain graph with respect to time for beam-column joint of ground story column

From the above graphs it can be seen that when the explosion takes place the progressive collapse failure is observed and stress value is maximum for the beam column joint also the stress concentration takes place. As the positive and negative waves generate the frame gets vibrates due to that we can see the variation of stress with time. The stress value goes up to 550Mpa which is more than the yield stress of steel and concrete. Although the stress in impact and blast analysis can be more than yield stress but the collapse cannot be prevented. Failure of

ground story beams parallel in the direction of blast loading is takes place due to compression while for beams perpendicular to the blast load direction the failure is due to high tensile stresses. Below is the Fig. 7 showing the compression failure of the ground story beams.



**Fig. 7 Compression failure of the ground story beams.**

## CONCLUSIONS

The following conclusions have been made from the analysis of building frame-

1. The ground story elements of building are the critically loaded elements as compared to upper storey elements.
2. When we compared the result of three different points of ground storey (i.e. Bottom most point of column, midpoint of column and beam-column joint), the beam column joint is found to be most critically loaded.
3. The collapse of the frame cannot be prevented, therefore the provisions for further strengthening of structure is required.
4. From previous literature reviews we have observed that SIFCON and CFST has been already used to reduce the stress concentration and deflections and we can use CFRP sheets on beam column joints. Results of building frame with and without CFRP sheets can be compare.
5. Compressive forces are observed in the ground story beams while tensile forces are observed in upper story beams,
6. This study can be extended by increasing the number of bays and floors and effect of non-structural elements (slab, wall) on structural elements (beam, column) can be worked out. Hence the present paper can be served as the benchmark for future works.

## REFERENCES

- Amy Coffield and H. Adeli, "An Investigation of the Effectiveness of the Framing Systems in Steel Structures subjected to Blast Loading" *Journal of Civil Engineering and Management*, vol. 20, no. 6 (2014), pp. 767-777, ISSN: 1392-3730.
- Amol B. Unde 1, Dr. S. C. Potnis "Blast Analysis of Structures", *International Journal of Engineering Research & Technology (IJERT)*, vol. 2, no. 7, (2013), pp. 2120-2126, ISSN: 2278-0181.
- B S SHARMA, M A IQBAL, P BHARGAVA and P GUNDLAPLLI "Response of containment Subjected to Missile Penetration" *proc Indian Natn Sci Acad* 79 no. 4 December 2013 Spl. Issue, Part A, pp.687-694.
- IS 4991-1968, Criteria for blast resistant design of structures for explosions above ground.
- Jayashree.S.M, R. Rakul Bharatwaj, Helen Santhi.M, "Dynamic response of a space framed structure subjected to blast load", *international journal of civil and structural engineering*, vol. 4, no. 1, (2013), pp. 98-105, ISSN 0976-4399.

- Mostafa A. Ismail, Yasser E. Ibrahim, Marwa Nabil, Mohamed M. Ismail, “Response of A 3-D reinforced concrete structure to blast loading”, International Journal of Advanced and Applied Sciences, vol. 4, no.10, (2017), pp.46-53.
- Sarita Singla, Pankaj Singla and Anmol Singla, “Computation of Blast Loading for a Multi-Storeyed Framed Building” International Journal of Research in Engineering and Technology. Vol. 4, no. 2(2015), pp.760-766, e-ISSN: 2319 – 1163, p-ISSN: 2321 – 7308.
- UFC 3-340-02, Unified Facilities Criteria, Structures to resist the effects of accidental explosions, Department of Defense, USA, 2002.
- UMESH JAMAKHANDI, Dr. S. B. VANAKUDRE, “Design and Analysis of blast load on structures” International Research Journal of Engineering and Technology (IRJET), vol.2, no.7, (2015), pp.745-747, e-ISSN: 2395-0056, p-ISSN: 2395-0072.
- Yasser E. Ibrahim, mostafa A. Ismail, Marwa Nabil, “Response of Reinforced concrete structures under blast loading”, journal of Elsevier Ltd., Procedia Engineering 171 (2017) pp. 890-898.
- Zubair I. Syed, Osama A. Mohamed, Kumail Murad, Manish Kewalramani, “Performance of Earthquake-resistant RCC Frame Structures under Blast Explosions” journal of Elsevier Ltd, Procedia Engineering 171 (2017) pp. 82-90.



## Effect of High Temperature on Physical, Mechanical and Microstructural Properties of Concrete-A Review

S. K. Wagh<sup>1\*#</sup>, M. S. Endait<sup>\*2</sup>, and S. S. Kolhe<sup>1</sup>

<sup>1</sup>PG Student, Department of Civil Engineering, School of Engineering and Technology, Sandip University, Nasik;

e-mail:suyashwagh15@gmail.com

<sup>2</sup>Associate Professor, Department of Civil Engineering, School of Engineering and Technology, Sandip University, Nasik;

e-mail: mahesh.endait@sandipuniversity.edu.in (Corresponding Author)

### ABSTRACT

Concrete is the principal material which is responsible for wide infrastructural development from a very long time and still it is being used in the construction industry because of its dependable properties. Fire is considered to be extensive damaging parameter to concrete due to high temperature shock induced in during heating because of lack of fire protection and presence of material having large calorific value. Elevated temperature brings changes in properties of concrete and thereby reduces the integrity of the structure. Measuring these changes in properties of concrete by using destructive and non-destructive tests for determining the temperature for which the structure was exposed to fire and reduction in the performance of the structure when compared with original is presented in this paper. The main objective of this paper is to summarize an information about measuring the damaging effect of fire on concrete by using Ultrasonic Pulse Velocity test, compression test, impact-eco test, petrographic examination and also by considering the factors like exposure time, temperature and effect post fire curing on concrete. The extraction presented in this paper will prove to be informative in recognizing the future area of research in evaluating the properties of fire damaged concrete.

**KEYWORDS:** Fire; Concrete; Compressive Strength; Ultrasonic Pulse Velocity; Microstructure.

### INTRODUCTION

India is one of the rapidly developing economy in the world and contribution of construction industry plays a vital role in this economic development. Economic development brings large population to urban area from rural area which leads to rapid urbanization of cities and ultimately increases the load on basic facilities which are necessary for ordinary society. Rapid urbanization and scarcity of land puts the pressure on construction industry which leads to construction of multistoried skyscrapers and unplanned development of cities with scarcity of basic needs such as water, sanitation, roads, etc.

Fire is not a predictable phenomenon like earthquake but proper precaution may avoid the fire break out. Generally fire breaks out in three main stages such as growth period, burning period and decay period (Lie, 1992). Growth period can be indicated by relatively small increase in temperature which is strongly responsible for burning of the material in most active manner for representing the burning period. During burning period temperature increases considerably and during decay temperature decrease. The development of fire mainly depends upon fire load which mainly constitutes fuel, material with high calorific value and their amount, with strong affinity with degree of ventilation (Nassif et al. 1999).

In the past few decades, most of the cases of fire damage were recorded as a most destructive phenomenon in terms of loss of mankind and economic deprivation. Concrete with its properties like easy availability of constituent materials, mouldability i.e. capacity to acquire any desired shape, durability, better thermal resistance, it is largely used as a major constituent in infrastructure development. Not only the buildings constructed in wood suffering from fire damage but also the buildings constructed in reinforced concrete are the examples of fire damage despite of its good fire resisting properties; because of change in its physical properties and chemical composition brings changes in its mechanical properties. Construction of multistoried buildings involves mostly a construction material which helps in reducing the dead weight of the structure that may possess materials which can be damaged easily due to fire. Severity of fire in congested areas can be observed to be more because fire at one place travels more rapidly to other.

Most of the fire damaged structures does not lose its strength completely and according to research cited by (Alhadid and Youssef 2013) states that only 9% RCC structures loses their entire strength hence, they can be demolished but, rest of 91% can be repairable. Rehabilitation of fire damaged structures is one of the most promising challenge for civil engineers and for understanding the exact level of damage, it is necessary to evaluate the residual compressive strength. Many of the researchers tried to evaluate this residual compressive strength by using many destructive as well as non-destructive testings. Destructive tests generally involves compressive strength, core test, pull-off test and Schmidt hammer test which is a partially destructive test. Non-destructive

tests generally involves observation of colour change by visual inspection, Ultrasonic Pulse Velocity Test (UPV) are generally studied, by taking into consideration the effect of different elevated temperatures, their exposure time, rate of heating/cooling and water curing regime.

Damage assessment by using UPV, compressive strength and by studying microstructural properties, authors are providing a generic and updated knowledge in the above mentioned field of damage assessment of fire damaged concrete.

## **EFFECT OF FIRE ON ULTRA-SONIC PULSE VELOCITY OF CONCRETE**

Determining the residual strength of concrete by using Ultrasonic Pulse Velocity (UPV) which is a non-destructive test, many of the researchers around the world tried to develop the relationship between the UPV and residual strength of concrete. Chung (1985) has proposed the relationship between the residual pulse velocity and residual compressive strength. For the purpose of developing the relationship, six test specimens are casted from each batch of concrete made by taking into consideration eleven different concrete mixes, by varying the aggregate cement ratio and water cement ratio. Out of six test specimens, compressive test was performed on the two specimens which are cured for 7 days in water and air cured for the next 28 days. UPV test was performed on the remaining two concrete prisms out of four, before sending them in to the muffle furnace for 2 hours. After heating, two cubes are cooled down slowly in the furnace and then tested for UPV and compressive strength; and remaining two were immersed immediately in water for the period of 24 hours i.e. 'Quenching' was done and then tested for UPV and compressive strength. Graph of residual velocity ratio and residual strength ratio was used for correlation and regression analysis and two empirical equations were proposed for air cooled and quenched samples for determining residual strength ratio considering residual UPV ratio of fire damaged concrete. Decrease in pulse velocity with increase in temperature was observed. It was observed that pulse velocity measured after quenching the specimen was always on the higher side as compared to air cooled samples, while decrease in compressive strength of the quenched samples were observed, this was due to weakening of cement gel due to absorption of moisture. Author mentioned that non uniformity of temperature across the structural member and variation in moisture condition of concrete can affect the accuracy and usefulness of the method in strength assessment.

(Mohamedbhai 1986) carried out the similar kind of work that Chung (1985) had carried out earlier, in addition to that two methods of heating and two methods of cooling which are slow and fast were adopted. Four different exposure durations were considered. Casted cubes were cured in water for 7 days and then air-dried till the time of heating i.e.  $84 \pm 1$  days. Author concluded that effect of rate of heating and cooling has negligible effect on concrete between the temperature ranges of  $600^{\circ}\text{C}$  to  $800^{\circ}\text{C}$  and considerable effect between the temperature range of  $200^{\circ}\text{C}$  to  $400^{\circ}\text{C}$ . This was due to large amount of moisture lost during initial stage of exposure and this moisture lost results in affecting the strength of concrete. It has also mentioned that residual strength predicted from pulse velocity does not gives accurate results.

Chew (1993) presented the effect of concrete cover and diameter of reinforcement on pulse velocity. It has been found that inclusion of reinforcement increase the pulse velocity, because of better conductive properties and UPV is independent of diameter of reinforcement, but this effect reduces as the concrete cover increases.

To check the uniform distribution of temperature till the center of the specimen Nassif et al. (1995) used thermocouples which were fixed in to the place by using refractory cement. For this purpose three different samples were used for testing. In the observation authors have studied that there was reduction in travel velocity of the ultrasonic pulse as compared with standard unfired sample, due to number of cracks and increase in their width. This effect was observed to be more pronounced in the temperature range of  $320^{\circ}\text{C}$  to  $378^{\circ}\text{C}$ . Nassif et al. (1999) again studied the effect of rapid cooling on UPV which explains the exact condition of firefighting operation and stated that rapid cooling results in 10% reduction in UPV as a result of further development of micro cracking and propagation of existing one. These results are incoherent with the findings of previous researchers. The reason for this incoherence was given as, previous researchers have done the curing of samples for long hours which revealed an increase in moisture content, which leads to overestimation of UPV but, rapid cooling (i.e. application of water for 5 minutes) just to bring the temperature to test temperature and does not results in large change in the moisture content and hence underestimated the UPV.

Yang et al. (2009) followed the similar track of the previous researchers by making the changes in the size of specimen and they adopted the concrete specimens of diameter 10 cm and length 20 cm along with changes in exposure time and temperature. In the present research ambient air cooling was adopted and cooled down specimens were tested at the age of age of 7, 30, 90 and 180 days. Graph showing the residual strength ratio and residual UPV ratio were plotted and the data were correlated to establish the relationship between UPV and compressive strength by using linear regression method. Researchers does not found any noticeable change in UPV for extended air curing of concrete and similar trend in reduction of in UPV and compressive strength was observed.

In addition to above work of Yang et al. (2009), Lin et al. (2011) done the research in which, in addition to

prolonged air curing, effect of post fire water curing of fire damaged concrete on strength and pulse velocity relationship was studied for predicting the residual compressive strength. Thermocouples were embedded inside the concrete specimens for measuring the temperature of core. Heated specimens are categorized into two groups, namely water cured specimens and air-cured specimens. Water cured specimens were kept in water for 3 days after natural cooling and then tested at the age of 4, 27, 57, 177 days. Similarly specimens kept in ambient air are also tested at the same age of water cured specimens. UPV and compressive strength of the specimens were measured according to specifications and for comparison unheated specimen were tested. In the conclusion considerable impact in regaining the strength of post fire water cured concrete was observed up to 500°C temperature. Significant gain in UPV due to post fire water curing was observed. This was because of filling of micro-cracks due to rehydration of fire damaged concrete. Later Hager et al. (2013) developed the relationship between UPV and compressive strength for Ordinary concrete and High Performance concrete, but by considering two different transducers with exponential and cylindrical probes. Exponential transducer with concentrator tip with an advantage of its application on curved surfaces increase its applicability over the conventional transducer. But, the signals obtained on the cube sample of size 15 cm from these transducers are relatively weak than cylindrical one and hence the correlating factor was introduced for making good understanding between the measurements performed by cylindrical and exponential probes. Point by point analysis along the length of the core obtained from the thermally damaged slab was performed using exponential transducer in order to check the feasibility of damage assessment of the heated specimens. Results obtained from UPV by using exponential transducer predicts the compressive strength on higher side than the results obtained from direct compression test. Temperature effect on Reactive Powdered Concrete mixed with 0-3% of steel fibre with increase in dosage of 0.5%, it was observed that ultrasonic pulse velocity was not much affected due to steel fibre content but mainly affected due to temperature. Up to 300°C temperature gradual decrease in UPV was observed and sharp decrease in velocity was noted between the temperature ranges of 400 to 700°C and again gradual decrease in rate of pulse velocity was observed between 700 and 800°C temperature by Gong et al. (2017). Hwang et al. (2018) carried out the study to monitor continuously the integrity of concrete subjected to elevated temperatures. The ultrasonic pulse velocity and the mechanical properties of concrete were evaluated before, during and after heating of the specimen. Circular specimen of diameter 10 cm and length 20 cm was used in the present study. An electric heating furnace was installed on the universal testing machine by employing the heat transfer heating method. Adopting heating rate of 1°C/min specimens were heated for 100, 200, 300, 400, 500, 600 and 700°C temperature for 5 hours. For preventing the damage to LVDT due to high temperature, quartz pipe of diameter 1 cm was installed touching the upper and lower surface of specimen for measuring the constant strain. To transmit ultrasonic pulse into the concrete specimen located inside the heating furnace, the transducer/receiver and concrete were connected to each other using bar of a 2.5 cm diameter with good corrosion resistance property. Bar used for transmitting the pulse velocity was cooled continuously so as to avoid heating near transducer. The results indicated that higher residual strain in the concrete indicates higher heating temperature which leads to decreased elastic modulus of concrete. Decrease in ultrasonic pulse velocity of heated concrete was observed after cooling of the concrete, with the possible reason of increase in the crack width and these results are in contrary with the findings of previous researchers. No reduction in the compressive strength and ultrasonic pulse velocity of the fire degraded concrete was observed up to 300° C temperature.

## **EFFECT OF FIRE ON STRENGTH OF CONCRETE**

Compressive strength of concrete is being considered in the construction industry to be a most reliable parameter for assessing the safety of structure and it is a form of destructive test. For assessing the temperature effect on compressive strength of concrete Malhotra (1956) has initiated the work on the concrete sample of 5.08 cm diameter and 10.16 cm length by considering three different testing conditions which are heating to a high temperature and testing in the hot state, heating of the specimen under constant stress and testing in the hot state and testing of the specimen after cooling it down gradually to ambient temperature. Experimentation was done within the temperature range between 200° to 600°C. For the design of experiment, number of samples required for testing, for each temperature within the temperature range and for different mix proportions were decided to be three for obtaining the mean value of the test results. Thermocouple was incorporated inside the specimen for measuring the temperature of core and for measuring the temperature inside the furnace another thermocouple was provided at the center of the furnace. Heating and stressing of the sample was done with the help of furnace provided with heating elements, hydraulic jack and dial gauge of capacity 20 ton. Large temperature gradient causes excessive spalling and it was avoided by controlling the rate of heating. In the conclusion it was found that specimens under constant stress during heating, avoids the development of cracks in the specimen and hence results in smaller reduction in strength. While the effect of heating on reduction of compressive strength was found to be greater in unstressed specimen (Ma et al. 2015). Chung (1985) observed the effect of heating on the compressive strength of concrete in addition to Ultrasonic

Pulse Velocity. Due to micro cracking and decomposition of cement gel, fast decrease in compressive strength was observed at high temperature. But up to 400°C temperature, no reduction in compressive strength was noted rather than increasing trend of compressive strength due to dehydration of cement gel as observed. While Mohamedbhai (1986) reported that, loss of moisture up to the temperature 400°C for 1 and 2 hours of exposure can be roughly taken as 70% and 60% respectively of the unheated one.

The study of effect of high temperature on partial replacement of Portland cement with pozzolanic material was investigated by Papayianni and Valiasis (1991). Portland cement was replaced partially with three types of Pozzolanic materials. At 200°C temperature 25% reduction in strength of Portland cement concrete was observed while, 38% to 50% loss of strength was observed in concrete with pozzolanic materials. At 400°C, 50% and 65% reduction in strength was observed respectively in concrete with Portland cement and concrete with pozzolanic materials. Hence it was concluded that pozzolanic materials increases the sensitivity of concrete at high temperatures. Li et al. (2012) studied the application of Ground granulated blast furnace slag (GGBFS) as a replacement for cement and investigated its properties at high temperature. In four different mix proportions replacement was done in 0%, 10%, 30% and 50% by the weight of cement, by keeping the water cement ratio constant. Cylindrical specimens for measuring compressive strength and modulus of elasticity of concrete and cube specimens were casted for studying the carbonation depth. Specimens were heated to six different temperatures in between 150° to 700°C and cooled down naturally to room temperature. 10% replacement of cement with GGBFS give similar results when the OPC concrete exposed to similar high temperatures. Replacement of cement by 30% GGBFS confers lower compressive strength than OPC concrete above 400°C. 50% replacement of cement by GGBFS does not exhibit good results. Maximum falling trend of compressive strength was observed above 400°C temperature. Siddique and Kaur (2012) cited in the given research also presented the similar conclusion. Authors have also observed that modulus of elasticity of concrete decreases with increase in temperature as well as increase in content of GGBFS in cement. These findings are similar with the conclusion drawn by Xiao et al. (2006) and Yüksel et al. (2011). Similar work has been carried out by using coal ash for producing light weight concrete was done by Ahn et al. (2016). By using the bottom ash as aggregate and fly ash as a portion of binder, by using these materials concrete of density 1790 and 1825 kg/m<sup>3</sup> and approximately 75-80% of density of normal weight concrete was produced and subjected to temperature up to 800°C. Behavior of light weight concrete made with bottom ash and fly ash was compared with commonly used lightweight concrete which contains expanded shale as an aggregate. After exposing to high temperature concrete containing bottom ash which produces much denser structure, smaller content of SiO<sub>2</sub> and rough surface produces smaller volume expansion as compared to concrete with expanded shale. Dense structure reveals higher spalling but that spalling was avoided by pre drying of the specimen at 100°C temperature. Modulus of elasticity of the specimen was evaluated from free-free resonate column test which is based on principal of elastic wave propagation. An instrument consists of supporting frame from which a cylindrical specimen was suspended by using two pieces of string. Waves are generated inside the specimen by hitting a small mallet at one end and wave form was analyzed by the wave form analyzer at the other end. Decrease in resonate frequency was observed with increase in temperature.

Poon et al. (2001) performed the experimentation for investigating the effect of post fire curing of fire damaged concrete on its compressive strength. Under the experimentation twenty different normal strength concrete and high strength concrete mixes are investigated. Cube size 10 cm were considered and at the age of 60 days those samples were heated to 600°C and 800°C. Before keeping the samples for two different post fire air and water curing regimes, heated samples from the electric furnace allowed to cool down to the ambient temperature. For analyzing the compressive strength recovery specimens were tested before heating, immediately after cooling to room temperature and after 7, 28, and 56 days of recuring. Recovery of strength was observed to be faster in water cured samples as compared to air cured samples. In addition to this, recovery was greater during first 7 days of curing because greater rate of rehydration of lime to fills the capillaries was observed. 15-20% more strength gain in water cured samples was noted as compared to air cured samples. Temperature above 800°C almost destroys the concrete by forming large surface as well as internal cracks and hence less strength was recovered.

Low heating rate of electric furnace results in homogeneous heating of concrete. To check the exact effect of sudden rise in temperature on concrete during fire, Li et al. (2004) tried to study the same by using, oil burning furnace with high heating rate on Normal Strength Concrete (NSC) and High Performance Concrete (HPC). Three different size of specimen tested for compressive, split tensile and bending strength of concrete and effect of size of specimen on compressive strength of concrete was also studied. Less loss of strength was observed in large size specimen. Formation of cracks as a result of heating reduces the cross sectional area of the specimen and thereby reduces the splitting tensile strength of concrete. Sharp reduction in bending strength of concrete was observed in HPC than NSC in between temperature 200-400°C and concrete almost lose its bending strength

above 800°C temperature.

As elaborated earlier in the effect of fire on pulse velocity of concrete (Yang et al. 2009; Lin et al. 2011) also investigated that for different curing regimes i.e. air and water curing, prolonged air curing does not have any remarkable effect on restoring the properties but, the water curing leads to restore the concrete strength significantly.

Compressive strength of High Performance Concrete (HPC) and Normal Strength Concrete (NSC) at 800°C were studied by Chan et al. (2000) on the cube specimen of size 10 cm. Considering three different mix designs with plane HPC, HPC with steel fibres and HPC with polymer fibres. Thoroughly saturated specimens were heated to 800°C temperature which proved to be the most severe condition for spalling because, high density of HPC results in high water pressure in pores. From the experimentation it was observed that HPC losses its strength more rapidly as compared to NSC and similar loss of strength was observed in HPC with polypropylene fibre but strength loss in HPC with steel fibres was observed to be less when compared with Plane HPC and HPC with polypropylene fibres.

Noumowe (2005) also studied the effect of high temperature on compressive and split tensile strength of fibre reinforced concrete. Polypropylene fibre with a dosage of 1.8 kg/m<sup>3</sup> added to high strength concrete for casting cylindrical samples and for comparison another control high strength concrete cylinders were casted. Heating of the samples was done in the electrically heated kiln at 200°C for 3 hours. For avoiding thermal shock specimens cooled down to room temperature in the kiln only. Like Nassif et al. (1995) for measuring temperature inside the specimen, authors had also installed the thermocouple inside the specimen. Properties of test specimen were measured before testing and after heating when the temperature of the specimen cooled down to room temperature. Results indicated that heating affected the compressive strength of concrete to 29-37% than that of the non-heated one and this effect was observed to be more in fibre reinforced concrete. Elevated temperature resulted into formation of additional channels and thereby porosity in concrete which found to be responsible for lower split tensile strength of fibre mixed concrete.

By following the similar approach Lau and Anson (2006) studied the effect of high temperature on properties of NSC and HSC with addition of steel fibre and by considering three different percentage levels of saturation. Experimentation was done on cube specimen, beam specimen and cylindrical specimen for measuring compressive strength, flexural strength and elastic modulus respectively. Study has been done on the six different mix proportions of NSC and HPC, out of which three are steel fibre reinforced concrete mix and three are non-steel fibre reinforced concrete mix. After 28 days of curing period weight and density of concrete cube specimen was recorded under saturated surface dry condition and similarly weight of oven dried concrete cube specimen was recorded after heating the specimen at 105°C temperature. The water loss in the specimen was determined. By using dry unit weight of concrete specimen, saturation level in other concrete specimens was calculated. Specimens with full saturation level indicates 5 to 12 MPa strength lower than concrete with saturation level at 20%. Flexural strength of fibre reinforced concrete was observed to be always better than non-fibre mixes, but this phenomenon becomes less effective when concrete exposed to 1000°C. It was said by other researchers that HPC is prone to spalling but in the current research authors does not found any evidence of spalling. Slower rate of rise in temperature and effect of steel fibres is the possible reason authors have given for avoiding spalling. Static modulus of elasticity of steel fibre reinforced concrete was observed to be higher than non-fibre mixes in between 2 and 6 GPa.

Choumanidis et al. (2016) also studied the effect of Steel fibre, Polypropylene fibres of two types (with different diameters and different length) and combination of all three types. Exposure temperature in the present study being kept limited to 280°C. Compressive strength conducted on cylindrical specimen and flexural testing conducted on prismatic specimen revealed that, only steel fibre exhibits decent properties on virgin specimen and heated specimen. Combination of long length polypropylene fibre and steel fibres in concrete revealed enhanced properties than steel fibre reinforced concrete at ambient temperature; but after heating, considerable loss in enhanced characteristics were observed. Authors also observed that combination of long and short polypropylene fibres in concrete performed very poorly at the high temperature conditions.

Behavior of high performance micro concrete and ordinary micro concrete at elevated temperature in terms of compressive strength and split tensile strength was examined in the given research article (Husem 2006) . High performance concrete and ordinary concrete have been produced and ordinary micro concrete (OMC) and high performance micro concrete (HPMC) samples were produced in order to represent their mortar phase. Cylindrical sample of high performance and ordinary concrete of size 15 x 30 cm was casted by using maximum size of aggregate of 16 mm and tested at the age of 28 days. Micro-High performance and Micro-Ordinary concrete was prepared by using the maximum size of aggregate of 4 mm and casted in the mould of size 4x4x16 cm. Because of the high density of HPMC and its high conductivity as compared to OMC, the slope of time temperature curve was kept higher for high performance micro concrete. Effect of high temperature was determined by performing split tensile strength followed by compression test on the broken samples, by considering the effect of post fire

curing regime on the heated samples. Loss of strength both in split tensile test and compressive test, was observed to be higher in ordinary concrete as compared to High performance concrete. It was also mentioned that effect of heating was lower in water cooled samples. Similar trend of decrease in strength in both ordinary concrete with aggregate size 16 mm and micro concrete with aggregate size 4 mm was observed with increase in temperature. Arioz (2007) investigating the properties of concrete prepared with river gravel and crushed limestone at elevated temperature. In addition to that specimens were oven dried for 24 hours at 105°C before subjecting them to elevated temperature. Heated specimens allowed to cool down and then kept in dry condition at ambient temperature for 2 hours. Loss in strength and loss in weight were examined. Weight loss in the concrete at 200°C and 1200°C was observed around 5% and 45% respectively and maximum weight loss was noted at temperature above 800°C. Hertz and Sørensen (2005) cited by Arioz (2007) stated that thermal expansion of Lime stone aggregate was lower than siliceous aggregates and hence, siliceous concrete suffers maximum damage. Slightly decrease in relative compressive strength of crushed limestone aggregate concrete up to temperature of 600°C was observed; and beyond this temperature, sudden strength reduction was observed. This sharp reduction was due to decomposition of crushed limestone aggregate above 600°C temperature. About 40% lesser strength was observed in river gravel concrete than limestone concrete. At 1200°C temperature 6% and 0% strength of crushed limestone and river gravel concrete was noted when compared with the unheated strength of specimen.

Effect of temperature on early age concrete where the concrete was incompletely hydrated was presented by Chen et al. (2009). Concrete cubes of dimension 10 cm were casted at the room temperature and after setting of concrete they were kept for curing for the next 1, 3, 7, 14, 28 days and heated in the furnace at the target temperature of 200, 400, 600, 800, 1000°C at the heating rate of 10°C/ minute for 3 hours. Temperature of the specimen was brought down to the temperature of 20°C by using slow and rapid cooling methods. Rapid cooling was done with the help of water spray and rapid cooling gives yellowish appearance to the concrete, while slow curing gives whitish appearance. Later cooled down specimens were kept for curing for the period of 28 days. Compressive strength and split tensile strength was carried out at different curing age. During heating large amount of water vapor was observed at the entrance of furnace because of incomplete hydration of the cement paste, while that release of water vapor was decreased with increase in curing period. Recovery of compressive strength of early age concrete i.e. 1 day, when heated up to temperature of 800°C was observed to be much higher as compared to 28 days cured concrete; which indicates the possibility of regaining the strength. This was because of, increase in age decreases the moisture content of concrete and thereby decreases the strength regaining capacity. And this recovery was observed to be highest in the concrete cured for 3 days. Elevated temperatures causes cracking of the concrete which reduces the effective cross sectional area and the applied tensile stresses causes expansion of cracks and hence, effect of temperature on split tensile strength was observed to be more severe as compared to effect of high temperature on compressive strength.

Impact-echo method, one of the form of non-destructive test was used for assessment of mechanical properties of fire damaged concrete were studied. Katarzyna and Hager (2015) was performed and experimentation to figure out the relationship between the mechanical properties of concrete such as compressive strength and static modulus of elasticity, and the parameters measured with the help of impact eco (IE) device. Heated specimens of size 15x15x15 cm were tested for IE test and destructive test for developing the relationship. Relationship obtained from cubical specimen later validated by conducting the additional test on concrete slab of size 1.2x1.0x0.3 m. As a result authors have found that results obtained by destructive tests are very consistent with results obtained from IE test and IE signal received in the time domain relates strongly with damage severity.

In continuation Park and Yim (2016) applied the Impact Resonance method for evaluating the residual mechanical properties and Dynamic Elastic Modulus of fire damaged concrete. In addition to above work done by Katarzyna and Hager (2015), different post fire curing regimes and post fire storing periods were considered. Concrete cylinders of diameter 10 X 20 cm length were casted and cured for 28 days and then a disk shaped sample were obtained of thickness 25mm by cutting the concrete cylinder by using a diamond saw. Samples were kept in drying oven for 24 hours at 80°C temperature before sending them to furnace and then heated to elevated temperatures. Cooling of the samples was done immediately after heating by immersing the samples directly into the water for 30 minutes and then tested at the age of 7, 30, 180, 360 days. Correlation was performed between measured dynamic modulus of elasticity, split tensile strength and residual compressive strength by using linear regression analysis. The relation developed was independent of mix proportion, exposure temperature and storing period. Post fire air curing was not resulted into restoring the dynamic elastic modulus of the fire damaged concrete and ultimately the compressive strength.

Along with UPV Gong et al. (2017) also studied the effect of high temperature on compressive strength of reactive powder concrete (RPC) with different percentage of steel fibre. Brittle failure of unheated reference test specimen made with plain RPC was observed. While the reduction in degree of brittle failure was observed in reference specimen made with steel fibre reinforced RPC. Similar failure characteristics were observed between heated specimens and reference test specimen, with same volume of steel fibers in the temperature range of 100 to 400°C. Beyond 400°C temperature sudden decrease in compressive strength was noted. This sudden reduction in

compressive strength was due to decomposition of calcium silicate hydrate gel (C-S-H) beyond temperature 560°C. Between 700 to 800°C temperature, steel fibre softened gradually and further depletion in concrete strength was observed.

### **EFFECT OF FIRE ON MICROSTRUCTURE OF CONCRETE**

Elevated temperatures causes' thermal deformation by forming micro-cracks in the hardened cement matrix and interfacial transition zone (ITZ) i.e. bond between cement paste and aggregate. Cracks at ITZ were observed to be wider in fire damaged specimen as compared to reference specimen. At 400°C Cracks appears first and then propagates considerably in the specimen in between temperature 600°C and 800°C (Papayianni and Valiasis 1991; Nassif et al. 1995). In SEM photographs, cracks in cement past were observed, some of them are passing around the unhydrated cement clinkers while in severely damaged specimen, cracks propagates through unhydrated cement clinkers. Nassif et al. (1999) studied the structural integrity of post fire rapidly cooled down concrete. From SEM photographs it was concluded that cracks are arrested at the ITZ if their orientation is perpendicular to ITZ, and they run along ITZ if their orientation is parallel.

As the effect of dehydration of calcium hydroxide and changes in crystalline structure of fired specimen observed in XRD, causes internal stresses because of shrinkage and volume change and thereby cracks in concrete. These micro-cracks and honeycombs caused by high temperature can be filled by rehydration products, this phenomenon were studied under SEM by Poon et al. (2001). Width of cracks measured before and after rehydration, and better recovery was observed in water cured specimen for 56 days of post fire water-recurring. It was mentioned that further recurring may result in additional recovery or decrease in crack width.

Examination carried out on the high strength concrete and high strength concrete with polypropylene fibre heated up to 200°C temperature revealed that, melting of fibres forming additional cavities and channels which may become an additional space to relieve high pressure of internal moisture. Furthermore, melting of fibre and decrease in length of fibre results in relaxation of concrete (Noumowe 2005).

Ahn et al. (2016) studied the microstructure of light weight concrete containing bottom ash as an aggregate and fly ash, at the interface between aggregate and paste before and after the thermal exposure. It was noted that rough surface of bottom ash exhibits greater interlocking effect between aggregate and paste which leads to slower fracturing of concrete.

Ingham (2009) conducted a case study of fire damaged reinforced concrete structure (during its construction stage). Investigation was carried out in two stages by, visual inspection and petrographic examination to figure out the detailed repair strategy. The observations compiled by the author from the review of (Hajpál and Török 2004; Sippel et al. 2007; Chakrabarti et al. 1996; Koca et al. 2006) it has been found that, in the temperature range between 250-300°C the change in colour normal to pink and reddish brown was observed in limestone and sandstone which may not be visible until 400°C, and at this temperature expansion takes place in marble which was observed to be non-reversible in nature but, the expansion in granite was observed to be reversible if heated at the slow rate. Development of pink and reddish brown colour reflects the substantial reduction in compressive strength (Short et al. 2001). At 600°C temperature calcination of calcium carbonate commences in limestone and at the same temperature, sandstone and marble exhibits brittle properties, while granite develops cracks. Temperature above 1000°C melting starts in almost all stone types such as Limestone, Sandstone, Marble and Granite. Mineralogical changes in the cement matrix are noted at 500°C temperature.

Microstructural changes of hardened cement paste are studied under SEM by Peng and Huang (2008) in high performance concrete (HPC). Pore structure coarsening was exhibited as result of elevated temperature at 200 to 600°C; below 600°C temperature effect of coarsening was observed to be more responsible for decrement in mechanical strength of concrete due to formation of cracks, than the decomposition of calcium silicate hydrate.

### **CONCLUSION**

Exposure of concrete to fire brings various changes in properties of concrete. From the above content following conclusions can be drawn:

- Ultrasonic pulse velocity decreases with increase in temperature, this is because microcracks reduces the travelling speed of pulse and increased pulse velocity can be observed in the fire damaged quenched sample which contains high moisture content through which pulse can travel more easily as compared to unquenched one.
- Decrease in residual strength of concrete with increase in temperature. Significant strength loss was observed in the temperature range between 400-600°C because of decomposition Calcium Silicate Hydrate. Compressive strength of concrete was observed to be higher under stressed state than unstressed state under elevated temperature conditions.
- Loss of moisture content during heating causes coarsening of microstructure of concrete which increase

- the porosity and increase in porosity means decrease in mechanical properties of concrete.
- Post fire curing of fire damaged concrete results in recovering the lost strength due to filling of microcracks as a result of rehydration process that generates the calcium silicate hydrate. Rehydration rate of concrete exposed to elevated temperature predominates within first 7 days.
  - Size of specimen controls the effect of fire, more the size of concrete specimen less will be the temperature effect and vice versa.
  - Steel fibres provides better fire protection in terms of residual mechanical properties of concrete as compared to polypropylene fibre because, polypropylene fibres melts at 200°C temperature by forming additional small channels/cavities in concrete which ultimately results in reduced strength.
  - High performance concrete causes explosive spalling when it is subjected to higher rate of rise in temperature. The higher rate of rising temperature, evaporates the moisture more rapidly and creates a vapour pressure which cannot go outside the concrete easily because of higher density of concrete. Hence more spalling was observed in High Performance Concrete and saturated samples as compared to Normal Strength Concrete and dry concrete.

## REFERENCES

- Ahn, Y. B., Jang, J. G., and Lee, H. K. (2016). "Mechanical properties of lightweight concrete made with coal ashes after exposure to elevated temperatures." *Cement and Concrete Composites*, Elsevier Ltd, 72, 27–38.
- Alhadid, M. M. A., and Youssef, M. A. (2013). "Structural Behavior of Jacketed Fire-Damaged Reinforced Concrete Members\_ A Review (PDF Download Available).pdf." *3rd Specialty Conference on Disaster Prevention and Mitigation*, 1–12.
- Arioz, O. (2007). "Effects of elevated temperatures on properties of concrete." *Fire Safety Journal*, 42(8), 516–522.
- Chakrabarti, B., Yates, T., and Lewry, A. (1996). "Effect of fire damage on natural stonework in buildings." *Construction and Building Materials*, 10(7), 539–544.
- Chan, Y. N., Luo, X., and Sun, W. (2000). "Compressive strength and pore structure of high-performance concrete after exposure to high temperature up to 800 H C." *Cement and Concrete Research*, 30(2), 247–251.
- Chen, B., Li, C., and Chen, L. (2009). "Experimental study of mechanical properties of normal-strength concrete exposed to high temperatures at an early age." *Fire Safety Journal*, Elsevier, 44(7), 997–1002.
- Chew, M. Y. L. (1993). "The Assessment of Fire Damaged Concrete." *Building and Environment*, 28(1), 97–102.
- Choumanidis, D., Badogiannis, E., Nomikos, P., and Sofianos, A. (2016). "The effect of different fibres on the flexural behaviour of concrete exposed to normal and elevated temperatures." *Construction and Building Materials*, Elsevier Ltd, 129, 266–277.
- Chung, H. W. (1985). "Ultrasonic testing of concrete after exposure to high temperatures." *NDT International*, 18(5), 275–278.
- Gong, J., Deng, G., and Shan, B. (2017). "Performance evaluation of RPC exposed to high temperature combining ultrasonic test : A case study." *Construction and Building Materials*, Elsevier Ltd, 157, 194–202.
- Hager, I., Carré, H., and Krzemie, K. (2013). "Damage Assessment of Concrete Subjected To High Temperature By Means of the Ultrasonic Pulse Velocity – Upv Method." *Studies and Researches*, 32, 197–211.
- Hajpál, M., and Török, Á. (2004). "Mineralogical and colour changes of quartz sandstones by heat." *Environmental Geology*, 46, 311–322.
- Hertz, K. D. Å., and Sørensen, L. S. (2005). "Test method for spalling of fire exposed concrete." *Fire Safety Journal*, 40(5), 466–476.
- Husem, M. (2006). "The effects of high temperature on compressive and flexural strengths of ordinary and high-performance concrete." *Fire Safety Journal*, 41(2), 155–163.
- Hwang, E., Kim, G., Choe, G., Yoon, M., Gucunski, N., and Nam, J. (2018). "Evaluation of concrete degradation depending on heating conditions by ultrasonic pulse velocity." *Construction and Building Materials*, Elsevier Ltd, 171, 511–520.
- Ingham, J. P. (2009). "Application of petrographic examination techniques to the assessment of fire-damaged concrete and masonry structures." *Materials Characterization*, Elsevier Inc., 60(7), 700–709.
- Katarzynna, K., and Hager, I. (2015). "Post-fire assessment of mechanical properties of concrete with the use of the impact-echo method." *Construction and Building Materials*, 96, 155–163.
- Koca, M. Y., Ozden, G., Yavuz, A. B., Kincal, C., Onargan, T., and Kucuk, K. (2006). "Changes in the engineering properties of marble in fire-exposed columns." *International Journal of Rock Mechanics and Mining Sciences*, 43(4), 520–530.
- Lau, A., and Anson, M. (2006). "Effect of high temperatures on high performance steel fibre reinforced concrete." *Cement and Concrete Research*, 36(9), 1698–1707.

- Lie, T. T. (1992). "Structural Fire Protection." *ASCE Manuals and Reports on Engineering Practice*, New York, NY, USA.
- Li, M., Qian, C., and Sun, W. (2004). "Mechanical properties of high-strength concrete after fire." *Cement and Concrete Research*, 34(6), 1001–1005.
- Li, Q., Li, Z., and Yuan, G. (2012). "Effects of elevated temperatures on properties of concrete containing ground granulated blast furnace slag as cementitious material." *Construction and Building Materials*, Elsevier Ltd, 35, 687–692.
- Lin, Y., Hsiao, C., Yang, H., and Lin, Y. (2011). "The effect of post-fire-curing on strength – velocity relationship for nondestructive assessment of fire-damaged concrete strength." *Fire Safety Journal*, Elsevier, 46(4), 178–185.
- Ma, Q., Guo, R., Zhao, Z., Lin, Z., and He, K. (2015). "Mechanical properties of concrete at high temperature — A review." *Construction and Building Materials*, Elsevier Ltd, 93, 371–383.
- Malhotra, H. . (1956). "The effect of temperature on the compressive strength of concrete." *Magazine of Concrete Research*, 85–94.
- Mohamedbhai, G. T. G. (1986). "Effect of exposure time and rates of heating -and cooling on residual strength of heated concrete." *Magazine of Concrete Research*, 38(136), 151–158.
- Nassif, A., Rigden, S., and Burley, E. (1999). "The effects of rapid cooling by water quenching on the stiffness properties of fire-damaged concrete." *Magazine of Concrete ...*, 51(4), 255–261.
- Nassif, A. Y., Burley, E., and Rigden, S. (1995). "A new quantitative method of assessing fire damage to concrete structures." *Magazine of Concrete Research*, 47(172), 271–278.
- Noumowe, A. (2005). "Mechanical properties and microstructure of high strength concrete containing polypropylene fibres exposed to temperatures up to 200 - C." *Cement and Concrete Research*, 35(11), 2192–2198.
- Papayianni, J., and Valiasis, T. (1991). "Residual mechanical properties of heated concrete incorporating different pozzolanic materials." *Materials and Structures*, 24(2), 115–121.
- Park, S. J., and Yim, H. J. (2016). "Evaluation of residual mechanical properties of concrete after exposure to high temperatures using impact resonance method." *Construction and Building Materials*, Elsevier Ltd, 129, 89–97.
- Peng, G. F., and Huang, Z. S. (2008). "Change in microstructure of hardened cement paste subjected to elevated temperatures." *Construction and Building Materials*, 22(4), 593–599.
- Poon, C. S., Azhar, S., Anson, M., and Wong, Y. L. (2001). "Strength and durability recovery of fire-damaged concrete after post-fire-curing." *Cement and Concrete Research*, 31(9), 1307–1318.
- Short, N. R. U., Purkiss, J. A., and Guise, S. E. (2001). "Assessment of fire damaged concrete using colour image analysis." *Construction and Building Materials*, 15(1), 9–15.
- Siddique, R., and Kaur, D. (2012). "Properties of concrete containing ground granulated blast furnace slag ( GGBFS ) at elevated temperatures." *Journal of Advanced Research*, Cairo University, 3, 45–51.
- Sippel, J., Siegesmund, S., Weiss, T., Nitsch, K. H., and Korzen, M. (2007). "Decay of natural stones caused by fire damage." *Building Stone Decay: From Diagnosis to Conservation*, 271(1), 139–151.
- Xiao, J., Xie, M., and Zhang, C. (2006). "Residual compressive behaviour of pre-heated high-performance concrete with blast-furnace-slag." *Fire Safety Journal*, 41(2), 91–98.
- Yang, H., Lin, Y., Hsiao, C., and Liu, J. Y. (2009). "Evaluating residual compressive strength of concrete at elevated temperatures using ultrasonic pulse velocity." *Fire Safety Journal*, 44(1), 121–130.
- Yüksel, I., Siddique, R., and Özkan, Ö. (2011). "Influence of high temperature on the properties of concretes made with industrial by-products as fine aggregate replacement." *Construction and Building Materials*, 25(2), 967–972.



## The effect of ceramic specimen shape in the Kolsky bar experiment: A numerical study

J. Venkatesan<sup>1</sup>, M. A. Iqbal\*<sup>1</sup>, V. Madhu<sup>2</sup>

<sup>1</sup>Department of Civil Engineering, Indian Institute of Technology Roorkee, Roorkee, India

<sup>2</sup>DRDO – Defence Metallurgical Research Laboratory, Hyderabad, India

\*jsvenkat.c@gmail.com (Corresponding Author)

### ABSTRACT

The advanced ceramic materials are well known for their high hardness, high compressive strength and low density which makes them suitable candidate for the armour design. These materials experience dynamic loading or high strain rate of loading during the projectile impact. Therefore, the dynamic response of ceramic was focus for several researchers. The uniaxial compressive strength of the ceramic materials at strain rate up to  $10^3 \text{ s}^{-1}$  is determined by Modified Kolsky bar experiment. In general, the recommended ceramic specimen L/D ratio for this test is 1 and the shape is cylinder. However, machining the cylindrical ceramic specimen out of the ceramic tile (the general form of ceramic produced for armour application) is difficult task than machining of square prism shape. Therefore, in the present study, the effect of ceramic specimen shape on the measured uniaxial compressive strength of ceramic using modified Kolsky bar experiment is assessed by numerical simulation. The outcome of the study was indicated that the shape of the ceramic specimen is not affecting the measurement of compressive strength using modified Kolsky bar experiment.

### INTRODUCTION

Advanced ceramics are well known for their excellent material properties such as high hardness, compressive strength, and low density. These properties are intrigued by the researchers to explore their application for the light weight armours. Despite of the above properties, ceramics has low tensile strength and toughness which demands an additional material to be placed along with them to produce an effective light weight armour. In general ceramics are used as a front layer and it is backed by ductile material in the armour. The armours undergo high rate of loading during the projectile impact. Therefore, it is important to study and understand ceramic failure mechanism under high rate of loading. Modified split Hopkinson pressure bar (MSHPB) apparatus has been used for testing the ceramics under high strain rate of loading of  $10^2$  to  $10^3 \text{ s}^{-1}$  in one dimensional stress condition [1]. For SHPB experiment, the maximum size of the specimen is calculated based on the strength of the bars used in the SHPB apparatus and the recommended specimen shape is cylindrical and the L/D ratio is 1 [2]. The ceramic specimens for the SHPB testing were machined from the ceramic tiles. Cylindrical specimens were core drilled using diamond tip core driller, whereas the cuboidal specimens can be easily machined using diamond disc cutters and also the use of cuboidal specimens allow visualization of failure during dynamic loading Hogan et al. (2016) [3].

There are few research works have been reported in the open literature concerning the effect of specimen dimension and shape on the measurement of material strength using SHPB. Rodriguez et al. [4] studied the effect of specimen diameter on the measurement of metal strength using SHPB apparatus through experimental and 2D numerical simulations. Aluminium 7017 was used for this study as the material which is not sensitive to the strain rate. Specimens with various diameter were tested and it was found that small size of the specimen can be used for SHPB test and it helps to achieve higher strain rate. Pankow et al. [5] carried out 3D finite element analysis on the cylindrical, square and elliptical cross section SHPB specimen of polymers. The difference in the cross section of polymer specimen significantly affected the stress concentration in the specimen during the high strain rate testing. However, it was negligible intensity for the cylindrical and square specimens and the stress strain curve for both the specimens were similar. Chen et al. [6] carried out 2D finite element simulation on ceramic testing using SHPB to study the stress concentration and stress distribution in ceramic specimens. Dog-bone and cylindrical shape of ceramic specimens were recommended to determine the failure strength of ceramic under high strain rate of loading due to the uniform stress distribution in these specimen shapes. Shih et al. [7] reported that the failure strength of cuboidal shape SiC specimen under quasi-static compression loading was lower than the cylindrical shape specimen due to the stress concentration. In the recent studies, the compressive strength and failure mechanism of ceramic under dynamic loading was determined using both cylindrical and cuboidal shape specimens [3,6–14]. The advantage of cuboidal specimens over cylindrical specimens are ease of ceramic machining with less damage, placing strain gauge on the specimen, and observe real time failure mechanism of ceramic during the testing using high speed camera or digital image correlation system. However, there is no study to justifying the use of cuboidal specimens for determining the failure strength of ceramic under high strain rate of loading.

Therefore, in this study, the uses of cuboidal shape specimen in SHPB apparatus were investigated using 3D finite element simulation. Comparison were made between cylindrical and cuboidal ceramic specimens failure strength under same strain rate. The finite element model was validated with the experimental results of Wang and Li (2015) [14] and the same model was extended for the current study.

### FINITE ELEMENT MODEL

In the present study, 3D finite element model was created using ABQUS/Explicit software which is capable to simulate the large deformation and dynamic related problems. Wang and Li (2015) carried out SHPB experiments and 3D numerical simulation on the alumina ceramic of cylindrical specimens to study the failure mechanism under dynamic loading. The SHPB apparatus used in the above experiment consist of 20 mm diameter and 2000 mm length of incident and transmission bar and the dimension of the striker bar was 20 mm diameter and 400 mm length. Two inserts of WC were used to protect the SHPB bars from the hard ceramic indentation and the dimension was 17 mm diameter and 17 mm length which is designed by considering the impedance matching between the bars and insert. The dimension of alumina ceramic was 5 mm diameter and 5 mm length. The length of incident and transmission bar was reduced to 1200 mm for the current finite element model and it is decided based on the minimum length required to replicate the SHPB and all other parts and testing conditions were same as it is in the Wang and Li (2015) SHPB experiment Fig. 1. The dimension of parallelepiped specimen considered in this study was 4.5 mm × 4.5 mm × 4.5 mm. The bar system of SHPB was meshed with 1 mm<sup>3</sup> size and the WC inserts were 0.5 mm<sup>3</sup>. The cylindrical and parallelepiped alumina ceramic specimen was meshed with 0.1 mm<sup>3</sup> Fig. 1. The material model used for the SHPB bars and WC inserts are linear elastic model as these parts are subjected to negligible deformation. Johnson-Holmquist (JH2) model was used for the alumina ceramic specimen. The material parameter for the above models are taken from the Wang and Li (2015).

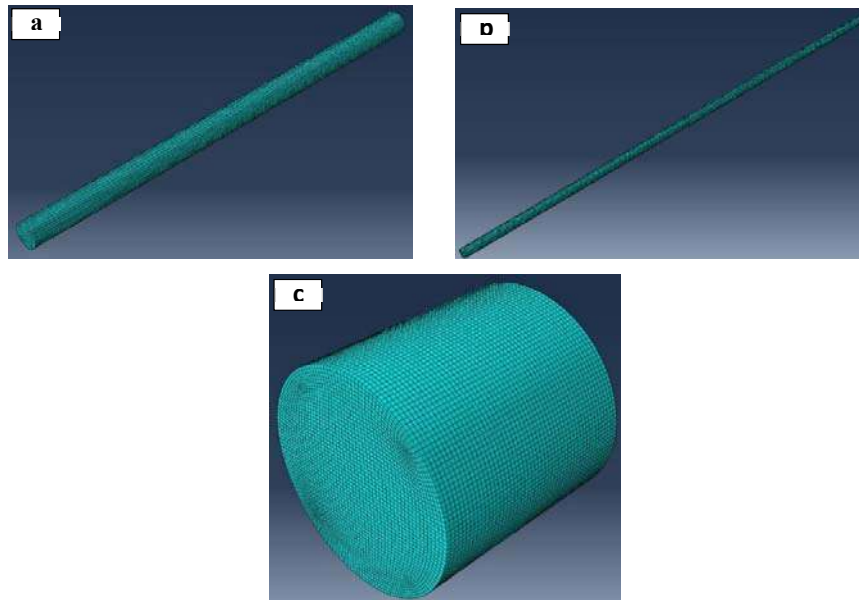


Fig. 1. Numerical model and meshing (a) 200 mm striker (b) 1200 mm incident and transmission bar and incident bar

The current numerical model was validated with the experimental results of Wang and Li (2015) of cylindrical shape ceramic specimen. As it can be seen from the Fig. 2 the current 3D numerical model is capable to predict the dynamic response of alumina ceramics, the same model was extended for parallelepiped shape ceramic specimen.

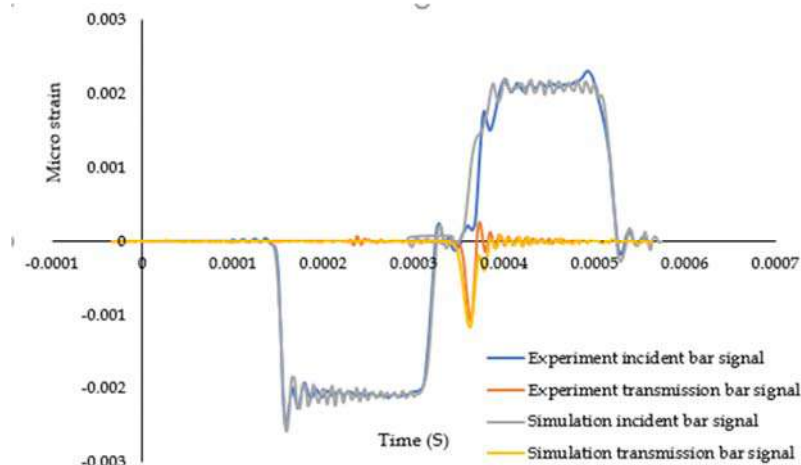


Fig. 2. Strain signal measured in experiment and numerical simulation

## RESULTS AND DISCUSSION

The objective of the SHPB experiment was to determine the material strength and failure mode and mechanism at higher strain rate loading. The strain signal measured at the centre of the SHPB bars have been shown in fig. 3. The parallelepiped and cylindrical shape specimen was not affecting the strain signal which denotes the negligible influence of specimen shape on the compressive strength measurement of ceramics at high strain rate of loading. The similar finding was observed by [4] for the metal specimens. However, in quasi-static compressive testing of ceramic material, the parallelepiped shape specimen gave less compressive strength than cylindrical specimen due to the stress concentration at the corner of the parallelepiped and the same was not seems to be true for high strain rate of loading. Therefore, based on the results of current study, it can be concluded that the specimen shape is having negligible influence on the strength measurement of the alumina ceramic material.

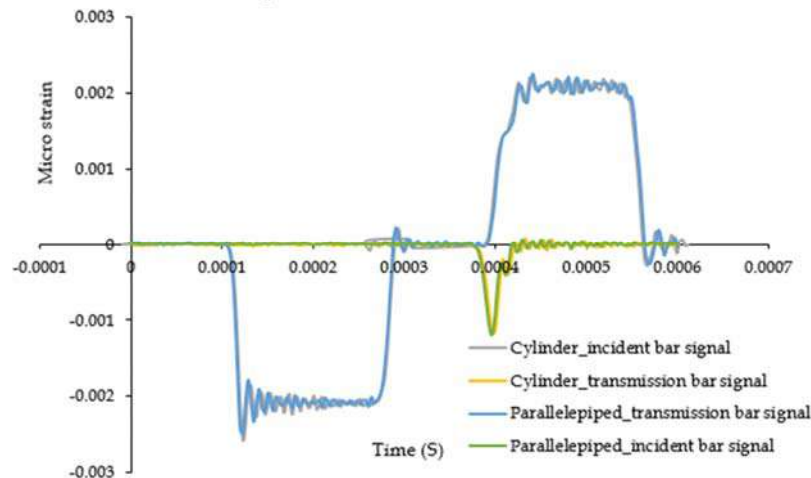


Fig. 3. Comparison of strain signal measured in the SHPB numerical simulation of cylinder and parallelepiped ceramic specimen

The failure process of the ceramic cylinder and parallelepiped specimen was shown in fig. 4. It could be observed that though the strain signal of both the specimens were similar, the failure process was different. The parallelepiped specimen failure was initially circular fracture at the centre of the specimen and the uniformity of the stress within the specimen before the failure was delayed as compare to the cylindrical specimen. Moreover, the corner of the parallelepiped specimen fractured completely at initial stage which indicates the failure process of ceramic depends on the specimen shape in the SHPB experiment.

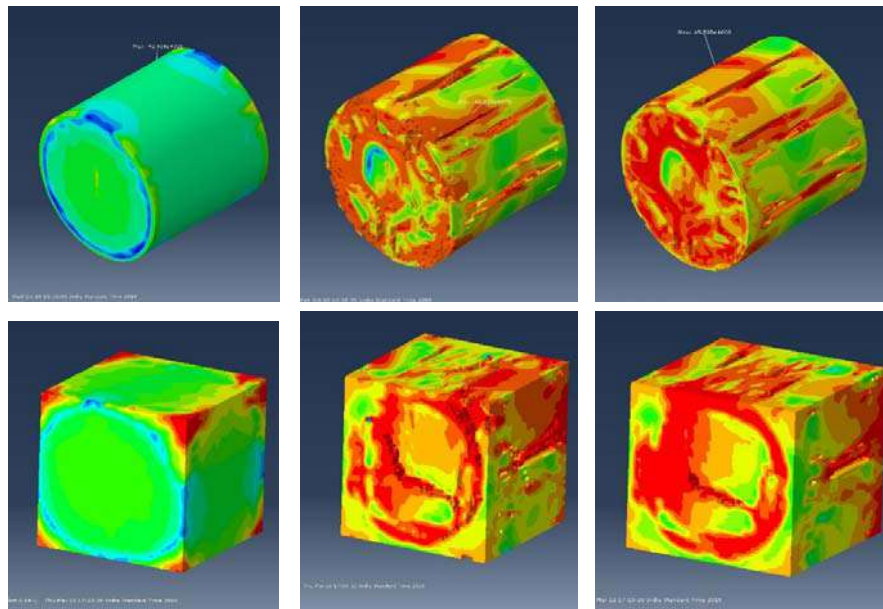


Fig. 4. Failure process of cylindrical and parallelepiped specimen in the SHPB experiment

## CONCLUSION

In this study, the effect of ceramic specimen shape on the measurement of compressive strength and failure process of ceramic under high strain rate of loading was studied using 3D numerical simulation. It was observed that the compressive strength measurement at high strain rate was not affected due to the specimen shape of ceramics. However, the failure process of ceramic was influenced by the ceramic specimen shape in the SHPB experiment. Further studies are required to explore the same for other ceramics

## REFERENCE

- G. Ravichandran, G. Subhash, Critical appraisal of limiting strain rates for compression testing of ceramics in a split Hopkinson pressure bar, *Journal of the American Ceramic Society*. 77 (1994) 263–267.
- W. Chen, B. Song, *Split Hopkinson (Kolsky) Bar - Design, Testing and Applications*, 2011.
- J.D. Hogan, L. Farbaniec, T. Sano, M. Shaeffer, K.T. Ramesh, The effects of defects on the uniaxial compressive strength and failure of an advanced ceramic, *Acta Materialia*. 102 (2016) 263–272. doi:10.1016/j.actamat.2015.09.028.
- J. Rodriguez, R. Cortes, M.A. Martinez, V. Sanchez-Galvez, C. Navarro, Numerical study of the specimen size effect in the split Hopkinson pressure bar tests, *Journal of Materials Science*. 30 (1995) 4720–4725. doi:10.1007/BF01153084.
- M. Pankow, C. Attard, A.M. Waas, Specimen size and shape effect in split Hopkinson pressure bar testing, *The Journal of Strain Analysis for Engineering Design*. 44 (2009) 689–698. doi:10.1243/03093247JSA538.
- W. Chen, G. Subhash, G. Ravichandran, Evaluation of ceramic specimen geometries used in a split Hopkinson pressure bar, *Dymat Journal*. 1 (1994) 193–210.
- C.J. Shih, M.A. Meyers, V.F. Nesterenko, S.J. Chen, Damage evolution in dynamic deformation of silicon carbide, *Acta Materialia*. 48 (2000) 2399–2420. doi:10.1016/S1359-6454(99)00409-7.
- G. Subhash, G. Subhash, Mechanical behaviour of a hot pressed aluminum nitride under uniaxial compression, *Journal of Materials Science*. 33 (1998) 1933–1939. doi:10.1023/A:1004325926287.
- H. Wang, K. Ramesh, Dynamic strength and fragmentation of hot-pressed silicon carbide under uniaxial compression, *Acta Materialia*. 52 (2004) 355–367. doi:10.1016/j.actamat.2003.09.036.
- S. Sarva, S. Nemat-Nasser, Dynamic compressive strength of silicon carbide under uniaxial compression, *Materials Science and Engineering: A*. 317 (2001) 140–144. doi:10.1016/S0921-5093(01)01172-8.
- L. Farbaniec, J.D. Hogan, K.Y. Xie, M. Shaeffer, K.J. Hemker, K.T. Ramesh, Damage evolution of hot-pressed boron carbide under confined dynamic compression, *International Journal of Impact Engineering*. 99

(2017) 75–84. doi:10.1016/j.ijimpeng.2016.09.008.

B. Paliwal, K.T. Ramesh, Effect of crack growth dynamics on the rate-sensitive behavior of hot-pressed boron carbide, *Scripta Materialia*. 57 (2007) 481–484. doi:10.1016/j.scriptamat.2007.05.028.

B. Paliwal, K.T. Ramesh, Dynamic Damage Nucleation and Growth in Boron Carbide, (2007).

Z. Wang, P. Li, Dynamic failure and fracture mechanism in alumina ceramics: Experimental observations and finite element modelling, *Ceramics International*. 41 (2015) 12763–12772. doi:10.1016/j.ceramint.2015.06.110.



## Influence of Boundary Condition and Mass of TNT on the Behaviour of Concrete Slab under Blast Loading

A. Singhal,<sup>1</sup> K. Senthil,<sup>2\*</sup> and B. Shailja<sup>3</sup>

<sup>1</sup>PG Student, Department of Civil Engineering, Dr. BR Ambedkar NIT Jalandhar, Punjab 144011;  
E-mail: eng.akhilsinghal92@gmail.com

<sup>2\*</sup> Assistant Professor, Department of Civil Engineering, Dr. BR Ambedkar NIT Jalandhar, Punjab 144011;  
E-mail: ursenthil85@yahoo.co.in; kasilingams@nitj.ac.in, Phone: +91-9458948743 (Corresponding Author)

<sup>3</sup> Assistant Professor, Department of Civil Engineering, Dr. BR Ambedkar NIT Jalandhar, Punjab 144011;  
E-mail: shailja.bawa@gmail.com

### ABSTRACT

The numerical simulation has been carried out on reinforced concrete slab against blast loading to demonstrate the accuracy of the finite element based numerical models using ABAQUS. The parameters such as weight of TNT and boundary conditions subjected surface blast have been studied. The results obtained from simulations were compared with the available experiments to validate the model and to examine the response of the reinforced concrete slab subjected to blast loading. The inelastic behavior of concrete and steel reinforcement bar has been incorporated through concrete damage plasticity model and Johnson-cook models available in ABAQUS were presented. The results of the present study were found in close agreement with the experimental results. It is observed that the maximum stress in the concrete was found to be in the range of 15 to 20 N/mm<sup>2</sup> and is almost constant for given charge weight. It is concluded that for every increase of 33.33% weight of TNT, the deflection increases by 52%. The slab with two short edge discontinuous end condition was found better and it may be utilized in designing important structures.

**KEYWORDS:** Finite element analysis, Reinforced concrete slab, Blast loading, Stresses and Deformation,

### INTRODUCTION

In the past few decades, damage to a structure due to explosion has increased as a result of increase in number and intensity of terrorist activities, manmade accident and natural explosion. In order to design structures which are able to withstand, it is necessary to first quantify the effects of such explosions. **Ettouney et al., (1996)** presented design of commercial building subjected to blast loading. It is observed that the design modifications and recommendations that improve ductility and structural response during occurrence of blast load. **Watson et al. (2005)** carried out experiments and measured the damages caused to reinforced concrete T beams and slabs by contact and close proximity explosive charges using different areas of contact and angles of inclination for the explosives. **Osteras et al., (2006)** discussed qualitative assessment of blast damage and collapse pattern of murrh Building bombing in 1995. **Ngo et al., (2007)** presents a comprehensive overview of the effects of explosion on structures. **King et al., (2009)** discussed typical building retrofit strategies for load bearing and non-load bearing structural members through strengthening, shielding, or controlling hazardous debris. In addition to that, many studies found on detailed experiments and finite element analysis using reinforced concrete slab subjected to blast loading [**Lu (2009), Lotfi and Zahrai (2018) and Senthil et al. (2018a, b, c)**], however, there are significant shortcomings and gaps which is derived from the previous studies. Based on the detailed literature survey, it is observed that most studies focused on simple experiments on simple slabs, column and bridge elements subjected to blast loading, however numerical investigations on slabs against blast loading has been found to be limited. Also response of the reinforced concrete slab subjected to blast loading under varying mass of TNT and boundary conditions has not been studied. In the present study, the numerical investigations has been carried out on reinforced concrete slab against blast loading through finite element method. The inelastic behavior of concrete and steel reinforced bar has been incorporated through concrete damage plasticity model and Johnson-cook model respectively. The results obtained from simulations were compared with the experiments available in literature, **Li et al., (2016)**. The simulations are carried out against varying mass of TNT and boundary conditions.

### CONSTITUTIVE MODELLING

In finite element modelling, inelastic behaviour of concrete was defined by using concrete damaged plasticity model (CDP) providing a general capability for modelling concrete and other quasi-brittle materials. The concrete damaged plasticity model is a continuum, plasticity-based, damage model for concrete. The stress strain relations under uniaxial compression and tension loading are given by the following equations where  $E_o$  is the initial (undamaged) elastic stiffness of the material:  $\sigma_t = (1-d_t)E_o(\epsilon_r - \epsilon_r^p)$  and  $\sigma_c = (1-d_c)E_o(\epsilon_c - \epsilon_c^p)$ , where  $d_t$  and  $d_c$  are

tension damage variable and compression damage variable respectively, **Senthil et al., (2017 and 2018c)**. The flow and fracture behavior of projectile and target material was predicted employing the **Johnson-Cook (1985)** elasto-viscoplastic material model available in ABAQUS finite element code. The material model is based on the von Mises yield criterion and associated flow rule. It includes the effect of linear thermo-elasticity, yielding, plastic flow, isotropic strain hardening, strain rate hardening, softening due to adiabatic heating and damage. The section of the reinforcement is assigned Fe250 steel and the ultimate tensile strength is 250 MPa is approximately equivalent to the ultimate tensile strength proposed by **Iqbal et al., (2015)**.

## FINITE ELEMENT MODELLING

The finite element model of the reinforced concrete slab was made using **ABAQUS/CAE**. The length and width of slab was 2.0 and 0.8 m respectively exactly proposed by **Li et al., (2016)**. The thickness of slab was 120 mm and clear cover is 20 mm on both the side of slab. The top and bottom steel reinforcement of main bar was 12 mm diameter placed at 95 mm center to centre distance. The size of stirrup reinforcement in slab was considered as 10 mm diameter placed at 196 mm centre to centre distance on shorter direction. The geometry of the concrete and steel reinforcement was modeled as solid deformable body. The interaction between concrete and steel was modeled using the tie constraint option available in ABAQUS/CAE wherein the concrete was assumed as host region and the steel as embedded region. The constitutive and fracture behavior of steel and concrete have been predicted using Johnson-Cook and Concrete damaged plasticity model respectively available in ABAQUS. The origin of blast considered against 1.5 m from the exterior top surface of slab and 8 kg mass of TNT, see **Fig. 1**.

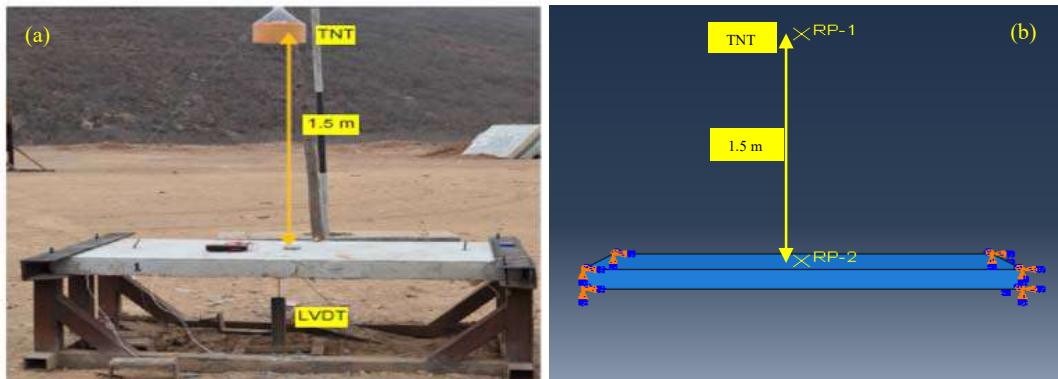


**Fig. 1** Picture showing (a) Experimental setup (Li et al., 2006) (b) Simulation

The blast load was incorporated using interaction module available in ABAQUS. The surface blast load was created using CONWEP definition and the surface blast was consigned with help of two reference point which is assigned based on standoff distance from point of response. The concrete elements of all the components were meshed using structured elements of 8 noded hexahedral linear brick element and steel reinforcement was meshed with linear beam element. Linear shape functions were used by elements and reduced integration was considered, i.e. per element one integration point. A linear element of type T3D2 (three dimensional two noded truss element) reduced integration. A detailed mesh sensitivity analysis has been carried out to understand the influence of mesh size. The size of element was varied as  $0.03 \times 0.03 \times 0.03$  m,  $0.02 \times 0.02 \times 0.02$  m,  $0.015 \times 0.015 \times 0.015$  m and  $0.01 \times 0.01 \times 0.01$  m and corresponding total number of elements were 7236, 24000, 56392 and 192000 respectively.

The predicted deflection of slab was compared with the experimental results, see **Fig. 2** corresponding to varying mesh size. The predicted deflection was 210, 190, 180 and 135 mm against 0.01, 0.015, 0.02 and 0.03 m mesh size respectively, whereas the measured deflection is 190 mm. It is observed that the deflection of slab corresponding element size of 0.015 and 0.02 m was found in good agreement with the experimental results. The mesh size 0.02 m was assigned, giving a total number of 24000 and 2688 elements for the concrete and reinforced steel bar respectively. The analysis was divided into 20 frames within a time frame of 0.08 second. A CPU time typical simulation for blast event took around 20 minutes.

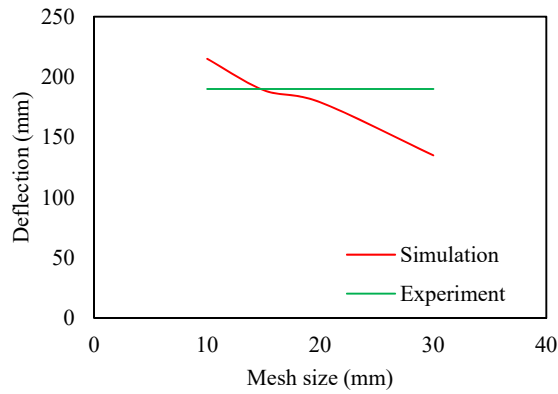


**Fig. 2** Deflection of slab function of varying mesh size

### COMPARISON OF EXPERIMENT AND SIMULATION

The simulations were carried out against 8 kg mass of TNT at a distance of 1.5 from the surface of the slab. The concrete damaged plasticity model has been employed for predicting the material behavior of the concrete, whereas the Johnson-Cook model has been used for predicting the material behavior of steel reinforcement. The simulated results thus obtained have been compared with the experiments carried out by Li *et al.* (2016) and discussed in this Section.

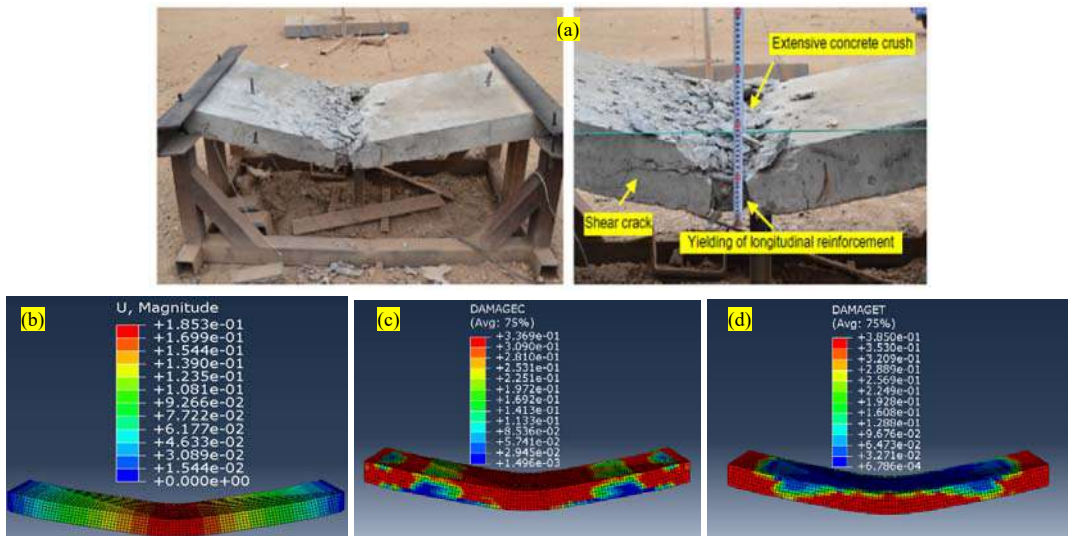


**Fig. 3** Deformed profile of (a) experiments and predicted results of (b) displacement (c) compression damage (d) tension damage

Fig. 3(a)-(d) shows the deformed profile of experiments and predicted results in light of displacement, compression damage, tension damage, Mises stress in concrete and steel and equivalent plastic strain in steel. It is observed that the maximum deflection obtained numerically is 185 mm, which is very close to the maximum deflection of 190 mm measured throughout the experiment. The predicted deflections are in close agreement to actual experimental results. However, the maximum difference between the actual and predicted deflection was found to be 3%. The actual and predicted deformation of the slab as a result of failure has been compared and almost exact pattern of deformation has been predicted through numerical simulations.

### RESULTS AND DISCUSSION

Three-dimensional finite element analysis has been carried out in order to study the response of reinforced concrete slab against blast loading using ABAQUS/CAE. The simulations were carried out against varying mass of TNT and different support condition. Also the response of slab have been studied against surface blast loading. The response of structural elements were observed in terms of deflection, von-Mises stresses, and compression

and tension damage therein were presented and discussed.

**Effect of varying mass of TNT**

The simulations were carried out against varying mass of TNT at constant standoff of distance, i.e. 1.5 m. The response of 120 mm thick slab was studied against varying mass of TNT and the mass considered as 6.0, 8.0 and 12 kg. The behaviour of reinforced concrete slab in terms of deflection, Mises stresses in concrete and steel bar and compression damage against varying mass of TNT is shown in **Figs. 4 and 5**.

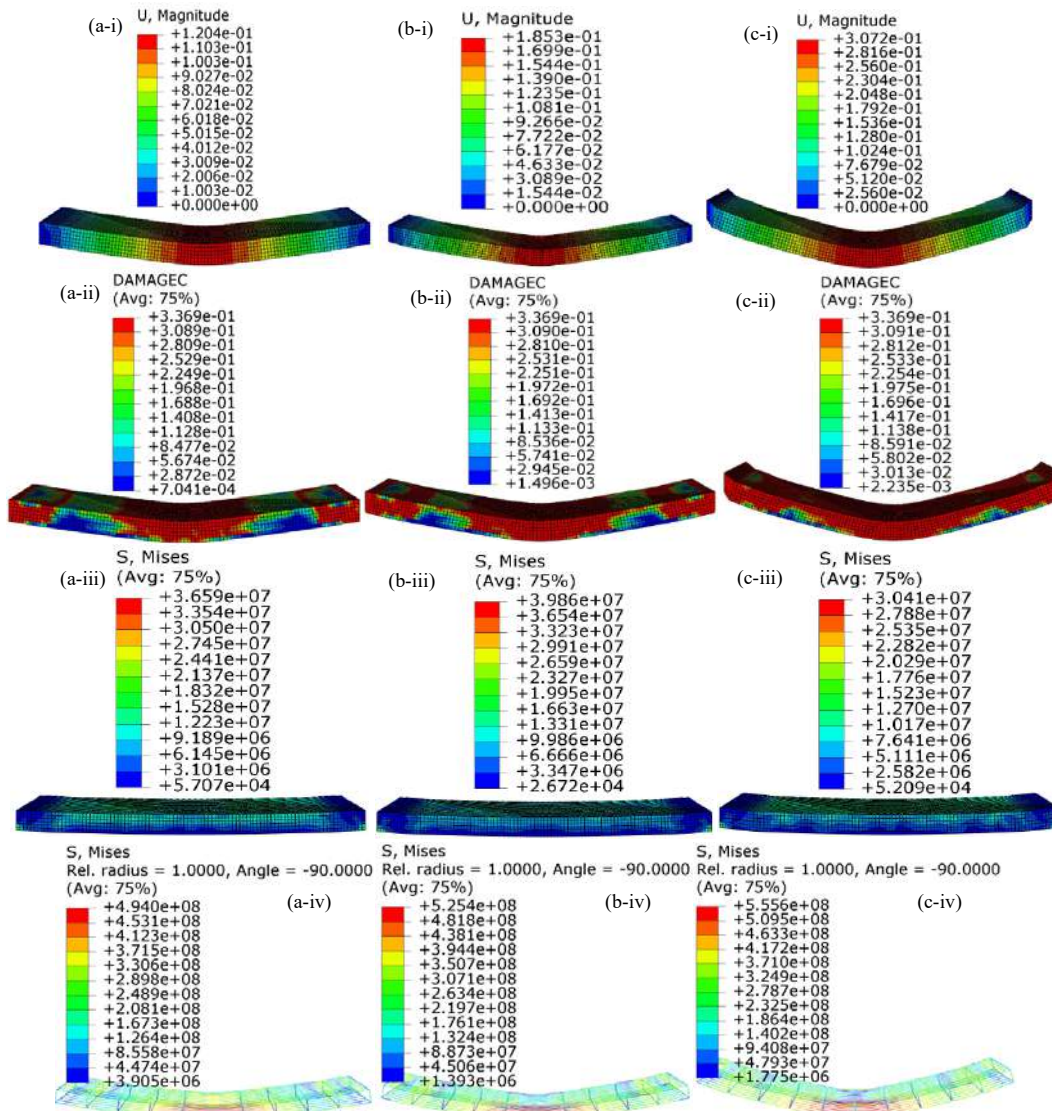


**Fig. 4 (i) Deflection of slab (ii) compression damage and Mises stresses in (iii) concrete and (iv) steel bar and against (a) 6 (b) 8 and (c) 12 kg mass TNT**

The displacement of slab against blast load of varying mass TNT originated at 1.5 m from the surface is shown in **Fig. 4(a-i)-(c-i)**. The unit of the displacement contours was “meter”. The maximum deflection was found to be 307, 185 and 120 mm against 12, 6 and 8 kg mass TNT respectively. It is observed that the deflection in the slab was found to be increased by 156% when the mass of TNT increased from 6 to 12 kg. It is concluded that for every increase of 33.33% weight of TNT, the deflection increases by 52% for a standoff distance of 1.5m. The maximum deflection on slab was about 307 mm against mass of 12 kg TNT and it is found to be more vulnerable.

The deflection of slab against 12 kg mass was found increased to 39 and 60% as compared to the deflection of slab by 6 and 8 kg mass TNT respectively. It is also clearly seen that the deflection reaches its peak value within 0.02 seconds i.e., from the time of detonation, see **Fig. 5**.

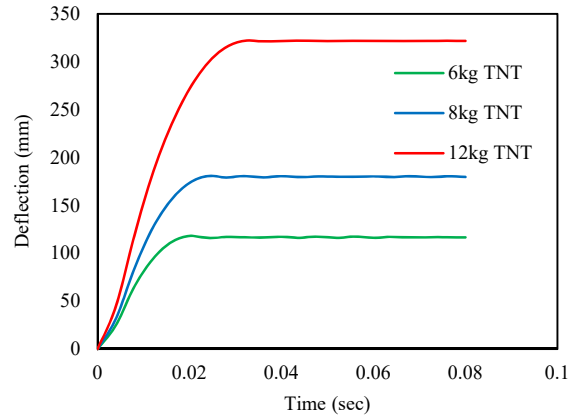


**Fig. 5** Response in terms of deflection function of time at varying mass of TNT

The compression damage of slab against blast load of varying mass TNT is shown in **Fig. 4(a-ii)-(c-ii)**. The compression damage contours described by unit less factor. The maximum damage due to compression was found to be 0.336 for against all chosen mass of TNT. The compression damage parameter was considered maximum of 0.351 in the present study. It is observed that the compression damage in the slab was found to reach maximum against 6, 8 and 12 kg mass TNT. From this observation, it is concluded that the slab was found to be more vulnerable against 6 kg mass of TNT and the slab may be safe if the mass of TNT below 6 kg.

The von-Mises stresses in concrete against blast load of varying mass TNT is shown in **Fig. 4(a-iii)-(c-iii)**. The unit of the von-Mises stress in the contours is “N/m<sup>2</sup>”. At 0.004 second time step, the maximum von-Mises stress at the concrete was found to be 36, 39.8 and 30.4 MPa for 6, 8 and 12 kg mass TNT respectively. However, it is observed that the stress in concrete was found to be almost 20 MPa after 0.004 second time step. Also, it is observed that the stress in concrete was found to be increased when the mass of TNT increased from 6 to 8 kg, whereas the trend is reverse when the mass of TNT increased from 8 to 12 kg. The von-Mises stresses in steel reinforcement against blast load of varying mass of TNT is shown in **Fig. 4(a-iv)-(c-iv)**. The von-Mises stress at the steel reinforced bar was found to be 494, 525 and 555 MPa for 6, 8 and 12 kg mass TNT respectively. It is observed that the stress was found to increase with increase in mass of TNT. Therefore, it is concluded that the steel reinforcement was found observing the stresses efficiently then the concrete when the mass of TNT is significantly higher. Therefore, it is concluded that the maximum stress in the concrete was found to be in the range of 15 to 20 N/mm<sup>2</sup> and is almost constant against 6, 8 and 12 kg charge weight.

#### **Effect of varying boundary condition**

Due to non-uniformity in buildings supports and structures one could find the different end boundary conditions. The support conditions of reinforced concrete slab was considered based on the provisions made by Indian standard practices, **IS 456:2000**. The behaviour of reinforced concrete slab in terms of deflection and Mises stresses in concrete element against varying boundary conditions are shown in **Figs. 6-8**.

The deflection of slab having different boundary conditions function of time is shown in **Fig. 6**. It was observed that maximum deflection reaches its peak value within the time step 0.02 seconds for all the boundary conditions except slab with three adjacent edge discontinuous. The deflection of slab having three adjacent edge discontinuous found increased upto time step 0.06 second, thereafter the deflection of slab is constant. The maximum deflection in slab of different boundary conditions such as all edges continuous, two long adjacent edges discontinuous, two short edge discontinuous, one short edge discontinuous, two adjacent edges discontinuous and three long edge discontinuous were shown in **Fig. 7**. The maximum deflection of slab subjected to all edges continuous, two long adjacent edges discontinuous, two short edge discontinuous, one short edge discontinuous, two adjacent edges discontinuous and three long edge discontinuous was observed 33.8, 185, 32, 33, 346 and 495 mm respectively. The maximum deflection was observed when the slab subjected to three edges

discontinuous and the minimum deflection when the slab subjected to two short edges discontinuous. However the deflection of slab having boundary of all edges continuous, two short edge discontinuous and one short edge discontinuous was found to be almost same, 33 mm.

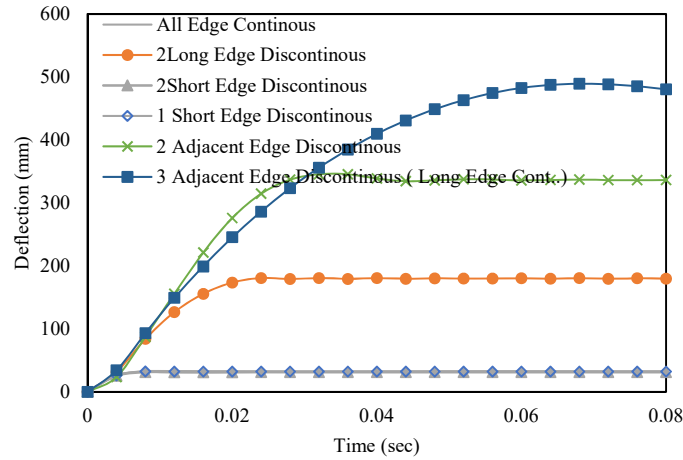


Fig. 6 Deflection of slab at different boundary conditions function of time

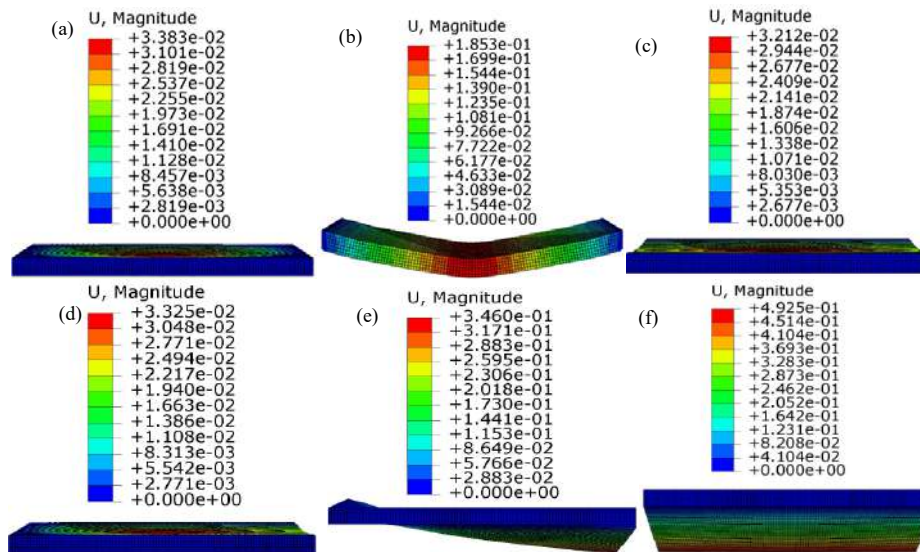
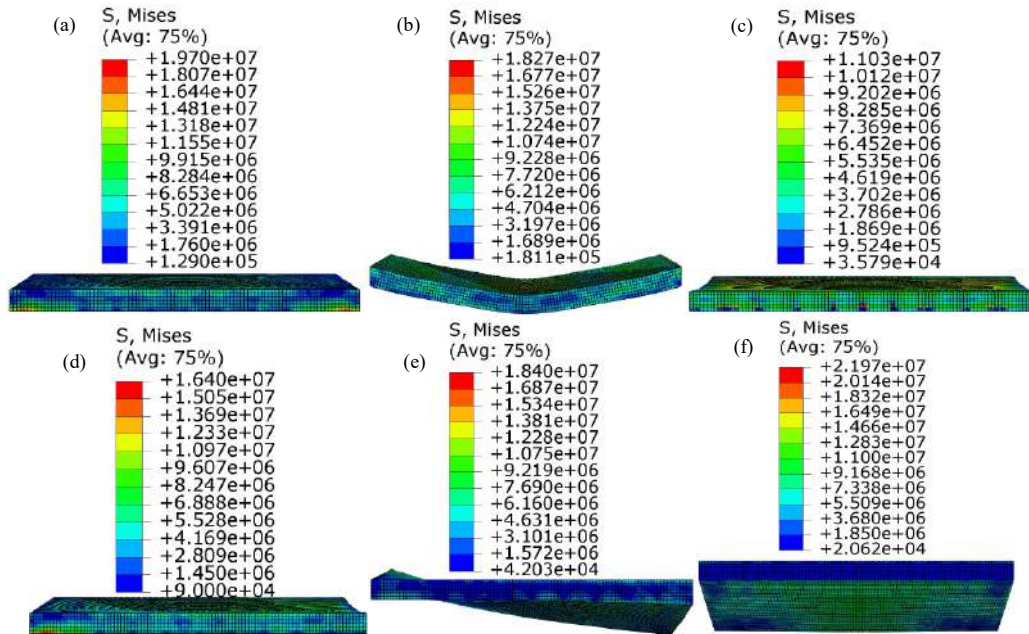


Fig. 7 Maximum deflection in slab having (a) all edges continuous (b) 2 long adjacent edges discontinuous (c) 2 short edge discontinuous (d) 1 short edge discontinuous (e) 2 adjacent edges discontinuous and (f) 3 adjacent edge discontinuous end conditions

The von-Mises stresses in concrete against blast load by 8 kg mass TNT at 1.5 m standoff distance and the response of slab having different boundary conditions at 0.08 second is shown in Fig. 8. It is observed that maximum stress reaches its peak value within 0.008 second irrespective of the boundary conditions. At 0.08 second, the maximum stress was observed when the slab having three adjacent edges discontinuous and the minimum stress was observed when the slab is discontinuous on two short edges discontinuous. The maximum stress developed by slab having all edges continuous, two long adjacent edges discontinuous, two short edge discontinuous, one short edge discontinuous, two adjacent edges discontinuous and three long edge discontinuous was observed 19.7, 18.2, 11.0, 16.4, 18.4 and 21.9 MPa respectively. It is observed that behaviour of slab in terms of von-Mises stress is almost similar for all edge conditions except two short edge discontinuous. The stress developed in the slab having two short edge discontinuous was found decreased by almost 30-50% as compared to other end conditions considered in the present study. It is also observed that the deflection and stress in slab having two short edge

discontinuous end conditions were 32 mm, 6.99 m/s and 11.03 MPa respectively and it seems to be the best boundary conditions among the chosen configurations. Therefore, it is concluded that the slab with two short edge discontinuous may be utilised in designing of important structures.



**Fig. 8 Mises stresses in slab having (a) all edges continuous (b) 2 long adjacent edges discontinuous (c) short edge discontinuous (d) 1 short edge discontinuous (e) 2 adjacent edges discontinuous and (f) 3 adjacent edge discontinuous end conditions at 0.08 second**

## CONCLUSION

The present study addresses the finite element investigation on the behavior of reinforced concrete slab against blast load. The numerical simulations were carried out using ABAQUS/Explicit finite element model to predict the response of slab and results are compared with the experimental available in literature. The simulations were carried out against varying mass of TNT and boundary conditions. The response of reinforced concrete slab was studied in terms of deflection, von-Mises stresses, compression and tension damage of concrete and the following conclusions have been drawn.

- The maximum deflection of slab obtained from simulation was 185 mm which is very close to the experimental results of 190 mm. The actual and predicted deformation of the slab as a result of failure has been compared and almost exact pattern of deformation has been predicted through numerical simulations.
- It is observed that the deflection in the slab was found to be increased by 156% when the mass of TNT increased from 6 to 12 kg. It is concluded that for every increase of 33.33% weight of TNT, the deflection increases by 52%. The maximum stress in the concrete was found to be in the range of 15 to 20 N/mm<sup>2</sup> and is almost constant for 6, 8 and 12 kg charge weight.
- It is also observed that the deflection and stress in slab having two short edge discontinuous end conditions were 32 mm, 6.99 m/s and 11.03 MPa respectively and it seems to be the best boundary conditions among the chosen configurations. The stress developed in the slab having two short edge discontinuous was found to decrease almost 30-50% as compared to other end conditions considered in the present study. Therefore, it is concluded that the slab with two short edge discontinuous may be utilised in designing of important structures.

## REFERENCES

ABAQUS, (2014) 6.14 Documentation. Dassault Systemes Simulia Corporation.  
 Ettouney, M., Smilowitz, R. and Rittenhouse, T. (1996), "Blast resistant design of commercial buildings", *Pract. Perio. Struct. Design Const., ASCE*, 1(1), 31-39.  
 Iqbal, M.A., Senthil, K., Bhargava, P. and Gupta, N.K., (2015), "The characterization and ballistic evaluation of mild steel", *Int. J. Impact Eng.*, 78, 98-113.

- IS 456:2000. Plain and reinforced concrete – Code of practice, Bureau of Indian Standard, New Delhi, 1-100.
- Johnson, G.R. and Cook, W.H. (1985), “Fracture characteristics of three metals subjected to various strains, strain rates, temperatures, and pressures”, *Eng. Fracture Mech.*, 21, 31–48.
- King, K.W., Wawelawczyk, J.H. and Ozbey, C. (2009), “Retrofit strategies to protect structures from blast loading”, *Canadian J. Civil Eng.*, 36(8), 1345–1355.
- Li, J., Wu, C., Hao, H., Su, Y. and Liu, Z. (2016), “Blast resistance of concrete slab reinforced with high performance fibre material”, *J. Structural Inte. Mainte.*, 1(2) 51-59.
- Lotfi, S. and Zahrai, S.M. (2018), “Blast behavior of steel infill panels with various thickness and stiffener arrangement”, *Struct. Eng. Mech.*, 65(5), 587-600.
- Lu, Y. (2009). “Modelling of concrete structures subjected to shock and blast loading: An overview and some recent studies”, *Struct. Eng. Mech.*, 32(2), 235-249.
- Ngo, T., Mendis, P., Gupta, A. and Ramsay, J. (2007), “Blast loading and blast effects on structures – An overview”, *Electronic J. Struct. Eng., Special Issue: Loading on Structures*, 76-91.
- Osteraas, J.D. (2006), “Murrah building bombing revisited: A qualitative assessment of blast damage and collapse patterns”, *J. Perform. Const. Facilities, ASCE*, 20(4), 330-335.
- Senthil, K., Rupali, S. and Satyanarayanan, K.S. (2017), “Experiments on ductile and non-ductile reinforced concrete frames under static and cyclic loading”, *J. Coupled Sys. Multiscale Dyn.*, 5(1), 38-50.
- Senthil, K., Rupali, S. and Kaur, N. (2018a). “The performance of monolithic reinforced concrete structure includes slab, beam and column against blast load”, *J. Mat. Eng. Struct.* 5(2), 137-151.
- Senthil K., Singhal A., Shailja B. (2018b). “Influence of mass of TNT and standoff distance on the response of reinforced concrete flat slab against blast loading”, *Jordan J. Civil Eng*, Under Review.
- Senthil, K., Gupta A. and Singh, S.P. (2018c) “Computation of stress-deformation of deep beam with openings using finite element method”, *Adv. Concrete Const.* 6(3), 245-268.
- Watson, S., Macpherson, W.N., Barton, J.S., Jones, J.D.C., Tyas, A., Pichugin, A.V., Hindle, A., Parkes, W., Dunare, C. and Stevenson, T. (2005), “Investigation of shock waves in explosive blasts using fibre optic pressure sensors”, *J. Physics: Conf. Series*, 15, 226–231.



# STRUCTURAL PERFORMANCE OF UHPC SLABS UNDER BLAST LOADING: A STATE ART REVIEW

Kunal<sup>1</sup>, H.K Sharma<sup>2</sup>

<sup>1</sup>M. Tech student, Deptt. Of Civil Engg., NIT Kurukshetra, Kurukshetra, kunald158@gmail.com

<sup>2</sup>Professor, Deptt. Of Civil Engg., NIT Kurukshetra, Kurukshetra, hksharma1010@yahoo.co.in (Corresponding Author)

## ABSTRACT

In recent decades blast loads have secured a lot attention. The objective of this paper is to overview of the blast effects on reinforced concrete slabs used for different structure. In case of explosion the public buildings are not secure area because terrorist attacks can takes place anywhere. The major reasons of injuries opposed to people are caused by heat of the detonation or blast and pressures there are further threats that can be dangerous at the same way. Slabs of any structure play an important role to withstand blast loading. Generally, when the conventional building structures are subjected to blast loading it will lead to progressive collapse of the structure. So, we need to design the structural element first which is located close to detonation point. To reduce the risk of collapse by the strengthening of slabs of the structure with the help of blast effects on structure the material is called Ultra-high-performance concrete (UHPC) which has good ductility, better toughness and more strength has been broadly used in modern construction. The dynamic response of the structure under blast loading is difficult to study due to the nonlinear nature of the material. A few of the experimentally and analytical is encapsulate on blast loading taken to slabs. This study will help to better understand on UHPC slabs under of blast loading.

**Keywords:** Ultra high-performance concrete, slabs, blast loading, analytical performance, terrorism.

## INTRODUCTION

In some previous years, reasonable importance has been given to blast load because intentional or accidental activities related to important structures. The threat of terrorism is in its peak in the entire world thus it is necessary to protect the civil infrastructures from the blast shock. Many researches are going throughout the world for studying the blast load on various structures. An explosion is defined as a sudden release of energy, rapid and large scale. According to the nature, blast can be classified as chemical or physical incident. A blast detonation is nearby or inside a structure is because of various reasons like quarry blasting or vehicle bomb pressure. This can produce external as well as internal damages to the building. This may result the progressive collapse of the building. The pressure wave's move with the temperature is around 2000-2500 °C, velocity of sound, pressure is nearly 250 kilo bar of the air causing this velocity to increase. The damage of building connection has been distinguished to fracture in brittle manner when subjected to blast. This progressive collapse can be decreased by strengthening slabs of the structure. Ultra-high-Performance concrete (UHPC) allows large compressive strength, high tensile strength, toughness and large energy absorption capacity as differentiate to the ordinary concrete and we get a reduced section of structural elements. So UHPC is very economical concrete having good resistance against the blast. Several works were reported on blast analysis of structural members. This research focuses to understand the effect of blast loading on slabs of structure. Slab will affect the progressive collapse of the building structure. It is very uneconomical to design every conventional building for blast loading but we can design some structural member such that it can resist the blast load and progressive collapse of a building at some extent. Dynamic response of structures subjected to blast loads is difficult to measure due to the non-linear nature of the material. Blast analysis may be performed with the help of finite element analysis by using the ANSYS modeling software.

## LITERATURE REVIEW

**Mike et al. (2006)** presented high explosive effect on building structure by case studies event from the explosion of huge vehicle borne materials in the Europe, Middle East as well as North America and World War II. When subjected to blast detonation damage building in which building joints have been discovered to fracture in a brittle way. The danger of the collapse may be decreased through strengthening beam column joints placed at closeness to a capacity design method for strengthening and potential vehicle borne devices is recommended.

**Ngo et al. (2007)** presented an analysis of results of the blast on structures. Illustration for mechanism of the blast wave with nature of explosions in free air is stated. This study also introduced different procedure to evaluate structural response and blast loads. It is very important that high-risks facilities like commercial and public

structure, design considerations opposed to high velocity impact and bomb blast. It is suggested that guidelines on provisions on progressive collapse and abnormal load cases avoidance should be admitted in Design Standards current Building adjustments. In the severe load conditions under building performance is enhanced with the help of Requirements on ductility levels.

**Yanchao et al. (2007)** Numerical simulations had been performed to study a standalone structure column with blast wave interaction. So it was also established that the blast wave–column interactions are considered; the interaction results will slightly increases the positive reflected impulse and decrease the positive reflected pressure. The result of column dimension on the blast wave–column interaction is important. Increasing the column dimension will decrease the blast wave strength behind the column. The effect of bottom on column is less important than the column breadth. Reducing the column dimension also reduces the time lag and as well as the time lag increase when the column dimension increases among the blast wave acts on the rear surface and column front.

**Nystrom et al. (2009)** had done the numerical studies of fragment loading and effects of blast. A numerical simulation apparatus had been applied to another analysis of the fragment loading and blast results on a reinforced concrete wall. The results were distinguished in the Simulations of the reaction of a wall strip is subjected to fragment loading, blast loading, both fragment loading and blast.

**Scheleyer et al. (2010)** conducted the full size explosive testing of fiber-reinforced concrete panels and the panels were containing inside a large concrete cover to minimize clearance over the faces from the blast wave it arranged in 100 kg TNT equivalent explosive charge between 7m and 12m. The two panels were constructed with various level of steel fibers dosage. Rest of the two panels was constructed with steel fibre with auxiliary steel bar reinforcement. Computer of numerical modeling was carried out applying the Autodyne package to estimate the behavior of four panels before measuring. Simplified modeling of the panels was also performed applying resistance-deflection together with single degree of freedom representation connection that took detail of feature ductile softening and brittle cracking behavior successive ultimate capacity.

**Na-Hyun et al. (2012)** presented the characteristics and behavior of reactive powder concrete (RPC) and ultra-high performance concrete (UHPC) subjected to blast load. They made an experimental analysis of UHPC structural elements with the explosions. Blast resistance abilities of RPC and UHPC were experimentally calculated to form the chance of applying RPC and UHPC in concrete structure capable to accidental impacts or terrorist attacks. Flexural strength, elastic modulus, compressive strength, Slump flow test were executed. Reflected pressure and incidental and as well as residual and maximum displacement and the strains of concrete and rebar were measured. The result presented that RPC and UHPC have high blast explosion resistance than normal strength concrete (NSC).

**Kamal et al. (2014)** focused on the evaluation of the performance of UHPC. 12 simple concrete beams were tested in flexure with and without shear reinforcements. The major variables were taken the kind of fibers and the percentage of web reinforcement and longitudinal both. Polypropylene fibers and Steel were used. The behavior like, ultimate load, initial cracking and cracking pattern was observed under different stages of loading. At the ending of loading large number of cracks were found because of the use of fibers that lead to the compact thickness of cracks. For check the experimental results ACI-code equations design were taken. Based on the analysis, it is found that by using of steel fibers and polypropylene the 28-day compressive strength increases by 6% and 2.5% as compared to mixes without fibers. Through web reinforcement and lower reinforcement ratios the increased ultimate loads percentage was 13% where steel fibers were used. Without web reinforcement, the increase in the ultimate loads was 15% and 48% where polypropylene fibers and steel were used.

**Quazi et al. (2014)** presents the study of five storey RCC building with the effect of Blast loading. For the calculation of effect of variable blast source weight a 30 meter distance from tip of detonation is helpful. In SAP2000 the blast loading was calculated analytically as a numerical model of the building and pressure-time history was constructed. The effects of the lateral load response caused by blast regarding inter storey drift, accelerations velocity, peak deflections is compared and determined.

**Shallan et al. (2014)** investigated, with different aspect ratios the effects of blast loads on three buildings through numerical simulations. The finite element program AUTODYN is helpful for the development of finite element models of these buildings. Blast loads spaced from the building and located at two different locations with many standoff distances were applied. The simulations have represented that increasing the standoff distance with effect of blast load decrease from the building and with variation. So that no variation occur in the displacement of the

column in the side of the blast load in aspect ratios of the buildings but the results of blast load reduces with the increasing aspect ratio in other element in the building.

**Li et al. (2015)** presented the investigation of slab under contact explosion in normal strength concrete (NSC) and ultra-high-performance concrete (UHPC). They conducted the experiment on both type of slab UHPC and NSC of contact explosion in the field. UHPC had been known for its better workability, high energy absorption capacity and good compressive and tensile strength. In their study they showed the dynamic behavior of NSC slab with contact detonation and estimated with the UHPC slab under similar loading plan. Numerical models (Finite Element Modeling) were also initiated to replicate both the previous contact explosion test and free air explosion test.

**Li et al. (2015)** investigates the segmental reinforced columns (RC) under blast loading resistance abilities. RC segmental columns energy dissipation bars and with or without shear keys are considered. The post tensioning forces of different levels and effect of the number of segments on column dynamic behavior are calculated. Commercial code LS-DYNA issued toper form blast loadings in segmental columns with numerical simulations. The present testing details on RC columns is compared against accuracy of the numerical model. Under many condition of blast loadings the numerical results of segmental columns are enumerated and estimated along the monolithic RC columns.

**Carufel et al. (2016)** examined the blast performance of UHPC column. In their study of blast loading UHPC were tested with the help of a shock tube they constructed eight columns along with ordinary concrete.

**Thomas et al. (2017)** studied the dynamic increase parameters for energy absorption, modulus of elasticity, ultimate tensile strength, other mechanical property and cracking strength. Data from existing research suggest that model use in this study underestimate tensile properties of UHPC from the strain rate sensitivity particularly on high strain rates. Developed models depends on available details are presented. The strain rate reactivity of the tensile strength of UHPC is homogeneous to that of intermediate strain rates and ordinary concrete at quasi-static. At high strain rates conventional concrete have less strain rate-sensitive than UHPC. The strain rate reactivity does not based on compressive strength fibre, fibre factor, fibre geometry and volume fraction, of UHPC of the structure stress concentration and damage in concrete and steel bars was observed. CFST improved the response of the structure though the collapse of the frame structure was not prevented.

## CONCLUSION

On the basis of the extensive literature survey it was found the blast loading has gained significance in the fields of reactor technology and military applications in past few decades. Many researches are being achieved on the blast analysis of various structures. UHPC, UHPFRC and other materials is taken to show their performances to resist the blast loadings. It is observed that UHPC succeeded in various manners to blast resistance. The major disadvantage of the experimental researches conducted currently is that there are no unifying criteria for the tests. Each researcher uses different standards for their experiments. If there are standard specifications for these blast tests, it would have been easier to compare the results obtained by various analyses. However, the intense research carried out on different concrete and concrete composites have indicated that the improved concrete composites have better blast resistance than conventional plain concrete.

## REFERENCE

- Carufel Sarah De, Dagenais Frederic, Melancon Christian and Aoude Hassan. "Effect of Design Parameters on the Blast Response of Ultra High-Performance Concrete Column" First International Interactive Symposium on UHPC – 2016.
- Kamal M.M, Safan M.A, Etman Z.A and Salama R.A. "Behavior and strength of beams cast with ultra-high strength concrete containing different types of fibers", HBRC Journal (2014) 10, pp 55, 63.
- Li Jun, Hao Hong, Wu Chengqing, "Numerical study of precast segmental column under blast loads" Elsevier @ Engineering Structures 102 (2015) pp 395–408
- Li Jun, Wu Chengqing, Hao Hong, "Investigation of ultra-high performance concrete (UHPC) and normal strength concrete (NSC) slab under contact explosion" Elsevier @ Engineering Structures 102 (2015) pp 395–408 <http://dx.doi.org/10.1016/j.engstruct.2015.08.032> 0141-0296/2015
- Mike P. Byfield, "Behaviour and design of commercial multi-storey buildings subjected to blast" Journal of Performance of Constructed Facilities © ASCE / November 2006 pp 324-329.
- Na Hyun Yi, Jay Kim Jang-Ho, Han Tong-Seok, Cho Yun-Gu, Lee Jang Hwa "Blast resistance characteristics of

ultra-high strength concrete and reactive powder concrete” Elsevier journal homepage: [www.elsevier.com/locate/conbuildmat](http://www.elsevier.com/locate/conbuildmat) Construction and Building Materials 28 (2012) pp 694–707

Ngo T, Mendis P, Gupta A. & Ramsay J. “Blast loading and blast effects on structures” EJSE Special Issue: Loading on Structures (2007) pp 76-79

Nystrom Ulrika, Gylltoft Kent, Numerical studies of the combined effects of blast and fragment loading. International Journal of Impact Engineering 36 (2009) pp 995–1005.

Quazi Kashif, Dr. Varma M.B “Effect of blast on G+4 RCC frame structure” International Journal of Emerging Technology and Advanced Engineering Website: [www.ijetae.com](http://www.ijetae.com) (ISSN 2250-2459, ISO 9001:2008 Certified Journal, Volume 4, Issue 11, November 2014)

Scheleyer G.K, Barnett S.J, Millard S.G. & Wight G., “Modelling the response of UHPFRC panels to explosive loading “WIT Transactions on The Built Environment, Vol 113, © 2010 WIT Press [www.witpress.com](http://www.witpress.com), ISSN pp 1743-3509 (on-line).

Shallan Osman, Eraky Atef, Sakr Tharwat, Emad Shimaa, “Response of building structures to blast effects” International Journal of Engineering and Innovative Technology (IJEIT) Volume 4, Issue 2, August 2014.

Thomas R.J. and Sorensen Andrew D., “Review of strain rate effects for UHPC in tension”, Construction and Building Materials (2017), pp. 1, 25, 26

Yanchao Shi Hao Hong, Li Zhong-Xian, “Numerical simulation to study the blast wave interaction with structure column”. 24 July 2007 © Springer-Verlag 2007



## Application of Encapsulated Carbonate Precipitating Bacteria For Self-Healing in Concrete

Mujahid Islam<sup>1</sup>, Rizwan A Khan<sup>2\*</sup>, Arbaz Hasan Khan<sup>1</sup> and, Iqbal K Khan<sup>3</sup>

<sup>1</sup>Post Graduate Student, Department of Civil Engineering, Z.H. College of Engg. & Tech., Aligarh Muslim University, Aligarh

<sup>2\*</sup> Associate Professor, Department of Civil Engineering, Z.H. College of Engg. & Tech., Aligarh Muslim University, Aligarh (Corresponding Author)

<sup>3</sup>Professor, Department of Civil Engineering, Z.H. College of Engg. & Tech., Aligarh Muslim University, Aligarh

### ABSTRACT

Formation of cracks in concrete decreases the service life of the structure. The Concrete strength as well as durability is also reduced by formation of cracks. It is therefore a need to develop the crack healing techniques to increase the service life of concrete structures. Addition of carbonate precipitating bacteria in concrete is very suitable and promising method for self healing of cracks. The bacterial spores of carbonate precipitating bacteria are either directly added in concrete or encapsulated and immobilized in different materials (hydrogels, silica gel, polyurethane, expanded perlite etc.). It has been reported that encapsulation of bacteria gives better results for self healing of cracks than bacteria directly added in concrete. This paper reviews the methods and materials used in the application of immobilizing and encapsulating the carbonate precipitating bacteria for self healing of cracks. Further, it also gives description of the different properties of concrete which vary with the materials used for immobilizing and encapsulating the bacterial spores.

**Keywords:** Self healing; MICP; Cracks; Bacterial Concrete; Encapsulation;

### INTRODUCTION

In today's modern world, concrete is widely used as a construction material. This is due to its unique characteristics of having high compressive strength, high durability, easily castable into desired shape, satisfactory fire resistance and most important is its inexpensiveness in comparison to other building construction materials. However major concern in concrete is its relatively low tensile strength which causes cracking in concrete [1,2]. These cracking reduces strength of concrete, causes hindrance to integrity of structure and durability of material and makes the concrete unsafe to adverse environmental conditions [3]. Cracks which are less than 0.2mm in concrete are filled by concrete itself. But the cracks which are more than 0.2mm then concrete fails to heal themselves. It is a well-known fact that these cracks provide an easy and simple path to different aggressive substance like sulphates, carbonates, chlorides etc. in concrete mix. These aggressive attacks causes corrosion of steel reinforcement and deterioration of concrete [4] which resulted in high maintenance cost. According to federal highway research, USA spends almost 4 billion dollars annually in terms of direct cost on maintenance of concrete highway bridges [5]. Whereas in UK about 45% of its annual construction cost is spent on maintenance of existing structures [6].

In order to enhance service life of concrete structures various strategies are used such as to retard crack propagation and bonding of cracks. This leads to increase in durability of concrete. But techniques like mixing of concrete with acrylic resins, silicon based polymers, epoxy resin contains materials that are incompatible with concrete and they are very expensive and mostly hazardous to environment [7]. Therefore, in present scenario it is urgent necessity to find a feasible way of crack healing methods which involve less cost and get rid of manual interference. Self-healing concrete (Fig. 1) or bio concrete is emerging as one of the feasible solution for controlling of cracks. Self healing concrete involves healing of crack by synthesis of mineral compounds through microbial activity. Self-healing through microbes involves precipitation of calcium carbonate in cracks by direct action of bacteria containing calcium compound such as calcium lactate [8]. This calcium carbonate precipitated by bacteria is compatible with concrete and during precipitation oxygen is consumed. Therefore, it reduces the chances of corrosion of reinforcement and increases its durability in reinforced concrete construction. The genus *Bacillus* (*B. subtilis*, *B. sphaericus*, *B. cohenii*, *B. pseudofirmus*, *B. haldurans*, *B. megaterium* etc) are mostly used in research purpose as bio agents for calcite precipitation due to its survival in high alkaline environment and capacity to form spores [8-10, 11-13]. Moreover these bacteria can lay in dormant stage upto 200 years. These spores get activated as soon as water is accessed in cracks and produces ample amount of crack filling  $\text{CaCO}_3$  based minerals through conversion of precursor organic compound (mostly calcium lactate) which are consciously added to the concrete mixture. When water comes in contact with unhydrated calcium in the concrete, then by the help of bacteria calcium hydroxide is produced. This calcium hydroxide reacts with atmospheric  $\text{CO}_2$  and forms limestone and

water. This consumption of water molecules drives chemical reaction in forward direction leading to production of limestone which seals the crack.

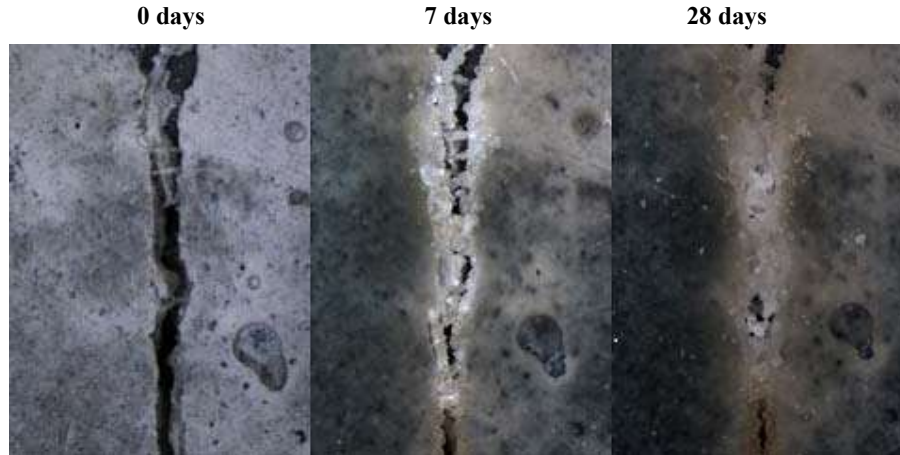
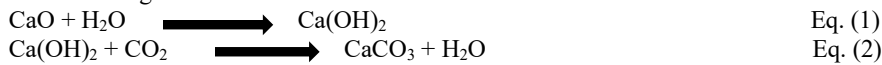


Fig.1.Self healing sample of concrete.

The following reaction is involved.



However it was observed that bacterial spores which are directly added to concrete matrix has very less viability and related activity approximately for two months. Hence productive self healing would be realised if bacteria survived for longer duration. This is achieved by encapsulating and immobilizing calcite precipitating bacteria using various encapsulation techniques. This review paper focus on evaluation of self healing of cracks by bacteriological action upon addition of carbonate precipitating bacteria to concrete after encapsulation and immobilization in different materials such as hydrogel, silica gel, polyurethane, and expanded perlite. Hydrogels are like hydrophilic gels that has network of long polymer chains and water is the dispersion medium [14]. In order to obtain good healing efficiency, sufficient water is essential for microbial activity. Hydrogel easily fulfils this task as they have higher water retaining capacity.

Silica gel has good mechanical, thermal and photochemical properties. They are basically colloidal dispersion of Silicic acid in water. Silica gel is good carrier for microorganisms like bacteria, yeast, algae. Silica gel immobilizes bacteria and protect them from harsh environment in the concrete. Polyurethane (PU) is widely used as waterproofing material. Immobilization of bacteria with PU is used as crack healing material [15]. Polyurethane shows higher healing capacity and lower permeability as compared to silica gel [16].

Perlite is used as a building material which is derived from volcanic rock. The volume of perlite gets expanded upto 4-20 times when subjected to heating above 870 °C and called as expanded perlite (EP) [17]. Immobilization of bacteria in EP shows considerable enhancement of crack healing. After 28 days it is seen that cracks are healed upto 0.79 mm when bacteria is immobilized in EP which is quite high.

These encapsulation methods, their preparation and their techniques of incorporation is discussed in this review. Apart from that their extent of crack healing and influence on compressive strength is also discussed in this paper review.

## ENCAPSULATION TECHNIQUES OF CARBONATE PRECIPITATING BACTERIA FOR SELF HEALING OF CONCRETE

### Encapsulation of bacteria in hydrogels

Hydrogels (Fig. 2) are deliquescent gels and have high capacity of absorbing water and it can retain large amount water in its structure without dissolving. The use of hydrogel for encapsulation of bacterial spores for self-healing provides three benefits. 1) During mixing and hydration stage bacterial spores are protected by hydrogels. 2) Hydrogel is used as water reservoir for spores germination and bacterial activity when cracking occurs. 3) The precipitated calcium carbonate can inhibit the re-opening of the cracks due to long exposure to dry environment. Bacteria used for encapsulation is *Bacillus sphaericus* LMG 22557. MBS medium [18] is used to cultivate *B. sphaericus* spores. The hydrogel used is synthesized based on commercial Pluronic® F-127 (Sigma Aldrich) is a

tri block copolymer and has a polymer chain of polyethylene oxide – polypropylene oxide – polyethylene oxide {(PEO)–(PPO)–(PEO)} units. Encapsulation process firstly includes mixing of a 20% weight by weight polymer solution (modified Pluronic® F-127) with bacterial spore suspension ( $10^9$  cells/ml) and bio reagents (yeast extract, urea etc) alongwith the initiator (Irga cure 2959) were mixed to the solution. The mixture is mixed for 5 minutes and then subjected to UV radiation for 1 hour resulting in formation of gel sheet. Dry powder is obtained from the hydrogel sheet by subjecting to force grinding and freeze drying.[19]. Thermogravimetric analysis (TGA) is used to show the formation of  $\text{CaCO}_3$  on hydrogels [20].

Mortar prism specimens ( $30\text{mm}\times 30\text{mm}\times 360\text{mm}$ ) with a reinforcement of ( $\phi = 6\text{mm}$  L= 660mm) in the centre are prepared. Multiple cracks are created in the prisms after 28 days by means of uniaxial tensile test. The cracked specimens are then subjected to the wet-dry cycle and crack healing efficiency is evaluated by microscope. It is observed that maximum crack width that is healed by hydrogel was about 0.5mm which is quite efficient. Water permeability is also decreased about 65%.

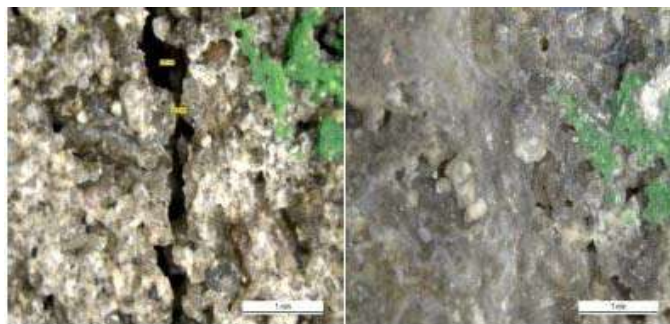


Fig.2 Healed crack (within 7d) in specimens with hydrogels.

### Encapsulation of bacteria into silica gel

Silica gels (Fig. 3) are colloidal dispersion of Silicic acid in water. Due to its stabilities in mechanical, thermal and photochemical properties, biological immobility and good matrix porosity for conveyance of molecules and ions, silica gel is used as a preferred carrier for microorganism [21, 22]. *Bacillus sphaericus* LMG 22557 is used as a bacterial strain for encapsulation. The concentration of bacterial cells are  $10^9$  cells/ml and is prepared according to Wang's method [16]. Silica gel is manufactured by using two raw materials, sodium silicate ( $\text{Na}_2\text{SiO}_3$ ) and mineral acid. These two are used in wet process to create a reaction generating monomeric silicic acid. These monomers upon polymerization generate primary silica particles called silica sol. These particles on further combination form a three dimensional structure in gel state called silica gel.

In order to mobilize bacteria into silica, gel two concentration of salt solutions are used. The salt solution with 8.5 g/l NaCl is used to resuspend centrifuged bacteria. Another salt solution with 60 g/l NaCl (represented as HS) is used to make silica sol become silica gel. Silica sol, bacterial suspension and HS are mixed together with volume ratio of 5:1:4. After two hours silica sol becomes gel and bacterial cells are thus merged inside gel. The incorporated bacteria along with culture medium and other agents are encapsulated in glass tube of length 40 mm and inner dia of 3 mm. Two set of glass tubes are taken. One is filled with bacterial suspension and silica-solution while other is filled with the deposition medium (DM) as described by Wang [16]. Both the glass tubes are glued together with their ends sealed by an adhesive (Schnellklebstoff X 60) (Fig.4). These glass tubes are embedded in mortar specimen during casting. Two kind of mortar specimens are cast. One is prismatic in shape with dimensions  $40\text{mm}\times 40\text{mm}\times 160\text{mm}$  for investigating strength regain. Other is cylindrical in shape ( $\phi = 80\text{ mm}$ , H = 22 mm) for measuring permeability of water. As soon as cracks develop, these glass tubes will break and healing agents are released in cracks. The silica gel combines with calcium ions from concrete matrix and calcium carbonate ( $\text{CaCO}_3$ ) precipitates into the crack there by healing the cracks. The cracks monitored by microscope and by thermogravimetric analysis it is found that around 25% by mass calcium carbonate is precipitated. Around 5% strength is regained and permeability of concrete is also decreased.

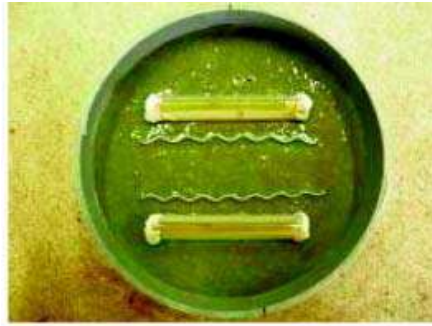


Fig.3.Specimens with glass tubes filled with silica sol as healing agent.

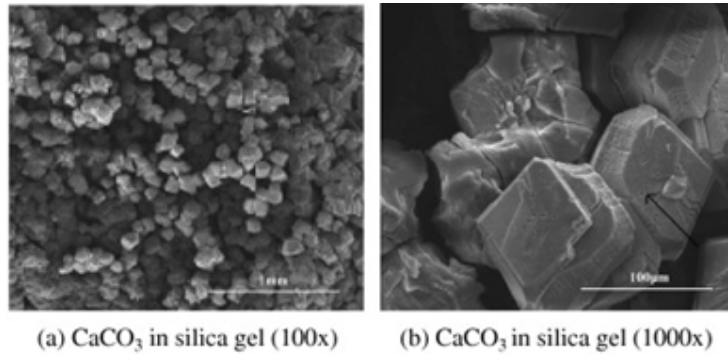


Fig. 4. Scanning electron microscopic images of CaCO<sub>3</sub> precipitation in silica gel.

#### Encapsulation of bacteria in polyurethane

Polyurethane (PU)(Fig.5) is extensively used as a water proofing material. Bacterial strain which is encapsulated in polyurethane is Bacillus sphaericus LMG 22557. The above strain has high urease deposition activity, long durability of bacteria and produces CaCO<sub>3</sub> in simple and manageable way. Bacillus Sphaericus is grown on medium consisting of urea and yeast extract. In order to encapsulate bacterial cell into polyurethane, a two component polyurethane ( MEYCO MP 355 1 K , BASF ) is used. Component A of PU (polyurethane prepolymer, PU A), component B of PU (accelerator, PU B) and bacterial suspension are mixed in the volume ratio of 5:0.5:1. After 15 minutes of mixing of all the three components, PU foam is formed and bacteria is embedded inside the foam. Bacteria are incorporated into mortar specimen through glass tubes of 40 mm length and 3mm of internal diameter. Three glass tubes are taken. One is filled with PU A. Second is filled with PU B together with deposition medium (DM) as described by Wang [16]. Third is filled with bacterial solution. All the three glass tubes are glued together and their ends were sealed by an adhesive (Schnellklebstoff X 60, HBM) (Fig.6). These glass tubes were embedded in mortar specimen during casting. Two kind of mortar specimens are cast. One is prismatic in shape with dimensions 40mm×40mm×160mm for investigating strength regain. Other is cylindrical in shape ( $\phi = 80$  mm, H = 22 mm) for measuring water permeability. As soon as cracks are developed these glass tubes will break and healing agents are released in cracks. The amount of calcium carbonate precipitated is measured by thermogravimetric analysis at different days interval. It is found that PU has more self healing capacity and lower permeability than silica gel. Strength regained is also much higher than silica gel.



Fig.5.Specimens with glass tubes filled with polyurethane as healing agent

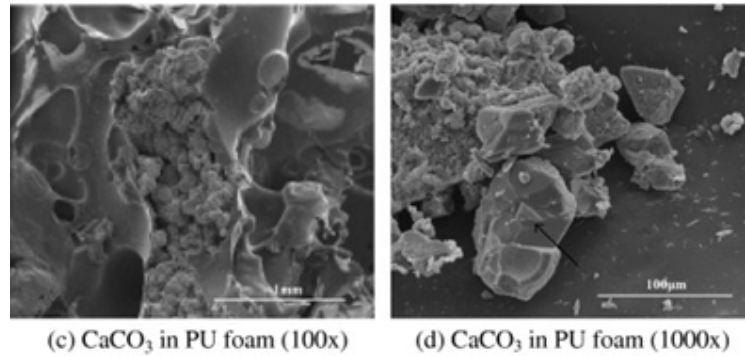


Fig. 6. Scanning electron microscopic images of CaCO<sub>3</sub> precipitation in silica gel.

### Encapsulation of bacteria in expanded perlite

Perlite (Fig.7) is a valuable and world wide used building material in construction industry. It is derived from volcanic rocks and are easily available in markets at very low cost. When subjected to heating above 870°C its volume gets expanded upto 4-20 times and called as expanded perlite. After above physical transformation, the expanded perlite (EP) displays splendid characteristics associated with higher porosity and higher water absorption. Therefore it is considered as an ideal bacterial immobilizing material. The bacteria which is immobilized in EP is alkaliphilic bacteria named *Bacillus cohnii*. The bacterial concentration is microscopically measured as  $3.6 \times 10^9$  cell/ml. In order to immobilize *Bacillus cohnii*, EP particles are first sprayed with the prepared bacterial suspension then they are dried in oven at 45°C for 2 days until a constant weight is achieved. A solution of calcium lactate (8 g/l) and yeast extract (1 g/l) is sprayed on the surface of particles and they are further oven dried at 45°C for 2 days. The particles are coated with geopolymer coating using a high pressure nozzle sprayer in order to reduce water absorption of EP particles. This coating also ensures that nutrients are not dissolved in water present in concrete mixtures. The coatings are prepared by mixing Metakaolin and Sodium silicate solution ( 15% by weight ) in the ratio of 1:1.

Prismatic concrete specimens are prepared with OPC, natural sand, coarse aggregate and calcium lactate with desired water cement ratio. The dimensions of prism that are casted is 15cm ×15cm ×30cm. After 3, 7, 14, 28 days of healing, all the specimens are removed from the water for microscopic inspection and crack width measurement. The maximum value for healed crack after 28 days is upto 0.79 mm. Microstructure analysis (Fig.8) of EP particle shows that the effective protection to bacteria during mixing of concrete is provided by geopolymer coating.

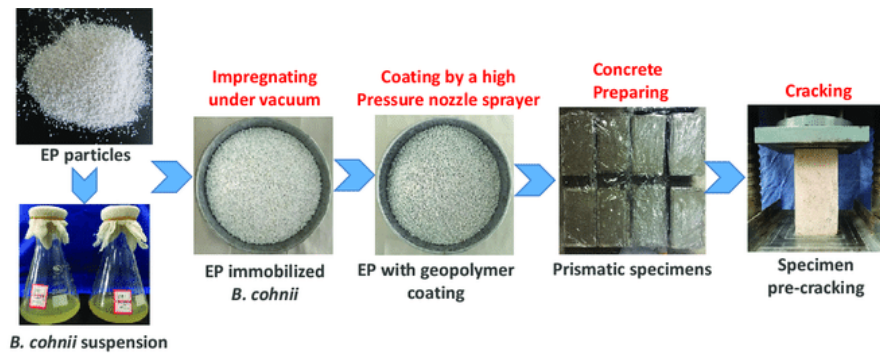


Fig.7. Steps for immobilization of *B. cohnii* spores in EP particles and experimental setup

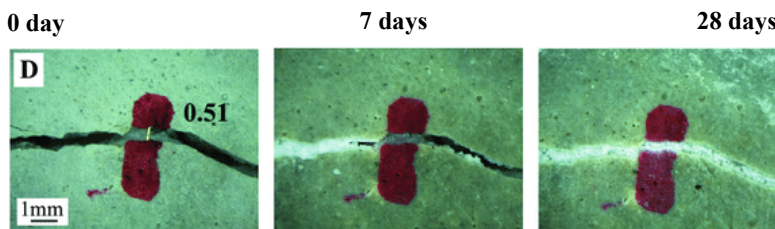


Fig. 8. Detailed Microscopic images of crack-healing processes in expanded perlite.

## CONCLUSIONS

In view of the considered properties, the traditional techniques to shield concrete from deterioration turns out to be a favorable property. Self-healing seems, by all accounts, to be a propitious method. The sort of bacterial culture and medium arrangement profoundly affected calcium carbonate crystal morphology. Metabolic exercises of some particular microbes in concrete are accountable to enhance general conduct of concrete. It has been theorized that all microscopic organisms are fit for  $\text{CaCO}_3$  generation since precipitation happens as a result of normal metabolic procedures, for example, photosynthesis, sulphate decrease, and hydrolysis of urea. Encapsulation of bacteria in hydrogels, silica gels, polyurethane and perlite shows around 40-70 % decrease in permeability as well as increase in strength due to precipitation of calcium in the range of 30-50 %. Higher bacteria content, lower incorporated amount and cost effectiveness makes them favourable bacteria carrier materials on large scale construction of concrete structures. In light of the examined properties like compressive strength, permeability, water ingestion, the self-healing approach using encapsulation seems to be a promising approach at this condition of improvement.

## References

- V. Wiktor, H.M. Jonkers, (2011). *Quantification of crack-healing in novel bacteriabased self-healing concrete* Cem. Concr. Compos. 33 (7) 763–770.
- W. Khaliq, M.B. Ehsan, (2016). *Crack healing in concrete using various bio influenced self-healing techniques*, Constr. Build. Mater. 102 349–357.
- H.M. Jonkers, E. Schlangen, (2007). *Crack repair by concrete-immobilized bacteria*, in: Proceedings of the First International Conference on Self Healing Materials, pp. 18–20.
- H.-W. Reinhardt, M. Jooss, (2003). *Permeability and self-healing of cracked concrete as a function of temperature and crack width*, Cem. Concr. Res 33 (7) (2003) 981-985.
- Federal Highway Administration, (2001). *Preventive Strategies in The United States, Report by CC Technologies Laboratories, Inc. to Federal Highway Administration (FHWA), Office of Infrastructure Research and Development. Report FHWA-RD-01-156.*
- M. De Rooij, K. Van Tittelboom, N. De Belie, (2011). *E. Schlangen, Self-healing phenomena in cement based materials*. Draft of State-of-the-Art report of RILEM Technical Committee.
- M.S. Vekariya, J. Pitroda, (2013). *Bacterial concrete: New Era for Construction Industry*, Int. J. Eng. Trend Technol. 4,4128–4137.
- H. Jonkers, (2011). *Bacteria-based self-healing concrete*, Heron 56 (1/2).
- J. Wang, H. Soens, W. Verstraete, N. De Belie, (2014). *Self-healing concrete by use of microencapsulated bacterial spores*, Cem. Concr. Res. 56, 139–152.
- J. Wang, K. Van Tittelboom, N. De Belie, W. Verstraete, (2012). *Use of silica gel or polyurethane immobilized bacteria for self-healing concrete*, Constr. Build. Mater. 26 (1) 532–540.
- H.M. Jonkers, A. Thijssen, G. Muyzer, O. Copuroglu, E. Schlangen, (2010). *Application of bacteria as self-healing agent for the development of sustainable concrete*, Ecol. Eng. 36 (2) 230–235.
- J. Wang, N. De Belie, W. Verstraete, (2012). *Diatomaceous earth as a protective vehicle for bacteria applied for self-healing concrete*, J. Ind. Microbiol. Biotechnol. 39 (4) 567–577.
- J. Wang, D. Snoeck, S. Van Vlierberghe, W. Verstraete, N. De Belie, (2014). *Application of hydrogel encapsulated carbonate precipitating bacteria for approaching a realistic self-healing in concrete*, Constr. Build. Mater. 68, 110–119.
- Zohuriaan-Mehr MJ, Kabiri K, (2008). *Superabsorbent polymer materials: a review*. Iran Polym J 17:451-77.
- Bang ss, Galinat JK, Ramakrishnan V, (2001). *Calcite precipitation induced by polyurethane-immobilized Bacillus pasteurii*. Enzyme Microb Technol 28:404-9.
- Jianyun Wang, Kim Van Tittelboom, Nele De Belie, Willy Verstraete, (2012). *Use of silica gel or polyurethane immobilized bacteria for self healing concrete* (26) 532-540.
- O. Sengul, S. Azizi, F. Karaosmanoglu, M.A. Tasmemir, (2011). *Effect of expanded perlite on the mechanical properties and thermal conductivity of lightweight concrete*, Energy Build. 43 (2) 671–676.
- Kalfon A, Larget-Thieri I, Charles JF, De Barjac H, (1983). *Growth, sporulation and larvicidal activity of Bacillus-sphaericus*. Eur J Appl Microbiol Biotechnol :18: 168-73.
- J.Y. Wang, S Van Vlierberghe, P Dubruel, W Verstraete, N De Belie, (2013). *Hydrogel encapsulated bacterial spores for self-healing concrete: Proof of concept*. ICSHM 606-9.
- Ivanov, V.M., et al. (2005). *Chromaticity characteristics of  $\text{NH}_2\text{Hg}_2\text{I}_3$  and  $\text{I}_2$ : Molecular iodine as a test form alternative to Nessler's reagent*, Journal of Analytical Chemistry, 60, 629-632.

- Soltmann U, Raff J, Selenska-Pobell S,(2003). *Biosorption of heavy metals by sol-gel immobilized Bacillus sphaericus cells, spores and s-layers*. J Sol-Gel Sci Technol 26:1209-12.
- Soltmann U, Bottcher H,(2008). *Utilization of sol-gel ceramics for the immobilization of living microorganisms* . J Sol-Gel Sci Technol;48:66-72.



## Distress Analysis of Jetty Structure Subjected to Dynamic Load – A Case Study

R. R. Gaikwad<sup>1</sup>, H. S. Chore<sup>2</sup> and S. A. Rasal<sup>3\*</sup>

<sup>1</sup>P. G. Student, Department of Civil Engineering, Datta Meghe College of Engineering, Sector-3, Airoli, Navi Mumbai - 400708, Email: rrgritu@gmail.com

<sup>2</sup>Associate Professor, Department of Civil Engineering, Dr. B. R. Ambedkar National Institute of Technology, Jalandhar - 144011, Email: chorehs@nitj.ac.in

<sup>3\*</sup> Assistant Professor, Dept. of Civil Engineering, Datta Meghe College of Engineering, Sector-3, Airoli, Navi Mumbai - 400708, Email: sarasal@rediffmail.com (Corresponding Author)

### ABSTRACT

The structural deterioration of jetty located in sea, depends upon various parameters such as exposure conditions, oceanographic conditions, salinity, ballast water contamination, wind velocity and its direction. Assessment of structural health of the jetty mainly corresponds to the corrosion of reinforcing steel embedded in the concrete. The present study is carried out to examine 27 years old existing jetty structure to ascertain its adequacy to withstand present service loading conditions including suggesting the remedial measures required if any. A comprehensive condition assessment of Jetty structure located at Jawaharlal Nehru Port Trust, Navi Mumbai (India) is carried out to understand the present status of the structure, assessment of residual service life; so that to suggest strengthening/rehabilitation scheme. Fissures and cervices in concrete cover cause ingress of saline environment in core concrete. To assess the distress and to understand the extent of deterioration caused to the concrete beams various tests were carried out. Sample size of 335 numbers of jetty beams considered for analysis. The Rebound hammer test, Ultrasonic pulse velocity test, compressive strength of core sample and various structural parameters used to calculate the structural strength and residual life. Non destructive test results segregated into three different types according to geometry and loading pattern of beams for statistical analysis. Statistical analysis showed highly significant difference in distress condition of crane beam and distress condition of secondary beam and main beam. No significant difference was observed between distress condition of main beam and secondary beam. It can be concluded that only Crane beams are subjected to huge dynamic load of moving crane used for loading and off-loading cargo. Hence distress in concrete was observed more in crane beam comparatively to other beams even though other parameters causing distress to all beams are constant.

**KEYWORDS:** jetty; oceanographic; crane beam; hammer test; Ultrasonic pulse velocity test; dynamic load.

### INTRODUCTION

Jetty is the interface between the land mode of transportation and waterways mode of transportation. The sea mode is very cheap mode compared to land mode for transporting huge quantity of material, raw material and passengers. There is various kind of jetties depending upon its location, material used for construction, purpose of it etc. The jetties constructed in river, river mouth and in sea are various location-based types. Jetties along with other infrastructure like breakwater, channel, ship anchorages, navigation aids, landside facilities including material handling equipment together form the Port. The tranquil waters in harbors facilitate safe berthing of ships/vessels at jetties where goods can be handled. At passenger jetties passenger can board the ship or can come on land from the ship safely. The jetties are constructed using Reinforced Concrete structures now days. Historically jetties were being constructed using wooden piles and wooden platforms, masonry structures, steel etc. There needs to be deeper waters near jetties to facilitate deeper draft vessel to come along and get berthed at jetty. These deeper portions are either channel or for taking advantage of tidal variation special berth pockets are provided near jetty for this purpose. While studying the existing jetty structure it is very much necessary to understand that the same structure has various degree of deterioration and the deterioration patterns also changes within the same structure. This happens because various parts of the structure have different exposure conditions, depending upon which the jetty structure can be bifurcated in different zones as Fig. 1.

While designing, constructing and maintaining the marine structures serviceability is one of the major aspect needs attention.

Serviceability Requirements:

- The marine environment is the most hostile environment under which the jetty structure has to serve.
- The structure is directly in contact with sea water which contains lot of corrosive agents and salinity.

- Surrounding air is saline, this causes the salt fumes getting sprayed on structure. With very strong sea breezes the same is impregnated in the concrete surface.
- Part of structure is in the intertidal zones: It leads to intermittent wetting and drying of the concrete surface which leads to deterioration of the concrete and steel very fast.
- Un-serviceability of jetty structures for example JNPT jetty' structure shall lead to loss of approx. Rs. 3 to 3.5 Crores per day. The economic cost to the nation shall more than Rs. 40 Crores per day.

Thus the port's structures needs exhaustive structural maintenance plan which needs to be followed scrupulously. The purpose of this study is to analyze this 27 years old existing jetty structure to ascertain its adequacy to withstand present service/loading conditions including suggesting the remedial measures required if any. However, design of these remedial measures would not be scope of this study.

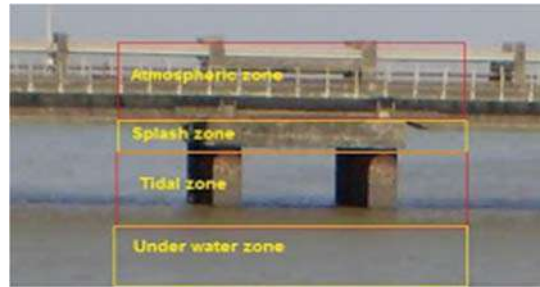


Fig. 1. Various Zones of Exposure of Jetty Structure

### STRUCTURES DETAILS

Jetty structure comprises of deck slab supported with grids of beams and piles, with fenders and bollard system including fender/breasting piles. The Jetty structure located at Jawaharlal Nehru Port Trust, Navi Mumbai has the following details:

#### Dimensions

Jetty size	:	685 m × 40.5 m
Slab Thickness	:	400 mm
Main Cross Beams	:	1600 mm × 1925 mm
Crane Beams	:	1000 mm × 1725 mm
Secondary Beams	:	750 mm × 1000 mm
Deck Slab Top	:	(+) 7.10 m RL (with respect to chart datum)
Sea bed level	:	(General – 13.0 m)
Rock encountered at	:	(-) 20 m
Founding Level of Piles	:	(-) 24 m

#### Grid of piles

The grid of piles is shown in Table 1. In horizontal X direction @6.4m c/c 06 Nos + @ 3.2m c/c 02 No.+ @ 6.4m/c/c 100 Nos, Z direction (In Plan perpendicular X direction). The grid, distance and details of pile diameter is shown in Table 1.

Table 1.Details of grid of piles

Grid		Distance	Pile Diameter
<b>Fender pile</b>			
Za	@	0.000 m	1000
<b>Crane Beam Pile</b>			
Z	@	3.750 m	1200
Y	@	7.000 m	1000
X	@	7.000 m	1000
<b>Crane Beam Pile</b>			
W	@	6.000 m	1200
V	@	7.000 m	1000
U	@	7.000 m	1000

### Grid of Beams

The details of the grid of beams are shown in Fig 2.

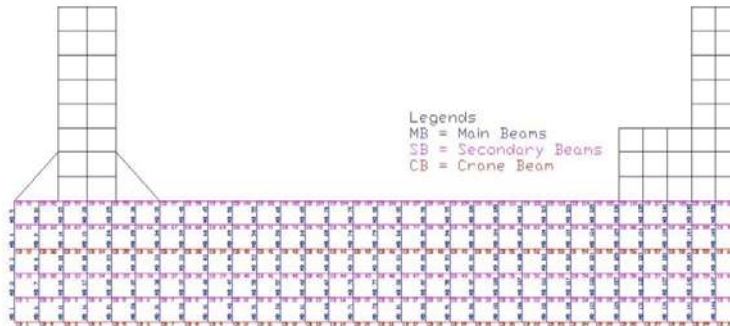


Fig. 2. Location and layout of Beams.

### LOADS ACTING ON THE JETTY STRUCTURE

#### Loads from Sea side

The loads from the sea side include the horizontal forces imparted by waves, by berthing and by vessel's pull on bollard/ mooring hooks. The velocity and angle of approach of the vessels determines the forces caused by berthing of vessels. The wind forces acting on the vessel body causes pushing/pulling of vessel which ultimately transferred to structure in form of bollard pull or fender push.

#### Landside Loads

Horizontal loads are caused from land side due to the earth pressures and differential water pressure which are not applicable in the present structure being the Jetty.

#### Loads coming from Deck

The important loads from the deck are the vertical loads caused by self weight of the deck superimposed loads from handling equipment. Horizontal loads are mostly due to wind forces on structures & cranes, and also due to the breaking force of cranes when break is applied. Also when cranes are parked using pins the strong wind force acting on crane imposes horizontal load on the rail thereby on jetty. But most vulnerable force act on jetty structure is when the crane is not moving but handling the containers. Various loads acting on jetty structure are shown schematically in Fig.3.

#### Dead Load

The dead load of the Berthing structure is due to the self weight of the structural members which includes slabs, beams, pile caps, piles, fender block, and retaining wall etc. for calculating this load physical dimension of the members are taken and then the load is calculated.

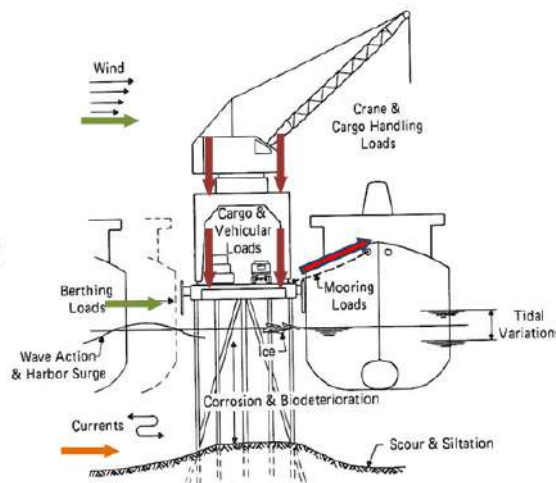


Fig. 3. Various loads acting on jetty structure are shown schematically in above figure

### ***Live Load***

The load of surcharges because of the stored and stacked cargo/material, such as general cargo, bulk cargo, containers and loads from vehicular traffic of all types, which includes trucks, trailers, railway, cranes, containers handling equipment and construction plant constitute vertical live loads. This is Container Jetty; railway load is absent in this case.

### ***Vessel Loads***

The present jetty is designed for 50,000 DWT container vessel.

### ***Mooring Forces***

The mooring loads are the lateral loads caused by the mooring lines when they pull the ship into or along the dock or hold it against the forces of wind or current. The load on any individual rope due to winds or currents acting on the ship or to checking the way of ship during berthing cannot be calculated with any accuracy. It depends on the tension in the rope and its angle to the berthing line. Thus mooring force will be two types

1. *Mooring Loads Due to Wind Forces:*
2. *Mooring Loads Due To Current Forces:*

### ***Forces due to Wind***

Wind force on structure shall be taken in accordance with IS: 875– 1987 as applicable. Wind force will act above the Sea water level.

After calculating for our site condition wind force acting over deck slab & piles are calculated & the maximum values obtained are 0.54 kN/m on deck slab & 0.32 kN/m on piles for normal wind speed while 4.07 kN/m on deck slab & 2.44 kN/m on piles for extreme wind speed. It is applied in both X and Z direction.

## **SITE INSPECTION AND NON DESTRUCTIVE TESTING**

### ***Site Inspection***

The site of the Port Civil (Marine) Infrastructure of JNPT was visited during August 12 & 26, 2016 and October 21-22, 2016 to assess their current structural health and stability. The structures are RCC Deck supported on piles in sea environment. The Non-destructive tests (NDT) of the sample RCC elements of the structures were carried out on all the above days. The locations of RCC elements were identified and surface preparations were carried out, prior to NDT.

Based on the inspections, the NDT selected for assessment of strength of RCC members include the Ultrasonic Pulse Velocity Test (UPVT), Rebound Hammer Test, Half Cell Potentiometer Test, and Concrete Core Compression Test. The marking of structural members were carried out based on the structure's plan and the locations of the structural members. The details of the tests and their guiding principle are summarized below.

### ***Rebound Hammer Test***

Rebound hammer test is done to find out the likely compressive strength of concrete by using rebound hammer as per IS 13311 (Part 2): 1992. The underlying principle of the rebound hammer test is "the rebound of an elastic mass depends on the hardness of the surface against which its mass strikes". When the plunger of the rebound hammer is pressed against the surface of the concrete, the spring-controlled mass rebounds and the extent of such a rebound depends upon the surface hardness of the concrete. The surface hardness and therefore, the rebound are taken to be related to the compressive strength of the concrete. The rebound value is read from a graduated scale and is designated as the rebound number or rebound index. The compressive strength can be read directly from the graph provided on the body of the hammer.

### ***Ultrasonic Pulse Velocity Test (UPVT)***

This test helps in assessing the quality of concrete. The time of travel for an ultrasonic pulse through a given path length of concrete is measured. For this purpose two probes (transducers) are used one transmitting and the other receiving. Thus,

$$\text{Ultrasonic Pulse Velocity (UPV)} = \text{Path Length} / \text{travel time}$$

It is best to have the two probes on opposite faces of concrete members. Thus, the signal passes through the entire thickness of the member. This is the direct (D) method of test and the same was used for the investigations of the RCC elements. On the other hand, when only one face of the structural element is available the two probes are kept on the same inspected face. This is the indirect (ID) method and the same was used when both sides of the RCC member was not accessible. As per the IS 13311 (Part 1): 1992, the measured indirect velocity can be lower than the direct velocity on the same concrete element. This difference may vary from 5 to 20 percent depending

largely on the quality of the concrete under test. Thus, the measured indirect velocity obtained from equation (1) is increased at least by 20 percent in the results reported. The UPV depends on the quality of concrete and is affected by all its ingredients. The IS 13311 (part 1):1992 uses only qualitative interpretation as given in Table 2.

**Table 2. Concrete Quality Grading Based on Ultrasonic Pulse Velocity as per IS 13311 (part 1):1992**

Range of Pulse Velocity	Concrete Quality
“V” Greater than 4.50 km/sec.	Excellent Quality
“V” In the range of 3.50 to 4.50 km/sec.	Good
“V” In the range of 3.00 to 3.50 km/sec.	Medium
“V” Less than 3.00 km/sec.	Doubtful

**Half-Cell Potentiometer Test**

The instrument measures the potential and the electrical resistance between the reinforcement and the surface to evaluate the corrosion activity as well as the actual condition of the cover layer during testing. The electrical activity of the steel reinforcement and the concrete leads them to be considered as one half of weak battery cell with the steel acting as one electrode and the concrete as the electrolyte. The name half-cell surveying derives from the fact that the one half of the battery cell is considered to be the steel reinforcing bar and the surrounding concrete.

The electrical potential of a point on the surface of steel reinforcing bar can be measured comparing its potential with that of copper – copper sulphate reference electrode on the surface. Practically, this is achieved by connecting a wire from one terminal of a voltmeter to the reinforcement and another wire to the copper sulphate reference electrode. This method may be used to indicate the corrosion activity associated with steel embedded in concrete and can be applied to members regardless of their size or the depth of concrete cover. It should be clearly noted that the test does not give actual corrosion rate or whether corrosion activity has already started, but it indicates the probability of the corrosion activity depending upon the actual surrounding conditions

The risk of corrosion is evaluated by means of the potential gradient obtained, the higher the gradient, and the higher risk of corrosion. The test results can be interpreted based on the following Tables 3 - 12.

**Table 3. Interpretation of Test Result (Half-Cell Potentiometer Test)**

Half – cell potential ( mV) relative to Cu-Cu sulphate Ref. electrode	% chance of corrosion activity
Less than - 200	10%
Between – 200 to – 350	50% (uncertain)
Above – 350	90%

**Table 4. Compressive Strength (N/mm<sup>2</sup>) of concrete cores taken from different structural member of the Main Beams**

Sr. No.	Location Main Beams	Length in mm	Diameter in mm	L/d	Weight in kg	Correction factor	Load in kN	Cylinder Compressive Stress in N/mm <sup>2</sup>	After Applying Correction Factor Cylinder Stress Value in N/mm <sup>2</sup>
1	SB 68	130	75	1.73	1.464	0.971	142	32.15	31.21
2	MB 83	120	75	1.6	1.364	0.956	151	34.19	32.69
3	CB 29	94	75	1.25	1.048	0.917	136	30.79	28.24



**Fig. 4. Concrete core drilling operation progress 3on beam**

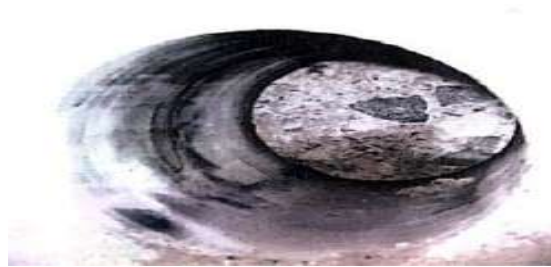


**Fig. 5. After taken of concrete core specimen from the drilled portion seen in the beam**



**Fig. 6 Collected undressed concrete core specimen before for dressing**



**Fig. 7 After dressing the concrete core specimen kept in the compressive testing machine for compression test**

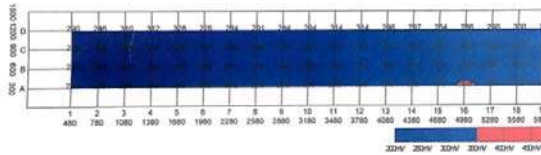


**Fig. 8 MB 141 (North Face)**

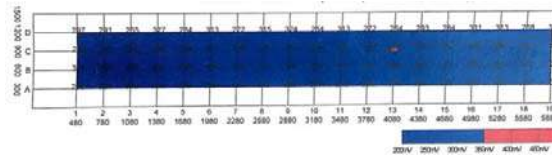


**Fig. 9 MB 141 (North Face)**

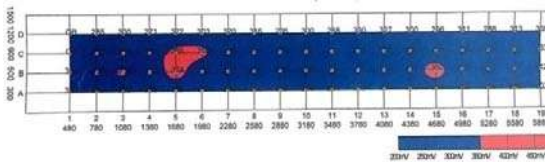


**Fig.10 MB 149 (North Face)**

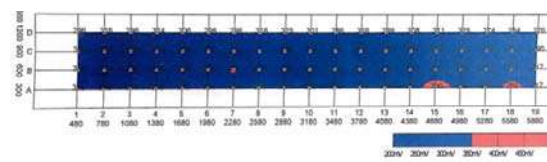


**Fig. 11 MB 149 (North Face)**

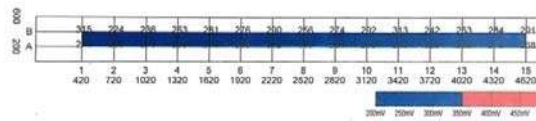


**Fig. 12 SB 29 (East Face)**

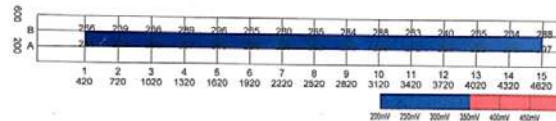


**Fig. 13 SB 29 (West Face)**

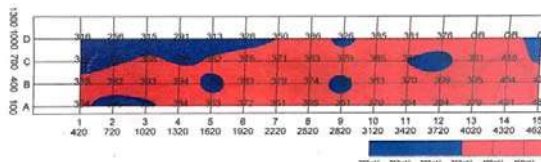


**Fig. 14 CB29 (East Face)**

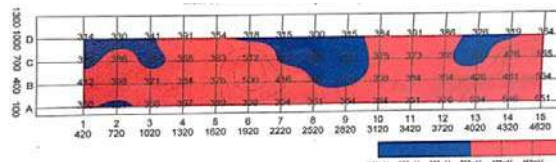


**Fig. 15 CB 29 (West Face)**

**Table 5 Ultrasonic Pulse Velocity Results**

ONEWAY						
	N	Mean	Std. Deviation	Std. Error	Minimum	Maximum
1 Main Beam	45	107.342	8.9405	1.3328	94.7	127.1
2 Secondary Beam	30	112.167	9.5688	1.7470	95.0	128.0
3 Crane Beam	15	122.680	9.8410	2.5409	110.3	135.4
Total	90	111.507	10.7025	1.1281	94.7	135.4
1 Main Beam	45	3.5767	0.29260	0.43620	2.93	4.00
2 Secondary Beam	30	3.4187	0.31265	0.05708	2.90	3.98
3 Crane Beam	15	3.0760	0.32006	0.08264	2.66	3.48
Total	90	3.4406	0.34960	0.03685	2.66	4.00

**Table 6 Statistical Analysis of Ultrasonic Pulse Velocity Tests-Anova**

ANOVA					
		Df	Mean Square	F	Sig.
UPV Time	Between Groups	2	1333.068	15.406	0.000
UPV Avg. Velocity	Between Groups	2	1.421	15.382	0.000

**Table 7 Statistical Analysis of Ultrasonic Pulse Velocity Tests-Post Hoc Test**

Post Hoc Test						
	Beam	Beam	Mean Difference	Std. Error	Sig.	Correlation
UPV Time	Main Beam	Crane Beam	15.3378	2.7734	0.000	Highly Significant
	Secondary Beam	Crane Beam	10.5133	2.9416	0.001	Highly Significant
	Main Beam	Secondary Beam	-4.8244	2.1925	0.006	Not Significant
UPV Avg. Velocity	Main Beam	Crane Beam	-0.50067	0.09061	0.000	Highly Significant
	Secondary Beam	Crane Beam	-0.34267	0.09611	0.001	Highly Significant
	Main Beam	Secondary Beam	0.158	0.07163	0.006	Not Significant

**Table 8 Statistical Analysis of Rebound Hammer Tests**

ONEWAY							
		N	Mean	Std. Deviation	Std. Error	Minimum	Maximum
RHT Comp. Strength	1 Main Beam	45	30.24936	2.154562	0.321183	26.340	34.560
	2 Secondary Beam	30	30.43004	1.881776	0.343564	27.780	34.560
	3 Crane Beam	15	25.95840	2.119745	0.547316	21.600	28.680
	Total	90	29.59443	2.614591	0.275602	21.600	34.560

**Table 9 Statistical Analysis of Rebound Hammer Tests-Anova**

ANOVA					
		Df	Mean Square	F	Sig.
RHT Comp. Strength	Between Groups	2	119.28	28.058	0.000

**Table 10 Statistical Analysis of Rebound Hammer Tests- Post Hoc Test**

Post Hoc Test						
	Beam	Beam	Mean Difference	Std. Error	Sig.	Corelation
RHT Comp. Strength	Main Beam	Cran Beam	-4.29096	0.614721	0.000	Highly Significant
	Secondary Beam	Cran Beam	-4.47164	0.65201	0.000	Highly Significant
	Main Beam	Secondary Beam	-0.18068	0.48598	0.711	Not Significant

**Table 11 velocity Comparison in Ultrasonic Pulse Velocity Test and its Cross Tabulation**

MEAN_VELOCITY VsMEAN_SGRP Crosstabulation						
			R.SGRP			Total
			1 Main Beam	2 Secondary Beam	3 Crane Beam	
MEAN_VELOCITY	1 Doubtful	Count	3	4	8	15
		% within R.SGRP	6.7%	13.3%	53.3%	16.7%
	2 Medium	Count	14	18	7	39
		% within R.SGRP	31.1%	60.0%	46.7%	43.3%
	3 Good	Count	28	8	0	36
		% within R.SGRP	62.2%	26.7%	0.0%	40.0%
Total		Count		45	30	15
		% within R.SGRP		100.0%	100.0%	100.0%

**Table 12 Chi- Square Test**

Chi-Square Tests			
	Value	df	Asymp. Sig. (2-sided)
Pearson Chi-Square	31.402	4	.000
Likelihood Ratio	33.057	4	.000
Linear-by-Linear Association	3.282	1	.070
N of Valid Cases	90		

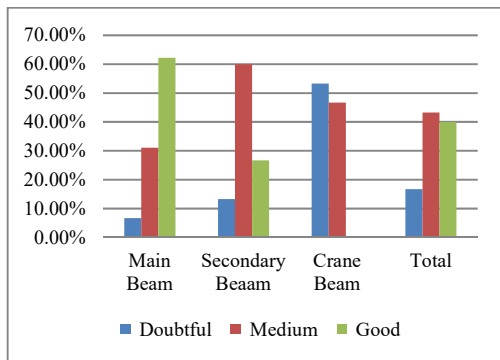


**Fig. 16 Beam Wise Comparison of UPV Results**

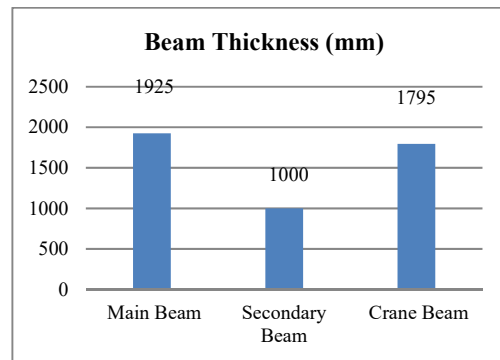


**Fig. 17 Comparison of Beam Thickness**

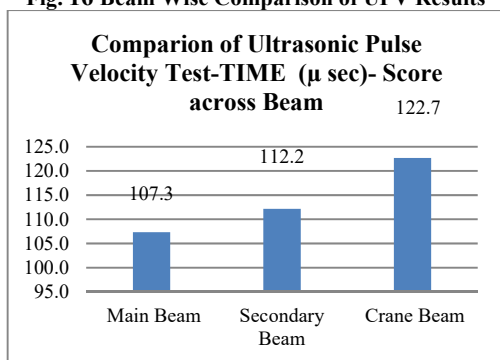


**Fig. 18 UPV Scores Across the Beams-Time Specific**

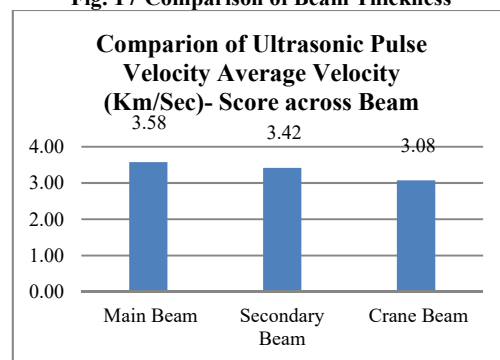


**Fig. 19 UPV Scores Across the Beams-Avg. Velocity Specific**

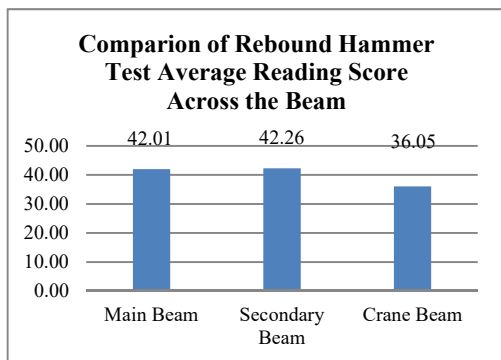


Fig. 20 Rebound Hammer Test Readings Across the Beams

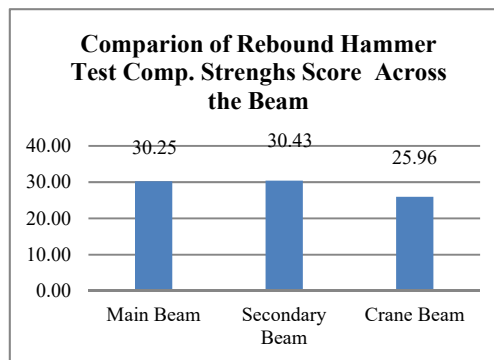


Fig. 21 Rebound Hammer Test Compressive Strength Across the Beams.

### Observations

The 27 year old jetty structure located as Jawaharlal Nehru Port Trust was studied visually and after careful inspections of structure and its drawings, number of beams was identified and categorized depending upon its structural utility. After visual inspection of the beams sample size was decided accordingly the test plan was devised. To ascertain the compressive strength of the concrete Ultrasonic Pulse Velocity tests and Rebound Hammer tests were conducted on 45 nos of Main Beams, 30 nos of Secondary Beams and 15 nos of Crane Beams, thus total sample size of 90 Nos of Beams. On perusal of these results, identified distress beams were tested for the Half Cell Potentiometer test. The both side facias of the beams were mapped for potential difference to ascertain the probability of corrosion. The concrete core samples were taken and the compressive test was conducted.

The statistical analysis and comparison of the results obtained from various Non Destructive Tests were carried out, Figs. 4-21. The SPSS Software was used and Anova and Post Hoc Tests were used for drawing conclusions.

To rule out size specific variance in the tests result the category wise comparison of the thickness of the beams is also done. On perusal of the statistical results it can be concluded that the concrete quality of the main beams and secondary beams are ranging from good to medium. The concrete quality of the crane beams is comparatively doubtful to medium. The travel time of the Ultrasonic waves is significantly hinger in crane beams that the main beams and secondary beams. The rebound hammer test revels that the compressive strength of concrete of Crane Beams is comparatively lower than that of main beams and secondary beams. The Half Cell Potential tests conducted indicated that the contours of potential difference on faces of the crane beams are higher than that of the faces of the main beams and secondary beams.

### CONCLUSION

From the above illustration it is concluded that the concrete of the Jetty Structure located in the sea deteriorated due to the ingress of elements causing corrosion present in marine environment and varied loading conditions. Through services and fissures in the cover concrete of the beams salt and salt fumes ingresses in the structure deteriorating concrete quality. Similarly the travel of 'element causing corrosion' till reinforcing steel induced potential difference thus the vulnerability of corrosion increased. The cover of the crane beam needs to be enhanced while designing the new jetty structures.

### REFERENCES

- Odd e. Gjorv (1969), "Durability of reinforced concrete wharves in Norwegian Harbours" *Proceedings of Conference Materiaux et Constructions*, volume 2, no.12, pp. 467-476.
- P Castro et. al. (2001) "Interpretation of chloride profiles from concrete exposed to tropical marine environments" *Journal of Cement and Concrete Research*, 31, pp. 529-537.
- P.S. Sengupta, (2009), "Special consideration in marine pile design and construction", *Indian Geodetic Society, conference at Guntur India*, pp. 709-711.
- P.Faulkner, P.Cutter and A.Owens, (2011), "Structural health monitoring system in difficult environments-

- Offshore wind turbines”, *6<sup>th</sup> European Workshop on Structural Health Monitoring- Fr.2.A.3*, pp.1-7.
- Chenna Rajaram, Pradeep Kumar Ramancharla, (2014), “Vulnerability assessment of coastal structure: A study on port buildings”, *International Journal of Education and Applied Research (IJEAR)*, volume.4, issue Spl-2, pp. 8-15.
- R.B. Singh, (2010), “Popular non-destructive testing of concrete structure-review of std. methods”, *National Seminar on Green Structures for Sustainability*, pp. 1-7.
- P.K. Satheesh Babu, A. Mathiazhagan, and C.G. Nandakumar, (2014), “Corrosion health monitoring system for steel ship structure”, *Journal of Environmental Science and Development*, Vol.5, pp. 491-495.



## Effect on Strength Parameters of Concrete on Partial Replacement of Cement by Sugarcane Bagasse Ash

Kaisir Ahmad Bhat<sup>1</sup>, Sadam Hussain shah<sup>2</sup>, Gurbir Kaur Jawanda<sup>3\*</sup>

<sup>1,2</sup> M.tech Student, Department of Civil Engineering, GNDEC Ludhiana, 141006, [kaisirbhat@gmail.com](mailto:kaisirbhat@gmail.com)

<sup>3\*</sup> Assistant Professor, Department of Civil Engineering, GNDEC Ludhiana, 141006 (Corresponding Author)

### ABSTRACT

Cement is most widely used product in construction industry and numerous studies have revealed the hazardous effects of cement on our environment. During manufacturing of cement emission of hazardous gases like CO<sub>2</sub> and dust with heavy metals that are highly poisonous in nature even in small quantities like Thallium, Cadmium, mercury takes place. The study aims at incorporating a secondary binder in concrete that shall suffice the rising demand of cement in construction industry and provide an eco-friendly alternative of cement. In this work, sugarcane bagasse ash (SCBA) is used as a binding material in concrete which is a waste material that facilitates to the waste regulation as well. SCBA is obtained after the sugarcane bagasse residue is burnt under uncontrolled conditions for generation of electricity in boilers. In this work, M25 design mix has been used with cement being partially replaced by sugarcane bagasse ash and varied as (0%, 3%, 6%, 9% and 12%) by weight of cement. Properties of hardened concrete were evaluated which involved in conduction of various tests like test for compressive strength at the age of 7 and 28 days, Flexural strength, Split tensile strength, Water absorption, Abrasion resistance and Water permeability test at the age of 28 days.

**KEYWORDS:** Sugarcane Bagasse Ash; Durability Tests; Mechanical tests; Fresh and hardened concrete;

### INTRODUCTION

Concrete is a mixture of cement, water, coarse aggregates, fine aggregates and admixtures. Cement is a binding agent between the components of concrete. Due to rising demand of cement and its harmful effects on environment lot of research studies have been carried out to find out its alternative. In a progressing country like India where construction is executed at very high rate since last 40 years, it is necessary to find an optimal solution for replacement of cement thus making it economically viable and environmentally safe. Sugarcane is the crucial crop in world which is used in sugar mills for the extraction of sugar, juice and jaggery. The remnant that remains after using sugarcane is utilized to form sugarcane bagasse. Sugarcane bagasse is used in sugar industries as fuel to generate the heat for boilers which in turn generates electricity. China has largest production of sugarcane that is more than 1500 million tons/year and India stands at second number with 300 million tons/year. Sugarcane bagasse ash is obtained after the sugarcane bagasse residue is burnt under uncontrolled conditions for generation of electricity in boilers. Sugarcane bagasse ash mainly has the constituents like Si, Al and Ca. From the past few years, sugarcane bagasse ash has been the topic of research for Pozzalone activity. Bangar Sayal S.(2017) used SCBA as a binding material in concrete. It has also been analyzed for workability, slump, compaction factor, compressive strength etc, in concrete. M. Sachin Raj et al.(2017), Ankur Anand et al. (2016) analysed the partly substituting the cement in concrete with bagasse ash and coir fibre. Sugarcane bagasse ash substituted in ratio of 0%, 5%, 10% and 20% and coir fibre was used 2% in concrete by the weight of cement. It inferred the results shows that after experimental study, the sugarcane bagasse ash and coir fibres gives the maximum strength as compared to normal concrete and SCBA gives the maximum strength at use of 15% and coir fibre is constant. The SCBA and CF both are increases the strength of concrete and decrease the density of concrete with increases the SCBA. K Sampath Kumar et al(2016), substituted opc with SCBA, rice husk ash and stone dust in concrete. For enhancing the workability of newly prepared concrete the cement is substituted in the ratio of 0%, 2%, 4%, 6%, 8% and 10% in concrete and slump value of concrete is recorded. The results reveal that the workability of concrete increases when its workability compared to concrete which made without admixtures. The compressive and split tensile strength tests have been performed on fresh and hardened concrete. The replacement of cement 6% gives similar compressive and tensile strength values as that of conventional concrete. The main purpose of this research is to work out the strength of sugarcane bagasse ash as a partly substitution with cement in concrete. Yashwanth. M. K(2014) Cement is a replacement material in concrete and sugarcane bagasse ash is used as a pozzalonic material in concrete. In this research, the determination of different parameters with different fractions of sugarcane bagasse ash is carried out. The parameters studied are as Compressive Strength, Split Tensile Strength, Flexural Strength, Water absorption, Abrasion Resistance Test and Water Permeability.

## Materials Used

Cement, fine aggregates, coarse aggregates, Sugarcane bagasse ash and water used in this study.

### Cement

In this current study, OPC of 53 grade is used for this research. Mostly, in total production OPC is used for 80 - 90 percent. It was fresh and free from lumps. The different parameter test of cement were conducted like consistency tests, Setting tests, fineness test, soundness tests etc. as per procedure arranged as per IS code 12269 - 2013 and properties of cement given in **Table1**.

**Table 1** Physical properties of cement

S No.	Physical Properties	Results Obtained
1	Normal Consistency	35%
2	Initial setting time	125 min.
3	Final setting time	270 min
4	Specific gravity	2.85

### Fine Aggregates

The sand was tested as per IS code 383-1970. the fine aggregates were free from the impurities like clay, organic matter and silt. The fine aggregates (sand) were also investigated for void ratio, as void ratio effects the water content for mixing, higher the void content higher will be the requirement of water and vice -versa. Various tests were conducted on sand as per the specification of IS code 2386 (Part I) – 1963(R2016) for determination of its physical properties gradation, fineness modulus and specific gravity.

### Coarse Aggregates

The crushed gravel aggregates were used in this study. Maximum nominal size was 20mm and 10mm that was used in this experimental study. Tests were conducted as per Indian Standard codes in this study. The physical properties of coarse aggregates are specified as per IS code 383-1970. IS codes are preferred for tests of coarse aggregates. The tests conducted were fineness modulus, specific gravity, soundness and water adsorption on coarse aggregates.

### Sugarcane Bagasse Ash

In this study, the sugarcane bagasse ash was collected from " The Budhewal Co Operative Sugar Mills Limited" in Ludhiana. The sugarcane bagasse ash contained unburnt, burnt and half burnt particles which was burnt in mills. sieving and grinding was done for removal of unwanted particles thus made suitable for use in concrete. In this present study, the sugarcane bagasse ash is used to substitute cement with different fractions as 0%, 3%, 6%, 9%, 12%. **Figure 1** depicts the pictorial view of sugarcane bagasse and sugarcane bagasse ash. **Table 2** and **Table 3** is the representation of SCBA.



**Figure. 1** Sugarcane Bagasse and Sugarcane Bagasse

**Table 2** Physical properties of Sugarcane Bagasse Ash (SCBA)

S No.	Property	Test Results
1	Density	572kg/m <sup>3</sup>
2	Specific gravity	2.15
3	Particle shape	spherical

**Table 3** Chemical properties of Sugarcane Bagasse Ash (SCBA)

S No.	Component	Mass %
1	SiO <sub>2</sub>	78.34
2	Al <sub>2</sub>	8.55
3	Fe <sub>2</sub> O	3.61
4	CaO	2.15
5	Na <sub>2</sub> O	0.12
6	K <sub>2</sub> O	3.46
7	MaO	0.13
8	TiO <sub>2</sub>	0.50
9	BaO	<0.16
10	P <sub>2</sub> O <sub>5</sub>	1.07

### Experimental Programme

Experimental work is executed in two step approach as per standard method. In first step physical properties, chemical composition of sugarcane bagasse ash and characterization of bagasse ash including initial setting time, final setting time of cement are studied. In second step, casted concrete specimen are studied, which involves tests on compressive strength, split tensile strength, water absorption, sorptivity, permeability and abrasion resistance. In order to attain the aim of the present work, the procedure follows as mixing, casting, curing and testing. Different factors effect the mixing of concrete. Mixed design of concrete is prepared as per IS code specification. First of all, sand, aggregates and cement were mixed in a mixer. After, mixing of these materials water was added and those materials were used which are replaced by cement in concrete. **Figure 2** and **Figure 3** represent the mixer and freshly prepared concrete.

### Mix design procedure for concrete

In this research, various strength parameters viz, compressive strength, split tensile strength, flexural strength, water adsorption, abrasion and permeability parameters were stipulated after partial replacement of cement with sugarcane bagasse ash in varied fractions as follows :0%, 3%, 6%, 9% and 12%. IS code 456-2000 was referred for desining the mixing proportions of plain concrete. Mix proportions were acquired and requisite number of specimens were casted for several tests at the duration of 7 and 28 days.



**Figure 2** Drum type mixer



**Figure 3** Freshly Prepared Concrete

### Casting

In present study, 150\*150\*150mm cubes specimens, 150mm dia. and 300mm long cylinders specimens, 100\*100\*500mm beams specimens and 70.8\*70.8 mm cubes specimens were casted in experimental work. The moulds were kept free from dust. Oil was applied on all sides of the moulds before concrete pouring, Figs.

2 and 3. Moulds were filled in several (3) layers of homogeneous height with adequate tamping. After this, the moulds were kept on vibrator table for small duration to ensure proper compaction in specimen. Excess concrete was removed from the moulds. After this removal, the top surface of samples were well finished and placed on safe place. **Figure 4** depicts the casting of specimen.



**Figure 4** casting of specimens

### **Curing**

After the casting of specimens is done the moulds were kept unmoved for 24 hours. The concrete moulds like cube moulds, beam moulds were unmounted after 24 hours for curing purposes. After demoulding of moulds the samples were placed in curing tank for the time period of 7 and 28 days in order to avoid the loss of moisture content. The casted specimens were cured under normal water which was free from harmful contaminants like oil, alkalis and acids etc.

### **Testing of specimens**

In this study, cured specimens were taken from curing tank at the age of 7 and 28 days. Thus tests were conducted on these specimens to determine the different parameters.

### **Compressive strength**

The compressive strength of the casted specimen is determined after the curing age of 7 and 28 days and tested instantly after the removal from water. Surface water was allowed to flow downward. The position of cubes while testing was at right angle to that of casting position. The load was consistently applied without any impact and incremented increase at constant rate of 14 N/mm<sup>2</sup> until failure of specimen took place. The test was conducted according to a IS code 516-1959. The test was conducted on compression testing machine. **Figure 5** shows the compressive strength testing method adopted in the study.



**Figure 5** Compressive strength testing (Before and after)

### **Split tensile strength**

Split tensile strength of casted specimen samples is determined after 7 days of curing and also after 28 days of curing. The load was applied gradually on the cylinders without shock and increased the constant rate of load in N/mm<sup>2</sup> until failure takes place on specimens. The test is conducted in compression testing machine. **Figure 6** shows the method of split tensile strength testing.



**Figure 6** Split tensile strength (Before and after)

### Flexural strength

For flexural strength the casted beams were taken from the curing tank at age of 7 and 28 days after wet curing and tested after the surface of specimens dries out. The tests were done on universal testing machine (UTM). **Figure 7** shows the flexural testing machine.



**Figure 7** Flexural strength Testing

### Water Absorption

In this test, the casted specimen 150\*150\*150 mm cubes of the age of 28 days curing period were used. After moist curing the specimen cubes were taken out and kept in an oven for 24 hours then the dry weight of the specimen was evaluated. The cube specimen were once again immersed in curing tank for 24 hours. The percentage of water absorption was measured and porosity, volume of voids in hardened concrete were determined. The test was executed on hardened concrete. The formula for water absorption is given as,  
 $\% \text{ water absorption} = \frac{(\text{Wet weight} - \text{Dry weight})}{\text{Dry weight}} \times 100$

### Abrasion resistance test

The abrasion test on hardened concrete was conducted as per IS code 9284-1979. 70\*70\*70mm size of cubes were casted for abrasion test. The test was conducted for the duration of 28 days after the curing. The surface of the specimens should be patted with mineral paper to remove cement laitance and expose aggregate particles from the surface of cubes, before executing the test. Scraped spot loss of solid shape example was taken as the decrease of mass in grams for two separate cubes under test. The procedure was repeated on the other three vertical faces of the same sample. The test was repeated on the same surface after rotating the sample at 180°. The abrasion loss of concrete is the average of the results obtained for the 12 surfaces (that is 4 surfaces for each cube in a sample of 3 cubes) and it is expressed in percent loss. **Figure 8** represent abrasion testing.

### Calculation

The loss in mass of sample for each surface shall be calculated as follows:

$$m = m_1 - m_2$$

$m$  = loss of mass in g,

$m_1$  = mass of the specimen before each test in g,

$m_2$  = mass of the specimens after each test in g.



Figure 8 Abrasion resistance test

## Results And Discussion

The current research aims at evaluation of concrete strength with ply of sugarcane bagasse ash as a partly substitution of cement in concrete. The different strength parameters viz compressive, flexural, Split tensile, water absorption, Abrasion resistance and Permeability test were done in the concrete lab by using different equipments. Table 4 and Figure 9 depicts and the comparative results of compressive strength after the age of 7 and 28 days.

Table 4 Compressive strength results

Mix Designation	% of SCBA	Average Compressive Strength at 7 days(MPa)	Average Compressive Strength at 28 days(MPa)
A <sub>0</sub>	0	22.15	31.74
A <sub>1</sub>	3	25.56	33.24
A <sub>2</sub>	6	27.14	34.42
A <sub>3</sub>	9	29.37	36.33
A <sub>4</sub>	12	28.72	35.67

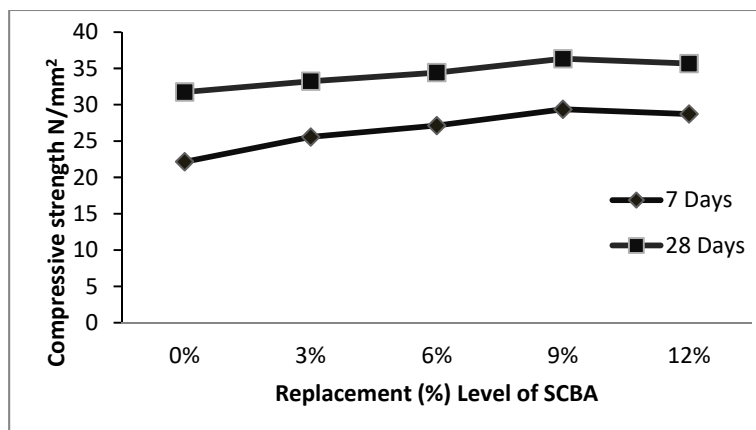


Figure 9 Variation in compressive strength of all mixes

The strength (compressive) acquired at 0% quantity of sugarcane bagasse ash is 31.74mpa, which is target mean strength of conventional concrete, now with the addition of sugarcane bagasse ash there is increase in compressive strength upto 9% and after that there is a gradual decrease in strength. This shows that 9% sugarcane bagasse ash can be added to concrete for good results and economic profitability. Silica in bagasse ash reacts with unused CH after the development of C-S-H gel, and increases the amount of C-S-H gel which aids in increasing the strength. As per the test results depicted in Table 5 the split tensile strength increases with addition of sugarcane bagasse upto 9% then again gradually decreases, thus 9% cement replacement in concrete can be done for optimal results.

in strength (split tensile) .

**Table 5** Variation of Split tensile strength with replacement of Sugarcane Bagasse Ash (SCBA) with cement.

Mix Designation	% of SCBA	Average Split tensile strength at 28 days(N/mm <sup>2</sup> )
A <sub>0</sub>	0	2.56
A <sub>1</sub>	3	3.37
A <sub>2</sub>	6	3.52
A <sub>3</sub>	9	3.73
A <sub>4</sub>	12	3.44

The tensile strength(split) represented by (ft) is calculated by using the formula. Split tensile strength (ft) = 2P / π LD, Where P = load at failure in Newton, L=length of the cylinder in mm D = diameter of the cylinder in mm

**Table 6** and **Figure 10** describes the flexural strength parameters of the specimen studied.By adopting BIS 516: 1959, the Prism specimens are tested for flexure in Universal testing machine of capacity 100kN. The flexural strength is calculated using the following expression.  $F_b = PL / BD^2$  N/mm<sup>2</sup> Where F<sub>b</sub> = Flexural strength N/mm<sup>2</sup>, P = Applied Load in Newtons B = Breadth in mm , D = Depth in mm. the flexural strength of nominal M25 grade concrete is 3.5N/mm<sup>2</sup>,it can be observed that flexural strength increases due to addition of sugarcane baggase upto certain limit i,e 9% replacement of cement and again value of flexural strength decreases due to further addition of sugarcane baggase ash , The flexure strength was increased due to the dense distribution of particles and low porosity in the concrete.

**Table 6** Variation of Flexural strength with replacement of Sugarcane Bagasse Ash (SCBA) with cement.

Mix Designation	% of SCBA	Average Flexural Strength at 28 days(N/mm <sup>2</sup> )
A <sub>0</sub>	0	5.23
A <sub>1</sub>	3	6.67
A <sub>2</sub>	6	7.14
A <sub>3</sub>	9	8.52
A <sub>4</sub>	12	7.28

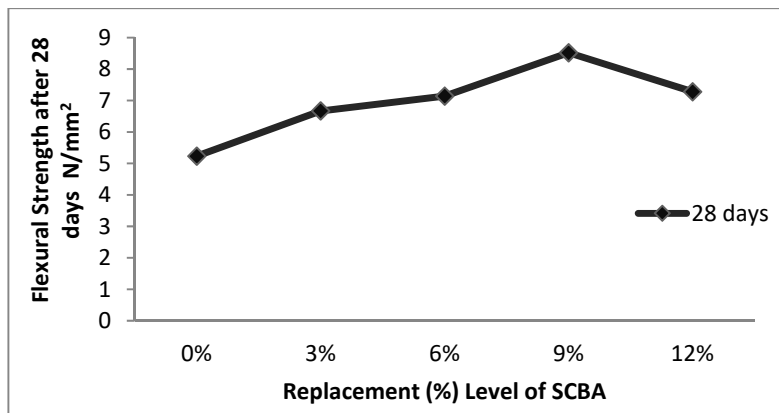


**Figure 10** Variation in flexural strength of all mixes

**Table 7** and **Figure 11** depicts the variation of water absorption in specimen afet 28 days. The water absorption of M25 grade of the conventional concrete is 3.30% after the duration of 28 days, it is observed that the water absorbtion of concrete cast with addition of sugarcane baggase ash is increased gradually, due to presence of un-burnt sugarcane baggase.

**Table 7** Variation of Water Absorption with replacement of Sugarcane Bagasse Ash (SCBA) with cement.

Mix Designation	% of SCBA	Average % of water absorption strength at 28 days
A <sub>0</sub>	0	1.07
A <sub>1</sub>	3	1.18
A <sub>2</sub>	6	1.38
A <sub>3</sub>	9	1.78
A <sub>4</sub>	12	2.00

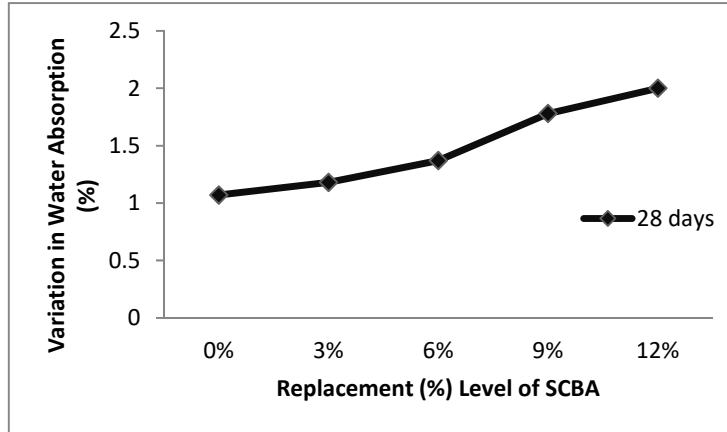


**Figure 11** Variations in Water Absorption

**Table 8** and **Figure 12** represent the Compressive Strength due to Abrasion Resistance in hardened concrete. Abrasion can be manifested on concrete in many forms and severities. Providing a concrete with high abrasion resistance relies on a variety of factors. The materials selected have a large influence on the resistance level, as does the mix composition, strength gain, and construction practices. It becomes necessary to estimate the compressive strength values of concrete when subjected to abrasion since, in real field practice concrete may be subjected to any kind of situation. It was observed that on replacement of 9% of cement by weight with SCBA compressive strength depicted its peak value as 15.68% and on further addition of SCBA compressive strength started to decrease.

**Table 8** Variation of compressive strength due to abrasion with replacement of Sugarcane Bagasse Ash (SCBA)

Mix Designation	% of SCBA	Average Compressive Strength at 28 days(N/mm <sup>2</sup> )
A <sub>0</sub>	0	9.24
A <sub>1</sub>	3	11.57
A <sub>2</sub>	6	13.92
A <sub>3</sub>	9	15.68
A <sub>4</sub>	12	13.37

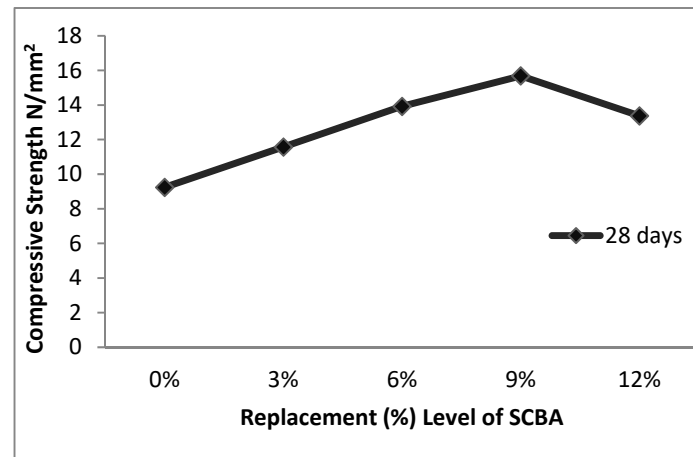


Figure 12 Compressive Strength due to Abrasion Resistance

### Conclusion

The present research work was done to investigate the different strength parameters viz Compressive, Split Tensile, Flexural Strength, Water Absorption, Abrasion Resistance and Permeability. Cubes (150\*150\*150mm) and cubes (70\*70\*70mm), Cylinders (300\*150mm) and beams (100\*500\*100mm) were casted and tested for these parameters to take the strength. The tests were done on fresh and hardened concrete. The significant end drawn from the present investigation:

- The compressive strength of the concrete increases with upto 9% of SCBA replaced with cement at 7 days 29.37 N/mm<sup>2</sup> and at 28 days 36.33N/mm<sup>2</sup>.
- The split tensile strength escalates upto 9% of SCBA substituted with cement in concrete at 28 days 3.73N/mm<sup>2</sup>.
- The flexural strength increases maximum up to 9% of SCBA replaced in concrete with cement at 28 days 8.52N/mm<sup>2</sup>.
- The various strength parameters viz compressive, split tensile, flexure etc increases with increases the percentages of SCBA upto a certain limit after this the strength of concrete decreases.
- The percentages of water absorption increases with increases the %age of SCBA in concrete because they have unburnt, burnt and half burnt particles. These particles also absorbed more water.

### References

- Anand.Ankur, Mishra.A.K.."Comparative study of concrete strength by partially replacement cement with sugarcane bagasse ash and fly ash" International Journal of Science, Engineering and Technology, Vol.5, (2016), P.(1063-1069).
- Bangar Sayall S. "An experimental study on replacement of cement with sugarcane bagasse ash" International Journal of Engineering and Science Management, Vol.1, (2017), P.(127-131).
- BIS- IS 456 : 2000 "Indian Standard code of practice for general structural use of plain and reinforced concrete". Bureau of Indian Standards, New Delhi, India.
- BIS- IS 12269 : 2013 "Specification for 53 grade ordinary portland cement" Bureau of Indian Standards, New Delhi, India.
- BIS IS 383:1970 "Specification for coarse and fine aggregates from natural sources for concrete" Bureau of Indian Standards, New Delhi, India.
- BIS IS 516:1959 "Method of test for strength of concrete" Bureau of Indian Standards, New Delhi, India.
- BIS IS: 2386 (Part I) – 1963(R2016) "Indian standard of test for concrete part I particle size and shape", Bureau of Indian Standards, New Delhi, India.
- BIS IS 9284:1979 "Method of test for abrasion resistance of concrete" Bureau of Indian Standards, New Delhi, India.
- Sachin .M, Subbavarshni.D, Nabendu.R and Ramesh.D "Study on replacement of cement in concrete with sugarcane bagasse ash and coir fibre" Imperial Journal of Interdisciplinary Research, Vol. 3,(2017), P.(1204-1207).
- Sampath.K, Prathyusha.A, Akhila.V, Sasidhar.P and Praveen U.M. "A comprehensive study on partial

replacement of cement with sugarcane bagasse ash, rice husk ash and stone dust" International Journal of Civil Engineering and Technology, Vol. 7,(2016),P.(163-172)  
Yahwanth M. K. Avinash. G.B., Raghavendra A. and Naresh Kumar.B.G (2014) "An experimental study on sugarcane bagasse ash as replacement for cement in lightweight concrete" International Journal of Latest Trends in Engineering and Technology, Vol. 3, (2014), P. (51-58).



## Strengthening of Heat-damaged R/C Members with Different Techniques

A.B. Danie Roy\*<sup>1</sup>, U. K. Sharma<sup>2</sup> and P. Bhargava<sup>3</sup>

<sup>1</sup>\*Assistant Professor, Department of Civil Engineering, TIET Patiala, India (Corresponding Author)

<sup>2</sup> Associate Professor, Department of Civil Engineering, IIT Roorkee, India

<sup>3</sup> Professor, Department of Civil Engineering, IIT Roorkee, India

### ABSTRACT

To examine the efficiency of different strengthening methods in reinstating heat-damaged concrete short columns and beams was evaluated experimentally. In this study the strengthening schemes namely Glass Fibre Reinforced Polymer (GFRP), High Strength Fibre Reinforced Concrete (HSFRC), Ferrocement (FC) and steel plate (SP) jacketing were employed. A total of Forty- eight reinforced concrete columns and twenty- four T-Beams were first subjected to different elevated temperatures. The heated and cooled specimens were strengthened using one of the chosen techniques. Thereafter, all specimens were tested under monotonic loading to determine the ultimate strength, stiffness, ductility and energy absorption behaviour. The strengthened columns and beams showed significant improvement in ultimate strength over the heat damaged unstrengthened columns and beams and in some cases, the strength enhancement was even more than the unheated control columns and beams. It was observed that while the GFRP jacketing is quite effective in improving compressive and flexural strength. GFRP jacketing was found to be the most effective method of strengthening fire or heat damaged concrete columns and beams.

### INTRODUCTION

Concrete structures generally perform well in fire and exhibit reasonably high resistance to temperature transients. However, extremely rapid heating and simultaneous cooling can cause large volume change due to thermal dilation, shrinkage due to moisture migration and eventual spalling due to high thermal stress and pore pressure build – up. Larger volume changes produce stresses resulting in microcracking and large fractures. Majority of concrete structures are not destroyed due to fire or a thermal exposure, thereby providing the advantage of easy reparability and reusability. Apart from improvement in the service life of buildings and low maintenance cost, Fibre Reinforced Polymer (FRP) wrapping has various benefits e.g. high strength, lightweight, resistance to corrosion, low cost, and versatility [1]. Significant research has been undertaken and reported on the repair and strengthening of RC elements with FRP confinement under ambient room-temperature conditions [2-4]. Unfortunately, due to the uncertainties regarding the behaviour of FRP in any subsequent fire following repair, limited research has been reported on the repairing of fire-damaged concrete elements. However, with the invention of many fireproof surface coatings for FRP, it has now been reported in the literature that FRP can be used to strengthen even the fire- or heat-vulnerable concrete structures [5-7]. Similarly, though enough information exists in the literature on the strengthening of RC elements with Ferro Cement [8-9], there are hardly two studies on using this technique for restoring and strengthening fire damaged RC elements [5-7]. Recently, a new method has been used for strengthening concrete structures via thin jackets made of high strength fibre reinforced concrete [10 - 11]. The advantages of this method are a high compressive strength, high tensile strength and there is no need to have reinforcement bars as rebars and stirrups and no specified concrete cover, and the thickness of the jacket can be as small as 15 – 40 mm. Several studies have previously been undertaken into the feasibility of using HSFRC for the rehabilitation and strengthening of damaged members but very few authors have reported on the repairing of fire damaged concrete elements [5,12]. The strengthening and repair of RC elements with steel jackets is a common engineering practice because it is inexpensive, does not require highly trained labour, is unobtrusive, does not reduce space, is easy to inspect and can be applied while the structure is still in use [ 13-14]. However, the application of steel jacketing in the repair of fire-damaged concrete has been reported by only one researcher [5]. The present study explored the potential of different strengthening schemes to restore the mechanical performance of RC elements that had been heat damaged at a certain temperature.

### EXPERIMENTAL PROGRAMME

The objective of this study was to investigate the effectiveness of different strengthening schemes in repairing heat-damaged concrete elements. Normal strength concrete was used for constructing reinforced concrete columns and beams. The details of the specimens are illustrated in Fig. 1 and Table 1. A different pattern of strengthening and

temperature of exposure were included in experimental variables and. Crushed limestone aggregate of 12.5 mm (maximum size) along with ordinary Portland cement and natural river sand (zone 2) with potable water were used to prepare the concrete. Cylinder compressive strength of 37.19 MPa was obtained after 28 days. The concrete mix consisted of 450 kg/m<sup>3</sup> Portland cement, 658 kg/m<sup>3</sup> washed sand, 1034 kg/m<sup>3</sup> crushed limestone, and 202.5 kg/m<sup>3</sup> portable water.

Hook-end steel fibres were used to prepare the HSFRC jacket. The fibres were used at a volumetric fraction of 2%. The steel fibres used were 0.60mm in diameter, 30mm long and had a yield strength of 1120 MPa. The welded mesh used in the FC jacketing had square openings (13x13 mm), a wire diameter of 0.96mm and a yield strength of 385MPa. The HSFRC and FC jackets were prepared using slurry which encompassed ordinary Portland cement, natural sand (<600 μm) and silica fume. The slurry mix proportions were 1:0.6:0.15:0.35:0.01 by weight of cement, sand, silica fume, water, and superplasticizer, respectively. The prepared slurry mix had a compressive strength of 68.06 MPa and high flowability (32 s), as measured in a standard ASTM C939 flow cone test (ASTM, 2010). The fabrics were held together by GFRP which was uni directional and in secondary direction having nonstructural weaves. The FRP was about 0.324mm thick, with an average tensile strength of 3400 N/mm<sup>2</sup> and an ultimate elongation of 4.33%. The SP jackets were 410mm long, 150mm wide and 2.3mm thick. The SPs were bonded to the sides of the prisms using epoxy adhesive.

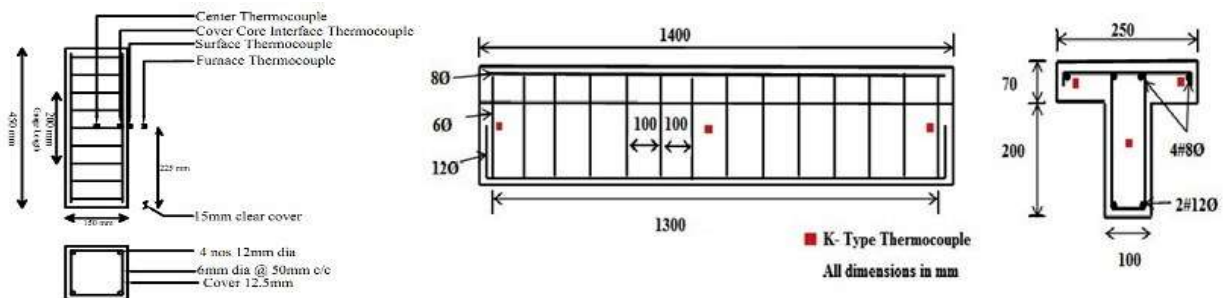


Fig. 1 Size of column and beam, reinforcement details and position of thermocouples

### Curing and Thermal Testing

The water curing period lasted for 28 days after which the specimens were kept in the laboratory at ambient temperature and humidity conditions for another 122 days. A programmable electrical furnace intended for a maximum temperature of 1200°C was used for heating the specimens. The temperature inside the furnace was measured and recorded with specially installed thermocouples. After 150 days, the specimens are heated in the furnace to different target temperatures ranging from ambient temperature to 900°C. The rate of heating was set at 10°C/min and each target temperature was maintained for 3 hrs to achieve a thermal steady state Fig. 2. After exposing the specimens to target temperatures for the desired time duration, the specimens were allowed in the furnace for natural cooling till room temperature.

### Observations after heating

Assessment of heat damaged concrete usually starts with visual observation of colour change, cracking and spalling of the concrete surface. The colour of the concrete columns changed to pink when the specimens were exposed to 300°C temperature and became light greyish at 600°C. However, the specimen's changed to ash white colour when exposed to 900°C. There was no visible crack on the surface of the specimens heated up to 300°C. However, while insignificant hairline cracks were observed at 600°C. The number of cracks became relatively pronounced at 900°C. No spalling was observed at 300°C and 600°C temperatures. On exposure to a temperature of 900°C no instant spalling was recorded in any of the specimens. The damage accumulated during the cooling process further reduces the residual strength, which leads to further expansion of any cracks day by day Fig 3.

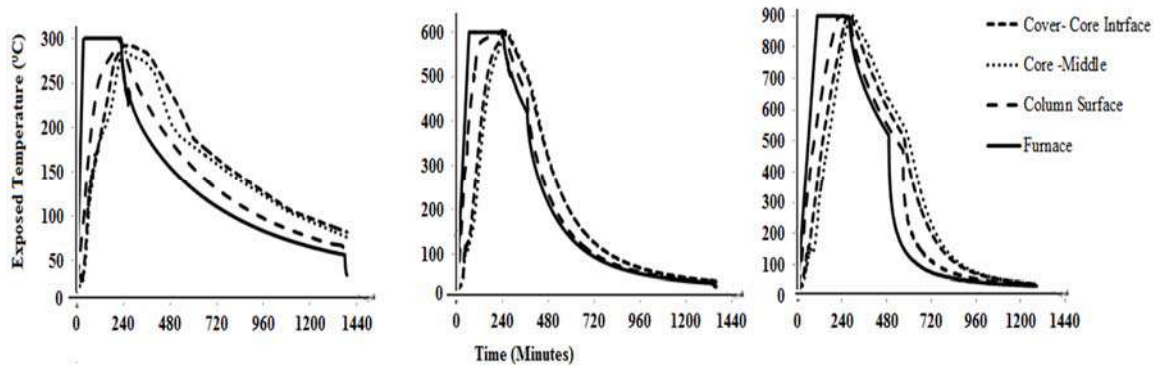


Fig. 2 Heating Regimes

Table 1 Details of Columns and beam specimens

Temperature	Control	300°C	600°C	900°C
Designation and wrapping methods for columns	SCA	SC3, SC3 GFRP, SC3 HSFRC, SC3 FC, SC3 SP	SC6, SC6 GFRP, SC6 HSFRC, SC6 FC, SC6 SP	SC9, SC9 GFRP, SC9 HSFRC, SC9 FC, SC9 SP
Designation and wrapping methods for Beams	TBA	---	TB6, TB6 GFRP, TB6 HSFC, TB6 FC	TB9, TB9 GFRP, TB9 HSFC, TB9 FC



Fig. 3 Surface cracking observed in test specimens exposed to 900 °C

### Installation of Strengthening Schemes

After heating and cooling the heat damaged specimens were strengthened with various techniques namely HSFRC, FC, GFRP and SP jacketing. The specimens which were heated to 900°C temperature were first repaired and their section was restored before wrapping. The loose concrete was removed using a steel wire brush, chisels, and hammer. The surfaces of the specimen were cleaned thoroughly to ensure no dust. A primer coat was applied on the spalled surface to attain good bonding between the old concrete and new restoration material i.e. micro concrete. In the samples presented to 300°C and 600°C, a preliminary epoxy holding was connected after the surface was cleaned so as to give great holding between the substrate and the new reinforcing material.

The heat harmed samples implied for fortifying with HSFRC jacketing were set inside the molds. HSFRC slurry reinforced with snared steel fiber at a volume division of 2% was filled the shape to frame a 25 mm thick coat around the samples. The FC jacketing was done with two layers of welded wire mesh. At several places, the first and the second layers of the wire mesh were tied together with the same diameter of steel wire. An overlap of 100 mm was provided in the lateral direction of the wire mesh. Slurry with high compressive strength of about 68.06 MPa was filled into the mould to form 25mm thick FC coat. The strengthened samples were secured with damped gunny packs for 14 days subsequent to demoulding. Before GFRP jacketing the outside of the samples was scratched delicately to expel surface contaminants. Firstly, the surface of the concrete was coated with a layer of epoxy primer on the external

surfaces of the concrete to fill air voids and to provide good bond strength. Thereafter, a thin layer of the saturant solution was applied over the specimens., the second layer of the saturant solution was applied on the surface of the first layer with a lap of 100 mm in length. The SP jacketing consisted of four steel plates, each one covering one of the four adjacent Then the first layer of GFRP sheets was wrapped around the specimen carefully. A roller was utilized to expel the entrapped air between the fiber and overabundance saturant in order to permit better impregnation of the saturant. Exceptional consideration was taken to ensure that no air voids were left between the fiber and the solid concrete surface. After the use of the first wrap faces of the sample, fortified longitudinally to the heat harmed surface. Before bonding the plates, the sides of the columns were roughened using a mechanical grinding machine, and the bonding faces of the plates were cleaned with acetone. The steel plates were fixed to the sides of the square column using an epoxy adhesive. To ensure that the steel plates were fixed tightly to the square column, the gaps at the corners of the plates were sealed with epoxy adhesive. After the gaps had been fully filled, the plates were tightened using binding wire. The strengthened columns and beams were cured in the laboratory for at least 28 days before loading Fig. 4.



Fig. 4 Strengthening process of GFRP jacketing and HSFRC jacketing

## INSTRUMENTATION AND TEST SETUP

Mechanical testing of the columns and beams was conducted after they had been heated, cooled and strengthened. The columns were loaded using a 2500 kN capacity universal testing machine (UTM) with displacement-control capabilities and beams were loaded using a 200 Ton capacity hydraulically hand operated jacks connected to a data acquisition system through load cells. The columns and beams were tested under monotonic increasing load. The axial contraction and deflection were noted using a linear variable differential transducer (LVDT) Fig. 5. Two horizontal LVDTs were also fixed on opposite faces of the specimen with the help of steel clamps. The mean lateral displacements were measured at the center of the specimen. Loads were recorded through inbuilt load cell in the UTM. The recorded data from the LVDTs, strain gauges and load cell were fed into a data acquisition system and stored on a computer.

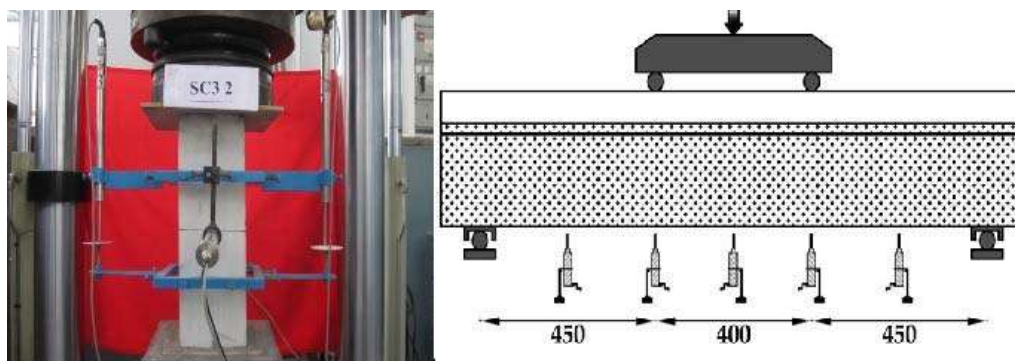


Fig. 5 Test setup for columns and beams

## RESULTS AND DISCUSSION

The test results for all the columns and beams are given in Table 2 and 3. Table 2 gives the peak load, peak strain,

secant stiffness, and energy dissipation as the average for three specimens. Tables 3 furnish the various measured and computed key parameters of the beam specimens. The load corresponding to the yield point,  $P_y$ , and the load corresponding to the ultimate point,  $P_u$  are shown in Table 3. The  $\mu_\Delta$  is the deflection ductility index, while  $\Delta_y$  and  $\Delta_u$  are the mid-span deflections at yield load and ultimate load respectively. The  $\mu_E$  is the energy absorption capacity and  $E_y$  and  $E_u$  are the areas under the load-deflection diagram at the yield load and ultimate load of beam respectively. Each result is the average of three tests.

Table 2 Test results of columns

Specimen Designation	Peak Load Pu(kN)	Strain at Peak $\epsilon_{cc}$	Strain at 0.8 Peak $\epsilon_{c80c}$	Secant Stiffness (kN/mm)	Energy Dissipation (kN.mm)
SCA	916	0.0060	0.0110	688.872	1932
SC3	883	0.0098	0.0140	450.683	1813
SC3 HSFRC	958	0.00400	0.00630	1066.815	976
SC3 FC	1055	0.00230	0.00330	2397.727	506
SC3 GFRP	1423	0.01004	0.0137	711.500	3214
SC3 SP	888	0.0090	0.0127	458.242	1516
SC6	648	0.00900	0.0179	344.680	1329
SC6 HSFRC	724	0.0064	0.0100	579.200	1284
SC6 FC	809	0.00420	0.00730	963.095	971
SC6 GFRP	1180	0.0183	0.02650	321.525	4431
SC6 SP	664	0.0103	0.0140	321.014	1491
SC9	193	0.0170	0.0249	55.619	725
SC9 HSFRC	483	0.0094	0.0154	256.914	1045
SC9 FC	565	0.0040	0.00922	614.130	862
SC9 GFRP	835	0.0337	0.0346	110.449	5674
SC9 SP	425	0.0127	0.0166	167.322	981
SC9 MC	347	0.0406	0.0560	70.242	1720

### Failure Modes of Columns and Beams

The columns were tested under monotonic compression up to failure. Different failure modes were observed in the various control and heat-damaged columns. The failure was particularly brittle, sudden and explosive in nature in the control specimens, while in the heat-damaged specimens the failure was gradual and exhibited ductile behaviour with increasing load. The exposure of concrete to high temperatures results in softening due to deterioration in the chemical and physical make-up of concrete. It is believed that these changes, along with the cracking observed at high temperatures, are what make concrete ductile. In the case of the specimens heated to 900°C, the lateral ties became exposed due to spalling of the cover concrete, resulting in crushing failure. In both the control and heat-damaged specimens, vertical cracks started at the top, followed by crushing of the concrete.

For specimens strengthened with HSFRC and FC, the failure initiated at the top and the bottom of the specimens due to the concentration of stress during loading. Diagonal and vertical cracks were observed in HSFRC specimens, and there was propagation and widening of the vertical cracks with increasing load after the specimen had reached its ultimate loading capacity. At this point, an increase in load created noise due to the breaking of the steel fibres, indicating a transfer of stress from the dilated concrete to the jacket. The bonding between the HSFRC and FC jacket and the concrete remained good enough during testing, as no debonding was observed during the process. For the specimens strengthened with FC jacketing, as the ultimate stages of loading were approached a bursting sound was heard. The welded mesh began to bulge out, and there was a cracking sound towards the ultimate stages of loading. The fact that failure occurred without a sudden and explosive noise indicates very ductile behaviour of the columns. The failure observed in the corners indicates that the stress in the square jacket is likely to be concentrated at the corners. The wires of the weld mesh in the horizontal direction were broken, while those in the vertical direction were buckled and broken at the corners.

For the specimens strengthened with GFRP a cracking noise was heard prior to failure. The failure of these specimens

took a long time but ended with a sudden and explosive noise. The GFRP jackets ruptured externally at the overlap position at the top and bottom ends. This is attributed to the concentration of stress in these regions. Conversely, in the specimens strengthened with SP jacketing, debonding did occur during loading. The failure of these specimens was gradual, with ductile behaviour with increasing load.

The failure modes of beams are shown earlier in Table 3. It can be noted that the undamaged beams developed a flexural tensile crack in the hinge region at an average load of 43kN. The flexural tensile cracks gradually propagated at the bottom of the beam within the middle third of the span. As the load was increased, shear cracks also began to develop between the support and loading points. Around 153kN, the beam started to yield and the beam finally failed in flexure at a load of 195kN. In specimens heated to 600°C, the first crack load was noted to be 26kN and flexural cracks developed pre-maturely in the mid-span region and then subsequent shear cracks were noted in shear span region but the beams finally failed in flexure at an average load of 166kN. As the temperature of exposure increased the failure load further decreased and in specimens subjected to a temperature of 900°C the first crack load got reduced to 21kN. The behavior and failure pattern of the beams heated at 900°C was also different. Though the failure started with flexural cracking in middle flexural region, the shear cracks started relatively earlier and the number of shear cracks was considerably more than the flexural cracks. Interestingly, the 900°C heat damaged beams exhibited a sudden failure in the shear region possibly due to a significant decrease in shear strength of concrete due to heating.

Table 3 Test results of beams

T-Beam Designation	Load(kN)		Deflection		Deflection Ductility Factor $\mu_{\Delta}=\Delta_u/\Delta_y$	Energy		Energy Ductility Factor $\mu_E=E_u/E_y$	Energy Dissipation (kN.mm)	Failure Mode
	Yield Load $P_y$ (kN)	Ultimate Load $P_u$ (kN)	$\Delta_y$ (mm)	$\Delta_u$ (mm)		$E_y$ (kN.mm)	$E_u$ (kN.mm)			
TBA	153	195.36	6.84	20.01	2.925	1457	4292	2.944	4292	Flexural
TB6	141	166.00	9.13	25.77	2.822	1031	3859	3.740	3859	Flexural
TB9	60	76.09	9.03	17.86	1.977	1096	2269	2.070	2269	Shear failure at support
TB6 HSFRC	142	197.63	7.82	28.81	3.684	720	4136	5.700	4136	Flexural
TB6 FC	153	201.30	7.71	23.7	3.073	832	3683	4.426	3683	Flexural
TB6 GFRP	194	225.90	7.48	10.89	1.455	1205	2121	1.760	2121	Flexural failure and debonding of shear fabric
TB9 HSFRC	98	138.88	3.68	12.14	3.298	456	1749	3.835	1749	Flexural
TB9 FC	106	141.43	3.68	15.65	4.252	360	1949	5.415	1949	Flexural
TB9 GFRP	140	195.91	6.99	14.29	2.044	1103	2428	2.201	2428	Debonding of fabric in shear region

The HSFRC strengthened heat damaged beams failed in flexure. The vertical flexural cracks generated in the middle region of beam, though with gradual increasing load these cracks traded towards the compression area and resulted in crushing of concrete in the compression zone. In comparison with unheated and heat damaged beams the strengthened beams encountered lesser number of cracks. In HSFRC strengthened beams, the width of cracks generated vertically was smaller at a given phase of loading compared to un-strengthened undamaged and damaged beams. However, at the final phase of loading just before failure, the cracks got broadened in strengthened beams and the width was more than that in undamaged beams. The un-strengthened beams failed in shear whereas the failure of 900°C heat damaged beams and strengthened with HSFRC was in flexure.

The failure of HSFRC strengthened specimens as well as heat damaged beams strengthened with Ferrocement jacketing was nearly similar. On either side of the repair where the bending moment was high, the cracks were mainly concentrated in that area. Ultimate failure was found to be due to the breakdown of the welded steel mesh in the tension

zone. More hairline cracks were seen in 600°C heat damaged FC beams, while relatively less hairline cracks were seen in 900°C heat damaged FC beams. After encountering the widening of some cracks in the middle it was considered as the failure of heat damaged beams.

Failure modes of the heat damaged beams strengthened with GFRP the development and propagation of cracks were relatively slower in GFRP strengthened beams compared to that in undamaged control beams, heated un-strengthened beams and HSFRC & FC strengthened beams. The GFRP strengthened beams underwent relatively lesser deflection during the test and the cracks were mainly confined in the flange of beams. The deflections were mainly concentrated in the middle region between the load points. The load carrying capacity of the beams kept on increasing until the appearance of cracks and thereafter the beams failed suddenly in brittle fashion. The ultimate failure of GFRP strengthened beams, which were heated at 600°C temperature, was a flexural failure and debonding of fabric in the shear region. In 900°C heat damaged and GFRP strengthened beams, debonding of GFRP fabric was observed in the shear region as the beam failed to indicate a shear failure.

### Strength of Heat Damaged Strengthened Columns and Beams

It can be seen from Tables 2 and Fig.6 that the heat-damaged columns SC3, SC6, and SC9 had ultimate failure loads of 883, 648 and 193 kN, respectively, compared with 916 kN for the corresponding unheated control specimen (SCA). This indicates that there was a decrease of 4%, 29% and 79% in the ultimate load carrying capacity of columns exposed to 300°C, 600°C, and 900°C, respectively. The degraded strength was restored when the heat-damaged short columns were strengthened with different strengthening techniques, which had a good confining effect on the specimens. The increase in strength was due to the expansion of the concrete laterally under axial compression, causing tensile stresses in the HSFRC, FC, GFRP, and SP jackets. Owing to this tensile stress, the jackets confined the column and kept them in a stressed state. Consequently, the load-carrying capacity of the column increased significantly

As expected, the strength of HSFRC, FC, GFRP, and SP jacketed specimens exposed to different temperatures was higher than that of the corresponding unstrengthened heated columns. The strength of the HSFRC jacketed heated specimens was 8%, 12% and 150% more for specimens heated at 300°C, 600°C, and 900°C, respectively, than the unstrengthened heated specimen. However, the HSFRC, FC, and SP strengthening could not restore the strength of the specimens heated to 600°C and 900°C to their corresponding room-temperature strengths, although the strength of the specimen heated to 300°C could be restored to its corresponding room-temperature strength. The strength of HSFRC, FC, and SP -strengthened specimens heated to 600°C and 900°C was less than the comparable unheated control specimens. The strength of the GFRP-jacketed specimens was higher than the corresponding heat-damaged unstrengthened specimens and control unheated specimens at both 300°C and 600°C exposure temperatures. Only for the strengthened specimen heated to 900°C was the GFRP strengthening notable to restore the room-temperature strength. The strength of GFRP strengthened specimens heated to 300°C and 600°C was 55% and 29% more than the unheated control specimens.

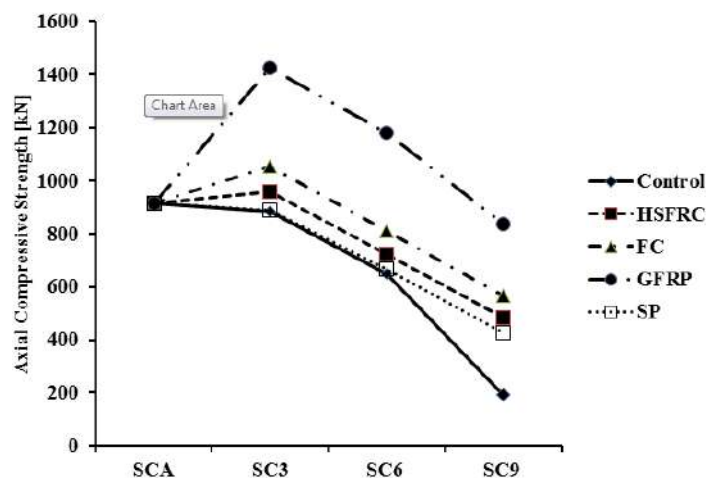


Fig. 6 Axial compressive strength of square columns

The results presented Tables 3 and Fig 7 indicate a clear decrease in the ultimate load capacity, ductility, and energy

dissipation of beams due to exposure at elevated temperatures when heated to temperatures of 600°C and 900°C. The results indicate a loss of about 14% and 61% in the ultimate flexural capacity after heating to 600°C and 900°C temperatures respectively. It can be noted that only GFRP strengthening was capable of restoring the room temperature strength of beams damaged at 900°C temperatures, while FC and HSFRC schemes could not restore the room temperature flexural strength of such heated beams. In case of beams heated at 600°C temperature, all the strengthening schemes restored the room temperature strength though GFRP strengthening still showed more efficient performance. In case of specimens heated at 600°C, the entire strengthening types showed reasonable enhancement in strength if compared with the strength of heat damaged unstrengthen beams, though the capability of various strengthening designs in restoring the room temperature strength was just sufficient at 600°C temperature. The GFRP strengthening showed better enhancements in strength compared with FC and HSFRC strengthening. On the contrary, while all the three strengthening schemes showed a tremendous increase in strength of 900°C heat damaged un-strengthened beams, it was GFRP which was able to restore the room temperature strength of beams heated at 900°C with other two techniques falling short in restoring the room temperature strength of heated beams at this temperature.

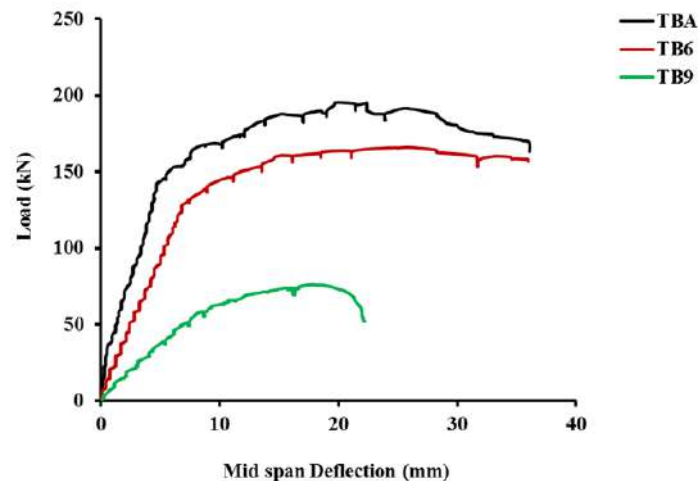


Fig. 7 Load-deflection relationships of control and heat-damaged specimens

## CONCLUSIONS

The results of tests examining the behaviour of RC square short columns and T Beam subjected to elevated temperatures and strengthened with different schemes have been reported. Within the scope of the present investigation, the following conclusions can be drawn.

1. This study proves that the strength of reinforced concrete compression and flexural elements degrade when exposed to elevated temperatures. The axial compressive strength of square columns was found to have reduced by 4%, 29%, 79% respectively after exposing to temperatures of 300°C, 600°C and 900°C respectively. The reinforced concrete T-beams experienced a reduction of 14% and 61% in their ultimate flexural strength after an exposure at 600°C and 900°C temperatures respectively. Thus, the results of this study show that the detrimental effects of elevated temperature on strength become significant only when the temperature reaches 600°C and more.
2. The axial compressive strength of heat damaged reinforced concrete columns increased significantly in case of GFRP strengthened specimens. HSFRC, SP, and FC jacketing techniques were found to be relatively less effective in increasing the compressive strength of heat damaged columns compared to GFRP jacketing.
3. All the strengthening techniques employed in this study showed reasonable enhancement in strength compared to the strength of heat damaged un-strengthened beams in case of beams heated at 600°C, though the capability of various strengthening designs in restoring the room temperature strength was just sufficient at 600°C temperature. The GFRP strengthening showed better enhancements in the strength of heat damaged beams compared with FC and HSFRC strengthening. While all the three strengthening schemes showed a significant increase in strength of 900°C heat damaged un-strengthened beams, it was GFRP which was able to restore the room temperature strength of beams heated at 900°C with other two techniques falling short in restoring the room temperature strength of heated beams at this temperature.

## REFERENCES

- Ehsani, M. R., & Jin, L., Repair of Earthquake-Damaged RC Columns with FRP Wraps, *ACI Structural Journal*, 1998, 94(2), 206–214.
- Luca, A. D., Asce, M., Nardone, F., Matta, F., Asce, A. M., Nanni, A., Asce, F., et al., Structural Evaluation of Full-Scale FRP-Confined Reinforced Concrete Columns. *Journal of Composites for Construction*, 2011, 15(1), 112–123.
- Lam, L., and Teng, J. G. Design–Oriented Stress-Strain Model for FRP Confined Concrete. *Construction and Building Materials*, 2003, 17, 471–489.
- Eid, R., Roy, N., Paultre, P., & Asce, M., Normal- and High-Strength Concrete Circular Elements Wrapped with FRP Composites. *Journal of Composites for Construction*, 2009, 13(2), 113–124.
- Danie Roy A.B., Sharma U.K., and Bhargava P. Strengthening of heat damaged reinforced concrete short columns. *Journal Structural Fire Engineering*, 2014, 5 (4), 381-398.
- Yaqub M., Bailey C.G., Nedwell P., Khan Q.U.Z., Javed I. Strength and stiffness of post-heated columns repaired with ferrocement and fibre reinforced polymer jackets. *Composites: Part B*. 2013, 44, 200–211.
- Haddad, R H, Shannag, M. J., & Hamad, R. J., Repair of heat-damaged reinforced concrete T-beams using FRC jackets. *Magazine of Concrete Research*, 2011, 59 (3), 223–231.
- Kondraivendhan, B., & Pradhan, B., Effect of ferrocement confinement on behavior of concrete. *Construction and Building Materials*, 2009, 23(3), 1218–1222.
- Mourad, S. M., & Shannag, M. J., Repair and strengthening of reinforced concrete square columns using ferrocement jackets. *Cement and Concrete Composites*, 2012, 34(2), 288–294.
- Martinola, G., Meda, A., Plizzari, G. A., & Rinaldi, Z., Strengthening and Repair of RC Beams with Fiber Reinforced Concrete. *Cement and Concrete Composites*, 2010, 32(9), 731–739.
- Shannag, M.J., High-Performance Cementitious Grouts for Structural Repair. *Cement and Concrete Research*, 2002, 32, 803–808.
- Haddad, R H, Al-mekhlafy, N., & Ashteyat, A. M., Repair of heat-damaged reinforced concrete slabs using fibrous composite materials. *Construction and Building Materials*, 2011, 25(3), 1213–1221.
- Priestley M.J.N, Seible F, Xiao. Y. et al., Steel jacket retrofitting of reinforced concrete bridge columns for enhanced shear strength. *ACI Structural Journal*, 1994, 91(4): 394–405.
- Ramirez J.L, Bleen J.M, Urreta J.I et al. Efficiency of short steel jackets for strengthening square section concrete columns. *Construction and Building Materials*, 1997, 34(5): 345–352



## Study of Impact Behavior of Polymeric Foams Using Numerical Simulation of Drop Weight Impact

Y. M. Chordiya,<sup>1</sup> and M. D. Goel<sup>2\*</sup>

<sup>1</sup>#Postgraduate Student, Department of Applied Mechanics, Visvesvaraya National Institute of Technology (VNIT) Nagpur, Maharashtra, India

<sup>2</sup>\*Assistant Professor, Department of Applied Mechanics, Visvesvaraya National Institute of Technology (VNIT) Nagpur, Maharashtra, India; e-mail: mdgoel@apm.vnit.ac.in (Corresponding Author)

### ABSTRACT

Vehicular occupant safety is amongst the prime concerns in transportation industry and hence, various parts of the automobiles, protection gears etc. are examined for the post-collision energy absorption. Other forms of protection against impact include helmet, knee protector, elbow band etc. Thus it is important to design such parts/equipments with sole purpose of safety in case of accident. Under these circumstances, selection of material is crucial because it's important to know the behavior of the material subjected to impact. This study investigates impact behavior and energy absorption for two different types of foams. In the present study, FE model is developed in LS-DYNA® for drop weight impact wherein, a bilinear material model is used for hammer and crushable foam material model is used to model the foams. Effect of drop height on the impact for two different foam i.e., Dytherm foam (DF) and Polyurethane foam (PU) is studied. A comparative study is presented for the response of the foam for varying drop heights. From the present study, it is observed that PU foam is optimum for low velocity impact considered in the present investigation.

**KEYWORDS:** Impact test; Numerical simulation; LS-DYNA; Foams.

### INTRODUCTION

Based on transport research wing, Ministry of Road Transport & Highways, GOI report on road accidents at least 4,80,652 accidents happened in year 2016, leading to 1,50,785 deaths. There is substantial increase in number of accidents in year 2016 in comparison with those happened in year 2015. Vehicular occupant safety is an important concern which needs to be accounted in vehicle parts design and thus tests are carried out to study collision behavior of vehicle parts for calculating the absorbed energy during the collision. These parts are called as crash boxes which are specially designed with a motive of colliding them so that we get an idea about what will be the response of the vehicles on collision.

In the past several researchers has investigated the drop weigh behavior of different materials such as concrete, graphite-fiber-reinforced composite, fiber-reinforced composite, metal foams, hybrid-fiber engineered cementitious composite (Bowles, 1986; Barr and Bouamrata, 1988; Rajendran et al., 2005; Zhang et al., 2007; Zhang et al., 2017). Apart from above experimental and numerical investigation, many authors developed different variation of this basic test for investigating the stress-strain behavior of various materials (Banthia et al., 1989; Roesset et al., 1994; Aymerich et al., 1996; Goyal and Buratynski, 2000; Browne and Johnson, 2002; Bhattacharya et al., 2006; Gunawan et al., 2011; Taheri-Behrooz et al., 2013). Thus, there exists a scope of numerical simulation of drop weight test for understating the stress-strain behavior of different materials as real experiments are costly and time consuming.

Materials which are light, durable, impact resistant are the optimum choice for such testing. Polymeric foams are the excellent choice because of their light weight composition and impact resistance properties. Helmets, cars, blast lining materials are the important areas where these foams are widely used (Goel et al., 2012). The cyclists and bike riders use elbow and knee pads made out of foam which is an important safety gear and absorb impact energy in case of fall/accident.

There are many impact testing methods but most widely used is drop weight impact hammer testing this is due to its ease and flexibility in its working. This method is widely used for determining impact resistance (Barr and Boumrata, 1988). But testing requires lot of manpower and even a minor change results in a huge change in the setup. To create a mathematical model in any Finite Element (FE) package and do the numerical simulation is better option under such circumstances. Hence, in the present investigation, two types of foams are investigated using numerical simulation at low velocities for their impact behavior and energy absorption.

## FE MODELLING AND MATERIAL PROPERTIES

In drop weight test, main component is impact hammer which is guided through two vertical posts and allowed to fall freely from a pre-decided height. This fall of hammer strikes the material with an impact force and by suitable data acquisition system this data is captured in real test. In the numerical simulation, hammer is modeled and it is allowed to fall freely from a predicted height to impact the material. In this study, 720 mm long and 155 mm diameter impact hammer with a self weight of 106 kg is modeled in LS-DYNA (LS-DYNA, 2018). For FE modeling, eight noded hexahedral solid elements with a bilinear material model are applied. The material properties are reported in the Table 1. Hammer is modeled using elastic plastic material/ model, i.e. MAT\_003 (MAT\_PLASTIC\_KINEMATIC) of LS-DYNA material library (LS-DYNA, 2018). The foam is modeled with dimensions of 80 mm diameter and 100 mm length using eight noded hexahedral solid elements. The assembly of finite element model of foam and hammer is shown in Fig. 1.

Clamped boundary condition is applied at the bottom of the foam. Two types of foam material i.e. DF and PU foam are considered. The properties of the foams are reported in Table 2 and these are modeled using MAT\_063 (MAT\_CRUSHABLE\_FOAM) i.e., crushable foam material model (LS-DYNA, 2018). Automatic surface to surface contact algorithm is applied between top surface of foam and bottom surface of hammer. The stress-strain behavior of the foams is shown in Fig. 2. Based on convergence study, a mesh size of 20 mm for hammer and 10 mm for foam is used. Thus, the hammer has a total of 18400 elements and foam has 1050 elements, respectively.

**Table 1 Material properties of the hammer**

Property	Value
Young's Modulus, $E$ (GPa)	210
Poisson's ratio, $\nu$	0.3
Yield stress, $\sigma_y$ (MPa)	230
Tangent Modulus (MPa)	800
Density, $\rho_0$ (kg/m <sup>3</sup> )	7800

FE simulation is carried out for impact velocities of 3.13, 3.84, 4.43, 4.95, 5.42 m/s corresponding to drop heights of 0.5, 0.75, 1, 1.25, 1.5 m, respectively. Simulation is carried out for a total time of 0.025s and the results are obtained at an interval ( $\Delta t$ ) of 0.0025 s. The  $\Delta t$  is chosen to satisfy the relation  $\Delta t \leq l/C_L$ ,  $l$  is the length of the smallest division and  $C_L$  is wave speed which travels through the material (Johnson, 1983).

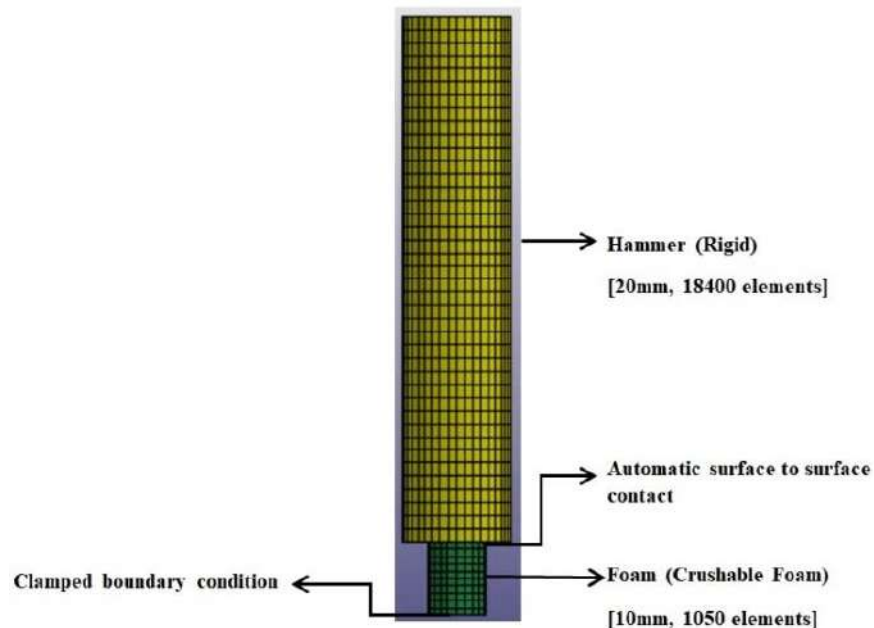


**Fig. 1 Finite element model of hammer impacting foam**

**Table 2 Material properties of the foam (ABAQUS, 2016)**

Property	DF	PU
Young's Modulus, $E$ (MPa)	3	7.5
Poisson's ratio, $\nu$	0	0
Yield stress, $\sigma_y$ (MPa)	0.22	0.2
Tension cutoff, $p_t$ (MPa)	0.02	0.02
Density, $\rho$ (kg/m <sup>3</sup> )	100	60

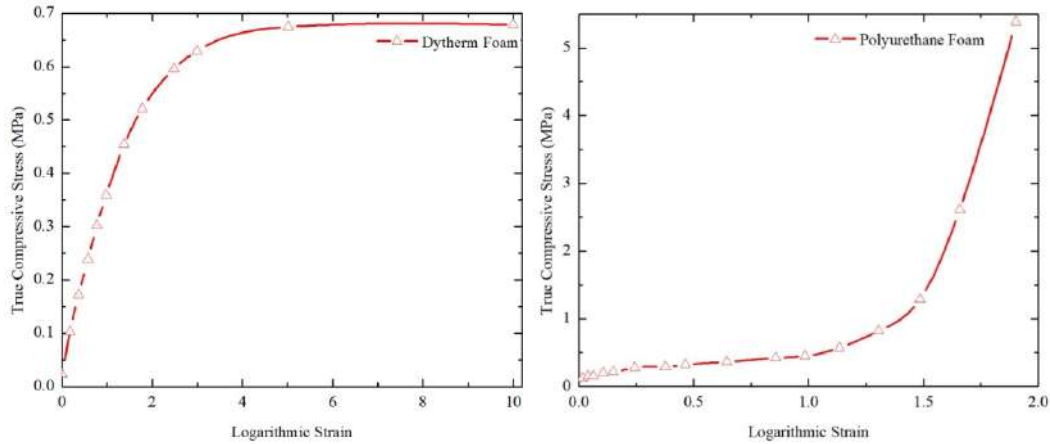


Fig. 2 True stress-strain curve for dytherm and polyurethane foam

## RESULTS AND DISCUSSIONS

The effect of height on displacement and reaction force of foam is studied. Moreover, displacement time history and reaction force time history is studied on top surface of foam and bottom surface of hammer, respectively. It is important to mention here that these parameters give an idea of the response of the material subjected to impact and hence focus is kept for these parameters. Fig. 3 shows the displacement time history for dytherm foam which depicts a maximum displacement of 50.24 mm for a drop velocity of 5.42 m/s. From this figure, it can be observed that maximum displacement for all drop heights is in same range but it is achieved at a minimum time for drop velocity of 5.42 m/s. Further, similar trend is observed wherein there is an increase up to a certain time then there is decrease and again there is increase as shown in Fig. 3. This is attributed to the fact of compression and relaxation in the foam structure under the impact loading. Similarly, Fig. 4 shows the displacement time history for PU foam. It can be observed from this figure that maximum displacement of 78.04 mm is observed for drop velocity of 5.42 m/s but here there is a change in variation, first the displacement increases then it decreases and again there is a small increase but it is not substantial in comparison with that of DF. The reason for such a behavior is attributed to the foam microstructure which is denser in the DF.

Further, reaction force time history is studied for both the foams and it is observed that both the foams follow the same trend as there is steep increase up to a certain time and then there is a decrease in reaction force with time as shown in Fig. 5 and Fig. 6 for PU foam and dytherm foam, respectively. From this figure, a peak reaction force of 2760 N is observed at an impact velocity of 5.42 m/s whereas, for dytherm foam this reaction force is found to be 1067 N at an impact velocity of 4.95 m/s.

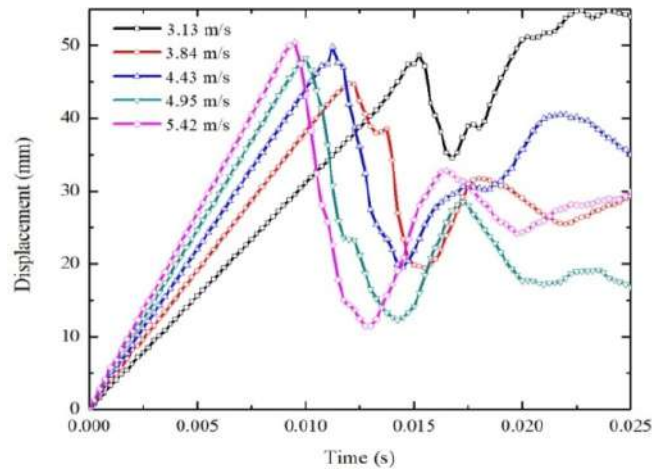


Fig. 3 Variation of displacement time history at top of foam for dytherm foam considering different drop velocities

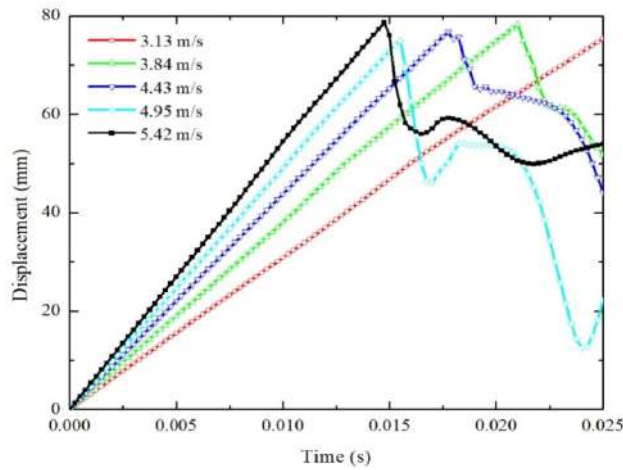


Fig. 4 Variation of displacement time history at top of foam for PU foam considering different drop velocities

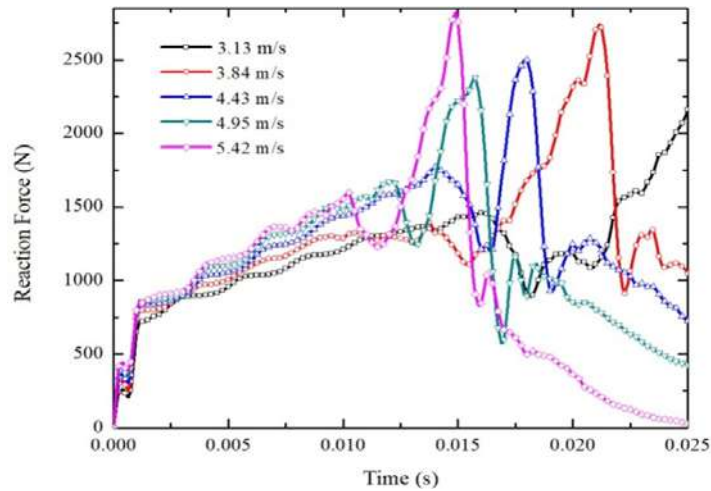
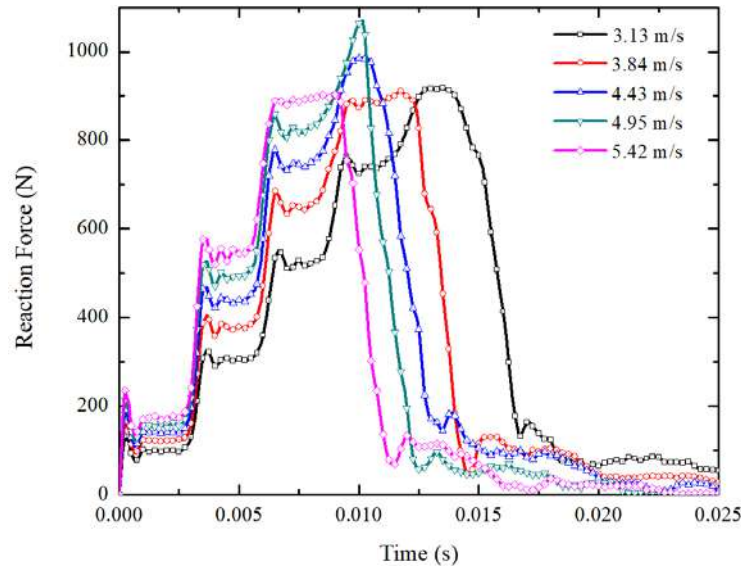
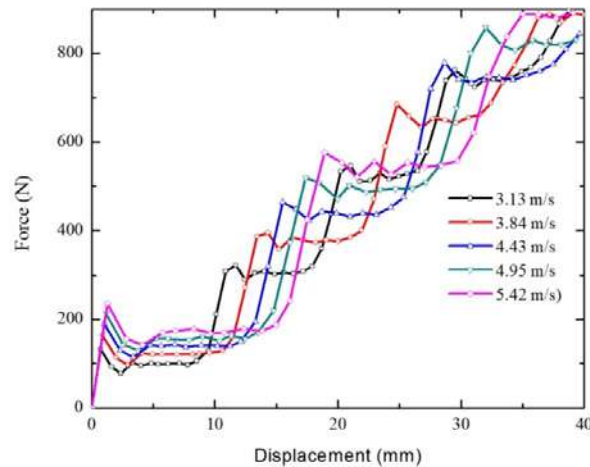


Fig. 5 Variation of reaction force time history at bottom of hammer for PU foam considering different drop velocities



**Fig. 6 Variation of reaction force time history at bottom of hammer for dytherm foam considering different drop velocities**

Fig. 7 and Fig. 8 show the variation of force with the displacement for dytherm and PU foam, respectively. For energy absorption, the area under these curves is computed. For computation of energy and comparison a common displacement of 40 mm is taken in the present study and this depicts the maximum deformation for energy absorption computation. Energy absorbed by the foams under varying velocities is reported in Table 3. It can be observed from this table that there almost no effect of variation of velocity on energy absorption for the parameters and foams considered in the present investigation. However, PU foam absorbs almost two times higher energy in comparison with dytherm foam for all other parameters being same.



**Fig. 7 Variation of force with displacement for dytherm foam considering different drop velocities**

**Table 3 Energy absorbed by the foams for varying drop impact velocities**

Drop velocities	DF (J)	PU (J)
3.13 m/s	17.45	39.19
3.84 m/s	17.96	39.82
4.43 m/s	17.40	39.13
4.95 m/s	17.42	38.90
5.42 m/s	17.32	40.39

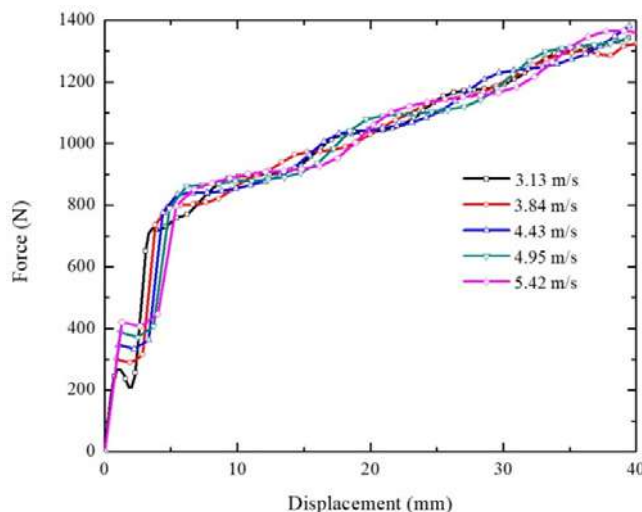


Fig. 8 Variation of force with displacement for PU foam considering different drop velocities

## CONCLUSIONS

This study investigates crashworthiness and energy absorption for two different types of foams. In the present study, FE model is developed in LS-DYNA® for drop weight impact wherein, a bilinear material model is used for hammer and crushable foam material to model the foams. Effect of drop height on the impact for two different foam i.e., dytherm foam (DF) and Polyurethane foam (PU) is studied. A comparative study is presented for the response of the foam for varying drop heights. Based on this study, following conclusion are drawn,

1. Increase in drop height leads to increase in all the parameters considered i.e., displacement, reaction force etc.
2. Lower density foam i.e. PU foam absorbs higher energy in comparison with dytherm foam for the foam and impact velocities considered in the present investigation.

## REFERENCES

- ABAQUS/Explicit user's manual, V 6.14. *Dassault Systemes Simulia Corporation*, France. 2016.
- Aymerich, F., Marcialis, P., Meili, S., & Priolo, P. (1970). "An instrumented drop-weight machine for low-velocity impact testing." *WIT Transactions on the Built Environment*, 25.
- Banthia, N., Mindess, S., Bentur, A., and Pigeon, M. (1989). "Impact testing of concrete using a drop-weight impact machine." *Experimental Mechanics*, 29(1), 63-69.1.
- Barr, B., and Bouamrata, A. (1988). "Development of a repeated drop-weight impact testing apparatus for studying fibre reinforced concrete materials." *Composites.*, 19(6), 453-466.
- Bhattacharya, S., Krishnamurthy, K. C., Rajendran, R., Prem Sai, K., and Basu, S. (2006). "Impact studies on structural components using a free-flight drop tower." *Experimental Techniques*, 30(2), 52-58
- Bowles, K. J. (1988). "The correlation of low-velocity impact resistance of graphite-fiber-reinforced composites with matrix properties." *Composite Materials: Testing and Design (Eighth Conference)*, ASTM International.
- Browne, A. L., and Johnson, N. L. (2002). "Dynamic crush tests using a "free-flight" drop tower: theory." *Experimental Techniques*, 26(5), 43-46.
- Goel, M. D., Matsagar, V. A., Marburg, S., and Gupta, A. K. (2012). "Comparative performance of stiffened sandwich foam panels under impulsive loading." *Journal of Performance of Constructed Facilities.*, 27(5), 540-549
- Goyal, S., & Buratynski, E. K. (2000). "Methods for realistic drop-testing." *International Journal of Microcircuits and Electronic Packaging*, 23(1), 45-52.
- Gunawan, L., Dirgantara, T., and Putra, I. S. (2011). "Development of a dropped weight impact testing machine." *International Journal of Engineering and Technology*, 11(6), 120-126.
- Johnson, W. (1983). "Elementary one-dimensional elastic stress waves in long uniform bars due to impact." In *Impact strength of materials* (pp. 2-35). London: Edward Arnold.
- Livermore Software Technology Corporation. (2018). "LS-DYNA: keyword user's manual (vol. 2)." Livermore,

California, U.S.A.

- Rajendran, R., Sai, K. P., Bhattacharya, S., and Basu, S. (2005). "Shock assessment of cylindrical bodies impacting on a rigid unyielding surface." *Journal of Structural Engineering*, 32(2), 139-142.
- Roesset, J. M., Kausel, E., Cuellar, V., Monte, J. L., and Valerio, J. (1994). "Impact of weight falling onto the ground". *Journal of Geotechnical Engineering*, 120(8), 1394-1412.
- Taheri-Behrooz, F., Shokrieh, M., and Abdolvand, H. (2013). "Designing and manufacturing of a drop weight impact test machine." *Engineering Solid Mechanics*, 1(2), 69-76.
- Zhang, J., Maalej, M., and Quek, S. T. (2007). "Performance of hybrid-fiber ECC blast/shelter panels subjected to drop weight impact." *Journal of Materials in Civil Engineering*, 19(10), 855-863.
- Zhang, W., Chen, S., and Liu, Y. (2017). "Effect of weight and drop height of hammer on the flexural impact performance of fiber-reinforced concrete." *Construction and Building Materials*, 140, 31-35.



## Comparison of Different Methods for Blast Load Application Using Numerical Simulation

V. S. Phulari,<sup>1</sup> and M. D. Goel<sup>2\*</sup>

<sup>1</sup>Postgraduate Student, Department of Applied Mechanics, Visvesvaraya National Institute of Technology (VNIT) Nagpur, Maharashtra, India

<sup>2\*</sup>Assistant Professor, Department of Applied Mechanics, Visvesvaraya National Institute of Technology (VNIT) Nagpur, Maharashtra, India; e-mail: mdgoel@apm.vnit.ac.in (Corresponding Author)

### ABSTRACT

A numerical investigation is carried out to examine the response of a rectangular steel plate subjected to air blast loading under three different methods i.e. ConWep (Conventional Weapon), SPH (Smooth Particle Hydrodynamics), and CEL (Coupled Eulerian-Lagrangian). Dynamic response of the plate under air blast is analyzed using ABAQUS<sup>®</sup>/Explicit. In SPH and CEL methods, explosive material i.e. TNT (Tri Nitro Toluene) is modeled using JWL (Jones-Wilkens-Lee) equation of state, whereas in ConWep method, it is defined directly using ABAQUS function. Response of the plate in terms of its peak central point displacement is computed for the comparison. It is observed from the results that response of plate from ConWep method and SPH method follow similar trends. However, peak response of the plate using CEL method is lower than the ConWep and SPH method.

**KEYWORDS:** Blast loading; Numerical Simulation; CEL; SPH; ConWep; FE Analysis; ABAQUS<sup>®</sup>/Explicit.

### INTRODUCTION

Due to increase in population, lots of infrastructure facilities are being developed throughout the world. This requires detailed analysis of such facilities for different types of loadings. Apart from conventional loadings, explosion induced loading are posing a serious challenge to the designers and engineers. In the past, several facilities were destroyed due to such loadings and many were turned into useless. This lead to research need for their detailed analysis and design under such extreme loadings. Moreover, many casualties were reported due to failure of structures which were not designed by proper consideration of effect of such loadings. Hence, to minimize casualties under such extreme loadings, it is very important to understand the response of structures under these loadings. This demands the need to analyze the structure behavior using various methods and choose the simpler one considering the requirements of designers and engineers.

In the past several researchers had studied behavior of plates using experimental and numerical simulation. These include investigation carried out by Nurick and Martin (1989a; 1989b), Cichocki and Perego (1997), Schubak (1991), Louca et al. (1996), Pan and Louca (1999), Rudrapatna et al., (2000), Lam et al. (2004), Gupta and Nagesh (2007), Goel et al. (2011). In numerical simulation, researchers have used ABAQUS and L-DYNA most commonly for simulation of blast response of plates. In those investigations, researchers used different method and material models for the response analysis and no comparison with different method was presented. Further, it is important to note that plates of various configurations are most frequently used structural elements to resist high amplitude loading such as that due to the explosions or impact. Hence, in the present investigation a plate is investigated under blast loading using different approach as available in ABAQUS. In ABAQUS<sup>®</sup>/Explicit, there exist different methods to apply and model the blast load. It is to be noted that all the methods are good to analyze and understand the response of the structure under explosion, but every method possess its own pros and cons (ABAQUS<sup>®</sup>, 2014).

Hence, in the present work, a FE analysis is carried out to understand the response of steel plate under air blast using three different methods i.e.

1. ConWep (Conventional Weapon),
2. SPH (Smooth Particle Hydrodynamics), and
3. CEL (Coupled Eulerian-Lagrangian)

Emphasis is put to understand the various challenges involved in modeling of blast loading using above methods and effect of these methods on final results. In the present investigation, FE analysis is carried out using explicit non-linear finite element package ABAQUS<sup>®</sup>/Explicit.

## PLATE GEOMETRY AND FE MODELLING

The steel plate used is 2 m × 2 m in size with a thickness of 20 mm. This plate is pinned at boundary condition i.e. it is not allowed to move in any direction but rotation is allowed at its boundary. In the present investigation, 1 kg of TNT (Tri Nitro Toluene) is applied at a stand-off distance of 1.5 m from the centre of the plate. Fig. 1 shows the plate and location of the explosive material. The plate is modeled using three-dimensional, deformable part with an extruded solid base feature available in ABAQUS®. In ConWep method, plate is modeled using four-node reduced integration shell elements (S4R) available in ABAQUS® element library. The explosive TNT is applied directly by charge weight and its location using ConWep module available in ABAQUS®. Herein, interaction is applied between TNT and plate which in turns, applies blast in the form of incident wave on the plate. Fine meshing was done to avoid mesh convergence issues and converged mesh results are reported herein. Enhanced hourglass control is used for the plate and other materials mesh to control hourglass effects.

For SPH model, two parts i.e. TNT and steel plate is modeled. Herein, TNT is modeled as Lagrangian 3D deformable equivalent solid sphere of 0.0525m radius and steel plate is modeled as Lagrangian 3D deformable 2 m × 2 m plate.

In CEL method, air, TNT and steel plate is modeled separately. Herein, TNT and air is modeled as Eulerian element, and steel plate is modeled as Lagrangian element. For air modeling Eulerian domain of 5 m × 5 m × 5 m cube is developed, and ideal gas EOS is used to define the material properties. TNT is modeled as Eulerian part with 1 kg mass which is equivalent to 0.0525 m sphere radius, and properties are assigned by using JWL EOS. Herein, Eulerian elements are completely filled with their respective properties. In the Eulerian analysis, the material is filled by means of Eulerian volume fractions (EVF) and it represents the ratio by which each element is filled with Eulerian material. Further, steel plate is modeled as Lagrangian part in CEL method.

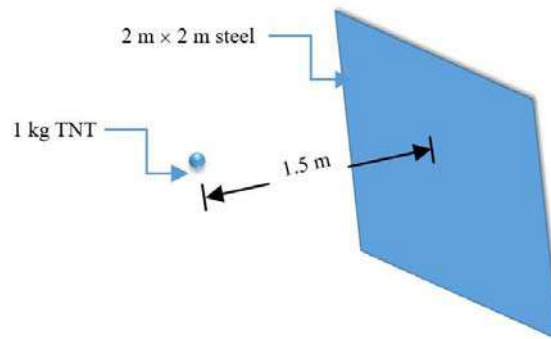


Fig. 2 Steel plate with 1 kg of TNT at a distance of 1.5 m from the centre of plate

## MATERIAL PROPERTIES

In this section, materials properties used for simulation are discussed. The plate is made of mild steel with Young's modulus,  $E = 210$  GPa, Poisson's ratio,  $\mu = 0.3$  and density,  $\rho = 7800$  kg/m<sup>3</sup> (Goel et al., 2011). The static yield stress of the plate material is 300 MPa (Goel et al., 2011). For explosive material, JWL (Jones-Wilkens-Lee) equation of state (EOS) is used as reported in Eq. 1. The material properties for JWL EOS are reported in Table 1.

$$P = A \left( 1 - \frac{\omega}{R_1 \rho} \right) e^{-R_1 \rho} + B \left( 1 - \frac{\omega}{R_1 \rho} \right) e^{-R_2 \rho} + \omega \rho e_{\text{int}} \quad \text{Eq. (1)}$$

Where,  $A$ ,  $B$ ,  $R_1$ ,  $R_2$  and  $\omega$  are user defined material constant, and  $\rho$  is the density of the detonation products.

To model the air, ideal gas EOS is used as reported in Eq. 2 and the properties for the ideal gas EOS are reported in Table 2.

$$PV = RT \quad \text{or} \quad P = \rho RT \quad \text{Eq. (2)}$$

Where,  $P$ ,  $V$ ,  $R$ ,  $T$  and  $\rho$  are pressure, volume, gas constant, temperature and density, respectively.

**Table 1 JWL material properties for TNT explosive (Tiwari et al., 2014)**

Detonation wave speed	6930 m/s
Density( $\rho$ )	1630 kg/m <sup>3</sup>
$A$	$3.738 \times 10^{11}$ Pa
$B$	$3.747 \times 10^9$ Pa
$\Omega$	0.35
$R_1$	4.15
$R_2$	0.9
Detonation energy density	$3.68 \times 10^6$ J/kg

**Table 2 Material properties for Ideal gas**

Density ( $\rho$ )	1.225kg/m <sup>3</sup>
Gas constant	287.058
Ambient pressure	101325 Pa
Specific heat	718 J/kg
Dynamic viscosity	$1.7894 \times 10^{-5}$ N-s/m <sup>2</sup>

## RESULTS AND DISCUSSIONS

After numerical model is developed, it is submitted for processing by defining the explicit dynamic analysis. The deformation of plate is studied carefully to understand its behavior under three different methods of blast load application. The results are computed in the form of central point displacement for comparison amongst three different methods as discussed. The complete process is carried out using ABAQUS®/Explicit and result by different methods are discussed in this section.

### SPH method

Smooth particle hydrodynamics (SPH) is a computational method used for simulating the mechanics of continuum media, such as solid mechanics and fluid flows. It is a mesh free Lagrangian method and the resolution of the method can easily be adjusted with respect to variables. This SPH model involves the quasi incompressible fluid through the EOS. Its meshless formulation makes the method easy for physical problems and which might be difficult for conventional methods. In the SPH method, computational domain is represented by a finite set of inter points with set of coordinates in the material frame. The SPH particles give a finite mass of continuum and carry the particulars about all physical changes which are evaluated at their points (ABAQUS®, 2014). Fig. 2 shows effect of 1 kg TNT on steel plate at variable time interval by SPH method. Fig. 3 shows variation of central point displacement-time history by SPH method.

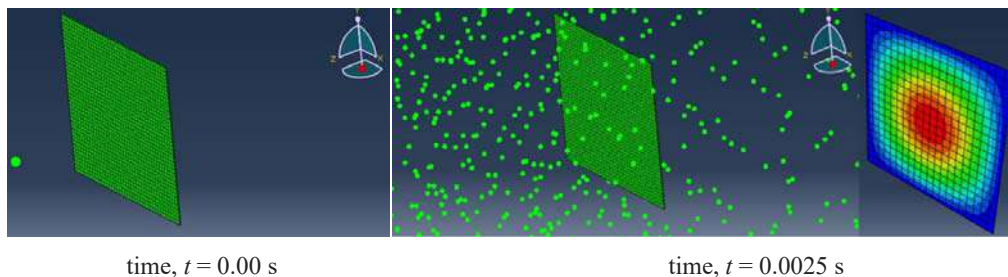


**Fig. 2 Effect of 1 kg TNT on steel plate at variable time interval by SPH method**

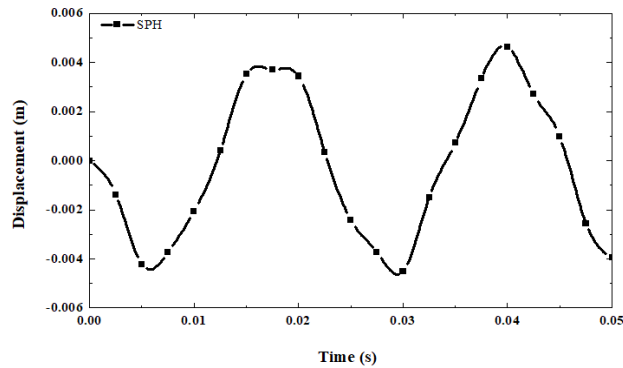


Fig. 3 Variation of central point displacement-time history by SPH method

**ConWep Method**

The blast load is applied on the front face of the door using CONWEP function as follows:

$$P(t) = P_r \cos^2 \theta + P_i(1 + \cos^2 \theta - 2 \cos \theta) \quad \text{Eq. (3)}$$

This function considers the enhancement of pressure due to reflection of waves. The pressure,  $P(t)$  on the face is determined based on the input amount of TNT, the stand-off distance, and angle of incidence “ $\theta$ ”. The final pressure is computed using Eq.3 and applied on the face of the plate. The whole assembly and the pressure response of steel plate at variable time interval are shown in Fig. 4. Fig. 5 shows the variation of central point displacement-time history by ConWep method for the plate and explosive charge considered in the present investigation.

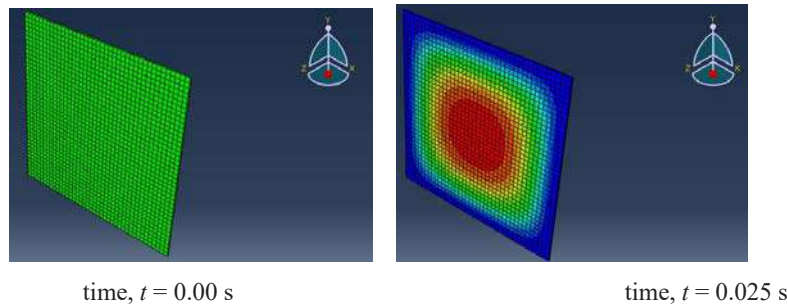


Fig. 4 Effect of 1 kg TNT on steel plate at variable time interval by ConWep method

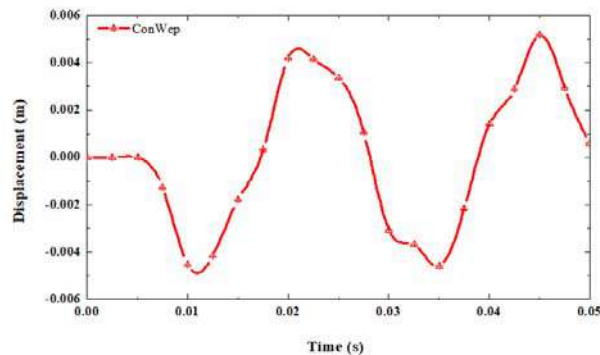


Fig. 5 Variation of central point displacement-time history by ConWep method

### CEL Method

Coupled Eulerian and Lagrangian (CEL) analysis technique merges two mesh approaches i.e. Eulerian and Lagrangian in the same analysis. The aim of this approach is to avoid mesh problems when performing simulations that involve extreme deformations. Lagrangian approach is the most commonly used finite element approach. It is to be noted that Lagrangian approach is not suitable for cases where high distortion of element is expected. In such conditions, Eulerian approach is preferred and large deformations can be meshed using Eulerian method. The interaction behavior between these two methods is modeled by interaction contact condition (ABAQUS®, 2014). The whole assembly and the pressure response of steel plate at variable time interval are shown in Fig. 6. Fig. 7 shows the variation of central point displacement-time history by CEL method for the plate and explosive charge considered in the present investigation.

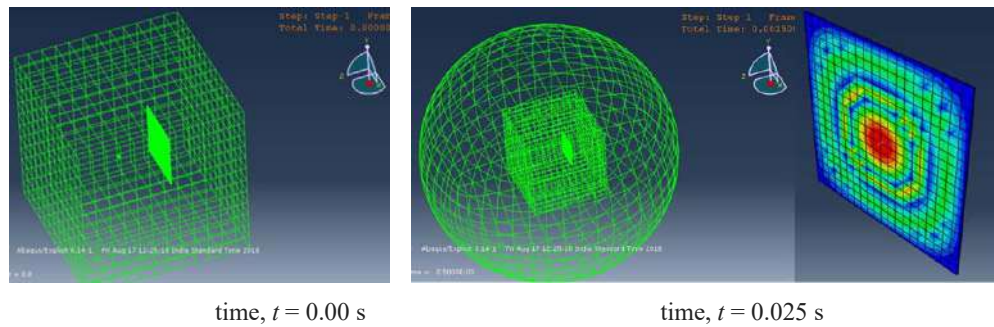


Fig 6 Effect of 1 kg TNT on steel plate at variable time interval by CEL method

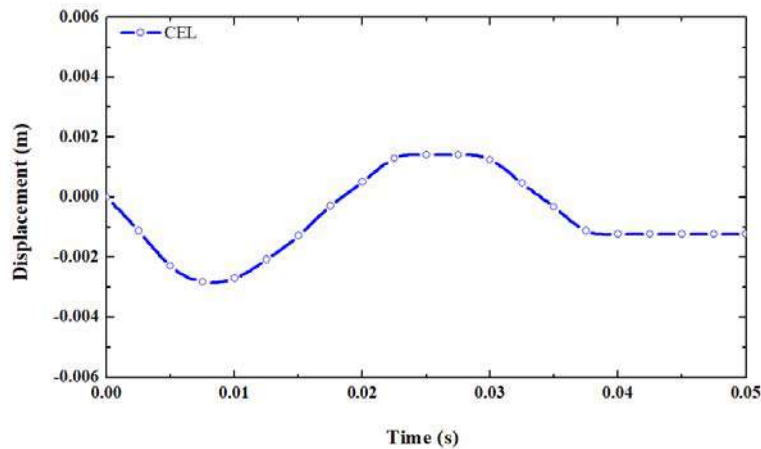
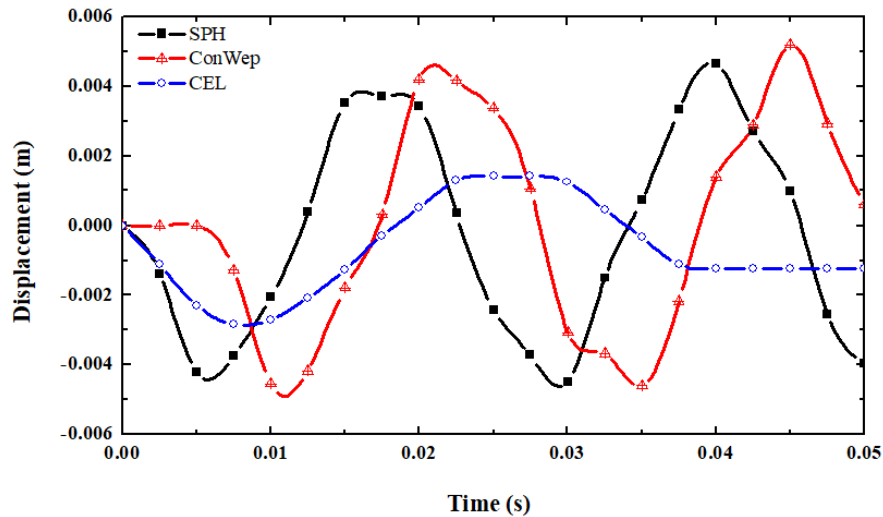


Fig 7 Variation of central point displacement-time history by CEL method

Combined variation of central point displacement-time history as computed using three methods i.e. SPH, ConWep and CEL are presented in Fig. 8. It can be observed from this figure that results of SPH and ConWep are in agreement with each other, whereas results of CEL shows substantial deviation are with the results obtained by SPH and ConWep methods. The reason for such behavior may be attributed to the fact that EOS is used in CEL method. Thus, based on this analysis, it is observed that ConWep method is simplest form for modeling the blast loading and can be used for computing the various parameters required for analysis. Further, SPH method requires more effort in comparison with ConWep method although the results obtained by these two methods are well in agreement with each other. Moreover, SPH method gives more accurate results as compared to other methods. This method is suitable for surface free or large boundary conditions. It is to be noted that results computed using CEL differs considerably with other two methods but this formation takes into account the physical behavior of various elements actually available in the real domain and thus required in details understanding of the modeling. Thus, it is recommended that for in-depth analysis CEL is best suited and ConWep method can be used as a quick method to understand the response of any structure. Further, ConWep method is best suitable for air blast and surface blast loading on structure as this method do not requires modelling of TNT and air media as required in

other two methods. Further, SPH method is more suitable for large blast loading for simple structures as used in the present investigation. The peak central point displacement for ConWep method is 4.6 mm and for SPH method it is observed as 4.5 mm. In case of CEL method, peak central point displacement is 1.41 mm. Thus, CEL results are 2.19 times lower in comparison with the ConWep and SPH results with loading and boundary conditions being same.



**Fig. 8 Comparison of variation of central point displacement-time history for three different methods i.e. SPH, ConWep and CEL**

## CONCLUSIONS

A numerical investigation is carried out to examine the response of a rectangular steel plate subjected to air blast loading under three different methods i.e. ConWep (Conventional Weapon), SPH (Smooth Particle Hydrodynamics), and CEL (Coupled Eulerian-Lagrangian). Dynamic response of the plate under air blast is analyzed using ABAQUS®/Explicit. In SPH and CEL methods, explosive material i.e. TNT (Tri Nitro Toluene) is modeled using JWL (Jones-Wilkens-Lee) equation of state, whereas in ConWep method, it is defined directly using ABAQUS function. Response of the plate in terms of its peak central point displacement is computed for the comparison. Based on this investigation, following observations are made,

1. ConWep method is best suitable for air blast and surface blast loading on structure as this method do not requires modeling of TNT and air media as required in other two methods.
2. ConWep method shows slightly higher response as compared to other methods. This method analyze the structure quickly but give approximate results.
3. SPH method gives more accurate results as compared to other methods. This method is suitable for surface free or large boundary conditions. But setting boundary condition is difficult and it takes extra time for analysis of structure.
4. CEL method is most commonly used under blast loading condition. It is best suitable for complicated structures under blast loading. This method shows lower response as compared to other methods.

## REFERENCES

- ABAQUS®/Explicit user's manual, V6.14. *Dassault Systemes Simulia Corporation*, France. 2014.
- Cichocki, K. and Perego, U. (1997). "Rectangular plates subjected to blast loading: the comparison between experimental results, numerical analysis and simplified analytical approach." *Journal of Physics IV France*, 7, C3761-C3766.
- Goel, M. D., Matsagar, V. A., and Gupta, A. K. (2011). "Dynamic response of stiffened plates under air blast." *International Journal of Protective Structures*, 2(1), 139-155.
- Gupta, N. K. and Nagesh (2007). "Deformation and tearing of circular plates with varying support conditions

- under uniform impulsive loads.” *International Journal of Impact Engineering*, 34(1), 42-59.
- Lam, N., Mendis, P. and Ngo, T. (2004). “Response spectrum solutions for blast loading.” *Electronic Journal of Structural Engineering*, 4, 28-44.
- Louca, L. A., Punjani, M. and Harding, J. E. (1996). “Non-linear analysis of blast walls and stiffened to hydrocarbon explosion.” *Journal of Constructional Steel Research*, 37(2), 93-113.
- Nurick, G. N. and Martin, J. B. (1989a). “Deformations of thin plates subjected to impulsive loading-a review; Part I theoretical consideration.” *International Journal of Impact Engineering*, 18(2): 159-170.
- Nurick, G. N. and Martin, J. B. (1989b). “Deformations of thin plates subjected to impulsive loading-a review; Part II experimental studies.” *International Journal of Impact Engineering*, 18(2): 170-186.
- Pan, Y. and Louca, L. A. (1999). “Experimental and numerical studies on the response of stiffened plates subjected to gas explosions.” *Journal of Constructional Steel Research*, 52(2), 171-193.
- Rudrapatna, N. S., Vaziri, R. and Olson, M. D (2000). “Deformation and failure of blast-loaded stiffened plates.” *International Journal of Impact Engineering*, 24, 457-474.
- Schubak, R. B. (1991). “Nonlinear rigid-plastic modelling of blast loaded stiffened plates.” PhD. Thesis, *University of British Columbia, Vancouver*.
- Tiwari, R., Chakraborty, T., and Matsagar, V. (2014). “Dynamic analysis of underground tunnels subjected to internal blast loading.” In *11<sup>th</sup> World Congress of Computational Mechanics (WCCM XI)*, 20-25 July 2014, Barcelona, Spain.



## Eco-friendly Pervious Concrete for Low Volume Traffic Pavements

Rekha Singh<sup>1</sup>, Sanjay Goel<sup>2</sup>

<sup>1</sup>\* Research scholar, I.K.G Punjab Technical University, Jalandhar, India; rekhasingh14@gmail.com (Corresponding Author)  
<sup>2</sup>. DAV Institute of engineering and Technology, Jalandhar, India; goelsanjay100@yahoo.com

### ABSTRACT

In cities, every major road is topped with normal concrete and shoulder drains are built using concrete technology. As a result the rainwater has no space to percolate down to the soil and ground water is not being recharged. Pervious concrete is popularly known for storm water controller, but they also assist in minimizing the urban heat island effects as it contain interconnected network of pore structure. Since Pervious pavements do not soak and hoard heat and then diffuse it to environment similar to asphalt pavements. The research paper provide characteristics of pervious concrete by interpreting the research work which has been in use since 19th century but has been in focus now days due to increasing ecological and environmental issues with uncontrolled use of normal concrete. The paper emphasizes the applications, benefits and challenges of using pervious concrete. It also highlights preparation of pervious concrete. An investigation of proportioning of pervious concrete has also been discussed.

**KEYWORDS:** Pervious concrete; Aggregates; Mix proportion; porosity; permeability.

### INTRODUCTION

Rapid urbanization and widespread use of cement concrete is creating several ecological and environmental challenges in India. With hasty improvement in infrastructure, housing and industrial development, concrete is occupying large spaces of our cities. Concretization at such pace is causing decline to ground water recharging, discharge of industrial wastes to ground water, heat island, constant fall of water table, weakening of tree roots and tree fall, frequent urban floods, the cumulative effects of which are making life at major cities troubled. The viable alternative suggested to cut down these problems is using pervious concrete at least to areas with low traffic volumes and discourage using normal concrete.

**Pervious Concrete** is a distinct category of concrete procured by a synthesis of distinctively defined mixture of cement, water and coarse aggregates. Usually, it has slight to nil fine aggregate quantity and contain precise cement paste to cover the aggregate pieces while preserving the linkages of the pores. According to ACI 522R the void content in the pervious concrete lies in the span of 15-22% in comparison to 3-5% in normal concrete. The compressive strength lies in the range 2.8 to 28MPa with drainage rate 0.14 to 1.22 cm/s.

It allows water to pass through it. It minimizes the runoff from paved areas, thus additional drainage for storm water is not required. It is also termed as porous concrete, permeable concrete, no fine concrete, gap-graded concrete, enhanced-porosity concrete, and zero-fines concrete. No fine concrete has wide no of usages in real life but the biggest use is in pavement systems for lesser movement traffic spaces such as motor parking, non-commercial roads, and tracks (Sonebi et al. 2016).

#### *From Pervious to impervious*

Pavement systems constituting about 30-40 per cent of the total urban fabric have converted pervious natural ground into impervious systems, which have created a negative impact on the environment. The use of pervious pavement increase the infiltration and recharge ground water whereas impervious surface like asphalt pavement reduce the infiltration as shown in Fig.1. These impacts are categorized as variations in hydrological aspect and temperature in the surrounding ambience. With regard to the hydrological aspects, the existing dense pavement system being impervious in nature, increases the quantity of runoff and reduces the infiltration of rainwater into the ground, which may create a flood-like situation in low-lying areas. The runoff, which occurs immediately during rainfall, termed as the first flush, is highly-polluted and requires large treatment facilities before being discharged into natural water bodies. Further, the problems of water logging, hydroplaning and skidding, which affect road users, exist when the pavement is wet. With regard to temperature in the surrounding ambience, impervious pavement systems act as a heat storage media that stores heat and releases it back to the atmosphere, increasing ambient temperature. This creates a phenomenon termed urban heat island (UHI), which results in an increase in the urban temperature by about 2-6°C compared to the surrounding rural areas. UHI results in thermal discomfort, which increases the consumption of electricity for cooling systems and other energy sources (Sreedhar & biligiri).

As per Malhotra (1976) the initial application of pervious concrete started in England in 1852 for constructing residential buildings. The construction material shortage in World War II catalyzed the popularity and adoption. USA and Japan started the focus on pervious concrete in 1980s and started using it for constructing pavements. Extensive research on porous concretes has been carried out in last two decades in many countries.



**Fig. 1 Eco-friendly Pervious concrete concept**

#### **APPLICATION AND ENVIRONMENTAL BENEFITS OF PERVIOUS CONCRETE**

The porous concrete pavement materials have voids or pores enabling heat exchange. These concrete can consume automobile noise and help in making peaceful and silent environment. Since such concrete do not retain water, it remove splash on the surface and sparkle at night thus driving become more convenient and safe. The main benefit of it lies in letting water pass rapidly through pavement and helping in real time ground water recharge. Due to high permeability almost entire water pass into pavement without runoff from paved surface (Tennis et al. (2004). It augments the environment of road surface. These concrete are beneficial for growth and suitability of trees also. Air and water can pass to tree roots and help in tree flourishing in highly urbanized areas as well. Since no sand is used, it helps in saving the valuable construction materials. Less cement usage also reduce cement requirement and hence less CO<sub>2</sub> is produced in manufacturing cement. With installation of pervious concrete, construction cost, construction time and adverse environmental impacts can be greatly reduced, (Sharma 2008, Avishreshth et al. 2017).

Some of other benefits are listed as following (ACI 522R):

1. Low usage pavements
2. Non-commercial roads
3. Tracks
4. Vehicle parking spaces
5. Sports grounds
6. Well linings
7. Foundations
8. Noise barriers
9. Walls
10. Architectural & Sculpture objects
11. Landscaping

The research studies carried out till date indicate that the pervious concrete can be a promising sustainable pavement material, which has positive effects towards low-impact development. Schaefer et al. (2006) determined the ill-effects of present and future urbanization can be reduced by implementing such pavement technologies that can be beneficial from different prospects. Several investigations have shown that mix parameters influence pore and strength properties to a large extent. Water-to-cement and cement-to-aggregate ratios as well as material density were found to be important mix parameters with significant effect on permeability; however, the numbers of proposed studies on mix design of porous concrete are very less. The design methods reported in past literature have many disadvantages, li (2009), Zheng et al. (2012), Schaefer et al. (2006). for e.g. there is no standard method to derive the w/c ratio or impact of compaction on properties of concrete has not been taken into consideration as well there are no appropriated technique to determine the mix design of porous concrete.

Park & Tia (2004) studied that there are certain drawbacks of porous concrete mixes, which are being studied to counter those problems. For example, porosity could be reduced over time with the accumulation of dust particles. Hence, such pavements require intermittent and frequent cleaning and maintenance. To overcome this bottleneck, a multi-layered pavement system with a removable or replaceable top layer; this particular wearing course will have the provision to be changed when damaged beyond repair.

## MATERIALS AND MIXTURE PROPORTIONING

The pervious concrete is primarily cement and coarse aggregates, with little or no-fine aggregates. The size of aggregates gradation in pervious application varies from 19mm to 9.5mm. The cement to aggregate ratio varies from 1:4 to 1:10. Ordinary Portland cement has been generally used as major binder in making concrete. Industrial wastes like Fly Ash, blast furnace slag and Silica Fume are also used in addition to Portland cement as Supplementary cementitious material. Aspects such as rate of strength development, setting time and permeability also need to be studied for respective Supplementary cementitious material. The thickness of cementitious layer is in direct relationship with mechanical and hydrological properties of pervious concrete.

From past research studies it is seen that pervious concrete can be produced by varying the w/c ratio, a/c ratio, size of aggregate and binder material type. Mix proportions are selected from experimental basis; however, the numbers of proposed studies on mix design of pervious concrete are very less. As per ACI 522R, the Table 1 gives typical range of material used in the pervious concrete application. The water to cement ratio is in between 0.26 to 0.40. Proper water to cement ration is necessary for the sufficient bond between the aggregates, MCIA (2002). The porosity span between 25% and 35% which mainly depends upon the aggregate to cement ratio of the mix proportion Joshaghani et al. (2015). The pervious concrete is lightweight compared to normal concrete and density varies between 1600 and 1900 kg/m<sup>3</sup>.

**Table1. Summary of mix proportions used in pervious concrete in accordance with ACI-522 R.**

Items	Proportions (Kg/m <sup>3</sup> )
Cementitious Material	270 to 415
Coarse Aggregate	1190 to 1480
W/C	0.27 to 0.34
Aggregate to cementitious ratio	4 to 4.5:1
Fine and coarse aggregate ratio	0 to 1:1

## PRIMARY CHARACTERISTICS OF PERVIOUS CONCRETE

The porosity and density of pervious concrete depend upon the properties of aggregates which are in direct relation to aggregate to cement ratio and compaction effort applied, Ibrahim et al. (2014), Putman & Neptune (2011), Murray et al. (2014). Deo et al. (2010) found reduction in porosity with an increase in the compressive energy absorbed by compactive efforts in porous concrete mixtures. The size of pores increase with increase in size of aggregate. The mixes can have the similar porosity or identical porosity regardless of the nominal maximum size of aggregate used. The size of pores increase with large size aggregate (12.5) and large no of small pores in small size aggregate (4.75mm) and combination of large and small pores in (9.5mm). Cosic et al. (2015) reported that to produce large size pores, large aggregate could be used resulting into higher value of overall porosity but it also reduce the chance of clogging. Large amount of smaller size fraction (4-8 mm) increase the density and strength properties in porous concrete.

The strength of the pervious concrete is primarily controlled by nature of the cement paste (paste thickness and strength) and the interface between the paste and the aggregate. Many researchers have reported that higher compressive strength could be achieved for mixtures containing smaller size aggregate and increase in cement paste.

The compressive strength of range 3-40 MPa can be achieved in pervious concrete, but the common range is between 3 and 10MPa, Crouch et al. (2007), Cosic et al. (2015), Zhong & Wille (2016), Yang & Jiang (2003). The compressive strength increases with decrease in porosity, Kim & Lee (2010). The typical view of Pervious concrete is represented in Figure 2.



Fig.2 Close view of pervious concrete

### PERVIOUS CONCRETE PAVEMENT SYSTEM

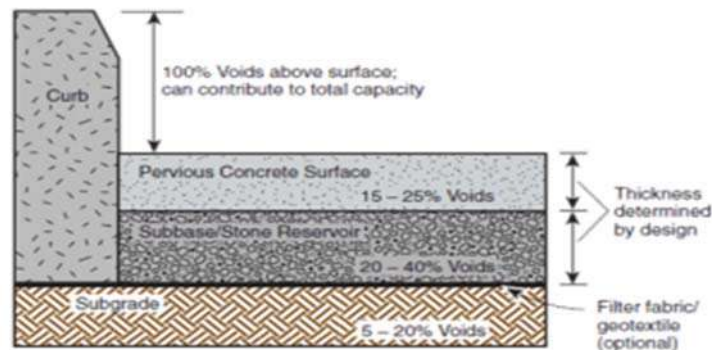


Fig. 3 Standard cross-section of Pervious concrete.

A standard cross section of pervious concrete pavement system has been shown in fig. 3. The top layer is pervious concrete layer (15-25% voids) of thickness four to six inches, second layer is permeable base of thickness 18 inches (20-40% voids) and last is permeable subgrade containing 5-20% voids, Tennis et al. (2004).

### CONCLUSIONS

Pervious concrete is in use since 1852 but in recent years, a lot of research studies have been carried out on it. Pervious concrete because of its ability to let water pass through it make it a valuable construction material for construction industry and environmental agencies for its ability in recharging ground water table. It is being highly used in pavement construction in USA and in Europe as a structural construction material, for walls in two story houses, load bearing walls for high rise buildings, infill panels for high rise buildings, roads, and parking lots. Along with major advantages, there are several limitations to usage of pervious concrete. Specific research is required to make it more usable for common applications. Regular maintenance of pervious pavement is required for proper functioning. In India, its testing is limited to R&D labs only and practical application is still not on the ground. Hence more practical research is required to be conducted to start using pervious concrete effectively and efficiently for diverse applications.

### ACKNOWLEDGEMENTS

Acknowledgments may be made to those individuals or institutions not mentioned elsewhere in the paper that made an important contribution.

### REFERENCES

- ACI (American Concrete Institute). (2011). "Report on Pervious concrete." ACI 522R-08, Farmington Hills, MI.
- Sonebi, M. , Bassuoni, M. , Yahia, A. (2016), "Pervious concrete: Mix Design, Properties and Applications", RILEM Technical Letters, 1 109 –115.
- Sreedhar, S., Biligiri, K. P.,(2017) "Comprehensive Laboratory Evaluation of Thermophysical Properties of Pavement Materials: Effects on Urban Heat Island", J. Mater. Civ. Eng., 04016026, DOI: 10 .1061/(ASCE)MT.1943-5533.0001531.
- Malhotra, V.M. (1976) No-Fines Concrete-Its Properties and Applications ACI Journal 73.11:628-644.
- Tennis, P., M. Leming and D. Akers (2004) "Previous Concrete Pavements", Portland Cement Association.

- Li J, (2009), "Mix design of pervious recycled concrete". In: Presented at the Geo Hunan international conference, Changsha, China, June, 2009.
- Zheng, M., Chen, S. and Wang, B. (2012), "Mix Design Method for Permeable Base of Porous Concrete". *Int. J. Pavement Res. Technol* Vol.5 No. 2102-107.
- Schaefer, V. R., Wang, K., Suleiman, M.T., Kevern J.T. (2006) "Mix design development for Pervious concrete in cold climates", Technical report, IOWA Department of Transportation.
- Park, S., and M. Tia (2004) "An Experimental Study on the water-Purification properties of porous Concrete". *Cement and Concrete Research* 34: 177–184.
- Joshaghani, A., Ramezani-pour, A., Ataei, O., Golroo, A., "Optimizing Pervious concrete pavement mixture design by using the Taguchi method". *Constr. Build Mater.* 101 (2015) 317–325.
- Ibrahim, A., Mahmoud, E., Yamin, Moh., Patibandla, V. C., (2014) "Experimental study on Portland cement Pervious concrete mechanical and hydrological properties", *Constr. Build Mater.* 50 524–529.
- Putman, B.J., Neptune, A.I. (2011) "Comparison of test specimen preparation techniques for Pervious concrete pavements", *Constr. Build Mater.* 25) 3480–3485.
- Murray, C. A., Snyder, K.S., Marion, B.A. (2014) "Characterization of permeable pavement materials based on recycled rubber and chitosan". *Constr. Build Mater.* 69 221–231.
- Deo, O., Neithalath, N., (2010) "Compressive behavior of Pervious concrete and a quantification of the influence of random pore structure features", *Mater Sci Eng* 528 402–412.
- Cosic, K., Korat, L., Ducman, V., Netinger, I., (2015)" Influence of aggregate type and size on properties of pervious concrete", *Constr. Build Mater.* 78, 69–76.
- Kim, H.K., Lee, H.K., (2010)"Influence of cement flow and aggregate type on the mechanical and acoustic characteristics of porous concrete", *Applied Acoustics* 71 607–615.
- Crouch, L.K. , Pitt, J., Hewitt, (2007)"Aggregate effects on pervious Portland cement concrete static modulus of elasticity". *J Mater Civ Eng.*, 19, 561–568.
- Zhong, R., Wille, K., (2016)"Compression response of normal and high strength Pervious concrete", *Constr. Build Mater.* 109, 177–187.
- Yang, J., Jiang, G., (2003) "Experimental study on properties of Pervious concrete pavement materials". *Cement and Concrete Research*, 33, P381–386.
- Avishreshth, A. K., Chandrappa, A., Prasanna, V. S., Biligiri, K. P., (2017) "Sustainable Solution to Mitigate Waterlogging and Flashfloods in Urban Conglomerates", [www.ncbw.com](http://www.ncbw.com)
- Mississippi Concrete Industries Association (MCIA). (2002) Pervious concrete: The pavement that drinks <http://www.mississippiconcrete.com>.
- Sharma, P.C.,(2008) "Pervious concrete for low volume Traffic Pavements-National Seminar on Highway Development"-Design, const, operation and Repairs-Lucknow-16thNov, 08.



## Recent Aspects of Municipal Solid Waste Management of Allahabad, India

Himanshu Yadav,<sup>1</sup> and V. P. Singh,<sup>2</sup>

<sup>1</sup>Research Scholar, Department of Civil Engineering, Indian Institute of Technology Guwahati, Guwahati, Assam; e-mail: [yadav.himanshu1234@gmail.com](mailto:yadav.himanshu1234@gmail.com) , Corresponding Author

<sup>2</sup> Assistant Professor, Department of Civil Engineering, Motilal Nehru National Institute of Technology Allahabad, Allahabad, Uttar Pradesh; e-mail: [vps15783@mnnit.ac.in](mailto:vps15783@mnnit.ac.in)

### ABSTRACT

With the rapid growth in population and urbanization, the generation of waste in Indian cities has increased. Improper solid waste management causes various hazards to the inhabitants. Qualitative and quantitative characteristics of the MSW are studied. The office of Allahabad Municipal Corporation was contacted for recent information. Data from some government websites and literatures are also studied. Various information of different zones, their wards and quantity of waste from each zone is estimated. Allahabad MSW is divided into 5 zones, which further divided into 80 wards. Recent population trends, Administrative setup of Municipal Corporation responsible for waste management, composition of domestic waste, commercial and institutional waste and waste from vegetable shop and restaurants of Allahabad city and status of waste disposal are studied.

**KEYWORDS:** *Waste management; Solid waste; Waste composition; Waste disposal; Allahabad.*

### INTRODUCTION

Rapid industrialization and tremendous population growth in India has led to the migration of peoples from villages to the cities and results in the generation of large quantity of municipal solid waste. India is the second most populous country in the world. The management of solid waste is going through a critical stage due to larger quantity of waste and non-availability of the facilities for treatment and disposal of solid waste in various cities. Improper disposal of solid waste causes various hazards to the environment and human health. It causes pollution in groundwater, surface water, air, soil contamination and loss of vegetation etc. (B. Jhamnani and SK Singh, 2009; Vijaya Singh and A.K. Mittal; 2009; A.O. Aderemi and T.C. Falade; 2012; S. M. Ali et al; 2014). MSWM is the one of the major environmental problem in Indian cities. Proper management requires construction and installation of facilities. This becomes expensive and and complex due to unplanned growth of urban areas (M. Sharholly et al., 2007a). Therefore, the present study aims to determine the composition of mixed waste, domestic waste, commercial and industrial waste, waste from the vegetable and restaurants, quantity of waste from various zones and wards, administrative setup of municipal corporation responsible for waste management in Allahabad.

### STUDY AREA

The city of Allahabad is among largest cities of eastern Uttar Pradesh and situated at the confluence of three rivers – Ganga, Yamuna and the invisible Saraswati (City Profile, AMC). The Allahabad city is connected to Varanasi and Kanpur by NH-2 at distance of 116 km and 187 km respectively. Allahabad is enclosed by Pratapgarh and Jaunpur in North, Mirzapur and Varanasi in East, Banda and Fatehpur in West. Southern boundary separates it from Madhya Pradesh (AMC, 2017). It is one of the four sites of Kumbha Mela. Allahabad city has an area of 82 km<sup>2</sup>. The city has population of about 12, 71,000 inhabitants (AMC 2017). Management of solid waste generated by city is done by Allahabad Municipal Corporation (AMC). The city is divided into 5 administrative zones, which are further divided into 80 wards. There are around 1, 88,406 household in the city of Allahabad. Allahabad receives approximately 1076 mm rainfall annually have approximately 108 rainy days annually.

### POPULATION TRENDS OF ALLAHABAD CITY

Allahabad's population growth in 2011 was 14.06 %. Population growth of Allahabad city is shown in Table 1 (Census of India, 2011).

**Table 1. Population trend of Allahabad city**

Census Year	Population	Decadal change	Growth rate (%)
1971	5, 13, 036		
1981	6, 50, 070	1, 37, 034	26.71
1991	8, 44, 546	1, 94, 476	29.92
2001	9, 75, 393	1, 30, 847	15.49
2011	11, 12, 544	1, 37, 151	14.06

Population density of Allahabad city is 157 persons per hectare. Ward 78 has highest population density of 1115, followed by ward 61 with population density of 825. Ward 24 and ward 43 has the lowest population density of 22 persons per hectares. Ward 76 has the maximum population of 28, 852 individuals and ward 48 has the minimum population of 5, 173 individuals. (AMC, 2015).

### WASTE GENERATION UNITS

Allahabad city is divided in five zones, which is further divided in 80 sanitary wards (Table 2). Ward wise maximum and minimum waste is generated from ward 76 and ward 48 respectively and the amount of solid waste is 12.983 and 2.328 tons/day respectively. Waste generation from all the wards is shown in Figure 1. Zone wise waste generation is maximum for Zone 1 and minimum for Zone 5 and the quantity is 184.24 and 40.97 tons/day respectively. Waste generation from all five zones of Allahabad is shown in Figure 2.

**Table 2. Zone wise wards of Allahabad city (AMC, 2017)**

Zone	Ward No.	Number of Wards
Zone 1	1, 3, 13, 49, 29, 15, 16, 20, 35, 63, 57, 80, 72, 52, 76, 40, 33, 64, 34, 78, 77, 19, 8	23
Zone 2	62, 65, 69, 70, 51, 58, 73, 79, 66, 71, 75, 47, 60, 68, 74	15
Zone 3	26, 9, 21, 17, 6, 32, 4, 10, 45, 14, 39, 27, 22, 5, 43, 38, 30, 31, 28, 2, 48, 54, 7, 18	24
Zone 4	24, 23, 67, 37, 12, 41, 25, 44, 61, 55, 59, 56, 53	13
Zone 5	36, 46, 50, 42, 11	5

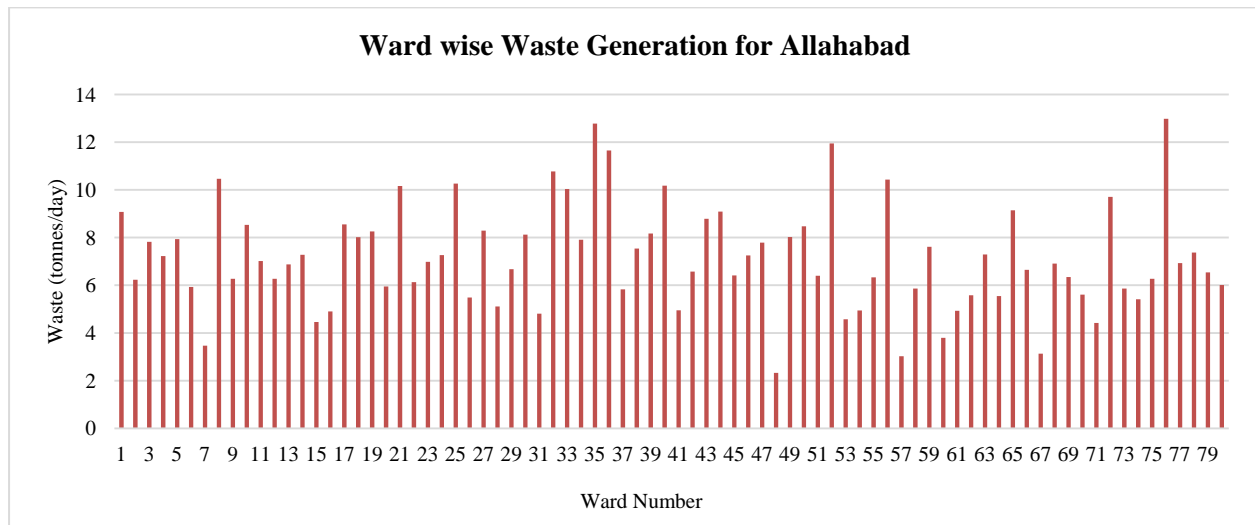


**Fig. 1 Ward wise waste generation for Allahabad (AMC, 2017)**

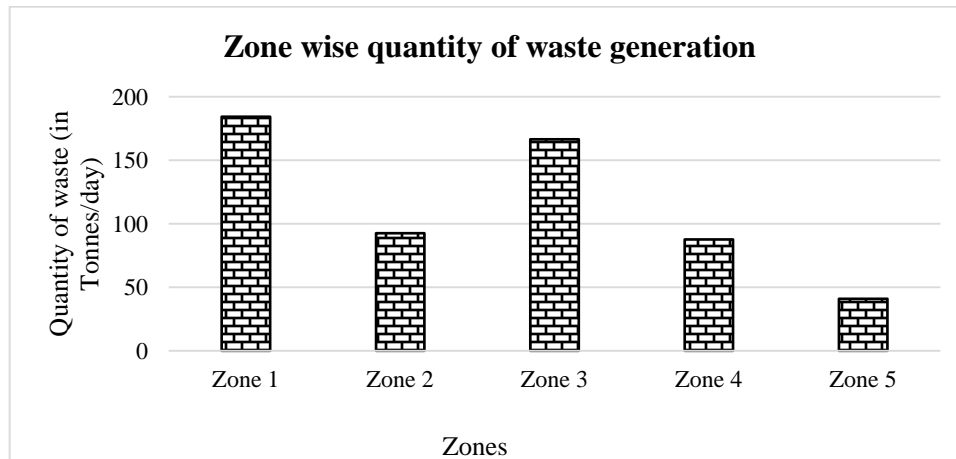


**Fig. 2 Zone wise quantity of waste generation for Allahabad**

### **ADMINISTRATIVE SETUP OF MUNICIPAL CORPORATION**

Allahabad Nagar Nigam is responsible for solid waste management of Allahabad city. The Mayor of Allahabad is the elected head of Allahabad Nagar Nigam. There are various functional departments under the administration of the Mayor i.e. Health and Engineering, Accounts, Animal husbandry, Street light, Tax department etc. (S. Saxena et al, 2010). Health and Engineering Departments working under Municipal Commissioner are directly associated to the Municipal Solid Waste Management. Organizational structure of Allahabad Nagar Nigam is shown in Figure 3.

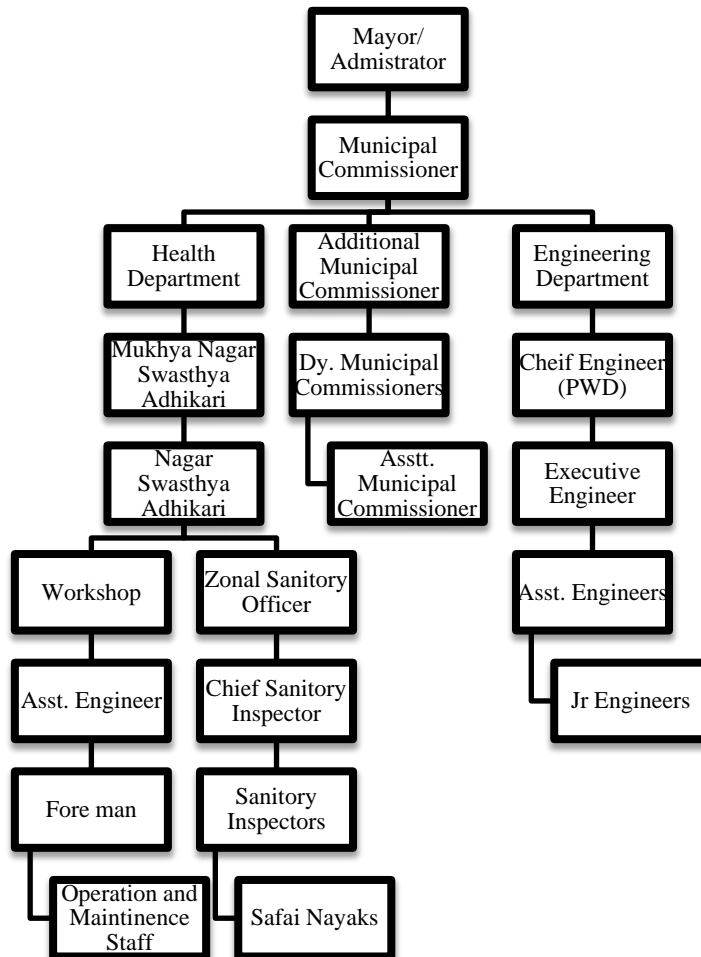


Fig. 3 Organizational Structure of Allahabad Nagar Nigam responsible for Solid Waste Management

### SOURCES AND COMPOSITION OF MUNICIPAL SOLID WASTE

Waste from the Allahabad city is approximately 572 ton per day. The average generation of solid waste is 450 grams per capita per day (AMC, 2015). The percentage of Municipal Solid waste generated from various sources for Allahabad city as shown in Table 3. (M. Sharholly et al. 2007b). The city generates the approximately 572 ton per day of municipal solid waste.

Table 3 MSW Sources of Allahabad (Sharholly, M. et al. 2007b)

Sources of waste in Allahabad	Percentage
Household	40
Restaurants	27.2
Street sweeping	9.1
Market	9.0
Shops and workshop	6.1
Offices	5.8
Hospitals	1.5
Hotels	1.3
Total	100

The solid waste generated in Allahabad comprises of paper, textile, food and vegetables, dry matter, wooden pieces , green matter, brick, glass, soil dust, metal, dry matter, medical waste and plastic etc. Data of composition of waste is obtained from Allahabad Municipal Corporation (AMC, 2017). Composition of domestic waste, composition of commercial and institutional waste, composition of vegetable and restaurants waste and composition of mixed waste is shown in Fig. 4 – 7.

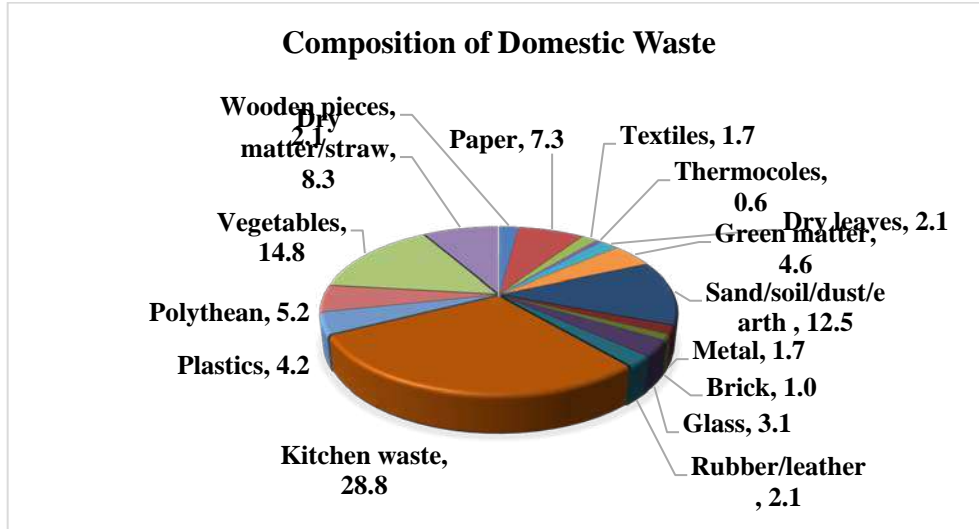


Fig. 4 Composition of domestic waste of Allahabad (AMC, 2017)

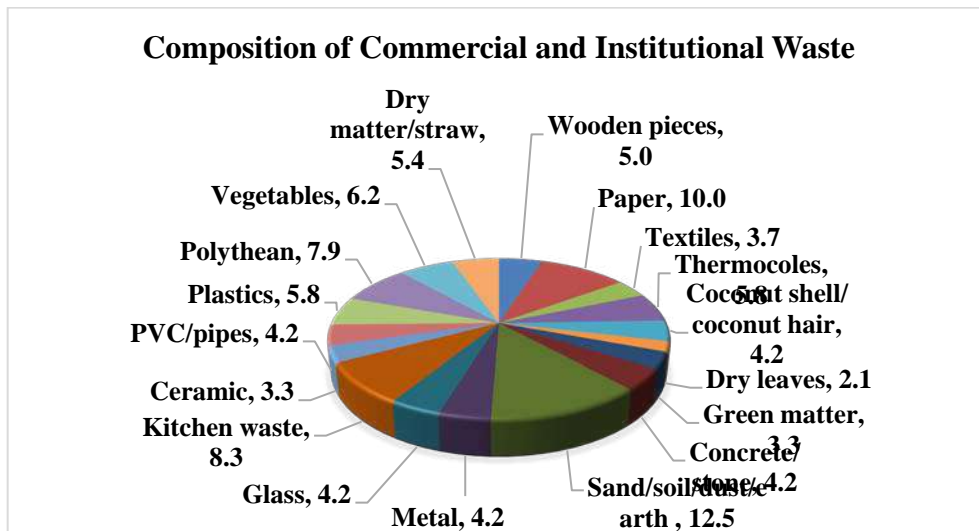


Fig. 5 Composition of Commercial and Institutional Waste of Allahabad (AMC,2017)



Fig. 6 Composition of waste from vegetable shops and restaurants (AMC, 2017)

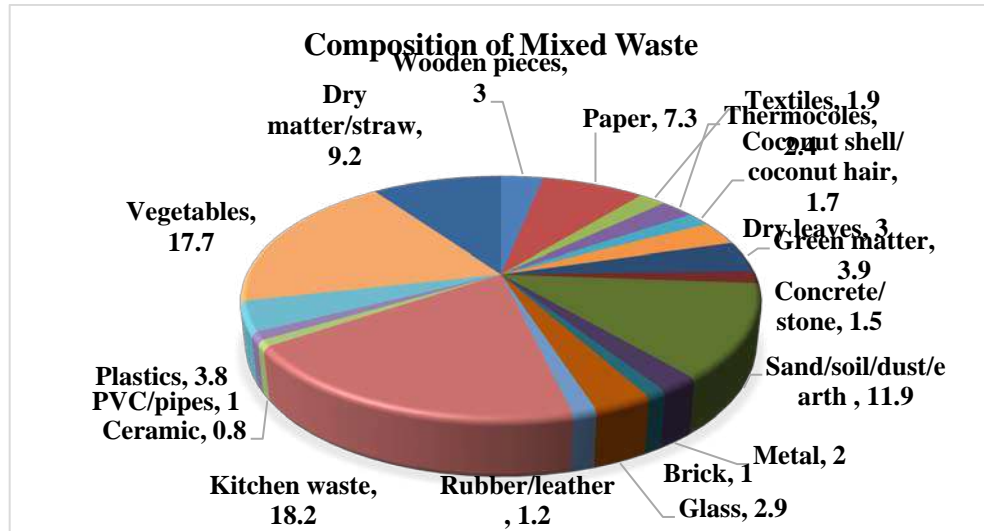


Fig. 7 Composition of mixed waste of Allahabad (AMC, 2017)

### STATUS OF DISPOSAL SYSTEM

Unsegregated waste is transported to the treatment site in Baswar. Site is located at a distance of 19 km from the city on area of 25 hectares. Facility comprises of 500 TPD mechanical composting plant and a landfill site maintained by AMC.

At present, an engineered landfill at Baswar is used for disposal of MSW. But Allahabad city has various dumpsites (M. Sharholy et al, 2007b), some of them are shown in Figure 8.

Phaphamau dumpsite is located on Allahabad – Lucknow highway, near the Ganga Bridge in Allahabad. This dumpsite is small, having an area of 0.6 hectare and height of 8.5 meters. This site is in low-lying area near the Ganga River. Bakshi Band dumpsite is located near chhota bhagara colony in Allahabad. This site lies near the Ganga River and has an area of 5.5 hectares and height 10 meters. The Allahabad city has various other small dumpsites.

Suitable closure of these sites need to be planned. Various alternatives for the closure of old dump sites are identified as local soil cover, MSW cover, HW cover, HW cover with gas recovery, HW cover with gas recovery and GW extraction, waste into new landfill and mining and processing of old waste and rejects into new landfill (Datta and Kumar, 2015). Suitable method of closure of old dump site can be planned based on hazard posed by the dumpsites.

Bio-medical waste collected from Allahabad is treated at a common facility for Allahabad and neighboring district

Pratapgarh at Maheva Murabpatti, Mirzapur. The treatment capacity is 60 kg/hour (AMC, 2015).



**Fig. 8 Illegal dumpsites of Allahabad**

## CONCLUSIONS

The study presents the recent scenarios of MSW management of Allahabad city, which will be helpful in creating awareness among the peoples and it can provide relevant information to the environmental engineers, researchers and decision makers about MSW management, which is required for improvement and future planning.

Overall waste generated from Allahabad city is 572 TPD. Maximum waste is generated from Zone 1 and minimum from Zone 5 and the amount is 184.24 and 40.97 tons/day respectively. Ward wise maximum and minimum waste is generated from ward 76 and ward 48 respectively and the amount of solid waste is 12.983 and 2.328 tons/day respectively.

The community should be aware about the importance of source segregation at the generation point as biodegradable, inert and recyclables for proper waste management. Segregation of waste at the source should be encouraged.

Technical assistance from various academic institutions (like MNNIT Allahabad, IIT Kanpur and IIT BHU etc.) should be encouraged.

Major portion of waste is generated from residential, restaurants, markets, street, offices, shops and workshops.

Suitable closure of illegal dumpsites of the city should be done by considering relative hazard caused dumpsites to the groundwater, surface water and air.

## ACKNOWLEDGEMENTS

Author wants to acknowledge the support from the environmental engineer, Allahabad Nagar Nigam (AMC) for providing with the required information.

## REFERENCES

- Allahabad Municipal Corporation AMC, (2017). Allahabad Nagar Nigam, Uttar Pradesh, India, unpublished data.
- Saxena S., Srivasatava R.K., and Samaddar A.B., (2010). Towards sustainable municipal solid waste management in Allahabad City. *Management of Environmental Quality: An International Journal*, Vol. 21 Issue: 3, pp.308-323, <https://doi.org/10.1108/14777831011036876>
- Jhamnani, B., and Singh, S. (2009). Groundwater contamination due to Bhalaswa landfill site in New Delhi. *International Journal of Environmental Sciences and Engineering*, 121-125.
- Singh V., and Mittal A.K., (2009). Toxicity Analysis and Public Health Aspects of Municipal Landfill Leachate: A Case Study of Okhla Landfill, Delhi. 8th World Wide Workshop for Young Environmental Scientists WWW-

- YES 2009: Urban waters: resource or risks? 2-5 June 2009.
- Aderemi, A.O., and Falade, T.C., (2012). Environmental and health concerns associated with the open dumping of Municipal solid waste: A Lagos, Nigeria Experience. *American Journal of Environmental Engineering*. 2012; 2(6): 160-165.
- Ali, S.M., Pervaiz, A., Afzal, B., Hamid, N., and Yasmin, A., (2014). Open dumping of Municipal solid waste and its hazardous impacts on soil and vegetation diversity of waste dumping site of Islamabad city. *Journal of King Saud University-Science* (2014)26, 59-65.
- Sharholly, M., Ahmad, K., Mahmood, G., and Trivedi, R.C., (2007). Municipal solid waste management in Indian cities – A review. *International Journal of Waste Management*. doi:10.1016/j.wasman.2007.02.008
- Sharholly, M., Ahmad, K., Vaishya, R. C. and Gupta, R.D. (2007). Municipal solid waste characteristics and management in Allahabad, India. *International Journal of Waste management*. doi:10.1016/j.wasman.2006.03.001
- Datta, M. and Kumar, A. (2015). Hazard rating of MSW dumps and geoenvironmental measures for closure. 50<sup>th</sup> Indian Geotechnical Conference 17<sup>th</sup> – 19<sup>th</sup> Dec. 2015. Pune, India.
- City Development Plan, 2015 for Allahabad city, (AMC, 2015).



## Surface Jet Aerators in Waste Water Treatment: A Comprehensive Review

Anit Raj Bhowmik<sup>1#</sup> and Bishnu Kant Shukla<sup>2\*</sup>

<sup>1</sup>School of Civil Engineering, Lovely Professional University, Phagwara, Punjab-144411, E-Mail: [anitrajbhowmik@gmail.com](mailto:anitrajbhowmik@gmail.com)

<sup>2</sup>School of Civil Engineering, Lovely Professional University, Phagwara, Punjab-144411, E-Mail:

[bishnukantshukla@gmail.com](mailto:bishnukantshukla@gmail.com) \*Corresponding author; #Presenting Author

### ABSTRACT

Aeration is a major process of waste water treatment. There are many types of aerators available out of which, mechanical surface jet aerators have been found to be most efficient and easy to operate. These aerators constitute a closed system and are simple in construction as well as working. Out of many types of surface jet aerators available, solid jet, hollow jet and expansion types aerators are frequently used. There have been many works on such types of aerators but a little study is available which may compare different types of aerators and suggest a particular type of aerator under a given situation. A number of studies have been included in this paper which comprise of single and multiple solid plunging jet aerators having circular, elliptical, rectangular, square and rectangular shaped having rounded edges, hollow jet aerators with different inclinations and expansion type aerators. It was observed that elliptical shaped solid jet aerators have maximum penetration into the pool which is most suitable for deep tanks where as hollow jet aerators having 60° plunge angle are best suited for shallow tanks. It was also concluded that solid jet aerators having eight rectangular shaped openings with rounded ends demonstrate highest oxygen transfer efficiency. However, aerators with single opening are most effective for lower discharges whereas aerators having multiple openings are suited for higher discharges. At the end, different types of aerators were compared on the basis of their performances and appropriate aerators were suggested for diverse types of flow and discharge conditions.

**KEYWORDS:** *Jet Aerator; Oxygenation Efficiency; Wastewater Treatment; Oxygen Transfer; Wastewater Treatment*

### INTRODUCTION

Oxygenation is a major step during waste water treatment process. There are several processes of oxygenation in which, surface jets aerators have proved to be cost effective and efficient. A water jet always forms a double-phased region when it plunges into pool after passing through atmosphere which has considerable air-water interfacial area. The process is named as plunging jet aeration in which aerodynamic and hydro-dynamic forces interact between jet of water with ambient atmospheric air. Plunging jets are used for floatation and floatation during wastewater and water treatment, plunging columns, bio-reactors, to increase gas-liquid transfer, minerals' bubble floatation, in cooling systems of power plants (Leung *et al.*, 2006), aerated filters, dipping beakers fermentation and waterfall etc. (Chanson *et al.* 2004; Bin, 2003). Application of dropping jets for aeration is considered a elegant way to get oxygenation as compared to other methods due to several reasons (Bin, 1993), because in such a method, no requirement of air compressor arises (Emiroglu and Baylar, 2003). Plunging water jet system produces a "closed system" which facilitates complete utilization of oxygen and volatile reactants. The system is very easy to design and operate. Also, it does not require any additional aeration device as water jet accomplishes mixing and aeration both. As a result of these advantages, aeration by such a method has become popular in recent years.

Mass transfer mechanism was center of study recently for many authors (van de Sande and Smith, 1975; Tojo *et al.* 1982; Bin and Smith, 1982; Ohkawa *et al.* 1986; Funatsu *et al.* 1988). Further, study has already been done on effect of liquid property on air transfer rate (Bonsignore *et al.* 1985) into water pool by aerators and in biological reactors (Yamagiwa *et al.* 2001; Leung *et al.* 2006). Many empirical reactions were suggested by researchers as a result of their study out of which the simplest relationships (Bin and Smith, 1982, Tojo *et al.* 1982) are given by Eq. 1, 2 and 3 respectively.

$$K_L a_{(20)} = 3.1 \times 10^{-4} + 4.85 \times 10^{-2} v_j^3 d_j^2 \quad (1)$$

$$K_L a_{(20)} = 9 \times 10^{-5} P \quad (2)$$

$$K_L a_{(20)} = 0.029 \times (P/V)^{0.65} \quad (3)$$

Where  $K_L a_{20}$  denotes volumetric oxygen-transfer factor at standard condition ( $m^3/h$ );  $v_j$  represents velocity of jet at exit end ( $m/s$ );  $d_j$  represents jet's diameter ( $m$ ) and  $(P/V)$ , jet power per unit volume ( $kW/m^3$ ). Thus a great deal of useful information is accessible on the falling water jet's oxygen-transfer characteristics. Majority of the researchers concluded

that there are mainly four factors which govern oxygenation by a dipping water jet and these are diameter of jet, velocity of jet, jet power (which depends on diameter of jet and its velocity) and angle of jet w.r.t. vertical axis. Though, shape of opening of aerator also affects its performance to a very great extent in oxygenation system.

As it was observed that researchers mostly carried out study on conventional type shapes of water jets, there have been efforts recently to study the effect of shapes and amount of entrainment of air by two dimensional jets (Chanson and Brattberg, 1998), air entry by oval (Shukla *et. al.*, 2018b) and rectangular (with circular ends) plunging jets (Begatur *et al.* 2002; Shukla and Goel, 2018) and ventury shaped circular jets (Emiroglu and Baylar, 2003).

In the current paper, the earlier works done on plunging jet aeration techniques have been critically reviewed and were compared based on oxygen transfer rates and efficiencies as compared to traditional aeration methods and untouched areas were recognized to facilitate new research works.

## THEORY OF OXYGEN TRANSFER BY WATER JET

The plunging or falling jet aeration system produces a “closed” system where it can safely be assumed that there is perfect mixing of liquid phase and a plug flow in the flow-movement pipe (Bin, 1993). In such a case, oxygen transfer factor (volumetric) may be given (achieved by integration of oxygen equilibrium equation) as by Eq. 4.

$$K_L a = (1/t) \ln [(C_s - C_o)/(C_s - C_t)] \quad (4)$$

In Eq. 4,  $C_o$  represents the dissolved oxygen (DO) concentration of water in the tank at the beginning and  $C_t$  after time  $t$  in the process of aeration, respectively with  $C_s$  being DO concentration at saturation;  $K_L a$  is the oxygenation coefficient (volumetric) which depends on temperature and is represented as in Eq. 5 (.Daniil and Gulliver, 1988).

$$K_L a_{(20)} = K_L a_{(T)} \times (1.024)^{(20-T)} \quad (5)$$

Where  $K_L a_{(T)}$  shows the term known as oxygen transfer factor or co-efficient at the temperature of  $T^\circ\text{C}$  (expressed in  $\text{s}^{-1}$ ) and  $K_L a_{(20)}$  shows the term known as the similar co-efficient at the standard condition (expressed in  $\text{s}^{-1}$ ),  $T$  being the temperature of the water (in  $^\circ\text{C}$ ).

The oxygen-transfer performance of plunging jets is communicated by Eq. 6 in the terms of OTE ( $\text{kgO}_2/\text{kWh}$ ).

$$OTE = \frac{O_R V}{P} \quad (6)$$

Where oxygen-transfer ( $\text{mg/L/h}$ ) at  $20^\circ\text{C}$  is denoted by  $O_R$  at one atmospheric pressure (standard condition);  $P$  denotes jet power ( $\text{kW}$ ). The parameters are calculated as in Eq. 7 and 8 respectively.

$$O_R = K_L a_{(20)} \times 3600 \times C_s^* \quad (7)$$

$$P(\text{in kW}) = \frac{1}{2(\rho Q v_j^2)} \times 10^{-3} = \frac{\pi}{8} \times (\rho n d_j^2 v_j^3) \times 10^{-3} \quad (8)$$

Where, saturation concentration of DO at the standard condition in water ( $\text{mg/L}$ ) is shown by  $C_s^*$ ;  $\rho$  shows density of water ( $\text{kg/m}^3$ );  $v_j$  depicts velocity of jet ( $\text{m/s}$ );  $d_j$  represents jet diameter ( $\text{m}$ ) and  $Q$  shows jet discharge ( $\text{kg/m}^3$ ). In the subsequent sections, details of a variety of surface jet aerators are reviewed.

## A. SINGLE PLUNGING JET AERATOR

Single plunging jet aerators have been examined under subsequent segments:

### (1) Single Vertical Solid Plunging Jet Aerator

According to latest works on plumb plunging jet having various width, input power, velocities as changeable parameter (Deswal, 2009), it was concluded that  $K_L a_{(20)}$  rises outstandingly with rise in the value of  $v_j$  and for constant velocity, jets having more thickness produce higher  $K_L a_{(20)}$  values. Also, it was noticed that jet power per unit volume increases,  $K_L a_{(20)}$  also rises in all tests. Standard oxygen transfer co-efficient value can be expressed, integrating the compound

effects of thickness and velocity as expressed in Eq. 9

$$K_L a_{(20)} = 0.103n^{0.81}v_j^{2.11}d_j^{1.43} \quad (9)$$

In above equation,  $n$  represents count of openings of jet, which is one in current scenario. Further, as a result of careful observations, it was found that OTE decreases with increase in jet power per unit volume which was in the range of 1.91-10.04 kgO<sub>2</sub>/kWh. As a result of recent study (Shukla *et.al.*, 2018) on elliptical shaped solid jet aerator, it was observed that elliptical shaped aerators depicted oxygen transfer value equal to  $9.52 \times 10^{-2-1}$  for flow area of 50.65 mms<sup>2</sup> at a velocity of 11.82 m/s corresponding to jet length of 470 mm and OTE of 16.18 kgO<sub>2</sub>/kW-hr for flow area of 75.97 mm<sup>2</sup> at jet velocity of 1.21 m/s corresponding to jet length of 470 mm.

## (2) Single Conical Hollow Plunging Jet Aerator

As a result of exhaustive study,  $\pi/3$  was found to be optimum angle for aeration (Tojo *et al.* 1982) and based on this, several works were carried out (Deswal and Verma, 2007; Ranjan, 2007) for plunging jet aerators with cone angle  $\pi/3$  and varying annular thickness ( $t_j$ ), input power and velocity as changeable parameter in the models of aerators which showed that  $K_L a_{(20)}$  rises drastically with rise in  $v_j$  where more the thickness of jet implied more achievement in the value of  $K_L a_{(20)}$ . With the rise in power per unit volume,  $K_L a_{(20)}$  also showed rising trend in all setups of experimental process. Upon the application of multivariate linear-regression, an empirical relationship was developed for  $K_L a_{(20)}$  for aerator having  $\pi/3$  plunge angle and other parameters of jet, P (i.e.,  $v_j$  and  $t_j$ ) (Deswal and Verma, 2007) expressed in Eq. 10

$$K_L a_{(20)} = 0.023 \times v_j^{1.98} t_j^{1.43} \quad (10)$$

The values obtained in Eq. 10 when plotted using SVM technique, it showed a dispersion of  $\pm 15\%$  with agreement line (Deswal and Verma, 2007). In the current case, optimum oxygenation factor equal to 9.0 l/s for discharge of 3.6 l/s with velocity equal to 4.78 m/s for aerator making  $\pi/3$  angle w.r.t. vertical axis (Ranjan, 2007) was observed. Another work on hollow conical aerator having angle  $\pi/3$  w.r.t. vertical axis showed OTE to be equal to 2.56-10.73 kg-O<sub>2</sub>/kW-hr (.Deswal and Verma, 2007).

## (B) SUDDEN EXPANSION TYPE JET AERATOR

Significantly elevated magnitude of  $K_L a_{(20)}$  was demonstrated by rapid expansion-type aerators. A rapid expansion-type aerator with span of 0.95 cm corresponding to discharge of 0.21 l/s to 0.33 l/s under customary settings was experimented (Pillai *et al.* 1971) and uppermost assessment of OTE was achieved to be 2.13 kgO<sub>2</sub>/kWh. Additional modified aerator depicted highest oxygenation factor of 2.06 l/s for discharge of 3.1 l/s, velocity of 1.9 m/s and aspiration rate of air equal to 7.5 liters/min (Ranjan, 2007). In this work, it was shown that at more discharges or for larger device, OTE rises. In this setting,  $K_L a_{(20)}$  was found to increase with rise in velocity of jet for all the discharges and for constant jet velocity, with rise in the magnitude of discharge.

## (C) MULTIPLE PLUNGING JET AERATORS

There have been several studies on multiple jets and the findings of major studies are presented in subsequent subsections.

### (1) Vertical Multiple Solid Jet Aerators

Many combinations in terms of varying numbers of jets showed that multiple jets depicted higher oxygenation as well as efficiency than single plunging jets under comparable conditions. Study on three aeration devices (single, jet with two units and jet having three units) having two jet thicknesses of 20 and 25 mm corresponding to discharges in the range of 2.0-12.5 l/s (Gupta *et al.* 2012) showed that OTE and  $K_L a_{(20)}$  parameters were found to be much more for jets with double aeration units than single unit jet and jet having three aeration units corresponding to discharge varying from 3.25 to 10.40 l/s, furthermore, at significantly less discharges, single jet aerators outperformed multiple jet aerators. Again, another study included aerators in four sets with one, four, eight and sixteen units (Deswal and Verma,

2007) for varying power, jet velocities, and discharges, and there was considerable effect of number of jet on O.T.E and  $K_L a_{(20)}$ . These parameters rise with rise in velocity corresponding to whole range of discharges and for constant jet velocity ( $v_j$ ), rise with rise in jet number ( $n$ ). An empirical relations showing relation of number of jets, velocity and jet diameter with  $K_L a_{(20)}$  was derived as in Eq. 11 (Deswal and Verma, 2007):

$$K_L a_{(20)} = 0.113n^{0.84}v_j^{2.14}d_j^{1.53} \quad (11)$$

Relationship shown by Eq. 11 showed a scatter of  $\pm 15\%$  with line of agreement. The highest OTE for multiple plunging devices was found to lie between 6.0 and 21.3 kg-O<sub>2</sub>/kW-hr (Deswal and Verma, 2007). As a result of exhaustive works on multiple solid rectangular shaped jet aerators having opening with rounded boundaries (Shukla and Goel, 2018), it was found that aerators having eight openings produce highest oxygen transfer of  $2 \times 10^{-2} \text{ s}^{-1}$  at a discharge of 4.69 l/s while aerator having single opening produced OTE equal to 21.53 kg-O<sub>2</sub>/kW-hr at a discharge of 1.11 l/s.

## (2) Inclined Multiple Solid Jet Aerators

Study was carried out on multiple inclined jets having  $\pi/3$  plunge angle (Deswal, 2008). Study on several combinations with different number of jets (1, 4, 8 and 16) was done and compared with other types of aerators having plumb jets under same condition. The study revealed greater values of  $K_L a_{(20)}$  for inclined aerator having multiple openings as compared to vertical jets for same value of jet power (P/V). Further, it was found that  $K_L a_{(20)}$  rises with rise in number of jets ( $n$ ), rise in power per unit volume (P/V) and rise in velocity ( $v_j$ ) as per Eq. 12, empirical equation was generated for multiple inclined jet aerator making angle  $\pi/3$  w.r.t. vertical axis, between different jet parameters (i.e.,  $n$ ,  $v_j$ ,  $d_j$ ) and  $K_L a_{(20)}$  (Deswal, 2008):

$$K_L a_{(20)} = 0.103n^{0.81}v_j^{2.11}d_j^{1.43} \quad (12)$$

In the above relationship, velocity of jet is denoted by  $v_j$  and  $d_j$  denotes diameter of jet. Conclusion revealed that by increasing (P/V), OTE diminishes. Also, O.T.E usually rises with rise in  $n$ , however at low value of (P/V), multiple jet aerator with 16 jets showed diminishing tendency for O.T.E. As a result, conclusion was made that at a specified jet power, there exists optimal combination of multiplicity of openings, regarding  $n$  and  $d$  which is worked out by Eq. 12. Current study showed highest OTE was found to lie in between 8.2 and 24.5 kg-O<sub>2</sub>/kW-hr.

## (D) PLUNGING JETS WITH DIFFERENT GEOMETRIES

As a result of exhaustive study by a number of authors (Begatur *et al.* 2002; Singh *et al.* 2011) on several geometries of openings, which were, square, circular, rectangular nozzles with rounded edges, elliptical and rectangular, it was concluded that shape of the opening significantly affects the oxygen transfer factor, OTE and also depth of penetration of jet into pool. Elliptical shaped openings showed highest penetration depth whereas least depth was shown by rectangular shaped nozzle jets. On the other hand rectangular shaped aerators with rounded ends, aerators having square and circular openings were found to show these parameters in between above for a constant jet power per unit volume (Begatur *et al.* 2002). Aerators with rectangular aerators having rounded boundaries demonstrated highest magnitude of oxygen transfer rate for a specified jet power (which was 1.45 times the circular aerators) whereas circular aerators showed minimum OTE values. As a results of these studies, empirical relationships were developed (Singh *et al.* 2011) which are presented in Table 1.

**Table 1: Comparison of  $H_p$  and  $K_L a_{(20)}$  values for different shaped nozzles**

Sr. No.	Nozzle type	$H_p$ (penetration depth)	$K_L a_{(20)}$ (oxygen transfer factor)
1	Circular	$671(P/V)^{0.067}$	$0.096(P/V)^{0.69}$
2	Square	$630(P/V)^{0.071}$	$0.077(P/V)^{0.67}$
3	Rectangular	$570(P/V)^{0.067}$	$0.116(P/V)^{0.73}$
4	Rectangular having rounded edges	$632(P/V)^{0.067}$	$0.177(P/V)^{0.76}$

## COMPARISION OF DIFFERENT AERATORS

Upon comparison, it was concluded that elliptical and circular were fit for larger penetration depth ( $H_p$ ) but showed smaller values of oxygen transfer efficiency (O.T.E.). Further, with more perimeter and larger air water interfacial area, the aerators with rectangular shaped openings having rounded edges showed utmost magnitude of oxygen transfer efficiency and appropriate for big tanks. Prominent aerator models were compared and presented in Table 2.

**Table 2: Comparison of aerator models based on oxygenation efficiency**

Sr. No	Aeration device type	Opening geometry	Angle with vertical axis	No. of openings	O.T.E. (kg-O <sub>2</sub> /kW-hr)
1	Single plunge jet	Circular	-	1	0.92 to 3.90
2	Plunging type ventury device	Circular	-	1	2.20 to 8.80
3	Aerator with only vertical jet	Circular	90°	1	5.20-19.30
4	Aerator with hollow plunging jet	Circular	60°	1	1.91-10.04
5	Conical shaped plunging jet	Circular with diverging jet	60°	1	2.56-10.73
6	Aerator having vertical multiple plunging jet	Circular	90°	1-16	6.00-21.30
7	Aerator having inclined jet with multiple openings	Circular with diverging jet	60°	1-16	8.20-24.50
8	Rectangular Aerator having rounded edge	Rectangular with rounded edges	90°	1	1.45 times of circular jet under similar condition
9	Elliptical aerator having varying jet length	Elliptical	90°	1	2.05-16.18
10	Rectangular aerator with rounded edge	Rectangular with rounded edges	90°	1-8	1.27-21.53

## GAP AREAS IDENTIFIED

Following gap areas were noticed during the review of the past works related to waste water treatment using surface jet aerators:

- 1) Aerators models with circular or rectangular openings with rounded edges were tested with diversity in the counts of opening only. Aerators having other opening shapes like elliptical, rectangular, square etc. were not tested in groups by any authors (i.e., more than one jet in a single aerator).
- 2) Literatures on just three angles (30°, 45° and 60°) were found. No work is available for aerators with other angles. However, it was been proved, hypothetically, that aerator with jets making 60° angle with vertical axis produces highest oxygen transfer efficiency.
- 3) No exertion was made to consolidate distinctive geometric shapes in a single model of aerator.
- 4) No study was found where effect of common impedance of at least two number of aerators in a single model have been studied.
- 5) Air-water mixing may not be perfect and uniform as assumed.

## CONCLUSIONS

This study investigation numerous models of surface jet aerators having varying inclinations, opening outline, number of jets and as a result of this review, following conclusions may be drawn:

- Single vertical jet aerator showed minimum value of oxygen transfer efficiency equal to 1.91-10.04 kg-O<sub>2</sub>/kW-hr.
- Inclined aerator making 60° angle w.r.t. vertical axis with 16 numbers of jets showed highest oxygen conveyance efficiency of 8.2-24.5 kgO<sub>2</sub>/kWh.
- At low discharge ranges (up to 6.0 l/s) and deep tanks, single jet aerators outperformed multiple jet aerators but at higher discharges, reverse trend was obtained.
- Aerators with rectangular opening having rounded ends demonstrated overall highest OTE (1.45 times of aerator having circular, 1.68 times aerator having square and 1.36 times aerator having rectangular openings) shapes at comparable conditions of power per unit volume and discharge.

## REFERENCES

- Bagatur, T., Baylar, A., and Sekardag, N. (2002) The effect of nozzle type on air entrainment by plunging water jets, *Water Qual. Res. J. Canada*, 37, 599-612.
- Bin, A.K., (1993) Gas entrainment by plunging liquid jets, *Chem. Eng. Sci. J. Great Britain*, 48, 3585-3630.
- Bin, A.K. and Smith, J.M. (1982) Mass transfer in a plunging liquid jet absorber, *Chem. Engng. Commun.*, 15, 367-383.
- Bonsignore, D., Volpicelli, G., Campanile, A., Santoro, L. and Valentino, R. (1985) Mass transfer in plunging jet absorbers, *Chem. Eng. Process*, 19, 85-94.
- Chanson, H., Aoki, S. and Hoque, A. (2004) Physical modelling and similitude of air bubble entrainment at vertical circular plunging jets, *Chem. Eng. Sc.*, 59, 747-758
- Chanson, H., and Brattberg, T. (1998) Air entrainment by two-dimensional plunging jets: the impingement region and the very-near flow field, in *Proc. ASME FEDSM'98. Washington DC*, 1-8.
- Daniil, E.I. and Gulliver, J.S. (1988) Temperature dependence of liquid film coefficient for gas transfer, *J. Environ. Eng.*, 114, 1224-1229.
- Deswal, S. (2008) Oxygen Transfer by Multiple Inclined Plunging Water Jets, *proceedings of world academy of science, engineering and technology*, 29
- Deswal, S. (2009) Oxygenation by hollow plunging water jet, *Journal of the Institute of Engineering*, 7(1), 1-8.
- Deswal, S. and Verma, D.V.S. (2007) Air-Water Oxygen Transfer with Multiple Plunging Jets, *Water Qual. Res. J. Canada*, 42(4), 194-201.
- Deswal, S., & Verma, D. V. S. (2007). Performance Evaluation and Modeling of a Conical Plunging Jet Aerator, *World Academy of Science, Engineering and Technology, International Journal of Aerospace and Mechanical Engineering I*(11), 616–620..
- Emiroglu, M. E. and Baylar, A. (2003) Study of the influence of air holes along length of convergent-divergent passage of a venture device on aeration, *J. Hyd. Res.*, 41, 513-520.
- Funatsu, K., Ch. Hsu, Y., Noda, M. and Sugawa, S. (1988) Oxygen transfer in the water jet vessel, *Chem. Eng. Commun.*, 73, 121-139.
- Gupta, R., Ranjan, S. and Kalra, A.M. (2012) Performance of multiple plunging hollow jets, *Journal of Indian Water Resources Society*, 32(1- 2), 50-55.
- Leung, S.M., Little, J.C., Hoist, T. and Love, N.G. (2006) Air/water oxygen transfer in a biological aerated filter, *J. Environmental Eng.*, 132, 181-189.

- Ohkawa, A., Kusabiraki, D., Shiokawa, Y., Sakal, M. and Fujii, M. (1986) Flow and oxygen transfer in a plunging water system using inclined short nozzles in performance characteristics of its system in aerobic treatment of wastewater, *Biotech. Bioeng.*, 28, 1845-1856.
- Pillai, N. N., Wheeler, W. C. and Prince, R. P. (1971) Design and Operation of an Extended Aeration Plant, *J. WPCF*, 43(7).
- Ranjan, S. (2007) Hydraulics of hollow jet aerators, *Journal of Indian Water Resources Society* 27(1-2).
- Ranjan, S. (2007) Performance evaluation of expansion aerators, *Journal of Indian Water Resources Society*, 27(1-2).
- Singh, S., Deswal S. and Pal, M. (2011) Performance analysis of plunging jets having different geometries, *International Journal Of Env. Sciences*, 1(6), 1154-1167.
- Shukla, B. K., & Goel, A. (2018). Study on oxygen transfer by solid jet aerator with multiple openings. *Engineering Science and Technology, an International Journal*, 21(2), 255–260. <https://doi.org/10.1016/j.jestch.2018.03.007>
- Shukla, B. K., Rajesh Kumar, V., & Goel, A. (2018). Experimental Studies on the Effect of Variation in Jet Length on Oxygenation Performance of Elliptical Shaped Solid Jet Aerator, *Jour of Adv Research in Dynamical & Control Systems* 10(08-special issue), 1037–1044.
- Tojo, K., Naruko, N. and Miyanami, K. (1982) Oxygen transfer and liquid mixing characteristics of plunging jet reactors, *Chem. Eng. J. Netherlands*, 25, 107-109.
- Tojo, K. and Miyanami, K. (1982) Oxygen transfer in jet mixers, *Chem. Eng. J. Netherlands*, 24, 89-97.
- van de Sande, E. and Smith, J.M. (1975) Mass transfer from plunging water jets, *Chem. Eng. J. Netherlands*, 10, 225-233.
- Yamagiwa, K., Ito, A., Kato, Y., Yoshida, M. and Ohkawa, A. (2001) Effects of liquid property on air entrainment and oxygen transfer rates of plunging jet reactor, *J. Chem. Eng. Japan*, 34, 506-512.



## **A New Decision Support System for Assessing Bird-hit Hazard from municipal Waste Dumps**

Amit Kumar

Assistant Professor, Department of Civil Engineering, Dr. B R Ambedkar National Institute of Technology, Jalandhar - 144011, India. (corresponding author). E-mail: [amitrathi.ucf@gmail.com](mailto:amitrathi.ucf@gmail.com); Phone: +91-965-414-0757

R. K. Tomar

Associate Professor, Department of Civil Engineering, Amity University, NOIDA - 201313, India. Email: [rktomar67@gmail.com](mailto:rktomar67@gmail.com)

### **Abstract:**

Municipal waste sites having organic content attract birds and vultures, and in turn pose a major hazard to the aircrafts. As the existing rating systems do not have the provision of assessing bird-hit hazard, the study proposes a new rating system for hazard assessment. After developing the system, the system is evaluated based on the ratings obtained for a set of five hypothetical sites. Finally the new rating system is applied to five waste sites, selected from Indian cities. The system assigns distinct ratings for the five waste sites, indicating its usefulness.

Keywords: bird, accidents, Waste Dumps, municipal waste, Rating System

### **Introduction**

Municipal waste dumps cause a number of problems in their vicinity e.g. pollution of groundwater, surface water and air (Hafeez et al. 2016) (Jhamnani and Singh 2009), (Papadopoulou et al. 2007), odorous emissions (Shusterman 1992), waste slope failure (Blight 2008), bird-hit accidents involving aircrafts (USEPA 1971) and steep reduction in property prices (Farber 1998). Out of these hazards, bird-hit hazard may be given special importance because of the fact that if occurred, it results in hundreds of human fatalities and big loss of resources in terms of damage to the aircraft.

This study focuses on bird-hit hazard from waste dumps sites in developing countries and attempts to develop a novel decision support system. The system is designed to assist policy-makers in deciding the priority of closure of the waste dumps based on the relative magnitude of bird-hit hazard from these dumps.

### **Literature Review**

This section describes the literature review regarding aircraft accidents hit by birds and the role of waste dumps in these accidents.

#### **Accidents involving birds and aircrafts**

A number of accidents have been reported in the literature involving aircraft and birds (Thorpe 2003)(USEPA 1971). In a duration of forty-four years (i.e. between 1955 and 1999), 33 aircrafts were written off and 21 lives were lost. Moreover, the financial losses amounted to US\$ 70 million for the period of 1980 and 1994. The bird species involved in the aviation accidents varies from region to region. In India, the main species responsible for the aircraft accidents are: white-backed vulture *Pseudogyps bengalensis*, Long-billed Griffon *Gyps indicus* and the Egyptian Vulture *Neophron percnopterus*, whereas in USA, the aircraft accidents are mainly attributed to Turkey Vulture *Cathartes aura* and the Black Vulture *Coragyps atratus* (Satheesan and Satheesan 2000).

Vultures are generally communally feeding scavenging raptors. The main reasons for the accident between vultures and the aircrafts are: habit of communal soaring, heavy body (1.5 - 12 Kg) and poor reflexes. Generally vultures fly high because of the large foraging area. As a result, the accident between aircrafts and the vulture have been even observed at very high altitudes e.g. at more than 30,000 ft height (Thorpe 2003).

#### **Role of MSW dumps in aircraft accidents**

Landfills are Table 1 lists the news reporting accidents involving aircraft and birds near waste disposal sites.

**Table 1 News reporting accidents involving aircraft and birds near waste disposal sites**

Year	Place	Description	Reference
2018	Kolkata	22 recorded instances of bird hits at Kolkata airport in the past six months	(TNN 2018)
2015	New Delhi	Delhi airport had most number of bird hits in 2014	(Philip and Ayyappan 2015)
2013	Chennai, India	8 bird-hits near airport because of illegal dumping around the airport	
2009	Bangalore, India	One bird-hit every month at Yelahanka Air Force Station which is situated close to Mavallipura landfill	(Gandhi 2009)
2009	St. John's Airport, St John's, Newfoundland and Labrador	Bird strikes about once a month; That rate ranks the city airport second worst of the top 20 airports in the country,	(The Canadian Press 2009)
2005	Bangalore, India	Pilot killed as MiG crashes in Bangalore	(The Hindu 2005)
2000	New Delhi	Bird hit caused MiG crash	(The Hindu 2000)

For hazard assessment from solid waste disposal sites, three methodologies are generally used: deterministic, stochastic and rating approaches (Nixon and Murphy 1998). As the deterministic and stochastic approaches require a lot of data, rating approach is preferred in case the purpose is relative ranking of the alternatives.

A number of ranking systems are available in literature for assessing the hazards from waste sites (Kumar et al. 2017). None of these systems take into account the bird-hit hazard from the waste sites.

#### Development of the new system for hazard assessment

The parameters that may be important for affecting the bird-hit hazard from a waste site are as following: (i) Waste height above ground (m), (ii) Waste disposed/day, (iii) Distance to airport and (iv) Scale of operations (airport). While waste height above ground denotes the propensity of the birds/vultures to locate a waste site, the waste disposed/day indicates the amount of feed available for the birds/vultures. The distance to airport and scale of operation of the nearest airport affects the degree of occurrence of collision between the birds feeding on the waste site and an aircraft.

Initially, the best and worst values of the selected parameters are decided to determine the boundary conditions for the parameters. The best and worst values of the parameters are given in Table 2.

**Table 2: Best and worst values of the system parameters**

Parameter	Best Value	Worst Value
Waste height above ground (m)	5	40
Waste disposed/day	0	1000
Distance to airport (km)	20	10
Scale of operations (aircraft movements/year) for the nearby airport	1500	150000

Subsequent step in the system development is assigning the rating values to individual parameters. All the system parameters are assigned rating values between 0.1 and 1. While three parameters i.e. waste height, waste disposed/day and distance to airport, are assigned ordinal values between 0.1 and 1, one parameter i.e. scale of operations is assigned

continuous rating values using a equation. The equation is derived using the best and worst values of the parameter. Next step in the rating system development is combining the system parameters using a suitable algorithm. A review of existing rating systems show that there are three types of algorithms used for the purpose: (i) Additive, (ii) Multiplicative, and (iii) Additive-multiplicative (Kumar et al. 2017). For this rating system, the additive-multiplicative algorithm is used for combining the system parameters. Three out of four parameters i.e. waste height, distance to airport and scale of operations are in addition, waste disposed/day is in multiplication. Final rating is obtained as given below:

$$FR_{bh} = (R_{wh} + R_{da} + R_{soo}) \times R_{wd}$$

$FR_{bh}$  – final rating for the waste site;  $R_{wh}$  – rating for waste height;  $R_{da}$  – rating for distance to airport;  $R_{soo}$  – rating for scale of operation.

So the final rating of a waste site is on a scale of 0-1. Higher the rating, higher is the relative hazard from a waste site.

### System Evaluation

After the development, the rating system needs to be evaluated. The new rating system was developed by applying it to a set of continuously varying waste sites. The site characteristics of the waste sites were conceptualized taking into consideration the field conditions. Table 3 shows the site conditions for the waste sites.

**Table 3: Site characteristics for hypothetical sites**

Parameter	W-1	W-2	W-3	W-4	W-5
Waste height above ground (m)	5	10	20	25	30
Waste disposed/day (tons/day)	0	400	800	900	1000
Distance to airport	30	20	15	12	10
Scale of operations (airport)	1500	50000	100000	130000	150000

The ratings obtained from the new system are shown in Fig.1. The range of the ratings is 0.1-0.95, which is practically the full range of the system. It indicates that the system responds to changes in site conditions.

### System Application

Finally the new system was applied to five waste sites, selected from Indian cities. The data for waste sites were taken from existing literature (Datta and Kumar 2016). All of these waste sites are uncontrolled and have the average waste heights varying from 5m to more than 40m. The site characteristics for these sites have been provided in Table 4.

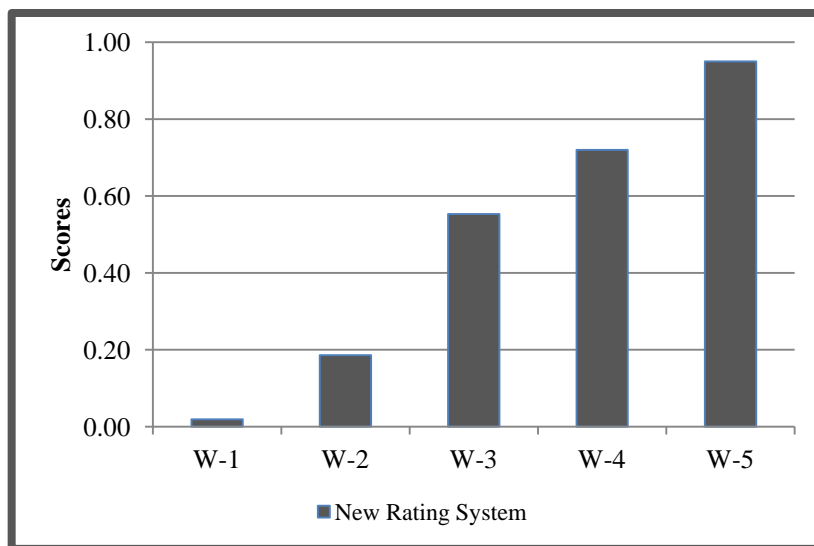


**Fig. 1 Final ratings for bird-hit hazard for the hypothetical waste sites**

**Table 4: Site characteristics for waste sites from Indian cities**

Site	S-1	S-2	S-3	S-4	S-5
Region	Northern	Eastern	North-west	Central	Western
Waste height above ground	40	30	5	5	30
Waste disposed/day	2500	3500	400	800	4000
Distance to airport	21	12	25	13	7
Scale of operations	282460	117134	19809	12990	260666

The results from the application of the new rating system on the waste sites selected from Indian cities have been shown in Fig. 2. The new rating system gives distinct score for all the sites in the range of 0.14 – 0.95. Three out of the five waste sites are having a rating of above 0.5. While site S-3 has the lowest rating, site S-5 has the highest rating. Although it receives 400 tons/day of fresh waste, the other parameters for site S-3 are on the safer side, e.g. the waste height is very low and it is located at a far-off distance from the nearby airport. On the other hand, site S-5 has waste pile of more height and is located only 7km from the airport,

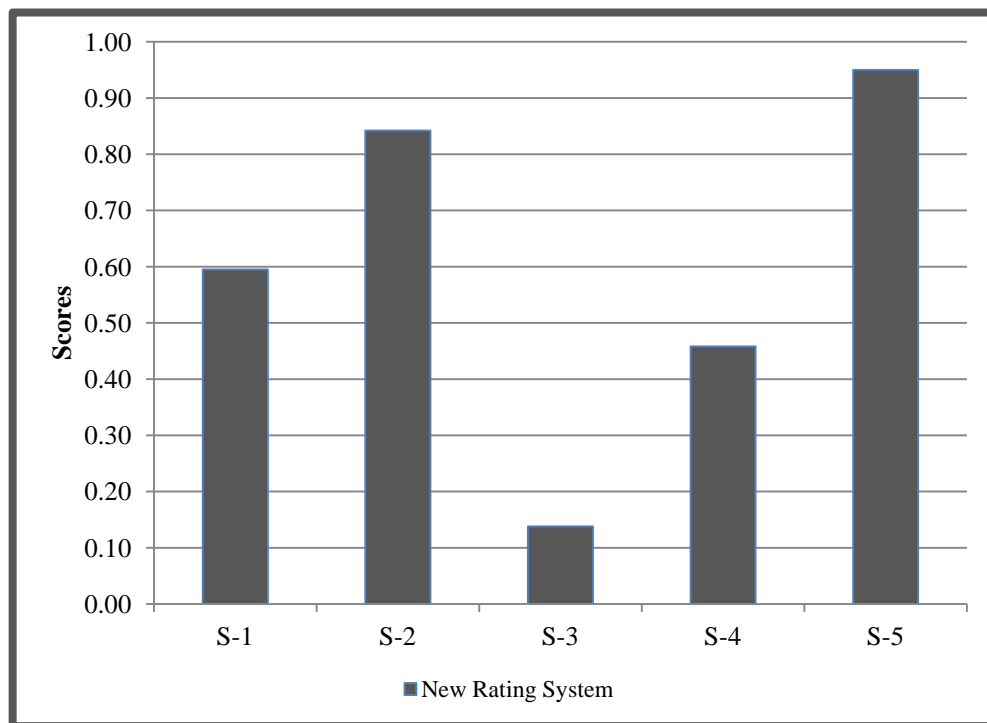


**Figure 2: Final bird-hit hazard ratings for the waste sites in Indian cities**

### Conclusions

Existing Rating system for ranking of sites does not have the rating system for bird-hit hazard. A new system has been developed in the study taking into consideration the four parameters: (i) Waste height above ground, (ii) Waste disposed/day, (iii) Distance to airport and (iv) Scale of operations. The system was evaluated by determining the ratings for a set of hypothetical sites. After the system was found responding to the variation in site conditions, the system was applied to five waste sites selected from Indian cities. Out of the five sites, site S-3 has the lowest rating owing to low

waste height and large distance from the airport. Site S-5 has the highest rating due to the higher waste pile on the site and close proximity to the nearby airport.

## References

- Blight, G. (2008). "Slope failures in municipal solid waste dumps and landfills: a review." *Waste management & research : the journal of the International Solid Wastes and Public Cleansing Association, ISWA*, 26(5), 448–63.
- Datta, M., and Kumar, A. (2016). "Waste Dumps and Contaminated Sites in India-Status and Framework for Remediation and Control." *Geotechnical Special Publication*.
- Farber, S. (1998). "Undesirable facilities and property values: a summary of empirical studies." *Ecological Economics*, 24(1), 1–14.
- Gandhi, D. (2009). "One bird hit a month at the Yelahanka Air Force Station." *The Hindu*, Bangalore, India, 165793.
- Hafeez, S., Mahmood, A., Syed, J. H., Li, J., Ali, U., Malik, R. N., and Zhang, G. (2016). "Waste dumping sites as a potential source of POPs and associated health risks in perspective of current waste management practices in Lahore city, Pakistan." *Science of the Total Environment*, 562.
- Jhamnani, B., and Singh, S. (2009). "Groundwater contamination due to Bhalaswa landfill site in New Delhi." *Int. J. Environ. Sci. Eng.*, 121–125.
- Kumar, A., Datta, M., Nema, A. K., and Singh, R. K. (2017). "Suitability of hazard rating systems for air contamination from municipal solid waste (MSW) dumps and improvements to enhance performance." *Canadian Journal of Civil Engineering*, 44, 549–557.
- Nixon, W. B., and Murphy, R. J. (1998). "Waste site hazard assessment: a taxonomy of current methods and criteria." *Environmental Engineering and Policy*, 1(1), 59–74.
- Papadopoulou, M. P., Karatzas, G. P., and Bougioukou, G. G. (2007). "Numerical modelling of the environmental impact of landfill leachate leakage on groundwater quality – a field application." *Environmental Modeling & Assessment*, 12, 43–54.
- Philip, C. M., and Ayyappan, V. (2015). "Delhi airport had most number of bird hits in 2014." *Times of India*, New Delhi.
- Satheesan, S. M., and Satheesan, M. (2000). "Serious Vulture-Hits To Aircraft Over the World." *INTERNATIONAL BIRD STRIKE COMMITTEE IBSC25/WP-SA3 Amsterdam, 2000*, 113–126.
- Shusterman, D. (1992). "Critical review: the health significance of environmental odor pollution." *Archives of Environmental Health: An International Journal*, 47(1), 76–87.
- The Canadian Press. (2009). "Landfill taking measures to reduce bird strikes at St . Johns airport." *The Guardian*, St. John's.
- The Hindu. (2000). "Bird hit caused MiG crash." 25–26.
- The Hindu. (2005). "Pilot killed as MiG crashes in Bangalore." *The Hindu*, Bangalore, India.
- Thorpe, J. (2003). "Fatalities and destroyed civil aircraft due to bird strike , 1912 – 2002." *Proceedings of the International bird strike committee*, (May), 28.
- TNN. (2018). "Kolkata airport tops in bird hits among metros." *Times of India*, Kolkata.
- USEPA. (1971). *Land Disposal Sites Near Airports Reporting Bird/Aircraft Hazards: a Survey for the Inter-Agency Bird Hazard Committee*.



## Natural treatment of domestic wastewater-Review on different media

Amit Kumar<sup>1</sup>, Simranjit Singh<sup>2</sup>, A.K. Agnihotri<sup>3</sup>

1. Assistant Professor, Department of Civil Engineering, Dr. B R Ambedkar National Institute of Technology, Jalandhar - 144011, India. E-mail: [amitrathi.ucf@gmail.com](mailto:amitrathi.ucf@gmail.com), Corresponding Author
2. Research Scholar, Department of Civil Engineering, Dr. B R Ambedkar National Institute of Technology, Jalandhar - 144011, India. E-mail: [simranjit32@gmail.com](mailto:simranjit32@gmail.com)
3. Professor, Department of Civil Engineering, Dr. B R Ambedkar National Institute of Technology, Jalandhar - 144011, India. E-mail: [agnihotriak@nitj.ac.in](mailto:agnihotriak@nitj.ac.in)

### Abstract

This study was conducted to review the process of treating domestic wastewater through sub surface constructed wetlands using different media. The role of media used in constructed wetland is reviewed based on various parameters such as the pollutant removal efficiency, operation and maintenance cost etc. It was concluded that the media with greater specific surface area are more suitable to remove nutrients from wastewater while the materials having low specific surface area are suitable to remove organic and suspended load without any clogging but deficient in removing nutrients. However industrial waste products are used as medium in CWs are more economical whereas the CWs whose medium filled with virgin materials are little bit costly.

Keywords: constructed wetlands; domestic wastewater; wetland media

### Introduction

Conventional treatment of wastewater involves a large financial investments and operation cost(Avellán & Gremillion, 2019). These conventional systems are out of range for countryside communities so constructed wetland comes out to be a better alternative for such treatment(Ali, Rousseau, & Ahmed, 2018). CW offer low cost(Yang, Zhao, Liu, & Morgan, 2018) of operation and negligible maintenance(Dotro et al., 2017) since there is no use of mechanical machines or any other external supply of energy(Hua, Haynes, & Zhou, 2018)(Liu, Zhao, Doherty, Hu, & Hao, 2015).

Ecosystems of wetland are used as sources, sinks, or transformers of nutrients and carbon. This capability of wetlands has lead to a large extent use of natural and constructed wetlands for enhancement of water quality(Barco & Borin, 2017)(Heal, 2014).

There are many type of CWs used now a days depending upon the purpose and land requirement aspects but the most common type is sub surface flow type (Gopalan, 2016) in which the flow may be horizontal or it may be vertical or sometimes a combination of both, which are generally known as hybrid constructed wetlands(Kadlec & Wallace, 2008). The basic design of subsurface type CWs include a filler media in which the flow may be vertical (down flow or up flow) or it may be the horizontal one. This media plays significant role in treatment, in other words this media is the home of the most physical and biological processes involved in wastewater treatment in CWs. In addition to better hydraulic conductivity of the media, its chemical composition is also a critical factor in design of CW(Kadlec & Wallace, 2008)(Lu, Zhang, Wang, & Pei, 2016).

With advancement of technology, humans have added more in the CWs in terms of their design, operation and management aspects to get extensive range of applications, more processing ability and the most important is high treatment efficiency. In recent times, due to increase in burden on water resources most of the countries now thinking about sustainability aspect along with economic growth(Goonetilleke et al., 2017). In this time CWs have allured the attention around the globe due to their low cost, high efficiency and excellent performance to treat wastewater and to relieve burden on freshwater resources(J. Vymazal, 2009).

Constructed wetland systems have already been used for processing enormous forms of wastewaters, specially

industrial, rural domestic household, urban household and other nonpoint-source pollution(Gopalan, 2016)(Dotro et al., 2017). Now a day, CWs have been developed as a technology to treat wastewater that bears high economic capability and environmental sustainability(Masi, 2009) that is particularly matched to sewage treatment in countryside areas.

The objective of this study is to review the use of sub surface flow constructed wetland in treating municipal/domestic wastewater using different media and to analyze the operation and maintenance of different mediums in constructed wetlands and the most important is the cost involved for using different media in CW.

### **Filter media for constructed wetland**

Literature shows that the researchers use vast varieties of media as subsurface so as to get desired results of efficiency for various pollutant removal. Now a day, typical constructed wetland matrices are vermiculite and zeolite(Zhao, Zhao, Xu, Doherty, & Liu, 2016), gravel, lava sands(Bruch et al., 2011), limestone, clay minerals, slag(Park et al., 2017), coal ash, grit and soil and some byproducts from industries(Vohla, Kõiv, Bavor, Chazarenc, & Mander, 2011).

Filtration media used in a CW mainly vary in surface area, so the process of removal of pollutants may alter according to media used. Use of media having greater surface area or uplifting the specific surface area of different media types can enhance the rate of removal of organic matter by multiplying the adsorption capacity of matrix of wetland to many folds. On the other hand, microorganisms activities connected with the treatment of wastewater in wetland matrix may depend on characteristics of media and the composition of influent coming. In this respect, the large variation of surface area of filtration media which is conveyed by small particle size can enhance the subsequent development of biofilm on these substrates, and thus enhances high microbial activity in the wetland matrix which facilitates removal of organic matter and other pollutants(Lu et al., 2016).

Medium act as the catalyst in constructed wetland, its physical and chemical attribute may straightly influence the efficiency of sewage treatment of whole system. In addition to this when the inside stretch of CW is filled with porous medium that bears large specific surface area, this can enhance hydraulic and mechanical capacities of the wetland and it also provide sufficient area to microorganisms for adhesion thus elevating the pollutant removal capacity of system(Vohla et al., 2011). Therefore, the medium selection in CW has great prominence for the effective efficiency of the CW treatment system.

### **Treatment Efficiency**

Currently, the wetlands treatment systems make use of gravel, grit sands, soil and other substrate media. This investment is very much effective, but nitrogen and phosphorus removal rate of these mediums are not sufficient; therefore, scientists have continuously developing new wetland mediums and carrying enormous levels of tests. The use of gravel and gravel-soil combined as constructed wetland medium to test domestic sewage treatment shows that phosphorus removal rate of gravel-soil combined medium is very good but removal rate of ammonia nitrogen is too less(Zidan, El-Gamal, Rashed, & El-Hady Eid, 2015). Moreover natural zeolite have the capacity to absorb ammonia nitrogen from wastewater, thus efficiently reducing the concentration of ammonia nitrogen. The use of fly ash as a substrate media in CW system is significant now a day because of its removal efficiency of organic matter, phosphorous and the most important is the ammonia nitrogen removal rate which is much larger than that of system in which gravel media is used(Vohla et al., 2011).

BOD and COD removal is necessary because organic matter present in the wastewater deadly affect the aquatic life if discharged directly to freshwater body like lakes and rivers etc. This is due to the reason that organic matter lowers the dissolved oxygen present in any water body so its removal is mandatory before disposal. CWs are extremely capable to remove organic matter from any type of wastewater. VFCW are more efficient than HFCW in case of subsurface flow when gravel and sand is used as medium in CW(Abou-elela, Golinielli, Abou-taleb, & Hellal, 2013). This is because of the reason that both gravel and sand are porous enough to give room for air supply and root growth. Also gravels are good adsorbents. Gravels allow enough space for the roots to develop fine biofilm in rhizosphere zone(J. Vymazal, 2009).

Coming to Nitrogen and Phosphorous, these two elements are major cause of concern in wastewater treatment as most of the conventional treatment systems are out of reach to catch these from wastewater. Their presence in water leads to eutrophication in water bodies so their treatment is need of hour. In CW system both nitrification and denitrification takes place where as the phosphorous removal is done through adsorption by media and uptake by CW plants. Nitrogen removal is better when we use industrial byproducts/waste as CW medium mostly zeolite, steel slag, coal slag/fly ash(Lu et al., 2016). Ammonia nitrogen removal is mainly done through adsorption and by nitrifying bacteria, these industrial products have larger specific surface area which provides enough area for the growth of bacteria and adsorption. Same is the case of phosphorous removal that high adsorption capacity of these industrial byproducts leads to high removal rates as compared to natural sand and gravel(Vohla et al., 2011). Si it is concluded that industrial waste like Coal ash has high removal efficiency in terms of phosphorous when used under subsurface conditions, whereas zeolite is widely used as medium to remove ammonia nitrogen under subsurface conditions(Lu et al., 2016).

Removal of suspended solids purely depends upon the loading rate of influent, filtration and sedimentation process(Jan Vymazal, 2010) whereas CW media is also significant in removing suspensions. Higher the voids in the material less will the removal. In this case sand, soil and other fine industrial byproducts are better alternative to filter suspended solids from wastewater(Andreo-Martínez, García-Martínez, Quesada-Medina, & Almela, 2017)(Abou-elela et al., 2013).

Heavy metals are toxic in nature and deadly affects the food chain so their removal is a major concern now a day. In CWs removal of heavy metals are mainly done by plants in CW but the medium of CW act as catalyst in various reactions. In this case the medium with higher void ratio are more capable as they transfer more oxygen to the system thus enhances the chemical reactions in the system and uptake is mainly done through plants(Khan, Ahmad, Shah, Rehman, & Khaliq, 2009).

### **Operation and Maintenance**

The challenges that are associated with the utilization of CWs do not end with their design and construction, but also go beyond to their subsequent operation and maintenance. Properly and carefully managed wetlands are passive and are low-maintenance treatment systems(Wu, Austin, Liu, & Dong, 2011). However, this does not mean that they do not require any maintenance.

CWs are designed and constructed to meet a vast number of goals from wastewater treatment to habitat creation and environment management. Other factor involved in the maintenance and operation is type of media and vegetation used, however most CW plants are water resistant, longer growing period and easy to grow so the onus of operation and maintenance of CW is mostly dependent on media used in CW. Gravels are most favorable materials and require minimum maintenance because of its high porosity and less clogging, but the materials who have high specific surface area are more prone to clogging and require proper operation and maintenance plans. The water should be pretreated to remove suspensions before CW treatment if we are using sand, coal slag, steel slag as CW media because of its high specific surface area.

To enhance the life of wetland system, its operation and maintenance must be planned according to its specific goals which are to be achieved. Generally sub surface flow type CWs require least maintenance.

Cost wise, CWs are very economical, easy to construct and are very cost effective as compared to conventional wastewater treatments operations(J. Vymazal, 2009)(Arias & Brown, 2009). CWs require negligible amount of external energy during its operation, a simple pump with flow regulator is sufficient to operate these systems. However the main cost of CW system constitutes its construction, material used as substrate and land costs but these problems are out ruled when subsurface type CWs came into light which reduces the construction and land costs(Lu et al., 2016)(Konnerup, Koottatep, & Brix, 2009)(Arias & Brown, 2009). If the CW media is filled with virgin material that is the material is to be freshly borrowed/purchased from market then the cost might increase however CW media from industrial waste, wood chips, soil make it very economical.

### **Conclusions:-**

Firstly, it has been concluded that CWs are cost effective than conventional treatment systems in treating domestic wastewaters. The pollutant removal efficiency in CW system depends upon the influent loading, plants used and the most important is the media used.

In terms of media gravels are most abundantly used media in sub surface type CW systems because of their high removal efficiency in terms of BOD and COD, require low maintenance, no clogging problem by using this media,

however nutrients can better be removed by industrial wastes like steel slag, coal slag etc. because of their large specific surface area which enhances adsorption and elevates bacteria growth. Their operation requires proper plan as clogging problem sometimes occurs but still they are low cost, low maintenance systems when properly managed. Heavy metals are mostly removed by plants but CW media act as catalyst in this case, it provides space for roots to grow and form biofilm to elevate uptake ability. In this case gravel and sand are most suitable.

## References:-

- Abou-elela, S. I., Golinielli, G., Abou-taleb, E. M., & Hellal, M. S. (2013). Municipal wastewater treatment in horizontal and vertical flows constructed wetlands. *Ecological Engineering*, 61(March 2018), 460–468. <https://doi.org/10.1016/j.ecoleng.2013.10.010>
- Ali, M., Rousseau, D. P. L., & Ahmed, S. (2018). A full-scale comparison of two hybrid constructed wetlands treating domestic wastewater in Pakistan. *Journal of Environmental Management*, 210, 349–358. <https://doi.org/10.1016/j.jenvman.2018.01.040>
- Andreo-Martínez, P., García-Martínez, N., Quesada-Medina, J., & Almela, L. (2017). Domestic wastewaters reuse reclaimed by an improved horizontal subsurface-flow constructed wetland: A case study in the southeast of Spain. *Bioresource Technology*, 233, 236–246. <https://doi.org/10.1016/j.biortech.2017.02.123>
- Arias, M. E., & Brown, M. T. (2009). Feasibility of using constructed treatment wetlands for municipal wastewater treatment in the Bogotá Savannah, Colombia. *Ecological Engineering*, 35(7), 1070–1078. <https://doi.org/10.1016/j.ecoleng.2009.03.017>
- Avellán, T., & Gremillion, P. (2019). Constructed wetlands for resource recovery in developing countries. *Renewable and Sustainable Energy Reviews*, 99(August 2018), 42–57. <https://doi.org/10.1016/j.rser.2018.09.024>
- Barco, A., & Borin, M. (2017). Treatment performance and macrophytes growth in a restored hybrid constructed wetland for municipal wastewater treatment. *Ecological Engineering*, 107, 160–171. <https://doi.org/10.1016/j.ecoleng.2017.07.004>
- Bruch, I., Fritsche, J., Bänninger, D., Alewell, U., Sendelov, M., Hürlimann, H., ... Alewell, C. (2011). Bioresource Technology Improving the treatment efficiency of constructed wetlands with zeolite-containing filter sands. *Bioresource Technology*, 102(2), 937–941. <https://doi.org/10.1016/j.biortech.2010.09.041>
- Dotro, G., Langergraber, G., Molle, P., Nivala, J., Puigagut, J., Stein, O., & von Sperling, M. (2017). *Treatment Wetlands*. *Water Intelligence Online* (Vol. 16). <https://doi.org/10.2166/9781780408774>
- Goonetilleke, A., Liu, A., Managi, S., Wilson, C., Gardner, T., Bandala, E. R., ... Rajapaksa, D. (2017). Stormwater reuse, a viable option: Fact or fiction? *Economic Analysis and Policy*. <https://doi.org/10.1016/j.eap.2017.08.001>
- Gopalan, B. (2016). COMPARISON OF TREATMENT PERFORMANCE BETWEEN CONSTRUCTED WETLANDS WITH DIFFERENT PLANTS, (October). <https://doi.org/10.15623/ijret.2014.0304037>
- Heal, K. V. (2014). *Constructed Wetlands for Wastewater Management*. *Water Resources in the Built Environment: Management Issues and Solutions* (2nd ed., Vol. 9780470670). Elsevier Inc. <https://doi.org/10.1002/9781118809167.ch25>
- Hua, T., Haynes, R. J., & Zhou, Y. F. (2018). Potential use of two filter media in constructed wetlands for

- simultaneous removal of As, V and Mo from alkaline wastewater - Batch adsorption and column studies. *Journal of Environmental Management*, 218, 190–199. <https://doi.org/10.1016/j.jenvman.2018.04.038>
- Kadlec, R., & Wallace, S. (2008). *Treatment Wetlands, Second Edition*. <https://doi.org/10.1201/9781420012514>
- Khan, S., Ahmad, I., Shah, M. T., Rehman, S., & Khaliq, A. (2009). Use of constructed wetland for the removal of heavy metals from industrial wastewater. *Journal of Environmental Management*, 90(11), 3451–3457. <https://doi.org/10.1016/j.jenvman.2009.05.026>
- Konnerup, D., Koottatop, T., & Brix, H. (2009). Treatment of domestic wastewater in tropical, subsurface flow constructed wetlands planted with Canna and Heliconia. *Ecological Engineering*, 35(2), 248–257. <https://doi.org/10.1016/j.ecoleng.2008.04.018>
- Liu, R., Zhao, Y., Doherty, L., Hu, Y., & Hao, X. (2015). A review of incorporation of constructed wetland with other treatment processes. *Chemical Engineering Journal*, 279, 220–230. <https://doi.org/10.1016/j.cej.2015.05.023>
- Lu, S., Zhang, X., Wang, J., & Pei, L. (2016). Impacts of different media on constructed wetlands for rural household sewage treatment. *Journal of Cleaner Production*, 127, 325–330. <https://doi.org/10.1016/j.jclepro.2016.03.166>
- Masi, F. (2009). Water reuse and resources recovery : the role of constructed wetlands in the Ecosan approach. *DES*, 246(1–3), 27–34. <https://doi.org/10.1016/j.desal.2008.03.041>
- Park, J. H., Wang, J. J., Kim, S. H., Cho, J. S., Kang, S. W., Delaune, R. D., & Seo, D. C. (2017). Phosphate removal in constructed wetland with rapid cooled basic oxygen furnace slag. *Chemical Engineering Journal*, 327, 713–724. <https://doi.org/10.1016/j.cej.2017.06.155>
- Vohla, C., Köiv, M., Bavor, H. J., Chazarenc, F., & Mander, Ü. (2011). Filter materials for phosphorus removal from wastewater in treatment wetlands-A review. *Ecological Engineering*, 37(1), 70–89. <https://doi.org/10.1016/j.ecoleng.2009.08.003>
- Vymazal, J. (2009). The use constructed wetlands with horizontal sub-surface flow for various types of wastewater. *Ecological Engineering*, 35(1), 1–17. <https://doi.org/10.1016/j.ecoleng.2008.08.016>
- Vymazal, J. (2010). Constructed Wetlands for Wastewater Treatment, 530–549. <https://doi.org/10.3390/w2030530>
- Wu, S., Austin, D., Liu, L., & Dong, R. (2011). Performance of integrated household constructed wetland for domestic wastewater treatment in rural areas. *Ecological Engineering*, 37(6), 948–954. <https://doi.org/10.1016/j.ecoleng.2011.02.002>
- Yang, Y., Zhao, Y., Liu, R., & Morgan, D. (2018). Global development of various emerged substrates utilized in constructed wetlands. *Bioresour Technol*. <https://doi.org/10.1016/j.biortech.2018.03.085>
- Zhao, J., Zhao, Y., Xu, Z., Doherty, L., & Liu, R. (2016). Highway runoff treatment by hybrid adsorptive media-baffled subsurface flow constructed wetland. *Ecological Engineering*, 91, 231–239. <https://doi.org/10.1016/j.ecoleng.2016.02.020>
- Zidan, A. R. A., El-Gamal, M. M., Rashed, A. A., & El-Hady Eid, M. A. A. (2015). Wastewater treatment in horizontal subsurface flow constructed wetlands using different media (setup stage). *Water Science*, 29(1), 26–35. <https://doi.org/10.1016/j.wsj.2015.02.003>



## EFFECT OF RICE HUSK ASH ON GEOTECHNICAL PROPERTIES OF CLAYEY SOIL: AN EXPERIMENTAL STUDY

\*Abhishek,<sup>1</sup> Vaibhav Sharma,<sup>2</sup> Ravi Kumar Sharma,<sup>3</sup> and Arvind Kumar<sup>4</sup>

<sup>1</sup>\*Research Scholar, Department of Civil Engineering, NIT Hamirpur; e-mail: [abhishek1@nith.ac.in](mailto:abhishek1@nith.ac.in) (Corresponding Author)

<sup>2</sup> Faculty, Department of Civil Engineering, NIT Hamirpur; e-mail: [civil.vaibhav.sharma@gmail.com](mailto:civil.vaibhav.sharma@gmail.com)

<sup>3</sup> Faculty, Department of Civil Engineering, NIT Hamirpur; e-mail: [rksnithp61@gmail.com](mailto:rksnithp61@gmail.com)

<sup>4</sup> Faculty, Department of Civil Engineering, NIT Jalandhar; e-mail: [agnihotriak@nitj.ac.in](mailto:agnihotriak@nitj.ac.in)

### ABSTRACT

Clayey soils are considered poor from construction point of view due to their large volumetric change on changing moisture content. The structures found on these soils often pose the problem of cracking which leads to instability of these structures. Rice husk is a waste product obtained from fields which is generally used a fuel in the boilers for processing of paddy. These boilers produce a tremendous amount of ash on burning of rice husk whose disposal is a big problem. The present experimental study deals with the effect of addition of rice husk ash on various geotechnical properties of poor clayey soils. Laboratory tests such as differential free swell, pH, Atterberg's limit, compaction and unconfined compressive strength tests on virgin soil and soil modified with varying percentage of rice husk ash have been conducted. The tests results reveal that on addition of 10% rice husk ash in virgin soil, the modified soil attains non- plastic nature. The pH value is found to be neutral and differential free swell index is also found to be zero on adding 10% rice husk ash in virgin soil. Thus an optimum content of 10% rice husk ash is found suitable to be mixed in virgin soil. Further, compaction tests for varying percentages of rice husk ash have been conducted and found that maximum dry density goes on decreasing and optimum moisture content increases. The unconfined compressive strength is found maximum for soil: rice husk ash:: 90: 10. Thus it can be stated that, rice husk ash can be used in soil stabilization which will solve the problem of its disposal and will help in protecting the environment.

**Keywords:** Clay, rice husk ash, Atterberg's limits; maximum dry density; optimum moisture content; unconfined compressive strength.

### INTRODUCTION

The geotechnical assets of poor clayey soils are influenced by the presence of water and these soils expand and lose strength on wetting. The foundations constructed over such soils are subjected to cracking and damage and often cause heavy economic losses. If the characteristics of poor soils can be improved by addition of various wastes such as rice husk ash in an appropriate amount, then it will bring environmental and economic benefits. India's economy is mainly based on the agriculture and rice is majorly cropped in India. According to a report by USDA Foreign Agriculture Service, total production of rice in year 2016- 17 was 105 million metric ton. It is estimated that about 70 million tons of RHA is produced annually worldwide. This RHA is a great environment threat causing damage to the land and the surrounding area in which it is being dumped. During milling of paddy, about 78% of weight is received as rice, broken rice and bran. Rest 22% of the weight of paddy is received as husk. This husk is used as fuel in the rice mills to generate steam for the parboiling process. This husk contains about 75% organic volatile matter and the balanced 25% of husk is converted into ash during the firing process and is known as rice husk ash (RHA). This RHA contains around 90% silica. So for every 1000 kgs of paddy milled, about 220 kgs (22%) of husk is produced, and when this husk is burnt in the boilers, about 55 kgs (25%) of RHA is generated. Bhasin et al. (1988) studied the effect of addition of RHA, fly ash, baggasse ash, sludge of lime on geotechnical properties of black cotton soil. The presence of high silica content in RHA, addition of lime improved the geotechnical properties. Muntohar and Hantoro (2000) used lime and RHA to stabilize the expansive soil and revealed that plasticity index, California bearing ratio and unconfined shear strength of the various composites enhanced. Basha et al. (2003) used cement and RHA to improve the plasticity and compaction characteristics of the bentonite soil and found that RHA content up to 10- 15 % and cement content up to 6- 8 % respectively are suitable for enhancing the soil properties. Ramakrishna and Kumar (2006) used RHA and cement to enhance the properties of the expansive black cotton soil

and recommended that RHA content up to 10 % and cement content up to 8 % are best suitable for increasing the unconfined compressive strength of soil. Sharma et al. (2008) used RHA, calcium chloride and lime to improve the geotechnical properties of the expansive clay and recommended that calcium chloride and lime in percentages 1 % and 4 % respectively without addition of RHA proved to be economical. Further, 12 % RHA content was found to be optimum for California bearing ratio and unconfined compressive strength tests. Rao et al. (2011) used RHA, lime and gypsum to enhance various properties of the expansive clay and revealed that unconfined compressive strength of composite increased 5 times than virgin soil; whereas, soaked CBR of composite increased 13 times than that of virgin soil. Sabat (2011) found that clay: RHA: lime: fiber mixture in ratio 84.5: 10: 4: 1.5 attained highest value for unconfined compressive strength and California bearing ratio. Sabat (2012) used soil, RHA and lime sludge in ratio 75:10:15 and found that soil characteristics improved with addition of these materials. Ashango and Patra (2014) found that 10 % RHA and 7.5 % Portland cement improved geotechnical properties of poor soils. This paper deals with the effect of addition of RHA in virgin clayey soil to improve the geotechnical properties of clayey soil.

## MATERIAL USED

### Clayey soil

The soil used in the present investigation was brought from Distt. Rohtak, Haryana. The soil was tightly packed in air tight bags and then was brought into laboratory and then dried in temperature controlled oven. The soil was then pulverized and sieved through 4.75 mm sieve. According to Indian Soil Classification system, soil used in the present study is classified as CH. The gradation curve of the clayey soil is presented in Figure 1. Table 1 presents various properties of the clayey soil.

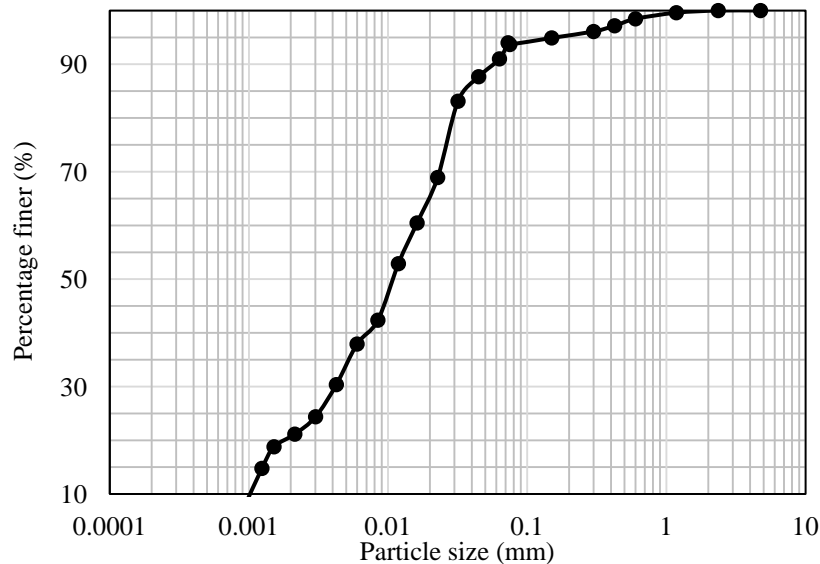


Figure 1. Gradation curve of virgin soil

Table 1. Geotechnical properties of virgin soil

Properties tested	Clay
Specific gravity	2.62
Soil classification	CH
Liquid limit (%)	51.9
Plastic limit (%)	27.1
Plasticity index (PI) (%)	24.8
Maximum dry density, (g/cc)	1.769
Optimum moisture content, (%)	15

**Rice husk ash**

RHA used in this investigation was brought from paddy industry, Mandi Gobindgarh, Punjab. Rice husk ash was transported in polyethene bags to laboratory and was dried for 24 hours and passed through 150 micron sieve and after that it was stored in cool and dry environment in polyethene bags to prevent any reaction with surrounding moisture. Chemical properties of RHA used in the present investigation are given in Table 2.

**Table 2. Chemical properties of rice husk ash**

Property	Value
SiO <sub>2</sub>	85-90%
Humidity	2%
Particle size	25 Microns
Color	Grey
Loss on ignition	3-4%

**RESULTS AND DISCUSSIONS**

**Differential free swell test**

Rice husk ash was added in soil in varying percentages of 5 %, 10 %, 15 %, and 20 %. Figure 2 shows the variation of DFS on varying percentages of RHA. The results of DFS showed that on addition of 10 % RHA in virgin soil, the DFS of composite became zero. Further addition of RHA beyond 10 % did not affect the DFS of soil. From the results, optimum value of RHA was observed to be 10 %. The reduction in value of DFS on increasing RHA content was due to having coarser particles of RHA which resulted in decreasing specific surface area and hence DFS. The relationship established between RHA content in clay: RHA mix and DFS can be expressed by a third degree polynomial equation expressed as below:

$$DFS = 2E-05(RHA)^3 + 0.0002(RHA)^2 - 0.0209(RHA) + 0.1936$$

$$R^2 = 0.9731$$

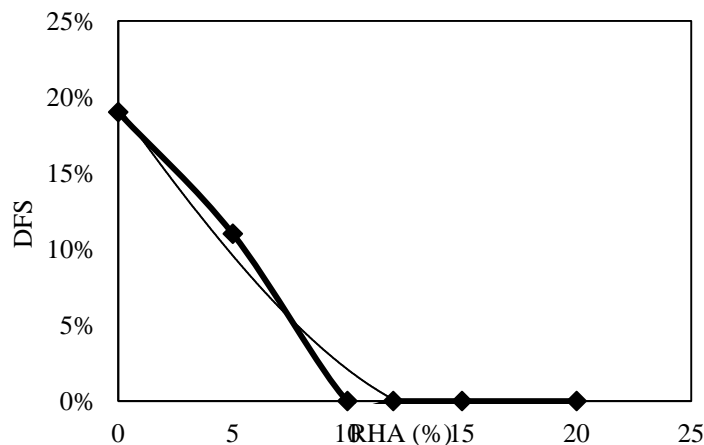


**Figure 2.** Variation in DFS of clay with addition of rice husk ash

**pH test**

pH test was conducted on the mixture of clay and RHA for 95:5, 90:10, 85:15, and 80:20 (Clay: RHA) variations as shown in Figure 3. It was revealed from Figure 3 that the pH of soil increased linearly on increasing RHA content. The pH of the soil: RHA composite attained neutral value (7.0) at 10 % RHA content and therefore, 12 % RHA content can be taken as optimum content for clay: RHA mixture.

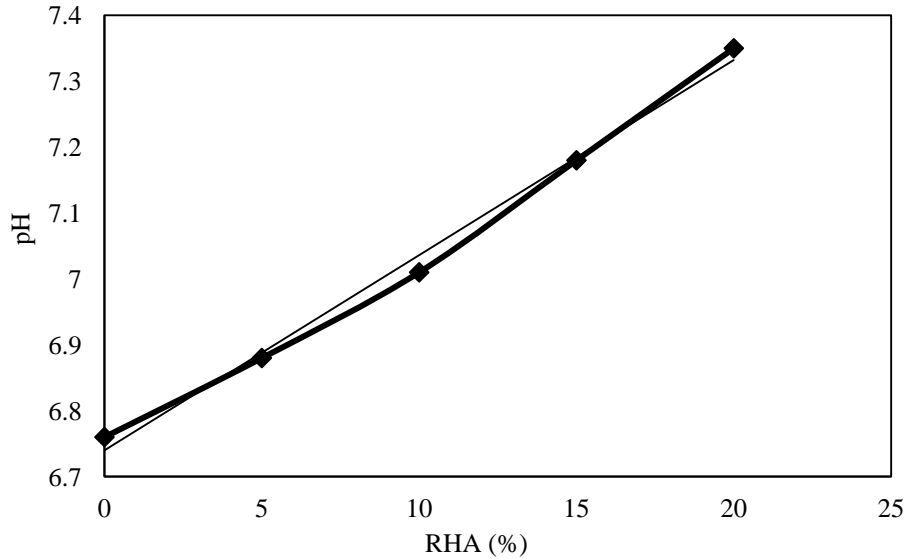


**Figure 3.** pH value with varying percentages of RHA

*Atterberg's limits test*

Rice husk ash was added to the clayey soil in various percentages of 5, 10, 15, and 20 % and tests were conducted to determine the liquid limit, plastic limit and plasticity index. Figure 4 shows the graph for various Atterberg's limits presented between consistency limit and corresponding RHA percentages added to the clayey soil. With the increase in RHA percentage in virgin soil, the liquid limit of various composites decreased. The liquid limit of virgin soil was 51.9 % which reduced to a value of 41.1 % on addition of 10 % RHA in virgin soil. The plastic limit of the RHA mixed soil increased constantly on increasing the percentage of RHA up to 10 % and further addition of RHA beyond 10 % decreased plastic limit of the composite. The plasticity index of RHA mixed clay composite at 10 % RHA content was 7.8 (which lies in the range of 6- 8).

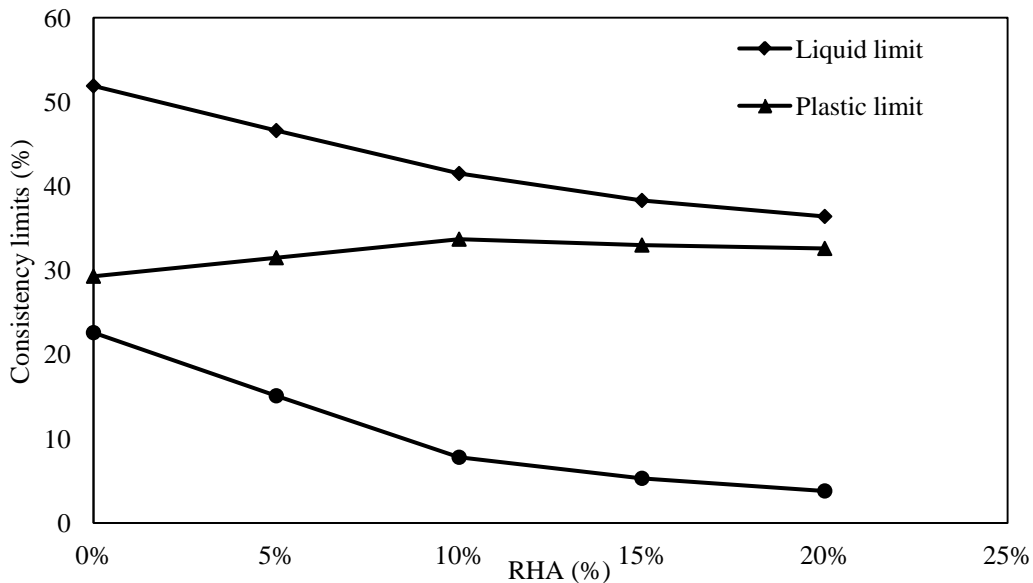


**Figure 4.** Atterberg's limits with varying RHA percentages

### Compaction tests

The compaction tests were carried out for the measurement of maximum dry density and optimum moisture content. The compaction tests were used for determining the maximum dry density (MDD) and optimum moisture content (OMC). The compaction curves for virgin soil, RHA, and various mixes of virgin soil and rice husk ash are presented in Figure 5. The maximum dry density of virgin soil and corresponding optimum moisture content was found to be 1.769 g/cc and 15 % respectively. On adding percentage of RHA in virgin soil, there was decrease in the value of maximum dry density and increase in optimum moisture content was noticed. On increasing RHA content up to 10 %, the maximum dry density decreased from 1.769 to 1.580 g/cc and the optimum moisture content increased from 15 to 18. % as shown in Figure 5. The decrease in value of MDD may be due to lower value of specific gravity of RHA in comparison to virgin soil.

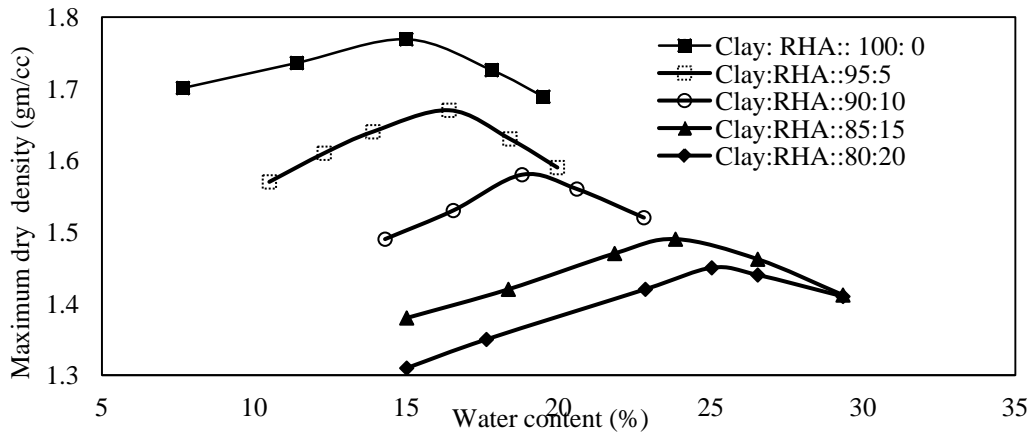


Figure 5. Compaction curves for clay and various mixes of clay: RHA composite

### Unconfined compressive strength

Figures 6, 7, and 8 present the effect of varying percentages of RHA on stress- strain characteristics for 3, 7, 28 days respectively. The UCS value of virgin soil after 3- days was 89.63 kPa; the UCS value of RHA stabilized soil after 3- days curing was 125.70 kPa for RHA content 5 %, 190.18 kPa for RHA 10 %, and 209.86 kPa for RHA 15 % as shown in Figure 9. The UCS value of virgin soil after 7- days was 139.63 kPa; the UCS value of RHA stabilized soil after 7- days curing was 214.23 kPa for RHA 5 %, 301.67 kPa for RHA 10 %, and 322.44 kPa for RHA 15 % as shown in Figure 9. The UCS value of virgin soil after 28- days was 209.86 kPa; the UCS value of RHA stabilized soil after 28- days curing was 292.93 kPa for RHA 5 %, 395.67 kPa for RHA 10 %, and 413.16 kPa for RHA 15 % as shown in Figure 9. Thus, from the above results it is revealed that the addition of RHA in virgin soil increased the UCS value of the composite. The increase in the UCS value on RHA mixed soil may be attributed to the pozzolanic reaction among virgin soil and RHA particles.

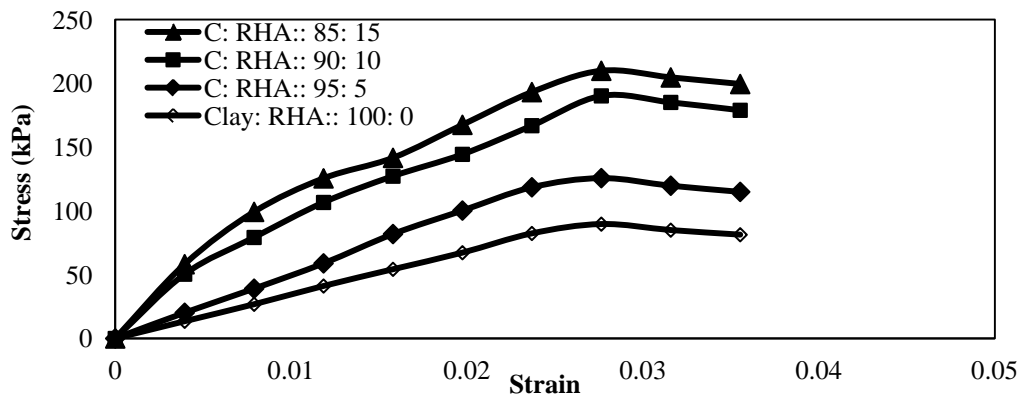


Figure 6. Stress versus strain plot for curing period of 3 days

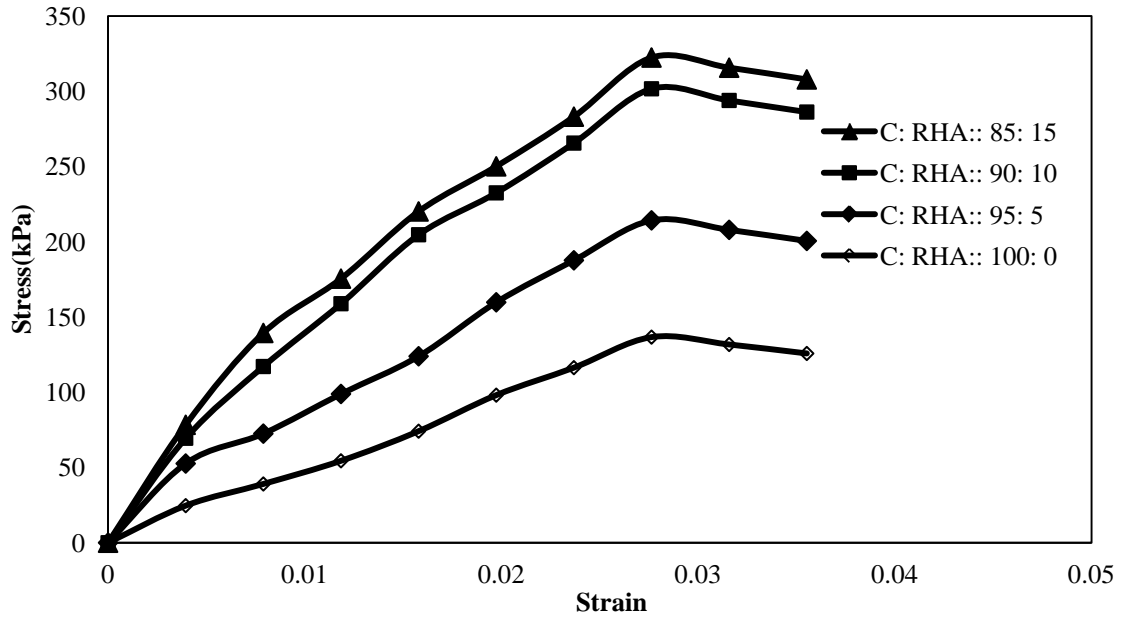


Figure 7. Stress versus strain plot for curing period of 7 days

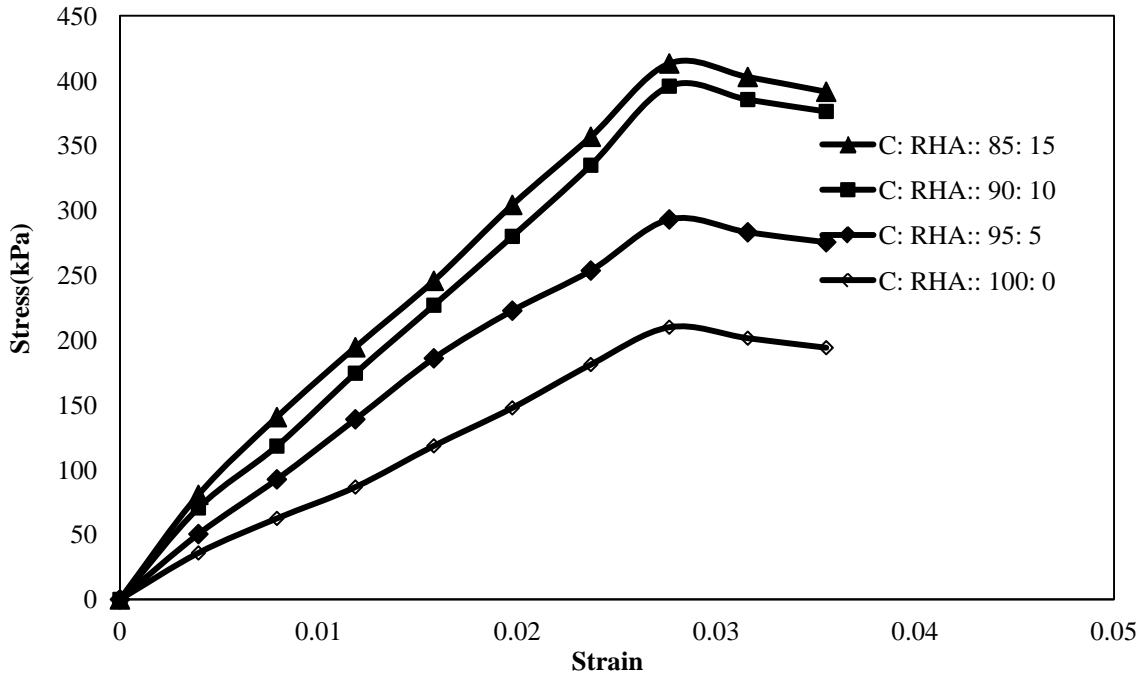
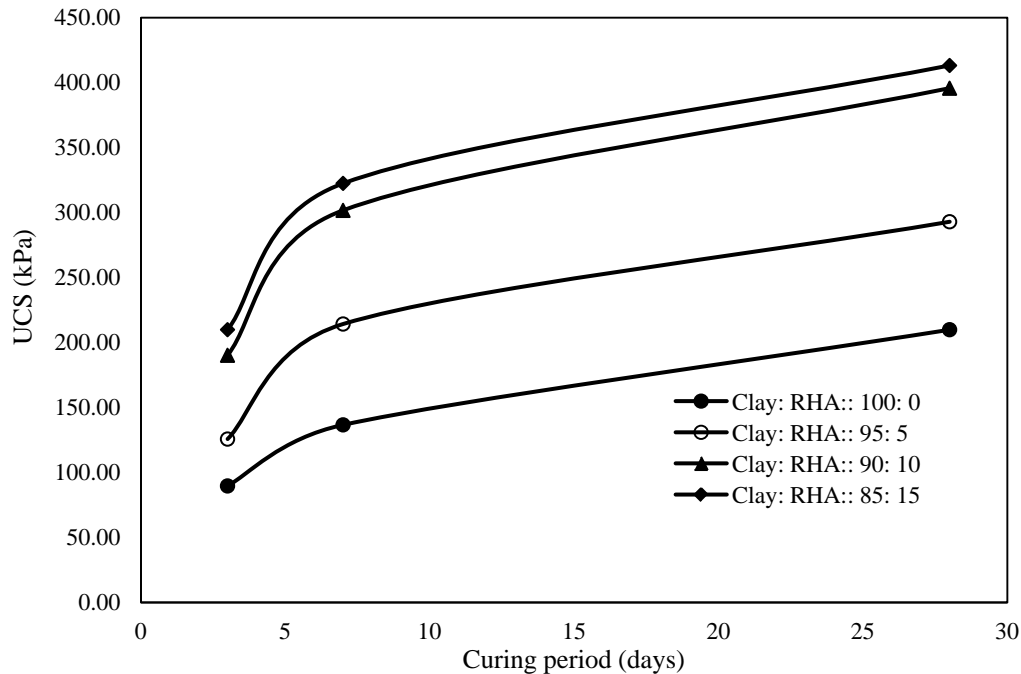


Figure 8. Stress versus strain plot for curing period of 28 days



**Figure 9.** UCS value versus curing period for various composites of clay and RHA

## CONCLUSIONS

Based on the laboratory test results, following conclusions were drawn:

1. The addition of RHA to clayey soil decreased the value of DFS. The DFS was observed to be zero for clay: RHA composite having RHA 10 %.
2. The pH of the clay: RHA composites increased with increasing RHA content and became neutral at 10 % RHA content.
3. The liquid limit of the composite decreased with increase in RHA content. The plastic limit of the composite increased up to RHA content 10 % and thereafter it started decreasing.
4. The maximum dry density of clay mixed with RHA composite decreased and optimum moisture content increased on increasing percentage of RHA in the mix.
5. The UCS value of the composite increased on increasing RHA content for curing period of 3, 7, and 28 days. The increase in UCS value was significant up to RHA content 10 % and thereafter on increasing RHA content beyond 10 %, the UCS value of composite did not show much increases.
6. Based on the above results, it can be concluded that an optimum content of 10 % RHA is best for stabilization of poor clayey soils.

## REFERENCES

1. Bhasin, N. K. "A Laboratory Study on the Utilization of Waste Materials for the Construction of Roads in Black Cotton Soil Areas." ROAD RESEARCH PAPERS; N225, 1988.
2. A.S. Muntohar, and G. Hantoro, "Influence of Rice Husk Ash and Lime on Engineering Properties of a Clayey Subgrade," Electronic Journal of Geotechnical engineering, 2000.
3. E.A Basha, R Hashim, and A.S Muntohar, 'Effect of the Cement- Rice Husk Ash on the Plasticity and Compaction of soil,' Electronic Journal of Geotechnical Engineering, 8 (A), 2003.
4. A.N. Ramkrishna, and A.V. Pradeepkumar, "Stabilization of Black Cotton Soil using Rice Husk Ash and Cement," Proceedings of National conference, Civil Engineering meeting the challenges of Tomorrow, page 215-220, 2006.

5. R.S. Sharma, B.R. Phanikumar, and B.V. Rao, "Engineering Behavior of a Remolded Expansive Clay Blended with Lime, Calcium Chloride and Rice- Husk Ash," *Journal of Materials in Civil Engineering*, vol. 20(8), page 509-515, 2008.
6. D.K. Rao, P.R.T. Pranav, and M. Anusha, "Stabilization of Expansive Soil using Rice Husk Ash, Lime and Gypsum- an Experimental Study," *International Journal of Engineering Science and Technology*, vol. 3(11), page 8076-8085, 2011.
7. A.K. Sabat, and R.P. Nanda, "Effect of Marble Dust on Strength and Durability of Rice Husk Ash Stabilised Expansive Soil," *International Journal of Civil and Structural Engineering*, vol. 1(4), page 939-948, 2011.
8. A.K. Sabat, "Effect of Polypropylene Fiber on Engineering Properties of Rice Husk Ash – Lime Stabilized Expansive Soil," *Electronic Journal of Geotechnical Engineering*, vol. 17(E), page 651-660, 2012.A.A.
9. Ashango, and N.R. Patra, (2014) "Static and Cyclic Properties of Clay Subgrade Stabilised with Rice Husk Ash and Portland Slag Cement," *International Journal of Pavement Engineering*, 2014.



## 3D Numerical Analyses of Geosynthetic Encased Floating Granular Piles in Soft Soil

Murtaza Hasan,<sup>1</sup> N. K Samadhiya,<sup>2</sup> and Amit Daiya<sup>3</sup>

<sup>1</sup>Assistant Professor, Department of Civil Engineering, Government Engineering College Bharatpur, Bharatpur, India-321001; e-mail: murtazadce@gmail.com, Corresponding Author

<sup>2</sup>Professor, Department of Civil Engineering, Indian Institute of Technology Roorkee, Roorkee, India – 247667; e-mail: nksamfce@iitr.ac.in

<sup>3</sup>Assistant Professor, Department of Civil Engineering, Government Engineering College Bharatpur, Bharatpur, India-321001; e-mail: amitdaiya@gmail.com

### ABSTRACT

The granular piles do not achieve significant load carrying capacity in very soft clays due to low lateral confinement. In recent years, geosynthetic reinforced granular piles have been widely used to provide additional confinement from geosynthetic. In the present paper, numerical analyses have been performed on vertical encased granular piles installed in very soft clays. The analyses have been carried out by using a finite element software, Plaxis 3D. The effect of various parameters such as geotextile stiffness and shear strength of clay were studied. A linear elastic perfectly plastic Mohr Coulomb model was used for clay and stone aggregates. Vertical load-settlement relationships of geotextile reinforced granular piles treated ground were obtained and compared that obtained from untreated ground. The results show significant improvement in the failure load of granular piles due to the incorporation of geotextile.

**KEYWORDS:** *Plaxis 3D; FEM; ground improvement; stone columns; geotextile; soft clay*

### INTRODUCTION

Ground improvement of soft clayey soils using granular piles, also known as stone columns has been a relatively new innovation, becoming popular in the last forty years. Recently, the technique has become widely used to support lightly and moderately loaded structures. Granular piles have been adopted for improving the load capacity, reducing total settlement, obtaining higher shear strength and increasing the unit weight of treated ground (Greenwood, 1970; Hughes et al., 1975; Hasan and Samadhiya 2015). Granular piles are commonly effective in clays having undrained shear strength in the range of 7-50 kPa (Barksdale and Bachus, 1983; IS: 15284-2003). Due to low lateral confinement, granular piles do not achieve significant load carrying capacity in very soft clays. Therefore, granular piles with additional confinement are required for the better performance. Geosynthetic reinforced granular piles have been successfully adopted in very soft soils throughout the world. The reinforcement effect in the form of either horizontal strips or vertical encasement has been very well established through various laboratory studies, fields and numerical analyses. Vertical encased granular piles have several advantages such as increment in load carrying capacity of pile by mobilisation of hoop stress in reinforced material; preventing the loss of pile material into surrounding soft clays; preserving frictional properties and the drainage of the stone aggregates. In the past, various researchers such as Murugesan and Rajagopal (2006, 2007), Wu and Hong (2009), Pulko et al. (2011), Yoo and Lee (2012), Almeida et al. (2014), Zhang and Zhao (2015), Mohapatra et al. (2016) and Hasan and Samadhiya (2016, 2017) have conducted large and small-scale laboratory tests, numerical analyses and field tests on vertical encased granular piles in very soft clays. Most of the laboratory studies on granular piles installed in soft clay are associated with end bearing piles; however limited information is available on the behavior of floating granular piles. In the present paper, numerical analyses have been carried out on ordinary and vertically reinforced floating granular piles installed in very soft clay to investigate the qualitative and quantitative improvement in the load carrying capacity of granular piles. Numerical analyses have been extended to the study effect of undrained shear strength of clay and geotextile stiffness using Finite-element analysis (FEM) software, Plaxis 3D.

### OUTLINE OF NUMERICAL ANALYSES

The numerical analyses have been performed on 75 mm diameter and 375 mm (5d) length single floating GP, where d is the diameter of the pile. Unit cell concept was simulated around each granular pile by assuming piles in a triangular pattern. The area replacement ratio was found to be 14% with spacing (s) of 2.5d. The granular piles were

installed in clay bed in a 200 mm diameter cylindrical tank and depth of clay bed was kept 525 mm (7d) throughout analyses. The encasement up to entire length of pile was assumed for vertical reinforced granular piles. Undrained shear strength ( $c_u$ ) of the soft clay taken as 5 kPa.

### Materials Used

Clay crushed stone aggregates and geotextile were used in the present analyses. These materials were collected from locally available sites and tested in Geotechnical Engineering Laboratories, Department of Civil Engineering, Indian Institute of Technology Roorkee. The physical properties of clay are specific gravity = 2.73, optimum moisture content = 17.56%, maximum dry unit weight = 17.22 kN/m<sup>3</sup>, liquid limit = 48%, Plastic limit = 18% and Plasticity index = 30 %. The dry unit weight and undrained shear strength corresponding to 34% water content were 13.85 kN/m<sup>3</sup> and close to 5 kPa respectively. It was classified as CI as per IS: 1498:2000. The Poisson's ratio for soft clay and aggregates were taken as per typical values suggested by Bowles (1997). The crushed stone aggregates made of granite and were 2–6.3 mm in size. The maximum and minimum dry unit weights of the aggregate are 15.04 kN/m<sup>3</sup> and 13.41 kN/m<sup>3</sup> respectively. The dry unit weight and angle of internal friction of stone aggregates at 70% relative density were 14.51 kN/m<sup>3</sup> and 43° respectively. The ultimate tensile strength of geosynthetic was determined from standard wide-width tension tests (ASTM D4595). The ultimate tensile strength and axial stiffness of geotextile used in the present study were found to be 4.41 kN/m and 8.07 kN/m. The strain corresponding to ultimate tensile force of geotextile was found to be 54.42%. The thickness of geotextile was found to be 2 mm.

### FINITE ELEMENT ANALYSES

FEM study was carried out by finite element software, Plaxis 3D. The vertical load-settlement behaviour of GP was obtained from Plaxis models. Plaxis 3D model was validated by simulating load settlement behaviour of single sand-fibre mixed GP by Basu (2009). Basu (2009) conducted laboratory test on rectangular tank of size 0.2625 m × 0.2625 m × 0.6 m. A GP having diameter of 75 mm and 600 mm length was installed in the centre of tank and loaded alone. In present study, a model was generated and analysed using Mohr–Coulomb failure criterion. The steps of modelling such as generation of the testing tank, formation of the granular pile and application of the load in the form surface prescribed displacement are presented in Fig. 1. The material properties used in the modelling are given in Table 1. The comparison of experimental and Plaxis 3D results is shown in Fig. 2. The results were found to be in reasonably good agreement.

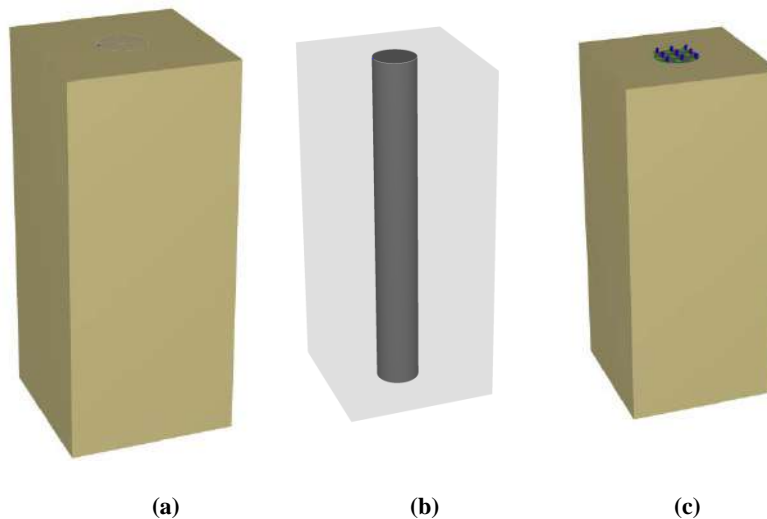
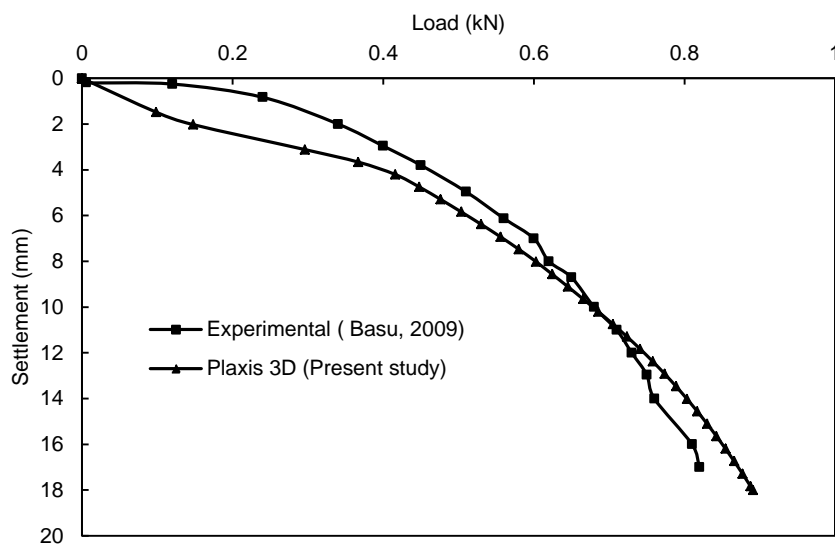


Fig. 1 Modelling of testing tank with (a) clay bed (b) granular pile and (c) surface displacement

**Table 1. Material properties used in Plaxis 3D**

Parameters	Basu (2009)		Present study	
	Clay	Sand-fibre mix	Clay	Stone aggregates
Young's modulus, E (kPa)	250	6700	420	42500
Cohesion (kPa)	16.0	15.55	5	0
Angle of internal friction, $\phi$ ( $^{\circ}$ )	0	34.47	0	43
Poisson's ratio, $\mu$	0.3	0.3	0.48	0.3
Dry unit weight ( $\text{kN/m}^3$ )	14.90	18.0	13.85	14.51
Bulk unit weight ( $\text{kN/m}^3$ )	19.37	-	18.58	-



**Fig. 2 Plaxis validation (Basu, 2009)**

In the present study, consolidation effect of clay was not taken into account. The linear elastic perfectly plastic Mohr Coulomb model, which was used by various authors (Ambily and Gandhi, 2007; Ghazavi and Afshar, 2013; Pulko et al., 2011) for similar study, has been adopted for clay and stone aggregates. Geotextile has been modelled as elastic material. In the modeling of tank, vertical boundaries can move only in the vertical directions and the bottom boundary of tank was kept restricted to move in all the three directions. The load on the GP was applied in the form of prescribed displacement by assuming rigid behaviour of loading plate. Loading period was kept short to ensure undrained loading condition. The material parameters used in present analyses ( $E$ ,  $c_u$ ,  $\phi$ ,  $\gamma_d$ ,  $\psi$ ) have been determined from relevant laboratory model tests and are given in Table. 1. The dilation angle for stone aggregates was determined from the relationship  $\Psi \approx \phi - 30^{\circ}$ . In the present analysis,  $\Psi$  has been taken as  $10^{\circ}$ . Plastic strain increments are computed using a non-associated flow rule. The interface between a GP and clay is a mixed zone where the shear strength properties of bed can vary, depending on the method of installation. Therefore an interface element has not been taken in the present paper. Generated mesh with nodes and stress points in the form volume and connectivity plot under medium element distribution for vertical encased floating granular pile are shown in Fig. 3.

## RESULTS AND DISCUSSION

The numerical analysis has been performed to estimate the ultimate load or failure load of ordinary and vertical encased floating granular piles. The results in terms of vertical load-settlement behaviour of clay bed, unreinforced and vertical encased floating granular piles are shown in Fig. 4. As may be seen from the figure, the unreinforced and reinforced floating granular piles exhibit clear ultimate load. The vertical load corresponding to 30 mm settlement was assumed to be ultimate load or load carrying capacity of GP.

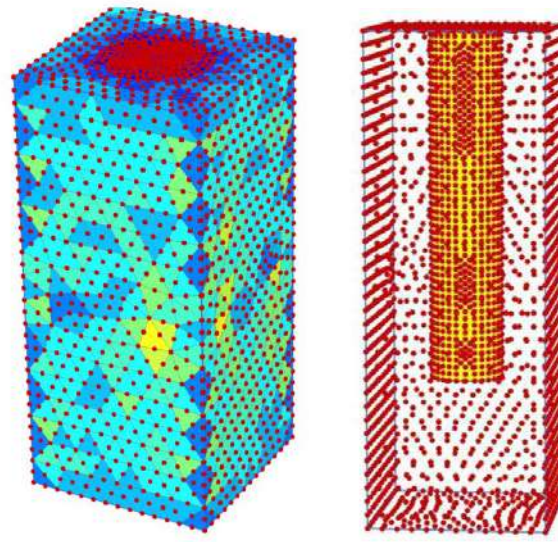


**Fig. 3 Mesh generation for vertical encased floating granular pile**

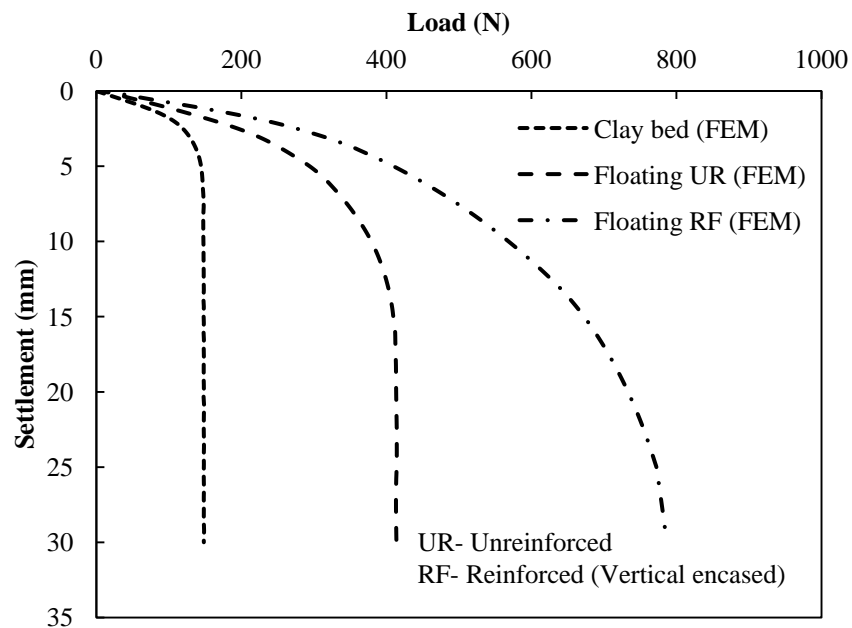


**Fig. 4 Load-settlement behaviour of unreinforced and vertical encased floating granular pile**

The load carrying capacity for unreinforced and vertical encased floating GP has been found to increase by 183% and 430% respectively as compared to clay bed. However, the increase in load carrying capacity for encased floating GP was found to increase 88% as that of unreinforced GP. The influence of shear strength of the soft clay on the behaviour of encased floating granular piles was studied. The shear strength of the clay bed was varied in the range 2 kPa-15 kPa. The axial stiffness of geotextile was taken as 7.32 kN/m. The variation of load carrying capacity with shear strength of encased floating GP is shown in Fig. 5. The load carrying capacity of encased floating GP has been found to increase with an increase in the shear strength of clay, which may be attributed to higher lateral confining pressure. The influence of the stiffness of geotextile on the behaviour of encased floating GP was also studied by numerical analyses. The encasement stiffness of geotextile was taken between 7 and 250 kN/m. The effect of stiffness on the load carrying capacity encased floating GP is shown in Fig. 6. The load carrying capacity has been

found to increase up to 50 kN/m stiffness of encasement, and then is constant for higher stiffness. It was observed that granular pile penetrated into clay rather than bulging due to higher stiffness of encasement.

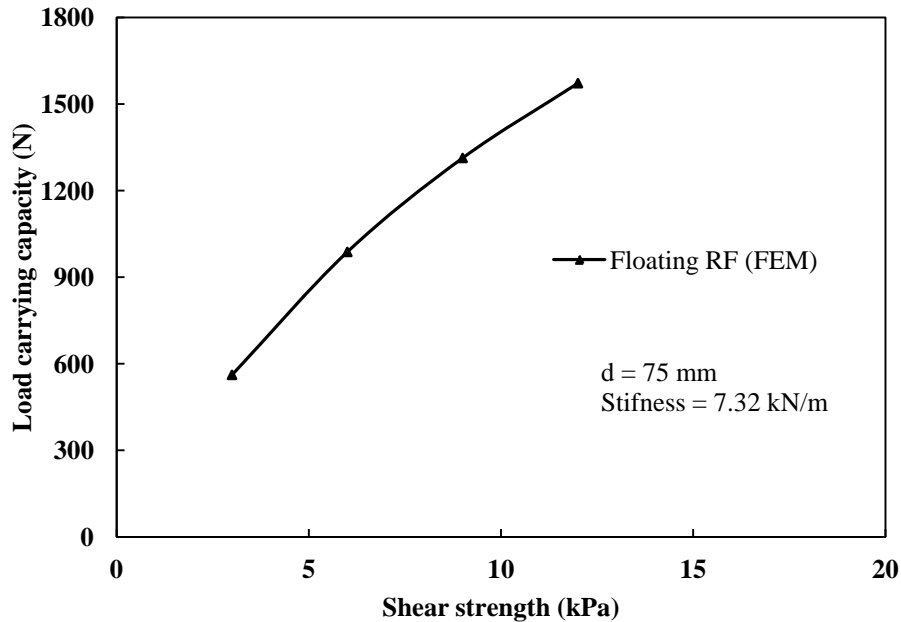


Fig. 5 Variation of the load carrying capacity with undrained shear strength

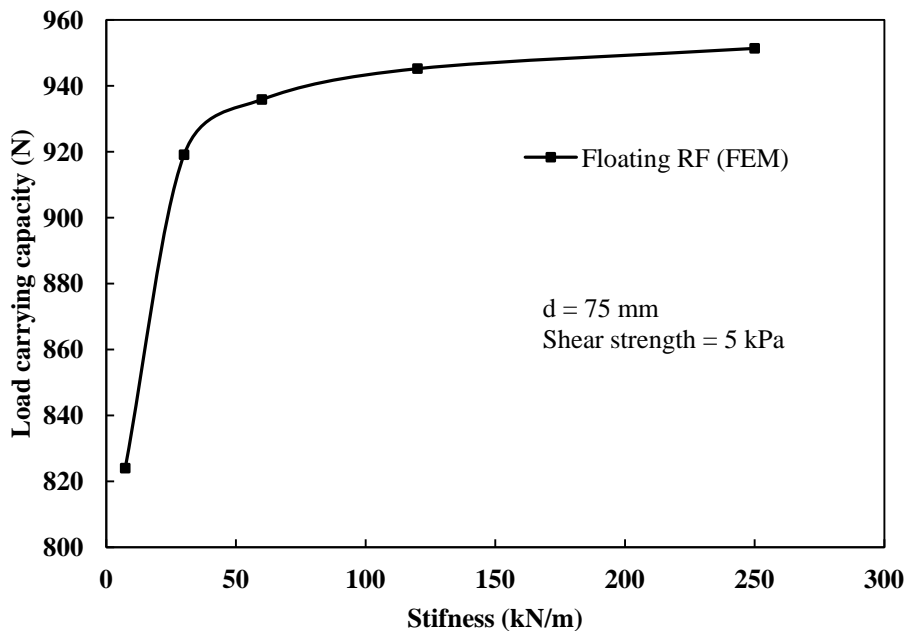


Fig. 6 Variation of the load carrying capacity with axial stiffness of geotextile

## CONCLUSIONS

In the present investigation, numerical analyses were carried out on 75 mm diameter encased floating granular piles. The effects undrained shear strength of clay and geogrid stiffness was also studied. The vertical load-settlement plots of unreinforced and vertical encased granular piles from Plaxis 3D numerical models were compared with that obtained from untreated ground. The following conclusions can be drawn:

1. The load carrying capacity of GP installed in very soft clay has been found to further improve due to inclusion of geosynthetic materials.
2. The load carrying capacity for unreinforced and encased floating GP was found to increase by 183% and 430% respectively as compared to clay bed.
3. The load carrying capacity of encased granular piles has been found to improve with increase in the shear strength of clay bed.
4. The load carrying capacity of floating encased GP has been found to increase up to 50 kN/m stiffness of geotextile, and then is constant for higher stiffness.
5. The reinforcement provided in the granular piles controls bulging of the granular piles.

## REFERENCES

- Almeida, M., Hosseinpour, I., Ricci, M., and Alexiew, D. (2014). "Behavior of Geotextile-Encased Granular Columns Supporting Test Embankment on Soft Deposit." *J. Geotech. Geoenviron. Eng. ASCE*, 1943-5606.0001256, 04014116
- Ambily, A. P. and Gandhi, S. R. (2007). "Behavior of stone columns based on experimental and FEM analysis." *Journal of Geotechnical and Geoenvironmental Engineering, ASCE*, 133(4), 405-415.
- ASTM D4595 (1986). *Standard test method for tensile properties of geotextiles by the wide-width strip method*, ASTM International, West Conshohocken, PA, USA.
- Barksdale, R. D. and Bachus, R. C. (1983). *Design and construction of stone columns: Final Report SCEGIT-83-104*. Federal Highway Administration, Washington D.C. 20590.
- Basu, P. (2009). *Behaviour of sand-fibre mixed granular piles*. Ph.d Thesis, Indian Institute of Technology Roorkee, Roorkee.
- Bowles, J. E. (1997). *Foundation analysis and design*, Mc Graw Hill International Editions, Singapore.
- Ghazavi, M. and Afshar, J. N. (2013). "Bearing capacity of geosynthetic encased stone columns." *Geotextiles and Geomembranes*, 38, 26-36.
- Greenwood, D. A. (1970). "Mechanical improvement of soils below ground surfaces". *Proceedings of ground engineering conference*, institution of civil engineers, London, 11-22.
- Hasan, M. and Samadhiya, N. K. (2015). "Experimental study on performance of floating granular piles in soft clay." *Indian geotechnical conference*, Pune, Maharashtra, India.
- Hasan, M. and Samadhiya, N. K. (2016). "Experimental and numerical analysis of geosynthetic-reinforced floating granular piles in soft clays." *Int. J. of Geosynth. and Ground Eng.* 2: 22. doi:10.1007/s40891-016-0062-6.
- Hasan, M. and Samadhiya, N. K. (2017). "Performance of geosynthetic-reinforced granular piles in soft clays: Model tests and numerical analysis." *Computers and Geotechnics* 87, 178-187.
- Hughes, J. M. O., Withers, N. J. and Greenwood, D. A. (1975). "A field trial of the reinforcing effect of a stone column in soil". *Geotechnique* 25(1), 31-44.
- IS: 1498 (2000). *Classification and identification of soils for general engineering purposes*, Indian Standards Institution, New Delhi, India.
- Mohapatra, S.R., Rajagopal, K., and Sharma, J. (2016). "Direct shear tests on geosynthetic-encased granular columns". *Geotextiles and Geomembranes*, 44, 396-405.
- Murugesan, S. and Rajagopal, K. (2006). "Geosynthetic-encased stone columns: numerical evaluation". *Geotextiles and Geomembranes*, 24, 349-358.
- Murugesan, S. and Rajagopal, K. (2007). "Model tests on geosynthetic encased stone columns". *Geosynthetics International*, 24(6), 346-354.
- Pulko, B., Majes, B. and Logar, J. (2011). "Geosynthetic-encased stone columns: analytical calculation model". *Geotextiles and Geomembranes*, 29(1), 29-39.
- Wu, C. S. and Hong, Y. S. (2009). "Laboratory tests on geosynthetic encapsulated sand columns". *Geotextiles and Geomembranes*, 27(2), 107-120.
- Yoo, C. and Lee, D. (2012). "Performance of geogrid-encased stone columns in soft ground: full-scale load tests". *Geosynthetics International*, 19(6), 480-490.
- Zhang, L. and Zhao, M. (2015). "Deformation analysis of geotextile-encased stone columns". *Int. J. Geomech, ASCE*, 15(3):04014053.



## IMPROVEMENT OF SHEAR STRENGTH OF SOIL BY MIXING OPTIMUM PERCENTAGE OF BITUMEN EMULSION AND CEMENT CONTENT

Dilshad Ahmad Idrisi<sup>1</sup>, Arushi Rawat<sup>1</sup>, and Siddharth Mehndiratta<sup>2</sup>

<sup>1</sup>UG Student, Department of Civil Engineering, G. B. Pant Institute of Engineering and Technology, Pauri

<sup>2</sup>Assistant Professor, Department of Civil Engineering, G. B. Pant Institute of Engineering and Technology, Pauri

Corresponding Author: siddharth14feb@gmail.com

### ABSTRACT

Soil is the most abundant naturally occurring material on earth surface in which almost all of the civil engineering work has been initiated. Soil shows variation in its properties and behaviour from place to place. Thus, there is a requirement to enhance the soil properties for long term success of construction project. One of the most important property of soil is shear strength which is due to cohesion and internal friction. It must be sufficient enough so that load coming from superstructures, bridges etc. can be easily dispersed to the soil without harming the structures. Even sometime it is observed that soil having good shear strength can also get failed due to differential settlement. Therefore, in order to overcome this problem different experimental study has been performed on soil to get the knowledge of physical properties of soil. In the present study, many attempts have been made to strengthen the soil properties using traditional materials which include bitumen emulsion and cement content in some proportion and then the results from both the materials has been compared and analyzed. The soil used in this study is clayey sand from Ghurdauri located near Pauri, Gharwal, and Uttarakhand. The results show that the cement is more effective for stabilization where more bearing strength is required and Bitumen Emulsion most likely to use for stabilization where more shear strength is required. In contrast to traditional material, bitumen emulsion is costly. Though it can be used in places having poor soil due to its shear strength enhancing property.

**Keywords:** Bitumen Emulsion, Cement, Shear Strength, Direct Shear Test

### INTRODUCTION

In a country like INDIA where soil types vary from section to section in different zones, it is very important to consider the behaviour of soil. Soil is one of the raw materials used in the construction process which plays an effective role in the designing of all kind of construction projects. An advance understanding of the soil behaviour can help in evaluation of strength of soil. A structure can only be strong if soil below it having good shear strength properties. Therefore, to obtain the engineering durability the understanding of engineering properties of soil is crucial.

Soil stabilization has often been the main concern of researchers in geotechnical engineering. Geotechnical engineers have always looked for solutions to stabilize and sustain the soil besides having an economical design.

In present study, the soil stabilization is done using bituminous emulsion and cement. The strength of soil from both the material is analysed. Initially the soil properties are determined by conducting sieve analysis, plastic limit, liquid limit, specific gravity and shrinkage limit test. thereafter strength of soil is determined by conducting standard proctor test, CBR test and the shear strength is determined by conducting direct shear test.

Bitumen emulsion is a mixture of water and bitumen but bitumen doesn't mix with water directly due to its oily nature. Hence, an emulsion is added with water before bitumen. Addition of emulsion with water before addition of bitumen into particles and keeps it dispersed in suspension. Bitumen emulsion is a two-phase system, one phase is of bitumen and other phase is of water, the proportion of bitumen are varied from 30-70 % depending upon our requirement.

Previously lots of research work has done on soil bitumen and gravel soil bitumen stabilization in different places. The present study is being inspired from the studies discussed below

Conway (1993) conducted laboratory bench-scale demonstration to comprehensively evaluate and demonstrate the effectiveness of the process in immobilizing the environmental contaminants of soil resulting from four common petroleum products: fuel oil (2-oil), fuel, oil (6-oil), gasoline and jet fuel (JP4).

Mosaddeghi et al. (1999) worked on soil compatibility by increasing the organic content in soil which could help not only in reducing compatibility but also increase soil traffic ability.

Ramit et al. (2017) worked on implementation of hydrocarbon emulsion in gravel road to boost strength and geotechnical property of soil. Several modifiers have been tried to improve the properties of soil subgrade in terms of engineering properties and performance criteria to derive the maximum benefits to withstand the modern-day heavy traffic stresses.

Kumar et al. (2017) worked on laterite soil using bitumen emulsion and ESP, CSA (egg shell powder and coconut shell ash) to strengthen the soil. CSA used as soil stabilizer to increase such as durability, high toughness, abrasion resistance etc. CSA has long standing use and it is environment friendly.

### OBJECTIVE

Objective of the present study is to stabilize the soil using bitumen emulsion and cement admixtures. The optimum percentage of bitumen emulsion and cement admixture is concluded by comparing the results with original soil sample. Different laboratory test is performed to get the index properties and engineering properties of soil. Direct shear test is used to measure the shear strength parameter of soil whereas California Bearing Ratio (CBR) test is used for the evaluation of subgrade strength of roads and pavements.

### MATERIAL USED

The materials used in this project are *Natural Soil*, *Cement* and *Bitumen Emulsion*. The local soil is obtained from G. B. Pant Institute of Engineering and Technology, Pauri Garhwal (Uttarakhand). Experimental study on the natural soil is conducted to know the physical property of soil. Initially Sieve analysis, liquid limit, plastic limit, standard Proctor test, specific gravity tests are conducted for soil classification. The properties of the soil are mentioned in below Table 1.



Fig. 1 Location of Soil Sample

Table 1: Properties of natural soil

S. No.	Property	Value
1.	Specific Gravity	2.654
2.	Liquid Limit (%)	32.69
3.	Plastic Limit (%)	23.853
4.	Plasticity Index (%)	8.837
5.	IS Classification	SC (Clayey Sand)
6.	Optimum Moisture Content (%)	14
7.	Density at OMC (g/cm <sup>3</sup> )	2.008
8.	Maximum Dry Density (g/ cm <sup>3</sup> )	1.7614

**Cement:** Cement is a binder, a substance used for construction that sets, hardens and adheres to other material, binding them together. Cement is use as a traditional material for soil stabilization or to improve geotechnical properties such as plasticity, compaction, and unconfined compressive strength. The Cement used in this project has following properties given in the Table 2.

**Table. 2** Properties of Cement

Type of Cement	Portland Pozzolana Cement
Specific Gravity	2.7
Fineness	2.1 %
Initial Setting Time	128 min
Soundness	5 mm

**Bitumen emulsions:** Bitumen emulsions consist of small droplets of bitumen dispersed in water and may be either anionic or cationic depending on the chemicals used to emulsify the bitumen. When bitumen emulsion is applied to the surface of the soil, the water evaporates, and the emulsion changes color from brown to black. The Bitumen Emulsion used in this project has following properties given in the Table 3.

**Table. 3** Properties of Bitumen Emulsion

Name of Product	Bitumen Emulsion
Type of Product	RS-1 (Rapid Setting)
Ionic Behavior	Cationic
Water Content	50 %
Average Setting Time	15 min

## RESULT AND DISCUSSION

### Comparison of Shear Strength of Soil with Different Percentage of Cement and Bitumen Emulsion

Various Direct Shear Test was performed to estimate the shear strength of soil with  $x\%$  increase in quantity of cement and Bitumen Emulsion in different manner. Each test was performed with different normal loads i.e.  $0.5 \text{ Kg/m}^2$ ,  $1.0 \text{ Kg/m}^2$ ,  $1.5 \text{ Kg/m}^2$ . Figure 2 shows the variation of shear strength of soil with different percentage of cement content. It is observed that shear strength is continuously increasing with increase in cement content.

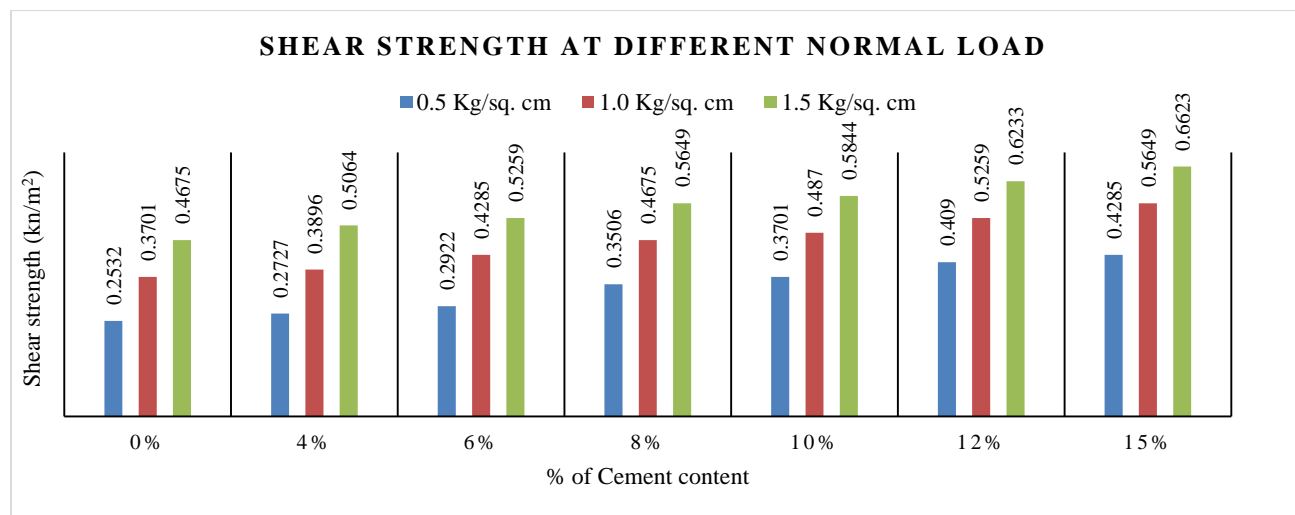


Fig. 2 Shear Strength at different Normal Stress (varying cement content)

Figure 3 display the variation of shear strength of soil with different percentage of Bitumen Emulsion. It is attributed from this figure that shear strength of soil will increase up to 8% of Bitumen emulsion and thereafter it will start reducing. Same trend has been observed for each normal load i.e.  $0.5 \text{ Kg/m}^2$ ,  $1.0 \text{ Kg/m}^2$ ,  $1.5 \text{ Kg/m}^2$ . Therefore, it is

concluded from this figure that 8% Bitumen emulsion is the optimum percentage of Bitumen emulsion at which maximum shear strength of soil is achieved. It is also observed from this figure that as the percentage of Bitumen Emulsion content reaches to 25, shear strength and shear strength parameter attained the values slightly equal as natural soil.

### COMPARISON OF SHEAR STRENGTH AT DIFFERENT PERCENTAGE OF BITUMEN EMULSION MIX

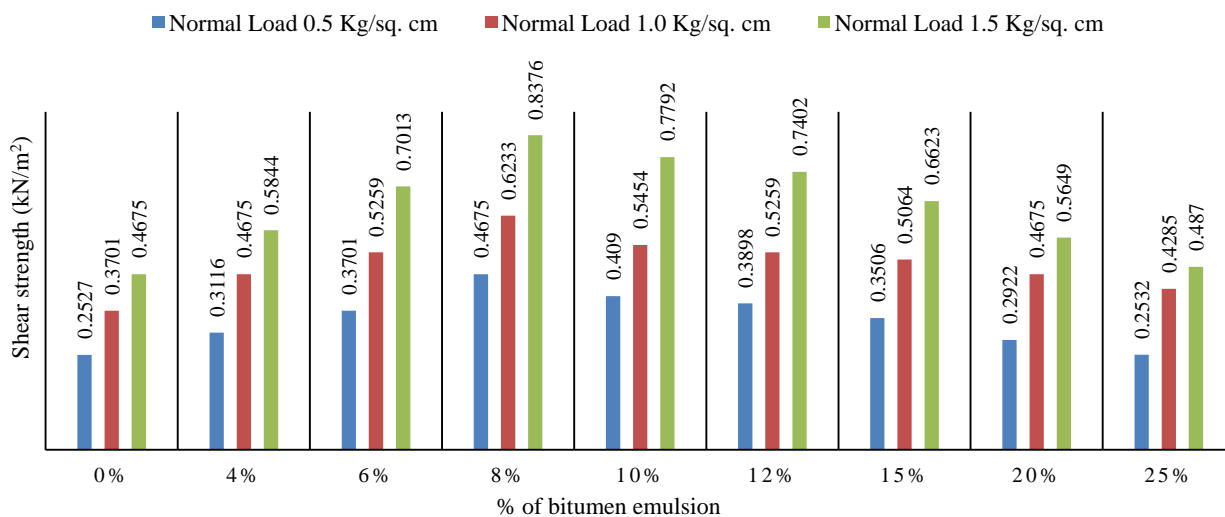


Fig. 3 Shear Strength at different Normal Stress (varying bitumen emulsion)

### Comparison of Shear Strength Parameter Cohesion and Angle of Internal Friction of Soil with Addition of Different Percentage of Cement and Bitumen Emulsion

Various Direct Shear Test was performed to estimate the shear strength parameters (Cohesion and Angle of internal friction) of soil with  $x\%$  increase in quantity of cement and Bitumen Emulsion in different manner. Figure 4-7 shows the variation of cohesion and angle of internal friction respectively with different percentage of Cement and Bitumen emulsion. Results indicates that shear strength parameter will increase in addition of each % increase of cement but shear strength parameter get maximum value at 8% of Bitumen Emulsion i.e. optimum percentage.

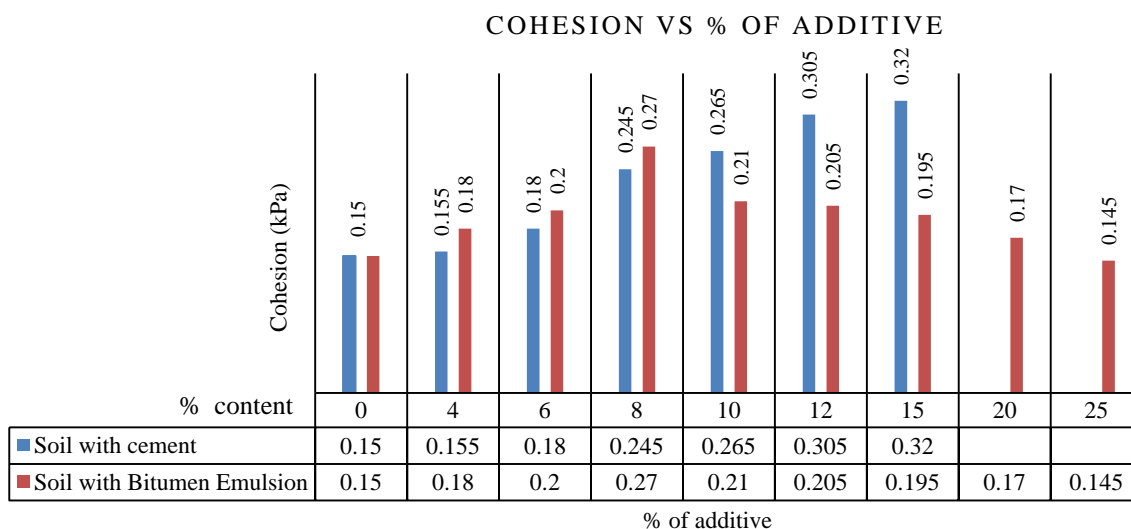


Fig. 4. Cohesion at different percentage of additives

### ANGLE OF INTERNAL FRICTION VS % OF ADDITIVE

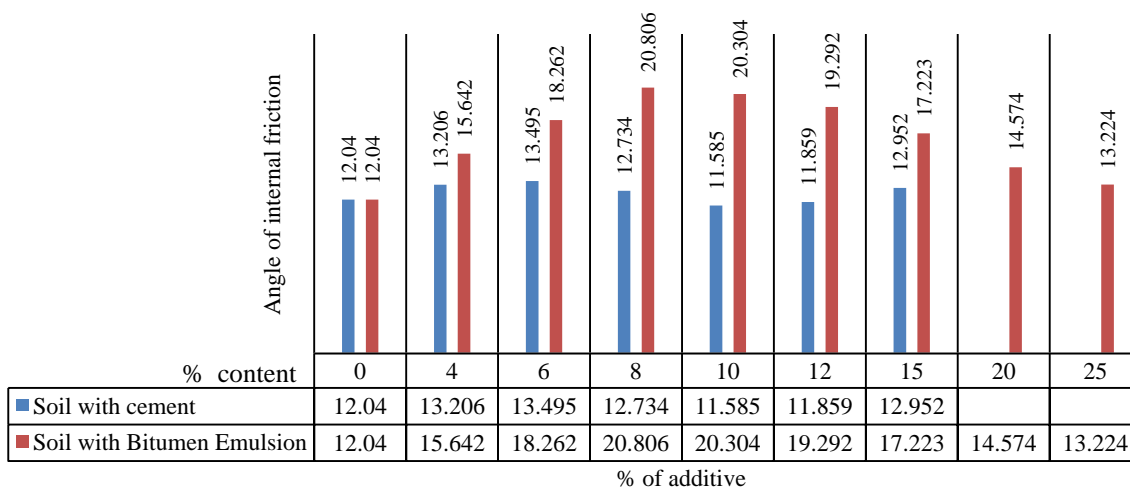


Fig. 5 Angle of internal friction at different percentage of additives

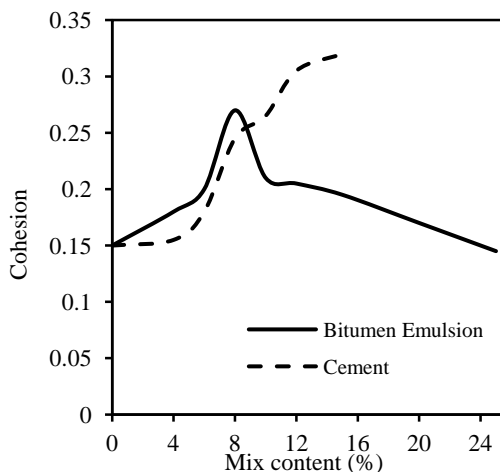


Fig. 6 Cohesion vs % of Content

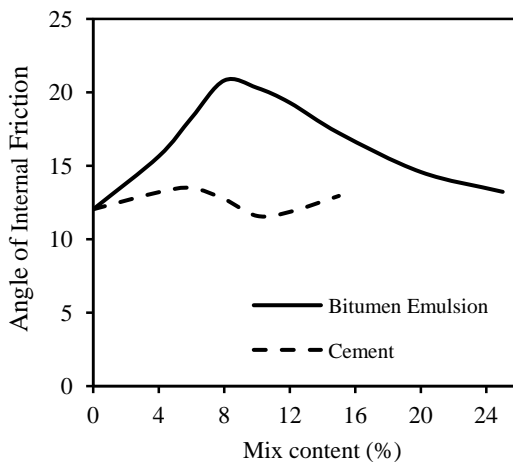


Fig. 7 Angle of internal friction (°) vs % of Content

### Comparison of CBR Value of Soil for Design of Soil Subgrade with Addition of Different Percentage of Cement and Bitumen Emulsion

Various CBR Test (California Bearing Ratio Test) was performed to estimate the Soil Subgrade with different percentage of cement and Bitumen Emulsion. Figure 8 shows that subgrade strength continuously increases with increase in cement content but subgrade strength will be maximum when 8% of Bitumen Emulsion is added to the soil i.e. optimum percentage because after 8%, CBR value start reducing.

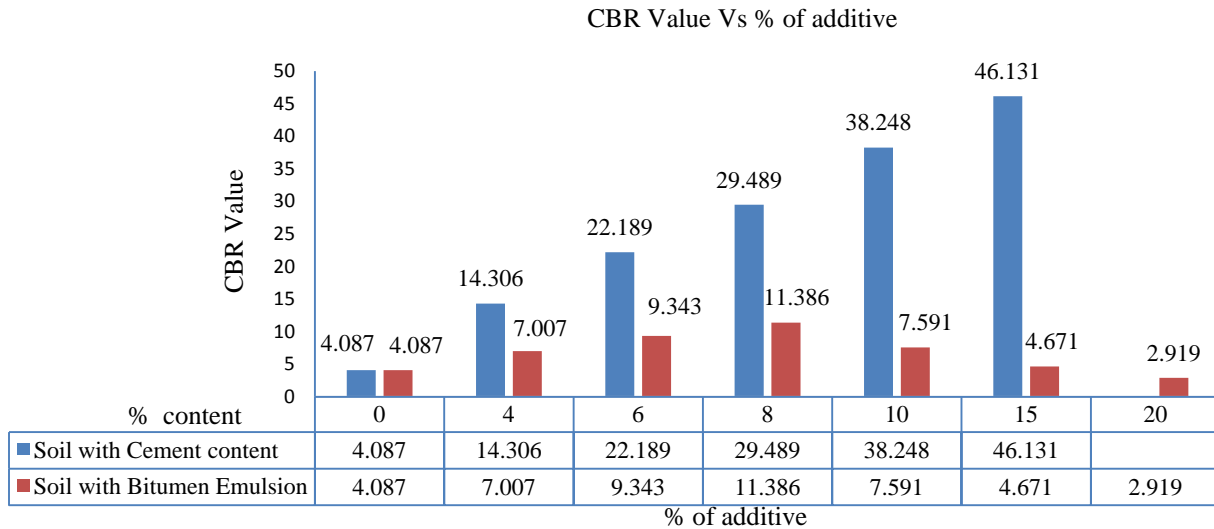


Fig. 8 CBR with different percentage of additives

## CONCLUSION

- The cost of Bitumen Emulsion is more than various traditional materials used for the soil stabilization but it can be used in places having very poor soil due to its shear strength enhancing property.
- The results indicate that with the increase of Bitumen Emulsion content in the soil sample, there is a rise in shear strength of soil up to 8 % proportion ratio thereafter shear strength of soil decreases with further increase in bitumen emulsion content. Correspondingly with the increase of cement content in the soil sample, the strength of soil continuously increases.
- CBR value at 20 % Bitumen emulsion proportion ratio is less than CBR value of natural soil.
- As the percentage of Bitumen Emulsion content reaches to 25, shear strength and shear strength parameter attained the values slightly equal as natural soil.
- Cement is more effective for stabilization where more bearing strength is required and Bitumen Emulsion is most likely to use for stabilization where more shear strength is required.

## REFERENCES

1. Asphalt emulsion-conditioner. U.S. Patent 4, 293,459, issued October 6, 1981.
2. Conway, M. F. (1993). Bench-scale evaluation of asphalt emulsion stabilization of contaminated soils. *Soil and Sediment Contamination*, 2(2), 157-165.
3. IS: 2720-Part 13 (1986), Indian standard methods of test for soils: Methods of test for soils-Direct shear test, Bureau of Indian Standards, New Delhi.
4. IS: 2720-Part 16 (1987), Indian standard methods of test for soils: Methods of test for soils-Laboratory determination of CBR, Bureau of Indian Standards, New Delhi.
5. IS: 2720-Part 3 (1980), Indian standard methods of test for soils: Determination of Specific gravity. Bureau of Indian Standards, New Delhi.
6. IS: 2720-Part 4 (1985), Indian standard methods of test for soils: Grain size analysis. Bureau of Indian Standards, New Delhi.
7. IS: 2720-Part 5 (1985), Indian standard methods of test for soils: Determination of liquid limit and plastic limit (second revision). Bureau of Indian Standards, New Delhi.
8. IS: 2720-Part 7 (1980), Indian standard methods of test for soils: Determination of water content-density relation using light compaction (Second revision), Bureau of Indian Standards, New Delhi.
9. Kumar, N. V., Asadi, S. S., Prasad, A. V. S., Kumar, G. P., and Vaddeswaram (2017), G. Study on strength of laterite soil using bitumen emulsion and esp, CSA.
10. Mosaddeghi, M. R., Hajabbasi, M. A., Hemmat, A., and Afyuni, M. (2000). Soil compactibility as affected by soil moisture content and farmyard manure in central Iran. *Soil and Tillage Research*, 55(1-2), 87-97.



## Influence of Vibrations by Rolling Stock Metro Rail on Pile-Soil Interaction

S. Rupali<sup>1a</sup>, T. R. Arvind<sup>b</sup>, I. Bhat<sup>c</sup>, K. Senthil<sup>d</sup>, A. K. Agnihotri<sup>e</sup>

<sup>a, d</sup> Assistant Professor, Department of Civil Engineering, Dr BR Ambedkar NIT Jalandhar, Punjab 144011, India

<sup>b</sup> Post Graduate, Department of Civil Engineering, Dr BR Ambedkar NIT Jalandhar, Punjab 144011, India

<sup>c</sup> Research Scholar, Department of Civil Engineering, Dr BR Ambedkar NIT Jalandhar, Punjab 144011, India

<sup>e</sup> Professor, Department of Civil Engineering, Dr BR Ambedkar NIT Jalandhar, Punjab 144011, India

### Abstract

Metro rail is the most popular rapid transport system which usually commutes along major arterial roads of urban areas. The close proximity of metro alignment to a building foundation will induce vibration on the structure. The vibration transfer greatly depends on the behaviour of soil and foundation system. The behaviour of soil becomes much more complex when the highly complex loading interacts with the substructure, making the soil-structure interaction analysis as an important factor of consideration in dynamic analysis. In view of this, it becomes a matter of utmost priority to understand the complex behaviour of the interaction effect of substructure and the sub soil strata. The main objective of this study is to contribute to the understanding of the response of soil-substructure system considering the soil-pile interaction under dynamic load from an overhead rolling stock. In this context, the numerical investigation has been carried out to analyse the soil-substructure interaction of pile foundation by modelling in ABAQUS that is a commercial finite element tool. The response of soil has been studied against acceleration versus time history of vibration produced by a light rolling stock at 50 kmph. The Mohr-Coulomb yield criterion has been used to model the inelastic behaviour of soil. The studies are carried out to understand the influence of varying peripheral distance from pile and varying depth of pile on well graded medium dense sand under dynamic loading. The post processing results predicted in terms of deformation induced in the soil are studied. The results clearly depict the interaction between pile and soil in vibration transfer. However there are also some notable differences mainly dependent on soil composition and material properties. The boundary dimension was found to have prominent effect on continuum soil modelling and it depends on the type of soil. The length of the pile has also an effect on vibration transfer.

**KEYWORDS:** Soil-pile interaction, Finite element analysis, Continuum soil modelling, Dynamic loading.

### INTRODUCTION

Rapid urbanisation and intense commercial developments in the recent past have resulted in steep rise in travel demand, resulting in pressure on our urban transport infrastructure. Metro rails are proposed as one solution to strengthen the transport infrastructure in cities. One of the main challenge regarding this is the metro alignment passing along major arterial roads of city road network which serve institutional, commercial and residential areas. The metro runs very close to the building foundation, inducing vibration and radiated noise in buildings. This problem consists of the emission of vibration, wave propagation in soil and the building emission of incident wave field. Vibration levels on attached buildings to Metro Rail depend on the distance to the road, transmitted load by the train, train speed, characteristics of the track and dynamic properties of the soil. In general it can be said that the problem of excessive ground-borne vibration due to train traffic has three links, i.e. the source, the path and the receiver. After being generated in the track, and propagating through the media, the vibrations are received by the foundations of nearby buildings. From the foundations the vibrations then propagate to the other parts of the buildings. The term vibration describes repetitive motion that can be measured and observed in a structure. Vibration creates dynamic stresses and strains which can cause fatigue and failure of the structure, fretting corrosion between

---

<sup>1a</sup>Corresponding Author : Email: satavalekarr@nitj.ac.in

<sup>b</sup> Post Graduate Student : Email: aravindr94@gmail.com

<sup>c</sup> Research Scholar : Email: er.ilyasbhat@gmail.com

<sup>d</sup> Assistant Professor : Email: kasilingams@nitj.ac.in

<sup>e</sup> Professor : Email: agnihotriak@gmail.com

contacting elements and noise in the environment. These vibrations can also affect the human response, working of sensitive equipments etc. Moreover, structural characteristics of the building and the foundation determine the dynamic response. The work on frame structures supported on pile foundations was first proposed by Buragohain and Shah (1977) who evaluated the space frames resting on pile foundation by means of stiffness matrix method to quantify the effect of soil-structure interaction. The stiffness matrix for the entire pile group was derived from the principle of superposition using the rigid body transformation. The foundation stiffness matrix was then combined with the superstructure matrix to perform the interactive analysis which was carried out in single step to assess the effect of soil structure interaction on the response of structure in terms of changes in member forces and settlements. Cai et al. (2000) developed a three-dimensional nonlinear finite element subsystem methodology, in which a plasticity-based constitutive model was developed to study the seismic soil-pile-structure interaction effects. The pile-soil subsystem is idealised as an assemblage of solid elements. A 3D version of the hierarchical single surface (HiSS) modelling approach for formulation of the problem is been adopted and it was concluded that with plasticity-based soil model, the motion of the pile foundation deviated significantly from the bedrock motion and this departure from the ground motion should not be overlooked in evaluating the seismic kinematic response of pile-supported structures. Chore et al. (2010) studied the effect of soil-structure interaction on a single-storey, two-bay space frame resting on a pile group embedded in the cohesive soil (clay) with flexible cap. For this purpose three dimensional Finite Element Analysis was carried out independently for the frame and pile foundation. A parametric study was conducted to study the effects of pile spacing, pile configuration, and pile diameter of the pile group on the response of superstructure for different pile tip conditions. In the present study response of soil against acceleration versus time history of vibration produced by a light rolling stock at 50 kmph was evaluated, behaviour of stiff clay and sand on Soil-Pile interaction under vibration was determined and a parametric study was carried out to understand the pile soil behaviour under vibration by varying peripheral distance from pile and varying depth of pile.

## NUMERICAL AND CONSTITUTIVE MODELLING

The modelling was done in a step by step approach. The constitutive modelling of soil, concrete and steel was carried out using ABAQUS/CAE.

### Geometric Modelling

The model consists of soil, pile, pile cap, and reinforcement. But a simplified geometry of the pile and pile cap was used, because the thesis focuses on soil-structure interaction and the modelling of soil. Three different lengths of pile were considered for parametric study. Therefore piles of three different lengths were modelled. The geometric model of the pile and pile cap is as shown in Fig.1. And the model of reinforcement is shown in Fig 2.



Fig.1. Geometric model of pile and pile cap

### Contact Properties

There are two contact areas for the soil and the pile, namely the circumferential boundary of the pile and pile cap in contact with the surrounding soil and the lower boundary of the pile in contact with the soil below the pile. The most important contact is the circumferential one, where the normal and tangential behaviour must be specified in ABAQUS//CAE. For the normal behaviour it was decided to use a "hard" contact together with the penalty constraint enforcement method. The default settings for the contact stiffness were used, meaning a linear relationship with contact stiffness ten times higher than representative underlying element stiffness. Also, the surfaces in contact were allowed to separate. Regarding the tangential behaviour, penalty algorithm was chosen as the constraint enforcement method. The directionality of the friction was assumed to be isotropic and a value of  $\mu = 0.5$  was used. The second contact involves the lower boundary of the pile and the underlying soil. This contact is modelled using a tie constraint, meaning that the two surfaces will undergo the same deformation. For both contact pairs surface-to-surface discretization was used with the pile as the master surface and the soil as the slave surface. The same

constraint is used to model the contact between lower surface of pile cap and soil. The contact between pile and pile cap was also modelled using a tie constraint. And the reinforcement bars were embedded in the concrete. In the ABAQUS manual it is specified that embedded element can be used to model rebar reinforcement but it only simulate a perfect bond condition.

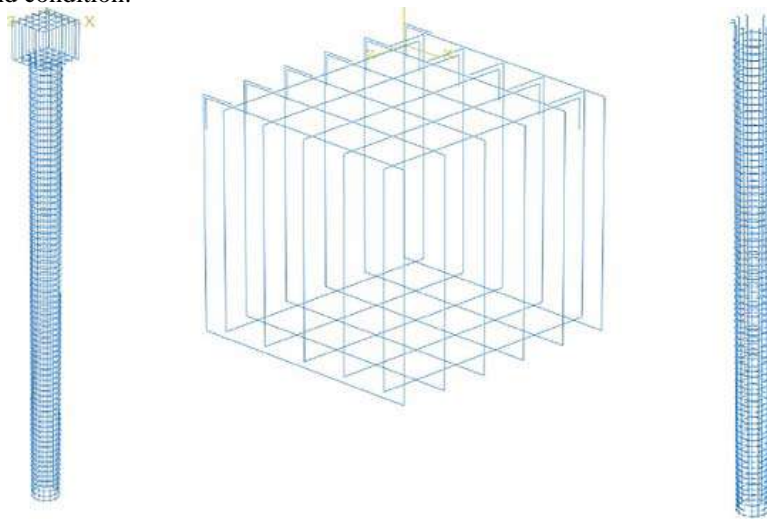


Fig.2. Geometric model of the reinforcement of (a) combined (b) pile cap and (c) pile

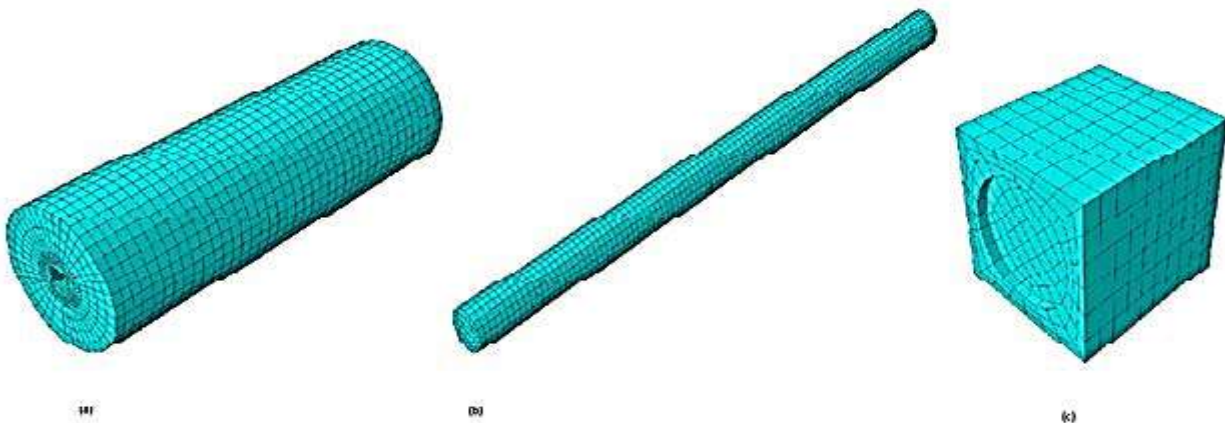


Fig.3. Models of (a) soil, (b) pile and (c) pile cap after meshing.

### Meshing

The pile and pile cap were modelled with solid elements, entitled C3D8R in ABAQUS/CAE, meaning brick elements with quadratic approximation with 8 nodes and reduced integration. A preliminary mesh for the full model was generated. And the elements had a global size of approximately 0.1 meters. Coarse mesh is used because we are interested in the results from soil. The reinforcements were modelled with beam elements, entitled B31 in ABAQUS/CAE, meaning one dimensional linear element with 2 nodes and element size 1m. Moving on to the mesh for the soil, solid C3D8R-elements were used, just as for the pile and pile cap. Regarding the mesh size, smaller mesh size (0.2 m) is modelled close to the pile and a larger mesh size (0.4 m) far away from the most stressed region is used. In order to establish these different mesh size a cylindrical partition in between the two different size mesh regions was modelled with tetrahedral elements. A 10 node modified tetrahedron element C3D10M was used, because, in finite element modelling a finer mesh gives more accurate solution but finer mesh demands lot of computation time. Since the results from the soil are considered here, finer mesh was used at the regions where maximum stress is expected. **Fig 3** depicts different mesh models.

### Application of loading

The loading was applied on the pile cap. The applied loading consist of dead load of the pile and pile cap system, a live load of 1500 kN on the pile cap as pressure distributed over column area (Kochi Metro DPR, 2015).

Acceleration time history of a train composed of 6 cars running on a track of continuous welded rails of 50 kg/m is considered that is shown in **Fig 4**. The mass of concrete sleeper is 251 kg, and the sleeper space is  $d = 0.55\text{m}$ . The distributed rail spring stiffness is  $k_s = 202.46 \times 10^6 \text{ N/m}^2$ , and the wheel-rail contact stiffness coefficient is  $k_H = 1421 \times 10^6 \text{ N/m}$  (Lezin et al., 2013).

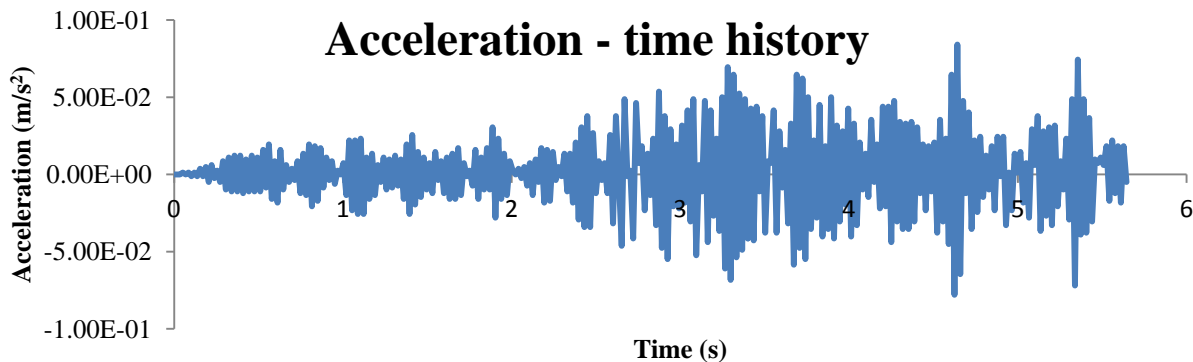


**Fig.4.** Acceleration-Time history of train considered for analysis (Lezin et al., 2013)

### Mesh Convergence Study

The main objective of the mesh convergence study was to find out a mesh size which was good enough to obtain accurate solution with mesh that is sufficiently dense and not overlay demanding computing resources. A mesh that satisfactorily balances accuracy and computing resources are required. To perform the mesh convergence study manually a mesh using the fewest reasonable number of elements was created and the model was analysed. Then the mesh was recreated with a denser element distribution and was analysed and compared with the previous mesh results. The mesh density was changed again until the results were found to converge. Since the study is mainly focused on the results from soil, for the mesh convergence study only the element size in the soil model was varied. Particularly element size of the inner finely meshed cylindrical portion of soil model was varied. Element sizes of all other parts were taken same in the analyses. The element sizes considered are given in **Table1**. And mesh models of soil with varying mesh sizes are shown in **Fig.5**.

**Table 1** Different cases considered for mesh convergence study.

	Case 1	Case 2	Case 3	Case 4
Inner C3D8R elements	0.05 m	0.1 m	0.2 m	0.3 m
Tetrahedral elements	0.1 m	0.2 m	0.3 m	0.3 m
Outer C3D8R Elements	0.4 m	0.4 m	0.4 m	0.4 m

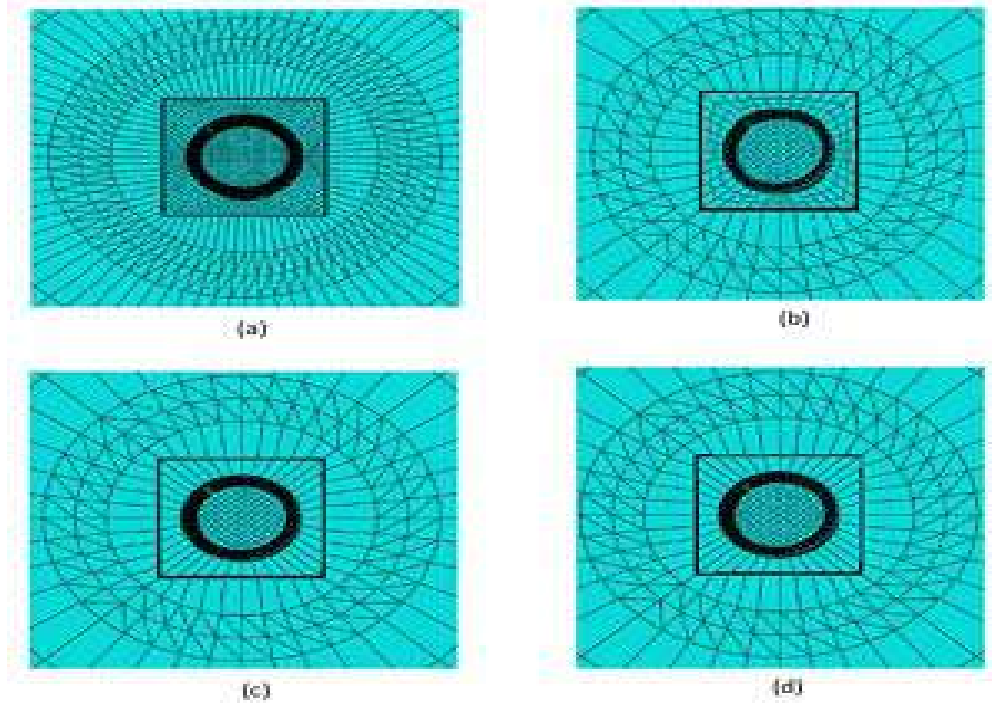


Fig.5. Different mesh sizes of soil model (a) Case1, (b) Case2, (c) Case3 & (d) Case

### VALIDATION OF MODEL

The results of the present study were validated against the P-y curve proposed by Reese and Welch (1975). A P - y relationship is used to model the interaction between a pile and the surrounding soil, denoted soil-pile interaction, where P is the lateral soil resistance and y is the lateral soil deflection. In practice, the relationship is used when designing laterally loaded piles. The main idea is to calculate the ultimate soil resistance with analytical methods and relate this to the actual lateral soil resistance P. P - y relationships are usually derived empirically and relate the lateral soil resistance P to the lateral soil deflection y. These non-linear P - y curves describe the behaviour of the soil when the pile is subjected to lateral loads.

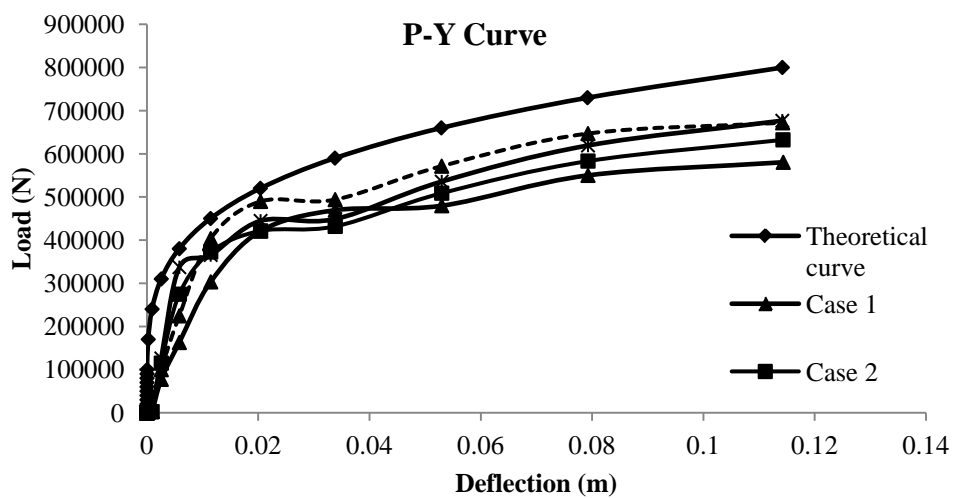


Fig.6. Comparison of results obtained from mesh convergence study.

## COMPARISON OF THEORETICAL AND FINITE ELEMENT RESULTS

Mesh convergence study was performed for four cases mentioned above. The P-y curves obtained were compared with the curve proposed by Reese and Welch (1975). The comparison is presented in **Fig 6**. Unlike usual trend best results were obtained for case 3 in which 0.2 m mesh size is considered for the inner C3D8R elements, 0.3m mesh size is considered for tetrahedral elements and 0.4m mesh size for outer C3D8R elements. The results obtained from other finer and coarser elements were not as good as the results obtained from case 3. But even the best result holds a 12 to 15 % difference from the theoretical curve.

From the mesh convergence study, it is concluded that the case 3 gave most accurate results. Therefore mesh size of case 3 is selected as the standard mesh size to model the soil for the vibration analysis.

## RESULTS AND DISCUSSION

The validated finite element model was used to study the effects in soil due to vibration from train a moving at 50kmph. And the parameters influencing vibration transfer through soil is also identified. The results of the parametric study on vibration analysis are given as under. The parameters considered for the study were boundary dimensions (peripheral distance from pile to the soil boundary), pile depth, and type of soil (well graded medium dense sand). The arrangement of parametric study is summarized in **Table 2**.

**Table 2** Arrangement of parametric study

Soil	Pile length	Peripheral Distance from Centre of pile to the boundary of soil model
Homogeneous well graded medium dense sand	10m	2.5m
		5m
		7.5m
	15m	2.5m
		5m
		7.5m
	20m	2.5m
		5m
		7.5m

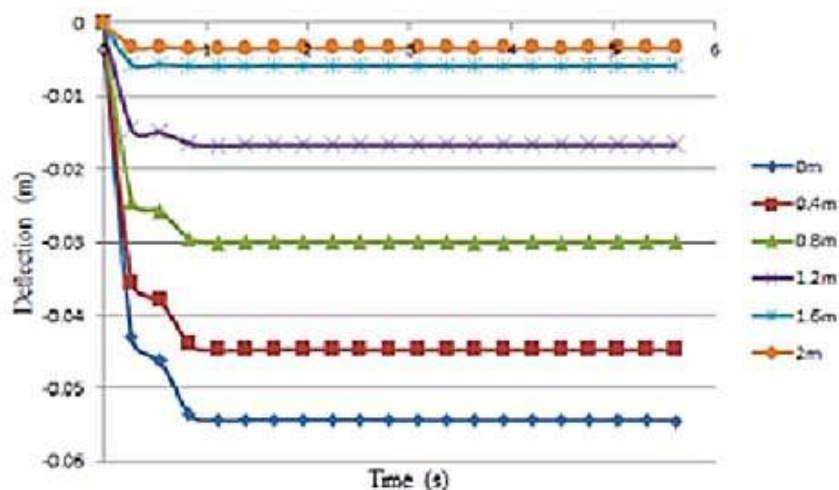


**Fig.7.** Vertical deflection vs. Time curve of stiff clay in model with 15m pile length and 5m radius boundary dimension

Maximum vertical deflection of pile due to the loads acting on it is studied here. The initial settlement is mainly due

to the axial load on pile but after that the vibration aided settlement is taking place. The vibration aided settlement is found significant in sand which is due to the vibration induced soil densification. From **Fig 7** it is clear that the initial linear part of the graph shows the deflection due to axial load and the remaining part of the curve is deflection from vibration. It can be also inferred from the fig. that vibration settlement in sand is more than 10mm. **Fig 8** show the deflection pattern of sand at the pile end. From the figure it is clear that the sand around pile lateral surface is also deflected due to more effective frictional contact. Detailed parametric study of the vertical deflection is given below.

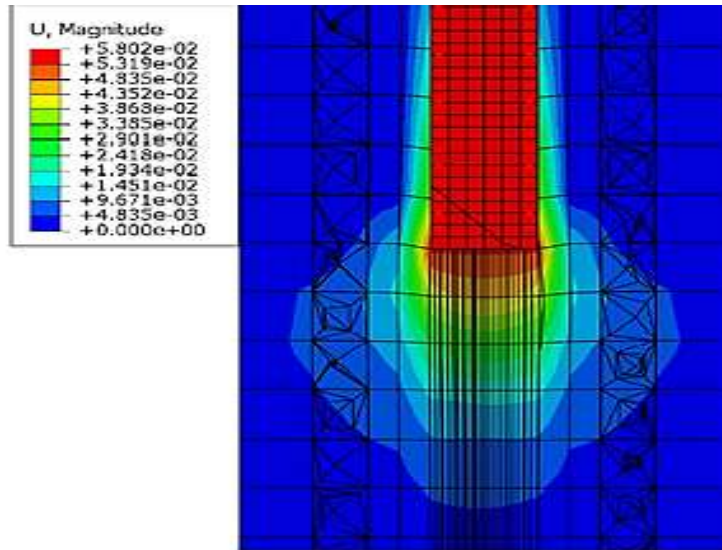


**Fig.8.** Deflection pattern of soil at pile end in well graded medium dense sand (deflection in m).

Fig 9, 10 and 11 show the vertical deflection of well graded medium dense sand in different models with different pile lengths and boundary dimensions. As mentioned before vibration induced deflection in sand is more compared to that of clay. And the effects of boundary dimension and pile length were found more prominent in sand which is discussed in detail in corresponding sections. The deflection pattern is also found to spread over more area in sand compared to clay. And the results justify the fact that vibrations have more influence on granular soil.

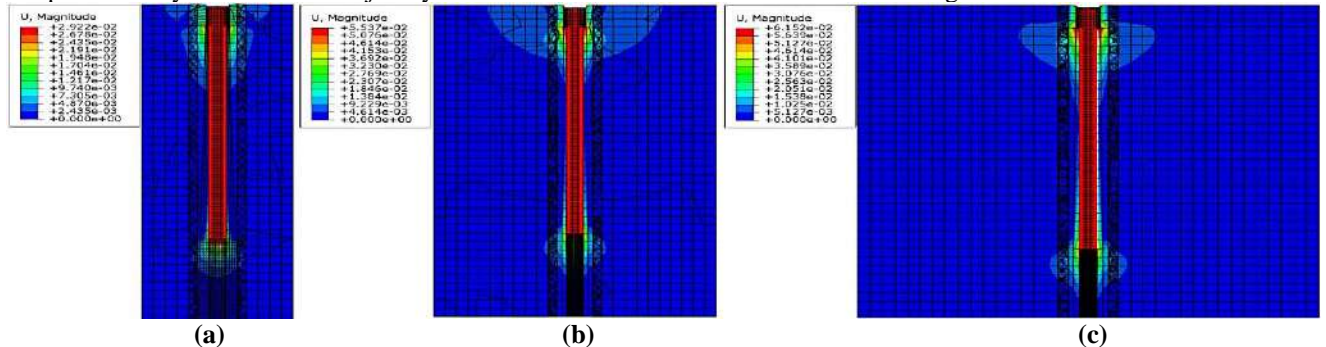


**Fig.9.** Vertical deflections (in m) of well graded medium dense sand with 10m pile model and boundary dimensions of (a) 2.5m radius, (b) 5m radius and (c) 7.5m radius

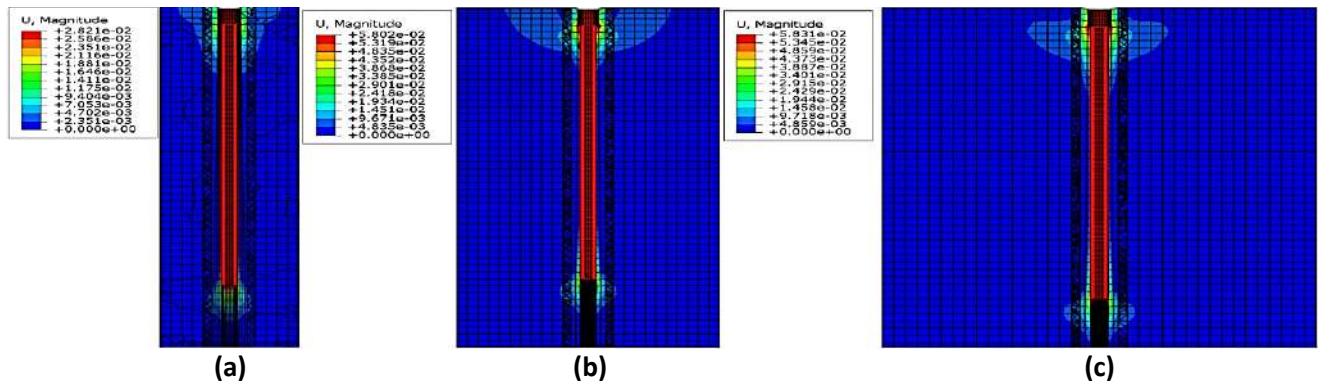


**Fig.10.** Vertical deflection (in m) of well graded medium dense sand with 15m pile model and boundary dimensions of (a) 2.5m radius, (b) 5m radius and (c) 7.5m radius.

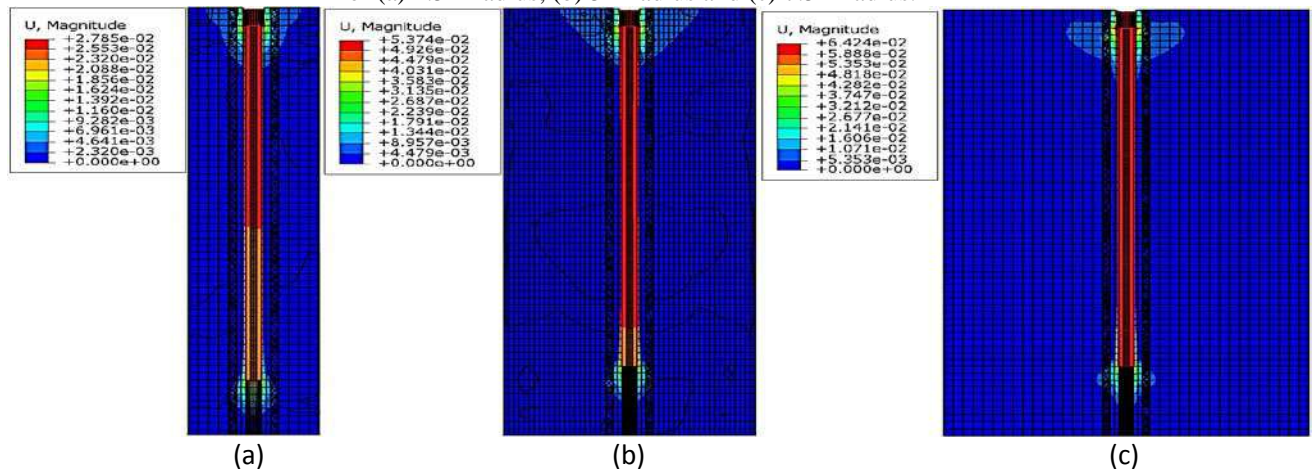


**Fig.11.** Vertical deflection (in m) of well graded medium dense sand with 20m pile model and boundary dimensions of (a) 2.5m radius, (b) 5m radius and (c) 7.5m radius.

**Effect of Boundary Dimension**

Comparison of maximum deflection values obtained for 3 boundary dimensions (2.5m radius, 5m radius and 7.5m radius) for 3 different pile lengths is shown in Fig 12. In case of vertical deflection, the 2.5m radius model gave very low deflection values compared to that of 5m radius model and 7.5m radius model. The variation is up to 50%. This is because of the fixed boundary condition given at the lateral boundaries which cannot simulate the actual infinite boundary nature. This effect is reduced as the radius of soil model increased. And for 5m radius model and 7.5m radius model comparable results are obtained.

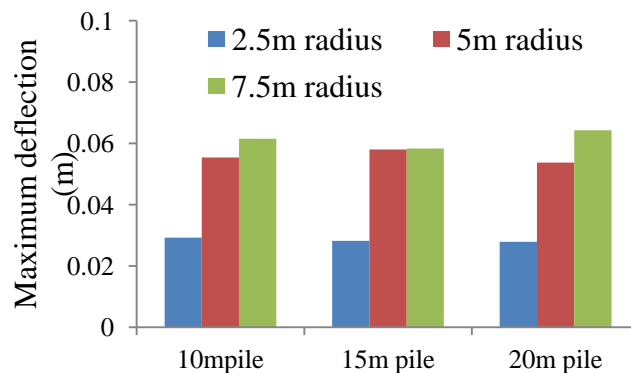


**Fig.12.** Comparison of maximum vertical deflection value obtained for different boundary dimensions with different pile lengths in well graded medium dense sand.

### Effect of Pile Length

After the comparison of vertical deflection against different pile lengths, as expected the deflection value is decreasing as the pile length increases. This is because of the increase in frictional resistance between pile and sand along the lateral surface, see Fig. 13. Therefore it can be concluded that the definition of interaction between pile and sand was effective.

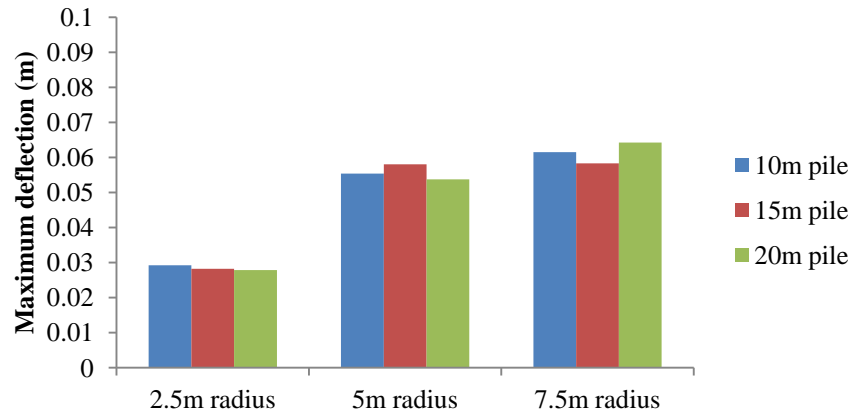


**Fig.13.** Comparison of maximum vertical deflection value obtained for different pile lengths with different boundary dimensions in well graded medium dense sand.

### Conclusion

The finite element software ABAQUS was capable of modeling the pile-soil interaction. When soil is modeled as a continuum model using solid elements, the most important part is the material model of the soil. An appropriate constitutive model to predict the inelastic behavior of the soil is required. As soils are highly non-linear, the constitutive model largely influences the results. Other important factors are the dimensions of the model and meshing of the soil in the finite element model.

- It was observed that results obtained from finite element analysis were in good agreement with theoretical P-y curve results as proposed by Reese and Welch for the pile-soil model.
- The vertical settlement of pile increased with the presence of train induced vibration. This establishes the fact that granular soils are more prone to vibration induced densification.
- It can be concluded that an accurate finite element model is unique for each soil type, which leads to a long optimization process in terms of modelling.
- When only finite elements are used to model the soil, the dimensions of the outer boundary have to be significantly large to eliminate artificial soil boundary effects on the results.

### REFERENCES

- Buragohain D.N. and Shah V.L. (1977). "Curved interface elements for interaction problems." Proc. Int. *Symposium on Soil-Structure Interaction*, Roorkee, India, 197-202.
- Cai Y.X., Gould P.L. and Desai C.S. (2000). "Nonlinear analysis of 3D seismic interaction of soil-pile-structure systems and application." *Engg Struct.*, 22, 191-199.
- Chore H.S., Ingle R.K. and Sawant V.A. (2010). "Building frame-pile foundation-soil interaction analysis: A Parametric study." *Int. Multi scale Mech.*, 3(1), 55-79.
- Reese, L.C. and Welch, R.C. (1975). "Lateral Loading of Deep foundations in stiff clay." *J Geotech Engg Div.*, 101(7), 633-649.



## NUMERICAL MODELLING OF MECHANICAL BEHAVIOUR OF PARTIALLY SATURATED SOILS USING UNCOUPLED APPROACH

Siddharth Mehndiratta<sup>1</sup>, Suvarna Nautiyal<sup>2</sup>, Vishwas A Sawant<sup>3</sup>

<sup>1</sup>Assistant Professor, GBPIET, Pauri, Uttarakhand, Email: siddharth14feb@gmail.com, Corresponding Author

<sup>2</sup>UG Student, GBPIET, Pauri, Uttarakhand, Email: Suvarna1234.sn@gmail.com

<sup>3</sup>Associate Professor, Indian Institute of Technology, Roorkee, Uttarakhand, Email:sawntfce@iitr.ac.in

### ABSTRACT

Changes in volume and degree of saturation of partially saturated soil due to capillarity give rise to many geotechnical problems. Fluctuations in water table can bring considerable impact on the ground response. The solutions to the consolidation problems associated with partially saturated soil can be obtained using both uncoupled and coupled approach. The motive of this study is to examine the effect of partially saturated soil zones on the behaviour of shallow foundations considering uncoupled approach using the finite element method. The fundamental equations governing the fully uncoupled constitutive behaviour of partially saturated soils are presented. A computer code has been developed in FORTRAN that is capable of performing consolidation analysis. The behaviour of partially saturated soils under strip footing is considered as an example. The capability of uncoupled approach in estimation of pore water pressure and settlement and to show Mandel-Crayner's effect in soil consolidation is discussed.

**Keywords:** Partially Saturated Soil, Finite Element Method, Uncoupled approach, Shallow Foundation

### INTRODUCTION

Consolidation analysis of saturated soils may be conducted by two different approaches. In the first approach, simultaneously solution is obtained for the displacement and pore water pressure in soil structure considering Biot's Theory. This approach is called as Coupled approach. A little approximate way of simplifying the coupled analysis is to perform seepage analysis first for prediction of pore water pressure. In this process, volumetric strains associated with the effective stresses acting on element are neglected in fluid continuity equation. During solution of the flow equations, the soil structure is assumed to be rigid, i.e. constant stress state and displacements. Then predicted value of pore water pressure is used as input to stress equilibrium equations. This approach is called uncoupled approach because the flow equations and equilibrium equations are solved separately (Corapeioglou 1984). Dependent variable in seepage analysis is pore water pressure (or hydraulic head). Similarly, dependent variables in stress deformation analysis are horizontal and vertical displacement. In uncoupled approach, pore water pressure is first determined by solving water flow continuity (seepage) equation. Then the calculated pore water pressure is used as input to determine the deformation over the domain by solving equilibrium (stress deformation) equation. Advantage with coupled or uncoupled approach is in their ability to predict displacement as well as generation and dissipation of excess pore pressure.

### UNCOUPLED APPROACH

#### *Governing Equation*

The continuity equation for the fluid phase can be expressed as

$$\frac{k_x}{\gamma_w} \frac{\partial^2 u_w}{\partial x^2} + \frac{k_y}{\gamma_w} \frac{\partial^2 u_w}{\partial y^2} + \frac{\partial \theta_w}{\partial t} = 0 \quad (1)$$

Volumetric water content  $\theta_w$  can be expressed as  $\theta_w = \beta_1 \varepsilon_v - \beta_2 u_w$

$$\frac{k_x}{\gamma_w} \frac{\partial^2 u_w}{\partial x^2} + \frac{k_y}{\gamma_w} \frac{\partial^2 u_w}{\partial y^2} + \frac{\partial (\beta_1 \varepsilon_v - \beta_2 u_w)}{\partial t} = 0$$

$$\frac{k_x}{\gamma_w} \frac{\partial^2 u_w}{\partial x^2} + \frac{k_y}{\gamma_w} \frac{\partial^2 u_w}{\partial y^2} = \beta_2 \frac{\partial u_w}{\partial t} - \beta_1 \frac{\partial \varepsilon_v}{\partial t}$$

(2)

The variation of pore water pressure  $u_w$  within the element is defined with shape functions as

$$u_w = \sum N_i^p u_{wi}$$

(3)

Similarly, the volumetric strain  $\varepsilon_v$  of the element is related to nodal displacement  $q_e$  as follows:

$$\varepsilon_v = \varepsilon_x + \varepsilon_y = \frac{\partial u}{\partial x} + \frac{\partial v}{\partial y} = \begin{bmatrix} \frac{\partial}{\partial x} & \frac{\partial}{\partial y} \end{bmatrix} \begin{Bmatrix} u \\ v \end{Bmatrix}$$

$$\text{But, } u = \sum N_i u_i \quad \text{and} \quad v = \sum N_i v_i$$

$$\varepsilon_v = \begin{bmatrix} \frac{\partial}{\partial x} & \frac{\partial}{\partial y} \end{bmatrix} \begin{bmatrix} N_1 & 0 & N_2 & 0 & \dots & N_i & 0 \\ 0 & N_1 & 0 & N_2 & \dots & 0 & N_i \end{bmatrix} \mathbf{q}_e$$

$$\varepsilon_v = \begin{bmatrix} \frac{\partial N_1}{\partial x} & \frac{\partial N_1}{\partial y} & \frac{\partial N_2}{\partial x} & \frac{\partial N_2}{\partial y} & \dots & \frac{\partial N_i}{\partial x} & \frac{\partial N_i}{\partial y} \end{bmatrix} \mathbf{q}_e = [1 \quad 1 \quad 0] \mathbf{B} \mathbf{q}_e$$

(4)

In which,  $\mathbf{B}$  is strain displacement transformation matrix for continuum element.

Equation (2) can be simplified as:

$$\begin{bmatrix} \frac{\partial}{\partial x} & \frac{\partial}{\partial y} \end{bmatrix} \frac{1}{\gamma_w} \begin{bmatrix} k_x & 0 \\ 0 & k_y \end{bmatrix} \begin{bmatrix} \frac{\partial N_1^p}{\partial x} & \frac{\partial N_2^p}{\partial x} & \frac{\partial N_3^p}{\partial x} & \frac{\partial N_4^p}{\partial x} \\ \frac{\partial N_1^p}{\partial y} & \frac{\partial N_2^p}{\partial y} & \frac{\partial N_3^p}{\partial y} & \frac{\partial N_4^p}{\partial y} \end{bmatrix} \mathbf{u}_{we} = \beta_2 \mathbf{N}_p \dot{\mathbf{u}}_{we} - \beta_1 [1 \quad 1 \quad 0] \mathbf{B} \dot{\mathbf{q}}_e$$

$$\begin{bmatrix} \frac{\partial}{\partial x} & \frac{\partial}{\partial y} \end{bmatrix} \frac{1}{\gamma_w} [k] \mathbf{B}_p \mathbf{u}_{we} = \beta_2 \mathbf{N}_p \dot{\mathbf{u}}_{we} - \beta_1 [1 \quad 1 \quad 0] \mathbf{B} \dot{\mathbf{q}}_e$$

(5)

In which,  $\mathbf{B}_p$  relates derivatives of pore water pressure and  $[k]$  is permeability matrix given as follows:

Applying variational approach,

$$\int \mathbf{u}_{we}^T \mathbf{N}_p^T \begin{bmatrix} \frac{\partial}{\partial x} & \frac{\partial}{\partial y} \end{bmatrix} \frac{1}{\gamma_w} [k] \mathbf{B}_p \mathbf{u}_{we} dv = \int \mathbf{u}_{we}^T \mathbf{N}_p^T (\beta_2 \mathbf{N}_p \dot{\mathbf{u}}_{we} - \beta_1 [1 \quad 1 \quad 0] \mathbf{B} \dot{\mathbf{q}}_e) dv$$

$$\mathbf{u}_{we}^T \mathbf{N}_p^T \frac{1}{\gamma_w} [k] \mathbf{B}_p \mathbf{u}_{we} - \int \mathbf{u}_{we}^T \mathbf{B}_p^T \frac{1}{\gamma_w} [k] \mathbf{B}_p \mathbf{u}_{we} dv = \mathbf{u}_{we}^T \int \beta_2 \mathbf{N}_p^T \mathbf{N}_p dv \dot{\mathbf{u}}_{we} - \mathbf{u}_{we}^T \beta_1 \int \mathbf{N}_p^T [1 \quad 1 \quad 0] \mathbf{B} dv \dot{\mathbf{q}}_e$$

Simplifying

$$\int \mathbf{B}_p^T \frac{1}{\gamma_w} [k] \mathbf{B}_p dv \mathbf{u}_{we} + \int \beta_2 \mathbf{N}_p^T \mathbf{N}_p dv \dot{\mathbf{u}}_{we} = \beta_1 \int \mathbf{N}_p^T [1 \quad 1 \quad 0] \mathbf{B} dv \dot{\mathbf{q}}_e$$

(6)

$$\mathbf{K}_f \mathbf{u}_{we} + \mathbf{M}_f \dot{\mathbf{u}}_{we} = \mathbf{L} \dot{\mathbf{q}}_e$$

(7)

Individual matrices  $\mathbf{K}_f$ ,  $\mathbf{M}_f$  and  $\mathbf{L}$  are defined by following relationship:

$$\mathbf{K}_f = \int \mathbf{B}_p^T \frac{1}{\gamma_w} [k] \mathbf{B}_p dv \quad \text{and} \quad \mathbf{M}_f = \int \beta_2 \mathbf{N}_p^T \mathbf{N}_p dv \quad \text{and} \quad \mathbf{L} = \beta_1 \int \mathbf{N}_p^T [1 \ 1 \ 0] \mathbf{B} dv$$

(8)

Applying Crank Nicolson time marching scheme,

$$\Delta t \mathbf{K}_f \mathbf{u}_{we}^{t+\Delta t} + \mathbf{M}_f (\mathbf{u}_{we}^{t+\Delta t} - \mathbf{u}_{we}^t) = \mathbf{L} (\mathbf{q}_e^{t+\Delta t} - \mathbf{q}_e^t)$$

$$[\mathbf{M}_f + \Delta t \mathbf{K}_f] \mathbf{u}_{we}^{t+\Delta t} = \mathbf{M}_f \mathbf{u}_{we}^t + \mathbf{L} (\mathbf{q}_e^{t+\Delta t} - \mathbf{q}_e^t)$$

(9)

In above relationship, matrix  $\mathbf{M}_f$  and  $\mathbf{L}$  are dependent on factors  $\beta_1$  and  $\beta_2$  which can be evaluated from soil properties.

$$\beta_1 = \frac{E}{H} \left( \frac{1}{1-2\mu} \right) \quad \text{and} \quad \beta_2 = \left( \frac{1}{R} - \frac{3\beta_1}{H} \right)$$

(10)

While solving flow equation in the uncoupled approach, the net normal stress is not to be considered. Consequently, the water volumetric modulus associated with increment in net normal stress approaches infinity. This will set the value of factor  $\beta_1$  as zero. Other factor  $\beta_2$  is given by reciprocal of the water volumetric modulus associated with a change in soil suction. In short, the factor  $\beta_2$  is the slope of soil water characteristic curve  $R$ . In summary, five soil parameters are required for the uncoupled analysis of partially saturated soil. These parameters are  $E$ ,  $H$ ,  $H_1$ ,  $\mu$  and  $K_w$ .

In the present study, to get initial values of unknown nodal displacements and pore water pressure, following procedure is adopted:

#### Numerical Procedure

- 1 Solve force equilibrium equation using total stress parameter. Constitutive matrix  $\mathbf{D}$  is based on undrained parameter ( $E_u$  and  $\mu_u$ ).

$$\mathbf{K} \mathbf{q}^0 = \mathbf{f}_u \quad \text{where} \quad \mathbf{K} = \int \mathbf{B}^T \mathbf{D} \mathbf{B} dV \quad \text{and} \quad \mathbf{D} = \mathbf{D}(E_u, \mu_u)$$

- 2 To obtain initial pore water pressure, force equilibrium equation is expressed in terms of effective stress and pore water pressure. In the expression of stiffness matrix, constitutive matrix  $\mathbf{D}$  is based on effective stress parameter ( $E$  and  $\mu$ ). As initial displacements  $\mathbf{q}^0$  are already evaluated in step 1, initial pore pressures can be computed.

$$\mathbf{K}^{\text{eff}} \mathbf{q}^0 + \mathbf{L} \mathbf{u}_w^0 = \mathbf{f}_u \quad \text{where} \quad \mathbf{K}^{\text{eff}} = \int \mathbf{B}^T \mathbf{D}^{\text{eff}} \mathbf{B} dV \quad \text{and} \quad \mathbf{D}^{\text{eff}} = \mathbf{D}^{\text{eff}}(E, \mu)$$

- 3 Now, displacements and pore water pressure are calculated at each time step.
- 4 Pore water pressures are estimated first using Eq. (9)

$$[\mathbf{M}_f + \Delta t \mathbf{K}_f] \mathbf{u}_{we}^{t+\Delta t} = \mathbf{M}_f \mathbf{u}_{we}^t + \mathbf{L} (\mathbf{q}_e^{t+\Delta t} - \mathbf{q}_e^t)$$

- 5 Then using values of these pore water pressures, nodal displacements are evaluated

$$\mathbf{K}^{\text{eff}} \mathbf{q}^{t+\Delta t} + \mathbf{L} \mathbf{u}_w^{t+\Delta t} = \mathbf{f}_u$$

- 6 Steps 4 and 5 are repeated till dissipation of excess pore water pressure.

#### PROBLEM GEOMETRY

A general engineering problem which usually involves the partially saturated soils is a shallow foundation resting above the ground water table. The analysis involved a 4 m wide flexible strip footing on a 10 m thick and 20 m wide

partially saturated soil, the soil media has been modelled as shown in Fig. 1. Soil foundation system has been modelled as plain strain model. Only transverse displacements are restrained on vertical boundaries on either side and bottom horizontal boundary. The magnitude of the instantaneous loading applied over the footing is set equal to -100 kPa. For simplicity, the soil resting below the footing is assumed to behave linearly elastic and have a constant modulus of elasticity and permeability for different initial conditions. The material properties of the unconsolidated soil are Young's modulus which is set at 10000 kPa, Poisson's ratio of 0.0,  $H$  parameter is assumed constant with suction at  $E/(1-2\mu)$ , and permeability is non-suction dependent at 1m/year. The coupled and uncoupled finite element method used for the analysis comprises of 8 - 4 node mixed element. The mixed element has 8 displacement nodes and 4 pore pressure nodes.

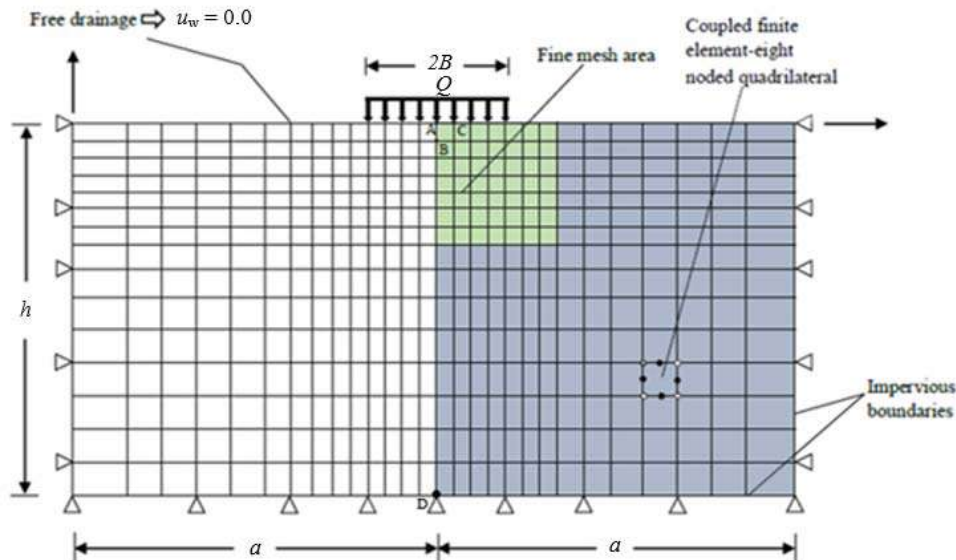


Fig. 1. Schematic representation of the problem statement and finite element mesh

## RESULTS AND DISCUSSION

### Effect of Water Table Depth

The relation between degree of saturation and negative pore-water pressure (above water table) is given by Brooks and Corey (1964) has been used (Eq. 11).

$$S_r = S_{wr} + (1 - S_{wr}) \left( \frac{P}{P_a} \right)^{-\lambda_p}, \quad (P < P_a) \quad (11)$$

where,  $S_{wr}$  is the residual degree of saturation ( $S_{wr} = 0.27$ ),  $P_a$  is the air-entry pressure ( $P_a = -7.35 \text{ kN/m}^2$ ), and  $\lambda_p$  is the pore-size distribution index ( $\lambda_p = 1.8$ ). The air-entry pressure  $P_a$  defines the capillary pressure above the water table.

In this section, for the assumed plane strain model (Fig. 1), both immediate vertical settlement and excess pore water pressure are obtained from uncoupled approach. The effect of water table (WT) level on the behaviour of partially saturated soil is presented in Figs. 2-3. Figure 2 shows the variation of immediate vertical displacement at the ground surface for different water table depth. It is observed that immediate displacement of soil near the centre line of footing increased (89.6%) by reducing water table from 10m to 7m. The same trend continues as the water table further reduces to 5m from the ground surface, below which there is no significant change is observed in displacement. At a distance away from the footing upward displacement is observed and this displacement reduces as the water table goes down, this is due to presence of negative pore water pressure that increases the shear strength of soil hence reduces the displacement.

With time, consolidation process causes decrease in pore water pressure within the saturated soil and increase in pore pressure in partially saturated soil, (becomes less tensile) as shown in Fig. 3. This indicates that flow is occurring upwards, from saturated to partially saturated region hence water-table fluctuates, initially rises and then diminish with time.

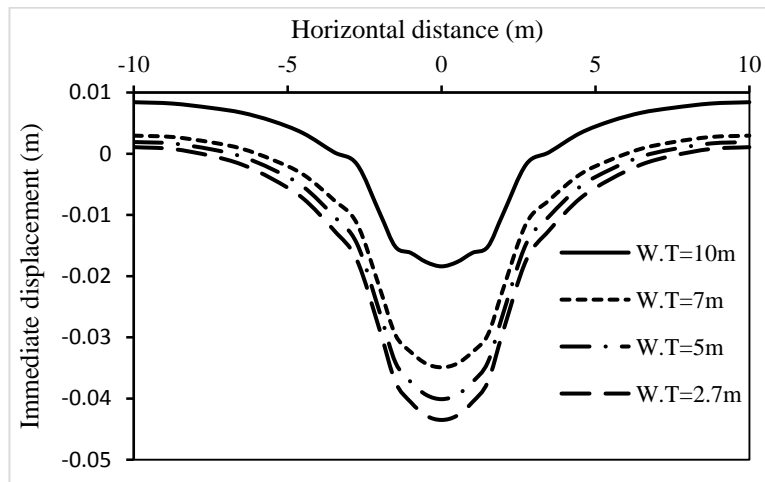


Fig. 2 Immediate displacement profile at ground surface for different water table depth

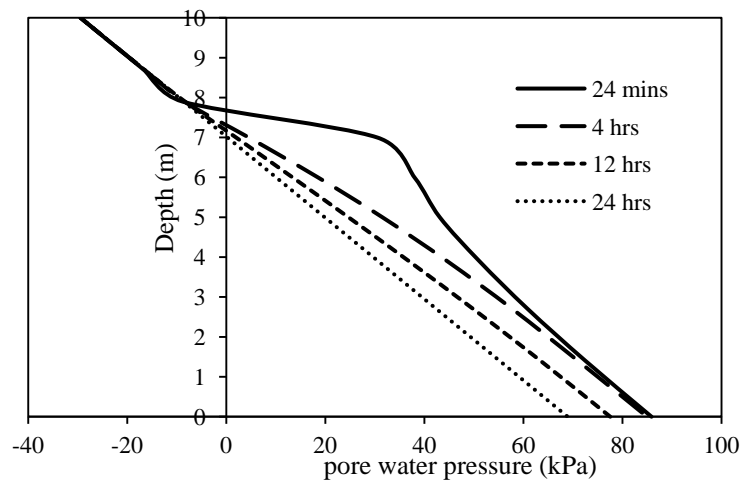


Fig. 3 Variation of pore water pressure with depth along the centre line of footing (initial water table at 7m)

### ***Effect of initial degree of saturation***

To define partially saturated soil, a relationship between the degree of saturation and the pore water pressure is required to characterize the partially saturated hydraulic property and the compressibility of the pore air fluid. A relationship that describe the variation in  $S_r$  with positive pore water pressure  $u_w$  and initial degree of saturation  $S_{r0}$  was suggested by Lowe and Johnson (1960) as

$$S_r = \frac{0.0099u_w + 0.98S_{r0}}{0.98 + 0.0097u_w} \quad (12)$$

The initial degree of saturation  $S_{r0}$  is varied as 85%, 95% and 100%. Variations of displacement with horizontal distance for different initial degree of saturation (85%, 95% and 100%) at time  $t = 24\text{min}$  are presented in Fig. 4. It is observed that the displacement in partially saturated soil is considerably higher than that in fully saturated soil. It is also observed that for fully saturated soil the displacement near the centre line of the footing are negative (i.e. downward), while at a distance away from the footing, they are positive (i.e. upward movement). Same trend can be seen for lesser degree of saturation near the centre line of footing with higher displacement whereas lesser upward movement noticed at a distance away from the footing. The ultimate displacement is stress path independent because soil is idealized as an elastic medium therefore ultimate displacement is found to be same for all three cases.

Distribution of excess pore pressure under footing with time is presented in Fig. 5. At a particular degree of

saturation, excess pore water pressure first increases with time and it declines eventually. This type of pore water pressure response is known as the Mandel Cryer effect. In general, with reduction in initial degree of saturation the excess pore water pressure decreases and dissipates at the end of consolidation.

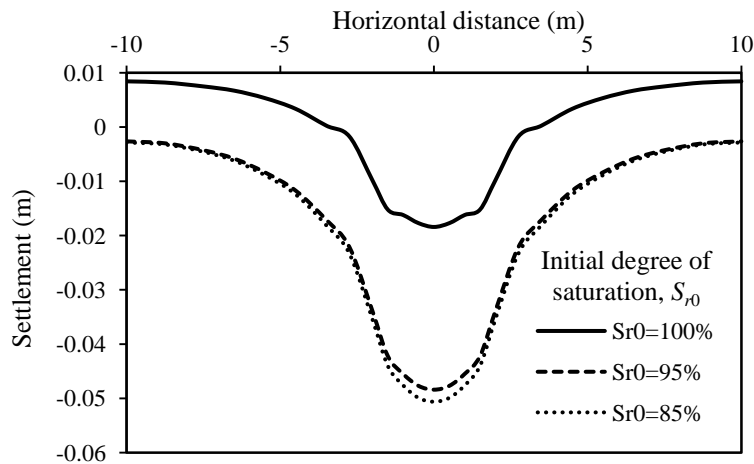


Fig. 4 Displacement profile at ground surface for different initial degree of saturation

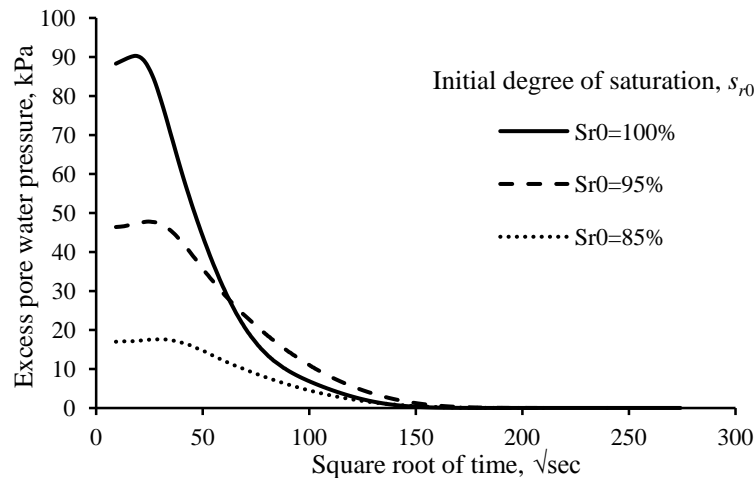


Fig. 5 Variation of excess pore water pressure with time for different initial degree of saturation

## CONCLUSION

A fully uncoupled finite element formulation has been proposed to analyse the effect of initial degree of saturation and water table level in partially saturated soils in response to loaded strip footing. The results demonstrate that the initial degree of saturation and water table level has great effect on the behaviour of partially saturated soil. These phenomena may have adverse effects on the safety and reliability of engineering designs involving soil consolidation calculations. Therefore, to simplify the problem numerically, the partially saturated zone should not be ignored with an assumption of full saturation.

## REFERENCES

1. Alonso, E.E., Gens, A. and Josa, A. (1990). "Constitutive model for partially saturated soils." *Geotechnique*, 40(3), 405-430.
2. Biot, M.A. 1941. General theory of three-dimensional consolidation, *J. Appl. Phys.*, **12**, 155-164.
3. Brooks, R.H. and Corey, A.T. (1964). "Hydraulic properties of porous media and their relation to drainage design." *Transactions of the ASAE*, 7(1), 26-28.
4. Dakshanamurthy, V and Fredlund, D. G. 1981. A mathematical model for predicting moisture flow in an unsaturated soil under hydraulic and temperature gradients, *The Water Resources Research*, **17**, (3), 714-722.

5. Kim, J. M. 2000. A fully coupled finite element analysis of water table fluctuation and land deformation in partially saturated soils due to surface loading, *Int. J. numerical methods in engineering*, **49**, 1101-1119.
6. Lowe, J. and Johnson, T. C. 1960. Use of Back Pressure to Increase the Degree of Saturation of Triaxial Test Specimens, ASCE Research Conference on Shear Strength of Cohesive Soils, Colorado, 819-836.
7. Mehndiratta, S. and Sawant, V. A. (2017a). "Numerical modelling of mechanical behaviour of partially saturated soils using coupled FEA. *International Journal of Geotechnical Engineering*, *11*(5), 452-466.
8. Mehndiratta, S. and Sawant, V. A. (2017b). "Behaviour of Partially Saturated Soil Under Isotropic and Triaxial Condition Using Modified BBM". *Indian Geotechnical Journal*, *47*(3), 219-232.
9. Ng, A. K. L. and Small, J. C. 2000. Use of Coupled Finite Element Analysis in Unsaturated Soil Problems, *Int. J. Numerical and Analytical Methods in Geomechanics*, **24**, 73-94.
10. Potts, D. M. and Zdravkovi, L. 1999. Finite element analysis in geotechnical engineering: Theory, Thomas Telford.



## Effect of Non-linearity of Soil on Displacement of Building Frame Resting on Different Foundations

S. A. Rasal<sup>1</sup>, H.S.Chore<sup>2</sup> and V.A. Sawant<sup>3</sup>

<sup>1</sup> Research Scholar, Dept. of Civil Engineering, Datta Meghe College of Engineering, Sector-3, Airoli, Navi Mumbai-400708,  
Email: sarasal@rediffmail.com.

<sup>2</sup> Associate Professor, Dept. of Civil Engineering, Dr. B. R. Ambedkar National Institute of Technology, Jalandhar – 144011,  
Email: chorehs@nitj.ac.in, Corresponding Author

<sup>3</sup> Associate Professor, Dept. of Civil Engineering, Indian Institute of Technology Roorkee, Roorkee-247667,  
Email: sawntfce@iitr.ac.in

### ABSTRACT

The study deals with physical modeling of a three storeyed building frame supported by three different foundations and using three dimensional finite elements. The foundations comprises of pile groups, raft and piled-raft embedded in cohesive soil mass. For the purpose of modeling, the elements of the superstructure frame such as beams, columns and slab; and that of the pile foundation such as pile and pile cap are discretized using twenty noded isoparametric continuum element. The interface between the pile and the soil is idealized using sixteen node isoparametric surface element. Three different elements are used for discretizing the soil. The soil elements are modeled using eight nodes, nine nodes and twelve node continuum elements. The parametric study is carried out for studying the effect of soil-structure interaction on response of the frame. The frame is analyzed initially without considering the effect of the foundation and then, the three different. The response of the frame included the displacement at each storey level of the frame. Further non-linear behaviour of soil is considered for the analysis. The effect of the soil- structure interaction is observed to be significant for the types of foundations and soil considered in the present study.

**KEYWORDS:** Soil-structure interaction; non-linear behaviour of soil; pile spacing; raft; piled-raft; top displacement.

### INTRODUCTION

The framed structures are normally analyzed on the assumption of rigid or hinged column bases for the purpose of the structural design. However, in actual practice, the foundation embedded in soil strata undergoes deformation depending on the relative rigidities of the foundation, superstructure and soil. In view of this, an interactive analysis, is required to be carried out for the accurate assessment of the response of such structures. Several researchers such as Chameski (1956), Morris (1966), Lee and Brown (1972), King and Chandrasekaran (1974), Buragohain et.al (1977) reported interaction analyses in the decade of 1960's and 1970's and few in recent studies. Most of the above mentioned studies quantified the effect of soil structure interaction on the response of framed structures in the context of isolated footings or combined footings or raft foundation. Some of these studies were analytical in nature; few of them were experimental. Buragohain *et al.* (1977) was the only researchers to have dealt with soil- structure interaction analysis of framed structure resting on pile foundation until recent past. The simplified assumptions and relatively less realistic approach were resorted to in this study.

Based on the lacunae in this study as is evident from the critical findings presented by Ingle and Chore (2008), Chore and co-authors (2009, 2010, 2013 and 2014) reported the methodology for the interaction analysis of a single storeyed building frame embedded in clayey soil on the rational approach and realistic assumptions. While most of the analyses were carried out using sub-structure approach, in some of the analysis the foundation (pile groups) was idealized as the completely three dimensional model whereas in few, it was idealized using simplified finite element models. The building frame was, however, modeled as the complete three dimensional model. Though, in most of these analyses, the linear elastic behavior of soil of soil was considered, a study considered non-linear elastic behavior of soil wherein the non-linearity was incorporated  $p$ - $y$  curve concept. Further, Chore and Sawant (2013) reported the analysis of the same frame using coupled approach and suggested that the sub-structure approach is more realistic. Chore (2014) reported the analysis of a single storeyed building frame supported on pile foundation, as done used in his earlier studies, using SAP-IV. Recently, Dode *et al.* (2014 and 2015) reported the interaction analysis of the single storeyed building frame using more improved finite element model for the foundation, i.e., pile

group and soil. Even many interaction studies (Agrawal, and Hora 2009; Thangaraj and Illampurthy 2010 and 2012; Dalili et. al 2011; Rajsekarswamy et.al 2011) have been reported in the recent past. However, these studies were confined to the analysis of frames or allied structure supported by isolated footings or raft foundation to quantify the effect of soil- structure interaction.

Considerable work is reported in the literature on axially loaded as well as laterally loaded single pile and pile groups. The approaches available for the analysis of axially loaded pile foundations include the elastic continuum method ( Polous 1968 and Butterfield and Banerjee 1971); and load transfer method (Coyle and Reese 1966; Hazarika and Ramasamy 2000; Basarkar and Dewaikar 2005) while those for analyzing the laterally loaded pile foundations include the elastic continuum approach (Coyle and Reese 1966 and Hazarika, and Ramasamy 2000) and modulus of subgrade reaction approach (Banerjee, and Davis1978; Matlock and Reese1956; Matlock 1970; Georgiadis et. al1992; Dewaikar and Patil 2006). In the decade of early 1970s, versatile finite element method (Desai and Abel 1974 and 1976; Desai et. al 1981; Zhang, L.M. 2001; Krishnamoorthy and Rao 2005; Chore et.al 2010 and 2012; Krishnamoorthy 2010; Baziar, et.al 2009) has become popular for analyzing the problem of pile foundations in the context of linear and non-linear analysis.

In the past few decades, there is an increasing recognition that the utilization of pile groups in conjunction with raft foundation could lead to considerable economy without compromising the safety and performance of the foundation. Such a foundation is referred to as the *piled raft*. The concept of piled-raft improves the serviceability of foundation performance by reducing settlements to acceptable levels. Although the piled-raft concept has been most notably applied to new construction involving high-rise buildings, it is also potentially useful for remedial works and moderate height structures. Methods that have been used for the analysis range from simplified calculations to numerical methods such as the boundary element method (Butterfield and Banerjee 1971; Brown and Wiesner 1975; Kuwabara 1989; Mendonca and De Paiva 2003) and the finite element method (Hooper 1973; Ottaviani 1975; Chow 1987; Liu and Novak 1991; Katzenbach and Reul 1997; Prakoso and Kulhawy 2001; Reul and Randolph 2003). In early years, the use of numerical methods was confined to simple problems. In last three decades, owing to rapid development in computer technologies, full three dimensional finite element methods are often used to solve the complex problems.

The foundation concept of piled rafts differs from traditional foundation design, where the loads are assumed to be carried either by the raft or by the piles, considering the safety factors in each case. Several methods of analyzing piled rafts have developed over the years. These include approximation methods, finite element method, boundary element method, combined boundary element and finite element method, combined finite layer and finite element method; and variational approach. In recent years, a variety of approaches for analyzing the piled- raft foundation system as mentioned in the preceding section have been developed over the years. All these approaches vary in the degree of sophistication of the formulations amount and the type of input parameters required, assumptions made; and in the applicability to realistic pile-soil-raft situations. Some of the significant studies are briefed approach wise in the subsequent paragraphs.

The approximation approach as presented by Chen *et. al.* (1974) treated the raft as a thin plate, the piles as springs and the soil as an elastic continuum; and further, the interaction effects between the piles were ignored. Randolph (1983) presented a method to compute the interaction between a single pile and a circular raft. Clancy and Randolph (1993) employed a hybrid method in which analytical solution was combined with the finite elements. The raft was modeled by two-dimensional thin plate finite elements, the piles were modeled by one-dimensional rod finite elements and the soil response was calculated by using an analytical solution. Poulos (1994) employed a finite difference method for the raft with the consideration of the interaction effects between the piles and raft. Kitiyodom and Matsumoto (2003) developed a simplified method of numerical analysis using a hybrid model in which the flexible raft is modelled as thin plates and the piles as elastic beams and the soil is treated as springs.

The finite element method is one of the powerful tools for the analysis of the complex problems of piled raft. In order to reduce the computational efforts, the problems are sometimes simplified to an axi-symmetric problem or a plane- strain problem. Some of the noteworthy contributions using this method include those by Hooper (1973), Madhav and Karmarkar (1982), Kakurai and Tomono (1987), Chow and Teh (1991), Wiesner (1991), Gandhi and Maharaj (1996), Smith and Wang (1998), Franke (2000), Katzenbach *et al.* (2000), Reul and Randolph (2003), Maharaj and Gandhi (2004), Poulos *et al.* (2006), Thoiba Singh and Balweshwar Singh (2008), Noh *et al.* (2008), Cheng (2011); Xie *et al.* (2012) and Sawant *et al.* (2012). Some of the researchers analyzed the circular piled rafts

while few of them, reported the performance of piled raft foundation for a multi-storeyed building. Some of the analyses were carried out in the context of non-linear behaviour of soil, few of them even used finite elements in conjunction with infinite elements. While some investigations considered sandy soil, few of them considered the cohesive sub-soil. Even, a study considered layered soil. Some studies were carried out using complete three dimensional finite element analysis; few studies were carried out in the context of simplified finite element models.

The boundary element method is a powerful tool that can be applied in engineering applications as only the boundary has to be discretized which reduces the amount of computer memory and the time to solve the problem as compared to that in finite element or finite difference method. This method provides a direct and accurate solution for the analysis. Moreover, it is fast and requires a moderate amount of computer storage space. The method has been used by many researchers (Brown and Wiesner 1975, Kuwabara 1989, Baziar *et al.* 2009, Sales *et al.* 2010) in the solution of the problem of piled raft embedded in different types of soil. Different idealizations were made for modelling different components of the foundation in question.

Integrating pros and cons some of the researchers (Hain and Lee 1978, Kakurai *et al.* 1987, Sinha 1997, Franke *et al.* 2000; and Mendonca and De Paiva 2003) even made use of combined boundary element and finite element method. Small and Booker (1984, 1986) developed an approach based on the finite layer technique in conjunction with the finite element method for analyzing the piled raft in layered soil. Maharaj and Gandhi (2004), Tan *et al.* (2005) and Chow *et al.* (2011) worked on the similar lines as that of Small and Booker (1984). The variational approach developed by Shen *et al.* (1999) makes use of the principle of minimum potential energy to simulate the response of the foundation system. Discretizations are required only at the interface between the raft and the soil. The method was extended later by many researchers (Shen and Teh 2002, Liang and Chen 2004 and Chow *et al.* 2011)

It is observed from the literature review that in most of the soil- structure interaction analyses, the linear elastic behaviour of the soil was considered. Hardly, any study reported the analysis involving the non-linearity of the soil mass. Further, in most of the earlier studies, piles in series and parallel arrangement were considered. On this backdrop, the present study reports the interaction analysis of a three storeyed building frame resting upon the different types of foundations. Firstly, the pile foundation comprising square pile group ( $2 \times 2$ ) is considered followed by raft and then piled raft foundation is considered. The interaction analysis incorporating non-linear behavior of soil is presented wherein the non-linearity is incorporated with *von Mises* yield criterion at each interaction. The effect of three different foundations is evaluated on the response of the typical building frame considered in the present study. The effect of the constant pile diameter, spacing between the piles and modulus of elasticity of soil is considered in case of pile foundation on the response of frame. Similarly, effects of the parameters such as varying raft thicknesses and soil modulus in case of raft foundation; and varying thicknesses for the constant pile diameter and soil modulus in respect of piled raft foundation is examined on the response of the frame.

## MODELING AND ANALYSIS METHODOLOGY

### ***Building frame on pile foundation***

The interaction analysis of a three storeyed frame resting on the pile group is carried out using complete three-dimensional finite element method. Initially, the frame is analyzed separately without considering the effect of foundation. This analysis is referred to as the non-interactive analysis (NIA). Later, the pile foundations are analyzed separately to obtain the equivalent stiffness of the foundation head. Further, these stiffnesses are used in the analysis of the frame to quantify the effect of SSI on the response of the frame. The analysis carried out considering the effect of SSI is referred to as the interactive analysis (IA). The interactive analysis is carried out incorporating the linear and non-linear behavior of the soil media. The non-linearity of the soil is incorporated in the analysis using *von Mises* yield criterion. The study aims at bringing out the effect of the non-linearity of the soil media on the response of the super-structure.

A full three dimensional geometric model of the sub-structure (pile foundation-soil system) is considered in the present study as against the half model for the sub-structure system considered in Chore and Ingle (2008). The elements of the framed structures such as beam, column and slab and that of pile foundation such as pile and pile cap are idealized as 20 node iso-parametric continuum elements. On the other hand, soil elements are discretized using eight node, nine node and twelve node continuum elements. Further, three degrees of freedom at each node, i.e.,

displacement in three directions in X, Y and Z of these different elements, are considered in the present analysis. For the proper mechanics of stress transfer between soil and pile under lateral load, 16 node iso-parametric surface elements is introduced between the interface of the pile and soil. The normal and tangential stiffness of these elements are assumed in such a way that shearing at the soil and pile interface is allowed; but separation of pile and soil node is not possible.

The selection of the appropriate finite element to represent the medium is one of the very important aspects in finite element analysis when the three dimensional geometric model is used to represent the soil- pile system. In the soil-pile system, two materials, viz. Soil and reinforced concrete are to be modelled. Both the materials exhibit different behaviours under loading. The shear failure is predominant in soil whereas the bending failure is significant in reinforced concrete. Therefore, pile and pile cap along with the superstructure elements are modeled using twenty node continuum elements having quadratic shape function which is well suited to model the medium with bending dominated deformation. Eight node continuum elements are used to model the soil which has linear shape functions. These elements are suitable for the medium whose deformations are dominated by shear strength. In order to maintain the continuity of displacements between these two types of elements in the discretised soil- pile domain, two more elements are formulated, viz. Twelve node and nine node solid elements. The shape functions of these two elements are formulated by using degrading technique. The shape functions are derived for these elements by degrading the twenty node solid elements. Twelve node elements are used at the junction where eight node and twenty node element meets. Further, nine node elements are used where twelve node element and twenty node element meets perpendicularly (Dode et al. 2014).

#### ***Building frame on raft foundation***

The non-interactive analysis of the building frame is carried out along lines similar to that in case of the analysis of the frame resting on pile group. The complete three dimensional finite element analysis is carried out. A parametric study is carried out to examine the effect of raft thickness and the soil modulus on the response of building frame. In the first approach, the soil behaviour is considered linear. That will define the relation between soil reaction ( $p$ ) and transverse displacement ( $w$ ) through modulus of subgrade reaction  $k_s$ . As  $p = k_s w$ . In the second approach, the relation between soil reaction ( $p$ ) and transverse displacement ( $w$ ) is expressed through an hyperbolic relationship.

$$p = \frac{k_{\max} w}{1 + \frac{k_{\max} w}{p_u}}$$

In which,  $k_{\max}$  is initial tangent modulus and  $p_u$  is the ultimate soil resistance.

#### ***Building frame on piled-raft foundation***

Initially, the frame is analyzed separately without considering the effect of foundation. Then, raft foundation is analyzed separately. The pile foundation comprising of single pile below the raft are worked out independently to get the equivalent stiffness of the foundation head. Further, they are used in the analysis of the frame to evaluate the effect of SSI on the response of the frame. The analysis carried out considering the effect of SSI is referred to as the interactive analysis (IA). The interactive analysis is carried out incorporating the linear and non-linear behavior of the soil media. The non-linearity of the soil is incorporated in the analysis using *von Mises* yield criterion. The study aims at bringing out the effect of the non-linearity of the soil media on the response of the super-structure.

### **PROBLEM DESCRIPTION**

A 3-D three storeyed building frame resting on pile foundation is considered for the study. The frame is 3 m high and 10 m × 10 m in plan. Each bay are 5m × 5m. The slab (200 mm thick) is provided at top as well as at the floor level. The slab at the top of the first, second and third storey is supported over 300 mm wide and 400 mm deep beams. The beams are supported by columns of size 300 mm × 300 mm. The pile foundation comprises of the group of four piles (2×2) embedded in soft marine clay, a cohesive type of soil mass.

All the piles in a group are circular piles. These are connected by a 500 mm thick pile cap. The behavior of the cap is assumed to be flexible. The properties of the material for pile and pile cap are given in Table 1. Typical building frame with fixed base and pile considered for non-interactive analysis is shown in Fig. 1

The interface shear stiffness ( $k_s$ ) is taken as  $G/10$  and the interface normal stiffness is taken as  $100G$ , in which  $G$  is the shear modulus of soil. The octahedral ( $\tau_{oct}$ ) shear stress is limited to undrained cohesion of clay soil (using half unconfined compressive strength of soil).

**Table 1. Pile and soil properties for parametric study**

<b>Soil properties</b>	
Modulus of Elasticity, $E_s$	20000 kPa
Poisson's ratio, $\mu_s$	0.4
Density, $\gamma_s$	18 kN/m <sup>3</sup>
Yield stress, $\sigma_y$	100 kPa
<b>Pile properties</b>	
Modulus of Elasticity, $E_p$	25 GPa
Poisson's ratio, $\mu_p$	0.2
Density, $\gamma_p$	25 kN/m <sup>3</sup>
Pile cap thickness, $t_p$	0.5 m
Pile diameter, $D$	1.0
$L/D$ ratio	20
$s/D$ ratio	2
<b>Interface element</b>	
Normal stiffness, $K_n$	$1.0 \times 10^6$ kN/m <sup>3</sup>
Tangential stiffness, $K_s$	1000 kN/m <sup>3</sup>
<b>Raft properties</b>	
Modulus of Elasticity, $E_p$	25 GPa
Poisson's ratio, $\mu_p$	0.2
Density, $\gamma_p$	25 kN/m <sup>3</sup>
Thickness	0.5m
<b>Piled-raft properties</b>	
Modulus of Elasticity, $E_p$	25 GPa
Poisson's ratio, $\mu_p$	0.2
Density, $\gamma_p$	25 kN/m <sup>3</sup>
Thickness	0.5 m

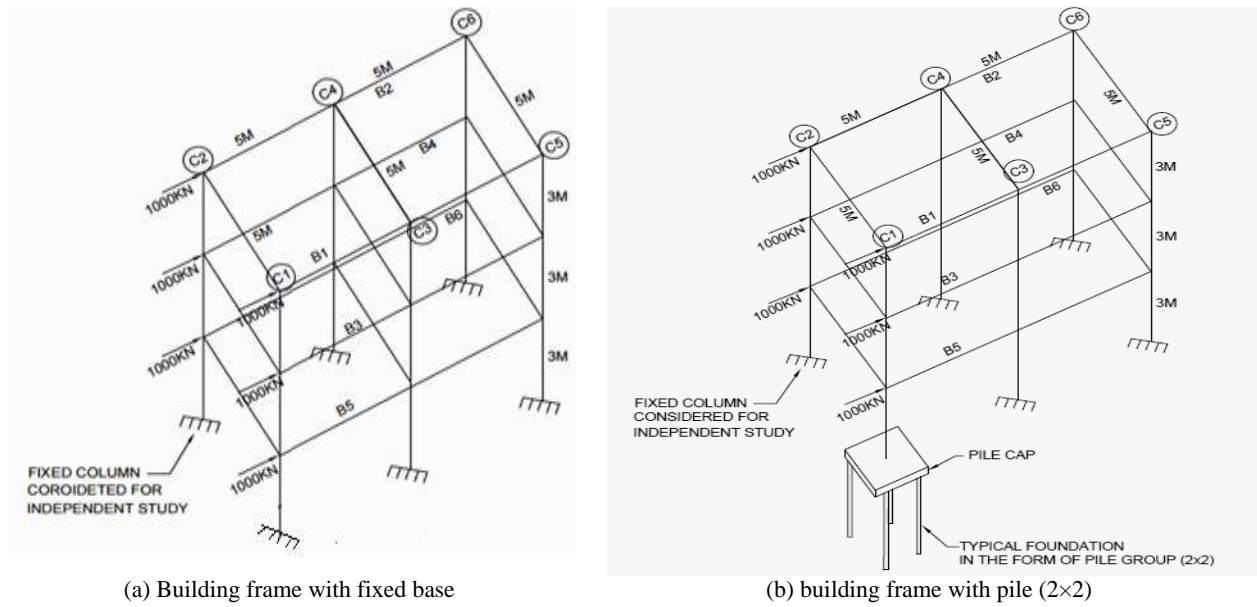


**Fig. 1 Typical building frame with Fixed base and Pile considered for non-interactive analysis.**

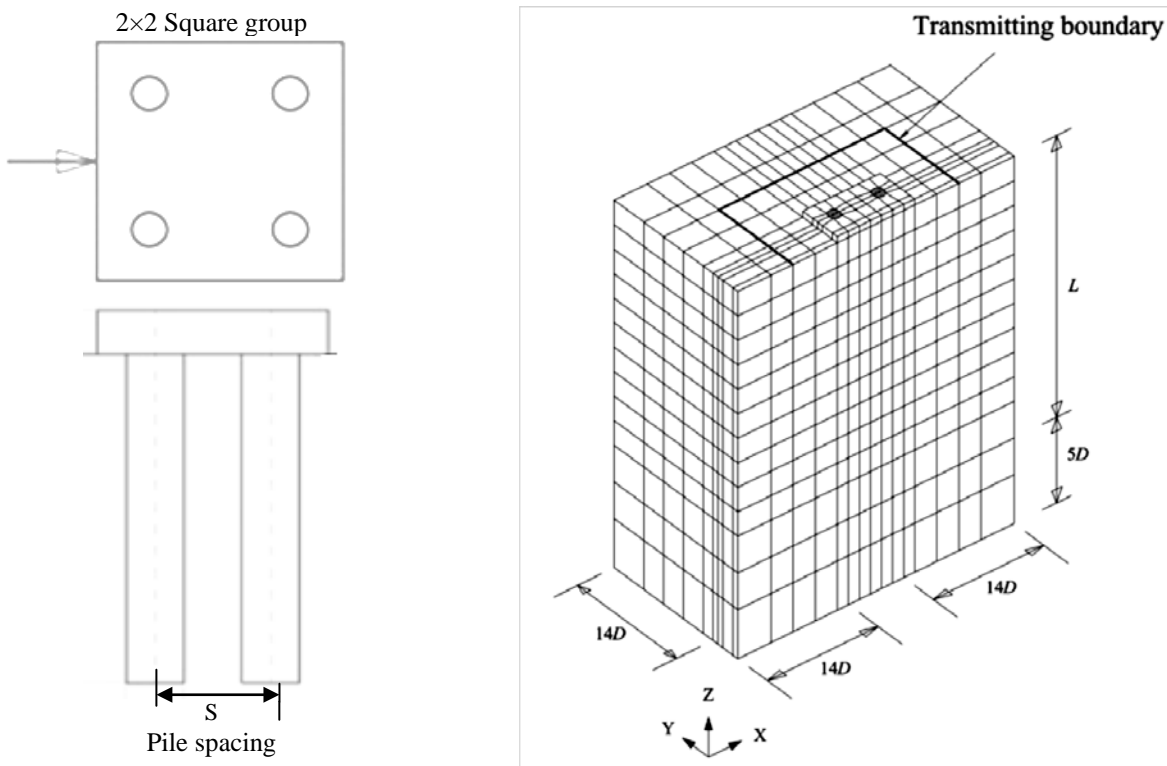


**Fig. 2 Typical finite element mesh for a square group of four piles (2x2) (After Dode et al. 2014)**

The group of four piles (2x2) that is considered in the present study is shown in Fig. 2. The discretized soil-pile domain for the half three dimensional geometrical model, which is used for the analysis of pile groups, is also shown in Fig 2. Half geometrical model is used for the square configurations so as to take the advantage of the symmetry. Along X and Y directions, the boundary is kept at 14D from the outermost pile of the pile group in each respective direction, as is apparent from Fig. 2. The three different foundations i.e pile, raft and piled-raft considered in the present study. The typical building frame with raft and piled-raft considered in the present study is shown in Fig.3.

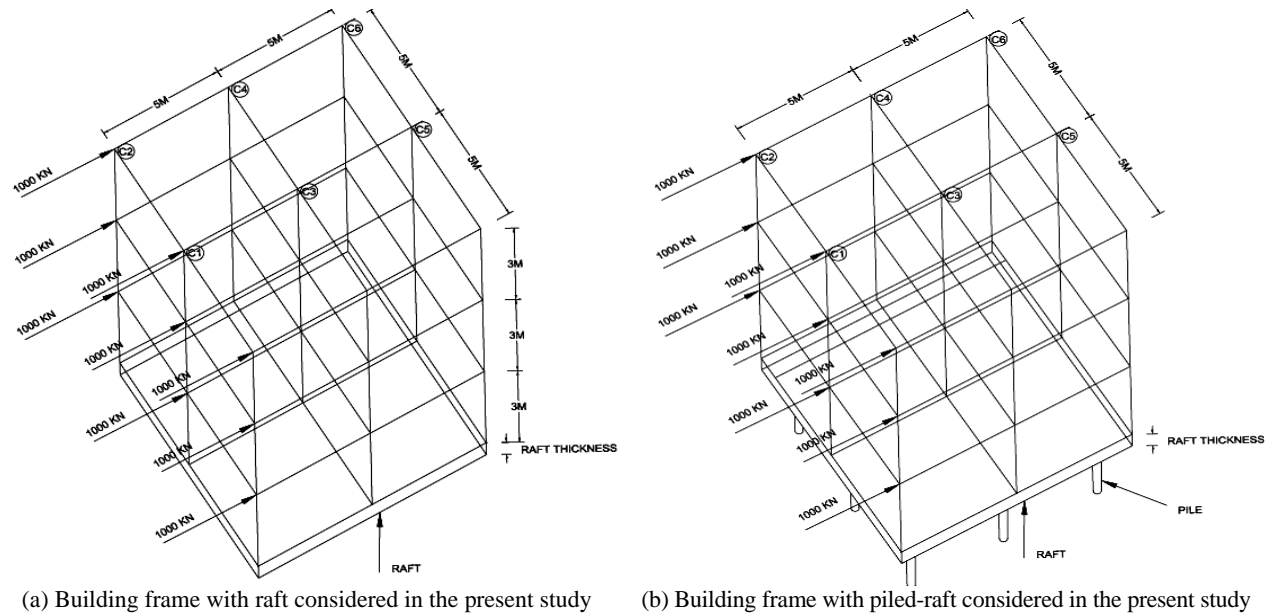


**Fig. 3: Typical building frame with raft and piled-raft considered in the present study**

In the initial convergence study, boundaries are varied from  $5D$  to  $15D$  and the solutions are observed to converge at a distance of  $10D$ . hence, in this study, the boundaries are assumed at  $10D$  where transverse displacement is assumed to be zero. For pile, 20 nodes element is considered which can model bending of pile in more effective manner. Failure of soil is dominated by shear characteristics. For soil, 8 node brick element having linear shape functions is considered. These elements are suitable for medium whose deformations are dominated by shear strength.

To study the effect of key parameters, the response is considered in terms of storey displacement, moments and shear in the frame resting on raft for different thickness and soil modulus; the same are compared with the fixed base analysis. It is observed that the response of raft foundation is significantly influenced by the material non-linearity of soil. A 3-D finite element program is developed for the analysis of a pile groups in clay considering the above aspects. Soil and raft media are discretised into 3-D isoparametric continuum elements. The raft elements are assumed to remain in elastic state at all the time. On the other hand, the soil elements are assumed to undergo plastic yielding according to the *von Mises* yield criterion. This model is selected because it is suitable for analyzing the behaviour of purely cohesive soils under undrained condition.

## RESULTS AND DISCUSSION

For the interaction analysis, a software program Build-Frame is developed using *FORTRAN 90*. In the parametric study conducted for the framed structure presented here, the response of the superstructure considered for the purpose of comparison includes the horizontal displacement at the top of the frame corresponding to each storey, shear force in beams, moment in beams and columns along with the axial force in columns. The response is evaluated initially for two conditions- without considering the effect of SSI and another by considering it. Hence, two analyses are reported, non- interactive analysis and the interactive analysis. Further, the interactive analysis is extended to incorporate the non-linear behaviour of soil and the results obtained using linear and non-linear behaviour of soil are compared.

### *Effect on the storey displacement*

The values of the horizontal displacement at each storey level of the frame in respect of pile, raft and piled-raft considered in the study is shown in Table 2. The corresponding percentage increase in displacement due to consideration of SSI (linear-interactive w.r.t. non-interactive, i.e., fixed base, and further, non-linear-interactive w.r.t. linear-interactive) is indicated in brackets in Table 2. Similarly, the variation in the storey displacement with storey height in respect of three different foundations considered in the present investigations is shown in Fig. 4.

**Table 2. Effect of different foundations on the storey displacement**

Type of Foundation	Storey Height (m)	9.0	6.0	3.0	0.0
	Analysis	Displacement (mm)			
Pile	Non-interactive	363.99	294.9	162.53	0.0
	Linear	423.78 (16.42 %)	347.58 (17.86 %)	214.14 (31.75 %)	11.39 (100%)
Raft	Nonlinear	423.87 (16.45 %)	352.09 (19.39 %)	215.34 (32.49 %)	11.61 (100%)
	Linear	395.00 (8.52 %)	317.00 (7.49 %)	175.00 (7.67 %)	10.11 (100 %)
Piled-raft	Nonlinear	468.00 (28.57 %)	347.00 (17.67 %)	197.00 (21.21 %)	11.06 (100 %)
	Linear	392.15 (7.74 %)	295.24 (0.12 %)	173.24 (6.59 %)	9.98 (100 %)
Piled-raft	Nonlinear	370.67 (1.84 %)	299.84 (1.68 %)	165.47 (1.81 %)	11.16 (100 %)

The general trend observed for all types of foundations (pile, raft and piled-raft) considered in this investigation is that horizontal displacement at each storey level increases due to the effect of soil structure interaction (SSI). It is seen that the displacement at top of each storey is on higher side corresponding to different foundations considered in the present investigation when compared with the values of top displacement obtained in non interactive analysis. The displacement is maximum at the top of the frame in respect of types of foundations, i.e., third storey. The SSI is found to increase the percentage displacement in the range of 16.42 – 31.75, 7.67 – 8.52 and 6.59 – 7.74 in respect of pile, raft and piled-raft foundation. Further, it is seen that the increase in displacement due to consideration of SSI at top storey of the frame is found 16.42, 8.52 and 7.74% respectively for pile, raft and piled-raft; the increase in displacement goes on decreasing with respect to pile, raft and piled-raft foundation. The variation in storey displacement with respect to linear analysis is shown Fig.4 (a).

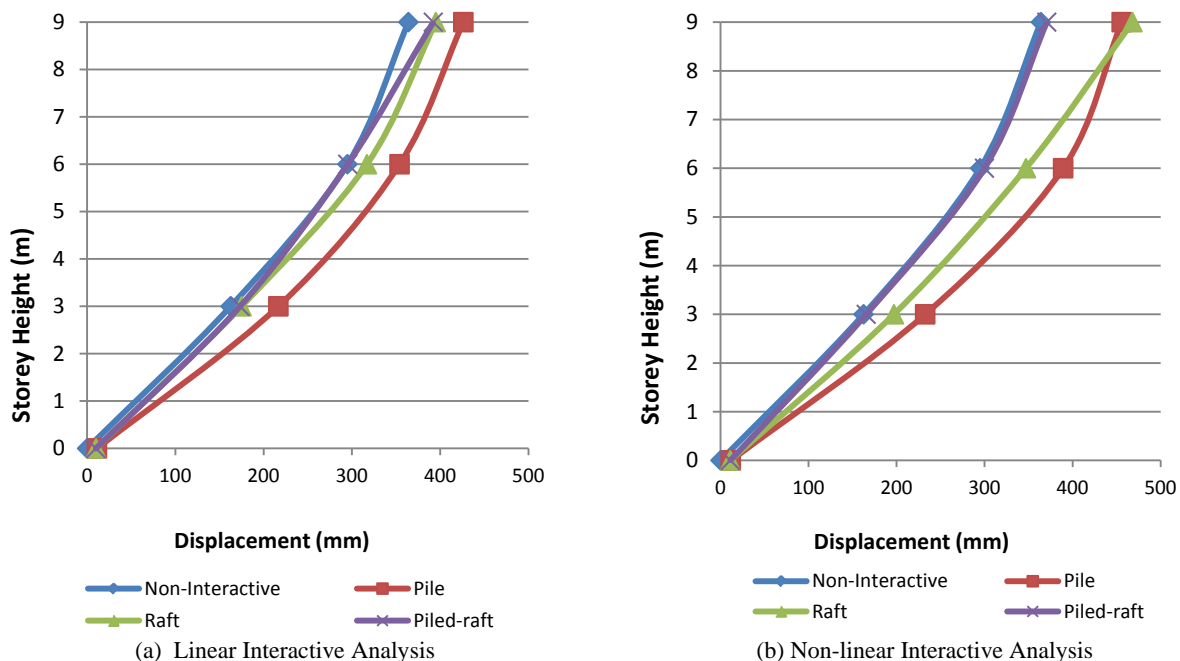


**Fig. 4 Effect of different foundations on the displacement**

**Effect of non-linearity of soil on storey displacement**

The analysis carried out in the context of linear behavior of soil is extended further to account for the non-linearity

of the soil using *von Mises* yield criterion. The values of the displacement obtained at the each storey level with respect to non-linear behavior of soil are also indicated in Table 2 for three different types of foundations (pile, raft and piled-raft).

The values of the displacements obtained in the present study are on a higher side in respect of either condition-linear and non-linear with soil- structure interaction for the foundations except piled-raft. The percentage increase in the displacement at top storey of the frame is observed to be 16.45 and 28.57 respectively for pile and raft foundation, while the percent increase in the storey displacement is found to be 1.84%; seems to be very marginal. The increase in the displacement is observed for raft foundation in comparison with pile and piled-raft. Figure 4 (b) shows the variation in storey displacement with respect to non-linear analysis.

## CONCLUSIONS

Some of the significant conclusions emerging from the interaction analysis reported in the present investigations are given below.

- The effect of soil- structure interaction (SSI) is significant on the storey displacement. The linear SSI is found to increase the displacement in the range of 17.1 – 33.31%.
- The non-linearity of soil is found to increase the displacement in the range of 2.84 – 9.71 % with respect to that obtained in the context of linear SSI.
- The displacement at each storey level decreases with pile, raft and piled-raft foundation in respect of linear and non-linear analysis.
- The increase in displacement due to consideration of SSI is more on the bottom storey and with increase in storey, the displacement goes on decreasing.
- The displacement at top of each storey is on higher side corresponding to different foundations considered in the present investigation when compared with the values of top displacement obtained in non interactive analysis in respect of linear and non-linear analysis.

## REFERENCES

- Agrawal, R. and Hora, M.S. 2009. "Coupled finite- infinite elements modeling of building frame- soil interaction system." *ARPJ Journal of Engineering and Applied Sciences*, 4(10), 47-54.
- Buragohain, D.N., Raghavan, N. and Chandrasekaran, V.S. 1977. "Interaction of frames with pile foundation." *Proc. Int. Symp. Soil- Structure Interaction, Roorkee, India*, 109-115.
- Brown, P. T. and Wiesner, T. J. 1975. "The behaviour of uniformly loaded piled strip footings." *Soils and Foundations*, 15 (4), 13-21.
- Butterfield, R. and Banerjee, P. K. 1971. "The problem of pile group - pile cap interaction." *Geotechnique*, 21(2), 135-142.
- Banerjee, P.K. and Davis, T.G. 1978. "The behaviour of axially and laterally loaded single piles embedded in non-homogeneous soils." *Geotechnique*, 28(3), 309-326.
- Basarkar, S.S. and Dewaikar, D.M. 2005. "Development of load transfer model for socketted tubular piles." *Proc. Int. Geotech. Conf. on Soil- Structure Interaction- Calculation Methods and Engineering Practice, St. Petersburg*, 117-122.
- Chameski, C. 1956. "Structural rigidity in calculating settlements." *Jl. Soil Mech. and Foundation Engineering, ASCE*, 82 (1), 1-9.
- Chore H.S. 2014. "Interactive Analysis of a Building Frame resting on Pile Foundation." *Coupled Systems Mechanics: An International Journal (Techno Press)*, 3(4), 367-384.
- Chore, H.S. and Ingle, R.K. 2008. "Interaction analysis of building frame supported on pile group." *Indian Geotechnical Jl.*, 38(4), 483-501.
- Chore, H.S. and Ingle, R.K. 2008. "Interactive analysis of building frame supported on pile group using a simplified F.E. model." *Jl. Struct. Engg. (JoSE), SERC, Chennai (India)*, 34(6), 460-464.
- Chore, H.S., Ingle, R.K. and Sawant, V.A. 2009. "Building frame- pile foundation- soil interactive analysis." *Interaction and Multiscale Mechanics: An International Journal*, 2(4), 397-412.
- Chore, H.S., Ingle, R.K. and Sawant, V.A. 2010. "Building frame-pile foundation- soil interaction analysis: a parametric study." *Interaction and Multiscale Mechanics: An International Journal*, 3(1), 55-80.
- Coyle, H.M. and Reese, L.C. 1966. "Load transfer for axially loaded pile in clay." *Proc. ASCE*, 92(SM- 2), 1-26.
- Chen, K. S., Karasudhi, P. and Lee, S. L. 1974. "Force at a point in the interior of layered elastic half-space", *Int. Jl. Solids Struct.*, 10 (11), 1179-1199.

- Cheng, Z. 2011 “Prediction and measurement of settlement of a piled raft foundation over thick soft ground”, *E- JI. Geot. Engg. (EJGE)*, 16(A), 125-136.
- Chore, H.S., Ingle, R.K. and Sawant, V.A. 2010, “Parametric study of pile groups subjected to lateral loads”, *Structural Engg. and Mech.: An Int. JI.*, 26 (2), 243-246.
- Chore, H.S. , Ingle, R.K. and Sawant, V.A. 2012. “Parametric study of laterally loaded pile groups using simplified F.E. models”, *Coupled Systems Mech.: An Int. JI.*, 1(1), 1-18.
- Chow, Y. K. 1987. “Axial and lateral response of pile groups embedded in non-homogeneous soil”, *Int. JI. Num. Analyt. Meth. Geomech.*, (11) 6, 621-638
- Chow, Y. K. and Teh, C. I. 1991. “Pile-cap-pile-group interaction in non- homogeneous soil”, *JI. Geotech. Engg., ASCE.*, 117 (11), 1655-1667.
- Chow, Y.K., Poulos, H.G. and Small, J.C. 2011. “Piled Raft Foundations for Tall Buildings”, *Geot. Engg. JI. (South East Asian Geotechnical Society)*, 42(2).
- Clancy, P. and Randolph, M. F. 1993. “An approximate analysis procedure for piled raft foundations”, *Int. JI. Num. and Analyt. Meth. in Geomech.*, 17(12), 849–869.
- Deshmukh, A.M. and Karmarkar, S.R. 1991. “Interaction of plane frames with soil”, *Proc. Indian Geotechnical Conference, Surat, India*, 323-326.
- Dewaikar, D.M. and Patil, P.A. 2006. “Analysis of a laterally loaded pile in cohesion-less soil under static and cyclic loading”, *Indian Geotech. JI.*, 36(2).
- Desai, C.S. and Abel, J.F. 1974. “*Introduction to finite element method*”, CBS Publishers, New Delhi.
- Desai, C.S. and Appel, G.C. 1976. “3-D analysis of laterally loaded structures”, *Proc. 2<sup>nd</sup> Int. Conf. on Numerical Methods in Geomechanics, Blacksburg*, 405-418.
- Desai, C.S., Kuppusamy, T. and Allameddine, A.R. 1981. “Pile cap- pile group- soil interaction”, *JI. Structural Engg., ASCE*, 107 (ST -5), 817-834.
- Dasgupta, S., Dutta. S.C. and Bhattacharya, G. 1998. “Effect of soil- structure interaction on building frames on isolated footings”, *JI. Struct. Engg. (JoSE), SERC, Chennai (India)*, 26 (2), 129-134.
- Dalili, M., Alkarami, A., Noorzai, J., Paknahad, M., Jaafar, M.S. and Huat, B. 2011. “Numerical simulation of soil-structure interaction in framed and shear wall structures”, *Interaction and Multiscale Mechanics: An International Journal*, 4(1) pp 17-34.
- Dode P. A, Chore H.S. and Agrawal D.K., 2014. “Interaction Analysis of a Building Frame Supported on Pile Groups”, *Coupled Systems Mechanics: An International Journal (Techno Press)*, 3 (3), 305-318.
- Dode P. A, Chore H.S. and Agrawal D.K. 2015. “Space Frame- Pile Foundation- Soil Interaction Analysis”, *Journal of Structural Engineering (JoSE), Structural Engineering Research Center, Chennai (India)*, 42(3), 246-255.
- Franke, E., El-Mossallamy, Y. and Wittmann, P. 2000. “Calculation methods for raft foundation in Germany”, *Design Applications of Raft Foundation*, Thomas Telford, 283-322.
- Georgiadis, M., Anagnostopoulos, C. and Saflekou, S. 1992. “Cyclic lateral loading of piles in soft clay”, *J. Geotech. Engg., SEAGS*, 23, 47- 60.
- Gandhi, S.R. and Maharaj, D.K. 1996. “Analysis of piled raft foundation”, *Proc. Sixth Int. Conf. on Piling and Deep Foundations, Mumbai, India*, 1.11, 1-7.
- Hain, S. J. and Lee, I. K. 1978. “The Analysis of flexible raft-pile systems”, *Geotechnique*, 28 (1), 65-83.
- Hooper, J. A. 1973. “Observations on the behaviour of a piled-raft foundation on London Clay”, *Proc. Int. JI. Civ. Eng.*, 55 (2), 855-877.
- H.G. Polous. 1968. “Analysis of settlement of pile.” *Geotechnique*, 18(4), 449-471.
- Hazarika, P.J. and Ramasamy, G. 2000. “Response of piles under vertical loading.” *Indian Geotech. JI.*, 30(2), 73-91.
- King, G.J.W. and Chandrasekaran, V.S. 1974. “Interactive analysis of a rafted multi-storeyed space frame resting on an inhomogeneous clay stratum”, *Proc. Int. Conf. Finite Element Methods, Australia*, 493-509.
- Krishnamoorthy; Rao, N.B.S. and Rao, N. 2005. “Analysis of group of piles subjected to lateral loads”, *Indian Geotechnical Journal*, 35(2), 154-175.
- Krishnamoorthy, C.S. 2010. “*Finite Element Analysis: Theory and Programming*”, Tata Mc-Graw Hill Publications, New Delhi (2<sup>nd</sup> Edition).
- Kakurai, M., Yamashita, K. and Tomono, M. 1987. “Settlement behaviour of piled raft foundation on soft ground”, *Proc. 8<sup>th</sup> Asian Regional Conf. Soil Mech. and Foundation Engg., Kyoto, Japan*, 1, 373-376.
- Katzenbach, R. and Reul, O. 1997. “Design and performance of piled rafts”, *Proc. XIV<sup>th</sup> Int. Conf. Soil Mech. and Foundation Engg., 97, Hamburg*, 4, 2253-2256.

- Katzenbach, R., Arslan, U. and Moormann, C. 2000. "Piled raft foundation projects in Germany", *Design Applications of Raft Foundation, Thomas Telford*, 323-391.
- Kitiyodom, P. and Matsumoto, T. 2003. "A simplified analysis method for piled raft foundations in non-homogeneous Soils", *Int. Jl. Num. Analyt. Meth. in Geomech.*, 27(2), 88-109.
- Kuwabara, F. 1989. "An elastic analysis for piled raft foundations in a homogeneous soil", *Soils and Foundations*, 29(1), 82-92.
- Lee, I.K. and Brown, P.T. 1972. "Structures and foundation interaction analysis", *Jl. Structural Engineering, ASCE*, 11, 2413-2431.
- Liu, W, and Novak, M. 1991. "Soil-pile-cap static interaction analysis by finite and infinite elements", *Canadian Geotech. Jl.*, 28, 771-783.
- Liang, F. Y. and Chen, L. Z. 2004. "A modified variation approach for the analysis of piled raft Foundation", *Mechanics Research Comm.*, 31, 593-604.
- Madhav, M.R. and Karmarkar, R.S. 1982. "Elasto-plastic settlement of rigid footings", *Journal Geotechnical Engineering Division, ASCE*, 108 (GT-3), 483-488.
- Maharaj, D. K. and Gandhi, S. R. 2004. "Non-linear Finite Element Analysis of Piled Raft Foundations", *Proc. Inst. Civ. Eng., Geotech. Engg.*, 157, 107-113.
- Morris, D. 1996. "Interaction of continuous frames and soil media", *Jl. Structural Engineering, ASCE*, 5(1), 13-43.
- Mandal, A., Moitra, D. and Dutta, S.C. 1999. "Soil- structure interaction on building frame: a small scale model study", *Int. Jl. Struct., Roorkee (India)*, 18(2), 92-107.
- Matlock, H. and Reese, L.C. 1956. "Foundation analysis of Offshore pile supported structures." *Proc. 5<sup>th</sup> Int. Conf. Soil Mech. and Foundation Engg., Paris*, 91-97.
- Matlock, H. 1970. "Correlations for design of laterally loaded piles in soft clay", *Proc. 2<sup>nd</sup> Offshore Tech. Conf., Houston*, 577-594.
- Mendonca, A. V. and De Paiva, J. B. 2003. "A Boundary element method for the static analysis of raft foundations on piles", *Engg. Analysis with Boundary Elements*, 24, 237-247.
- Ng, C.W.W. Zhang, L.M. 2001. "Three dimensional analysis of performance of laterally loaded sleeved piles in sloping ground." *Jl. Geotech. and Geoenv. Engg., ASCE*, 127, 499-509.
- Noorzaei, J., Viladkar, M.N. and Godbole, P.N. 1991. "Soil-structure interaction of space frame-raft –soil system: parametric study", *Computers and structures*, 40, (5), 235-1241.
- Noh, E. Y., Huang, M., Surarak, C., Adamec, R. and Balasurbamaniam, A. S. 2008. "Finite element modeling for piled-raft in sand", *Proc. of Eleventh East Asia-Pacific Conf. Structural, Engineering and Construction (EASEC-11)*, Taipei, Taiwan.
- Ottaviani, M. 1975. "Three-dimensional finite element analysis of vertically loaded pile groups", *Geotechnique*, 25 (2), 159-174.
- Poulos, H.G. 1971. "Behaviour of laterally loaded piles: II- group of piles." *Jl. Soil Mechanics and Foundation Engg., ACSE*, 97(5), 733-751.
- Poulos H.G. (1994), "An approximate numerical analysis of piled raft interaction" *Int. Jl. Num. and Analyt. Meth. in Geomech.*, 18 (2), 73-92.
- Poulos, H.G., Badelow, F., Small, J.C., Moyes, P. 2006. "Economic foundation design for tall buildings". *Proc. 10<sup>th</sup> Int. Conf. on Piling and Deep Foundations, Amsterdam*, 200-209.
- Prakoso, W. A. and Kulhawy, F. H. 2001. "Contribution to piled raft foundation design", *Jl. Geotech. and Geoenv. Engg., ASCE*, 127(1), 17-24.
- RajsekarSwamy, H.M., Krishnamorthy, A., Prabhakara, D.L. and Bhavikatti, S.S. 2011. "Evaluation of the influence of interface elements for structure- isolated footing- soil interaction analysis." *Interaction and Multiscale Mechanics: An International Journal*, 5, (3) 65-83.
- R. Butterfield and P.K. Banerjee 1971. "The problem of pile group and pile cap interaction." *Geotechnique*, 21(2), 135-142.
- Randolph, M. F. 1983. "Design of piled raft foundations", *Proc. Int. Symposium on Recent Developments in Laboratory and Field Tests and Analysis of Geotechnical Problems, Bangkok*, 525-537.
- Reul, O. and Randolph, M. F. 2003 "Piled rafts in over consolidated clay: Comparison of in- situ measurements and numerical analyses", *Geotechnique*, 53(3), 301-315.
- Srinivasraghavan, R. and Sankaran, K.S. 1981. "Settlement analysis for combined effect of superstructure- footings-soil system", *Jl. Institution of Engineers (India)*, 6, 194-198.
- Subbarao, K.S., ShradaBai, H. and Raghunatham, B.V. 1985. "Interaction analysis of frames with beam footing", *Proc. Indian Geotech. Conf., Roorkee, India*, 389-395.
- Sawant, V.A. and Chore, H.S. 2013. "Building frame-pile foundation –soil interactive analysis Using 3-D FEM',

- Journal of Structural Engineering (JoSE), SERC Chennai*, 36(6), 318-325.
- Spiller, W.R. and Stoll, R.D. 1964. "Lateral response of piles", *Jl. Soil Mech. and Foundation Engg., ASCE*, 90, 1-9.
- Sales, M.M., Small, J. C. and Poulos, H.G. 2010. "Compensated piled rafts in clayey soils: behaviour, measurements, and predictions", *Canadian Geotech. Jl.*, 47, 327-345.
- Sawant, V. A., Ladhane, K. and Pawar, S. 2012. "Parametric study of piled raft for three load-patterns", *Coupled System Mech.: An Int. Jl.*, 1(2), 115-131.
- Sinha, J. 1997. "*Piled raft foundations subjected to swelling and shrinking soils*", Ph.D. Thesis (Unpublished), University of Sydney, Australia.
- Small, J. C. and Booker, J. R. 1984. "Finite layer analysis of layered elastic materials using flexibility approach, Part I. — Strip Loadings", *Int. Jl. Num. Meth. Eng.*, 20, 1025-1037.
- Small, J. C. and Booker, J. R. 1986. "Finite layer analysis of layered elastic materials using flexibility approach, Part II. - Circular and Rectangular Loadings", *Int. Jl. Num. Meth. Eng.*, 23, 959-978.
- Smith I. M. and A. Wang 1998. "Analysis of piled rafts", *Int. Jl. Num. and Analyt. Meth. Geomech.*, 22 (10), 777-790.
- Shen, W. Y., Chow, Y. K. and Yong, K. Y. 1999. "Variational solution for vertically loaded pile groups in an elastic half-space", *Geotechnique*, 49 (2), 199-213.
- Shen, W. Y. and Teh, C. I. 2002. "Analysis of laterally loaded pile groups using a variational approach", *Geotechnique*, 52 (3), 201-208
- Tan, Y.C., Chow, C.M. and Gue, S.S. 2005. "Piled raft with different pile length for medium rise buildings on very soft clay", *Proceedings 16<sup>th</sup> Int. Conf. Soil Mech. and Geot. Engg. (ICSMGE), Osaka, Japan*, September 12-16.
- Thangaraj, D.D. and Illampurthy, K. 2010. "Parametric study on the performance of raft foundation with interaction of frame." *Electronic Journal of Geotechnical Engineering*, 15(H) 861-878.
- Thoiba Singh, N. and Baleshwar Singh 2008. "Interaction analysis for piled rafts in cohesive soils" *The 12th Int. Conf. Int. Association for Comp. Meth. and Advances in Geomechanics (IACMAG), Goa, India*.
- Viladkar, M.N., Godbole, P.N. and Noorzaeei, J. 1991. "Soil-structure interaction in plane frames using coupled finite-infinite elements", *Computers and Structures*, 39 (5), 1991, 535-546.
- Wiesner, T. J. 1991. "Various applications of piled raft analysis", *Proc. Int. Conf. on Comp. Meth. and Advances in Geomech., (Ed.: Beer, Booker and Carter), Balkema, Rotterdam*, 1035-1039
- Xie X., Shou M. and Huang J. 2012. "Application Study of Long-short-piled Raft Foundation", *Applied Mechanics and Materials*, 70, 242-245.



## INTERACTION ANALYSIS OF BUILDING FRAME WITH PILE FOUNDATION

Varnika Srivastava,<sup>1</sup> Hemant S. Chore<sup>2</sup>, Prasad A. Dode<sup>3</sup>

<sup>1</sup>Assistant Professor, Deptt. of Civil Engg., Thakur College of Engineering, Mumbai; e-mail:vrnkasrivastava@gmail.com

<sup>2</sup>Associate Professor, Deptt. of Civil Engg., Dr.B.R. Ambedkar National Institute of Tech. Jalandhar; e-mail:chorehs@nitj.ac.in,  
Corresponding Author

<sup>3</sup>Professor, Deptt. of Civil Engg., Datta Meghe College of Engineering, Navi Mumbai; padode@rediffmail.com

### ABSTRACT

The three dimensional finite element analysis of the single storeyed building frame resting on a pile group embedded in cohesive soil mass is presented in this paper. The elements of the superstructure frame and that of the pile foundation is discretized using twenty node isoparametric continuum elements. The interface between the pile and pile cap is idealized using sixteen node isoparametric surface elements. The more improved finite element mesh is used for modeling soil element as compared to the one used in the study reported in the literature. The soil elements are discretized using eight node, nine node and twelve nod continuum elements. Both the elements of superstructure and substructure (*i.e.*, foundation) including soil are assumed to remain in elastic state at all the time. The interaction analysis is carried out using sub-structure approach to attempt a parametric study. The effect of spacing between the piles in a group and arrangement of the piles in a group of two piles is evaluated on the response of building frame. The response includes the displacement at the top of the frame and bending moment in columns. The effect of the soil-structure interaction is observed to be significant for the type of foundation and soil considered in the present study.

**KEYWORDS:** Soil-structure interaction; pile groups; pile spacing; pile diameter; top displacement; bending moment.

### INTRODUCTION

The framed structures are normally analyzed with their bases considered to be either completely rigid or hinged. However, the foundation resting on deformable soils also undergoes deformation depending on the relative rigidities of the foundation, superstructure and soil. Interactive analysis is, therefore, necessary for the accurate assessment of the response of the superstructure. Numerous interactive analyses (Chameski, 1956; Morris, 1966; Lee and Brown 1972; King and Chandrasekaran, 1974; Buragohain *et al.* 1977) have been reported in many studies in the 1960's and 1970's and few (Srinivasraghavan and Sankaran, 1981; Subbarao *et al.*, 1985; Deshmukh and Karmarkar 1991; Noorzai *et al.* 1991; Dasgupta *et al.*, 1998; and Mandal *et al.*, 1999 in the decade of 1980's and 1990's. While most of the above mentioned studies dealt with the quantification of the effect of interaction of frames with isolated footings or combined footings or raft foundation in the context of supporting sub-soil either analytically or experimentally; only the study by Buragohain *et al.* (1977) was found to deal with the interaction analysis of frames on piles until recent past.

The work presented by Buragohain *et al.* (1977) was carried out using the stiffness matrix method and moreover, it was based on the simplified assumptions and relatively less realistic approach. Pointing out the lacunae in the aforementioned interaction analysis of a framed structure resting on pile foundation, Chore and co-authors (2008<sup>a,b</sup>, 2009, 2010<sup>a,b</sup>) reported the methodology for the interaction analysis of a single storeyed building frame embedded in clayey soil on the rational approach and realistic assumptions. Although most of the analyses used sub-structure method (uncoupled approach), few of them used coupled approach where the structure and foundation were considered to be a single compatible unit. However, the investigations underscored that the sub-structure approach is preferred in such interaction analysis owing to simplicity in the method, less memory requirement on part of the computational resources and not much variation in the results obtained using sub-structure method and coupled approach. Recently along similar lines, Reddy and Rao (2011) reported an experimental work on a model building

frame supported by a pile group and compared the results analytically using finite element analysis. Even numerous studies by many researchers (Agrawal and Hora, 2009 and 2010; Thangaraj and Illampurthy, 2010; Dalili *et al.*, 2011; Rajsekar Swamy *et al.*, 2011; and Thangaraj and Illampurthy, 2012) have been reported most recently. However, these studies were confined to the interaction analysis of frames or allied structure supported by isolated footings or raft foundation.

On the backdrop of the considerable work of the interaction analyses of space frame- pile foundation-soil system reported in the recent past, the interaction analysis of a single storied frame resting on pile foundation is reported in this investigation. However, more refined 3-D F.E. mesh is used for pile foundation, wherein soil elements are discretized using three different elements—eight node, nine node and twelve node continuum elements, as compared to the mesh employed in the similar study (Chore and Ingle, 2008) wherein the soil mass was discretized using twenty node continuum elements. Further, the piles that were modeled were square for simplicity in modeling. However, while considering its effect, they were treated as the circular piles of the diameter equivalent to the size of the square piles. Further, the flexible pile cap along with its stiffness is considered and the stiffness matrix for the sub-structure is derived by considering the effect of all the piles in a group in the similar fashion as that considered in the previous work (Chore and Ingle, 2008). The behavior of elements of the superstructure and sub-structure including soil is considered to be linearly elastic. The total stress analysis is carried out and immediate behavior of the soil is considered.

Although Srivastava *et al.* (2016) reported the limited studies on displacement of the building frame resting on two pile groups consisting of two and three piles, respectively with series and parallel arrangement, only two spacings were considered. The present investigation deals with the comprehensive analysis that evaluates the displacement and bending moment in superstructure columns. However, only a group of two piles are considered along with series and parallel arrangement and more number of spacings. Further, the results are compared with those published in the literature (Chore and Ingle, 2008).

## **HYPOTHESIS IN MATHEMATICAL MODELING**

The interaction analysis is carried out using the finite element method. A typical frame is analyzed separately considering the fixed column bases. Later, the pile foundations are worked out independently to get the equivalent stiffness of the foundation head. Further, they are used in the interaction analysis to evaluate the effect of SSI on the response of the frame.

A three dimensional geometric model of the superstructure frame-pile foundation-soil system. The elements of the superstructure (beam, column and slab) and that of pile foundation (pile and pile cap) are discretized into 20 node isoparametric continuum elements. On the other hand, soil elements are discretized using eight node, nine node and twelve node continuum elements. Further, three degrees of freedom at each node, *i.e.*, displacement in three directions in X, Y and Z of these different elements are employed in the present investigation. To ensure proper mechanics of stress transfer between soil and pile under lateral load, 16 node isoparametric surface elements is introduced at the interface. The normal and tangential stiffness of these elements are assumed in such a way that shearing at the soil and pile interface is allowed but gapping will be restricted.

Since a 3-D geometric model is used to represent the soil-pile system, selection of the correct finite element to represent the medium is one of the very important aspects in finite element analysis. In the soil- pile system, two materials, *viz.* soil and reinforced concrete are to be modeled. The either material show different behaviors when subjected to loading. The failure of the soil is dominated by its shear characteristics, whereas the flexure dominated failure is shown by the reinforced concrete. Therefore, pile and pile cap along with the superstructure elements are modeled using twenty node continuum elements. This element has quadratic shape function which is well suited to model the medium with bending dominated deformation.

Eight node continuum elements are used to model the soil which has linear shape functions. These elements are suitable for the medium whose deformations are dominated by shear strength. To maintain the continuity of displacements between these two types of elements in the discretized soil-pile domain, two more elements were formulated, *viz.* twelve node and nine node solid elements. The shape functions of these two elements were formulated by using degrading technique as employed by Krishnamoorthy (2010). The shape functions are derived for these elements by degrading the twenty node solid elements. Twelve node elements are used at the junction

where eight node and twenty node element meets. Further, nine node elements are used where twelve node element and twenty node element meets perpendicularly.

### PROBLEM DESCRIPTION

A 3-D single storeyed building frame resting on pile foundation, as shown in Fig.1, is considered for the study. The frame, 3 m high is 10 m × 10 m in plan with each bay being, 5 m × 5 m. The slab, 200 mm thick, is provided at top as well as at the floor level. Slab at top is supported over 300 mm wide and 400 mm deep beam. The beams are resting on columns of size 300 mm × 300 mm. pile groups comprising two piles are considered in the present study. Further, two arrangements of piles with respect to the direction of load (series and parallel) are considered (Fig.2). All the piles in a group are circular piles, connected by a 500 mm thick flexible pile cap. While dead load is considered according to unit weight of the materials of which the structural components of frame is made up for the purpose of the parametric study presented here, lateral load as shown in the Fig. 2 is also considered. The properties of the material for pile and pile cap are given in Table 1.

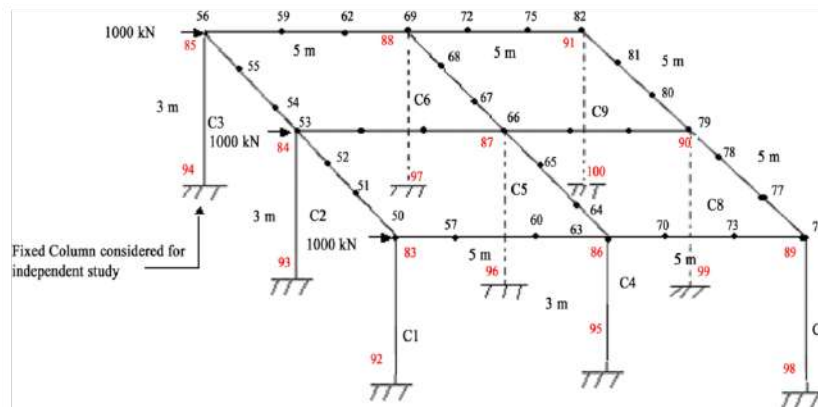


Fig.1 Typical building frame considered in the study (After Chore and Ingle, 2008)

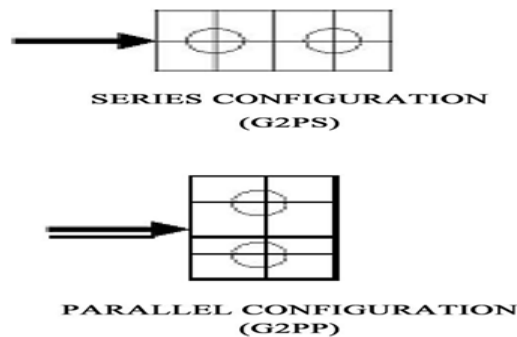
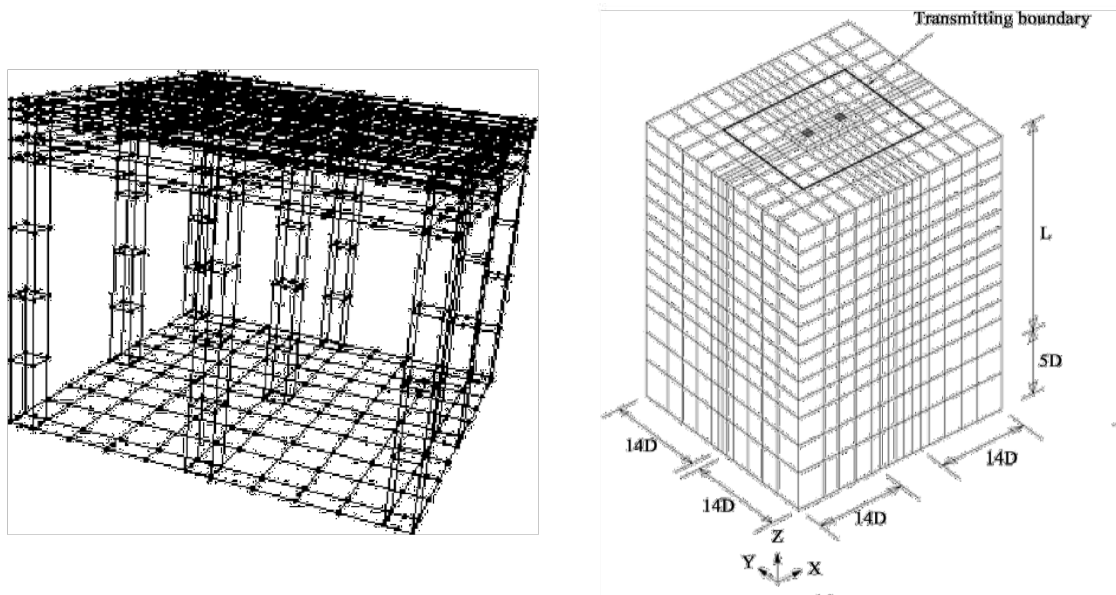


Fig.2 Group of two piles with different arrangements considered in the study

Fig. 3 shows the mathematical model of the building frame with the modeling idealizations mentioned in the preceding section. Fig. 3 also shows the discretized soil-pile domain for the full 3-D geometrical model which is used for the analysis of two piles groups viz. 2PP (two piles in parallel), 2PS (two piles in series). For group configuration in series and parallel arrangements, full 3-D geometric model is used. One subroutine is developed in the program to generate the geometrical and material properties required for finite element analysis.

**Table 1. Geometrical and material properties for the elements of the frame and foundation**

Properties	Corresponding Values
Pile diameter (D)	300 mm
Length of pile (L)	3 m (3000 mm)
Thickness of pile cap	500 mm
Grade of concrete used for frame elements	M-20 (as per Indian Specification) Characteristic compressive strength: 20 MPa
Young's modulus of elasticity for frame elements ( $E_c$ Frame)	$0.25491 \times 10^8$ kPa
Grade of concrete used for pile and pile cap	M-40 (as per Indian Specification) Characteristic compressive strength: 40 MPa
Young's modulus of elasticity for foundation ( $E_c$ Foundation)	$0.3605 \times 10^8$ kPa
Poisson's ratio for concrete ( $\mu_c$ )	0.15
Young's modulus of elasticity for soil ( $E_s$ )	4267 kPa
Poisson's ratio for soil ( $\mu_s$ )	0.45
Interface stiffness in tangential direction ( $k_s$ )	1000 kN/m <sup>3</sup>
Interface stiffness in normal direction ( $k_n$ )	$1 \times 10^6$ kN/m <sup>3</sup>



**Fig. 3 Typical F.E. mesh for a building frame and pile group**

When the load is acting along the line joining the center of pile then, it is called as series along X and Y directions,

the boundary is kept at  $14D$  ( $D$  being the diameter of the pile) from the outermost pile of the pile group in respective directions. The position of the transmitting boundary is also shown by thick line as is evident from the aforementioned figures. However, this boundary is meant to be used in the dynamic analysis and hence, is beyond the scope of the investigations reported in this paper. Four different spacing between the piles in a group ( $3D$ ,  $4D$ ,  $5D$  and  $6D$ ) are considered and pile diameter as 300 mm is considered.

## RESULTS AND DISCUSSION

For analyzing the pile foundation separately a software program Pile\_Routine was used. The analysis of the pile foundation is carried out for the lateral or vertical force ( $F_H$  or  $F_V$ ) of magnitude of 1000 kN applied on pile cap. The equivalent stiffness,  $k_h$  and  $k_v$ , are calculated and are further used in the interaction analysis of the frames structure. For the interaction analysis, a software programme Build\_Frame is developed. The software program is developed using FORTRAN 90. After assessing the accuracy of the programme in the context of simple problems of structural engineering and soil-structural engineering and further, implementing it on the published work, the said program is used in the present study. In the parametric study conducted for the specific frame presented here, the response of the superstructure considered for the comparison include the horizontal displacement of the frame at top of the frame as well as bending moment in superstructure columns, for both fixed base and soil-structure interaction (SSI) cases.

### Effect of SSI on Top Displacement of the Frame

The displacements of frame evaluated in respect of various arrangement of piles group is shown in Table 2. From the results of parametric study conducted on a specific building frame with pile foundation of different configurations as mentioned in the preceding section, it is observed that top displacement is very less (38.18 mm) when the column bases are assumed to be fixed and increases when the effect of soil- structure interaction is taken into consideration. The maximum values of top displacement are found to be 121 mm and 126 mm at the minimum spacing of  $3D$  for the group of two piles with series and parallel arrangement, respectively with respect to 300 mm pile diameter. The corresponding displacement at the higher spacing considered in the study. i. e.,  $6D$  is 102 mm and 114 mm, respectively. Incorporation of the aspect of soil-structure interaction is found to increase the displacement in the range of 97% - 230% when compared with the displacement obtained in view of the fixed column base condition. The general trend observed for all the configurations considered in the investigation in respect of all pile diameters is that horizontal displacement is more when the spacing between two piles is kept  $3D$  and thereafter, decreases for higher spacing, i.e.,  $3D$ ,  $4D$ ,  $5D$  and  $6D$ , in all the configurations considered in this study.

**Table 2 Top displacement and percentage increase in top displacement with SSI**

Top displacement				Percentage increase due to SSI			
$3D$	$4D$	$5D$	$6D$	$3D$	$4D$	$5D$	$6D$
Top displacement obtained assuming column bases to be fixed: 38.18 mm							
Group of two piles (Series arrangement)							
121	114	106	102	217	199	178	167
Group of two piles (Parallel arrangement)							
126	121	116	114	230	217	204	199

The trend of reduction in displacement with increase in spacing could be attributed to the overlapping of stressed zones of individual piles at closer spacing. When the piles are closer, combined action of pile and that of pile cap is more rigid; and moreover, in three dimensional formulations, it reflects block action. Owing to this, displacement is observed more for spacing of  $3D$ ; and thereafter, it goes on decreasing. Effect of the configuration of the pile group on response of the superstructure is quite significant. It is obvious from the results that for the parallel arrangement, displacements obtained are on higher side as compared to the series arrangement. The series arrangement offers stiffer behavior than parallel arrangement. This is because the combined structural stiffness of pile and pile cap in parallel arrangement is small as compared to that in series arrangement. This can be attributed to the larger area available for the development of passive resistance.

**Comparison with the results in published literature (Chore and Ingle 2008)**

The displacements obtained in the published literature (Chore and Ingle 2008) with respect to the 300 mm pile diameter and spacing common with those considered in the present study (3D, 4D and 5D) are compared further (Table 3).

**Table 3 Comparison of displacement (in mm) with published literature**

Particulars	Present study			Chore and Ingle (2008)		
	3D	4D	5D	3D	4D	5D
G2PS	121	114	106	95.57	90.78	86.89
	126	121	116	88.90	84.67	81.56

It is seen from Table 3 that the trend of reduction in displacement with increase in pile spacing is similar in the present investigation as well as reported in the present study. However, when the displacements are compared in the context of the configurations, it is observed that in the study reported in the literature, the displacements are on higher side for series arrangement as compared to the parallel arrangement. However, in the present investigation, the displacements are on higher side for parallel arrangement. This could be attributed to the different modeling idealizations as well as the boundaries of the area of mesh for modeling sub-structure components, i. e., and pile foundations. It may be noted that while modeling the pile group, the soil elements were modeled using 20 noded isoparametric continuum element in the study reported by Chore and Ingle, the soil elements are discretised using three different elements, viz. eight, nine and twelve node isoperimetric continuum elements. Further, 16 node isoparametric surface elements introduced at the interface of pile and soil, in the study by Chore and Ingle (2008, in order to ensure proper mechanics of stress transfer between soil and pile under lateral load are also considered in the present study.

As regards the finite element model for the sub-structure, half geometrical models were considered for the group of two piles and three piles in the study reported in the literature (Chore and Ingle 2008) by taking the advantage of the symmetry. However, in the present investigation, full models of the pile groups are considered. Along X and Y directions, the boundary is kept at 14 D (D being the diameter of the pile) from the outermost pile of the pile group in respective direction, as is apparent from Fig. 3 whereas in the study reported in the literature (Chore and Ingle 2008), along X direction, the boundary is kept at 7D and along Y-direction, 5.5D. Moreover, the piles considered in the present investigation are modeled truly as circular whereas the piles considered in the study reported in the literature (Chore and Ingle 2008) were modeled as the square piles, but its effect was taken as that of circular piles inscribed in a square.

These are the reasons which could have resulted in the different trend of displacements with respect to configuration as well as displacements being on higher side in the present study.

**Effect of SSI on Maximum B.M. in Superstructure Columns**

The Effect of soil-structure interaction (SSI) on B.M. at top and bottom of superstructure columns of the specific frame is evaluated. The percentage increase or decrease in moments in columns of the frame is evaluated. The absolute maximum moments in columns obtained in view of SSI and those obtained considering the column bases to be fixed are compared. The absolute maximum positive (sagging) and negative (hogging) moments in columns of the frame obtained considering the effect of SSI are shown in Table 4. The corresponding change in moments with respect to the moments obtained considering fixed column bases is also shown in Table 4.

From the values tabulated in Table3, the effect of SSI is found to increase the maximum positive moment in columns in the range of 14.82-16.18 % with respect to absolute maximum positive moment obtained in view of fixed base condition for group of two piles (series and parallel). Similarly, the effect of soil structure interaction is to increase the absolute negative bending moment in the range of group of two piles is 27.67-28.46%.

**Table 4 Absolute maximum positive and negative B.M. in columns (kN-m) and percentage increase with SSI**

Positive B.M.		% Increase		Negative B.M		% Increase	
3D	6 D	3D	6 D	3D	6 D	3D	6 D
Non-Interactive Analysis							
275.64		-	-	-283.41		-	-
Group of Two Piles (Series Arrangement) [G2PS]							
320.26	316.50	16.18	14.82	-364.08	-361.85	28.46	27.67
Group of Two Piles (Parallel Arrangement) [G2PP]							
320.27	316.52	16.18	14.82	-364.08	-361.86	28.46	27.68

**Comparison with the results in published literature (Chore and Ingle 2008)**

The increase in the absolute maximum positive moments due to SSI is found to be in the range of 14.82-16.18% in the present investigation considering the group of two piles with series as well as parallel arrangement whereas the corresponding increase is reported to be in the range of 14-15% in the published literature. Along similar lines, the increase in the absolute maximum negative moment is observed to be in the range of 27.38- 28.46% in the present study as against 26-27% reported in the published literature. From this, it may be inferred that there is no significant change in the absolute maximum moments in the present study and that reported in the literature.

**Effect of SSI on Maximum B.M. in Superstructure Columns**

Further, percentage increase or decrease in moments at top and bottom of individual columns of the frame due to incorporation of the effect of SSI in the analysis is evaluated. From this, the extent of the effect of SSI on columns placed on left and right hand side of the frame is found. It is obvious that the effect of SSI on moments in superstructure columns is significant when the values of moments are compared on the premise of fixed base approach. The effect of SSI on corresponding percentage increase or decrease in maximum moments of the individual columns in respect of various configurations and for all pile diameters is reported Table 5.

**Table 5 Maximum moment and percentage difference in individual columns**

Column	Fixed Bases	Group of Two Piles (Series)	Group of Two Piles (Parallel)	Column	Fixed Bases	Group of Two Piles (Series)	Group of two piles (Parallel)
C-1(T)	-188.77	-215.74 (14.29%)	-215.68 (14.26%)	C-1 (B)	230.17	143.12 (-37.82%)	143.1 (-37.83%)
C-2 (T)	-206.60	-213.67 (3.42%)	-236.65 (14.55%)	C-2 (B)	242.22	200.5 (-17.22%)	200.5 (-17.22%)
C-4 (T)	-280.51	-345.33 (23.11%)	-345.34 (23.12%)	C-4 (B)	270.12	260.64 (-3.51%)	260.65 (-3.51%)
C-5 (T)	-283.41	-365.67 (29.03%)	-365.68 (29.03%)	C-5 (B)	275.64	323.52 (17.37%)	323.53 (17.37%)
C-7 (T)	-154.03	-206.13 (33.83%)	-206.13 (33.83%)	C-7 (B)	217.54	159.78 (-26.55%)	159.76 (-26.56%)
C-8 (T)	-190.95	-271.59 (42.23%)	-271.61 (42.24%)	C-8 (B)	263.00	236.85 (-9.94%)	236.68 (-10.01%)

The effect of SSI in the columns placed on left hand side appears less and effect of SSI in columns placed on right hand side the effect seems to be more. Further, trend of variation in moments with pile spacing is studied for both the configurations of the pile groups considered in this investigation.

**EFFECT ON VARIATION OF B.M. IN COLUMNS WITH PILE DIAMETER AND SPACING**

The variation of B.M. at top and bottom of few typical columns for spacing in respect the two configurations of the group of two piles considered in the study is described in this section.

In the group with series arrangement of piles therein, hogging moment at top of corner columns (C-1 and C-3) placed on left hand side of the frame decreases on negative side at  $4D$  spacing, increases at  $5D$  spacing and again decreases at higher spacing of  $6D$ . The sagging bending moment at the bottom follows the same trend of variation as observed in case of hogging moment for these columns. For the central column (C-2), hogging moment decreases at the spacing of  $4D$  and thereafter, goes on increasing for next higher pile spacing whereas sagging moment follows the trend of increase, decrease and increase corresponding to the spacing of  $4D$ ,  $5D$  and  $6D$ , respectively. The hogging moment at top of the corner columns (C-4 and C-6) and the column placed in the centre (C-5) placed in the interior row follows the same trend as that seen in case of sagging moment in column C-2, but with the marginal difference in the values of moment at the respective pile spacing. However, at the bottom of the columns C-4 and C-6, exactly opposite trend of variation in moment (i.e., decrease-increase- decrease) as that seen at the top is observed. The sagging moment at bottom of the column C-5 follows the trend increase-decrease-increase of variation at the spacing of  $4D$ ,  $5D$  and  $6D$ , respectively. The trend of variation in hogging and sagging moment as seen case of the columns C-4, C-5 and C-6 is observed in case of the columns C-7, C-8 and C-9.

For the group having parallel arrangement of piles, the trend of variation in bending moment at top and bottom of the columns of the frame remains almost same as that seen in group piles with parallel arrangement, barring few exceptions such as B.M. at top of column C-2, top and bottom of columns C-7 (i.e. C-9) and at the bottom of column C-8. At the top of column C-2, the moment increases at the spacing of  $4D$ , decreases at  $5D$  and again increases at the next higher spacing of  $6D$ . At top of column C-7 (i.e. C-9), the moment increases initially up to the spacing of  $4D$  and then decreases for next two higher spacing considered in the study while at the bottom, decreases at the spacing of  $4D$ , increases at  $5D$  and again decreases at  $6D$ . At the bottom of column C-8, the variation of moment follows the trend of increase- decrease-increase at the spacing of  $4D$ ,  $5D$  and  $6D$ , respectively.

## CONCLUSIONS

Some of the prominent conclusions deduced from the parametric study presented in this paper to bring out the effect of soil- structure interaction on the response of the building frame in the context of the group of two piles with two different arrangements (series and parallel) of piles therein, are indicated below.

1. The effect of soil-structure interaction on top displacement of the frame is quite significant. Displacement is less for the conventional analysis, i.e., fixed base condition and increases in the range of 97% - 230% when the effect of SSI is taken into consideration
2. The displacement at top of frame decreases with increase in pile spacing. The effect of configuration of the pile group is significant on the displacement. The series arrangement offers stiffer behavior than parallel arrangement.
3. It is obvious that the effect of SSI on moments in superstructure columns is significant when the values of moments are compared on the premise of fixed base approach.
4. The effect of SSI is to increase the absolute maximum positive moment in columns in the range of 14.82-16.18 % for the pile group considered in the present study and absolute negative bending moment, 27.67-28.46%.
5. The effect of SSI on columns placed on the left hand side of the frame appears to be less and that on columns placed on the right hand side, more.

## REFERENCES

- Agrawal, R. and Hora, M.S. (2009) Coupled Finite-Infinite Elements Modeling of Building Frame-Soil Interaction System. *Journal of Engineering and Applied Sciences*, **4**, 47-54
- Agrawal, R. and Hora, M.S. (2010) Effect of Differential Settlements on Non-Linear Interaction Behaviour of Plane Frame-Soil System. *Journal of Engineering and Applied Sciences*, **5**, 75-87
- Buragohain, D.N., Raghavan, N. and Chandrasekaran, V.S. (1977) Interaction of Frames with Pile Foundation. *Proc.*

- Int. Symp. Soil-Structure Interaction*, Roorkee, 109-115
- Chameski, C. (1956) Structural Rigidity in Calculating Settlements. *Soil Mechanics and Foundation Engineering*, **82**, 1-9
- Chore, H.S. and Ingle, R.K. (2008) Interaction Analysis of Building Frame Supported on Pile Group. *Indian Geotechnical Journal*, **38**, 483-501
- Chore, H.S. and Ingle, R.K. (2008) Interactive Analysis of Building Frame Supported on Pile Group Using a Simplified F.E. Model. *Journal of Structural Engineering*, **34**, 460-464
- Chore, H.S., Ingle, R.K. and Sawant, V.A. (2009) Building Frame-Pile Foundation-Soil Interactive Analysis. *Interaction and Multiscale Mechanics: An International Journal*, **2**, 397-412
- Chore, H.S., Ingle, R.K. and Sawant, V.A. (2010) Building Frame-Pile Foundation-Soil Interaction Analysis: A Parametric Study. *Interaction and Multiscale Mechanics*, **3**, 55-80
- Dalili, M., Alkarami, A., Noorzai, J., Paknahad, M., Jaafar, M.S. and Huat, B. (2011) Numerical Simulation of Soil-Structure Interaction in Framed and Shear-Wall Structures. *Interaction and Multiscale Mechanics*, **4**, 17-34.
- Deshmukh, A.M. and Karmarkar, S.R. (1991) Interaction of Plane Frames with Soil. *Proc. Indian Geotechnical Conf.*, Surat, 323-326.
- Dasgupta, S., Dutta, S.C. and Bhattacharya, G. (1998) Effect of Soil-Structure Interaction on Building Frames on Iso-lated Footings. *Journal of Structural Engineering*, **26**, 129-134.
- King, G.J.W. and Chandrasekaran, V.S. (1974) Interactive Analysis of a Rafted Multi-Storeyed Space Frame Resting on an Inhomogeneous Clay Stratum. *Proc. Int. Conf. Finite Element Methods*.
- Krishnamoorthy, C.S., Rao, N.B.S. and Rao, N. (2005) Analysis of Group of Piles Subjected to Lateral Loads. *Indian Geotechnical Journal*, **35**, 154-175.
- Krishnamoorthy, C.S. (2010) Finite Element Analysis: Theory and Programming. 2nd Edition, Tata McGraw-Hill Publications, New Delhi.
- Lee, I.K. and Brown, P.T. (1972) Structures and Foundation Interaction Analysis. *Journal of Structural Engineering*, **11**, 2413-2431.
- Mandal, A., Moitra, D. and Dutta, S.C. (1999) Soil-Structure Interaction on Building Frame: A Small Scale Model Study. *Int.Jl. Struct., Roorkee (India)*, **18**, 92-107
- Morris, D. (1966) Interaction of Continuous Frames and Soil Media. *Journal of Structural Engineering*, **5**, 13-43.
- Noorzai, J., Viladkar, M.N. and Godbole, P.N. (1991) Soil-Structure Interaction of Space Frame-Raft-Soil System: Parametric Study. *Computers and Structures*, **40**, 235-241. [http://dx.doi.org/10.1016/0045-949\(91\)90394-2](http://dx.doi.org/10.1016/0045-949(91)90394-2)
- Reddy, R.C. and Rao, G.T.D. (2011) Experimental Study of a Modelled Building Frame Supported by a Pile Group Embedded in Cohesionless Soils. *Interaction and Multiscale Mechanics*, **4**, 321-336
- Rajsekar Swamy, H.M., Krishnamoorthy, A., Prabhakara, D.L. and Bhavikatti, S.S. (2011) Evaluation of the Influence of Interface Elements for Structure-Isolated Footing-Soil Interaction Analysis. *Interaction and Multiscale Mechanics*, **4**, 65-83. <http://dx.doi.org/10.12989/imm.2011.4.1.065>
- Sawant, V.A. and Chore, H.S. (2010) Building Frame-Pile Foundation-Soil Interactive Analysis Using 3-D FEM. *Journal of Structural Engineering (JoSE)*, **36**, 318-325
- Srinivasraghavan, R. and Sankaran, K.S. (1981) Settlement Analysis for Combined Effect of Superstructure-Footings-Soil System. *Journal of the Institution of Engineers (India)*, **6**, 194-198.
- Srivastava, V., Chore, H.S. and Dode, P.A. (2016) Interaction of Building Frame with Pile Foundation. *Open Journal of Civil Engineering*, **6**, 105-202. <http://dx.doi.org/10.4236/ojce.2016.62018>
- Subbarao, K.S., Shrada Bai, H. and Raghunatham, B.V. (1985) Interaction Analysis of Frames with Beam Footing. *Proc. Indian Geotech. Conf.*, Roorkee, 389-395.
- Thangaraj, D.D. and Illampurthy, K. (2010) Parametric Study on the Performance of Raft Foundation with Interaction of Frame. *Electronic Journal of Geotechnical Engineering*, **15**, 861-878.
- Thangaraj, D.D. and Illampurthy, K. (2012) Numerical Analysis of Soil-Mat Foundation of Space Frame System. *Interaction and Multiscale Mechanics*, **5**, 267-284. <http://dx.doi.org/10.12989/imm.2012.5.3.267>



## Effect of Dynamic Soil-Structure Interaction Analysis on Displacement of Building Frame Resting Raft Foundation

D.R. Suroshe<sup>1</sup>, H.S.Chore<sup>2</sup> and V.A. Sawant<sup>3</sup>

<sup>1</sup>Research Scholar, Dept. of Civil Engineering, DattaMeghe College of Engineering, Sector-3, Airoli, Navi Mumbai-400708,  
Email: drsuroshe@yahoo.co.in

<sup>2</sup>Associate Professor, Dept. of Civil Engineering, Dr. B. R. Ambedkar National Institute of Technology, Jalandhar – 144011,  
Email: chorehs@nitj.ac.in, Corresponding Author

<sup>3</sup>Associate Professor, Dept. of Civil Engineering, Indian Institute of Technology Roorkee, Roorkee-247667,  
Email: sawntfce@iitr.ac.in

### ABSTRACT

The available literature reports many interaction analyses of the framed structures in order to quantify the effect of soil- structure interaction on the response of the structure in the context of static as well as dynamic loading. Most of the structures are resting on either isolated footings or combined footings or mat foundations. However, there has been relatively lesser studies on the interaction analysis of building frame supported on raft foundation in respect of dynamic loading. The proposed paper presents the dynamic analysis of building frame supported on raft and brings out the effect of SSI on the response of the structure. Three dimensional finite element analysis is adopted. Three storeyed building frame resting on raft comprising of different thicknesses is considered in the present investigation. The components of the building frame such as beams, columns and slabs are modeled using 20 nodedisoparametric continuum elements. Further, the components of the superstructure and substructure including soil are treated to behave in the linear elastic manner. The soil surrounding the foundation is modelled with 8 node element. The interface of soil and raft has been accounted for by incorporating 16 node interface elements in the modeling. The result indicates that the dynamic loading and SSI has considerable effect on the response of the structure includes displacement at each storey level. The effect of the soil- structure interaction is observed to be significant for the raft foundations and soil considered in the present study.

**KEYWORDS:** Building Frame;raft foundation; transmitting boundary; Degradation technique.

### INTRODUCTION

The framed structures are normally analyzed considering their bases to be either completely rigid or hinged. However, the foundation resting on deformable soil also undergoes deformation depending on the relative rigidities of the foundation, the superstructure and soil. Interactive analysis is, therefore, necessary for the correct assessment of the response of the superstructure resulting into the realistic analysis. Many interactive analyses in the context of static loading have been reported in the literature. While majority of these analyses report either interaction of frames with isolated footings or the interaction of frame with raft foundation, few of them report interaction of frame with combined footings. Ingle and Chore 2007;reviewed the various analysis of the interaction of building frames with foundation accounting the interaction of building frames with foundation accounting for soil-structure interaction (SSI) available in the literature and pointed out hardly any work, except that by Buragohain et al1981; have been done on the interaction analysis of framed structures resting on pile foundation and underscored the necessity of the interaction analysis for such system using realistic assumptions and rational approach and further reported few such analyses either using simplified approach or complete 3-D analysis. Apart from many interaction analyses in evolving building frames- foundation interaction in the context of static loading, persual of the literature indicates many SSI analyses in the context of the dynamic loading which are reviewed briefly in the sub-sequent sections.

### REVIEW OF LITERATURE

Jennings and Bielek1973; studied the dynamics of building-soil interaction wherein soil was modeled by a linear elastic half space and building structure by n- degree of freedom oscillator for examining earthquake response and steady state

response under sinusoidal excitation. Vaish and Chopra 1974; proposed to analyze the sub-structure approach for analyzing the complex structure-foundation systems wherein foundation was first analyzed independently and dynamic compliance characteristics so obtained was incorporated into structural equations of motion. Luco et al 1974; presented an approximate numerical procedure for evaluating the vertical, rocking and the corresponding function obtained for elastic half space. Luco and Hadjian 1974; studied the feasibility of representing a 3-D SSI problem by plain strain model and errors involved in such representation Novak 1978; evaluated effect of piles on dynamic response of footings and Structures and underscored the importance of damping in the dynamic analysis aimed at quantifying the effect of SSI.

Chandrasekaran and Pankaj 1981; studied the dynamic behaviour of the framed buildings considering foundation interaction by considering 2-D structural system by considering the system as plain strain FE problem and treating the soil as linearly elastic. Citing computational difficulties in understanding the phenomenon of dynamic response of massive structures such as nuclear power plant building and offshore gravity towers, Gupta et al 1982; discussed the merits and demerits of various approaches available and proposed a three dimensional hybrid model incorporating good features of the various approaches and eliminating undesirable approaches.

Damping has a significant effect on the structural response to wind, earthquake and other dynamic loads. SSI contributes to the damping that ranges negligible for elastic structures on rigid foundation. Novak and Hifnawy 1983; tried to consider the aspect of soil damping in a rational manner and evaluated effects of SSI on damping of structures using simple but approximate energy consideration and complex eigen value analysis. Pais et al 1989; suggested two types of effects namely, kinematic interaction and inertial interaction while accounting for SSI. Ingle 1994; emphasized the need for the appropriate modeling techniques and methods for the analysis of building structures subjected to earthquake. Different building configurations were considered with different beam stiffness and analyses were carried out using seismic coefficient and response spectrum methods. Wu and Smith 1995; presented an efficient methodology which used modal analysis implemented in the frequency domain to obtain the structural response of a system with SSI.

Nogami 1996; developed a simplified mechanical model for the 3-D dynamic SSI analysis of surface foundation. The model comprising of 1-D vertical beams with distributed mass and horizontal spring was found capable of reproducing the 3-D SSI behaviour.

Markis et al 1996; examined the problem of dynamic soil- pile foundation- structure interaction and proposed a simple rational dynamic procedure for analyzing the dynamic response of a bridge structure supported on pile group, but at the same time pointed out that for the realistic results, non-linear analysis should be resorted to although the work reported linear analysis. Kulkarni et al 1997; reported modeling of building structures by considering symmetric and unsymmetric building configurations wherein analysis was attempted by various ways of modeling the structure and further, an eigen value analysis was also reported. Kumar and Praksh 1997; carried out a comprehensive parametric study using a simplified model in incorporating SSI. Effect of SSI was found to be significant on the fundamental natural frequencies of the system; but quite negligible on natural frequencies in higher modes for similar foundation characteristics. Aviles and Preez-Rocha 1998; reported numerical solution for evaluating the effects of foundation embedment on the effective period and the damping and the response of soil-structure systems.

Citing two possible mechanisms of interaction, as inertial and kinematic, that could take place between the structure, foundation and soil, Stewart et al 1999; described analysis procedure and system identification techniques for evaluating inertial SSI effects on seismic structural response. The procedure so developed was implemented with reference to earthquake data pertaining to 1994 Northridge earthquake. The analysis procedure predicted the observed SSI effects accurately. Curras et al 2001; reported experimental and analytical study for pile group supported structure. Experimental data on the seismic response of a pile group supported structure was obtained through dynamic centrifuge model tests and then used to evaluate a dynamic beam on a non-linear Winkler model foundation analysis. Wu et al 2001; brought out the effect of torsional coupling on the dynamic response of the structure and found the combined effect on SSI and torsional coupling to have a significant effect on the response of the structure interaction accounting the aspect of radiation damping. Roy and Dutta 2001; investigated the effect of SSI on dynamic behaviour of building frames on grid foundation by incorporating the aspect of infill brick wall.

The above review of literature also highlights little work having been done on building frame-pile foundation

interaction in the context of dynamic loading. In view of this, it is proposed to present the interaction analysis of a simple single storeyed space frame having two bays supported on pile group incorporating soil-structure interaction to examine the dynamic behaviour of the system. For attempting more rational analysis on the basis of realistic assumptions, pile cap has been assumed to be flexible and its stiffness has been considered. Stiffness matrix for the foundation has been derived at a time by considering the effect of all piles in a group. On this basis, analysis of the building frame supported on pile group embedded in soft marine clay has been attempted by using 3-D FEM. The effect of various foundation parameters like configuration of the pile group, spacing and number of piles along with the pile diameter is evaluated on the response of the frame. The analysis also takes into account the interaction between pile cap and soil.

**PROBLEM DESCRIPTION**

A 3-D three storeyed building frame resting on raft foundation with different thicknesses is considered for the study. The frame, 3 m high is 10 m × 10 m in plan with each bay being, 5m × 5m. The slab, 200 mm thick, is provided at top as well as at the floor level. The slab at the top of the first, second and third storey is supported over 300 mm wide and 400 mm deep beams. The beams are resting on columns of size 300 mm × 300 mm. The raft embedded in soft marine clay, a cohesive type of soil mass is considered for the present study. While the dead load is considered according to the unit weight of the materials of which the structural components of frame are made up of, for the purpose of the parametric study presented here. The soil properties, interface element and properties of raft are given in Table 1. Fig. 1 shows the half geometrical model of building frame with fixed column base and group of four piles.

**Table 1. Raft and soil properties for parametric study**

Soil properties	
Modulus of Elasticity, $E_s$	20000 kPa
Poisson's ratio, $\mu_s$	0.4
Density, $\gamma_s$	18 kN/m <sup>3</sup>
Yield stress, $\sigma_v$	100 kPa
Interface element	
Normal stiffness, $K_n$	$1.0 \times 10^6$ kN/m <sup>3</sup>
Tangential stiffness, $K_s$	1000 kN/m <sup>3</sup>
Raft properties	
Modulus of Elasticity, $E_p$	25 GPa
Poisson's ratio, $\mu_p$	0.2
Density, $\gamma_p$	25 kN/m <sup>3</sup>
Thickness	0.5m

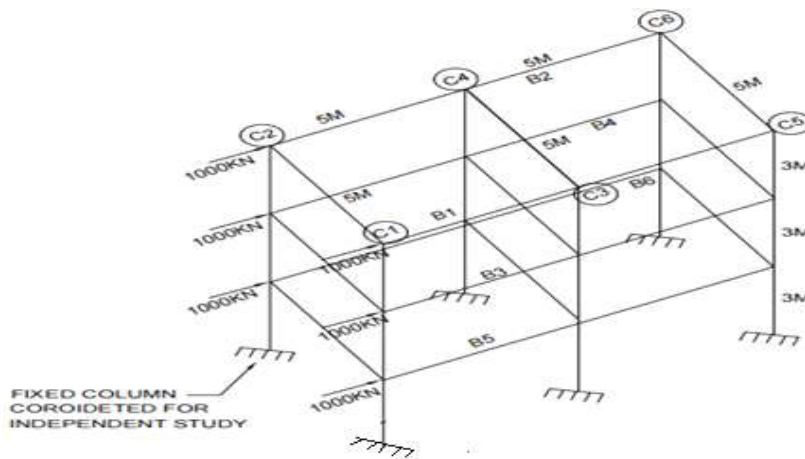


**Fig. 1 Typical building frame with fixed base considered for non-interactive analysis.**

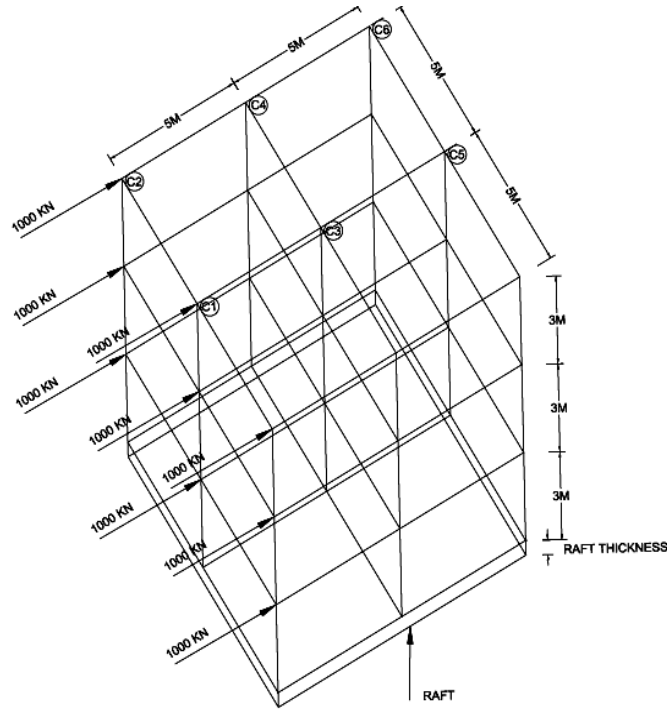


Fig. 2: Typical building frame with raft considered in the present study

## MODELING AND ANALYSIS METHODOLOGY

### *Building Frame on raft foundation*

The complete three dimensional finite element analysis is carried out. A parametric study is carried out to examine the effect of raft thickness and the soil modulus on the response of building frame. The soil behaviour is considered linear. That will define the relation between soil reaction ( $p$ ) and transverse displacement ( $w$ ) through modulus of subgrade reaction  $k_s$ . As  $p = k_s w$ . In the second approach, the relation between soil reaction ( $p$ ) and transverse displacement ( $w$ ) is expressed through an hyperbolic relationship.

$$p = \frac{k_{\max} w}{1 + \frac{k_{\max} w}{p_u}}$$

In which,  $k_{\max}$  is initial tangent modulus and  $p_u$  is the ultimate soil resistance.

## F. E. FORMULATION

Soil is considered as linear-elastic-perfectly-plastic material. The mesh size selected for a finite element solution can be optimized for both, accuracy and computational economy based on analyses of several meshes with different numbers of elements and mesh sizes.

### *Continuum Element*

Relation between strains and nodal displacements is expressed as,

$$\{\varepsilon\}_e = [B] \{\delta\}_e$$

where,  $\{\varepsilon\}_e$  is strain vector,

$\{\delta\}_e$  is vector of nodal displacements, and

[B] is strain displacement transformation matrix. The stress-strain relation is given by,

$$\{\sigma\}_e = [D] \{\varepsilon\}_e$$

where,  $\{\sigma\}_e$  is stress vector, and  $[D]$  is constitutive relation matrix.

The stiffness matrix of an element is given as expressed as,

$$[K]_e = \int_V [B]^T [D] [B] dv$$

### **Interface Element**

Relative displacements (strains) between the surface of soil and structure induce stresses in the interface element. These relative displacements are given as

$$\{\varepsilon\}_e = [B]_f \{\delta\}_e$$

where,  $[B]_f$  represents the strain displacement transformation matrix.

The element stiffness is obtained by the usual expression,

$$[K]_e = \int_S [B]_f^T [D]_f [B]_f ds$$

where,  $[D]_f$  is the constitutive relation matrix for the interface.

### **Equivalent Nodal Force Vector**

The lateral force  $F_H$ , acting on raft thickness, is considered as uniformly distributed force over the raft.

The intensity of this uniformly distributed force is,

$$q = F_H / A,$$

where,  $A$  is the area of raft. Equivalent nodal force vector,  $\{Q\}_e$ , is then expressed as,

$$\{Q\}_e = \int_A q [N]^T dA$$

where,  $[N]$  represents matrix of shape functions [8].

### **Constitutive Model**

The soil is replaced by an idealized material which behaves elastically up to some state of stress at which slip or yielding occurs and beyond yielding, the theory of plasticity is implemented to account for the constitutive law of the soil. The constitutive relationships arising from the theory of plasticity are incremental in nature due to the stress path dependence of the material behaviour. The essential features of the plasticity theory are:

- i) A yield function, separating the elastic and plastic states of stresses in the body under consideration. By means of a yield function, it is possible to decide whether plastic deformation takes place or indeed, is possible.
- ii) A plastic potential function defining the direction of plastic straining when yielding occurs (flow rule).
- iii) A hardening/softening law describing the dependence of the yield functions on the plastic strains.
- iv) Some assumed elastic behaviour within the yield surface.

### **Yield criterion**

The Yield criterion used in present study is explained here.

(i) *von Mises yield criterion*

$$\sqrt{3} (J_2')^{1/2} = K$$

where,  $\alpha$  and  $K$  are material constants, which may be related to Coulomb's material constants  $c$  and  $\phi$ .

### **Constitutive matrix**

The elasto-plastic  $[D]_{ep}$  matrix is expressed as:

$$[D]_{ep} = \left[ [D] - \frac{[D] \left\{ \frac{\partial Q}{\partial \sigma} \right\} \left\{ \frac{\partial F}{\partial \sigma} \right\}^T [D]}{\{A\} + \left\{ \frac{\partial F}{\partial \sigma} \right\}^T [D] \left\{ \frac{\partial F}{\partial \sigma} \right\}} \right]$$

where

F and Q = the yield and plastic potential functions, [D] = elasticity matrix,

F = Q (Associative flow rule) and A = hardening parameter.

Above Equation can be written as:

$$[D]_{ep} = \left[ [D] - \frac{[D] \{a\} \{a\}^T [D]}{\{A\} + \{a\}^T [D] \{a\}} \right]$$

where {a} is the plastic flow vector given by:

$$\{a\}^T = \left\{ \frac{\partial F}{\partial \sigma_x}, \frac{\partial F}{\partial \sigma_y}, \frac{\partial F}{\partial \sigma_z}, \frac{\partial F}{\partial \tau_{xy}}, \frac{\partial F}{\partial \tau_{yz}}, \frac{\partial F}{\partial \tau_{zx}} \right\}^T$$

### Non-linear analysis

Incremental analysis is carried out on raft foundation in which elasto-plastic constitutive matrix  $D_{ep}$  is calculated assuming von Mises yield criteria at each increment. In the present study *von Mises* yield criterion is considered.

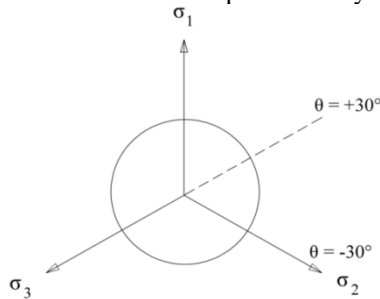


Fig. 3: Representation of *von Mises* yield criteria in deviatoric plane

Fig. 3 shows the Graphical representation of *von Mises* yield criteria in deviatoric plane. When plotted in principal stress space it appears as circular cylinder whose central axis coincides with space diagonal. *von-Mises* yield function is approximation to the Tresca yield function and expressed in terms of  $J_2$  and material constant  $K$  as,

$$\sqrt{3}(J_2)^{1/2} = K$$

The total load is applied in the ten equal increments and the stiffness matrix, [K] is kept constant for all the load increments. Following is the algorithm used for nonlinear analysis:

- i) Apply incremental load  $\Delta F$  and solve for incremental displacement,  $\Delta u$

$$\{\Delta F\} = [K] \cdot \{\Delta u\}$$

Update the total displacements by adding incremental displacement  $\Delta u$  in

$$u_i = u_{i-1} + \Delta u$$

$u_i$  = displacement for  $i^{\text{th}}$  increment

- ii) Set  $m_e = 0$ , where  $m_e$  indicates number of yielded elements.

- iii) For each element, set  $m_p = 0$  (number of yielded points within the given element), obtain the element incremental displacement vector  $\{\Delta \delta\}^e$  from global incremental displacement vector,  $\Delta u$ .

- iv) For each Gauss point, compute the incremental stress  $\{\Delta \sigma\}^e$  and total stress  $\{\sigma_{Ti}\}^e$  for  $i^{\text{th}}$  increment from following relations:

$$\{\Delta \sigma\}^e = [D] \cdot [B] \cdot \{\Delta \delta\}^e$$

$$\{\sigma_{Ti}\}^e = \{\sigma_{Ti-1}\}^e + \{\Delta \sigma\}^e$$

Check for yield, if the point have not yielded then go to next Gauss point, else, set  $m_p = m_p + 1$ , and calculate extra stress over yield stress,  $\{\Delta\sigma\}_{ext}$

$$\{\Delta\sigma\}_{ext} = [D - D_{ep}] \cdot \{\Delta\varepsilon\}^e$$

Set total stress at yield level

$$\{\sigma_{Ti}\}^e = \{\sigma_{Ti}\}^e - \{\Delta\sigma\}_{ext}$$

Update the additional force vector to be applied in next iteration

$$\{\Delta F\}^e = \iiint_V [B]^T \cdot \{\Delta\sigma\}_{ext} dV$$

Complete loop over the Gauss points of the element

- v) If  $m_p > 0$ , then assemble load vector  $\{\Delta F\}^e$  and set  $m_e = m_e + 1$ .
- vi) Repeat Step (iv) to (vi) for all the elements.
- vii) If  $m_e = 0$ , then not a single element have yielded, go to next load level.
- viii) If  $m_e > 0$ , then check for convergence using following displacement criteria,

$$e_d = \left( \sqrt{\sum(q_i)^2} - \sqrt{\sum(q_{i-1})^2} \right) / \sqrt{\sum(q_i)^2}$$

where,  $e_d$  = displacement norm,  $q_i$  = total displacement at the  $i^{\text{th}}$  iteration and  $u_{i-1}$  = total displacement at the  $i-1^{\text{th}}$  iteration.

If the convergence criterion is satisfied, then apply next load increment. If a convergence criterion is not satisfied then repeat the procedure from step (i) to step (ix), till the displacements are converged.

## RESULTS AND DISCUSSION

For the interaction analysis, a software program Build-Frame is developed using *FORTRAN 90*. After assessing the accuracy of the program in the context of simple problems of structural engineering and soil- structure interaction and further, implementing it on the published work, the said program is used in the present study. In the parametric study conducted for the specific frame presented here, the response of the superstructure considered for the purpose of comparison includes the horizontal displacement at the top of the frame corresponding to each storey. The response is evaluated initially for two conditions- without considering the effect of SSI and another by considering it. Hence, two analyses are reported, non- interactive analysis (NIA) and the interactive analysis (IA).

The values of the horizontal displacement obtained in respect of the non-interactive analysis at each storey level of the frame for the various raft thicknesses considered in the study are shown in Table 2. The corresponding percentage increase in displacement due to consideration of SSI (interactive) for different raft thicknesses keeping constant soil modulus ( $E_s=20000\text{kPa}$ ), considered in the present study is also indicated in the afore-mentioned table. Similarly, the variation in the storey displacement with storey height in respect of different raft thicknesses considered in the present investigations is shown in Fig. 3.

**Table.2. Storey displacement for various raft thicknesses ( $E_s=20000\text{kPa}$ )**

Storey height (m)	Fixed Base	Raft thk = 0.25m	% variation	Raft thk = 0.5m	% variation	Raft thk = 0.75m	% variation
9	0.363	1.09	282.43	1.37	276.85	1.52	317.59
6	0.294	1.32	200.42	1.52	416.07	1.73	484.94
3	0.162	0.35	116.56	0.65	298.63	0.70	332.23
Storey height (m)	Fixed Base	Raft thk = 1.0m	% variation	Raft thk = 1.25m	% variation	Raft thk = 1.5m	% variation
9	0.363	1.66	355.73	1.80	394.64	1.98	444.58
6	0.294	1.90	543.27	1.91	548.25	1.97	567.79
3	0.162	0.89	447.47	1.00	513.79	1.05	544.31

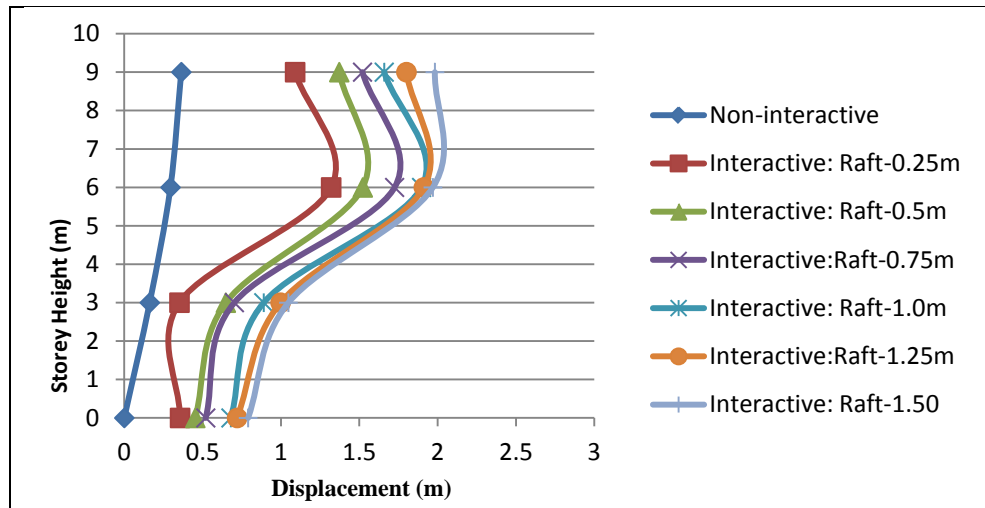


Fig. 4 Variation in storey displacement in respect of various raft thicknesses

The general trend observed for all the raft thicknesses considered in present investigation is that horizontal displacement at each storey level increases due to the effect of soil structure interaction (SSI). It is seen that, with increase in raft thickness the percentage displacement increases. For raft of thickness 0.25 m the percentage variation is found to be in the range of 116.56 – 282.43% from bottom to top storey. Similarly, for the raft of thickness 0.5, 0.75, 1.0, 1.25 and 1.5m the percentage variation is observed to be in the range of 276.85 – 298.63%, 317.58 – 484.94%, 355.73 – 453.27%, 394.64 – 548.25% and 444.58 – 567.79% respectively. Further it is observed that the variation in the storey displacement at the first storey increases with increase in raft thickness, but in case of raft of thickness 0.25m and 0.5m it goes on decreasing. As regards the percentage variation in the storey displacement after raft of thickness 0.75m to 1.5m it found to increase in the displacement.

## CONCLUSIONS

Some of the broad conclusions emerging from the interaction analysis reported in the present investigations are given below.

- The effect of soil-structure interaction (SSI) is significant on the storey displacement.
- The SSI is found to increase the displacement at top storey in the range of 282.43-444.58%.
- The displacement at each storey level increases with increase in raft thickness.
- The increase in displacement due to consideration of SSI is more at middle storey and, the displacement goes on decreasing for bottom and top storey.

## REFERENCES

- Aviles, J. and Perez-Rocha, L. E.1998 “Effects of foundation embedment during building soil interaction”, *Jl.of earthquake Engg.and Struct.Dyns*.Vol.27,Pp 1523-1540.
- Buragohain, D. N., Raghavan, N. and Chandrasekaran, V. S.1981, “Interaction of frames with pole foundation”, *Proces. Of Intern. Symposium on Soil-Structure Interaction, Roorkee*, pp 109-115.
- Chandrasekaran, A. R. and Pankaj.1981, “Dynamic behavior of framed buildings considering foundation interaction”, *Proc. VIIth Symposium on Earthquake Engg., Roorkee*, Vol. I, pp167-172.
- Curras, C. J., Ross, W. B., Kutter, B.L. and Wilson, D. W.,2001 “Dynamic Experiments and analysis of a pile group supported structures”, *Jl. Of Geot. And GeoenvironmentalEngg., ASCE*, Vol. 127,No. 7, pp 585-596.
- Gupta, S., Penzein, J., Lin, T. W. and Yeh, C. S.,1985 “Three dimensional hybrid modeling of soil-structure interaction”, *Jl. Of Earthquake Engg. And Struct. Dyn.*, Vol. 10, pp 69-87.
- Ingle, R. K.1994, “Earthquakek analysis of buildings structures: a comparative study”, *Proc. Tenth Symposium on earthquake Engg., Roorkee*, 1994, pp 435-444.

- Ingle, R.K. and Chore, H.S. 2007. "Soil-structure interaction analysis of building frames: an overview", *Jl. of struct. Engg., Structural Engineering Research Centre, Chennai*, 34(5), 360-368.
- Jennings, P.C. and Bielek, J.1973, "Dynamics of buildingsoil interaction", *Bulletin of Seismolical Society of America*, Vol. 63, No. 1, pp 9-48.
- Kulkarni, S. S., Ingle, R. K. and Chandrikapure, S. P.1997, "Investigation into modeling of building structures", *Proc. Of the Struct. Engg. Convection*.
- Kumar, S. and Prakash, S.1997, "Natural frequency response of structures considering soil-structure interaction", *Proc. Seismic Behaviour of Ground and Geot. Struct.*, pp. 225-233.
- Luco, J. E. and Hadjian, A. H.1974, "Two dimensional approximations to the three dimensional soil-structure interaction problem", *Jl. Of NuclearEngg. And Design*, Vol. 31,pp 195-203.
- Luco, J. E., Hadjian, A H. and Boss, H. D.1974, "The dynamic modeling of half plane by finite elements" *Jl. Of Nuclear Engg. and Design*, Vol. 31, pp 184-194.
- Markis, N., Gazetas, G. and Delis, E.1996, "Dynamic soil-pile-foundation structure interaction: records and predictions", *Geotechnique*, Vol. I, pp 33-50.
- Nogami, T.1996, "Simplified subgrade model for three dimensional soil-foundation interaction analysis", *Soil Dyns. And Earthquake Engg.*, Vol. 15,pp 419-429.
- Novak, M. and Hifnawy El, L.1983, "Effect of soil interaction on damping of structures", *Jl. Of EarhquakeEngg. And Struct. Dyns.*, Vol. 11, pp 595-621.
- Novak, M.1978, "Effects of piles on dynamic response of footings and structures", *Proc. Dyn. Meth. For soil and Rock Mech.* , Rotterdam, Vol. I, pp 185-200.
- Pais, A. L. and Kausel, E.1989, "On rigid foundations subjected to seismic waves", *Jl. Of earthquake Engg. And struct. Dyn.* , Vol. 18,pp 475-489.
- Roy, R. and Dutta, S. C.2001, "Effect of soil structure interaction on dynamic behavior of building frames on grid foundation", *Proc. Of Struct. Engg. Convection (ACC)*, Roorkee, 2001, pp 694-703.
- Stewart, J. P., Genves, G. L. and Seed, R. B.1999, "Seismic soil-structure interaction in buildings- II: empirical findings", *Jl. Of Geot. And Geological Engg., ASCE.*, Vol. 125, No. 1, pp 26-27.
- Vaish, A. K. and Chopra, A. K.1974, "Earthquake finite element analysis of structure-foundation system", *Jl. Of Engg. Mech. Div., ASCE*. Vol. 100, No. EM-6, pp 184-194.
- Wolf, J. P. and Song, C.2002, "Some cornerstones of dynamic soil-structure interaction", *Jl. Engg. And Struct.*, Vol. 24, pp 13-28.
- Wu, W. H. and Smith, A. H.1995, "Efficient modal analysis for structures with soil-structure interaction", *Jl. Of earthquake Engg. And struct Dyn.*, Vol. 24, 1995, pp 283-299.
- Wu, W. H., Wang, J. F. and Lin, Chi-chang.2001, "Sys-tematic assessment of irregular building- soil interaction using efficient modal analysis", *Jl. Of Earthquake Engg. And Struct. Dyns.*, Vol. 30, pp 573-594.



## TO STUDY THE EFFECT OF BY-PRODUCTS OF INDUSTRIAL WASTE ON CONSTRUCTION INDUSTRY

Manjesh Srivastava<sup>1</sup>, Kuldeep Sharma<sup>2</sup>, Vikas Kumar<sup>3</sup> and Sunayana<sup>4</sup>

<sup>1</sup>M.M.M.U.T., Gorakhpur, e-mail: manjesh.srivastava396@gmail.com

<sup>2</sup>Dr.B.R.Ambedkar NIT, Jalandhar, e-mail: kuldeepsha333@gmail.com

<sup>3</sup>M.M.M.U.T., Gorakhpur, e-mail: vikaskumarnitk@gmail.com. Corresponding Author

<sup>4</sup>CSIR-NEERI, Mumbai Zonal Centre, e-mail: nayanahbti@gmail.com

### ABSTRACT

Sustainable infrastructure development includes the, building construction, transportation facilities, sustainable foundation, sewage and water supply facilities and environmental solution. Waste materials are the main source for environmental pollution so to overcome from this problem and considering the cost of construction, the uses of waste materials for new products and use in construction industry is increasing day by day. The industrial waste is the major problem for the sustainable infrastructure as they have adverse effect on land and water. This paper investigates the recycled waste materials and presents a critical review on properties and compressive strength of some of the building materials. The main objective of this study is to find out that which type of recycled and waste materials are currently used in the construction industry according to their compressive strength. Fly ashes (FA), Granulated Blast Furnace Slag (GBFS), Municipal Solid Waste (MSW), Metakaolin (MK), and Wood Ash (WA) are the common type of wastes which are generate from industries. It was observed from the study that FA is replaced by fine aggregate with 5 different percentages of its volume; GBFS replaced the cement with 40-65 % of its volume. It was observed that up to an addition of 5% MSW there will be no major effect was observed in the strength of concrete but there will be a significant contribution in strength take place when it is replaced by 15-20 %. MK is used in between 30 to 40% for remove all the cement hydration in Meta kaolin Pozzolana Cement paste .WA is used at level of 5-15% of its volume.

**KEYWORDS:** *Waste Materials, Sustainable Structure, Environmental Concerns, Natural Resources*

### INTRODUCTION

For any construction activity materials like concrete, steel, brick, stone, clay, wood etc. is required. So for the concrete mixture these are the main construction materials which are used in construction industries. During the designing of concrete structure durability is one of the most important properties which have to be considered. For achieving high strength, low permeability and durability it is compulsory to reduce the porosity of cement paste by adding some amount of admixture. Actually waste incinerators generate more CO<sub>2</sub>, oil or natural gas so for environmental concerns from several years' scientists and researchers searching a solution to overcome from this problems. Recycled waste material is a promising material in the construction industry due to its lightweight, elasticity, energy absorption, sound and heat insulating properties.

**This paper discusses the utilisation of different waste in construction industry. Also a comparative study has been done for compressive strength of concrete mix on the basis of replacement of cement by different waste materials.**

There are different types of industrial waste materials but most common type of waste materials with different properties and its advantages are as follows:

#### 1. Coal Fly Ash (CFA) :

CFA is the by product which is obtained by the combustion of pulverized coal, from thermal power plant as shown in figure 1. Main constituents used in CFA are Si, Al, Fe and CaO which are generally used in cement for the manufacturing of concrete mixture due to its fineness and pozzolanic material. Table 1 and Table 2 define the physical and chemical properties of CFA.



Fig. 1 Fly Ash and OPC

**Properties of Coal Fly Ash**

**Table 1. Physical properties**

Property	Range
$G_{FA}$ (Specific Gravity)	2.14 – 2.69
$M_c$ (Moisture Content %)	0.38
fineness ( $cm^2/gm$ )	1579 – 5550

**Table 2. Chemical Properties**

Constituents	Range
Silicon Dioxide	30.92 – 62.76
Aluminium Oxide	12.30 - 26.95
Iron Oxide	2.84 – 24.43
Calcium Oxide	1.10 – 30.53
Magnesium Oxide	0.69 – 6.69
Sulphur Trioxide	0.31- 3.85

**Advantages of Coal fly Ash (CFA):**

- In road way construction as sub base and base courses.
- In manufacturing of cement as raw materials.
- As an admixture in blended cement.
- In Soil Stabilization

**2. Granulated Blast Furnace Slag (GBFS):**

Hogan and Meusel et al. (1981) observed that when lime, iron and coke heated at the temperature of 1500°C and melt in blast furnace, molten iron and molten slag are obtained. For granulating the slag process involves to cool the molten slag with high water pressure through water jets. The granulated slag is further processed by drying and then ground to a very fine powder, which is GBFS as shown in figure 2. Table 3 and 4 defines the physical and chemical properties of GBFS.

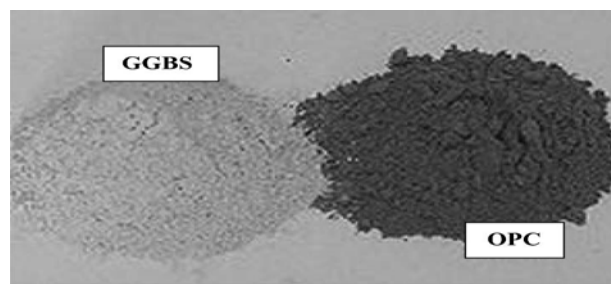


Fig. 2 Granulated Blast Furnace Slag (GBFS)

**Properties of GBFS:**

**Table 3. Physical Properties**

Property	Value
$G_{GBFS}$ (Specific Gravity)	2.9
$\gamma_b$ (Bulk Density)	1200 ( $kg/m^3$ )

**Table 4. Chemical Properties**

Constituents	Range
Silicon Dioxide	35.34
Aluminium Oxide	11.59
Iron Oxide	0.35
Calcium Oxide	42
Magnesium Oxide	8.04
Sulphur Dioxide	1.18

**Advantages of Using GBFS in cement and concrete:**

- For concrete placement it improves its workability and durability.
- Reduced permeability and more chemically stable.
- Improved surface finish.
- Reduce maintenance and repairing costs.

**3. Municipal Solid Waste Ash (MSW) :**

Lin et al. (2002) observed that MSW is obtained by the combustion of the by product of MSW as shown in figure 3. For this incineration is the only method for controlling the production of MSW. Refuse Derived Fuel (RDF) and Mass Burning Process are commonly used for the incineration of MSW. Table 5 and 6 defines the physical and chemical properties of MSW.



Fig. 3 Municipal solid waste Ash (MSW)

**Properties of MSW Ash**

**Table 5. Physical properties**

Property	Range
Bulk Density	1425 kg/m <sup>3</sup>
Specific Gravity	2.44
Moisture Content	24.71 %

**Table 6. Chemical properties**

Constituent	Range
Silica	13.8-20.5
Calcium	5.38-8.03
Iron	2.88-7.85
Magnesium	0.90-1.84
Potassium	0.84-1.15
Aluminium	3.26-5.44
Sodium	2.00-4.62

**Advantages of MSW Ash**

- In cement manufacturing.
- For concrete mixing
- In glass and Glass-Ceramics.
- In Road Pavement.
- In Embankment.

**4. Metakaolin (MK) :**

According to Wild et al. (1996) MK is a pozzolanic material which is obtained from kaolinitic clay by the process of calcination at 500° C and 800° C. Kaolin is a fine, white, clay mineral the most common constituents of kaolin is hydrated aluminum disilicate as shown in figure 4. Table 7 and 8 defines the physical and chemical properties of MK.



Fig. 4 Meta kaolin

**Properties of Metakaolin**

**Table 7. Physical Properties**

Property	Value
Specific Gravity	2.60
Bulk Density	0.3 – 0.4 (g/cm <sup>3</sup> )
Colour	White

**Table 8. Chemical Properties**

Constituents	Percentage (%)
Silicon Dioxide	51.52
Aluminium Oxide	40.18
Iron Oxide	1.23
Calcium Oxide	2.0
Magnesium Oxide	0.12

**Advantages of Using Metakaolin in cement and concrete:**

- Increased durability and chemical attack against resistance.
- Because of particle packing it's reduce shrinkage.
- Reduced permeability and efflorescence.

**5. Wood Ash (WA) :**

According to Etiegni and Campbell (1991) WA is obtained due to the combustion of wood and wood products i.e. chips saw dust, bark, etc. residual remains after the combustion of wood may be organic and inorganic as shown in figure 5. Hardwoods usually produce more ash than softwoods and the bark and leaves generally produce more ash than the inner woody parts of the tree. Table 9 and 10 defines the physical and chemical properties of WA.



Fig. 5 Wood Ash (WA)

**Properties of Wood Ash**

**Table 9. Physical Properties**

Parameter	Ash	Sludge
Moisture content (%)	38	83.4
pH	8.82	7.98
Carbon	280	6.64

**Table 10. Chemical Properties**

Constituents	Percentage (%)
Silicon Dioxide	31.8
Aluminium Oxide	28
Iron Oxide	2.34
Calcium Oxide	10.53
Magnesium Oxide	9.32
Potassium oxide	10.38
Sodium Oxide	6.5

**Advantages of Using Wood Ash**

- Etiegni and Campbell (1991) discuss the application of WA in the agriculture soil.
- NCASI use WA for the treatment of hazardous waste.
- Etiegni (1990) reported that WWA can be used as a feedstock in the manufacture of OPC.

**RESULTS AND DISCUSSIONS**

**1. Fly Ash (FA) :**

Siddique et al. (2003) observed the  $f_{ck}$  of concrete mixture increases by the replacement of OPC with 5 different percentages of class F FA by weight. There will be a significant improvement take place in the strength when cement is replaced by FA upto 40% but after that, effect was insignificant as shown in figure 6.

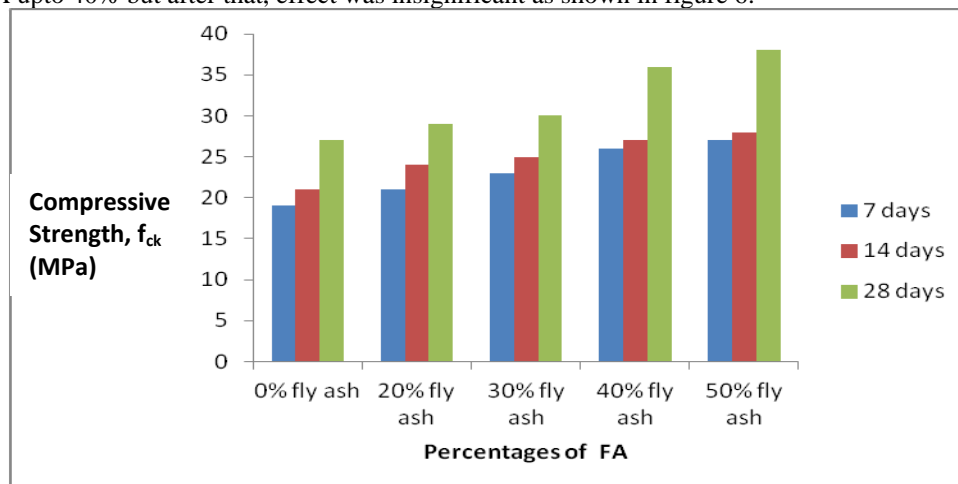


Fig. 6 Compressive Strength results for Fly ash

**2. Granulated Blast Furnace Slag (GBFS):**

Hogan and Meusel et al. (1981) observed that  $f_{ck}$  of concrete mix by the replacement of OPC with GBFS. It was observed from figure 7 that GBFS is more significant at 28 days when cement is replaced by GBFS upto a range of 40-60%.

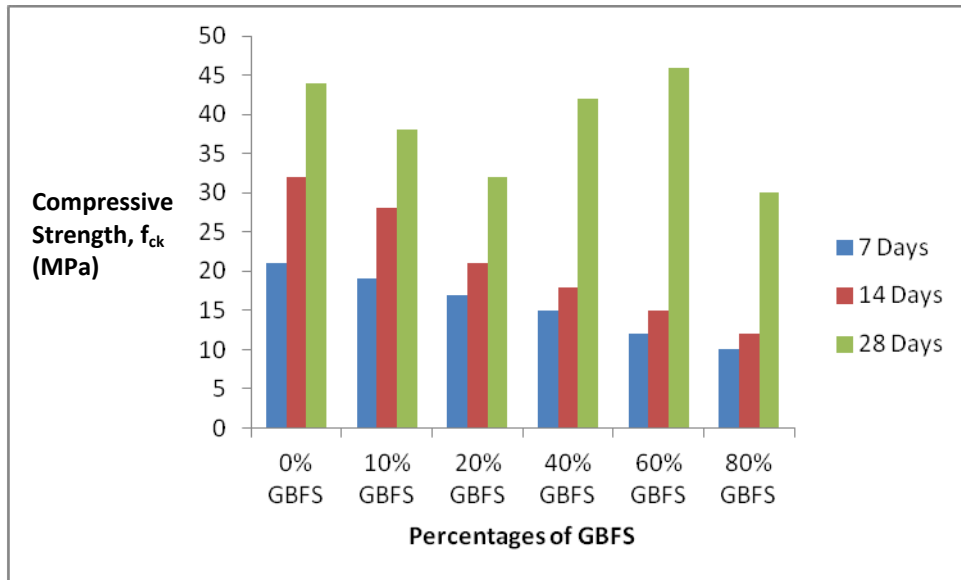


Fig. 7 Compressive Strength results for GBFS ash

**3. Municipal Solid Waste Ash (MSW):**

Lin et al. (2002) observed the effect of replacement of OPC with MSW on the  $f_{ck}$  of concrete mix. It was observed from figure 8 that the addition of MSW in the cement decrease the strength of concrete in early days but gain in strength is achieved at 60 days significantly when cement is replaced by MSW upto a range of 10-20%.

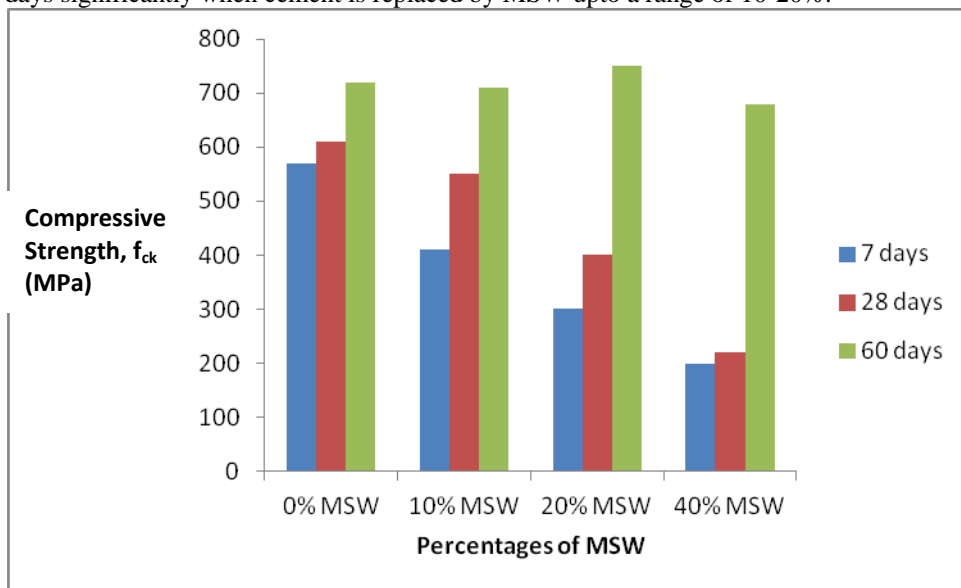


Fig. 8 Compressive Strength results for MSW ash

**4. Metakaolin (MK):**

Wild et al. (1996) observed that the  $f_{ck}$  of concrete increase with the addition of Metakaolin increases. It was studied that gain in the strength is take place as percentage of Metakaolin increases from 0 to 20% as shown in figure 9 after

that there will be decrease in strength take place.

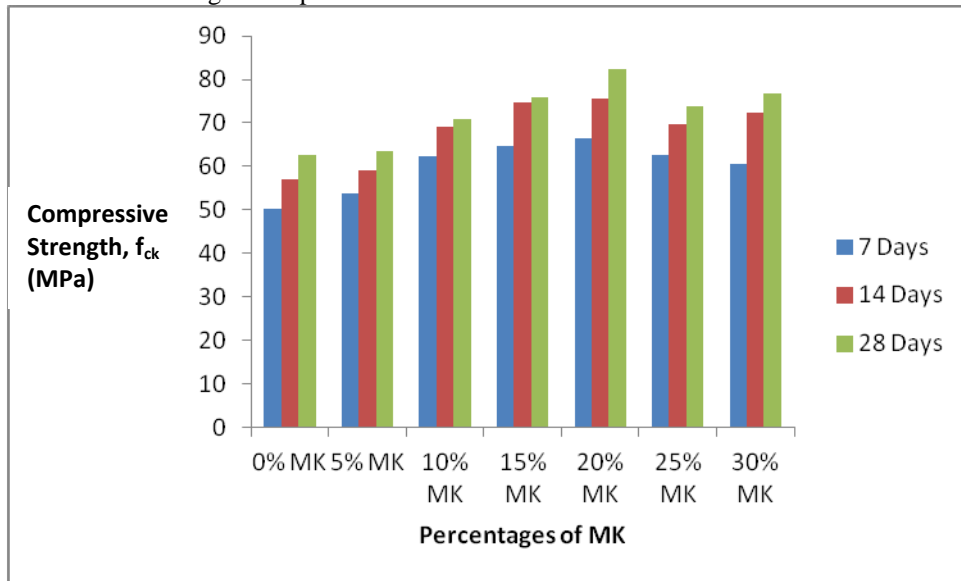


Fig 9 Compressive Strength results for MK

#### 5. Wood Ash (WA) :

Naik et al. (2002) discuss the  $f_{ck}$  of mix prepare by the replacement of OPC with WA at 365 days age of concreting. It was observed from figure 10 that cement can be replaced by WA upto range of 0-10% after that the effects in strength are not appropriate.

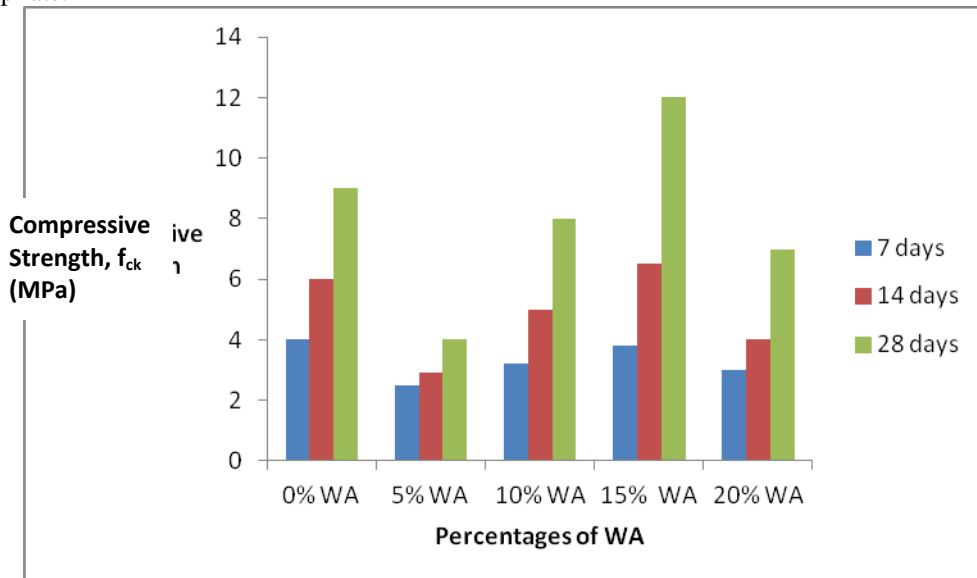


Fig. 10 Compressive Strength results for Wood Ash

## CONCLUSIONS

This research shows the properties of industrial waste materials and concludes the following results that compressive strength of some waste material likes GBFS and MSW decreases when the properties of quantity increases. Also, materials like Fly ash, Wood ash and Meta kaolin increases when the property of quantity increases.

1. It was observed that the increase in the quantity of GBFS at the time of hydration there was a slightly decrement take place in compressive strength of concrete but it was more effective after the age of days when 40-60% cement is replaced by GBFS.
2. From the literature study it was observed that the addition of MSW is not effective significantly in the early age of concrete but a significant achievement is observed after the 60 days.
3. It was observed that the optimum range for the replacement of cement with the fly ash is 0-40 % after that there will be less significant effect take place in the compressive strength of concrete.
4. It observed that there was an increment in compressive strength take place as the quantity of Metakaolin increases. The replacement of OPC with MK by 20% gives best result for the compressive strength.
5. There was an increment in compressive strength as the quantity of WWA increases. It was study that as the cement quantity replaced by 15 % of WWA, then maximum gain in the strength is take place.

So, we may improve the properties of mortar and concrete like mechanical and durability by the replacement of cement as industrial waste materials. For manufacturing of concrete mixture these waste materials is also used for the cost reduction and very useful for reduction in landfill cost for the protection of environment from the pollution effects.

### **ACKNOWLEDGMENTS**

The author is grateful to other co-authors of the paper for their constant support, guidance, encouragement and advice. This study carried out in Civil Engineering department of M.M.M.U.T. Gorakhpur.

### **REFERENCES**

- Abdullahi M et al. (2006), Characteristics of wood ash/OPC Concrete, Leonardo Electronic Journal of Practices and Technologies, 8: 9-16.
- Cook JE et al. (1982), Research and application of high strength concrete using class C fly ash, Concrete International, 4: 72-80.
- Curcio F et al. (1998), Dilatant behaviour of super plasticized cement pastes containing meta kaolin, Cement and Concrete Research, 28 (5): 629-634.
- Campbell AG (1990) Recycling and disposing of wood ash. TAPPI Journal 73 (9): 141–143.
- Etiegni L (1990) Wood ash recycling and land disposal. Ph.D. Thesis, Department of Forest Products, University of Idaho at Moscow, Idaho, USA, pp. 174.
- Etiegni L, Campbell AG (1991) Physical and chemical characteristics of wood ash. Bio resource Technology, Elsevier Science Publishers Ltd. 37 (2): 173–178.
- Hogan FJ et al.(1981),“Evaluation for durability and strength development of a ground granulated blast furnace slag, Cement Concrete Aggregate, 3 (1): 40-52.
- Haque MN et al. (1988), High fly ash concretes, ACI Materials, 8 (1): 54-60.
- Ikpong AA et al. (1992), Strength characteristics of medium workability ordinary Portland cement-rice husk ash concrete, Building and Environment, 27 (1) 105-111.
- Joshi RC et al. (1987), Effect of a sub-bituminous fly ash and its properties on sulphate resistance of sand cement mortars, Journal of Durability of Building Materials, 4: 271-286.
- Krammart P et al. (2004), Properties of cement made by partially replacing cement raw materials with municipal solid waste ashes and calcium carbide waste, Construction and Building Materials, 18: 579-583.
- Lin KL et al. (2004), “The hydration properties of pastes containing municipal solid waste incinerator fly ash slag”, Journal of Hazardous Materials, B109: 173-181.
- Naik TR et al. (2003), CLSM containing mixtures of coal ash and a new pozzolanic material, ACI Materials Journal, 100 (3): 208-215.
- Rafat Siddique et al. (2008), Waste Materials and By-Products in Concrete ISBN: 978-3-540-74293-7.
- Raba et al. (1981), Sub bituminous fly ash utilization in concrete, Materials Research Society, Boston, pp, 296-306.
- Srivastava, Kumar (2018), “The methods of using low cost housing techniques in India”, Journal of Building Engineering, ISSN: 2352-7102
- Wild S et al. (1996), Relative strength, pozzolanic activity and cement hydration in super plasticized meta kaolin concrete, Cement and Concrete Research, 26 (10): 1537-1544.
- Wainwright PJ et al. (2000), the influence of ground granulated blast furnace slag (GBFS) additions and time delay on the bleeding of concrete, Cement and Concrete Composites, 22: 253-257.



## INFLUENCE OF LIME AND CHICKEN MESH ON COMPACTION PROPERTIES OF SOIL

*R. Vipasha<sup>1</sup>, K. Senthil<sup>2\*</sup>, S. Rupali<sup>2</sup>, Jatin Anand<sup>1</sup>, Shailja Bawa<sup>2</sup>*

<sup>1</sup>(Dept. of Civil Engineering, Chandigarh University, SAS Nagar, Punjab, India)

<sup>2</sup>(Dept. of Civil Engineering, Dr. B.R. Ambedkar National Institute of Technology Jalandhar, Punjab-144011, India)

\*Corresponding Author

### ABSTRACT

For increasing the durability of pavements it has been observed that there was no such research on lime and chicken mesh which has been carried out till date. Although the initial cost of chicken mesh is more than geo mats, geotextiles or any other geosynthetic but the tensile strength is high for this material. Chicken mesh is a steel material which is galvanized with zinc which also holds the resistance to corrosion. The purpose of the research is to investigate the effect of lime and chicken mesh on compaction properties of soil and its application in the field. The tests on soil classification, compaction tests were performed. From the study the optimum lime content by weight was obtained as 2 % against double layers of chicken mesh combination. Standard Proctor tests were conducted to determine optimum moisture content and maximum dry density of the soil. For various % of lime content, maximum dry density value increased till 2%, after which it decreased till 6%. Optimum water content value decreased at 1%, increased at 2% and kept on decreasing till 6% of lime. Proctor curve became flatter at 2% whereas for other cases it was found to be normal. In case of use of chicken mesh, for double layers of chicken mesh, the value of MDD and OMC both decreased as compared to single layer of chicken mesh.

**KEYWORDS:** Chicken mesh; Standard Proctor test; MDD and OMC

### INTRODUCTION

Wet, poorly compacted soil give rise to poor pavement support and embankment/fil and hence soil needs to be stabilized. There is a lot of literature available regarding stabilization of soil using lime and other admixtures like geotextiles, fly ash, coconut, plastic waste, bitumen, rice husk ash, marble dust, saw dust ash, cement and many more [Aytekin and Nas 1998, Bhattacharja and Bhatta 2003, Choudhary et al. 2012]. A lot of experimental work has been done on soil using lime, cement, fly ash, geogrid and other amixtures. However, literature related to stabilization of soil using lime, fly ash, cement, jute geotextile and geogrid by performing several tests has been presented in this general, [Hussain and Dash 2009, Negi et al. 2013]. On the other hand chicken mesh is a galvanized iron drawn wire mesh having greater friction and bearing resistances than PVC coated wire, Moayedi et al. 2009. Its hexagonal shape prevents the creation of internal stresses. Due to its flexibility structure, chicken wire is fitting for mounting on curved and angled surfaces. The use of lime in soil stabilization has been discussed and its future use in this field is anticipated, but limited research was initiated to investigate the effects of chicken mesh on the stability of soil. A study of lime-chicken-mesh stabilization was, therefore, initiated.

### MATERIALS AND METHODOLOGY

For the visual identification of soils, normally rub the soil between the fingers or observe the various site conditions and get the type of soil. For more authentications, various tests need to carry out in order to identify the accurate type of soil. Tests like sieve analysis (IS 2720:1985 (part IV)), liquid limit, plastic limit (IS 2720:1985 (part V)) has been

performed. After getting the type of soil a study of lime and chicken mesh has been therefore initiated as there was no research ever initiated to investigate the effects of both lime and chicken mesh on compaction properties of soil. Lime in the form of quick lime is used, lime when added to the soil it hydrates and releases heat, water evaporates, decreases the water holding capacity and ultimately increases the stability.

The soil was chosen from a village mankheri near Chandigarh University, Gharuan, Chandigarh. The soil from the site was taken to the laboratory for testing work. For classification of soil, particle size analysis has been carried out, for knowing general properties specific gravity and atterberg's limit test has been conducted. The specific gravity (IS 2720:1980 (part III/Sec-1)) of the taken soil has been found to be 2.46. It has been noticed that the liquid limit of soil is 22.2%. In the plastic limit test, the soil begins to crumble before rolled into threads of 3mm diameter the soil is of no plastic type. It is sandy soil not the clayey. As per IS Classification it has been observed that more than half of the coarse fraction is smaller than 4.75mm therefore it is sand and the type is **SP (poorly graded sand with gravel)**. However, authors are extended the present investigations on SP soil considering major application of poorly graded sand with gravel on sub base and the present study is treated as most important in the field of highway and embankment.

**Standard proctor test (IS 2720:1980 (Part VII)):**

1. Sieve 4kg of soil through 4.75 mm sieve.
2. Clean, dry and grease the mould of proctor test.
3. 3 kg of soil specimen in the tray should be taken. Start adding water with the water content of 8%.
4. Calculate the weight and volume of empty mould. Fix the collar to the mould and Place the mould on a solid base.
5. The soil is to be added in 3 equal layers. Start the test by giving 25 numbers of blows with rammer to 1/3<sup>rd</sup> of the whole soil sample. The blows given should be uniformly extended over the surface of each layer; the top surface of the layer will be scratched with spatula before putting the second layer.
6. Add the final layer of soil and repeat the procedure.
7. The final layer of the soil should be added at least 5 mm above the top surface of collar to strike off when the collar is detached.
8. Using a straight edge the top surface of the soil should be trimmed off after removing the collar.
9. In the end the base plate and mould should be cleaned from the outside and the weight of mould should be taken without collar.
10. Bulk density ( $\gamma_d$ ) = Dry soil weight (g) / Soil volume ( $\text{cm}^3$ ).
11. (Dry density)  $\gamma_d = \gamma_w / (1+w)$ .
12. Take out the soil and add different % of water and repeat the whole procedure.
13.  $\gamma_d$  for various water contents is calculated and a graph between water content and  $\gamma_d$  is plotted to find the value of MDD (maximum dry density) and OMC (optimum water content).

*Proctor test using various % of lime-* using various % of lime from 2% to 8 % proctor test has been performed again to find the value of MDD and OMC.

*Proctor test using single layer and double layer chicken mesh-* using single layer and double layer of chicken mesh i.e. single layer of chicken mesh at the center of mould and for double layer; one layer of chicken mesh after compacting first layer of soil and second layer of chicken mesh after compacting the second layer of soil. Value of MDD and OMC has been calculated using single layer and double layered chicken mesh. Different combinations and designation of the mix proposed were shown in **Table 1**.

**Table 1** Designation of the Mixes

Name of Mix	M1	M2	M3	M4	M5	M6	M7	M8	M9
Soil (%)	100	99	99	97.5	96	94	100	100	98
Lime (%)	0	1	2	2.5	4	6	-	-	2
Chicken Mesh	-	-	-	-	-	-	Single Layer	Double Layer	Double Layer

**EXPERIMENTAL INVESTIGATIONS**

Standard proctor test has been conducted and a compaction curve has been made to find the values of optimum moisture

content (OMC) and maximum dry density (MDD). Compaction curve for basic soil and various sample mixes were shown in **Fig. 1(a)-(f)**. The maximum dry density of M1 mixes and corresponding optimum moisture content were 1.91 g/cm<sup>3</sup> and 13.8 % respectively. The maximum dry density of M1, M2, M3, M4, M5 and M6 mixes were found to be 1.91, 1.911, 2.06, 1.932, 1.962 and 1.835 g/cm<sup>3</sup> respectively. The optimum moisture content of M1, M2, M3, M4, M5 and M6 mixes were found to be 13.8, 12.3, 10.5, 11.6, 11.9 and 12.6 %, respectively. The maximum dry density and lowest optimum moisture content was achieved by the proportion M3 corresponding lime content was 2%. Therefore, it is concluded that 2% lime content was found to be effective and in case of addition of lime, causes increase of heat of hydration resulting increase optimum moisture content.

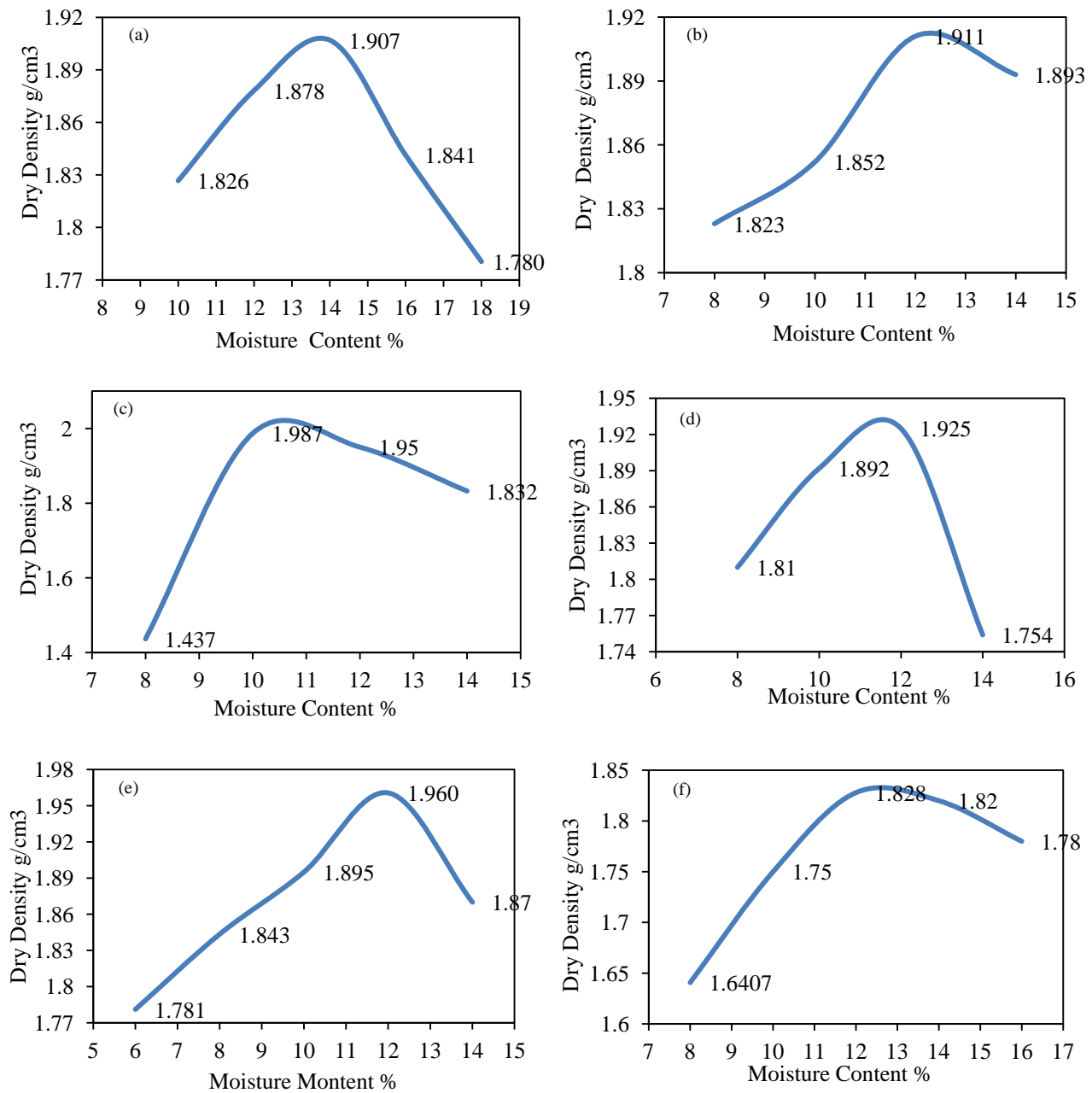


**Fig. 1. Maximum dry density corresponding varying moisture content of (a) M1 (b) M2 (c) M3 (d) M4 (e) M5 and (f) M6 mix**

Compaction curve for basic soil and various sample mixes were shown in **Fig. 2(a)-(c)**. The maximum dry density (MDD) of M7, M8 and M9 mixes were found to be 1.943, 1.936 and 1.865 g/cm<sup>3</sup> respectively. The optimum moisture content of M7, M8 and M9 mixes were found to be 13.6, 12.3 and 14.3 %, respectively. It is observed that the compaction value decreases on adding lime with double layered chicken mesh because there is formation of crystals of lime and soil which decreases the water content and ultimately decreases the compaction value. The highest maximum dry density and lowest optimum moisture content was achieved by the proportion M8 however, addition of lime on mix 9, resulting increasing moisture content and decreasing the MDD. Therefore, it is concluded that double layer chicken mesh without lime content on the specified sample was found to be effective. The detailed results of the MDD and OMC of various mixes are shown in **Table 2**.

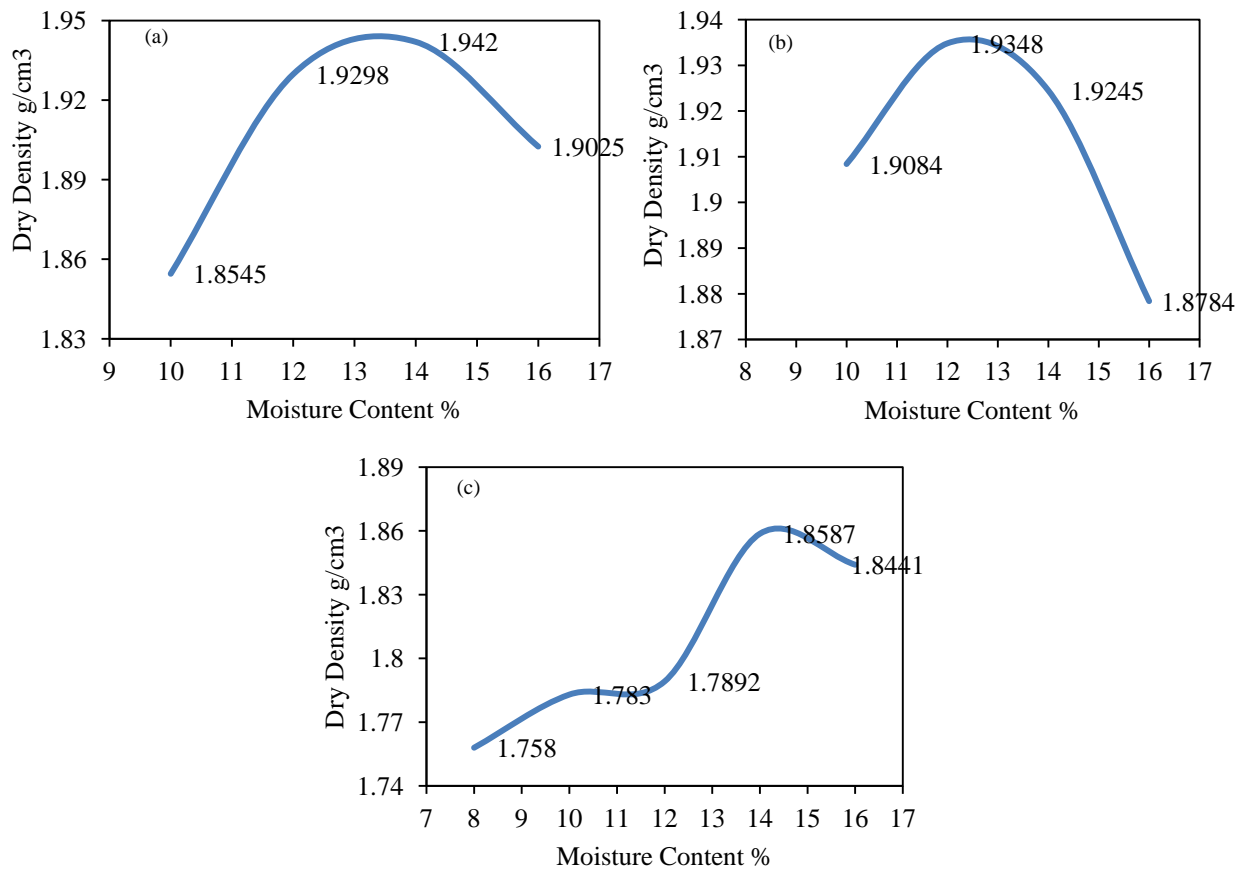


**Fig. 2.** Maximum dry density corresponding varying moisture content of (a) M7 (b) M8 and (c) M9 mix

**Table 2.** MDD values for varying content of lime and chicken mesh

Moisture content %	basic soil (g/cc)	1 % Lime (g/cc)	2 % Lime (g/cc)	2.5 % Lime (g/cc)	4 % lime (g/cc)	6 % Lime (g/cc)	Single layer of chicken mesh (g/cc)	Double layers of chicken Mesh (g/cc)	2% lime and double layers of chicken mesh (g/cc)
6	-	-	-	-	1.781	-	-	-	-
8	-	1.823	1.437	1.81	1.843	1.640	-	-	1.758
10	1.8267	1.852	1.987	1.892	1.895	1.75	1.854	1.908	1.783
12	1.878	1.911	1.95	1.925	1.960	1.828	1.929	1.934	1.789
14	1.907	1.893	1.8324	1.754	1.87	1.82	1.942	1.924	1.858
16	1.841	-	-	-	-	1.78	1.9025	1.878	1.844
18	1.780	-	-	-	-	-	-	-	-

## CONCLUSION

The experimental investigations has been performed on sand through stabilization technique. As stabilization agent, lime and chicken mesh were used in the present investigations. Authors have carried out basic material tests to identify the nature and property and it was concluded that chosen soil was poorly graded sand in nature.

- The highest maximum dry density and lowest optimum moisture content was achieved by the mix M3 corresponding lime content was 2%. Therefore, it is concluded that 2% lime content was found to be effective and in case of addition of lime, causes increase of heat of hydration resulting increase in optimum moisture content.
- The highest maximum dry density and lowest optimum moisture content was achieved by the proportion M8 however, addition of lime in mix 9, resulting in increasing moisture content and decreasing the MDD. Therefore, it is concluded that double layer chicken mesh without lime content on the specified sample was found to be effective.

## REFERENCES

- Aytekin, M., and Nas, E. (1998). "Soil Stabilization with lime and cement." Digest 98, pp, 471-477.
- Bhattacharja, S., and Bhatta, J.I. (2003). "Comparative Performance of Portland Cement and Lime Stabilization of Moderate to High Plasticity Clay Soils." Research and Development Bulletin RD125, Portland cement Association, Skokie, Illinois, USA. 26 pages.
- Choudhary, A.K., Gill, K.S., and Jha, J.N. (2012). "Improvement in CBR values of expansive soil sub-grades using geosynthetics." Indian Geotechnical Conference., J-233(155-160).
- Hussain, M., and S.K., Dash. (2009) "Influence of lime on compaction behaviour of soils." *Indian Geotechnical Conference.*, pp (15-17).
- Dash, S.K., and Hussain, M. (2012). "Lime Stabilization of Soils: Reappraisal." *American society of civil engineers.* Vol 707 -714.
- Negi, A., Faizan, M., Siddharth, D.P., and Singh, R., (2013). "Soil stabilization using lime." *International Journal of Innovative Research in Science, Engineering and Technology.* Vol. 2(2) 448-453.
- Moayed, H., Kazemian, S., Prasad, A., and Haut, B. (2009). "Effect of Geo-grid Reinforcement Location in Paved Road Improvement." *Electronic Journal of Geotechnical Engineering.*, Vol. 14, 1-11.
- IS 2720:1980 (part III/Sec-1), *Method of Test for Soils, Determination of Specific Gravity*, Bureau of Indian Standard, New Delhi.
- IS 2720:1985 (part IV), *Method of Test for Soils, Grain Size Analysis*, Bureau of Indian Standard, New Delhi.
- IS 2720:1985 (part V), *Method of Test for Soils, Determination of Liquid and Plastic Limit*, Bureau of Indian Standard, New Delhi.
- IS 2720:1980 (Part VII), *Method of Test for Soils, Determination of Water Content-Dry Density Relation Using Light Compaction*, Bureau of Indian Standard, New Delhi.
- IS 2720:1987 (Part XVI), *Method of Test for Soil, Laboratory Determination of CBR*, Bureau of Indian Standard, New Delhi.



## GIS-BASED LANDSLIDE SUSCEPTIBILITY MAPPING FROM NAGGAR TO ROHTANG IN DISTRICT KULLU, HIMACHAL PRADESH

Akhilesh Kumar<sup>1</sup>, Ravi Kumar Sharma<sup>2</sup>, Vijay Kumar Bansal<sup>3</sup>

<sup>1</sup>\*.#Research Scholar, Department of Civil Engineering, NIT, Hamirpur (HP), India; akhileshsharma54@gmail.com

<sup>2</sup>Professor, Department of Civil Engineering, NIT, Hamirpur (HP), India; rksnithp61@gmail.com

<sup>3</sup>Associate Professor, Department of Civil Engineering, NIT, Hamirpur (HP), India; vijaybansal18@yahoo.com

### ABSTRACT

Landslide susceptibility mapping means division of land into identical areas and rank according to their degrees of real potential hazard caused by mass movements. Steep slopes, high relative relief with unfavorable hydro-geological conditions are the major causes of landslides in mountainous terrain. The elimination of causative factors is difficult but damage and loss of lives caused by landslides can be minimized by adopting suitable measures. Identification of landslide susceptible regions helps in making strategic planning for the future developmental activities in landslide prone areas. In the present study, a part of Kullu district has been selected to trace landslide susceptibility areas. Geographical information system was used for preparation of database, analysis, modeling and output. Arc GIS 10.0 software has been used for integration of input layers by assigning appropriate weights. The analytical hierarchy process was used for assigning weightage to different causative factors as slope map, aspect map, landuse/ landcover map, soil map, drainage density map and lithology map. Subsequently, the landslide hazard zonation map is prepared. The resultant landslide hazard map has been categorized into three risk zones. The resultant map is useful for landslide hazard mitigation, prevention and improvement to society and proper land-use planning.

**KEYWORDS:** Landslides; Hazard; Geographical information system; Analytical hierarchy process; Zonation; Mitigation

### INTRODUCTION

Landslides are unexpectedly occurring natural phenomena. It is a hazard when it occurs in an uninhabited place; still it turns into a disaster causing extraordinary landscape changes and destruction of life. Landslides are particularly a massive damage phenomenon in tectonically active Himalayas. The present work conducts a landslide susceptibility zonation in western Himalayas in district Kullu of Himachal Pradesh using geographical information system (GIS). Landslide and related geomorphic processes pose a threat to people and property in Kullu district of Himachal Pradesh, India. Landslides are influenced by various geo-environmental factors such as movement of mass of rock, debris or earth down a slope. Mountainous areas experiences a dramatic economic and population growth in recent times resulting from tourism and agro-industrial development. The intensification of land use, expansion of built-up areas and physical infrastructure has raised the level of vulnerability to natural hazards. It increases the need of accurate information about the location and quantum of landslide hazards so that appropriate mitigation measures can be undertaken timely. The objective of identifying the landslide hazard prone areas around this town is due to tourist importance, and will help in minimizing the natural hazards causing substantial damages to life and property. The characteristics of the landslides include location, size, mechanics of the sliding, composition, velocity and travel distance. A landslide susceptibility zonation map classifies the land surface into zones of varying degrees of stability based on the estimated significance of causative factors including instability.

In this study, GIS and remote sensing capabilities has been utilized for landslide zonation mapping. GIS is a very fast and accurate method, which integrates landslide triggering, factors which in a certain extendable to predict the susceptibility of an area of landslides. In this study, GIS along with analytical hierarchy process (AHP) is used for landslide hazard zonation. AHP method has been used to calculate the weights of landslide influence parameters. The parameters used in this study area are IRS 1D LISS III Imagery, topographic maps, geological maps, soil map and field visits. GIS has been used for preparation of database, analysis, modeling and output. IRS 1D LISSIII dated October 31<sup>st</sup> 2011 have been used for landuse/landcover map. Arc GIS 10.0 software has been used for integration of input layers after assigning the appropriate weights. People are unaware of the disaster that can occur due to landslide and can harm them very adversely due to their wrong choice of selection of area for the construction of their shelter. Therefore, to

make the people aware about the landslide characteristic of area and to help them in selecting for the construction. In addition to this, the study area also includes NH-3 (NH-21) which connects the Kullu valley with the rest of the country. Entire inflow of tourists from various parts of the country is diverted to the valley during tourist season leads to heavy vehicular traffic on this highway from the beginning of May until the end of October. This highway has its additional importance as the supplies of defense equipment and essential commodities for defense personnel deployed at Leh has been diverted through this route. Military vehicles carry supplies of essential commodities and defense equipments to the border parts of Leh from Pathankot and Chandigarh from beginning of July and remain plying on this route to passes at "Rohtang" and "Baralacha". As such, it is of immense importance to study landslide prone areas along this highway.

### STUDY AREA AND DATA USED

The study area traced in and around Kullu town of Himachal Pradesh (Fig. 2). It runs from 32°00'00" to 32°30'00" Northern latitude and from 77°00'00" to 77°30'00" Eastern longitude with topological map numbers as shown in the Fig.(1)

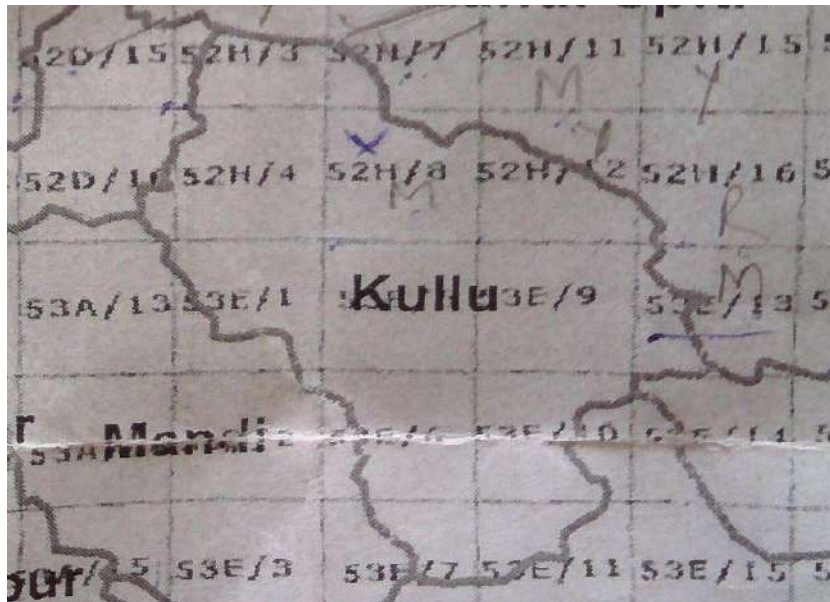


Fig. 1 Topological sheets numbers in which area lies (52H/3, 52H/4, 52H/7 and 52H/8)



Fig. 2 Google earth image showing location of study area (Image dated 16/11/2014)

## METHODOLOGY

The method utilizes an underlying scale with values from 0 to 9 to rate the relative preferences for two criterias as shown in table 1. In this the assumption made that the comparison matrix is reciprocal; that is, if criterion A is twice as preferred to criterion B, it is concluded that criterion B is preferred only one-half as much as criterion A. Thus, if criterion A receives a score of 2 relative to criterion B, criterion B should receive a score of 1/2 as compared to criterion A. Same logic can be used to complete the lower left side of matrix of pair-wise comparison. When comparing anything to it, the evaluation scale must be 1, representing equally preferred criteria. This pair wise comparison matrix of the criteria parameters has been incorporated to the online AHP calculator. Subsequently, criteria weights were computed using these score values, as given in Table 2.

In this study, weighted rating scheme was used. Subsequently, weights rating scheme for factors and their classes were computed as shown in Table 3. For investigation of all layers arithmetic weighted overlay approach was used, that is built in Arc GIS software. An arithmetic weighted overlay process accepts both continuous and discrete grid layers, and the resulted data was in continuous grid data layer. All the factors were re-classified based on the importance of each factor influencing landslide hazard, using Arc GIS spatial analyst module. Each sub-class is given rating between 0-9 in an increasing order of hazard; zero indicates low hazard and 9 indicates high hazard. Weights and its rating of landslide influence factors shown in Table 4. The weights were calculated by AHP. Lowest weight indicates low landslides and higher weight indicate high landslides.

**Table 1 Scale for pair wise comparison**

Intensity of importance	Definition
1	Equal importance
2	Equal to moderate importance
3	Moderate importance
4	Moderate to strong importance
5	Strong importance
6	Strong to very strong importance
7	Very strong importance
8	Very to extremely strong importance
9	Extreme importance

**Table 2 Pairwise comparison matrix**

	Slope	Drainage density	Lithology	Landuse/Landcover	Soil	Aspect
Slope	1	2	3	3	9	9
Drainage density	1/2	1	3	3	8	9
Lithology	1/3	1/3	1	2	4	5
Landuse/ Landcover	1/3	1/3	1/2	1	3	4
Soil	1/9	1/8	1/4	1/3	1	4
Aspect	1/9	1/9	1/5	1/4	1/4	1

**Table 3 Factor and weights**

Sr. No.	Factor	Weighted by pair wise comparison
1	Slope	38.1
2	Drainage density	29.6
3	Lithology	14.4
4	Landuse/Landcover	10.4
5	Soil	4.9
6	Aspect	2.7

**Table 4 Weights rating scheme for factors and their classes**

Factor	Classes	Rating	Weight
Slope	0-15	1	38.1
	15-25	3	
	25-35	5	
	35-45	7	
	>45	9	
Aspect	Flat	0	2.7
	North	1	
	North East	4	
	East	7	
	South East	8	
	South	9	
	South West	6	
	West	3	
Landuse/Landcover	North West	2	10.4
	Moderate cover forest	5	
	Sparsely vegetative land cover	9	
	Water Body	0	
	Agricultural & inhibited land	1	
	Snow Covered area	9	
	Barren land	7	
Drainage density	Rock outcrop	5	29.6
	Low	1	
	Medium	5	
Soil	High	9	4.9
	Sandy	7	
	Sandy with Loamy	6	
	Loamy	5	
	Calcareous loamy	7	
Lithology	Course loamy	6	14.4
	Assorted material	5	
	Granotoid gneiss	3	
	Slate with quartzite	2	
	Schist	4	

The consistency ratio of 0.10 or less indicates a reasonable level of consistency in pair wise comparisons; if consistency ratio is greater than 0.10, the values of the ratio are indicative of inconsistency judgment. Consistency ratio for the weights was calculated using the online AHP calculator.

### THEMATIC LAYERS

The present work involves six parameters: slope, drainage density, lithology, land use, soil and aspect. These were selected for assessing the relative importance of these causative factors. This has been done by pair wise comparison of each pair of parameters.

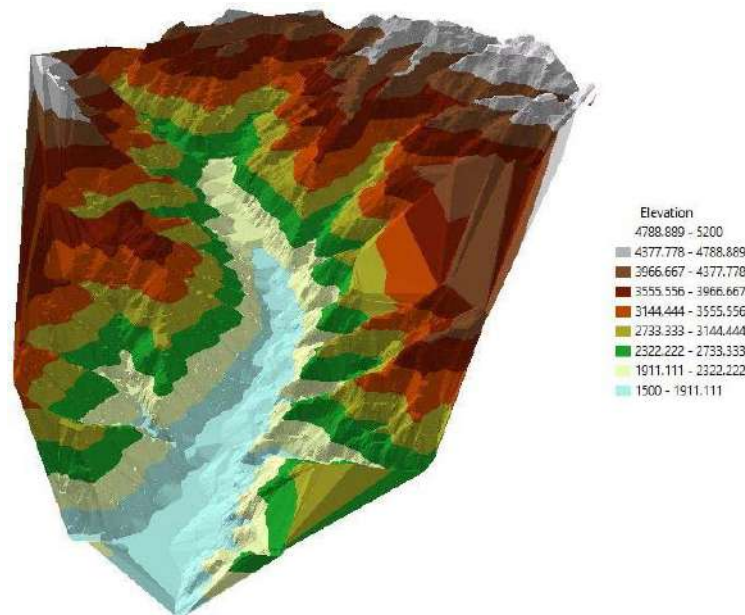


Fig. 3 IRS-1D LISS3 data (Dated 31<sup>st</sup> Oct 2011)

### Slope and Aspect

Slope and aspect are important causative factors that determine the hazardousness of an area. Slope degree refers to the rate of change in elevation over distance with higher values representing steeper terrain while lower the slope value representing flatter terrain. Aspect defines the down slope direction of the maximum rate of change or the direction of steepest slope (Sharma and Mehta 2013). In Kullu district gentle slopes (below 20°) form nearly 1/3 (34.25%) of total area of the district and such slopes has been found either along the river's course or on ridge tops. The moderately steep and steep slopes account for 35.35% and 24.55% area respectively; about 6% of the total area possesses very steep to precipitous (above 40°) slopes. The aspect distribution in the district has an even distribution as all nine directions have 10-15 % of total area. The aspect has significance in understanding the slope stability. Usually southeast (SE) to south (S) and southwest (SW) slopes are comparatively more prone to slope failure and sliding activities. Slope has been classified into 5 classes, 0-15°, 15-25°, 25-35°, 35-45°, >45° as shown in fig. 4.(a). The rating has been given on 0-9 scale based on the degrees of slope. On the other, aspect map was generated using aspect tool in GIS. It refers to the direction of maximum slope of the terrain surface. It influence solar, which is strongly related to the distribution and density of vegetation on mountainous slopes, as vegetation provides anchorage to the ground. The stability of slope is also related to the aspect, the aspect thus generated shows direction from 0° to 360°. The aspect values have been categorized into nine direction classes, namely N, NE, E, SE, S, SW, W, NW and flat as shown in fig. 4.(b).

### Physiography and Relief

The study area possesses high relative relief, which refers to the difference between the highest and the lowest altitude in an area. The lower relief signifies mature topography while higher values indicates rapid rise in altitude and presence of faults. For determining the morphological character of an area, relative relief has significant alliance with landslide by acting as a triggering factor. As a risk agent, relative relief plays a decisive role in the vulnerability of settlements, transport network and land. In study area, there is wide variation in relative relief ranging from low to very high as shown in fig.4.(c).

### Geological structure

In study area, a broad central zone of crystalline unfossiliferous rocks consisting of granite, gneisses, schist and other metamorphic rocks forms the axis of the Himalayas (Kayastha, 1964). Five major litho-tectonic units express the geology of the current area; (1) Vaikrita Group (2) Jutog Group (3) Kullu Group (4) Larji Group, and (5) Rampur Group. The area is dissected by several major thrusts, namely Jutogh Thrust, Kullu thrust and Vaikrita thrust along with

several local faults/lineaments. These thrusts are still active and play a major role in the neo-tectonics of the area (Choubey et al., 2007). The Jutogh thrust separates rocks belonging to Kullu group and Jutogh group while Kullu thrust or Chail thrust (Bhargava and Bassi, 1994) defines boundary between the rocks of Rampur-Larji group and Kullu group. Structurally, the mainly Kullu Valley is a gently folded antiform having river Beas following its axial plane along a fault running NNW-SSE from the upper catchment to near Aut, where it is intersected by a cross fault almost at right angles (Sah and Mazari, 2007). This fault is a dextral tear fault with a dislocation of nearly 1.5km (Shankar and Dua, 1978) fig 4.(d). The lithology map was derived from geological map. It is also one of main important parameters for occurrence of landslides. There are four types of rocks traced in the study area such as schist, slate with quartzite, granotoid gneiss and assorted material. The rock types are digitized as polygons and converted in to raster format. Based on susceptibility of rocks for landslides, rating has been given on 0-9 scale, 0 indicates no landslides, 9 indicates more susceptible for landslides.

### **Drainage character**

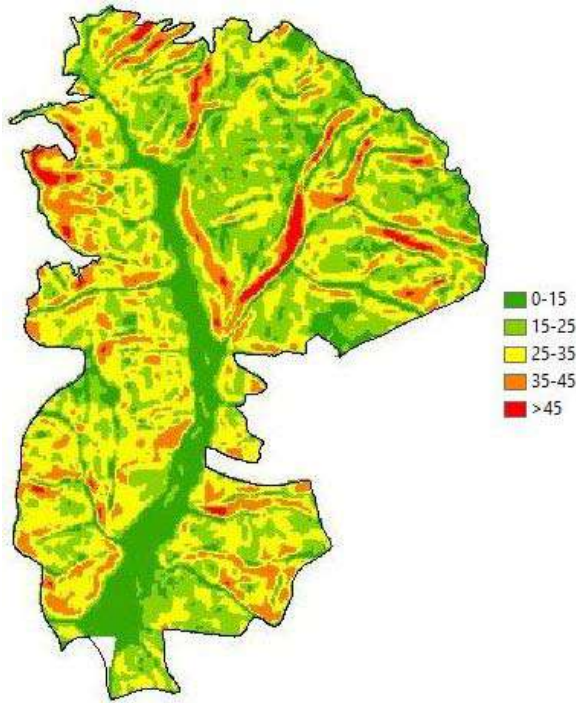
The drainage patterns in the study area is outcome of long time interaction between the geological structure, topography and slope. The overall drainage reflects early stage of dendritic pattern with visible traces of parallel dendritic and trellis patterns in between fig 4.(f). The measurement of drainage density is useful in determining landscape dissection and runoff potential. Higher values denote higher degree of dissection of land, as well as indicate the higher probability of slope failure. The drainage density map was prepared using topographic maps. The drainage density was computed considering a 250-by-250-m cell and classified into low, medium and high density as shown in fig 4. (e) The drainage superimposed on the drainage density map show relatively more numbers and closely spaced drainage channels in the high-density class than in the medium and low classes.

### **Land use/land cover**

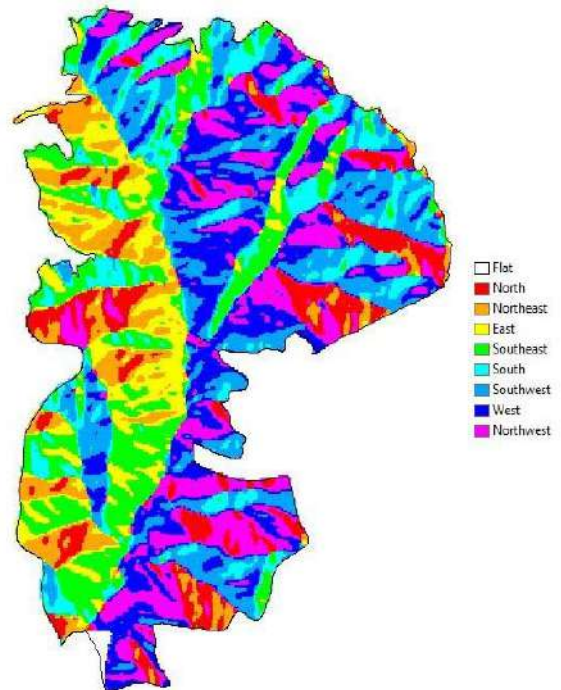
Land use/land cover analysis reflects relationships between land use, disaster risk and vulnerability to disaster events (Sharma and Mehta 2012). The landuse/ land cover analysis for this study is based upon IRS-1D LISS-III (2011). The landuse classification of mountainous terrains suffer from certain drawbacks as high relief results in shadow areas and confusion between land use classes like barren rocky surfaces, water bodies and settlements. The maximum likelihood classification (MLC) algorithm which is the most accurate classifier (Richards and Jia, 1999; Saha et al. 2005) has been used. Landuse/landcover map has been generated by multisource image classification of LISS III image. Multisource classification has been adopted to reduce the effect of shadows cast by high mountain peaks in the study area. Seven classes have been considered in this study as shown in fig.4.(h). These classes are water body, moderate cover forest area, sparsely vegetative land cover, agricultural cum inhibited land, snow covered area, barren land and rock outcrop. Digital elevation model (DEM) and normalized difference vegetation index (NDVI) have been included in the classification process to reduce the effect of shadows in the region to improve the difference among various classes.

### **Soil**

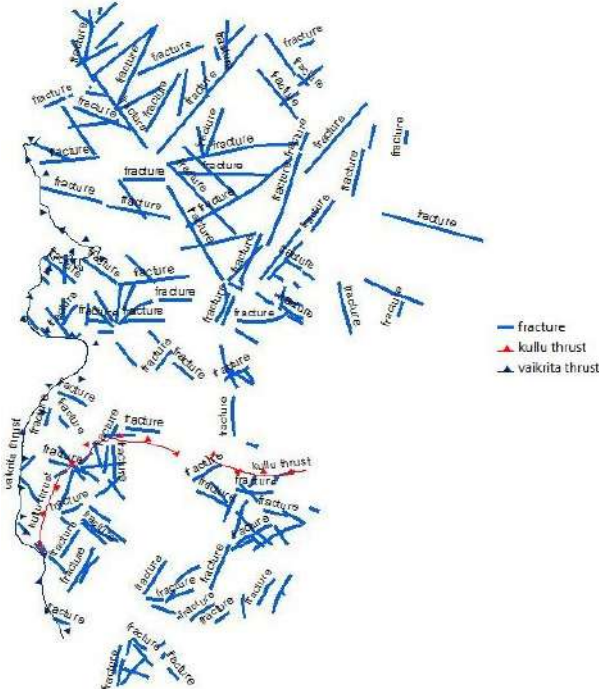
The topsoil cover on a slope has an influence on landslide occurrence as observed in the field (Mehta et al. 2010). The soil map was derived from regional soil map. The soil present in the area is sandy, sandy with loamy, loamy, calcareous loamy and course loamy as shown in fig.4.(g). The soil types are digitized as polygon from registered soil map and converted into raster; the rating has been given based on susceptibility of soil type for occurrence of landslides.



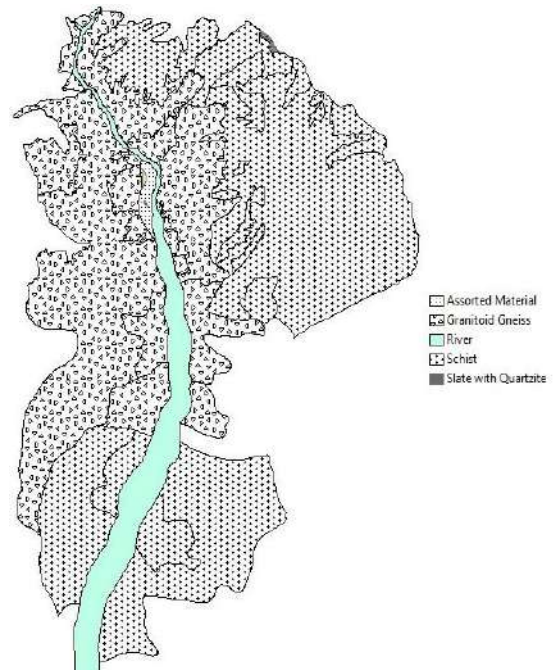
4. (a) Slope degree map



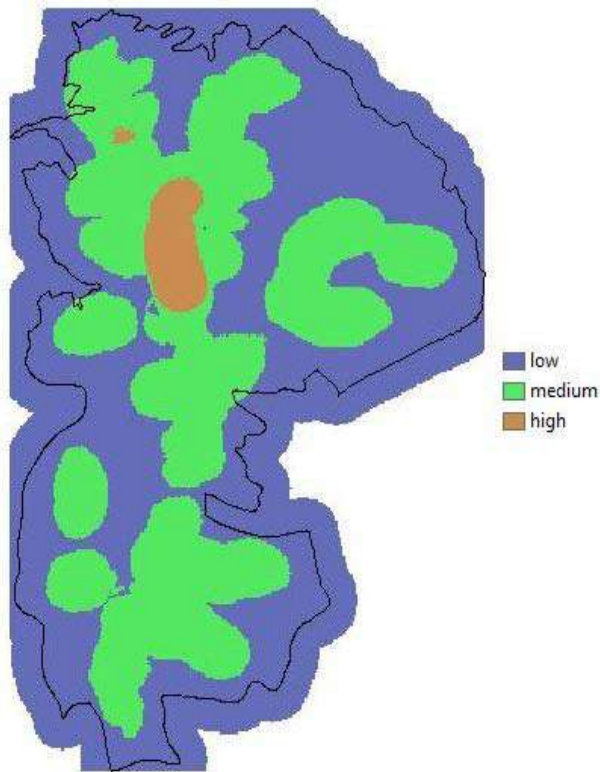
4. (b) Aspect map



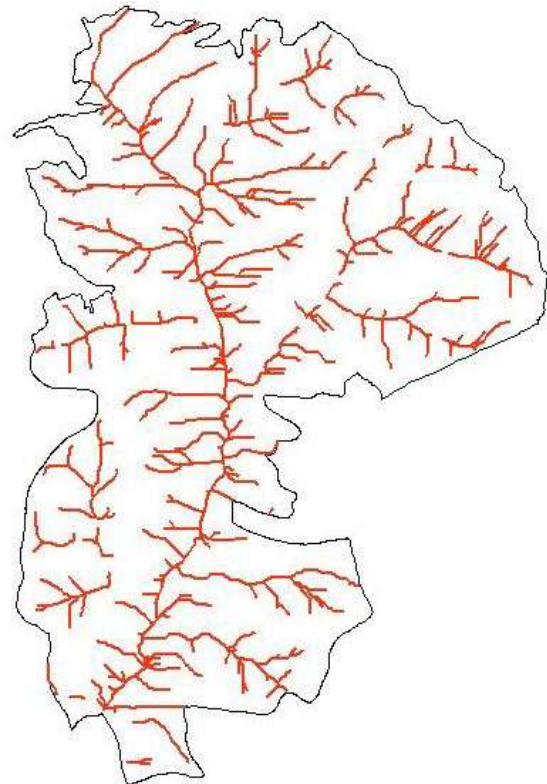
4. (c) Structural map



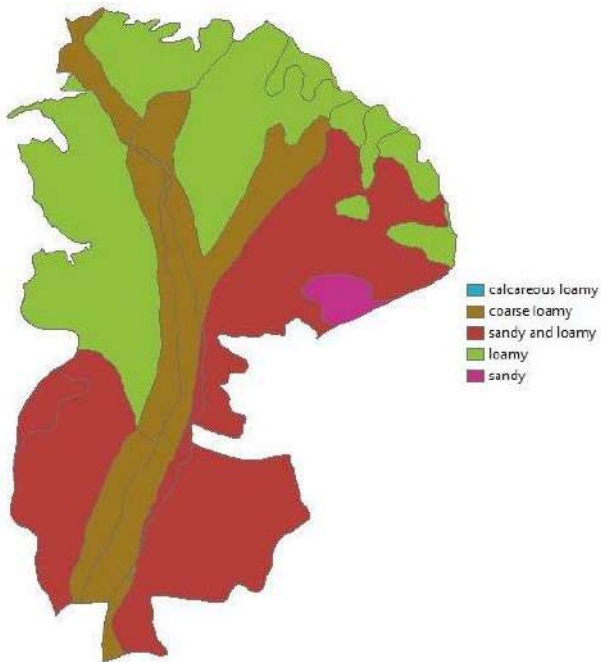
4.(d) Lithology map



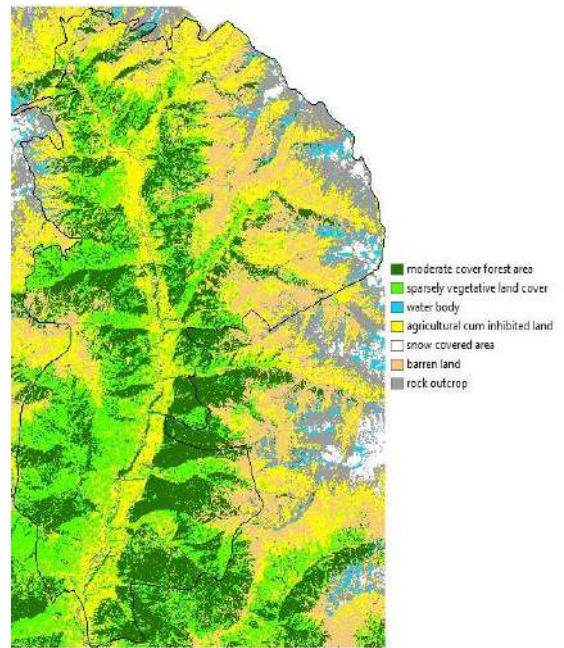
4.(e) Drainage map



4.(f) Stream network



4.(g) Soil map



4.(h) Landuse/landcover map

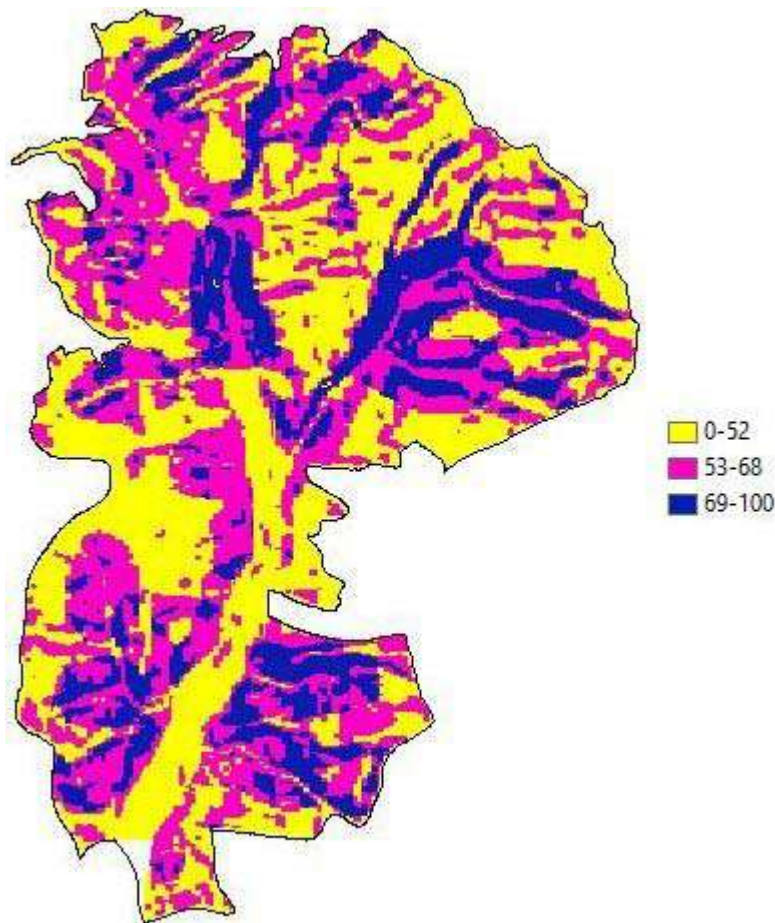


Fig. 5 Final landslide hazard zonation map

## CONCLUSION

The output map is categorized into three classes low, medium and high risks of landslide in study area. This study has focused an application of GIS and AHP in landslide susceptibility zonation mapping. In this study, weighted rating approach was carried out using arithmetic overlay analysis and the weights are calculated using online AHP calculator. The resulting map is classified into three classes low, medium and high risks of landslide in study area fig.5. The percentage wise classification of the study area has been divided into three different regions. From 0-52% chances of low landslide hazard are there, from 53-68% chances of medium landslide hazard are there and from >68% chances of high landslide hazard are there.

## REFERENCES

- Bhargava, O. N., and Bassi, U. K. (1994) "The crystalline thrust sheets in the Himachal Himalaya and the age of amphibolite facies metamorphism". *J Geol Soc Ind*, 43(4), 343–352.
- Choubey, V. M., Mukherjee, P. K., Bajwa, B. S., and Walia, V. (2007) "Geological and tectonic influence on water–soil–radon relationship in Mandi–Manali area, Himachal Himalaya" *Envir geo*, 52(6), 1163–1171.
- Kayastha, S. L. (1964) "The Himalayan Beas Basin: A Study in Habitat, Economy, and Society". Banaras Hindu University.
- Mehta, B. S., Parti, R. A. M. A. N., and Sharma, R. K. (2010) "Landslide Hazard Analysis and Zonation on National

- Highway-21 from Panasra to Manali, HP, India” *Internat. Jour. Earth Sci. Engg*, 3(3), 376-381.
- Richards, J. A., and Jia, X. (1999) “Error correction and registration of image data. In Remote sensing digital image analysis” *Springer, Berlin, Heidelberg* 39–74.
- Sah, M. P., and Mazari, R. K. (2007) “An overview of the geoenvironmental status of the Kullu Valley, Himachal Pradesh, India” *Journal of Mountain Science*, 4(1), 003–023.
- Saha, A. K., Arora, M. K., Csaplovics, E., and Gupta, R. P. (2005) “Land cover classification using IRS LISS III image and DEM in a rugged terrain: a case study in Himalayas” *Geocarto International*, 20(2), 33–40.
- Shanker, R. A. V. I., and Dua, K. J. S. (1978) “On the existence of a tear fault along upper Beas valley, District Kulu, Himachel Pradesh, and its bearing on the thermal activity” *Himalayan Geology*, 8(1), 466–472.
- Sharma, R. K., and Mehta, B. S. (2012) “Macro-zonation of landslide susceptibility in Garamaura-Swarghat-Gambhar section of national highway 21, Bilaspur District, Himachal Pradesh (India)” *Natural hazards*, 60(2), 671–688.
- Sharma, R. K., Mehta, B. S., and Jamwal, C. S. (2013) “Cut slope stability evaluation of NH-21 along Nalayan-Gambhrola section, Bilaspur district, Himachal Pradesh, India” *Natural hazards*, 66(2), 249270.



## **Influence of silica from rice husk ash on swelling and shrinkage behavior of different lake soils in Hyderabad**

**P.Pradeep Kumar<sup>1</sup> and R. Sandhya Rani<sup>2</sup>**

<sup>1</sup>Associate Professor, Department of Civil Engineering, Anurag Group of Institutions, Hyderabad;  
e-mail:ppkumar1985@gmail.com, Corresponding Author

<sup>2</sup>Associate Professor, Department of Civil Engineering, MVSR Engineering College, Hyderabad;  
e-mail: sandhyaupendar@gmail.com

### **ABSTRACT**

Urbanization and growth in population have been the well-known reasons for using expansive soils for the constructions, although they are considered as problematic soils for stability of infrastructure on them. Identification of swell/shrink behavior of expansive soils and methods reduce them is one of the important aspect of study to achieve the accurate assessment of expansive soil on foundations. Recent studies of using environmental waste like rice husk ash, fly ash etc. rice husk ash is one of the byproduct of brick industry where rice husk is used as fuel for burning bricks. For improving the properties of expansive soil will enable to reduce pollution in the current study rice husk treated with HCL acid solution burnt above 400 degrees in furnace produces silica which is mixed with expansive soils from different lakes to study the swelling and shrinkage behaviour. The swelling behaviour of for lake soils found to reduce with addition of silica. The influence silica on liquid limit, plastic limit and plasticity index has been studied .

**KEYWORDS:** silica, rice husk, swelling soils, liquid limit, plastic limit, plasticity index.

### **INTRODUCTION**

Expansive clays exist in many places in the world, being particularly noticeable recently in some Asian countries such as India (Katti et al., 2002; Shelke and Murty, 2010), China (Rama swamy and Anirudhan, 2009), Bangladesh (Siddique and Hossian, 2013), Indonesia (Java, Sumatra, and Sulawesi) (Bukit et al., 2013), and Thailand (Sawang suriya et al., 2011). They were often formed from volcanic ashes by in-situ alteration through hydrothermal processes. Expansive clays' features, the significant volumetric expansion upon wetting and shrinkage upon drying, are a very common cause of problems which have long been recognised in these clays because they could cause failure of structures constructed above them (Louafi and Bahar, 2012; Puppala et al., 2013; Lim et al., 2013). The damages are mainly on building foundations (Dasgupta, 2013), slopes (Zhan et al., 2006), roadway subgrades (Muntohar, 2006), highways, airports seaports and other residential buildings (Ramadas et al., 2012).

Because of the variation of water content or suction in the ground, expansive clays experience changes in volume. Such volume changes and resulting shrink-swell movements often distress the infrastructure that is not designed to resist those swelling pressures or forced movements (Sudjianto et al., 2011). Shrinkage characterisation of expansive clays was attempted by Puppala et al. (2006), among others, on natural and stabilised expansive clayey soils using two different measurement methods, manual and digital imaging which focused on linear and three dimensional volumetric shrinkages.

The swelling pressures depend on the loading and wetting conditions as a consequence of the different microstructure changes that occur under different conditions (Wang et al., 2012). Wetting of expansive clays causes such a great uplift force that suppressing their actions on structures purely by mechanical means (with piles and rigid linings, for example) is not a realistic option. An ultimate countermeasure would be a total replacement of problematic expansive clays with non-expansive ones. However, it will be more practical and cost-effective to alleviate the expansive characteristics by mixing the clays in problem with less active, non-expansive soils at an appropriate ratio, thus limiting the amounts of both newly purchased soils and surplus soils that would be generated upon full replacement. If added soils have a cementing effect, it is considered to be more advantageous in restricting the swelling. This project focuses on the 'diluting' effects of adding a non-expansive clay on expansive characteristics of an expansive clay, while the authors' ongoing research also considers cementation as an additional variable.

This study attempts to show and characterise the influence of the Silica content on physical and mechanical properties of the swelling clay by paying particular attention to its effect on swelling and shrinkage potential. To approach the above objectives, different lake soils in the Medchal Region are tested, by Adding Silica in different percentages such as 0%, 0.5%, 1%, 2% to know the behaviour of different lake soils, Namely Bowrampet, Bachupally, Pochampally, Dundigal in the Region of Medchal District. A number of experiments were performed on both physical and mechanical properties of the natural lake soils, including the Atterberg limits, specific gravity, Sieve

Analysis, swelling and linear shrinkage behaviour.

**MATERIALS:**

**Soils:**

To know the shrinkage and swelling behaviour of lake soils, which are collected from different lakes namely Bowrampet, Bachupally, Pochampally, Dundigal. These lakes are located in Medchal district Region.

**Silica:**

The silica particles which are produced from rice husk treated HCL and burned t 600 degrees.

**Results and Discussion:**

The soil samples collected from various lakes from medchal region, Hyderabad. Swell index test has been performed on all the soil samples. It has been found that all the samples have found to be low swell soils except Bowrampet sample which is moderate expansive soil. The swell index of soils is gradually decreased with increasing of silica particles content.the results indicating decreasing of swell index has been shown in the Fig 1. The swell index of Bowrampet sample is found to be 8.33% is decreased, at 2% of adding silica particles with respect to 0% adding of silica to the soil sample. The swell index of Bachupally sample is found to be 9.6% is decreased, at 2% of adding silica particles with respect to 0% adding of silica to the soil sample. The swell index of Pochampally sample is found to be 11.03% is decreased, at 2% of adding silica particles with respect to 0% adding of silica to the soil sample. The swell index of Dundigal sample is found to be 11.14% is decreased, at 2% of adding silica particles with respect to 0% adding of silica to the soil sample.

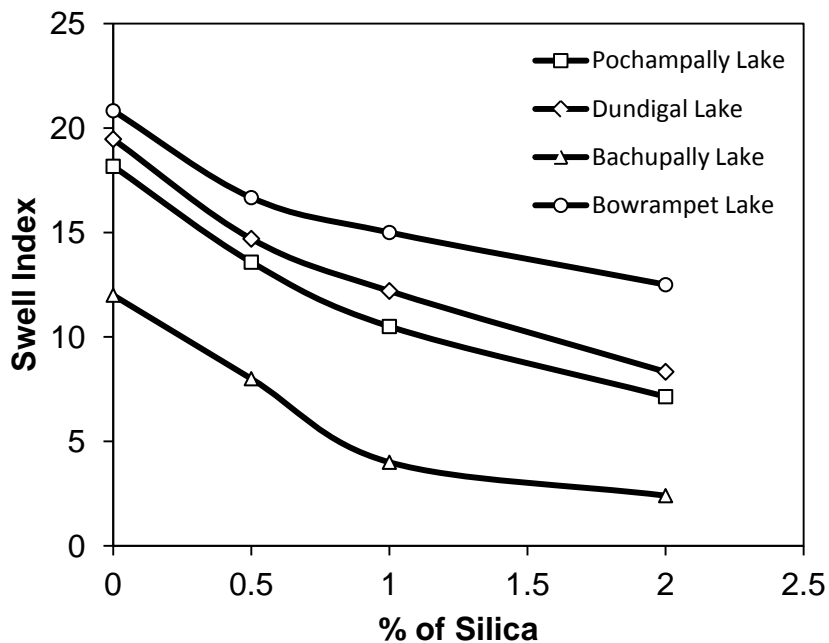
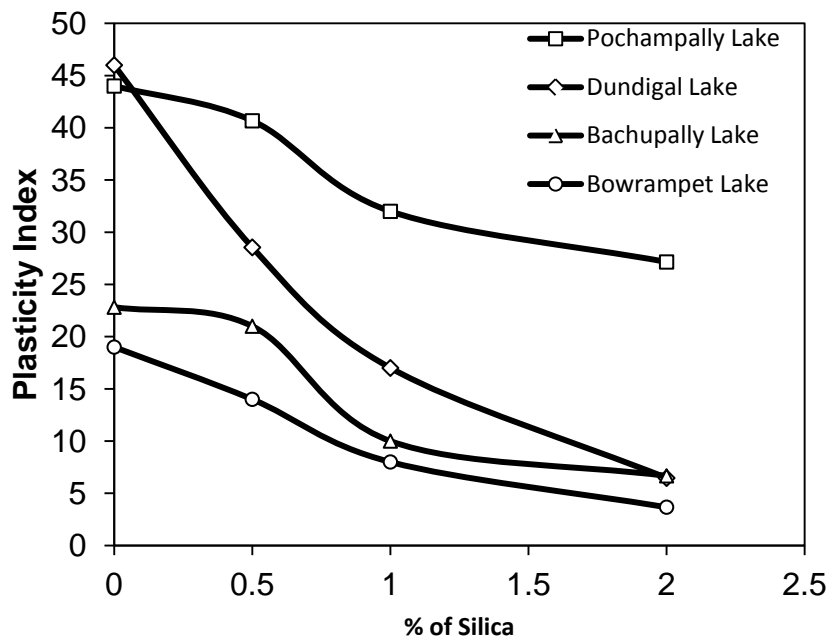


Fig.1. Swell Index versus percentage of Silica of Different Lake Soils.



**Fig.2. Plasticity Index versus percentage of Silica of Different Lake Soils.**

The plasticity index of soils is gradually decreased with increasing of silica particles content. The plasticity index of Bowrampet sample is found to be 15.33% is decreased, at 2% of adding silica particles with respect to 0% adding of silica to the soil sample. The plasticity index of Bachupally sample is found to be 16.15% is decreased, at 2% of adding silica particles with respect to 0% adding of silica to the soil sample. The plasticity index of Pochampally sample is found to be 16.85% is decreased, at 2% of adding silica particles with respect to 0% adding of silica to the soil sample. The plasticity index of Dundigal sample is found to be 39.54% is decreased, at 2% of adding silica particles with respect to 0% adding of silica to the soil sample.

**Conclusions:**

- Rice husk which is usually used as a fuel in brick industry treated with hydrochloric acid converts in to silica. Therefore rice husk ash which is a byproduct of brick industry can be used as an admixture to improve properties swell soils.
- The swell index of Bowrampet, Bachupally, Pochampally and Dundigal soils are found to reduce by 8.33, 9.6, 11.03 and 11.14 percent respectively
- Similarly, The Plasticity index of Bowrampet, Bachupally, Pochampally and Dundigal soils are found to reduce by 15.33,16.15, 16.85 and 39.54 percent respectively

**REFERENCES**

Bukit N, Frida E and Harahap MH (2013) Preparation Natural Bentonite in Nano Particle Material as Filler Nanocomposite High Density Polyethylene. Chemistry and Materials Reserch 3(13):10-20.

Dasgupta T (2013) Geotechnical Aspects of Building on Expansive Soils. University JournalAISECT 2(4):1-6.

Katti RK, Katti DR and Katti AR (2002) Behaviour of Saturated Expansive Soil and Control Methods. Published by: A.A. Balkema, a member of Swets & Zeitlinger Publishers,Indian, pp.1.

Lim SC, Gomes C and Kadir MZAA (2013) Characterising of Bentonite with Chemical, Physical and Electrical Perspectives for Improvement of Electrical Grounding Systems. International Journal Electrochemical Science 8:11429-11447.

- Louafi B and Bahar R (2012) Sand: An Additive for Stabilisation of Swelling Clay Soils. *International Journal of Geosciences* 3(4): 719-725.
- Muntohar AS (2006) The Swelling of Expansive Subgrade at Wates-Purworejo Roadway, Sta. 8+127. *Civil Engineering Dimension* 8( 2): 106-110.
- Puppala AJ, Pathivada S, Bhadriraju V and Hoyos LR (2006) Shrinkage strain characterisation of expansive soils using digital imaging technology. *Expansive Soils, Recent advances in Characterisation and Treatment. Proceedings and Monographs in Engineering, Water and Earth Sciences* (Al-Rawas, A. A., Goosen, M. F. A). Taylor & Francis Group, London, UK, pp.258-270.
- Puppala A, Manosuthikij T and Chittoori BCS (2013) Swell and Shrinkage Characterisations of Unsaturated Expansive Clays From Texas. *Engineering Geology* 164: 1-23.
- Ramadas TL, Kumar ND and Yesuratnam G (2012) A Study on Strength and Swelling Characteristics of Three Expansive Soils Treated with CaCl<sub>2</sub>. *Academic Research Journals* 1(1):77-86.
- Ramaswamy SV and Anirudhan IV (2009) Experience with Expansive Soils and Shales in and Around Chennai. *Indian Geotechnical Society* 2(7):873-881.
- Sawangsurinya A, Jotisankasa A, Vadhanabhuti B and Lousuphap K (2011) Identification of Potentially Expansive Soils causing Longitudinal Cracks along pavement shoulder in central Thailand. *Unsaturated Soils: Theory and Practice*. Kasetsart University, Thailand, pp. 693-698.
- Shelke AP and Murty DS (2010) Reduction of Swelling Pressure of Expansive Soils Using EPS Geofoam. *Indian Geotechnical Conference, GEO trendz, December 16-18, 2010, IGS Mumbai Chapter & IIT Bombay*, pp.495-498.
- Siddique A and Hossain MA (2013) Effects of Lime Stabilisation on Engineering Properties of an Expansive Soil for use in Road Construction. *Journal of Society for Transportation and Traffic Studies* 2(4):1-9.
- Sudjianto AT, Suryolelono KB, Rifa'i A and Mochtar IB (2011) The Effect of Variation Index Plasticity and Activity in Swelling Vertical of Expansive Soils. *International Journal of Engineering & Technology* 11(6):142-148.
- Wang Q, Tang AM, Cui YJ, Delage P and Gatmiri B (2012) Experimental Study on the Swelling Behaviour of Bentonite/Claystone Mixture. *Engineering Geology* 124(1):59-66.
- Zhan TL, Ng CWW and Fredlund DG (2006) Instrumentation of an Unsaturated Expansive Soil Slope. *Geotechnical Testing Journal* 30(2):1-11.



## Effect of Marble Dust and Lime on Unconfined Compression Strength of Stabilized Marine Clay

B. Manjuladevi<sup>1</sup>, H.S.Chore<sup>2</sup>, S. Dutta<sup>3</sup> and P.Kousitha<sup>4</sup>

<sup>1</sup>Research Scholar, Dept. of Civil Engineering, Datta Meghe College of Engineering, Sector-3, Airoli, Navi Mumbai-400708, Email: mdevibala10@gmail.com

<sup>2</sup>Associate Professor, Dept. of Civil Engineering, Dr. B. R. Ambedkar National Institute of Technology, Jalandhar – 144011, Email: chorehs@nitj.ac.in, Corresponding Author

<sup>3</sup>Assistant Professor, Dept. of Civil Engineering, Datta Meghe College of Engineering, Sector-3, Airoli, Navi Mumbai -400708, Email:sus.iitbcivil@gmail.com

<sup>4</sup>Assistant Professor, Dept. of Civil Engineering, Datta Meghe College of Engineering, Sector-3, Airoli, Navi Mumbai -400708, Email: kousitha@gmail.com

### ABSTRACT

Marine clay is found widely along the coastal area and had demanded for expensive solutions in the construction of coastal highways. Marine clay has a poor supporting capacity and experience large change in volume on variations of moisture content, thereby such soils may need to be improved to make them suitable for Road construction activities. Accumulation and safe disposal of various waste materials is now becoming a major concern to the environmentalist. India has a large network of industries which are producing million metric tons of industrial waste. Marble dust is one such product from marble Industry. A range of tests that include standard Proctor tests (SPT), unconfined compressive strength (UCS) tests and micro-structural analyses by using X-ray diffraction (XRD) were conducted to investigate the properties of marine clay stabilized with stabilizers (Marble Dust and Lime) in varying proportions. From the present study, it is observed that UCS value of the stabilized marine clay has been increased by 130% on addition of 20% Marble dust and it has been improved by 297.45% for stabilized soil-Marble dust-Lime (76:20:4) mixture.

**KEYWORDS:** Marine clay, Marble dust, Lime, SPT, UCS, XRD

### INTRODUCTION

The disposal of waste materials coming out of industry now days is posing a great environmental and ecological problem. These waste materials can be effectively used in the pavement construction as they have got good potential in improving the strength of subgrade soil of pavement whereby there can be reduction in thickness of the pavement. Such construction may prove to be economical. Vast areas, particularly along the coastal are covered with thick soft marine clay deposit having very low shear strength and high compressibility. In view of development of coastal areas in recent past, large number of ports and industries are being built. The viability of land for the development of commercial, housing, industrial and transportation, infrastructure etc in urban areas is a moot question. This necessitated the use of land, which has weak strata where in the geotechnical engineers are challenged by presents of different problematic soils with varied engineering characteristics.

Continuous efforts have been made all over the world to devise ways to solve the problems of marine clay. Placement of adequate surcharge load, chemical stabilization and use of various reinforcement techniques are some of the tried and tested remedial measures to avoid problem posed by marine clay. Expansive soils cause more damage to structures, particularly light buildings and pavements than any other natural hazard, including earthquakes and floods (Jones and Holtz, 1973).

On the other hand, marble (natural stone) production world-wide was 21.7 million tons in the year of 1986; however in 1998 this amount increased to 51 million tons(DPT, 2001). Increasing demand for marble product raises the generation

of waste marble material (Muthu Kumar and Tamilarasan 2015). The proportion of marble discharged as waste during block production at the quarries is equal to 40 - 60 % of the overall production volume (Çelik 1996). In India, Rajasthan is the richest state in the country with regards to marble deposits (1100 Million Tons) both in quality and quantity. The ever increasing popularity of the marbles of Rajasthan, growing demand for finished/unfinished products, discovery of new marble deposits and growing private & public supports have led to a significant growth in Marble Industry of this State. As a result, numbers of marble quarries as well as marble processing units have significant been increased mainly during last one decade. Around 3600 marble queries/mines and 1200 marble processing (gang saws) units spread all over the 16 Districts of Rajasthan. The important regions of marble deposits are Udaipur - Rajsamand - Chittorgarh region, Makrana - Kishangarh region, Banswara - Dungarpur region, Andhi (Jaipur) - Jhiri (Alwar) region and Jaisalmer region. The marble dust gets generated from cutting and polishing of marble stone. The amount of marble slurry produced every year is in the range of 5-6 million tons (cpcb.nic).

The aim of present study is to explore the utilization of the marble dust as a stabilizing aent (in conjunction with lime) for soil subgrade material owing to economy and utilization of waste with the use of marble dust.

## **BACKGROUND**

Many literatures are available on soil improvement by the application of additives, notably cement and lime. Lately, other materials were also used as s a soil modifier. Such materials are fly ash (Indraratna *et al.* 1991, 1995, Çokça 1999), rice husk (Muntohar 1999; Muntohar and Hantoro 2000), marble dust (Okagbue and Onyeobi, 1999), and limestone ash (Okagbue and Yakubu 2000). Marble dust has very high lime (CaO) content up to 55 % by weight (Çelik and Sabah 2007; Zorluer and Usta 2003; Oates 1998; Almedia *et al.* 2007; Tegethoff 2001).

Okagbue and Onyeobi (1999) studied the potential of marble dust as a stabilizing additive to red tropical soils while they reported reduction in plasticity by 20 % to 33 %, increase in strength by 30 % to 46 % and increase in CBR by 27% to 55%. Altugsaygili (2015) investigated the possibility of utilizing waste marble dust in stabilizing clayey soils. Marble dust was added in increment of 5% up to 30% by weight. The optimum moisture content ranged between 16.5% and 15.5%. Addition of waste marble dust to the soil resulted in increase in unconfined compressive strength from 110 kPa (5% addition) to 220 kPa (30% addition).

Shyam Singh and Yadav(2014) investigated the effect of marble dust addition in varying proportions (10, 20, 30, 40, 50%) on the properties of black cotton soil. The liquid limit value decreased from 57.67% to 33.9% and shrinkage limit value increased from 8.06% to 18.39% .The differential free swell was decreased from 66.6% to 20.0%. Muthu Kumar.M and Tamilarasan (2015) observed an increase in unconfined compressive strength values by the addition of marble dust in varying percentages (5, 10, 15, 20, 25).

Dhruv Saxena (2017) studied the effects of marble powder and sand to improve the properties of Expansive soils. The clay soil was mixed with marble powder and sand from 20% to 40% and 30% to 50% respectively at an interval of 10%. The results, shows that, liquid limit, plasticity index, optimum moisture content, permeability and cohesion decreased and plastic limit, shrinkage limit, maximum dry density, California bearing ratio and angle of internal friction increased with an increase in marble powder content. From the economic analysis it was found that, marble powder up to 20% is optimum (56:24:20) for sand mixed with clayey soil which can be used in strengthening the sub grade of flexible pavements to save the cost of construction. Yilmaz and Yurdakul (2016) studied soil stabilization in the scope of utilization of waste material. Marble dust increases the geotechnical properties, such as compaction, Atterberg limits, unconfined compressive strength of the mixtures. Application of wastes dust for soil stabilization may be an efficient practice in terms of solid waste management.

## **MATERIALS AND EXPERIMENTAL PROGRAM**

### **Materials**

#### ***Soil: Marine clay***

It is collected from the JNPT (Jawaharlal Nehru Port Trust), Maharashtra State, India by approximately 50m-60m form the banks of the Uran River at a depth of 3m-3.5m. The location of the site in Google map is shown Fig.1. The index properties of soil are given in table.1.

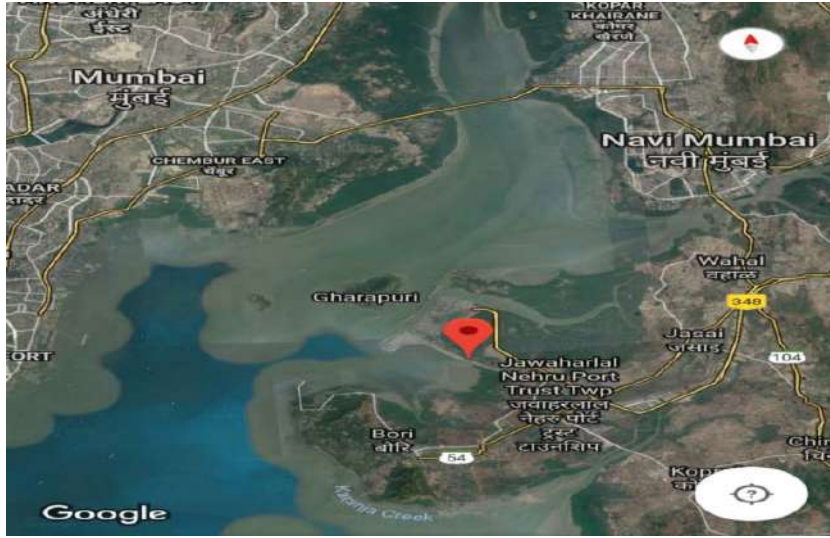


**Fig 1. Site location**

**Table 1. Physical properties of soil sample**

Sr.No.	Parameters	Value
1	Specific gravity	2.45
2	Liquid limit (%)	77
3	Plastic limit (%)	35
4	Sand (%)	3.90
5	Silt + Clay (%)	96.10
6	Soil Classification	CH
7	Soil specification as per AASHTO	A-7-5(24)
8	Optimum moisture content (%)	31
9	Maximum dry unit weight (kN/m <sup>3</sup> )	13.73

**Marble dust**

Marble dust is the by-product of the marble industry which is generated during cutting and grinding of marble .The waste generation is approximately 40% of the total marble handled per annum. It has relevance because annually about 68 million of marbles are manufactured all over the world. The disposal of marble waste on open ground creates serious threats for the public health and for the environment alongside occupying a lot of space that may be used for other purposes. Besides, marble wastes may contaminate the water and cause diseases if gets mixed with the surface water sources. It may also percolate through the soil and affects the ground water. It also causes clogging of soil by lowering its permeability and reduces the productivity of the soil (Bansal and Sidhu2016).

Rajasthan is the richest state in India with regards to marble deposits (1100 Million Tons) both in quality and quantity. Around 4000 marble mines and 1100 marble processing units spread over 16 Districts out of 33 Districts of Rajasthan. The state has 95% of the total marble processing units (cpcb.nic). The Marble dust, obtained from a marble cutting and polishing industry located in the Kishangarh region (Rajasthan), has a specific gravity of 2.65, sand sized particles74.716%,siltsized particles25.28%.

**Lime**

Lime is a general term that includes three different types, such as quick lime (CaO), hydrated Lime [Ca(OH)<sub>2</sub>] and

carbonate of lime ( $\text{CaCO}_3$ ). Quick lime and hydrated lime are commonly used in soil stabilization. Lime used for this study was locally available quick lime. The main contribution of lime to strength of soil is forming its ability decrease the apparent amount of fines in a soil causing flocculation and agglomeration of clay particles. Lime also create cementation between soil particles, higher the surface area of soil the more effective the process of lime cementation. Lime is easily available and thus it was used in our study.

### Testing Procedure

To find optimum percentage of marble dust, for stabilization of marine clay, marble dust was varied from 5 percent to 30 percent by dry weight of soil in increments of 5 percent. Standard Proctor Compaction tests, UCS tests, were conducted on these samples/mixes according to the relevant Indian Standard codes. Further the lime was added from 0 to 10% at an increment of 2% to study the effect of lime on expansive soil stabilized with optimum percentage of marble dust. Standard Proctor tests and UCS tests were conducted on these samples according to relevant Indian Standard Codes. To establish the mineralogical composition of Marine clay and marble dust, X-ray diffraction (XRD) tests were performed.

### XRD

The XRD patterns of Marine clay and Marble dust are shown in Figs. 2 and 3, respectively. The major mineral components found in the marble dust are Dolomite [ $\text{CaMg}(\text{CO}_3)_2$ ], Quartz ( $\text{SiO}_2$ ) and Calcite ( $\text{CaCO}_3$ ). The major mineral components found in the Marine clay are Quartz ( $\text{SiO}_2$ ), Andesine ( $(\text{Na,Ca})\text{Al}_{1-2}\text{Si}_{3-2}\text{O}_8$ ), Illite  $2\text{M1}(\text{K}_{0.65}\text{Al}_{2.0}[\text{Al}_{0.65}\text{Si}_{3.35}\text{O}_{10}](\text{OH})_2)$ , Kaolinite [ $\text{M}(\text{Al}_2\text{Si}_2\text{O}_5(\text{OH})_4)$ ].

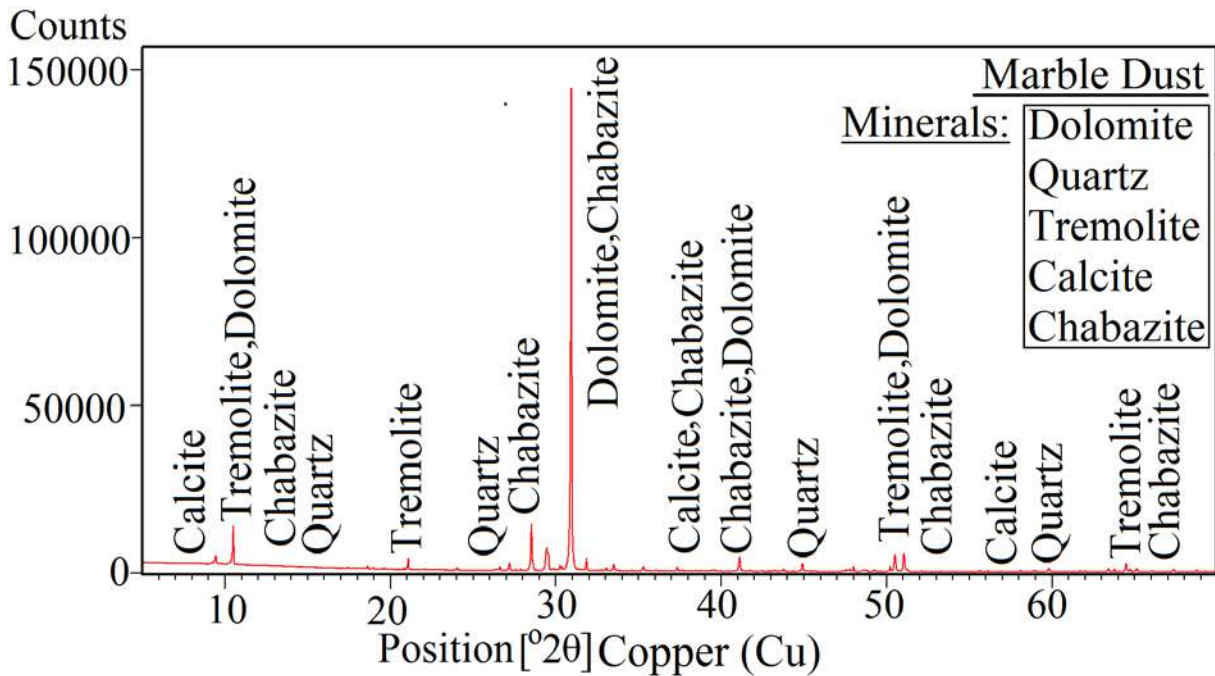


Fig. 2. X-Ray Diffraction Patterns for Marble Dust

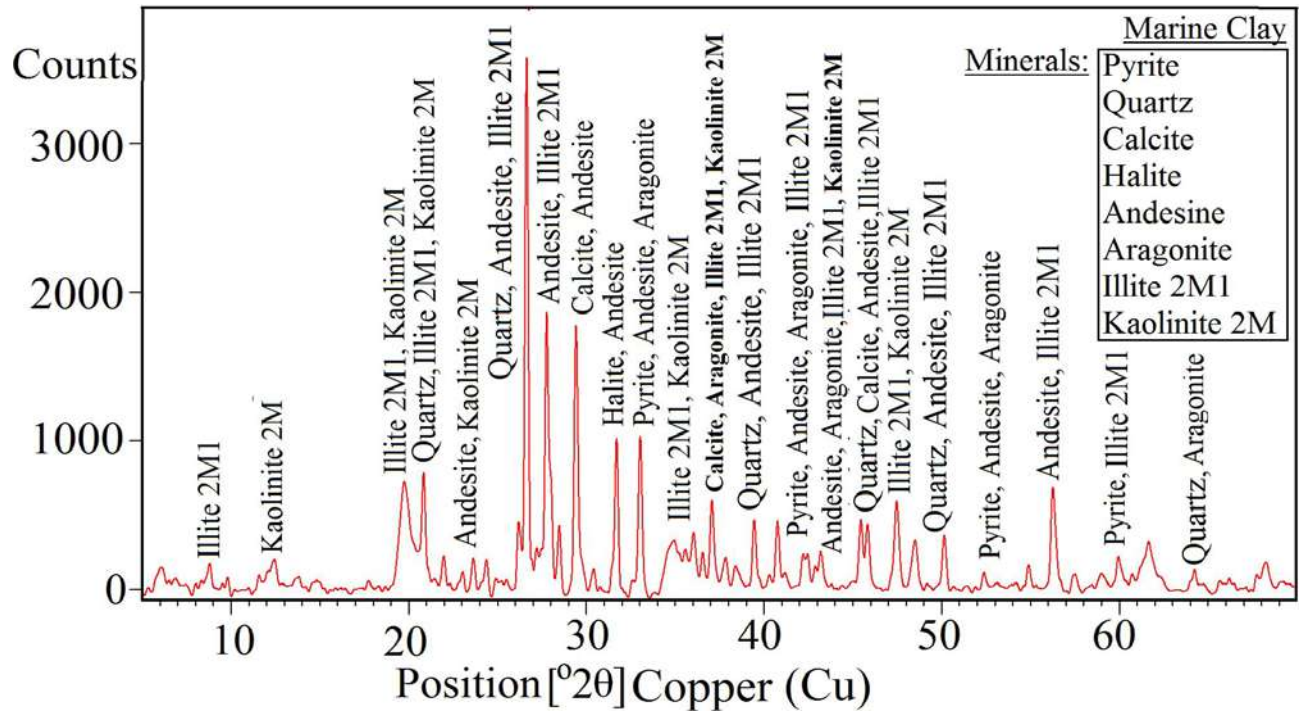


Fig 3. X-Ray Diffraction Patterns for Marine Clay

### ANALYSIS OF TEST RESULTS

The results of the Standard Proctor Test and UCS Test values of Marine Clay- Marble Dust-Lime specimens are presented in Table 2.

Table 2 Standard proctor and UCS Test Result

Marine Clay + Marble Dust + Lime	Optimum moisture content %	Maximum dry unit weight (kN/m <sup>3</sup> )	UCS value (kN/m <sup>2</sup> )	Percentage increase in strength (%)
(100+0+0)%	0.31	13.729	23.045	---
(95+5+0)%	0.3	14.249	24.644	6.936
(90+10+0)%	0.29	14.435	40.893	77.446
(85+15+0)%	0.27	14.611	48.140	108.89
(80+20+0)%	0.25	14.906	53.083	130.344
(75+25+0)%	0.245	15.102	46.179	100.383
(70+30+0)%	0.24	15.396	41.776	81.276
(78+20+2)%	0.236	15.317	87.279	278.723
(76+20+4)%	0.2029	15.808	91.591	297.446
(74+20+6)%	0.2197	15.435	85.317	270.212
(72+20+8)%	0.245	15.004	77.472	236.170
(70+20+10)%	0.282	14.101	72.569	214.893

Figure 4 shows the variation of maximum dry unit weight (MDU) of expansive soil with addition of different percentage of marble dust and lime. MDU goes on increasing irrespective of the increase in percentage of addition of marble dust and lime. MDU of soil increase from 13.72kN/m<sup>3</sup> to 15.808kN/m<sup>3</sup> for stabilized soil with 20% marble dust and 4% lime. Further, the addition of lime increases the OMC and decreases the maximum dry density. The reduction in dry density is due to the replacement of soil by lime in the mixture which has relatively lower specific gravity compared to that of the soil (Koya 2017). The increase in MDU is an indicator of the improved properties of stabilized soil.

The OMC goes on decreasing irrespective of percentage addition of Marble dust and Lime as shown in Figure 5. The OMC decreases to a value of 20.29% from 31%, when 20% marble dust and 4% lime were added to marine clay.

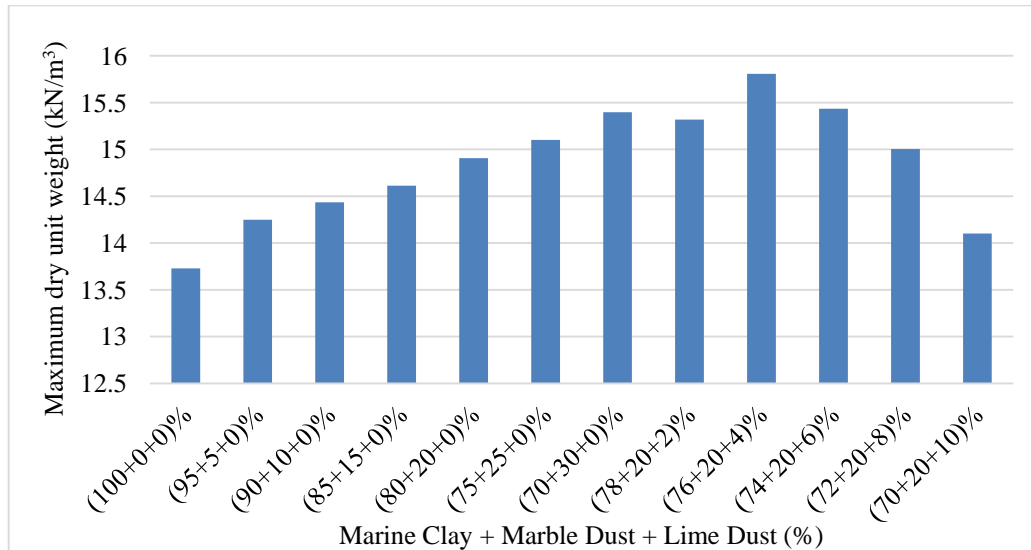


Fig. 4. Variation of MDD with % of Marble dust and Lime

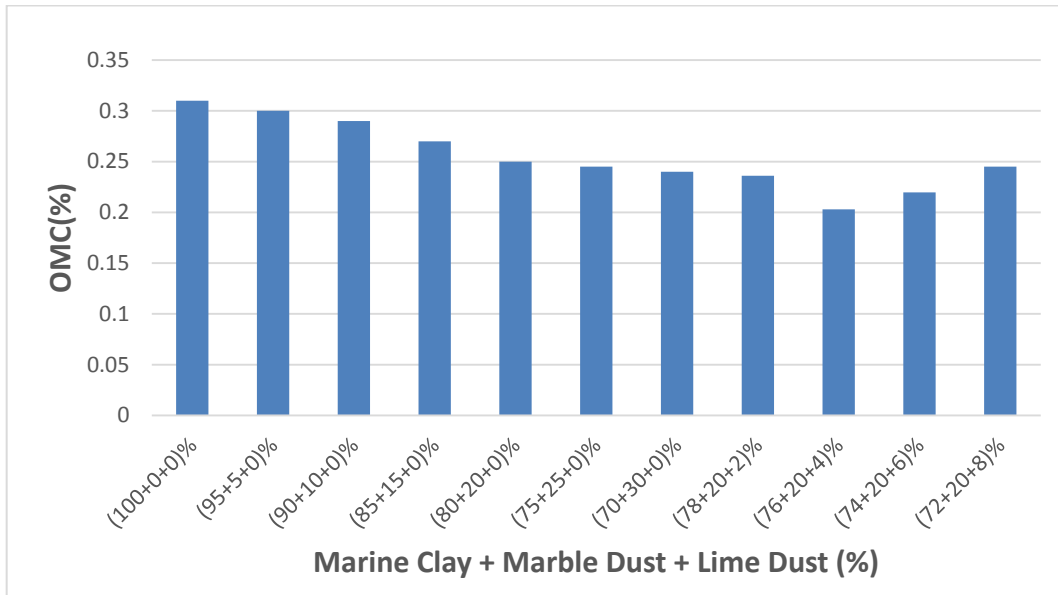


Fig.5. Variation of OMC with % of Marble dust and Lime

### Unconfined Compressive Strength

UCS test is the main test recommended for the determination of the required amount of additive to be used in the stabilization of soil. The unconfined compression test is a quick and relatively inexpensive mean to obtain undrained shear strength of cohesive soils. In this test, the confining pressure  $\sigma_3$  is kept zero. This test is commonly used in

practice because of its simplicity and it provides a basic indicator of the strength of compacted samples and is used for quality control in construction in the field. In most cases, undrained strength results from an unconfined compression test are conservative. The maximum stress measured at failure ( $\sigma_1 \text{ max.}$ ) is equal to unconfined compression strength ( $q_u$ ). For conducting the UCS test, cylindrical specimens of size 38 mm diameter and 76 mm length were prepared under static compaction at optimum moisture content and maximum dry density. The test was conducted in accordance with IS: 2720 (Part 10)-1991.

The UCS values for different combinations are presented in Fig.6. It is observed that the highest value of UCS is obtained for 20% marble dust and 4% lime content which increases from 23.045 kN/m<sup>2</sup> to 91.594 kN/m<sup>2</sup>. The increase in UCS value at 20% marble dust and 4% lime was 297.45%.

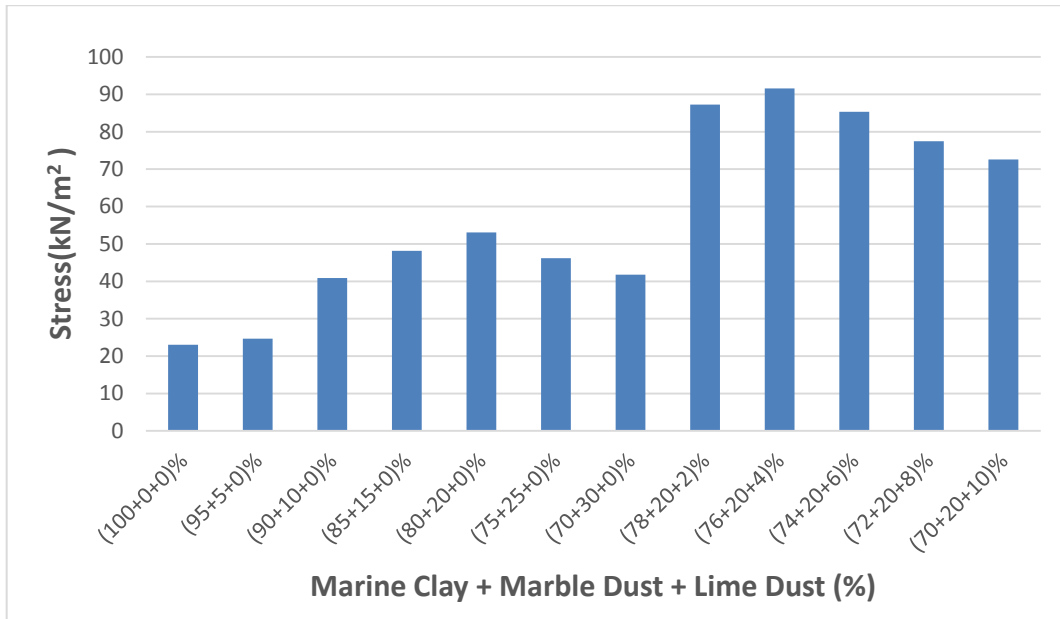


Fig.6. Variation of UCS with % of Marble dust and Lime

The initial increase in the UCS value is attributed to the gradual formation of cementitious compounds (calcium silicate hydrate) due to the reaction between the calcium carbonate present in the marble powder, soil and water (Muthu Kumar and Tamolarizine, 2015).

Table 3. Properties of the Stabilized Marine clay with an optimum of 15 % Sawdust and 4 % Lime

Sr.No.	Property	Marine Clay	MC + 20%MD	76%MC+20%MD+ 4%LIME
1	Liquid Limit (%)	80	53	49
2	Plastic Limit (%)	35	27	30
3	Plasticity Index (%)	45	26	19
4	Specific gravity	2.5	2.59	2.48
5	Optimum moisture content (%)	31%	25	20.29
6	Maximum dry density (kN/m <sup>3</sup> )	13.729	14.906	15.808
7	Maximum dry density (kN/m <sup>3</sup> ) (Monowar Hussain,2015) $\gamma_{dmax}=35.2 (PL)^{-0.25}$	14.471	15.441	15.11
8	Maximum dry density (KN/m <sup>3</sup> ) (Monowar Hussain,2015) $\gamma_{dmax}=70.44 (OMC)^{-0.497}$	12.782	14.221	15.77
9	Unconfined compressive strength(kN/m <sup>2</sup> )	23.045	53.083	91.594

However, it is very interesting to note that, further addition of marble dust beyond 20% and lime 4% led to reduction in UCS values. Several mechanisms are responsible for strength development in soil stabilized with marble dust and lime. The main generator of UCS in conjunction with the marble dust and lime admixed soils is the formation of cementitious products under Pozzolanic reaction and the additional strength is mobilized by granular packing in the matrix formed with lime acting as filler (Consoli *et al.* 2001). On other hand, the decrease in the UCS value beyond 20% marble dust and lime 4% may be due to extra marble dust that could not be mobilized for the chemical reaction which consequently occupies spaces within the sample.

The reduction in the plasticity index value is an indication of an improvement of soil property. These results are consistent with previous researcher (Shyamsingh *et al.* 2014 ; Ali *et al.* 2014 ; Amit *et al.* 2013) and are in agreement that the marble powder can be utilised as additives in soil stabilization. The soil samples were changed from having high plasticity to silty behavior, which is in terms of favorable workability (Muthu Kumar and Tamolarizine 2015).

The above study has been validated with the equation proposed by (Monowar Hussain 2015). The equation proposed by Monowar Hussain between  $\gamma_{dmax}$  and PL, with a correlation coefficient ( $R^2$ ) of 0.9 is found to be  $\gamma_{dmax} = 35.2 (PL)^{-0.25}$ , wherein  $\gamma_{dmax}$  is in  $\text{kN/m}^3$  and PL is in percent. Correspondingly, another correlation between  $\gamma_{dmax}$  and OMC with a correlation coefficient ( $R^2$ ) of 0.9 is  $\gamma_{dmax} = 70.44 (OMC)^{-0.497}$ , wherein  $\gamma_{dmax}$  is in  $\text{kN/m}^3$  and OMC is in percent.

## CONCLUSIONS

There are a lot of soft soil stabilizers that can be used to treat soft problematic soils. However, different type of soil and location play an important role in order to determine the suitability and quantity of additive that will be used.

Some of the broad conclusions deduced from the present experimental work are given below.

- The liquid limit of the marine clay is found to be decreased by 33.86% on addition of 20% marble Dust and it further decreased by 38.86% on addition of 4% of lime.
- The plastic limit of the marine clay is found to be improved by 22.85% on addition of 20% Marble dust and it further improved by 16% when 4% lime is added.
- The plasticity index of the marine clay is found to be decreased by 42% on addition of 20% Marble dust and it further decreased by 57.77% when 4% lime is added.
- The O.M.C of the marine clay is found to be decreased by 19.33% on addition of 20% Marble dust and further decreased by 34.54% on addition of 4% of lime.
- The M.D.D of the marine clay is found to be improved by 8.57% on addition of 15% Marble dust and improved by 15.14% when 4% lime is added.
- The compressive strength (UCS) value of the marine clay is found to be increased by 130.34% on addition of 20% marble dust and further, improved by 297.466% when 4% lime is added.
- For the best stabilization effect, the optimum proportion of Marble Dust-Lime is found to be 20 % - 4 %.
- The industrial waste like marble dust has a potential to modify the characteristics of expansive clay like marine clay and to be suitable in many geotechnical applications

## REFERENCES

- Agrawal. V., Gupta .M. (2011). "Expansive Soil Stabilization Using Marble Dust," *International Journal of Earth Sciences and Engineering ISSN 0974 - 5904*, Volume 04, No 06 SPL, October 2011, pp 59.
- Ali .R. Khan H and Shah A .A (2014). " Expansive Soil Stabilization Using Marble Dust and Bagasse Ash", *International Journal of Science and Research (IJSR)*, ISSN 2319-7064 Volume 3 Issue 6, PP 2812- 2816.
- Almeida N., Branco, F., Santos, J.R.(2007). "Recycling of Stone Slurry in Industrial Activities: Application to Concrete Mixtures" *Building and Environment*, Vol. 42, pp. 810–819, 2007.
- Altug.S.(2015). "Use of Waste Marble Dust for Stabilization of Clayey Soil' *ISSN 1392–1320 materials science (Medziagotyra)*. 21(4).
- Amit.V. and Singh R.R.(2013). "Utilization of marble slurry to enhance Soil properties and protect environment"

- Balasubramaniam, A. S., Kamruzzaman, A. H. M., Uddin, K., Lin, D. G., Phienwij, N. & Bergado, D. T. (1998). "Chemical stabilization of Bangkok clay with cement, lime and fly ash additives". *Proceedings of the 13th Southeast Asian Geotechnical Conference*, Taipei, Taiwan, R.O.C., pp. 253–258
- Baser O (2009), "Stabilization of Expansive Soils Using Waste Marble Dust", *Master of Science Thesis*, Submitted to Civil Engineering Department, Middle East, Technical University.
- Çelik, M.Y.(1996)., *M. S. Thesis*, Afyon Kocatepe University, *Natural and Applied Sciences*, 119 pages, 1996.
- Çelik, M.Y., Sabah, E.(2008). "Geological and Technical Characterization of İscehisar (Afyon-Turkey) Marble Deposits and the Impact of Marble Waste on Environmental Pollution", *Journal of Environmental Management*, Vol. 87, No.1, pp. 106-116,
- Central Pollution Control Board (2012) "Guidelines for Management and Handling of Marble Slurry generated from Marble Processing Plants in Rajasthan (Final Draft)," New Delhi, India.
- Chu J, Chang M.F, Choa V (2002). "Consolidation and permeability properties of Singapore marine clay". *J Geotech Geoenviron Eng ASCE*, 128(9):724–732.
- Çokça, E(2001), "Use of Class C Fly Ashes for the Stabilization of an Expansive Soil", *Journal of Geotechnical and Geoenvironmental Engineering*, Vol. 127, No.7, pp. 568-573.
- Consoli, N. C., Prietto, P. D. M., Carraro, J. A. H., and Heineck, K. S. (2001). "Behavior of compacted soil-fly ash-carbide lime-fly ash mixtures." *J. Geotech. Geoenviron. Eng.*, 10.1061/(ASCE)1090-0241,127:9(774), 774–782.
- Hitesh Bansal and Gurtej Singh Sidhu(2016), "Influence of Waste Marble Powder on Characteristics of Clayey Soil", *International Journal of Science and Research (IJSR)*, Volume 5 Issue 8.
- Hussain. M. and Dash S.K (2015), "The influence of lime on the compaction behaviour of soils", *Journal of Environmental Geotechnics*.
- Hyde, AFL, Yasuhara, K, and Hirao, K (1993). "Stability Criteria for Marine Clay Under One Way Cyclic Loading," *J Geotech Eng, ASCE*, Vol 119, No 11, pp 1771–1889.
- İpek, T. "Stabilization of Expansive Soils Using Lime, Cement and Fly Ash, *M.S. Thesis, METU, Turkey*, 119 pages, 1998.
- IS-2720 (Part X)(1991). "Methods of test for soils, Laboratory determination of Unconfined compressive strength(UCS)." *Bureau of Indian Standards*, New Delhi, India.
- J. Environ. Res. Develop.* Vol. 7, No. 4A, pp 1479- 1483.
- Jijo.J.and Pandian.K.(2015). "Soil Stabilization as an Avenue for Reuse of Solid Wastes: A Review" *Acta Technica Napocensis: Civil Engineering & Architecture* Vol. 58, No. 1.
- Jones, D. E., and Holtz, W. G (1973). "Expansive Soils - the hidden disaster, Civil Engineering, *ASCE* 43(8), pp. 49-51.
- Muntohar, A. S(1999). "Behaviour of engineering properties of the clay blended with LRHA (lime rice husk ash)". *Research Rep. from Grant, Muhammadiyah Univ. of Yogya-Karta, Yogya-Karta, Indonesia*.
- Muntohar, A.S. and Hantoro(2000). "Influence of rice husk ash and lime on engineering properties of clayey subgrade" *Electronical Journal of Geotechnical Engineering*, 2000.
- Muthu Kumar M and Tamolarizine V.S.(2015). "Experimental Study on Expansive Soil with Marble Powder", *International Journal of Engineering Trends and Technology*, Volume 22 Number 11, 504- 507.
- Noohu.K.Nusly(2017). "Effect of Lime on Geotechnical Properties of Marine Clay" *International Journal of Innovative Research in Science, Engineering and Technology An ISO 3297: 2007 Certified Organization , National Conference on Technological Advancements in Civil and Mechanical Engineering – (NCTACME'17)* 17th - 18th , Volume 6, Special Issue 4, pp85-88.
- Oates, J. A. H(1998). "Lime and Limestone", Wiley-VCH, Weinheim.
- Okagbue, C. O and Yakubu, J.A (2000). "Limestone ash waste as a substitute for lime in soil improvement for engineering construction", *Bulletin of Engineering Geology and the Environment*, Vol. 58, No.2, 107-113..
- Okagbue, C. O., and Onyeobi(1999). "Potentials of marble dust to stabilize red tropical soils for road construction, *Engineering Geology*, 53, pp. 371-380, 1999.
- Palaniappan, K. A and Stalin, V. K. (2009). "Utility effect of solid wastes in problematic soils", *International Journal of Engineering Research and Industrial. Applications*, 2(1), pp 313-321.
- Sabat, A.K (2012). "Stabilization of expansive soil using waste ceramic dust", *Article in Electronic Journal of Geotechnical Engineering*, Vol. 17, pp 3915 -3926.
- Sabat, A.K., and Nanda, R.P. (2011). "Effect of marble dust on strength and durability of rice husk ash stabilised expansive soil", *International Journal of Civil and Structural Engineering*, Vol.1 (4), pp 939-948.

- Saxena. D. (2017), "Effects of Marble Powder and Fine Sand on Properties of Expansive Soil", *International Journal of Engineering Trends and Technology (IJETT)* – Volume 52.
- Singh.P.S and Yadav R K (2014). "Effect of marble dust on index Properties of black cotton soil", *Int. J. Engg. Res. & Sci. & Tech, ISSN 2319 -5991*, Vol. 3, No. 3, pp, 158 – 163.
- Swami, B. L.(2002). "Feasibility study of marble dust in highway sector", *Highway Research Bulletin*, 67, pp. 2736.
- Tegethoff, F.W, Rohleder.J. and Kroker(2001). "Calcium Carbonate: From the Cretaceous Period into the 21st Century; Birkhauser Verlag" *Boston, MA, USA*, p. 342.
- Yilmaz.F.and Yurdakul. M. (2016), "Evaluation of Marble Dust for Soil Stabilization", *Special issue of the 3rd International Conference on Computational and Experimental Science and Engineering (ICCESEN 2016)*, Vol. 132.



## IMPROVEMENT IN ENGINEERING BEHAVIOUR OF EXPANSIVE SOILS TREATED WITH DISCRETE FIBRES – A REVIEW

*Pavan Kumar Meena<sup>1</sup>, Ashwani Jain<sup>2</sup>*

<sup>1</sup>M.Tech student, Department of Civil Engineering, National Institute of Technology Kurukshetra, Haryana-136119, India, Email: pavan\_31702214@nitkkr.ac.in

<sup>2</sup>\*Professor, Department of Civil Engineering, National Institute of Technology, Kurukshetra, Haryana-136119, India, Email:ashwani.jain@nitkkr.ac.in, Corresponding Author

### ABSTRACT

The black cotton soil is expansive clay with high potential of shrinkage and swelling. There are many materials and methods by which we can improve the properties to counteract the swelling-shrinkage problem of expansive soil. Some of these include physical alteration, sand cushioning, cohesive non-swelling soil (CNS) layer, belled pier, under-reamed pile, granular pile anchor and chemical stabilization. Many other innovative ideas have been presented and implemented successfully. Some of the techniques include stabilization using admixtures, cement waste, lime, fly ash, rice husk, and reinforcing of soil with natural fibres and synthetic fibres. This paper presents a critical review the history, benefits and possible execution problems of using a different type of natural and synthetic fibres, as randomly oriented and uniformly oriented soil reinforcement, to reduce swelling and shrinkage characteristics of expansive soils.

Keywords: expansive soil, stabilization, natural and synthetic fibres, swell potential

### INTRODUCTION

As a consequence of their inherent characteristics including low strength, high compressibility and a high potential for swelling and shrinkage, expansive soil is often characterized as an unsuitable construction material for civil engineering applications. The soil was not suitable in the present form for construction due to following reasons-Poor workability for compaction, High compressibility and leading to settlement, Inadequate shear strength for required slop stability. Expansive soils usually exhibit complications more for lightly loaded structures than moderately loaded structures. Such soil often requires modification to satisfy design criteria prior to application stabilization of expansive soil can be achieved through two approaches i.e. chemical and mechanical techniques. Therefore, soil reinforcement is defined as a technique to improve the engineering characteristics of soil in order to develop parameters such as shear strength, compressibility, density and hydraulic conductivity. A reinforced soil is a composite material in which tension-resisting elements are embedded in a soil mass, which is weak in tension.

Chemical techniques mainly involve the addition of chemical binders (i.e. cement, lime and polymers) to the soil, thereby amending the soil fabric heave and induced strength. The mechanical approaches make use of compaction with the aid of reinforcement. Alternate stabilization techniques capable of replacing or minimizing the use of traditional cementitious agents have been highly encouraged. The use of fibres may be regarded amongst the most well received positions in this context. However, fibre geometrical properties, mainly defined in terms of aspect ratio (i.e. fibre length to the diameter/width ratio) has also been reported to portray an equally important role in yielding an effective stabilization scheme. With respect to stiffness, steel and fibreglass reinforcements in the form of strips and bars having a high modulus of elasticity are often categorized as ideally inextensible reinforcement, while the geosynthetic and geo-natural reinforcements, including plants roots, having relatively low modulus of elasticity, are considered ideally extensible reinforcement.

Several laboratory tests and some field tests have been used to investigate the behaviour of fibre-reinforced soil. Some of these tests are, Direct shear test, static and cyclic triaxial compression tests, Unconfined compression test, Compaction test, Hydraulic conductivity test, Consolidation test, California bearing ratio test, Plate load test, Brazilian indirect/Splitting tensile strength test, Durability test, Ring shear test, Torsional shear test, Bender column test, Resonant column test, Flexural strength test, Fibre pull-out test.

### Soil Reinforcement with fibres

Soil reinforcement is not a new technique it is used since prehistoric time. Soil reinforcement is often used nowadays in the form of continuous geosynthetic or geo-natural reinforcement inclusion. The effect of fibre content on dry density for any particular fibre content, an increase in fibre content causes in reduction in dry density. This is due to the

reduction of average unit weight of the solids in the soil fibre mixture. Soil are strong in compression but weak in tension, therefore to improve the tensile strength some fibres were mixed in to the soil either by uniformly distribution or by randomly orientation. Fibres in soil are works as reinforcement and modify the properties of soil. Fibre used in reinforcement of three types natural, synthetic. Natural fibres are i.e. coir fibre, jute fibre, bamboo fibre, sisal fibre, cotton fibre, flax fibre, manila fibre, palm fibre, grasses wood chips etc., some of these natural fibres are biodegradable so to we are using some additives and chemicals. Human and animal hairs are also available as natural fibres. The different fibres are presented in Figs. 1-10.

		
Fig.1 Jute Fibre	Fig.2 Palm Fibre	Fig.3 Sisal Fibre
		
Fig.4 Coir Fibre	Fig.5 Cotton Fibre	Fig.6 Grass Fibre
		
Fig. 7 Polypropylene Fibre	Fig. 8 Metal Fibre	Fig. 9 Glass Fibre
		
Fig. 10 Carbon Fibre		

Synthetic fibres are i.e. polypropylene fibre, Glass fibre, polyester fibre, polyethylene fibre, nylon fibre, carbon fibre, metal fibre etc. there are several environmental factors that are affect the durability of fibres i.e. UV rays, heat, oxygen

and humidity, chemicals etc.

## REVIEW OF LITERATURE

**Sajal pachauri (2016)** discuss the use of synthetic fibre and natural fibre and their comparison. In this study, the strength characteristics. of the soil coir fibre composite have been compared with the same soil reinforced with synthetic polypropylene fibre. Study shows that fibre inclusion increased not only the peak strength of the samples but also its ductility. It was also noted that water content of 5% dry of optimum moisture content showed the maximum strength. Moreover, soil samples reinforced with coir fibres and showed higher strength characteristics than polypropylene reinforced soil sample. This study concludes that coir as natural fibre reinforcement could be successfully employed in field where short term and effective fibre reinforcement is designed.

**Panpan Guo (2017)** Jute is mainly eco-friendly fibre that is used for producing porous textiles which are widely used for filtration, drainage and soil stabilization. The study presents discussion related the fibre content, fibre length, fibre orientation, water content, and dry density. The direct shear strength, cohesion and strength ratio increases with increasing fibre content until reaching a fibre content of 0.6% after which further increases in fibre content tends to reduce fibre reinforcing effects due to replacement of soil particles by too many fibres.

**Aggarwal and Sharma (2010)** used different lengths of jute fibres in different percentages to reinforced soil. Bitumen was used for coating fibres to protect them from microbial attack and degradation. According to their conclusion jute fibre reduces the MDD while increases the OMC. Jute fibre also increases the CBR value of reinforced soil 2.5 times of the plain soil CBR value. mortar strength is also increased by using jute fibres.

**Rajesh Prasad Shukla (2018)** Effect of various proportions of randomly oriented polyester fibre on the shear strength of expansive soil. The unconfined compressive strength of reinforced soil was determined by incorporative four fibre contacts with varying aspect ratios. In almost all the cases, maximum enhancement in the strength of the soil was achieved with fibre with an aspect ratio of 40. Peak strength of untreated soil is found at strain level of 6-8%, whereas it increases to 10-12% in reinforced soil. The rate of the increases in the soil strength is relatively large with an aspect ratio of 40 as compared to aspect ratio of 20 or 60. For a fibre content of 0.75% the unconfined compressive strength increased by approximately 1.5, 2 and 1.7 times the strength of the unreinforced soil for fibre of aspect ratio 20, 40 and 60 respectively. The strain level is also increased with an increase in fibre content. For a fibre content 0.75% the strain failure increased by 1.5 times compared to that of unreinforced soil.

**Moghal and Chittoori (2017)** Two type of synthetic fibres, fibre cast and fibre mesh, were studied by conduction one-dimensional fixed ring oedometer swell-consolidation and bar linear shrinkage tests. Three dosages and two lengths of fibres were evaluated with or without lime treatment. The results indicated that fibre cast fibres had batter swell restricting performance in the absence of lime treatment, while in the presence of lime both the fibres had similar performance in reducing swelling. Shrinkage tests results showed that irrespective of dosages levels, both the fibres had pronounced effect in reducing the liner shrinkage strain up on lime treatment. The  $C_c$  values increases with increase in fibre length. The  $C_r$  values either stayed the same or reduced with increasing fibre content depending on the absence or presence of lime. Similar behaviour was observed in  $C_r$  values with increases in fibre length. Longer fibres performed better compared to shorter fibres due to greater mobilisation of friction levels.

**Zhuang (2015)** The test results show that the maximum dry density and plasticity index of reinforced expansive soil were decreased along with the increased lime mixed rates. Liquid limit of reinforced expansive soil gradually decreased and plastic limit increased gradually and the plasticity index decreases gradually with the increasing amount of lime. Basalt fibre mixed into expansive soil can make the ductility of expansive soil improved, corresponding to the axial strain under the damage state was in the desired state with the increasing of the additional amount of the basalt fibres.

**Subba Rao (2018)** Coir fibre can be effectively used as reinforcing material but it has less durability and hence coir fibre coated with kerosene is used as reinforcement. Water absorption test were conducted on uncoated and kerosene coated coir fibres. It concludes water absorption capacity of kerosene coated coir fibre reduced by 32% as that of uncoated coir and the addition of kerosene coated coir fibre decreased MDD and increased OMC. UCC strength of kerosene coated coir fibre reinforced soil increases to about 2.5 times in comparison to that of unreinforced soil UCC strength value.

**Dang and Khabbaz (2018)** Bagasse fibre was employed in this investigation as reinforcing components for expansive soil reinforcement. The test results indicated that bagasse fibre reinforcement not only significantly improved the compressive strength, the initial deformation modulus and the shear strength of reinforced soil, but it also considerably transformed the reinforced soil behaviour from strain softening to strain hardening by curtailing the post-peak shear strength loss.

**Prabakar (2002)** outcomes shows that, sisal fibre has been chosen as the reinforced material and it was randomly included into the soil in four different percentages of fibre contents and different fibre lengths. The reinforced soil sample were subjected to compaction and triaxial compression test. Results shows that the sisal fibre reinforced soil reduces the dry density of the soil due to a low specific gravity and unit weight of sisal fibre and shear stress improved. Initial introduction of fibre into the soil causes an increase in OMC, and a further increase in both length and fibre content reduces OMC. The further increase in length of fibre fails to interlock the soil particles and therefor, soil-fibre particles do not act as a single coherent matrix. The shear stress of reinforced soil is also increased with increase in confining pressure. The value of cohesion is increased due to the inclusion of sisal fibre.

**Gao et al. (2015)** Effects and mechanism of carbon fibre reinforced soil in which carbon fibre is mixed into soil and water was added in soil to achieve the optimum soil water content. Unconfine compression test were performed on soil sample and results showed that the addition of carbon fibre to the soil improve the UCS, plasticity and brittle failure of soil. The strength increases in starting then decreases with further increases in fibre content.

**Estabragh (2014)** Treatment of an expansive soil by mechanical and chemical techniques against swelling. In mechanical treatment, reinforcing the soil with randomly distributed fibres and chemical treatment by using cement or lime as a chemical agent. experiments on untreated and treated samples were conducted in an oedometer. The experimental programme consisted of two groups.

- The first group involved the tests on expansive soil reinforced with randomly distributed fibres (mechanical improvement), different percentages (0.5, 1 and 1.5%), and different lengths (10, 20 and 30 mm), in bar shape or tape shape.
- The second group that were mixed with different percentages (5, 8 and 10%) of cement or lime (chemical improvement) for different curing times.
- The results showed that, compared with the natural soil, the swelling behaviour (swelling potential and swelling pressure) was reduced by adding randomly mixed discrete fibres. The reduction of swelling potential and swelling pressure is also a function of percentage, length and type of fibre (bar or tape shape). The results also indicated that the addition of cement and lime caused reduction in swelling potential and its effect was considerably more than the influence of fibre.

**Seda et al. (2007)** shows that, the effect of adding small particles of waste tire rubber on the swelling potential of an expansive soil was evaluated. The index properties and compaction parameters of the rubber, expansive soil, and expansive soil-rubber (ESR) mixture tested were determined. The ESR mixture is more compressible than the untreated soil, both the swell percent and the swelling pressure are significantly reduced by the addition of rubber to the expansive soil. Atterberg limits and plasticity indices of the soil and ESR mixture are very similar. The optimum water contents of the soil and ESR mixture are the same. The addition of 20% rubber by weight to the soil decreases the maximum dry unit weight of the ESR mixture due to the lower specific gravity of the rubber material. ) The addition of 20% waste tire rubber by weight to the soil increases the compressibility of the ESR mixture but significantly reduces both its swell percent and swelling pressure.

**Viswanadham et al. (2008)** study performed on expansive soil reinforced with geo-fibres, discrete and randomly distributed geo-fibres are useful in restraining the swelling tendency of expansive soils. Swelling characteristics of remoulded expansive soil specimens reinforced with varying fibre content and aspect ratio were studied. One dimensional swell-consolidation tests were conducted on oedometer specimens. Reduction in heave and swelling pressure was the maximum at low aspect ratios at both the fiber contents of 0.25% and 0.50%. Reinforcing expansive clay specimens with polypropylene fiber reduced heave. Heave was reduced more at lower aspect ratios than at higher aspect ratios.

## CONCLUSION

This paper will going to review the concept of using discrete fibres in soil both natural and synthetic. The addition of fibres is in different percentages by dry weight of soil and mixed into silt, clay, sand or lime and cement stabilization. All the papers listed above was conclude that strength and stiffness of soil is improved by fibre reinforcement increases with increases in aspect ratio, fibre content, fibre modulus and soil fibre surface friction.

It was observed that addition of fibre in soil increases peak strength and ductility of soil sample and decreases in settlement at the ultimate load. The maximum dry density (MDD) of the soil decreases with addition of fibre and the value of optimum moisture content (OMC) of the soil increases with increases in percentage fibre content.

On the basis above listed papers it is clearly seen that the compressive strength, CBR value, bearing capacity and safe bearing pressure increases with increases in fibre content then it decreases with further inclusion of fibres. The subject of fibre and their applications in conjunction with soils and other similar materials, such as coal ashes, mine wastes etc., is known as the fibre reinforced soil engineering, which provides cost-effective and environmentally friendly solution in a sustainable manner for several construction projects in civil engineering and some other related areas.

## REFERENCES

- Pachauri, S., Priya, M.I. and Garg, A., (2019). "Comparative Analysis of Strength Characteristics of Soil Reinforced with Coir and Polypropylene Fibres". In *Ground Improvement Techniques and Geosynthetics* (pp. 355-361). Springer, Singapore.
- Wang, Y.X., Guo, P.P., Ren, W.X., Yuan, B.X., Yuan, H.P., Zhao, Y.L., Shan, S.B. and Cao, P., (2017). "Laboratory investigation on strength characteristics of expansive soil treated with jute fiber reinforcement". *International Journal of Geomechanics*, 17(11), p.04017101.
- Aggarwal, P., & Sharma, B. (2010,September). "Application of jute fiber in the improvement of subgrade characteristics". In *Proc of int conf on adva in civ eng, Trabzon, Turkey* (pp. 27-30).
- Parihar, N.S., Shukla, R.P. and Gupta, A.K.,( 2018). "Shear Strength of Medium Plastic Expansive Soil Reinforced with Polyester Fibers". *Slovak Journal of Civil Engineering*, 26(2), pp.1-8.
- Moghal, A.A.B., Chittoori, B.C., Basha, B.M. and Al-Mahbashi, A.M., (2018). "Effect of polypropylene fibre reinforcement on the consolidation, swell and shrinkage behaviour of lime-blended expansive soil". *International Journal of Geotechnical Engineering*, 12(5), pp.462-471.
- Zhuang, X.S. and Yu, X.Y., (2015). "Experimental Study on Strength Characteristics of Lime-basalt Fiber Reinforced Expansive Soil". In *Applied Mechanics and Materials* (Vol. 744, pp. 495-498). Trans Tech Publications.
- Ramasubbarao, G.V., (2014). "Strength behaviour of kerosene coated coir fiber-reinforced expansive soil". *Facta universitatis-series: Architecture and Civil Engineering*, 12(2), pp.113-120.
- Dang, L.C. and Khabbaz, H., (2018). "Enhancing the Strength Characteristics of Expansive Soil Using Bagasse Fibre". In *Proceedings of China-Europe Conference on Geotechnical Engineering* (pp. 792-796). Springer, Cham.
- Prabakar, J. and Sridhar, R.S., (2002). "Effect of random inclusion of sisal fibre on strength behaviour of soil". *Construction and Building Materials*, 16(2), pp.123-131.
- Gao, L., Zhou, Q., Yu, X., Wu, K. and Mahfouz, A.H., (2017). "Experimental study on the unconfined compressive strength of carbon fiber reinforced clay soil". *Marine Georesources & Geotechnology*, 35(1), pp.143-148.
- Estabragh, A.R., Rafatjo, H. and Javadi, A.A., (2014). "Treatment of an expansive soil by mechanical and chemical techniques". *Geosynthetics International*, 21(3), pp.233-243.
- Seda, J.H., Lee, J.C. and Carraro, J.A.H., (2007). "Beneficial use of waste tire rubber for swelling potential mitigation in expansive soils". In *Soil improvement* (pp. 1-9).
- Viswanadham, B.V.S., Phanikumar, B.R. and Mukherjee, R.V., (2009). "Swelling behaviour of a geofiber-reinforced expansive soil". *Geotextiles and Geomembranes*, 27(1), pp.73-76.



## A REVIEW OF THE IMPROVEMENT IN SOIL BEHAVIOUR USING DIFFERENT SOIL REINFORCEMENT TECHNIQUES

*Sumit Rawat<sup>1</sup>, Ashwani Jain<sup>2</sup>*

<sup>1</sup>M. Tech student, Department of Civil Engineering, National Institute of Technology Kurukshetra, Haryana-136119, India, Email: sumitrawt110693@gmail.com

<sup>2</sup>Professor, Department of Civil Engineering, National Institute of Technology, Kurukshetra, Haryana-136119, India, Email: ashwani.jain@nitkkr.ac.in, Corresponding Author

### ABSTRACT

Since from the dawn of civilization, soil improvement is a major part of concern in the construction activities. Engineers from the past have endeavored to find solution to many soil-related distresses such as settlement, slope failures, slides, and soil erosion. Soil reinforcement is a technique where soil properties improve upon its reinforcement with natural or synthetic additives. Reinforcement of soils can be done with different type of fibres, e.g. with natural fibres like Jute, Sisal, coir, palm etc. and synthetic fibres like as polypropylene, glass, nylon etc. Development of Geosynthetics over the years helped technologists in manufacturing various types of textiles to tackle from such kind of problems. This paper reviews the literature for different soil reinforcement techniques used to improve engineering performance of soil. This paper focuses on use of fibres as geo reinforcement bed between the layers of a soil mass, to fulfill this purpose various types of geo-synthetic such as geogrid, geocell, geonets etc. had been used to improve engineering behaviour of soil mass and their results been reviewed. From the literature review, it has been noticed that reinforcing soil with single or multiple layers of geotextile bed is an effective solution to various soil related problems. Moreover, synthetic geotextiles are preferred over natural geotextiles because of their non-biodegradability and durability. However, eco-compatibility and developing ecological concerns have provoked researchers and technologists to opt for natural, biodegradable alternatives for various aspects of geotechnical applications.

**KEYWORDS:** Soil Improvement; Soil Reinforcement; Natural Fibre; Biodegradable; Geotextile.

### INTRODUCTION

Soil improvement is a prime issue of concern in the construction activities due to rapid increase in urbanization and industrialization. Man, since advancement of engineering trying to overcome such problems. Development of building and other civil engineering structures on weak or soft soil is highly perilous on geo-specialized grounds because such soil is prone to differential settlements, poor shear strength and high compressibility. Soil reinforcement is considered as effective technique of ground improvement to tackle with several soil related problems. Reinforced soil is composite material formed by the contact between frictional soil & tension resisting materials such as sheets, strips and grids made of synthetic and natural fibres in order to reduce the tensile strain developed because of gravity & boundary forces. Basically, soil reinforcement friction is a fundamental concept behind technique of reinforced earth. Also, the flexible nature of reinforced soil mass enables it resist large amount of differential settlement, increment in bearing capacity and horizontal deformation of soil mass without any distress. Reinforcement of soils can be done with different type of fibres, e.g. with natural fibres like Jute, Sisal, coir, palm etc. and synthetic fibres like as polypropylene, glass, nylon etc. Use of such types of fibres and Development of Geosynthetics over the years helped technologists in manufacturing various types of soil reinforcement materials (such as geogrid, geocell, geonets etc.) to tackle various soil related problems. Geosynthetics defined as a planar textile fabric or material used in the improvement of engineering properties of soil. The term geosynthetics embrace both natural and man-made geotextiles. Geosynthetics gained popularity due to quality, ease in construction, simplicity, durability, less time consumption etc. These materials finds their application in Stabilizing Embankments, Strengthening of Road Sub-grade, controlling soil erosion developed due to weather actions, Consolidation of Soft Soil, Settlement of Rails, Controlling Riverbank Erosion, and many more. But the high cost of polymeric geosynthetics and its environment concordance makes it imperative to explore natural fibres (viz. geofabrics) to make construction work more cost efficient and eco-friendly. One of the significant reasons of the insignificant consumption of natural geotextiles could be the absence of framework and thorough think about on performance and behaviour in soil of changing characteristics and conduct under various nature and extent of external loads. The studies

directed so far in the field of characteristic geotextiles were not as intensive as was desired. Things however have begun changing in so far as Geo material is concerned. The mechanism of Geo materials in transforming soil conduct has been investigated through laboratory thinks about and more than 260 field trials/applications as of date in India [Sanyal, 2017].

## REVIEW OF LITERATURE

The review of literature is conducted on three major grounds as follows: -

### ***DEVELOPMENT AND USE OF GEOSYNTHETICS IN INDIA***

**Mandal (1987)** mainly discuss about the advancement and utilization of geotextiles in India Investigator through the study finds that for large settlements, reinforcement of soil with geotextile play a significant role . This paper concludes that geotextiles proves economic and feasible in terms of improving engineering performance of soil, reduction in construction cost, providing adequate factor of safety. This paper also examines that Reinforcement of soil by natural geotextiles are comparatively cheaper and economic than synthetic geotextiles. However, any economic advantage in the uses of synthetic geotextiles proves well before adoption into their wider use.

**kaniraj and Rao (1994)** reviews about the trends in the practice of geotextile and related products in geotechnical. applications. in India This paper likewise includes temperate and specialized perspectives to control potential for the development of geotextiles and their item in India This paper talked about five noteworthy point on geotextiles, in particular, Manufacture of geotextile in India and their properties, testing gear and detail of geotextiles in India, Application of geotextiles in India, Research on geotextile in India, utilization of geotextile made of natural fibres and materials in India. This paper likewise gives data about assembling of various sorts of gear utilized for testing geotextiles in India. The department of Indian guidelines has set up panels and sub councils to make particulars and strategies for testing geotextiles.

### ***SOIL REINFORCEMENT USING SYNTHETIC FIBRE BED***

**Adams and Collin (1997)** explored the potential advantages of foundation of soil strengthened with geosynthetic using large-scale model footing load tests. This paper evaluated the effect of single and multiple layers of geosynthetics reinforcement set underneath shallow spread footings. For evaluation two distinct types of geotextiles taken for experiment, one is stiff biaxial geogrid and another one geocell. Test results indicate that inclusion of layer of geosynthetic reinforcing soil foundations may lead to increment in the ultimate bearing capacity by a certain factor. Clearly demonstrate Substantial increase in the ultimate Bearing capacity of shallow spread footings on sand reinforced with geosynthetics.

**Vercueil et al. (1997)** Studied the effect of geosynthetics on the liquefaction resistance of a saturated sand reinforced. cyclic triaxial test is performed on saturated Hostun RF sand and circular sheets of geosynthetic as a reinforcement. A Series of test were conducted to analyze undrained behaviour of saturated sand reinforced with non-woven geotextiles have varying compressive, rigid and roughness properties. Test results indicate that liquefaction resistance of sand reinforced with circular layer of geosynthetic undergone a noticeable increment and furthermore the impact of reinforcing geotextiles have delayed liquefaction with the reduction in the interstitial pressure of sand.

**Haeri et al. (2000)** led arrangement of examinations to analyze the impact of geotextile support on the mechanical conduct of sand. The mechanical conduct was examined through fluctuating the quantity of geotextiles layers, kind of geotextile, confing pressure, and geotextile course of action. Tests were done on samples with two different diameters for the determination of stress-strain & dilation conduct of geotextile strengthened dry shoreline sand. Through results it has been observed that inclusion of geotextiles made increment in the axial strain at failure, peak strength, and ductility and reduction in dilation. Such enhancements in the conduct of Reinforced sand are more significant for small size examples.

**Kumar and Saran (2003)** talk about technique for evaluation of pressure intensity corresponding to a given settlement for a rectangular footing laying on fortified soil footing. Analysis has been simplified by introducing non-dimensional charts for the various terms used, directly been used by practicing engineers. An empirical method has been recommended for the calculation of ultimate bearing capacity of Reinforced soil foundation were performed to approve aftereffects of experiment.

**Yoon (2004)** demonstrated the effect of inclusion of tire waste on Bearing capacity and settlement sandy soil. Laboratory plate load tests were conducted on sandy soil reinforcing it with waste tire fibre as reinforcement to

investigate its effective use. Investigation is done by introducing several testing parameters such as size, segments, density, depth of Reinforcing material. Noticeable reduction in settlement has been observed for lower sand density along with two times increment in load B.C. The effect of single layer of reinforcement on medium density soil show considerable reduction in settlement and improvement in bearing capacity by a factor of 2. Moreover, their combination gives the best results as a reinforcing material.

**Basudhar (2007)** did a test consider on circular footings laid on semi-infinite geotextiles sand bed Idea of homogenization of such soils has been used for prediction of the load settlement behavior along with the comparison with experimental values by performing both analytical and numerical analyses. Effect of various parameters such as size, layers, position of placement and pattern of geotextile reinforcement size on the load-settlement behaviour of the footings have been observed.

**Dash et al. (2007)** conducted series of test on laboratory model to evaluate the effect on sand bed reinforced with geocell laying down beneath strip loading. Mechanism of geocell have been comprehended by estimating strain characteristics of geocell walls, pressure force transferred to the soil subgrade and deformation behavior of soil subgrade. Variation in the strain characteristics of geocell wall evaluated that the geocell mattress behaves as a composite beam upheld by the subgrade soil. Parameters like shape of geocell layer and its arrangement position beneath the soil footing found to be governing factor in dispersion of load in the geocell mattress.

**SNM & AR (2010)** had performed experiment on laboratory model of strip footings laid on the geocell and planar reinforced sand beds. The various parameters such as the width of reinforcement, no. of geo-textile layers and depth of geocell below the base of footing had been studied during testing. Incongruous to other researches, effect of reinforcing sand with both types of reinforcement was evaluated for various level of settlements. Results from testing show that increment in number, height and width of geocell reinforcement beyond a certain limit doesn't shows a significant improvement. On the other hand, system consisting geocell reinforcement proves better than equivalent planar reinforcement system in terms of loading as well as in settlement behavior.

**Badakhshan et al. (2016)** directed a series of test evaluating the effect of geogrid on sandy soil by the application of centric and eccentric loading through circular & square footings laid on sandy soil. Meyerhof's Effective Width Concept, laboratory model tests, numerical analyses data had been used to validate approach for eccentric loading in unreinforced and reinforced conditions. The results of this study had shown that decrement in circular footing's ultimate Bearing capacity had been observed less with increment of load eccentricity in comparison of square footing in same reinforced condition. Improvement index examined that inclusion of geogrid layers increases U.B.C in both types loading condition and their contributions increased with increasing the load eccentricity.

**Abbas (2018)** examined the effect of inclined load on strip footing on reinforced sandy soil utilizing exploratory model. A total of 48 plate load test were conducted, eight tests without reinforcement and remaining with the reinforcement of geogrid. The effect of the load inclination angle ( $\alpha$ ), number of geogrid layers (N) and the relative density (RD) on the bearing capacity, settlement and horizontal displacement were examines. Experimental results gave major conclusions as outlined, significant increase in bearing capacity is observed using geogrid reinforcement, bearing capacity increased with increasing no. of layers attaining an optimum value of N=4-5 along with decrease in horizontal displacement of footing.

**Lakshmi et al. (2018)** have conducted a comparative study to improve the strength of soil by reinforcing the soil by means of non-woven randomly distributed polypropylene fibres (PF) and by using geosynthetics such as Geotextiles, Geonets and Geogrids. Laboratory tests like Unconfined Compression (UCC) test and soaked CBR test were performed to evaluate the strength of reinforced soil sample. Different percentage of PF were mix in soil sample to determine the optimum percentage of PF at which maximum strength of soil was observed in UCC test and soaked CBR test. Placement of Geosynthetics like Geotextiles, Geonets and Geogrids at various depths from the top in order to determine the optimum depth at which maximum strength of soil was observed in UCC test and soaked CBR test. From test results it can be observed that soil with 1 % PF showed maximum increase in UCC strength of about 41.66 % and soaked CBR value was found to increase by 1.5 times that of unreinforced soil. Geotextiles, Geonets and Geogrids when placed at three fourth the depth from the top showed maximum strength gain in UCC test and soaked CBR test.

#### ***SOIL REINFORCEMENT USING NATURAL FIBRE BED***

**Ghosh et al. (2005)** conducted the experiment for enhancing the bearing Capacity of pond ash on inclusion of jute

textile. Pond ash is waste product of thermal power plant its storage and disposal are very problematic as it requires vast area and above all its environmental hazards. This study aims to mitigate all such distresses. pond ash powder can be adopted as structural fills for the development of residential and industrial sites situated in low lying areas. This experiment studies the effect on B.C of square footing reinforced with jute geotextile. Results of testing program demonstrated that increment in bearing capacity of square footing with the increase in layers of jute geotextile, attains a maximum value at certain number of layers of reinforcement relying upon  $u/B$  proportion

**Subaida et al. (2009)** demonstrated the behavior of unpaved roads with inclusion woven coir geotextiles. Experiment was performed to examine the effect of reinforcing laboratory sample pavement with coir fibre sheet in a two-layers section. Monotonic and repeated loads had been applied on coir sand bed by rigid circular plate. The test results indicate that load bearing capacity is significantly improved with reinforcement of thin sheet of coir fibre. Experimental results have shown significant increment in load carrying capacity by laying down geotextile between the bond of the subgrade and base course. Additionally, Placement of coir geotextile beneath the base course at all levels of distortions have demonstrated a Considerable improvement in bearing capacity.

**Waruwu, and Susanti (2015)** studied that construction of foundation on peat soil is suitable regarding its stability concern, in view of the, high pressure low shear quality, low bearing capacity high water content and Utilizing of bamboo grid is a choice to enhance stability of the construction on the peat soil. Treated framework can be made to enhance the strength durability of bamboo. The tests were led in the research lab utilizing a test box length 120 cm, width 90 cm, and depth 90 cm. The plate size of  $15 \times 15 \text{ cm}^2$  and thickness of 1 cm was taken for application of load . Reinforcement material utilizing bamboo lattices without and with the treated of which is put under the establishment plate separately 1 layer, 2 layers, and 3 layers. Peat soil fortified of bamboo matrix with and without treated produce a critical bearing capacity contrasted and peat without support. By and large, the greater reinforcement is utilized, the bearing capacity of the foundation on peat soil will undergone increment. Advantages treated of grid of bamboo isn't noticeable on the adjustment in estimation of the bearing capacity of peat. It very well may be inferred that the impact was not noteworthy treated of bamboo lattice to expand the bearing capacity of a peat soil on foundation.

**Shaia et al. (2016)** investigated the effect of natural jute fibre sheet coated with bitumen material on the CBR value of soil .CBR test have been conducted on unreinforced soil sample and soil sample reinforced with natural jute fibre sheet. Test results have shown inclusion of jute fibre sheet increases CBR value of soil and also placement of jute fibre sheet at second layer have considerable effect than placing it anywhere else in the soil sample the coating of Jute fibre has not shown No significant improvement in CBR value of soil been observed due application of bitumen coating; however, longevity of jute fibre can be improved.

**Dharmesh et. al (2017)** examines the behavior of shallow foundation laying on coir geotextile sand bed. Significant change in the bearing capacity and settlement were noticed. Bearing capacity is Improved by a factor of 5 and decrease in settlement by 87% by placement of three layers. Same sort of improvement been observed with the arrangement of single layer of coir geotextile.

## CONCLUSION

This paper reviews that inclusion of different types geosynthetic and geo materials as fibre bed to reinforce soil to improves various engineering properties of soil. Major conclusion made from review of literature are-

- Friction between the interface of soil mass and reinforcing material is essential phenomenon in the reinforced earth.
- By obtaining optimum depth of reinforcement layer by choosing different  $u/B$  ratio results in Significant increase in bearing capacity of soil mass and also placement of optimum no. of layers of reinforcement in soil mass results in improvement of B.C of soil.
- Shape of footing, direction of application of load and geometry of reinforcing materials also improves performance of reinforced earth.
- Considerable reduction in differential settlement and horizontal displacement had been observed.

- One of the real reasons of the insignificant consumption of natural geotextiles could be the absence of frameworkatic and thorough examine on performance and behaviour in soil of changing characteristics and conduct under various nature and extent of external loads.

Use of Geotextiles is a feasible and temperate alternative for a soil reinforcement. However, growing environmental issues prompted engineers and technologist to opt for natural geotextiles. The exploration led so far in the field of natural geotextiles were not as concentrated as desired. Be that as it may, developing ecological issues incited architects and technologist to settle on characteristic geotextiles.

## REFERENCES

- Abbas, J. (2018). "Behavior of a strip footing on reinforced soil subjected to inclined load." *In MATEC Web of Conferences* (Vol. 162, p. 01022). *EDP Sciences*.
- Adams, M. T., & Collin, J. G. (1997). "Large model spread footing load tests on geosynthetic reinforced soil foundations." *Journal of Geotechnical and Geoenvironmental Engineering*, 123(1), 66-72.
- Badakhshan, E., Noorzad, A., & Zameni, S. (2018). "Eccentric behavior of square and circular footings resting on geogrid-reinforced sand." *International Journal of Geotechnical Engineering*, 1-11.
- Basudhar, P. K., Saha, S., & Deb, K. (2007). "Circular footings resting on geotextile-reinforced sand bed." *Geotextiles and Geomembranes*, 25(6), 377-384.
- Dash, S. K., Rajagopal, K., & Krishnaswamy, N. R. (2007). Behaviour of geocell-reinforced sand beds under strip loading. *Canadian Geotechnical Journal*, 44(7), 905-916.
- Ghosh, A., Ghosh, A., & Bera, A. K. (2005). "Bearing capacity of square footing on pond ash reinforced with jute-geotextile." *Geotextiles and Geomembranes*, 23(2), 144-173.
- Haeri, S. M., Noorzad, R., & Oskoorouchi, A. M. (2000). "Effect of geotextile reinforcement on the mechanical behavior of sand." *Geotextiles and Geomembranes*, 18(6), 385-402.
- Kaniraj, S. R., & Rao, G. V. (1994). "Trends in the use of geotextiles in India." *Geotextiles and Geomembranes*, 13(6-7), 389-402.
- Kumar, A., & Saran, S. (2003). "Bearing capacity of rectangular footing on reinforced soil." *Geotechnical & Geological Engineering*, 21(3), 201-224.
- Lakshmi, S. M., Gayathri, S., Susanna, K. D., Ammaiappan, M., & Manoharan, M. (2018). "An Experimental Study On Soil Strength Enhancement Using Geosynthetics." *International Journal Of Innovative Research Explorer*, 5(4), 433-442.
- Lal, D., Sankar, N., & Chandrakaran, S. (2017). "Performance of shallow foundations resting on coir geotextile reinforced sand bed." *Soil Mechanics and Foundation Engineering*, 54(1), 60-64.
- Mandal, J. N. (1987). "Geotextiles in India." *Geotextiles and Geomembranes*, 6(4), 253-274.
- Shaia, H., Aodah, H. H., & AL-Hameidawi, B. H. (2016). "Improvement of Sub-grade Soil using Natural Jute Fiber Sheet at Various Layers." *journal of kerbala university*, 14(3), 170-177.
- Subaida, E. A., Chandrakaran, S., & Sankar, N. (2009). Laboratory performance of unpaved roads reinforced with woven coir geotextiles. *Geotextiles and Geomembranes*, 27(3), 204-210.
- Tafreshi, S. M., & Dawson, A. R. (2010). "Comparison of bearing capacity of a strip footing on sand with geocell and with planar forms of geotextile reinforcement." *Geotextiles and Geomembranes*, 28(1), 72-84.
- Vercueil, D., Billet, P., & Cordary, D. (1997). "Study of the liquefaction resistance of a saturated sand reinforced with geosynthetics." *Soil Dynamics and Earthquake Engineering*, 16(7-8), 417-425.
- Waruwu, A., & Susanti, R. D. (2015). Behavior of Soil Peat with Reinforcement of Bamboo Grid. *IOSR J. Eng*, 5, 29-36.
- Yoon, Y. W., Cheon, S. H., & Kang, D. S. (2004). "Bearing capacity and settlement of tire-reinforced sands." *Geotextiles and Geomembranes*, 22(5), 439-453.



## Experimental Investigation of Contaminant Transport through Porous Media

S. B. Patil<sup>1</sup>, H. S. Chore<sup>2</sup>, V.A.Sawant<sup>3</sup>

<sup>1</sup>Associate Professor, <sup>2</sup>Associate Professor, <sup>3</sup>Associate Professor

Department of Civil Engineering

<sup>1</sup>Datta Meghe College of Engineering, Airoli, Navi Mumbai-400708

<sup>2</sup>Dr. B. R. Ambedkar National Institute of Technology, Jalandhar – 144011, Corresponding Author

<sup>3</sup>Indian Institute of Technology, Roorkee-247667

Email: <sup>1</sup>sbpatil\_2009@rediffmail.com, <sup>2</sup>chorehs@nitj.ac.in, <sup>3</sup>sawantfce@gmail.com

### ABSTRACT

Groundwater is a valuable natural resource. During the past few decades, it has been experienced that many types of contaminants can infiltrate into the ground and pollute the soil media and groundwater. In many practical situations, one needs to predict the time behavior of a contaminated groundwater layer. Most of the groundwater contaminants are reactive in nature and they infiltrate through the vadoze zone, reach the water-table; and continue to migrate in the direction of groundwater flow. Therefore, it is essential to understand the transport process of contaminants through the subsurface porous media. In this study, an attempt is made to investigate the behavior of solute transport through porous media using laboratory experiments. A Soil Column is constructed to represent porous media. Experiments were carried out on different soil media using chloride and fluoride. The maximum value of the relative concentration is observed to be in the range of 0.90 to 0.96 and 0.68 - 0.79 for chloride and fluoride respectively. It is known that fluoride is a reactive chemical; hence while transporting through the soil media, some amount of fluoride is adsorbed through soil. When the effect of velocity on the relative concentration of solute is considered, it is observed that higher the velocity, the attainment of the peak will be earlier.

**KEYWORDS:** *Groundwater contamination; Soil column; Solute transport; Fluoride; Chloride*

### INTRODUCTION

The groundwater is a very important part of the environment and must be protected for the benefit of the present and future generation. Its contamination is one of the most typical hydro-geological and environmental problems. Geotechnical engineers are becoming increasingly involved with the problems of pollutants migration through the soil. This involvement arises from concerned regarding the contamination of groundwater system by toxics substances which have been, or are being, stored in landfills and lagoons. Since the movement of pollutant through relatively impermeable soil is slow, time required for several contaminants to reach the surrounding groundwater may range from several to hundreds of years. The transport of solute in the soil and groundwater is under increasing threat from growing demands, wasteful use and contamination. In order to protect the environment from contamination by pollutants, waste materials are usually placed in engineered landfills.

Most of the groundwater contaminants are reactive in nature and they infiltrate through the vadoze zone, reach the water-table; and continue to migrate in the direction of groundwater flow. Therefore, it is essential to understand the transport process of contaminants through the subsurface porous media.

#### *Sources of Contamination*

A groundwater contaminant is defined by most regulatory agencies as any physical, chemical, biological or radiological substance or matter in the groundwater. The contamination can occur by natural processes, agricultural operations urban run offs, waste disposal practices, spills and leaks etc.

The solid wastes include buried waste that is subjected to leaching by percolating rain water and surface water or by groundwater contact with the fill. This generated Leachate (Fig. 1) can contain high levels of BOD, COD, nitrate, chloride, alkalinity, trace elements and even toxic constituents.

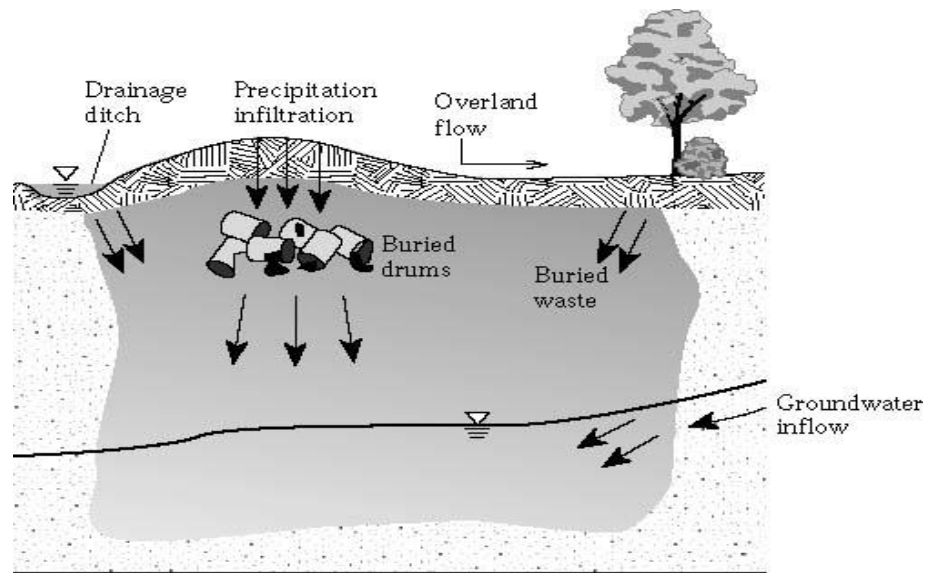


**Fig. 1 Sources of fluid for the generation of landfill leachate**

### ***Transport Process***

To predict the environmental consequences of groundwater contamination one ought to know as to where the contaminant would interfere, when it would arrive; and what are the potential concentrations. The contaminant is introduced in groundwater by (i) advection which is caused by flow of groundwater (ii) dispersion which is caused by mechanical mixing and molecular diffusion; and (iii) Sorption

Solute transport in soil and groundwater is affected by a large number of physical, chemical and microbial processes and media properties. Advection carries the contaminant at an average rate as a plug flow. However, in reality, the solute is seen to spread out from the flow path. This spreading or mixing phenomenon is called dispersion. At the microscopic level, the fluid flow within a porous medium is actually a movement along the tortuous three dimensional passages in voids. The molecular diffusion is caused by the non-homogeneous distribution of contaminant in a fluid. The contaminant molecules in high concentration will move to the low concentration areas to form a uniform concentration distribution. An advection dispersion transport equation is generally used for estimating the level of contamination in groundwater.

### ***Advection***

The advection is the movement of dissolved solute with flowing groundwater at the seepage velocity in porous media. Advection and hydrodynamic dispersion are the physical properties that control the solute flux.

### ***Dispersion***

It is the result of two processes – firstly, molecular diffusion and secondly, mechanical mixing. The mechanical dispersion (Fig.2) or mechanical mixing occurs when contaminated groundwater mixes with non-contaminated groundwater resulting in a dilution of the contaminant, which is called dispersion.

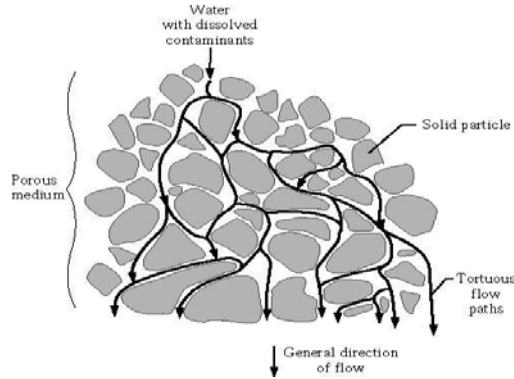


**Fig. 2 Schematic of mechanical dispersion**

**Sorption**

Sorption is the process by which chemicals are retained on to the surface of soil particles. It is the exchange of molecules and ions between solid phase and liquid phase, including adsorption and desorption.

The one-dimensional form of the governing equation for contaminant migration through a saturated porous medium is expressed as

$$\left(1 + \frac{\rho_d}{n} k_d\right) \frac{\partial C}{\partial t} = D \frac{\partial^2 C}{\partial x^2} - \bar{v}_x \frac{\partial C}{\partial x} - \lambda C \dots\dots\dots (1)$$

Where

$\rho_d$  – bulk density of porous medium (ML<sup>-3</sup>)

$n$  – Porosity (L<sup>3</sup>/L<sup>3</sup>)

$k_d$  – distribution constant (ML<sup>-3</sup>)

$C$  – Concentration of contaminant (ML<sup>-3</sup>)

$D$  – Dispersion coefficient (L<sup>2</sup>/T)

$\lambda$  – is the decay constant (1/T)

$\bar{v}_x$  – Seepage velocity (L/T)

$R$  – Retardation factor =  $\left(1 + \frac{\rho_d}{n} K_d\right)$

**LITERATURE REVIEW**

Experimental studies are essential tools in the geo-environmental engineering for understanding transport of adsorbed and non-adsorbed solutes through soil. Experiments can be used to obtain the properties necessary to model the movement of contaminant in porous media in a realistic situation. In all, the experiments provide valuable insight about the porous medium, the behavior of chemicals, and associated processes such as diffusion, dispersion, anion exchange and sorption during transport.

This article provides a critical review of the various approaches available for analytical, experimental and numerical studies of contaminant transport through porous media.

Several analytical solutions for the movement of chemicals in a one dimensional semi-infinite system using Laplace transform techniques has been developed by van Genuchten (1981). The governing transport equation includes terms accounting for linear equilibrium adsorption, zero-order production and first-order decay. An analytical solution for contaminant transport from a finite and continuous source in a continuous flow regime has been developed by Domenico and Robbins (1985). The significance of the approach is that it provides a closed form solution without involving numerical integration procedures.

Domenico (1987) developed a mathematical model for a finite source that incorporates one dimensional groundwater velocity, longitudinal and transverse dispersion, and some form of decay for either radionuclide's or biodegradable organics. This solution is one of the most widely used analytical solutions for three dimensional solute transport in the field of contaminant hydrogeology and has been implemented in several risk assessment codes.

Wexler (1992) presented analytical solutions to the advection-dispersion solute equation for a variety of boundary condition types and solute-source configurations in one, two and three dimensional systems having uniform groundwater flow. Solutions were presented in a simplified format, together with information on important assumptions in derivation and limitations to their use.

Barone *et al.* (1992) described a laboratory diffusion-test for estimation of the diffusion coefficient ( $D$ ) and the adsorption coefficient ( $Kd$ ) for several volatile organic species in a clayey soil.

Rowe and Badv (1996) conducted a series of chloride diffusion tests on clayey silt, silt and sand, both for single layer and two layer systems. Based on the experimental results, authors suggested that the existing solute transport theory can adequately predict the chloride migration through landfill liners at near saturated conditions. They noted that the effective porosity can be taken to be the volumetric water content for the soils for all practical purposes.

Rowe *et al.* (2000) performed the several inorganic diffusion tests on Geo synthetic Clay Liners (GCL) and bentonite specimens; and stated that 'there is a linear correlation between the diffusion coefficient and the final bentonite void ratio for both sodium and chloride'.

Rosqvist and Destouni (2000) modelled lithium transport through an undisturbed solid waste sample and a pilot-scale experimental landfill by use of probabilistic Lagrangian approach. The relevant conceptualization and quantification of the water and solute movement through preferential pathways is found to be critical for meaningful extrapolation of observations in environmental assessments of long-term landfill performance.

Sheu T.W.H. and Chen Y.H. (2002) developed a finite element model for predicting the contaminant concentration governed by the advective-dispersive equation. The results obtained have a much greater range of validity in the sense that no oscillations were observed in circumstances in which advection becomes dominant over other competing terms.

William J. and Ning Lu (2004) described a new lecture module and laboratory experiment for demonstrating chemical transport phenomena in soils. Simple colored dye was used to simulate a contaminant in a flowing soil-water system, thus precluding the requirement for expensive and complex analytical equipment involved in traditional chemical transport testing and creating a highly visually oriented learning environment.

Praveen Kumar R. and Dodagoudar G.R (2009) proposed a methodology for modeling the one dimensional advection-dispersion equation involving first-order degradation through a saturated porous medium using EFGM. Numerical results of the EFGM are compared with experimental data reported in the literature for two types of one-dimensional contaminant transport process. It is found that EFGM results agree well with those obtained from the experiments, this ensures the accurate formulation of the EFGM.

Patrick J.*et al.* (2011) presented an experimental and numerical investigation of coupled consolidation and contaminant transport in porous media. Diffusion and large strain consolidation-induced transport tests were conducted on composite specimens of kaolinite slurry consisting of an upper uncontaminated layer and a lower layer contaminated with potassium bromide. Effluent concentrations and mass outflows were higher for the boundary nearest to the contaminated layer in the double-drained case. Simulations also indicated that, for the conditions of this investigation, a reduction in specimen height yielded earlier breakthrough and higher levels of contaminant mass outflow.

Ballarini E. *et al.* (2012) described the detailed numerical simulation of highly controlled laboratory experiments using uranine, bromide and oxygen depleted water as conservative tracers for the quantification of transverse mixing in porous media. Synthetic numerical experiments reproducing an existing laboratory experimental set-up of quasi two dimensional flow through tank were performed to assess the applicability of an analytical solution of the 2D advection-dispersion equation for the estimation of transverse dispersivity as fitting parameter. From the results, an improved experimental set-up as well as a numerical evaluation procedure could be developed, which allow for a precise and

reliable determination of dispersivities.

Massimo Rolle *et al.* (2012) performed multi-tracer laboratory bench-scale experiments and pore-scale simulations in different homogeneous saturated porous media. The results show that a non-linear compound-dependent parameterization of transverse hydrodynamic dispersion is required to capture the observed lateral displacement over a wide range of seepage velocities.

Sharma *et al.* (2013) reported the experimental investigation of contaminant transport through saturated layered soil using the soil column experiment. An implicit finite difference numerical analysis was also carried out to get the numerical solution of advective dispersive transport including equilibrium sorption and first order degradation constant for the multi-layered soil. The results of experimental breakthrough curves (BTCs) showed that the order in which the soil layers were stratified in a water-saturated profile did not influence the effluent solute concentration distribution.

Deepak Swami *et al.* (2013) have performed laboratory experiments to investigate the behavior of solute transport through stratified porous media. A numerical model is used to simulate the breakthrough curves of experimental data of chloride and fluoride. It is seen that the peak of breakthrough curves is higher for the non-reactive solute compared to that of the reactive solute. The values of effective diffusion coefficient and retardation coefficient are estimated by simulation of experimental breakthrough curves.

Hulagabali *et al.* (2014) described an alternative numerical method to model the two dimensional contaminant transport through saturated porous media using a finite difference method (FDM) and finite element method (FEM). Results of the FDM and FEM are compared and it is found that they agree well.

## RESEARCH GAP AND FINDINGS

Several researchers conducted experimental investigations either in laboratory or in field besides carrying out the analytical studies and numerical modelling for understanding the behavior of contaminants in porous media and for predicting the future contamination level. The experimental studies are regarded as complimentary to the analytical and numerical studies. Even though there is considerable number of research works available in the literature pertaining to the contaminant transport; still, there is scope for more experimental work in that area.

## MATERIALS AND METHODS

### Various Methods for Determination of Solute Transport

#### 1. *Experimental method*

Experimental studies are essential tools in the geo environmental engineering for understanding transport of adsorbed and non-adsorbed solutes through soil. Experiments can be used to obtain the properties necessary to model the movement of contaminant in porous media in a realistic situation. A model can be constructed to study the flow of contaminants in soil using various boundary conditions. Soil Column model is widely used for this purpose.

#### 2. *Numerical modeling*

Numerical modeling of pollutant migration in porous media has recently received a great deal of attention due to an increased interest in the preservation of the quality of the environment and particularly the protection of groundwater from various pollutants. Numerical models are able to account for the complexity of the subsurface and accommodate complicated boundary conditions

#### 3. *Software simulation*

Various softwares are now available in market which combines the benefits of both numerical and experimental modeling. Various data & parameters for solute transport can be obtained from these softwares by simulating the flow in a stated boundary condition.

#### 4. *Remote sensing of groundwater*

Remote sensing and GIS are effective tools for water quality mapping and land cover mapping essential for monitoring, modeling and environmental change detection. GIS can be a powerful tool for developing solutions for water resources problems for assessing water quality, determining water availability, preventing flooding, understanding the natural environment, and managing water resources on a local or regional scale. However it is rarely

carried out due to the huge cost involved in it.

### EXPERIMENTAL SETUP AND PROCEDURE

Laboratory tracer experiments were conducted to investigate solute transport in soil column during steady saturated water flow. The experimental set-up consists of column, made up of an acrylic pipe with thickness of 8mm, 100mm diameter and 1600mm length. (as shown in Fig. 3). The cross section area of pipe was  $78.50\text{cm}^2$ .

Tank was filled with granular medium using a funnel and during the filling dry soil was carefully packed in small increments into column avoiding any soil particle –size segregation. Tap water was tested prior to performing the experiments to measure concentrations of free chloride. After measuring the concentration of tap water, a storage tank was used to store the prepared solution of known concentration. The prepared solution was introduced into the soil column at a constant flux, keeping the head constant of input solution. First the soil column was saturated by the tap water so that the steady-state water flow condition established. The water level was always kept above the grains to achieve a uniform packing and to avoid the entrapment of air bubbles. Then sodium chloride solution (NaCl) with known concentration as tracer is injected into the column as the input for 30 minutes. Concentration of the tracer NaCl during the experiment was measured in the column with a constant time interval. The solute samples were collected at the outlet of the column and concentration were measured by the titration procedure. The effluent solutions were collected in fractions of each 15 minutes into the collector. After measuring cylinder was used to collect a fraction of water sample for accurate measurement and to cross-check the volume collected in particular duration of time for velocity calculations.

All collected samples were stored in air-tight bottles to protect from direct sunlight. After the sampling each sample was labeled and tested. For measuring chloride in the fraction collected. All the samples were titrated with potassium chromate as indicator and silver nitrate as a titrant. For the measurement of fluoride, the spectrophotometer is used. The effluent solute concentration was expressed as relative concentrations( $C/C_0$ ), where C and  $C_0$  are the solute concentration in the effluent fraction and input pulse, respectively.

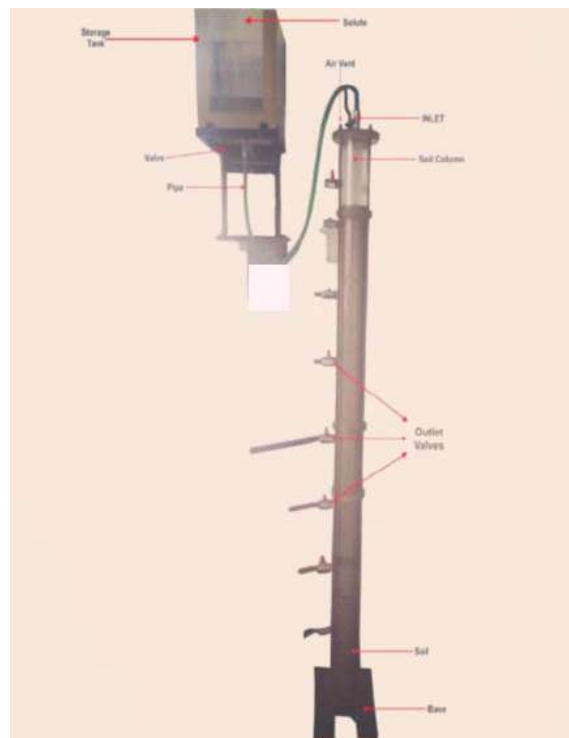


**Fig. 3 Soil column**

Various experiments were conducted on different soil samples obtained from field to determine its various properties as mentioned in Table 1.

**Table 1. Summary of geotechnical investigations for different soils used as a media**

Sr. No.	Soil	Specific Gravity	Porosity	Moisture Content %	Bulk density gm/cm <sup>3</sup>	Hydraulic Conductivity (mm/sec)
1.	Soil A	2.67	0.48	8	2.56	10 <sup>-1</sup>
2.	Soil B	2.64	0.38	10	2.62	10 <sup>-1</sup>

### RESULTS AND DISCUSSIONS

Experiments were carried out on different soils using chloride and Fluoride. If the supplied solute source at the inlet has a constant concentration and it remains throughout the experiment, it is known as the continuous solute source.

#### Concentration of Fluoride for continuous type boundary condition

##### Soil A

First fluoride was allowed to pass through soil A and the samples were collected at a depth of 120 cm. For the given soil sample, the initial concentration of fluoride was 1.4 mg/lit with different velocities as shown in figure.

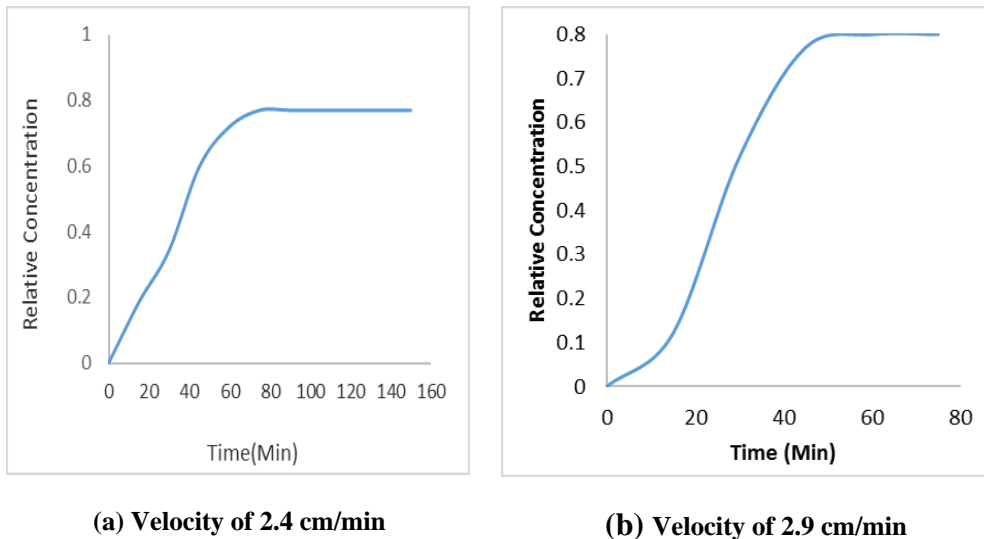
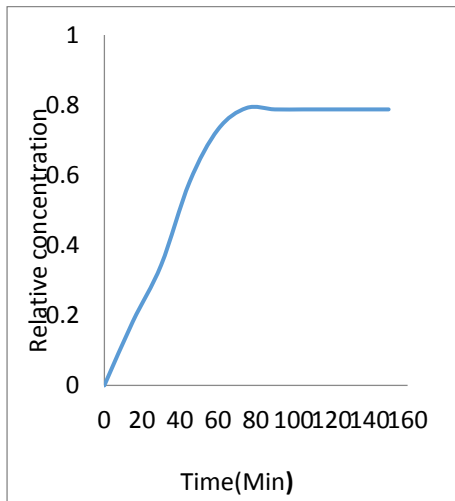


**Fig. 4 Variation of relative concentration of fluoride with an initial concentration of 1.4 mg/lit with different velocities**

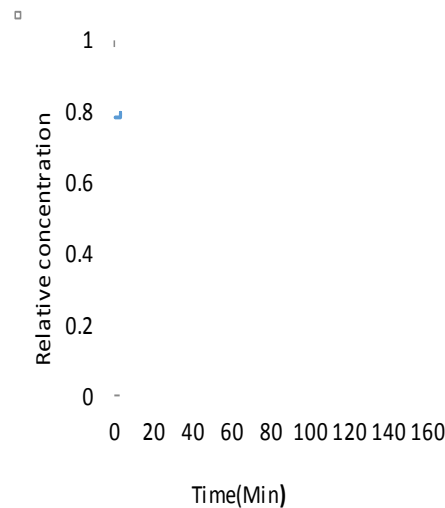
From Fig. 4(a), it is found that, the relative concentration in respect of case (a), increases with time up to 75 minutes and the corresponding concentration is observed to be 0.77. The concentration is found to be constant beyond the time interval of 75 minutes. Similarly, the relative concentration with respect to case (b) is found to increase with time up to 60 minutes, where it is observed to be 0.80(Fig 4.b). Thereafter, it is found to be constant. When the effect of velocity on the relative concentration of Fluoride solute is considered, it is observed that higher the velocity, the attainment of the peak will be earlier.

**Soil B**

From (Fig. 5 a), it is found that, the relative concentration in respect of case (a), increases with time up to 90 minutes and the corresponding concentration is observed to be 0.78.



(a) Velocity of 2.4 cm/min



(b) Velocity of 2.9 cm/min

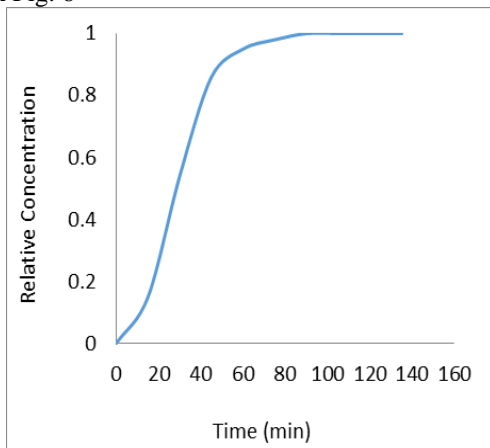
**Fig.5 Variation of relative concentration of fluoride with an initial concentration of 1.4 mg/lit with different velocities**

The concentration is found to be constant beyond the time interval of 90 minutes. Similarly, the relative concentration with respect to case (b) is found to increase with time up to 75 minutes, where it is observed to be 0.77 (Fig 5 b). Thereafter, it is found to be constant.

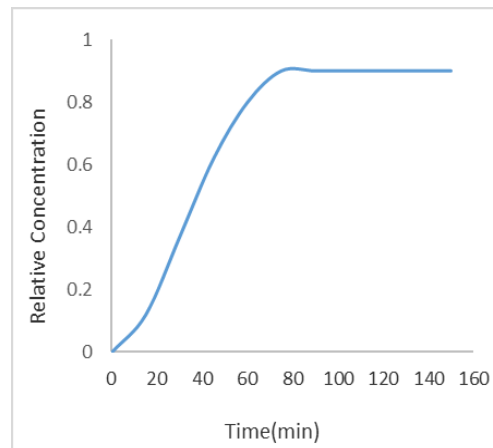
**Concentration of chloride for continuous type boundary condition**

**Soil A**

The variation of relative concentration of chloride with initial concentration of 150 mg/lit with different velocities is shown in Fig. 6



(a) Velocity of 2.4 cm/min



(b) Velocity of 2.9 cm/min

**Fig.6 Variation of relative concentration of chloride with time for an initial concentration of 150 mg/lit**

The relative concentration with respect to the case (a) is found to increase with time up to 90 minutes (Fig. 6 a). The corresponding relative concentration is observed to be 1. The concentration is found to be constant beyond the time interval of 90 minutes. The relative concentration with respect to case (b) is found to increase with time up to 75 minutes, where it is observed to be 0.90 (Fig 6b). Thereafter, it is found to be constant. The comparison of two plots reveals the effect of velocity on transport to be significant. It is revealed that if the velocity is more, concentration will attain the peak earlier.

### Soil B

The relative concentration with respect to case (a) is found to increase with time up to 120 minutes (Fig. 7 a). The corresponding relative concentration is observed to be 0.96.

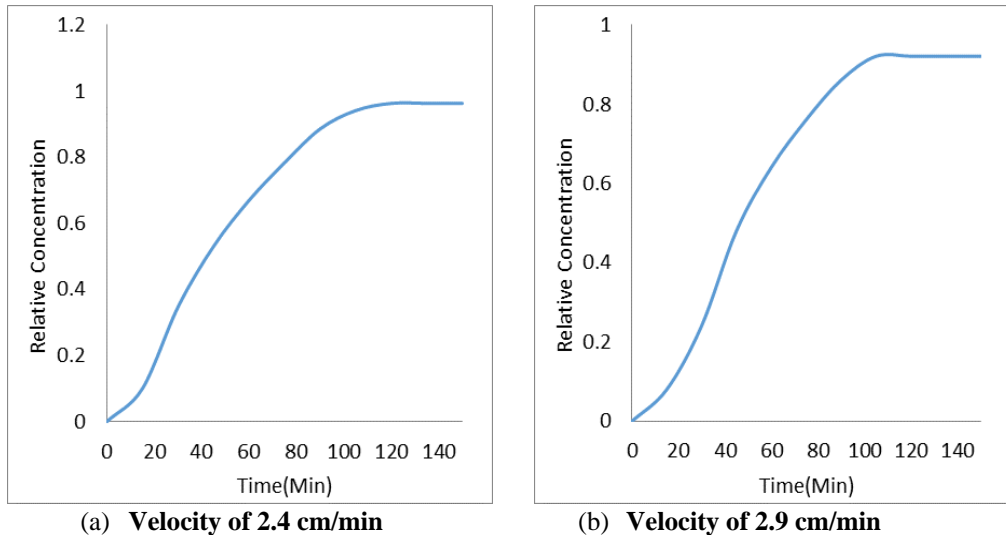


Fig.7 Variation of relative concentration of chloride with time for an initial concentration of 150 mg/lit

The concentration is found to be constant beyond the time interval of 120 minutes. The relative concentration with respect to case (b) is found to increase with time up to 105 minutes, where it is observed to be 0.92 (Fig 7b). Thereafter, it is found to be constant. The comparison of two plots reveals the effect of velocity to be significant on the transport of the contaminants, i.e., solutes. It is revealed that if the velocity is more, concentration will attain the peak earlier.

### SUMMARY AND CONCLUSIONS

An experimental investigation was carried out on the solute transport to study the behavior of solute through porous media. In the study, the transport of two types of solutes, i.e., chloride and fluoride was studied. The maximum value of the relative concentration is observed to be in the range of 0.90 to 0.96 and 0.68 - 0.79 for chloride and fluoride respectively. It is known that fluoride is a reactive chemical i.e. non conservative; hence while transporting through the soil media, some amount of fluoride is adsorbed through soil. When the effect of velocity on the relative concentration of solute is considered, it is observed that higher the velocity, the attainment of the peak will be earlier. In nutshell, the experiments provide valuable insight about the porous medium and the behavior of chemicals.

### ACKNOWLEDGEMENT

The authors gratefully acknowledge the financial support rendered by the University of Mumbai under the scheme of 'Minor Research Grant' (Project No. 321) for the experimental set up during the academic year 2013-14.

## REFERENCES

- Ballarini, E., Bauer S., Eberhardt C. and Beyer C. (2012), "Evaluation of transverse dispersion effects in tank experiments by numerical modeling: Parameter estimation, sensitivity analysis and revision of experimental design", *J. Contam. Hydrol.*, **134** (6), 22–36.
- Barone, F. S., Rowe, R. K. and Quigley, R. M. (1992), "A laboratory estimation of diffusion and adsorption coefficients for several volatile organics in a natural clayey soil", *J. Contam. Hydrol.*, **10**(3), 225-250.
- Domenico, P. A. and Robbins, G. A. (1985), "A new method of contaminant plume analysis", *Ground Water*, **23**(4), 476-485.
- Domenico, P. A. (1987), "An analytical model for multidimensional transport of a decaying contaminant species", *J. Hydrol.*, **91**(2), 49-58.
- Hulagabali, A.M., Solanki, C. H. and Dodagoudar G. R. (2014), "Contaminant Transport Modeling through Saturated Porous Media Using Finite Difference and Finite Element Methods", *IOSR Journal of Mechanical and Civil Engineering*, pp. 29-33.
- Patrick J. Fox, Janguen Lee and John J. Lenhart (2011) "Coupled Consolidation and Contaminant Transport in Compressible Porous Media", *Int. J. Geomech.*, **11**(2), 113-123.
- Praveen Kumar and Dodagoudar G.R, (2009) "Modeling of contaminant transport through landfill liners using EFGM", *Int J. for numerical and analytical methods in geomechanics*, **34**, pp. 661-688..
- Rosqvist, H., and Destouni, G. (2000) "Solute transport through preferential pathways in municipal solid waste." *J. Contam. Hydrol.*, **46**, 39-60.
- Rowe, R.K. and Badv, K., (1996) "Chloride migration through clayey silt underlain by fine sand or silt", *J. Geotech. Eng., ASCE*, **122**(1), pp. 60-68.
- Rowe, R. K., Lake, C. B. and Petrov, R. J., (2000) "Apparatus and procedures for assessing inorganic diffusion coefficients for geosynthetic clay liners", *Geotech. Testing J.*, **23**(2), pp. 206-214..
- Sharma, P.K., Sawant, V.A., Shukla, S.K. and Khan, Z. (2013) "Experimental and numerical simulation of contaminant transport through layered soil", *Int. J. Geotech. Engg.*,
- Sheu, T.W.H. and Chen, Y.H. (2002) "Finite element analysis of contaminant transport in groundwater", *Appl. Math. Comput.* **127**, pp. 23–43.
- Swami Deepak, P.K. Sharma and C.S.P. Ojha, (2013) "Experimental investigation of solute transport in stratified porous media", *ISH Journal of Hydraulic Engineering*, **19**(3), pp. 145–153..
- van Genuchten, M. Th. (1981), "A closed-form equation for predicting the hydraulic conductivity of unsaturated soils." *Soil Sci. Soc. Am. J.*, **44**(5), 892-898.
- Wexler, E.J. (1992), "Analytical solutions for one-, two-, and three-dimensional solute transport in ground-water systems with uniform flow", *Techniques of Water Resources Investigations of the U.S. Geol. Surv., Chapter B7, Book 3: Applications of Hydraulics*, Reston, Virginia.
- William J. and Ning, Lu, (2004) "Integrated lecture and laboratory modules for contaminant transport studies in Undergraduate geotechnical engineering", *J. Prof. Issues Eng. Educ. Pract.*, **130**(3), pp. 19-25.



## Development of Methodology for Design of Foundation for Small Size Windmills on Existing Structure

Hemanshu A. Badgujar,<sup>1</sup> Smita B. Patil,<sup>2</sup> and  
Abhishek R. Deshmukh<sup>3</sup>

<sup>1</sup>P. G. Student, Department of Civil Engineering, Datta Meghe College of Engineering, Navi Mumbai; email: hemanshubadgujar@gmail.com

<sup>2</sup> Associate Prof, Department of Civil Engineering, Datta Meghe College of Engineering, Navi Mumbai; e-mail: sbpatil\_2009@rediffmail.com, Corresponding Author

<sup>3</sup> Assistant Prof, Department of Civil Engineering, Datta Meghe College of Engineering, Navi Mumbai; e-mail: abhishek.deshmukh890@gmail.com

### ABSTRACT

In India the average per capita electricity consumption is from 1-1.5kWhrs for domestic utilities, it means a small wind mill of 1 kWp is reasonably adequate to survive up with every day necessity of a family. Smaller wind mills are being used in stand-alone systems to supply localized needs. Wind energy is non-conventional source of energy. Due to the recent technological improvements wind energy outshines all other renewable energy resources. Vibrations of a wind turbine have a negative impact on its performance, so, in this study vibrations are controlled by using various methods. The vibrations of a wind turbine originate at various sources, the foundation's only task is to confirm the constancy for the wind turbine, and to do so over its life time. This is done by shifting and scattering the loads acting on the foundation to the ground structure. It was observed from analysis that for a windmill having 455 rpm and 7.58 Hz of rotational frequency, the vibrations obtained were having frequency of 13.188 Hz, the rotational frequency and vibrational frequency are distinct, thus there will not be resonance and windmill will not be damaged.

**KEYWORDS:** *small size windmills; methodology for windmill; vibrations of windmill; renewable energy.*

### INTRODUCTION

For at least 3000years windmills have been used, mainly for crushing grain or impelling water, while in navigating ships the wind has been an important source of power for even longer. Locally, due to obstacles such as trees or buildings wind velocities are significantly reduced. The survey states that the energy consumption per capita per day ranges from 5 to 6 units (kWhrs) for domestic applications. This leads to energy source/supply @ 1 to 1.5 kW per day available for 5 to 6 hrs. A renewable energy source will be preferably suited to fulfill these energy requirements. The sources existing easily are biogas, wind, solar, etc. out of which wind energy is studied in this paper.

Wind power currently shares about 4% of global electricity demand as per the fourth edition of Global Wind Energy Outlook which was released in 2014 and it is likely that in 2020 the share could reach up to 17% to 19%. Also, it is producing 2 million jobs and reducing CO<sub>2</sub> emission by 3 billion tonnes per year. In the of year 2014, the capacity was 336 giga watts (GW) in world-wide total wind power, viewing a growth of around 18.7 % (44 GW) over the earlier year. 25-30% of global energy requirement could provide wind energy by 2050. More than 83 countries are utilizes wind energy to supply their electricity grids.

### REVIEW OF LITERATURE

Past literature work closely relating with the present study is presented in this section. The literature review related to windmill vibration, aerodynamics rotor blade and performance analysis of mini wind turbines are discussed.

Kocer and Arora (1996) formulated the design of steel transmission poles as an optimization problem. In 1997 they extend the work in an effort to standardize steel pole design by using discrete optimization. In this work, the selected design was optimal and pole of prefabricated section.

Negm and Maalawi (1999) developed and tested optimization strategies in an effort to obtain the optimal design of a

wind turbine tower made up of multiple uniform Segments.

Murtagh *et al.* (2005) studied the structural model are incorporated with soil structure interaction effects at the time of vibration response of wind turbine towers. They found that the flexibility of soil incorporating into the model introduces amount of damping into the system considerable. It suggests that calculations of natural frequency not to be consider for damping due to interaction of soil structure will be uneconomical design and unrealistic.

Silva *et al.* (2008) presented a non-linear model of reinforced concrete slender structures which based on experimental data of dynamic analysis. Additionally, they transcribed optimal design of reinforced concrete wind turbine towers in this model into optimization constraints.

Murtagh *et al.* (2008) investigated the use of a passive control device, namely, a tuned mass damper (TMD), for the mitigation of vibrations due to the along-wind forced vibration response of a simplified wind turbine. The wind turbine assembly constituting a multi-body dynamic system consists of three rotating uniform rotor blades connected to the top of a flexible uniform annular tower. Using a discrete parameter approach, the free vibration properties of the tower and rotating blades are each obtained separately. Including the effects of centrifugal stiffening due to blade rotation and self-weight, a rigid mass at the top, representing the nacelle, for the tower.

Svensson (2010) examining the foundations for onshore wind turbines where both the more conventional method with a large concrete slab are investigated, but also alternative foundation methods are studied, mainly piled foundations.

Wagh and Shinde (2012) conducted a new design methodology was established for indigenous development of small wind machine technology, which considers aerodynamic rotor blade design for rotor blade performance and finite element design practices for strength of rotor blades. For 1kW power of small wind machine, this paper valuable for design, manufacturing also the performance testing of aerodynamic rotor blade.

Fitzgerald and Basu (2013) developed an active structural control scheme to control wind turbine nacelle/tower out-of-plane vibration. An active tuned mass damper (ATMD) is designed a placed inside the turbine nacelle. An Euler-Lagrangian wind turbine model considers the structural dynamics of the system and the interaction between in-plane and out-of-plane vibrations.

Kekezoglu *et al.* (2015) conducted a new mini wind turbine concept suitable for urban use and low wind speeds is demonstrated. The mini wind turbine concept consist of modular structure and can be improved for different conditions and wind sites. In this study, performance analyses of the mini wind turbine concept are performed and the results are summarized.

Alpman (2015) conducted Aerodynamic performance of two small-scale horizontal axis wind turbines are analyzed under the extreme operating gust and extreme direction change conditions with initial wind speeds of 7, 10, 13, 15 and 20 m/s.

Ramesh *et al.* (2017) conducted Modeling and analysis of small wind turbine blades by using a standard NACA air foil, in that work an attempt is made to evaluate the performance of small wind turbine blade models, through FEA.

## AIMS AND OBJECTIVES

The current study includes installation of mini wind turbine on an existing structure and calculating the vibrations induced and re-strengthening of structure. Some of the objectives emanating from the aim of the present study are outlined as follows.

1. Collecting information about windmill design and parameter values.
2. Deciding how to analyze the structure and Formulating the optimization problem.
3. Main objective of this paper is to minimize the vibrations of windmill which are harmful for existing structure.

## RESEARCH METHODOLOGY

### Study of Windmill Structure

#### a) Rotor Design

The rotor is the part of the wind turbine in charge of convert power taken from the wind flow to the rotational power of the main low-speed shaft.

When considering the installation of the wind turbine a chosen site has enough wind to generate the power needed. The power from the wind is proportional to the cube of the wind speed:

$$P_{\text{wind}} = \frac{1}{2} \rho S V^3 \quad (\text{Eq. 1})$$

Where:

$\rho$  is the air density ( $\text{kg/m}^3$ )  
 $S$  is a rotor area ( $\text{m}^2$ )  
 $V$  is the wind speed ( $\text{m/s}$ )

### b) The Tip Speed Ratio

The tip speed ratio  $\lambda$  (lambda) or TSR for wind turbines is the ratio between the rotational speed of the tip of a blade and the actual velocity of the wind.

$$\text{Tip speed ratio } \lambda = \text{speed of rotor tip} / \text{wind speed} = v / V = \omega r / V \quad (\text{Eq. 2})$$

Where:

$V$  is the wind speed ( $\text{m/s}$ )  
 $v = \omega r$  is velocity of rotor tip ( $\text{m/sec}$ )  
 $r$  = rotor radius ( $\text{m}$ )  
 $\omega = 2\pi f$  is the angular velocity ( $\text{radian/sec}$ )  
 $f$  = frequency of rotation ( $\text{Hz}$ ) or ( $\text{sec}^{-1}$ )

### c) Number of Blades

Usually flat objects are connected to a centre shaft that converts the push of the wind into a circular motion in a wind turbine. Most wind turbines have three blades. Two blades are used for small windmills in case of construction and installation. Larger numbers of blades decrease vibration intensity. Instead of two blades if three blades are used, noise and wear are generally lesser and effectiveness higher. Some people find that the three-bladed rotor is more attractive to look at than a one or two-bladed rotor. Considering all those characteristics the numbers of blades have been carefully chosen as 3 see, Fig. 1

### d) Length of the Blades

The length of the blade is a distance from the tip of the blade till the center of rotor.

### e) Aerodynamics

The two primary aerodynamic forces at work in wind-turbine rotors are lift, which acts perpendicular to the direction of wind flow; and drag, which acts parallel to the direction of wind flow.

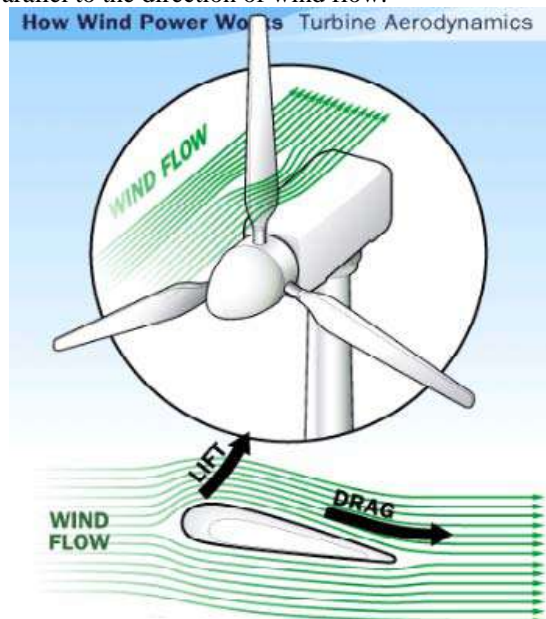


Fig. 1 Working principle of wind power turbine

In an airfoil structure, one surface of the blade is somewhat rounded, whereas the other is comparatively flat. Lift is a pretty complex phenomenon, but in general words when wind travels over the rounded, downwind face of the blade, it

has to move faster to reach the end of the blade in time to encounter the wind traveling over the plane, upwind face. In many aerodynamics problems, lift and drag are aerodynamic forces.

Lift and drag forces depend on the coefficient of lift and coefficients of drag, which in turn depend on the cross section of the used blade, and on the angle of attack  $\alpha$ , at which the wind strikes the blade. We cannot calculate the lift and drag coefficients. They are measured experimentally in the wind tunnels and recorded in the table of the individual of the blade profile.

#### *f) Angle of Attack*

The difference between where the wing is pointed and the direction of the air flowing over the wing is the angle of attack.

### **Study of Effect of Vibrations on Foundation of Windmill**

The general methodology used to transcribe the design of wind turbine towers and foundations into an optimization problem includes:

- 1) Collecting information on design requirements and parameter values
- 2) Deciding how to analyze the structure
- 3) Formulating the optimization problem

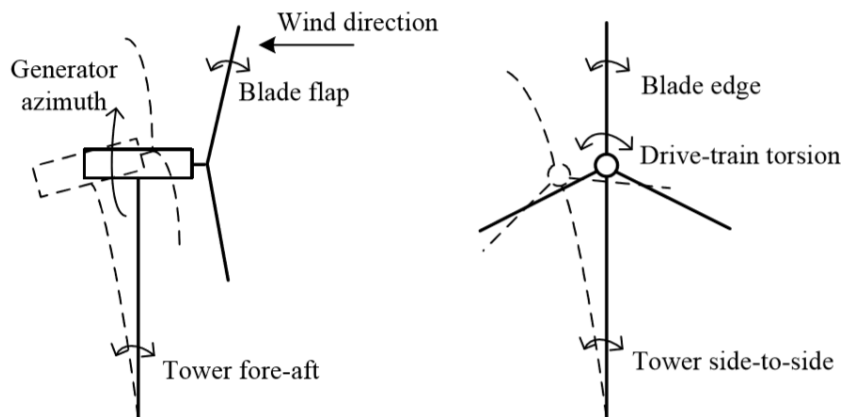


Fig. 2 Schematic representation of a wind turbine tower

The left picture in Fig. 2 shows the vibrations in the plane of the turbine axis, while the right picture shows the vibrations in the plane of the turbine blades. and thus, cause fatigue. The fluctuating loads and vibrations will also reduce the life expectancy of other components such as the low speed shaft and the gearbox, and thus increase the maintenance cost of the turbine, which is a critical problem in the wind energy industry.

### **Study on Vibrations of Small Size Windmills**

#### *a) Design Parameters of Windmill*

ANSYS R18.0 software has been used to carry out Vibrations study of Small size windmills of 1 kW Power output by using following design parameters. The modelling of the windmill is presented in Figs. 3-6.

- 1) Propeller diameter = 1.75 m
- 2) Effective blade length = 0.875 m
- 3) Rotational speed = 455 r.p.m.
- 4) Height of Post = 2.5 m
- 5) Density of the air ( $\rho$ ) = 1.125 kg/m<sup>3</sup>
- 6) Design Wind Speed = 44 m/s (As per IS 875 Part III)

*b) Details of ANSYS work*

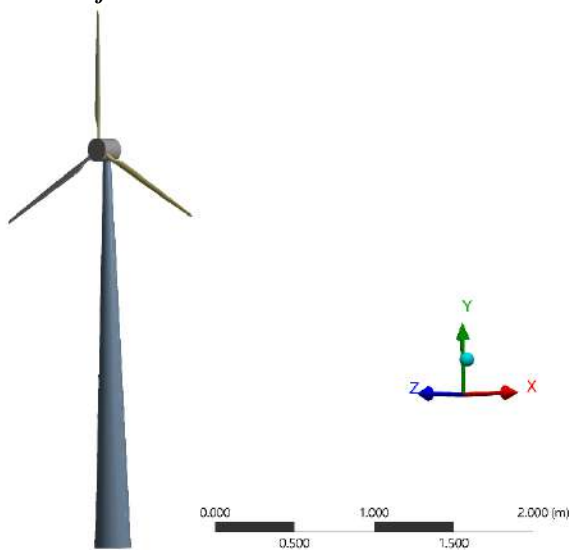


Fig. 3 Windmill model in Ansys

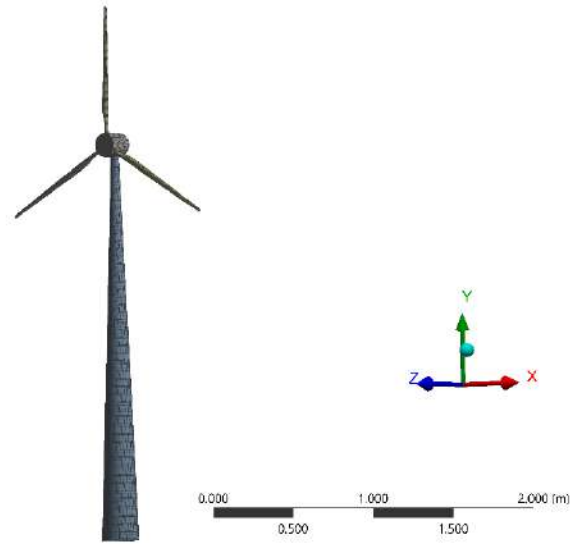


Fig. 4 Meshing of windmill

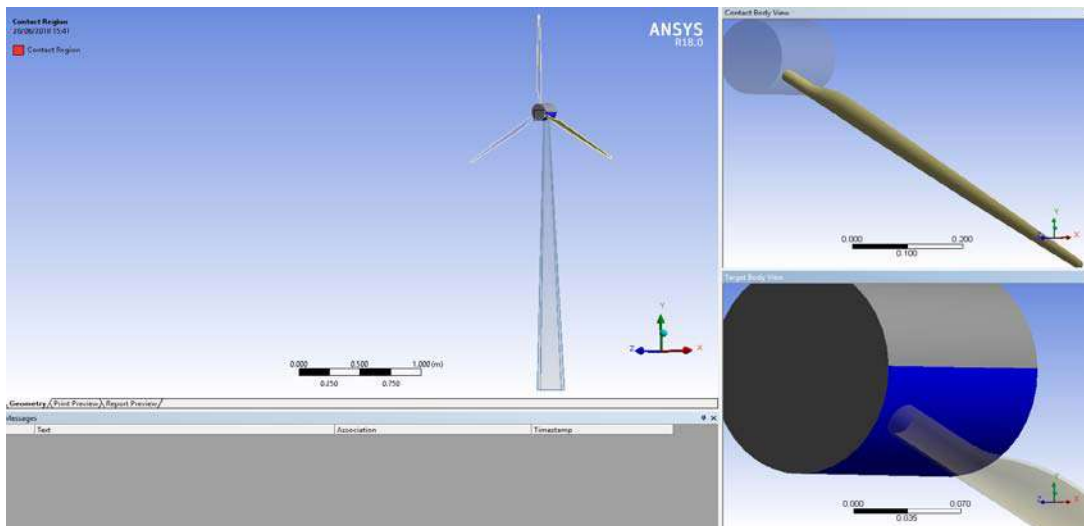


Fig. 5 Connection of windmill

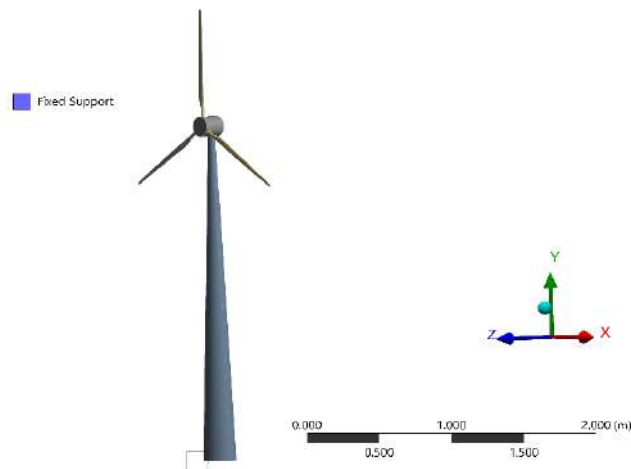


Fig. 6 Fixed support of windmill

## RESULTS AND ANALYSIS

### Stability of Structures on Resonance Frequency

A frequency capable of stimulating a resonance determined in a given body or system. It was observed from analysis in Ansys that for a windmill having 455 rpm or 7.58 Hz of rotational frequency, The vibrations obtained were having frequency of 13.188 Hz as shown in Fig. 7.

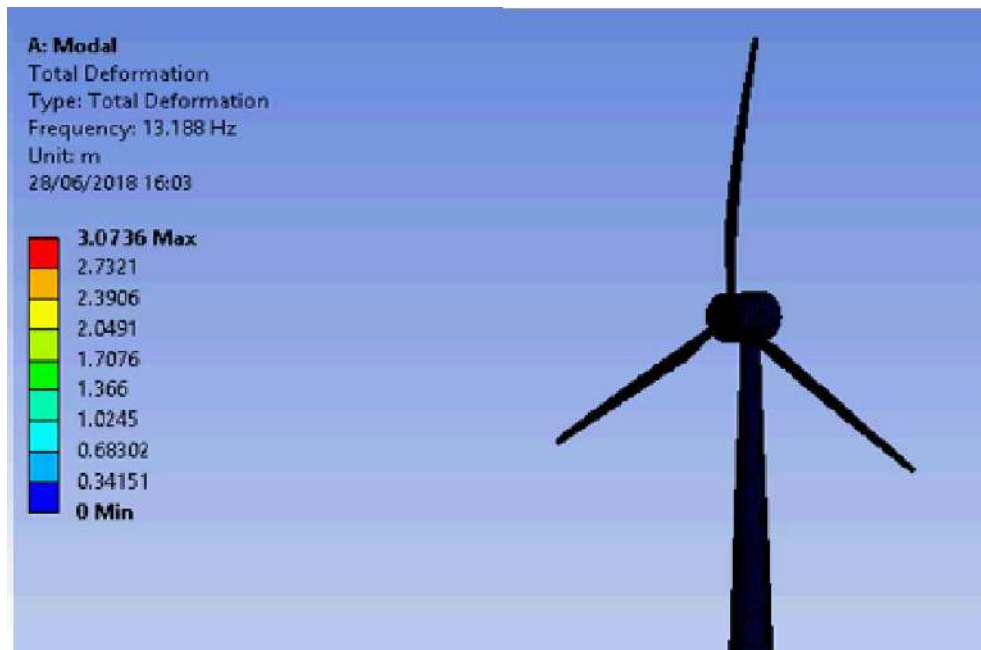


Fig. 7 Vibrational analysis in Ansys

The rotational frequency and vibrational frequency are distinct, thus there will not be resonance and windmill will not be damaged.

## Reaction Force Develop at the Base of Windmill

Table 1: Reaction force

Maximum value over time	
x-axis	0 N
y-axis	584.69 N
z-axis	794.33 N
Total	983.32 N

As observed from Table no. 1 the vertical reaction is 584.69 N which is being transferred on single column on the structure. The horizontal reaction force due to vibrations is 794.33 N.

## SUMMARY AND CONCLUSION

- The rotational frequency and vibrational frequency are distinct, thus there will not be resonance and windmill will not be damaged.
- For development of small wind machine technology, new design methodology was established which considers aerodynamic rotor blade design for rotor blade performance. The way of combining ANSYS and STAAD.Pro was adopted to establish the methodology for small size windmills on existing structure.
- In this paper, a new wind turbine concept that can be mounted on roofs, is presented. With the developed wind turbine system, wind energy potential can be used more efficiently in supplying city demands.

## REFERENCES

- Bedri Kekezoglu, Mugdeşem Tanrıoven, Ali Erduman (2015), "A New Wind Turbine Concept: Design and Implementation", *Acta Polytechnica Hungarica*, Vol. 12, No. 3, 2015
- Breifffni Fitzgerald, Biswajit Basu (2013), "Active Tuned Mass Damper Control of Wind Turbine Nacelle/Tower Vibrations with Damaged Foundations", *Key Engineering Materials* Vols. 569-570 (2013) pp 660-667 (2013) Trans Tech Publications, Switzerland.
- Henrik Svensson (2010), "Design of Foundations for Wind Turbines", Department of Construction Sciences Structural Mechanics, ISRN LUTVDG/TVSM--10/5173--SE (1-158) ISSN 0281-6679, Division of Structural Mechanics, LTH, Lund University, Box 118, SE-221 00 Lund, Sweden.
- John Corbett Nicholson, University of Iowa (2011), "Design of wind turbine tower and foundation systems: optimization approach", University of Iowa Iowa Research Online, Spring 2011
- Kocer, Fatma Y. and Arora, Jasbir S. (1996), "Optimal Design of Steel Transmission Poles", *Journal of Structural Engineering* 122, no. 11 (November): 1347-1356
- M. M. Wagh, N. N. Shinde (2012), "Design, Development, Manufacturing and Testing of Aerofoil Blades for Small Wind Mill", *International Journal of Renewable Energy Research*, Vol.2, No.4, 2012
- Maryam Refan and Horia Hangan, (2012), "Aerodynamic Performance of a Small Horizontal Axis Wind Turbine", *Journal of Solar Energy Engineering*, Vol. 134 / 021013-1, May 2012
- Murtagh P.J., Basu B., and Broderick B.M. (2005), "Response of Wind Turbines Including Soil-Structure Interaction", Proceedings of the Tenth International Conference on Civil, Structural and Environmental Engineering Computing, paper 270: 1-17
- Murtagh P.J., Basu B., and Broderick B.M., Ghosh A., (2008), "Passive control of wind turbine vibrations including blade/tower interaction and rotationally sampled turbulence", *Wind Energy*, 11 (4) (2008) 305–317
- Negm, Hani M. and Maalawi, Karam Y. (1999), "Structural Design Optimization of Wind Turbine Towers", *Computers and Structures* 74 (2000): 649-666
- Ramesh J., Rathna Kumar P., Md Umar, Mallikarjuna M. V. (2017) "Static and Dynamic analysis of 1kw small wind turbine blades by various materials" *Indian J. Sci. Res.* 17(2): 161-165, 2017

Proceedings of National Conference: Advanced Structures, Materials and Methodology in Civil Engineering  
(ASMMCE – 2018), 03 - 04th November, 2018  
PAPER CODE: G-319

Silva, Marcelo, Arora, Jasbir, and Brasil, Reyolando MLRF. (2008), "Formulations for the Optimal Design of RC Wind Turbine Towers", Engineering Optimization 2008 – *International Conference on Engineering Optimization (June)*

Zijun Zhang, University of Iowa (2009), "Wind turbine vibration study: a data driven methodology", University of Iowa Iowa Research Online, Fall 2009



## Stability Assessment of Slope for Vertical Rock Cut - A Case Study

R. G. Vagal,<sup>1</sup>A.R. Katti<sup>2</sup>

<sup>1</sup># P.G Student, Department of Civil Engineering, Datta Meghe College of Engineering, Sector-3, Airoli, NAVI MUMBAI-400708, Email: rajeshvagal@gmail.com

<sup>2</sup> Professor, Department of Civil Engineering, Datta Meghe College of Engineering, Sector-3, Airoli, Navi Mumbai-400708, Email: drkattianand@gmail.com, Corresponding Author

### ABSTRACT

The stability of slopes for vertical rock cut is most imperative aspect of vehicular safety on Indian highways. India's first six-lane concrete, high-speed, Mumbai Pune Expressway 94.5 km long, frequently eclipsed by landslides experiences persistent problem of rock fall. The present study aims to understand the behaviour of the strike, the dip, and the jointing pattern, of rock mass, to assess stability of slope for vertical rock cut. Occurrence of slope failures depend on factors such as adverse slope geometries, geological discontinuities, weak or weathered slope materials and severe weather conditions. External loads like heavy precipitation and seismicity could play a significant role in slope failure. Khandala monkey hill rock cut 405m long, ranges between 15m to 20m in height is segregated in three layers top, middle, and bottom for statistical analysis. Four numbers of boreholes driven 15m deep from existing ground level to collect NX size core. Photographs for vertical rock cut clicked and mapped with 5m × 5m grid, segregated in three layers, top, middle, and bottom for statistical analysis. The length and height of rock cut physically measured. The study of rock classification illustrate peculiar behaviour of rock mass. The RQD and RMI values (243 sections) show significant correlation between layers when statistically analysed. Upper layer consisting of soil and highly jointed rock is extremely susceptible to slide (RMI mean value is 0.400 with 0.0908 standard deviation for sample size, N=80.). Middle layer with poor RQD and strong RMI show the signs of sliding and toppling with upper layer (RMI mean value for middle section is 5.638 with 0.807 standard deviation for sample size, N=80). Bottom layer having very strong RMI and excellent RQD is most stable (RMI mean value 12.242 and 4.199 standard deviation for sample N=80).

**KEYWORDS:**RQD; RMI; rock cut; rock fall; dip; strike.

### INTRODUCTION

The Mumbai-Pune Expressway, officially known as the “Yashwantrao Chavan Mumbai Pune Expressway” is India's first six-lane concrete, high-speed, access controlled tolled expressway. It spans a distance of 94.5 km, frequently eclipsed by landslides in the *ghats*, experiences persistent problems of rock fall. A reconnaissance inventory carried out by the Central Road Research Institute, New Delhi, India revealed that about 90% of the slope failures along the stretch are due to rock fall, and the remaining 10% are due to debris flows, subsidence, and sliding. Based on frequency and magnitude of the recorded incidences, more than seventeen problematic rock fall prone areas have been identified. These critical areas of rock fall are located at km 14, km 18, km 21.5, km 29.8, km 26.491, km 38.9, km 41, km 41.679, km 42.36, km 47.5, km 68, and km 70. Investigations of all the identified areas have been carried out from various aspects that were thought critical to slope stability, including geological, geomorphologic and geotechnical aspects.

#### *Basic Geology*

The geological conditions in the study area are dominated by basalt, an extrusive rock created by the outpouring of volcanic magma. Successive eruptions of basalt have formed the Deccan plateau region of South West India. The condition of the rock can be defined as amygdaloidal basalt with vesicles and coarse grains having unconfined strength of 150 MPa and the compact, fine-grained basalt with an unconfined strength of 180 MPa (MSRDC Report, 1995). The strength of the intact rock does not contribute significantly in the case of fractured or jointed rocks. In these rocks, the discontinuities play a major role in forming favourable conditions for failure along mostly its day lighted surfaces. The weathered mass in this layer is highly susceptible to erosion in the presence of water, which leads to scouring at the base of the upper layer and, ultimately, failure of the overhanging rocks see Fig. 1.

#### Literature Review

The Rock Quality Designation Index (RQD) was developed by Deere (Deere et al. 1967) to provide a quantitative estimate of rock mass quality from drill core logs.

Palmstrom et al., (1982, 1996, 2000, 2001, 2002, 2003, 2005, 2009, 2010) proposed a rock mass index (RMI) to

characterize rock mass strength as a construction material. The presence of various defects (discontinuities) in a rock mass that tend to reduce its inherent strength are taken care of in rock mass index (RMi), which is expressed as

$$\mathbf{RMi} = \mathbf{q_c} \times \mathbf{Jp} \quad \dots(2.2)$$

$q_c$ -the uniaxial compressive strength (UCS) of the intact rock material in MPa,  $Jp$ -the jointing parameter composed of mainly four jointing characteristics, namely, block volume or density of joints, joint roughness, joint alteration, and joint size.

The value of  $Jp$  varies from almost “0” for crushed rock masses to “1” for intact rocks

Palmstrom (1974) presented simple expression between volumetric joint count ( $J_v$ ) and RQD.

$$\mathbf{RQD} = \mathbf{115 - 3.3 J_v} \quad \dots (2.3)$$

( $RQD = 0$  for  $J_v > 35$ , and  $RQD = 100$  for  $J_v < 4.5$ )

Based on the literature pertaining to the classification of rock mass and stability of slope reviewed here, we can presume that adopting proper precautionary measures to tackle the hazardous problems needs thorough investigation. A list of all rock parameters and an understanding of all rock properties and rock mechanics are necessary for any rock-engineering project. Then an objective-based method of planning should be undertaken. A procedure for identifying causes of failure is most relevant to the project within the scope of the objective, and finally the ability to select relevant engineering techniques rounds out the process. Taking these steps, we can utilize existing knowledge in an optimal way to develop stable design, construction, and monitoring procedures for any project.

Bases on the above, one need to map the entire area and understand the jointing pattern and rock mass classification

The first case of rock and debris fall at this location reportedly occurred in the year 2003-2004, during monsoon. Since the rocky blocks are intermittently falling from the face, as well as from top of the slope. The size of the block varies from a few centimeter to a meter and sometimes even more in diameter. The incidences of the rock fall are frequent during rainy season. The impact of the falling as noticed is very high.



Fig 1: Rock fall at Adoshi in Sept. 2015

The sliding material itself blocks a part of the expressway, thereby causing inconvenience to the traffic. The direct fall makes the impact more dangerous and is most of the times fatal when rock block hit running vehicle.

The sliding material itself blocks a part of the expressway, thereby causing inconvenience to the traffic. The direct fall makes the impact more dangerous and is most of the times fatal when rock block hit running vehicle resulting to the loss of life, which cannot be valued.

The primary causes of rock-fall include:

- Dip and strike of the bedding plane,
- Weathering of the rock,
- Presence of soil in the weak joints and bedding planes,
- Vertical rock cutting with inadequate dressing of rock face after blasting,
- The intersection of the joints exposed on the face of the slope forming wedges,
- The presence of a prominent oblique joint/fracture between the two separate layers of basalt,
- A weak sub-horizontal layer dividing two basaltic most of the material slides down,
- A large amount of precipitation with high intensity,
- Seepage of water into the weathered and weak layers that are exposed on the surface after the construction of the expressway,

- A high gradient of slope and a steep vertical cut,  
Hence requires detailed classification and stability analysis of rock slope at Adoshi and Khandala

### ***Aims & Objectives of the present study***

To study the behaviour of rock mass by understanding

1. The jointing pattern
2. The dip
3. The strike and

The other engineering properties of rock and rock mass.

### ***Methodology***

Geotechnical engineering properties of rock influence the shear strength, permeability, susceptibility to chemical and physical weathering etc. and the mineralogical characteristics. The attitude of bedding or jointing relative to the adjacent slope is an important factor for geological formations of slope where the direction of the bedding planes and density of particular set of joints can induce slope failure.

The site investigation for the Khandala site includes

- 1) Borehole drilling and sampling,
- 2) Photographic survey for Khandala rock cut.

### ***Rock cut***

Photographic survey for Khandala hills and desk study to collect previous site investigations and the history of development of the site.

- To undertake a visual inspection of the ground conditions.
- To identify areas of slope movement where there may be a risk of slope failure.
- To identify areas of slope instability.

The ultimate aim of a site investigation was to obtain the maximum amount of good quality data at minimum cost. Different techniques used as the basis for defining the site conditions, in combination to give a range of results. The limitations of each method was important to get control on output of the data quality.

### ***Rock Mass Classification***

Rock Mass Classification is useful for empirical design approach that correlates the practical experiences encountered at the previous site to the situation that one can expect at the proposed site. Various measurements and the characterization of the degree of jointing, i.e. the density and condition of joints within a rock mass volume. Block size is the most important feature influencing the behaviour of rock masses in surface cuttings. Therefore, reliable measurements of the rock blocks govern the quality of assessments in rock mechanics, rock engineering, and numerical modelling.

The following methods for measuring the degree of jointing and the block size, together with correlations between them,

1. Observation of exposed (sound) rocks in the surface or in excavations.
2. Logging of drill cores, where the distance between joints (joint intercept), the RQD, joint frequency (number of joints per meter) are noted.
3. The weighted jointing method, which improves measurements made on rock surfaces and on drill cores.

The following measurements of the joint conditions:

- 1 Joint roughness, composed of smoothness of joint surface and waviness of joint plane.
- 2 Joint alteration, composed of the condition of the joint wall and possible joint filling or coating on joint wall.
- 3 Joint size and termination.

The following rock mass parameters have generally the strongest impact on the behaviour and strength properties of a rock mass,

A. The degree of jointing, including:

1. Density of joints (measured as joint set spacing, block size, RQD);

2. Block shape or jointing pattern;
  3. Orientation of joint set or main discontinuities;
- B. The joint characteristics, consisting of:
- 1 Joint roughness (smoothness and waviness or planarity);
  - 2 Joint condition or alteration (condition of joint walls, possible filling material)
- C. The rock material through which the joints intersect:
- 1 Strength and elastic properties of the rock;
  - 2 Rock anisotropy;
  - 3 Rock durability;
  - 4 Content of certain minerals with special properties (swelling, elastic, soluble, etc.).

**Block Types & Shapes**

The types of blocks delineated by joints have characterized in different ways and by different terms. Where relatively regular jointing exists, it may be possible to give adequate characterization of the jointing pattern according to the system presented by Dearman (1991) see Fig. 3.

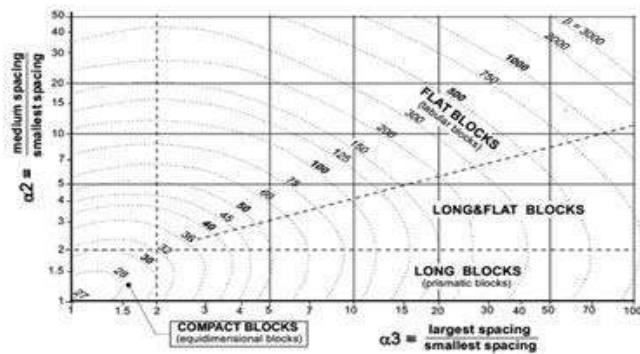


Fig 2: Block type characterized by the block shape factor ( $\beta$ )

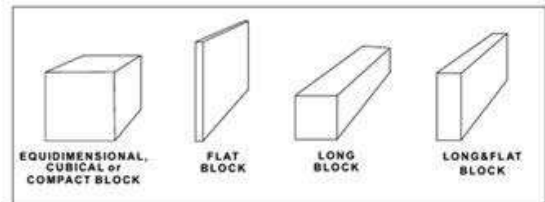


Fig 3: Main types of blocks (Palmstrom 1995)

The block shape depends mainly on the differences between the joint set spacing. The block shape factor ( $\beta$ ), gives numerical expression as follows. As block may be form by more than six faces or may have irregular shape, it can be difficult to find the value of ( $\beta$ ) see, Fig.2. A simplified expression is:

$$(\beta) = 20 + 7a_3/a_1 \dots (3.1)$$

Where  $a_3$  is the longest and  $a_1$  the shortest dimension of the block

For very flat to extremely flat blocks above equation has limited accuracy. Where ( $\beta$ ) is not known, it is recommended to use a 'common' value of ( $\beta$ ) = 36. (Palmstrom 1995)

**Block volume ( $V_b$ )**

The volumes of individual blocks in a surface can be directly measured from relevant dimensions by selecting several representative blocks and measuring their average dimensions. It is not possible to observe the entire individual block in an rock cut or outcrop or in the surface of an underground opening, especially where less than three joint sets occur. Random joints and/or cracks formed during the excavation process will often result in defined blocks. In such cases a spacing of random joints, 5 to 10 times the spacing of the main joint set can often be use to estimate the block volume.

Where only one joint set ( $S_1$ ):

$$V_b \approx S_1 \times 5 S_1 \times 10 S_1 = 50 S_1^3 \dots (3.2)$$

For two joint sets ( $S_1$  and  $S_2$ ):

$$V_b \approx S_1 \times S_2 \times 5 S_1 = 5 S_1^2 \times S_2 \dots (3.3)$$

**Volumetric Joint Count ( $J_v$ )**

The volumetric joint count ( $J_v$ ) has been described by Palmstrom (1982, 1985, 1986). It is a measure of the number of joints within a unit volume of rock mass, defined by

$$J_v = \frac{1}{s_1} + \frac{1}{s_2} + \frac{1}{s_3} + \dots + \frac{N_r}{s_3} \quad \dots (3.4)$$

$s_1, s_2, s_3$  are the joint spacing &  
 $N_r$  = the number of random joints.

$J_v$  can easily be calculated from common joint observations, since it is based on measurements of joint spacing or frequencies. In the cases where mostly random or irregular jointing occurs,  $J_v$  can be found by counting all the joints observed in an area of known size.

**Correlation between block volume ( $V_b$ ) and volumetric joint count ( $J_v$ )**

The block volume for three joint sets with intersecting angles  $90^\circ$  express as  
 $V_{b_0} = \beta \times J_v^{-3} \quad \dots (3.5)$

**Rock quality designation (RQD)**

RQD is by its original definition (Deere, 1966) the length in percent of measured length of the un-weathered drill core bits longer than 10 cm.

The RQD is easy and quick to measure. It is the only method used for measuring the jointing density along the core drill hole. In rock engineering and core logging, the RQD has several limits. Therefore, it is more important to consider joint density measurements of drill cores than RQD in the core log.

**Correlation between RQD and  $J_v$**

It is not possible to obtain good correlations between RQD and Palmstrom (1982), see Fig. 4 presented the following simple expression, which is frequently used:

$$RQD = 115 - 3.3 J_v \quad \text{ref. (2.3)}$$

Here,  $RQD = 0$  for  $J_v > 35$ , and  $RQD = 100$  for  $J_v < 4.5$

**Weighted jointing density measurements ( $w_j d$ )**

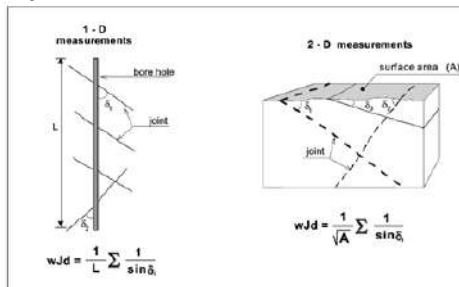


Fig 4: Shows the intersection between joints and drilled core hole (Palmstrom 1995)

The weighted joint density method developed to achieve better information from borehole and surface observations. Based on the measurement of the angle between each joint and the surface or the borehole, divide the angles into the four intervals; rating of  $f_i$  is given, to simplify the observations see Table 1.

Table 1: Angle intervals and ratings of the factor  $f_i$

Angle ( $\delta$ ) between joint and surface	Rating of the factor $f_i$
$\delta > 60^\circ$	1
$\delta = 31 - 60^\circ$	1.5
$\delta = 16 - 30^\circ$	3.5
$\delta < 16^\circ$	6

To simplify the observations, the angles have been divided into intervals for which average ratings of  $f_i$  have been selected. The definition of  $w_j d$  is:

For 2-D measurement in rock surface:  $w_j d = \frac{1}{\sqrt{A}} \sum f_i \quad \dots (3.6)$

For 2-D measurement in rock surface:  $w_j d = \frac{1}{L} \sum f_i \quad \dots (3.7)$

$\delta$  = the inter section angle, i.e. the angle between the observation plane or borehole and the individual joint:

$A$  = the size of the observed area in  $m^2$

$L$  = the length of the measured section along the drill core  
 $f_i$  = A rating factor,

The weighted jointing density ( $wjd$ ) value is approximately similar to the volumetric joint ( $J_v$ ) count ( $wjd \approx J_v$ ).

**Weighted jointing measurements made on drill cores**

The 5 m long, part of the core divided into the 3 sections with similar density of joints:

For each section the number of joints within each angle interval has been counted and the results are shown in

Fig.5

Section 1, length L = 2.17 m			
Interval	Rating $f_i$	Number of joints	Number of weighted
$> 60^\circ$	1	11	11
$31- 60^\circ$	1.5	6	9
$16- 30^\circ$	3.5	2	7
$< 16^\circ$	6	1	6
			$N_w = \sum n$

Result  
 $wjd = \frac{N_w}{\sqrt{A}} = 6.6$

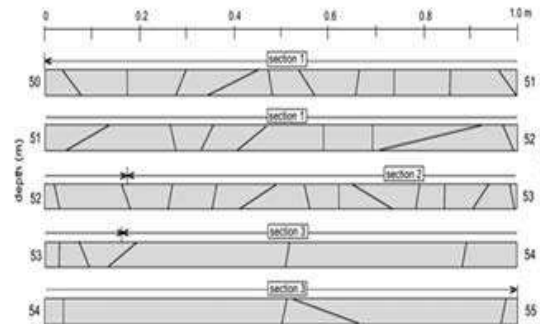


Fig 5: Calculation of the weighted joint density from registration of jointing in the borehole

**The Rock Mass Index System (RMI)**

Arild Palmstrom proposed a rock mass index (RMI) to characterize rock mass strength as a construction material. Rock mass index (RMI) took care of various defects (discontinuities) present in a rock mass that tend to reduce its inherent strength (Palmstrom 1996), see Table 2.

RMI system in rock mechanics and rock engineering enhances the accuracy of the input data required in rock engineering by its systematic approach of rock mass characterizations.

The presence of various defects (discontinuities) in a rock mass that tend to reduce the inherent strength of the rock constitutes the main feature in its behaviour. This main principle of the Rock Mass index is as follows

$RMI = \sigma_c \times JP$  for jointed rock mass ..... (3.8)

$\sigma_c$  = the uniaxial compressive strength of the intact rock material;

$JP$  = the jointing parameter. It is a reduction coefficient representing the effect of the joints in a rock mass. The value of  $JP$  varies from almost zero for crushed rocks to one for intact rock.

$RMI = \sigma_c \times F\sigma$  for massive rock having rock size larger than approx.  $5m^3$  ..... (3.9)

$F\sigma$  = The massivity parameter represents the scale effect of the uniaxial compressive strength (massive rock has value of approximately  $F\sigma \approx 0.5$ ).

The combination of the input parameters in R M i

The uniaxial compressive strength of intact rock ( $\sigma_c$ ) can be determined from laboratory tests,

The larger joints have a markedly stronger impact on the behaviour of a rock mass than smaller joints hence a factor for the joint size and termination is included as a size correction factor for joints. The influence of a discontinuous joint, i.e. joints that terminate in massive rock, is much less, as the failure plane must partly pass through intact rock.

**The joint parameter (JP)**

The jointing parameter (JP) is by empirical relations related to the joint condition factor,  $jC$ , and the block volume,  $V_b$ .

$JP = 0.2 \sqrt{jC} \times V_b^D$  ..... (3.10)

Where,  $V_b$  = the block volume, given in  $m^3$

$D = 0.37 jC^{-0.2}$  ..... (3.11)

The jointing parameter by the following expression, which derived from the lines representing  $jC$   
 The joint condition,  $jC$ , is as follows:

$$jC = jL - jR/jA \quad \dots (3.12)$$

$jL$  = the joint size and continuity factor.

$jR$  = the joint roughness factor of the joint wall surface and joint planarity.

$jA$  = the joint alteration factor, representing the character of the joint wall, i.e. the presence of coating or weathering and possible filling.

### ***The joint roughness factor (jR)***

The roughness factor includes the small-scale asperities (smoothness) on the joint surface and the large-scale planarity (waviness) of the joint plane.

$$jR = jw \times js \quad \dots (3.13)$$

The ratings of the joint waviness factor ( $jw$ ).

The ratings of the smoothness factor ( $js$ ).

Surface smoothness or unevenness is the nature of the asperities in the joint surface, which one can feel by touch. This is an important parameter contributing to the condition of joints; asperities that occur on joint surfaces interlock, if the surfaces are clean and closed, and inhibit shear movement along joint surfaces. Asperities usually have a wavelength and amplitude measured in millimeters.

### ***The joint alteration factor (jA)***

This factor represents the strength of the joint wall and the effect of filling and coating materials. The strength of the surface of a joint is a very important component of shear strength and deform- ability where the surfaces are in direct rock to rock contact as in the case of unfilled (clean and coated) joints (Bieniawski, 1984, 1989). The strength of the joint surface is determined by the following:

- The condition of the surface in clean joints,
- The type of coating on the surface in closed joints,
- The type, form and thickness of filling in joints with separation.

Weathering or alteration is more pronounce along the joint wall than in the block. This result in a wall strength, is some fraction of what would be measured on the fresher rock found in the interior of the rock blocks. The state of weathering or alteration of the joint surface where it is different from that of the intact rock, is therefore essential in the characterization of the joint condition

### ***The joint length and continuity factor (jL)***

To measure the joint length observes the discontinuity trace lengths on surface exposures.

Palmstrom (1995) described feature to evaluate the exact length of a joint, a solution is to estimate the size range of the joint. The factor  $jL$  include the effect of the *joint continuity*, which is divided into two main groups:

- Continuous joints that terminate against other joints
- Discontinuous joints that terminate in massive rock.

$$jL = 1.5 \times jC \times L^{-0.3} \quad \dots (3.14)$$

$L$  = the length of the joint in meter, and

$jC$  = joint continuity ( $jC = 1$  for continuous and  $jC = 2$  for discontinuous joints)

The measurements other than block volume can be applied directly. These are located in the upper left part of the figure. Here, the volumetric joint count ( $J_v$ ) for various block shapes (or numbers of joint sets) can be used instead of the block volume.

RQD can be used with the limitations of the accuracy. Numerical values alone are seldom sufficient for characterizing the properties of a complex material such as a rock mass.

**Table 2: Classification of RMI**

Characterization		RMI Value
Term for RMI	Term for rock mass strength	
Extremely low	Extremely weak	< 0.001
Very low	Very Weak	0.001 - 0.01
low	Weak	0.01 - 0.1
Moderately high	Moderately Strong	0.1 - 1
high	Strong	1 - 10
Very high	Very Strong	10 - 100
Extremely high	Extremely strong	> 100

**Result & Analysis**

Field observational methods are one of the most useful and effective investigation techniques. Based on the results acquired by implementing these techniques, one can accurately evaluate the actual site conditions and make conclusions regarding the type of investigation, analysis and protective measures required. A thorough field investigation has been carried out to identify the causes and mechanism of the failures. Field data collected in form of bore logs driven 15 m deep above rock fall section of Khandala hill. Photographs clicked with high resolution (DSLR) camera to procure exact and clear picture for mapping joints. Rock type, jointing pattern, joint size, etc. carefully observed and notes prepared for Adoshi and Khandala rock cut. Observations and results tabulated and statistically analysed on IBM SSPS Version 2 software see Tables 3-5.

Four numbers of boreholes were driven 15m deep from existing ground level to collect NX size core. Selection of location for borehole was planned with objective to get comprehensive impression of physical and chemical properties of rock subject to mapping.

Bore log data revealed that the topmost layer constituted of murrum followed with highly weathered and highly fractured amygdaloidal basalt with recovery in form of rock fragments and nil RQD (core pieces length > 10cm). This layer ranged between ground and 4m to 7m depth. Middle layer showed moderate recovery in form of core pieces with moderate RQD of 35 % to 70 % .This layer ranged between 6m to 11m depth and constituted fairly jointed amygdaloidal basalt. Bottom layer post 10m to 11m depth was found to be the strongest with above 80% to 90 % recovery and similar percentage of RQD.

No. of bore holes: 4

Depth of termination: 15m to 20m (at least 5m in good quality hard rock)

Bore Log No. 1 (Sample calculation)

Table -3: Shows input parameters required to calculate RQD and RMI

Input Parameters				
	A	B	C	Remark
<b>jR</b>	<b>1</b>	<b>1.5</b>	<b>4</b>	<b>From Table</b>
<b>jL</b>	<b>1</b>	<b>4</b>	<b>1</b>	<b>From Table</b>
<b>jA</b>	<b>4</b>	<b>2</b>	<b>4</b>	<b>From Table</b>
<b>jC= (jR x jL)/jA</b>	<b>0.25</b>	<b>3</b>	<b>1</b>	<b>From calculation</b>
<b>D=0.37jC<sup>-0.2</sup></b>	<b>0.4882</b>	<b>0.2970</b>	<b>0.3700</b>	<b>From calculation</b>
<b>σC</b>	<b>8.43</b>	<b>8.43</b>	<b>18.31</b>	<b>From Lab results</b>
<b>β</b>	<b>36</b>	<b>36</b>	<b>36</b>	<b>for a-common block shape From Table</b>

Photographs for Khandala of vertical rock cut with previous history of rockslide clicked on high resolution (DSLR) camera for mapping & analysis. The length and height of rock cut physically measured. The photos mapped with 5m × 5m grid. For statistical analysis purpose, 5m × 5m grid sections further segregated in three layers top, middle, and bottom

Khandala Section of Rock cut:

Length: 405m  
 Height: 15m to 22m  
 Number of Mapping sections (5m × 5m grid): 243

Table 4: Shows descriptive statistics for RQD

Layers	Mean	Std. Deviation	N
Top	25.50	12.19	80
Middle	32.09	12.25	80
Bottom	82.70	11.73	80

Table -5: Shows Pearson Correlation & Sig. for RQD

Layer	Layer	N	Pearson Correlation	Sig. (2-tailed)	Correlation
Top	Middle	80	0.553**	0.000	Highly Significant
Top	Bottom	80	0.312**	0.005	Highly Significant
Middle	Bottom	80	0.371**	0.001	Highly Significant

A Pearson product-moment correlation coefficient computed to assess the relationship between the RQD top layer and RQD middle layer as shown in Tables 6-7.

Highly significant positive correlation between the two variables i.e.,  $r = 0.553$ ,  $n = 80$ ,  $p = 0.000$  i.e.  $< 0.005$  is seen.

Table 6: Shows descriptive statistics for RMi

Layers	Mean	Std. Deviation	N
Top	0.400	0.0908	80
Middle	5.638	0.807	80
Bottom	12.242	4.199	80

Table -7: Shows Pearson Correlation & Sig. for RMi

Layer	Layer	N	Pearson Correlation	Sig. (2-tailed)	Correlation
Top	Middle	80	0.530**	0.000	Highly Significant
Top	Bottom	80	0.271*	0.015	Significant
Middle	Bottom	80	0.356**	0.001	Highly Significant

A Pearson product-moment correlation coefficient computed to assess the relationship between the RMi values of top layer and RMi values of middle layer. Highly significant positive correlation between the two variables,  $r = 0.530$ ,  $n = 80$ ,  $p = 0.000$  i.e.  $< 0.05$  is seen.

A Pearson product-moment correlation coefficient computed to assess the relationship between the RMi values of top layer and RMi values of bottom layer. Significant positive correlation between the two variables,  $r = 0.271$ ,  $n = 80$ ,  $p = 0.015$  i.e.  $< 0.05$  is seen.

A Pearson product-moment correlation coefficient computed to assess the relationship between the RMi values of middle layer and RMi values of bottom layer. Significant positive correlation between the two variables,  $r = 0.356$ ,  $n = 80$ ,  $p = 0.001$  i.e.  $< 0.005$  is seen.

Khandala monkey hill topmost portion consist of lose soil, lose boulders covered with carpet of heavy vegetation.. The present study is for the vertical rock cut along express highway and do not include scope to study this topmost layer with lose boulders and soil. It is very important to comprehend the presence of lose boulders which roll

down the vertical rock cut during monsoon leading to major accidents. This layer primarily constitute of loose soil, small rock fragment and boulders and thus ingress of water leads to subsidence.

The study of rock classification for Khandala rock cut section illustrates that the RQD and RMI values (243 for Khandala Section) show significant correlation between layers when statistically analyzed. Three different layers top, middle and bottom display different properties that leads to collapse.

Top section RMI mean value is 0.400 with 0.0908 standard deviation for sample size, N=80. This layer with extremely low mean value of RMI classified as extremely weak is seen completely isolated at top in the graph; clearly demarcate highly jointed rock layer susceptible to slide.

RMI mean value for middle section is 5.638 with 0.807 standard deviation for sample size, N=80. This layer with high RMI mean value and strong rock classification acquire specific area demarcated on rock cut. This middle layer with its columnar jointing pattern and sharp dyke angle is most prone to overturning and falling down with highly jointed top layer overburden.

Bottom section with RMI mean value 12.242 and 4.199 standard deviation for sample N=80; rock classification is defined as very strong and is most stable layer in the rock cut. Graph line can be seen intermittently rising and trying to touch middle layer graph. This portion of rock cut seems to having low RMI value compare to the very strong rock abutting it and one can evaluate as probable rock material in bottom layer susceptible to overturn or fall.

From the above it can be summarized that Top most layer of the rock cut having very poor RQD and very low RMI value, is found to have highly jointed columnar jointing pattern with silty clay stuffed in wide joint spacing making this layer prone to slide. Water ingress during heavy rains in this layer make it more perilous for subsidence.

Middle layer which holds burden of highly fragmented top layer show similar jointing pattern with columnar set of joints but larger block volume making it more stable from sliding. Poor RQD value but high RMI and steep dyke angle towards rock cut make this layer precarious and prone to toppling.

Bottom layer the most stable layer is found to have different joining pattern that of above two layers. It shows rhombohedral block pattern with less joint density. Greater block volume, good to excellent RQD and strong to very strong RMI values make this layer more established and firm.

## CONCLUSION

From the above study it can be concluded that

- Top layer consisting of soil and rock fragments is highly susceptible to slide.
- Middle layer with poor RQD and high RMI show the tendency of toppling with upper layer.
- Bottom layer having very strong RMI and excellent RQD is found to be most stable.

## REFERENCES

- Central Road Research Institute, New Delhi (2005) Draft Final report on “Study of Landslide & Rock fall Problem on Mumbai-Pune Expressway”: Submitted to MSRDC Ltd. Mumbai.
- Deere D.U., Deere D.W., (1988) “The rock quality designation (RQD) index in practice”, Rock Classification System for Engineering Purpose, *ASTM STP 984*, Louis Kirkaldie, Ed., American Society for Testing and Material, Philadelphia, pp91-101.
- Kumar K., Prasad P.S., Mathur S., Kimothi S., (2010) “Rock fall and subsidence on Mumbai Pune Expressway, *International Journal of Geoenvironment Case Histories*”, October, Vol. 2, Issue 1, p24-39.
- Palmstrom A., (2009) “Combining the RMR, Q and RMI classification system”, Paper published February. *in www.rockmass.net*
- Palmstrom A., (2005) “Measurement of and correlations between block size and rock quality designation (RQD). *Tunnelling and Underground Space Technology*, 20, p.362-377.

- Palmstrom A., (2002) "Measurement and characterisation of rock mass jointing, in situ characterisation of rock".in V.M. Verma& R.K. Saxena (Eds), Chap. 2, p.358 New Delhi: *Oxford & IBH Publishing Co. Pvt. Ltd. And Rotterdam: A.A.Balkema.*
- Palmstrom A., Singh R., (2001) "The deformation modulus of rock masses- comparison between in situ test and indirect estimates", *Tunnelling and Underground Space Technology*, Vol.16, No.3, 2001, pp. 115-131.
- Palmstrom A., Stille H., (2010) "Rock Engineering", *Published by Thomas Teleford Limited*, 40 Marsh Wall London E14 9TP.
- Palmstrom A., (2000) "Block size and block size distribution", Presented at the Workshop on "Reliability of classification system" in connection with the *GeoEng 2000 conference*, Melbourne, 18-20 November.
- Palmstrom A., (1996) "RMi- A system for characterising rock mass strength for use in rock engineering", *Journal of Rock Mechanics and Tunnelling Technology*, 20, pp362-377.
- Palmstrom A., (1982) "The volumetric joint count-a useful and simple measure of the degree of rock mass jointing", *Proc. Int. Congr. IAEG*, New Delhi, V.211-228,
- Stille H., Palmstrom A., (2003) "Classification as a tool in rock engineering" *Tunnelling and Underground Space Technology*, Vol.18, pp. 331-345.

## THE EFFECT OF CALCIUM EXCHANGE CAPACITY ON THE PROPERTIES OF BLACK COTTON SOIL

Raju Mandal<sup>1</sup>, V K Arora<sup>2</sup>

<sup>1</sup>M.Tech scholar, Department of Civil Engineering, NIT Kurukshetra, Haryana 136119, India ;email:mandal.raju.sindri@gmail.com

<sup>2</sup>Professor, Department of Civil engineering, NIT Kurukshetra ,Haryana 136119, India; email:aroravk1@gmail.com, Corresponding

Author

### ABSTRACT

In this exploration work Calcium chloride and fly ash remains is utilized as an added substance to enhance the building properties of Black cotton soil. As we know that black cotton soil shows swelling and shrinkage behavior due to the change in water content in soil so in this research work Calcium chloride (CaCl<sub>2</sub>) is used with 1, 2 and 3 percentage to reduce the expansive behavior of black cotton soil and fly ash is also used with 20 and 30 percentage to compare the results obtained from CaCl<sub>2</sub> treated soil. Here three laboratory test or investigations named liquid limit test, plastic limit test and standard proctor test were performed. The soil samples were also subjected to wet and dry cycle to check the change in properties of soil. In this test five times soil was left to air dry with and without CaCl<sub>2</sub> addition and test were performed in each times. To compare the results the same processes were also repeated with fly ash addition and the values of liquid limit, plastic limit and standard proctor test were noted in the observation table. After the tests it was observed that with the increase in CaCl<sub>2</sub> percentage liquid limit was decreased and plastic limit was increased so plasticity index diminished and thus swell qualities also diminished. The outcomes obtained from CaCl<sub>2</sub> addition proved better for reduction of expansive nature of black cotton soil.

**KEYWORDS:** expansive soil; calcium chloride; fly ash ; liquid limit; plastic limit; proctor test.

### 1. INTRODUCTION

#### 1.1 Black cotton soil

Black cotton soils indicate swell and shrink quality which have propensity to shrink or swell with the difference in dampness content. In numerous parts of the world these soils are prevalent. Because of progress of water content breaking of the structures happens which are based on them. The swelling property of dark cotton soil causes the loss of property as well as loss of the lives. Black cotton soils likewise called regur in a few parts of the world.

Black cotton soils are found immeasurably in locales of center India like Andhra Pradesh, Gujarat, Madhya Pradesh and Maharashtra and in a few spots of Orissa, far reaching soils are accessible in the areas of Narmada, Tapi, Krishna, and Godavari. The profundity of accessibility of black cotton soil is high in north western india. This kind of soils are the residual soils which are framed because of weathering or compound disintegration of the stone, left at that put itself after arrangement from the stones. This sort of soil comprises of high level of montmorillonite mineral substance which is reason for swell and shrinkage conduct of expansive soil. By and by in India almost 25 percentage of the soils are covered by the expansive soils.

#### 1.2 Fly Ash

Since we realize that control usage has been expanded because of fast development of populace and industrialization. As we know that coal is utilized by Thermal power plants for creation of power, and it is crushed to fine powder frame, before it is singed. After consuming the coal and by this entire procedure the waste material is delivered is called fly ash. The principle issue with fly ash remains is safe administration and transfer. Safe transfer and administration of fly ash remains is exceptionally troublesome in light of the fact that it possesses tremendous territory of land and it will effortlessly spread around then results in the contamination. The wastes that are produced by industries have the hurtful and extremely complex synthetic concoctions and it is exceptionally hard to treat them so the transfer and management in eco-friendly manner of fly ash remains is extremely significant focuses. The fly ash transfer and disposal ought to be so as to not damage to natural framework and life. Therefore it should be treated and after that it should be disposed. Fly ash usage in our nation is around 57% in the year 2011-13, at that point staying fly ash remains moves as a waste material which causes ecological issues. Presently, the time has come to use fly ash that are generated and that will generate, by considering its unfavorable impact on eco framework. To utilize fly ash add up to creation usage, world nations pronounced second world summit for fly ash on 2012 remains utilize. The very much kept up coal utilize, focused on its mass utilize.

**Table 1 fly ash utilization in India**

Different field	Use in percentage
Ground improvement	16
Dykes	36
Miscellaneous	4
Construction	16
Cement	28

### 1.3 Pore Water

In this examination or study, water is blended for various extents of CaCl<sub>2</sub> for assurance of index and engineering properties of the soil. As we realize that calcium chloride is formed by calcium and chloride. CaCl<sub>2</sub> is a solid electrolyte and it carries on as ionic halide. What's more, at room temperature it is strong and exceptionally dissolvable in water. It is additionally utilized for saline solution in coolers and it controls the residue on asphalts because of hygroscopic nature. Anhydrous CaCl<sub>2</sub> must be kept in such way that air ought not be permitted. Calcium chloride is solvent in water and dissolvable in liquor and kerosene. It is exceptionally basic chemical in modern and assembling production lines. see Fig. 1.

It is a solid electrolyte and in the present examination distinctive level of CaCl<sub>2</sub> is utilized and decided conduct of the black cotton soil exposed to wet and dry cycles.

In aqueous solution CaCl<sub>2</sub> behaves as calcium ions source. It's soluble property in water is valuable for changing ions from water.

For example,

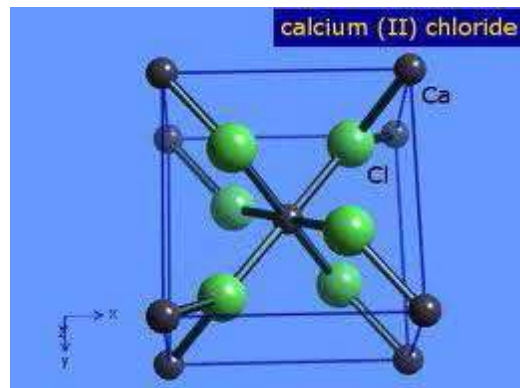
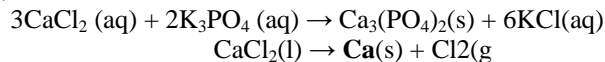


**Figure 1 structure of calcium chloride**

## 2. LITERATURE REVIEW

### Stabilization using chemicals

**Bouazza (2006)** in land field cover framework the clay liner may be exposed to the cations badly, for example, Mg, Na and Al changes bentonite material property in the event that it is exposed to cycles drying and wetting due to nonstop precipitation and temperature. To decide the impact of cycles of wet and dry on as far as possible and plastic farthest point of the bentonite material and far reaching attributes of the bentonite were found at various cycles of wetting and drying with various extents of CaCl<sub>2</sub> arrangement utilized for these cycles. Diverse extents of CaCl<sub>2</sub> blended at each wetting stage, and decided level of particle trade of calcium for sodium on mud for each stage. Though others writers researched properties of the soil with various extent of the synthetic concoctions and have not been resolved level of calcium trade accomplished. They viewed as two arrangements, for example, 0.0125M and 0.125M of CaCl<sub>2</sub> and decided calcium trade on each wet cycle. It has additionally verified that in the lab may be impractical to accomplish the full trade limit however in the event that field it is conceivable to accomplish the full cation trade limit. On the off chance that it is important to accomplish the full trade in the lab the soil ought to be pressed a few wet and

dry cycles.

**Ramesh et al. (2011)** Since mixing of acids also changes the property of expansive soil so here salts were mixed in the soil and results showed enhancement of soil density and decrement of OMC. And furthermore quality properties of the soil has been moved forward.  $\text{CaCO}_3$  more viable to expansive soil in quality enhancement perspective contrasted with the Shedi soil. Defilement of ideal level of antacids treated soils by 1N acids decreased the dry density and expanded OMC for expansive soil while in case of Shedi soil dry density and moisture content was decreased. From the research center investigation it is realized that soluble bases of 15% and 5% individually for Black Cotton soil and 15% if there should be an occurrence of Shedi soil are compelling.

**Kalkan (2011)** Due to subjection of to wet and dry cycle it is observed that wet and dry cycle causes cracks in the soil which results in increment of permeability which consequently results in the side drainage and footing distress. This type of soil mainly contains montmorillonite mineral that leads to change in volume due to change in water content in soil. So it is necessary to stabilize the soil with chemicals or by using waste materials. He mixed silica fume waste material in expansive soil and subjected it to various wet and dry cycle and found enhancement of strength and decrement of swelling and shrinkage behavior.

**Ramdas et al. (2012)** calculated increasing strength of swelling soil by the use of  $\text{CaCl}_2$ . They utilized diverse extents  $\text{CaCl}_2$  and discovered the quality and strength properties of soil. They included 0.5, 1, 2 and 2.5 %  $\text{CaCl}_2$  in soil and found index properties of expansive soil. They watched expansion of  $\text{CaCl}_2$  builds the UCS strength and declines the expansive conduct of the soil and furthermore diminish in liquid limit and increment in plastic limit. They were resolved unconfined compressive strength enhancement for the curing time of 14 days and 28 days. Results shows, ideal measurements of  $\text{CaCl}_2$  that was seen, is 1 percentage by dry weight of the soil.

**Mohan et al. (2013)** it isn't surely knew of soluble bases and acids on change in volume properties of soils. Endeavors have been made paper to think about soils stabilized with max level of soluble bases and polluted with one typical acids. In the results it is demonstrated that the diminishing in proportion of void in case of Red earth is little contrasted with that of swelling soil. When soil was  $\text{MgCO}_3$  treated with  $\text{H}_2\text{SO}_4$  expands the void proportions in peripheral contrasts with soil treated by  $\text{CaCO}_3$  with  $\text{H}_3\text{PO}_4$  at all viable weight. The investigation demonstrates that the corrosive's impact on the soil mineralogy and furthermore soil conduct relies upon the term of soil association with acids.

### 3. MATERIALS AND METHODOLOGY

#### 3.1 Materials

##### Black cotton soil

In my thesis work, expansive soil is gotten from Nagpur, Maharashtra. The far reaching soil was gotten in the wake of evacuating 0.5 m profundity top soil by the technique for irritated testing and transported in sacks to the research facility. To decide the dampness substance of soil it is transported painstakingly to the lab without losing dampness content. The dirt is dried and crushed and sieved by the help of 4.75 mm sieve to do research facility tries. The different geotechnical properties are presented in Table 1.

Table 2 physical properties of black cotton soil

SL.NO	PROPERTIES	VALUE
1	MDD	1.56g/cc
2	OMC	25.10%
3	NATURAL MOISTURE	9.2%
4	LIQUID LIMIT	75%
5	SPECIFIC GRAVITY	2.57
6	PLASTIC LIMIT	27%

##### Calcium Chloride

For my test, I took  $\text{CaCl}_2$  from lab of NIT kurukshetra. It's atomic wt was 110.97 gm. In this examination distinctive extents of  $\text{CaCl}_2$  is blended with water, tests were performed and discovered the conduct of the black cotton soil. Typically broad soil swells because of the arrangement of twofold layer of water in the soil. When I added  $\text{CaCl}_2$  solution in soil, it has replaced ions from the soil as max as possible however it is watched that swelling pressure was

decreasing due to diminishing of twofold layer. From the writing overview it is realized that the swelling conduct of the soil absolutely relies upon the amount of ion exchange happens in the entire procedure.

In my test procedure when I added different % of CaCl<sub>2</sub> solution in soil and subjected this in five wet and dry cycle and performed tests, I found cation exchange conduct goes on increasing with cycles of wet and dry due to decrease in double bond thickness of water and consequently its swelling property was also decreased.

### **Fly ash**

As we know that fly ash is a byproduct of various power plant. It is an of sort squander material shaped because of the burning of bituminous coal. In my experiments it is used for doing three test by mixing it in 20 and 30 % in the expansive soil and it is used to compare the results obtained from calcium chloride and fly ash. It is also subjected to wet and dry cycle with mixing fly ash and without mixing fly ash and all the three test were performed and results were noted.

### **3.2 Methodology**

For the assessment of behavior of expansive soil with CaCl<sub>2</sub> and fly ash, three distinct amount of CaCl<sub>2</sub> and two diverse proportions of fly ash were utilized. The calcium proportions were 1, 2 and 3 percentage and 20 and 30 % of fly ash utilizes in the present examination. The soil was blended with CaCl<sub>2</sub> and fly ash separately before the exploratory projects directed. Every one of the tests were led by the IS code technique. The accompanying investigations were led in lab.

### **Wet and Dry Cycles**

Wet and dry cycle means that after every test soil was subjected to air dry in lab condition i.e in the temperature of lab until the point when the loss of dampness stopped then the soil was rewetted with indistinguishable centralization of water from utilized at first. This process was done for all the cycles and in each cycle experiments were done and found the results.

### **3.3 Determination of Index Properties**

#### **Determination of Liquid Limit**

300 grams of black cotton soil was taken after sieving through 425 micron sieve and water was added to it and blended completely and paste was made and soil was taken to the cup and a groove was made at the centre, groove size was 2mm. Now handle of Casagrande tool was rotated and revolution speed was 2 revolution per second, now the no of blows required to close the groove was found and soil sample was taken near the groove to find water content. Some water was added and repeated the whole procedure. Five readings were taken in the range of 15 to 35 blows and finally graph was plotted between log of number of blows in x-axis and water content in y-axis. We got a straight line and water content corresponding to 25 number of blows was found from the graph that represented liquid limit, see Table 2.

**Table 3 Liquid limit in % at different cycles**

<b>CYCLE</b>	<b>BCS</b>	<b>BCS+1%CaCl<sub>2</sub></b>	<b>BCS+2%CaCl<sub>2</sub></b>	<b>BCS+3%CaCl<sub>2</sub></b>	<b>BCS+20%FA</b>	<b>BCS+30%FA</b>
<b>0</b>	68.52	64.20	59.36	57.58	54.42	45.90
<b>1</b>	69.00	63.45	58.19	56.61	54.40	46.07
<b>2</b>	69.04	60.30	57.30	55.78	53.82	45.69
<b>3</b>	69.61	59.99	55.66	54.46	54.04	45.25
<b>4</b>	70.00	57.19	54.52	53.23	53.87	46.29
<b>5</b>	70.66	56.80	53.10	51.80	53.79	45.77

#### **Determination of Plastic Limit**

We know that plastic limit is characterized as the water content at which soil can be rolled to a thread of diameter 3 mm without disintegration. For this test 20 gm soil was taken and water was added and soil was blended so that it comes in plastic state and 10 gm of soil was taken and it was rolled on the glass plate till it breaks with a thread diameter of 3 mm. Finally when this condition was reached then soil was taken from the thread and allowed to dry in the oven to find out water content. This process was repeated by adding CaCl<sub>2</sub> and fly ash and results were noted in the Table 3.

**Table 4 plastic limit in % at different cycles**

CYCLE	BCS	BCS+1%CaCl <sub>2</sub>	BCS+2%CaCl <sub>2</sub>	BCS+3%CaCl <sub>2</sub>	BCS+20%FA	BCS+30%FA
0	27.10	33.05	39.55	40.53	24.23	22.33
1	27.45	35.50	41.24	42.10	23.45	22.95
2	28.00	37.85	42.28	43.75	24.12	21.22
3	29.84	39.27	43.13	43.93	25.05	22.59
4	30.50	40.95	43.15	44.36	24.44	22.65
5	31.20	41.10	43.97	44.51	24.97	23.00

### 3.4 Compaction Methods and Characteristics

For compaction test I used standard proctor test to find out dry density and OMC. Around 5 kg of black cotton soil was taken and it was put in the oven and after oven drying 4-6% of water was added to the soil and mixed it properly and soil was filled in the proctor mould in 3 layers and each layer was given 25 number of blow and then collar was removed and soil along with mould was taken out and soil was leveled by cutting with knife and finally soil and mould was weighed. Now mould weight was subtracted from the total weight and weight of compacted soil was obtained. Now weight of compacted soil was divided by volume of mould i.e 944cc to get bulk unit weight of compacted soil and some soil was taken and kept in oven to find water content. Now water content was increased and whole process was repeated and finally dry unit weight was calculated by knowing the water content and finally graph was plotted to find maximum dry density and OMC. This whole procedure was repeated for different percentage of CaCl<sub>2</sub> as well as for Fly ash and by the help of bulk unit wt and water content dry unit wt was found and finally graph was drawn to determine max dry density and OMC for all cases, see Table 4.

The following table shows the data for various cases:

**Table 5 Proctor test data of black cotton soil**

CYCLE	BCS		BCS+1% CaCl <sub>2</sub>		BCS+2%CaCl <sub>2</sub>		BCS+3%CaCl <sub>2</sub>		BCS+20%FA		BCS+30%FA	
	D	OMC	D	OMC	D	OMC	D	OMC	D	OMC	D	OMC
0	1.57	24.10	1.590	22.37	1.612	20.73	1.620	20.05	1.522	26.58	1.611	25.39
1	1.56	23.83	1.600	21.45	1.621	20.17	1.625	19.44	1.531	26.18	1.604	25.49
2	1.57	23.55	1.605	20.86	1.625	18.90	1.630	18.55	1.527	26.42	1.615	25.11
3	1.57	23.16	1.610	20.68	1.625	18.90	1.634	17.84	1.519	27.12	1.614	25.13
4	1.58	22.82	1.617	20.16	1.627	18.66	1.634	17.84	1.523	26.46	1.615	25.11
5	1.59	21.00	1.625	19.81	1.630	18.00	1.640	17.18	1.530	26.36	1.622	24.87

D=Maximum Dry Density in g/cc, OMC=Optimum Moisture Content in %

## 4. RESULT AND CONCLUSION

### 4.1 Liquid Limit

With the increase in the cycle of wet and dry, liquid limit of soil (without any CaCl<sub>2</sub> or Fly ash addition) was increasing slightly it means that wet and dry cycle helps to enhance the cation exchange phenomenon in expansive soil, so due to slight increase in liquid limit swelling nature of soil also increases. Therefore to reduce this effect calcium chloride was added. With the increase in CaCl<sub>2</sub> percentage the Liquid limit of the soil decreases and wet and dry cycle also helps to decrease the liquid limit value by enhancing the cation exchange process. And 2% calcium chloride was economically effective to decrease the liquid limit.

#### 4.2 Plastic Limit

By the test of plastic limit it was observed that with the proceeding of cycles of wet and dry the value of plastic limit shows increments. With the increase in wet and dry cycle plastic limit of expansive soil was also increasing slightly. And with the addition of  $\text{CaCl}_2$  Plastic limit was increasing more rapidly and 2 percentage of  $\text{CaCl}_2$  was found economical to enhance plastic limit.

#### 4.3 Compaction Characteristics

Graph has been plotted by the experimental test data for standard proctor test, see Figs 2-5

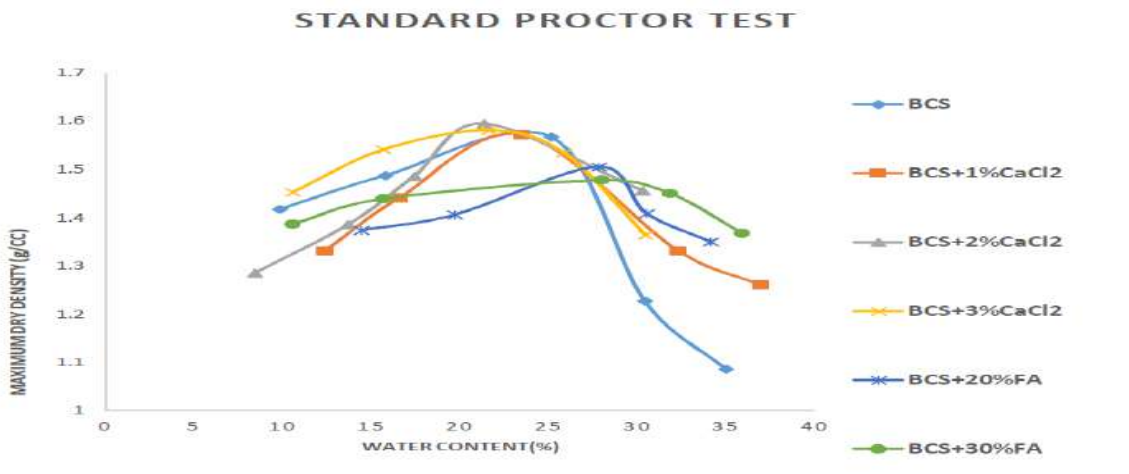


Figure 2 combined standard proctor test graph for different proportions of calcium chloride and fly ash

It is seen from the combined graph plotted above that 3 %  $\text{CaCl}_2$  has more density as compared to 2%  $\text{CaCl}_2$  but the difference in both the densities is very small so for economical point of view stabilizing by 2%  $\text{CaCl}_2$  is suggested.

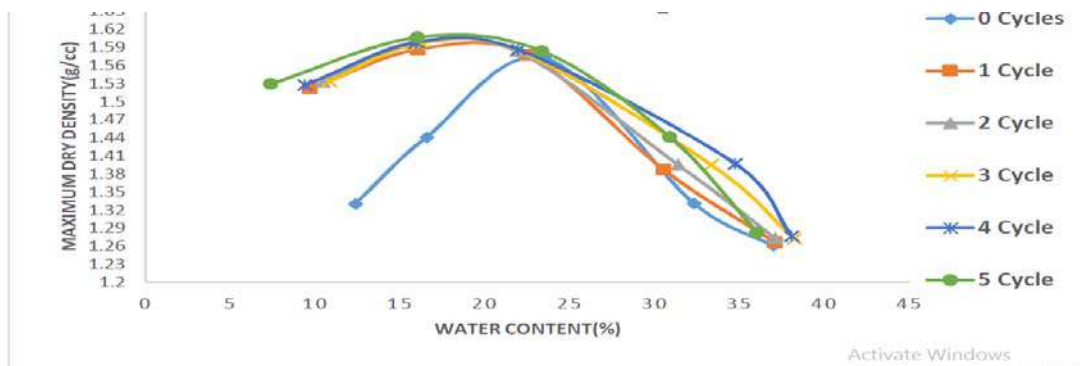


Figure 3 standard proctor test graph for five different cycles of BCS+1%CaCl<sub>2</sub>

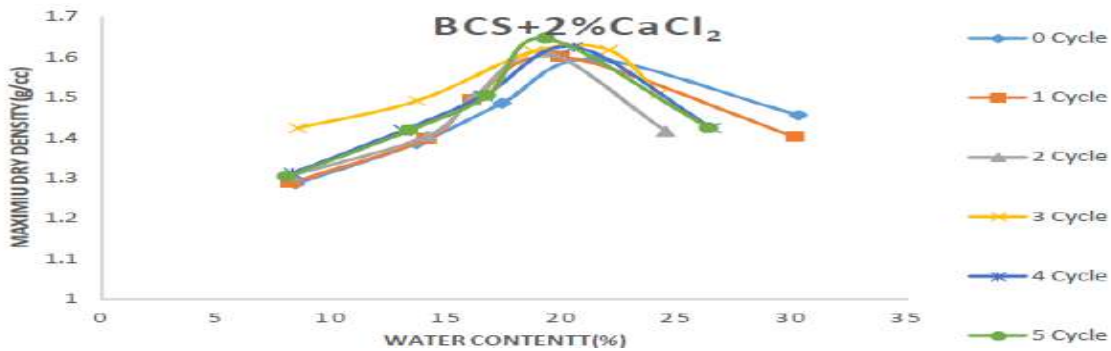


Figure 4 standard proctor test graph for five different cycles of BCS+2%CaCl<sub>2</sub>

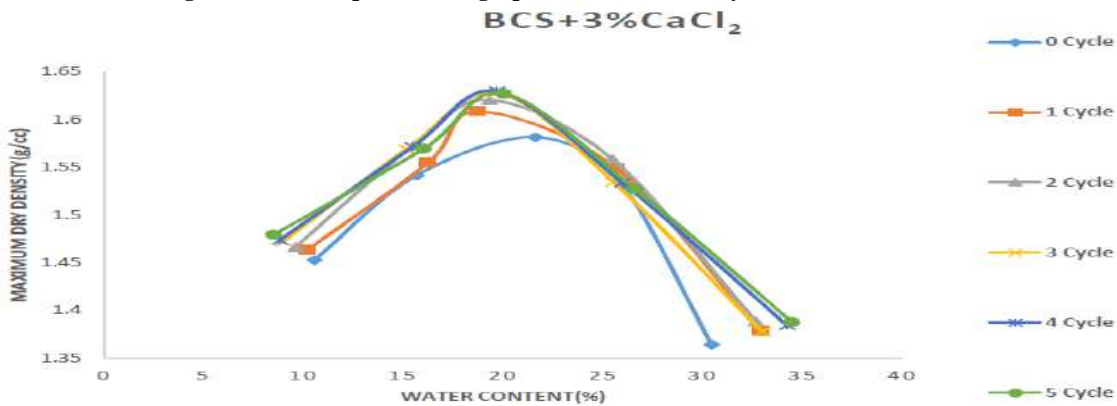


Figure 5 standard proctor test for five different cycles of BCS+3%CaCl<sub>2</sub>

Above three graphs show graphs for 1,2 and 3% of CaCl<sub>2</sub> solution addition to the expansive soil and in graph dry density and water content for all the five cycles are also shown and by analyzing the graph we can say that with the increase in cycle, change in the dry density is very small or it shows very slight change and when CaCl<sub>2</sub> percentage is increasing then soil is becoming dense slightly and at less moisture content and it is also observed from the graph that there is slight change in compacted density with 2 and 3% CaCl<sub>2</sub>, so 2% CaCl<sub>2</sub> is recommended for density improvement as well.

## 5. CONCLUSION AND SCOPE

In view of the exploratory examination and investigation of results following ends are made:

- With the increase in the cycle of wet and dry, liquid limit of soil (without any CaCl<sub>2</sub> or Fly ash addition) was increasing slightly it means that wet and dry cycle helps to enhance the cation exchange phenomenon in expansive soil, so due to slight increase in liquid limit swelling nature of soil also increases. Therefore to reduce this effect calcium chloride was added.
- With the increase in CaCl<sub>2</sub> percentage the Liquid limit of the soil decreases and wet and dry cycle also helps to decrease the liquid limit value by enhancing the cation exchange process. And 2% calcium chloride was economically effective to decrease the liquid limit.
- When calcium chloride was added to the soil and tested for liquid limit It was found that when cycles of wet and dry was proceeding then the liquid limit was decreasing, it shows that full cation exchange does not occur in the soil instantly after adding CaCl<sub>2</sub> in black cotton soil..
- With the increase in wet and dry cycle plastic limit of expansive soil was also increasing slightly. And with the addition of CaCl<sub>2</sub> Plastic limit was increasing more rapidly and 2 percentage of CaCl<sub>2</sub> was found economical to enhance plastic limit.
- Hence by addition of CaCl<sub>2</sub> liquid limit was decreasing and plastic limit was increasing and since we know that

plasticity index= liquid limit-plastic limit so, we found that plasticity index was decreasing. Therefore we can conclude that swelling nature of black cotton soil can be reduced by addition of CaCl<sub>2</sub>.

- With the increase in cycle, change in the dry density is very small or it shows very slight change and when CaCl<sub>2</sub> percentage is increasing then soil is becoming dense slightly and at less moisture content and it is also observed that there is slight change in compacted density with 2 and 3% CaCl<sub>2</sub>.
- At 2% of calcium chloride BCS has maximum dry density, henceforth 2 % calcium chloride is best to get maximum dry density by calcium exchange process.
- Endeavors ought to be made to find out those material having less cost and having the property of cation exchange other than CaCl<sub>2</sub>.
- Use of different chemicals for their behavior on swelling nature on soil to decrease expansive property.
- Use of CaCl<sub>2</sub> for other profoundly expansive soil .

## REFERENCES

- Geotextiles and Geomembranes 25 (2007) 170–185 “ Investigation of the effects and degree of calcium exchange on the Atterberg limits and swelling of geosynthetic clay liners when subjected to wet–dry cycles ” Abdelmalek Bouazza, Stephan Jefferis, Thaveesak Vangpaisal.
- Applied Clay Science 52 (2011) 345–352 “Impact of wetting–drying cycles on swelling behavior of clayey soils modified by silica fume” Ekrem Kalkan.
- J. Geotech. Geoenviron. Eng. 2000.126:40-49. “effect of wet-dry cycling on welling and hydraulic conductivity of gcls” Ling-Chu Lin<sup>1</sup> and Craig Benson.
- Academic Research Journals (India), pp.77-86 “A study on strength and swelling characteristics of three expansive soils treated with cacl<sub>2</sub>” Ramadas.T.L , Darga Kumar.N And Yesuratnam.G.
- Proceedings of Indian Geotechnical Conference, December 15-17, 2011, Kochi (Paper No. L-254.) “ Compaction characteristics of alkalis treated expansive and non expansive soil contaminated with acids ” Ramesh h.n., venkataraja mohan s.d.
- ISSN 2250-2459, Volume 2, Issue 10, October 2012 “ Efficacy of sodium carbonate and calcium carbonate in stabilizing a black cotton soil ” Ramesh.P, Narasimha Rao.A. V., Krishna Murthy.N.
- engineering geology 60(2001) 223-233 “The impact of cyclic wetting and drying on the swelling behaviour of the expansive soils” Reddy.B.V.V, ram.S.M, muttharam.
- IGC 2009, Guntur, India “ Effects of soil pollution on geotechnical behaviour of soils ” Sivapullaiah.P.V.
- Proceedings of Indian Geotechnical Conference December 22-24, 2013, Roorkee “volume change behaviour of alkalis treated expansive and non-expansive soils contaminated with acids” S.D.V.Mohan, H.N.Ramesh

## SOLOPE STABILIZATION BY SOIL NAILING – A REVIEW

Abhijeet Kanungo<sup>1</sup>, Sujata Gupta<sup>2</sup>, Anupam mital<sup>3</sup>

<sup>1</sup>#MTEchScholar, Department of Civil Engineering, National Institute of Technology, Kurukshetra, Haryana-136119, India; email:abhijeet\_31702106@nitkkr.ac.in

<sup>2</sup>\* Ph.D. Scholar, Department of Civil Engineering, National Institute of Technology, Kurukshetra, Harayana-136119, India; email: sujata\_6160052@nitkkr.ac.in

<sup>3</sup>\* Professor, Department of Civil Engineering, National Institute of Technology, Kurukshetra, Harayana-136119, India; email:anupam.mittal@rediffmail.com, Corresponding Author

### ABSTRACT

Soil nailing is a method of soil reinforcement, by the use of steel rods and other materials. The process of reinforcement is done by using the shear strength of in situ soil and pull out resistance of soil nails. As a slope is prone to failure during construction and reformatory work, if any by the constructor, may lead to high risk, engineers must look forward for an effective method. Soil nailing may prove to be efficient and cost effective. This paper investigates the study of experimental and analytical analysis of design and construction of nailed slope that has been done in past few years. Study shows that there is quite difference in the failure pattern and load characteristic of unreinforced and reinforced soil slopes, which has different inclination with the horizontal. Nail characteristic such as inclination, length, and frictional behaviour also influence the slope stability and nail strength. It was observed that the deformation of soil slope was less in reinforced slopes as compared to unreinforced soil slopes. An increase in tensile and shear strength of soil was observed due to the reinforcement of soil.

**KEYWORDS:** Soil nailing; reinforcement; slope stability; shear strength.

### INTRODUCTION

In recent years world has experienced a lot of fatalities and economic loss due to number of landslides and slope instabilities. Slope stability is one of the important facets of geotechnical engineering and engineers should focus on stable design and construction of slopes which should be economical as well. Slope failure and landslides can be contained by using proper slope stabilization techniques. Various slope stabilization methods include retaining walls, sheet piling, counter berms, shear key, rock bolting, water control and drainage but soil nailing is an advance method of slope stabilization amongst other methods. Soil nailing is the technique used in slope stabilization and excavation with the use of passive inclusions, usually steel bars, termed as soil nail. Soil nailing is typically used to stabilize existing slopes or excavations where top-to-bottom construction is preferred over other retaining wall systems. The function of soil nailing is to increase the shear and tensile strength and stabilize the existing steep slopes and excavations as construction take place from the top to bottom. The ground deformation leads to the soil-nails interaction, which develops the reinforcing action of soil nails which contributes in development of tensile forces in soil nail.

Improvement in the stability of slopes achieved by soil nailing due to:

- a) Increase in the shear resistance along slip plane in friction soil, by increasing the normal force on shear plane
- b) Reduction of the driving force along slip surface both in friction and cohesive soil.

As shown in fig.1, the soil nail system can be divided into two regions active and passive. At the time slope failure, active region tends to deform which leads to axial deformation along soil nails, which are placed across the slip surface, which causes the development of tensile forces in soil nail in the passive zone, which resists the deformation of active zone.

Various types of soil nails used in soil nailing are:

- a) Grouted nails
- b) Driven nails
- c) Self-drilling soil nails
- d) Jet grouted soil nails.

Failure modes in soil nailing are as follow:

- a) Pull out failure
- b) Nail tendon failure
- c) Face failure

d) Overall failure (slope instability).

To make the soil nailing a more efficient and cost-effective stabilization method we need proper design and analysis methods. This paper investigates previous work done, in the analysis of slopes stability using soil nailing. Analysis of soil nails can be done using experimental setup or various laboratory tests such as pull out test or sliding shear test, and numerical analysis of slopes stability may be carried out using various software such as Optum G2, SLOPE/W, FLAC, PLAXIS 2D AND 3D.

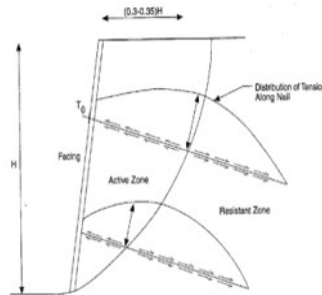


Fig.1 Conceptual soils nail behaviour (Byrne et al., 1998)

## LITERATURE REVIEW

### Grouted Soil Nail

Jeon (2012) carried out field test on two different nail arrangements and their numerical analysis. The name given to the arrangement of the nails was type A and type B. The embedded length for type A was 9.6 m and for type B, it was 10.7 m. A single nail was used in type A arrangement and four nails with circular plate attached to them was used in type B arrangement. The field test was done to investigate the pullout capacities and slope stability reinforcement efficiency in both rock and soil slopes. Through the test, the factors influencing shear resistance at soil-nail interface and the mobilized nail forces were investigated. Based on previous studies, it was observed that bending resistance of nails is less than 15%, most of the resistance is contributed by shear resistance. In the test soil depth tested was in the range of 9-11 m. In numerical analysis, which is carried out on FLAC 2D, factor of safety was estimated using cable and pile element for both type A and type B, with respect to, number of nails and their diameter. When field pullout test was conducted, test was divided into three types verification test, proof test and creep test. The field test indicated that pullout resistance of type B was greater than type A (concluded by graph in fig.2). The results of creep test show that maximum displacement for type A was 0.4 mm and for type B, it was 0.6 mm. creep test results satisfies the specification of FHWA, for both the types.

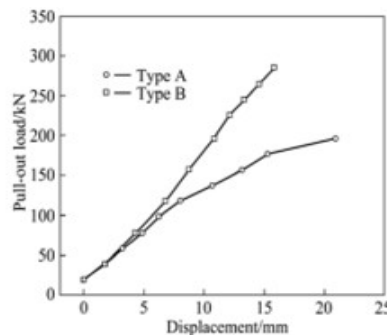


Fig.2 Load-Displacement Relationship

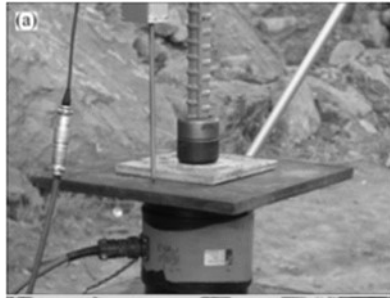


Fig. 3 System of Nail Arrangement, type A

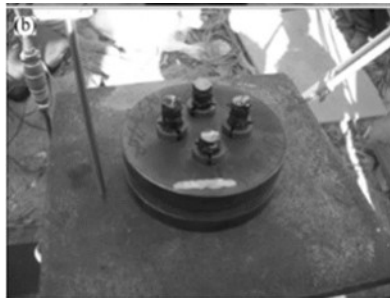


Fig. 4 System of Nail Arrangement type B

From the numerical analysis it was observed that the stability of rock slopes was increased as diameter of nails was increase, as 9% and 15% increase in FOS was observed for 120 mm and 150 mm diameter when it was compared with 90 mm diameter. The study conclude that the type B was more effective than type A, and diameter of nails affect the resistance by the nails up to a great extent, especially is case of rock slopes. Type A and B of nails arrangement used in test shown in figs. 3-4.

**Wang et al. (2016)** studied the effect of variation of degree of saturation on the shear strength of interface of cement grout and sand. The author conducted direct shear test on grouted soil nails. Soil water retention curve was accordingly determined as it demonstrates the unsaturated soil behaviour. While the cement-sand interface obtained at different water content was observed by using microscope, which helps to explain the differences in shear stress. Tensiometer was used to obtain the water retention curve. Direct shear box was used to study the interface shear stress between the unsaturated sand and cement grout. The results investigated from water retention curves and interface microstructure show that with increase in degree of saturation, both the peak and residual shear stress decrease, followed by almost constant stage; afterwards. It was also observed that, less the cohesiveness between sand particles, larger the interface shears stress.

**Isaka1 et al. (2016)** conducted a laboratory test and numerical analysis on nails to analyse the effect of saturation condition, grout interface and overburden pressure. Lateritic soil was used in test and overburden pressure was applied by hydraulic jacks. Numerical analysis was done by using PLAXIS. Pullout forces and interface forces were obtained by numerical analysis. The results of study show that the theoretical pullout forces were smaller than that of the experimental pullout forces. To study the effect of saturation on pullout resistance two different saturation conditions were used and it show that on increasing the degree of saturation the pullout resistance decreases. Results also concluded that the cement grout is the most influencing factor for pullout test of all the factors undertaken in this study, cement grout leads to large increase in pullout resistance of soil nail. Results of numerical analysis show that the mobilized shear stress is not a constant value along the nail length; it is an important conclusion in evaluation of the failure plane of the model.

**Ye et al. (2017)** compared the results of model test and numerical analysis. The study was focused on understanding the pullout mechanism of soil nails with cement bulks provided along the length of soil nails. Cement bulks were provided with different shape angles ( $\beta$ ) and friction coefficient ( $\mu$ ). Laboratory tests were carried out to observe the influence of some factors such as overburden pressure, grouts, degree of saturation on nailing mechanism of soil. For experiment purpose, a soil box of 1000 mm length, 600 mm width, and 800 mm height was used, and nail consist of 500 mm long

nail rod and 200 mm long nail head with a diameter of 34 mm. Numerical modelling was done using ABAQUS (8 node model).

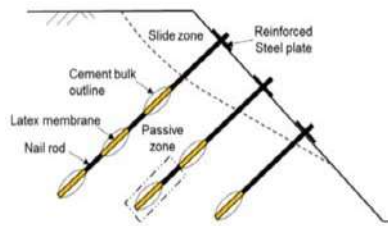


Fig.5 Compaction grouted soil nail.

Similar arrangement as that of lab was simulated on software and comparisons were carried out. From numerical analysis it was observed that pull out force for different  $\beta$  appears almost equal for small displacement, but they gradually increase for higher value of  $\beta$ , the pullout force rises faster. Further conclusion from the study shows that the parameters,  $\beta$  and  $\mu$  affect the total pull out force of soil nail. Enlargement of diameter can also result in increase in pull out force, the larger diameter also leads to remarkable hardening behaviour. Fig.5 shows the arrangement of cement bulk used in the test.

### Screw Nail

**Rawat and Gupta (2018)** carried out a study of screw soil nails on two soil slopes which are at an angle of  $45^\circ$  and  $90^\circ$  with the horizontal. It is a comparative study of conventional smooth nails and screw nails. Their factor of safety and load-displacement characteristics are compared. In this modelling the author used the tank of 60 cm(length)\* 40 cm(width)\* 60 cm(height) and screwed nails used were of mild steel solid bar having diameter of 16 mm and thread height of 0.15 mm, as shown in fig.6. To study the interface friction Direct Shear Test (DST) was conducted, the author concluded that screw nails can produce better sliding friction than conventional smooth nails. This study concludes that the minimum amount of soil movement requires to start the reinforcing action of soil nails. Numerical analysis was done on SLOPE/W and PLAXIS. Study shows that the stability of active zone leads to stability of slope. Global stability of soil slopes was achieved as FOS was greater than 2 for both the soil slopes. Conclusion drawn from study shows that screw nails are more effective in slopes stabilization of steep slopes and screw nails are also advantageous in terms of performance, serviceability, and ease of installation as compare to that of smooth nails.

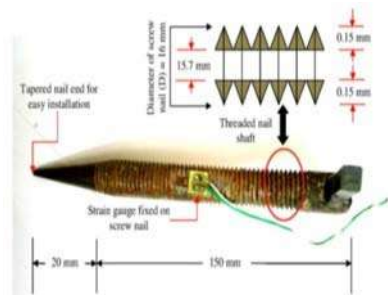


Fig.6 Screw Nail used in Experiment

### Nails in Clay

**Azzam and Basha (2017)** have done the assessment of the soil nailing technique to improve the strength of cohesive soil. Direct shear test and unconfined compression test were carried out on reinforced clay. To study the effect of soil nail on clay, number, depth, and inclination of nails were varied in this study. Stiff clay soil was used in this study. The nails were used as vertical inclusions in the clay; steel smooth bars were used as nails. Result of UCS shows that a gradual increase in resistance to ultimate stress with smaller strain is achieved as the number of inclusions is increased. It was observed that, the improvement in the shear strength of the clay is due to the reinforced elements that are installed in a highly sheared zone and resist the induced tensile strains associated with compressive loads. Inclusion of minimum number of nails up to a shallow depth results in incomplete increase in sample stiffness, hence nails should be

extended up to deeper depth in sufficient numbers. Previous studies on soil nailing in clay show that the soil nailing techniques are not suitable to clay due to the low cohesion of clay which leads to small friction between the ground and soil nails.

### Design of Soil Nails

**Pei et al. (2013)** measured the strains on soil by fiber Bragg grating (FBG) sensor and evaluate the factor of safety. To evaluate the stability of a slope, an optimal model was proposed to search the potential slip surfaces based on measured strain values. Maximum sum of strains on soil nails at different elevations of the same cross section was taken as the objective. Positions of soil nails, circular slip surface, and boundary conditions of the soil nails were summarized and taken as constraints. Wavelength shifts of FBG sensor help in computation of strains along nail length. FBG sensor works on the Bragg's law. The strains measured by FBG sensors help in computation of axial forces in nails. This optimal method is the modified form of limit equilibrium method. This method can be used to modify the analysis of nailed slopes, further development is required to correlate the strains measured by FBG sensors and factor of safety.

**Seo et al. (2014)** studied the types of failure in soil nails. Failure in soil nails is of three types, pullout failure, shear failure, and face failure. In the design of soil nails only two failures are considered, the face failure is not considered for design. Authors in this study carried out an optimized design procedure of soil nailing considering not only pullout and shear failures but also the face failure. In an actual site condition, multi face excavation is executed rather than full face excavation, and face failure can therefore occur due to decrease in confining pressure on excavated face. Theoretical verification of mechanical behaviour of face failure as well as pullout failure and shear failure have been done in this study. The study shows that the face failure can be prevented by maintaining the confining pressure, in this study prestress was used for additional confining pressure. In the optimized design procedure, the optimum amount of prestress was determined to prevent the face failure. Finally, in the design procedure proposed in this study, used the four constrain conditions three for failure and one for construction condition and the optimum number on nails and prestress was determined.

**Gunawan et al. (2017)** conducted a study to relate the length and diameter ratio of the nail with FOS to optimize the designing procedure of soil nailing. The safety factor was analysed by the simplified bishop method. Data simulation was used to relate the length diameter ratio with the FOS. The study was done on  $45^{\circ}$   $60^{\circ}$  and  $90^{\circ}$  slopes. It was observed that as the length to diameter ratio increases the FOS also increases. Effective length diameter ratio depends on the steepness of the slope. Study also concludes that the large diameter nails are more affective in reinforcing action; hence an optimum length to diameter ratio comes out to be around 450-600.

### Soil Nail Parameters

**Junaideen et al. (2004)** conducted the test to improve the understanding of soil-nail interaction in loose fills. Pullout test was conducted in a displacement-rate-controlled manner, on steel bars embedded in loose, completely decomposed granitic soils. The results of test showed that the normal stress acting on nails is function of the volume-change tendency and arching effect of soil. In the test the direct shear box was used as pullout device, and experiment was performed on ribbed bars, knurled tube and round smooth bar. The test was conducted with various overburden pressures shows a significant influence of ribs on the pullout resistance. It was observed that the pullout resistance of the round smooth bars and knurled tube increase with an increase in overburden pressure, and the results were different for ribbed bar. The load-displacement curves show that all the curves have a distinct pick value and followed by a downfall in pullout force. The reduction in pullout force after the peak value could be due to combined effects of reduction in normal stress and strain softening of the material. Results of test show that the average apparent friction angle was  $20^{\circ}$  and apparent adhesion was 2.2KPa, and for knurled tubes values of apparent friction angle and cohesion was found to be  $20.8^{\circ}$  and 7.2 KPa, friction angle was quite low for a knurled tube, which has rough surface. For ribbed bar, it was observed that, there was not much increase in pull out resistance as the overburden pressure increased. The study show that nailing action is caused by the soil movement in the active zone and laboratory results show that the peak pull out forces are mobilized in a few millimetres of relative displacement. The test was conducted in multistage manner in the laboratory, but it is quite difficult to estimate the exact interface between soil and nails, because of the uncertainty involved in calculation of in situ forced on nails.

**Kwong and Lee (2008)** carried out a field test to study the development of passive load along the full length of soil nails when subjected to induced rise in groundwater table. A slope of height 10 m and slope angle  $55^{\circ}$  was formed in the field to carry out the test. Nails were inclined at an angle of  $15^{\circ}$  to horizontal. This test was conducted to study the

development of loads along soil nail when ground water was raised to the ground surface. Strain gauges were connected to nails so that effect of increase in ground water on nails can be computed. Numerical analysis was carried out on GeoStudio and results were compared with field test. The factor of safety comes out to be near about 1, at highest water level. Although the factor of safety was near to 1 but soil nails prevent failure as nails have prevented the formation of shear band or slip surface.

**Hong et al. (2015)** studies the effect of different interface roughness conditions on pullout resistance on soil nails. To establish a correlation between the frictional resistance and roughness angles of internal drill hole surface, cross-sectional shapes of internal drill hole surfaces were created using four plastic rods with various shapes of external threads. The shapes of the drill hole involve rectangular and triangular threads. The relation between pullout resistance and roughness angle shows that, the increase of roughness angle leads to a related rise of pullout resistance of soil nails and therefore improves the safety condition of reinforced structures. The drill holes in field are rougher than that of laboratory; hence we may not exactly interpretate the result of field in the laboratory. Pullout test results show that, the increase of pullout displacement results in a related linear reduction of the shear stress of the interface. Observations show that soil nail diameter values are found to expand significantly compared with the drill hole diameter values in all pullout tests, which result in large increase in pullout resistance of soil nails. The triangular type soil nail is found to be effective in increasing the mobilized pullout resistance of model soil nails.

**Tang and Jiang (2015)** investigate the effect of various soil parameters on factor of safety of a slope. GeoStudio software was used for stability analysis. The study was conducted for a slope of 9 m in height and slope angle of  $74.5^\circ$ . Outputs of software analysis show that, with increase in soil-nail dip angle safety factor first increases and then decreases. Most effective soil-nail dip angle comes out to be  $15^\circ$ . Factor of safety decreases with increase in soil-nail horizontal spacing, it should not exceed 2 m in any case. Analysis showed that there was a linear increase in safety factor with increase in nail diameter up to a certain extent. When the variation of factor of safety was studied with respect to nail length it was observed that, the safety factor increases with the increase of nail length, but, when the nail length equals approximately the height of the slope, the safety factor almost stops increasing.

**Rawat and Gupta (2016)** observed the behaviour of unreinforced and reinforced slopes of sandy soil, which are tested under slowly increasing surcharge load. The study of soil nailing is done both, experimentally and numerically. Various soil slopes were examined under different nail inclination. Failure pattern and load settlement curve were observed on the basis of experimental observation and FE analysis output. The test was done on  $45^\circ$  and  $60^\circ$  soil slopes with nails inclined at  $0^\circ$ ,  $15^\circ$ , and  $30^\circ$ . Observation of tests showed that slopes have circular slip surface and slope failure occurred in  $45^\circ$  soil slope and toe failure took place in  $60^\circ$  soil slope.

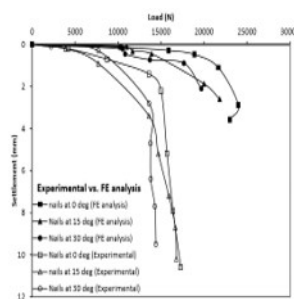


Fig. 7 Comparison of FE analysis and experimental test on a  $45^\circ$  slope

Maximum load capacity was observed in  $0^\circ$  nails for  $45^\circ$  slope; it was also seen that minimum load was carried by bottommost nail. Finite element analysis results on PLAXIS shows that nails are experiencing bending and shear stress and failure of slopes starts from top (crest) and move towards toe of slopes. Fig.7, showing the comparison between the results obtained from experiments and numerical analysis of PLAXIS. Fig. 8, showing the failure pattern output from PLAXIS for  $60^\circ$  soil slope.

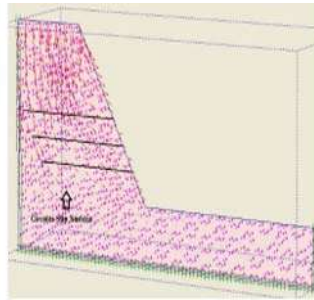


Fig.8 Failure pattern output from PLAXIS for  $60^\circ$  soil slope.

**Rawat et al. (2017)** investigate the pullout behaviour of soil nails with circular discs along the shaft. To study the effect of circular disc finite element analysis was carried out using Abaqus. Number and spacing of circular disc were varied during the analysis. The results of analysis show that as the number of disc increases the pullout force also increase. This increase in pullout force is due to densification of soil, which is in between the discs. A load displacement curve shows an unsmooth pattern due to strain softening of soil. Stress distribution also gets affected due to introduction of disc in nails. Further effect of overburden pressure on nails with circular disc can be studied in future work.

## CONCLUSION

In this paper, study of some previous work has been done to study the issues and aspects of slope stabilization using soil nailing. Soil nailing prove to be cost effective and risk-free technique of slope stabilization. More research work can be done to optimize its design and construction. Various conclusions from this review are as follows:

- a) Soil nailing is much more efficient in case of steep slopes as compare to that of gentle or shallow slopes.
- b) Various factors such as nail length, nail inclination, spacing effect the functioning of nails and different software can be used to find out the optimum number of variables.
- c) Results of experimental work and numerical analysis in the previous studies were identical up to a large extent, hence numerical analysis can be used, aptly for further study in this field.
- d) Less number of works has been done in case of screw nails and nails in clayey soils. More number of studied can be conducted in these cases.
- e) Some recent studies show that nails arrangement can also affect pullout resistance and nail capacity; also the diameter of nail has important impact on its shear resistance.
- f) Study shows that nail efficiency also depends on nail parameters, such as length diameter ratio, roughness of drill holes, roughness of nails; hence detailed studies can be done to find out the optimum nail parameters.
- g) Soil nails attains a peak value of pullout resistance force on varying the overburden pressure, which is due to the decrease in normal stress.

Previous studies show that there is quite less work has been done in case of screw nails, further work in the case of driven nails or screw nails can be done to find out the optimum number of different nail parameters, mainly for steep slopes. A detailed study may lead to better understanding of soil-nail interaction. Increasing need of slope stability prompted designers and constructors to adapt for an effective method such as soil nailing. The work done in case of soil nailing so far is not as satisfying as desired.

## REFERENCES

- Azzam, W. R., & Basha, A. (2017). "Utilization of soil nailing technique to increase shear strength of cohesive soil and reduce settlement." *Journal of Rock Mechanics and Geotechnical Engineering*, 9(6), 1104-1111.
- Budania, R., Arora, R.P. and CE, C., (2016). "Soil Nailing for Slope Stabilization: An Overview." *International Journal of Engineering Science*, 3877.
- Gunawan, I., Surjandari, N. S., & Purwana, Y. M. (2017, November). "The study on length and diameter ratio of nail as preliminary design for slope stabilization." In *Journal of Physics: Conference Series* (Vol. 909, No. 1, p. 012073). IOP Publishing.
- Hong, C. Y., Zhang, Y. F., Guo, J. W., & Li, G. Y. (2015). "Experimental study on the influence of drillhole roughness on the pullout resistance of model soil nails." *International Journal of Geomechanics*, 16(2), 04015047.
- Isaka, Avanthi & C Madushanka, B & Priyankara, Nadeej. (2016). "Analysis of Pullout Resistance of Soil-Nailing in Lateritic Soil." *Advances in Civil and Environmental Engineering Practices, for Sustainable Development*

(ACEPS)

- Jeon, S. S. (2012). "Pullout tests and slope stability analyses of nailing systems comprising single and multi rebars with grouted cement." *Journal of Central South University*, 19(1), 262-272.
- Junaideen, S. M., Tham, L. G., Law, K. T., Lee, C. F., & Yue, Z. Q. (2004). "Laboratory study of soil nail interaction in loose, completely decomposed granite." *Canadian Geotechnical Journal*, 41(2), 274-286.
- Kwong, A. K. L., & Lee, C. F. (2008). "A field test study on instrumented soil nail installed in cut slope." International Conference on Case Histories in Geotechnical Engineering. 2.
- Pei, H. F., Li, C., Zhu, H. H., & Wang, Y. J. (2013). "Slope stability analysis based on measured strains along soil nails using FBG sensing technology." *Mathematical Problems in Engineering*, 2013.
- Rawat, S., & Gupta, A. K. (2016). "An experimental and analytical study of slope stability by soil nailing." *Electron J Geotech Eng*, 21(17), 5577-5597.
- Rawat, S., & Gupta, A. K. (2018). "Testing and Modelling of Screw Nailed Soil Slopes." *Indian Geotechnical Journal*, 48(1), 52-71.
- Rawat, S., Gupta, A. K., & Kumar, A. (2017). "Pullout of soil nail with circular discs: A three-dimensional finite element analysis." *Journal of Rock Mechanics and Geotechnical Engineering*, 9(5), 967-980.
- Seo, H. J., Lee, I. M., & Lee, S. W. (2014). "Optimization of soil nailing design considering three failure modes." *KSCE Journal of Civil Engineering*, 18(2), 488-496.
- Tang, O. L., & Jiang, Q. M. (2015). "Stability analysis of slope under different soil nailing parameters based on the Geostudio." *International Journal of Georesources and Environment-IJGE (formerly Int'l J of Geohazards and Environment)*, 1(2), 88-92.
- Wang, Q., Ye, X., Wang, S., Sloan, S. W., & Sheng, D. (2016). "Degree of saturation effect on the grout-soil interface shear strength of soil nailing." In *E3S Web of Conferences* (Vol. 9, p. 15007). EDP Sciences.
- Ye, X., Wang, S., Wang, Q., Sloan, S. W., & Sheng, D. (2017). "Numerical and experimental studies of the mechanical behaviour for compaction grouted soil nails in sandy soil." *Computers and Geotechnics*, 90, 202-214.



## CFD Analysis of Bridge-Pier Model for Local Scouring

Atul Ailawadhi<sup>1</sup> and Baldev Setia<sup>2</sup>

<sup>1</sup>M.Tech. Student, Department of Civil Engineering, National Institute of Technology, Kurukshetra, Haryana;

<sup>2</sup>Professor, Department of Civil Engineering, National Institute of Technology, Kurukshetra, Haryana, Corresponding Author

### ABSTRACT

Scouring around bridge piers is a prominent problem that has been persisting since a long time. Significant experimental research has been carried out in this field. Based on experimental results aided by computational simulations, it has been observed that a sound correlation can be established between both the methods. However, owing to the increasing cost, effort and time required for long laboratory experiments in this field, it has been felt necessary to rely heavily on computational techniques. Keeping in view this necessary aspect a computational study has been planned and is under execution in NIT Kurukshetra. Objective of the study intends to make use of ANSYS-FLUENT based software simulation of a cylindrical bridge pier model for clear-water conditions. The software works on the principle of CFD. The variables chosen for the study include average flow velocity, diameter of the pier and the corresponding dependent parameters are stresses & velocities in the vicinity of the pier. The obtained flow patterns & results based on the k-epsilon turbulence model, are also to be visualized using graphs, contours and streamlines for different pier diameters. This study may be useful in reduction of the efforts required in the similar experimental works to check scouring.

**KEYWORDS:** *CFD-Computational Fluid Dynamics; local scouring; bridge-pier model; clear-water conditions.*

### INTRODUCTION

The term scour in a hydraulic structure signifies the erosion that occurs in the soil that surrounds the structure. There are generally three types of scours that affect the performance and safety of bridges, namely, local scour, contraction scour and degradation scour (Parker et al. 1997). The local scour is the most critical in scour consequences for bridges amongst all types. A typical scour pattern at a circular pier can be observed in Fig. 1.

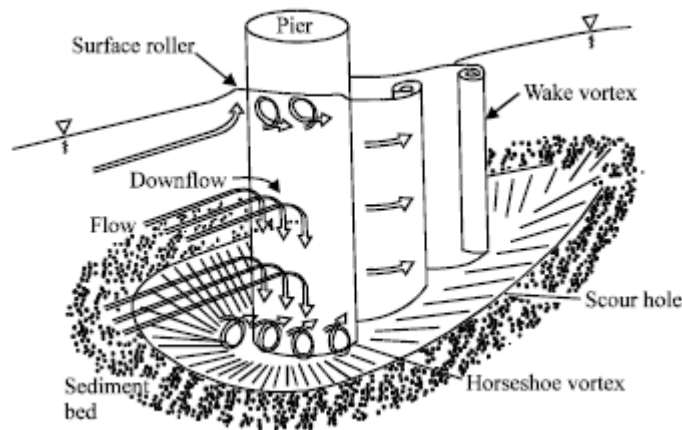


Fig.1: Illustration of the flow and scour pattern at a circular pier (Hammil 1999)

Interfering structures, in the river flow direction cause the local scour that results in formation of a scour hole in the vicinity of the pier. Since bridge failure is most commonly caused by local scour, in past years, numerous significant experimental research works have been carried out in this field as scouring around bridge piers is a prominent problem that has been persisting since bridges over rivers came into existence. A study conducted by Shirhole and Holt (1991) shows that scouring has been a cause in more than 60% cases in 1,000 bridge failures in U.S.

The methods and techniques that have been undertaken for the analysis of the local scour involve analytical solutions,

experimental tests and numerical simulations. However, most of these methodologies possess their own drawbacks, limiting the practical applicability. The experimental one being most tedious and expensive is only suited for the bridges that are highly valuable. This leaves the most affected regular bridges that are more in numbers when considered in time of flooding.

On the other side the scour-depth is solely assumed to be an independent variable making the scouring process a one-dimensional event, in analytical solutions. Whereas, scouring usually occurs in a complicated three-dimensional (3D) form, consisting of various time-dependent parameters like depth, 3D shape, influence area, and water flow condition. Thus a significant error in the scour calculation may be observed due to this dimensional discrepancy.

Besides all the expense of money, time and efforts made for scour development analysis, it still involves a great uncertainty to warn about the disaster prior to failure. Since the strength of local flow field is a major factor that determines the magnitude of local scour process which in turn is primarily governed by the obstruction to the flow caused by the bridge pier it becomes a necessity to first cling to its analysis.

For the simulation of complex flow patterns around the pier, a solution for the three-dimensional Navier-Stokes equations and the equation of continuity was obtained by Cheng et.al. using Large Eddy Simulation method. It was observed that at the nose of the pier, the created down flow affects the development of the horseshoe vortex. Turbulent structures, lift coefficient, and drag coefficient were also compared with the experimental results by them. With the extent and pace of development of computational resources and numerical methods, it has become more reliable alternative for the bridge-scour problem. The study aims at making use of the software resources for the observation of flow field patterns and magnitudes and its further applications to the determination of various quantities related to scour hole.

## PROBLEM DESCRIPTION

The problem basically consisted of a cylindrical bridge pier depicted by a circular section in 2-D plane erected in a stream of flowing water setup in a flume, modelled using demarcating the boundaries for the flow model. The boundaries were setup with no-slip condition between which a transient flow of the viscous fluid (water) was assumed. The analysis consisted usage of Finite-Volume-Method with the k-epsilon turbulence model, the model being most common for the simulation of the mean flow characteristics for turbulent flow conditions.

The model uses the following couple of equations in fig. 2 for the Turbulence Kinetic Energy (k) and Rate of Dissipation of Turbulence Energy (ε), respectively:

$$\frac{\partial(\rho k)}{\partial t} + \frac{\partial(\rho k u_i)}{\partial x_i} = \frac{\partial}{\partial x_j} \left[ \frac{\mu_t}{\sigma_k} \frac{\partial k}{\partial x_j} \right] + 2\mu_t E_{ij} E_{ij} - \rho \epsilon \quad \text{Eq. (1)}$$

$$\frac{\partial(\rho \epsilon)}{\partial t} + \frac{\partial(\rho \epsilon u_i)}{\partial x_i} = \frac{\partial}{\partial x_j} \left[ \frac{\mu_t}{\sigma_\epsilon} \frac{\partial \epsilon}{\partial x_j} \right] + C_{1\epsilon} \frac{\epsilon}{k} 2\mu_t E_{ij} E_{ij} - C_{2\epsilon} \rho \frac{\epsilon^2}{k} \quad \text{Eq. (2)}$$

**Fig. 2: Equations for Turbulence Kinetic Energy (k) and Rate of Dissipation of Turbulence Energy (ε) (Source: [https://en.wikipedia.org/wiki/K-epsilon\\_turbulence\\_model#cite\\_note-versteeg2007introduction-4](https://en.wikipedia.org/wiki/K-epsilon_turbulence_model#cite_note-versteeg2007introduction-4))**

, where the notations have their usual meanings.

The diameter of the pier is described as of the order of 1/6<sup>th</sup> of the width of the flume (Whitehouse1998) and the average inlet velocity (V<sub>in</sub>) set to the stated value by experimental setup in the same flume to create clear water conditions corresponding to a specific discharge.

Further carrying the same study, on the basis of the values of maximum velocities, flow patterns and the various other parameters like grain size distribution, bed slope, hydraulic mean radius, etc. the prediction of dependent bed shear stresses, the thresholds for incipience and resulting quantum of scour parameters may be made through Shield's curve.

### SIMULATION MODEL FOR SINGLE CIRCULAR SECTION PIER

For a model of flume used in experimental study in the Fluid Mechanics Laboratory of NIT Kurukshetra the setup is modelled with the following parameters, see Fig.3 and Table 1.

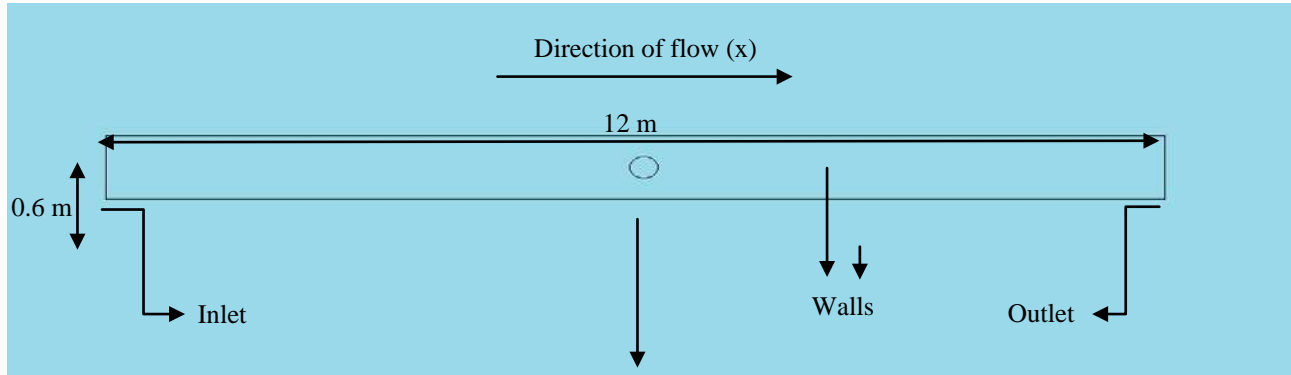


Fig. 3: Geometric layout of the model

Table 1: Various parametric values used for modeling

S. No.	Parameter	Value(Units)	
		Case-I	Case-II
1	Length of Flume (L)	12 m	12 m
2	Width of Flume (B)	0.6 m	0.6 m
3	Diameter of Circular Pier (d)	0.1 m	0.15 m
4	Average Flow Velocity(inlet) ( $V_{in}$ )	0.25 m/s	0.25 m/s
5	Dynamic Viscosity of the Fluid ( $\mu$ )	0.001003 kg/ms	0.001003 kg/ms
6	Density of the Fluid	998.2 kg/m <sup>3</sup>	998.2 kg/m <sup>3</sup>

Based on the above values the modeling was started in 2-D using the “Design Modeler” and surface from the sketches was obtained. This was followed by Mesh generation using “Method of Triangles”. The boundary conditions were then created including the circular edge of the pier and the rectangular flume edges in 2-D and the named selections made. The quality and sizing parameters were then edited to the requirement, see Figs. 4-5.

The setup was then started using double precision further setting the model as viscous and transient with the aforementioned material (fluid-water) properties. The boundary conditions then set for the named selections as “Cylinder” & “Wall” as Walls, “Inlet” as Velocity Inlet and “Outlet” as Pressure Outlet. The calculation was initialized with “Time Step” value as 0.01 and the “Number of Time Steps” value as 200 resulting into following iteration graphs, indicating converging values of various quantities like continuity, x-velocity, y-velocity, k-value, epsilon value:

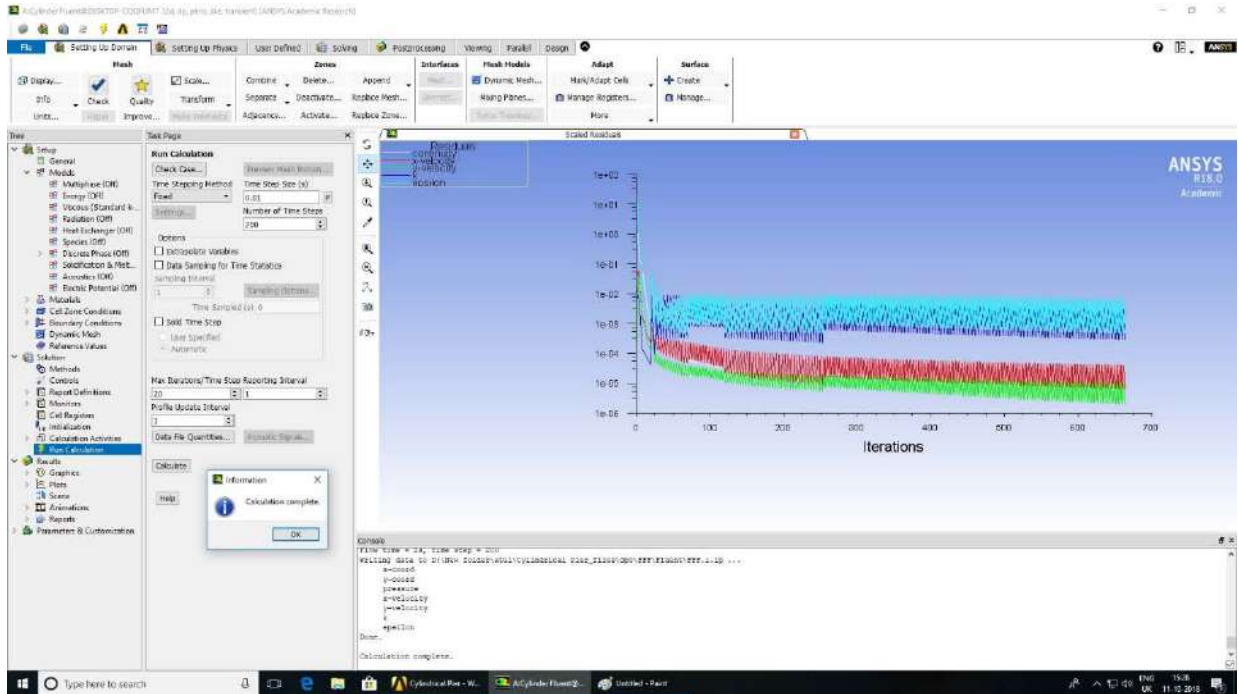


Fig. 4: Iteration Graph (for d= 0.1 m)

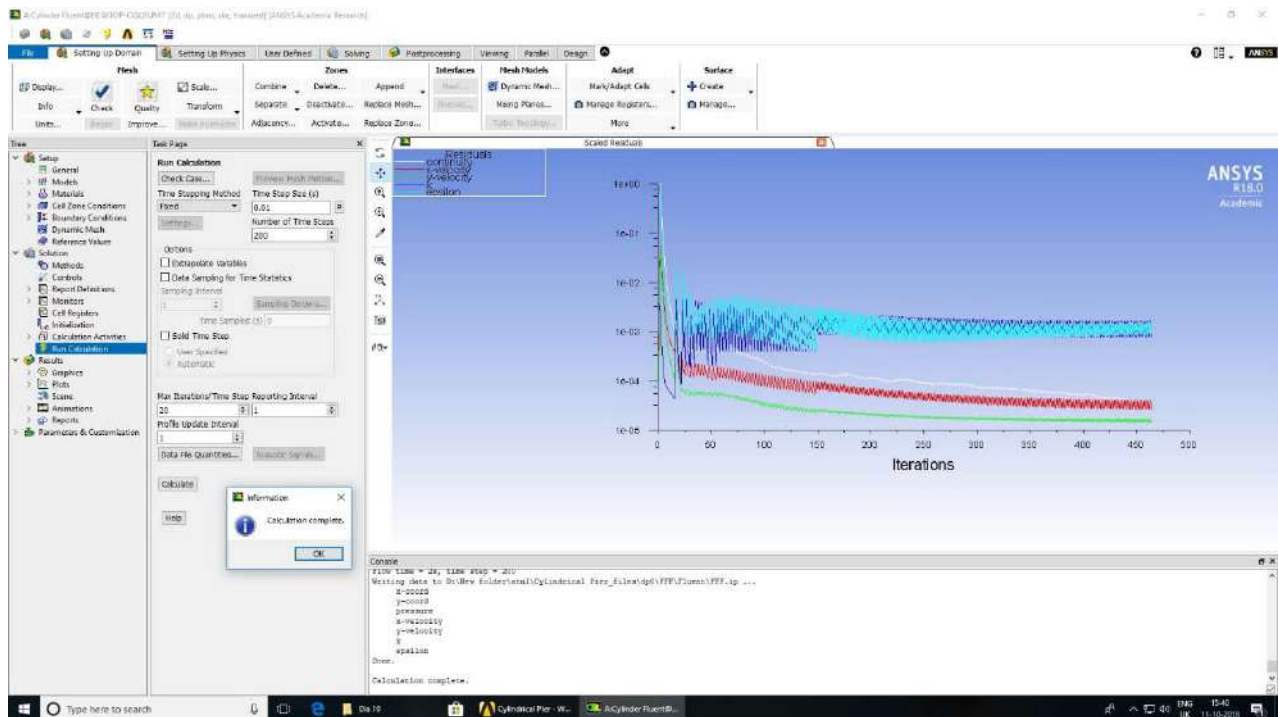


Fig. 5: Iteration Graph (for d= 0.15 m)

Since the simulation was carried out on a pier with circular section keeping its diameter as a variable parameter in this primitive phase of study, a non-dimensional parameter( $\pi$ ) using the width of the flume (B) and the pier diameter (d) may be derived to observe the trends for maximum velocity( $u_{max}$ ) in x-direction i.e. the direction of flow as:

Eq. (3)

$$\pi = \frac{(B - d)}{B}$$

## RESULTS

For **Diameter 0.1m**, the following contours were obtained for streamlines and the x-direction velocity (u), see Figs. 6-9.

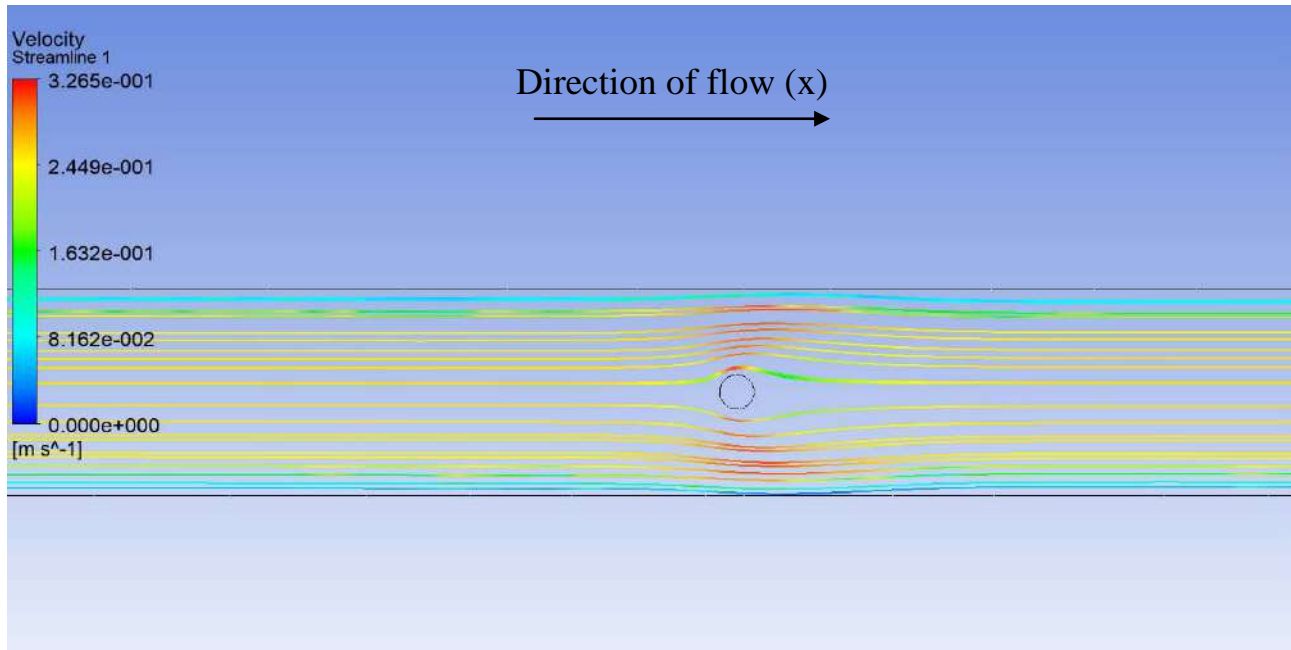


Fig. 6: Contours of velocity streamline (for d= 0.1 m)

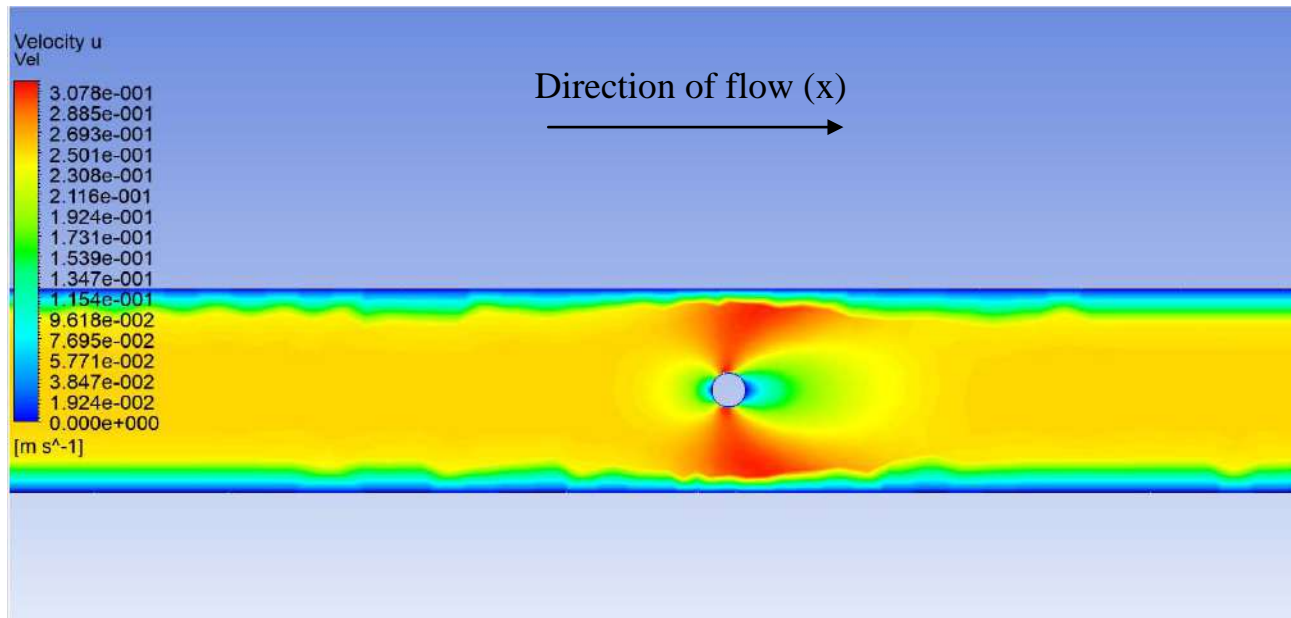


Fig. 7: Contours of velocity (u) in x-direction (for d= 0.1 m)

For **Diameter 0.15m**, the following contours were obtained for streamlines and the x-direction velocity (u).

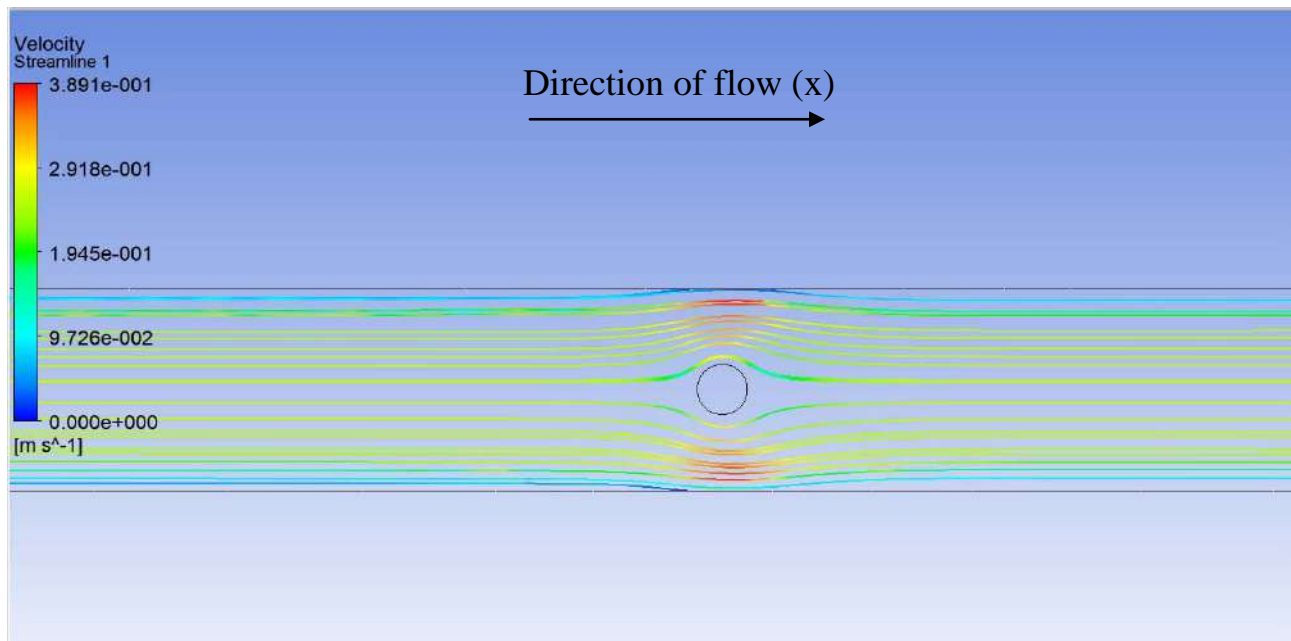


Fig. 8: Contours of velocity streamline (for d= 0.15 m)

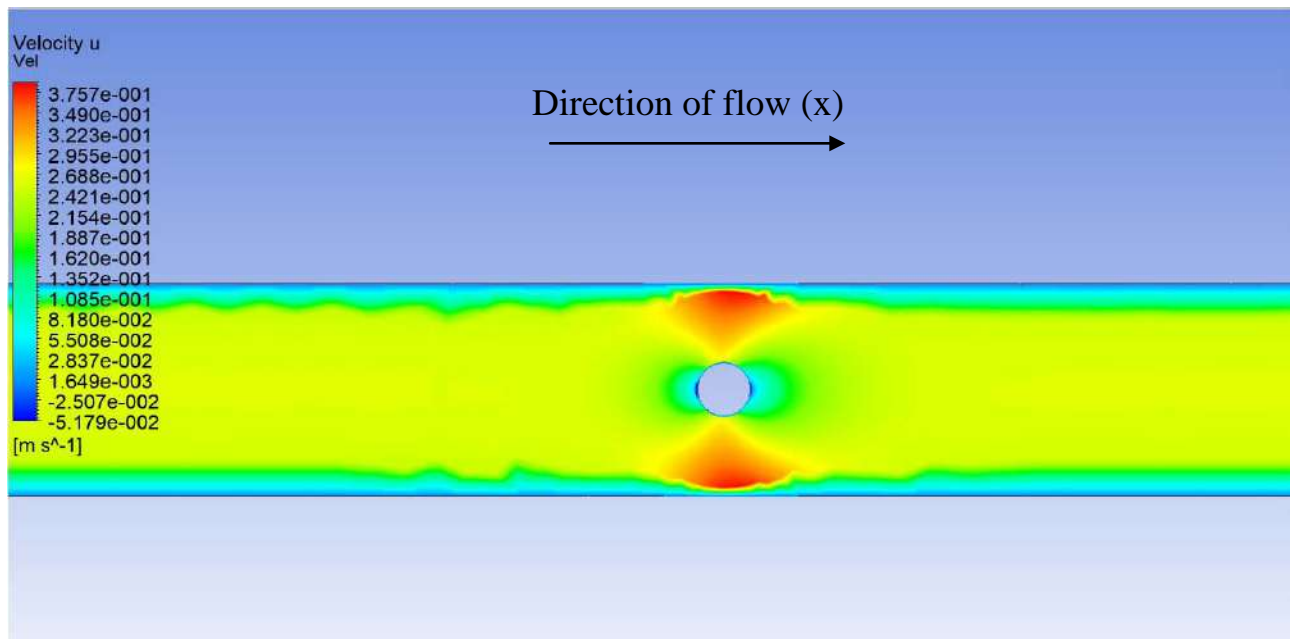


Fig. 9: Contours of velocity (u) in x-direction (for d= 0.15 m)

The contours above show that for an average inlet velocity of 0.25 m/s, the maximum velocity obtained in the vicinity of the pier is 0.3078 m/s in case of 0.1 m pier diameter and 0.3757 m/s for 0.15 m pier diameter.

The streamlines are more converging at the downstream end of pier in case of pier diameter 0.15 m as compared to pier diameter 0.1 m.

Value of  $u_{max}$  is 0.3078 m/s for  $\pi = 0.8333$  whereas  $u_{max}$  is 0.3757 m/s for  $\pi = 0.75$  (from eq<sup>n</sup>. 3)

### CONCLUSION:

The relation between the defined non-dimensional parameter ( $\pi$ ) and the maximum velocity in the direction of flow  $u_{max}$  is inversely proportionate i.e. keeping the flume width constant and increasing the pier diameter increases the magnitude of maximum velocity in direction of flow near the pier (obstruction).

Also the decreasing value of  $\pi$ , increases the convergence of streamlines at the downstream end of the obstruction.

The increasing value of  $u_{max}$ , in case of pier with higher diameter also indicates relatively higher magnitude of scouring.

### REFERENCES:

- K Chen, Weibing F, Liyuan Xu. (2014). *Three-Dimensional CFD Modeling of Local Scour around Bridge Piers*. IEEE International Conference on Progress in Informatics and Computing.
- HEC 18. (2012) - [www.fhwa.dot.gov/engineering/hydraulics/pubs/hif12012](http://www.fhwa.dot.gov/engineering/hydraulics/pubs/hif12012).
- Masjedi A, Bejestan MS. (2010). *Effect of Bridge Pier Position in a 180 Degree Flume Bend on Scour Hole Depth*. Journal of Applied Sciences 10(8): 670-675, 2010.
- Adhikary B.D, Majumdar P, and Kostic M. (2009). *CFD Simulation of Open Channel Flooding Flows and Scouring Around Bridge Structures*. Proceedings of the 6th WSEAS International Conference on FLUID MECHANICS (FLUIDS'09)
- Zhu Z, Liu Z (2012). *CFD prediction of local scour hole around bridge piers*. © Central South University Press and Springer-Verlag Berlin Heidelberg 2012
- Whitehouse, R.J.S. (1998) *Scour at Marine Structures: A Manual for Practical Applications*. Thomas Telford, London. <http://dx.doi.org/10.1680/sams.26551>
- [https://en.wikipedia.org/wiki/K-epsilon\\_turbulence\\_model#cite\\_note-versteeg2007introduction-4](https://en.wikipedia.org/wiki/K-epsilon_turbulence_model#cite_note-versteeg2007introduction-4)



## A REVIEW ON DIFFERENT MATERIALS AS LINERS AT LANDFILL SITES

*Taqi Adeel<sup>1</sup>, D.K. Soni<sup>2</sup>*

<sup>1</sup>M.Tech student, Department of Civil Engineering, National Institute of Technology Kurukshetra, Haryana-136119, India,  
Email:engtaqiadeel@gmail.com

<sup>2</sup>Professor, Department of Civil Engineering, National Institute of Technology, Kurukshetra, Haryana-136119, India,  
Email: dksoni@nitkkr.ac.in, Corresponding Author

### ABSTRACT

Landfilling is the method of disposal used most commonly for municipal wastes and land farming throughout the world. Quick urbanization and populace development prompt tremendous generation of solid waste that should be overseen. A municipal landfill gets a wide range of waste. Leachate is the liquid created from waste because of physical, biological and chemical process inside the landfill. The effect of a waste dump on the environment can be lessened by giving an impermeable boundary. Liners in a waste contaminant site assume an imperative job to hinder relocation of leachate and its toxic constituents into the groundwater or adjacent aquifer. A typical landfill liner ought to have low penetrability, obstruction against shearing, limit poison relocation, ought to withstand disintegration, low swelling, and shrinkage. Porousness and quality of a liner material utilized in the landfill site. For this to be done various technical methods should be adopted which decreasing the percolation of leachate in a landfill liner. The main goal is to decrease porosity and soil permeability. The availability of local soil, satisfying the engineering properties of a liner material for waste contaminant site is decreasing day by day. So this paper reviews about various kinds of materials used as liner in landfill such as This paper also mention about different types of liner system such as single liner system, composite liner system and double liner system to provide isolation of landfill from environment. From this literature review it can be noticed that the adoption of such method led to confinement of leachate in the very layer of disposed waste which percolates through landfill sites and contaminate the landfill soil which alter the various engineering properties of soil and makes it unfit fulfilling the required purposes. Use of these techniques prove an effective solution to various landfill related problems.

**KEYWORDS:** landfill; leachate; landfill improvement; liner system; liner materials.

### INTRODUCTION

Modern landfills are highly engineered containment framework, intended to limit the effect of solid waste (refuse, trash, and garbage) on the environment and human wellbeing. In present-day landfills, the waste is contained by a liner system. The basic role of the liner system is to disengage the landfill substance from environment and, in this manner, to shield the soil and groundwater from contamination beginning in the landfill. The best risk to groundwater presented by current landfills is leachate. Leachate comprises of water and water-solvent mixes in the decline that gathers as water transfer through the landfill. This water might be from rainfall or from the waste itself. Leachate may move from the landfill and sully soil and groundwater, in this way showing a hazard to human and environmental health. Landfill liners are planned and developed to make a barrier between the waste and the environment and to deplete the leachate to gathering and treatment facilities. This is done to keep the uncontrolled arrival of leachate into nature. Society produces a wide range of different solid wastes that posture diverse threats to environment and to community health. Distinctive disposal sites are accessible for these diverse kinds of waste. The potential threat posed by the waste decides the sort of liner system required for each kind of landfill. Liners might be portrayed as single (likewise alluded to as simple), composite, or double liners. Single liners comprise of a clay liner, a Geosynthetics clay liner or a geomembrane. Single liners are some of the time utilized in landfills containing construction debris. Clay liner is effectively accessible and is tough. Engineered geo-membranes are made out of polymers, for example, thermoplastics; crystalline thermoplastics; thermoplastic elastomers (chlorinated polyethylene, chlorylsulphonated polyethylene); elastomers (neoprene, ethylene propene diene monomer). The composite liner comprises of a geomembrane in the mix with a clay liner. These are more viable at constraining leachate movement into the subsoil. A twofold liner comprises of either two single liners, two composite liners, or a solitary and a composite liner. The double liners gather the leachate, while the lower liner goes about as a hole discovery system. Double liners are to be utilized in metropolitan solid waste landfills and particularly in unsafe waste landfills. A double liner is more impervious to stretch splitting and raised strain because of malleable yield. Liner frameworks are utilized some municipal solid waste landfills and in all hazardous waste landfills it can be observed that the use of such these techniques for increase of maximum dry density and unconfined

compressive strength has been noticed whereas the optimum moisture content and hydraulic conductivity decrease. So these techniques prove an effective solution to various landfill related problems.

## REVIEW OF LITERATURE

**Benson et al. (1994)** explained that contains research center estimated water hydraulic conductivities and related file estimations gathered amid the structure of concentrated soil liners. The screening was led to wiping out destinations where scale-subordinate hydraulic conductivities were known or prone to exist. Just liners compacted drip of the line of ideal states were incorporated.

**Kayabali K. (1997)** considered goes for explored certain highlights of a novel material proposed to fill in as an impenetrable liner in clean landfills. The characteristic zeolites of (Turkey) and the business powdered bentonite were utilized in different examinations, for example, compaction, hydraulic conductivity, and strength. Different proportions of bentonites and zeolites compacted at the ideal water content were tried to decide the quality parameters. The research facility tests compacted under ideal water content and marginally higher water contents were tried for hydraulic conductivity. For the bentonite content over 5%, the subsequent normal hydraulic conductivity esteems ran from  $2 \times 10^{-8}$  to  $4 \times 10^{-5}$  cm s<sup>-1</sup>. Cation trade limit, an imperative chemical property of a liner material, of bentonite and natural zeolite were observed to be 60 and 95 meq/100g, individually. The bentonite zeolite proportion of 0.05-0.10 was observed to be a perfect landfill liner material with respect to its low hydraulic conductivity and high cation trade limit. The utilization of bentonite zeolite proportion blends as an option in contrast to mud liners would fundamentally diminish the thickness of baseliner for sterile landfills.

**Tyrer et al. (2000)** assessed of the leaching properties of a considerable lot of these materials demonstrate them to be generally inert in both landfill leachates and in the synthetic condition winning in bond pore arrangements. Quickened leach testing of these materials, utilizing high-weight stream cells, proposes that they are commonly good with one another and with the clay hydraulic barrier boundary in the liner framework.

**Plamer et al. (2000)** demonstrated that blends of class F and class C fly ashes remains alongside coarse aggregate can be compacted to hydraulic conductivities required for landfill liners gave compaction is wit of optimum water content. The field tests demonstrated that developing a fly ash remains liner with hydraulic conductivities like those found in the lab is testing, and requires watchful consideration regarding factors that outcome in splits and porous entomb lift regions that outcome in high field hydraulic conductivity. Leachate gathered from the base of the test cushion likewise demonstrated that metal filtering must be viewed as when planning a liner with fly ash.

**Prashanth et al. (2001)** were viewed as the capability of pozzolanic fly ash debris as a hydraulic obstruction in the landfill. The conduct of three unique kind of fly ashes, demonstrating a scope of physical properties and chemical arrangement from three types of sources are accounted for in the examination. Geotechnical properties expected to assess the utilization of fly ashes remains as hindrance, for example, shrinkage, compaction, porousness, solidification and strength characteristics are accounted for. The demonstrate that fly ashes debris have low shrinkage and henceforth don't split. Compacted fly ashes undergo next to no volume changes.

**Güney and Özdemir (2005)** directed, the examinations of usage of sepiolite mud in landfill liner were explored. The regular soil was utilized close to sepiolite. Accordingly, the thought regarding the utilization of the sepiolite blend with characteristic soil, which can be effortlessly acquired from where the landfill region is to be developed, was explored. Record, mechanical and physicochemical tests were done to check the use of sepiolite in the landfill liner region.

**Quadri et al. (2009)** utilized Kolar soil and Granite polish wastes are utilized as essential materials. The properties of these materials are changed by adding sodium bentonite to accomplish the required properties of a skilled material for landfill liners and covers. Likewise, the execution of these materials is tried under various physicochemical situations. The consequences of the examination demonstrate that expansion of sodium bentonite conveys the penetrability to the expected range to use as an elective material for landfill liners and spreads.

**Budihardjo et al. (2012)** talked about the favorable circumstances and confinement of Geosynthetics clay liners as landfill leachate obstructions to ensure the environment. Geosynthetics clay liners have a few points of interest in their shape, accessibility, simple in the establishment and for the most part hydraulic execution. In any case, the Geosynthetics clay liners likewise have some impediment for their obstruction toward puncture, the shear strength and

bentonite loss in transport and taking care of. During their installation, more consideration ought to be put on to decrease the risk of Geosynthetic clay liners damage that can bargain their execution.

**Wu et al. (2017)** coal gangue is one of the biggest modern strong waste everywhere throughout the world, and numerous techniques have been proposed for the reusing of coal gangue. In the present investigation, the possibility of utilizing coal gangue as landfill liner material is considered through a progression of lab tests as far as pressure driven conductivity, sorption qualities and filtering conduct.

**Anuar and Chan. (2017)** explored the impact scope of pH esteem on the development of marker microscopic organisms, *Escherichia coli* (*E. coli*) disconnected from landfill leachate. The outcomes demonstrated that the quantity of *E. coli* became higher in basic contrasted with acidic condition. Discoveries from this examination will fill in as a base for future investigations for expelling microscopic organisms in leachate utilizing DMS as geosorbent in a landfill site.

**Banar et al. (2017)** considered was to research the potential use of waste clay from boron generation in sterile landfills. The waste clay (CW) was blended with bentonite (B) and waste tire (TW) at various proportions. Results demonstrate that any of the CW-TW blends were not worthy to use in landfills in view of lacking bearing capacity clues. Then again, CW and 2B/98CW blends have adequate qualities from the purpose of trial tests. As an end, it has been presumed that CW can be utilized as a liner material for landfills without an expansion.

**Akgun et al. (2017)** because of the current requirement for new landfill destinations in Ankara, the appropriateness of Ankara Clay as a liner material for landfill locales was explored. A mineralogical and geotechnical database was made by gathering the aftereffects of past tests by the present creators and in addition, those of tests performed. The examination researched tentatively the mineralogical and geotechnical qualities of the clayey soil tests acquired from the Ankara district. These examples had a normal water powered conductivity of  $\sim 2.68 \times 10^{-10}$  m/s which is not as much as the most extreme estimation of  $1 \times 10^{-9}$  m/s, as indicated by ecological controls in Turkey.

**Oluremi et al. (2017)** reported it is evident that municipal solid waste leachate would have a detrimental influence on the compacted clay liner formed from natural lateritic soil. Treatment of natural lateritic soil with waste wood ash minimizes the detrimental effect of the leachate on compacted soil as liner material. It also shows that waste wood ash treatment of lateritic soil beyond 4 % by dry weight of soil in waste containment application will have a negative effect on its compatibility with municipal solid waste leachate.

**Widomski et al. (2018)** examined the use of seven clay substrates of different particle composition and plasticity, tested locally in rustic areas, as materials permitting reasonable development of the waste landfill liners, which meet the primary standards of supportability, use locally accessible materials and farthest point the natural threats presented via landfill leachate to water, general health, and arable land.

## CONCLUSION

In this review paper, study of some previous work has been done to study the issues and aspects of landfill characteristic using clay liner.

The conclusion based on present study in given below:

1. Some specialist examined the potential use of the liner in landfills. In view of the reason for improving geotechnical properties of waste materials to impervious of the landfill.
2. Bentonite inappropriate amount mixed with fly-fiery remains might be utilized as a base liner of a landfill site.
3. The maximum dry density of landfill is expanded and optimum moisture content diminished with the expanding of bentonite.
4. Using of clay liner in landfill maintain a strategic distance from to the relocation and compressible and furthermore brings down the hydraulic conductivity which makes the liner essentially impenetrable.
5. The fly slag can be designed to get great quality and the most extreme adequate hydraulic conductivity for use as landfill liners.

6. Landfill liner can be cover and it is likewise locally accessible materials, which can achieve low penetrability and high quality.
7. Landfill liners are basic for shielding the environment from landfill waste contamination. Utilizing just the best quality landfill liner materials is vital since keeping any break from happening ought to be of the need. A landfill liner keeps the relocation of leachate and toxic results into topsoil, and guard against entrance into aquifers of close-by rivers and the tainting of other nearby water sources.
8. Using liners in municipal solid waste landfills can enhance the hydraulic conductivity, bearing capacity, slop steadiness, and long-term reliability.
9. With the end goal to acquire an elective landfill liner material for solid waste disposal areas equipped for chemical filtering and having a low hydraulic conductivity, characteristic zeolite was blended with a business powdered bentonite.
10. Geosynthetics clay liner as landfill liner and substitute compacted mud liner in some landfill site. The low pressure driven conductivity, thin thickness, effectively in transport and establishment are some of advantages of Geosynthetics clay liners among compacted clay liner. Regardless of its focal points, Geosynthetics clay liners additionally has some constraint such us shear quality which is identified with insecurity when introduced on the incline and its thickness that make more powerless toward cut.

## REFERENCES

- Benson, C.H., Zhai, H. and Wang, X., 1994. "Estimating hydraulic conductivity of compacted clay liners". *Journal of geotechnical engineering*, 120(2), pp.366-387.
- Kayabali, K., 1997. "Engineering aspects of a novel landfill liner material: bentonite-amended natural zeolite". *Engineering Geology*, 46(2), pp.105-114.
- Tyrer, M., Atkinson, A., Claisse, P.A. and Ganjian, E., 2000, June. "Novel composite landfill liners." In *Proceedings of the "Green3", 3rd international symposium on geotechnics related to the European environment, Berlin* (pp. 21-4).
- Palmer, B.G., Edil, T.B. and Benson, C.H., 2000. "Liners for waste containment constructed with class F and C fly ashes". *Journal of Hazardous Materials*, 76(2-3), pp.193-216.
- Prashanth, J.P., Sivapullaiah, P.V. and Sridharan, A., 2001. "Pozzolanic fly ash as a hydraulic barrier in landfills". *Engineering Geology*, 60(1-4), pp.245-252.
- Güney, Y. and Özdemir, H.V., 2005. "The utilization of sepiolite in landfill liners". *Environmental technology*, 26(5), pp.561-570.
- Patil, M.R., Quadri, S.S. and Lakshmikantha, H., 2009. "ALTERNATIVE MATERIALS FOR LANDFILL LINERS AND COVERS".
- Budihardjo, M., Chegenizadeh, A. and Nikraz, H., 2012. "Geosynthetic clay liner as landfill's leachate barrier". In *Proceedings of the International Conference on Civil and Architectural applications (ICCAA'2012)* (pp. 98-100). Planetary Scientific Research Center.
- Wu, H., Wen, Q., Hu, L., Gong, M. and Tang, Z., 2017. "Feasibility study on the application of coal gangue as landfill liner material". *Waste management*, 63, pp.161-171.
- Anuar, N.M. and Chan, C.M., 2017, November. "Reuse of dredged marine soils as landfill liner: Effect of pH on Escherichia coli growth". In *IOP Conference Series: Materials Science and Engineering* (Vol. 271, No. 1, p.

012071). IOP Publishing.

- Banar, M., Güney, Y., Özkan, A., Günkaya, Z., Bayrakçı, E. and Ulutaş, D., 2017. "Utilisation of waste clay from boron production as a landfill liner material". *International Journal of Mining, Reclamation and Environment*, pp.1-17.
- Osinubi, K.J., Oluremi, J.R., Eberemu, A.O. and Ijimdiya, S.T., 2017, October. "Interaction of landfill leachate with compacted lateritic soil–waste wood ash mixture". In *Proceedings of the Institution of Civil Engineers-Waste and Resource Management* (Vol. 170, No. 3+ 4, pp. 128-138). Thomas Telford Ltd.
- Akgün, H., Türkmenoglu, A.G., Met, İ., Yal, G.P. and Koçkar, M.K., 2017. "The use of Ankara Clay as a compacted clay liner for landfill sites". *Clay Minerals*, 52(3), pp.391-412.
- Widomski, M., Stępniewski, W. and Musz-Pomorska, A., 2018. "Clays of Different Plasticity as Materials for Landfill Liners in Rural Systems of Sustainable Waste Management". *Sustainability*, 10(7), p.2489.



## EFFECT OF GEOGRID REINFORCEMENT ON THE BEHAVIOR OF SQUARE FOOTINGS ON SAND - A REVIEW

*Mohit Chahar<sup>1</sup>, V.K. Arora<sup>2</sup>*

<sup>1</sup>M.Tech scholar, Department of Civil Engineering, NIT Kurukshetra, Haryana

<sup>2</sup>Professor, Department of Civil Engineering, NIT Kurukshetra, Haryana, Corresponding Author

### ABSTRACT

Soil reinforcement is the method of improving the bearing capacity and other engineering properties of soil. This study summarizes the previous investigations done on the geogrid reinforced sandy soil square model footings. The study considered various parameters like the depth of reinforcement layer below the footing, number of reinforcement layers used and the spacing between the geogrid sheets all of which contributed to the effect on the performance of the model footing and its load settlement response. It was revealed that the performance of the footing is enhanced if the reinforcing was done within the significant depth and with the optimum number of geogrid sheets in comparison to the case when the sand was unreinforced. The results demonstrated the potential benefit of the layout and configuration of geogrid reinforcement in improving the bearing capacity and settlement resistance of the model footing. The study also included the numerical models using PLAXIS 3D, whose results were validated using the experimental results. The numerical model results were found to be in good relation with those of the tests performed.

**KEYWORDS-** Geogrid, reinforced soil, bearing capacity, square footing, PLAXIS 3D, model testing, settlement reduction.

### INTRODUCTION

The weak soil under shallow foundation results in excessive settlement. Structural damage, reduction in durability and deterioration are the expected causes. In conventional treatment, the increasing of the dimension of the footing is a common method used to improve the performance level. However, reinforcement elements are an alternative and economical solution to improve performance of the soil. Inclusion of reinforcement generally increases the ultimate bearing capacity of soil and reduces the footing settlement. The usage of the reinforcements in a soil medium became especially popular after the pioneering work of Vidal (1966).

As granular soil is weak in tension therefore to improve its tensile properties it is reinforced with various type of reinforcements (see Fig. 1):

- a) Strip,
- b) Bar,
- c) Sheet, and
- d) Grid

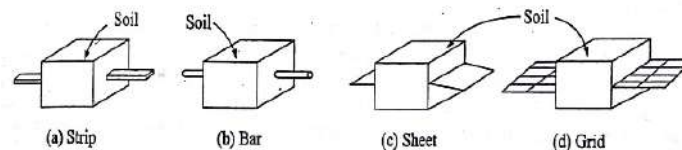


**Fig. 1. Types of Reinforcing Elements**

The working principal of reinforced soil mass is that when the soil mass is in unstable zone tries to move, it tries to pull out reinforcements along with it. However, the movement of the reinforcement is prevented by the soil of the stable zone. This ensures that the soil in the failure zone is unable to move since it cannot slip past the reinforcement. Hence the entire soil in which reinforcement is provided remains stable and its strength improves. This is shown in Fig. 2(d).

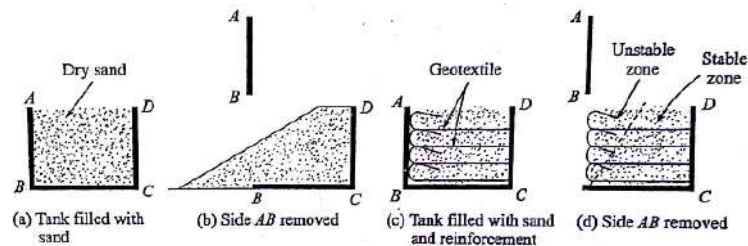


**Fig. 2. Mechanism of reinforcement in soil mass**

The concept of soil reinforcement is being used extensively in the field of geotechnical engineering. Earlier, the concept commenced with the use of metallic grid reinforcements in the geotechnical structures and a more recent one is the use of synthetic reinforcements. In the cases of poor to marginal ground conditions, geosynthetic reinforcement is proved to be a cost-effective solution and in some cases geosynthetics open up the possibility of constructing shallow foundations in lieu of expensive deep foundations. Among the range of geosynthetics available on the market, geogrids are the most preferred type of geosynthetic materials for reinforcing the foundation beds. The influences of different variables and parameters such as the type of geosynthetic, depth of reinforced zone, spacing between two reinforcement layers, width of reinforcing layer, and those contributing to the improved performance of reinforced soil foundation were examined (i) to reduce footing settlements, and (ii) to increase the ultimate bearing capacity of foundations.

Primarily, geogrids and geocells are the two different forms of synthetic reinforcements, which are being used in the construction industry. The research carried out over the last two decades reveals that geogrid is the most advantageous form of synthetic reinforcement, and thus the work in this direction needs to be carried out more extensively. The primary objective of this study is to summarize the work carried out by the different authors.

## LITERATURE REVIEW

**Latha and Somwanshi (2009):** They did the investigation and discovered the effects of various reinforcement parameters like the type and tensile strength of geosynthetic (geogrid and geonet) material, amount of reinforcement, layout and configuration of reinforcement layers below the footing on the bearing capacity improvement of the footings. For this they used rigid steel plate to model the square footing over loose sand (Poorly graded Sand, SP). The results showed that the bearing capacity value changed more drastically with the spacing of reinforcement layers than any other parameter. Spacing ratio ( $h/B$ ) (where,  $h$  is spacing between the two consecutive reinforcement layers and  $B$  is width of the footing) of 0.5 corresponds to the highest bearing capacity value and gives about 4 layers in the significant depth below model footing. But they were unable to give the optimum depth of the first reinforcement layer below model footing. A term improvement factor ( $I_r$ ) was used to represent the improvements due to the provision of reinforcement which is similar to the bearing capacity ratio (BCR value). They also performed the numerical modelling on FLAC 3D and the results were found to be in well relation with the experimental readings.

**Latha et al. (2009):** Presented the results from the laboratory model test and numerical simulations on square footing resting on geosynthetic reinforced sand. It was noted that the tensile strength alone is not the governing factor but

composite action between the soil and the reinforcements also plays a vital role. The effect of parameter like the type of geosynthetic reinforcement revealed that geonets and biaxial geogrids perform similarly up to settlement ratio of about 7 to 8 but after that geogrids goes up to a settlement ratio of 11 without failure (Fig. 3(a)), also they were able to achieve a higher Improvement factor ( $I_f$ ) as compared to geonets (Fig. 3(b)).

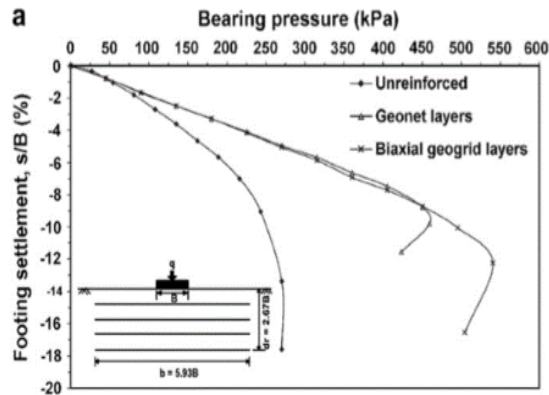


Fig. 3(a). Variation of Bearing pressure with Footing settlement

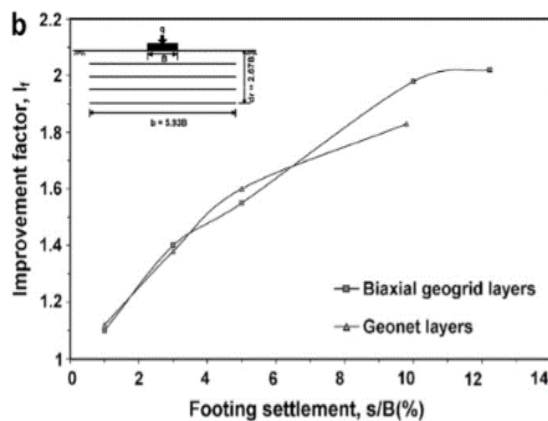


Fig. 3(b). Variation of Improvement factor with Footing settlement

Their other main finding was the effect of the depth of top layer of reinforcement on to the BCR value of footing, but it was quoted that no specific optimum depth of the top layer was determined. Generally at the ultimate loads BCR values decreases as top layer spacing increases. No clear optimum depth of the top layer spacing was obtained for geogrid reinforced sand, which can be clearly seen by Fig. 4.

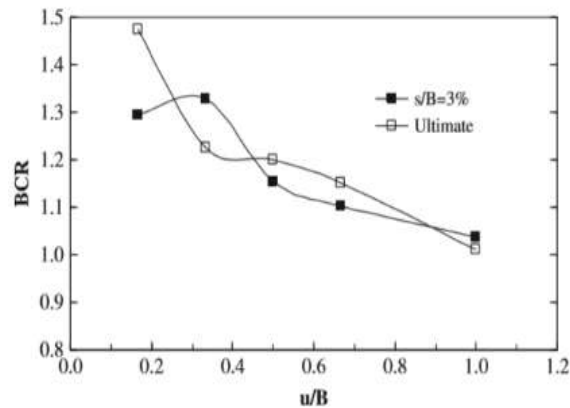


Fig. 4. BCR vs u/B for one layer of reinforcement

Moreover the random distribution of reinforcements was found to be inferior to the oriented distribution. Also the problem of rupture of geocell during the testing was observed, which made its application limited as compared to geogrids and geonets.

**Farsakh et al. (2013):** Investigated and evaluated the behavior of square and rectangular footings on the geogrid reinforced sandy soil. They used three different types of geogrids and one geosynthetic and lastly the combination of the two. They represented the variation of Bearing Capacity Ratio (BCR) with respect to u/B (top reinforcement spacing ratio), N (number of reinforcement layers), h/B (vertical spacing ratio) and s/b (settlement ratio) (where, u: Top layer spacing, h: Vertical spacing between layers, d: Total depth of reinforced zone, s: Settlement of the footing, B: Width of footing) to get a precise idea of the effect of the various parameters on the response of the footing. The effect of the number of reinforcement layers and depth of reinforced zone is shown below in Fig. 5.

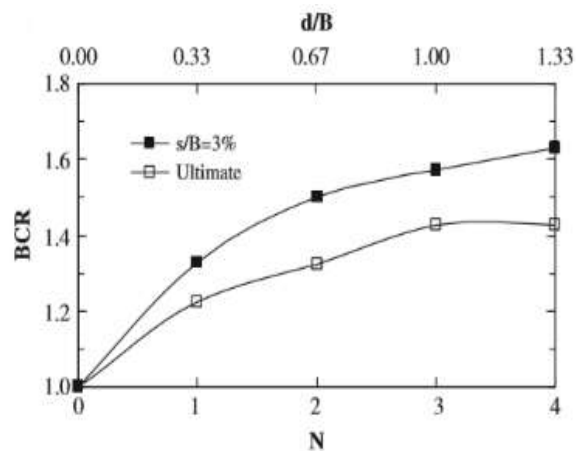


Fig. 5. BCR vs N and d/B

They showed that the bearing capacity increased as the number of layers increased. However, the significance of an additional reinforcement layer decreased as the number of layers increased. The effect of the spacing between the reinforcement layers (h) with respect to the width of the footing (B) is also presented in Fig. 6. However, no optimum vertical spacing was obtained for the geogrid reinforced sand, but it was obvious that the BCR values decreased as the vertical spacing (h) increased with maximum BCR at  $h=0.167B$ . The authors also believed that a value of  $h=0.2B$  can be taken as a reasonable value for use in design of reinforced sand foundations.

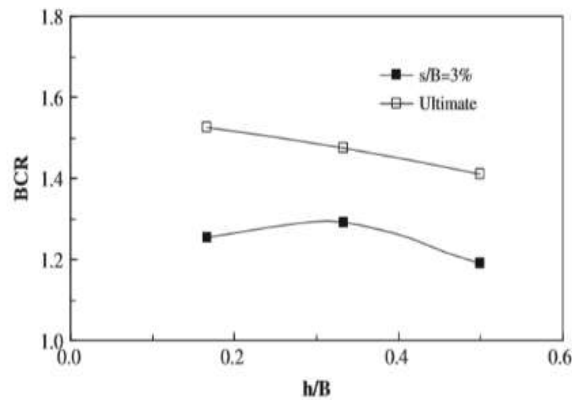


Fig. 6. BCR vs h/B

**Hegde and Sitharam (2013):** Focused on the experimental and numerical study of the square footings supported on geocell reinforced sand and clay beds and by comparing them found that the trend in the variation of the BCR values with settlement is different for the two beds. BCR values increased with settlement for sands while it was reduced for the clays. They used ECA for composite modelling and numerical analysis was carried out using FLAC-2D, thus the results did not hold good with field works.

**Kumar and Chakraborty (2014):** Proposed that the improvement in the bearing capacity becomes quite extensive for two layers of the reinforcements as compared to the single layer of the reinforcement for geogrid reinforced foundations. They carried their work on a circular footing with circular shaped reinforcement layers. They also studied the behavior of footing if the angle of shear resistance ( $\phi$ ) of sand was changed and discovered that the increment in  $\phi$  resulted in increment in the bearing capacity efficiency factors ( $N_c$  and  $N_\gamma$ ).

**Hegde et al. (2014):** Performed the numerical modelling of the geocell reinforced sand beds using FLAC-3D and found out that the ECA is very unrealistic for the modelling purpose. They quantified the reduction of settlement in terms of a factor known as percentage reduction in settlement (PRS), and showed that reinforcement helps in reducing the permanent settlement under the footing.

**Sanjei (2016):** Studied the behavior of model shallow foundation of timber on geocell reinforced sand. The study aims to build an accurate numerical model for the bearing capacity of square footing on geocell reinforced soil. The study employed PLAXIS 3D. The method is improvement over the Equivalent Composite Approach-ECA used to model geocell till now. His study proposed that 4 layers were optimum for sand reinforcement using geogrid and the reinforcement located beyond  $d/B=2$  does not contribute to the increase in the bearing capacity of the footing. Similar values were shown by **Farsakh et al. (2013)**. The final results were shown as in Fig. 7, where it was observed that the PLAXIS 3D gave somewhat exaggerated results in every case. He concluded that significant improvement in bearing pressure was only when  $U/B$  ranges in between 0.5 and 1.0 .

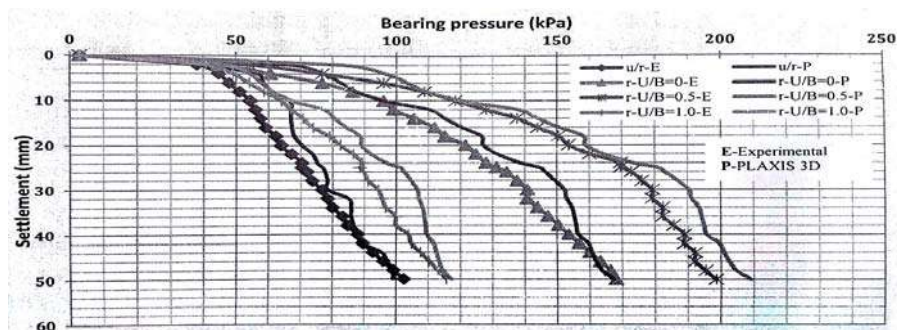


Fig. 7. Bearing pressure –settlement behavior of footing under various conditions

## CONCLUSION

This study summarizes the work carried out by the different authors as follows:

- a) Better performance of geogrids as compared to geotextile and geonet for sandy soil foundations.
- b) An optimum to layer depth was not obtained, however studies indicate increasing it, decreases the  $I_f$  value.
- c) The BCR value was found to be increased owing to the redistribution of the foundation loads over a wider area (i.e., more uniformly) below the reinforced zone.
- d) Settlement reduction was observed to be of decreased as compared to the unreinforced case.
- e) Some optimum number of reinforcement layers were observed over an influence depth.
- f) There was also a proposed optimum spacing between the reinforcing layers, increasing which further has no prime effect towards improving the performance of footing.

As increasing need of improving engineering properties of sands prompted designers and constructors to adapt for an effective method such as geogrid reinforcements. Thus, there is need for more extensive study in this direction to establish precise design procedures for geogrid reinforced square footings in the field. More research can be done on numerical modelling using PLAXIS 3D which will result in better understanding of the reinforcing property of geogrids and the most advantageous use of them in geotechnical engineering.

## REFERENCES

- C. Sanjei (2016) "Numerical modelling of the behavior of shallow foundations on geocell reinforced sand" IEEE, 978-1-5090-0645-8/16.
- A. Hegde and T.G. Sitharam (2015) "3-Dimensional numerical modelling of geocell reinforced sand beds." Geotextiles and Geomembranes, vol. 43, pp. 171-181.
- G. Madhavi Latha, and S. Amit Somwanshi (2009) "Bearing capacity of square footings on geosynthetic reinforced sand." Geotextiles and Geomembranes, vol. 27, no. 4, pp. 281-294.
- G. Madhavi Latha and Amit Somwanshi (2009) "Effect of reinforcement form on the bearing capacity of square footings on sand." Geotextiles and Geomembranes, vol. 27, pp. 409-422.
- G. Latha Madhavi (2000) "Investigation on the behaviour of geocell supported embankments." Madras, India.
- G. Madhavi Latha, Sujit Kumar Dash and K. Rajagopal (2009) "Numerical Simulation of the Behavior of Geocell Reinforced Sand in Foundations." International Journal of Geomechanics, no. August, pp. 143-152.
- M.Y. Abu-Farsakh and Q. Chen (2008) "Use of Reinforced Soil Foundation (RSF) to Support Shallow Foundation." Louisiana Transportation Research Center-FHWA, Louisiana, USA, FHWA/LA. 07/423.
- Murad Abu-Farsakh, Qiming Chen and Radhey Sharma (2013) "An experimental evaluation of the behavior of footings on geosynthetic-reinforced sand." The Japanese Geotechnical Society, Soil and Foundations 53(2):335-348.
- A. Hegde and T.G. Sitharam (2013) "Experimental and numerical studies on footings supported on geocell reinforced sand and clay bed." International Journal of Geotechnical Engineering, vol. 7, no. 4, pp. 347-354.
- Manash Chakraborty and Jyant Kumar (2014) "Bearing capacity of circular foundations reinforced with geogrid sheets" The Japanese Geotechnical Society, Soil and Foundations 54(4):820-832.
- A. Hegde and T.G. Sitharam (2015) "Three-dimensional numerical analysis of geocell-reinforced soft clay beds by considering the actual geometry of geocell pockets." Canadian Geotechnical, vol. 52, pp. 112.
- T.G. Sitharam, S. Sireesh, and Sujit Kumar Dash (2005) "Model studies of a circular footing supported on geocell-reinforced clay" Canadian Geotechnical, vol. 42, pp. 693-703.
- T.G. Sitharam and S. Sireesh (2005) "Behaviour of embedded footings supported on geogrid reinforced foundations beds." Geotechnical Testing Journal, vol. 25, no. 5, pp. 452-463.



## A REVIEW ON EFFECT OF SLOPING GROUND ON BEARING CAPACITY OF FOOTING

*Rahul Verma,<sup>1</sup> Sujata Gupta,<sup>2</sup> Anupam Mital<sup>3</sup>*

<sup>1</sup>M.Tech Scholar, Department of Civil Engineering, N.I.T Kurukshetra, Kurukshetra, Haryana136119;  
e-mail: [rahul\\_31702217@nitkkr.ac.in](mailto:rahul_31702217@nitkkr.ac.in)

<sup>2</sup>Ph.D Scholar, Department of Civil Engineering, N.I.T Kurukshetra, Kurukshetra, Haryana136119;  
e-mail: [sujata\\_6160052@nitkkr.ac.in](mailto:sujata_6160052@nitkkr.ac.in)

<sup>3</sup>Professor, Department of Civil Engineering, N.I.T Kurukshetra, Kurukshetra, Haryana-136119;  
e-mail: [anupam.mital@rediffmail.com](mailto:anupam.mital@rediffmail.com), Corresponding Author

### ABSTRACT

In developing country like India, development of infrastructure in hilly region, the safety on slope has to be given more importance for designing shallow foundations resting on slopes. Depending upon the position of the footing, steepness of the slope and due to development of plastic region of failure, a significant reduction in the bearing capacity of the foundation takes place. As the slope angle increase bearing capacity is reduce. For design of foundation, bearing capacity is most important parameter which depends upon the various factors i.e. location of footing, shear strength of soil, presence of water table, type of loading and allowable settlement of footing. Slope stability is a prime issue in sloping ground rather than foundation settlement. Estimation of bearing capacity of foundation on highly slope is very complex. During the last two decades, many researchers have study to find the bearing capacity of footing resting on or near slope by using different methods. i.e. slip line method, limit equilibrium method, limit analysis method and numerical method. This paper reviews the various available literatures on the analysis of shallow foundation on sloping ground.

Keywords: Bearing Capacity; Shallow Foundation; Slope Stability.

### Introduction

A foundation is as a part of the substructure used to transmit the loading of the structure to the strata underlying below it. The bearing capacity of foundation is a primary concern in geotechnical engineering. In foundation design, the ultimate bearing capacity of strip footing is expressed as sum of the three main factors related to cohesion, surcharge, and unit weight of soil according to TARZAGHI's equation (1943). Several other methods may predict the bearing capacity of foundation resting on or in level grounds (MEYERHOF,1963; HANSEN,1970; VESIC,1975). These are either based on laboratory experiment or in-situ test results. Due to land limitation, structures are generally placed on the slope crest or at a distance from slope crest. Examples are bridge piers supported on approach embankments, foundation of transmission tower and some buildings. Slopes are very common in hilly region. Hilly regions cover more than 15% of total land area of India (Joshi et al, 2011). Construction of foundation on slope or near slope is a complex and difficult problem for civil engineer. Slopes are affected the ultimate bearing capacity of foundation. So stability of slope is most important factor in performance of structure on or near the slope. Some factors like location of footing, the edge distance, shear strength of soil, slope angle, depth of embedment of footing, rainfall intensity, water table etc, affect the stability of footing on or near the slope. For footing on or near slope, the bearing capacity of footing is reduced due to development of curtailed zone of passive resistance towards the slope face. Analysis of bearing capacity of foundation can be done by four approaches; slip-line methods, limit equilibrium methods, limits analysis methods and finite-element methods. According to problem of interest and its complexity, method to analysis the bearing capacity is select. An attempt has been made in this paper to review the available literature on the analysis of shallow foundation on sloping ground. Based on literature study some suggestion have been made as well to determine bearing capacity of footing on or near the slope more efficiently.

### LITERATURE REVIEW

Evaluation of bearing capacity of foundation is required for the following two purposes:

1. The safety factor against ultimate shear failure must be adequate.
2. The settlements under allowable bearing pressure should not exceed tolerable values.

Bearing capacity can be determined by experimental study and theoretical study. Experimental studies can be conducted as model study or full scale testing. Theoretical studies can be further classified into four categories; limit equilibrium method, limits analysis method, slip-line method, and numerical methods.

Based on laboratory tests

**Shields et al. (1977)** determined the bearing capacity factor  $N_{\gamma q}$  for a footing resting on a constant slope of 2H:1V in a granular soil and concluded that Meyerhof (1957) has overestimated the  $N_{\gamma q}$  values. Design charts were presented for  $N_{\gamma q}$  value in correlation with depth of footing and offset distance between slope crest and footing.

**Garnier et al. (1994)** proposed coefficients of reduction due to slope based on experimental test. Three slopes of 3V:2H, 2V:1H and 3V:1H were assumed on sand with an angle of internal friction of  $40.5^\circ$ . The peak load at the time of failure was measured and the coefficient of reduction of bearing capacity was calculated as the percentage of the reference peak load.

**Yoo (2001)** determined the bearing capacity behavior of a strip footing on a geogrid-reinforced earth slope. Length, spacing and number of layer of reinforcements were varied for different depth of reinforcement location. Results of laboratory study are compared with the finite element analyses results of computer programme Plaxis. Bearing capacity and settlement increased and decreased respectively by considerable amount with increase in length and number of geogrid layers. Optimum value of different reinforcement parameters were presented as well for maximum benefits of reinforcement.

**Kumar et al. (2007)** conducted a series of model tests to examine the bearing capacity of foundations over a dense sand layer overlying loose sand deposit with and without the inclusion of geogrid reinforcements in the densified layer and concluded that the bearing capacity is increased up to 3 to 4 times with reduction in settlement.

**Sawwaf (2007)** determined the effect of depth of replaced sand layer and offset distance between footing and slope crest under sinusoidal loading. Length, spacing and number of layer of reinforcements were varied for different depth of reinforcement location. The test results showed that stabilizing the sand slope by the partial replacement with the inclusion of soil reinforcement not only increases the stability of the slope itself but also significantly decreases the footing settlement and provides greater stability to the footing under both the monotonic and dynamic loading conditions.

**Alamshahi and Hataf (2009)** conducted laboratory model test and results are compared with finite element results. The bearing capacity of rigid strip footings on sloping ground is increased by providing the grid anchor layer in ground and effect of reinforcement depends on distribution of reinforcement. By the reinforcement, settlement is also reduced.

**Kumar and Ilamparuthi (2009)** conduct the laboratory study to find the response of strip footing on unreinforced and reinforced model slopes. Finite element analysis was carried out using Plaxis to validate the experimental results. They concluded that by inclusion of geosynthetic reinforcement under the footing, load-settlement behavior and bearing capacity can be improved.

**Sommers and Viswanadham (2009)** evaluated the stability of footing on geo-textile-reinforced slopes by centrifuge test under the acceleration of 40g and concluded that reinforcements cause the increase in the stability of slope.

**Castelli and Lentini (2012)** performed model laboratory testing of footing on a well-graded compacted sandy slope and found that bearing capacity increases with increase in distance between footing and slope crest. Finally they concluded that by the slope the failure mechanism is affected and bearing capacity reduced of about 50%.

**Keskin and Luman (2013)** investigated the effect of setback distance of footing, slope angle, relative density of sand and footing width on ultimate bearing capacity of strip footing and the results with the finite element analysis. They concluded that the bearing capacity increases with increase in setback distance, relative density of sand, footing width and decrease in slope angle.

Based on Theoretical and Analytical Method

Most of earlier studies are conducted by theoretical analysis. Theoretical analysis consists of limit equilibrium analysis, limit analysis, slip line method and numerical methods.

**Limit Equilibrium Method**

In this method by using of shear surface of any shape, internal stresses and average factory of safety of slopes is computed.

**Meyerhof (1957)** Reported that when a foundation located on the face or top of a slope is loaded to failure, the plastic zone developed on the slope side is relatively smaller size compared to the similar foundation on level ground and the bearing capacity is reduced. It means that length of failure surface have been reduced and that will reduce the resistance of soil. Slope has reduced the bearing capacity of the strip footing in cohesive and granular soil as well. Bearing capacity is increased with increase in offset distance between slope edge and footing. Meyerhof indicated Plastic Zones near rough strip foundation on face of slope and Plastic zones and slip surfaces near rough strip foundation on top of slope listed in Fig 1 and Fig 2

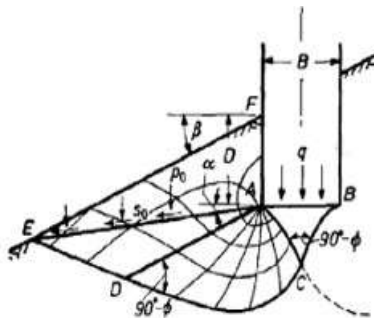


Fig.1 Plastic Zones near rough strip foundation on face of slope by Meyerhof's theory

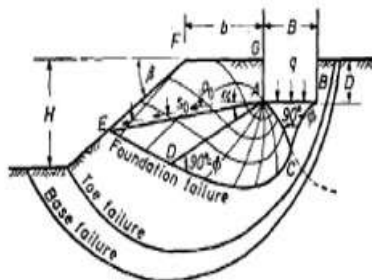


Fig.2 Plastic zones and slip surfaces near rough strip foundation on top of slope

**Saran et al. (1989)** were considered only one sided failure surface. Equivalent surcharge takes place the footing load and at a time of failure, it was assumed that strength of sloping side has mobilized fully one side but on other side only some percentage of strength is mobilized and a mobilization factor 'm' on opposite to slope side used as shown in Fig. 3 and Fig. 4. When  $\phi$  value reached some limit for a particular value of slope angle, bearing capacity become independent of offset distance between slope crest and footing.

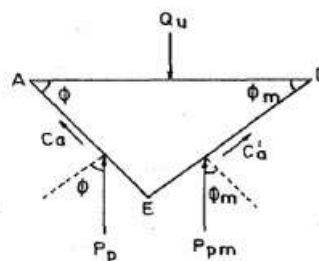


Fig. 3 Assumed rupture surface

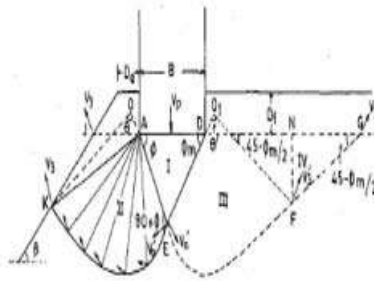


Fig. 4 failure surface in sloping ground by Saran, Sud, and Handa (1989)

**Sarma and Chen (1995)** concluded that the inertia force of the soil mass underneath a footing induced by earthquake has significant influence on the bearing capacity of the footing i.e. bearing capacity is reduced.

**Choudhury and Rao (2005)** to determine seismic bearing capacity factors considered composite failure surface. Principle of superposition was validated as well and it was concluded that the capacity of footing reduced by horizontal acceleration as well as vertical acceleration.

**Chen et al. (2007)** concluded that the seismic bearing factors increased when intermediate principal stress was considered in analysis. Seismic bearing capacity was increases by 16% to 40%. Bearing capacity factor  $N_\gamma$  increase more in compared to  $N_q$  and  $N_c$ .

**Castelli and Motta (2010)** used limit equilibrium method to develop a model for footing with circular failure surface. Analyzed kinematic and inertial effects of the seismic loading on footing. Presented seismic and static bearing capacity as a function of seismic coefficient, soil friction angle. Embedment depth have considerable influence in case of soil having low friction angle. Effect of distance of the footing from the edge of the slope on bearing capacity was also considered in analysis.

**Shukla and Jakka (2014)** conducted a simple parametric analysis considering various factors such as depth ratio of footing, offset distance between footing ( $B'$ ) and slope edge and slope angle using limit equilibrium method. It was concluded that bearing capacity factors have been increased with increase in depth of foundation. When  $B'/B$  ratio approaches approximately equal to or more than 5 then effect of slope angles becomes negligible. The effect of offset is very less at the low slope angle value as compared to higher slope angle. The effect of depth ratio is very prominent at a lower slope angle compared to high value of inclination.

#### **Limit Analysis Method**

Without carrying out the analysis of stage which required in limit equilibrium analysis, limit analysis directly gives the ultimate capacity. Evaluation of upper bound and lower bound collapse load is referred to as limit analysis. In addition to yield condition, the limit analysis methods consider the soil stress-strain relationship in idealized manner and this is referred as a flow rule or normality in limit analysis. Result of a limit analysis study is depends on flow rules. In upper bound analysis collapse load are evaluated by equating rate of internal work done and the rate of external work done. Lower bound analysis gives a collapse load less than that true collapse load and it consider only force equilibrium of soil. A true collapse load can be evaluated by using upper bound and lower bound analysis simultaneously. Limit analysis is more versatile and complicated method compared to limit equilibrium with an assumed stress-stain. In general, value of ultimate bearing capacity in limit analysis method is more accurate as compared to limit equilibrium analysis. Limit analysis gives the higher value of bearing capacity as compared to limit equilibrium.

**Michalowski (1989)** determined three dimensional stability analysis of locally loaded drained  $c - \phi$  soil with consideration of all possible failure modes in conjunction with upper bound theorem.

**Sawada (1994)** using upper bound theorem in association with pseudo-static approach, they were evaluated seismic bearing capacity and results were found very close to Bishop and Kotter. Failure surface was changed with incorporation of reinforcement and consideration of horizontal earthquake coefficient.

**Yang et al. (2007)** analyzed footing on sloping ground using energy dissipation method (upper bound solution) and results are compared with laboratory model testing results. It was assumed that soil failure is governed by a linear Mohr-Coulomb yield criterion, and soil deformation follows an associated flow rule. Bearing capacity values were

presented for various values of angle of internal friction and slope angle.

**Yamamoto (2010)** introduced the shear transfer coefficient to evaluate the seismic bearing capacity of spread foundations with consideration of variable shear transfer at the base of foundations. It has been shown that increment of horizontal seismic coefficient, the seismic bearing capacity factors reduce considerably. In addition, the magnitude of bearing capacity factors decreases further with increase in slope inclination and increase with the embedment and the distance of slope crest from the beginning of loading.

**Kumar and Chakraborty (2012)** using lower bound solution in conjunction with finite element and nonlinear optimization to determined the bearing capacity factors of smooth and rigid footing. Variation of the bearing capacity factor were presented with changes in slope angle ( $\beta$ ) for various internal friction angle ( $\phi$ ). This method is a very rigorous compared to other available method as it does not require an assumed failure mechanism.

**Ausilio, E. (2014)** investigated the seismic bearing capacity of shallow strip footing. It is placed near to the crest of the geo-reinforced soil structures and capacity of footing determined by the kinematic theorem of the limit analysis set up within the framework of the pseudo-static process. It concluded that with an raise in edge distance, the ultimate bearing capacity of the footing placed on both unreinforced and reinforced slopes increases and it diminished with an increase in slope angle.

**Kumar and Chakraborty (2015)** determined the bearing capacity of circular footing resting over fully cohesive strata covered with sand layer, using axisymmetric lower bound limit analysis with finite element sand linear optimization. They concluded that the bearing capacity improves significantly with cover of a sand layer. The bearing capacity has been shown in terms of the variation in the non-dimensional efficiency factor with changes in the thickness of the sand layer for several combinations of  $\phi$ ,  $c_u/(\gamma b)$ , and  $q/(\gamma b)$ . The efficiency factors increase with increases in  $\phi$  and  $q/(\gamma b)$  and decreases in  $c_u/(\gamma b)$ .

### *Slip Line Method*

Slip line method or Stress characteristics method is a well-known approach to solve stress boundary value problem on their limit state. This method assumes equilibrium of stresses everywhere in the system while components of stress at every point of the body satisfy the yield criterion. This method does not provide any allowance for creep or strain-rate effects so it is applicable for only non-strain-hardening materials. This method can model the boundary and field condition for the failure mechanism of cohesion less soil mass very accurately.

**Kumar and Rao (2002)** examine the effect of slope angle, angle of internal friction and coefficient of earthquake acceleration on bearing capacity factors applying the technique of stress characteristic.

**Kumar and Rao (2003)** used slip line technique to correlate factors such as angle of internal friction, slope angle and earthquake acceleration coefficient with seismic bearing capacity of strip footing. The value and amount of  $N_\gamma$  based on the both-sides failure mechanism, for smaller values of earthquake acceleration coefficient ( $\alpha_h$ ), observed to be significantly less than that obtained using the single-side mechanism. All the bearing capacity elements reduce greatly with increase in  $\alpha_h$  for various ground inclinations.

**Jahanandish et al. (2008)** used slip line method to show the impact of second side on the bearing capacity of footing beneath the both fixed and dynamic loads. Horizontal and vertical earthquake coefficients were reviewed for analysis and concluded that vertical bearing capacity decreases with increasing the second side slope angle and horizontal seismic coefficient in direction of first side slope.

**Keshavarz et al. (2011)** used a computer to analyze the slip line net and find the maximum load distribution under the foundation. Bearing capacity of the reinforced foundations has been expressed in the form of bearing capacity factors. Increase in the ultimate bearing capacity due to soil reinforcement is expressed in another bearing capacity factor called  $N_r$ . Design charts have been provided for practical applications.

**Keshavarz and Kumar (2018)** used the method of stress characteristics for determined the bearing capacity of strip and circular footings placed on rocky mass with using failure criteria of the modified Hoek-and-Brown. The bearing capacity has been shown in the form of non dimensional bearing capacity factors which are function of various input data for rock mass. They concluded that decreasing in the value of  $\sigma_c/(\gamma b)$ , the factor  $N_c$  increase continuously and the footing roughness have more significant effect for a circular footing as compared with a strip footing.

### *Numerical method*

Traditional methods such as limit equilibrium, slip line and limit analysis gives just either upper bound or lower yet numerical strategies give both lower-bound and upper bound collapse load of footing. Numerical methods are more accurate as compared to other available method but same time these methods are very complex in application and analysis.

**Paul and Kumar (1997)** determines the factor of safety and developed a procedure to performed seismic stability analysis of slope with a building loads using a computer program.

**Kai Wing Ip (2005)** developed a numerical model using the FEM program “PLAXIS. Variation of bearing capacity factors with slope angle, depth ratio, distance between the top of slope and footing edge presented as well.

**Jao et al. (2008)** using finite element analysis based on the theory of elastic-plasticity to evaluated the stability of eccentrically loaded strip footings on sloping ground. Observed that load eccentricity is not much affect the pressure and settlement parameters but it affect the ultimate bearing capacity of footing. For a value of slope 2H: 1V, effect of slope angles value becomes negligible when the magnitude of offset distance between slope crest and footing become more than 5 times of width of footing.

**Alamshahi and Hataf (2009)** performed a series of finite element analyses and conduct model tests in laboratory on reinforced soil. Finally results comes from both analysis were compared and it was confirmed that after the inclusion of grid-anchor layers in the ground (reinforced soil),the bearing capacity of footing increased and it depend on the position of reinforcement.

**Keskin and Luman (2013)** determined the effect of setback distance, relative density ,footing width and slope inclination on bearing capacity of footing by comparing the results of finite element method with experimental test and concluded that if setback distance, relative density of sand footing width increase and slope angle decrease, bearing capacity of footing increased.

**Acharyya et al. (2018)** examine the bearing capacity of square footing resting on slope with finite element method using Plaxis 3D vAE.01. An optimal 7-10-1 artificial neural network (ANN) used to determine the bearing capacity of footing based on input parameters. From these test results they concluded that increasing in the shear strength parameters of soil, footing width and embedment depth and decreasing in sloping angle, bearing capacity of footing increased.

### conclusion

In this paper, study of some previous work has been done to study the issues and aspects of sloping ground on bearing capacity of footing.

The conclusion based on present study is given below:

1. The magnitude of bearing capacity factor predicted by design chart is provided by theories of Meyerhof (1957), Graham et al (1987), and Saran et al. (1989) and the experimental work from Shields et al. (1977) and Gamier et al. (1994).
2. Some researchers (Shields et al. 1977, Saran et al.1989, Kai Wing Ip, 2005, Jao et al. 2008, Shukla and Jakka, 2014) concluded that the bearing capacity up to b/B ratio 5 or 6 affected by offset distance.
3. Upper bound analysis or limit equilibrium method and most of studies done by limit analysis method used.
4. Finite element and numerical methods can help the researcher to simulate seismic analysis more accurately.
5. Each method depends upon several factor involved in estimating the ultimate bearing capacity of the shallow foundation on the top of slope, hence it is difficult to identify a single common factor dominating the ultimate bearing capacity.
6. Still today, there is no worldwide accepted techniques available to determine bearing capacity of footing resting on or near the slope.
7. Results of experimental work and numerical analysis in previous studies were identical up to large extent, hence numerical analysis can be used for further study of bearing capacity of footing.
8. The settlement criteria and global stability of slope, which can be major deciding factors in slopes not considered in previous studies. Only shear failure criteria considered. These factors need to be considered in determination of bearing capacity of footings in future.

## References

- Acharyya, R., Dey, A. and Kumar, B. (2018). "Finite element and ANN-based prediction of bearing capacity of square footing resting on the crest of c- $\phi$  soil slope." *International Journal of Geotechnical Engineering*, pp.1-12.
- Alamshahi, S. and Hataf, N. (2009). "Bearing capacity of strip footings on sand slopes reinforced with geogrid and grid-anchor." *Geotextiles and Geomembranes*, 27(3), pp.217-226.
- Alamshahi, S. and Hataf, N. (2009). "Bearing capacity of strip footings on sand slopes reinforced with geogrid and grid-anchor." *Geotextiles and Geomembranes*, 27(3), pp.217-226.
- Ausilio, E. (2014). "Seismic bearing capacity of strip footings located close to the crest of geosynthetic reinforced soil structures." *Geotechnical and Geological Engineering*, 32(4), pp.885-899.
- Castelli, F. and Lentini, V. (2012). "Evaluation of the bearing capacity of footings on slopes." *International Journal of Physical Modelling in Geotechnics*, 12(3), pp.112-118.
- Castelli, F. and Motta, E. (2010). "Bearing capacity of strip footings near slopes." *Geotechnical and Geological Engineering*, 28(2), pp.187-198.
- Castelli, F. and Motta, E. (2010). "Bearing capacity of strip footings near slopes." *Geotechnical and Geological Engineering*, 28(2), pp.187-198.
- Chen, C.F., Dong, W.Z. and Tang, Y.Z. (2007). "Seismic ultimate bearing capacity of strip footings on slope." *Journal of Central South University of Technology*, 14(5), p.730.
- Chen, W.F. and McCarron, W.O. (1991). "Bearing capacity of shallow foundations." In *Foundation Engineering Handbook* (pp. 144-165). Springer, Boston, MA..
- Choudhury, D. and Rao, K.S.S. (2005). "Seismic bearing capacity of shallow strip footings." *Geotechnical and Geological Engineering*, 23(4), pp.403-418.
- El Sawwaf, M. A. (2007). Behavior of strip footing on geogrid-reinforced sand over a soft clay slope. *Geotextiles and Geomembranes*, 25(1), 50-60.
- Garnier, J., Canepa, Y., Corte, J.F. and Bakir, N.E. (1994), January. "Etude de la portance de fondations en bord de talus." In *Proc. XIIIth International Conference on Soil Mechanics and Foundation Engineering* (pp. 705-708).
- Georgiadis K.(2009). "Undrained bearing capacity of strip footings on slopes". *Journal of geotechnical and geoenvironmental engineering*. 2009 Oct 15;136(5):677-85.
- Ip, K.W. (2005). "*Bearing capacity for foundation near slope*" (Doctoral dissertation, Concordia University).
- Jahanandish, M. and Arvin, M.R. (2008). "Seismic stability analysis of footing adjacent to slopes by slip line method." In *Proc. of the 14 th World Conference on Earthquake Engineering* (pp. 12-17).
- Janbu, N. (1973). "Slope stability computations." *Publication of: Wiley (John) and Sons, Incorporated*.
- Jao, M., Ahmed, F., Muninarayana, G. and Wang, M.C. (2008). "Stability of eccentrically loaded footings on slopes." *Geomechanics and Geoengineering: An International Journal*, 3(2), pp.107-111.
- Keshavarz, A. and Kumar, J. (2018). "Bearing capacity of foundations on rock mass using the method of characteristics." *International Journal for Numerical and Analytical Methods in Geomechanics*, 42(3), pp.542-557.
- Keshavarz, A., Jahanandish, M. and Ghahramani, A. (2011). "Seismic bearing capacity analysis of reinforced soils by the method of stress characteristics."
- Keskin, M.S. and Laman, M. (2013). "Model studies of bearing capacity of strip footing on sand slope." *KSCE Journal of Civil Engineering*, 17(4), pp.699-711.
- Kumar, A., Ohri, M.L. and Bansal, R.K. (2007). "Bearing capacity tests of strip footings on reinforced layered soil." *Geotechnical and geological Engineering*, 25(2), pp.139-150.
- Kumar, J. and Chakraborty, D. (2012). "Bearing capacity of foundations with inclined groundwater seepage." *International Journal of Geomechanics*, 13(5), pp.611-624.
- Kumar, J. and Chakraborty, M. (2015). "Bearing capacity of a circular foundation on layered sand-clay media." *Soils and Foundations*, 55(5), pp.1058-1068.
- Kumar, J. and Mohan Rao, V.B.K. (2002). "Seismic bearing capacity factors for spread foundations." *Geotechnique*, 52(2), pp.79-88.
- Kumar, J. and Mohan Rao, V.B.K. (2003). "Seismic bearing capacity of foundations on slopes." *Geotechnique*, 53(3), pp.347-361.

- Kumar, S.A. and Ilamparuthi, K. (2009). "Response of footing on sand slopes." *Indian Geotechnical Society Chennai Chapter, Students Paper Competition*, pp.9-12.
- Meyerhof, G.G. (1957), August. "The ultimate bearing capacity of foundations on slopes." In *Proc., 4th Int. Conf. on Soil Mechanics and Foundation Engineering* (Vol. 1, pp. 384-386).
- Michalowski, R.L. (1989). "Three-dimensional analysis of locally loaded slopes." *Geotechnique*, 39(1), pp.27-38.
- Paul, D.K. and Kumar, S. (1997). "Stability analysis of slope with building loads." *Soil Dynamics and Earthquake Engineering*, 16(6), pp.395-405.
- Saran, S., Sud, V.K. and Handa, S.C. (1989). "Bearing capacity of footings adjacent to slopes." *Journal of geotechnical engineering*, 115(4), pp.553-573.
- Sarma, S.K. and Chen, Y.C. (1995). "Seismic bearing capacity of shallow strip footings near sloping ground." In *Proceedings of the 5th SECED conference on European seismic design practice. Balkema, Rotterdam* (pp. 505-512).
- Sawada, T., Nomachi, S.G. and CHEN, W.F. (1994). "Seismic bearing capacity of a mounded foundation near a down-hill slope by pseudo-static analysis." *Soils and Foundations*, 34(1), pp.11-17.
- Shields, D.H., Scott, J.D., Bauer, G.E., Deschenes, J.H. and Barsvary, A.K. (1977) July. "Bearing capacity of foundations near slopes." In *Proceedings of the ninth international conference on soil mechanics and foundation engineering*(Vol. 1, pp. 715-720).
- Shukla, R.P. and Jakk, R.S. (2014). "Bearing capacity of footings on slopes." In *Proceedings of Indian Geotechnical Conference* (pp. 1993-1996)
- Viswanadham, B.V.S. and König, D. (2009). "Centrifuge modeling of geotextile-reinforced slopes subjected to differential settlements." *Geotextiles and Geomembranes*, 27(2), pp.77-88.
- Yamamoto, K. (2010). "Seismic bearing capacity of shallow foundations near slopes using the upper-bound method." *International Journal of Geotechnical Engineering*, 4(2), pp.255-267.
- Yang, X.L., Wang, Z.B., Zou, J.F. and Li, L. (2007). "Bearing capacity of foundation on slope determined by energy dissipation method and model experiments." *Journal of Central South University of Technology*, 14(1), pp.125-128.
- Yoo, C. (2001). "Laboratory investigation of bearing capacity behavior of strip footing on geogrid-reinforced sand slope." *Geotextiles and Geomembranes*, 19(5), pp.279-298.



# SOIL STABILIZATION USING POLYPROPYLENE FIBER – A REVIEW

*Rashi Singh<sup>1</sup>, V.K. Arora<sup>2</sup>*

<sup>1</sup>M.Tech scholar, Department of Civil Engineering, NIT Kurukshetra, Haryana

<sup>2</sup>Professor, Department of Civil Engineering, NIT Kurukshetra, Haryana, Corresponding Author

## ABSTRACT

The objective of this study is to find out the application of the waste fiber (polypropylene) fiber materials in the geotechnical engineering and to analyze the waste polypropylene fiber effects on the shear strength of the unsaturated soil. Using stabilization of soil we can improve its bearing capacity, strength, durability and to prevent from erosion. The unconfined compressive strength, Proctor test and CBR test are performed first. After that the fiber is included in the soil and check the fiber effectiveness in strength characteristics of soils through performed a test of UCS, Proctor and CBR tests. The results have been interpreted in terms of stress-strain behavior, failure variation in strain-stress, effect of fiber content and other strength parameters. This study shows that the use of polypropylene fiber is very effective in civil engineering field for improving the properties of the soil because it causes the sufficiently great improvement in shear and compressive strength of soil. Now using Genetic programming formulate the models based on the measured data. The formulated GP model will be useful to determine optimum input values for achieving strong and bearing strata.

**KEYWORDS:** Polypropylene (PP) fiber, unsaturated soil, strength, UCS, Genetic programming (GP) model.

## INTRODUCTION

Germinating the use of waste material in soil stabilization (strengthening the soil) is spread in present scenario all over the world. The mainly objective due to which stabilization of soil using waste materials is extensively used nowadays due to extensive production of waste like fly ash, plastics, rice husk ash which is hazards for environment and also developing the problems of deposition. So, here in this project we are going to discussing about the stabilization of soil using randomly distributed polypropylene fibers (PP) which obtain from the waste material. Important thing is foundation for any land based structure, foundation should be strong and the soil around it plays a very critical role. So, the process of soil stabilization helps to achieve the required properties in a soil needed for the construction work. Now a day's various types of soil stabilization techniques are used:

- a) Steel wire reinforcement
- b) Geosynthetic reinforcement
- c) Addition of lime
- d) Randomly mix fibres into the soil

Polypropylene (PP) fibers are used in present scenario due their availability with desired property and durability. PP exhibit excellent resistance to abrasion, chemicals and biological entities investigated the micro-mechanical interactive nature between the soil particle and reinforced polypropylene fibers (PP).

In this study, we also utilized genetic programming (GP) to generate the models for prediction of unconfined compressive strength (UCS) of polypropylene stabilized cohesive soils.

## Genetic Programming (GP)

Genetic Programming is one of the most recently developed artificial intelligence (AI) technique based on generating a random set of equations, testing their fitness to the available data, choosing the most fitting equations, merging them using some certain mechanism (like living beings) to generate the next generation which continues the cycles until the target accuracy conducted. The result of this technique is closed form solutions which can be applied or included easily in engineering software. GP is a revolutionary soft-computing method which based on the Darwinian Theory. GP includes a high level diversification by breeding of randomly different computer programs as populations. The programs are structured like trees and having functions and terminals. Two sets must be defined as the sources of functions and terminals. Tree structures are reach any complexity if the sets of functions and terminals are rich. The function set includes arithmetic functions like (+, ×, or ÷), Boolean logic functions (AND, OR, NOT, etc.), mathematical functions (sin, cos, log), conditional functions (IF, THEN, ELSE). Terminal set consist of variables, numerical constants, functions with no argument, etc. Tree like structure program formed by Random functions and terminals. Branches which contain functions and terminals are connected to the root point. Blind search start by the genetic programming(GP) within the search area for solutions by creating random initial population. GP determines fitness of each individual & ones & also measures next generation with better fitness through the following process like by mutation (see Fig.1.), crossover (see Fig.2.) or by direct reproduction.

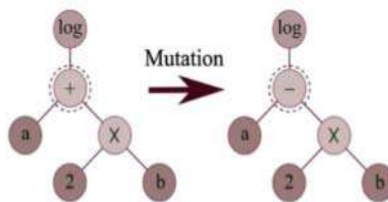


Fig. 1. Typical mutation model

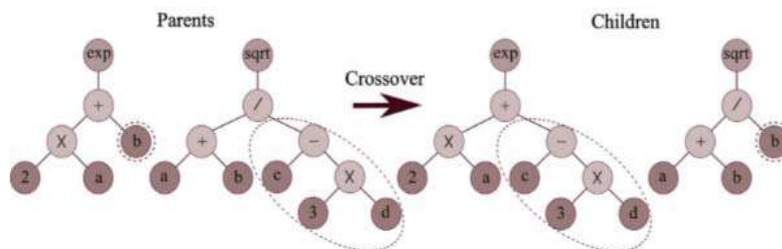


Fig. 2. Typical cross over operation

Without any changes few population transfer to new generation during the process of the reproduction. Individuals having with improved fitness with higher chances of selection. For generating the next generation, firstly from each individual one random node from each is selected & then swapping of sub-tree with one another have to be done when the cross over procedure and to generate a new population. According to initial type of node sometimes GP choose random node and then mutates it into a new function or terminal. Multi-Gene-Genetic-Programming (MGGP) is modified form of GP which consists of various GP models linearly. MGGP gives the linear weighted combination of the GP trees commonly known as 'gene'.

## LITERATURE REVIEW

**Alavi and Gandomi (2011):** For the evaluation of the performance characteristics of the soil stabilization they employed the approach for the characteristics of modelling in the civil engineering problems, i.e. Genetic Programming. They provided an overview of the application of GP in geotechnical engineering problems with emphasis on methodology suitable for assessing the comparative accuracy of each application. They using a linear variant of G.P, called Linear Genetic Programming (LGP) and hybrid search algorithm combining LGP & Simulated Annealing (AG) known as LGP/SA were employed for the prediction UCS, MDD&OMC of soil-stabilizer-mixers. They developed models using a various types of soils & stabilizers and slightly variations in their properties. Six sets are provided for the prediction models for analyses the results of LPG & LPG/SA which shows the proposed models which gives the accuracy in the estimation of target UCS, MDD and OMC values. LPG shows the better behavior compared with LPG/SA. They showed that the using the LPG& LPG/SA approaches gives accuracy in result and UCS, MDD & OMC can be evaluated without examine the time consuming & sophisticated lab or field tests..

**Trivedi et al. (2013):** Their study resulted in the formulation of a model which can be used to predict the CBR variation with the percentage of stabilizer used based on Genetic Algorithms. Fly ash used as a stabilizer in soil having different proportions varying 10% to 40% by soil weight sample & added to the sample of soil which collected from the site near Godhra (Eastern Gujarat). Experiments were conducted on the collected soil sample which is loamy in nature. Soil sample properties like LL, PL, OMC and CBR were observed for the samples containing addition different proportion of fly ash in them. The data collected for these properties from laboratory experiments when putted into the Evolver 5.7 will provide the predicted values of the CBR for various proportions of Fly ash added to the soil samples.

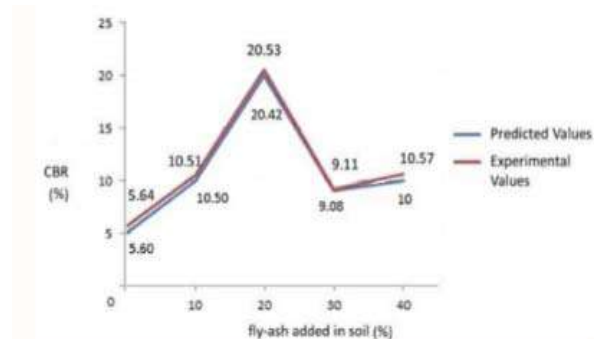


**Fig. 3. Comparison of Experimental and Predicted CBR values**

The graph above (Fig. 3) shows that the Experimental and Predicted values of CBR are almost overlapping indicating the accuracy of the Evolver Model formulated in the research study. They showed that experimental values of all index properties reaches to their maximum with the adding 20% of fly ash except for Optimum moisture content (OMC). OMC reaches to its maximum value by the addition of 29.27% fly ash. For 10% to 20% of fly ash added MDD value remains the same at 1.41 gm/cc. For UCS on addition of 20% fly ash its value varies from 0.152N/mm<sup>2</sup> to 0.148N/mm<sup>2</sup> and CBR values from 20.53% to 5.64%. Results shows that 20% fly ash containing soil gives the best results compared to other proportions of the soil stabilization. They created Evolver model to apply Genetic Algorithm for predicting CBR values with good amount of accuracy.

**Nangia et al. (2015):** Studied the strength characteristics of the sand stabilized using polypropylene fiber (also known as nylon). For the study PP fibers of diameter 0.25 mm and pieces of average length of 25 mm were used and were mixed (randomly) with soil in varying percentages (0 to 2.5) by dry weight of soil. They performed the direct shear test and Standard proctor test on three different places of soils. Result showed that optimum moisture content (OMC) increased in case of fine soils due to increase in surface area. Addition of fibers gave better strength characteristics in

case of well graded soil samples when compared with poorly graded samples. Shear strength for a particular normal stress increased with additional percentage of PP fibers.

**Harsha Vardhan et al. (2015):** Performed investigation on Red soil (mainly available at North Eastern part of India) using Polypropylene (PP) fiber formulate models for estimation of UCS using the genetic programming(GP). They employed the use of light compaction standard proctor to estimate the values of optimum moisture content (OMC) and maximum dry densities (MDD) to be 1.72g/cc & 16.92%. UCS test performed on both reinforced and unreinforced soils to get an estimate of the improvement in the strength properties. Then data was prepared for training of GP model. The parameter settings for Multi-Gene-Genetic-Programming (MGGP) is a set based on trial & error approach. They proposed that to analyses the soil parameters effects and fiber content, best way is to formulate the UCS models with ratio of change in strength (UCS of reinforced soil to the UCS of unreinforced soil) due to the inclusion of natural fiber as output and soil density, soil moisture content & fiber content as inputs. Their study also demonstrated the advance approach of soft computing (SoC) known as genetic programming (GP), see Figs. 4-5.

**Statistical plot of model on the training and testing phase UCS data**

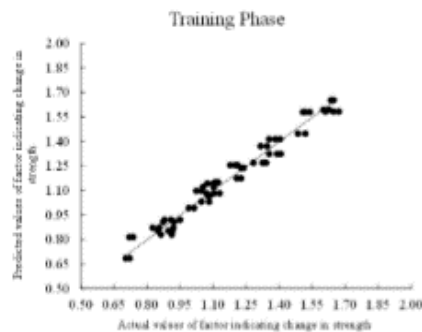


**Fig. 4.** Plot of predicted vs actual values of strength factor (reinforced/unreinforced strength) on training data.

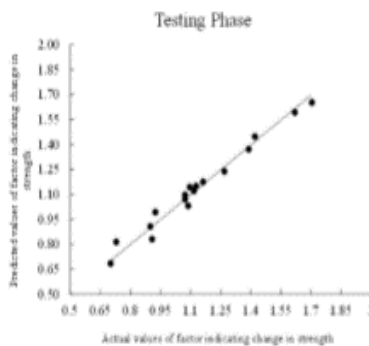


**Fig. 5.** Plot of predicted vs actual values of strength factor (reinforced/unreinforced strength) on testing data.

**Table 1.** GP model shows Error metrics

Error metrics	Training Data	Testing Data
R <sup>2</sup>	0.9689	0.9766
MAPE	3.5930	3.3245
RMSE	0.0469	0.0422

This Table 1. shows that the higher values of correlation coefficients & lower values of Mean absolute probability error (MAPE) and Root mean square error (RMSE) indicates that model obtained is in good relation with the dynamics of phenomenon have a high prediction accuracy.

**Teja (2016):** Evaluated the polypropylene fiber effects on strength characteristics of unsaturated soil .Tests on the soil nd evaluation of effect of polypropylene fiber were carried out by direct shear test and UCS test. They prepared two soil samples using different maximum dry density (MDD) and optimum moisture content(OMC) and tested these two soil samples using different proportions of fiber reinforcement (0.05%,0.15%& 0.25%) .For Direct shear test, on sample 1 the net percentage improvement in values of  $c$  &  $\phi$  observed was 19.6% from  $0.325\text{kg/cm}^2$  to  $0.3887\text{kg/cm}^2$  & 15.9% from  $47.72^\circ$  to  $48.483^\circ$  respectively. Randomly distributed PP fiber reinforcement is not recommended. For sample 2, net percentage improvement in values of  $c$  &  $\phi$  were observed to be 53% from  $0.3513\text{kg/cm}^2$  & 15.2% from  $27.82^\circ$  to  $32^\circ$  respectively. Hence, use of PP fiber as reinforcement is recommended, see Fig. 6

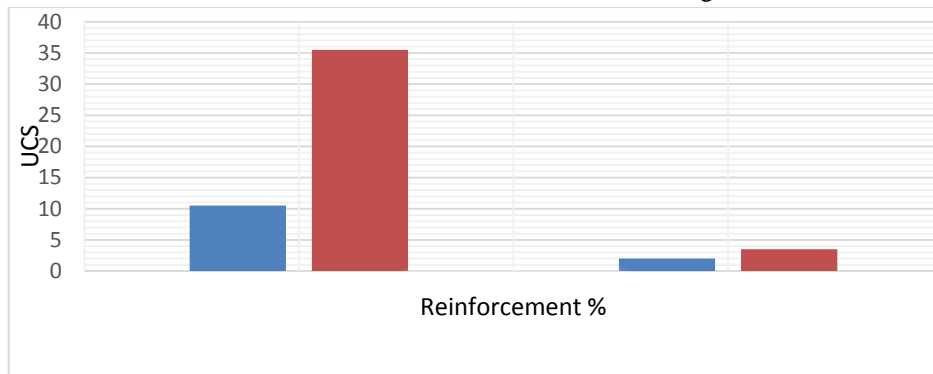


**Fig. 6. Comparison between sample 1 and sample 2 for UCS test**

For sample 1, UCS value increases from 0.0643MPa to 0.0562Mpa, net 14.4%, graph shows that continuously decreasing with initially steep slope. For sample 2, UCS value increases from 0.0692MPa to 0.1037MPa, net 49.8%, shows alternate rise & fall.

**Jiao et al. (2017):** Modelled the geopolymer stabilized clayey soil using multi-gene genetic programming (MGGP) for prediction of UCS. UCS was related with the percentage of ground granulated blast furnace slag (GGBS), liquid limit (LL), plastic limit (PL), plasticity index ( $I_p$ ), fly ash, proportion of alkali to binder and ratios of sodium (Na) & silicon (Si) to aluminum (Al). They implemented Multi gene genetic programming (MGGP) to determine the UCS of the clayey soil stabilized with polypropylene fiber (PP). Now, derived the equations for effective parameters of different combinations. MGGP based models give accuracy in the results of UCS. The proposed models were cable of estimating the UCS test without carrying out any laboratory tests. Sensitivity analysis results illustrates that S, plastic limit (PL) & silica to aluminum ratio (Si/Al) are most important factor affecting UCS. Any increase in ratios of Na/Al and Si/Al leads to the increased value of UCS.

**Balagoudra et al. (2017):** Proposed the stabilization of clayey soil using lime in addition to polypropylene fibers. The various tests performed on Black cotton soil with increment of 0.25% polypropylene fiber (PPF) up to 1% and constant 4% lime by weight of soil. They conducted the test on black cotton soil and find out the increasing the strength characteristics of soil by adding polypropylene (PP) fiber and lime and then compare the strength properties of between black cotton soil with fibers & without fiber using unconfined shear strength test (UCS), direct shear test (DST) & California bearing ratio test (CBR).

#### **Effect of Percentage of PP Fiber on OMC**

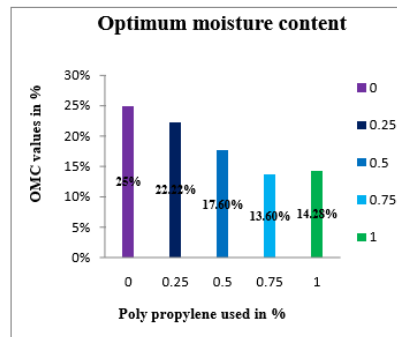


**Fig. 7. Optimum moisture content vs Polypropylene fiber used**

The graph (see Fig. 7) shows that the different percentages of polypropylene fiber with lime (4%) shows the decrement in the Optimum moisture content (OMC). The OMC decreased upto 0.75% and then OMC gradually increased when further addition of polypropylene fiber. Hence, at 0.75% of polypropylene fiber optimum dosage is found.

#### Effect of Percentage of PP Fiber on MDD

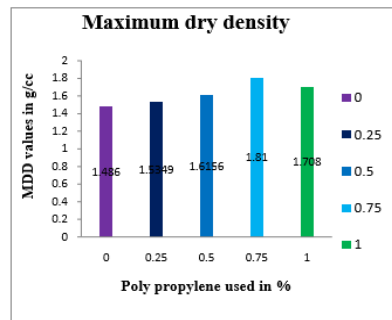


**Fig. 8. Maximum dry density vs Polypropylene fiber used**

This graph (refer Fig. 8) shows that the percentage of polypropylene fiber with lime (4%) resulted in the increment in the Maximum dry density (MDD). As MDD increases strength of soil also increases. The MDD increased up to 0.75% after which it gradually decreased if any further addition of polypropylene fiber was done. Hence, at 0.75% of polypropylene fiber optimum dosage is found.

#### Effect of Percentage of PP Fiber on UCS

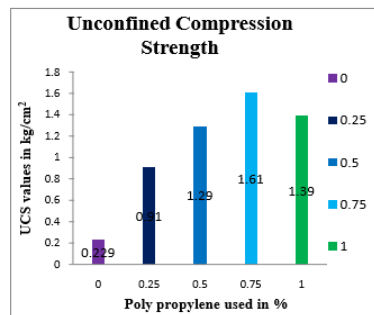


**Fig. 9. Unconfined Compressive Strength vs Polypropylene fiber used**

Above graph (see Fig. 9) is shown for different percentages polypropylene with lime (4%), which shows the increment in compression strength. The compression strength was found to be increased up to 0.75% then further addition of

polypropylene fiber it shows decrement in the graph .Hence, at 0.75% of polypropylene fiber addition optimum dosage is found.

#### Effect of Percentage of PP Fiber on CBR Value

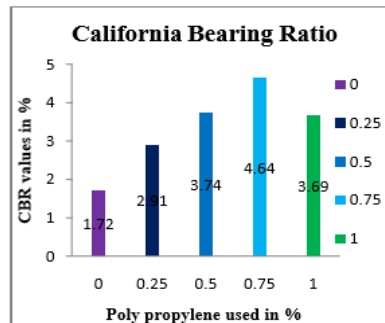


**Fig. 10. California Bearing Ratio vs Polypropylene fiber used**

Above graph (see Fig. 10) is for different percentages of polypropylene fiber with lime (4%) and shows increment in the CBR value. The CBR value increased upto 0.75% after that it drastically decreased when further addition of polypropylene fiber. Hence, at 0.75% addition of polypropylene found the optimum dosage. Thus obtained the optimum percentage of lime and polypropylene fiber as 4% and 0.75% for soil stabilization.

#### CONCLUSION

The study summarized the work carried out by the different authors as follows:

- Using the application of Genetic Programming (GP) in geotechnical engineering problems for assessing comparative accuracy of each applications.
- Using the fibre reinforcing soil, improves soil strength and also bearing capacity of soil. Moreover it is economical in both terms whether it is capital or energy, both increases the bearing capacity of soil rather than going for a deep foundation & raft foundation.
- Polypropylene fibre as a stabilizer in soil stabilization is advantageous, because it causes significant advancement in compressive and shear strength of the soil.
- By using the application of Genetic Programming (GP), Multi-Gene-Genetic-Programming (MGGP) predict UCS of geopolymer stabilized clayey soil model.
- Stabilization of Black cotton soil on addition of polypropylene (PP) fibre & lime performing UCS, CBR test. Improving bearing capacity & engineering properties of the soil.

As increasing need of enhance the engineering properties of soils prompted designers & constructors to adapt for an effective method such as stabilization of soil using polypropylene fiber (PP). Thus, there is need for more extensive study in this direction to establish precise design procedures for polypropylene (PP) reinforced fiber in the stabilization of soil. More research can be done on using Genetic Programming (GP) which will result in better understanding and accuracy in the reinforcing soil tests and the most advantageous use of them in geotechnical engineering.

#### REFERENCES

- Zhang, X.J., Zhou, K.J. & Zhou, J.X. (1998) "Experimental study on dynamic properties of cohesive soil reinforced with fibres." Chinese Journal of Geotechnical Engineering, Vol. 20(3), pp 45-49.
- Yetimoglu, T., Inanir, M., Inanir, O.E. (2005) "A study on bearing capacity of randomly distributed fiber-reinforced sand fills overlying soft clay." Geotextiles and Geomembranes 23 (2), 174–183.
- A. Naeini and S. M. Sadjadi (2008) "Effect of Waste Polymer Materials on Shear Strength of Unsaturated Clays", EJGE Bund k, (1-12).
- Sabat, A. K., Nanda, R. P. (2011) "Effect of marble dust on strength and durability of Rice husk ash stabilized expansive soil." International Journal of Civil and Structural Engineering, Volume 1, No 4, pp. 939 948.
- Alavi and Gandomi (2011) "Genetic programming based approach for performance characteristics assessment of stabilized soil, Chemical stabilization, simulated annealing, nonlinear modelling."
- Trivedi, Nair and Iyyunni (2013) "Optimum genetic algorithm, fly ash, soil stabilization." 3<sup>rd</sup> Nirma University International Conference. In: ELSEVIER 51, 250 - 258.
- Vardhan, Jha, Bordoloi, Garg (2015) "Factor of change in strength, unconfined compressive strength, reinforced soil, polypropylene fiber, Genetic programming." 50<sup>th</sup> Indian Geotechnical conference.
- Nangia, Nigam, Tiwari (2015) "Shear, Fiber, Random, Polypropylene, Distribution, Strain, Compression, characteristics strength of the soils along Yamuna River Bank." International Journal of Engineering and Technical Research (IJETR).ISSN:2321-0869.
- Teja (2016) "Direct shear test, unconfined compression test, polypropylene fiber, fiber reinforcement, Soil stabilization using polypropylene fiber materials." International Journal of Innovation Research in Science Engineering and Technology (IJIRSET). Vol.5, issue9. ISO 3297: 2007.
- Soleimani, Rajaei, Jiao (2017) "New prediction models for unconfined compressive strength of geo polymer stabilized soil using multi-gen genetic programming." In: ELSEVIER (2018) 99-107.
- Balagoudr, Krishna, yaligar, Shwetha .G.C. (2017) "Soil stabilization, fibers, lime, raft foundation, Stabilization of Black Cotton soil using Lime." International Journal of Engineering Science and Computing (IJESC) Vol.7 Issue No.5.
- M. Hinchliffe, H. Hiden, B. McKay, M. Willis, M. Tham, G. Barton, J.R. Koza (1996) "Modelling chemical process systems using a multi-gene," Late Breaking Papers at the Genetic Programming, pp.56-65.



## LOAD ECCENTRICITY EFFECTS ON BEHAVIOUR OF CIRCULAR FOOTING RESTING ON GEOGRID REINFORCED SAND –A REVIEW

*Sachin Dahiya<sup>1</sup>, Anupam Mital<sup>2</sup>*

<sup>1</sup>M.Tech scholar, Department of Civil Engineering, NIT Kurukshetra, Haryana

<sup>2</sup>Professor, Department of Civil Engineering, NIT Kurukshetra, Haryana, Corresponding Author

### ABSTRACT

The study was undertaken to investigate the effect of load eccentricity on the behavior of steel circular model footing resting on a geogrid reinforced sand bed. The study highlights the effect of number of reinforcement layers and various load eccentricity on the load settlement response and bearing capacity of the footing. There appear to be an optimum reinforcement spacing for multilayer reinforced sand. It was observed that when the reinforcement is placed in the optimum embedment spacing, the bearing capacity increases with load eccentricity within the core area of footing and it decreases outside core area. Study shows that the ultimate bearing capacity increases in comparison to unreinforced condition if the reinforcement layers were placed within a range of effective depths and the inclusion of soil reinforcement leads to significant reduction in the depth of sand layer and increase in bearing capacity of eccentrically loaded circular footing, leading to the cost effective design of the footing.

**Keywords:** Circular footings; Reinforced sand; Bearing capacity; Eccentric load; Geogrid sheets.

### INTRODUCTION

In civil engineering, the substructure like foundation is used to transfer the load of the structure safely to the soil lying below. It is also subjected to earthquake and wind load in addition to the normal loads. Designers always try to keep the load as symmetric or centric on the foundation because eccentricity of the loading results in the generation of the moment on the foundation which decreases the area of footing effective in resisting the stresses. Therefore eccentricity should be considered carefully during design only. Footing moves away from soil due to increase in the eccentricity because of the generation of the tension. Bearing capacity and the settlement of foundation are the two important parameters regarding the design of foundation. Both the parameters should be considered carefully for the safe design or safety of a structure.

Now due to eccentricity of loading, tensile stresses are generated in granular soil below along with footing. But as granular soil is weak in tension, therefore to improve its tensile properties it is reinforced with various types of reinforcement (Fig 1):

- (a) Strip
- (b) Bar
- (c) Sheet
- (d) Grid

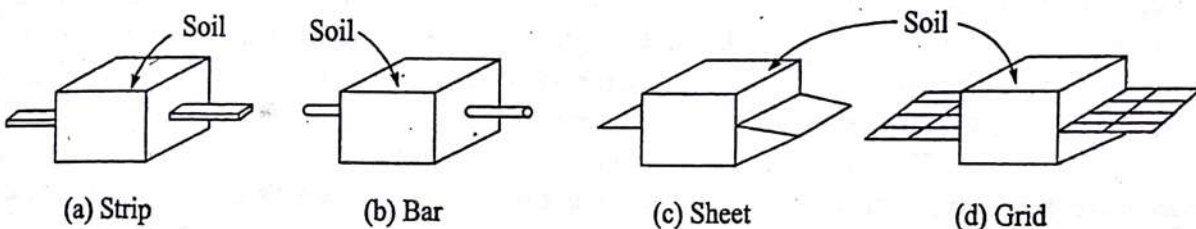


Fig.1. Types of reinforcement

The working principle of reinforced soil mass is that when the soil mass in unstable zone tries to move, it tries to pull out reinforcement along with it. However, the movement of the reinforcement is prevented by the soil of the stable zone. This ensures that the soil in the failure zone is unable to move since it cannot slip past the reinforcement. Hence the entire soil in which reinforcement is provided remains stable and its strength improves, see Fig. 2.

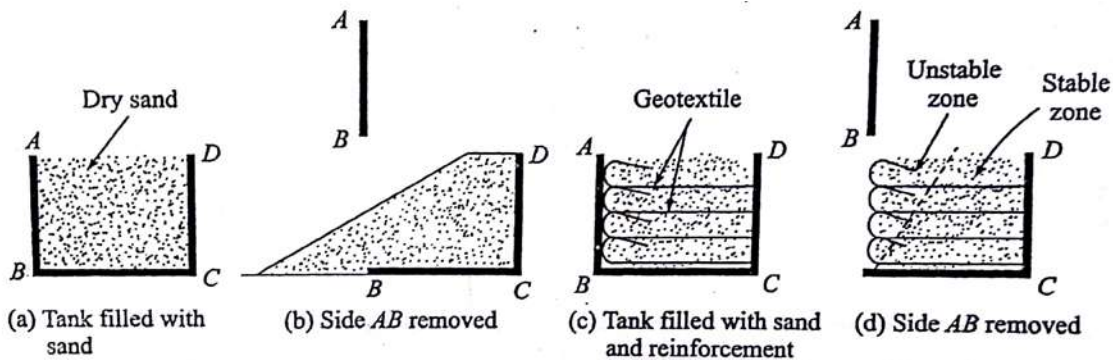


Fig.2.Mechanism of reinforcement in soil mass

Due to good interlocking and tensile properties of Geogrid reinforcement with the granular soil it has been used in present study to improve the strength of sand. Providing the geogrid in the foundation generally have following benefits, (a) reduction in the cost of construction material (b) serviceability of the developed model is greater when compared with unreinforced section (c) reduction of shear stress due to increase in the angle of internal friction as a result of provision of geogrid in the soil. Therefore to improve the tensile characteristics of the granular soil we provide geogrid as reinforcement.

The present study focuses on the effect of different parameters of geogrid layers, such as the depth of first and second layers of reinforcement, number of reinforcement layers, effect of relative density of soil and also the effect of load eccentricity on the bearing capacity and settlement of the circular footing resting on sand bed.

#### LITERATURE REVIEW

**Badakhshan and Noorzad (2015):** studied the effect of load eccentricity on the circular footing resting on the sand provided with geogrid layers as reinforcement. The study was carried out on poorly graded sand with relative density 60% reinforced with geogrid CE121 having oval shaped aperture and tensile strength of 7.68 KN/m. The model circular footing made up of steel plates having 120 mm diameter ( $D$ ) was taken for the study. The loading was applied within the core area of the footing i.e. within the distance of one-fourth of the radius of footing. They found that the depth ratio ( $u/D$ ) 0.42 (where  $u$  is the depth of 1<sup>st</sup> layer of reinforcement from the base of footing) gives the highest bearing capacity ratio (BCR) at all load eccentricities. For the 2<sup>nd</sup> layer of reinforcement, depth ratio ( $h/D$ ) 0.42 (where  $h$  is the spacing between the geogrid layers) gives the maximum BCR. BCR in case of centric loading condition increases by increasing number of layers ( $N$ ) of geogrid upto 4 in number but in case of eccentric loading conditions the corresponding number of layers were 3. Results show that the BCR decreases by increasing the load eccentricity in both reinforced and unreinforced condition. The settlement was also decreased by increasing the number of geogrid layers and it was maximum in case of one geogrid layer. Effect of few parameters like density of soil, depth of embedment of footing, scale effect has not been taken into account in this study and the results were limited to poorly graded sand.

**Sawwaf and Nazir (2012):** studied the effect of load eccentricity on the small-scale ring footings resting on reinforced soil layer. Medium to coarse sand reinforced with biaxial geogrid layer having rectangular aperture and tensile strength of 30.7 KN/m was taken for carrying out the research. The model footing used in the study was made up of mild steel having outer diameter ( $D$ ) of 120 mm and various internal diameters. The test series was conducted by replacing the soil by dense sand. The BCR increases with the increase in the depth ( $d$ ) of replaced sand upto a value of  $d/D=1.5$ . Optimum number of layers of reinforcement for the increase in BCR with the increase in number of layers ( $N$ ) were 3 along with replaced sand after that BCR becomes constant. BCR increases with eccentricity ( $e$ ) upto a ratio of  $e/D=0.15$ , after which the effect of eccentricity is not so great and bearing capacity also increases with increase in relative density. They also studied that the bearing capacity was increased in case of stiff geogrid as compare to the flexible one. This study was limited only for one type of geogrid, sand and ring footing of one outer diameter, see Fig. 3

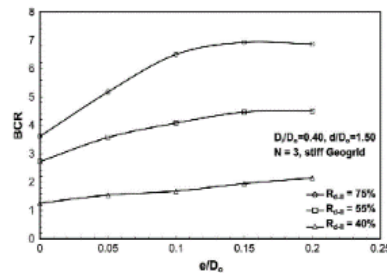


**Fig.3. Variation of BCR vs Eccentricity**

**Basudhar, Saha and Deb(2007):** conducted the study on circular footings resting on geotextile reinforced sand bed. Dry Ganga sand with specific gravity 2.68 and various relative density of 45%, 73% and 84% reinforced with geotextile (having 0.48 mm thickness and bursting strength of 2000 KPa) was taken for carrying out the study. Model circular footings having diameter of 30, 45 and 60 mm were used. At the same settlement with the increase in relative density of sand, bearing capacity of footing increases. As the number of reinforcement layer increases bearing capacity also increases. For the same reinforced conditions with the increase in the size of footing BCR decreases and laterly it becomes constant. The numerical prediction of the settlement of the footing was done using fast lagrangian analysis of continua (FLAC) and a error of 16% in the value of settlement was observed, see Fig. 4.

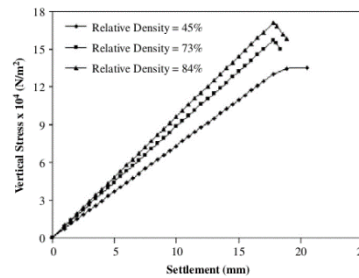


**Fig.4. Variation of Vertical Stress vs Settlement**

**Boushehrian and Hataf(2003):** carried out experimental and numerical investigation of the bearing capacity of model circular footings on reinforced sand. Well graded sand with relative density of 50% reinforced with biaxial geogrid (having elastic stiffness of 28 KN/m and 5mm\*5mm size openings) was taken for carrying out the study. Model circular footing of diameter 15 cm was taken for conducting test. They found out the optimum depth of single layer of reinforcement and multilayer reinforcement for achieving the maximum BCR. The effect of number of layers of reinforcement on BCR is negligible when N=4. They also varied the elastic normal stiffness of reinforcement and results shows that by electing the more rigid reinforcement does not always lead to favourable results in terms of BCR. The numerical analysis of the same footing and soil was carried out by using PLAXIS software and there was variations in the results as compare to experimental study, see Figs. 5-7

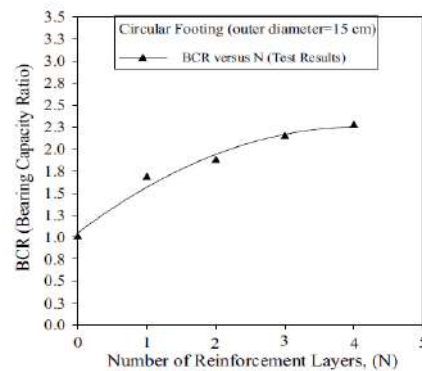


**Fig.5. Variation of BCR vs Number of Reinforcement Layers**

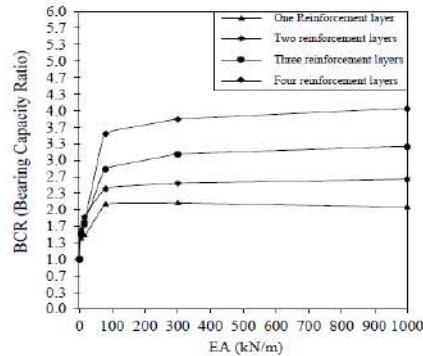


Fig.6.Variation of BCR vs Effective Stiffness of Reinforcement Layers

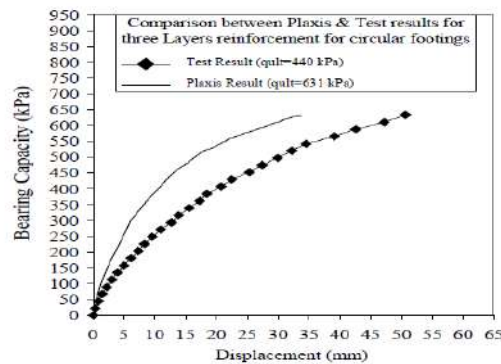


Fig.7.Variation of Bearing Capacity vs Displacement

Yetimoglu, Jonathan and Saglamer(1994):studied the bearing capacity of rectangular footing resting on geogrid reinforced sand. The sand used in the test was oven dried uniform quartz sand having a relative density of 70 to 73% and it was reinforced with uniaxial geogrid GS1000 made by using polypropylene. The size of rectangular footing used was  $B=101.5$  mm and  $L=127$  mm. Finite element analysis was carried out using a computer program, DACSAR( deformation analysis considering stress anisotropy and reorientation).The depth ratio of 0.3 in case of single layer reinforcement was found to be optimum by the both test and analysis. The corresponding ratio was 0.25 in case of multilayer reinforcement. Optimum vertical spacing was around  $0.2B$  and the value of BCR calculated by test is slightly different from that obtained by software. The results indicated by the test and analysis shows that the bearing capacity ratio increases with a proportional rate with the number of reinforcement layers upto  $N=4$ . But the values of BCR were in a good agreement for  $N=1-4$ . By increasing the size of reinforcement there was a slight increase in the BCR as shown by the both test and analysis. The study of effect of reinforcement stiffness on the BCR was done on finite element only and the result shows that by increasing the effective stiffness the BCR of a footing increases, see Fig. 8

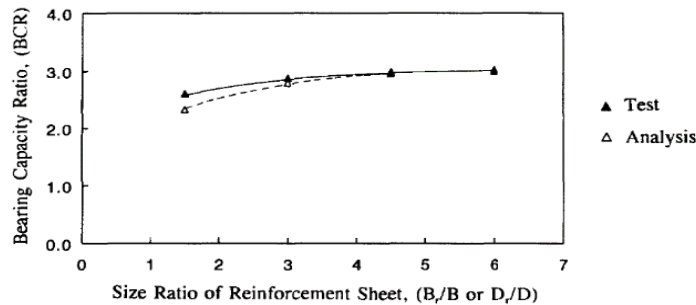


Fig.8.Variation of BCR vs Size of Reinforcement

**Sitharam et al. (2005):** carried out number of tests on embedded circular footing resting on geogrid cell reinforced foundation bed. The embedment depth of the footing was varied from 0 to 0.6D over foundation beds of dry sand and saturated silty clay. The load-Settlement curve of the embedded circular footing resting on on cellular reinforced beds is almost linear up to a settlement range of 12– 15% of the footing width in sand bed and about 8–10 % in clay bed. The load carrying capacity of the reinforced sand beds increased by 9.5 times with increase in the embedment depth of foundation and about 6.5 times in the surface case. In case of reinforced soft clay beds, bearing capacity increased against the unreinforced bed, and it increased up to 5.5 with the footing embedment depth. In sand, it could be said that at allowable settlement range of isolated footings, the footing embedment depth equal to 0.3D gives optimal performance.

**Chakraborty and Kumar (2014):** Studied the Bearing capacity of circular foundation reinforced with geogrid sheets. The test were carried out on a rigid footing centrally loaded. Horizontal circular reinforcement was used for reinforcing the soil mass. The reinforcement was assumed to have no resistance against bending. The study does not take into account the stiffness parameters of the soil and reinforcement. It was based on the shear strength parameters of soil and soil reinforcement interface. The diameter of the reinforcement was found to increase with an increase in the value of friction angle. The optimum value of friction angle was found to be between 30 degree and 45 degree for achieving optimum diameter of reinforcement sheets and good strength. The analysis clearly reveals that the inclusion of the reinforcement causes significant increase in bearing capacity especially when the soil medium is reinforced with two layers of the reinforcement sheets. There is a critical depth of reinforcement for which bearing capacity factors of soil achieves maximum value and bearing capacity of soil improves.

**Lovisa et al. (2010) :** They studied the behaviour of loaded circular footing resting on the prestressed geotextile reinforced sand bed. Results shown by them indicates that the effect of the prestressed geotextile is evident at greater depths of footing in comparison to the counterparts i.e. reinforced and unreinforced sand beds. The effect of load eccentricity was not considered in this case. The case was limited for centric loading conditions only.

**Sawwaf(2009):** studied the effect of load eccentricity on the strip footing resting on geogrid reinforced sand . The test were conducted and the results indicated that the effect of reinforcement on BCR is greater at lower value of eccentricity and high value of relative densities. The optimum depth ratios indicated by the test were  $u/B=0.33$  and  $h/B=0.5$  for achieving the maximum BCR.

**Patra et al. (2006):** studied the effect of load effect of load eccentricity on the strip footing resting on geogrid reinforced sand bed. They derived an empirical relationships from model loading tests and reported that the ultimate bearing capacity achieved in case of reinforced sand is greater as compare to unreinforced conditions. This effect becomes much lower with increasing load eccentricity. Results indicates that the optimum value of  $u/B$  is 0.35-0.45 for the first layer of geogrid depending on the load eccentricity value. They also shows that the rigid reinforcement not always leads to a better effect on bearing capacity.

## CONCLUSIONS

The effect of load eccentricity and the number of layers of geogrid on the various parameters of circular footing was studied by researchers based on a series of tests. Different values of eccentricity were considered to understand the changes in the bearing capacity and settlement of the circular footing with respect to number of layers of geogrid reinforcement. The following conclusions were drawn from this study:

- (1) The maximum value of bearing capacity for circular footing resting on reinforced sand was achieved at optimum values of single layer reinforcement and multilayer reinforcement for both centric and eccentric loading conditions.
- (2) For eccentrically loaded circular footing, BCR increases upto four layers of reinforcement in case of centric loading and it increases upto three layers of reinforcement in case of eccentric loading and fourth layer has a reducing effect.
- (3) With the increase in the settlement of the footing BCR ratio keeps on decreasing in both reinforced and unreinforced conditions.
- (4) With the increase in number of geogrid layers, the settlement was maximum initially upto one layer and then decreases afterwards.

- (5) With the increase in the effective stiffness of reinforcement, BCR increases but few research shows that taking rigid reinforcement into consideration does not always lead to better results.
- (6) With the increase in the relative density of the soil BCR increases and settlement decreases.
- (7) By replacing the loose soil with dense soil and further providing geogrid reinforcement in replaced part gave good results of increased BCR and decreased settlement.
- (8) Size of reinforcement has also effect on the BCR of footing, with the increase in the size of the footing BCR increases.
- (9) When different reinforcement were compared, geogrid was found to be the most effective one in increasing the BCR and decreasing Settlement of footing.
- (10) There was always a difference between the results of experiment study and finite element analysis. A marginal error was observed in BCR value.

By studying the effect of load eccentricity on the circular footing we can derive a relation between BCR in eccentric loading and BCR in centric loading conditions. By this we have to work on centric loading only and we can derive the eccentric BCR by the derived relationship which will save our lot of time in designing part.

## REFERENCES

- Basudhar PK, Saha S, Deb K. (2007) "Circular footings resting on geotextile-reinforced sand bed." *Geotextiles and Geomembranes*; 25 (6):377-84.
- Boushehrian J, Hataf N. (2003) "Experimental and numerical investigation of the bearing capacity of model circular and ring footing on reinforced sand." *Geotextiles and Geomembranes*; 21 (4):241-56.
- Sawwaf ME, Nazir A. (2012) "Behavior of eccentrically loaded small-scale ring footings resting on reinforced layered soil." *Journal of Geotechnical and Geo-environmental Engineering*; 138 (3):376-84.
- Yetimuglu T, Wu JTH, Saglamar A. (1994) "Bearing capacity of rectangular footings on geogrid-reinforced sand." *Journal of Geotechnical Engineering, ASCE*; 120 (12):2083-99.
- Sitharam TG, Sireesh S. (2004) "Model studies of embedded circular footing on geogrid-reinforced sand beds." *Ground Improvement*; 8 (2):69-75.
- Alawaji HA. (2001) "Settlement and bearing capacity of geogrid-reinforced sand over collapsible soil." *Geotextiles and Geomembranes*; 19 (2):75-88.
- Dhillon GS. (1961) "Settlement, tilt and bearing capacity of footings under central and eccentric loads." *Journal of the National Building Organisation*; 6 (2):66-78.
- Eastwood W. (1995) "The bearing capacity of eccentrically loaded foundations on sandy soil." *Structural Engineer*; 33(6):181-7.
- Badakhshan E, Noorzad A. (2015) "Load eccentric effects on behaviour of circular footings reinforced with geogrid sheets." *Journal of Rock Mechanics and Geotechnical Engineering* 7691-699.
- Moghaddas Tafreshi SN, Dawson AR. (2010) "Comparison of bearing capacity of a strip footing on sand with geocell and with planar forms of geotextile reinforcement." *Geotextiles and Geomembranes*; 28(1):72e84.
- Prakash S, Saran S. (1971) "Bearing capacity of eccentrically loaded footings." *Journal of the Soil Mechanics and Foundations Division, ASCE*; 97(1):95e103.
- Al-Tirkity J, Al-Taay A. (2012) "Bearing capacity of eccentrically loaded strip footing on geogrid reinforced sand." *Journal of Engineering Sciences*; 19(1):14e22

## A REVIEW PAPER ON THE IMPACT ON SOIL AND WATER QUALITY IN VICINITY OF LANDFILL SITE AREA

*Shubham K Tiwari<sup>1</sup>, Surinder Deswal<sup>2</sup>*

<sup>1</sup>M.Tech scholar, Department of Civil Engineering, NIT Kurukshetra, Haryana, India 136119  
Email: tiwari729374@gmail.com

<sup>2</sup>Professor, Department of Civil Engineering, NIT Kurukshetra, Haryana, India 136119  
Email: deswal.leo@gmail.com, Corresponding Author

### ABSTRACT

The generation of municipal solid waste (MSW) in India is close around 115000 Ton/day. The disposal of MSW into landfill has been perceived as the real wellspring of soil, surface and groundwater contamination. The greater part of the disposal site in India flooding because of unpredictable dumping of solid waste. The leachate delivered via landfill site contains a lot of high concentration of organic and inorganic constituents beyond admissible points of confinement which additionally changes the nature of soil and water (surface and ground water) in the region of landfill site. This paper aims to review work done on study of soil and water contamination close to the landfill site region. The impact of separation on soil source from landfill site, contamination level of soil and impact with passage of time on soil quality additionally checked on.

**KEYWORDS:** Leachate; Landfilling; Municipal solid waste; soil contamination; water contamination.

### INTRODUCTION

SWM is such a field where India needs to do lot of work either through law enforcement or public awareness because India feed almost 1.21 billion populations which is around 18% of world's population. Although there is lot of method for SWM sites are: "incineration, landfilling and composting" but these methods are still harming environment up to certain extent and not reducing its effect at all. So there is need of hour to change the approach the disposal-based towards the reduction/recovery-based of waste management. Although landfilling is one of the inexpensive and commonly used method in India and various parts of world for MSW. This practice of solid waste landfilling is not only occupying the large and expensive properties nearby the built up area but also make worsen the quality of soil and water around its vicinity. The open dumps are unpleasant, dull, messy, unhygienic, polluted and generally stinky. Every single city in India has one or two MSW landfill site. The problem of landfills is worsening in metropolitan cities because of high rate of waste generation and higher population density. These waste are disposed off on landfill sites without proper processing and segregation so its poses large quantity of valued things in it. A review on previous literature shows that landfills are a fundamental piece of compelling waste management methodology which takes waste which can't be further processed. It is an effective method to reduce biodegradable waste up to certain extent if operated in engineered way but if don't take engineered consideration while operating can be turn disastrous for water and soil quality nearby its radial distances and make unacceptable changes in their quality. Municipal committees must get ready for future landfill needs by figuring full proof long term plan and allocating landfill land which causes minimum effect in its vicinity and prove to be sustainable operating process. Not properly handled waste create nuisance like leachate produced from landfill seep through waste and affect the soil and water ( surface and ground water ) which directly affect ground water supply. This chemical infiltration additionally prompts a loss in composted soil, rendering the ground unfertile for significant lots of time. Many researchers have been investigated the vicinity of landfill sites situated in different parts of country to study the impact of landfill leachate on soil and groundwater. Here this review paper is trying to figure out various conclusions about the sanitary landfill and its adjoining areas which is not fully engineered operated and causing so many causalities in both physically and chemically. The basic significance of this review paper is taking the consideration of open dumping, various environmental impacts due to landfill sites and the leachate produced from it, to discuss the intensity of contamination around various landfill sites.

### LITERATURE REVIEW

**Ei-Fadel et al. (1997)**, presented an overview on the gasses and leachate produced from landfill site and try to fix them by developing mechanism and author also try to show their environmental consequences . Author also showed the way to eradicate or minimize these effects or consequences and also depiction of control. In maximum cases, installation of collection as well as treatment and reclamation of venting gasses from landfill can help in preventing the gas movement from different critical point of landfill. In this paper author suggested various methods can be employed for collection

and extraction of gasses like extraction and relief wells, trenches and gradient control wells.

**Mufeed Sharholly et al. (2007)**, made an attempt to review the scenario of generation, segregation and transportation mechanism as well as disposal along with treatment feasibility of MSW in India. Author's study tries to relate municipal solid waste management (MSWM) status in present as well in future and to point out various complications. Various attempts have been made to critically review the waste management process and status of their execution. Author also concluded how the situation of infrastructures, process of planning and lack of funding with inappropriate data collection affecting the solid waste management in Indian cities. Municipalities are not well equipped and advanced to tackle the problem related to MSWM.

**A.Tripathi et al. (2012)**, the examination evaluates the characteristics of contaminated soils of three municipal dumpsite of Allahabad city, Uttar Pradesh. The pH of the dumpsite soils extended from  $6.42 \pm 0.46$  to  $7.16 \pm 0.81$  which is moving to neutral or alkaline ph. Water retaining capacity and moisture content at landfill were in great sums ( $30.43 \pm 1.33$  to  $48.58 \pm 1.19$  and  $35.53 \pm 1.79$  to  $50.77 \pm 1.32$  % separately). Landfill had higher organic matter ( $1.60 \pm 0.39$  to  $2.55 \pm 0.48$ %) when contrasted with their abutting territories. Clay texture assumed a noteworthy job in separating ordinary soils of abutting territory than landfill soils. The concentration of total metal Cr, Cu, Fe, Ni, Pb and Zn were likewise studied and lifted limit of heavy metals were found at landfill site ( $32.46 \pm 1.07$  to  $108.85 \pm 3.99$  mg/kg). Metal contamination at landfill site was in the request of  $Pb > Zn > Fe > Ni > Cu > Cr > Cd$  bestowing most elevated tainting to Daraganj dumpsite while Phaphamau dumpsite was slightest debased. Cr and Cd were not discernible from all abutting zones while Pb, Zn, Fe, Ni and Cu were available in minimum sums ( $7.32 \pm 0.30$  to  $37.94 \pm 4.22$  mg/kg). Physio-chemical characteristics and heavy metal fixations at every dumpsite were additionally corresponded with one another and numerous critical relationships were watched. Concentration of Zn were very corresponded with the groupings of Cu, Ni and Pb ( $r = -0.66$  to  $0.86$ ,  $p < 0.05$ ). Concentration of Cr were additionally essentially related with Ni and Pb ( $r = -0.62$ ,  $-0.69$ ,  $p < 0.05$ ). The examination clearly shows that the limit of heavy metal contamination is greater at dumpsites which might be a reason for worry for their encompassing condition and life forms. This study will demonstrate significant in giving gauge data to additionally soil quality checking ponders in study zone.

**Tapan Narayan (2009)**, in this paper author learned that main fault that led to the ineffective established of treatment plants was the deficiency of the application i.e., of modest scientific techniques to select the matter to be composted. Due to absurd Indian scenario landfills also becomes ineffective because landfills are operated in time restricted frame which lacking India. Various Indian landfill sites are operated beyond their saturation period which leads to various adversaries and affects the nearby population and topography in various ways. Although India is developing country which faces rapid urbanization with disturbing features with very less waste management strategies which adversely affect the functioning of landfill sites. Due to rapid increment in population quantity of waste also increases and finally leads to depletion of landfill sites. Here in this paper found that public participation plays a major role in dealing with municipal solid waste management (MSWM) and in Indian scenario public awareness and participation is missing which is causing huge problem which need to address soon to achieve objective of waste management. So there is need of public participation that should be made attractive.

**Aderemi Adeolu et al. (2011)**, has conducted extensive experiment to analyze physio-chemical and microbial constraints of leachate produced from landfill and as well as on soil samples. He accessed various samples from site and its various radial distances by marking most contaminated zones and to assess the penetration of leachate in ground water quality. Various parameters like as TDS, EC, and  $Na^+$  beyond the WHO acceptance limits in drinking water for 62.50, 100, and 38.05 percent of groundwater test, respectively pH as well as Fe beyond WHO limit in 75 percent of water test obtained from various points. "In appreciable negative relationship of  $-0.80$ ,  $-0.59$ , and  $-0.59$  were shown by  $Na^+$ , TDS, and EC respectively distance from the dumpsite. The outcome from analysis found that the leachate produced from the site had a trifling effect on groundwater aquifers which can be accredited to the prevailing soil stratigraphy at the landfill site and containing of clay which had derived to have an important on the natural decrement of landfill leachate into groundwater.

**Bhalla et al. (2014)**, investigated the properties of landfill leachate produced from MSW landfill site situated in Ludhiana, Punjab (India) which is operated in non-engineered way. Obviously this dump site is low laying dump type. Leachate test are obtained from the periphery of site and examined for various parameters that include physio-chemical parameters to check out the changes happened in water quality and found that leachate samples had been contaminated with lifted concentration of organic and inorganic constituents beyond their acceptable limit. It was found that concentration of heavy metal was very trace because of domestic nature of MSW. In this study he also carried out effect of leachate percolation on soil quality i.e. its changes in engineering properties. Author also compared the effect of

seasonal variation on soil quality and contamination level of soil. The time span of variation is around six months which clearly shows contamination level increase with time of various parameters like pH, organic carbon, Nitrate, Total Phosphorous and Phosphate. Author suggests the remedial measures to control contamination level is public awareness on waste sorting, adoption of clean technology, serious steps from concerned authorities and employment of sound engineered techniques while operating landfill sites.

**Loveleen Gupta et al. (2014)**, an experimental study is conducted for knowing the characteristics of leachate from dumpsite and groundwater in the nearby of sanitary landfill Narela- Bawana (New Delhi, India). Leachate and ground water test are collected in the vicinity of landfill site. The study of physio- chemical parameter of water sample reported that high contamination of water sample consisting heavy metals like Cr, Cu, Fe, Cd, Ni, and Zn. She also studied the likely contamination of hazardous substances in ground water samples because of discharging of such contaminant over the large period of time with leachate. Results for various compared with the acceptable limit of BIS, WHO standards under normal circumstances there should be no variation in the concentration of the constituents of water. Analysis concluded that landfill site contribute significant amount of leachate which contains higher concentration of heavy metals and other cations. The concentration of heavy metals and cations more than the suggested furthest reaches of BIS and WHO. The distributions of cations and metals are spatial which possess serious threat for ground water in the vicinity of site, concentration of contaminant decreases as distant from landfill site.

**Naveen et al. (2013)**, performed experimental study which was aimed to determine the characteristics of the leachate test from a landfill site in Mavallipura, near Bangalore. The experiments were carried out by standard procedure and pollutants present in leachate is characterized into four groups i.e., dissolved organic matter, inorganic macro components, heavy metals and organic compounds. The pH measured from procedure comes out which is 7.4, directly shows the little alkaline nature in the landfill site. Experiment findings showed presence of various metal but highest in concentration was iron which is 11.16 ppm. BOD<sub>5</sub> as well as COD of the dumpsite were 1500 mg/l and 10400 mg/l, respectively

**Manju Rawat Ranjan et al. (2014)**, conducted the field study to estimate methane as well as nitrous oxide discharge from landfill site situated in Ghazipur and the array of methane gas emission flux was 18 mg/m<sup>2</sup>/h which was very low in winter samples and highest 265 mg/m<sup>2</sup>/h in summer samples. The span of nitrous oxide gas emission was estimated between 265 – 1728 mg/m<sup>2</sup>/h and although extraction rate as well as calorific value of gaseous discharge is so great that it can be used in electricity production. Then, there was also estimated that waste from landfill site contributed roughly 5 percent to greenhouse gases (GHG) discharge which suggest that there is need of hour to start reduction of GHG emission from landfill site because GHG responsible for global warming. Although due to haphazard urbanization, open land in Indian cities has been shrinking which is creating problem in allocation of fresh land for dumping site that's why mining of precious resources from saturated or old operational landfill sites must be one of the step to recycle MSW and also reduction of GHG discharge. In his study, he has forced for the utilization and confinement of GHG from Ghazipur landfill site. Regarding this, various agencies from New Delhi has come out for the excavation as well as processing of resources. Which can be used for making RDF i.e., green electricity, and the collected CH<sub>4</sub> as biofuel.

**B.S Badmus et al. (2014)**, Geochemical impact assessment of groundwater test from hand-burrowed dug holes inside the region of Aba-Eku landfill was done for residential and agricultural purposes. Ten groundwater test were obtained both in dry season and wet season for examination of physio-chemical parameters: pH, EC, TDS, Na<sup>+</sup>, K<sup>+</sup>, Ca<sup>2+</sup>, Mg<sup>2+</sup>, HCO<sub>3</sub><sup>-</sup>, CO<sub>3</sub><sup>2-</sup>, Cl<sup>-</sup>, SO<sub>4</sub><sup>2-</sup> and NO<sub>3</sub><sup>-</sup>. The aftereffects of demonstrated the test groundwater tests to be in the given permissible limit of WHO/NSDWQ. In any case, lifted values of concentrations of the chemical constituents were seen in well 5 meter closer to the landfill. Translation of Piper diagram demonstrated CaHCO<sub>3</sub> to be prevailing in the region. Alkaline earth metals (Ca<sup>2+</sup>, Mg<sup>2+</sup>) and weak acids (HCO<sub>3</sub><sup>-</sup>, CO<sub>3</sub><sup>2-</sup>) are predominant cations and anions over the alkaline and strong acids in the both seasons. Groundwater in the investigation zone is of hard, fresh, and alkaline in nature. Determination for agriculture demonstrated that the vast majority of the water test was appropriate for water system reason aside from in a couple of areas.

**Sruti Pillai et al. (2014)**, The Municipal Solid Waste transfer site for the city of Thrissur, in Kerala, India, has transformed into an over flooding landfill in perspective of the eccentric dumping of solid waste at the site. Gas and leachate production are unavoidable outcomes of routine with regards to solid waste transfer in landfills. The migration of gas and leachate far from the landfill present genuine environmental concerns which incorporate, and are not restricted to, flames and blasts, vegetation damages, unpleasant odor, landfill settlement, ground water contamination, soil contamination and an unnatural weather change. Leachate and soil test were collected from this dumpsite and its adjoining territory to examine the likely effect of leachate percolation on soil characteristics. Concentration of different physio-chemical characteristics and engineering properties were examined in soil test. The examination of

Conductivity and compaction characteristics of soil was also done. The examination showed that leachate can change the properties of soil. The results of study showed that leachate can alter the property of soil. The physio-chemical and geo-engineering properties of soil were taken into under consideration by treating the soil with synthetic leachate There is decrement in the property of soil which directly indicate the chemical interaction aspect of leachate and soil.

**Sayeed Shakeel Afsar et al. ( 2015)**, carried out a study which related with various chemical aspects of leachate concentration of heavy metals and pH; TDS; TS. Test samples are collected from three landfill sites Bhalswa, Ghazipur and Okhla and various parameters like electrical conductivity, Total sulfate and Total chlorides were found out. The findings of the experiment showed that Bhalswa landfill site is most contaminated with leachate highest having concentration of various parameters like total dissolved solid, total solid and electrical conductivity having numerical values i.e. 9637 mg/l, 10071 mg/l and 14631 mho/cm res respectively. The outcome from the experiment will be helpful to determine the impact on groundwater due to seeping of leachate through soil strata.

**Shubham S. Hilwale et al. (2017)**, The produced quantity of municipal solid waste (MSW) in India is close around 115000 Ton/day. Municipal solid waste (MSW) and its management is greatest challenge which on looking by the administrator, engineer and planner. Management of MSW incorporates different steps, for example, collection, transportation and deposition, treatment and disposal yet the impact which is MSW on different elements won't end with its disposal. This paper center around the product come after the landfill of MSW i.e. leachate it is the viscous fluid which is drawn out from landfill MSW which is most continuous part of MSW. The management of leachate properties and its effect on different factor is additionally been concentrated in this paper.

**Jhamnani and Singh (2009)**, Testing and investigation of leachate from Bhalaswa landfill and groundwater tests from adjoining regions, likely demonstrated the tainting of groundwater due to landfill leachate. The consequences of recreation of Chloride from landfill exhibits that the reproduction results are in consonance with the watched grouping of Chloride in the district of landfill site. The strong waste transfer structure eventually being penetrated in Delhi contains unimportant dumping of misuses made, at three territories Bhalaswa, Ghazipur, and Okhla with no regard to authentic thought for the protection of enveloping condition. Bhalaswa landfill site in Delhi, or, as it were as a dump site, is depended upon to wind up explanation behind bona fide groundwater tainting in its area. The leachate from Bhalaswa landfill was seen to have a high grouping of chlorides, and furthermore DOC, COD. The present examination was endeavored to choose the conceivable grouping of standard contaminants in the groundwater over some stretch of time due to the arrival of such contaminants from landfill leachates to the groundwater. The watched convergence of chlorides in the groundwater inside 75m of landfill of site was seen to be in consonance with the reenacted grouping of chloride in groundwater considering one dimensional transport appear, with restricted mass of contaminant source. Administering condition of contaminant transport including shift in weather conditions and dissemination scattering was explained in matlab7.0 utilizing limited distinction technique.

## CONCLUSION

This paper reviews the impact on the soil and water quality in the vicinity of landfill site area. Paper also reviews the environmental consequences due to absurd operation of landfill site and what corrective measure can be considered to reduce these effects. Major conclusion can be made from above studies are-

- Leachate contains organic and inorganic constituents along with heavy metals which are completely depend on the composition of solid waste.
- The contamination in the vicinity of landfill site area increases with the passage of time, reason being with time the solid waste material gets degraded and the waste constituents percolate down along with rainwater thus polluting soil and groundwater.
- The studies are valuable in giving pointers contaminant at such open dumpsites and in this way will be useful in making any remediation arrangement for contaminated soils.
- In this way the open dumping of waste ought to be debilitated and an appropriate checking and remediation plan is expected to diminish the chances of ground water contamination by filtering of these contaminants.
- Since India is developing nation and have huge assets of systems and offices yet because of absence of mindfulness, political issues, absence of consideration toward the obligations which allot to the govt. officers, and so on are a portion of the obstacles because of which India can't adapt up in waste administration when contrasted with different nations.

## REFERENCES

- El-Fadel, M., Findikakis, A. N., & Leckie, J. O. (1997). "Modeling leachate generation and transport in solid waste landfills." *Environmental technology*, 18(7), 669-686.
- Sharholly, M., Ahmad, K., Vaishya, R. C., & Gupta, R. D. (2007). "Municipal solid waste characteristics and management in Allahabad, India." *Waste management*, 27(4), 490-496.
- Tripathi, A., & Misra, D. R. (2012). "A study of physico-chemical properties and heavy metals in contaminated soils of municipal waste dumpsites at Allahabad, India." *International Journal of Environmental Sciences*, 2(4), 2031-2040.
- Narayana, T. (2009). "Municipal solid waste management in India: From waste disposal to recovery of resources?." *Waste management*, 29(3), 1163-1166.
- Aderemi, A. O., Oriaku, A. V., Adewumi, G. A., & Otitoloju, A. A. (2011). "Assessment of groundwater contamination by leachate near a municipal solid waste landfill." *African Journal of Environmental Science and Technology*, 5(11), 933-940.
- Bhalla, B., Saini, M. S., & Jha, M. K. (2014). "Assessment of Soil Contamination near Unlined Municipal SolidWaste Landfill." *International Journal of Current Engineering and Technology*, 4(4), 2678-2683.
- Gupta, L., & Rani, S. (2014). "Leachate characterization and evaluating its impact on groundwater quality in vicinity of landfill site area." *J Environ Sci Toxicol Food Technol*, 8(10), 1-7.
- Naveen, B. P., Sharma, A. K., Sivapullaiah, P. V., Sitharam, T. G., & Narayana, M. A. (2013). "CHARACTERISTICS OF THE LEACHATE FROM MSW LANDFILL, BANGALORE." *K. Sharma, PV Sivapullaiah, TG Sitharam, Ms Ashwath Narayana. Geosynthetics india.*
- Ranjan, M. R., Ramanathan, A. L., Tripathi, A., & Jha, P. K. (2014). "Landfill mining: a case study from Ghazipur landfill area of Delhi." *International Journal of Environmental Sciences*, 4(5), 919-925.
- Badmus, B. S., Ozebo, V. C., Idowu, O. A., Ganiyu, S. A., & Olurin, O. T. (2014). "Groundwater Assessment of Hand Dug Wells around Open Landfill in Ibadan Metropolis for Domestic and Irrigation Purposes." *Journal of water resource and protection*, 6(15), 1412-1424.
- Pillai, S., Peter, A. E., Sunil, B. M., & Shrihari, S. (2014). "Soil pollution near a municipal solid waste disposal site in India." In *International Conference on Biological, Civil and Environmental Engineering, (BCEE-2014) March* (Vol. 1718), 148-152.
- Afsar, S. S., Kumar, S., & Alam, P. (2015). "Characterization of Leachate At Various Landfill Site of Delhi, India." *International conference on Science, Technology and Management, Magnesium*, 250, 1078-1085.
- Hiwale, S. S., Adbane, S. T., Joshi, K. S., Khandare, V. D., & Pophalkar, P. A. (2017). "Study on the Leachate management." *International Journal of Research in Advent Technology Carbon*, 1000(20000), 5000, 288-292.
- Jhamnani, B., & Singh, S. K. (2009). "Groundwater contamination due to Bhalaswa landfill site in New Delhi." *International Journal of Civil and Environmental Engineering*, 1(3), 121-125.



## Slope Stability of Road Embankment

Vaibhav Garg\*<sup>#1</sup>, S.N. Sachdeva<sup>2</sup>

<sup>1</sup>M.Tech student, Department of Civil Engineering, National Institute of Technology Kurukshetra, Haryana-136119, India,  
e-mail:vaibhavgarg2801@gmail.com (Corresponding Author)

<sup>2</sup>Professor, Department of Civil Engineering, National Institute of Technology, Kurukshetra, Haryana-136119, India,  
e-mail:snsachdeva@nitkkr.ac.in

### ABSTRACT

Construction of highways often involves raising the level of existing ground to build a stable road sub grade. The embankment for the road is needed due to topographical requirements of the area as well as to make the road safe against any possible flooding and damage to pavement structure due to seepage from standing water by the side of the road. The embankments are constructed with different heights and side slopes. For the purpose of road transportation, an embankment of height 6.0 m and above is termed as high embankment. Guidelines for the design of high embankments are covered in IRC: 75-2015 which recommends Swedish Circle and Bishop's method among various available methods for the analysis of slope stability of road embankments. This paper presents an overview of the stability of different slopes provided for various heights of embankments with design aspects related to slope stability of typical highway embankments.

**KEYWORDS:** *Embankment; Topographical; Bishop's Method; Swedish Circle; Slope Stability.*

### INTRODUCTION

Due to human's activities or natural procedures, the variation in the rise of the surface of earth, there exist forces which are responsible to reestablish the earth to a leveled surface and this process referred as mass movement. Under the influence of gravity force the analysis of stability of slopes provides the safe designing of earthen slopes. The high road embankment stability depends on various other factors like foundation profile, fill material quality, extent of compaction, drainage arrangement both surface and sub-surface, and embankment geometry like height of embankment, slope angle, ground profile etc., external factors like traffic or earthquake load or presence of any water body by the side of the embankment or development of pore water pressure due to infiltration from heavy rain. All these parameters and conditions will make significant impact on overall stability of the embankment.

To know the most probable failure geometry from the point of view of the shape of the critical slip surface, specialists mostly use analysis of slope stability. To assess the stability of human made or natural slopes they additionally make utilization of a wide range of different analytical techniques. These failures can become disastrous and in some cases it includes the broad misfortune in monetary and in addition a social and environmental condition. For determination of most sliding surface related with minimum value of safety factor is generally performed to find out slope circular failures. In such manner, the necessary steps to calculate are the forces approaching to make failure of slope, the potential mass which is balanced by restored forces. To calculate stability of slope various methods have been adopted like limit equilibrium method, probabilistic analysis approach, rigid element method, limit analysis method and finite element method. Among this different technique, for the assessment of slope stability, the method which has turned out to be broadly utilized is limit equilibrium method and this method accounts for the forces and moments acted on an assumed critical or slip surface went through a mass of soil.

Some methods such as; Fellenius (or Swedish Slip Circle), Bishop, Morgenstem and Price, Janbu, Spencer method and many others as mentioned in IRC: 75-2015 compute factor of safety of sliding mass. For the available resisting moment along the sliding surface and deriving moment are to be easily evaluated, the different methods accounts the entire potential mass to bifurcate into a number of vertical slices. To define factor of safety in terms of stability of slope is referred as the ratio of the final shear strength divided by the maximum shear stress value at initiation of failure. The weight of the sliding mass soil, loads on surface and earthquake forces are the driving forces whereas force of internal friction and the soil cohesion at the failure surface are resisting forces. Minimum factor of safety for stability analysis is shown in Table1 as per IRC: 75-2015.

In order to identify the surface of critical slip sliding mass, diverse searching and improvement techniques have been adopted as made reference to above. They all had the trouble in using them for hand counts and these iterative procedures are tedious that is the reason the utilization of software's is usually adopted with the end goal to complete the analysis rapidly and reliably. Different software's like GEO5, SLOPE/W and FLAC/Slope software's etc. were utilized to perform the slope stability problems and decide the critical failure surface.

**Table.1: Recommended Minimum Factors of safety (FOS) For Stability Analysis**

Loading Condition	FOS under static loads	FOS under seismic loads
Static Case	1.4 (at the end of construction)	1.1
	1.2 (*initial factor of safety)	
Sudden Drawdown	1.3	1.0
Steady Seepage	1.3	1.0

\*Initial factor of safety 1.2 is applicable to situations where there is a gain in shear strength of sub soils due to ground improvement methods leading to increase in factor of safety with time. In such cases it is important that construction is continuously monitored for changes in pore water pressures, progress of settlements and occurrence of lateral deformations.

### IMPORTANCE OF STUDY

The basic purpose of slope stability analysis in application of engineering field is lead to the safety of road. The results of this study are of importance in planning detailed investigations of major projects. Engineers must account all the aspects of geotechnical affecting their design along with properties of soil material, slope stability and possible natural disasters which can have obliterating social and monetary impacts. Stability of slopes is important throughout all aspects of construction and a small difference in the calculated safety factor can result in a noteworthy increment in costs both in construction and ongoing maintenance.

### LITERATURE REVIEW

**Ameta et al (2016)** this paper aims to design of slope for road embankment with the help of software for fine sand with sanitary ware waste material and it includes laboratory experimental work, software work, as well as cost analysis work. Different laboratory experiments were performed on fine sand with direct mixing of fine sand of different dry densities 1.50 gm/cc, 1.55 gm/cc and 1.58 gm/cc and different percentage 0%, 2%, 4%, 8% and 12% of sanitary ware waste material having particles size range between 2.36 mm to 4.75 mm. A geotechnical software (SLOPE/W) was used for stability analysis of road embankments of various heights of 6 m, 7.5 m and 9 m. Slope/w model formed with the help of slope geometry soil properties. With the use of Bishop simplified method the safety factor is calculated. According to IRC: 75-1979, the acceptable factor of safety for the design of low embankments is 1.25. Investigation is done for two lane road embankment of height 6 m, 7.5 m, 9 m and width 8 m (taking allowance for shoulders) by steeping of side slope to the maximum extent till the value of safety factor of the critical sliding surface remains within the recommended limit of 1.25 as per IRC: 75-1979. Tables 2-4 shows the slope stability analysis results.

**Table 2: Results of Mix Compositions of Fine Sand of 1.50 gm/cc Dry Density and Different Percentages of Sanitary Ware Waste Material of slope stability analysis**

S.No.	Height of Embankment (m)	Admixture (%)	Angle of Internal Friction ( $\phi$ )	Slope (H:V)	Factor of Safety
1.	6.0	0	29.29°	2.24:1	1.259
2.	6.0	2	35.96°	1.72:1	1.250
3.	6.0	4	38.36°	1.58:1	1.253
4.	6.0	8	40.61°	1.46:1	1.254
5.	6.0	12	43.73°	1.31:1	1.256
6.	7.5	0	29.29°	2.24:1	1.259
7.	7.5	2	35.96°	1.72:1	1.250
8.	7.5	4	38.36°	1.58:1	1.253
9.	7.5	8	40.61°	1.46:1	1.254
10.	7.5	12	43.73°	1.31:1	1.256
11.	9.0	0	29.29°	2.24:1	1.259
12.	9.0	2	35.96°	1.72:1	1.250
13.	9.0	4	38.36°	1.58:1	1.253
14.	9.0	8	40.61°	1.46:1	1.254
15.	9.0	12	43.73°	1.31:1	1.256

**Table 3: Results of Slope Stability Analysis of Mix Compositions of Fine Sand of 1.55 gm/cc Dry Density and Different Percentages of Sanitary Ware Waste Material**

S. No.	Height of Embankment (m)	Admixture (%)	Angle of Internal Friction ( $\phi$ )	Slope (H:V)	Factor of Safety
1.	6.0	0	32.09°	2:01	1.257
2.	6.0	2	39.52°	1.52:1	1.256
3.	6.0	4	42.73°	1.36:1	1.259
4.	6.0	8	45.65°	1.22:1	1.250
5.	6.0	12	47.43°	1.15:1	1.254
6.	7.5	0	32.09°	2:01	1.257
7.	7.5	2	39.52°	1.52:1	1.256
8.	7.5	4	42.73°	1.36:1	1.259

9.	7.5	8	45.65°	1.22:1	1.250
10.	7.5	12	47.43°	1.15:1	1.254
11.	9.0	0	32.09°	2:01	1.257
12.	9.0	2	39.52°	1.52:1	1.256
13.	9.0	4	42.73°	1.36:1	1.259
14.	9.0	8	45.65°	1.22:1	1.250
15.	9.0	12	47.43°	1.15:1	1.254

**Table 4: Results of Slope Stability Analysis of Mix Compositions of Fine Sand of 1.58 gm/cc Dry Density and Different Percentages of Sanitary Ware Waste Material**

S.No.	Height of Embankment (m)	Admixture (%)	Angle of Internal Friction ( $\phi$ )	Slope (H:V)	Factor of Safety
1.	6.0	0	34.72°	1.8:1	1.250
2.	6.0	2	41.70°	1.40:1	1.250
3.	6.0	4	44.70°	1.27:1	1.259
4.	6.0	8	46.55°	1.19:1	1.258
5.	6.0	12	49.10°	1.09:1	1.257
6.	7.5	0	34.72°	1.8:1	1.250
7.	7.5	2	41.70°	1.40:1	1.250
8.	7.5	4	44.70°	1.27:1	1.259
9.	7.5	8	46.55°	1.19:1	1.258
10.	7.5	12	49.10°	1.09:1	1.257
11.	9.0	0	34.72°	1.8:1	1.250
12.	9.0	2	41.70°	1.40:1	1.250
13.	9.0	4	44.70°	1.27:1	1.259
14.	9.0	8	46.55°	1.19:1	1.258
15.	9.0	12	49.10°	1.09:1	1.257

**Gupta et al (2016)** to observe the effect of density and moisture on property of cohesive soil this study has been carried out. Since the soil are to be used for making road pavement, embankments, dams etc so at a constant grading of a soil its impact on swelling pressure, strength, CBR value and permeability has been considered. Its slope stability analysis has been done by SLOPE/W software and is used in under various conditions to evaluate slope stability.

Bishop method is used for analysis of embankment at different heights of each slope. To decide the properties of cohesive soil specifically expansive black cotton soil, the impact of changing the density and moisture has been carried out. Fig.1. represents factor of safety in short-term analysis or of homogeneous embankments at different heights on different water content and different density.

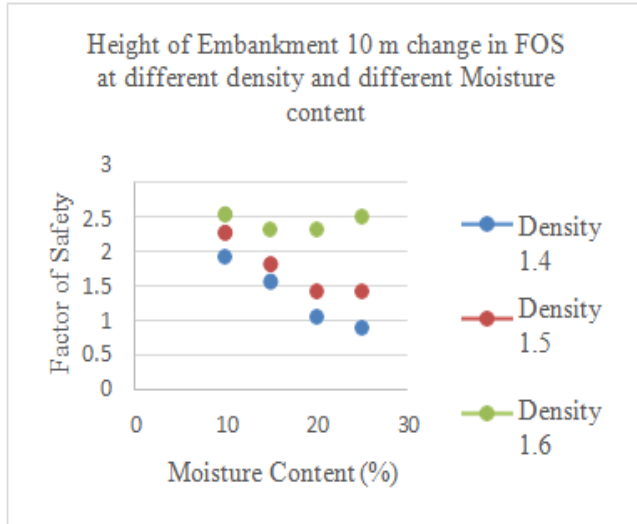


Fig.1 (a) at an embankment height of 10 m

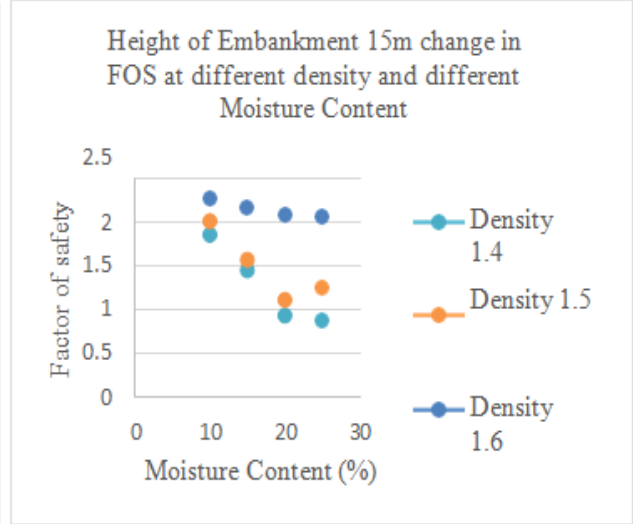


Fig.1 (b) at an embankment height of 15 m

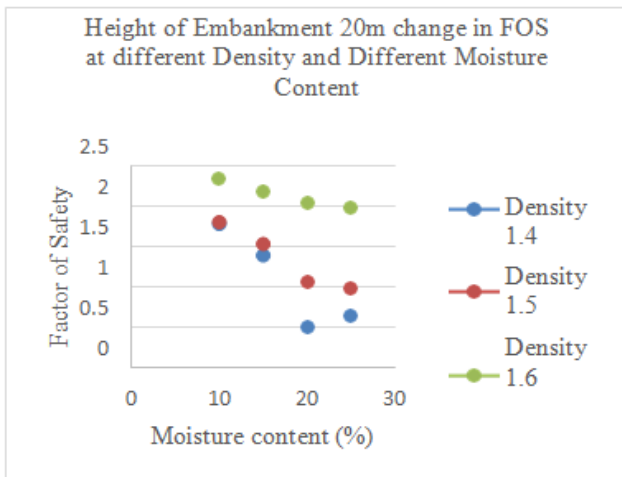


Fig.1 (c) at an embankment height of 20m

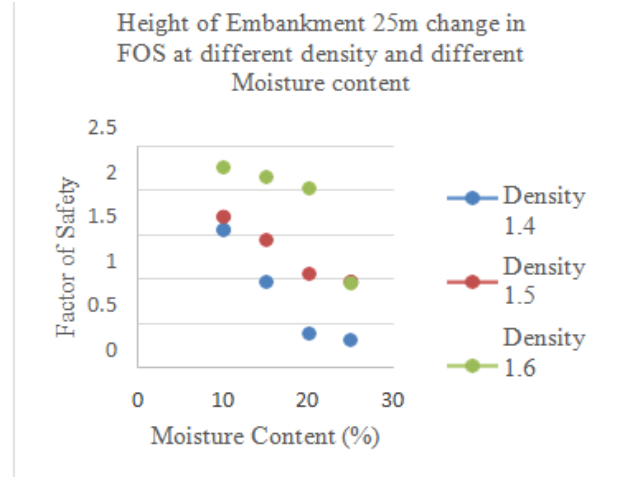


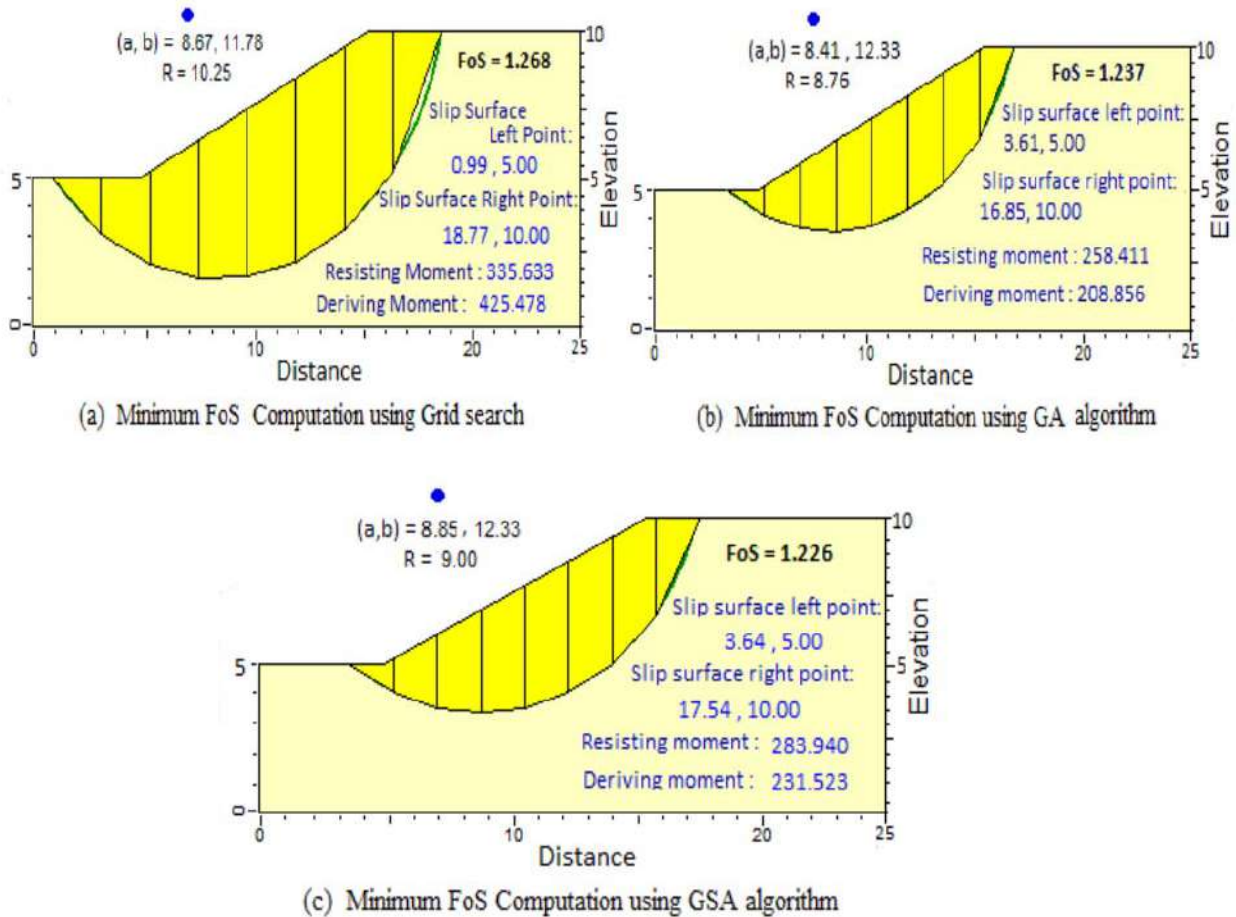
Fig.1 (d) at an embankment height of 25 m

Fig.1: The Variation of factor of safety with moisture content at different heights of embankments.

**Laxminarayana and Naresh (2017)** the clear idea of this paper is to know the best suitability of locally available fill material. For this particular analysis done in latest version of 2016 PLAXIS-2D. Analysis contains usage of different fill materials and different slope angles with different heights and this slope study includes the homogeneous soils, as well as slope section with different soils layers. The result obtained of study is if embankment height increases the factor of safety decreases, but within the same height of embankment, slope increases then the factor of safety increases.

**Fawaz et al (2014)** this paper means to examine the stability of slope, dependent on the numerical simulation utilizing software named PLAXIS. The parameters of soil mechanical properties establishing the slope are assessed from the laboratory outcomes and numerical simulations of in-situ pressure meter test. The slope investigation comprises to decide the critical surface failure and the related safety factor. This factor is ascertained by considering over the impact of components that contribute instability of slope as well as they worked on the use of various techniques for the slope strength.

**Singh et al (2018)** in this research by the use of the gravitational search algorithm failure surface which is critical is identified and it is used for evaluating the safety factor. With the quantitative assessment and execution outcomes, it is accounted that the GSA calculation could procure result more steady with higher accuracy. By settling a benchmark investigation of the literature this algorithm is analysed on the other hand, simulation outline for model of slope and geometry is validated using software named 'slide a rock-science'. Figure 2 shows value of different factor of safety by different approaches using grid search, Genetic algorithm (GA) and Gravitational Search algorithm (GSA).



**Fig.2** On different generation by Fellenius method shows critical failure surface

**Goliya and Gour (2014)** in this research, study has been carried out for identifying, not just slope failure reason based on investigations of site, test and analysis of design to give the of materials standard geotechnical properties with the appropriate side slope yet additionally a step with most recent accessible meta computing tools. Some attributes of soil such as grain size, optimum moisture content and cohesive strength has been taken in thought to design and construct the high embankment of height up to 20 m. In the present study as per IRC guideline, the optimisation of side slope with required safety factor has been also considered. Various soil tests have been performed on excavated local soil and analysed in software the outcomes are appeared in Fig 3.

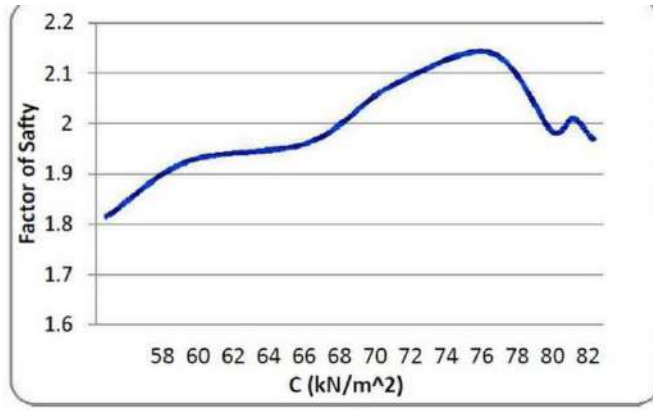


Fig.3 (i)

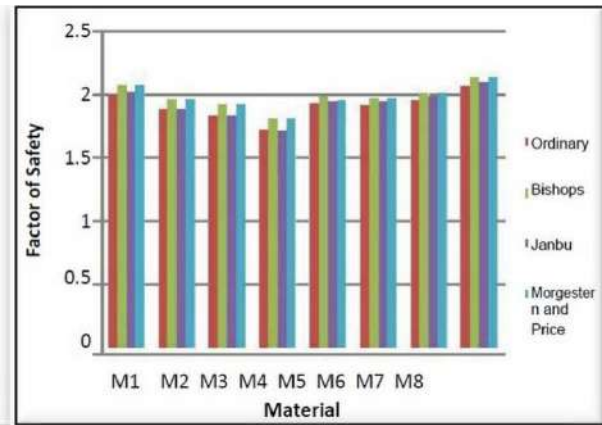


Fig.3 (ii)

Fig3. (i) Soil of side slope 1:1.75 showing variation of factor of Safety with Cohesion value, & (ii) By different methods variation of factor of safety of modified material.

### METHODOLOGY TO CALCULATE STABILITY OF SLOPE

Analysis of stability of slope is generally done by using the method of slices. This method gives, through the safety

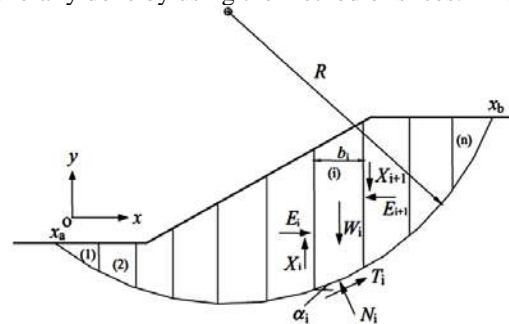


Fig.4 Bishop's method.

Factor, a view of the balance condition of the studied slope with respect to the limit equilibrium. Figure 4 indicates embankment design with number of slices. Either it is a plane, round or some other failure, the equation of the safety factor is distinctive accordingly. Short-term total stresses, long-term effective stresses these are one or both of the condition in which the calculations of stability in all cases are performed. The accuracy of the results will depend, in any case, on the shear parameters determination quality. The numerous lengthy methods can be solved out with the use of software's easily. These methods can be classified into those which accept irregular surface failure (Janbu, Bjerrum) and those which expect circular surface failure (Bishop, Fellenius). Mostly the failure occurs in slope is portrays in Figure 5 as failure of continuum as appeared. The vast majority of the slipping in the mass is an aftereffect of ominous discontinuities Introduction, where the discontinuities are pursue by the rupture surface. The slope stability that is not in the state of limit equilibrium is expressed using the safety factor. The safety factor can be defined as the ratio of resisting forces and deriving forces.

The reliable technique for calculations for PC programming and taking care of the common issue of stability of slope, and also to characterize the mechanism of fracture, is theoretical bifurcation into slices of the sliding body. Figure 6 shows forces acting on slice of a sliding body.

- T: shear force

- E: interslice force normal component
- e: Eccentricity of normal force
- r: The height of interslice force normal component
- X: The sizes of interslice force shearing component
- N: Normal effective force in basis

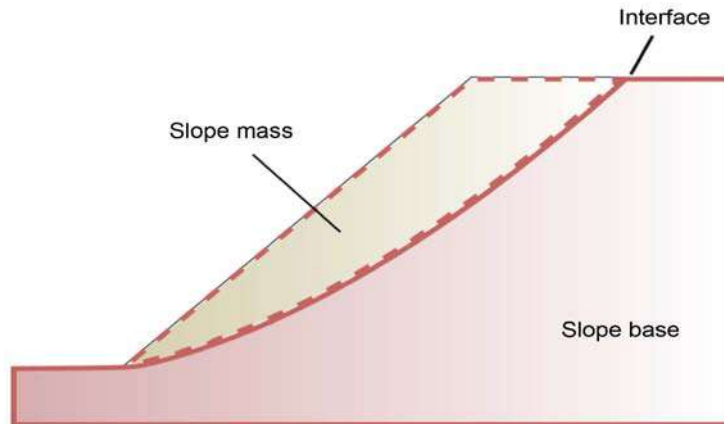


Fig.5 The soil mass not having stability that acts as an equivalent continuum.

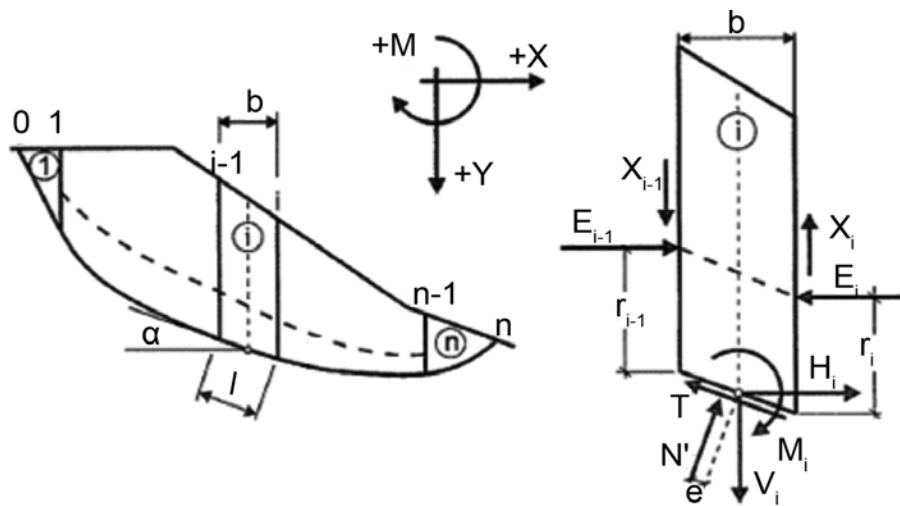


Fig.6 Forces and Stresses acting on a typical slices

## CONCLUSIONS

- The manuscript written exhibits a methodology to assess the road embankments stability having various high height and specific slope embankments.
- The failure of slope relies upon slope geometric property, shear parameter and mechanical properties of soil.
- The slope stability analysis conducted by the software provides results in a very short time and thus can be used easily for the design of slope of road embankments.
- When the percentage of sanitary ware waste material by weight mixed with fine sand is increased from 0% to 12%, irrespective of the height of the road embankment, its slope is steepened from 2.24:1 to 1.31:1, 2:1 to 1.15:1 and 1.8:1 to 1.09:1 for density 1.50 gm/cc, 1.55 gm/cc and 1.58 gm/cc respectively.
- The safety factor decreases with increase in moisture content for a specific density and height of

- embankment.
- There is decreases in the safety factor with increment of embankment height for given moisture content and dry density of embankment.
- The GSA approach could perform productively and deliver outcomes all the more reliably with greater exact value.
- Among these methods such as Bishop's Simplified Method, Janbu Method, Ordinary Swedish Circle method and Morgenstern and Price Method, the lower factor of safety is estimated by Ordinary Swedish Circle method.

## REFERENCES

- Ameta, D., Gupta, A and Sharma, P. (2016). "Design of slope for road embankment with the help of software for fine sand with sanitary ware waste material" *International Journal of Advanced Research*, Vol.4 (Issue 10), pp.889-897.
- Bishop, A.W. (1955). "The Use of Slip Circles in the Stability Analysis of Earth Slopes", *Geotechnique*, Vol.5 (Issue 1) pp.7-17.
- Fawaz Ali, Farah Elias, Hagechade Fadi (2014). "Slope stability analysis using numerical modelling", *American Journal of Civil Engineering*, 2014; Vol.2 (Issue 3): pp.60-67.
- Goliya, H. and Gour, P. (2014). "Slope stability analysis for high embankment with metacomputing technique-a Case study of Natrax high speed track", *International Journal of Core Engineering & Management (IJCEM)*, Vol.1 (Issue 2), pp.68-78.
- Gupta, P., Raghuvanshi, A. K., and Bhargava, S. (2016). "Effect of density and moisture on the slope stability of Highway embankment", *International journal of engineering sciences & research technology*, Vol.5 (Issue7), pp.10-16.
- IRC (The Indian Roads Congress). (2015) "Guidelines for The Design of High Embankments", IRC:75-2015, New Delhi.
- Janbu, N. (1954). "Stability analysis of slopes with dimensionless parameters. Harvard Soil Mechanics Series", Vol.6 (Issue3).
- Laxminarayana, A. and Naresh, M. (2017). "Analysis of Embankments with Different Fill Materials using Plaxis-2D", *International Journal of Engineering Trends and Technology*, Vol.45 (Issue 6), pp.280-284.
- Morgenstern, N.R. and Price, V.E. (1965). "The Analysis of the Stability of Generalized Slip Surfaces. *Geotechnique*", Volume15, pp79-93.
- J. Singh, H. Banka and A. K. Verma (2018). "Analysis of slope stability and detection of critical failure surface using gravitational search algorithm," *4th International Conference on Recent Advances in Information Technology (RAIT)*, Dhanbad, 2018, pp.1-6. doi: 10.1109/RAIT.2018.8389049.
- Spencer, E. (1967). "A Method for Analysis of the Stability of Embankments Assuming Parallel Interslice Forces", *Geotechnique*, Vol.17, pp.11-26



## Cost Analysis of Continuously Reinforced and Conventional Concrete Pavement

Lokit Bansal\*<sup>#1</sup>, S.N. Sachdeva<sup>2</sup>

<sup>1</sup>M.Tech student, Department of Civil Engineering, National Institute of Technology Kurukshetra, Haryana-136119, India,  
Email:24lokit@gmail.com (Corresponding Author)

<sup>2</sup>Professor, Department of Civil Engineering, National Institute of Technology, Kurukshetra, Haryana-136119, India,  
Email:snsachdeva@nitkr.ac.in

### ABSTRACT

Continuously Reinforced Concrete Pavement (C.R.C.P) is used for roads carrying very high volume of commercial traffic and where maintenance of road is difficult. This type of pavement is provided with main reinforcement in longitudinal direction. This pavement theoretically has no transverse joints except construction joints provided at the end of a day's job. A longitudinal joint is provided only if the road is wider than 4.5m. Approximately 0.3-0.4 percent of the sectional area of concrete slab is provided as longitudinal steel in pavements with elastic joints whereas without joints this reinforcement is 0.6-0.85 percent. Due to less number of joints smoothness and riding comfort of CRCP is better which results in low vehicle operation cost. Also CRCP road has longer life if properly constructed and care is taken while placement of steel. The demerits of CRCP are its high initial cost but merit is that it is maintenance free. This paper presents an overview of the cost of CRCP versus the conventional concrete pavement.

**KEYWORDS:** *CRCP; Transverse joints; Longitudinal joint; Vehicle operation cost*

### INTRODUCTION:

Continuously Reinforced Concrete Pavement, CRCP is a concrete pavement in which reinforced is provided in the direction of traffic. CRCP is a durable pavement, modified version of plain concrete pavement. Reinforcement is used in CRCP, to remove the problem of concrete slab cracking, eliminate the joints, and improve the strength and life span of pavement. Maintenance is virtually eliminated in CRCP. The Bureau of Public Roads on the Columbia Pike in Arlington, Virginia first use the CRCP in 1921.

Flexible pavement is commonly used in India for pavement design. As we know that traffic volume is increasing so main focus in pavement design to improve the quality of road pavement; Continuous Reinforced Concrete Pavement (CRCP) technique is better alternative to overcome the disadvantage of other type of pavement the continuous reinforced concrete pavement it is clear from the name continuous reinforcement is provided. These reinforcement provided in longitudinal as well as transverse direction, without transverse joint(theoretically) except terminal joints and construction joints necessitated by existing conditions at the site.

Designing a CRCP involves the dimensioning of pavement thickness, longitudinal and transverse reinforcement, slab width construction joints, shoulders, climatic and foundation parameters. In CRCP, reinforcement used to keep the cracks closed and tight together. The demerits in using CRCP as a paving alternative is its high initial cost due to the large amount of reinforcing steel used in this type of pavement.

The following two basic types of concrete pavements and flexible pavement are designed and cost comparisons were made at initial direct cost and LCC basis to assess the economic benefits of CRCP over other pavement types.

1. Jointed un-reinforced or plain concrete pavements (JPCP)
2. Continuously reinforced concrete pavements (CRCP)
3. Flexible pavement

The life cycle cost analysis was made considering annual and major maintenance, fuel savings, and early completion benefits in addition to initial direct cost consisting of materials, labour, equipment cost and interest during construction.

However, based on full life-cycle cost analysis, in some of the cases present value of CRCP can be lower than that of Jointed Plain Concrete Pavement (JPCP). It is depend on the amount of traffic to be carried. It is found for one particular project that the life-cycle cost of CRCP was about five percent lower than that of Jointed Plain Concrete Pavement (JPCP) based on a 50 Year analysis period (Savings due to low maintenance, low vehicle operating cost, low delay cost). Due to little or no maintenance required in CRCP life-cycle cost of CRCP is reduced and also reduces user delay cost.

## **LITERATURE REVIEW**

Now a days CRCP is widespread in the world especially in the United States and Europe. These pavement firstly used by United States in. Several road tests were conducted during the 1940 to 1950. Today over 50,000 kilometres of highway length have been built in CRCP, according to a Federal Highway Administration report published in October 1998, the technology started to be used more extensively in 1960's. In Canada, in 1958, multiple CRCP sections with various designs were constructed on portion of the Trans-Canada Highway near Calgary, Alberta. In Europe CRCP has been used in France, Belgium, Netherland, United Kingdom and Spain. In 1950 Belgium built its first CRCP section. Several projects were conducted since then to arrive at the current design. Belgium use CRCP not only in its highway but also on its country roads and National Highway. France has used CRCP since 1983 and to date; it has over 600 kilometres as well as several rehabilitations project underway.

### **History of CRCP IN USA**

- 1921 : U.S. Bureau of Public Roads - first CRC - Columbia Pike near Washington (60 m)
- 1938 : U.S. 40 at Stilesville, Indiana (400 m)
- 1947 : U.S. 40 at Vandalia, Illinois Route 130 near Hightstown, New Jersey
- 1949 : U.S. 40 near Fairfield, California
- 1950's : Texas - Pennsylvania, Michigan, Maryland
- 1960 : 162 km of lanes built CRCP is no longer considered experimental and becomes a current practice

In India, first CRCP sample stretch road executed on old Pune-Mumbai Highway under Pimpri chinchwad Municipal Corporation (PCMC), Pune having traffic @200 Maximum Single Axle Load (MSAL). Further six more projects have been executed with private developers in Pune (Maharashtra) region and some are under construction

## **LIFE CYCLE COST ANALYSIS**

Life Cycle Cost Analysis (LCCA) of pavement includes not only present and future maintenance and Rehabilitation costs, but also related costs such as vehicle operation, vehicle maintenance, delays and interest during construction and loss of revenue through road closure and long construction period etc.

The following main costs are calculated for all the 4 options mentioned above:

**Initial Direct Cost:** The initial direct cost consists of materials, labour for constructing the road including design cost and interest on capital during the construction period.

**Maintenance:** Maintenance costs for a concrete pavement are negligible. Nominal regular maintenance cost of Rs. 5000/ per km has been considered apart from joint sealing cost. The concrete roads can stand more than 40 years without any major repair and hence there will not be any major repair in 30 years life considered. Joint sealing at every five years has been considered in case of JPCP. Flexible Pavement suffers deformations, rutting and weathering. Major maintenance will be required after every 5 years apart from regular maintenance. Hence the maintenance cost of road after 5, 10 & 15 years from the commissioning has been worked out.

**Fuel Saving:** The concrete roads, which are rigid pavements, save fuel of loaded trucks plying upon them. Heavier the trucks, more is the saving. This fact was first documented in USA, by the Federal Highway Administration (FHWA) after trials carried out by them in 1982 while comparing the fuel consumption by load carriers on different

types of pavements. A saving of up to 20% fuel was obtained on concrete roads by FHWA. Similar experiments were carried out in India first in 1992 and again in March 1997. The trials carried under the supervision of Central Road Research Institute, CRRI, New Delhi and the results confirm the findings of FHWA. The fuel cost, about 21% is one of the major components of vehicle operating cost (VOC) and any reduction in fuel consumption contributes larger savings in overall VOC of trucks and other vehicles.

Construction Period: Any reduction in construction period facilitates the fast all-round development of that area and also helps to reduce interest during construction, generate revenue from toll charges and fuel savings etc.

Cost of materials, reinforced steel, fly ash and different type of construction like G.S.B, W.M.M, W.B.M etc. are given in Table-1

**Table 1 – Unit's rates**

SL	Material	Units	Rate (rs.)
1	Pavement Quality Concrete (PQC)	Cum	4000
2	Reinforcement Steel – Basic cost	Tonne	21000
3	Extra for corrosion resistant property	Tonne	800
4	Reinforcement cost in RCC	Tonne	28893
5	Dry lean concrete (with & without fly ash)	Cum	2400
6	Drainage layer (DL)	Cum	1000
7	Granular sub base (GSB)	Cum	850
8	Wet mix macadam (WMM)	Cum	1400
9	Water bound macadam (WBM)	Cum	900
10	Dense bituminous macadam (DBM)	Cum	4000
11	Bituminous concrete (BC)	Cum	4500
12	Premier granular layer	Sq.m	16
13	Track coat on primed granular layer	Sq.m	10.00
14	Track coat on bituminous layer	Sq.m	5.00

Rough estimation of cost items for the various rigid pavement & flexible pavement options (Cost of 1km length road of 18m wide-4lanes) were indicated in Table 2.

**Table 2 - Cost Comparison of Various Types of Pavements (Rs. in Lac)**

Pavement Type	Flexible	JPCP	CRCP
Item of Cost			
Material & Labour	281.03	355.27	373.61
Interest during Construction	23.08	14.21	14.94
Initial Direct Cost	304.11	369.48	388.56
Extra in Direct Initial Cost over Flexible	--	65.37	84.44
Percentage of initial direct cost	100%	121%	128%
Extra in VOC over Flexible	605.78	0.00	0.00
Maintenance Cost	126.15	32.50	1.30
Revenue due to early Completion	--	33.39	33.39
Total Life Cycle Cost	1036.05	368.59	356.47

## DESIGN ESSENTIALS

Designing a CRCP involves dimensioning the different geometric pavement features such as thickness, longitudinal and transverse reinforcement, construction joints, slab width, shoulders, pavement transitions based on site-specific traffic, climatic and foundation parameters. The spacing of crack, width of crack, steel stresses, and bond development length generated as function of reinforcement, each affect the CRCP structural stability in the long terms. The percentage of longitudinal reinforcement is determined so as to control cracking and to ensure structural stability of the pavement. In CRCP the presence of continuous reinforcement set into the cement concrete and by the omission of transverse joints other than construction and terminal joints. Whereas in pavement quality concrete (PQC) volumetric changes (due to temperature and moisture) results in the development of large numbers of evenly distributed hairline cracks appearing at random. It is important that precautions must be taken during the CRCP design, selection of material and construction process so that a crack pattern develops that minimize development of pavement distresses. The main problems of CRCP are transverse cracking, spalling, punch-out and steel rupture.  
**Use MS-excel to find percentage and spacing of longitudinal and transverse reinforcement**

### INPUT

Give thickness and width of pavement and grade of concrete and steel etc. in Table-3

**Table 3 –Data of pavement**

	Given data for crcp pavement	unit
	thickness	300 mm
	concrete grade	40 N/mm <sup>2</sup>
	width of pavement	7 m
	longitudnal steel %	0.7
	steel grade	500 N/mm <sup>2</sup>
	diameter of longitudinal bar	20 mm
	leaving space for bars from edge	10 cm
	diameter of transverse bar	12 mm

**OUTPUT**

From MS-excel with the help of formulas putting in cells you can get the spacing and percentage of longitudinal and transverse reinforcement from Table-4

**Table 4 – percentage and spacing of longitudinal and transverse reinforcement**

Longitudnal steel design	
steel required	73.5
no. of steel bars	24
spacing of bars	14.34783
transverse steel design	
% of transverse steel	0.02016
sapcing of bars	186.9048

**CONCLUSION**

From the above study following conclusion can be drawn

1. CRCP saves fuel & money: The major part of the benefit (about 80%) in respect of rigid pavement over flexible is on account of well-established fuel saving and considerable saving in vehicle operating cost comprising reduced consumption of fuel, lubricants and vehicle maintenance cost.
2. Excellence Qualities: CRCP provides all the attributes a roadway designer seeks: Strength, Durability, Smoothness, Traction, Very Low Maintenance require, Longer Life and Low Life Cycle Cost. Further, it offers much better riding quality (smooth surface).
3. Use of CRCP & JPCP can reduce import of bitumen there by leading to saving of foreign currency.
4. In joint less concrete pavement, excellent smooth Riding offered by CRCP. That maximizes the comfort for the passengers.
5. Disadvantage of CRCP is its high initial cost & difficulty in repair works required (in comparison of JPCP) to be done if not constructed properly.

**REFERENCES**

National Highway Authority of India, NHAI web site  
 “CRCP design and construction practices in USA”, Web Site of Cement Reinforcing Steel Institute (CRSI)  
 Life Cycle Cost analysis & Techno-Economic Study for the use of Reinforced Concrete Roads in National

Highways & Expressways, INS/Pub/035

IRC: 101-1988 Guidelines for design of continuously reinforced concrete pavements with elastic joints.

Pydi Lakshmana Rao, Continuously Reinforced Concrete Pavements – The Path of Wisdom (Durable, Virtually Maintenance Free, Environmental Friendly, Saves Fuel & Money), Journal IRC

L.R. Kadiyali, Fuel Savings on Cement Concrete Pavement by CMA

The beau, D., Davidson, F. First Experience with Continuously Reinforced Concrete Pavement (CRCP) in Canada. Quebec Ministry of Transport, Quebec, Canada.2008.

Kathleen Hall, Dan Dawood, Suneel Vanikar, Robert Tally, Jr., Tom Cackler, Angel Correa, Peter Deem, James Duit, Georgene Geary, Andrew Gisi, Amir Hanna, Steven Kosmatka, Robert Rasmussen, Shiraz Tayabji, and Gerald Voigt. Long Life Concrete Pavements in Europe and Canada. Federal Highway Administration (FHWA), August 2007.

History of Design and Construction Practice of CRCP in Belgium Luc Rens, C.E. FEBELCEM – Consulting Engineer [l.rens@febelcem.be](mailto:l.rens@febelcem.be)

Shiraz D. Tayabji, Dan G. Zollinger, George T. Korovesis, Peter I. Stephanos, Jeffrey S. Gaenon. Performance of Continuously Reinforced Concrete Pavements. Summary of Practice & Annotated Bibliography. Vol 1, FHWA-RD-94-178, Federal Highway Administration (FHWA), October 1998.

B. E. Gite., Yogesh S. Nagare. Continuous Reinforced Concrete Pavement. 2002.  
<http://www.engineeringcivil.com/continuously-reinforced-concrete-pavement.html#more-5203>(Paper submitted to web portal)

Sanjay Nayak. Continuous Reinforced Concrete Pavement-The Most Advance Rigid Pavement Technology on Global Arena. ICST-2K14-CE-179.

Ludomir Uzarowski, Imran Bashir, Rabiah Rizvi, Design of CRCP with Heat Transfer System for A Bus Terminal in Hamilton. 2010.

Stock, A.F. Concrete Pavement. Elsevier Applied Science, crown house, Linton road, Banking Essex, England 1998.



## Design Aspects of Reinforced Earth Wall for Road Over Bridges

Nida Nasir\*<sup>1</sup>, S.N. Sachdeva<sup>2</sup>

<sup>1</sup>M.Tech student, Department of Civil Engineering, National Institute of Technology Kurukshetra, Haryana-136119, India, Email: [nidanasir453@gmail.com](mailto:nidanasir453@gmail.com) (Corresponding Author)

<sup>2</sup>Professor, Department of Civil Engineering, National Institute of Technology, Kurukshetra, Haryana-136119, India, Email: [snsachdeva@nitkr.ac.in](mailto:snsachdeva@nitkr.ac.in)

### ABSTRACT

Reinforced Earth Walls are being used extensively these days for retaining the approaches of road over bridges. The necessity of the Reinforced Earth walls assumes significance due to the increasing rate of dynamic loads of traffic on our roads. Reinforced earth walls have high load carrying capacity and theoretically can be constructed to any height. The Reinforced Earth walls are more durable and aesthetically better finished when compared to conventional retaining walls. The structural flexibility of Reinforced Earth walls allows for significant differential movement along the wall. It's simple and repetitive construction technique simplifies control and management and helps to minimize wastage and pilferage on the site. The most common design of reinforced earth walls is based on lateral earth pressure approach. This paper highlights the design aspects of a Reinforced Earth wall versus a conventional retaining wall that make the Reinforced Earth wall more economical and cost effective.

**KEYWORDS:** *Reinforced Earth Walls; Stability; Cost Effectiveness; Reinforcing material; Economical*

### INTRODUCTION

Reinforced Earth wall is merely a composition of stabilized soil and reinforcement. It is used to retain the substantial loads and its simple control and management technology makes it more economical over other alternatives. The facing panels of the Reinforced Earth wall is made of precast concrete which makes it aesthetical. However, facing panels are least significant structurally.

In highways and bridge grade separations, Reinforced Earth wall is most economical structure for earth retention. Similarly, it can also be used for very high structures or in limited space availability as well. The most significant and cost effective parameters of the Reinforced Earth wall are reinforcement length, no. of layers of reinforcement, spacing between reinforcements and height of the wall. These parameters are also responsible for the variation in forces developed in the reinforcement. Before the invention of the Reinforced Earth wall, the retaining walls were used as the supporting member. Further, the Geogrids or Geotextiles came in to practice for development of reinforced earthen concept.

The Reinforced Earth wall is most economical among all conventional retaining walls. Furthermore, each system has its own significance in construction. The Reinforced Earth technology serve the purposes more effectively as high adherence galvanized steel and mechanically stabilized earth is used in it.

Hence, Reinforced Earth wall is one of the examples of advanced structures in construction. The complete structure of reinforced earth walls includes number of components which are shown in Fig 1.

Components of reinforced soil retaining walls

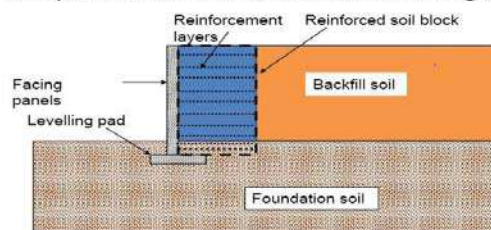


Fig. 1 Diagram showing components of Reinforced Earth retaining wall

## LITERATURE REVIEW

**R.D. Nalawade (2008)** compared cost involved in the construction of RE wall by Geogrid & Metallic strip with that of the conventional RCC cantilever retaining wall; wall height of 7 m is selected. In the study researcher had estimated the overall cost of Reinforced Earth wall by using different reinforcing materials and the design process.

Cost of Reinforced Earth wall by Geogrid:

- a) As per design calculation total number of layer of Geogrid = 14
  - b) Total quantity of Geogrid per layer =  $5 \times 1 = 5 \text{ m}^2$  and total area of for 7m height =  $70 \text{ m}^2$
  - c) i) Cost of Geogrid upto 6th layer =  $30 \times \text{Rs.}110/\text{m}^2 = \text{Rs.}3300/-$ 
    - ii) Cost of Geogrid from 7th to 10th layer =  $20 \times \text{Rs.}130/\text{m}^2 = \text{Rs.}2600/-$
    - iii) Cost of Geogrid from 11th to 13th layer =  $15 \times \text{Rs.}190/\text{m}^2 = \text{Rs.}2850/-$
    - iv) Cost of Geogrid upto 14th layer =  $5 \times \text{Rs.}260/\text{m}^2 = \text{Rs.}1300/-$
  - d) Total cost of Geogrid =  $\text{Rs.}10050/-$
  - e) Cost of precast panel of thickness 14 cm =  $7 \times 800/\text{m}^2 = \text{Rs.}5600/-$
  - f) Cost of accessories per meter length of wall 5% of total cost =  $\text{Rs.}785/-$
- Total Cost of Reinforced Earth wall by Geogrid per meter length =  $\text{Rs.}16435/-$

Cost of Reinforced Earth wall by Metallic strips

As per design calculation,

- a) Total number of strips for 7m height per meter length = 54
  - b) Total length of strips =  $54 \times 5 = 270 \text{ Meter}$
  - c) i) Weight of strip per meter length = 0.71 kg.
    - ii) Weight of strips = 192 kg.
    - iii) Cost of strips =  $192 \times \text{Rs.}35/\text{kg} = \text{Rs.}6720/-$
    - iv) Rate of galvanization for strip =  $192 \times 25 / \text{kg} = \text{Rs.}4800/-$
  - d) Cost of precast panel of thickness 14 cm =  $7 \times 800/\text{m}^2 = \text{Rs.}5600/-$
  - f) Cost of accessories per meter length of wall 5% of total cost
- Total cost =  $17120 + 850 = \text{Rs.}17970/-$
- Total cost of Reinforced Earth wall by metallic strip per meter length =  $\text{Rs.}17970/-$

Cost of R.C.C Cantilever wall

As per design calculation,

- a) i) Total length of 8  $\Phi$  for 7m height per meter length = 174m. Weight = 0.395 kg/m.
    - ii) Total length of 25  $\Phi$  for 7m height per meter length = 65m. Weight = 3.85 kg/m.
    - iii) Quantity of steel =  $(174 \times 0.395) + (65 \times 3.85) = 320 \text{ kg}$ .
    - iv) Total cost of tor steel =  $320 \times 35 = \text{Rs.} 11200/-$
  - b) i) Quantity of M20 concrete per meter length of wall = 4.23 M3. Rate =  $\text{Rs.} 2500/\text{M}^3$ 
    - ii) Cost of concrete =  $2500 \times 4.24 = \text{Rs.}10600/-$
  - c) Add 10% towards shuttering, bar bending, form work and curing etc. = 2180/-
- Total cost of R.C.C Cantilever wall per meter length =  $\text{Rs.}23980/-$

From above calculation it is observed that deployment of the Reinforced Earth wall by Geogrid reduce the cost 32% and by metallic strips reduce cost upto 25% as compared to conventional RCC cantilever retaining wall. It has been experienced that the saving in terms of time was about 50%.

**Harangad Singh and Saleem Akhtar(2015)** have taken rates for different heights and experimental results as shown in Fig 2.In the study researchers have calculated the cost of Reinforced Earth walls which were reinforced with different reinforcing material at different heights to analyze the effect of change of reinforcing material.

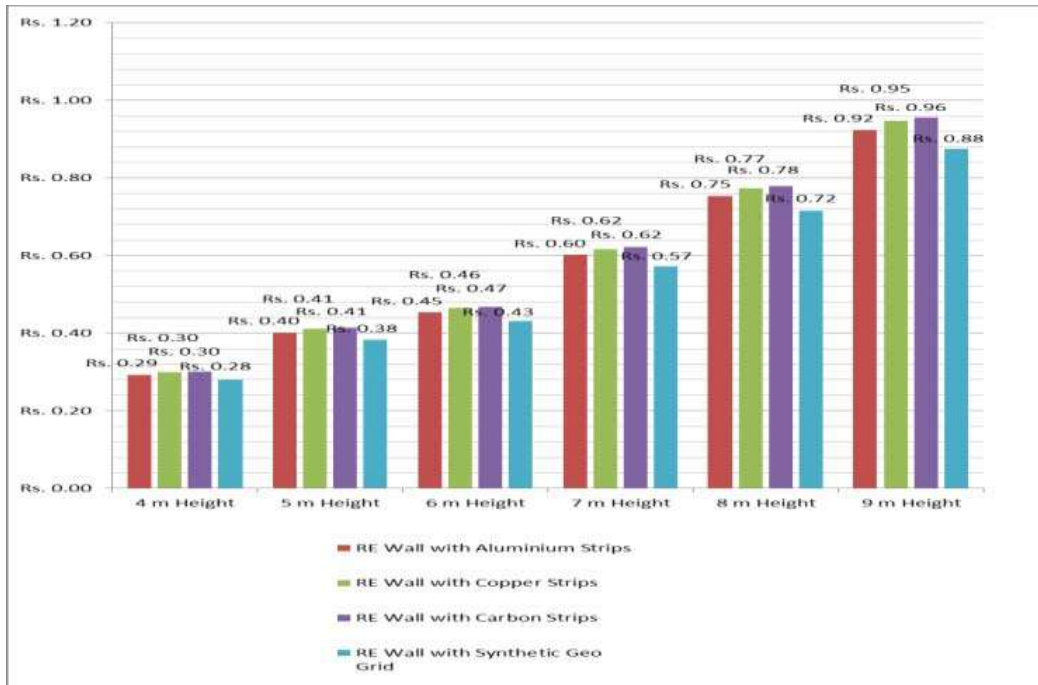


Fig .2 Comparison of Reinforced Earth Walls with Different types of Reinforcing Elements

Further researchers have filled GSB, sand and local earth in which they found that using local earth in Reinforced Earth wall structures was most economical. It is shown in table 1.

Table.1 Cost of Reinforced Earth Wall with Different Filling Alternatives

Item	Leveling Pad (m-15)	Surface Area	Filling Alternatives		
			GSB	Sand	Local Earth
	(cum)	(Sqm)	(cum)	(cum)	(cum)
RE wall	36	2,231	13,386	13,386	13,386
Unit Direct Rate (Rs.)	4,268	1,224	998	248	154
Amount (Rs.)	1,53,648	27,30,744	1,33,59,228	33,19,728	20,61,444

Amount for Reinforced Earth Wall (using GSB) = Rs. 1,33,59,228/-  
 Amount for Reinforced Earth Wall (using Sand) = Rs. 33,19,728/-  
 Amount for Reinforced Earth Wall (using local Earth) = Rs. 20,61,444/-

Mahi Sharma and H.S. Goliya(2014) have also analyzed and designed the walls with different alternatives and material for various heights are given in table 2.

**Table 2 Cost of various retaining walls at different heights**

Height of wall	Cost of retaining wall(Rs.)	Cost of Reinforced Earth wall steel strips(Rs.)	Cost of geogrid RE wall(Rs.)
5m	40250	17000	14500
6m	43952	22082	16580
7m	48780	24165	20700
8m	56605	27722	23840
9m	73620	35335	30200

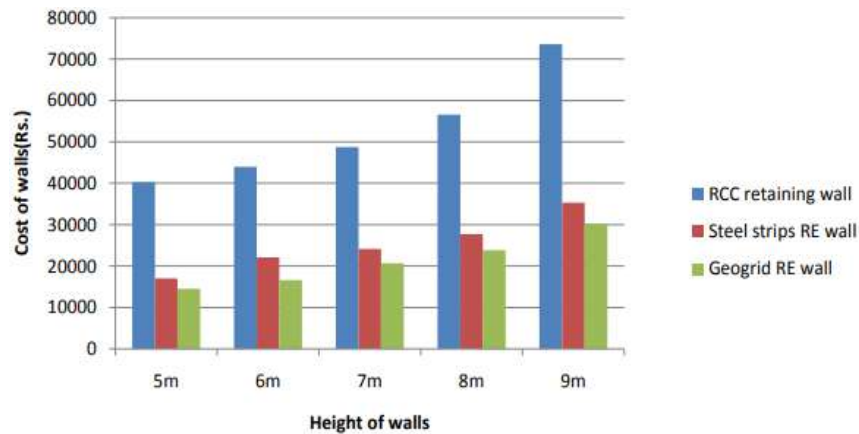


**Fig. 3 Relationship between Height of walls and Cost of walls**

The figure 3 graph shows the RCC Retaining walls are costlier and Geogrid Reinforced Earth walls are the cheapest one. On increasing the height of walls, the rate of savings starts declining.

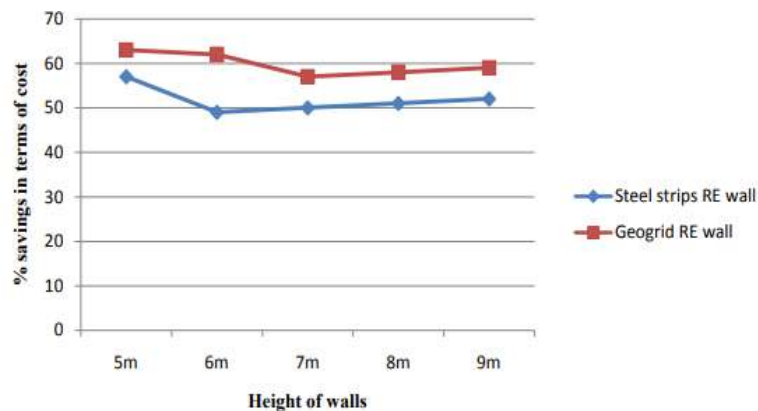


**Fig. 4 Relationship between height of walls and % savings in terms of cost**

The graph in figure 4 shows the comparison of Steel strips Reinforced Earth wall and Geogrid Reinforced Earth wall partially. The Steel strips Reinforced Earth wall and Geogrid Reinforced Earth wall were nearly equally economical.

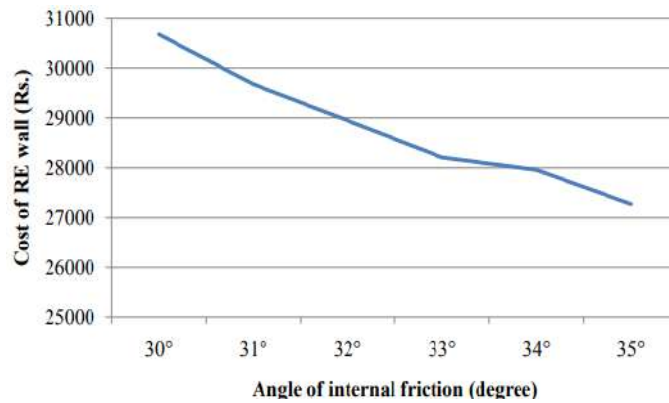


**Fig. 5 Relationship between angle of internal friction of Silty Gravel soil and cost of Geogrid Reinforced Earth wall**

In the fig.5 graphs we can see as the internal friction angle was increased the cost of Reinforced Earth wall decreased.

**Orabi Al Rawi and Maale Al Abade(2017)** estimated the whole cost of implementing the Reinforced Cement Concrete Retaining wall including equipments, material and labor cost which gave precise cost of the wall in table 3.

**Table.3 Costs of Implementing the Reinforced Concrete Retaining Wall**

Activity ID	Equipment	Equipment Cost, JD	Number of Labors	Labors Cost, JD	Material Amount	Material Cost, JD	Total Cost, JD
A1000	2 Rock breakers + 2 Loaders and 1 Bulldozer	A lump sum of 15680 JD					15680
A1010	Concrete Mixer	100	4	140	61 m <sup>3</sup>	4340	4580
A1020	---	---	2	250	150 m <sup>2</sup>	900	1150
A1030	---	---	4	560	60 tons	24000	24560
A1040	1 Pumpcrete + 4 Vibrators	100 (for vibrators)	2	100	330 m <sup>3</sup>	24750 (including Pumpcrete cost)	24850
A1050	---	---	4	700	1500 m <sup>2</sup>	1000	1700
A1060	---	---	4	2100	68 tons	27200	29300
A1070	1 Pumpcrete + 4 Vibrators	100 (for vibrators)	4	560	370 m <sup>3</sup>	27750 (including Pumpcrete cost)	28310
A1080	---	---	6	2100	800 m <sup>2</sup>	2500	4600
A1090	1 Bulldozer and 2 Compactors	A lump sum of 6300 JD					6300
<b>Total Costs</b>							<b>141030</b>

**Zeynep Durukan and Semih S. Tezcan(1992)** has done analysis of cost of Reinforced Soil walls by partially breaking down the total cost in to sub parts so that the cost could be estimated easily.

**Table.4 Cost analysis of Reinforced soil walls (break down of cost)**

Type	Work	Total	Percent
Materials	Facing	21%	67%
	Moulds	4	
	Reinforcement	36	
	Drainage	2	
	Others	4	
Labor	Site	1%	17%
	Wall	11	
	drainage	5	
Plant	Site	1%	16%
	Wall	10	
	drainage	5	
Total		100%	100%

## CONCLUSION

1. From the cost analysis of Reinforced Earth walls at various heights it can be concluded that on varying the composite material i.e. backfill and reinforcing material, the Reinforced Earth wall will give the optimum cost.
2. If we change the geometry and loading conditions, the Reinforced Earth wall will give better results and will be more economical as compared to RCC retaining wall.
3. On the basis of prefabrication technology, it can be strongly assumed that Reinforced Earth wall would take less time during construction as compared to RCC retaining wall.
4. From the estimated costs of different alternatives, it can be concluded that the Reinforced Earth wall is the best alternative among all in terms of technology, aesthetics, economy and applications.
5. The Reinforced Earth walls are not restricted for some heights. These can be used in cases of high vertical cuts for the stabilization of active earth pressure which stabilizes the earth without any structural damage in long period of time.

## REFERENCE

- Chonkar, R.R. (2001). "Review of design of reinforced earth retaining walls for flyovers." in The Indian Concrete Journal, pp 782-786.
- Govinda, K. M., Ingle, R.K. (2014). "A Review on Design of Reinforced Earth Wall" in International Journal of Advanced Trends in Computer Science and Engineering (IJATCSE), Vol.3, Mysore, India.
- Guidelines for Design and Construction of Reinforced soil walls by IRC: SP: 102-2014.
- Singh,H., Akhtar, S.(2015). "A Review on Economic Analysis of Reinforced Earth Wall with different types of Reinforcing Materials" in International Journal of Latest Technology in Engineering, Management & Applied Science Volume IV, Issue XII.
- Sharma, M., Goliya, H.S. (2014). "Design and Economic analysis of reinforced earth wall" in International Journal of Emerging Trends in Engineering and Development Issue 4, Vol.6 Oct. –Nov, (2014).
- Rawi, O.A., Abade, M.A. (2017). "Cost Evaluation and Management for Adopting Reinforced Earth Retaining Structures in Jordan" in Civil and Environmental Research www.iiste.org ISSN 2224-5790 (Paper) ISSN 2225-0514 (Online) Vol.9, No.9.
- Basudhar ,P.K., Vashistha,A., Kousik, D.,Dey,A.(2008) "Cost Optimization of Reinforced Earth Walls" in Geotechnical and Geological Engineering.
- Nalawade,R.D.(2008). "Stability and Cost Aspects of Geogrid Reinforced Earth Wall of Flyover" in the 12th International Conference of International Association for Computer Methods and Advance in Geomechanics (IACMAG).
- Durukan,Z.,Tezcan,S.S.(1992).proposed "Cost analysis of Rreinforced soil walls"Geotextiles and Geomembrane.



## Roller Compacted Concrete (RCC) as a Material in Rigid Pavement- A Review

Raksha J. Khare<sup>1</sup>, Hemant.S.Chore<sup>2</sup> and Rajendra B Magar<sup>3</sup>

<sup>1</sup>Research Scholar Civil Engineering Department, School of Engineering and Technology, Anjuman-I-Islam's Kalsekar Technical Campus, New Panvel-410206 (Maharashtra), India.(Corresponding Author)

<sup>2</sup>Associate Professor, Department of Civil Engineering, Dr. B.R. Ambedkar National Institute of Technology, Jalandhar-144011 (Punjab), India.

<sup>3</sup>Professor and HoD Civil Engineering, School of Engineering and Technology, Anjuman-I-Islam's Kalsekar Technical Campus, New Panvel-410206 (Maharashtra), India.

### ABSTRACT

The heavy wheel loads of the road traffic should move with the least possible rolling resistance. It becomes necessary to maintain the road profile so that the vehicle can move safely. The natural soil is seldom strong enough to support repeated applications of wheel loads without significant deformations. It is, therefore, necessary to interpose between the wheels and the soil, a structure to support loads. This structure is called as the *pavement*. Different types of pavements like flexible and rigid are used as the pavement. Nowadays, there are few pavements which are constructed using materials exhibiting the properties of flexible as well as rigid pavement. However, the studies on the application of RCC as a paving material are very scarce and scanty. The material has got the potential to be used in the pavement as an alternative to the conventional concrete pavement, despite its some of the limitations. However, their use is not that common in India as a highway pavement on large scale and on large trafficked road although they are recommended for the low volume roads being constructed in the rural parts of the country under Rural Roads Development Programme and Pradhan Mantri Gram Sadak Yojana (PMGSY). However, there are hardly any studies, describing the comprehensive investigation on the performance of RCC as a material in general and in pavement in particular. The paper presents a brief review of the work pursued by the researchers in this context.

**KEYWORDS:** *Roller Compacted Concrete; Flexible Pavement; Rigid Pavement; Rolling Resistance.*

### INTRODUCTION

The heavy wheel loads of the road traffic should move with the least possible rolling resistance. Hence, the road profile should be such that the fast vehicle should move safely and comfortably along the longitudinal profile. The natural soil is seldom strong enough to support repeated applications of wheel loads without significant deformations. It is, therefore, necessary to interpose between the wheels and the soil, a structure to support loads. This structure is called as the *pavement*. Alternatively, the cross-section of the carriageway is referred to as the pavement (Saxena 2014). The objective of pavement is to support the wheel loads and to transfer the load stresses through a wider area on the soil subgrade below. Thus, the magnitude of the stresses transferred to the sub grade soil through the pavement layers are considerably lower than the contact pressure or the compressive stresses directly under the wheel load applied on the pavement surface. The reduction in the wheel load stresses due to the pavement depends both on its thickness and the characteristics of the materials used in different component pavement layers placed over the soil subgrade. A pavement layer material is considered more effective or superior, if it is able to distribute the wheel load stress through a larger area per unit thickness of the layer (Khanna *et al.* 2014).

### Requirements of Highway Pavements

The highway pavements are designed and constructed such that the road vehicles are able to travel at the design speed without undue discomfort to the occupants and also the pavement structure remains stable. The highway pavements have to fulfil two major requirements, namely –

- (i) Functional requirements from the point of view of road users, and
- (ii) Structural requirements from the point of view of the highway engineer.

These two major requirements can be, further, classified as under.

- (a) The pavement structure should provide a firm and unyielding surface with good acceptable riding quality, with adequate skid resistance and do not deform excessively
- (b) The pavement should have favourable light reflecting characteristic and low noise generation.
- (c) The pavement structure should ensure that transmitted stresses are reduced to an extent that they will not exceed the supporting capacity of the sub grade and pavement course.
- (d) The pavement should possess sufficient stability to support without damage, the abrasive action of traffic.
- (e) The pavement should withstand adverse weather and environmental conditions and other damaging elements.
- (f) The pavement should aim at the balance between construction cost, road user and maintenance costs.

## TYPES OF PAVEMENTS

Depending upon the structural behaviour of the pavement structures or component parts thereof, the pavements are broadly classified as. the Flexible and the Rigid. Apart from these two, the other categories of pavements include. Semi-rigid type of pavements and composite pavements.

The conventional rigid pavement (Fig .1) comprises mainly of cement concrete slab, i.e., pavement quality concrete (PQC) which itself serves as the wearing course. It may rest on the subgrade directly or sometimes a base or sub-base may be interposed between the slab and the subgrade. However, it is advisable to rest the slab on the base course which is normally of dry lean concrete (DLC) which in turn should be constructed on the granular sub-base(GSB), which also acts the drainage later. This GSB eventually rests on the soil subgrade, the base course or the granular sub-base does not impart any structural action unlike that in flexible pavement. The role of base course is to provide a firm surface for the PQC which also prevents the entry of the surface (roof water), if any through joints or cracks, into the subgrade and to prevent the mud pumping. To some extent, the base course provides the support to the concrete slab. The role of granular sub-base (GSB) is to prepare the platform for the construction of DLC and to facilitate the drainage of the water entered in the pavement structure through any mode of ingress of water and to prevent it from entering the soil subgrade. Many a time, a membrane layer (may be of thin polyethene sheet or the bitumen) is introduced between the DLC and the PQC to reduce the stresses getting induced in the pavement due to an interfacial friction.

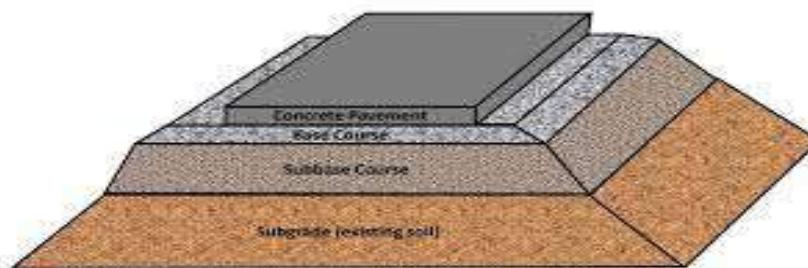


**Fig. 1. Components of Cement Concrete Pavement**

At times, the bonded materials like the ‘Pozzolanic Concrete’ (lime -fly ash -aggregates mix), lean cement concrete or soil- cement are used in the sub-base courses or base courses of the pavement. Some chemicals that are being used for soil stabilization also form a semi-rigid layer. In a nutshell, when either base and/ or sub-base course of the pavement comprises of the cement or Pozzolanic treated materials, the pavement is referred to as the semi-rigid material (Khanna *et al.* 2014)

Nowadays, there are few pavements which are constructed using materials exhibiting the properties of flexible as well as rigid pavement, e.g., wearing course of the pavement is constructed by spreading bricks or precast rectangular cement concrete blocks or interlocking concrete blocks laid on the base course. The joints between them are filled with fine sand of standard gradation. These pieces of blocks act as small rigid plates. Hence, the wearing course constructed of these blocks is neither truly flexible nor it is truly rigid layer. It possesses dual properties and is suitable for low volume village roads or foot paths or many a time, collector streets or local streets in the urban road network (Srinivasan Kumar 2014)

### **Structural Behaviour of Different Types of Pavements**

The flexible pavements are those, which on the whole have low or negligible flexural strength and are rather flexible in their structural action under the loads. The flexible pavement layers may reflect the non-recoverable as well as recoverable deformations of the lower layers including the subgrade on to the upper layers and also to the pavement surface. Thus, if the lower layer of the pavement or the soil subgrade gets deformed or undulated due to the permanent deformation, the flexible pavement layers and also the pavement surface may get undulated to somewhat similar pattern (Khanna *et al.* 2014).

On the contrary to this, the rigid pavements are those which possess noteworthy flexural strength or flexural rigidity. The rigid pavements are generally made of Portland Cement Concrete and are, therefore, called as the Cement Concrete Pavements. Plain cement concrete pavement slabs made of specified strength characteristics are laid, with or without steel reinforcements at the joints. In rigid pavements, the stresses are not transferred from grain to grain to the lower layers unlike in case of flexible pavement layers. The rigid pavement has the slab/ beam action and is capable of transmitting the wheel load stresses through a much wider area below the pavement slab. The rigid pavement does not get deformed to the shape of the supporting layer below, as the pavement slab can bridge the gap or minor variations of the surface of the supporting layer below (Khanna *et al.* 2014).

### **Types of Rigid Pavements**

The conventional rigid pavements, i.e., concrete pavements, are normally classified as under.

1. Plain Jointed Cement Concrete Pavements (Dowelled or Un-Dowelled)
2. Jointed Reinforced Cement Concrete Pavements (JRCP)
3. Continuously reinforced Cement Concrete Pavement (CRCP)
4. Pre-stressed Concrete Pavements (PCP)

Apart from these, the other types of pavements can also be provided using cement concrete. They are listed below.

- i. Fibre reinforced concrete pavements.
- ii. Prestressed concrete pavements.
- iii. Roller compacted concrete pavements.

### **ROLLER COMPACTED CONCRETE PAVEMENTS**

Roller Compacted concrete (RCC) is different from conventional concrete primarily because of the zero slump consistency while mixing and placing .ACI 116 defines RCC as “concrete compacted by roller compaction. Concrete that, in its unhardened state, will support a vibratory roller while being compacted. RCC is placed by asphalt pavers and compacted by vibratory rollers and hardened into concrete. RCC is used for construction of dams and pavements. It contains small amount of water and hence, not possible to be placed by the same method as for the conventional Portland cement concrete (CVC).

Roller compacted concrete has been receiving prominence recently once again, but now as a surfacing layer, as compared to its use in earlier times as a sub-base under concrete or bituminous surfacing. In the earlier usages, lean cement concrete mixes with very low workability, were laid and compacted by roller for serving as a sub-base.

The roller compacted concrete pavement (RCCP) currently receiving attention makes use of pavement quality concrete of zero slump and a vibratory roller. As such, RCCP is not an innovation in concrete paving, but further development and adoption of technology evolved earlier for lean concrete sub-base /soil-cement. The speed of construction using conventional machinery (as in asphalt paving), the higher strength because of low water –cement ratio, and the economy arising out of these factors, still cannot lead to outright adoption of RCCP as a high way or airfield surfacing, since the problems associated with provision of joints as well as a good riding surface do not lead themselves to easy solutions. Nevertheless, there have been studies undertaken in several countries on this technique, and several useful observations have been made. Significant experience on construction aspects has also been gained through adoption of RCCP for parking areas of docks, storage yards, log sorting and storage yards of timber industry and haul roads in USA and Canada. However, the major use of roller compacted concrete has been in the construction of dams.

The basic mix design procedure for conventional concrete is applicable to RCCP also expecting for the lower water-cement ratio and higher density in the case of RCCP, which brings in additional advantage in its usage. The maximum size of aggregate has to be limited, since larger sizes will result in segregation and honeycombing. The aim of the RCCP is to achieve an impervious surface with a nominal macro-texture similar to that of asphalt concrete, which is obtained with 20 mm maximum aggregate size. Reducing the maximum size below 20 mm is likely to increase costs. The consistency, water cement and density to be achieved in the field, are predetermined in the laboratory. For consistency, the Vee Be apparatus used in conventional concrete tests can be used with some modifications. The optimum moisture content and the maximum density can be determined as per modified AASHTO. The field density can be fixed as a percentage of maximum dry density obtained in the laboratory. Generally, the value used is 97%. The use of Fly ash as part replacement of cement is also finding its place in such construction.

**Advantages of Roller compacted Concrete Construction are as follows.**

- Ease in construction and rapid in construction.
- No Joints or dowels required.
- Relatively cost effective.

**Methodologies of RCC Design**

Unlike the design of flexible pavements, where several changes took place through the years, the design of rigid pavements has followed empirical principles from the beginning. The input parameters relate to the subgrade support, material characteristics, traffic loads and climate. Several researchers (Older 1925, Goldbeck 1925, Westergaard 1925, Teller and Sutherland 1935, Spangler 1937, Bradbury 1938, Pickett and Ray 1951, Freberg 1955, Ioannides *et al.* 1985 and Shie *et al.* 1993) significantly contributed to the thickness design of rigid pavements. However, Westergaard's theory (1925, 1933 and 1948) is the basis on which many modifications took place in the analysis and design of rigid pavements. Further, with the advent in the computers and numerical methods, mechanistic- empirical (M-E) approach is being followed nowadays. In M-E approach, the slab thickness is determined by considering the fatigue failure of the slab due to damage caused by cumulative axle load passes. These modifications have provided reasonably good agreement with the performance of in-service pavements (Srinivasa Kumar 2014).

A few widely used design methods for RCC pavements include

- 1) The Portland Association Method (PCA) (1984).
- 2) The AASHTO Design Method of Rigid Pavement (1993).
- 3) Indian roads Congress (IRC) (1974, 1988, 2002 and 2015).

**Applications**

Due to the low water-cement ratio and good aggregate interlocking, RCC pavement is generally very strong and can carry heavy loads. As the same equipment as for asphalt pavement are used, rapid construction is done in short time, and since the strength growth is fast enough the opening for traffic in a short time can be permitted. Due to small drying shrinkage the interval between joints can be maximized. RCC has adequate resistance to freezing and thawing. It has established itself as a fast-economical construction method for dams, off-highway pavement

Projects, heavy duty parking and storage areas, and as a base for conventional pavement. Other common applications are in ordinary roads, roads in factories, temporary roads for construction works, parking areas, service areas, container yards, material-handling yards, apron and carriageway of airports, for binder course of expressway and heavily trafficked roads.

### **Construction of Roller Compacted Concrete Pavement (RCCP)**

RCC is weigh-batched and mixed in a continuous mixing pug mill or a normal mixer such as used for soil-cement treated base or asphalt concrete construction. The pavement is initially constructed in lifts of 150-200 mm for a pavement thickness of more than 400 mm with an elapse of time of 30 minutes to 2 hours between the lifts. The lower lift requires more compactive effort with more passes of the roller, to achieve the desired density. If a smooth pavement surface is not obtained, a layer of asphalt may be used to cover the Surface and smooth out the roadway.

Vee-Bee consistometer apparatus with some modification can be used to evaluate RCC' s consistency. The curing of RCCP is accomplished by keeping the surface of the pavement wet for seven days. Water spray or fine mist is most appropriate and is commonly used. Wet sand can also be used for curing RCC. Due to very low drying shrinkage of RCC as compared to PCC, the contraction joints are provided at a spacing of 10 to 20 meters whereas the spacing between contraction joints is 4.5 meter in PCCP.

RCCP as a result of the high stability achieved by the mineral skeleton formed by the aggregates after compaction can be opened to traffic almost immediately. Further, the stability of the mineral structure allows high volume of mineral binders to be used than that used in the vibrated concrete pavements. The total thickness of an RCCP structure is much less than an asphalt/gravel pavement of the same load-carrying capacity. Due to its advantages as a comparatively low cost and durable Paving material, RCC is also emerging as a common base for conventional highway and street pavements. Thus RCC is a material that has the longevity of concrete at price of asphalt.

### **Limitations**

Unlike concrete pavement, the surface of RCCP is uneven as in the case of flexible pavement. It is, therefore, necessary to add a wearing course several centimetres thick made of bituminous concrete or, at least, a surface treatment to provide a non-skid finish for heavy traffic moving at high speeds. Due to the fact that the RCC is highly sensitive to loss of strength, the compaction has to be carried out energetically with a sufficient number of passes of the rollers and that the densities required are to be carefully controlled. To achieve high density, material to be compacted must be on a solid base. RCC placed on resilient sub-grade such as clay cannot achieve high level of compaction. In case the cement used in RCC has a high content of pozzolanas they develop their strength rather slowly. This makes RCC sensitive to freezing temperature during setting in cold weather.

In the Early 1970's, the attention of researchers was drawn to a new construction material called Roller compacted concrete (RCC). The First use of RCC was an experimental study carried out by U.S army in 1972. The new material, thus, gained popularity and was used in dam construction not only in U.S., but in other countries also. In 1980's, the RCC was used as a heavy -duty material for log sorting yards, tank hardstands, railroad sorting yards and other industrial pavements. The use of RCC for pavements is relatively new and growing interest. RCC has traditionally been used for pavements carrying heavy loads in low-speed areas, such as parking, storage areas, port, airport service areas, intermodal and military facilities. With improved paving and compaction methods as well as surface texturing techniques, recent applications of RCC can be found for interstate highway shoulders, city streets, and rural highways.

### **REVIEW OF LITERATURE ON RCC AS A MATERIAL FOR RIGID PAVEMENTS**

The review of various research works carried out on facets of RCC as a paving material is reported briefly in the following section. For the purpose of clarity, the literature survey is presented in four broad categories, mentioned as under.

- a) Experimental Studies to Evaluate the Properties of RCC as a Paving Material
- b) Numerical Modelling and Analysis
- c) Analysis and Design
- d) Comparative Studies

### Experimental Studies

Kajorncheapunngam and Stewart (1992) reported Rise husk ash (RHA) as cementitious Roller Compacted Concrete material due to high silica content. The use of RHA is not only to solve the problem of shortage of cement in the developing countries like ours, but also to help to conserve energy, resources, and the environment. The use of RHA with 50% of replacement of cement in RCC was found to improve the compressive strength of concrete. Tsutomu *et al.* (1994) performed experiment to study the effect of classified fly ash (CFA) on improving the performance of RCCP, they concluded that the CFA can contribute to increase RCC slab thickness up to 35 cm in one layer without loss of flexural strength. They also concluded that these results are desirable to apply RCC for heavy duty pavements in airports and seaports.

Pittman and Ragan (1998) carried out laboratory investigations on the drying shrinkage of RCC for pavement application. The combined effect of the moisture content and aggregate grading on the drying shrinkage was statistically significant whereas the individual effects were not that significant. Ghafoori and Cai (1999) conducted experiments on Laboratory made roller compacted concrete with various combinations of cement (Type I and Type V for surface-resistant concrete), lignite dry bottom ash, and crushed limestone coarse to determine the suitability of use of bottom fly ash to manufacture long-term durability bottom ash roller compacted concretes. Gage *et al.* (1999) highlighted the OPP fines (mining by-product referred to as OPP fines means Ore Pretreatment Plant Fines) is a very effective filler in RCC because its particle-size distribution is very similar to that of the cement.

Hamzah and Mohamed Baqer (2008) studied the experimental and analytical behaviour of various mixes of RCC using different materials. They concluded that the magnitude of density of RCC decreases when using crushed aggregate and when using admixtures  $w/c$  reaches 0.83 in uncrushed aggregate mixes.

Krishna Rao *et al.* (2014) evaluated the properties of RCCP with the help of soil compaction method. The results showed that RCCP mixes can be proportioned using soil compaction method and they concluded that from the strength behaviour of RCC, it is recommended for paving applications. Pavan and Krishna Rao (2014) carried out experimental investigation to study the effect of fly ash on strength characteristics of RCCP. The results indicated that the mixture where cement was substituted by fly ash, when increasing the fly ash caused reduction in compressive strength, splitting tensile and flexural strength values at all of the ages up to 28 days.

Krishna Rao *et al.* (2016) carried out experimental investigations of ultrasonic pulse velocity on roller compacted concrete containing GGBS and M-Sand. A new model was proposed to determine the dynamic elastic modulus of GRCC as a function of age of concrete and percentage replacement of GGBS by ultrasonic Method. Hossain and Ozyildirim (2016) investigated the properties of RCC for use in pavements. The special provision for use of RCC developed in this study was workable and was planned to be incorporated as a standard provision in VDOT's *Road and Bridge Specifications* with minor modifications. The study summarized the research that led to the development of VDOT's RCC specification.

### Numerical Analysis and Modelling

Ouezdou and Loulizi (2009) carried out numerical modelling of RCCP under vehicular loading. In the study, a 3-D numerical model was developed using F.E. software ABAQUS. This modelled pavement was analysed under a single tier load of 60kN with certain tire pressure. The results obtained were compared with the closed form solutions and Portland Cement Association procedure. The comparison showed that the FE model gives lower stresses and higher displacements. It concluded that 3-D F.E. modelling is a reliable method for calculation of stresses and displacement in RCCP. Zidri *et al.* (2009) studied a 3-D numerical model by introducing the computer code ABAQUS. Also, other methods of 2-D were applied for determination of stresses and strains. It was concluded that the 3-D modelling gives results slightly lower than those given by 2-D methods'.

Afshin Famili (2016) carried out the numerical analysis of Roller Compacted Concrete Pavement where a 3-D finite element (FE) model of RCC pavement was developed. Using finite element software ABAQUS software, the study investigated the effects of changes speed in vertical displacement. Rupnow *et al.* (2016) studied the performance of thin roller compacted concrete under accelerated loading to determine the structural performance with failure mechanics and load carrying capacity also stating the applicability of RCC pavement with cement treated base .

Vahidi *et al.* (2017) carried out the modelling of mechanical properties of roller compacted concrete containing RHA using ANFIS. The test results and performed modelling showed that the optimal value for obtaining the maximum compressive strength and minimum permeability is offered by substituting 9% and 18% of the cement by RHA, respectively.

### **Analysis and Design**

Schrader (1987) presented the effect of compaction methods, water content, and other variables on density, pore pressure, practical construction problems in RCC construction. Muller (1990) reviewed the state of the art studies in RCCP. Further, the study was extended to determine the performance of various types of pavements made and determine if a basis exists to build RCCP in Arizona, on an experimental basis, for both new roads and street connections.

Naik *et al.* (2001) studied the state-of-the-art information on strength and durability of roller compacted concrete for pavement design with and without supplementary cementitious materials with two case studies (using HVFA). Kim (2006) employed RCC for the interstate - 285 shoulder reconstructions in Atlanta, GA. Halsted (2009) studied the application, benefits, design, construction, testing, performance and sustainability of RCC pavement with successful example across North America.

Williams (2014) selected RCCP as a potential solution for failing pavements in the Arkansas area. The RCC pavement designed for two lanes was successfully constructed. Krishna Rao *et al.* (2015) carried out the analysis and design of RCCP for low volume roads in India. Design curves for low volume were presented and the proposed RCCP was found suitable for subgrade having low modulus of reaction.

### **Comparative Studies**

Haque *et al.* (1987) reported conceptive analysis of many inferior and marginal aggregates, waste products, and other deleterious materials which do not meet standards and specifications to be used in the manufacturing of Roller Compacted Concrete Pavement construction. It was observed that RCC containing marginal aggregates becoming cost effective and competitive. Mechanically weak and poorly graded materials can be used to manufacture the RCC of adequate strength for use in pavement structures.

Mehdi Koohmishi (2013) made a comparison between the properties of flexible pavement and RCCP by conducting experiments. The investigation showed that RCCP can be used instead of flexible pavements for warm weather conditions. Zarrinkafsh and Shirazi (2014) studied the different aspects of RCCP such as mix design, flexural strength, compressive strength and focus on the different part of RCCP in detail was investigated. It was concluded that for low speed, the RCCP can be the best choice. It is also economical on freeways and highways.

Alikhani and Nejad (2015) studied the properties of RCCP and its economic evaluation. It was concluded that RCCP can be used first in steep slopes and hot weather with a heavy and slow loading that in which asphalt pavements have problems and cannot be amenable.

### **SUMMARY**

Many studies pointed out the advantages of RCCP over the conventional flexible pavement. The studies on the application of RCC as a paving material are very scarce and scanty. The literature indicates that the material has got the potential to be used in the pavement as an alternative to the conventional concrete pavement, despite its some of the limitations. However, there use is not that common in India as a highway pavement on large scale on large trafficked road although they are recommended for the low volume roads being constructed in the rural parts of the country under Rural Roads Development Programme and Pradhan Mantri Gram Sadak Yojana (PMGSY). However, there are hardly any studies, describing the comprehensive investigation on the performance of RCC as a material in general and in pavement in particular. Although there are few studies on modelling and analysis, limited studies are available wherein various aspects of the RCC pavements are linked by considering various aspects involved in the analysis, design, construction, modelling and assessment of the performance of the RCCP for different traffic conditions and weather conditions that would be prevalent in different parts of the country. It is an established fact

that the RCC would be comparatively economical vis-a-vis conventional concrete when used in pavement. Moreover, it can be an economical option in a part of the country like ours where the industrial waste material containing Pozzolanic properties is available in abundance. Given the problem of safe disposal of such materials raising environmental concern, such material can be used advantageously in the RCC.

## REFERENCES

- ACI Committee 309(1998).“Compaction of Roller-Compacted Concrete”, ACI 309.5R-XX -final draft 6, 56 Pages.
- ACI 325 10R-95,(2000).“State of the Art report on Roller Compacted Concrete Pavements”, ACI manual of concrete practice, ACI, USA, 32PP
- AASHTO (1993).“AASHTO Guide for Design of Pavement Structures”, American Association of State Highway and Transportation Officials, Washington, D.C.
- Bradbury,R.D.(1938).“Reinforced Concrete Pavements”,Washington,D.C.Wire Reinforcement Inst.
- Dolen ,T. P.(1991).“Freezing and Thawing Durability of Roller-Compacted Concrete”, Durability of Concrete, Second CANMET/ACI International Conference, SP-126, 101-114
- Famili,A. and Vafaei, M.(2016).“Numerical Analysis of Roller Compacted Concrete Pavement”, Saudi Journal of Engineering and Technology ,1(1),20-25.
- Goldbeck,A.T.(1925) .“The Design of concrete pavements”,Concrete.
- Goldbeck, A. T. (1925).“Researches on the structural design of highways by the United States Bureau of Public Roads.Transactions of ASCE ,88. 264-300.
- Goldbeck, A. T.(1925).“The interrelation of longitudinal steel and transverse cracks in concrete roads”, Public Roads.
- Friberg, B. F.(1955).“Stresses in concrete pavements by sector analysis”, Proceedings of the Highway Research Board.
- Huang, Y.H. (2004).“Pavement Analysis and Design”, 2nd Edition, Prentice Hall,147-166, University of Kentucky, USA
- Hamzah,A.A and Al-Shadeedi,M.B.(2008).“Evaluation of Properties of Roller Compacted Concrete”, The 1st Regional Conference of Eng. Sci, NUCEJ, 11(33),366-373
- Handbook on Cement Concrete Roads (2000). Cement Manufacturers’ Association, New Delhi
- Ioannides, A. M., Thompson, M.R and Barenberg,E.J. (1985).“Westergaard solutions reconsidered”,Transportation Research Record No. 1043. Washington, D.C. Transportation Research Board, 13-23.
- IRC. 58-2002. Guidelines for the design of plain jointed rigid pavements for highways. New Delhi.
- IRC. 58-2015. Guidelines for the design of plain jointed rigid pavements for highways. New Delhi.
- Jahi,H.(2014).“Roller compacted concrete pavements”, A Journal of multidisciplinary Research,3(8), 121-13
- Krishna Rao, S. Sarika, P. Sravana, P.and Chandra Sekhara Rao, T. (2014), “Evaluation of Properties of roller compacted concrete Pavement”, International Journal of Education and Applied Research, ISSN.2348-0033, 4(2),88-90.
- Krishna Rao, S.,Dr.Chandra Sekhara Rao,T.and Dr.Sravana,P.(2013).“Effect of manufactured sand on strength characteristics of Roller compacted Concrete”, International Journal of Engineering Research and Technology, ISSN. 2278-0181, 2(2).
- Krishna Rao,S.Dr.Chandra Sekhara Rao,T.and Dr.Sravana,P (2015).“Design & Construction of Roller Compacted Concrete Pavements for low volume roads in India” ,International Manager Journal of Civil Engineering Research ,5(2).
- Khanna, S.K., Justo C.E.G. and Veeraragavan, A. (2014).“Highway Engineering”, Nem Chand and Bros., Roorkee (India) (10th Revised Edition)
- Kadiyali, L.R. and Lal, N.B. (2009).“Practice and Principles of Highway Engineering”, Standard Publishers, New Delhi
- Kajorncheapunngam, S. and Stewart, D.F. (1992).“Rice Husk Ash in Roller Compacted Concrete”,Concrete International, 14(4),38-44.
- Naik, T. R., Kraus, R. N., Chun, Y.M., Ramme, B. R., and Singh, S.S.(1997).“Strength and Durability of Roller-Compacted HVFA Concrete Pavements”,International conference on Durability of Concrete.
- PCA (1984).“Thickness Design of Concrete Pavements”,Portland Cement Association ,PCA.

- Pickett, G. and Ray, G.K. (1953). "Influence charts for concrete pavement", *Transaction of ASCE*, 110, 49-73.
- Shi, X., Fwa, T.W. and Tan, S.A. (1993). "Warping stresses in concrete pavements on Pasternak Foundation", *ASCE. of Transportation Engineering*, 119(6), 905-913.
- Spangler, M. G. (1937). "Stresses in the corner region of concrete pavements", *Iowa Eng. Exp. Station Bulletin No. 157*. Iowa State University.
- Saxena, S. (2014). "A Text Book of Highway and Traffic Engineering", CBS Publishers, New Delhi
- Srinivasa Kumar, R. (2014). "Pavement Design", University Press, Hyderabad.
- Schrader, E.K. (1987). "Compaction of Roller Compacted Concrete", *Special Publication, ACI SP96-06*, 96.
- Teller, L. W. and Sutherland E. C. (1935). "The structural design of concrete pavements, Part II. Observed effects of variations in temperature and moisture on the size, shape and stress resistance of concrete pavement slabs". *Public Roads* 16(9). 1935, October 1936, and April 1943
- Vineela, P., Krishna Rao, S., Panduranga Rao, B. and Ramesh, V. (2015). "2D Analysis of Stresses and Displacements of Roller Compacted Concrete Pavements (RCCP) for Low Volume Road under Vehicular Loading", *International Journal of Research in Engineering and Technology*, 2319-1163.
- Vahidi, E.K., Malekabadi, M.M., Rezaei, A., Roshani, M.M. and Roshani, G.H. (2017). "Modelling of mechanical properties of roller compacted concrete containing RHA using ANFIS", *Computer and Concrete*, 19(4), 435-442
- Westergaard, H.M. (1925). "Computation of stresses in concrete roads", *Proc. of HRB. Part I*, 90-112,
- Westergaard, H. M. (1993). "Analytical tools for judging results of structural tests of concrete pavements", *Public Roads*, 14(10), 185-188
- Westergaard, H. M. (1925). "Computation of stresses in concrete roads", *Proc. of HRB. 5(Part I)*. 90-112. National Research Council, Washington, D.C.
- Westergaard, H. M. (1948). "New formulas for stresses in concrete pavements of airfields", *ASCE Transactions* 113, Paper No. 2340, 425-444.
- Zdiri, M., Abriak, N., Neji, J., and Ouedou, M.B. (2009). "Modelling of Stresses and Strains Distribution in an RCC Pavement using the Computer Code "ABAQUS"", *Electronic Journal of Structural Engineering*, 9, 37-44.
- Zdiri, M., Abriak, N., Ouedou, M.B. & Loulizi, A. and Neji, J. (2009). "Numerical Modeling of a Roller Compacted Concrete Pavement under vehicular loading", *International Journal of Pavement Research and Technology*, 2(5), 188-195.
- Zarrinkafsh, O. and Shirazi, M.R. (2015). "Design of Roller Compacted Concrete Pavement", *International Journal of Civil, Environmental, Structural, constructional and Architectural Engineering*, 9(6), 785-788.



## Transportation System Modelling of Chennai City using Object Oriented Simulation

Anit Raj Bhowmik<sup>1</sup>, Bishnu Kant Shukla<sup>2</sup> and  
Gandu Srikanth<sup>3</sup>

<sup>1</sup>School of Civil Engineering, Lovely Professional University, Phagwara, Punjab-144411, E-Mail: [anitrajbhowmik@gmail.com](mailto:anitrajbhowmik@gmail.com)

<sup>2</sup>School of Civil Engineering, Lovely Professional University, Phagwara, Punjab-144411, E-Mail: [bishnukantshukla@gmail.com](mailto:bishnukantshukla@gmail.com)  
(Corresponding Author)

<sup>3</sup>School of Civil Engineering, Lovely Professional University, Phagwara, Punjab-144411, E-Mail: [gandusreekanth@gmail.com](mailto:gandusreekanth@gmail.com)

### ABSTRACT

A competent transportation system is crucial to economic development and social integration of a country. As per 2015 statistics, GDP of India is about 2.1 Trillion USD and annual growth rate of GDP in India is averaged as 7.4%. Transport sector accounts for a share of 6.4% in India's GDP. India's road transport contributes to approximately 4.8% of the GDP which carries 60% of freight and 87% of passenger traffic. India's fuel imports are growing at an average of 14% annually for which India spends equivalent to 3% of GDP on fuel imports and can lose 1% of its GDP due to the rising fuel prices, thereby posing a major threat to the economy of the country in the future. This study carries out interdisciplinary work involving the sectors of Transportation, Energy, Economy and Environmental interaction considering the parameters such as model split, fuel consumption, fuel costs and GDP by building a System Dynamics (SD) model using STELLA software to forecast the GDP and Environmental impact levels pertaining to transportation system in the upcoming years. A scenario of augmenting the growth rate of public transportation and simultaneously restricting the growth rate of private transportation showed a substantial decrease of fuel consumption and fuel cost which resulted in an increase in the GDP as well as reduction in the environment impact levels in the transportation system in Chennai city for the future years.

**KEYWORDS:** *Transportation System; System Dynamics; Model Split; Fuel cost; GDP*

### INTRODUCTION

Road transport, together with the other modes of transport, provides indispensable mobility for all citizens and goods and contributes to the economic prosperity of a nation (Babcock and Davalos, 2004). Hence it is a key factor to social, regional and economic cohesion, including the development of rural areas. The economy is one of the factors that influence the size and the type of transport (Brail, 1987; Burrell, 1996). An improvement of road infrastructure implies lower transport costs like lower maintenance cost and lower accident cost, so that more or longer trips with the same quantity of labour, equipment and fuel are possible (Jacobsen, 2012). The relationship between transport and economy arises as soon as one considers the exact significance of transport for economic development (Litman, 2009; Litman, and Colman, 2001). Road transport is vital to India's economy as it contributes nearly 4.8% share towards Gross Domestic Product of the nation. The transport sector is greatly influenced by the availability and affordability of infrastructure and fuel. India produces only 15% of its fuel demand and the remaining 85% of demand is met through imports. During the year 2014-2015, the crude oil import accounted for 3% of the country's GDP. The limited availability of resources within the country and the need for import affects the price dynamics (Kadiyali, 1985). Hence a collective effort and unified policy direction is the need of the hour to face the challenges and minimize these economic losses and achieve efficiency in usage of transportation systems simultaneously reducing environmental pollution and contribute to economy of the nation.

## **SYSTEM DYNAMICS THEORY**

System Dynamics is a methodology, whereby complex, dynamic and nonlinear interactions in social systems can be understood and analysed and new structures and policies can be designed to improve the system behaviour. System Dynamics presents Systems Approach and prescribes a coherent set of steps for conducting a system inquiry. System Dynamics is the result of 'Cross Fertilization' among elements of Traditional Management, Feedback Control Theory and Computer Simulation. The principal concern of a System Dynamics study is to understand the forces operating in a system in order to determine their influence on the stability growth of the system. System Dynamics modelling requires explicit recognition of two types of flows namely Physical Flow and Information Flow. SD models are always tested for their ability to generate behaviour similar to that of the real system only then they are deemed to be valid representation of reality. The model emphasizes more on the structure than on the parameter values.

The System Dynamics approach to modelling uses two important schemes. The first scheme is thinking about the problem in terms of how the quantities vary through time (the very word dynamics implies an emphasis on change through time). The second perspective is the thinking about whether there exists a substantial feedback relationship.

## **METHODOLOGY**

In this study, a System Dynamics model relating Transport, Energy and Economy has been built. Data relating to economic parameters in present scenario has been collected and simulated to find the future levels of the same in transport sector. The present levels and future simulated levels are compared. The models have been subjected to various scenario analysis aimed at studying and understanding the interaction between Transport and Economy sectors at a micro level (Rephann and Isserman, 1994). The impact of the policies framed by the government to achieve sustainability in transportation with respect to economic development has been analyzed.

The model of the Transport and Economy interaction using the System Dynamics (SD) approach is to be implemented in the 'STELLA' ('STELLA 9.1' package). The modelling tool which is an object-oriented simulation environment, allows the development of interaction models with significantly less effort than using traditional programming languages. Using this tool, the modeller defines objects representing physical or conceptual system components and indicates the functional relationships among these objects. The comparison of results under various scenarios has been carried out to determine the advantages of the policy measures adopted. Based on which, suitable recommendations of the policies have been provided.

The various sectors under consideration for model building are vehicle population sector, energy sector and economy sector. The secondary data pertaining to the above mentioned sectors have been collected from Transport Department, Chennai.

The area selected for study is Chennai city which is the fourth most populous metropolitan area and the sixth most populous city in India. Chennai's vehicle population has been accelerating steadily which has reached 4.37 million in 2015. Daily, about 1,500 new vehicles hit the roads, with two-wheelers constituting more than 75 percent of them. With respect to the transport sector, the data which are of prime concern are vehicle population and the existing Modal Split in the city which have been obtained from the Second Master Plan for Chennai, CMDA report. The modal split between public and private transportation in the city was 35:65 in the year 2004 which has been projected to reach 55:45 in 2011, 60:40 in 2016 and 70:30 in 2026. These projected values have been considered for various scenario analyses. The vehicle population in Chennai city between the years 2010 to 2015 was collected from the Statistics of Transport Department, Chennai which gives the data regarding the total number of commercial and non-commercial vehicles in the city and the data is considered for this study which is given in the Table 1.

**Table 1: Vehicle Population in Chennai City**

YEARS/ VEHICLES	2010	2011	2012	2013	2014	2015
BUSES	3421	3464	3527	3654	3798	4257
AUTO RICKSHAW	49062	63340	66679	68599	70933	73854
TAXI	1259	1268	1354	1475	1517	1628
PRIVATE BUS	2702	2906	2962	2991	3015	3043
MINI BUS	2095	2217	2355	2406	2491	2575
LCV	11836	12736	19123	21469	33136	41248
HCV	12846	17928	22165	33571	40833	49124
MOTOR CYCLES	13.71	15.63	17.06	19.42	21.18	22.67
SCOOTERS	3.33	4.03	4.69	4.90	5.10	5.75
MOPEDS	4.97	6.15	6.27	6.39	6.45	6.66
TWO WHEELERS (IN LAKHS)	22.01	25.81	28.91	30.53	32.79	35.09
CARS (IN LAKHS)	4.82	5.80	5.98	6.15	6.59	6.87
TOTAL (IN LAKHS)	27.61	32.64	37.60	38.81	40.11	43.72

With respect to the energy sector, the fuels which were of prime concern were petrol and diesel. Hence data pertaining to the fuel consumption per day by petrol and diesel driven vehicles have been collected from earlier studies and presented in Table 2.

**Table 2: Average Fuel Consumption by Different Classes of Vehicles**

TYPE OF VEHICLE	AVERAGE DISTANCE COVERED (KM/DAY)	FUEL EFFICIENCY (KM/LTR)	FUEL CONSUMED (LITERS/VEHICLE / YEAR)
BUS	151	4.1	13415
AUTO	96	21	1669
TAXI	21	13	534
PRIVATE BUS	111	5	11863
MINI BUS	22	8.7	897
LCV	51	14	1330
HCV	55	4.33	4637
CARS	22	13.5(PETROL)	593
		14.0(DIESEL)	571
TWO WHEELERS	18	53	124

**Source : Report of the Expert Group, Government of India Report.**

In 2015, Chennai had a GDP of \$66 Billion i.e., 4, 03,260 crore rupees, ranking fifth in the cities of India based on GDP. According to Confederation of Indian Industries (CII), it is estimated to grow to a \$100 Billion economy by the year 2025 (Statistical Organization and State Directorate of Statistics.), see Table 3.

**Table 3: Annual GDP And GDP Growth Rate of Chennai City**

Year	GDP (Crore Rupees)	Growth Rate (%)
2012-13	348338	6.94
2013-14	374498	7.51
2014-15	403260	7.68

## RESULTS AND DISCUSSION

### SCENARIO I- DO MINIMUM (Allowing the existing trend to continue)

In the Do Minimum scenario, the existing trend of growth rates of MTC buses, Auto Rickshaws, Taxis, LCVs, HCVs, Private buses, Mini buses, Two Wheelers and Cars along with the Accident cost and NPI values has been allowed to continue till the year 2026. Based on the existing growth rate, the amount of fuel consumed and fuel costs by each transport sector have been simulated.

**Table 4: Results of Scenario I – Vehicle Population**

Year	Bus	Auto	Taxi	LCV	HCV	Pvt Bus	MiniBus	Cars	TW
2015	4257	73854	1628	41248	49124	3043	2575	687598	3509159
2016	4436	78211	1939	49126	50057	3442	2858	752232	3801472
2017	4622	82826	2309	58510	51008	3892	3173	822942	4118135
2018	4816	87713	2750	69685	51978	4402	3522	900299	4461175
2019	5019	92888	3276	82995	52965	4979	3909	984927	4832791
2020	5229	98368	3901	98847	53972	5631	4339	1077510	5235363
2021	5449	104172	4646	117726	54997	6369	4816	1178796	5671468
2022	5678	110318	5534	140212	56042	7203	5346	1289602	6143902
2023	5916	116827	6591	166993	57107	8147	5934	1410825	6655689
2024	6165	123719	7850	198888	58192	9214	6587	1543443	7210107
2025	6424	131019	9349	236876	59297	10421	7312	1688526	7810709
2026	6693	138749	11135	282119	60424	11787	8116	1847248	8461341

It could be observed from the table 4 that if the existing trend is allowed to continue, the number of cars and two wheelers would reach 18.47 lakh and 84.61 lakh respectively in 2026. Whereas the public transport vehicles constituting the MTC buses have increased only to a fleet size of around 6693 in 2026.

**Table 5: Results of Scenario I –Fuel Consumption by Vehicles**

Year	Bus	Auto	Taxi	LCV	HCV	Private Bus	Mini Bus	Cars	TW
	In liters per day								
2015	148454	337618	5931	150261	623977	106118	6511	1098520	865272
2016	154689	357538	7063	178960	635832	120020	7228	1201781	937349
2017	161186	378632	8412	213142	647913	135743	8023	1314748	1015430
2018	167956	400972	10019	253852	660224	153525	8905	1438334	1100016
2019	175010	424629	11933	302338	672768	173637	9885	1573538	1191647
2020	182361	449682	14212	360084	685550	196383	10972	1721450	1290911
2021	190020	476214	16926	428860	698576	222109	12179	1883266	1398444
2022	198001	504310	20159	510772	711849	251206	13519	2060293	1514935
2023	206317	534064	24010	608330	725374	284113	15006	2253961	1641129
2024	214982	565574	28596	724521	739156	321332	16657	2465833	1777835
2025	224011	598943	34058	862904	753200	363427	18489	2697622	1925928
2026	233420	634281	40563	1027719	767511	411036	20523	2951198	2086358

The fuel consumed by cars is 29.51 lakh liters per day and two wheelers is 20.86 lakh liters per day, and that of MTC buses is just 2.33 lakh liters per day in 2026. Finally the total fuel that would be consumed by all the vehicles in 2026 would be 298.81 crore liters per annum.

**Table 6: Results of Scenario I –Fuel Cost by Vehicles**

Year	Bus	Auto	Taxi	LCV	HCV	Private Bus	Mini Bus	Cars	TW
	In Rupees per day								
2015	5690252	18342464	322202	5759488	23917035	4067521	249586	50173571	47009367
2016	6308714	20366766	400052	7298561	25931232	4894790	294771	57758487	53395122
2017	6994396	22614472	496711	9248912	28115056	5890312	348136	66496922	60648318
2018	7754603	25110240	616725	11720443	30482794	7088307	411162	76565353	68886788
2019	8597435	27881443	765737	14852427	33049933	8529955	485599	88167416	78244373
2020	9531873	3095848	950752	1882135	3583326	1026481	573512	10153810	88873093

		1		1	6	2		5	
2021	1056787 3	3437510 6	118047 1	2385086 8	3885100 0	1235251 0	677341	11694863 8	10094561 8
2022	1171647 4	3816879 4	146569 3	3022439 3	4212287 6	1486481 3	799966	13471206 0	11465807 6
2023	1298991 5	4238115 9	181983 0	3830107 6	4567029 6	1788807 8	944792	15518974 4	13023323 4
2024	1440176 2	4705840 7	225953 3	4853604 2	4951646 6	2152622 7	111583 7	17879887 9	14792412 3
2025	1596706 1	5225184 4	280547 6	6150603 8	5368654 5	2590431 7	131784 9	20602115 2	16801814 4
2026	1770248 9	5801843 6	348332 8	7794192 7	5820781 1	3117284 1	155643 2	23741276 7	19084173 7

In accordance with the increase in number of vehicles and fuel consumption between the public and private transport, the fuel cost incurred by cars is 23.74 Crore Rupees per day and two wheelers is 19.08 Crore Rupees per day, and that of MTC buses is just 1.77 Crore Rupees per day in 2026 (Table 6). The total fuel cost that would be incurred by all the vehicles in 2026 would be 24679 Crore Rupees per annum.

**Table 7: Results of Scenario I – Final GDP for Chennai City**

<b>Year</b>	<b>Chennai GDP (Crore Rupees)</b>	<b>Total Accident Cost (Crore Rupees)</b>	<b>Total Fuel Cost (Crore Rupees)</b>	<b>Final GDP (Crore Rupees)</b>
2015	403260	263	5673	397323
2016	434230	278	6485	427468
2017	467579	294	7412	459874
2018	503489	310	8472	494708
2019	542157	327	9683	532147
2020	583795	346	11068	572381
2021	628630	365	12651	615615
2022	676909	385	14460	662064
2023	728896	407	16528	711962
2024	784875	429	18891	765555
2025	845154	453	21592	823108
2026	910061	479	24680	884903

It could be observed from the table 7 that if the existing trend is allowed to continue, the accident cost and fuel cost would reach to 479 crore rupees and 24,680 crore rupees and the Final GDP would reach to nearly 8.85 Lakh Crore Rupees in 2026. Thus the Do Minimum Scenario emphasizes the need to adopt proper planning measure and preventive methodologies to minimize the threats of loss to GDP and improve the GDP. Hence scenario II and scenario III has been tried using 'STELLA' package.

## SCENARIO II- PARTIAL EFFORTS

In the Partial Efforts scenario (Scenario II), simulation has been carried out such that minimal efforts are undertaken by the government to achieve a Modal Split of 50:50 between Public and Private Mode of transport. The simulated value of the vehicle population based on the above mentioned values have been shown in the table 8-11 below:

**Table 8: Results of Scenario II – Vehicle Population**

Year	Bus	Auto	Taxi	LCV	HCV	Private Bus	Mini Bus	Cars	TW
2015	4257	73854	1628	41248	49124	3043	2575	687598	3509159
2016	4704	78211	1939	49126	50057	3442	2858	714302	3592326
2017	5198	82826	2309	58510	51008	3892	3173	742045	3677464
2018	5744	87713	2750	69685	51978	4402	3522	770868	3764620
2019	6347	92888	3276	82995	52965	4979	3909	800813	3853842
2020	7013	98368	3901	98847	53972	5631	4339	831922	3945178
2021	7750	104172	4646	117726	54997	6369	4816	864243	4038678
2022	8563	110318	5534	140212	56042	7203	5346	897821	4134395
2023	9462	116827	6591	166993	57107	8147	5934	932706	4232380
2024	10456	123719	7850	198888	58192	9214	6587	968950	4332688
2025	11554	131019	9349	236876	59297	10421	7312	1006604	4435372
2026	12767	138749	11135	282119	60424	11787	8116	1045724	4540491

It could be observed from the Table 8 that if minimal efforts are undertaken, the number of cars and two wheelers would reach 10.45 Lakh and 45.40 Lakh respectively from 18.47 Lakh cars and 84.61 Lakh two wheelers (scenario I values) in 2026, whereas the public transport vehicles constituting the MTC buses have increased only to a fleet size of around 12,767 from 6,693 (scenario I value) in 2026. The hypothesis considered is that one bus will replace 19 cars and 38 two wheelers.

**Table 9: Results of Scenario II –Fuel Consumption by Vehicles**

Year	Bus	Auto	Taxi	LCV	HCV	Private Bus	Mini Bus	Cars	TW
In liters per day									
2015	148454	337618	5931	150261	623977	106118	6511	1098520	865272

2016	164042	357538	7063	178960	635832	120020	7228	1141150	885779
2017	181266	378632	8412	213142	647913	135743	8023	1185437	906772
2018	200299	400972	10019	253852	660224	153525	8905	1231447	928262
2019	221331	424629	11933	302338	672768	173637	9885	1279245	950262
2020	244571	449682	14212	360084	685550	196383	10972	1328902	972784
2021	270250	476214	16926	428860	698576	222109	12179	1380491	995838
2022	298627	504310	20159	510772	711849	251206	13519	1434085	1019440
2023	329983	534064	24010	608330	725374	284113	15006	1489764	1043601
2024	364631	565574	28596	724521	739156	321332	16657	1547609	1068334
2025	402917	598943	34058	862904	753200	363427	18489	1607704	1093653
2026	445223	634281	40563	1027719	767511	411036	20523	1670137	1119573

In accordance with the alteration of growth rate in number of vehicles between the public and private transport, the fuel consumed by cars decreases to 16.70 Lakh liters per day from scenario I's 29.51 lakh liters per day and the fuel consumed by two wheelers decreases to 11.19 lakh liters per day from scenario I's 20.86 lakh liters per day and the fuel consumed by MTC buses increases to 4.45 lakh liters per day from scenario I's 2.33 lakh liters per day in 2026. The total fuel consumption by the private transport is 27.89 lakh liters per day where as that of public transport is just 4.45 Lakh liters per day. So the total saving in the fuel consumption is 23.44 lakh liters per day.

**Table 10: Results of Scenario II –Fuel Cost by Vehicles**

Year	Bus	Auto	Taxi	LCV	HCV	Private Bus	Mini Bus	Cars	TW
	In Rupees per day								
2015	5690252	18342464	322202	5759488	23917035	4067521	249586	50173571	47009367
2016	6690143	20366766	400052	7298561	25931232	4894790	294771	54830083	50457478
2017	7865735	22614472	496711	9248912	28115056	5890312	348136	59927067	54158506
2018	9247902	25110240	616725	11720443	30482794	7088307	411162	65506965	58131003
2019	10872944	27881443	765737	14852427	33049933	8529955	485599	71616379	62394880
2020	12783538	30958481	950752	18821351	35833266	10264812	573512	78306486	66971510
2021	15029861	34375106	1180471	23850868	38851000	12352510	677341	85633495	71883834
2022	17670908	38168794	1465693	30224393	42122876	14864813	799966	93659146	77156473
2023	20776040	42381159	1819830	38301076	45670296	17888078	944792	102451267	82815858
2024	24426805	47058407	2259533	48536042	49516466	21526227	1115837	112084379	88890356
2025	28719084	52251844	2805476	61506038	53686545	25904317	1317849	122640372	95410415
2026	33765601	58018436	3483328	77941927	58207811	31172841	1556432	134209237	102408716

In accordance with the alteration in the growth rates, the total fuel cost incurred by the private transport is 23.66 Crore Rupees per day where as that of public transport is just 3.37 Crore Rupees per day (Table 10). So the total saving in the fuel cost is 20.29 Crore Rupees per day which shows a reduction of 28.94% of fuel cost incurred by all the vehicles in scenario I.

**Table 11: Results of Scenario II – Final GDP for Chennai City**

<b>Year</b>	<b>Chennai GDP (Crore Rupees)</b>	<b>Total Accident Cost (Crore Rupees)</b>	<b>Total Fuel Cost (Crore Rupees)</b>	<b>Final GDP (Crore Rupees)</b>
2015	403260	263	5673	397323
2016	434230	263	6310	427657
2017	467579	264	7018	460298
2018	503489	264	7805	495420
2019	542157	264	8681	533213
2020	583795	264	9655	573876
2021	628630	264	10738	617628
2022	676909	264	11943	664702
2023	728896	264	13283	715349
2024	784875	264	14774	769837
2025	845154	264	16431	828458
2026	910061	264	18275	891522

It could be observed from the Table 11 that when the partial efforts are applied to the existing trend, the accident cost and fuel cost would reach to 264 crore rupees and 18,275 crore rupees and the final GDP would reach to nearly 8.91 lakh crore rupees in 2026 in scenario II from scenario I's 8.85 lakh crore rupees which higher by 6,619 crore rupees when compared with Scenario I.

### **SCENARIO III- DESIRABLE SCENARIO**

In the desirable scenario, simulation has been carried out such that minimal efforts are undertaken by the government to achieve a Modal Split of 70:30 between Public and Private Mode of transport. In order to facilitate the above condition, the Public transport has been augmented in a phase wise manner to reach a growth rate of 17.34% and simultaneously the growth rate of cars and two wheelers have been restricted to 2.33% and 3.19% respectively.

**Table 12: Results of Scenario III – Vehicle Population**

<b>Year</b>	<b>Bus</b>	<b>Auto</b>	<b>Taxi</b>	<b>LCV</b>	<b>HCV</b>	<b>Private Bus</b>	<b>Mini Bus</b>	<b>Cars</b>	<b>TW</b>
2015	4257	73854	1628	41248	49124	3043	2575	687598	3509159
2016	4812	78211	1939	49126	50057	3442	2858	698665	3548462
2017	5440	82826	2309	58510	51008	3892	3173	709931	3588204
2018	6149	87713	2750	69685	51978	4402	3522	721400	3628392
2019	6951	92888	3276	82995	52965	4979	3909	733076	3669030
2020	7857	98368	3901	98847	53972	5631	4339	744963	3710123
2021	8882	104172	4646	117726	54997	6369	4816	757065	3751677
2022	10040	110318	5534	140212	56042	7203	5346	769387	3793696
2023	11349	116827	6591	166993	57107	8147	5934	781932	3836185
2024	12829	123719	7850	198888	58192	9214	6587	794705	3879150
2025	14502	131019	9349	236876	59297	10421	7312	807712	3922597
2026	16393	138749	11135	282119	60424	11787	8116	820955	3966530

It could be observed from the Table 12 that the number of cars and two wheelers would reach 8.20 Lakh and 39.66 Lakh respectively from 18.47 lakh cars and 84.61 lakh two wheelers (scenario I values) in 2026, whereas the public transport vehicles constituting the MTC buses have increased only to a fleet size of around 16,393 from 6,693 (scenario I value) in 2026.

**Table 13: Results of Scenario III –Fuel Consumption by Vehicles**

<b>Year</b>	<b>Bus</b>	<b>Auto</b>	<b>Taxi</b>	<b>LCV</b>	<b>HCV</b>	<b>Private Bus</b>	<b>Mini Bus</b>	<b>Cars</b>	<b>TW</b>
	<b>In liters per day</b>								
2015	148454	337618	5931	150261	623977	106118	6511	1098520	865272
2016	167813	357538	7063	178960	635832	120020	7228	1116310	874963
2017	189695	378632	8412	213142	647913	135743	8023	1134423	884763
2018	214432	400972	10019	253852	660224	153525	8905	1152863	894672
2019	242394	424629	11933	302338	672768	173637	9885	1171638	904692
2020	274002	449682	14212	360084	685550	196383	10972	1190754	914825
2021	309732	476214	16926	428860	698576	222109	12179	1210218	925071

2022	350121	504310	20159	510772	711849	251206	13519	1230037	935432
2023	395776	534064	24010	608330	725374	284113	15006	1250217	945909
2024	447386	565574	28596	724521	739156	321332	16657	1270766	956503
2025	505725	598943	34058	862904	753200	363427	18489	1291692	967216
2026	571671	634281	40563	1027719	767511	411036	20523	1313001	978048

The total fuel consumption by the private transport is 22.91 lakh liters per day where as that of public transport is just 5.71 lakh liters per day (Table 13). So the total saving in the fuel consumption is 17.20 lakh liters per day. On comparison with Scenario I, the total fuel consumed by all the vehicles in scenario III decreases to 210.67 crore litres per annum from scenario I's 298.81 crore litres per annum in 2026, which shows a reduction of 29.49% of fuel consumption by all the vehicles in scenario I.

**Table 14: Results of Scenario III –Fuel Cost by Vehicles**

Year	Bus	Auto	Taxi	LCV	HCV	Private Bus	Mini Bus	Cars	TW
	In Rupees per day								
2015	5690252	18342464	322202	5759488	23917035	4067521	249586	50173571	47009367
2016	6843926	20366766	400052	7298561	25931232	4894790	294771	53698729	49841362
2017	8231502	22614472	496711	9248912	28115056	5890312	348136	57472849	52843965
2018	9900402	25110240	616725	11720443	30482794	7088307	411162	61513602	56027454
2019	11907666	27881443	765737	14852427	33049933	8529955	485599	65839925	59402727
2020	14321892	30958481	950752	18821351	35833266	10264812	573512	70472102	62981338
2021	17225593	34375106	1180471	23850868	38851000	12352510	677341	75431870	66775535
2022	20718006	38168794	1465693	30224393	42122876	14864813	799966	80742514	70798307
2023	24918491	42381159	1819830	38301076	45670296	17888078	944792	86428987	75063424
2024	29970605	47058407	2259533	48536042	49516466	21526227	1115837	92518020	79585484
2025	36047013	52251844	2805476	61506038	53686545	25904317	1317849	99038261	84379969
2026	43355387	58018436	3483328	77941927	58207811	31172841	1556432	106020404	89463288

The total fuel cost incurred by the private transport is 19.54 crore rupees per day where as that of public transport is just 4.35 crore rupees per day (Table 14). So the total saving in the fuel cost is 15.19 crore rupees per day. On comparison with Scenario I, the total fuel cost incurred by all the vehicles in scenario III decreases to 10,353 crore rupees per annum from scenario I's 24,679 crore rupees per annum in 2026, which shows a reduction of 58.04% of fuel cost incurred by all the vehicles in scenario I.

**Table 15: Results of Scenario III – Final GDP for Chennai City**

<b>Year</b>	<b>Chennai GDP (Crore Rupees)</b>	<b>Total Accident Cost (Crore Rupees)</b>	<b>Total Fuel Cost (Crore Rupees)</b>	<b>Final GDP (Crore Rupees)</b>
2015	403260	263	5673	397323
2016	434230	254	5992	427984
2017	467579	245	6329	461005
2018	503489	236	6685	496568
2019	542157	228	7060	534869
2020	583795	220	7457	576118
2021	628630	212	7876	620542
2022	676909	205	8319	668386
2023	728896	197	8786	719912
2024	784875	190	9280	775405
2025	845154	184	9802	835168
2026	910061	177	10353	899532

It could be observed from the Table 15 that when the desirable efforts are applied to the existing trend, the accident cost and fuel cost would reach to 177 crore rupees and 10,353 crore rupees and the final GDP would reach to nearly 8.99 lakh crore rupees in 2026 in scenario III from scenario I's 8.85 lakh crore rupees which is higher by 14,629 crore rupees when compared with Scenario I. Thus from the analysis it could be found that achieving modal split of 70:30 has a greater impact on fuel consumption and fuel cost as well as on the economy generated by the city.

## **RECOMMENDATIONS**

From the study carried out, the following recommendations are given.

- There is an immediate need to restrict the growth of private transport and to augment the public transport. This augmentation can be attributed by increasing the MTC buses fleet size in the city.
- In order to achieve the Modal Split of 70:30, the MTC fleet size should not be lesser than 16,393 and should be implemented on time with efficient services and to be operated with maximum efficiency.
- The growth rate of two wheelers and cars should be restricted implying that the number of vehicles should be contained within and 39.66 lakh and 8.20 lakh in the year 2026 to achieve the above mentioned policy of the government.
- These policies lead to a considerable reduction in the fuel consumption and fuel cost in the city making it a place with reduced economic losses due to fuel imports.
- This study also recommends that besides implementing the conventional measures of 4E's - Engineering, Enforcement, Education and Emergency medical response to the overall transportation sector it is always advisable and better to add an additional E also i.e., the Ethical Values for a prosperous and sustainable economy of the city.
- Finally it could be suggested from the study that not only the quantitative economic indicator like the GDP of the nation has to be considered for representing the economic growth of the city but also the qualitative economic indicators like the Value System and Quality of Life of the people is also to be considered for representing the real economic growth and prosperity of the city.

## REFERENCES

- Babcock, M. and Davalos, J. (2004), 'Case Studies of the Economic Impact of Highway Bypasses in Kansas', *Kansas Department of Transportation, Kansas State University*, 21-25.
- Brail, R.K. (1987). "Microcomputers in Urban Planning and Management." *Center for Urban Policy Research, New Brunswick, NJ*. Burrell, D. (1996). "Impacts of Highway Bypasses on Kansas Towns." As prepared for the Kansas Department of Transportation, October 1996, Report No. 226. Retrieved 9/4/06 from [www.ipsr.ku.edu/resrep/bypass.htm](http://www.ipsr.ku.edu/resrep/bypass.htm).
- Centre for Economic and Business Research* (1994), 'The Economic Impact of Different Levels of Expenditure on the Roads Programme', 2, 41-65.
- Jacobsen, M. (2012), 'Evaluating U.S. Fuel Economy Standards in a Model with Producer and Household Heterogeneity', *University of California at San Diego*, 29-66.
- Litman, T. (2009), 'Transportation Cost and Benefit Analysis', *Victoria Transport Policy Institute*, 2, 78-164.
- Litman, T. and Colman, S. B. (2001), "Generated traffic: Implications for transport planning". *Institute of Transportation Engineers. ITE Journal*, 71(4), 38-47.
- Kadiyali.L.R (1985), 'Traffic and Transportation Planning', *Khanna Publishers, New Delhi*.
- Rephann, T., and A. Isserman (1994). "New Highways as Economic Development Tools: An Evaluation Using Quasi-Experimental Matching Methods." *Regional Research Institute, West Virginia University*.
- [www.cmdachennai.gov.in/Economy.pdf](http://www.cmdachennai.gov.in/Economy.pdf), 3(4), 4-22.
- [www.cmdachennai.gov.in/Traffic and Transport.pdf](http://www.cmdachennai.gov.in/Traffic%20and%20Transport.pdf), 3(5), 2-26.
- [www.dieselnet.com/standards/in/](http://www.dieselnet.com/standards/in/).



## Effect of Axle Load Spectrum on Design of Rigid Pavement

Ezatullah Rahimi<sup>1</sup>, S.N. Sachdeva<sup>2</sup>

<sup>1</sup>M.Tech student, Department of Civil Engineering, National Institute of Technology Kurukshetra, Haryana-136119, India,  
Email:Ezatullah.rahimi888@gmail.com (Corresponding Author)

<sup>2</sup>Professor, Department of Civil Engineering, National Institute of Technology, Kurukshetra, Haryana-136119, India,  
Email:snsachdeva@nitkkr.ac.in

### ABSTRACT

Design of rigid pavements is done considering the flexural stress under the simultaneous action of load and temperature gradient for different categories of axles. Sum of cumulative fatigue damage caused by single, tandem and tridem axle load applications causing tensile flexural stress at the top and the bottom of the pavement slab should be less than one for the design to be safe. The legal axle load limits in India are 10.2 tonnes (100KN), 19tonnes (186KN) and 24 tonnes (235KN) for single, tandem and tridem axle respectively. In service cement concrete pavements are subjected to stress due to a variety of factors acting simultaneously. The severest combination of different factors that induce the maximum stress in the pavement will give the critical stress condition. The flexural stress due to the simultaneous application of traffic loads and temperature differential between the top and bottom fibres of concrete slab is considered for design of pavement thickness. The influence of traffic as an input parameter for mechanistic-empirical pavement analysis on the percentage of fatigue cracks on slabs determines the required slab thickness for jointed concrete pavement. The traffic is considered in the design in terms of number of commercial vehicles per day and the axle load spectrum of the vehicles. Most often, the number of commercial vehicles is known but the axle load of the vehicles or the axle load spectrum is not known. This paper presents an overview of the effect of variation in axle load spectrum on thickness design of a rigid pavement which will help us understand the need of how accurately the axle load spectrum is required for the design.

**KEYWORDS:** *Axle load spectrum; cumulative fatigue damage analysis; thickness design of rigid pavement; ESAL*

### INTRODUCTION

A rigid pavement is constructed from cement concrete or reinforced concrete slabs. The design of rigid pavement is based on providing a structural cement concrete slab of sufficient strength to resist the loads from traffic. The concept of axle load spectrum is the computation of cumulative fatigue damage for thickness design of rigid pavement. The basic factors governing design of concrete pavements are design period, design commercial traffic volume, composition of commercial traffic in terms of single, tandem, tridem and multi-axles, axle load spectrum, tyre pressure, lateral placement characteristic, directional distribution, strength of foundation and climatic consideration. The legal axle load limits in India are 10.2 tonnes, 19tonnes and 24 tonnes for single, tandem and tridem axle respectively, a huge number of axles operating on NH convey much weighty loading than the valid limits. Data on axle load spectra of the commercial vehicles is need to count the repetitions of single, tandem and tridem axles in each orientation attended pending the design term. Axle load survey may be conducted for a continuous 48-hour period. The vehicle to be surveyed may be selected randomly to avoid bias. Information on typical spacing among repeated axles of commercial vehicles is needed to clarify the proportionality of axles that should be weighed for top-down cracking caused by axle loads during night time. The slab has the Disposition of curling up due to minus temperature differential. Data on the spacing of axles may be collected during the traffic survey. If the spacing between any pair of consecutive axles is less than the spacing of transverse joints, such axles need to be considered in the design traffic for computing top-down cracking damage. Cement concrete pavement may be designed to have a life span of 30 years or more.

For safe thickness design the cumulative fatigue damage due to wheel load and curling stresses at the bottom and top is less than one. In other words, a pavement is deemed to have failed if sum of cumulative damages is greater than one. This paper represent the effect of axle load on thickness design of rigid pavement, by increasing the axle load frequency the thickness will increase and by increasing the thickness, the cumulative fatigue damage will decrease. Load spectrum consist the distribution of loading for different classes of vehicles (class 4 to class 13) and different axle types (single, tandem and tridem) with these detailed loading data the design procedure can quantify the

accumulated damage from any particular type of loading that a cumulated traffic index (e.g. equivalent single axle load ESAL) was not capable of. However, using load spectra enhance some particle challenges for pavement engineers. The object of this study was to explore approaches that can provide a meaningful about load spectra and relate cumulative traffic loading to pavement performance(Yanqing Zhao , Yiqiu Tan & Changhong Zho, 2012).

## LITERATURE REVIEW

**Chen-Mingkue et al (2001)** reported that the concept of single axle load equivalency factor (LEF) was studied and developed by AASHO. The model was used to simulate the AASHO road test pavement section and developed by different formula for various pavement under axle loading. Some factors effected on design of pavement thickness like base course, joint and subgrade strength. One of the most famous method for evaluating stress, surface deflection and fatigue damage is equivalent single axle load (ESAL), it was developed by American Association of State Highway Official (AASHO). To improve and calculate accumulative traffic, a new regression formula was isolated by using 3-D finite element modeling. The ESWL concept was conducted by US corps engineer in 1950, between many procedures of counting equivalent wheel load factor (EWLF), the (ESAL) concept was one of the important procedures for pavement design.

This methodology was based on some the relationship between serviceability of pavement and wheel repetition. The equations shown the relationship between equivalent single axle repetition, slab thickness D (inch), axle load L1 (kips), axle type L2 (single axle=1, tandem=2 and tridem=3) and terminal serviceability of pavement Pt. So 80 kN (18kips) single axle was accepted as standard axle. LEF of different type of axle calculated by equation (1).

$$LEF_x = \frac{dx}{d18} = \frac{\frac{1}{wx}}{\frac{1}{w18}} = \frac{w18}{wx} = \left[ \frac{(l1+l2)^{4.62}}{(18+1)^{4.62} \times l2^{3.28}} \right] \times \left[ \frac{10^{Gt/\beta 18}}{10^{Gt/\beta x}} \right] \quad \text{Eq. (1)}$$

$$\beta = 1.00 + \frac{3.63(L1+L2)^{5.2}}{(D+1)^{8.46} \times L2^{3.52}} \quad \text{Eq. (2)}$$

$$Gt = \log \left[ \frac{4.5 - Pt}{4.5 - 1.5} \right] \quad \text{Eq. (3)}$$

Where

$\beta$  – Factors depends upon the thickness of slab, axle load and axle type

Gt – it's depend upon the terminal serviceability of pavement

$LEF_x$  – equivalent load factor of the x axle load type

dx- the damage caused by one application of the axle type x

d18- the damage caused by one application of the standard axle load

$\beta_x$ - the  $\beta$  of the axle type x

$\beta_{18}$ - the  $\beta$  of the standard axle 80KN

$W_x$  – the number of load application at Pt for the axle type x

$W_{18}$  - the number of load application at Pt for the standard axle

Pt - terminal serviceability of pavement (2 and 2.5)

Table 1 shows the material properties of a typical pavement.

**Table.1 Material properties of PCC slab and base course in AASHO road test (1962)**

Pavement Type	Young's modulus (static 28 days)	Poisson's ratio	Unit weight (kg/cm <sup>3</sup> )	Thermal expansion coefficient
---------------	-------------------------------------	-----------------	--------------------------------------	-------------------------------

PCC slab	28.9 Gpa	0.15	$2.41 \times 10^{-3}$	$9.9 \times 10^{-6} 1/C^{\circ}$
Base	0.289 Gpa	0.40	$1.98 \times 10^{-3}$	$14.4 \times 10^{-6} 1/C^{\circ}$

The figures 1 to 4 show the relationship between equivalency load factor, slab thickness, terminal serviceability and axle loads.

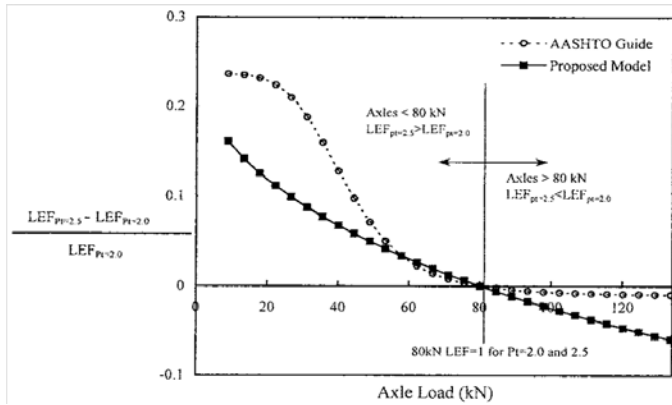


Fig.1 LEF variation ratio for Pt. Change

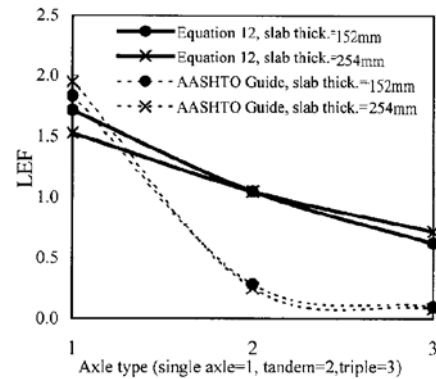


Fig.2 LEF variation due to different axle

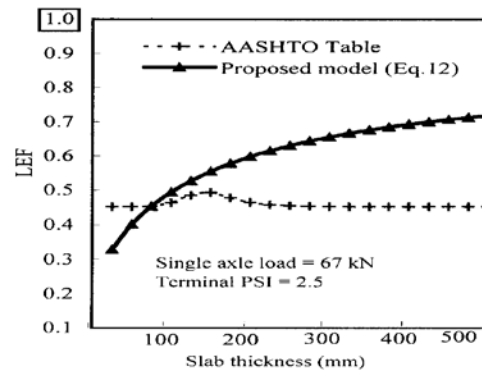
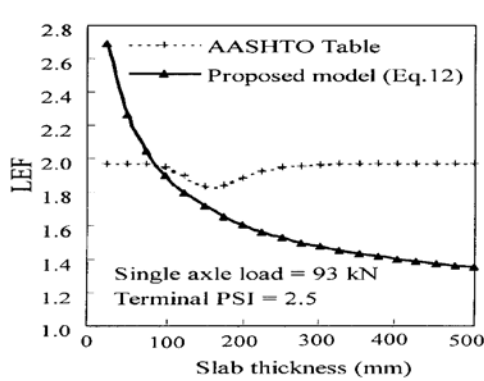


Fig.3 LEF variation for different slab thickness

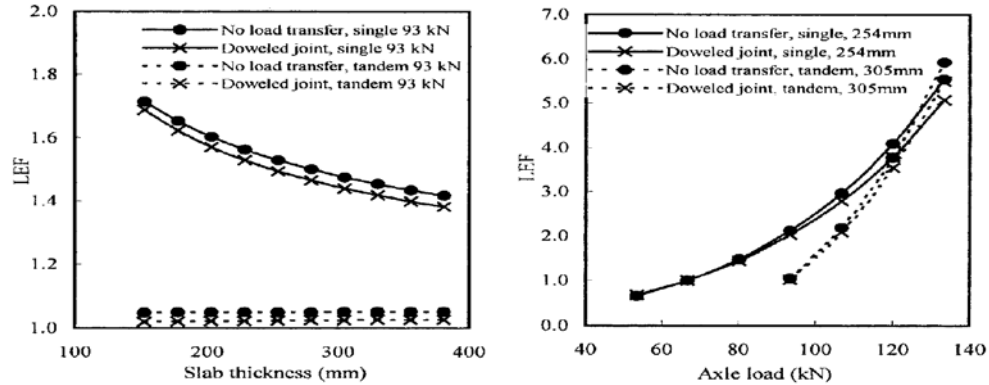


Fig.4 The effect of dowel joints on LEF for various situations

Danny x. Xiao et al (2016) have studied that the truck axle load spectrum in the Mechanistic Empirical pavement Design Guide (MEPDG) had advancement in pavement design due to individual axle load. In this issue it was reported that characterized three image of loading to pavement design volume, load and damage. Four Epitome indicators were investigated in this study, cumulative truck volume (CTV), cumulative truck load (CTL), equivalent single axle load (ESAL) and relative pavement performance impact (RPPI).

(CTV)- is the volume of traffic that the engineers who need to know how many vehicles travel on a road at what time and it's depend upon on annual average daily traffic (AADT).

(CTL)- It is a new index about loading information of traffic flow.

(ESAL)- It is an equivalent axle loading for calculating the different axle load of traffic.

(RPPI)- It is to identify normalized axle load spectrum in each vehicle class and axle type.

Sara I.R. Amorim et al (2015) reported that most of pavement need to the design traffic, based on the alteration of the traffic spectrum to be counted in to a number of equivalent passages of a standard axle using the (ESALF). In general these factors considered only the type of axle like (single, tandem and tridem), but they do not consider the types of wheels like single and dual wheel. The first equivalency factors used to determine the number of ESAL were based on present serviceability index and it is depend upon on the type of pavement and thickness of the pavement surface. Table2 shows the different axles load spectrum by various frequency of axles it has done as the example on IRC: 58-2015.

Table.2 Different types of axle load spectrum

Rear Single Axle			Rear Tandem Axle			Rear Tridem Axle		
Load Group (kN)	Mid-Point of Load Group (kN)	Frequency (%)	Load Group (kN)	Mid-Point of Load Group (kN)	Frequency (%)	Load Group (kN)	Mid-Point of Load Group (kN)	Frequency (%)
185-195	190	18.15	380 - 400	390	14.5	530-560	545	5.23
175-185	180	17.43	360 - 380	370	10.5	500-530	515	4.85
165-175	170	18.27	340 - 360	350	3.63	470-500	485	3.44
155-165	160	12.98	320 - 340	330	2.5	440-470	455	7.12
145-155	150	2.98	300 - 320	310	2.69	410-440	425	10.11
135-145	140	1.62	280 - 300	290	1.26	380-410	395	12.01
125-135	130	2.62	260 - 280	270	3.9	350-380	365	15.57
115-125	120	2.65	240 - 260	250	5.19	320-350	335	13.28
105-115	110	2.65	220 - 240	230	6.3	290-320	305	4.55
95-105	100	3.25	200 - 220	210	6.4	260-290	275	3.16
85-95	90	3.25	180 - 200	190	8.9	230-260	245	3.1
< 85	80	14.15	< 180	170	34.23	< 230	215	17.58
		100			100			100

**Surya Teja Swarna et al (2017)** it have been reported that for finding the stress in concrete pavement using westergard's & Bradbury's theory has not given correct values. Thus in IRC: 58-2011 and IRC: 58-2015 has given some chart for design based on KGPSLAB software. Table 3 shows the stress in CCP for different type of load.

**Table.3 Stress in concrete pavement without concrete shoulder for 250mm PQC and k=300Mpa/m**

Wheel Loads, kN	Temperature Differential, °C	Stresses (MPa) in Slab without CONTA175	Stresses (MPa) in Slab with CONTA175	Stress (MPa) from Charts of IRC:58-2015
120	00	1.290	1.280	1.250
	09	1.840	1.940	1.980
	15	2.310	2.380	2.420
	21	2.620	2.700	2.750
160	00	1.720	1.680	1.650
	09	2.290	2.320	2.310
	15	2.660	2.780	2.720
	21	3.070	3.180	3.000
200	00	2.160	2.080	2.000
	09	2.640	2.710	2.690
	15	3.160	3.170	3.170
	21	3.420	3.590	3.500

**A.C.Bordelon et al (2015)** reported that the influence of traffic loading for Mechanistic-Empirical (ME) pavement analysis was investigated for finding percentage of fatigue cracking & thickness of slab. This investigation has developed on the Illinois weigh station of United States. The load spectrum for many sites were developed by changing the (AADTT) volume to generate the same (ESALs).

**B.S Morton et al (2004)** reported that for designing the concrete pavement there are several parameter, two of these important are axle load and contact stress, which that these are directly depended upon on tyre inflation pressure. It was investigated on South African and international load variation in maximum axle load is between 8-9 tonne and the grass combination mass is 56 tonnes with the maximum axle load 9 tonnes. Figure 5 and 6 shows Axle Load Distribution and Tyre Inflation Pressure Distribution in pavement.

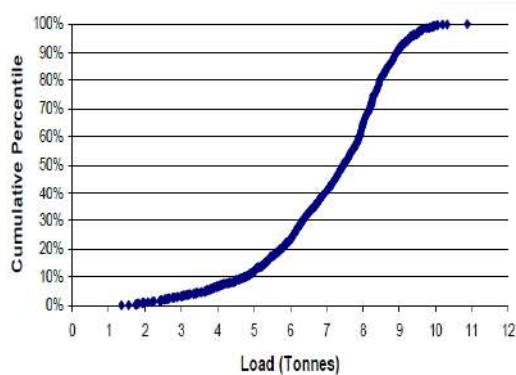


**Fig 5 cumulative distribution of axle load**

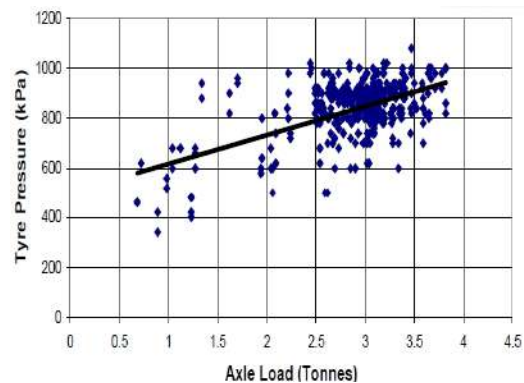


**Fig.6 axle load versus tyre inflation pressure (steering axles)**

As per IRC: 58-2015 the cumulative number of commercial vehicles during the design period may be estimated from the equation (2).

$$C = \frac{365 \times A \{ (1+r)^n - 1 \}}{r} \quad \text{Eq. (4)}$$

C = Cumulative number of commercial vehicles during the design period

A = initial number of commercial vehicles per day in the year when the road is opened to traffic

r = annual rate of growth of commercial traffic volume (expressed as decimal)

n = design period in year

**Design of slab thickness:** thickness design depends upon the flexural stress due to loading and temperature. The flexural stress at the bottom layer of the CC slab is the high during the day time when the axle loads act midway on the pavement slab while there is a positive temperature as illustrated in fig 7 and 8. This condition is likely to produce Bottom-Up cracking.

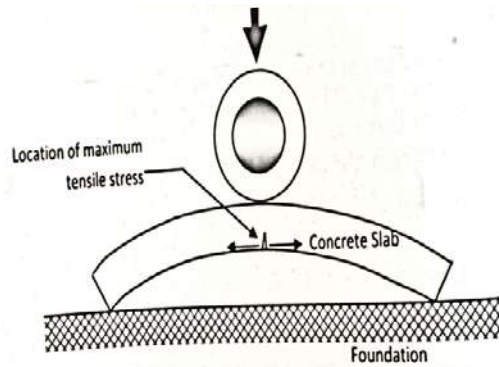


Fig 7 Axle load placed in the middle of the slab during mid-day

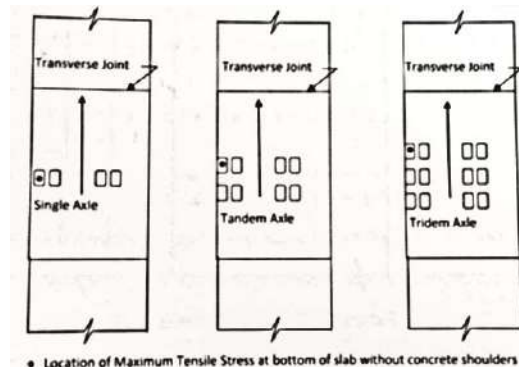


Fig 8 placement of axles for maximum edge flexural stress at bottom of the slab without concrete shoulder

During the night hours, the top surface is cooler than the bottom surface and the end of the slab curl up a concave shape resulting in loss of support for the slab as shown in fig 9. Positioning of axles of different configurations on the slab with successive axles placed close to the transverse joints is shown in fig 10. These axle positions can initiate Top-Down cracking during night hours.

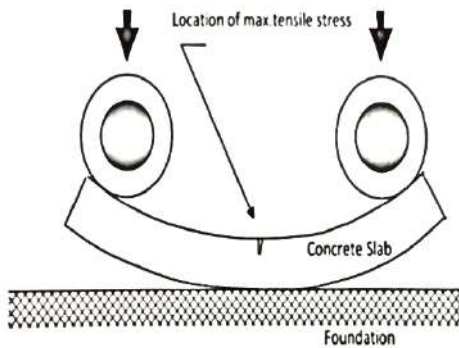


Fig.9 Placement of two axles commercial vehicle

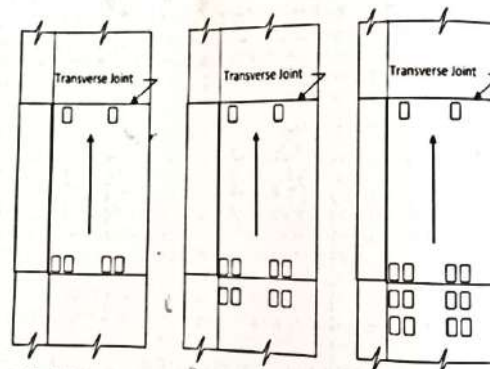


Fig.10 Different axle load positions causing tensile stress at the top fiber of the slab with tied concrete shoulder.

**Cumulative fatigue damage analysis:**

For a typical slab thickness and other design factors, the pavement shall be checked for cumulative top-down and bottom-up fatigue damage. For bottom-up cracking, the flexural stress at the edge due to the combined action of single or tandem rear axle load and positive temperature differential is considered as the equation (5).

For top-down cracking the flexural stress due to combined action of single, tandem and tridem rear axle load and negative temperature differential is calculated as the equation (6).

$$CFD (BUC) = \sum_i^j \frac{n_i}{N_i} (10AM \text{ to } 4PM) \quad \text{Eq. (5)}$$

$$CFD (TDC) = \sum_i^j \frac{n_i}{N_i} (0AM \text{ to } 6AM) \quad \text{Eq. (6)}$$

Where,

$N_i$  – allowable of number load repetitions for the  $i^{\text{th}}$  load group during the specified six-hour period

$n_i$  – predicated number of load repetitions for the  $i^{\text{th}}$  load group during the specified six-hour period

$j$  – Total number of load group

If the sum of cumulative fatigue damages (1) due to wheel load and curling stresses at the bottom and (2) wheel load and curling stresses at the top is less than 1, the pavement is safe. In other words, a pavement is deemed to have failed if sum of cumulative damages is greater than one.

Thus if  $CFD (BUC) + CFD (TDC) \leq 1$ , the pavement is save from large scale cracking. The design thickness may be increased by 10mm to (1) to permit two retexturing and (2) grinding to rectify faulting during the service life.

Fig 11 shows the relationship between flexural stress and slab thickness due to single axle load of 80 kN at  $\Delta T = 0^\circ\text{C}$  without concrete shoulders and fig 12 shows the relationship between flexural stress and slab thickness due to Tandem axle load of 480 kN at  $\Delta T = 21^\circ\text{C}$  with tied concrete shoulders.

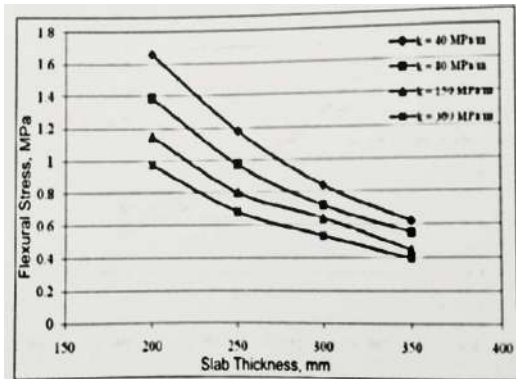


Fig. 11 stress due to single axle load of 80kN

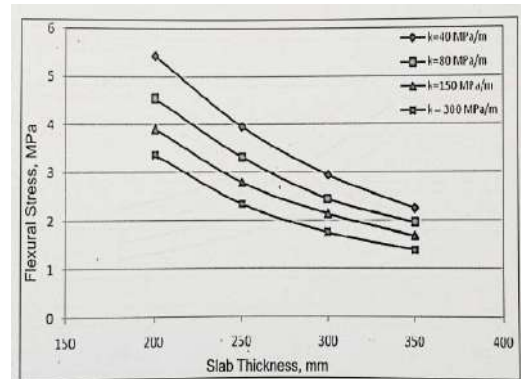


Fig. 12 stress due to Tandem axle load of 480kN

## CONCLUSIONS

On the basis of above mentioned studies it can be concludes that:

1. Design of rigid pavements is done considering the flexural stress under the simultaneous action of load and temperature gradient for different categories of axles.
2. Sum of cumulative fatigue damage caused by single, tandem and tridem axle load applications causing tensile flexural stress at the top and the bottom of the pavement slab should be less than one for the design to be safe. Thus if  $CFD (BUC) + CFD (TDC) \leq 1$ , the pavement is save from large scale cracking.
3. By increasing of slab thickness, the cumulative fatigue damage will decrease and by decreasing slab thickness it is versa.
4. The main factors governing design of concrete pavements are design period, design commercial traffic volume, composition of commercial traffic in terms of single, tandem, tridem and multi-axles, axle load spectrum, tyre pressure, lateral replacement characteristic, directional distribution, strength of foundation and climatic consideration.
5. Axle load spectrum affects the thickness of concrete pavement. More severe the axle load frequency in the higher categories of load spectrum like 150 kN and higher, more is the flexural stress and fatigue damage which requires more thickness of the pavements. However, more frequency of axles loads in the lower

categories of axle load spectrum of value less than 150 kN does not lead to a higher thickness of the pavement.

6. The function of  $LEF_s$  is to change repetitions of particular axle to the equivalent utilization of the standard axle.
7. The flexural stress at the bottom layer of the concrete slab is the maximum during the day hours, there is a positive temperature gradient. This condition is likely to produce Bottom-Up cracking. The flexural stress at the top layer of the concrete slab is the maximum during night hours, so the temperature of the top layer is cooler the bottom layer, than this condition is likely to produce Top-Down cracking.
8. By the increasing of load repetition the flexural stress will increase and by increasing flexural stress, fatigue damage also increases.

## REFERENCE

- AASHO ([American Association of State Officials](#)) road test (1962).
- A. C. Bordelon<sup>1</sup>; J. E. Hiller<sup>2</sup>; J. R. Roesler<sup>3</sup>; and V. G Cervantes<sup>4</sup> (2015) “Investigation of ESALs versus Load Spectra for Rigid Pavement Design” *Airfield and Highway Pavements 2015* © ASCE 2015.
- B.S Morton<sup>1</sup>, E. Luttig<sup>1</sup>, E. Horak<sup>2</sup> and A.T. Visser<sup>2</sup> (2004), “The Effect of Axle Load Spectra and Tyre Inflation Pressures on Standard Pavement Design Methods”, *Proceedings of the 8th Conference on Asphalt Pavements for Southern Africa (CAPSA'04)*.
- Chen-Ming kue and Shen-Hsian Lin (2001) “An analytical study of axle load equivalency factors of concrete pavements” *Journal of the Chinese Institute of Engineers*.
- Danny x. Xiao, Zhong Wu (2016) “Using systematic indices to relate traffic load spectra to pavement performance” *International Journal of Pavement Research and Technology* 9 (2016) 302–312.
- Indian Roads Congress (IRC: 58-2015) “Guidelines for the Design of Plain Jointed Rigid Pavements for Highways” (Fourth Revision).
- Jorge A. Prozzi & Feng Hong (2009) “Optimum statistical characterization of axle load spectra based on load associated pavement damage” *International Journal of Pavement Engineering*.
- Sara I.R. Amorim, Jorge C. Pais, Aline C. Vale & Manuel J.C. Minhoto (2015) “A model for equivalent axle load factors” *International Journal of Pavement Engineering*.
- Surya Teja Swarna, Braj Bhushan Pandey (2017) “Analysis and design of concrete pavements: A new approach” *Invitation International seminar on Repair, Rehabilitation and Retrofitting of Bridge & Structures*.
- Yanqing Zhao, Yiqiu Tan & Changhong Zhou (2012) “Determination of axle load spectra based on percentage of overloaded trucks for mechanistic empirical pavement design” *Road Materials and Pavement Design*.



## A Review on Warm Mix Asphalt

Gandu Srikanth,<sup>1</sup> Rajiv Kumar <sup>2</sup>  
Rohit Vasudeva <sup>3</sup>

M.Tech Student<sup>1</sup>\*, Department of Civil Engineering, Lovely Professional University, 144411, Punjab, India.  
[gandusreekanth@gmail.com](mailto:gandusreekanth@gmail.com)

Assistant Professor <sup>2</sup> Department of Civil Engineering, National Institute of Technology- Jalandhar, 144011, Punjab, India.  
[kumarr@nitj.ac.in](mailto:kumarr@nitj.ac.in), Corresponding Author

Assistant Professor<sup>3</sup> Department of Civil Engineering, Lovely Professional University, 144411, Punjab, India.  
[rohit.22225@lpu.co.in](mailto:rohit.22225@lpu.co.in)

### ABSTRACT

Warm Mix Asphalt (WMA) is a new trend developed in Europe and after successful implementation in Europe USA also accepted the warm mix technology in all 50 states. Presently in India Central Road Research Institute – Delhi and some of the other organization working on this trend. To reduce the emission of various hazardous gas fumes, consumption of fuel, compaction & placing Temperature and haul distance industries have Warm Mix Asphalt instead of hot mix asphalt (HMA). Here they achieve all the properties similar to HMA meanwhile reducing demerits of HMA by adding various types of additives like emulsions, wax based, chemical & foam technologies etc. By the order of Supreme Court of India to shut down HMA plants in metropolitan cities so, WMA is an alternative mix type in metropolitan cities. This paper is the review about various trends, merits & de-merits, technical aspects, various temperatures of additives while adding with binders, various live examples where this technology implemented, mix design, performance tests on WMA

**KEYWORDS:** *Warm; Cold and Hot mixes; Mixing and Compaction Global Warming; Haul Distance.*

### INTRODUCTION

The hot mix asphalt industries constantly working to develop various technologies to enhance pavement performance, construction efficiency, conserve resources, material improvement and environmental aspects (Newcomb 2007). In that case, Hot mix asphalt also has a significant role in fuel consumption for heating aggregates and binder and release various hazardous air pollutants. So, manufacturers need an alternative mix type that can reduce these effects with same or better results. In HMA, temperature maintenance of aggregates, binder and mix is a major issue so, to defeat that, asphalt industries constantly working on various asphalt mixes (Ex: Warm & Half-Warm, Cold, LEA etc.) by reducing mixing & compaction temperature which will lead to reduce energy consumption and environment pollutants. Mixing temperature of WMA is 110 to 140 °C compare to HMA of 150 to 180 °C (Behl et al. 2013). To safeguard the fossil fuel utilization, strong environmental acts, economical, haul distances and global warming researchers are focusing on the warm mix technology (Figure 1).



Figure 1 Sustainable Development (D'Angelo 2008)

WMA is a generic term for various technologies and products that are incorporated into plant produced HMA to decrease the plant mixing, roadway paving and compaction temperatures while maintaining workability. It's a compaction aid for HMA. Warm mix is produced by decreasing the viscosity of binder or Surface Tension at Asphalt Aggregate Interface or by increasing workability of mix in less temperature. WMA allow mixing, placing and transporting process at low temperature. It's not a mix type it is a technology that can use in any mix type where to decrease mixing & compaction temperature (*MS-2 2014*).

The main goal of this paper is to write a review on the aspects associated with WMA involving background, history, advantages and dis-advantages, various WMA technologies & mechanism's, mix design, best practices for producing WMA, lab experiments of warm mix asphalt and Various projects in India.

**Background** (Button et al. 2007) & (Table-1)

Warm mix technology was developed in Europe (1997) then by US (2002) the first trial took place in Europe (1999), USA(2004), India (2009). Many countries like USA, Canada, Germany, France, India etc countries adopted this technology on public roads after successful field tests like the Central Road Research Institute -New Delhi for India.

Table 1: Various Trend Developments (Button et al. 2007)

Sl.No	Year	Details/Place	Type of Technology	Remarks
1	1956	LadisCsanyi, Iowa State University	Foamed	Foamed bitumen for use as a soil binder
2	1968	Mobil Oil Australia	Foamed	Adding cold water rather than steam into the hot bitumen
3	1970	Chevron	*	He developed mixing & Thickness Design
4	1997	Chevron	*	He published full detailed code "Bitumen mix manual ".
5	1994	Maccarrone, G.Holleran	Foamed (Cold Mix)	He introduced Cold Mix Asphalt using Foamed Technology
6	1995	Shell Bitumen		They filed a patent on Warm mix asphalt
7	1997	Sasol Wax International, Europe	Wax	They introduced Sasobit in WMA
8	1999	Jenkins, A.A.A.Molenaaretc		They introduced Half Warm-Mix technology.
9	2000	Koenders		He introduced this WMA in open & Gap Graded and stone mastic asphalt

**Advantages :-**(D'Angelo et al 2008),(AmbikaBehl 2016),(EAPA 2010), (Sangiorgi 2018), &(Prowell et al. 2014).

- a) **General:** Significant less mixing & compaction temperature, less energy consumption, reduce hazardous fumes emission, due to less difference between placing and surrounding ambient temperature we can have long-haul distances, paving in un-attainable places, reduce thermal segregation, less aging effect, faster construction i.e, compaction temperature is less (less curing time) so we can open traffic in less time only , Improved deep lift & thin lift in Asphalt pavement, WMA has good compatibility with RAP so there is reduction in usage of virgin materials and give good kick start to recycle theme (Zaumanis 2010)
- b) **Environment:** Mainly it decreases greenhouse gases by 25-30%. So, this would earn tradable carbon credits (IRC:SP:101- 2014). It is quite compactable with reclaimed asphalt pavement technology (RAP) that saves utilizing virgin materials and reduce the hazardous effect of dumping the damaged pavement materials. Typically 30-40 % of CO<sub>2</sub> & SO<sub>2</sub>, 50 % of Volatile Organic Compounds, 10-30 % or CO, 60-70 % of NO<sub>x</sub> and 20-25 % of dust reduced by using WMA(D'Angelo et al 2008)(Table-2). Decreasing the mixing temperature leads to the energy consumption of 35 % and more based on process.

Table 2: Various pollutant % in Various Countries (D'Angelo et al 2008)

<b>Emission</b>	<b>Norway</b>	<b>Italy</b>	<b>Netherlands</b>	<b>France</b>
<b>CO<sub>2</sub></b>	31.5	30-40	15-30	23
<b>SO<sub>2</sub></b>	NA	35	NA	18
<b>VOC</b>	NA	50	NA	19
<b>CO</b>	28.5	10-30	NA	NA
<b>NO<sub>x</sub></b>	61.5	60-70	NA	18
<b>Dust</b>	54.0	25-55	NA	NA

- c) **Health Benefits:** During mixing PAH fumes contain carcinogenic, mutagenic and teratogenic elements that cause severe health issue for workers.30-50 % of aerosol/fumes and polycyclic aromatic hydrocarbons (PAH) that affect the workers and surrounding area peoples also get reduced(Prowell et al 2014).
- d) **Technical Advantages:** Less aging& oxidation of bitumen that delay fatigue cracks of pavement, high workability, enough compaction time, longer haul distances, allow construction during cold weather condition also.
- e) **Economical:** Average production temperature of WMA is 27-30°C that results an average 22.1 % decrease in fuel consumption and rest temperature maintain vehicles, burners etc make the value 35 % energy consumption so parallely the cost also reduced. Decrease load on Mixing Plant leads to less maintenance and extend plant life.
- f)

**Drawbacks:** WMA is susceptibility to moisture damage. Due to less mixing temperature leads to incomplete drying of aggregates the moisture may get trapped in the pavement and leads to moisture damage. WAM have less aging (Stiffness) of binder so it faces rutting. The initial production cost of WMA is high (Ex: Production at Iceland per-ton \$0.30 for WAM-Foam, \$3.50 for Sasobit, and \$4.00 for Aspha-Min).

**Classification of Warm mix technologies & Mechanisms** :(Capitão et al. 2012),(D'Angelo et al 2008),(Button et al. 2007)& (Rubio et al. 2012).

The basic principle of this technology is to add additives to the final mix, in this coating of aggregates with the binder is highly achieved within less temperature typically ( $30^{\circ}\text{C}$  less) than of hot mix temperature. Viscosity plays an important key role in the coating of aggregates. To achieve this warm mix by a) lowering the viscosity of binder b) reduction of surface tension at aggregates and bitumen interface.

Many authors have classified this warm mix technologies by many types based on Purpose type of additives etc. Here in this paper considering the classification according to Indian Standard Code for WMA IRC-SP:101-2014, CRRI -Delhi authored Papers and (MS-2 2014) (Dinis-almeida 2010)& (IRC:SP:101- 2014).

**There are mainly two classifications of Warm mix technologies.**

1) Based on temperature parameter (Figure 2). A) Cold Mix: It is produced in ambient temperature by using foam and emulsions B) Half -Warm Mix Asphalt have these temperatures ranges from 65 to  $100^{\circ}\text{C}$  C) Warm Mix Asphalt: It has the mixing & compaction temperature is 110 to  $140^{\circ}\text{C}$  just above water boiling point. D) Hot Mix: it has a production temperature of  $150\text{-}180^{\circ}\text{C}$ .

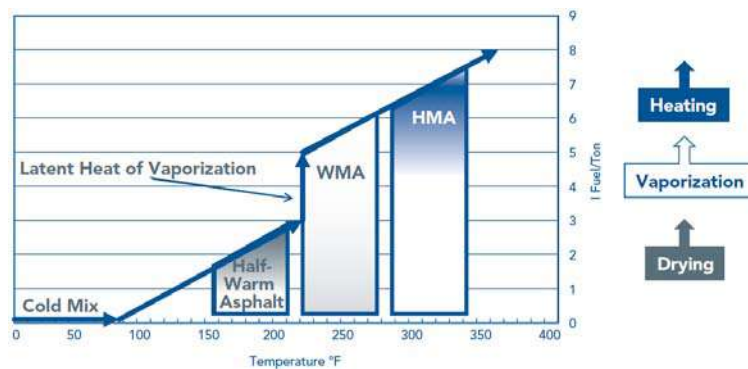


**Figure 2: Classification by temperature range, temperatures, and fuel usage are approx. (D'Angelo et al 2008)**

2) Based on the type of additive we have three types a) Foaming (Water containing & Water based) b) Chemical (polymers & Emulsification agents) c) Organic (synthetic wax, fatty acids, amides).

3) Based on purpose: a) Hybrid b) Rheological Modifiers c) Others

**a) Foaming** :(Zaumanis 2010) (Hurley et al. 2005) water expand 1600 times when converted into steam at atmospheric pressure when this steam gets entrapped with viscous bitumen it produces foam then results in an increase in its volume and decrease in viscosity(AmbikaBehl 2016). When preheated aggregates combine with this foam (high volume bitumen or high surface area bitumen) enable coating of aggregates at a lower temperature. Foaming technology is subcategorized into two types a) water-based b) water combined. In the water-based water is injected with a foam generating machine and on other hand water combined here we use zeolites like aluminosilicates of alkali metals (have 20% water content) when this type of zeolites gets combined with preheated binder water get release and the same process continue to produce foam and warm mix. These synthetic zeolites are added to the binder at the rate of 0.25 % by weight. Due to the presence of water stripping may occur so to overcome this issue it is recommended to have chemical additives that promote the coating of aggregates and decrease water sensitivity of mix.

Foaming technology is also used in Low Emission Asphalt (LEA) process. Here coarse and a portion of fine aggregates are heated at normal HMA temperature and a coating and adhesion additives approx 0.50 % by weight of binder after adding them heated, wet, coated and remaining fine aggregates or RAP mix together during this vapors of 3-4 % is released and turn into foam and process continue up to aggregate coating.

Foam asphalt is also used in two-stage WMA process. It has two binders soft and hard binder. Soft binder ranges between 20-30 % to total binder content first they make completely coat coarse aggregates and on second hard binder get a coat to pre-coated aggregates.

Ex: Aspha Min, Advera, Double barrell green, Ultrafoam GX

**b) Chemical** :(Hurley et al. 2006) Generally this technology doesn't depend on viscosity or foaming to make changes in mixing and compaction temperature it uses improves chemical additives as surface agents, improve aggregate coating, anti-stripping agent's. It mostly contains polymers and emulsification agents etc. Generally, these chemicals will get mix with binder directly. At normal temperature, it improves interfacial adhesion.

Ex: Rediset&Cecabase improve wetting of aggregates by bitumen, Evotherm is an American technology which absorbs less water than emulsions. Evotherm 3G is the latest technology which is a water-free warm technology.

Ex: Evotherm, rediset& Table 3

**c) Organic** :(Hurley and Prowell 2005)

When this additive's heated to a temperature above its melting point and increase binder's stiffness at normal temperature reduces the viscosity of binder at a lower temperature and maintain the same for a long time that allows proper compaction. Generally, most of this organic additive has a crystalline structure like sasobit that consist 45-115 carbon atoms & paraffin waxes have 25-40 carbon atoms(AmbikaBehl 2013). Waxes have long molecular hydrocarbon chain when they combine with bitumen there is a chance of changing binder carbon chain length that alters few properties of bitumen in terms of stiffness & viscosity etc. While adding organic additives (Wax type) to binder firstly heat the additive to its softening point and then add to binder this allows to reduce viscosity of the binder in lower temperature.

Ex: Sasobit, Asphaltan-B,Cecabase& Table 3

**d) Hybrid** :( IRC: SP: 101- 2014) It's a combination of two more technologies to achieve required results.

Ex: Low Energy Asphalt is a combination of Chemical and water based on improving aggregate coating at less temperature.

**e) Rheological Modifiers** :( IRC: SP: 101- 2014) Here industries use such an additive to improve the rheological properties of asphalt mix.

Ex: - Wax based additives modify the viscosity of binder.

**f) Others** :-( IRC: SP: 101- 2014) These are such products manufactured for other purposes but we incorporating them to produce warm mix.

Ex:- Sulfur & Trinidad Lake Asphalt

**Table 3: Summary of Warm Mix Additives with Usage & Mixing Temperatures**

Foaming Additive			
WMA Technology	Company	Recommended Additive/ Usage	Mixing Temperature (°C)
Aspha-min®	Eurovia and MHI	0.3% by total mass of the mixture	130-170 based on Binder Stiffness
ADVERA® WMA	PQ Corporation	0.25% by total mass of the mixture	130-170 based on Binder Stiffness
WAM-Foam®	KoloVeidekke Shell Bitumen	No additive. It is a two-component binder system that introduces a soft and hard foamed binder at different stages during plant production.	110 - 120
LEA®	LEA-CO	0.2-0.5% by weight of the binder	<100
LEA, also EBE and EBT	LEACO, Fairco, and EIFFAGETravauxPublics	0.2 to 0.5 % by weight of Bitumen	<100
ECOMAC	Screg	Unknown Quality & Quantity	Placed at above 45
LT Asphalt	Nynas	0.5–1.0% of a hygroscopic filler	90
LEAB®	BAM	0.1% by weight of the binder	90
Organic Additives			
WMA Technology	Company	Recommended Additive/ Usage	Mixing Temperature (°C)
Sasobit®	Sasol	0.8-3.0% by weight of asphalt	130-170 based on Binder Stiffness
Asphaltan-B®	Romonta	2.5% by weight of asphalt	130-170 based on Binder Stiffness
Licomont BS 100®	Clariant	3% by weight of asphalt mixture	130-170 based on Binder Stiffness
3E LT or Ecoflex	Colas	Unknown quantity	30-40 drop from HMA
Chemical Additives			
WMA Technology	Company	Recommended Additive/ Usage	Mixing Temperature (°C)
CECABASE RT®	Arkema Group	0.2-0.4% by weight of asphalt	90-100
Evotherm®	Meadwestvaco Asphalt Innovations	Improve coating, workability, and adhesion at lower temperatures.	85-115
HyperTherm/QualiTherm	Coco Asphalt Engineering	0.2-0.3 % by weight of the binder	120
Rediset WMX®	Akzo Nobel	2% by weight of the mixture	120-130
Emerging US technology			
WMA Technology	Company	Recommended Additive/ Usage	Mixing Temperature (°C)
Evotherm™	Mead-Westvaco	Unknown quantity	85-115
Double- Barrel Green	Astec	Not necessary; an antistripping agent may be added similar to normal HMA	116-135

**Mix Design Method:-** NCHRP 691 report “*Mix Design Practices for Warm Mix Asphalt*” recommended mix design process for WMA. These recommendations have already drafted in AASHTO R35 under “*Special Mixture Design Consideration and Models for Warm Mix Asphalt* “. These are the following conclusions given by NCHRP :

- a) HMA volumetric results will applicable to WMA if-and-only-if the binder absorption is less than or equal to 1 % of HMA.
- b) Coating, compatibility, moisture sensitivity, and rutting results are not similar to HMA & WMA.
- c) Compatibility was found to be different based technology, Production temperature used particularly when RAP is used.
- d) WMA is more susceptible to moisture damage than HMA so using any anti-stripping additives can decrease that due to less mixing temperature WMA is less resistance to rutting.
- e) Even aggregates & binder content is similar for both WMA & HMA specimen prepared under lab condition for stiffness test exhibiting different results after short-term aging.

**Best Practice for Producing WMA** (Prowell et al. 2014)

- a) Reduce Stockpile moisture content: On average 1% reduction of the moisture content of aggregates utilize 10% fuel saving for that we have two ways 1) Cover with any temporary/Permanent structure 2) grading of stockpiles
- b) Tune burners to ensure complete combustion: Mostly burners contain modulating actuator motor with the mechanical link with dampers and fuel valves. The disadvantage is at full firing range the maintenance of air to fuel ratio. Before starting it go through trail mix for ensuring that ratio if the ratio is not proper ie, incomplete combustion it can easily detect by brown coloration of coated aggregates.
- c) Drying aggregates with maintaining baghouse temperatures: The one most tough challenge in the production of WMA is stockpile temperature high to avoid condensation that results in corrosion of baghouse & formation of mud.

**Lab tests for Warm Mix Asphalt:** (Bonaquist 2011) & (IRC:SP:101- 2014)NCHRP: 691 & WMA IRC-SP:101-2014 have specified few performance tests for WMA although quality and performance tests are similar for both WMA & HMA as per IRC:111 guidelines but mixing and compaction temperature of WMA is 30 °C lesser than HMA.

They are three tests for WMA 1) Coating 2) Compatibility 3) Moisture Sensitivity.

- a) Compacting: AASHTO T 195 : Min 95 % of coarse aggregate shall be coated.
- b) Compatibility: AASHTO T245 : Ratio shall be such that  $0.9 < R < 1.1$
- c) Moisture Susceptibility: AASHTO T245 : Tensile Strength Ratio shall be greater than 80% as per IRC: 111

**Indian Scenario** :(Behl et al. 2013) & (Kumar 2016) India adopt this Warm Mix Asphalt since 2009 by Central Road Research Institute -New Delhi its first trail begins with 0.50 KM stretch road using Thiopave additive at Bavana Industrial area owned by DSIDC.

Basically, we have two WMA suppliers they are Shell and MWV (MeanWestvaco). Shell provide Thiopave and MWV supply Evotherm. Shell Thiopave get accreditation by IRC because they are improving the mechanical properties of AshokaBuildcon Ltd under gridlines of Ashoka Highway Research Center working on Thiopave since 2010. Since 2009 they are few projects constructed using WMA they are Bhavana Industrial Area (0.5 KM, 2009), NH-3 (210 KM, Thiopave, 2010), NH-10 (Evotherm,2011), SH-5 Gujarat (1KM, VG-30,2011).

## CONCLUSION:

Based upon the literature review its very clear that it has many advantages and for disadvantages, here have solutions to reduce its negative effect. It's an alternative way for HMA in metropolitan cities. WMA exhibiting same positive results of HMA (Approx). Due to lower mixing temperature, it is reducing the aging of binder that that

results in resistance towards thermal and fatigue cracks. WMA has good compatibility with waste & recycling materials like RAP, various plastic polymers, replaceable materials with aggregates and with binders so it's a user-friendly technology. As environmental, economic, health benefits of WMA compared with HMA have much better results that result in US, UK, Germany, Canada, and India etc like giant countries to adopt this technology in their public transportation infrastructure.

There is no evidence of reduction of CO in case of WMA; there is a reduction of 36% of total organic matter (Prowell et al. 2014).

In India Organic & chemical additive are better because for using they not required huge modifications of existing HMA plants (Prowell et al. 2011).

## ACKNOWLEDGEMENTS

With the grace of my parent's Srinivas Rao & Annapurna, my supporting faculty Mr.Charanjot Singh and Dr. Rajiv Kumar, I have been constantly empowering myself, professionally and personally. Mr.RohitVasudeva & Ms.Banita Sharma sustained and encouraged me in this field and encouraged me to write this paper. So, I would like to extend my heartfelt gratitude to all of them.

## REFERENCES

- AmbikaBehl., 2016. "Performance Characteristics Of Warm Mix Asphalt." PhD Thesis, IIT-Roorkee, India.<http://shodhbhagirathi.iitr.ac.in:8081/jspui/image/pdf/web/viewer.html?file=/jspui/bitstream/123456789/13851/1/thesis%20final%2014.4.pdf>
- AmbikaBehl. (2013). "Rheological Characterization of Bituminous Binder containing Wax based Warm Mix Asphalt Additive." *IOSR Journal of Mechanical and Civil Engineering*, 9(1), 16–22.<http://www.iosrjournals.org/iosr-jmce/papers/vol9-issue1/C0911622.pdf>
- Behl, A., Kumar, G., Sharma, G., and Jain, P. K. (2013). "Evaluation of field performance of warm-mix asphalt pavements in India." *Procedia - Social and Behavioral Sciences*, Elsevier B.V., 104, 158–167.<https://www.sciencedirect.com/science/article/pii/S1877042813044996>
- Bonaquist, R. (2011). *Mix design practices for warm mix asphalt. NCHRP Report 691*. Available online at [http://co-asphalt.com/wp-content/uploads/2015/03/nchrp\\_rpt\\_691.pdf](http://co-asphalt.com/wp-content/uploads/2015/03/nchrp_rpt_691.pdf) Accessed August 25, 2015.
- Button, J. W., Estakhri, C., and Wimsatt, A. (2007). "This synthesis documents the results of a comprehensive review of worldwide information dealing with the following issues as related to warm-mix asphalt ( WMA ) technology : current state of the art / practice of WMA , benefits and costs of WMA technology." 7(2).<https://static.tti.tamu.edu/swutc.tamu.edu/publications/technicalreports/0-5597-1.pdf>
- Capitão, S. D., Picado-santos, L. G., and Martinho, F. (2012). "Pavement engineering materials : Review on the use of warm-mix asphalt." 36, 1016–1024.<https://www.sciencedirect.com/science/article/pii/S0950061812004308>
- D'Angelo J, Harm E, Bartoszek J, Baumgardner G, Corrigan M, Cowsert J, Harman T, Jamshidi M, Jones W, Newcomb D, Prowell B, Sines R, Yeaton B. Warm-Mix Asphalt: European Practice FHWA Report No. FHWA-PL-08-007; 2008. <https://international.fhwa.dot.gov/pubs/pl08007/pl08007.pdf>
- Dinis-almeida, M. (2010). "Mix Design Criteria for Half Warm Asphalt Recycling ( HWMR ) - Case Study Mix Design Criteria for Half Warm Asphalt Recycling ( HWMR ) - Case Study." (May).[https://www.researchgate.net/publication/236118336\\_Mix\\_Design\\_Criteria\\_for\\_Half\\_Warm\\_Asphalt\\_Recycling\\_HWMR\\_-\\_Case\\_Study](https://www.researchgate.net/publication/236118336_Mix_Design_Criteria_for_Half_Warm_Asphalt_Recycling_HWMR_-_Case_Study)

- EAPA. (2010). "The Use of Warm Mix Asphalt." *Masterbuilder.Co.in*, (January), 1–13.<http://www.asfaltblij.nl/media/1416/2009june-the-use-of-warm-mix-asphalt.pdf>
- Hurley, G. C., and Prowell, B. D. (2005). "Evaluation of Aspha-Min ® Zeolite For Use In Warm Mix Asphalt." (June).<http://dsp2002.eng.auburn.edu/research/centers/ncat/files/reports/2005/rep05-04.pdf>
- Hurley, G. C., Prowell, B. D., and Hurley, G. C. (2005). "Evaluation of Sasobit ® For Use In Warm Mix Asphalt." (June).[http://www.warmmixasphalt.org/submissions/11\\_20071127\\_evaluation\\_of\\_sasobit.pdf](http://www.warmmixasphalt.org/submissions/11_20071127_evaluation_of_sasobit.pdf)
- Hurley, G. C., Prowell, B. D., and Hurley, G. C. (2006). "Evaluation Of Evotherm ® For Use In Warm Mix Asphalt." (June).<http://www.surveying-courses.bece.auburn.edu/research/centers/ncat/files/reports/2006/rep06-02.pdf>
- IRC:SP:101- 2014. "Interim Guidelines For Warm Mix Asphalt." Available online :<https://archive.org/details/govlawircy2014sp101> Accessed August 2014.
- Kumar, R. (2016). "Warm Mix Asphalt Investigation on Public Roads -A Review." (June).<http://airccse.com/civej/papers/3216civej06.pdf>
- MS-2 7 th Edition (2014) Asphalt Mix Design Methods*. Manual Series No. 2. Asphalt Institute, Lexington, KY.<https://www.slideshare.net/QasimMasood1/ms-2-7th-edition>
- Prowell, B. D., Hurley, G. c., and Frank, B. (2011). "Warm-Mix Asphalt : Best Practices." *National Asphalt Pavement Association Napa*, 1–5.[http://driveasphalt.org/assets/content/resources/QIP-125\\_Warm\\_Mix\\_Asphalt\\_3rd\\_edition.pdf](http://driveasphalt.org/assets/content/resources/QIP-125_Warm_Mix_Asphalt_3rd_edition.pdf)
- Prowell, B., Frank, B., Osborne, L., Kriech, T., and West, R. (2014). "Effects of WMA on Plant Energy and Emissions and Worker Exposures to Respirable Fumes." II, 64.<https://www.nap.edu/read/22272/chapter/3>
- Rubio, M. C., Martínez, G., Baena, L., and Moreno, F. (2012). "Warm mix asphalt : an overview." *Journal of Cleaner Production*, Elsevier Ltd, 24,7684.<https://www.sciencedirect.com/science/article/pii/S0959652611004926>
- Sangiorgi, C. (2018). "Warm Mix Asphalt (WMA ) technologies : Benefits and drawbacks — a literature review." (June 2016).[https://www.researchgate.net/profile/Aboelkasim\\_Diab/publication/309537669\\_Warm\\_Mix\\_Asphalt\\_WMA\\_technologies\\_Benefits\\_and\\_drawbacksa\\_literature\\_review/links/5a91e0a5aca27214056430cc/Warm-Mix-Asphalt-WMA-technologies-Benefits-and-drawbacks-a-literature-review.pdf](https://www.researchgate.net/profile/Aboelkasim_Diab/publication/309537669_Warm_Mix_Asphalt_WMA_technologies_Benefits_and_drawbacksa_literature_review/links/5a91e0a5aca27214056430cc/Warm-Mix-Asphalt-WMA-technologies-Benefits-and-drawbacks-a-literature-review.pdf)
- Zaumanis, M., 2010. Warm Mix Asphalt Investigation. PhD Thesis, Riga Technical University, Kgs,Lengby, Denmark.[http://www.warmmixasphalt.org/submissions/117\\_20100630\\_M.Zaumanis\\_WMA\\_Master\\_thesis.pdf](http://www.warmmixasphalt.org/submissions/117_20100630_M.Zaumanis_WMA_Master_thesis.pdf)



## Pedestrian Flow Characteristics: A Review Study

Ashish Kumar<sup>1</sup>, S.N. Sachdeva<sup>2</sup>

<sup>1</sup>M.Tech student, Department of Civil Engineering, National Institute of Technology Kurukshetra, Haryana- 136119, India, Email: [ashishthakurniist@gmail.com](mailto:ashishthakurniist@gmail.com) (Corresponding Author)

<sup>2</sup>Professor, Department of Civil Engineering, National Institute of Technology, Kurukshetra, Haryana-136119, India, Email: [snsachdeva@nitkkr.ac.in](mailto:snsachdeva@nitkkr.ac.in)

### ABSTRACT

Due to increase in number of vehicles on road, rapid urbanisation and not following traffic rules traffic accidents have become a major concern for road users especially to pedestrians. Vulnerable road users (VRUs) consisting of pedestrians, cyclists and motorised two wheeler drivers are the groups majorly involved and affected by it. About 1.50 lakh persons get killed every year in road accidents in India. Facilities to safeguard the pedestrians from the heavy traffic are not provided on most of the roads. Walking speed, volume, volume to capacity ratio etc. are the pedestrian flow characteristics which help to understand the pedestrian flow behaviour and thus facilities can be designed accordingly. Little attention has been given in India towards study of such pedestrian behaviour. The study of pedestrian flow characteristics under heterogeneous traffic condition is very important. This paper presents the results of the research work taken up in the past in respect of pedestrian flow characteristics under mixed traffic flow conditions.

**KEYWORDS:** *Urbanization; Accidents; Vulnerable road users; Pedestrian flow; Mixed Traffic Conditions.*

### INTRODUCTION

A person who travels on his foot instead of using any vehicle is called a pedestrian. People on wheelchair or those using roller stakes to travel are also termed as pedestrian. Basically anyone walking on footpath, crosswalk or on road are called pedestrian. Walking where on one hand saves fuel which results in less pollution emission, it has also health benefits. Nowadays commercial and residential areas are being developed which is more walk able so as to reduce pollution emission and to also make surrounding safe and secure. For short trips up to 1-2 km it is the most adequate and suitable mode of transportation. The initiation and termination of every journey is by walking. In between the walking trips other modes of transportation are also involved. Walking as a sustainable and suitable mode of travel is understood worldwide and cannot be neglected. About 64.7% trips are made on foot in walking trips. Tiruchirappalli, India, **Arasan et al. (1994)**. In cities like Kinshasa and Dar Es Salaam around 66% trips are walking trips. In cities like Beijing 61% of the total trips were made on foot, **Tanaboriboon and Jing (1994)**. Walking share of different cities of India is shown in Fig.1.

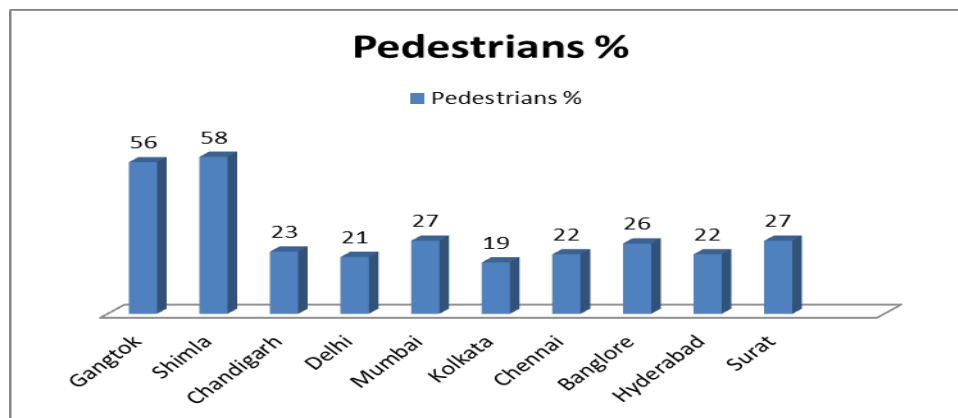
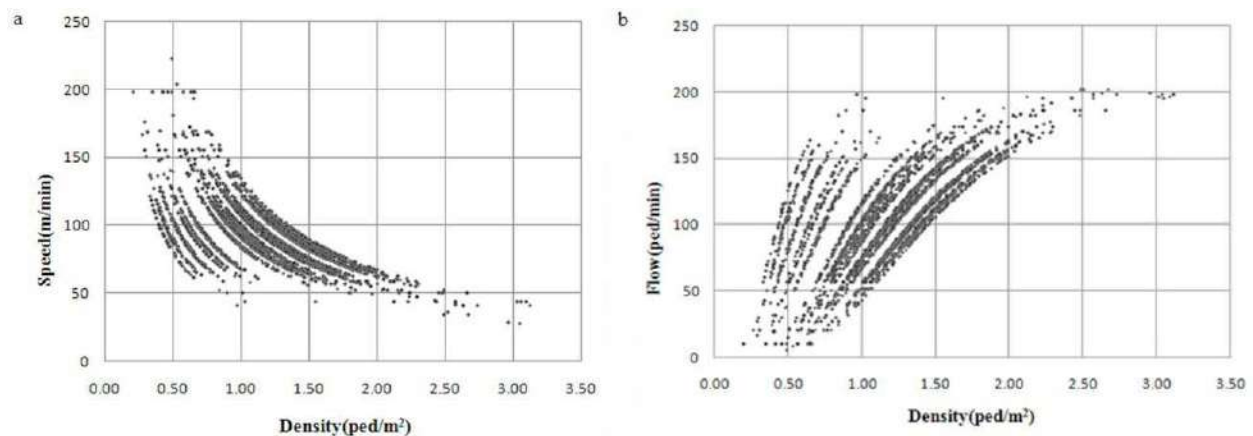


Figure1: Percentage Trips Made on Foot Out of Total Trips Made in Indian Cities

Traffic rules are not fully respected In India, thus their behaviour under mixed traffic conditions flow is different from that of developed countries. Even after providing proper signals and controls people tentatively decline to use it. Also no separate phase is provided at any signalised intersection for pedestrian to cross. Hence, traffic engineers should give utmost priority to safety of pedestrian. Very limited study has been done on this topic especially when Indian circumstances come into picture.

## LITERATURE REVIEW

**Soumyadip Das (2018)** Green shield's linear model govern the relationship between speed and density at sidewalk but Greenberg's logarithmic model is better representative for relationship between speed-density for signalised crosswalk, see Fig. 2



**Figure 2 (a) Speed- Density relationship**

**(b) Flow- Density relationship**

**Moreno (2011)** A noteworthy effects on pedestrian movement can be seen with the increase in population density and use of commercial space. Children depend more on their parents for crossing the roads as it becomes hard for them to evaluate the safe gap acceptance.

**Hediye H (2014)** Pedestrian gender, age, squad, crosswalk length and signals affecta pedestrian manner of walking such as stride length and its frequency. Pedestrians instead of increasing step frequency increases stride length to speed up their walking on crosswalk. They travel at comparatively lower rate for initial half of the crosswalk and then increase their rate. Signalised intersections without countdown displays notice higher number of pedestrian offenders as these intersections have limited time which encourages them to walk faster.

**Rastogi R (2011)** Two way flow of vehicles increases psychophysical activity of pedestrians and thus increases their speed at crosswalk. Whereas in case one way movement of traffic such activity reduces to a great extent.

**Kotkar K L (2010)** Crossing behaviour is influenced by pedestrian characteristics such as age, gender etc., and delay faced due to other vehicles and thus speed of pedestrian while crossing is comparatively higher than on sidewalk. Averagespeed of older pedestrians (age group 50+) is found to be lowest, whereas average speed of younger pedestrians (age group 16-25) is found to be highest.

**Polus (1983)** Walking speed is affected by not only age but gender also. Average speed of men is found to be greater than women.

**Gowri Asaithambi (2016)** A comparative study of pedestrian flow characteristics was done before and after installation of traffic signals and following were the observations.

- After installation of signals there was an increase in pedestrian's waiting time by about 53% from 4.67 sec to 7.09 sec.
- Due to safety concerns in both the cases females were slower than males while crossing the road.
- Installation of signals reduces panic stricken pedestrians and thus their speed reduces by about 25% from 1.39 to 1.07 m/sec.
- After installation of signals accepted gaps by both male and female reduces.

### Based on Accepted Gaps

**Moore (1953)** Crossing speeds were increased by the pedestrian who accepted shorter gaps. Pedestrians crossing when the gap is less than 3 sec crossed at a speed of 1.57m/sec while those crossing when the gap is more than 7 sec crossed at speed of 1.2m/s.

**Cohen (1955)** for a 7m wide road, all pedestrian crossed the road when gap was greater than or equal to 10.5 sec. When the gap was less than 1.5 sec no pedestrian crosses the road while when the gap increases to 7 sec about 92% pedestrian crossed the road.

**DiPietro and King (1970)** Waiting time of pedestrian at the kerb is affected by accepted gap and with the increase in accepted gaps waiting time also increases.

**Zhao and Wu (2003)** At signalised intersections, 5.79 sec was found to be the average acceptable gap and 3.62 sec was found to be the lag for the pedestrians.

**Das (2005)** Size of intersection influences the critical gaps. While crossing from median pedestrian accepted smaller gaps than crossing from the side walk curb. A gap of 8 sec was accepted by most of the pedestrian.

**Das (2005)** Gaps rejected by older persons were accepted by children and younger people however no difference was found in accepted gaps by both genders.

**Brewer (2006)** the pedestrian crossing pattern can be classified into three categories. In first case pedestrian crosses the road in one crossing movement irrespective of its width and this manoeuvre was called single stage crossing.

In second case, pedestrian crosses up to the median in one and then crosses to the other side in second go. And this movement was called two stage crossing.

In the third case between continuous flow of vehicles pedestrian crosses the road by continuously looking for space between the flow of vehicles by changing their speed and direction and was called rolling manoeuvre.

**Oxley (1997)** The average gap accepted by younger pedestrian was 51.3 metre and 119.2 metre and that by older pedestrians it was 69.1 metre and 134.1 metre, for two way and one way road respectively.

The summary of all past studies i.e., gap acceptance in terms of time (sec) and space (metre) is shown in Table 1. According to the data the lower and upper limit for gap acceptance was 1.5 sec and 10.5 sec.

**Table 1: Summary of all past studies i.e., gap acceptance in terms of time (sec) and space (meter)**

Researcher (year)	Country	Accepted Gaps (sec)
Moore	U.K	3.05 to 7.06
Cohen	U.K	1.57 to 7.1
Dipietro and King	U.S.A	3.08 to 10.05
Oxley	Australia	51.30m to 134.10m
Zhao and Wu	China	5.8
Das	India	8
Brewer	U.S.A	5.32 to 9.39

### LOS MODEL DEVELOPED BY VARIOUS AUTHORS BASED ON QUANTITATIVE SURVEY

Various parameters were used by researchers to develop the level of service model based on quantitative survey which is shown in Table 2.

**Table 2 Parameters Used by Various Researchers**

AUTHOR	LOCATION	FACILITY	REMARKS
Nagraj and Vedagiri (2013)	Mumbai, India	Signalised crosswalk	<b>l</b> =left-turning vehicles (PCU /15min), <b>r</b> =vehicles turning right (PCU /15min), <b>t</b> =through vehicles (PCU /15min), <b>p</b> =pedestrians crossing every 15 mins
Marisamynathan and Vedagiri (2017)	Mumbai, India	Signalised crosswalk	<b>Dped</b> =pedestrian delay (sec), <b>Vtraffic</b> =traffic volume in the direction of pedestrian crossing <b>P(yn)</b> =chances of collision between pedestrians and vehicles
Muraleetharan (2005)	Sapporo, Japan	Crosswalk	<b>Dij</b> =Categorical score associated with jth level of the ith attribute, <b>δij</b> = 1 if the jth level of the ith attribute is present, <b>pd</b> =Pedestrian delay in seconds, <b>pb</b> =Number of pedestrian-bicycle conflict
Zhao	Anhui,	Unsignalised	<b>Vm</b> =number of vehicles flowing in both the direction

(2014)	China	crosswalk	<b>Lb</b> =crossing length <b>Nm</b> =number of marked crosswalks, <b>Nu</b> =number of unmarked crosswalks
Kadali and Vedagiri (2015)	Mumbai, India	Mumbai, India	<b>LU</b> =Land-use type, <b>PPCD</b> =crossing difficulty perceived by pedestrian, <b>PPCS</b> = crossing safety perceived by pedestrian, <b>WOM</b> =width of median, <b>NOL</b> = number of lanes, <b>NOVE</b> =number of vehicles encountered while crossing
Archana (2015)	India	Signalised crosswalk	<b>CSR</b> =crosswalk surface condition rating, <b>PCT</b> =pedestrian crossing time (sec), <b>PFH</b> =pedestrian flow (ped/hr)

## CONCLUSION

From the above study following conclusions can be drawn.

1. At sidewalks Green shield's linear model govern speed-density relationship but in case of signalized crosswalk Greenberg's logarithmic model is found to be more suitable. Since crosswalk segment does not have definite effective width and thus is not a constraint area unlike footpaths, hence with the increase in density pedestrian instead of lowering their rate of walking they start to move more swiftly.
2. Crossing behavior is influenced by pedestrian characteristics such as age, gender etc., and delay faced due to other vehicles and thus speed of pedestrian while crossing is comparatively higher than on sidewalk. Average speed of older pedestrians (age group 50+) is found to be lowest, whereas average speed of younger pedestrians (age group 16-25) is found to be highest. This is owing to the fact that with old age energy level decreases which affect speed of the pedestrian. Also females were found to be slower than males.
3. After the signals are installed pedestrian have to wait for the red signal to cross the road and thus their waiting time increased by 53 % (from 4.67 to 7.09 s). Also with increase in waiting time more pedestrians offenders were noticed.
4. After installation of the signal pedestrian feel more safety and so panic stricken pedestrian reduces thus the average crossing speed gets reduced by 24 % (from 1.39 to 1.07 m/s). Pedestrian follow one step crossing manoeuvre to cross the road and thus their speed reduces.

5. According to the graph shown in fig.1. We saw that walking share of Shimla and Gangtok is much more than other Indian cities. The reason could be that both the areas are hilly areas which steep terrain and on such terrain vehicles movement becomes more difficult so people give priority to walking. Moreover both the cities are also tourist's areas.
6. The average gap accepted by young pedestrian was 51.3 m and 119.2m and that by older pedestrians it was 69.1m and 134.1 m, for two way and one way road respectively. Accepted gap in terms of time varied between 1.5sec and 10sec. With the increase in waiting time at the curb accepted gap also increases.

## REFERENCES

- Arasan, V. T., Rengaraju, V. R., and Rao, K. V. K. 1994. "Characteristics of trips by foot and bicycle modes in Indian city." *J. Transp. Eng.*, 120 2, 283–294.
- Arcana, G.: Analysis of pedestrian level of service for crosswalk at intersections for urban condition. *International Journal of Students' Research in Technology & Management* 1(6), 604–609 (2015)
- Bennet MK, Manal H, Van Houten R. A comparison of gateway in-street sign configuration to other driver prompts to increase yielding to pedestrians at crosswalks. *J Appl Behav Anal* 2014; 47(1):3-15.
- Brewer, A. M., Fitzpatrick, K., Whitaker, A. J., and Lord, D. (2006). "Exploration of pedestrian Gap-acceptance behaviour at selected locations." *Transportation Research Record* 1982, National Research Council, Washington, D.C, pp. 132-140.
- Cohen, J., Dearnaley, E. J., and Hansel, C. E. M. (1955). "The risk taken in crossing a road." *Journal of the Operational Research Society*, Vol. 6, No. 2, pp. 120-128.
- Das, S., Mansk, C. F., and Manuszak, M. D. (2005). "Walk or wait? An empirical analysis of street crossing decisions." *Journal of Applied Econometrics*, Vol. 20, pp. 529-548.
- DiPietro, C. M. and King, L. E. (1970). "Pedestrian gap-acceptance." *Highway Research Record*, No. 308, NCHRP, Washington, D.C., pp. 80-91.
- Hediye H, Sayed T, Zaki MH. The use of gait parameters to evaluate pedestrian behaviour at scramble phase signalized intersections. *J Adv. Transp* 2014; 49(4):523-534.
- Kadali, B.R., Vedagiri, P.: Evaluation of pedestrian crosswalk level of service (LOS) in perspective of type of land-use. *Transportation Research Part A: Pol- icy and Practice* 73, 113–124 (2015)
- Kotkar K L, Rastogi R, Chandra S. Pedestrian flow characteristics in mixed traffic conditions. *J Urban Plan D* 2010; 136(1):23-33. doi: 10.1061(ASCE)0733-9488(2010)136:1(23)
- Marisamynathan, S., Vedagiri, P.: Modelling pedestrian level of service at signalized intersection under mixed traffic conditions. *Transportation Research Record: Journal of the Transportation Research Board* (2634), 86–94 (2017)
- Ministry of Urban Development (2008), *Traffic and Transportation Policies and Strategies in Urban Areas in India*, Government of India, New Delhi.
- Miranda-Moreno LF, Fernandez D. Modelling of pedestrian activity at signalized intersections: land use, urban form, weather and spatiotemporal patterns. *Trans Res Rec* 2011; 2264:74-82. doi: 10.3141/2264-09
- Moore, R. L. (1953). "Pedestrian choice and judgment." *Journal of the Operational Research Society*, Vol. 4, pp. 3-10.
- Muraleetharan, T., Adachi, T., Hagiwara, T., Kagaya, S.: Method to determine pedestrian level-of-service for crosswalks at urban intersections. *Journal of the EasternAsiaSociety for Transportation Studies* 6, 127–136 (2005)
- Nagraj, R., Vedagiri, P.: Modelling pedestrian delay and level of service at signalized intersection crosswalks under mixed traffic conditions. *Transportation Research Record: Journal of the Transportation Research Board* (2394), 70–76 (2013)
- Oxley, J., Brian Fildes, Elfriede Ihsen, Judith Charlton and Ross Day, (1997). "Differences in traffic judgments between young and old adult pedestrians." *Accident Analysis and Prevention*, Vol. 129, No. 6, pp. 839-847.
- Rastogi R, Chandra S, Vamsheedhar J, Das VR. Parametric study of pedestrian speeds at midblock crossings. *J*

- Urban Plan D 2011; 137(4):381-389. doi:10.1061/(ASCE)UP.1943-5444.0000083
- Soumyadip Das, Deotima Mukherjee, Pritam Saha, Sudip kumar Roy. Pedestrian Flow Characteristics at Signalised Intersection in Mixed Traffic Situations: A case study of Kolkata, India. The 9<sup>th</sup> International Conference on Ambient Systems, Network and Technologies (ANT 2018)
- Tanaboriboon, Y., and Jing, Q. 1994. "Chinese pedestrians and their walking characteristics: Case study in Beijing." *Transp. Res. Rec.*, 1441, 16–26.
- West Perth pedestrian study. 2006. Curtin Univ. of Technology, City of Perth and Geographia, Australia.
- Zhao, Jiali and Jiaping, Wu (2003). "Analysis of pedestrian behaviour with mixed traffic flow at intersection." *Intelligent Transportation Systems Journal, IEEE*, Vol. 1, pp. 323-327.
- Zhao, L., Bian, Y., Lu, J., Rong, J.: Method to determine pedestrian level of service for the overall unsignalized midblock crossings of road segments. *Advances in Mechanical Engineering* 6, 652986 (2014)
- Polus, A., Schofer, J. L., and Ushpiz, A. (1983). "Pedestrian flow and level of service." *J. Transp. Eng.*, 109(1), 46–56.
- Gowri Asaithambi, Manu O. Kuttan, Sarath Chandra (2016) "Pedestrian Road Crossing Behaviour Under Mixed Traffic Condition: A Comparative Study of an Intersection Before and After Implementing Control Measures" *Trans. In Dev. Econ.* (2016)



## Performance of various rejuvenators with RAP material in road construction

Ankit Sharma<sup>1</sup>, Praveen Kumar,<sup>2</sup> and  
G.D. Ransinchung R.N.<sup>3</sup>

<sup>1</sup>Research Scholar, Department of Civil Engineering, Indian Institute of Technology Roorkee, Roorkee;  
e-mail:sharmaankit.sharma65@gmail.com (Corresponding Author)

<sup>2</sup> Director, National Institute of Technology Delhi, Delhi; e-mail: praveenaeron@gmail.com

<sup>3</sup> Associate Professor, Department of Civil Engineering, Indian Institute of Technology Roorkee, Roorkee;  
e-mail: gdranjan@gmail.com

### ABSTRACT

Excavated road material which goes into landfills is generally reutilized by many countries. This practice is sustainable, eco-friendly and save the cost of construction. This recycling technology is called Reclaimed Asphalt Pavement (RAP). The main hurdle in recycling of old pavement is it's stiffer bitumen which got aged in pavement's service life. This decreased flexibility results into early cracking of pavement or less durable pavement. To improve the softness of aged binder, rejuvenator can be added into RAP extracted binder. Many countries are recycling RAP material up to a certain proportion e.g. 50%. Many studies have conducted for evaluating the performance of incorporating RAP material up to 100%. This paper will review the studies on high proportion of RAP material with various rejuvenators. It will help to understand the performance of rejuvenators in RAP mixes.

**KEYWORDS:** *Recycled Asphalt Pavement; RAP; Rejuvenator; Asphalt softener; Ageing.*

### INTRODUCTION

Recycling of limited reservoir of natural aggregates and crude oil by product i.e. bitumen is essential for sustainable development. Many countries have started recycling since the beginning of the twentieth century. In India first Reclaimed Asphalt Pavement (RAP) have constructed in 1948. RAP material can be efficiently recycled up to 100%. A survey indicates that on using 100% RAP, there is 35% reductions in carbon footprints and 50% saving in cost of construction materials (**Zaumanis et al., 2014**). In addition to this due to quality concern of RAP material its use in surface course is less e.g. 10% whereas in base course its proportion can be up to 50% (**NRA, Specification for Road Works, 2011** and **NSAI, Standard Recommendation SR 28, 2009**).

There are many recommendations available on maximum limit of RAP to be used in recycling. According to **Dony A. et al., (2013)** and **X.D. Hu et al., (2012)**, the upper limit of RAP material is 30% whereas lower limit of RAP is 10% (**Moneron P. et al., 1999**). The main problem with use of high proportion of RAP material is the early cracking of asphalt mix. During service life of pavement, it get subjected to traffic (sometimes more than design traffic), summer, winter, rain and different weathering actions as per the site conditions. Bitumen binder available in 'asphalt mix matrix' work as glue to bind the aggregates and filler together. On loading over flexible pavement, load gets transfer by mechanism of grain to grain transfer and taken by skelton of aggregate and asphalt binder. With service life of pavement, bitumen gets stiffer due to loss of its lighter oils (volatile material i.e. maltenes) due to continuous oxidation under heat & sun rays and on recycling, it's durability gets decreased. Recycling with high proportion of RAP is possible by addition of the rejuvenators/ softeners, which reduces the stiffness of aged binder and improve the resistance against cracking (**Booshehrian A. at al., 2013**). Rejuvenators restore the original properties of virgin binder and increase the design life of flexible pavement (**Nahar S et al., 2014** and **Xu X et al., 2014**). There are various studies available on the use of rejuvenators with RAP material.

**Zaumanis at al., (2014)** conducted a study in which six rejuvenators have used, out of which 5 were generic and 1 was commercial as shown in fig. 1. The commercial rejuvenator i.e. Hydrogreen S<sup>TM</sup> was formerly known as BituTech RAP<sup>TM</sup>.

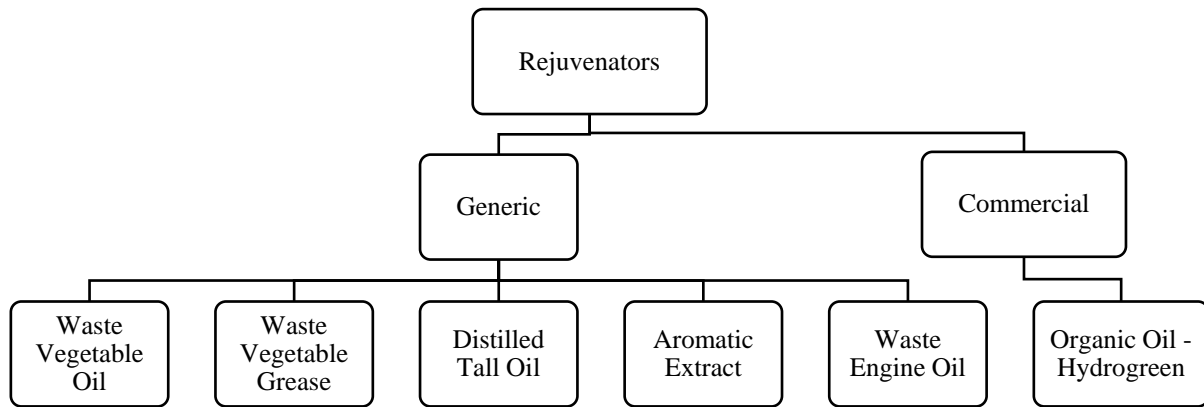


Fig. 1 Type of rejuvenators used in study by **Zaumanis et al., (2014)**.

As shown in fig.2, except waste engine oil (WEO), all five rejuvenators ensured required grade of PG 64-22 at dosages of 12% by weight of the binder, whereas for waste engine oil dosages found to be more than 12%. WV oil, WV grease, organic oil and distilled tall oil found to be more efficient in reducing PG temperature compared to virgin bitumen, aromatic extract and WE oil. Superpave fatigue and workability criteria have also been satisfied by all six rejuvenators. It is clear that the rutting resistance of all rejuvenated samples got improved than virgin bitumen due to high PG temperature than virgin bitumen, Hamburg WTT shows similar results. Except WE oil, all rejuvenators have shown better low temperature thermal cracking potential compare to virgin binder.

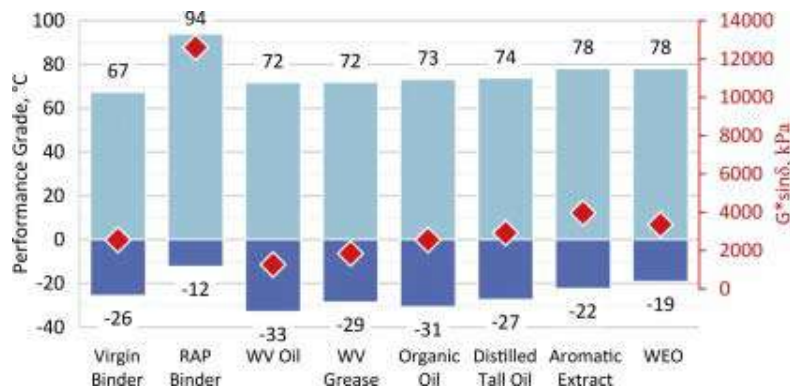


Fig.2 Performance Grade and  $G^* \sin\delta$  variation w.r.t. various rejuvenators at 12% dosage and 25 ° C.

**Farooq et al. (2018)** conducted a study using Used-Mobile Engine Oil (UMEO) as a rejuvenator to produce warm mix asphalt from RAP with Evotherm as a chemical additive. The use of UMEO enabled to increase the RAP proportion from 20% to 60% in contrast to warm mixes produced without UMEO.

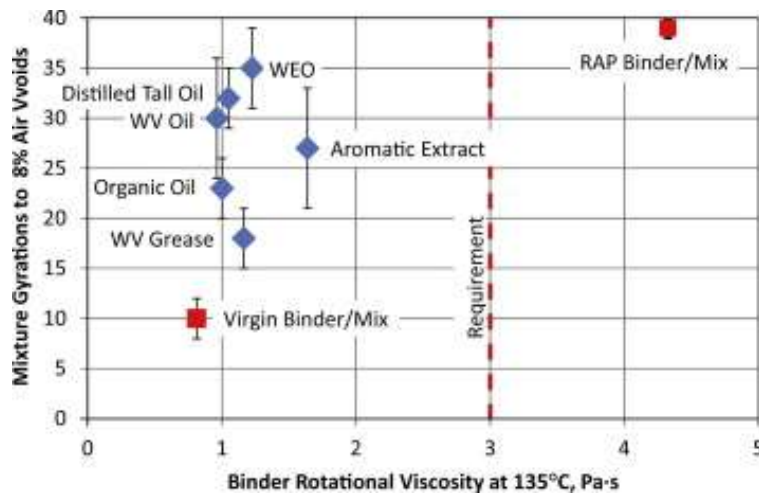


Fig.3 Gyration to 8% air voids VS binder rotational viscosity.

From fig. 3 it is clear that all the rejuvenators improved the workability of RAP mixture but none of them improve it to the level of virgin bitumen. Also, all rejuvenators satisfied the Superpave design criteria of rotational viscosity less than 3 Pa.s at 135°C.

This paper will help to understand the performance of rejuvenators with RAP material. In this paper Waste Engine Oil (WEO), organic oil, petrochemical oil, aromatic oil's performance have discussed as rejuvenators in RAP mixes. Diffusion- Penetration test, Diffusion- DSR test, Asphalt Mortar Transfer ratio test describe the optimal dosages of rejuvenators.

## LITERATURE REVIEW

Fatigue performance of RAP incorporated asphalt mixes is important to calibrate the life of pavement under repeated loading cycles (Bernier et al., 2012). In a study conducted by Widyatmoko (2008), RAP material has used in proportion of 10, 30 and 50% both in surface and base course. Results showed that fatigue performance of mixes were improved than control mixes on using soft grade bitumen. In an another study conducted by Arvind and Das (2007) fatigue performance of RAP incorporated asphalt mixes found out to be improved or at least equivalent to the control mixes.

Moisture resistance of RAP incorporated asphalt mixes is checked by Widyatmoko (2008) and found that overall RAP mixes were not sensitive to moisture induce damage. Whereas in an another study conducted by Su et al., (2009) incorporate 40% and 70% RAP in asphalt mixes and results indicated the equivalent to slightly lower resistance to moisture resistance of RAP- mixes. The effect of RAP on raveling of RAP-mixes was also evaluated and found not be an issue. Rutting performance of RAP-mixes was observe and recommended that 40% and 70% RAP was successfully used in airport surface course and 70% RAP-mixes has improved rutting performance that 40% due to the increased stiffness of binder in the recycled mix. It was also concluded that 40% incorporation of RAP can be used as airport class surface course whereas 70% incorporated RAP-mixes are not recommended to use due to higher potential of fatigue damage. One other airport sureface course study examined by Hajj et al., (2010) revealed that incorporation of 17% and 20% RAP results in good performance up to 8 years of service life.

Aged bitumen is extracted from RAP and added with recommended dosages of rejuvenators, this blend is called recycled binder. Performance tests including conventional (penetration, softening point, ductility and viscosity) and rheological tests determine the optimum dosages of rejuvenator. Mixing of rejuvenator in such proportion with RAP material that it leads to the formation of the desired grade of final binder is a process to determine the required rejuvenator dosages (West et al., 2013). Literature survey shows that when 10–50% of the rejuvenator/ softener by the weight of the aged binder in the RAP was mixed into the RAP directly, it will take 48–144 hour for fully diffuse the rejuvenator into the RAP (R. Karlsson and U.L.F. Isacsson, 2003). The research conducted by Dony et al., (2013) informs that on increasing rejuvenator dosages, penetration increases exponentially and softening efficiency

of organic oils are more than petrochemical recycling agents. To improve the diffusion of RAP binder with rejuvenator, the following actions can be considered (**Bonaquist, 2007**):

- For improving interaction between materials, mixing and storing time can be increased.
- Add WMA additive for reducing the viscosity of binder without lowering the mixing and compaction temperature.
- The increment in mixing and compaction temperature.

Fig.4 indicates diffusion process of rejuvenator, at first rejuvenator has applied and slowly diffusion get initiated and after certain time i.e. curing time aged binder converted to recycled binder. A rejuvenator should satisfy these criteria (**Zaumanis et al., 2014**):

1. It should allow 100% RAP utilization by diffusing into aged RAP binder and mobilizing binder's original properties so that all aggregates can be coated.
2. It should soften the aged binder so that asphalt mixture can be compacted sufficiently without excessive emissions.
3. The diffusion process (as shown in Fig. 4) should be completed before opening to traffic to reduce the chances skidding and increased rutting susceptibility.

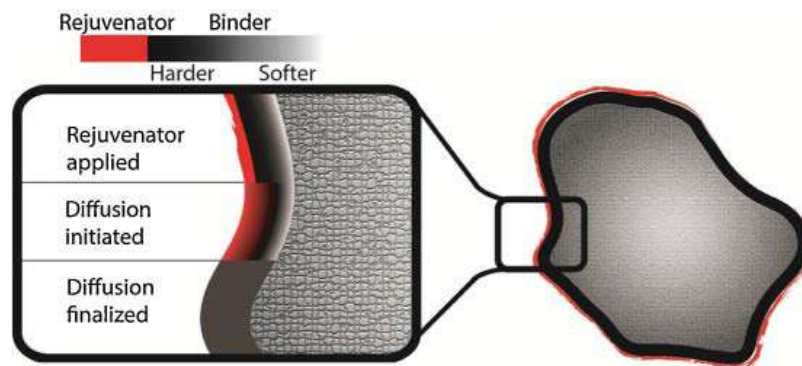


Fig. 4: Recycling agent diffusion into binder film and binder layer viscosities.  
Credit: <https://www.sciencedirect.com/science/article/pii/S0921344914001505>

4. The Blend of rejuvenator and aged binder should reconstitute its chemical and physical properties so that it can work for another service life.
5. The binder rheology should be altered in a way that it will reduce cracking potential of binder whereas improving rutting resistance (**Tran et al., 2012**).

According to **Bailey and Zoorob, (2012)** on using waste and virgin vegetable oil as a rejuvenator, RAP binder viscosity have reduced to target viscosity of virgin binder. Use of vegetable oil is recommended for restoring the rheological behavior of aged binder, reducing mixture's stiffness to the level of virgin binder and improving resistance to ageing.

Waste edible oil is the potential rejuvenator in improving the low-temperature grade of binder (**Gordon et al., 2009**). Low-temperature thermal cracking has reduced and softening efficiency have increased for RAP mixtures on the addition of organic blend, distilled tall oil and refined tallow oil.

Table 1. Rejuvenator optimum dose based on Superpave PG tests (**National Renderers Association Inc.**)

S.No.	Rejuvenator	Max dose (%)	Min dose (%)
1	WV Oil	16.4	7.4 <sup>a</sup>
2	WV Grease	16.4	8.1 <sup>a</sup>
3	Organic Blend	18.4	9.1 <sup>a</sup>
4	Distilled Tall Oil	18.8	9.4 <sup>a</sup>
5	Aromatic Extract	27.8	11.5 <sup>b</sup>
6	WEO	25	16 <sup>b</sup>

<sup>a</sup> Based on intermediate PG requirement.

<sup>b</sup> Based on Low PG.

Table.1 indicates maximum and minimum dosages of various rejuvenators based on intermediate and low Performance Grade temperature criteria.

#### OPTIMUM DOSAGES AND RATE OF DIFFUSION OF REJUVENATOR FOR RAP MATERIAL

The percentage of rejuvenator by weight of aged binder affect both the performance of the final binder and recycled RAP mixture (**Shan et al., 2007**). It means it is necessary to determine the optimal dosages of rejuvenator for the efficient performance of recycled asphalt mixture. In a study conducted by **Tao Ma et al., (2015)** the performance of rejuvenator has checked for artificially laboratory aged asphalt and its artificial RAP mixtures. Four rejuvenators say A, B, C and D have viscosity values as 4, 15, 190 and 215 mPa s respectively. Each rejuvenator's dosages vary as 2, 4, 6 and 8% by weight of aged asphalt binder. Results of conventional test on aged asphalt binder indicate that all four rejuvenators successfully soften the aged binder. But the optimal % of rejuvenators A, B, C and D for rejuvenating aged asphalt, found out to be 4%, 5%, 6% and 8% by weight of aged asphalt.

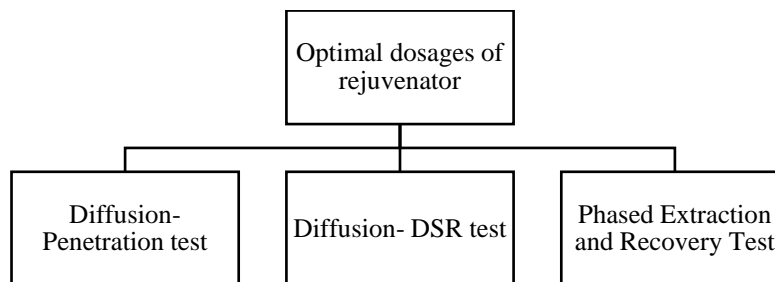


Fig. 5 Methods to determine optimum dosages of rejuvenators.

Fig. 5 indicates three methods of identification of optimum dosages of rejuvenators which are described below :

**Diffusion Penetration test** In this test Penetration values of recycled asphalt binder (i.e. rejuvenated aged asphalt binder) determined concerning curing time. Penetration value w.r.t. curing time indicates the percentage of diffusion of rejuvenator into the aged binder.

**Diffusion DSR test** In this test,  $G^*/\sin\delta$  is calculated for varying curing time of recycled binder. This test also indicates the diffusion of rejuvenator in aged RAP binder.

**Phased Extraction and Recovery Test:** RAP mix is put into trichloroethylene solvent for 45 minutes, the amount of RAP binder dissolved into solvent represents phase extraction and the performance tests on binder recovered from this solution represents recovery test. This method also represents the diffusion ability of rejuvenator into RAP.

**Note:** The slope of results e.g. Penetration values w.r.t. curing time represents the rate of diffusion of rejuvenator.

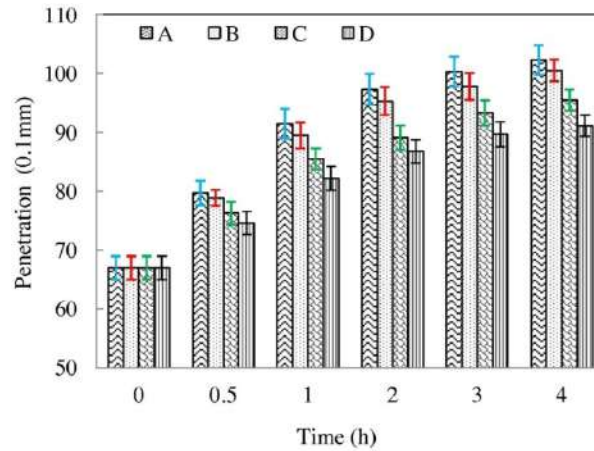


Fig. 6 Diffusion-penetration test for different rejuvenators.

As shown in fig.6 the penetration values of lighter oil containing rejuvenators i.e. A and B (having low viscosity) are increasing at a steeper slope than that of tackifying resin containing more viscous rejuvenators C and D. This statement is justified with the equations given in the table. 2 below.

Table. 2 Fitting formulas for different rejuvenators.

Rejuvenator	Fitting formula	Slope	R <sup>2</sup>
A	$P = 10.5\ln(t) + 89.0$	10.5	0.96
B	$P = 10.0\ln(T) + 87.4$	10	0.97
C	$P = 9.0\ln(T) + 83.7$	9	0.98
D	$P = 7.8\ln(T) + 81.0$	7.8	0.98

From table.2, it is clear that the slope of 'A' and 'B' are more than that of 'C' and 'D'. Here, slope indicates diffusivity of the rejuvenator. The greater slope means more diffusivity of softener in the aged binder, hence rejuvenator 'A' has most diffusivity than 'B', 'C' and 'D'.

The asphalt film thickness of new and RAP aggregate can be calculated as follow:

$$h = \left( \frac{P_b}{Y_b \cdot (S A_a \cdot m_a + S A_m \cdot m_m)} \right) * 10^6 \quad \dots \text{Eq. 1}$$

Where,

$h$  = thickness of the asphalt film ( $\mu\text{m}$ )

$P_b$  = weight of the asphalt in kg

$Y_b$  = Density of the asphalt  $\text{kg/m}^3$

$S A_a$  and  $S A_m$  = Specific surface area of aggregates and mineral filler

$m_a$  and  $m_m$  = weight of aggregates and mineral fillers.

There are two approaches to determine optimal rejuvenator content of aged binder. One is ideal condition RAP mix where, rejuvenator has blended with aged bitumen, this is called diffusion- recycled asphalt whereas another is actual condition RAP mix where, rejuvenator is added directly into the RAP aggregates and recycled asphalt is extracted for testing, this recycled binder is called mix- recycled asphalt.

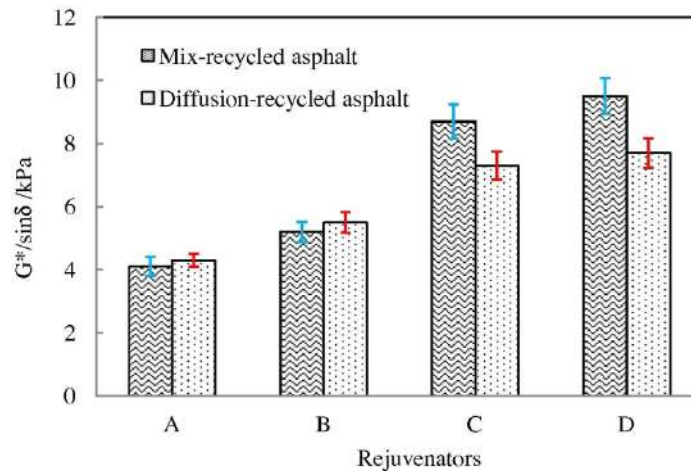


Fig. 7 Rutting parameter ( $G^*/\text{Sin}\delta$ ) variation for mix-recycled asphalt and the diffusion-recycled asphalt.

As showed in fig. 7, test results of the diffusion-DSR test on diffused RAP binder (ideal) and recycled RAP binder (actual) indicates that for rejuvenators 'A' and 'B' have more " $G^*/\text{Sin}\delta$ " in comparison to 'C' and 'D'. This is because the diffusion of lighter oil is more in comparison to tackifying resin rejuvenators i.e. 'C' and 'D'.

The rate of diffusion of rejuvenator in aged binder follows **Fick's Law** according to which the rejuvenator mingle with aged RAP rapidly during initial one hour and after that the rate of diffusion got slow which indicates that the difference in viscosity values of rejuvenator and aged RAP decreased with curing time.

**Mortar Transfer Ratio** test describe the rejuvenation of aged RAP by any rejuvenator diffusion in aged RAP material. In the study conducted by due to rejuvenation by **Tao Ma et al., (2015)** following Mortar transfer ratio found out which indicates that lighter oil rejuvenator rapidly increases rejuvenation on increment in their dosages w.r.t. the tackifying resins rejuvenator as shown in table 3.

Table. 3 Mortar Transfer Ratio for lighter oil (A &B) and tackfying resins (C&D).

Rejuvenator	Content (%)	Transferred asphalt mortar (%)
Non	0	15.4
A	4	19.4
	10	31.8
B	5	17.5
	10	29.9
C	6	21.4
	10	26.4
D	8	23.6
	10	25.4

### Mix Design method of RAP recycling

As per the literature review, it has found that there is no standard method available for mix design guidelines of RAP or Reclaimed Asphalt Shingles (RAS) material till date. The rejuvenator's dosages and their guidelines need to be developed specially for performance grade binder specifications (Soohyok Im et al., 2016). Warm Mix Asphalt technology guidelines about RAP recycling are not defined. WMA additive can work as a rejuvenator. WMA additives reduce the viscosity of binder at 30°C lower temperature than of Hot Mix Asphalt (HMA) technology. Due to reduced temperature absorption of light oils of binder and rejuvenators got decreased and it leads to flexibility of RAP recycled asphalt mixture performance.

### CONCLUSIONS

Optimum dosages of organic and petroleum rejuvenators lie in between 5 to 12% by weight of the binder and optimum performance of RAP mix found to be up to 70% incorporation of RAP material in asphalt mix. The performance of rejuvenator depends on its viscosity and curing time. There is desire need to research on the curing time of rejuvenator with the RAP material. Mortar Transfer Ratio test is found out to be best suitable for determination of the effectiveness of rejuvenator in rejuvenating RAP recycled material. The diffusion of lighter oil is more than tackfying resin rejuvenators into the aged binder. It is also observed that properties of aged asphalt changes concerning the viscosity of rejuvenator used. Generally, lower viscosity rejuvenators lead to higher rate of change of results and vice versa.

### REFERENCES

- Bernier A., Zofka A., Yut I. (2012). "Laboratory evaluation of rutting susceptibility of polymer-modified asphalt mixtures containing recycled pavements", *Constr. Build. Mater.* 31, 58–66.
- Bonaquist R. (2007). "Can I run more RAP? Hot Mix Asphalt Technol", Vol. 12.
- Booshehrian A., Mogawer W.S., Vahidi S. (2013), "Evaluating the effect of rejuvenators on the degree of blending and performance of high RAP, RAS, RAP/RAS mixtures", *J. Assoc. Asphalt Paving Technol.*, 82.
- Dony A, Colin J, Bruneau D, Drouadaine I, Navaro J. (2013). "Reclaimed asphalt concretes with high recycling rates: changes in reclaimed binder properties according to rejuvenating agent", *Constr Build Mater*,

41:175–81.

- Farooq M.A., Mir M.S., Sharma A. (2018). "Laboratory study on use of RAP in WMA pavements using rejuvenator", *Construction and Building Materials*, Volume 168, Pages 61-72.
- Hajj E.Y., Sebaaly P.E., Kandiah P. (2010). "Evaluation of the use of reclaimed asphalt pavement in airfield HMA pavements", *J. Transp. Eng.*, 136 (3), 181–189.
- K. Aravind, A. Das. (2007). "Pavement design with central plant hot-mix recycled asphalt mixes", *Constr. Build. Mater.*, 21 (5), 928–936.
- Moneron P, Baudu Y, Guieysse B and Quaranta G. (1999). "La suppression des études préalables dans le cadre du recyclage des enrobés à 10%. Revue Générale des routes et aérodromes";785:57.
- Nahar S, Qiu J, Schlangen E, Shirazi M, van de Ven M, Schitter G and Scarpas A. (2014). "Turning back time: rheological and microstructural assessment of rejuvenated bitumen." In: 93rd Annual Meeting of the Transportation Research Board, Washington, D.C.
- National Renderers Association Inc. (2008), A buyer's guide to rendered products, Alexandria, VA.
- NRA (National Roads Authority, Dublin), Specification for Road Works Volume 1 Series 900 (2011). "Road Pavements – Bituminous Bound Materials".
- NSAI (National Standards Authority of Ireland, Dublin), Standard Recommendation SR 28 (2009) . "Recommendation for the use and implementation of the I.S. EN 13108 series bituminous mixtures – material specifications".
- R. Karlsson and U.L.F. (2003). "Isacson, Application of FTIR-ATR to characterization of bitumen rejuvenator diffusion", *J. Mater. Civil Eng.* 15 (2) 157–165.
- Shen J., Amirkhanian S., Tang B. (2007). "Effects of rejuvenator on performance-based properties of rejuvenated asphalt binder and mixtures", *Constr. Build. Mater.*, 21, 958–964.
- Soohyok I., Pravat K., Fujie Z. (2016). "Development of new mix design method for asphalt mixtures containing RAP and rejuvenators", *Construction and Building Materials*, Volume 115, Pages 727-734, ISSN 0950-0618.
- Su K., Hachiya Y., Maekawa R. (2009) "Study on recycled asphalt concrete for use in surface course in airport pavement", *Resour. Conserv. Recycl.*, 54 (1), 37–44.
- Tao Ma, Xiaoming H., Yongli Z. and Yao Z. (2015). "Evaluation of the diffusion and distribution of the rejuvenator for hot asphalt recycling", *Construction and Building Materials*, Volume 98, Pages 530-536, ISSN 0950-0618.
- Tran N.H, Taylor A, Willis R. (2012), "Effect of rejuvenator on performance properties of HMA mixtures with high RAP and RAS contents", Auburn, AL: National Center for Asphalt Technology.
- West R, Willis J.R, Marasteanu M. (2013), "Improved mix design, evaluation, and materials management practices for hot mix asphalt with high reclaimed asphalt pavement content", NCHRP Report.
- Widyatmoko I. (2008). "Mechanistic-empirical mixture design for hot mix asphalt pavement recycling", *Constr. Build. Mater.*, 22 (2) , 77–87.
- X.D. Hu, Y.H. Nie, Y. Feng and Q.S. Zheng. (2012). "Pavement performance of asphalt surface course containing reclaimed asphalt pavement (RAP)", *J. Test. Eval.*, 40 (7) 181–189.
- Xu X, Zaumanis M, dos Santos S and Poulidakos L. (2014). "Rheological, microscopic, and chemical characterization of the rejuvenating effect on asphalt binders", *Fuel*;135, 162–71.
- Zaumanis M., Mallick R. B. and Frank R. (2014). "100% recycled hot mix asphalt: A review and analysis, Resources, Conservation and Recycling", Volume 92, Pages 230-245, ISSN 0921-3449.



## Utilization of Waste Materials in Construction of Cool Pavements: A Review Study

Mohit Thakur<sup>#1</sup> and Amardeep Boora<sup>\*2</sup>

<sup>1</sup>M-Tech student, Department of Civil Engineering, Jaypee University of Information Technology, Waknaghat-173234, India,  
E-mail: mohit.thakur6786@gmail.com

<sup>\*2</sup>Assistant Professor, Department of Civil Engineering, Jaypee University of Information Technology, Waknaghat-173234,  
India, E-mail: [amardeepboora9@gmail.com](mailto:amardeepboora9@gmail.com) (Corresponding Author)

### ABSTRACT

Fast and improper development in urban areas is remarkably expanding in order to satisfy human requirements. Due to the lack of observations, the process includes the mitigation of energy balance of the Earth. Therefore, improper development or development without planning will create many problems which is going to effect the health, quality and solace of neighbouring bodies. The everyday intimation of such habitat related issues is the urban heat island (UHI) event. Building structures and pavements in urban areas are made up of low reflective power materials which ultimately can captivate great amount of heat from solar radiations and then deliver it back to the surroundings at night-time. There are several learnings already done to look for a change in technology that can help in lessening the UHI. Reduction in urban heat island effect can be attained by (1) increasing permeability to actuate cooling effect through evaporation; (2) reducing uproar by composite structure; (3) increasing the surface reflectance of pavement to reduce heat tapping and hoarding. Thus, because of the outcome of heat island in insertion to the whole world's climatic change, increases the urban ambient temperature and hence increases temperature of urban winds. Thus the building materials plays very important role at balancing and maintaining the urban environment. The main objective of this study is to highlight different methods of utilization of waste materials and their application in pavement construction.

**KEYWORDS:** *Heat island; waste materials and cool pavement.*

### INTRODUCTION

The event of urban heat island (UHI) is quiet chronicle case of climate difference. The precise occurrence is because of the raised urban temperatures contrast in periphery rural regions, due to the swelled anthropogenic heat, decline in the air drift, deficiency of heat descends and raised blotting up of solar radiation by urban canyon. To mitigate the heat island effect, coherent mitigation approaches has blossomed and auditioned.

Construction materials showing higher insulation to sun's rays and radiation altogether with a raised emissivity factor are called as cool construction materials. We can use such materials in construction of footpaths, building structures, roads and rooftops of the buildings. Recent studies conclude in reducing the material temperature to quiet convincing degrees. Cool construction materials can be the materials having white color which leads to major reflectance and emittance, or can have different color showing a large reflectance and emittance. So also, asphaltic materials exhibiting a significantly higher reflectivity than ordinary black-top have been produced and are accessible for use in urban structures, when fundamental. Aside from the improvement of exceedingly intelligent materials for urban communities and structures, propelled materials dependent on Nano-mechanical parts like thermo-chromic or Phase Change Material (PCM) doped surfaces have additionally been created. The present paper incorporates the writing survey and some old writing considers with respect to the offset.

### BACKGROUND STUDIES

Most of the structures and pavements are made up of low reflective power materials which ultimately can captivate great amount of heat from solar radiations and then deliver it back to the surroundings at night-time

(Guntor et al. 2007). Several studies have been carried out across the world to identify a new technology that can help in lessening the urban heat island effect. According to Syneffa et al. (2011), reduction in UHI effect can be attained by (1) increasing permeability to actuate cooling effect through evaporation; (2) reducing uproar by composite structure; (3) increasing the surface reflectance of pavement to reduce heat tapping and accumulation. Prototype made up of wasted tiles, sand and epoxy resin can enhance the surface reflectance of the pavement and hence can reduce the heat accumulation. In an experimental study carried out by Guntor et al. (2014), the prototype made up of wasted tiles mixed with epoxy resin when applied as a coating in a parking lot has given optimizing results for both the surface temperature and the underground soil temperatures. The results for reduction of surface temperature are shown in the table 1 below. UHI is the most documented phenomenon of climatic changes and high urban temperatures and this is majorly due to the higher urban temperatures when compared to the surrounding sub urban and rural areas (Santamouris et al. 2012). Thus to counterbalance the impact UHI having on urban areas, efficient mitigation techniques have been developed and applied (Santamouris et al. 2007).

Table 1: Temperature difference of coated and uncoated pavement surfaces.

Date	Coated Surface Temperature (°C)	Uncoated Surface Temperature (°C)	Temperature Difference (°C)	% Reduction
Nov 9, 2011	46.2	49.9	3.7	7.41
Nov 10, 2011	45.3	48.5	3.2	6.60
Nov 11, 2011	31.8	32.7	0.9	2.75
Nov 12, 2011	39.0	41.7	2.7	6.47
Nov 13, 2011	38.7	42.1	3.4	8.08
Nov 14, 2011	47.1	51.5	4.4	8.54
Nov 15, 2011	41.3	44.2	2.9	6.56
Nov 16, 2011	48.3	52.7	4.4	8.35

Utilization of many propelled materials for the urban condition, disperse and reflect warm and sun oriented radiation have been incorporated to these systems. Some different variables like key finishing of urban areas including suitable choice and putting of green zones and sun powered control frameworks were likewise considered. Some numeric demonstrating has demonstrated that the utilization of intelligent material when connected all through the zone can lessen the encompassing temperature up to 2° C, or, in other words critical factor against a dangerous atmospheric deviation (Santamouris et al. 2009; Syneffa et al. 2007). Other than these exceptionally intelligent materials, the created and propelled materials dependent on nanotechnology like PCM doped surfaces or thermo chromic surfaces have been delivered. The intelligent materials for clearing were chosen with the end goal to fulfil a few criteria; a) to show the most noteworthy conceivable toughness and to tastefully satisfying, b) to introduce the most astounding conceivable emissivity factor, c) to display the least conceivable abatement of the reflectivity in view of the maturing impact, d) to exhibit the higher conceivable non specular reflectivity to the sun oriented radiations. Santamouris et al. (2011) presumed that the warmth island notwithstanding the worldwide climatic change expands the urban temperature and henceforth builds the temperature of warmth waves. In this manner the building materials assumes vital job at adjusting and keeping up the urban condition. Research for such materials that can be utilized in development can be characterized in four general stages. The primary stage, brilliant materials exhibiting high emissivity

and reflectivity have been produced and examined. Amid the second stage, cool hued materials have been created utilizing infrared intelligent shades. Third and fourth stage was stage change materials and dynamic cool materials separately. Diverse examinations have been done for the better comprehension of warm and optical qualities and properties of such materials and also their effect on the urban atmosphere and condition. High sun based reflectance (SR) and higher infrared emittance are two noteworthy properties influencing the temperature of a surface. The warm attributes of clearing materials are truly critical as they hugely affect air temperature of lower layers of environment adding to the marvel of warmth island impact. Ordinary asphalts are for the most part comprised of the material like stone, solid, black-top, elastic, marble, rock and so forth and these asphalts can achieve the surface temperature of 48-67° C. Brilliant et al. (2007) proposed a few rules with the end goal to introduce photovoltaic shelters for shading asphalts in parking garages which could likewise help in delivering power. Kinouchi et al. (2004) built up a particular sort of asphalt by using chip seals and sap blended totals that fulfils low splendour and high albedo. Discoveries of the investigation uncovered that the surface temperature of the covered asphalt is very nearly 15o C lower than the traditional asphalt. Exceptionally intelligent materials demonstrates a high cooling property amid hot days. Based on the discoveries it was reasoned that the creation of materials with dynamic optical properties can be considered as a proficient answer for the issue of UHI. Be that as it may, these materials likewise indicates optical corruption and maturing issues.

In another examination, **Li et al. (2013)** reasoned that because of the urban warmth island wonder, enhancing the road and clearing warm condition is drawing in the consideration from training individuals, scholastics, and focused enterprises. Likewise, different strategies, for example, emissivity and reflectance, penetrable asphalts could be a compelling route through for upgrading the encompassing warm condition and lessening the warmth island impact in summers. Porous asphalt has a greater number of voids than regular impermeable asphalt and is intended to enable water to pass by means of surface to the sub-layers and into the ground down. Penetrable asphalts incorporate penetrable black-top asphalts, permeable solid asphalts, pervious cast solid asphalts, and interlocking solid asphalts (**Hunt et al. 2008**). Vegetated porous asphalts, for example, grass pavers and solid matrix pavers, utilize plastic, metal, or solid grids for help and to enable grass or other vegetation to develop in the interstices are a few interchanges as well. A few urban areas, for example, Tokyo and Osaka, have tried the adequacy of water-retentive asphalts as a major aspect of utilizing penetrable asphalts to decrease the warmth island impact. A portion of these frameworks include underground water funnelling or surface water sprinkling to improve the vanishing from the asphalts. This examination inferred that the unpleasantness and void structure is dependable in expanding convection and the cooling impact, they may likewise lessen the surface's net sunlight based reflectance, warm conductivity, and warmth limit (**U.S. Ecological Protection Agency, 2008**).

As per the **Leadership in Energy and Environmental Design (2013)**,the solar reflective index is the scale used in measuring the emittance & reflectivity of a material, and thus includes both solar reflectance and thermal emittance in measuring the heat effects from the solar energy, see Table 2.

Table 2: Albedo values for different type of pavements.

Type of Pavement	Albedo Values
White Portland Cement Concrete	0.70 - 0.80 (new)
	0.40 – 0.60 (old)
Asphalt	0.05 – 0.10 (new)
	0.10 – 0.15 (old)
Grey Portland Cement Concrete	0.35 – 0.40 (new)
	0.20 – 0.30 (old)

Administration in Energy and Environmental Design (LEED) confirmation framework has another definition for cool asphalts; (1) Shading hard surfaces with finishing or plan components; (2) Using materials with a Surface Reflectance Index (SRI) of 29 or more prominent; (3) Using an open-lattice clearing framework that is no less than half pervious.

The investigation directed by **Syneffa et al. (2005)** speaks to the outcomes led on white shading coatings and aluminium pigmented coatings which were contemplated on a 24 h premise. Albeit both the coatings were portrayed by a high sun based reflectance, aluminium-pigmented coatings were less attractive in light of the fact that they have a tendency to stay more smoking because of their low infrared emittance when contrasted with white shaded coatings. Results acquired by surface temperature sensors and information logging frameworks inferred that cool covering can lessen a white solid tile's surface temperature under sweltering summer conditions by 4oC and amid the night by 2oC. It tends to be hotter, than the encompassing air by just 2oC amid the day and cooler than the surrounding air by 5.9oC amid the night. In this way as per this examination, cool coatings (white shading coatings and aluminium color coatings) present better warm execution even looked at than other cool materials like white marble and white mosaic and their application to the urban condition has incredible potential in lessening surface temperatures.

**Akbari et al. (2001)** has learned about cool surfaces (cool rooftops and cool asphalts) and urban trees that can majorly affect urban warmth island and, consequently, can lessen cooling-vitality utilization. The investigation evaluated that 20% of the national cooling request can be kept away from through a substantial scale usage of this is to be seen when a higher review fastener is replaceable by a white surface. This must be assessed by the requests out and about and the atmosphere.

**Syneffa et al. (2011)** led an examination in which five shaded thin layer black-top examples that can be connected on existing and new black-top asphalts have been created and tried with the end goal to assess their optical and warm execution. It was discovered that every one of the examples has given higher sun powered reflectance esteems and lower surface temperatures contrasted with traditional dark black-top. This investigation demonstrated that supplanting ordinary black-top in a street could prompt a normal air temperature reduction of 5oC under low breeze speed conditions. The aftereffects of this examination show that the utilization of thin layer black-top in streets and asphalts can have critical effect in bringing down surface and encompassing temperature.

**Global Cool Cities Alliance (2012)** has recorded a scope of materials that are accessible for standard clearing needs. Asphalt criteria can differ enormously relying upon the utilization. Thruways, interstate shoulders, civil lanes, parking areas, walkways, play areas, garages, connect decks, and squares all have particular usefulness necessities that can be met by a scope of cool asphalt choices. Numerous sorts of penetrable asphalts, including pervious concrete, permeable black-top, and fortified grass asphalts, are likewise viewed as cool since they can cool an asphalt surface through the dissipation of dampness put away in the asphalt. Porous asphalts have the additional advantage of giving tempest water administration. Some normal asphalt composes are depicted in the table on the confronting page.

**Akbari and Matthews (2012)** paper infers that expanding the sun powered reflectance of the urban surface lessens its sun powered warmth gain, brings down its temperatures, and abatements its outpouring of warm radiation into the environment. This procedure of "negative radiative compelling" can help counter the impacts of an unnatural weather change. Also, cool rooftops and cool asphalts alleviate summer urban warmth islands, enhancing open air quality and solace. An ongoing report presumed that the utilization of white rooftops increments sun powered reflectance by around 0.40, respecting a diminished barometrical temperature equal to decreasing CO<sub>2</sub> outflows by 10t/100 m. Cool-hued rooftops that expansion sun oriented reflectance by around 0.20, yield a one-time CO<sub>2</sub> counterbalance of 5t/100m. The sun based reflectance of asphalts can be raise by and large by around 0.15. Utilizing cool rooftops and cool asphalts in urban regions, by and large, can build the mean albedo of a urban zone by around 0.1. This examination gauge that expanding the albedo of urban rooftops and cleared surfaces worldwide will actuate a negative radiative driving equal to counterbalancing something like 40– 160Gt of transmitted CO<sub>2</sub>.

In research done by **Pomerantz and Akbari (1998)** they found that, in urban regions, expanding the albedo from 0.1 to 0.35, could give a cooling sparing of \$0.012/m<sup>2</sup>-yr. what's more, brown haze reserve funds of

about \$0.06/m<sup>2</sup>-yr. In this manner one could buy a cooler material whose additional expense is this sum, with no net cost. On the off chance that streets are cooler they may likewise last more and in this way set aside extra cash. In this investigation an expansion in lifetime by 30% speaks to a colossal sparing in development, upkeep, accommodation and transfer. One kind of reasonable cool surface, chip seal, is standard in the asphalt business. Notwithstanding the ecological advantages, cooler streets can be less expensive to develop, and may likewise last impressively longer than streets that are not covered with light shaded fixings.

The goal of the examination done by **Tran et al. (2009)** was to distinguish and approve high-reflectance black-top materials that (a) are reasonable for use in parking areas and other extensive cleared surfaces; (b) have a SRI estimation of no less than 29 (the LEED least prerequisite); and (c) are practical. In this investigation the impact of material properties on SRI is additionally talked about, i.e. for new ordinary black-top asphalts, the SRI is for the most part low on the grounds that there is little reflectance of the dark fastener layer and little presentation of total after development. On the off chance that light-hued total is utilized in the black-top blend, the SRI can increment over a time of 5 to 10 years. In this manner, SRI will increment after some time in view of weathering of fastener and more presentation of total. Competitor innovations that can be considered for enhancing SRI of an asphalt talked about are; (a) Surface Gritting with Light-Colored Aggregate, (b) Sand-or Shot-Blasting and Abraded Binder Surface, (c) Chip Seals with Light-Colored Aggregate, (d) Colourless and Reflective Synthetic Binders with Light -Colored Aggregate, (e) Micro-surfacing with Light-Colored Materials, (f) Surface Painting with Light-Colored Paint, (g) Sand Seals with Light-Colored Aggregate and (h) Grouting of Open-Graded Course with Cementitious Materials. The first seven innovations were assessed by utilizing new test areas worked off the track away territory of the National Centre for Asphalt Technology (NCAT). For the last innovation, the examination group worked with EUCO Densit LLC to recognize a test segment for densiphalt and acquire the surface reflectance record results.

The cooling impact of little urban green lush destinations of different geometric setups in summer was the target of the examination led by **Shashua-Bar and Hoffman (2000)**. It was considered tentatively at 11 diverse lush locales. Two elements were found to clarify more than 70% of the air temperature difference inside the concentrated green site, the incomplete shaded territory under the tree overhang and the air temperature of the non-lush surroundings abutting the site. Vegetation surfaces demonstrate bring down radiative temperatures than other non-vegetated ones of a similar shading. The distinction in most extreme temperature may surpass 20 K. On account of extensive green zones, for example, parks, vegetation influences the air temperature above it and in this way enhances the warm condition of the urban zone. The destinations contemplated here have different geometric designs: two greenhouses, four roads, one green square, two yards and two lanes. The examination was done on estimated air temperature information at twelve assembled amid July– August 1996.

**Wilmers (1990)** examined that vegetation has an imperative influence with some restraint of urban atmosphere. Along these lines, Wilmers in his "idealistic meteorologically arranged city", Metutopia, saw the vegetation as the fundamental and first arranging component of the town. In this investigation the principle parameters of the microclimatic contrasts in urban atmosphere are the article to coordinate sun oriented radiation, its span and the matter of the ground surface and the encompassing structures. Vegetation assumes a critical job by its unique appropriate ties with vitality parity and wind. Contingent upon evapotranspiration, vegetation cover and water surfaces reduce the pinnacles of temperature amid the day. The utilization of green components together with poleoclimatopes and choroclimatopes nearby arranging is an essential arranging gadget to enhance urban atmosphere, particularly in the mild atmospheres yet in addition in hot atmospheres.

**Doulos et al. (2004)** attempted to explore the effect of the materials' optical and warm qualities on the urban temperature and in addition the conceivable vitality preservation amid the mid-year time frame. The materials mulled over were marble, rock, stone, clear stone and mosaic. The surface temperature estimations were gone up against hourly premise from 09:00 AM to 06:00 PM. The example materials were utilized on the outside period of the asphalt and rooftops. The surface temperatures of the example materials were estimated with an IR camera that is an infrared condition checking framework. Amid pragmatic, the emissivity esteems for the aggregate number of the considered materials were near 0.9 that exists in the scope of 0 to 1. From the investigation of the aggregate number of the asphalt materials as per their surface shading material it was discovered that the light hued materials were cooler than the others. Not surprisingly the white shaded materials were the coldest, while the dark hued were the hottest, see Table 3.

Table 3: Various construction materials as cool paving materials.

Paving Materials	Colour	Absolute maximum surface temperature (°C)	Absolute minimum surface temperature (°C)
Marble	Grey and White	36.6	22.0
Granite	White-Green	36.8	22.8
Pebble	White	38	23.0
Pave Stone	Black	49.2	28.2
Mosaic	White and Grey	37.7	22.2

**Uemoto et al. (2010)** contemplated that paints have four principle constituents: cover, solvents, added substances, and color. Shade gives shading, as well as controls sparkle, concealing force, quality, and porousness of the paint film. There are two fundamental classes of regular colours: natural, with a somewhat restricted administration life and haziness, and inorganic, which are for the most part more sturdy and less helpless to the photochemical debasement. Inorganic colours likewise have greater strength under higher temperatures and are artificially inactive to acids, soluble base, and so forth. The most essential innovation in the creation of cool paints is the definition with Complex Inorganic Colored Pigments (CICPs) or Mixed Metal Oxide (MMO) shades. These colours likewise present a long administration life in typical conditions, are warm steady and artificially latent. Concrete based materials present unwanted warm properties and cool paints can enhance warm solace states of ease lodging, modern structures and ranch structures developed with fibre bond material sheets. Cool paints can likewise prompt a more extended administration life cycle for this sort of rooftop. Latent cooling of structures is an innovation portrayed by minimal effort and simple application.

In urban territory, green vegetation is helpful to enhance the warm condition in summer, **Saito et al. (1990)**. Nonetheless, the green regions in urban areas are bit by bit diminishing attributable to populace increment and urbanization. In this way, air temperatures in urban territories rise and a warmth island happens. The reason for this investigation is elucidation of the impact of a green territory on the warm condition in a urban region, especially the cooling impact in summer. In this paper, the connection between green dissemination and warm condition is explored. The field perceptions in extensive territories and in little regions were taken. There were high temperatures zones in a few thickly developed areas secured with black-top, solid, slate and tiles. Amid the evening time, the air temperature in suburbia is 2 °C lower than the air temperature downtown. There is a high temperature district in the focal zone of the city which is secured with black-top and solid that has a high warm limit.

**Jauregui (1990)** has considered that the little green territories in urban communities, for example, shade trees along avenues and gardens in rural areas, are a wonderful and attractive piece of the urban scene; they give shade in the warm hours and, as **Landsberg (1981)** out, their impact is constrained to the microclimate.

Extensive urban parks, then again, ex-tend a quantifiable and good impact be-yond their points of confinement over the encompassing urban region. Urbanization in these urban areas develops at a quicker pace than the planting of trees in urban parks. Different purposes behind the poor thickness of green territories saw in third world urban communities are the surprising expense of urban land, stop support and, the shortage of water for water system aftereffect of bigger cooling rates in the green territory, least temperatures are 3-4°C cooler in the recreation centre. The littler warm dormancy of the lush region results in a higher warming rate at the recreation centre amid the morning and at early afternoon hours. Greatest temperatures are then equivalent or even a small amount of a degree higher in the green zone.

This investigation by **Golden and Kaloush (2005)** comprises of mesoscale satellite remote detecting symbolism and microscale handheld IR thermography. Both these instruments are valuable in characterizing

and reevaluating asphalt surfaces temperatures and their commitment to the Urban Heat Island. This examination has talked about the systems that have been now inspected the effects that asphalt have on encompassing temperatures and surfaces. In mesoscale remote detecting parameters like (a) Soil and Vegetation Index; (b) Albedo; (c) Surface Temperatures and (d) advantages of remote detecting were examined. Mesoscale remote detecting was done as such as to distinguish the job of surface asphalts on the Urban Heat Island Effect. A consistent field imaging work was directed to distinguish warming and cooling surface temperature conditions for the distinctive asphalt materials.

**Lawson and Senadheera (2009)** considered and helped in distinguishing and keeping up arrangements with chip seals for flushed asphalts and draining asphalt. Components like totals, fasteners, condition, activity and development adds to draining and flushing of chip seals. In this audit paper, it was talked about that, making asphalts colder or applying cool asphalt systems diminishes the impact of draining and flushing of asphalts. It was additionally talked about that while making the solid blend, water blended with lime and different added substances was utilized in order to utilize it as a cool asphalt. This strategy is material in a crisis to capture seeping on a naturally put asphalt. The exploration findings recommend three promising territories for further research and execution with respect to answers for draining and flushing. They are the utilization of lime water, water-cutting, and racked-in seal.

Due to rapid urbanization the high temperatures has led to problem of UHI. One way to handle this problem is by using paving materials that has high albedo and provide low surface temperatures. **Benrazaviet al. (2016)** conducted a study in Malaysia. The study had three phases: First, exploring theories regarding temperature reduction through pavement materials. Second, collecting related plans and maps for the area to conduct a field study. The last phase involved the measuring of surface temperatures by FLIR E60, an infrared thermal camera imaging device. The study conducted by Benrazavi provides the reference for taking values for surface temperatures of different pavement materials in different area and landscape weathers and environments.

In the examination directed by **Li (2015)** the warm execution for a few asphalt composites has been finished. The asphalt composites significantly utilized, including solid material, square paver and black-top material. In this investigation, two standard testing strategies for deciding sun powered reflectance has been made reference to: (1) ASTM C1549 Standard Test Method for assurance of sun oriented reflectance close surrounding temperature utilizing a Portable Solar Reflectometer (2009) and (2) ASTM E1918 Standard Test Method for estimating sun based reflectance of even and low-inclined surfaces in field (2006).

In an examination directed by **Qin (2015)**, the structures at both side of the road make a gulch like condition that is called road gorge or urban ravine. This examination proposes a numerical model to anticipate the Urban Canyon Albedo (UCA) and approves the model with exploratory perceptions. The model thinks about the various reflections between various surfaces in the urban ravine. Utilizations of the model are loped on two points: (1) if expanding the asphalt albedo successfully raises the albedo of the road gorge; and (2) if an intelligent asphalt mirrors a sizable extra diffuse radiation to adjoining structures' dividers. Parameters of the model found that the gorge perspective proportion overwhelms the UCA while different parameters assume auxiliary job. Expanding the albedo of the asphalt could successfully raise the UCA.

**Taleghani et al. (2014)** has quickly considered the impact of vegetation and water in summer and all the more vitally in winter. The late spring examination demonstrates that a green territory has a 4.7oC lower air temperature toward the evening in correlation with an exposed zone. The winter think about demonstrates that the air temperature over a green rooftop is higher than over a white rock rooftop. Both the late spring and winter ponders demonstrate that parks in urban communities have a lower and more steady air temperature contrasted with rural areas, both in summer and winter. This paper recommends that the urban communities and their open spaces can possibly moderate urban warmth island by including more vegetation and water bodies. The two examinations in summer and winter demonstrated that spots with trees have a more steady air temperature amid multi day in correlation with rural areas. The temperature in a recreation centre in the downtown area was for the most part lower than the temperature in uncovered rural areas.

The examination by **Wang et al. (2016)** assesses diverse UHI alleviation systems in various urban neighbours of Toronto, chose by their building thickness. The impacts of cool surfaces, that is, on the rooftops, in the city asphalts or as vegetation territories are assessed through numerical re-enactments utilizing the product ENVI-met. Results likewise demonstrated that by expanding the albedo of houses by 0.2, from moderate-dim to

medium-light shading, the cooling-vitality utilize can be lessened by around 30– 40%. In other investigation by Taleghani et al. (2014) demonstrated that in the mild atmosphere of Portland white material which has albedo over 0.9, expanded the globe and mean brilliant temperature and created a cooler air temperature in examination with a dull asphalt. The outcomes from the examination demonstrates that utilizing cool asphalt with higher surface albedo from 0.2 to 0.4 and bring down warmth limit from 0.62 to 0.49 J/K, the ground surface temperature could be diminished maximally 7.9oC in the early afternoon at 12:00pm.

This investigation by **Salata et al. (2017)** needed to analyse diverse alleviation procedures of the urban microclimate by mulling over the grounds of the Sapienza University in Rome. It was helped out through the product ENVI-met V 3.1. The circumstance of urban warmth deteriorated with the urban development which now and then happened without an appropriate arranging as far as morphology and materials. Amid the post war period, an expansion in the quantity of building structures with a subsequent difference in the scene, a few materials turned out to be more typical, as black-top and solid, in this way deciding a Urban Heat Island (UHI) which could cause an expansion noticeable all around temperature of 3.6°C to 5°C in the covering layer. This examination analysed the exhibitions of various relief systems which were, cool rooftops, cool asphalt, more urban vegetation and a mix of each of the three arrangements, doing a correlation with the present setup of the site. The most profitable arrangement is the one with the usage of the cool rooftops, cool asphalt and more urban vegetation.

The investigation by **O'Malley et al. (2015)** embarks to set up UHI alleviation procedures, their viability and strength to help give proposals to use of such methodologies in future. Many have recommended that urbanization has restricted to no impact concerning environmental change (**Parker, 2004; Peterson, 2003**), some others show that urban areas are adequately fit for reacting to it. This examination means to explore relief techniques. The current writing was basically inspected with a mean to examine the idea of UHI all in all and all the more particularly in relationship with the idea of manageability and flexibility at city scale for Urban Heat Island (UHI) wonder to check strength and advance urban maintainability.

## CONCLUSION

Change in atmosphere all inclusive or the urban warmth island process bring the temperature up in the urban regions and upgrades the recurrence of warmth waves. Materials assume an imperative job and communicates the warm equalization in the urban condition. Utilization of materials demonstrating high reflectivity to sun based radiation and high emissivity esteems contributes very to the relief of the warmth island process.

In this review paper we discussed about various studies that has been conducted by various researchers and the materials that has shown high reflectance and emissivity were of light color. As both of our asphalt and concrete pavements have low reflectance & emissivity because of the black color of bitumen and high heat absorption of aggregates respectively, the addition of some new material or the replacement of conventional materials will be a great contribution. Materials like white or grey colored marble powder, white or grey colored pebble, white-brown colored granite, etc. has shown great results when applied as a coating on existing pavements. Mixing these materials in design concrete and noticing the changes in temperature might lead to some new outcome. According to this study, the process of mitigation of urban heat must have three phases; first, specifying the new reflective materials; second, developing those materials and third, applying those materials for positive results.

The general survey contemplate has demonstrated that the utilization of cool asphalts is an effective moderation procedure with the end goal to diminish the power of warmth island in urban regions and enhance the worldwide ecological nature of open territories.

## REFERENCES

- Kreith, F. and Kreider, J.F., 1976. "Preliminary design and economic analysis of solar energy systems for heating and cooling of buildings". *Energy*, 1(1), pp.63-76.
- Saito, I., Ishihara, O. and Katayama, T., 1990. "Study of the effect of green areas on the thermal environment in an urban area". *Energy and Buildings*, 15(3-4), pp.493-498.
- Jauregui, E., 1990. "Influence of a large urban park on temperature and convective precipitation in a

- tropical city”. *Energy and buildings*, 15(3-4), pp.457-463.
- Wilmers, F., 1990. “Effects of vegetation on urban climate and buildings”. *Energy and Buildings*, 15(3-4), pp.507-514.
- Kennedy, T.W., Huber, G.A., Harrigan, E.T., Cominsky, R.J., Hughes, C.S., Von Quintus, H. and Moulthrop, J.S., 1994. “Superior performing asphalt pavements (Superpave): The product of the SHRP asphalt research program”.
- Pomerantz, M. and Akbari, H., 1998, July. “Cooler paving materials for heat island mitigation”. In *Proceedings of the 1998 ACEEE summer study on energy efficiency in buildings* (Vol. 9, p. 135).
- Shashua-Bar, L. and Hoffman, M.E., 2000. “Vegetation as a climatic component in the design of an urban street: An empirical model for predicting the cooling effect of urban green areas with trees”. *Energy and buildings*, 31(3), pp.221-235.
- Akbari, H., Pomerantz, M. and Taha, H., 2001. “Cool surfaces and shade trees to reduce energy use and improve air quality in urban areas”. *Solar energy*, 70(3), pp.295-310.
- Doulos, L., Santamouris, M. and Livada, I., 2004. “Passive cooling of outdoor urban spaces. The role of materials”. *Solar energy*, 77(2), pp.231-249.
- Synnefa, A., Santamouris, M. and Livada, I., 2006. “A study of the thermal performance of reflective coatings for the urban environment”. *Solar Energy*, 80(8), pp.968-981.
- Golden, J.S. and Kaloush, K.E., 2006. “Mesoscale and microscale evaluation of surface pavement impacts on the urban heat island effects”. *The international journal of pavement engineering*, 7(1), pp.37-52.
- Lawson, W. and Senadheera, S., 2009. “Chip seal maintenance: solutions for bleeding and flushed pavement surfaces”. *Transportation Research Record: Journal of the Transportation Research Board*, (2108), pp.61-68.
- Tran, N., Powell, B., Marks, H., West, R. and Kvasnak, A., 2009. “Strategies for design and construction of high-reflectance asphalt pavements”. *Transportation Research Record: Journal of the Transportation Research Board*, (2098), pp.124-130.
- Akbari, H., Menon, S. and Rosenfeld, A., 2009. “Global cooling: increasing world-wide urban albedos to offset CO<sub>2</sub>”. *Climatic change*, 94(3-4), pp.275-286.
- Uemoto, K.L., Sato, N.M. and John, V.M., 2010. “Estimating thermal performance of cool colored paints”. *Energy and Buildings*, 42(1), pp.17-22.
- Lee, K.W., Craver, V.O., Kohm, S. and Chango, H., 2010. “Cool pavements as a sustainable approach to green streets and highways”. In *Green Streets and Highways 2010: An Interactive Conference on the State of the Art and How to Achieve Sustainable Outcomes* (pp. 235-247).
- Synnefa, A., Karlessi, T., Gaitani, N., Santamouris, M., Assimakopoulos, D.N. and Papakatsikas, C., 2011. “Experimental testing of cool colour thin layer asphalt and estimation of its potential to improve the urban microclimate”. *Building and Environment*, 46(1), pp.38-44.
- Santamouris, M., Synnefa, A. and Karlessi, T., 2011. “Using advanced cool materials in the urban built environment to mitigate heat islands and improve thermal comfort conditions”. *Solar Energy*, 85(12), pp.3085-3102.
- Akbari, H. and Matthews, H.D., 2012. “Global cooling updates: Reflective roofs and pavements”. *Energy and Buildings*, 55, pp.2-6.
- Santamouris, M., Gaitani, N., Spanou, A., Saliari, M., Giannopoulou, K., Vasilakopoulou, K. and Kardomateas, T., 2012. “Using cool paving materials to improve microclimate of urban areas—Design realization and results of the flisvos project”. *Building and Environment*, 53, pp.128-136.
- Li, H., Harvey, J.T., Holland, T.J. and Kayhanian, M., 2013. “The use of reflective and permeable pavements as a potential practice for heat island mitigation and stormwater management”. *Environmental Research Letters*, 8(1), p.015023.
- Anak Guntor, N.A., Md Din, M.F., Ponraj, M. and Iwao, K., 2013. “Thermal performance of developed coating material as cool pavement material for tropical regions”. *Journal of Materials in Civil Engineering*, 26(4), pp.755-760.

- Taleghani, M., Tenpierik, M., van den Dobbelsteen, A. and Sailor, D.J., 2014. "Heat mitigation strategies in winter and summer: Field measurements in temperate climates". *Building and environment*, 81, pp.309-319.
- Li, H., 2015. "A comparison of thermal performance of different pavement materials". In *Eco-Efficient Materials for Mitigating Building Cooling Needs* (pp. 63-124).
- Qin, Y., 2015. "Urban canyon albedo and its implication on the use of reflective cool pavements". *Energy and Buildings*, 96, pp.86-94.
- O'Malley, C., Piroozfar, P., Farr, E.R. and Pomponi, F., 2015. "Urban Heat Island (UHI) mitigating strategies: A case-based comparative analysis". *Sustainable Cities and Society*, 19, pp.222-235.
- Benrazavi, R.S., Dola, K.B., Ujang, N. and Benrazavi, N.S., 2016. "Effect of pavement materials on surface temperatures in tropical environment". *Sustainable cities and society*, 22, pp.94-103.
- Wang, Y., Berardi, U. and Akbari, H., 2016. Comparing the effects of urban heat island mitigation strategies for Toronto, Canada. *Energy and Buildings*, 114, pp.2-19.
- Salata, F., Golasi, I., Petitti, D., de Lieto Vollaro, E., Coppi, M. and de Lieto Vollaro, A., 2017. "Relating microclimate, human thermal comfort and health during heat waves: An analysis of heat island mitigation strategies through a case study in an urban outdoor environment". *Sustainable cities and society*, 30, pp.79-96.



## Effect of Waste Material on Properties of Bituminous Mix: A Review Study

Unique Vaidya<sup>#1</sup> and Amardeep Boora,<sup>\*2</sup>

<sup>1</sup>M-Tech student, Department of Civil Engineering, Jaypee University of Information Technology, Waknaghat-173234, India E-mail: [uniquevaidya09@gmail.com](mailto:uniquevaidya09@gmail.com)

<sup>2</sup>Assistant Professor, Department of Civil Engineering, Jaypee University of Information Technology, Waknaghat-173234 E-mail: [amardeepboora9@gmail.com](mailto:amardeepboora9@gmail.com) (Corresponding Author)

### ABSTRACT

In the present scenario, road plays an important role by connecting different cities to main national highways and state highways. However, the construction cost of the road by using the conventional method is quite high. Therefore, it is the need of the situation to propose an alternative material as the replacement of conventional ones in order to reduce the overall construction cost of the road without compromising with its required properties. As per the report of ministry of road transport and highway (MORT&H2015-2016), India has the second largest road network. While, Jambeck (2015) mentioned that India is standing on the 12<sup>th</sup> place in production of the waste. The quantum of plastic in solid waste is increasing due to an increase in the population, urbanization and other development activities. The disposal of waste plastic has thus become a serious problem globally due to their non-biodegradability. Therefore, utilization of the waste materials in the construction of flexible pavement that will prove as a cost-effective method as well as eco-friendly. Various studies were conducted across the world by focusing on the utilization of different waste materials like a plastic waste i.e. low-density polyethylene (LDPE), high-density polyethylene (HDPE), waste tire rubber etc. Based on the findings of these studies it was concluded that these waste materials could be used in the flexible pavements. On the basis of the literature review, it is concluded that the plastic waste can be utilized as the replacement of bitumen up to 30% without compromising its properties.

**KEYWORDS:** *Waste plastic; crumb rubber; bitumen; aggregates; flexible pavement.*

### INTRODUCTION

Plastic and other waste material becomes real concern for everyone in today's life. The main issue is to Decomposition of these waste materials is a real challenge as these are the responsible for polluting the environment. Because of that this problem becomes the point of interest of the researchers across the world. Therefore, utilization of non-biodegradable waste material in construction is rapidly growing. It was observed that the waste material can be unchanged on earth for hundreds of decade without degradation and this issue of disposal of non-biodegradable waste will not solve itself and certain practical steps have to be taken for solving this problem. Due to time, traffic is increasing day by day. Hence it's a time of increasing strength and stability of roads by utilizing waste material and reduce the overall cost of road. In the road construction, bitumen is coated over stone aggregates mix, laid and rolled. But when water takes place over roads, it penetrates into the road and it is known by potholes. For this different kind of anti-stripping agents are used but these have their limitation also as the construction cost will increased. So as an alternative, it is found that the use of waste plastic, crumb rubber and other waste for coating on aggregates could improve the overall performance of the pavement (i.e. abrasion, resistance of slip, fatigue life and durability of pavement) will be improved. On the basis of previous studies, bituminous mix design with recycled plastics mainly high density polyethylene (HDPE), low density polyethylene (LDPE) and other waste material showed an increase in Marshall Stability and reduction in mix design. On the basis of previous studies, improvement in indirect tensile strength (ITS) also noted. By heating at temperature 100°C to 160°C low

density polyethylene and high density polyethylene becomes soften and show good binding properties and utilizing it with bitumen results in a mix which is perfect for road construction. The main of the present study is to identify and highlight different techniques to utilise (up to maximum extent) these waste material as the partial replacement of bitumen or as a coating material for the aggregate.

## BACKGROUND STUDIES

Several types of waste materials i.e. waste plastic, crumb rubber and many more were used in bituminous mix design by researchers across the world. It was observed that the utilization of waste material as the replacement of bitumen can improve the service life of the flexible pavement too. Different guidelines were proposed by the researchers across the world regarding the utilization of waste material in the different proportion which is discussed in detail below.

In a recent study, Ahmadiania et al. (2011) investigated on waste polymer like plastic bottles for stone mastic asphalt and said asphalt mixture with a polymer is a costly mixture for pavement of roads so it's better to use waste polymers. In this theory plastic bottles were used which is a type of polyethylene terephthalate and it is a polymer which is used for disposable dishes plastic bottles containers and other. In this research material used was waste polymer portland cement bitumen and crushed aggregates. The waste polymer was used as an additive to the mixture for increased durability and stability. For testing, the wet and dry process was performed. First was a wet process and in this waste, the polymer was added with the binder or in the second test which was dry process waste polymer blended with crushed aggregates but there were certain steps which were also taken that aggregates were first heated for two hours at 200°C temperature. Bitumen content was 5% to 7%. After selecting appropriate content, it was heated up for 1hour at temperature 150°C. After that bitumen aggregates and filler was mixed. The waste polymer was blended for a few minutes and its percentage varies between 2% to 10%. Marshall compactor was used them for compaction at a temperature of 145°C. After that marshal stability test was performed where polymer stability value increases to a maximum 6% after that it started decreasing. Stability value was higher with all the sample except sample with 10% PET. In marshal flow sample of polyethylene terephthalate (PET) until 4% decreasing after that it starts increasing which means stability of high percentage PET decreased. In this analysis of variance is used for comparing the different asphalt mixtures and the result of this theory was stability started decreasing after 6% of Polyethylene terephthalate and PET also increases and stiffness and a perfect match was 6% of PET mixture. Earlier, Arabani et.al. (2010) examined the effect of the waste tire on asphalt mixture or pavement. According to the author, cracking is the main issue in normal pavement and cracking can occur in after several years in every type of pavement, so for increasing the service life of the pavement, author used a high modulus tire cord mesh, Bitumen of 60/70 grade and different size of aggregate according to the passing percentage is used as a material in this experiment and different test like marshal test, indirect tensile stiffness modulus test, the dynamic creep test, and indirect test was done on this by taking different tire thread sample of content 0%,1%,3%,5% on the basis of overall weight of bitumen. These tests are done by using standard marshal apparatus and Nottingham asphalt tester. In this binder content was taken off 5.3%, 5.5% and 5.7% for all samples and according to marshal test optimum bitumen content for sample 0% or 1% was 5.3% and for the sample, 3% or 5% was 5.7%. In this indirect tensile fatigue test was done for finding out the fatigue characteristics, indirect tensile strength and for examination of material cracking ITFT test was used. According to the resulting sample having 3% of waste, tire thread is having better stiffness than other samples. The conclusion of using waste tire thread material is having desirable properties of pavements. Its stiffness is also high as compare to non-reinforcement samples. On the basis of the resultsof creep test, rutting depth was found to decrease after600 MPa. It is due to increase in sample content after 3%. while fatigue life was increasing due to gradually increasein waste tire thread content. Utilization of waste tire thread was resultant in the improvement in the mechanical properties of bitumen. While, Akbulut et al. (2012) conducted a research study to utilize granite sludge as a filler material in bituminous hot mixtures. They focused on using a waste material as fillers material in the bituminous mix for increasing the ratio of fine aggregate and stress-bearing capacity, decreasing the void ratio. In the study, granite sludge (sludge is formed during cutting and polishing of granite) was used as a filler material. Initially, different tests were conducted to examine the properties of aggregate i.e. abrasion, impact value, presence of voids and many more. It is to note that the weak aggregate should not be included in the mix as these aggregates can warp under the effect of freezing and thawing. On the basis of the test results, aggregates stripping and adhesion resistance values were found within the limit. In bituminous hot mix test, recycled filler material was added in five different quantitative values for testing. Tests were scheduled for each 0.5% bitumen increment and flow test was conducted. In the test weight of specimen,weight in water & surface dry saturated to water were measured. Different curves were plotted to examine

the relationships between percentage of bitumen content and stability, bulk specific gravity, percentage of void filled with bitumen, and percentage of void. Resultant optimum bitumen ratios for different design groups i.e. 0%, 2%, 4%, 6% and 8% were found out around 3.83%, 4.04%, 4.10%, 4.76% and 5.11% respectively). These tests told about the use of waste granite filler materials in bituminous mix. In this, increase in durability shown by using 6.4 % filler material in bituminous mix. On the basis of result, the maximum stability values came with 0%, 2%, 4%, 6% and 8% mix. The filler additives came out to be 1360, 1260, 1480, 1600 and 1640 kg respectively. The Maximum value came with 8% filler Content which was around 1650 kg. The percentage of voids for different samples containing filler additives in different proportion i.e. 0%, 2%, 4%, 6% and 8% were found out around 3.8%, 3.0%, 3.2% and 2.5% respectively. Tests samples containing ideal bitumen content were relieved in a water shower at 60°C for 48 hours. Then, the marshall stability test was performed. According to this, the stability loss was lower in 8% filler specimens than in others. After that Indirect filler test was conducted to determine the resistance to plastic deformation of the bituminous hot mixtures at a varying range of temperatures. (5°C, 25°C and 40°C) and the stiffness modulus of bituminous mixes. Indirect tensile strength at 40°C was lower than that at 25°C. change in filler level from 6% to 8% at 40°C showed Change in Indirect tensile strength from 264.0kPa to 264.6kPa. at 5°C, the Maximum stiffness was with 8% filler particles, whereas at 25°C the maximum value was at 6% filler particles. Thus the serving period of 8% filler particles was concluded to be more. Therefore, it was concluded the granite sludge can be reused as a filler material. Optimum bitumen content levels were calibrated i.e. 5.11%, 4.76%, 4.10%, 4.04%, and 3.83% for varying proportion of filler material (i.e. 0%, 2%, 4%, 6% and 8% values respectively). Thus by increasing, recycled granite sludge bitumen level fell under the economical limits. Specimens with 8% filler contents had maximum stability values by filling micro voids in the bituminous hot mixture. Different properties of bituminous hot mixtures with variation in filler type and content indicated that fillers significantly affected the mixture properties. The capacity of bituminous hot mixtures in wearing courses was supposed to be better if the filler were to be used at 7.3%. Recently (Ahmad 2014), low-density polythene was utilized in the bituminous mix design. In this study material taken as waste plastic low-density polyethylene (LDPE), bitumen of VG30 grade and aggregates. Different samples were made with a percentage of 2%, 4%, 6%, 8%, 10%, 12%, according to the overall weight of bitumen. There was a various test conducted on the bitumen by following IS code. According to LDPE, in this polythene waste and plastic bottles are cut into small pieces for making different samples of size 2mm - 3mm. According to MORT&H specification stone aggregates and for filler material stone dust and cement was used in a ratio of 3:2. Various test conducted on samples and result was sample having 12% waste having better stability value. Inflow value tests the value was decreased by 34 % as compared to plain bitumen with 12% of LDPE waste which show more stability and in bulk density test value increased by 25% with the same sample. In an air void test, the value decreased by 44% with 12% of the plastic waste sample which shows more stability. So this study concludes that the overall quality improved by 14% by using 12% of LDPE waste sample.

Bhageerathy et al. (2014) conducted a study on the use of plastic waste in construction of road. The materials used in the study were bio-medical syringe plastic waste, bitumen, and aggregates. During the study three normal mix specimens were made and samples containing bitumen content of 4.5 %, 5%, and 5.5% respectively and conducted a marshall test on samples. The optimum bitumen content was found to be 5%. Marshall test was performed on four plastic modified mix specimens having plastic values in different proportion like 2%, 3%, 5%, and 7%. In this optimum plastic content (OPC) was recorded as 5 %. On the basis of static creep test, percentage of permanent strain for plastic and normal modified mix specimens were found around 0.33 and 0.54 respectively. The results of indirect tensile stiffness modulus (ITSM) tests revealed that the normal mix had less tensile stiffness modulus than the modified mix with plastic. Aggregates coated with 5% of plastic were tested to examine different properties like aggregate crushing value percentage (%), aggregate impact value percentage (%), los angeles abrasion value percentage (%), specific gravity of 13mm aggregates, specific gravity of 19mm aggregates, specific gravity of 9.5mm aggregates, water absorption of 19mm aggregates percentage (%), Water absorption of 13mm aggregate percentage (%), water absorption of 9.5mm aggregate (%). From the test results it was revealed that the aggregate crushing value get decreased by 27% after coating the aggregate with the plastic. While, the aggregate impact value was found to decrease upto 17.7 percent. Los angeles abrasion value of plastic coated aggregates were seen to be reduced by 8%, and water absorption for plastic coated aggregates was 0%. Thus, from this study, it was concluded that the optimum value of plastic content will be equal to 5% of weight of bitumen. The marshall stability value of normal mix was seen to be 51% less than a modified mix with plastic, indicating an increase in load carrying capacity. The reduction in crushing value and impact value of aggregate was found around 27% and 17.7% respectively. Reduction in los angeles abrasion value of coated aggregates with plastic indicated that, these have a superior abrasion resistance as compared to normal mix. In this the permanent strain was decreased by 0.21%, there was an indication towards the increased tensile strength of Plastic modified mix as its average tensile modulus was

found to be increased by 47.8% than the normal mix design. Hence, the biomedical waste can be disposed of easily and conveniently by incorporating it in bituminous mixes. While, Bansal et al. (2017) employed waste rubber and waste plastic material in the modified bituminous mix design as the replacement of bitumen. In this study, crushed plastic bottles, plastic bags, waste tire were used as a waste material. In the study, three samples were made by mixing of rubber, plastic with bitumen in individual and combined manner. In this study different type of test like penetration test, ductility test and softening point test was done. For the purpose of testing, different samples were made by utilizing the plastic and rubber in varying proportion i.e. 4%, 6%, 8%, 10% and 5%, 10%, 15 % respectively. Maximum stability value was obtained when the mix was prepared in different proportion i.e. 84% of bitumen, 6% plastic, and 10% rubber. In marshal flow value test, the higher value was obtained with the rubber content more than 10%. In case of bulk density, values were found higher for all mixes rather than the conventional method. However, mix having 8% of waste was depicting higher value than other mixes. While the air void found to be increased due to variation in the density of the waste material. This study reveals that the use of waste in road construction will prove more economical than the conventional method and also improves the quality of roads. Ghalyan and Rana (2017) partial replaced the bitumen by using plastic waste in bituminous concrete. In this study, plastic waste, aggregates, bitumen of 60/70 penetration grade was used as a material. According to study waste was collected from different resources and washed properly for the removal of impurities in the waste. After that waste plastic was cut out in small pieces of size 2.36mm to 4.75mm because small pieces can mix properly and give the better result. After this aggregates were heated at 160°C and waste plastic was added to the heating chamber for giving a coating to aggregates. After that bitumen was also added and heated at the same temperature. Several tests were carried out like an impact value test, ductility test, and marshal stability test according to proper guideline and with different percentage of plastic samples. So according to the test result, this study concludes that the increase of waste plastic in mix design increase the property of aggregates and enhance the strength. The advantage of using waste plastic is, it's economical and eco-friendly.

Hınışođlu and Agar (2004) investigated a study on the use of the waste plastic material in the bituminous mix design. The material used in this study was bitumen AC-20, waste high-density polyethylene (HDPE) and crushed limestone used as an aggregate. Marshal test method was used in this study for finding out the resistance with or without HDPE modified concrete. In this sample made by mixing waste HDPE in 4%,6%, and 8% according to the weight of bitumen content, HDPE, bitumen and aggregates heated up separately at the temperature of 155°C and 165°C and mixed with the help of the mechanical mixer. In this void ratio in samples were around 3.07% to 3.35%. After this process samples were kept in the room for cool down. After samples were kept in water at the temperature of 60°C for 30 minutes and tested with Marshall test apparatus. All the results were obtained from each mixed sample. According to the result, the stability decreases with increasing of waste HDPE content. The maximum stability increases with 4% of HDPE. In this flow increases according to the increase of HDPE content. According to flow result sample having 4%, bitumen content was having the smallest flow value of 3.8 mm. According to Marshall quotient result, the sample with 4% fulfilled all the specification of Marshall quotient. This study concludes that sample with 4% HDPE is having better stability for using in the construction of roads. Marble waste was used as a filler material in the construction of bituminous roads/ flexible pavement by Karasahin and Terzi (2007). It is to note that the limestone dust is utilizing across the world in large quantity which works as a filler material. However, there is a number of filler material which exhibits different properties. For the same purpose marble dust was treated first due to the presence of different marble content. Consequently, a marshal sample with 75-100 penetration asphalt cement was prepared. Later on, several samples were cast in order to carry out several tests. After doing several tests and analysis stability of limestone dust was found higher in comparison to marble dust. The void ratio was found higher in case of marble dust comparatively void ratio observed in the case of limestone. In this process, four type of marble dust sample was taken in which two was from the different place and other two was from the different place and used without doing any process on that sample and in the test the optimum bitumen content was 4.7 %. So according to the test result sample having limestone dust the plastic deformation decrease by 8% after that it started increasing which means plastic deformation decrease to a point after that, it starts increasing because the different type of filler material fills the void in the material and increase its stability but after some time. The second sample was which is having marble dust and the result was that it can be used directly without doing any process on it and according to the plastic deformation test marble dust is having higher plastic deformation. By doing all the test the conclusion for limestone dust sample and marble dust was that plastic deformation decreases by 7% after that it starts increasing and both the samples of lime dust and marble dust having the same plastic deformation but marble dust can be used directly in asphalt mix and it is having higher plastic deformation and this type of mix can be used for link roads or local roads.

Kumar and Vikranth (2017) conducted a study on the use of plastic waste polypropylene (PP) in flexible pavements. The material used in this study was aggregates, bitumen and waste plastic. Various tests were conducted to compare normal aggregate and plastic coated aggregate as well as normal bitumen and bitumen mixed with plastic waste. The value of specific gravity of plastic coated aggregate was more than the plain aggregate and the water absorption test showed that coating with plastic reduced the moisture absorption and increases the quality of the aggregate. The coating of plastic improved the Aggregate Impact value. The Aggregate crushing value was lower of plastic coated Aggregate thus; it could withstand more load. The Los Angeles abrasion test showed a decreased value of wear and tear for plastic coated Aggregates thus, indicating a longer life. When plastic was added to bitumen the penetration of bitumen decreased. With the increase in plastic content, the softening value increased. The viscosity value of plastic coated bitumen was Low as compared to conventional bitumen. On addition of polypropylene to bitumen fire point and flash point increased thus preventing hazards. The value of conventional bitumen was less as compared to plastic coated bitumen. From the study, it was concluded that the optimum value of plastic waste added was 9-10% by weight. On adding plastic waste to bitumen and aggregate, their properties increased by reducing bitumen up to 9-10% cost of construction of Flexible Pavements also decreases and moreover it's a useful way to preserve our environment. Recently, Kawade et al. (2018) conducted a study on design and qualitative analysis of flexible pavement containing waste materials. The waste materials used in the study as the replacement of natural aggregates were namely crushed stone, steel slag, recycled concrete and crumb rubber (by cutting waste rubber tires in pieces that could pass through 2.36mm sieve and were retained on 1.18mm sieve). Marshall Stability test was performed for each type of mixes containing different waste material as the replacement of aggregates and VG-30 bitumen mix. In the case of steel slag, the impact value and crushing value was found to be around 9.33% and 15.42% respectively which is appropriate for highways construction as per to Indian road congress (IRC). While impact value and crushing value of recycled concrete aggregate was 24.69% and 31.47% respectively which are not as per the IRC's specifications. Marshall stability and the flow value of mix containing steel slag was found to be 990.6kg and 2.1mm respectively, which satisfies the IRC's guidelines. On the other hand, stability and the flow value of the mix containing 100 % of recycled concrete aggregate (RCA) (692.33kg and 1.83mm respectively) was not found as per the IRC specifications. Though, the mix containing 50% RCA as the replacement of natural aggregates was showing the stability value around 1340.31 kg while flow value was found to be 1.96. Therefore, it can be concluded that properties of bitumen mix increase with the addition of rubber crumb up to 50% as the replacement of natural aggregate.

Prasad and Prasad (2009) conducted a study on the performance of waste tire rubber on the model flexible pavement. The materials used in the study were soil, fly ash gravel Road metal and waste tire rubber. Direct shear tests, California bearing ratio test and cyclic load tests were carried out. The results showed that Cohesion and angle of internal friction values for gravel materials were increased from 11.77 to 26.48Kn/m square. And 36°C to 43°C respectively with 5.0 percent of waste tire rubber and after that it decreased. The Cohesion and angle of internal friction values were decreased from 7.85 to 18.64 KN/ meter square and 33°C to 39°C respectively for the fly ash with 6.0 percent of waste tire rubber chips and after that, it decreased. From this test, it was concluded that the optimum range of waste tire rubber for gravel and fly ash were 5% and 6% respectively. California bearing ratio test results showed that for gravel and fly ash subbase materials, the values increased from 8.0 to 13.32 and 4.0 to 8.73 for 5.0% and 6.0 % of waste tire rubber respectively. Therefore, the optimum percentage of waste tire rubber for gravel and fly ash were 5% and 6% respectively. The cyclic load test results showed that the load carrying capacity had shown an upward increase in pavement made with waste tire rubber as a component. From the above study, it was concluded that the optimum percentage of waste tire rubber is 5% and 6 % of dry Unit Weight of soil respectively for gravel and fly ash material reinforced with waste tire rubber. The load carrying capacity of the pavement reinforced with waste tire rubber increased and the gravel reinforced waste tire rubber model flexible pavement showed better performance than fly ash subbase reinforced with waste tire rubber. Pasandin and Perez (2017) conducted a study on the performance of bituminous mixt made with recycled concrete aggregates and waste crumb tire rubber. The material used in this study were, bitumen, normal aggregates, and recycled concrete aggregates (RCA) and waste rubber tire. In this study samples were made with inclusion of 0 %, 35% and 42% RCA. The specimens were made with varying optimum bitumen content (OPC) value i.e. 4% to 6% for different samples. The stiffness of the bituminous mix and fatigue life prediction was calculated. The test results showed that the type of strip loading is responsible for the split pattern. Results of the stiffness test depicted that the primary stiffness of the mix will achieve at hundred cycles against the primary micro-strain at the tenth cycle and the same trend was observed for all the samples. Later, bituminous mix of 35/50 grade containing crumb rubber was prepared (without addition of recycled concrete aggregates i.e. 0%) which was depicting higher stiffness value in comparison to the mix of same grade having 0% of crumb rubber and RCA. Consequently, it was concluded that the bitumen

mixed having waste crumb rubber shows the higher stiffness. On addition of recycled concrete aggregate to the mixture in different proportion (35% and 42% recycled concrete aggregates), no difference was noticed in the property of the mix when compared to the normal mix (0% RCA and crumb rubber) and the bituminous mix of 35/50 grade having crumb rubber. However, when recycled aggregates were not added to the mixture the properties of the bitumen were more prominent. From the results, it could be seen that fatigue life of the bituminous mixtures was getting increased due to the inclusion of recycled aggregates. Fatigue life of the bitumen mix of 35/50 grade containing rubber was found lower than the conventional mix of 35/50 grade. For recycled concrete aggregates, initial micro strain was found 303.1  $\mu\text{m}$  without addition of recycled concrete aggregates while addition of 35% recycled concrete aggregates was depicting 226.6  $\mu\text{m}$  initial micro-strain value. Consequently, increment in the initial macro strain value i.e. 264.7  $\mu\text{m}$  was observed with the addition of 42 % recycled concrete aggregates. Therefore, it could be seen that there was no co-relation between the initial macro-strain limit and recycled concrete aggregates percentage (%). The result also showed that the recycled concrete aggregates percentage produced more changes in fatigue loss than the type of bitumen used. Consequently, during the ITFT test, fatigue mechanism was found prevalent instead of permanent formation mechanism because of the use of recycled concrete aggregates and the waste tire rubber as a good modifier. Fatigue life of the bitumen in the mixture was found to be increase with the increase in the percentage of recycled concrete aggregates. When waste rubber tire was used as a modifier, the fatty performance of hot mix asphalt (HMA) made with recycled concrete aggregates was found to be affected. Initially, the mixtures made with bitumen containing rubber of 35/50 grade was showing more fatigue life as comparison to mix made with only bitumen 35/50 grade. However, for initial macro-strain mixtures with bitumen containing rubber of 35/50m grade was depicting higher fatigue life.

Rajmane et al. (2009) utilized waste plastic effectively in the construction of flexible pavement for improving their performance. The materials used in the study were waste plastics, bitumen, and aggregate. The tests conducted on bitumen were penetration test, ductility test, softening point test, flash and fire point test. For aggregate, the tests that were performed were specific gravity test, water absorption test, impact value test, and abrasion test. The relevant index and Engineering properties of plastic waste was determined and compared with conventional bitumen. Trial mixes were carried out with different percentage of plastic waste and were compared for the compressive strength. The optimum range of plastic waste that was to be mixed with the most common bitumen was selected that would produce the maximum compressive strength. These samples were then tested for various pavement properties. The study concluded that the plastics increased the melting point of the bitumen. The plastic waste, when mixed with bitumen, provides an improved material for the construction of pavements because this mixture has higher Marshall stability values and suitable Marshall Coefficient, therefore, it increases the road life and also it is one of the best ways for disposing of the waste plastics. Consequently, Rokade (2012) also utilized the waste plastic and waste rubber tires in Flexible highway pavements. The material used in the study was crumbled rubber, low-density polyethylene (LDPE) and bituminous mix. The semi dense bituminous concrete was made using marshall method of bituminous mix design, using conventional 60/70 grade bitumen to which varying percentages of LDPE was added and 60/70 grade bitumen added with different percentages of crumb rubber. The results depicted that with 5% bitumen content, density, and Marshall Stability value were higher. Values for Flow value, Bulk Density, Air Voids, Voids in mineral aggregate (VMA), Voids filled with bitumen were within the parameters of MORT&H. The test showed that 10% of crumb rubber of the weight of bitumen is the best dose for improving the strength of the SDBC mix. The study concluded that Marshall Stability value has shown ascending value and the maximum value has reached by about 25% on addition of low-density polyethylene (LPDE) and (crumb rubber modified bitumen (CRMB)). The density of mix has also increased in case of LDPE and CRMB when compared with 60/70 grade bitumen. Similarly, Rajput and Yadav (2016) replaced the bitumen with plastic waste in bituminous road construction. The materials used in the study were VG30 viscosity grade bitumen, hard and angular coarse aggregates of 9.5mm and 6mm size, and fine aggregates (dust) is used in varying quantity according to MORT&H specification and waste plastic shredded to the size of 2.36mm. For the preparation of plastic modified mix plastic contents of 6%, 8%, 10%, 12%, and 14% by weight of bitumen were added to hot aggregate. Marshall test was performed on plastic modified mix specimens as well as plain bitumen to study a number of parameters and compare them. The results depicted That Marshall stability value was increased and the Maximum value was for specimen containing 12% plastic by weight of bitumen. There was an increment inflow value with increase in plastic content. For 6% plastic waste, flow value was 2.7 and for 14% plastic waste by weight of bitumen flow value was 4.0. The value of void filled with bitumen (VFB) was recorded around 72.0 for 6% plastic waste by weight of bitumen and for 14% plastic waste it was found to be 75.9. Percentage of air voids decreased from 4.0 at 6% plastic waste to 3.2 at 14% plastic waste by weight of bitumen. Hence, it was concluded that by doing an increment in the percentage of waste plastic into the mix the Marshall stability values also up scaled. Thus, the optimum plastic

content was found as 12%. The flow value goes continued to increase with the addition of plastic content in the mix. The percent air voids in the mix showed a downfall while VFB continued to increase on the addition of the plastic waste. Therefore, it can be said that the addition of plastic waste to the bituminous mix increases the strength and durability of the roads. Reddy et al. (2017) performed a study on the properties of pavement using waste plastic in Road Construction. The materials used in the study were bitumen, waste polyethylene terephthalate, crushed granite (coarse aggregate). Marshall test was conducted to obtain a crushing value, impact value, los angeles abrasion value, flakiness index, Elongation index, the specific gravity of coarse aggregates, the specific gravity of fine aggregates, water absorption test values of aggregate. Similarly, physical properties of bitumen like penetration, softening point, ductility, flash point and fire point, specific gravity, and viscosity were also recorded. The optimum binder content was found to be 5.5% for 80/100 grade of bitumen with the stability value of 1190 kg. The flow value along with Maximum stability was 3.6mm. Gm was found to be maximum of 2.394 gm/cc at 5.5% of bitumen. Percent air void (Vv) varied from 2.5% to 4% by different percentage from 5% to 6%. Vv was found to be 3.5% with the bitumen content of 5.5%. Plastic was added to the hot aggregate mix with a varying range of 0-12%. The results showed that with the increase in the percentage of plastic waste the optimum stability was found to be in the range from 1930 to 1950 kg. The flow values varied from 4.0 to 4.5mm at 8% of plastic waste. The bulk density was found to be maximum between 2.29 to 2.35 gm/cc at 8% of waste plastic, and there was a decrease from 2.14 gm/cc at 12% plastic. The study concluded that the Vv was found to be 4.9% to 4.6% at 8% of plastic waste. The properties of bitumen were increased by adding 12%-14% plastic waste as compared to unmodified bitumen. This study also approached towards preserving our environment.

Sultana and Prasad (2012) performed a study on the use of waste plastic as a strength modifier in the surface course rigid and flexible pavement. The materials used in the study were waste polymer low-density polyethylene, High-density polyethylene and polypropylene (PP), bitumen 80/100 penetration grade, cement concrete and water. Plastic coated aggregates, polymer modified bitumen, and concrete cubes were prepared. Aggregate tests, Rheological tests, Performance tests were done on modified mix and unmodified mix. The results showed, increase in properties of aggregates like impact value, abrasion value, and los-angeles abrasion value. On the basis of result, penetration and ductility value decreases and softening point value increases. Marshall stability test was conducted both on plastic coated aggregates and modified bitumen with waste material and marshall stability value increased by addition of waste material in mix. Loss of stability test resulted that mixes with an index of more than 75% were approved. On the basis of test report, properties of aggregates were improved by using waste material with aggregates. The rheological properties were also improved by adding waste plastic material to unmodified bitumen mix. Penetration and ductility value decreases and softening point value increases. The marshall stability test concluded that low-density polyethylene (LDPE) showed better values as compare to polypropylene (PP). The optimum value for low density poly ethylene was noted 8% for sample made with waste plastic material. On the basis of performance test there was an improvement in flexible pavements than rigid pavements. Shedame and Pitale (2014) performed a study on bituminous concrete containing plastic waste material. The materials used in the study were aggregates of size (20mm, 10mm), bitumen (60/70grade), stone dust and cement as filler, waste plastic in shredded form. The penetration test, Ductility test, Specific gravity test, and Softening point test were performed on bitumen. On Aggregates Specific gravity, Water Absorption Test, Impact value test, Abrasion test, crushing value test, stripping value Test were conducted. Marshall stability test was carried out to determine the Optimum Binder content for bitumen content (BC) mixes. The properties that were checked in this test included stability, flow value, Bulk specific gravity, Air voids, Voids filled with bitumen and Voids in mineral aggregate. The Plastic Waste was added to 0% to 1% by the increment of 0.25%. Marshall specimen with varying waste plastic content was tested for Bulk density and Stability. The average Optimum Waste Plastic Content value was 0.76%. The study concluded that when 0.76% plastic by weight of aggregate and 3% filler was used, it improved the volumetric properties of bituminous mixes which resulted in better performance of BC with plastic waste. Addition of plastic increased the melting point of bitumen. Plastic roads idea was eco-friendly and also increased the road life along with being eco-friendly. Sutradhar et al. (2015) utilized stone dust, waste concrete, and brick dust as filler material in the bituminous mix design. In this study coarse aggregate of size 2.36 mm, bitumen of grade 85/100, fine aggregates which were kept in 0.075mm sieve and waste filler material like fine sand and stone dust mix, waste concrete dust and brick dust was used as a material. For testing purpose, the marshall test was conducted. According to the test result, the optimum bitumen content for brick dust and waste concrete dust was found similar to the conventional filler material. It was concluded that the waste concrete dust and brick dust is having the same properties as compared to conventional one and can be used as filler materials. Somani et al. (2016) conducted a study on strengthening of the flexible pavement by using waste plastic and Rubber. The materials that were used in the study were low-density polyethylene (LDPE), crumb rubber, aggregate, and bitumen. For aggregate, the tests that were carried out were

aggregate impact value test, aggregate crushing value test, flakiness, and elongation index test. For bitumen the tests that were carried out were penetration test, softening point test, ductility test, and viscosity test. Semi-dense bituminous concrete was prepared by adding conventional bitumen with different percentages of LDPE and bitumen with the addition of different percentages of crumb rubber. The results depicted that the Marshall stability and the density will be increased with the addition of vitamin content was up to 6 %. All the other parameters or properties were found as per the specification of MORT&H. It was observed that the mixing of 8% LDPE and 6% bitumen content will result in the higher Marshall stability value (i.e. 945 kg with 3.26 mm flow value). Shaikh et al. (2017) conducted a study on the Use of Plastic Waste in Road Construction. The materials used in the study were bitumen 60/70, aggregates, cement, and shredded plastic waste of 2.36mm size. Marshall stability test was performed on both the modified and unmodified bituminous mix. On aggregate the tests performed were aggregate impact value, los angeles abrasion test, water absorption test, specific gravity test, stripping value test. On bitumen the tests performed were penetration value test, ductility test, flashpoint test, fire point test, Softening point test. Marshall stability test was then performed by adding plastic waste. The specific gravity increased from 2.5 to 2.66 and 2.77 on the addition of 10% and 15% plastic content respectively. Aggregate impact value decreased from 10.79% to 8.94% on addition of 15% plastic. Los Angeles abrasion value declined from 12.85% to 10.65% on addition of 15% plastic waste. Water absorption value decreased to 1.1% at the plastic waste of 15% and stripping value was decreased to nil by adding 15% plastic waste. On addition of 15%, plastic waste by weight of bitumen the marshall stability value increased from 950kg to 1980kg, and the flow value increased from 3.1mm to 5mm at plastic waste of 15% by weight of bitumen. Thus, the study conducted that modified mix improved the marshall characteristics. With the addition of plastic waste marshall stability value increased, flow value decreased, thus it could withstand heavy loads, hence, increasing the durability of roads and also preserving the environment. Recently, Sharma et al. (2018) examined the performance of bituminous paving mix containing waste plastic. The material used was crushed basalt type of course aggregate 20 mm, crushed basalt type of fine aggregate 2.36 and down, 80/100 penetration grade bitumen, basalt stone dust, and cement as a mineral filler. While the waste plastics namely polyethylene terephthalate (PET), polypropylene (PP), polystyrene (PS), polyvinyl chloride (PVC), low-density polyethylene (LDPE), high-density polyethylene (HDPE) was used in the shredded form. Marshall Stability test was carried out with varying percentage of plastic waste in order to check the stability of the mix. Later, a comparison between the results of BC (Bituminous concrete) mix with waste plastic and plain BC mix was made. Consequently, the stability value of optimum plastic content OPC (optimum plastic content) was found to be 30.1, which was much higher than the optimum bitumen content OBC (optimum bitumen content). The volume of voids in BC mix containing plastic waste was found lower than the plain BC mix. These results were within the parameters of MORT&H-2001 specifications. The test concluded that the OPC mix showed higher stability as compared to OBC mix and intermolecular binding between bitumen and waste plastic enhances the strength, durability, and life of roads. While, Sharma and Srikanth (2018) utilized waste polythene in the bituminous paving mix design. The materials used in the study were bitumen, aggregate and waste plastic. Marshall stability test was performed and carried out in two parts to determine optimum bitumen content (OBC) and optimum plastic content (OPC). Different samples were made with different ratio of bitumen, aggregates, and plastic. After that test was conducted at the temperature of 60°C to check the OBC which was found to be 5.8%. Later, disposed milk packets were used to determine OPC. In this. The specific gravity and softening point were taken from the report of milk packets manufacturer and report specified the specific gravity and softening point value around 0.92 and 115°C respectively. So according to the result, the value for plastic content corresponding to maximum stability was equal to 10%. The value of binder content corresponding to maximum bulk specific gravity was found to be equal to 7.5%. Average of the above values came out to be 8.75%. The results from the test stated that, the OBC was 5.8% and the OPC was concluded to be 8.75%. Thus, it was concluded that addition of plastic waste material content in bitumen increases the stability as comparison to conventional bituminous mix.

Trimbakwala (2017) conducted a study on the use of waste plastic in road construction. The materials used in the study were aggregate, bitumen, the 8% of plastic waste to the weight of bitumen was added in the conveyor belt to coat the plastics efficiently. Marshall method was carried out the plastic was added to heated bitumen in different proportions (0-12% by weight of bitumen). The properties of modified and unmodified bitumen were compared. It was seen that penetration and ductility values of modified bitumen were decreased with the increase in contact of plastic additive, till 12% by weight. The softening point of the modifier was increased on addition of plastic waste up to 8% by weight. Marshall specimen having a different amount of waste plastic content were tested for bulk density and stability. The maximum value of stability was considered as the main criteria for optimum waste plastic contents. The average maximum stability value (MSV) of the mix by using the modified Binder was seen to be 1750 kg which led to three times increase in stability of the BC mix that comprised of 4.6 % bitumen and 8 % process

plastic by weight of Bitumen. The ability of the mix which was created with the above-modified bitumen was checked to withstand soaking under water in adverse conditions. The average MSV of the BC mix with the modified binder was seen to have an upscale value by about 2.6 Times of the mix which contained ordinary bitumen. Even the fatigue life increased of BC mixes that used this modified binder. Thus the comparison between normal roads and plastic roads was concluded that the durability of the roads having shredded plastic waste was quite higher as compared to the conventional roads. The plastic waste had a good binding property which made the life of the roads longer and also proved as an aid to the strength i.e. to bear more traffic load. Plastic addition to the bituminous mix also solved the problem of managing hazardous waste plus it is an eco-friendly method of construction. Tiwari et al. (2018) conducted a study on modified bituminous binder using plastic waste. The materials utilized in the study were bitumen 60/70 grade, plastic waste (LDPE) shredded into the size of 2.36mm. Bitumen was modified by melting at a temperature of 150°C and adding shredded pieces of low-density polyethylene (LDPE) ranging between 2.36mm to 4.75mm. Different tests like penetration test, softening point test, ductility test were performed on modified bitumen. The results showed that penetration value of plastic modified bitumen was reduced by 19.4% for LDPE waste. By adding 2% and 4% plastic the penetration values were 65mm and 62mm, this led to an increase in strength and load-bearing capacity. Ductility value was decreased by about 21.79% for plastic modified bitumen. For 2% to 10% addition of plastic ductility value decreased from 75cm to 61cm. Softening point value increased by 18.6% when plastic was added. The results showed that on the addition of 2% and 4% plastic the softening point increased to 49°C and 52°C respectively. The study concluded that use of plastic waste in the proportion of 2% -4% gave penetration values and softening point under the IS code (IS-1203-1978) specifications. Adding 2%-4% plastic higher softening value of 52°C was obtained which helped in withstanding higher temperature susceptibility. In the same way decrease in penetration value gave higher load-bearing capacity. Addition of plastic waste to the bituminous mix also reduced its aging. Thus, it was proved that using plastic waste modified bituminous mix in road construction increased the durability of roads.

Wayal and Wagle (2013) investigated a study on the use of waste plastic rubber in aggregate and bitumen for road materials. The material used in this study was aggregate, bitumen, plastic, and rubber. Different tests were performed to calibrate different properties i.e. crushing values, impact value, abrasion value, the specific gravity of aggregate and bitumen penetration value, ductility, softening point. For checking moisture absorption and void measurement hot stone aggregates (150°C) is mixed with hot bitumen (170°C) and coated with rubber and plastic. This showed a decrease in porosity and improve in quality with respect to soundness, voids and moisture absorption. The soundness test confirmed that the plastic and rubber-coated aggregate didn't show any weight loss. To study the aggregate impact value, the aggregate was coated with 1% and 2% plastics and rubber by weight and then subjected to aggregate impact value test. It was seen that the coating of plastic and rubber on aggregate improves the quality. Los Angeles abrasion test found out that there was less wear and tear values of 1% and 2% plastic and rubber-coated aggregate as compared to conventional aggregates. Softening point, ductility and penetration point of bitumen was studied by heating bitumen 10-140 degrees, to this 10% and 20% plastic and crumbled rubber (split in 5% and 10%) was taken in proportion by weight. Then these values were compared with the conventional values and found better. Hence proving that use of waste rubber and plastic increased the durability and life of roads lastly, Marshall stability test was performed to determine the stability of bituminous mix. For this 1200 GM's of mix was taken with thickness 63.5 mm, approximately 1200 GM's of filler and aggregate was heated at 180-200°C, the compaction mold assembly and rammer was preheated at 100-140°C, bitumen was heated at 130-140°C, 4% polymer and 4% crumbled rubber by weight is added, 80/100 bitumen was heated at 160-140°C. The values were compared with the conventional mix. This study concludes that on adding 8% polymer and crumbled rubber in the blended mix, the Marshall test, flow(mm), Gmb(gm/cm<sup>3</sup>), AV (%), VMA (%) VFB (%) increases compared to conventional mix. Vashisht and Saini (2017) utilized waste plastic and crumb rubber in the flexible pavement. In this study, the wet and dry process was adopted for preparing the modified bitumen. Samples were prepared according to the ministry of road transport and highway (MORT&H) specification. In the wet process, first bitumen was heated at the temperature of 160°C and temperature was recorded at the time of softening of material. Later, waste material was added in the mix for avoiding agglomeration in the material. In this percentage of modified agent vary from 1% to 16%. In the dry process, it was only done with plastic waste by cutting it into small size of around 3mm-6mm and mixed with the aggregate at the temperature of 165°C. On the other hand, bitumen was heated at a temperature of 160°C for having good binding strength. After that sample was made with 8% of plastic waste and 16% of plastic waste. In the present study, crumb rubber was not utilized in order to make the sample because of the poor bonding quality (i.e. between crumb rubber and aggregates). As per the result, impact value was found to be increased up to 10% due to the addition of plastic waste (i.e. worked as a coating material for aggregate). The specific gravity of

plain and modified aggregates was found to be same while penetration value and ductility value of modified bitumen was lower than the conventional one.

## CONCLUSION

On the basis of past studies, several methods were identified for utilizing different waste materials i.e. plastic waste, industrial waste, agricultural waste and many more in road construction resultant in a sustainable environment. Use of different waste materials as the replacement of bituminous was found appropriate for the road construction (flexible pavement) as different properties of bitumen were found to be increased or within the limit as specified by Indian standards. Therefore, waste material can be utilized in the construction of low volume roads (i.e. traffic movement will be minimum) which will be beneficial and economical. The main problem which hinders the development of such technologies is the absence of proper guideline of mix design procedures regarding the same. From the present study, it is revealed that the waste materials can be utilized to create a sustainable environment without compromising the actual requirements (i.e. strength). From the future point of view, a study can be extended by proposing an alternative of bitumen (based on waste material) for construction of flexible pavement or maximum utilization of waste material by mixing these wastes in the combined manner (by looking at their chemical properties) in order to replace the bitumen partially or fully.

## REFERENCES

- Ahmadinia, E., Zargar, M., Karim, M.R., Abdelaziz, M. and Shafiq, P. (2011). "Using waste plastic bottles as an additive for stone mastic asphalt". *Materials & Design*, 32(10), pp.4844-4849.
- Arabani, M., Mirabdolazimi, S.M. and Sasani, A.R. (2010). "The effect of waste tire thread mesh on the dynamic behavior of asphalt mixtures". *Construction and Building Materials*, 24(6), pp.1060-1068.
- Akbulut, H., Güreş, C., Çetin, S. and Elmacı, A. (2012). "Investigation of using granite sludge as filler in bituminous hot mixtures". *Construction and Building Materials*, 36, pp.430-436.
- Annual Report of ministry of road transport and highway (MORT&H). 2015-2016. Government of India
- Ahmad, M.S. (2014). "Low-density polyethylene modified dense graded bituminous macadam". *International Journal of Engineering Trends and Technology*, 16, pp.366-372.
- Bhageerathy, K.P., Alex, A.P., Manju, V.S. and Raji, A.K. (2014). "Use of biomedical plastic waste in bituminous road construction". (*IJEAT*), pp.2249-8958.
- Bansal, S., Misra, A.K. and Bajpai, P. (2017). "Evaluation of modified bituminous concrete mix developed using rubber and plastic waste materials". *International Journal of Sustainable Built Environment*, 6(2), pp.442-448
- Ghalayan, P. and Rana, E.S. (2017). "Partial replacement of bitumen by using plastic waste in bitumen concrete". *International Journal of Latest Research in Engineering and Computing*, 5(2), pp.7-12.
- Hınışlıođlu, S. and Ađar, E. (2004). "Use of waste high density polyethylene as bitumen modifier in asphalt concrete mix". 58(3-4), pp.267-271.
- Jambeck, J.R., Geyer, R., Wilcox, C., Siegler, T.R., Perryman, M., Andrady, A., Narayan, R. and Law, K.L. (2015). "Plastic waste inputs from land into the ocean". pp.768-771.
- Karaşahin, M. and Terzi, S. 2007. "Evaluation of marble waste dust in the mixture of asphaltic concrete". *Construction and Building Materials*, 21(3), pp.616-620
- Kawade, N, Chalke, S, Dawale, N., Jangam, U., and Parulekar. (2018). "Design and Qualitative Analysis of Flexible Pavement by Using Waste Material". *International engineering, science & Technology research journal*.
- Kumar, T.K. and Vikranth, J. (2017). "A Study on the use of plastic waste (Polypropylene) in flexible pavements". *International Journal of Engineering and Management Research*, Volume-7, Issue-3.
- Pasandín, A.R. and Pérez, I. (2017). "Fatigue performance of bituminous mixtures made with recycled concrete aggregates and waste tire rubber". *Construction and Building Materials*, 157, pp.26-33.
- Prasad, D.S.V. and Prasada Raju, G.V.R. 2009. "Performance of waste tire rubber on the model flexible pavement". *ARPN Journal of Engineering and Applied Sciences*, 4(6), pp.89-92.
- Rajmane, P.B., Gupta, A.K. and Desai, D.B. (2009). "Effective utilization of waste plastic in the construction of flexible pavement for improving their performance". *Journal of Mechanical and Civil Engineering*, pp.27-30.
- Rokade, S. (2012). "Use of waste plastic and waste rubber tires in flexible highway pavements". *International conference on future environment and energy, IPCBEE (Vol. 28)*.

- Reddy, M.S. Reddy, Y.R. and Takhelmayum, G. (2017). "Experimental Investigation on the Properties of Pavement using Waste Plastic in Road Construction". International Journal of Advances in Scientific Research and Engineering.
- Rajput, P.S., and Yadav, R.K. (2016). "Use of Plastic waste in bituminous road construction". International Journal of Science Technology & Engineering, 2(10), pp.509-513.
- Shedame, P.P. and Pitale, N.H. (2014). "Experimental study of bituminous concrete Containing plastic waste material". International Organization of Science and Research- Journal of mechanical and civil engineering, PP 37-45
- Sk, A.S. and Prasad, K.S.B. (2012). "Utilization of waste plastic as a strength modifier in the surface course of flexible and rigid pavements". International Journal of Engineering Research Application, 2(4), pp.185-91.
- Sharma, A. and Goud, M.M. (2018). International Journal of Technical Innovation in Modern Engineering & Science, 4(5).ISSN: 2455-2585
- Sarma, M.S., and Srikanth, B. (2018). "Study on the use of waste polythene in bituminous paving mix design". International Journal for Modern Trends in Science and Technology ISSN: 2455-3778 :: Volume: 04, Issue No: 06, June 2018
- Shaikh, A., Khan, N., Shah, F., Shukla, D. and Kale, G. (2017). "Use of plastic waste in road construction". International Journal of Advance Research and Development. Volume2, Issue5.
- Sutradhar, D., Miah, M., Chowdhury, G.J. and Sobhan, M.A. (2015). "Effect of using the waste material as a filler in the bituminous mix design". American Journal of Civil Engineering, 3(3), pp.88-94.
- Somani, maharaniya, Kumawat, Rangera. (2016). "Strengthen of the flexible pavement by using waste plastic and rubber".scholarly peer reviewed research publishing Journal- International Journal of Civil Engineering, Volume 3, Issue 5 – May-2016
- Tiwari, M.M., Singh, U.P., Gupta, P., Kumar, R. and Bharti, S. (2018). "Modify bituminous blinder using plastic waste". Journal of transportation systems, 3(1).
- Trimbakwala. (2017). Plastic Roads – "Use of waste plastic in road construction"; Int J Sci Res Publ 4) (ISSN: 2250-3153), International Journal of Scientific and Research Publications (IJSRP), Volume 7, Issue 4, April 2017 Edition [ISSN 2250-3153].
- Vashisht, R. and Saini, M. (2017). "Experimental Study of Materials Used in Flexible Pavement Using Waste Plastic and Crumb Rubber". Journal of Civil Engineering and Environmental Technology. Volume 4, Issue 2; April-June, 2017, pp. 121-123.
- Wayal, A.S., and Wagle, M.D. (2013). "Use of Waste Plastic and Waste Rubber in Aggregate and Bitumen for Road Materials. Polymer", 40(88), p.36, International Journal of Emerging Technology and Advanced Engineering (IJETE), ISSN 2250-2459, ISO 9001:2008 Certified Journal, Volume 3, Issue 7, July 2013.



## Use of Local Available Waste Materials in Road Construction - Problems & Possibilities

Jagjit Singh\*<sup>1</sup>, and Surinder Singh<sup>2</sup>

<sup>1</sup>B-Tech student, Department of Civil Engineering, NIT-Jalandhar, Jalandhar, India, 144011  
<sup>1</sup>sainijagjit@rocketmail.com (Corresponding Author)

<sup>2</sup> B-Tech student, Department of Civil Engineering, NIT-Jalandhar, Jalandhar, India, 144011  
98ssingh31@gmail.com

### ABSTRACT

Roads are the backbone for the development of any country. Nowadays good quality of roads like Expressway, National highway, state highway etc. has been constructing in our country. These bundles of roads are providing speed in development. The study of advanced construction materials a highway engineer tries to achieve these requirements by numbers of laboratory tests and finalize the best result obtained. This presentation tries to figure out the use of locally available in the construction of roads. In this presentation, we have focused on the highway construction materials its characteristics and qualities etc. Fly ash, blast furnace slag, cement kiln dust, municipal solid waste, bitumen etc. has been fully discussed. Fly ash is very important materials for construction of roads. A huge quantity of fly ash is accumulated by thermal power plants. Its consumption of road construction protects the environment. The analysis of these materials, its quality standards, and specifications are useful for construction of highway project. It replaces the granular material i.e. GSB material in subbase course and also consoled system reduces the demand for heavy wearing course save resources and construction time. In this presentation, we have focused on the locally available material to be used as highway construction material at appropriate layer.

**KEYWORDS:** *Fly ash; Cement Kiln Dust; Blast Furnace Slag; Rice Husk Ash.*

### INTRODUCTION

Transportation is a very important mode for the development of any country. The adequate transportation facilities/system facilitate within the development within the economic, industrial and social and overall development of the country.

There are four major modes of transport.

- Roadways and Highways
- Railways
- Waterways
- Airways

Construction of road pavement, its system, development, planning, alignment, geometric style, road traffic operation, and its management, pavement style, construction and maintenance materials, economic thought finance and admin systems area unit deals among the road engineering. Indian Road Congress has divided the roads into completely different classes like village road, Major district road, another district road, pike, National road, and freeway. Growth of a country greatly depends upon road network development. these days our government has centered on the development of roads. For the development of roads, several materials area unit used, it depends on the sort of road and on the market fund for construction of that road. IRC –SP 72 Clause 5.2 presents the rule for construction of roads with domestically on the market materials like selected granular soil for subgrade, stabilization of native soil, bricks and overburden brick metal, industrial waste, stone metal, present softer metals like kankar, mooram etc.

Waste is generated from all directions. it should be from business, Municipality, and Agriculture or from the other method of human or animal use. The waste could also be within the style of solid, liquid or in gases type. They not solely need immense area to stock it however additionally foul the atmosphere. The contaminated atmosphere is harmful to human health and for the property of the system. Thus, the generation of waste should be reduced or recycled for human use. Most of such waste is employed in business or human cycle once its correct process. 3 major amounts of wastes area unit from municipality, business and building demolition. Wastes like demolition waste, fly ash, industrial waste is simply employed in building.

### **GENERAL REQUIREMENT OF PAVING MATERIAL**

The pavement structure for a given set of style conditions should be decent to resist the varied forces to that it's subjected. the first forces to that it's subjected include those of transport loading and people because of varied environmental condition factors. environmental condition factors of significance include temperature and/or wet connected volume changes, freeze-thaw action, chemical attack, and stability changes related to temperature and wet fluctuations. Thus, the paving materials once employed in combination within the pavement structure:

- . must have adequate stability;
- . must resist wear of traffic; should resist or limit the results of the environmental condition and chemical action; and should resist or limit the results of internal structural changes like growth, contraction, temperature deformation, etc. and internal changes within the load carrying capability.

As a consequence of those necessities, most paving materials should meet sure quality standards. ordinarily these quality levels are developed supported a few years of expertise. In most instances, these quality standards replicate native expertise with materials, construction techniques, and environmental condition exposure. samples of easy quality indicators for paving materials include:

The impetus to be used of marginal or non-specification materials isn't new, however in recent years new twists, significantly energy conservation and material disposal, are added. The search has taken variety of various directions:

1. The utilization of regionally offered sands, gravels, and crushed stones which can not meet commonplace route specifications thanks to improper gradation, status, poor skid, etc., however that have potential as substitutes for base and moulding material once benefited by stabilization, blending, etc;
2. The utilization of in-situ or native fine-grained soil as a pavement structural part by rising strength and durability properties through some stabilization method;
3. The utilization of domestic, industrial, and mining wastes as combination replacements or supplements.
4. The utilization of existing paving materials (including mineral concrete, Portland cement concrete, etc).

The economic and energy edges of the utilization of the on top of materials in route construction area unit nevertheless to be firmly established, however all of those seem to possess tremendous potential.

### **TYPES OF LOCAL AVAILABLE MATERIAL & USES IN ROAD CONSTRUCTION**

Industrial wastes are used in construction in growing countries. The utilization of those materials in road making relies on technical, economic, and ecological criteria. The shortage of ancient road materials and therefore the protection of the atmosphere create it imperative to research the possible use of those materials fastidiously. India includes a giant network of industries set in numerous components of the country and many more area unit planned for the close to future. many million metric tons industrial wastes are produced in these institutions. historically soil, stone aggregates, sand, bitumen, cement etc. are used for construction. Natural materials being exhaustible in nature, its amount is declining bit by bit. Also, the price of extracting sensible quality of the natural material is increasing. Involved concerning this, the scientists are searching for different materials for main road construction, and industrial wastes product is one such class. Table 1. Shows the fly ash utilization in the year 2010 in million tonnes per annum (Bajpai et al.2017).

**Table 1 - Fly-ash utilization during the year**

S. no	Mode of Fly-ash utilization	Utilization (Million Tonnes per annum)	Percentage Utilization
1	Cement	17.45	48.13
2	Reclamation of low lying area	3.16	8.72
3	Roads and Embankments	4.72	13.02
4	Mine Filling	2.45	6.76
5	Bricks & Tiles	2.36	6.51
6	Agriculture	0.37	1.02
7	Others	5.74	15.83
	Total	36.26	100

### Fly Ash in Asphalt Pavements

Fly ash can be used as a filler material with Hot mix asphalt in the road pavements. It help in reducing the cost of the overall project. It has better resisting properties than other filler materials and provide better durability to the pavements. Following are the advantages of using fly ash in the pavement construction:

- Provide better resistance on the surface to heavy loads
- Economical

### Fly Ash in Grouts for Pavement Subsealing

Fly ash can be used as an filler material for filling the voids in the pavements. Mixture of fly ash, water and other materials can be used as an filling the voids in the road pavements. Following are the advantages of using fly ash an filler material;

- Take very less time in setting without disturbing the traffic on tha roads
- Final strength is very much high
- Very less costly as compared with other filler materials

### Blast furnace Slag

Blast furnace slag is generated with the help of melting technique in steel making operations. at the same time as metalworks slag has been used as a substitute for native coarse mixture in concrete mixtures, it's jointly been used in asphalt mixtures. In general, the slag is crushed so as that it will pass the ¾ in. sieve. After crushing to a required particle size slag can be easily used as a cementitious material in making concrete mixes. There are lot of plants in India generating tonnes of waste slag per year. Table 2 shows the plant wise capacity of production of slag from various industries in India;

**Table 2. Plant wise Capacity of Iron and Steel Slag in India (Tiwari et al. 2012)**

Name of Steel Plant	Capacity for granulation (T/Year)
Bhilai Steel Plant , DurgChattisgarh	2675
Bokaro Steel Plant, Bokaro, Jharkhand	5000
Rourkela Steel Plant, Rourkrla, Odisha	600
Durgpur Steel Plant, Durgpur West Bengal	NA
IISCO Steel Plant, Burnpur, West Bengal	400
Visvesvaraya Iron & Steel Plant, Bhadravati, Karnataka	68
RashtriyaIspat Nigam Ltd, Visakhapatnam, Andhra Pradesh	1440
IDCOL Kalinga Iron Works Ltd, Barbil, Odisha	53
JSW Steel Ltd, Bellary, Karnataka	NA
Tata Steel Ltd, Jamshedpur,Jharkhand	2100
Visa Steel Ltd, Kalinganagar	175
NeelachalIspat Nigam Ltd, Kalinganagar,Odisha	NA
Sona Alloys Pvt Ltd, Satata, Maharashtra	100.8

### Use of furnace slag as a building material binder for applications in main road construction

Following are the benefits of furnace slag as a building material binder:

- There's a development of higher strength;
- Low energy demand – solely grinding of fabric is needed;
- Less costly as comparison with cement
- Used in making concrete mixes and can used in making pavements
- Having better index properties than cement used as an filler materia in place of cement.

### Use of furnace slag as a rough mixture for asphalt for applications in main road construction

Even as metal works slag has been used as a substitute for native coarse mixture in concrete mixtures, it's additionally been employed in asphalt mixtures. Here again, the slag is typically crushed to achieve the specified particle size. the benefits of furnace slag as a coarse mixture for asphalt that are mentioned in the following:

- Less costlier than alternative mineral fillers; and
- Suitable for roads close to nearby steel plants, reduction in the transportation cost.

Figure 1. Shows the percentage of utilization of slag in the different working areas:

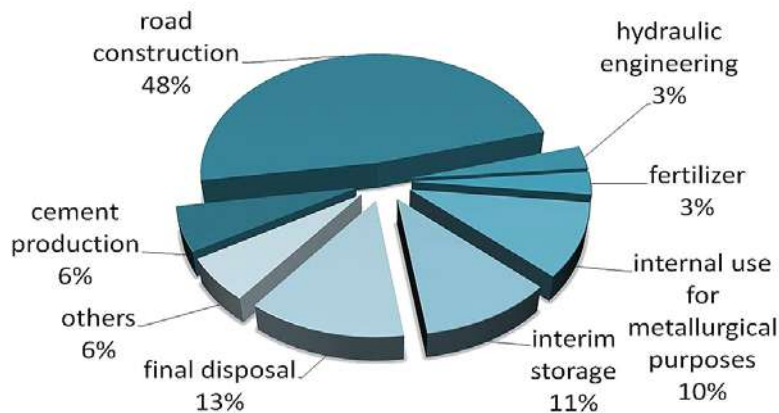


Figure 1: Shows the utilization of slag in different working areas (Tiwari2016)

### Cement kiln dirt

Cement kiln dust (CKD) is that the finely divided dry alkaline stuff carried from a cement kiln by the exhaust gas and captured by the kiln's air pollution system. In general, however, the composition of cement kiln dirt is comparable to it of cement and consists of carbonate, calcite, silicate, metal sulphate, salt, aluminium oxide, iron oxide, chloride, magnesia, sulphate, and metal halide. Cement kiln dirt features a chemical composition almost like that of cement; thus, the first worth of cement kiln dirt is its building material properties. Following are the uses of CKD in road construction

### Use of cement kiln dirt for soil stabilization for applications in road construction

Cement kiln dirt may be used to improve the properties of soil in situ, and as matter in pozzolanic stable base mixtures. The adsorbent capability and building material properties of cement kiln dirt enable it to cut back the wetness content and increase the bearing capability of the soft soil. Cement kiln dirt for soil stabilization have blessings that are shown below:

- Cement kiln dust effectively improves soil strength and conjointly reduces construction time and costs;

- once lime is employed as a stabilising agent, the soil should be remixed and compacted 48 hours once the lime is initial applied;
- Cement kiln dirt may be mixed with soil to change plastic limits or wetness content to supply the specified stable properties

### **Use of cement kiln dirt as mineral filler in asphalt paving for applications in road construction**

Hot-mixed asphalt (HMA) may be a common paving material. Hot-mixed asphalt is formed by coating of dried coarse and fine aggregates with hot asphalt cement that acts as a binder. Cement kiln dirt may be wont to replace some of the mineral filler employed in hot-mixed asphalt. Cement kiln dirt as mineral filler in asphalt paving has following advantages:

- Specifications for mineral filler in hot mixed asphalt (AASHTO M17) are for material passing the No. 50 sieve to be between 95 and 100%. Typically, the utmost particle size of cement kiln dirt is regarding 0.3 mm (No. 50 Sieve), that conforms to the mineral filler high size
- Better physical properties, the building material properties of cement kiln dirt are shown to extend the soundness and stiffening of hot-mixed asphalt.

### **Waste plastic bags**

In Asian country 310 Million individuals betting on Plastic bags. Asian country ranks 3<sup>rd</sup> within the world within the consumption of plastics. It's found that plastic waste of the size 2-8mm could also be incorporated handily in hydrocarbon mixes used for road constructions. The optimum dose is around 0.4- 0.5 you interested in weight of hydrocarbon combine and 6-8% by weight of hydrocarbon. Hydrocarbon Concrete (BC) may be a stuff largely employed in construction comes like road emergence, airports, parking tons etc. It consists of asphalt or hydrocarbon (used as a binder) and mineral mixture that is mixed along down in layers then compacted. The role of waste plastic bags within the combine was studied for numerous engineering properties by getting ready Marshall Samples of B.C. mixtures with and without compound. Marshall Properties like stability, flow value, unit weight, air voids were wont to confirm optimum polyethylene content for the given grade of hydrocarbon (80/100). skinny plastic luggage are principally composed of rarity Polyethylene (LDPE) and it's ordinarily used for packaging, protective and lots of alternative applications. Table 3. showing the changes in the properties the bitumen after varying the percentage of quantity of plastic waste in it:

Table 3. Properties after adding different amount of plastic in bitumen

% of Plastics	Ductility (cm)	Penetration (mm)	Softening Point (°C)
1%	64	95	54
2%	55	90	50
3%	20	80	50
5%	11	55	72

### **Use of Plastic Waste in Bituminous Pavement**

Advantages

- Minimize the requirement of bitumen by around 10%.
- Develop a technology which is eco-friendly.
- Improvements in fatigue life of roads.
- Boost the strength and better performance of the road.
- Use higher percentage of plastic waste.
- The gases exerted in traffic conditions are absorbed by smoke absorbent.

### **Foundry and colliery sand**

The metal works industry utilizes industrial grade silicon dioxide sand for moulds in metal casting. Waste foundry sand is a by-product of the foundry casting process of metallic element and nonferrous metals, 95th of this material is generated from the ferrous casting method. Spent foundry sand consists primarily of silicon dioxide sand, coated

with a skinny film of burnt carbon, residual binder (bentonite, sea coal, resins) and dust. ferrous industries account for the bulk of metalwork's sand used. Foundry sand can also contain some leachable contaminants, with non-ferrous foundry sands frequently containing high levels of significant metals classified as risky. colliery spoil is that the waste made from the method of extracting coal and rendering it marketable. once the coal is processed by laundry before sale to the client, colliery spoil is made within the form of coarse or fine discard. It often utilized in fill though a serious use is in infrastructure applications. Most colliery spoil is employed as bulk fill, notably for construction lagoons, stream banks and for capping lowland or general ground raising. it is additionally used for flood protection works, beach renewal, and construction. it is burnt and unburnt colliery spoil, that has terribly completely different properties. Burnt spoil is usually of upper strength than unburnt spoil and is consequently in higher demand.

From physical analysis the physical properties are somewhat similar to the natural sand & chemical analysis there is no harmful chemical in it which gives no hazardous to use in concrete.

1. Water absorption for foundry waste sand is higher than local sand
2. Foundry waste sand fineness is nearly same as that of the local sand
3. Foundry waste sand has lower specific gravity compared to local sand
4. From this test, replacement of fine aggregate with this used foundry sand material provides maximum compressive strength at 40% replacement.

### **Processed Municipal solid waste**

Management of Municipal Solid Wastes (MSW) continues to stay one among the foremost neglected major problems in Indian cities thanks to the speedy urbanization, urban increment, and industry. Most of the native administrations are directly dumping MSW with none segregation and treatment to the open dumping site, this way of inappropriate disposal of MSW becomes a serious threat to the environments and public health in developing countries like india(May 2000) of Ministry of Urban Development (MoUD), Government of India that 1,00,000 MT of Municipal Solid Waste was generated daily within the country. The survey conducted by the central institute of Plastics engineering and Technology (CIPET) at the instance of CPCB has reported generation of 50,592 tonnes of MSW per day within the year 2010-11 in some 59 cities. The MSW amount is anticipated to extend considerably by the year 2020 thanks to the expansion in population, living standards of the residents and degree of exploitation, industry and numerous different activities. It was often utilized in different construction and different activities which are given below to avoid the pollution and provides away for safe disposal. They are-

- Embankment fill
- Road use material
- Aggregate for asphalt
- Aggregate for concrete making concrete blocks
- Materials having same properties like cement
- Lime mixtures
- Land drainage media.

### **Rice Husk Ash (RHA)**

Rice husk ash is a oxide material obtained when burning of rice husk associate exceedingly on fire. This waste matter have high pozzolanic properties and often utilised within the stabilization for construction. It is fine-grained oxide in nature light in and grey in colour. Basically, this idea is initially followed within the rigid pavement of M15 grade concrete and also the combination of rice husk and chemical compound in correct proportion. The layer is provided below the primary layer that absorbs the percolated water through road cracks. once significant vehicles pass away this paved surface rice husk that underneath the concrete layer gets compressed and also the precipitated

water is thrown out that maintains the water level underneath the safe limit or could all water are often expelled out due to the spring action of rice husk layer and even when this action, the rice husk layer retains its original position. Figure 2. shows the use of rice husk in the sub base layer (Patil et al. 2014)



Figure 2: Model showing rice husk layer as a sub base

### Advantages of rice husk if used in road construction

- Compressive strength is comparatively more than normal rigid pavements.
- More flexible to normal loads
- Combination of rigid as well as flexible pavement.
- Better durability
- Free of coat available, so very economical to use in road construction.

### CONCLUSIONS

Additive of plastic waste at different content gives effect on the temperature status of the bitumen. because the content of plastic waste increase from 1.5% to 6%, the penetration range decreases gradually and softening point of modified bitumen increase. The addition of plastic waste content will increase the viscosity of the bitumen at extreme temperature i.e. 135 °C. High viscosity means less possibilities of rutting. according to obtained Marshall parameters, the addition of ash up to 4-dimensional in dense bituminous macadam combine, by replacing standard mineral filler like hydrated lime shows a 7.5% reduction in OBC compared to the control mix, which can give a substantial economy of bitumen in resulting mixture. it's possible to use metal slag as a binder material within the bituminous mix design. The 8-12% addition of metal slag provides the most value for plasticity test. Hence, 8-12% is that the optimum value. The softening point is higher than 110 that is desirable. in case of addition of rice husk, compressive strength is relatively more than normal rigid pavements.( 14 N/mm<sup>2</sup> >10 N/mm<sup>2</sup> ).

Use of innovative technology not solely strengthened the building however additionally increase the road life. However, one must proceed cautiously, as a result of potential environmental, health and safety issues related to the usage of a number of the waste materials. Thus, additional analysis is required before any specific material is finally approved as another building material. it's hoped that the availability of appropriate technology, applicable legislation, and awareness among all stakeholders would widen the probabilities of using some of the waste materials for sustainable building.

### REFERENCES

- Ahmed,A., andLovell,C. W.(2010). “Use of Waste Materials in HighwayConstruction: State of the Practice and Evaluation of the Selected Waste Products”*Transportation research record*1345:1-7.
- Al-Hadidy,A.I.,Tan, Y., (2009). “Effect of polyethylene on life of flexible pavements”, *Construction and Building Materials*(23): 1457-1460.
- Bajpai, R., Khan, M.L, Sami, O.M., Yadav, P.K, Srivastav, P.K, (2017).“Construction of Flexible Pavements using Plastic Waste Along with Bitumen” *International journal for scientific research and development*(5):563-564.
- Keflemariam, B.,Kotresh, K.M,(2018).“Reuse of waste plastic for flexible pavement construction-Green method”*Wolaitasodo university department of construction technology*,:1-8.
- Patil, S. R.,Bachhav, S.S.,Kshirsagar, D.Y.,(2016).“ Beneficial Use of Municipal Solid Waste Ash In Sub Base In Road Construction”*International Journal of Engineering Inventions e-ISSN: 2278-7461*,5(3):24-28.
- Patil,A.H., Shirsat,A. R., Phadke, R.A.,Mohire, A.A., Junawane, G.H, Hake, N.N,Lunkad, H., (2014).“ Use of Rice Husk In Road Construction” *Civil and Environmental Research ISSN 2224-5790*(6):1-5.
- Safiuddi,M., Jumaat, M. A., Salam, Islam,M. S. and Hashim, R.,(2010).“Utilization of solid wastes in construction materials” *International journal of the physical sciences* (5): 1952-1963.

Proceedings of National Conference: Advanced Structures, Materials And Methodology in Civil Engineering  
(ASMMCE – 2018), 03 - 04th November, 2018

PAPER CODE: T-412

Sawant, M.,Lokhande, L., Lokhande, P.,Kute, P.,Masi, S.,Khutwad,S.,(2017).“ Use of Steel slag in Bituminous Road Construction” *International Research Journal of Engineering and Technology*(4):2096-2097.

Tiwari, M.K, Bajpai S., Dewangan,K., (2016).“Steel Slag Utilization-Overview in Indian Perspective”*International Journal of Advanced Research*, 4(8):2232-2246.

Tiwari, M.K,(2016),“Fly ash utilization a brief review in Indian context ” *Indian research journal of engineering and Technology*,3(4):950-956.



## Laboratory Investigations on Stone Matrix Asphalt Containing Pet Bottles

Vinod Kumar Sharma<sup>1</sup>, Rajiv Kumar<sup>\*2</sup>

<sup>1</sup>Research Scholar, Department of Civil Engineering, Dr B R Ambedkar NIT Jalandhar, Punjab 144011, India, e-mail: vinodks.ce.18@nitj.ac.in

<sup>2</sup>Assistant Professor, Department of Civil Engineering, Dr B R Ambedkar NIT Jalandhar, Punjab 144011, India, e-mail: kumar.r@nitj.ac.in (Corresponding Author)

### ABSTRACT

Waste materials are being produced significantly throughout the world. One of the waste materials is plastic waste. There are different categories of plastic waste out of which one type of the plastic waste is the disposal bottle. Generating a disposable plastic bottle is becoming a major problem in different cities in India. PET (Polyethylene Terephthalate) bottle is one of the plastic wastes which can be recycled. Recycled PET bottle is also used by Nike for making the uniform of cricketers. In India, PET bottle is collected by kabadiwallas and they get Rs.14-15 per kg. The aim of this study is to investigate the effects of adding PET plastic bottles in bitumen and bituminous mix. The PET bottle was cut in to strips at the uniform size of 5mm × 5mm. In the present study, two methodologies have been carried out one is a wet mix and the second one is a dry mix. In the wetmix, it has blended with VG-10 (Viscosity Grade) bitumen. In the drymix, the PET has been added with aggregate. In the wetmix, the percentage of PET increases till the specification becomes similar to the PMB-40 (polymer modified bitumen) then the optimum dosage of PET was found. In dry mix PET directly added in aggregate and Marshall Sample was prepared and it was compared with the wet mix. The specific gravity and properties of asphalt mixture containing varied percentages of PET were evaluated through the conduction of Marshall Test. Optimum Bitumen Content (OBC) was calculated for each percentage of PET bottles used in the mixture. It was found that by adding waste PET bottles into the bituminous mix the stability and flow values of asphalt mixture is increased. Further, it was observed that by adding lower amount of PET bottles the bulk specific gravity of the mixtures increased. Hence it was concluded that the mixtures containing PET bottles have lower OBC values as compared to the conventional mixture, and this may reduce the amount of asphalt binder which can be used in road constructions.

**KEYWORDS:** *Polyethylene Terephthalate; Bitumen; Softening Point; Penetration Value; Marshall Stability; Polymer Modified Bitumen.*

### INTRODUCTION

Stone Mastic Asphalt (SMA) is developed in Germany in 1960(Vavrik et al. 2010). SMA has a high coarse aggregate content to resist the Permanent deformation. The stone skeleton is filled with mastic of bitumen and filler. To provide adequate stability and to prevent drainage of binder during transportation and placement fibers are added to bitumen. A typical Stone Mastic Asphalt mix consists of 0.3% fiber, 6-7% binder, 8-12% filler, and 70-80% of coarse aggregates(Sarang et al. 2015a). The deformation resistant capacity of SMA stems from a coarse stone skeleton providing more stone to stone contact than conventional Dense Graded Asphalt mixes (DGA). Higher bitumen content results in improved binder durability. A thicker bitumen film and lower air void content (Sarang et al. 2015b).

### Polyethylene Terephthalate

Polyethylene Terephthalate (PET) is thermoplastic in nature. It is also known by “Polyester,” PET is a transparent polymer, having dimensional stability under variable load and good mechanical properties. Moreover, PET has good chemical resistance along with gas barrier properties. PET is having wide applications like Manufacture of bottles, Electrical components and Thermally Stabilized Films (e.g. Graphics, Capacitors, Recording Tapes and Film Base etc.). Its applications are widely used by Textile industry also for the production of Fibers. It is having excellent physical properties and belongs to a thermoplastic. It constitutes around 18% of the total polymers produced worldwide. Over 60% of its production is used for synthetic fibers and bottles, which consume approximately 30% of global PET demand(Prasad et al. 2015).

### Structure and Properties of PET

The properties and structure of Polyethylene Terephthalate (PET) are given in Table 1(Sulyman et al. 2016). PET absorbs water from its surroundings hence it is hygroscopic. While heating this “Damp” PET the resilience is decreased as water gets hydrolyzed. Thus, before the resin can be processed in a molding machine, it must be dried. Drying is achieved using a desiccant or dryers are used for drying the PET before it is fed into the processing equipment. The physical and chemical properties of PET are given in Table 1.

**Table 1: Physical and Chemical Properties of PET**

Properties	Value
Young’s modulus of PET	2800-3100 MPa
Tensile strength of PET	55-75 MPa
Elastic limit of PET	50-150%
Notch Test Value	3.6 KJ/m <sup>2</sup>
Glass transition temperature(T <sub>g</sub> )	67-81°C
Vicat B	82°C
Linear expansion coefficient ( $\alpha$ )	0.00007 per K
Water absorption (ASTM)	0.16
Meting point	>250°C
Boiling point	>350°C (decomposes)
Density	1.38 g/cm <sup>3</sup>
Solubility in water	Practically insoluble
Molar mass	Variable

### Molecular Structure

Polyethylene Terephthalate, commonly abbreviated as PET. The most common thermoplastic polymer resin of the polyester family is PET. It is used in containers for Foods, Liquids, Fibers for clothing and Thermoforming for manufacturing. Its chemical formula is abbreviated as (C<sub>10</sub>H<sub>8</sub>O<sub>4</sub>)<sub>n</sub> as shown in Figure 1.

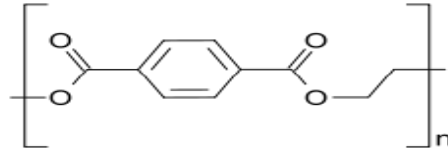


**Figure1: Molecular Structure of Polyethylene Terephthalate**

## EXPERIMENTAL PROGRAM

### Material Selection

- a) Binders: Various binders are available in market such as VG 10, VG 20 and VG 30 etc. These binders are categorized according to their viscosity. Binder which was used in this study is VG 10 added with chips of PET bottles and make it bitumen equivalent to PMB 40. VG-10 is most commonly used in applications like Surface Dressing and in cold climate paving instead of using 80/100 penetration bitumen grade(Prasad et al. 2012). The physical properties of VG 10 are shown in Table 2. Modified Bitumen products and Bitumen emulsions are also produced from it. The physical properties of PMB 40 are shown in Table 3.

**Table 2: Physical Properties of VG 10**

Property	Test Method	Specified limits as per IS:73-2006
Absolute Viscosity at 60° C (Poise)	IS 1206 (Part 1)	Min 800
Kinematic Viscosity at 135 °C (c St)	IS 1206 (Part 3)	250
Softening Point °C	IS 1205	Min 40
Flash Point °C	IS 1209	220
Penetration at 25 °C	IS 1203	80-100
Specific gravity	IS 1202	1.0

**Table 3: Physical Properties of PMB 40**

Property	Test Method	Specified limits in IRC: SP:53-2010
Penetration at 25 °C	IS 1203	30-50
Softening Point, °C, Min	IS 1205	60
Flash Point, °C, Min	IS 1209	220
Viscosity at 150 °C (Poise)	IS 1206 (Part 1)	3-9
Specific gravity	IS 1202	1.0

- b) Aggregates: Crushed stone aggregates (course and fine) were used to prepare the SMA mixture specimens. The materials used are clean, durable, and hard and these were from dust and soft specimens. Aggregate gradation adopted for stone matrix asphalt is the gradation recommended as per IRC: SP: 79-2008 for 13 mm nominal maximum aggregate size. This aggregate gradation is recommended for wearing course and for a nominal layer thickness of 40-50 mm. The aggregate gradation recommended and adopted is MORTH specification. The physical properties of aggregates and specified limits as per IRC: SP: 79-2008 are shown in Table 4. As per MORTH gradation samples of appropriate sizes were collected and stored after Sieve analysis(Roy et al. 2013). One sample weighs 1200 gms.

- c) Blending of Binder with PET: The modifier(PET) is mixed with base binder (VG 10) so that it disperses thoroughly before its use. First of all, the bitumen is heated until it became liquid. The molten bitumen was poured into four different pans with a volume of 500 ml. The PET waste in percentages of 2, 4, 6, and 8 % by weight of bitumen was added to bitumen and the mixture was heated up to 180 – 210 ° C till it attains homogeneity. Using Bitumen Stirrer the bitumen and PET Waste was mixed thoroughly. Immediately after mixing the various properties such as Viscosity, Ductility, Flash & Fire Point, Softening Point, Penetration and Stripping values changed(Ahmad et al. 2017).

### Marshall Mix Design for SMA

Stone Matrix Asphalt (SMA) relies on stone-to-stone contact to provide strength. It is a tough, stable, rut-resistant mixture. Rich mortar binder provides durability. The estimated 20-25% increase in cost is more than offset by the increase in life expectancy of the mix. Primarily through the increased durability and decreased rutting(Prasad et al. 2012). SMA is a premium mix to be used in areas where maintenance cost is comparatively high. Several design factors for mix that must be considered are as given in Table 4.

**Table 4: Physical Requirements of Coarse Aggregates for Stone Matrix Asphalt**

Properties	Test	Method	Specifications
Cleanliness	Grain Size Analysis	IS:2386 (P1)	< 2% passing (0.075 mm Sieve)
Particle Shape	Combined Flakiness& Elongation Index	IS:2386 (P-1)	< 30%
Strength	Los Angeles Abrasion Value	IS:2386 (P-4)	< 25%
Toughness	Aggregate Impact Value	IS:2386 (P-4)	< 18%
Polishing	Polished Stone Value	IS:2386 (P-1)	> 55%
Durability	Soundness (either Sodium or Magnesium) - 5 cycles		
	Sodium Sulphate	IS:2386(P5)	< 12%
	Magnesium Sulphate	IS:2386 (P-5)	< 18%
Water Absorption	Water Absorption	IS:2386 (P-3)	<2%

### Sample Preparation

Following steps were followed to prepare Samples:

- Weighing of sample - 3 samples were prepared with binder content 5.5%, 6%, 6.5% respectively. Firstly, weight of samples was taken according to the gradation.
- Heating of aggregates - After weighing, aggregates of all gradation were mixed together to make one sample of weight 1200gms. Further all samples were heated in oven at a temperature of 1300°C. Overheating of sample was avoided as shown in Figure 2.
- Heating of bitumen VG 10: Further Bitumen was heated at high temperature to attain molten state. As it will mix with aggregates and fibers with ease.



**Figure 2 (a) Heating of Aggregate**



**(b) Heating of bitumen VG10**

- Mixing of components - All components (Fiber, Aggregates & Bitumen) were mixed together to make a homogeneous mix of SMA sample.
  - ❖ Putting in mould–To prepare samples the Mix was put in mould. A standard iron cylindrical mould of 100mm diameter is taken. Mould was also heated before use so that mixture may not become cold before hammering. A typical mould is shown in Figure 3.



**Figure 3 (a) Marshall mould**



**(b) Marshall hammer for compaction**

- ❖ Compaction – Further specimens were poured into the moulds and hammering action was performed to compact the mix. In this a Standard Marshall hammer was used. Usually hammering can be done by giving 50 or 75 blows to each side of specimen. In this experimental study each sample was given 50 blows each on both faces.
- ❖ Finalizing the sample - After hammering the sample was taken out of mould. Tags specifying sample number and binder contents are attached to recognize them later. Further the sample was left in open to cool down at room temperature.

## **RESULTS AND OBSERVATIONS**

### **Determination of Penetration**

Penetration test is done to evaluate the consistency of bitumen. With the increase of PET content in neat bitumen the consistency value of bitumen increase. It has been observed that, penetration value decreases with PET content as shown in Table 5

**Table 5: Penetration Test results**

Sample	Trial 1	Trial 2	Trial 3	Avg.
VG 10	95	91	93	93
2%	58	56	59	58
4%	53	54	52	53
6%	45	47	48	47
8%	34	32	35	34

**Determination of Softening point**

The temperature at which Bitumen attains the degree of softening is known as Softening point. As per IS: 334-1982, ASTM E28-67, ASTM D36 and ASTM D6493 – 11, It is the temperature in °C at which a standard steel ball passes through a sample of bitumen in a mould and falls through a height of 2.5 cm, when heated under water or glycerin at specified conditions of test. It is an empirical test and shows the temperature at which bitumen would behave less like solid and more like liquid. The binder should have sufficient fluidity before it is used in Road construction. Softening point increases with PET content as shown in Table 6 and Figure 4.

**Table 6: Softening Point (SP) result**

Sample	SP,Ball-1	SP, Ball-2	Average SP
VG 10 Pure	45	44	44.5
PMB 40	-	-	60
2%	51.5	51.5	51.5
4%	54	55	54.5
6%	57	57	57
8%	63	64	63.5

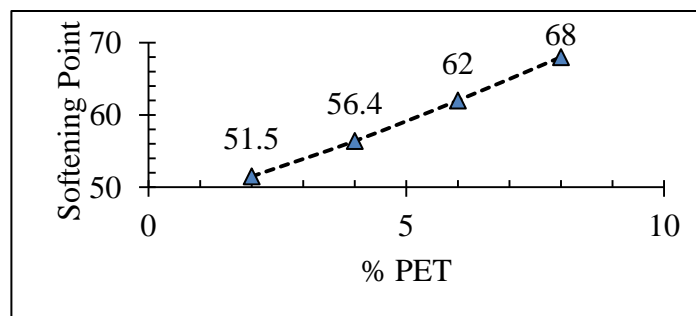


**Figure 4: %PET vs. softening point**

**Determination of Ductility**

The ductility test is an empirical test to measure the cohesive strength of bitumen. The ductility of bituminous material is the distance in centimeters to which it will elongate before breaking when a briquette specimen of the

materials is pulled at a constant rate and at constant temperature. The test temperature sometimes varies from grade to grade. The ductility value decreases with PET content and are shown in Table 7 and Figure 5.

**Table 7: Ductility Test Result**

Sample	Ductility Value
PMB 40	30
VG 10 Pure	More than 100mm
2%	46.3mm
4%	35.4mm
6%	28.5mm
8%	22.5mm

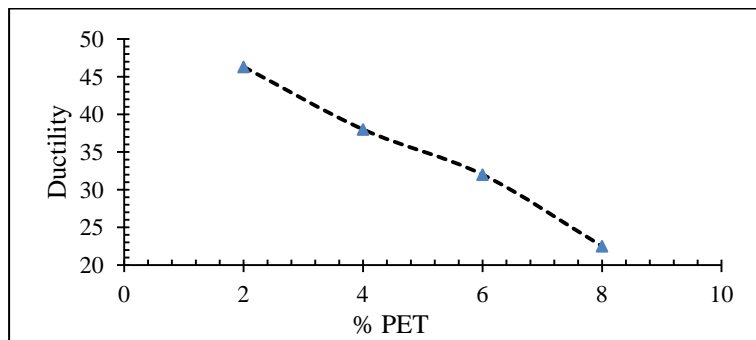


**Figure 5: % PET vs. Ductility**

### Marshall Mix Design

The Marshall Stability and flow test provides the performance prediction measure for the Marshall Mix design method. This stability test is applicable to Hot-Mix Design of bitumen and aggregates with maximum size of 2.5 cm. The stability portion of the test measures the maximum load supported by the test specimen at a loading rate of 50.8mm/min. It is the Maximum load at 60°C to cause deformation. Load is applied to the specimen till failure, and the maximum load is designated as stability. The flow value recorded in 0.25mm increments at the same time when the maximum load is recorded. Hence Flow value is the total deformation of Marshall Specimen under maximum load.

### Dry mix design

Dry mix design is done to resolute the amount of various sizes of mineral aggregates to use to get a mix of maximum density. The dry mix design involves three important steps which are as follows:

- Selection of Aggregates
- Proportion of Aggregates
- Gradation of Aggregates

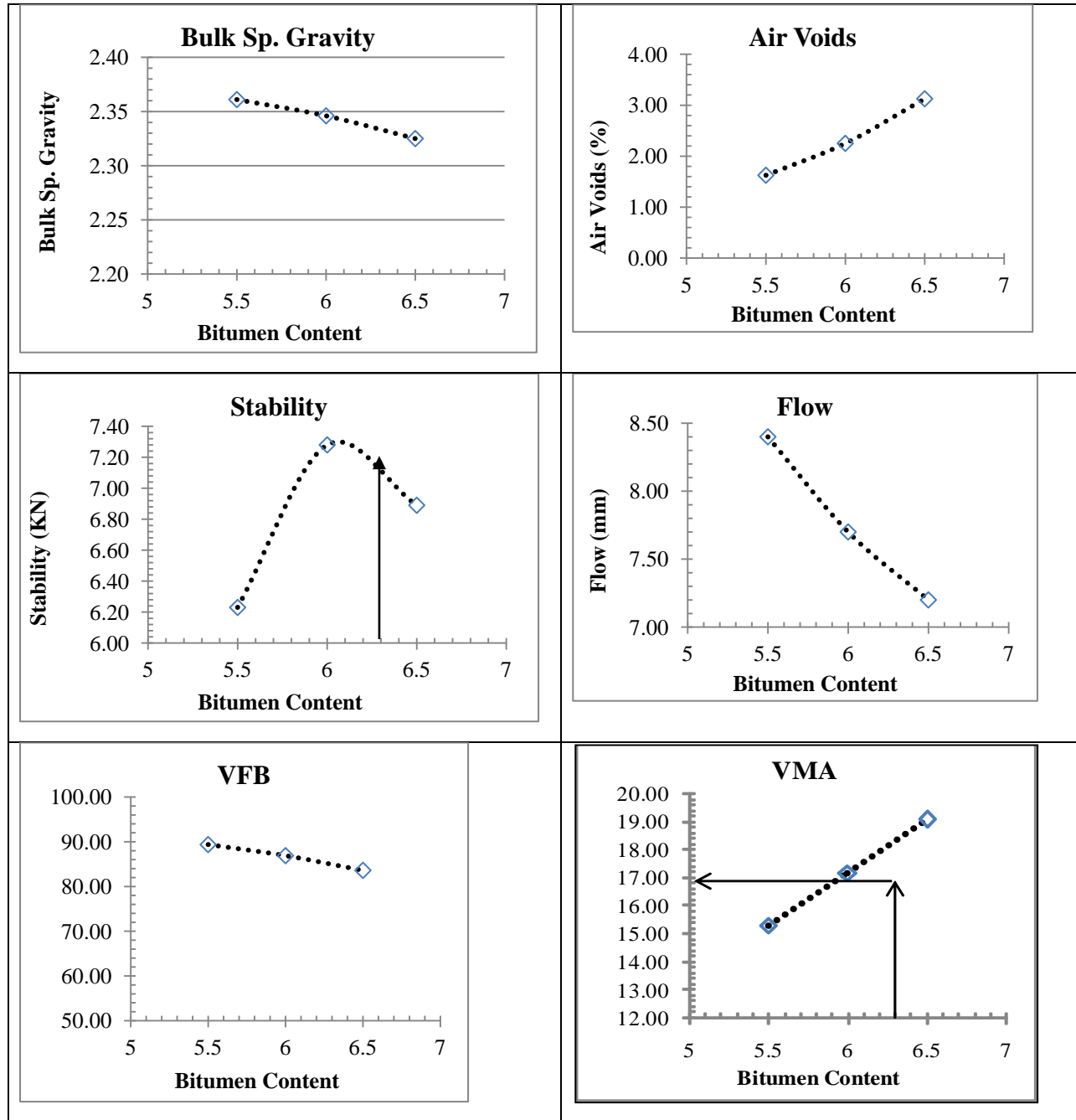


Figure 6: Marshall Mix Design Parameters by Dry Mix Process

### Wet mix design

The Wet mix design purposive the optimum bitumen content. This is done prior by the Dry Mix Design. The properties that are of interest are Theoretical Specific Gravity ( $G_t$ ), Bulk Specific Gravity ( $G_m$ ), Percentage Air Voids ( $V_v$ ), Percentage Volume of Bitumen ( $V_b$ ), VMA, VFA.

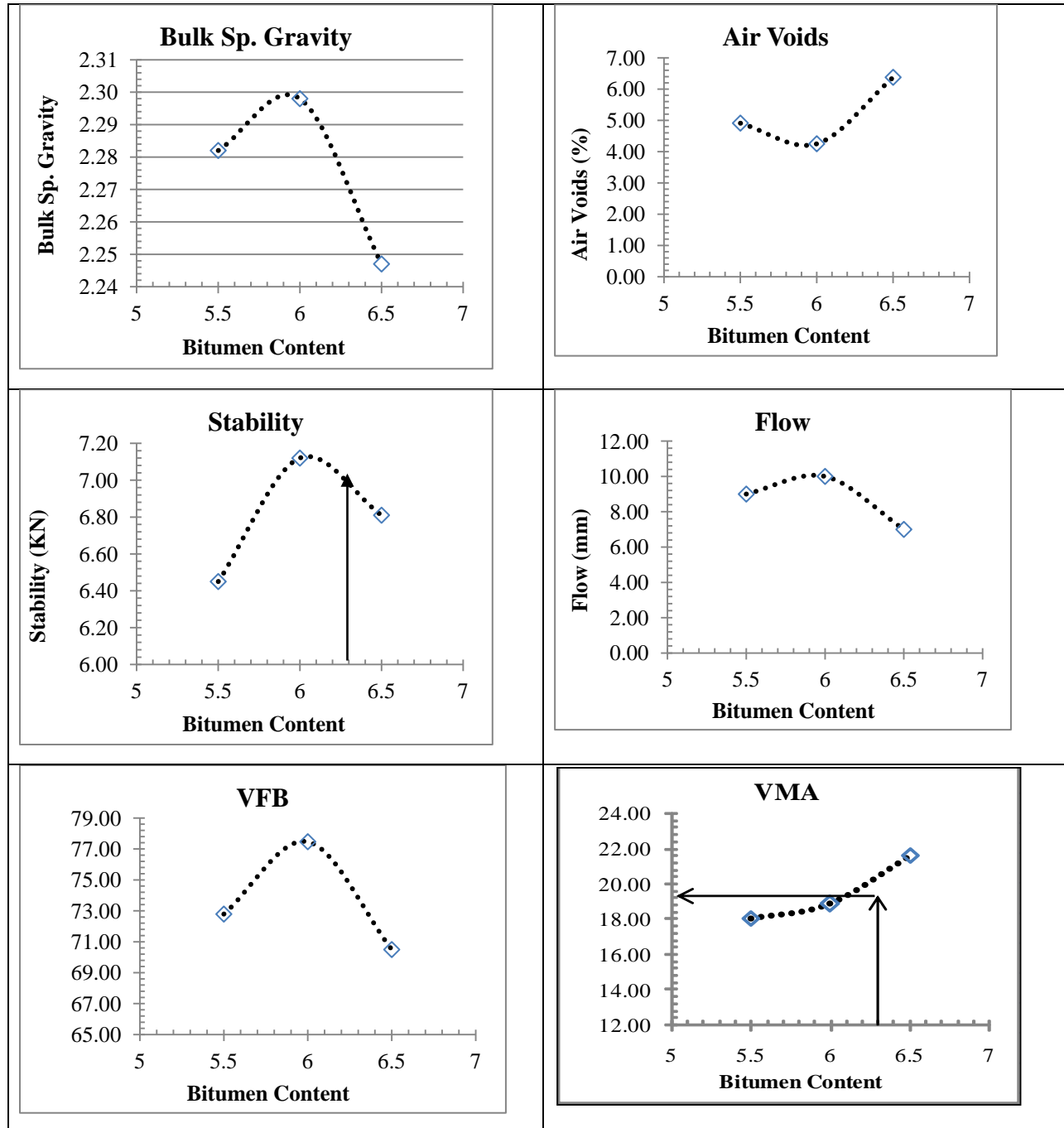


Figure 7: Marshall Mix Design Parameters by Wet Mix Process

**CONCLUSION AND FUTURE SCOPE**

- With the increment in PET content in VG 10 Ductility, Softening point, and Penetration values changed. At 6% PET the mix is equivalent to PMB 40.
- Price of PMB 40 is more than that of VG 10 containing 6% PET; hence it is economical in SMA design.
- Mixture containing PET had more stability values compared to conventional mixtures and the stability trends initially increasing by adding lower percentage of PET and decrease at higher amount of PET.

- Adding higher amount of PET results in higher flow value.
- With increase in bitumen content, VFB increases whereas VMA of Marshall sample decreases, as bitumen replaces the air voids in the mix.
- In present study it has been seen that VMA increases as binder increases. Due to thicker bitumen film, the aggregates move apart slightly resulting in increase of VMA.
- SMA is gaining more popularity among Highway authorities and asphalt industry as it has proved to be more superior on heavily trafficked highways in recent years.
- SMA is having longer service life and gives it a better return on investment though the initial costs may be high. At least 5–10 years increment in life span can be obtained. Hence the choice of SMA can be a good investment.
- With increase in the contents of waste plastics and polypropylene additives the bulk specific gravity of SMA decreases slightly due to the variations in air voids in the mixture as compared to the control mixture.

## REFERENCES

1. Ahmad, A. F., Razali, A. R., Razelan, I. S. M., Jalil, S. S. A., Noh, M. S. M., and Idris, A. A. (2017). “Utilization of polyethylene terephthalate (PET) in bituminous mixture for improved performance of roads.” *IOP Conference Series: Materials Science and Engineering*, 203(1).
2. Prasad, K. V. R., Mahendra, S. P., and Kumar, N. . (2015). “Use of PET (POLY ETHYLENE TERAPHTALATE) WASTE in Bituminous Road Construction –A Critical review.” *International Journal of Emerging Technologies and Engineering*, 2(4), 96–99.
3. Prasad, S. K., R. M. K., and R Prasad, K. V. (2012). “Study on Marshall Stability Properties of BC Mix Used In Road Construction by Adding Waste Plastic Bottles.” *IOSR Journal of Mechanical and Civil Engineering*, 2(2), 12–23.
4. Roy, N., Veeraragavan, A., and Krishnan, J. M. (2013). “Influence of Air Voids of Hot Mix Asphalt on Rutting within the Framework of Mechanistic-empirical Pavement Design.” *2nd Conference of Transportation Research Group of India (2nd CTRG)*, Elsevier B.V., 104, 99–108.
5. Sarang, G., Lekha, B. M., Geethu, J. S., and Shankar, A. U. R. (2015a). “Laboratory performance of stone matrix asphalt mixtures with two aggregate gradations.” *Journal of Modern Transportation*, Springer Berlin Heidelberg, 23(2), 130–136.
6. Sarang, G., Lekha, B. M., Krishna, G., and Ravi Shankar, A. U. (2015b). “Comparison of Stone Matrix Asphalt mixtures with polymer-modified bitumen and shredded waste plastics.” *Road Materials and Pavement Design*, 0629(January), 1–13.
7. Sulyman, M., Haponiuk, J., and Formela, K. (2016). “Utilization of Recycled Polyethylene Terephthalate (PET) in Engineering Materials: A Review.” *International Journal of Environmental Science and Development*, 7(2), 100–108.
8. Vavrik, W. R., Gillen, S., Behnke, J., Garrott, F., and Carpenter, S. H. (2010). “Evaluation of Field-Produced Warm Mix Stone Matrix Asphalt ( WMA-SMA ) Mixtures Prepared By.” (August).
9. Ahmad, A. F., Razali, A. R., Razelan, I. S. M., Jalil, S. S. A., Noh, M. S. M., and Idris, A. A. (2017). “Utilization of polyethylene terephthalate (PET) in bituminous mixture for improved performance of

- roads.” *IOP Conference Series: Materials Science and Engineering*, 203(1).
10. Prasad, K. V. R., Mahendra, S. P., and Kumar, N. . (2015). “Use of PET (POLY ETHYLENE TERAPHTALATE) WASTE in Bituminous Road Construction –A Critical review.” *International Journal of Emerging Technologies and Engineering*, 2(4), 96–99.
  11. Prasad, S. K., R. M. K., and R Prasad, K. V. (2012). ““Study on Marshall Stability Properties of BC Mix Used In Road Construction by Adding Waste Plastic Bottles.”” *IOSR Journal of Mechanical and Civil Engineering*, 2(2), 12–23.
  12. Roy, N., Veeraragavan, A., and Krishnan, J. M. (2013). “Influence of Air Voids of Hot Mix Asphalt on Rutting within the Framework of Mechanistic-empirical Pavement Design.” *2nd Conference of Transportation Research Group of India (2nd CTRG)*, Elsevier B.V., 104, 99–108.
  13. Sarang, G., Lekha, B. M., Geethu, J. S., and Shankar, A. U. R. (2015a). “Laboratory performance of stone matrix asphalt mixtures with two aggregate gradations.” *Journal of Modern Transportation*, Springer Berlin Heidelberg, 23(2), 130–136.
  14. Sarang, G., Lekha, B. M., Krishna, G., and Ravi Shankar, A. U. (2015b). “Comparison of Stone Matrix Asphalt mixtures with polymer-modified bitumen and shredded waste plastics.” *Road Materials and Pavement Design*, 0629(January), 1–13.
  15. Sulyman, M., Haponiuk, J., and Formela, K. (2016). “Utilization of Recycled Polyethylene Terephthalate (PET) in Engineering Materials: A Review.” *International Journal of Environmental Science and Development*, 7(2), 100–108.
  16. Vavrik, W. R., Gillen, S., Behnke, J., Garrott, F., and Carpenter, S. H. (2010). “Evaluation of Field-Produced Warm Mix Stone Matrix Asphalt ( WMA-SMA ) Mixtures Prepared By.” (August).



## **RUNOFF EROSION CONTROL USING BIODEGRADABLE GEOMESHES AT DIFFERENT RAINFALL INTENSITY**

**S Verma<sup>1</sup> and S Suresh Kumar,<sup>1</sup> and V K Midha<sup>2</sup>**

<sup>1</sup>PhD Research Scholar, Department of Textile Technology, Dr. B.R. Ambedkar National Institute of Technology, Jalandhar, [sushmal3verma@gmail.com](mailto:sushmal3verma@gmail.com), Corresponding Author

<sup>1</sup>PhD Research Scholar, Department of Textile Technology, Dr. B.R. Ambedkar National Institute of Technology, Jalandhar, [sureshkumar05t406@gmail.com](mailto:sureshkumar05t406@gmail.com)

<sup>2</sup>Professor, Department of Textile Technology, Dr. B.R. Ambedkar National Institute of Technology, Jalandhar, [midhav@nitj.ac.in](mailto:midhav@nitj.ac.in)

### **ABSTRACT**

One of the major problems to the terrestrial ecosystem is “Soil erosion”. It occurs due to wind, water, and other human activities; amongst them, most common is the erosion induced by water running down from the slopes during rainfall is known as “runoff soil erosion”. Worldwide, erosion on cropland averages about 30t/ha-yr and ranges from 0.5 to 400t/ha-yr. An agronomics method is used to mitigate this problem, in which geomeshes made from textile materials are laid over the soil slopes until the permanent vegetation is established. Effectiveness of such erosion control methods depends on various geographical conditions and properties of geomeshes. Therefore, in this study runoff erosion control performance of different geomeshes made from coir and jute fibers is studied at different rainfall intensities (i.e. 75, 100 and 125 mm/hr), at a slope angle of 45°. Erosion control test is performed in a modified Bench-scale erosion tester based on ASTM D 7101 standard. From the study, it is observed that increased rainfall intensity reduces the erosion control percentage in control samples due to the higher water flow velocity and increased soil detachment at higher rainfall intensity. However, geomeshes covered soil slopes provide better erosion control percentages than the bare surfaces, due to the canopy and storage effect of geomeshes. Amongst coir and jute geomeshes, jute geomeshes with better drapability and water retaining capacity provide better erosion control performance.

**KEYWORDS:** Runoff erosion, Erosion control; Geomeshes; Rainfall intensity.

### **INTRODUCTION**

Removal of the top layer of the soil is known as soil erosion. Soil erosion occurs due to the wind, water, and other human activities. It is a prevalent problem throughout the ecosystem. Half of the topsoil on this planet has been lost in the last 150 years. Currently, about 80% of the world’s agricultural land suffers moderate to severe erosion; while 10% experiences slight erosion. It has become a serious environmental problem as the consequences have affected the environment directly (Pimentel 2006). Around 56% of the erosion is due to the water. Most common erosion is the ‘runoff erosion’, which is due to the water running down from the slopes during rainfall. Heavy rainfall accelerates the problem of soil depth, organic matter content and soil acidity. Some other devastating problem occurs like landslide, desertification, flood, and sedimentation of reservoirs (Morgan et al. 1984; Allen 1996)

These problems of soil erosion can be controlled by soil management techniques by using natural vegetation and geomeshes. In the soil management techniques, geomeshes made from the natural fibres, laid over the soil surface which reduces the velocity of the water. It gives temporary reinforcement and holds the soil till the plant grows (Ghosh et al. 2004). Grown vegetation at the soil surface, increases the soil cover and reduces the impact of the rainfall. Whereas, deeper roots of the plants propagate into the soil structure and binds the soil particles due to which soil erosion is reduced. Biodegradable nature of the geomeshes makes it environment-friendly. Simultaneously, moisture regain of the natural geomeshes are higher than the other geomeshes (Saha et al. 2012). Jute and coir geomeshes are preferred over natural geomeshes because they can provide better microclimate to the vegetation by retaining more water into the soil (Midha et al. 2014). Both jute and coir geomeshes offer better tensile strength and facilitate better vegetation growth due to their open structure, whereas nonwoven geomeshes restrict the growth of vegetation due to lower opening size. Hence, in runoff erosion control application weaved geomeshes are preferred (Midha and Kumar 2013). Soil erosion is influenced by a number of parameters like rainfall intensity, slope angle, type of soil. Effect of these parameters are known but the detailed study has not been done. In this study, the effect of rainfall intensity on the soil erosion performance has been observed. The detailed analysis of this parameter is required to understanding the basis phenomenon of erosion and engineering the meshes structure. Therefore, in this study, five different geomeshes made of coir and jute are subjected to erosion control test under different rainfall intensities. Furthermore, to evaluate the restriction offered by geomeshes against the water flow velocity, geomeshes also tested under zero-infiltration.

## MATERIAL AND METHODS

Different coir and jute samples have been used in this study. Average mesh opening size for jute and coir geomeshes are taken 19 x 19 mm and 10x12 mm respectively. The mesh opening size is considered based on the commercially available geomeshes. The physical properties of the geomeshes are shown in Table 1.

**Table 1 Material specification of geomeshes**

Material	Sample no.	Yarn linear density (Tex)	Yarn diameter (mm)	Yarn density (ends per meter & picks per meter)	Mesh opening size (mm)	Weight per unit area (g/m <sup>2</sup> )	Fractional cover	Flexural rigidity	
								Dry	Wet
Coir	C1	4794	4	43	19x19	412.28	0.314	4380	1581
	C2	6765	5	42	19x19	568.26	0.376	5759	1987
	C3	7614	6.5	39	19x19	593.89	0.443	6501	2492
Jute	J1	2961	2.5	80	10x12	441.00	0.338	861	189
	J2	4773	3.9	72	10x12	644.00	0.457	972	196

## Methodology

Runoff erosion control test is performed on a modified runoff erosion control tester, which is based on ASTM D 7101 standard, as shown in Figure 1. The Instrument consists of PLC (Program logic controller) with V-jet nozzles, which are used to get the required rainfall intensity of 75, 100, and 125mm/hr. Water flow rate and pressure are throughout monitored to ensure the uniform rainfall simulation. Runoff erosion test is carried out at a fixed slope angle of 45°.



- A- Water tank
- B- PLC
- C- V- Jet Nozzles
- D- Testing space

**Fig. 1 Runoff erosion control tester**

To carry out the test, testing tray is filled with soil from shivalik region (lower Himalayan regions) and compacted based on the ASTM D 698 standard. Prepared soil trays are positioned at 45° angle on runoff erosion set up and subjected to different rainfall intensities. Eighteen such results are repeated for each sample, and results of initial three trials are not considered to avoid the initial error that generated due to the initial absorption of soil and geomesh. Rainfall is simulated for 3 minutes for each trial and runoff water with eroded soil is collected. The eroded soil from the runoff is separated by sedimentation process and the erosion control % of each sample is calculated by using equation

$$\text{Erosion control}(\%) = \frac{E - C}{E} \times 100 \quad (1)$$

C - Eroded soil with geomesh (gms).

Woven geomeshes control runoff erosion by offering restriction to the runoff velocity. But, under testing condition, absorption of water by the soil influences the water restriction properties of the geomeshes. Thus, to

avoid soil infiltration, testing is also carried out in zero infiltration condition (without soil) for better understanding of the geomeshes.

In zero infiltration condition testing, soil tray is replaced with a metallic surface as shown in Figure 2. Geomesh is placed on the metallic surface and rainfall is allowed for 3 minutes to collect runoff volume. After that, rainfall is ceased for three minutes to collect culmination discharge. Similar procedure is repeated to know the effect of different geomeshes at different rainfall intensity.



**Fig. 2 Sample placement for testing in soil infiltration and zero infiltration condition**

### RESULT AND DISCUSSION

The results of runoff erosion test performed with soil and without soil at 45° angle and different rain fall intensity (75,100, and 125mm/hr) are tabulated in Table 2, 3. Effect of different rainfall intensity on the different infiltration condition has been shown in Figures 3,4.

**Table 2 Runoff erosion test under soil infiltration condition**

Material	Sample code	Runoff Volume (ml)			Erosion Control (%)		
		75mm/hr	100mm/hr	125mm/hr	75mm/hr	100mm/hr	125mm/hr
Coir	C1	342	454	581	42.1	38.7	37.5
	C2	339	430	576	59.1	50.2	48.4
	C3	327	441	564	54.5	48.5	45.7
Jute	J1	292	388	448	68.5	68.5	61.2
	J2	260	341	387	74.3	71.3	66.2

**Table 3 Runoff erosion test under zero infiltration condition**

Material	Sample code	Runoff Volume(ml)			Culmination Discharge (ml)		
		75mm/hr	100mm/hr	125mm/hr	75mm/hr	100mm/hr	125mm/hr
Coir	C1	420	575	624	68	64	62
	C2	434	571	715	64	62	74
	C3	420	564	721	53	73	76
Jute	J1	313	435	592	197	206	201
	J2	290	390	552	212	228	231

**Influence of Rainfall Intensity on Erosion Control Performance of Geomeshes at Soil Infiltration Condition**

Figure 3 shows the effect of different rainfall intensity on erosion control (%). The rate of water simulated on the slope is higher as compared to the lower rainfall intensity. Therefore, runoff volume increases, as rainfall intensity increases. Further, at increased rainfall intensity, erosion control (%) decreases. Increased rainfall intensity increases the impact of rainfall on the soil surface due to that more detachment of soil particles from the soil surface, which results in reduced erosion control at increased rainfall intensity. Jute shows the better erosion control than the coir due to its better drapability behaviour.

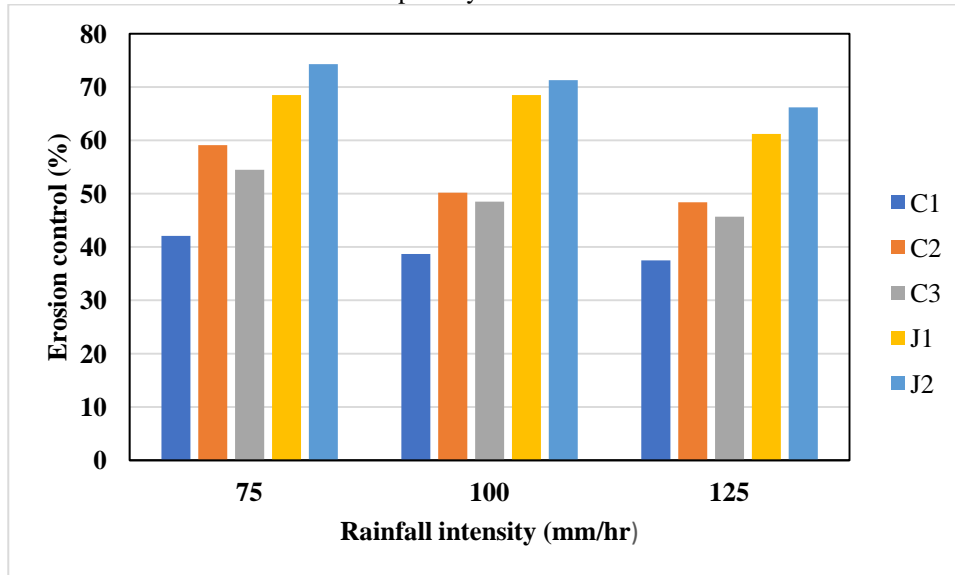


**Fig. 3 Effect of rainfall intensity on erosion control (%)**

**Influence of Rainfall Intensity on Erosion Control Performance of Geomeshes at Zero Infiltration Condition**

Figure 4 shows the effect of different rainfall intensity on culmination discharge. At increased rainfall intensity, coir geomeshes (C1, C2, and C3) show inconsistent culmination discharge due to the rigid coir fibres which protrude on the geomesh surface. But, Jute geomeshes (J1 and J2) show an insignificant increase in culmination discharge at increased rainfall intensity. Since culmination discharge occurs due to the geomesh’s absorption and storage effect, and both of them do not depend upon rainfall intensity. Therefore, at increased rainfall intensity, jute geomeshes with better drapability show a marginal difference in culmination discharge. However, geomeshes with higher mass show higher culmination discharge as compared to lower mass geomeshes

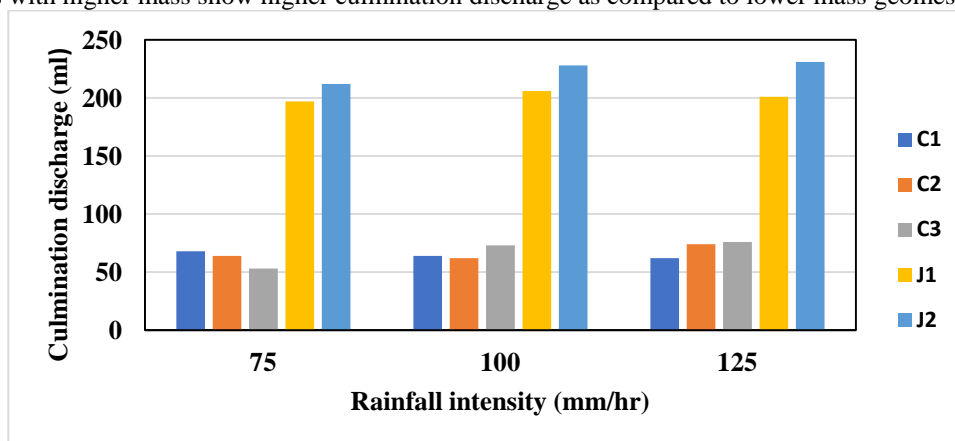


**Fig. 4 Effect of rainfall intensity on culmination discharge**

The culmination discharge of lower weight jute geomeshes (J1) at 125mm/hr rainfall intensity is 201 ml, but under the same condition culmination discharge of higher mass jute geomesh (J2) is 231 ml. It is due to the higher weft yarn diameter and higher absorbing capacity of geomesh (J2), which increases the storage capacity. Jute geomeshes show the better overall performance due to the better drapability behaviour of the jute. Flexural

rigidity of wet jute geomesh is higher than the dry geomesh. Due to this, draping behaviour of jute geomeshes increases and results in better erosion control performance

#### CONCLUSION

From the erosion control performances of geomeshes, it is observed that erosion control percentage and soil infiltration conditions are highly influenced by the rainfall intensity. As the rainfall intensity increases, runoff volume increases due to the impact of rainfall which results in more detachment of soil particles. At the increased level of rainfall, jute geomeshes (J2) show better erosion control than coir geomeshes because of its higher moisture regain. Jute geomeshes also performs better in infiltration conditions due to the higher storage volume and better drapability.

#### REFERENCES

- ASTM (American Society for Testing & Materials). (2013). Test Method D 7101-2013: Standard index test method for determination of unvegetated Rolled Erosion Control Product (RECP) ability to protect soil from rain splash and associated runoff under bench-scale conditions. West Conshohocken, PA: ASTM.
- Allen, S. (1996). "Evaluation and Standardization of Rolled Erosion Control Products." *Geotextiles and Geomembranes*, 14, 207–221.
- Ghosh, P., Samanta, A. K., and Basu, G. (2004). "Effect of selective chemical treatments of jute fibre on textile-related properties and processibility." *Indian Journal of Fibre & Textile Research*, 29, 85–99.
- Midha, V. K., Kumar, S. S., and Sharma, A. (2014). "Performance of transesterified jute rolled erosion-control products." *Geosynthetics International*, 21(5), 301–309.
- Midha, V. K., and Suresh Kumar, S. (2013). "Influence of woven structure on coir rolled erosion-control products." *Geosynthetics International*, 20(6), 396–407.
- Morgan, R. P. C., Morgan, D. D. V, and Finney, H. J. (1984). "A Predictive Model for the Assessment of Soil Erosion Risk." *J. agric. Engng Res.*, 30, 245–253.
- Pimentel, D. (2006). "Soil erosion: A food and environmental threat." *Environment, Development and Sustainability*, 8(1), 119–137.
- Saha, P., Roy, D., Manna, S., Adhikari, B., Sen, R., and Roy, S. (2012). "Geotextiles and Geomembranes Durability of transesterified jute geotextiles." *Geotextiles and Geomembranes*, 35, 69–75.



## Review on Fire Safety in Car Parking

Deepanshu Rajora,<sup>1</sup> B.P. Yadav,<sup>2</sup>

<sup>1</sup>\*,M.Tech Student, Department of Health, Safety and Environment, University of petroleum and Energy Studies, Dehradun

<sup>2</sup>Associate Professor, Department of Health, Safety and Environment, University of petroleum and Energy Studies, Dehradun

### Abstract:

This paper mainly highlights on car parking safety from fire. Nowadays many underground car parks are constructed in large residential, administrative and office buildings. A large portion of them are developed with a view of tackling the issues related to indoor air quality, for example, carbon monoxide emitted from vehicles. In such cases, mechanical ventilation frameworks must be introduced to supply air that is natural. An abundant number of fire mishaps involving car parking lots in the recent decades have brought a serious focus on this issue. There have been some concerns about the causes of fires in car parks associated with present day vehicle construction & the way these flames can spread to the automobiles that are parked close by. Thus, this paper will mainly highlight the various aspects on how these parking lots catch fire and also on how the fire spreads vigorously endangering the whole building. The safety measures using various engineering controls on how to curb the smoke and heat production will also be discussed. The study discusses one case study on major car parking fire accident and also alludes to the safer building design of a car parking lot taking into concerns regarding fire and .

Keywords: vehicles, car, fire safety, parking design

### Introduction

Nowadays, car parking structures are generally found in abundance in urban areas or cities. These structures are solitary, or sometimes co-exist with a residential compound. Structures can be many storey, above ground and may be open or closed; and be utilized to park and safely keep different kinds of vehicles (EC 1999). The increase in the rate of construction of underground parking lots, especially in crowded urban places leads to safety concerns related to fire hazards. As a result, a rigid set of restrictions has to be implemented which needs proper planning in advance. Due to crouched or low roofs, and absence of openings, there is an effect on the scenario of fire leading to higher temperature in these structures and more damage (Zhao and Kruppa 2004).

Parking garage fires are generally limited to a single vehicle. Only about 8 percent of incidents extend to the area beyond the footprint of the vehicle, where the fire has originally started. In simple words, the majority of fires are bound to a single vehicle in scope (MZ and Spearpoint 2014). However, it is difficult to predict when the fire will strike. The worries regarding human life and property damage have prompted the consideration of effects of fires in developing automobiles parking structures. The structural design and materials used for the parking lot play a vital role in controlling fire and ensuring a safe and sound car storage area. For the same reasons, it is important for a manufacturer or builder to keep in mind the various standards and codes necessary for a safe design while constructing parking lots

**Table 1: List of car parking fire**

S. No.	Fire accident and place	Number of vehicles damaged	Damage
1	Liverpool Echo arena Car park	1400	Nil (animals died)
2	Frolunda Square ,Sweden	100	Nil
3	Palace Vendome fire , Paris	40	Firemen affected by smoke
4	Raipur Railway station parking fire	200	Nil
5	Atlanta International Airport Parking	3	Nil

From Table 1, one can observe that that there have been many cases of car parking fire incidents in and around the world, but fortunately no people have been injured. It doesn't mean that the issue does not need attention. Instead, these events should be treated as a near miss incident for human lives.

### **Causes of Fire Occurrence in Car Parking Area**

In a car there is abundance of inflammable materials including flammable fluids like petrol, engine oil, seats and plastics used in the interior. As Oxygen is abundant in nature, it is very demanding to cut the supply of Oxygen to prevent the fire at the start or its spread after an accident. Depending on the miles the car has travelled before parking, weather, adjacent vehicle, state of the car machinery and human failure, the possible causes are as follows: (i) Arson: It is very much possible that someone may alight the car, which can be a deliberate Violation (whether Routine, Situational, or Exceptional),(ii) Electronic malfunction within the car, (iii) Static electricity: Static discharges of the car or adjacent cars, through friction build-up in the tyres, or wind blowing over the metal body causes ignition spark,(iv) Radiation: If the car is parked where there is a radiation leak from the buildings or other one off scenarios where the other vehicles are carrying unsafe illegal materials,(v) Electricity/arcing: This normally happens when we park the car under overhead electric lines, (vi) Flashpoint/auto-ignition: The flashpoint of gasoline is -43 degree C, and auto-ignition temperature is 280 degree C, hence car temperature matters a lot, (vii) Poor maintenance: Leaking fluids, Overheating engines, Overheating catalytic converters, battery issues, bad gasket are all examples of poor maintenance which may lead to fire(Chow 1998).

It becomes very important to carefully examine the parking lot involved in a fire accident to understand the basis of the origin & spread of fire. Since fresh air is abundant, open-sided parking areas may easily lead to fire due to easy availability of ventilation. It is possible for the fire to spread easily in case of availability of materials which can easily catch fire. On the other hand, enclosed parking lots have more probability to witness under-ventilated fires as a result of short-supply of air. Consequently, the material is left incompletely burnt resulting into production of harmful gases which affect the persons respiratory tract (DCLG 2010).

The format and structure of automobile parking premises imply that fire spread starting with one automobile then onto the next is a definite risk. Vehicles are for the most part stationed closely thereby facilitating flame to spread from one car to another. Moreover car parking premises mostly have rooftop which is quiet lower enabling warmth & smoke development simply over the vehicles (PJHJ et al. 2003).

### **Building Design of Parking Lot**

Car parking lot can be broadly classified into open and closed based on guidelines provided by European Convention for Constructional Steelwork (ECCS) which states that, a parking lot will be termed as “open” if the area of wall ventilation is present at two facades facing in opposite side. Usually open car parking area are highly ventilated which helps in keeping the fire in its zone of ignition thus avoiding flashover(Wang 2014).

In order to test the structural fire behaviour of steel members, a study was conducted in the year 2000 called the “three fire test”. This test was conducted in an unprotected real car park consisting of 3 cars, made of concrete steel. The duration of the fire test was one hour and twenty minutes and the maximum temperature that reached the ceiling just above the car was 1040 degree C. After cooling the structure only a slight deformation of twenty five millimetres was observed however the structure did not collapse. Thus this test successfully concluded that concrete steel is indeed resistant to fire.

One of the important requirements for a proper parking lot is the suitable number and size of columns in parking structures. It should be kept in mind seen that large columns do not congest the traffic lanes width and, the parking space. Furthermore, corrosion, chloride attack and leakage may occur in the floor deck joints. So the number of joints should be kept minimal. Manufacturers should provide impact resistance test and density hardness in order to verify if their structural product would stay in place if stressed over the design limits. Also, in order to protect the parking structure from harsh external weather conditions, roof insulation should be carried out and an external wall may need to be constructed. In order to overcome the expansion due to thermal energy, expansion joints can be used. These joints should be designed in such a manner that they are able to withstand vehicular weight (Fettah 2016)

### ***Liverpool echo arena car park fire***

A huge fire in Liverpool destroyed up to 1,400 vehicles in a multi-storey car park, forcing many people to spend New Year's Eve in a temporary shelter. The concerned fire department termed the blaze as one of the worst it had ever dealt with. As per the report filed by the police, an accidental fire in one car which spread to other vehicles appeared to have been the cause for the fire. Nearby apartments had to be evacuated due to smoke. People were

also frightened by the noise as car windows exploded during the fire. About 21 fire engines were put into service for dousing the fire. The risk of building collapse made the situation worse. All vehicles left in the 1,600-capacity car park were destroyed. The temperature reached during the blaze was between 800C and 1,000 degree C. Although crews attended within eight minutes of the alarm, the flames spread so quickly they were not able to control the blaze. A study conducted afterwards concluded that the sprinkler system would have stopped the fire in time. Moreover, a sprinkler system would certainly have limited the spread and given a much better opportunity to put the fire out before it spread to the extent it did.

### **Control Measures for Fire Prevention and Mitigation**

The sorts of fire protection framework introduced in parking lots have to be site-specific. The main control systems are smoke detection system, a sprinkler system and a programmed fire detection system (Merci and Shipp 2013). Investigations of previous accidents completed across various countries have demonstrated that sprinkler frameworks in parking structures help extraordinarily in protecting lives & lessen harm by fire. Automobile parking lots are outlined with lower rooftop stature, permitting sudden sprinkler action. But as vehicles do not allow the penetration of water, installing sprinkler system framework doesn't have any impact on the fires inside car. Sprinklers work by creating a cooling effect. As a result of the water emanating from sprinklers, the temperature gets cooler, which in turn, prevent the fire spread. However, sprinklers don't help in expelling the dangerous gases and smoke formed by fire (Jian-ping et al. 2011). At least one method for ventilation of smoke and warmth is needed in all vehicle parking areas. Ventilation is an important factor, clearly demonstrated by many researches to tremendously lessen the probability of flame spreading between neighbouring autos. As an extra measure of assurance, programmed fire detector is generally provided to provide a rapid reaction to the occurrence of fire. Impulse fan, if installed, assists drawing out harmful gas and smoke towards proper exit points (Wang and Yan 2008).

Apart from the above, other measures have significance for controlling fire in a parking lot are: passage for fire engine to enter and exit the parking in a quicker manner, private fire hydrant, hose reels, Firefighting staircase for cars with more height (Matsushita et al. 1993).

The parameters for a suitable car parking lot design should include: easy and simple entrance and exit to and from the car lot; uncomplicated flow of traffic in and around the parking lot; proper ventilation and low maintenance. In order to satisfy all these above requirements for a proper car parking design, steel construction is a very suitable solution. Thus various advantages of steel construction include: lower dead load, faster construction, low maintenance and highly resistant to fire (Wang 2014). For making general public aware, safety drills can also be conducted based on the different scenarios which are assumed to be found in the parking structures to calculate the best response to be useful in emergencies.

### **Conclusions**

This study reviews the fire in car parking lots and sheds light on the causes and solutions for the same. It is very important to identify and analyse the sources from which a fire could occur in a car parking lot. The sources like highly combustible material and loose wiring etc. need to be kept away or monitored intensively. The building design and the materials used in constructing the parking lot have a vital role to play and it is required on the part of the builders to keep fire safety in mind while constructing a parking lot. The relevant codes and standards should be followed while designing the parking lots. It would help control various hazards in parking structures. Various fire protection systems e.g. smoke and fire detection system and sprinkler systems in parking lots may control the fire in origin as well as its spread.

### **References**

- Chow, W. (1998). "On safety systems for underground car parks." *Tunneling and Underground Space Technology* 13(3): 281-287.
- Jian-ping, Y., Zheng, F., Zhi, T., Jia-yun, S. (2011). "Numerical Simulations on Sprinkler System and Impulse Ventilation in an Underground Car Park." *Procedia Engineering* 11: 634-639.
- Matsushita, K., Miura, S., Ojima, T. (1993). "An environmental study of underground parking lot developments in Japan." *Tunnelling and Underground Space Technology* 8(1): 65-73.
- Merci, B. and M. Shipp (2013). "Smoke and heat control for fires in large car parks: Lessons learnt from research?" *Fire safety journal* 57: 3-10.

Proceedings of National Conference: Advanced Structures, Materials and Methodology in Civil Engineering (ASMMCE – 2018), 03 - 04th November, 2018

PAPER CODE: C503

Mz, M. T. and Spearpoint, M. (2014). "Development of fire scenarios for car parking buildings using risk analysis." *Fire Safety Science* 11: 944-957.

EC (1999). Development of design rules for steel structures subjected to natural fires in Closed Car Parks. European Commission. ISBN: 92-828-7164-9

DCLG (2010). "Fire spread in car parks." BD2552, Department for Communities and Local Government.

PJHJ, W.V.D., Borgers, A.W.J., Timmermans, H.J.P. (2003). "Travelers micro-behavior at parking lots-a model of parking choice behavior."

Wang, Z. and Yan, Q. (2008). "The Study on the Fire Incipient Fault and the Fire Countermeasure of the Large-scale Underground Garage [J]." *Journal of Chinese People's Armed Police Force Academy* 8: 021.

Zhao, B. and J. Kruppa (2004). "Structural behaviour of an open car park under real fire scenarios." *Fire and materials* 28(2-4): 269-280.

Fettah, B. (2016). Fire analysis of car park building structures.

Wang, Y. C. (2014). *Steel and composite structures: Behaviour and design for fire safety*, CRC Press.



## NUMERICAL MODEL AND SIMULATION OF CRACK PROPAGATION IN FRC SLUICE GATES BY XFEM

Peerjada Jaffar Abass,<sup>1\*#</sup> Dr. S. Muthulingam<sup>2</sup>

<sup>1</sup>PhD Scholar, Department of Civil Engineering, Indian Institute of Technology Ropar; [2017cez0005@iitrpr.ac.in](mailto:2017cez0005@iitrpr.ac.in),  
Corresponding Author

<sup>2</sup>Assistant Professor, Department of Civil Engineering, Indian Institute of Technology Ropar

### ABSTRACT

A Sluice gate is a hydraulic structure used to control flow of water. Understanding the behavior of sluice gates can provide useful information for the economic design of same gates. The present paper combines numerical simulation of Fiber Reinforced Concrete sluice gates and XFEM approach to analyze the growth of cracks(tensile/shear) initiated from the pre-existing flaw using finite element tool, ABAQUS. The important feature of XFEM is that, without any remeshing, it can extend the crack. Experimental behavior is compared with the proposed numerical model.

The results from the analysis are compared with the available literature on sluice gates. The numerical model using ABAQUS shows good agreement with the experimental results.

**KEYWORDS:** crack propagation; Fiber-reinforced concrete; sluice gate; pendulum impact; impact resistance; XFEM; pre-existing crack.

### INTRODUCTION

Sluice gates are hydraulic structures commonly used for control of flow in irrigation canals, channels and stores water. Its supervision and functioning basic to ensure the safety of lives and public property too. As most of sluice gates are made of metal (cast iron, black iron, and stainless steel) they are customarily stolen and sold as scrap metal. These issues are common in scattered regions. Depending upon gate opening, flow conditions through a sluice gate can be categorized as:

1. Free flow condition: The condition in which free hydraulic jump is formed downstream the gate.
2. Submerged flow condition: It occurs when the tail water depth rises behind the conjugated depth, as shown in (Fig. 1).

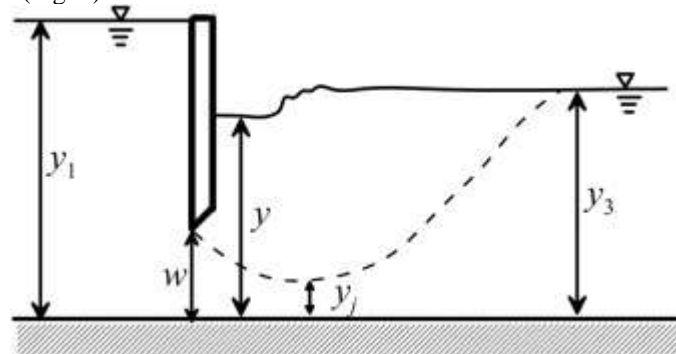


Fig. 1 Flow through submerged vertical sluice gates

The gates are barriers put normal to the flow direction. Different types of gates exist, as it is very appropriate to use them. It is well known that the laboratory experiments and modeling of hydraulic structures and costly and time-consuming. The numerical simulation of gates may be competent of providing explicit solutions for the efficient designing of hydraulic structures. Secondly they are difficult to discharge water inside of levee. Additional problem is malfunctioning of sluice gates which inhibit the effort to stop water. Because of these highlighted issues, it brings non-steel sluice gates into concern. As fiber reinforced concrete is characterized by high strength resistant to cracks, impacts, abrasion than normal concrete and low dead weight. This makes it proper choice for sluice gates as these is less likely to be stolen and easier to discharge water. Numerous researches have been done on sluice gates which include discharge through the sluice gates, flow, or experimental related like designing of gates (Liu and Cho, 2018). Few researches have been done on numerical simulation of sluice gates.

### Objectives

In the present study, computational model was developed based on the fracture mechanics theory to define crack growth in fiber reinforced concrete to show the validity of experimental analysis. Implementation and validation of numerical model involving pre-existing cracks in FRC. Studies in the past revealed the performance of plain, reinforced, fiber reinforced composites structures through impact analysis (Rajput and Iqbal, 2017), (Yu, Beer et al. 2016), (Aghdasi and Ostertag, 2018), blast loading on steel plates showed with increase in the tilt angle, the blast load being imparted on target plate was deflected (Yuen et al. 2018). The literature addressing the impact behavior of prestressed concrete is limited. Iqbal et al. (2018) proposed shear crack along with major tensile crack develops along the direction of pre-stress. The results suggested by (Ghahremannejad et al. 2018) revealed that increasing fibre improves serviceability by decreasing the number of cracks and crack widths. Bijankan et al. (2016) suggested that presently classical energy momentum methods failed to find out the flow rate in case of high submergences. Discharge through multiple submerged sluice gates is affected by various parameters. Sauida (2014) suggested that with the increase in expansion ratio, there was increase in discharge coefficient. To understand the crack initiation and propagation in brittle (concrete) structures many researchers conducted research based on experimental and numerical analysis. Most of the studies found the brittle nature of concrete and observed that initially primary wing cracks of tensile nature are seen followed by secondary cracks. Lajtai (1971) supervised uni-axial compression tests on POP having pre-existing flaw of different dimensions and orientations corresponding to loading conditions. The distinct crack patterns were observed as depicted in (Fig. 2) from the results, which comprise:

- Tensile crack: appears first after loading and are parallel to the loading direction.
- Normal shear crack: got initiated at the tip of the crack and is normal to loading direction.
- Additional shear zone: appeared around the crack tip when loading was further applied.
- Inclined shear crack got developed in the shear zone which results in loss of cohesive strength of material.

Alonso, Pedraza, Galvez and Cendon (2018) proposed a constitutive model to simulate fracture analysis of concrete and quasi-brittle materials. The corresponding model showed good accuracy in load deflection curves, fracture typologies and trajectories of crack. Farnam and Rezaie (2018) developed a model to simulate fracture mechanics in pre stressed concrete sleepers. Fracture mechanics parameters (stress intensity factor, CTOD and crack length) were analyzed, and the results found that flexural behavior is more reliable on crack length initiation rather than crack width and the cracks gets initiated from the centre portion.

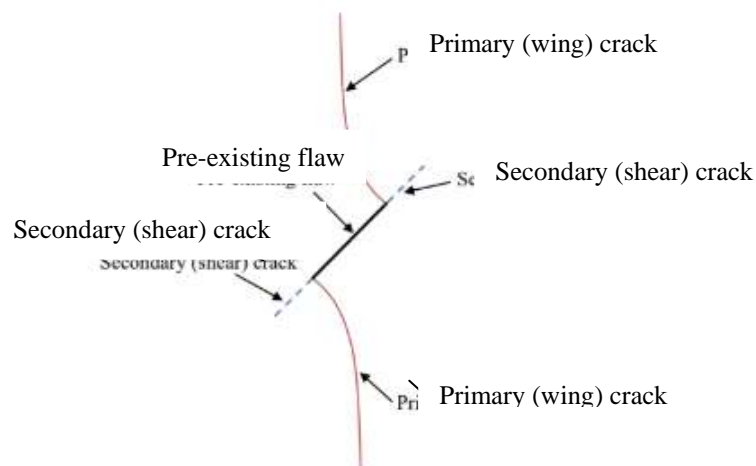


Fig. 2 Initiation of primary and secondary cracks from a pre-existing crack.

### DESIGN AND CONSTRUCTION OF SLUICE GATES:

#### Design of FRC Sluice Gates

A sluice gate comprises a gate unit and mechanical lifting system. Categorically the structure comprises the following components: (a) Gate: it is a movable steel device which comprises body structures, frame and fixed base. (b) Culvert: the structure which joins the discharge canals lying inside of river bank and river drainage structures lying outside the bank, having hole on both sides. (c) Lifting device: device which operates mechanically to open and close the gate. The device is driven hydraulically or electrically and manually.

(d) Derrick: it acts as a bridge between the gate and hoist. It is made of metal and screw thread or trapezoidal in shape. The gates can be operated manually or electrically. In manual gates, opening and closing of gates are done by human operators to activate a derrick. The gate is opened vertically and is installed on rivers for field irrigation. Automated gates are typically installed on river banks to avoid tides and floods. The difference in water levels along two sides of a bank is the driving force to lift the gate. The sluice gates proposed in this paper were automatically operated. The sluice gates are illustrated as shown in (Fig. 3).

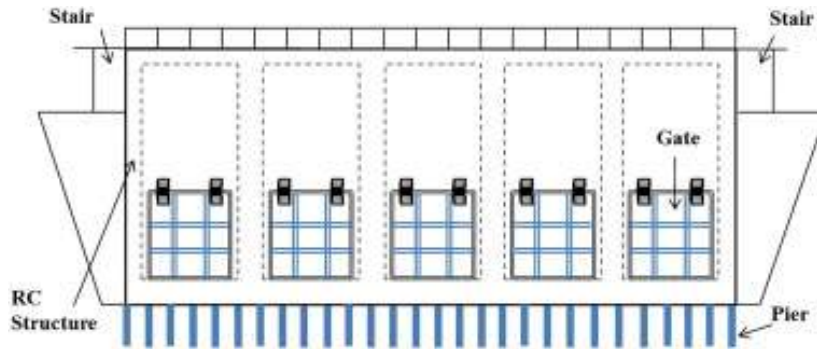


Fig. 3 Example of sluice gates.

**Construction of FRC Sluice Gates:**

Sluice gates comprise the given dynamic loads: hydrostatic pressure, mud-pressure, inertial force due to earthquakes, buoyancy, flowing and static pressure due to mud slides. The construction and the location of lugs and the constructed FRC gate is shown in (Fig. 4). The maximum principle stress (-2.67Mpa), shear stress (1.16Mpa) and maximum strain (0.31mm) of the sluice gate (Houanliao gate) based on two-way slab theory. The sluice gate contained double layered galvanized mesh (Liu and Cho, 2018). The results found slump test as 24cm, air content as 2% and unit weight as 2373kg/m<sup>3</sup>. The material composition of sluice gates is shown in the (Table 1).

Table 1. Composition of FRC sluice gate material (kg/m<sup>3</sup>).

w/cm	Water	Cement	Slag powder	Fly ash	Coarse aggregates	Carbon fiber	Fine aggregates	Super plasticizer
0.26	160	400	140	75	917	8	586	6



Fig. 4 Lifting lugs location and surface of FRC

NUMERICAL MODELING AND EXPERIMENTAL STUDIES

**Basic Concept of XFEM**

The extended finite element method (XFEM) is a numerical technique which extends classical FEM approach aiming on the crack propagation problems. It is based on the partition of unity. The concept permits local enrichment functions to be smoothly assimilates into a finite element approximation. It's the background of XFEM. More generally  $\sum_{i=1}^n f(x) = 1$ . Special enrichment functions in concurrence with additional DoFs

ensuring discontinuities present. Simulating crack propagation with XFEM doesn't need initial crack and crack path definitions to comply with the structural mesh. The approximation for a displacement vector function with partition of unity enrichment is:

$$\mathbf{u}^h(\mathbf{x}) = \sum_{i=1}^n N_i(\mathbf{x})\mathbf{u}_i + \sum_i M_i(\mathbf{x})\mathbf{a}_i + \dots \quad \text{Eq. (1)}$$

With  $M_i(\mathbf{x}) = N_i(\mathbf{x})\cdot\psi(\mathbf{x})$

Where  $\psi(\mathbf{x})$  is the enrichment function,  $\mathbf{u}_i$  is the nodal displacement vector and  $N_i$  is the nodal shape function.

## Experimental Studies

For the experimental study, FRC is adopted to notice the crack growth proceeding. The FRC sample is prepared (Liu and Cho, 2018) with the dimensions 500\*500\*60 mm<sup>3</sup>. The method of impact test was adopted to check the ability of FRC. In this 13.5kg steel ball was allowed to hit the sample on the centre through a distance of 200cm. The rate at which length of FRC changed is 0.005. The sample construction involved concoction of wooden mold, sorting wire meshes, welding of steel plates and concrete mixing, and introducing steel bolts for rubber water seals. Young's modulus, compressive strength, tensile strength and coefficient of thermal expansion were obtained as shown in (Table 2).

**Table 2. Material parameter used in numerical model of FRC**

Test Item	Test Method	Unit	No.1	No.2	No.3	Average
Compressive Strength	ASTM <a href="#">C39</a>	MPa	102	99	97	99.3
Flexural Strength	ASTM <a href="#">C78</a>	MPa	18.4	18.0	18.1	18.2
Splitting Tensile Strength	ASTM <a href="#">C496</a>	MPa	7.6	7.9	7.3	7.6
Elastic Modulus	ASTM <a href="#">C469</a>	GPa	37.7	40.7	41.6	40.0
Coefficient of Thermal Expansion	ASTM <a href="#">T336</a>	$\times 10^{-5} \text{ }^\circ\text{C}^{-1}$	2.14	2.15	2.19	2.16

## NUMERICAL ANALYSIS OF THE MODEL

The numerical analysis of FRC sluice gates adopts XFEM approach to represent the behavior and crack growth process by using the finite element tool ABAQUS. Sluice gates behave elastically till the crack is initiated after that traction separation law comes into picture.

### FRC Model without Pre-Existing Flaw

The model is meshed finer to get the more accuracy of deflected part. Element type (R3D4) of 4-node bilinear quadrilateral was used. And for shell it was 4- node doubly curved shells (S4R). The boundary conditions chosen were according to the field conditions. The plate is hit by a rigid ball from a reference point of 400mm vertically and 100mm axially at an angle of 45<sup>0</sup>. The gate is hit by number of blows to check the crack initiation and growth. The ball hit the gate automatically as of high impact problem. The rotational velocity is 750 rad/sec. Friction has been taken into account as coefficient of friction is 0.3.

### FRC Model with Pre-Existing Flaw

The model with the pre-existing flaw was used to simulate the crack propagation in FRC. The crack is at an angle of 45<sup>0</sup> with the radial axis of specimen. The crack length was 65mm.

The model for both validation and crack analysis are depicted in (Fig. 5).

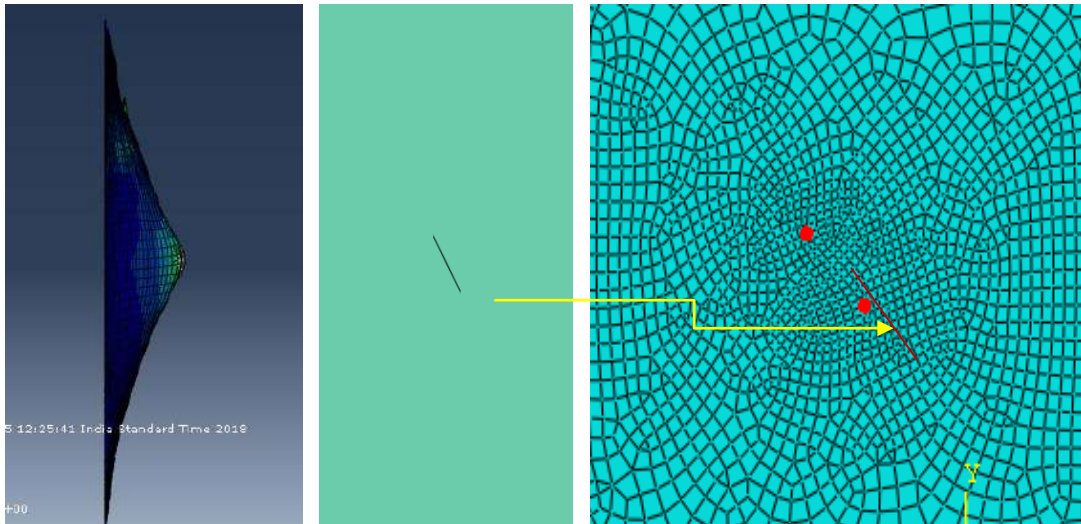
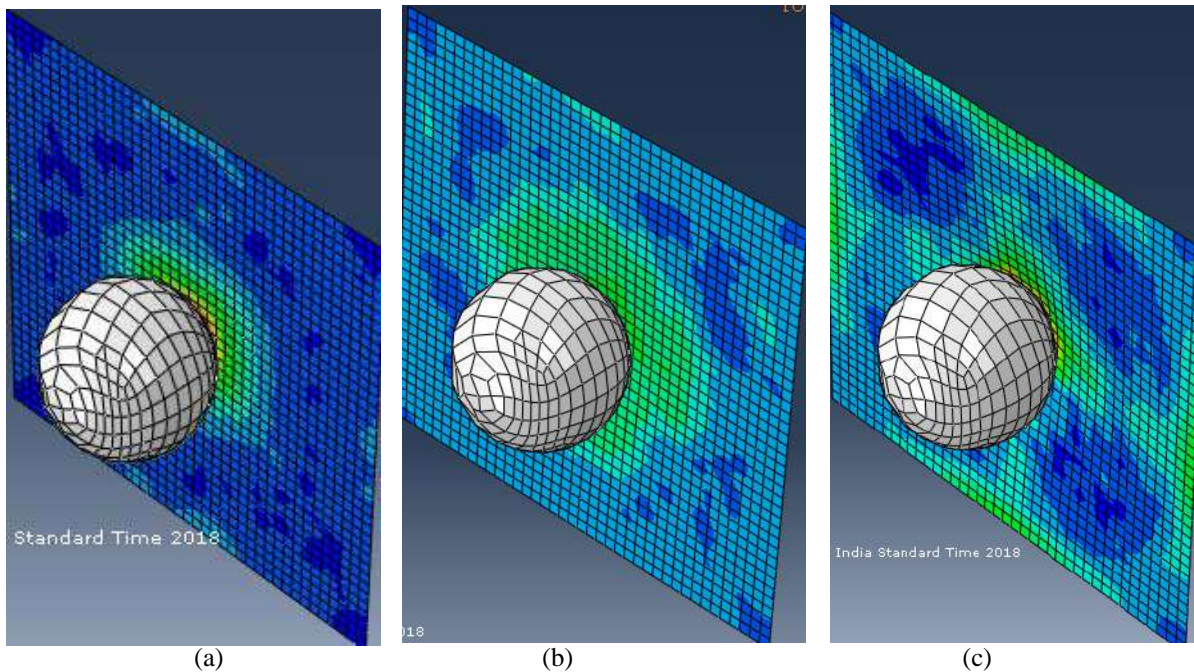


Fig.5 model in ABAQUS representing flaw size at  $45^\circ$

## RESULTS AND OBSERVATION

The proposed model found can simulate the field conditions and crack growth patterns. Initial hitting didn't correspond the deflected area but when it was approaching higher length (400mm), the deflected parts were clearly seen and showed the behavior of FRC. Impact of pendulum on FRC plate is shown in the (Fig. 6). Effect of the application of load (pendulum) on the FRC sluice gates consisting pre-existing crack is fully depicted in the (Fig. 7). The crack growth initiation and propagation can be easily observed. Primary cracks are easily depicted. Gate with pre-existing crack can be observed with the increase in tensile crack ahead of the crack tip. The crack growth was because of the blows ball hitting the gate. Shear zone was observed to be less as is depicted in figures (Fig. 7 a-d).



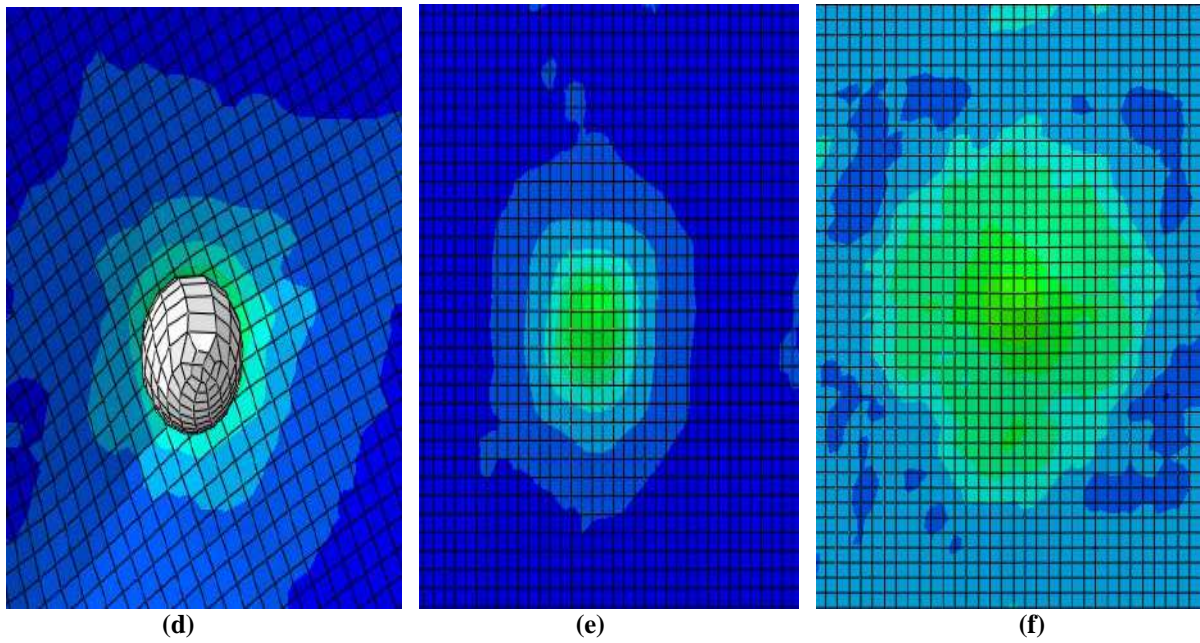


Fig. 6 Pictures of proposed model

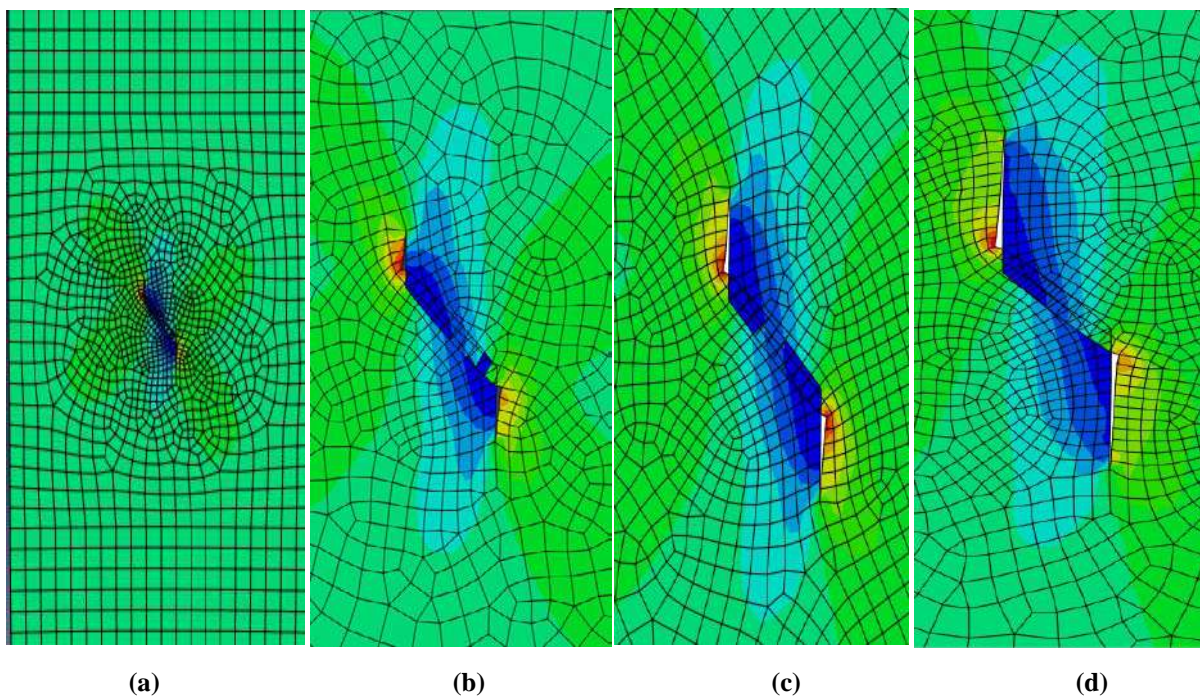


Fig.7 comparison between the crack growth observed in XFEM analysis

### CONCLUSION

Numerical model based on fracture mechanics was proposed and propagation of crack in FRC sluice gates with pre-existing flaw was analyzed using XFEM in Finite element software ABAQUS. Crack propagation parameter such as crack length is important in fractural behavior of elements. Fractural behavior of FRC sluice gates will be predictable by determining the crack length. It was clearly seen that which regions are in stress and how the material behaves. The contact was automatic because of high impact problem. The cracks in sluice gates followed fracture mechanics and grows along the enriched nodes. It has been depicted that with the increase in number of blows, crack length shows variation. Tensile cracks were easily observed while shear cracks were little limited. The numerical model showed good agreement with the shape and crack propagation. Further improvement in numerical simulation is under investigation for better accuracy.

## REFERENCES

- Aghdasi, Claudia P.Ostertag.(2018). “Green ultra-high performance fiber-reinforced concrete (G-UHP-FRC).” 10.1016/j.conbuildmat.2018.09.111
- Alonso, Victor Rey-de-Pedraza, Francisco Galvez and David A.Cendon. (2018). “Numerical simulation of fracture of concrete at different loading rates by using the cohesive crack model.” 10.1016/j.tafmec.2018.05.003.
- Bijankhan, Salah Kouchakzadeh, Gilles Belaud. (2016). “Application of the submerged experimental velocity profiles for the sluice gate's stage-discharge relationship.” 10.1016/j.flowmeasinst.2016.11.009.
- Farnam F.Rezaie.(2018) “Simulation of crack propagation in prestressed concrete sleepers by fracture mechanics.” 10.1016/j.engfailanal.2018.09.012
- Ghahremannejad, Maziar Mahdavi, Arash Emami Saleh, Sina Abhaee, Ali Abolmaali. (2018). “Experimental investigation and identification of single and multiple cracks in synthetic fiber concrete beams.” 10.1016/j.cscm.2018.e00182.
- Iqbal, A.K.Mittal, V.Kumar. (2018). “Experimental and numerical studies on the drop impact resistance of prestress-ed concrete plates”. 10.1016/j.ijimpeng.2018.09.013
- Lajtai. (1971). “A theoretical and experimental evaluation of the Griffith theory of brittle fracture.” 10.1016/0040-1951(71)90060-6.
- Liu, Shih Wei Cho.(2018). “Study on application of fiber-reinforced concrete in sluice gates.” 10.1016/j.conbuildmat.2018.05.004
- Maierhofer, M Krause, H Wigggenhauser. (1998). “Non-destructive investigation of sluices using radar and ultrasonic impulse echo.” 10.1016/S0963-8695(98)00040-1
- Rajput, M.A.Iqbal.(2016). “Impact behavior of plain, reinforced and prestressed concrete targets.” 10.1016/j.matdes.2016.10.073
- Sauida. (2014). “Calibration of submerged multi-sluice gates.” 10.1016/j.aej.2014.04.008.
- Shayan, J.Farhoudi. (2013). “Effective parameters for calculating discharge coefficient of sluice gates.” 10.1016/j.flowmeasinst.2013.06.001
- Yuen, A. Butler, H. Bornstein, A. Cholet. (2018). “The influence of orientation of blast loading on quadrangular plates.” 10.1016/j.tws.2018.08.004
- Yu, L. van Beers, P. Spiesz, c , H.J.H. Brouwers.(2015). “Impact resistance of a sustainable Ultra-High Performance Fibre Reinforced Concrete (UHPFRC) under pendulum impact loadings.” 10.1016/j.conbuildmat.2015.12.157.fibre reinforced concrete (UHPFRC)



## State of Art - Preparation of a Proposal & Estimate for a Mega Project as Per Good Engineering Practice

Rajesh Kataria<sup>1#</sup> and Aaditya Dogra<sup>2\*</sup>

<sup>1</sup>Ex Chief General Manager Indian Oil Corporation Ltd.& Associate Professor Civil Engineering DPGITM, Gurugram Email ID: kataria1957@gmail.com, Corresponding Author

<sup>2</sup>Graduate Student of DPGITM, Gurugram Email ID: [dograaditya4@gmail.com](mailto:dograaditya4@gmail.com)

### ABSTRACT

This paper has been written with aim, the quality of proposal for a mega project should be upto the mark so that Corporate level Board of Directors respective ministry, Govt. of India can approve them in one go after the scrutiny with or without query or minimum number of queries. This is intended for high value mega project of more than Rs. 1,000 crores. The proposal should have proper Justification, Technical Feasibility as well as appropriate Market and Commercial Assessment. The Project Cost Estimation with maximum level of accuracy needs to be done so that later on variations i.e. increase or decrease in cost should be minimum. The type contracts with special technical and commercial clauses must be conceived, implemented for minimum Project Cost variation at the time of physical completion and financial closure of project. The paper broadly covers: Justification, Market and Commercial Assessment, Technical Feasibility study, Project Cost, Financial Analysis, Sensitivity and Risk Analysis

**Keywords:** FEED: Front End Engineering Design; CPI/WPI : Consumer/Whole Sale Price Index; ROI : Rate of Return; NPV : Net Present Value; LSTK : Lump Sum Turnkey; PMC : Project Management Consultant; MIRR : Modified Internal Rate of Return.

### INTRODUCTION

The foremost issue that needs to be described in the Capital Investment Proposal pertains to identification of basic objective or need which is sought to be fulfilled by implementation of the proposed project. The Proposal shall present the complete perspective, rationale and background of need for the project.

It has been observed that in most of the proposals of above nature, the derivations observed from originally conceived one to the final execution are too many which result in drastic scope of words changes, cost increase and over runs

For a mega project of capital investment in nature the aspects to be taken care are:

- **Justification**
- **Market and Commercial Assessment**
- **Technical Feasibility study**
- **Project Cost**
- **Financial Analysis**
- **Sensitivity and Risk Analysis**

### JUSTIFICATION

#### Important Points to Ponder

A few important factors for the justification are ; types of needs, economic considerations, technical and financial considerations mentioned as detailed below

#### Type of Needs

The need for a project may be broadly on account of:

- Capacity enhancement due to demand and supply imbalances
- Economic considerations and Technical and/or operational necessity
- Marketing considerations
- Improvement in existing operations and Govt. of India Strategic policy decisions
- Safety, environmental and other statutory requirements

#### Economic Considerations

Capital investments may be required due to economic considerations. These include the projects, which directly lead to:

- Enhancement of profitability,
- Reduction in operating costs.

#### Technical and/or Operational Necessity

- The need for investments under this category may be due to constraints in sustaining existing level of operations like:
- Obsolescence of instrumentation, mechanical and electrical equipments due to some developments in technical field,
  - Changes in operating input and/or output requirements.
  - The proposal shall indicate:
    - *Developments, which caused operational necessity.*
    - *Constraints/ limitations presently being experienced.*
    - *Efforts made in the past to overcome these constraints.*
    - *Justification for proposed option.*
    - *Tangible/ Intangible benefits.*

However, the economic benefits may also be brought about in all such proposals.

#### **Marketing Consideration**

Capital investments may be required due to marketing considerations like better customer service, long range business commitments to take care of volatile market scenario.

In such cases, intangible benefits shall be clearly brought out, apart from outlining their synchronization with overall Corporate Marketing strategy. Demand projection should be based on latest available actual demand with projected growth rates.

Such investments should be analyzed through market share gain or avoidance of erosion of market share or for putting up entry barrier for new competitors.

#### **Safety, Environmental and Other Statutory Requirements**

The proposal shall clearly state:

- Background and statutory change and its implications.
- Impact on the safety of operations or on environment.

Product Quality improves:

- Background and decision of Govt. and Impact of Govt. decision in the form of action required.
- Likely benefits in form of capital/operating cost reimbursement, or through price change or subsidy.

## **MARKET AND COMMERCIAL ASSESSMENT**

### **Introduction**

Commercial or market viability is the starting point for assessing the feasibility of capital investment proposals. It determines the need for a new project or for the expansion of an existing project. Three critical questions that need to be asked are:

- Where and how much is the demand?
- At what price?
- Is this proposal consistent with the organizations expertise and strategy?

### **Assessment of Commercial viability**

Commercial viability should be based on an assessment of the existing and potential market demand and supply (both domestic and international) for the product proposed to be manufactured.

- The proposed product mix also needs to be examined and possible future changes in the volume and pattern of supply and demand should be estimated in order to assess the long-term prospects of the unit.
- In demand analysis, the demand for a product or service should be determined along with the share of the total market that can be secured by the company through appropriate marketing strategies.
- The reasonability of selling price of the product is another important factor, which should be looked into.

### **Buy-back Arrangements, Take or Pay Clause**

As part of assessing commercial viability, specific terms and conditions of the buy-back arrangements, Take or Pay clause, if any entered into by the company need to be carefully scrutinized.

It should be ensured that there are no lacunae in the buy-back arrangement/Take or Pay clause fall through at the time of commencement of actual production due to insufficient safeguards.

## **TECHNICAL FEASIBILITY STUDY**

### **Factors to be considered**

Technical appraisal of a project is essential to ensure that necessary physical facilities for production will be available and the best possible alternative is selected to procure them. While formulating the proposal, following indicative checklist may be taken into consideration. The checklist under broad heading is given below:

- Location and Site

- Technical Aspects

**Location**

- Distance from the nearest railway station, seaport and airport
- Need for railway siding and Distance from the nearest town
- Distance from the electrical sub-station or HT lines.
- Availability of drinking/ fire/ cooling water and Availability of skilled / unskilled workers
- NOC from the State Government for the proposed site
- Clearances from: State Pollution Control Board, Explosives Department and from environmental angle (Environmental impact assessment study to be carried out independently).

**Site**

- Particulars of land; whether freehold, leased, rented etc. If land is leased/ rented, terms thereof including the period of lease, etc. (Lender to be advised to initiate formalities for creation of security).
- Adequacy of land area proposed from the angle of future expansions. Size of the land vis-à-vis norms is also to be indicated justifying the size.
- Soil/water test reports from experienced consultants
- Load bearing capacity and type of foundation required.
- Electrical sub-station and its capacity to meet projects power requirement
- Whether dedicated sub-station / power line required and costs thereof
- Land prone to earthquake, floods, landslides.

**Technical Aspects**

Capacity

- Capacity to be synchronized with overall supply/ demand balance.
- Allowance for plant break down, down time and over handling time etc. to be considered.
- In multi plants/ units project, capacity balancing of various units/ facilities.

Technology/ technical arrangements

- Whether internally developed technology can be used.
- Whether technology is proven (more specifically to Indian conditions)
- Reference plants within and outside the country
- Performance data of plants based on the same technology

Process

- Flow chart and description
- Material balance, Utility balance and Off-site facilities

Plant & Machinery

- List of major equipment and machinery
- Capacity of individual identifiable sections; sectional balancing and reasons for imbalance, if any
- Whether the capacities are comparable with the international plant size.
- Reputation of machinery suppliers.
- Analysis of technical parameters considered vis-à-vis Statutory requirement, Govt. / Corporation policy or norms.

Input/ output requirement

- Details of major raw materials/ feedstock
- Output and their disposal
- Critical items of the input, which may affect the process/ operation, like gas availability for Turbo Generators.

Manpower requirement

- Basis of manpower estimates
- Details of manpower (managerial, supervisory, skilled etc.)
- Comparison of manpower strength with similar other projects.
- Training needs and facilities provided
- Comparative analysis of departmental vs. outsourcing

Implementation schedule

- **Mode of implementation i.e. Turnkey, conventional, hybrid, BOOT, BOO or departmental and reason for selection**
- Activity wise scheduling through PERT chart.
- Executing agency with consultancy requirement

- Comparison of implementation schedule with similar other project.
- Synchronization with linked projects.

## **PROJECT COST**

### **Introduction**

An accurate and realistic project cost estimate is vital for appraisal of the project since it has a direct relation with the economic viability of the project.

### **The following core projects are covered:**

- Refining/Petrochemical

### **Components of Project Cost**

Project cost represents the total of all items of outlay associated with a project. The project cost estimates shall be prepared including the following components while clearly indicating the breakup of Rupee and Foreign exchange Component:

- **Prime cost**
- **Provision for design and scope changes**
- **Provision for contingencies**
- **Construction period expenses**
- **Financing cost during construction period**

### **Prime Cost**

Prime cost of the project includes total cost of land, building, equipments, materials, civil construction, other items namely mechanical, electrical, instrumentation, safety, fire fighting, pollution control etc. required to complete the project.

### **Guiding Factors**

- **Mode of execution**

Mode of execution of the project (i.e. on Conventional, LSTK or hybrid basis) is to be determined first. In case mode of execution is decided to be conventional, the estimation of cost shall accordingly be done. However, if the mode of execution is LSTK mode cost estimate to be done with proper justification and based on cost benefit.

- **Component wise breakup of the prime cost**

The major component wise breakup of the prime cost of the project shall be annexed to the proposal. The details for major components of the project cost shall also be provided, wherever possible. The cost should be on net basis after adjustment of Cenvat/ EPCG benefit, if any. However, to take care of the uncertainty in continuance of such benefits, these shall be covered under risk/sensitivity analysis, Harrison. (1985).

- **List of equipments entitle for accelerated/ enhanced depreciation under IT Act.**

List of equipments for pollution control, energy savings, etc on which accelerated/enhanced depreciation under IT Act is available must be identified separately and benefits shall be considered in financial evaluation of the project.

- **Basis for cost estimation**

Generally, the cost estimates are compiled based on the data maintained by various units all over the country, latest quotations received for similar jobs etc. The base date (month/year) shall be clearly indicated.

- **Forward cost Escalation**

No forward cost escalation shall be considered. The cost estimates shall correspond to a fairly recent date not more than 3 months old from the date of the proposal. The base date (month/year) shall be clearly indicated.

- **Comparative Analysis**

The proposal shall provide a comparative analysis of the cost with similar projects under execution or already executed. The comparative analysis shall also provide reasons for abnormal variations, wherever applicable.

- **Completeness of Project facilities**

It must be ensured that all necessary facilities have been envisaged in the project cost. Necessary facilities are the ones absence of which would lead to underperformance post commissioning and would require supplementary scheme approval on ground of operational necessity to achieve optimal/ higher efficiency.

**The Proposal seeking approval for capital investment must cover a confirmation that this aspect has been specifically taken into consideration.**

- **Statutory Levies**

All taxes and duties like, Custom duty, counter veiling duty, Special Additional Duty (SAD), Excise duty, Central Sales Tax (CST)/ Value Added Tax (VAT), Withholding Tax and Service Tax in respect of Licensor payments & Service Tax (in respect of services portion of Contracts) has to be considered at the prevailing rate to arrive at the final investment cost. No works contract tax to be considered if LSTK methodology is adopted since our contracts do not envisage works contract tax as there is clear bifurcation between supply and services in our contracts.

- **Foreign Exchange Requirements**

The foreign exchange requirements for the project shall be separately reflected. The foreign exchange requirement along with the foreign currency conversion rate adopted shall also be provided.

**Components of Prime Cost**

**In case of refinery/ Petrochemical Projects**

Normally the following estimation methodology should be adopted under the following fourteen broad heads:

- **Land**

Land requirement for the project to be implemented is estimated and the cost is to be worked out as follows:

**Estimation of land requirement**

For estimation of land requirement, following factors to be considered:

- Plot area required for plant, off-sites and utilities, pipe racks, roads and culverts allowing for easy access to lifting equipment.
- Green belt coverage
- Area for fabrication yard.

**Estimation of land cost**

In case of outright purchase

Land cost is considered as per the cost per acre indicated by local municipal authorities/ state govt. according to the Land Act applicable at the time of estimation.

- Land cost should also include:
- charges for registration and compensation for standing crops, trees, tube wells,

In case of long lease

In case the marketing/ Pipeline installation is proposed at a site where land is owned by Port Authorities/ Railways/ Subsidiary, the terms of lease shall be taken into consideration.

- **Site Development**

Site development is the cost required for development of the land like land filling and leveling.

Cost of site development must also include:

- soil investigation, oceanographic investigation, environmental-related study cost
- sand stabilization expenditure, cost of borrow pit and cost of transportation, filling and leveling,
- In case of coastal land, sand filling by dredging will be considered under this head.

- **Royalty & Know How**

This represents the cost of know how related to the production process payable to the Licensors, in case of Refinery. In case the licensor selection has been done, estimation will be on the basis of agreement with licensor.

- **Process Design & Engineering**

Process design is the basic engineering fees payable to the Process licensor in case of Refinery. This includes the fees payable towards Front End Engineering Design (FEED) package, basic engg, charges towards training etc by the licensor.

In case of projects is to be executed on conventional mode, detailed engineering and construction supervision payable to Engineering, Procurement and Construction Management (EPCM) consultant is also included under this head.

In case of LSTK, charges payable to PMC is included under this head. PMC cost in case of LSTK mode of execution will be lower since engineering job will be done by the LSTK contractor. Basic engineering fees will be based on the contracts finalized with process licensor. Detailed engineering fee will be worked out on the basis of contract finalized with EPCM consultant.

- **Plant & Machinery (P&M)**

This is the major element of cost in any project cost estimate.

- ❖ **Components of cost :**

- all process units, utilities and Captive Power Plant (CPP),
- storage facilities, loading facilities and off site facilities & equipment foundation,
- control room buildings & detailed engineering cost of LSTK contractor,
- construction management cost of LSTK contractor including commissioning assistance (in some cases pre commissioning and commissioning manpower is also included in the scope LSTK contractor),
- cost of commissioning spares and mandatory spares
- Annual Maintenance Contract (AMC) of selected instrumentation items like DCS/PLC/ECS/Analyzers/MMI till guarantee/warranty period,

- ❖ **Determination of cost :**

The estimated cost for P&M depends not only on the equipment costs but on the execution methodology also.

- In case of LSTK mode of execution, the total responsibility for engineering, procurement, supply, installation, testing & commissioning lies with LSTK contractor, with all associated risks.
- In conventional mode of execution, these activities are performed by owner with the help of EPCM consultant. Hence the risk gets passed on to owner from LSTK.

Hence cost estimate in both cases should reflect this shifting of risks and hence are different. Different PMCs adopt different methodologies to arrive at the base line plant cost.

After studying the different methodologies adopted by various PMCs, the following methodology and percentages are suggested. The exercise is to be undertaken after completion of FEED document and working out Bill of Quantity BOQ for bulk items. For  $\pm 10\%$  estimate important Material Take Off (MTO's) are required to be drawn so that accuracy of the estimate improves to  $\pm 10\%$

#### **Process plants**

- Cost for equipment and bulk supply (piping, electrical & instrument) to be worked out after FEED preparation and working out BOQ based on FEED and engineering required for working out the BOQ (We designate this cost as 'X')
- The following costs be added to 'X' as a %age under following subheads:
  - Spares : 3% and Erection : 8% (Mechanical + Electrical + instrumentation)
  - Civil works including insulation and painting : 25%
- The total cost thus worked out is the baseline cost 'Y'
- In case of LSTK mode of execution, the detailed Engg, construction management, start up & any specific construction site requirement by way of heavy lifting/ handling equipment, cranes etc are to be provided by LSTK contractor. Hence following provisions be added to above baseline cost in case of LSTK as a %age of baseline cost
  - a) Engineering: 5% and Construction management, supervision: 5%
  - b) Start up & commissioning : 0.3%
  - c) Construction site requirement of contractor: 0.5%
- Addition of above (~12%) to baseline cost will give the plant cost.
- In case of conventional method of execution, items under (a) to (d) are covered under scope of EPCM consultant / owner. Hence these costs are reflected in EPCM fee and owner expenses. Hence in conventional mode of execution, the base line cost can be considered as the plant cost.

#### **Offsites**

Compared to process plants, estimation for offsite facilities is project specific and difficult to compute as engg work involved is huge to arrive at realistic BOQs. Moreover there is wide variation in scope from project to project. Additionally, the offsite works are spread over larger areas calling for higher supervision manpower.

The following methodology and percentages are suggested based on previous experiences:

- Cost for equipment and bulk supply (piping, electrical & instrument) to be worked out after FEED preparation and working out BOQ based on FEED and engineering required for working out the BOQ (We designate this cost as 'X')
- The following costs be added to 'X' as a %age under following subheads:
  - Spares : 3% and Erection : 8% (Mechanical + Electrical + instrumentation)
  - Civil works including insulation and painting : 25%
- The total cost thus worked out is the baseline cost 'Y'
- In case of LSTK mode of execution, the detailed engg., construction management, start up & any specific construction site requirement by way of heavy lifting / handling equipment, cranes etc are to be provided by LSTK contractor. Hence following provisions be added to above baseline cost in case of LSTK as a %age of baseline cost.
  - d) Engineering: 5% and Construction management, supervision: 5%
  - e) Start up & commissioning : 0.3%
  - f) Construction site requirement of contractor: 0.5%
- Addition of above (~11%) to baseline cost will give the plant cost.
- In case of conventional method of execution, items under (a) to (d) are covered under scope of EPCM consultant/ owner. Hence these costs are reflected in EPCM fee and owner expenses. Hence in conventional mode of execution, the base line cost can be considered as the plant cost.

#### **Power plant & utility plants**

The scope of work varies widely from project to project. In some projects, it is only addition of 1-2 generating units where as in projects like PNCP, the scope is a total integrated power plant with all auxiliaries included and of medium size. For general guidance, it is recommended to used PNCP estimating factors as guidance:

- Cost for equipment and bulk supply ( piping, electrical & instrument) to be worked out after FEED preparation and working out BOQ based on FEED and engg required for working out the BOQ (We designate this cost as 'X')
- The following costs be added to 'X' as a %age under following subheads :

- spares : 3% and Erection : 8% (Mechanical + Electrical + instrumentation)
  - Civil works including insulation and painting : 15%
  - The total cost thus worked out becomes the baseline cost 'Y'
  - In case of LSTK mode of execution, the detailed engg, construction management, start up & any specific construction site requirement by way of heavy lifting / handling equipment, cranes etc are to be provided by LSTK contractor. Hence following provisions be added to above baseline cost in case of LSTK as a %age of baseline cost
    - a) Engineering : 3% and Construction management, supervision : 2%
    - b) Start up & commissioning : 0.3%
    - c) Construction site requirement of contractor : 0.3%
  - Addition of above (~6%) to baseline cost will give the plant cost.
  - In case of conventional method of execution, items under (a) to (d) are covered under scope of EPCM consultant/ owner. Hence these costs are reflected in EPCM fee and owner expenses. Hence in conventional mode of execution, the base line cost can be considered as the plant cost.
- ❖ **Guiding factors:**
- The P&M cost arrived at based on above guidelines should be cross verified (in case of process plants and CPP/ utility plants) by comparison with a recently executed similar plant cost (after correction for capacity and escalation for time of execution based on published indices as described below) for authenticity and ensuring capture of recent market trends. Alternatively, the plant cost provided by Licensors or independent estimators may also be used for the purpose of comparison.
- **Roads & Building**

This consist of internal road, culverts etc. in the battery area and other non plant building. The following shall be covered under this head:

    - The enabling jobs for making approach roads to site and internal roads in the plot area.
    - Buildings like construction site office, canteen etc.
    - In grass root projects, Admn. Building, technology buildings (cost of workshop, laboratory building, and warehouse, Oil Movement & Storage (OM&S), Occupational Health Centre (OHC) and Fire Station), compound wall, security gates, watch towers.
    - Cost of strengthening the roads for movement of heavy equipment to be included in cost of roads.

However, the roads within the plant area, equipment foundation and control room building, substation building etc are to be considered as a part of Plant & Machinery.
  - **Railway Siding**

This is the cost of railway siding if any to be provided for loading gantry Estimate should be based on budgetary quote obtained from Railways/ IRCON/ similar such agency.
  - **Construction Period Expenses**

This cost head includes salary and over head cost of personnel who will be directly deployed in the execution of the project both at site and HO.
  - **Start Up Expenses**

This element considers amount payable to Process licensors for commissioning assistance, the cost of commissioning fuel, any expenditure estimated to be incurred on test runs and experimental production net of any revenue before the plant begins commercial production.

In case of conventional contracts, where commissioning is in the scope of owner, this shall also include the amount payable to equipment vendor specialists for commissioning assistance. This is estimated on the basis of per diem rates agreed with Licensor/ equipment specialists with necessary escalation provision as per agreement.
  - **Township**

This element considers the cost of residential accommodation to be provided to operating/ maintenance/ support service personnel to be deployed after commissioning as per agreed satisfaction level. This should also include the CISF personnel accommodation like barracks etc.

This is to be worked out considering per unit cost of the dwelling unit based on the entitlement of personnel to be deployed and the number of dwelling units.
  - **Financing Cost (Includes Interest During Construction)**

This is the cost of financing the project. This element is normally estimated considering debt/ equity ratio of 1:1 and prevailing cost of long term debt. The phasing of the expenditure to be realistic based on our past experience. In case of change in the debt equity, financing cost should be calculated accordingly.

Projects taken up by the CPSU are partly financed through internal resources and partly through specific borrowings.

Debt equity ratio of 1:1 shall be assumed where no specific financing plans have been finalized. Where financing mode has been decided then the same shall be indicated. However, the ratio shall be reviewed on case to case basis. Non-plans schemes shall be assumed to be financed from internal resources.

**Provision for Design and Scope Change**

The provision for scope and design change needs to be justified on case-to-case basis. Normally no provision for scope and design change may be required in respect of repetitive projects where scope and design is amply clear at the time of preparation of project cost estimates. However, in case of grass root projects, such provision not exceeding 10% of the total cost of the project may be considered to take care of changes in the scope and design due to detailed engineering.

**Provision for Contingencies**

To take care of minor changes in process schemes, technical ambiguity and other unforeseen requirement of projects contingency is added to project cost to arrive at final project cost for investment approval. As per present practice, 5% of 14 head project cost is taken as contingency to arrive at final cost for investment approval in case of conventional mode of execution. In LSTK mode of execution, PMC considers 2 % to 3% contingency in P & M cost. Thus in case of LSTK mode of execution, balance of 5 % not considered in P&M cost is added under this head. See **Fig.1** for processes of proposal and estimation.

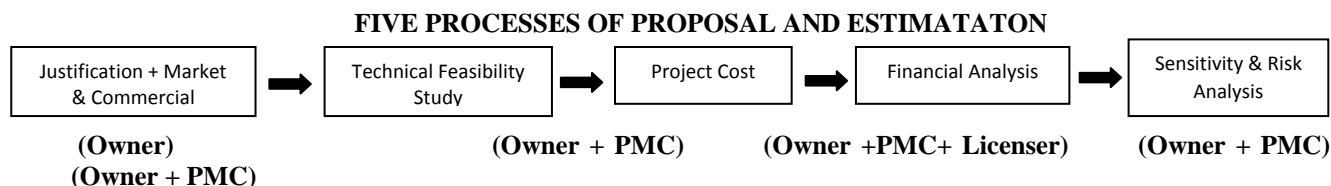


**Fig.1 Flow chart for Proposal & Estimation**

The author has 15 yrs. of experience in preparation of Capital Investment Proposals & Cost Estimation for Core Sector Projects i.e. Refining/Petrochemical, Pipelines and Marketing as senior executive.

**FINANCIAL ANALYSIS**

**Introduction**

The Financial analysis of a project is vital for assessing the viability of the project and hence provides valuable information to the decision-maker. Financial analysis produces an estimate of the financial gains, which will accrue, to the Corporation after implementation of the project.

The financial analysis entails determination of year-wise cash flow of the project, computation of key decision criterion like modified internal rate of return (ROI & ROE), net present value (NPV) of cash flows, debt service coverage ratio and break even (BE) analysis etc. Financial analysis of capital investment proposals shall be carried out based on realistic set of assumptions duly considering present prices of input/ output, market forces etc.

**Determination of Cash Flows**

**Components of Cash Flow**

Determination of year-wise cash flows is the most crucial step of the financial analysis. The cash flows shall be determined for three components namely:

- a. Initial Investment;
- b. Operating Cash Flows;
- c. Terminal Cash Flows

**Initial Investment**

This component of cash flow mainly represents net cash outlay in the period in which the asset is purchased or constructed. In other words, initial investment shall comprise of the total project cost as indicated in the capital investment proposal and shall also include incremental value of working capital, wherever required.

**Incremental working Capital:**

The incremental working capital shall included the followings as outflows in the year of incremental requirement and return of the same at the end of the project life cycle:

- Inventory of raw materials/ intermediates/ finished goods and Inventory of stores/ chemicals

**Operating Cash Flows**

This component of cash flow presents year-wise cash flow generated from operations after the project has been commissioned. The capacity utilization in case of Refinery/Petrochemical projects shall not be more than 60% in the first full completed year, at 80% in the second year and 100% from third year onwards till project life cycle subject to demand projections.

The determination of operating cash flows shall, therefore, entail estimating year-wise operating income, input/ raw material cost and operating expenses during the project life.

#### ***Operating Income***

- Operating income of a project represents total realization or savings from the operations, after implementation of the project, Jack Loftus.(1999).
- While computing the Gross operating income, following issues are to be kept in view:

#### ❖ Margins through Optimization

The Optimization Group set up by the Corporation carries out the exercise of determining the margins related to a particular Project by integrating the proposed Project into the existing set up. This process leads to determining the Corporate Margins which is a derivative of two scenarios, showing margins with the Project and Margins without the Project. The basis adopted by the Group for determining the margins is given below:

- Various Refinery Models (RPMS) are used along with the Integrated Planning Model (IP) which takes into account the existing capacities of all the IOCL refineries
- The demand for products are estimated based on long term Compound Annual Growth Rate (CAGR) projected by the Planning Department – Marketing HO, assuming a base year for location wise actual demand.

Prices of Crudes and Product RTP's, Assessable values and Transaction Values are considered based on 3 year weighted average price with a base Exchange conversion rate for the pricing.

#### ❖ Stand alone – Margins

Though the margins derived by Optimization group through the IP model will continue to be used for the financial analysis, it is mandatory that a standalone analysis is also carried out and be made a part of the proposal. Wide variations in results derived through the margins given by Optimization and margins of stand alone will have to be looked into and addressed accordingly in the proposal.

#### ***Input/ Raw Material Cost***

- Landed cost of inputs/ raw material shall include all incidental costs involved including present rate of custom duties.
- For refineries/ petrochemical projects, crude cost may be considered based on 3 years average import parity prices of identified crude (excluding abnormal fluctuation such as war situation, etc.). Crude quantity corresponding to internal fuel should be valued at current crude cost or 3 years average, whichever is higher. Similarly, external fuel, if any, should also be valued at current cost of respective fuel or 3 years average, whichever is higher, Goel (1987).

#### ***Operating Expenses***

- The operating expenditure of the project shall include the cost of chemicals and consumables, utilities (like power, water, and fuel) repairs and maintenance, wages and salaries, rent and insurance, depreciation, other administrative expenses etc.
- Process Plants requiring fixed bed catalysts need replacement of catalysts after 2-5 years depending upon the guaranteed life. Such incremental operating expenses shall be considered over the project life cycle.

#### **Terminal Cash Flow**

The cash flow in the terminal year of the project mainly represents the salvage value of the project plus release of incremental working capital. Salvage value shall be considered as under:

- Land to be valued at original cost.
- For items other than land, the terminal cash flow may be considered as the book value determined under the Companies Act, 2013.

**In respect to proposals for construction of retail outlets, basis for taking terminal values shall be as per policy finalized by Marketing Division from time to time and approved by the Planning and Projects Committee of the Board.**

#### **Project Life**

For cash flow determination and financial analysis, the life of assets from the date of completion of the project shall be assumed as per life determination given in Schedule-II of the Companies Act, 2013 or 25 years whichever is less.

#### **Issues Requiring Special Care – Cash Flows**

While determining the cash flows for the projects, special care need to be exercised in respect of following:

- Cash inflow can occur by increase in cash revenue and/ or cash saving through reduction in operating costs.
- Cash outflow can occur by increase in operating expenses and/ or decrease in cash revenue, apart from outgo for initial capital investment.
- The net cash flow shall be estimated on 'after tax basis', as payment of taxes is an outflow of cash.

- For calculation of MIRR, all financial charges arising due to financial leverage like interest payment/ dividend payment shall not be considered as cash outflows.
- For calculation of ROE, interest outgo on project loans, tax shield available and principle payments shall be considered. In this case, initial capital outgo shall be limited to equity outgo.
- Corporate tax to be considered as under:
  - Corporate tax to be considered on the project on stands alone basis.
  - Loss, if any, to be carried forward for adjustment with future profit.
  - Minimum Alternative Tax (MAT) to be considered, wherever regular tax liability does not arise.
  - All deductions / rebates/ benefits etc. wherever available under the income tax act to be considered.

#### **Cash Flows Based On Constant Prices**

- While preparing Cash Flow estimates, an issue, which is raised quite frequently, is whether such estimates shall be based on current prices or constant prices.
- Forecasts in current prices, which include the effects of inflation do not give a realistic picture of the true financial profitability of a project, since, inflation can artificially improve apparent profitability by increasing future.

#### **Financial Evaluation**

##### **Introduction**

After determination of cash flow as per methodology enumerated above, the next logical step is to financially evaluate the proposal. The evaluation shall be carried out through following two methods:

- Internal Rate of Return (ROI/ ROE)
- Net Present Value (NPV)

Both the above methods fully recognize the timing of cash flows through the process of discounted cash flows.

##### **Zero date for financial evaluation**

In case of projects involving two stage approvals (1st stage FR approval and 2nd stage DFR based final approval), zero date shall be based on DFR based 2nd stage approval. Expenses incurred between 1st stage and final stage approval shall be escalated to Present Value based on Hurdle Rate in the financial evaluation.

##### **Internal Rate Of Return (MIRR)**

- Internal Rate of Return (IRR) is the discounting rate at which present value of cash inflow is equal to the present value of cash outflow. In other words, the discount rate that yields a ZERO Net Present Value is called Internal Rate of Return.
- While calculating IRR, WACC of the Corporation existing as on the date of evaluation shall be considered for intermediate cash inflows. WACC shall be communicated by CO(PAG) every year after the finalization of the annual accounts of the Corporation
- MIRR shall be computed for all capital investment proposals and indicated in the Capital Investment Proposals.
- Normally projects having MIRR of less than Hurdle Rate (i.e. cost of capital + premium) shall not be considered as commercially viable and therefore, shall be fully justified on non-commercial grounds, wherever applicable.
- For calculation of Return on Equity, interest outgo along with principle repayment is to be considered.

##### **Net Present Value (NPV)**

- The present value of a future sum of money can be found by discounting it to the present point in time or Year 'O' at the required rate of return/ discount rate. Required rate of return shall not be less than cost of capital.
- Under this method, the present value of each years' net cash flow is calculated, starting from the year '0' till complete project life. This discounting rate adopted shall be the Hurdle Rate.
- The NPV method has a straight-forward rationale. An NPV of zero signifies that the benefits of the project (projected cash flows over time) are just enough to:
  - Recoup the capital employed, and
  - Earn the required rate of return on the capital employed
- If the project has a positive Net Present Value, the project is considered to be commercially viable.
- Divisions shall indicate Net Present Value of all the projects at a discount rate of Hurdle Rate duly enclosing workings with the capital investment proposal

#### **Summary Of Financial Analysis**

- For the purpose of financial analysis of capital investment proposals, cash flow estimates shall be prepared for the full project life. These cash flow estimates along with calculation of ROI/ROE, NPV, & Break Even analysis shall be attached to the proposal.
- A statement of assumptions made for Financial Analysis shall be enclosed.

- In summary it may be stated that the more sophisticated and mathematical methods of investment appraisal, particularly NPV and MIRR can have extremely useful applications so long as they are used appropriately.

#### **Other Intangible Benefits**

- Apart from carrying out the financial analysis of the proposal, it is equally important that the proposal shall also indicate other intangible benefits of the project. Normally, these are the benefits related to socio and strategic needs of the country. This includes projects for pollution control, safety needs, staff welfare etc.
- A care needs to be taken while listing the intangible benefits of the project. The benefits, which can be quantified and measured, shall not be treated as intangible benefits. For example, a project for modernization of equipment may have a number of intangible benefits like lesser pollution, better safety etc. but it may also lead to higher productivity. The higher productivity shall be measured, quantified and considered for the purpose of financial and economic analysis of the proposal.

## **SENSITIVITY AND RISK ANALYSIS**

### **Introduction**

After presentation of financial analysis of the project, the capital investment proposal shall indicate an analysis of risk and uncertainty involved in the proposal.

All capital investment proposals involve some risk or uncertainty with respect to their completion, capacity utilization, fulfillment of specified need, safety and profitability etc. as the underlying assumptions made at the project formulation stage may not hold good during the project life. Therefore, analysis of risk and uncertainty is an essential part of formulation of capital investment proposal. This not only facilitates the preparation of sound proposals but also helps in systematic consideration of risk by the approving authorities.

### **Type Of Risks**

Risks associated with capital investment proposals can be broadly classified as:

- Financial Risks
- Other risk

### **Financial Risk**

Impact of various risks finally affects the profitability as a result of change in cash flows from the values considered at proposal stage. Some quantification of financial risk involved with a proposal is possible. This quantification helps in decision-making.

Many techniques are available for determining financial risk involved with the Project like Risk Adjusted Discount Rate, Certainty Equivalent, Sensitivity Analysis, DCF, Break Even Analysis, Probability Assignment, Coefficient of Variation, Standard Deviation etc.

Most of above techniques rely heavily on the intuition of Project Planner, because he has to give factors for probability or for risk quantification. Hence, the results established through such techniques are subjective and therefore do not provide a clear insight to risk/ uncertainty involved, Madachy. (1995).

However, sensitivity analysis is subjective only with respect to the selection of range of variable for determining the sensitivity. Sensitivity Analysis is an excellent tool to know the financial impact of a variable on the proposal. Therefore, sensitivity analysis technique shall be used for determining financial risk of the project, Dennis Lock (1987).

### **Sensitivity Analysis**

Sensitivity analysis is a quantitative process of measuring change in value of a dependant variable consequent to change in the value of one or more other variables. A further aspect of such analysis is evaluation of its sensitivity to possible errors in estimation of each or some of the critical variable. This information is very valuable and shall be provided in the capital investment proposal so as to give an overview of the impact of changes in the value of those variables, which form an essential part of the analysis, Harold Kerzner ( 1979).

For the purpose of carrying out the sensitivity analysis, it is utmost necessary in the first place to identify the important variables of the projects. These may be assumptions regarding incremental throughput/ sales, capital cost, operating cost, completion schedule, prices of various input/ output, reduction in tariff/ duty protection (partly/fully), Cenvat benefit etc. After identification of these important variables, sensitivity analysis shall be carried out to assess the impact of marginal changes in these variables on final results of the project i.e. MIRR/ NPV of the project, Seon-Gyoo Kim (2010).

MIRR/ NPV of the project shall also be computed on completion Project Cost basis, taking into account average rate of inflation in the following manner:

- Labor component of the project cost may be updated using the average (of 12 months) of Consumer Price Index (CPI) for industrial workers, Meredith and Mantel. (1989).
- For all other components of cost except labour the average (of 12 months of Whole Sale Price Index (WPI) for all commodities may be used.

With the help of the sensitivity analysis, it will be possible to identify the variables with high sensitivity and low sensitivity. The Capital Investment Proposal shall give the full details of these variables and their degree of sensitivity.

#### **Proposals Mooted on Strategic Consideration**

All project proposals should have base case MIRR at least meeting the Hurdle Rate. However, there may be proposals with MIRR less than the Hurdle Rate but recommended on strategic consideration. In such cases, sensitivity of MIRR by escalating the constant prices, in a limited way, as discussed below shall be presented:

- Inflows of first 5 years of operation shall be escalated by previous 3 years average annual increase in prices of products/ services, Hemanta Kumar Doloi (2010).
- Outflows of first 5 years on account of service components shall be escalated based on previous 3 years average annual increase in CPI for industrial workers.
- Outflows of first 5 years on account of materials/ spares, etc shall be escalated based on previous 3 years annual increase in WPI.

#### **Worst Case Scenario**

Scenario analysis gives us several different ‘scenarios’ or likely outcomes for our project. We can analyze what will happen if we have a best-case, worst-case and most-likely-case scenario. This measures the variability of the returns and can present us with a variety of situations and financial outcomes so that we are adequately prepared for each one. In scenario analysis we can change many variables and estimate a new outcome, Gulsah and Dikmen (2008).

#### **Other Risks**

Other risks constitute all those risks which may jeopardize success/ completion of the project. In case where need is other than profit, like operational necessity, Government policy, safety, environment etc. there is a risk to the fulfillment of the same. Following shall come under other risks:

- Risk in getting input/ linkage with input sources.
- Risk in disposing output/ linkage with market, downstream plants.
- Risk in obtaining statutory clearances and Risk in obtaining Government clearances.
- Risk in capacity utilization due to change in demand/ supply situation.
- Performance risk associated with a new technology.
- Risk of technology obsolescence and Risk worthiness of Technical collaborator.
- Safety risk associated with the selected technology.

Above risks shall be enumerated by the Project Authorities in Capital Investment Proposals, wherever applicable. The impact of risk shall be quantified as far as possible, otherwise qualitative information shall be given. Sensitivity analysis shall also be provided in case of capacity utilization etc.

#### **Risk Mitigation Measures**

The proposal should include the various risks associated with the project/ investment in achieving the desired results. There should be a mitigation plan for each of the risks identified and in case these plans entail further financial outflows, the same should be indicated, Henok and Hua (2009).

#### **Conclusion:**

It is evident from the title of the paper, this paper has been written to take care of all vital, critical points optimally needed to prepare a Proposal and Estimate for a mega project. We have tried to cover LSTK, Conventional, Hybrid, BOO basis estimates, various factors for project costing, financial viability/feasibility in terms NPV, MIRR so that it can be approved by the ministry & corporate boards with least difficulty/queries.

#### **References:**

- FL Harrison.(1985). “*Advanced Project Management*“.PP 79-115; Gower.
- Jack Loftus.(1999). “ *Project Management Of Multiple Projects And Contracts*“. PP 71-83; Thomas Telford.
- B.B. Goel.(1987). “*Project Management: A Development Perspective*“.PP 145-186; Deep & Deep Press.
- Harold Kerzner.( 1979). “*Project Management: A System Approach, Scheduling and Controlling*“.PP 169-236; Van Nostrand Reinhold Company.
- Jack R. Meredith, Samuel J. Mantel.(1989). “ *Project Management: A Managerial Approach*“. PP 327-359; John Wiley & Sons.
- Dennis Lock.(1987). *Project Management Handbook*. PP 83-104; Grower.
- Raymond J. Madachy.(1995). “ *Knowledge-Based Risk Assessment and Cost Estimation*“.PP 220-225. University of Southern California, Los Angeles, CA 90089-0781; and SoJb, vare Engineering Process Group, Litton Data Systems, Agoura Hills, CA 91376-6008.

Proceedings of National Conference: Advanced Structures, Materials and Methodology in Civil Engineering  
(ASMMCE – 2018), 03 - 04th November, 2018

PAPER CODE: C 505

Seon-Gyoo Kim.(2010). “A Risk Performance Measurement System for the Mega-Project“.PP 588-592; Kangwon National University, Chuncheon, Korea.

Henok Minas and Lang Hua Chiu.(2009). “The Distinct Characteristics and Strategic Impact of Emergent Projects in Large Organizations“PP 16-20. Master Thesis European Masters in Strategic Project Management.

Seon-Gyoo Kim.(2010). “Risk Performance Indexes And Measurement Systems For Mega Construction Projects“.; Division of Architecture Vol 12, Kangwon National University, Chuncheon, Korea.

Hemanta Kumar Doloi. (2010).” *Understanding stakeholders' perspective of cost estimation in project management*”. International Journal of Project Management 29 (2011) 622–636.

Gulsah Fidah, Irem Dikmen.(2008).” A Risk And Vulnerability Ontology For Construction Projects.”PP 4-13.American Society of Civil Engineering.



## A Review on Structural Health Monitoring Using Piezoelectric Transducers

Avadhesh Sharma<sup>1</sup>, Awdhesh Kumar<sup>2</sup> and Harshit Varshney<sup>3</sup>

<sup>1</sup>Assistant Professor, Department of Applied Science, Invertis University, Bareilly (U.P.), avadhesh.s@invertis.org, Corresponding Author

<sup>2</sup>M.Tech First Year (Civil Engineering), Rajshree Institute of Management and Technology, Bareilly (U.P.), er.awd.civil@gmail.com

<sup>3</sup>Assistant Professor, Department of Civil Engineering, Rajshree Institute of Management and Technology, Bareilly (U.P.), harshit.civil@gmail.com

### Abstract

The paper presents a review of non-destructive smart structural health monitoring using piezoelectric transducers. It is possible to detect and repair using these smart materials the probable failure zone of a loaded structure specially the linear crack openings in significant hydraulic structures by employing efficient sensing systems based on piezoelectric transducers. This system works as embedded intelligence facilitating real time monitoring of structures, considering the problem of structure failure during after disaster phase paper also enquire about the complex damage assessment during post disaster period in a structure due to various catastrophic natural (seismic vibrations, wind load impact etc.) and anthropogenic (vibrations due to machine operations, various explosion etc.) calamities by using piezoelectric properties of material, piezoelectric materials as ceramics, polymers and composites presenting a promising solution that can contribute in a more diverse way in preventing huge losses of valuable property and human life.

**KEYWORDS-** *Structural, Health Monitoring, Piezoelectric, Transducers, Sensor, Piezoelectricity*

### INTRODUCTION

With increased trend of urbanization all over the globe construction industry took a significant boost during last few decades; with enhanced technology and market demand every day structures are going to be more complex day by day. In view of this scenario structure stability and safety becomes a challenging area. Significant structures like skyscrapers, dams and nuclear reactors needs a continuous monitoring as they affect a huge population and region in case of failure with an irreversible damage potential. These massive structures are difficult to monitor merely with implementing traditional approach since even a micro crack may cause severe radiation leak or creation of failure environment on site. Here we require a reliable and 24x7 hours real time monitoring mechanism which can enable us to access the entire structure assembly as well as its components against various cause of damage (natural as well as anthropogenic), so that necessary preventive measures shall be adopted before it's too late. Early damage detection saves loss of life and property. The state of the structure must remain in the domain specified in the design.

A structure failure is actually a step wise process that initiates from some initial stage. Long term damage accumulation increases the possibility of failure. And if it is not assisted well within the stipulated time then structure will certainly go out of order from the domain specified in the design. Therefore an effective and efficient monitoring system is inescapable for ensuring the integrity of structure safety.

There are several methods available for structural health monitoring such as impedance based structural monitoring, data fusion techniques, vibration control and wireless based structural monitoring etc. Structural health monitoring is not a new need for identification of cracks in buildings and hydraulic structures rather it has been practised from many centuries using various techniques. Qualitative and non-continuous methods have long been used to evaluate structures for their capacity to serve their intended purpose. For example, since the beginning of the 19th century, railroad wheel-tappers have used the sound of a hammer striking the train wheel to evaluate if damage was present. see **Fig.1**

### SENSOR BASED CONCEPT OF STRUCTURAL HEALTH MONITORING (SHM)

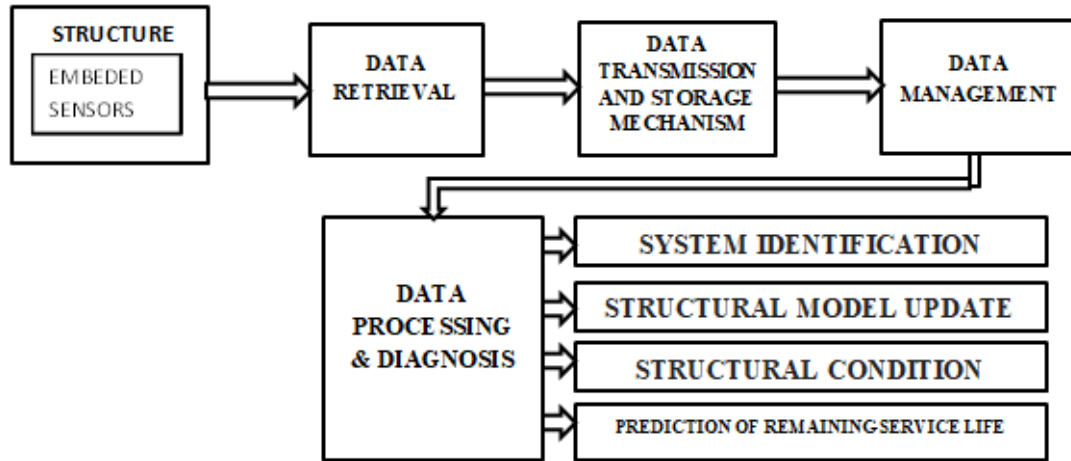


**Fig.1 Process flow of SHM**

#### **PIEZOELECTRIC MATERIALS:**

Although piezoelectric materials have been known for more than a century, the materials have gained importance over the last few decades because of their high potential as smart materials. The materials have inherent transducer characteristics, being capable of both sensing and actuation. They convert mechanical energy into electrical energy, which makes them useful as sensitive sensors of mechanical inputs such as pressure, strain, vibration, rotation, sound, ultrasound etc. They also convert electrical energy to mechanical energy, which makes them useful as actuators.

#### **Piezoelectric effect:**

The phenomenon of piezoelectricity was discovered as early as 1880 in a single crystal of quartz by Pierre and Jacques Curie. They found that on application of pressure certain crystals like quartz or ceramic, an electric voltage develops across the material. The piezoelectric effect is due to the asymmetry in the crystalline structure. This allows the ions to move along one axis than the others. When a mechanical stress is applied, each side of the crystal acquires opposite charges leading to a voltage drop across the crystal. This effect is linear and the voltage disappears when the mechanical or heat stress is removed.

They later reported piezoelectric behaviour in other materials such as Rochelle, salt, tourmaline and Topaz. The discovery of ferroelectric ceramics barium titanate and zirconate titanate (PZT) during the 1940s and 1950s led to a spate of research activities on these materials. Over the years a wide variety of transducers, sensors and actuators have been developed using the ceramic PZT, which is one of the most sensitive piezoelectric material, another important piezoelectric material that created a lot of interest is the polymer polyvinylidene fluoride (PVDF), which was discovered in 1969. A polymer exhibiting transducer characteristics has special advantages over the ceramics because of the more flexible and less brittle nature of polymers. **See Fig. 2**

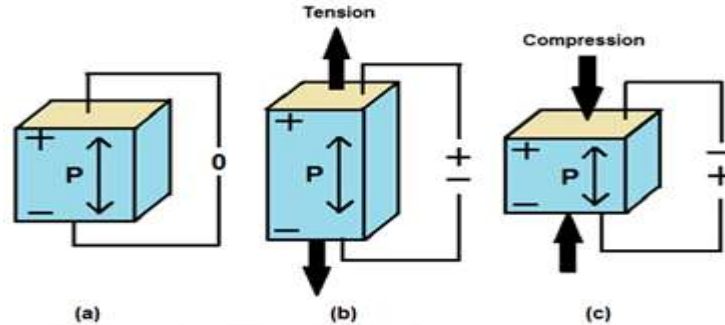


*Fig 2 Piezoelectric Effect*

### **STRUCTURAL HEALTH MONITORING USING PIEZO ELECTRIC MATERIALS-**

With all round development of science nowadays fusion of different disciplines opening the way for enhancing the problem handling ability including structural health monitoring, Civionics is such kind of fusion that redefining the meaning of modern structural Health Monitoring and asset management ,it's is the combination of civil engineering with electronics engineering It involves the integration of sensors, possibly smart materials, data transmission, computational power, and processing ability inside the structures that facilitate the automatic deformation monitoring , Sensor-Driven Predictive Analysis of structure emerges as the boon for deriving optimal repair programme and framing disaster management strategies, Nuclear power plants ,railway bridges ,skyscrapers ,buildings and pipelines can be enabled with piezo electric sensors who respond quickly when subjected to any stress on them and produce a continuous deformation monitoring of structures during the entire life of the structure, early detection of failure roots prevents abrupt failure and make it convenient to prevent or mitigate the damage.In Greece, Rio–Antirrio bridge using sensor based technology and here real time monitoring of structure and traffic is performed on real time basis, next in USA Huey P Long bridge where over eight hundred static and dynamic strain gauges are specially designed to measure axial and bending load effects, in continuation the foundation and column of Masjid al-Haram, Mecca, Saudi Arabia are equipped with more than six hundred sensors (Concrete pressure cell, Embedment type strain gauge, Sister bar strain gauge, etc.)There are various types as Mechanical, optical and electrical strain sensors are available now that use different methods of strain measurement for example a slide caliper is a Mechanical strain sensor, which is simple but generally have poor resolution. A device with levers to amplify strain to readable values can be devised, but it is prohibitively large. Optical sensors are typically costly and too delicate to be densely deployed on civil infrastructure. Electrical sensors, which include the piezoelectric sensor, semiconductor strain gage, and the widely used foil strain gage), have high resolution and are small, sturdy, and inexpensive. Thus, they are good candidates for developing a wireless strain sensor. other than Impedance based SHM techniques where Working principle is supplying electricity power, sensing through PZT patches, hence through the help of signature obtained, we can able to detect, monitor and giving the best solution option. There are several other techniques such as data fusion techniques in which used principle is same as in Impedance based approach but in this process of integrating data and knowledge representing the same real world object in consistent, accurate, and useful representation. Situation awareness, user refinement, and mission management, Finally finding root-mean-square deviation (RMSD) is the way of detection defect/fault , vibration control technique Mostly used technique from ancient time, is depends on Vibration applied from the sensors, Damping, and signature getting from system. Difference shown in signature through system can help to predict the defect/risk zone on the structure. Care should be taken in it, due to vibration structure may further damage, acoustics emission (AE) technique Used to diagnostic of overall structural integrity, detection, location, identification and assessment of flaws/faults. It is continuous or periodic monitoring used in wireless and wired technology. In this echo of sound is measured and smart sensor wireless technology.

## **DISASTER MANAGEMENT USING PIEZOMETRIC MATERIALS-**

Prevention of Huge destruction and loss of life is possible by developing effective and quick responsive early warning system, piezoelectric based sensors respond on stress variation that become abrupt during the pre-shock stage of the earthquake, these signals trigger the alarm and would allow businesses, residents and public agencies time to get ready against the main shock.

### **Earthquake sensor technology and piezoelectric material-**

Piezoelectric materials also used for designing a sound alarm certain piezoelectric materials as Lead Zirconate crystals present in the piezoelement can readily store current and can release the current when the orientations of the crystals are disturbed through mechanical vibrations. Signals from the piezoelectric material is amplified by an electronic scheme and high output is generated this high output is used to sound alarm and to light LED. [6] By embedding high precision sensors it is possible to detect weak ground movements Also, the sensors need to be installed in the correct orientation to perfectly detect the ground motion, and hence the alignment of the sensor is a factor that needs critical thinking. To detect the ground motion in the low frequency range, the system uses micro electro mechanical and piezoelectric system sensors.

The Micro-Electro-Mechanical Systems (MEMS) sensor is a high precision, digital 3-axis silicon accelerometer with an excellent sensitivity of 0.0039g/LSB, and similar models of these sensors are widely used in contemporary smart phones. The sensitivity of this sensor is superlative for detecting an earthquake of magnitude M 4.0 or higher which corresponds to peak ground acceleration. The second sensor is a piezoelectric sensor, which is a piezo film element laminated to a sheet of polyester (Mylar). It can produce a useable electrical signal output when forces (in this case ground movement) are applied to the sensing area. To fit this sensor in the design, a charge amplifier is incorporated that can detect ground movement in the frequency band [0.075-3] Hz. The output of this charge amplifier is limited to safe voltage levels. The piezo film sensor's response can be adjusted by adding test mass at the tip of the sensor. As test masses are added, the baseline sensitivity of the piezo film sensor increases. [7, 8]

## **CONCLUSION-**

After reviewing the existing literature there accessed a wide potential of piezoelectric material as a smart material in structural health monitoring also its application not only limited as sensors and actuators in a smart structural system, but also to dampers. A study on piezoelectric material also proposed a conceptual design for a smart structural system that uses Smart materials, and described how the innate performance of piezoelectric materials, called smart Materials, can be used to make actuators, sensors, and dampers. [9, 10]As a key element it can contribute in designing next generation early warning systems to detect and warn against pre shocks and seismic data acquisition, though there are many challenges yet to be deal as how to eliminate false input by creating algorithms that can differentiate between real and false seismic activity signals so that it become more reliable in future, moreover its sensitivity towards strain variations can detect the possible failure zone so huge loss of property and life can be prevented as per forewarned is forearmed concept.

## **REFERENCES-**

1. Dawson, Brian (1976), "Vibration Condition Monitoring Techniques For Rotating Machinery". The Shock And Vibration Digest (London: Springerlink) 8 (12): 3
2. Vijaya M.S. (2012), "*Piezoelectric Materials and Devices: Applications in Engineering and Medical Sciences.*" CRC Press Taylor and Francis group.
3. Nagayama, T. and Spencer, B.F. (2007), "Structural Health Monitoring Using Smart Sensors". Department Of Civil And Environmental Engineering, University Of Illinois At Urbana-Champaign
4. Dhakal, D.R., Neupane, K., Thapa, C and Ramanjaneyulu, G. V. (2013), "Different Techniques Of Structural Health Monitoring". *International Journal Of Civil, Structural, Environmental And Infrastructure Engineering Research And Development*, 3(2), 55-66
5. Kamble, P.P. (2007), "Wireless Sensor Networks For Earthquake Detection And Damage Mitigation System". *International Journal Of Innovative Research In Computer And Communication Engineering*, 4(3), 6209-6214.

6. Kitagawa, Y., Tamai, H Masaki. (2004), “Characterstics of piezoelectric Dampers & their application to tall buildings as a smart structural system”. 13th World Conference on Earthquake Engineering Vancouver, Canada August 1-6.
7. Kitagawa.Y, Tamai.H and Takeshita. M. (2000), “Smart Structural Systems For Exposed To External Disturbances –Concept And Technology”, 12th World Conference on Earthquake Engineering Auckland, New Zealand, Jan 30 – Feb 04.
8. Chung-Bang Yun And Jiyoung Min (2011), “Smart Sensing, Monitoring, And Damage Detection For Civil Infrastructures”, *KSCE Journal Of Civil Engineering*, 15(1):1-14
9. Blasch, E., Kadar, I., Salerno, J., Kokar, M., Dase, S., Powell, G., Corkill, D and Euspinni (2006), “Issues And Challenges In Situation Assessment”., *Defence and Security Analysis*, DOI: 10.1117/12.669779.



## AFFORDABLE HOUSING SOLUTION USING LEAN CONSTRUCTION TECHNIQUES

## Hamdaan Ansari<sup>1</sup>, R. B. Magar<sup>2</sup>, A. R. Honnutagi<sup>3</sup>, Fauwaz Parkar<sup>4</sup>

<sup>1</sup>Research Graduate, Department of Civil Engineering, Anjuman-I-Islam's Kalsekar Technical Campus, New Panvel;  
ansarihamdaan0@gmail.com:

<sup>2</sup>Professor and H.O.D, Department of Civil Engineering, Anjuman-I-Islam's Kalsekar Technical Campus, New Panvel;  
rajendramagar69@gmail.com, Corresponding Author

<sup>3</sup>Director, Anjuman-I-Islam's Kalsekar Technical Campus, New Panvel; director.aiktc@gmail.com

<sup>4</sup>Assistant Professor, Department of Civil Engineering, Anjuman-I-Islam's Kalsekar Technical Campus, New Panvel;  
[fouazfn@rediffmail.com](mailto:fouazfn@rediffmail.com):

### ABSTRACT

The population distribution of India is not uniform. People migrate to urban areas in search of better livelihood, healthcare, education etc. In India, almost half of the population lives in urban areas. Concentration of people in urban areas leads to severe land shortage and housing shortfall. There is an urgent need for low-cost housing to be constructed that is affordable to low-income groups of the society. On the other hand, due to increased competition and decline in profit margins in construction projects, the construction community is finding ways of eliminating wastes and increasing profit. This is exceptionally more critical under the current financial crisis and economic recession. Lean techniques, which are successfully utilized in manufacturing industry offer the promise to minimize wastage of materials and eliminate non-value adding work. This work is aimed at testing the Last Planner system, a lean technique for delivering affordable homes for the economically weaker sections of the society. The results show an astounding 38% decrease in construction time, 11% decrease in material wastage, 12% decrease in construction cost and better finished quality. The work concludes that lean techniques have the potential to optimize construction project duration and cost, which will ultimately lead to constructing affordable housing projects, without compromising on quality.

**KEYWORDS:** *Affordable Housing; Economically weaker sections; Housing Shortfall; Last Planner System; Lean Construction Techniques; Low-cost Housing; Population Distribution.*

### INTRODUCTION

International human rights law recognizes everyone's right to an acceptable standard of living, including adequate housing. Despite the fundamental place of this right within the international legal system, it is estimated that 828 million people from developing countries live in slums and sub-standard housing (Al-Saadi and Abdou, 2016). Consequently, accommodating people from the low-income group poses a significant challenge to developing countries during their urbanization. To address this issue, affordable housing has become the top priority of many governments in a bid to improve the living conditions of low-income households.

On the other hand, the construction industry goes through decrease in profit margins every year, due to the competition, the resources prices and other economic issues, as fees and taxes. This implies that the Construction Industry needs to improve managerial tools and reach adequate levels of efficiency and productivity to remain profitable (Reinbold, 2016). The construction of affordable housing is generally linked with lack of quality and non-profitable work for the developers. It is because of this reason that Private sector is reluctant to invest in the affordable housing sector. They target the middle-income group and high-income group due to more profit in respective sectors. The low-income group is left at the mercy of the government and the NGOs for housing. Many researches have indicated that Lean Techniques improve the efficiency of construction processes. There is a

tremendous scope for testing the utility of Lean Techniques in the construction of an affordable housing project. Lean Techniques, if appropriately applied, are bound to improve the construction processes and help in bringing down overall cost of the project. This will create a win-win situation for both, the developer- who shall make substantial profit, and the needy population- who shall get affordable low-cost housing.

Sivam and Karuppanan (2002) reviewed the role of the state, the market and non-governmental organizations (NGOs) in the provision of housing for low-income groups. It is found that formal housing agencies in both the public and the private sector are neither building fast enough to meet demand nor cheaply enough to reach the poor. Therefore, an informal sector has emerged in almost all cities in India. Gandhi (2012) stated that with increasing concentration of economic and commercial activities, rapid economic growth and influx of population in Indian cities, the pressure on affordable housing delivery is mounting, resulting in proliferation of slums. Gopalan and Venkataraman (2015) encouraged the government to provide incentives to private developers to develop affordable housing projects. Nair *et al.* (2015) stressed the need for including mass housing zones in city plans. Needham (2016) concluded that the involvement of private developers can help solve the problem of affordable housing. Ram (2016) stated that one way of improving housing for the poor households is that commercial developers build simple and decent housing for sale at prices which many of those household could afford. The author suggested that if certain constraints were to be lifted, developers would build such housing commercially.

Beary (2005) concluded that lean construction is a powerful tool which can improve any process. Their research was based on lean construction production planning concepts. Interviews with professionals from the homebuilding industry were conducted to study the prevalent practices, analyze the data and find areas of improvement. Bayfield and Roberts (2005) revealed how implementing Lean Techniques in the construction of Honda's New European plant has been rewarded with a construction cost of only 701 pound/sq.m. – 40% improvement on the cost of previous plant at Swindon and completed 9 years earlier (1173 pounds/sq.m., built virtually identical on the same site in Swindon). Fernandez (2009) suggested Lean theory for improving the productivity of construction process, underlining the fact that construction productivity lags behind that of the manufacturing; a crisis or a pre-crisis state that exists in the construction industry. To increase productivity, one should eliminate variation and the cause of variation. A systematic change must be achieved for eliminating the root cause of problems.

Mossman (2009) concluded that better quality of product was achieved by incorporating lean techniques in the construction process. As per studies on 9 industrialized housing plans to incorporate lean construction methods in their operation carried out by manufactured housing research alliance, it was revealed that lean implementations resulted in significant improvement in product quality by means of waste reduction-12% production place reduction, 10% Raw material damage reduction and 28% labor reduction. Nahmens and Ikuma (2009) have found out that lean based tools like Last-Planner System (LPS) reduced accident rates: crew that use lean construction tools, including Last Planner, had about 45% lower accident rates than crews in the same company performing similar work, but not using such tools. Court *et al.* (2009) concluded that creating value for customers and end users – is likely to result in more effective waste elimination and lead to more satisfied customers. Pastana and Gambatese (2016) concluded that Value Stream Mapping, a lean technique reduces frequent drawing revisions and rework at site. Ahuja (2016) concluded that Increased Visualization, a lean technique reduces chances of accidents on site. Reinbold (2017) concluded that Daily Huddle Meetings leads to better communication between workers on construction site. Hosseini *et al.* (2017) concluded that waste in the construction industry has been the subject of several researches around the world. Researchers implement different methods to reduce the amount of waste in the construction industry. One of the effective methods to reduce construction waste is the application of lean approach to the construction industry.

## METHODOLOGY

There will be four phases of this work. Fig. 1 shows the flow diagram adopted for study.

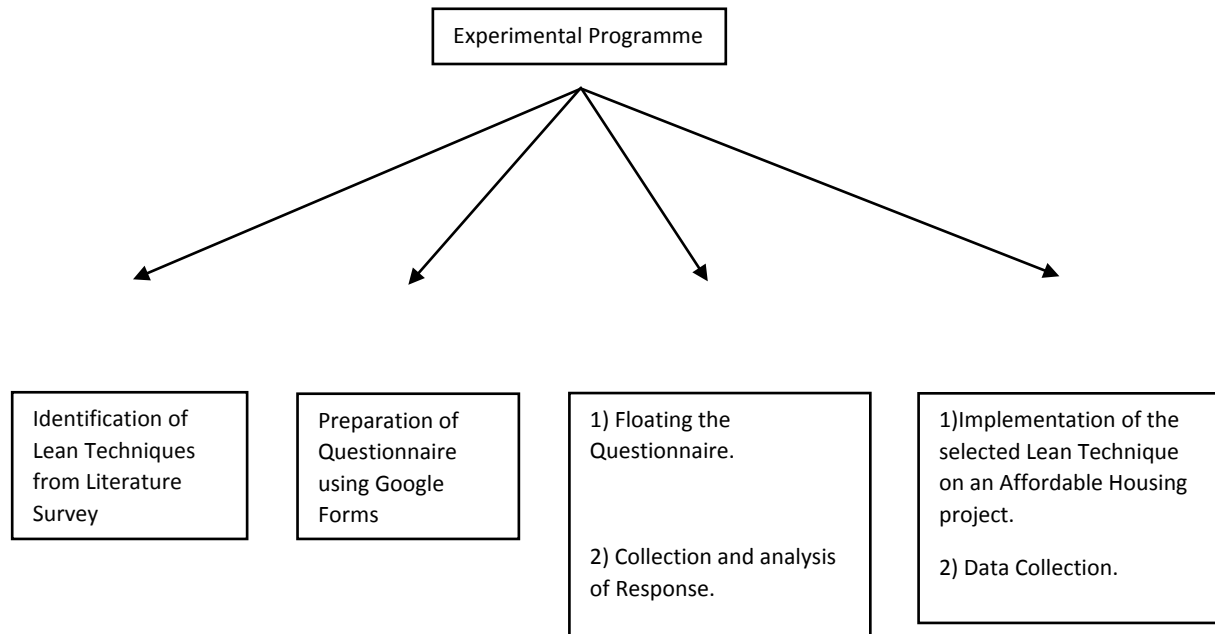


**Fig 1. Flow Diagram for Experimental Programme**

**Phase I** - Lean Techniques that have proven to improve the construction process were identified from Literature Survey. These include The Last Planner System, Increased Visualization, Work Standardization, Fail Safe for Quality, Just In Time (JIT), Kaizen, Value Stream Mapping, The Five S's, Total Quality Management, First Run Studies, Poka-Yoke and Daily Huddle Meetings.

**Phase II** – A Questionnaire based on the identified techniques was prepared using Google Forms. The first part of the questionnaire was related to personal and professional details of the respondents. In the second part, respondents were asked to rate Lean Techniques on a 5-point Likert's scale given below.

(1) =Technique Not Effective; (2) = Technique Less Effective; (3) = Effective Technique; (4) = Highly Effective Technique; (5) = Extremely Effective Technique.

**Phase III** – Google Forms was used to float the questionnaire in the Construction industry and collect the responses. The questionnaire targeted a sample audience of one hundred respondents, out of which sixty-seven responses were received, giving a response rate of 67%. Table 1 shows the response rate.

**Table 1. Response Rate**

Kind of survey	Targeted Respondents	Response	No-response	Percentage of Response
Questionnaire	100	67	33	67%

38% of the respondents were from a Client firm, followed by Contractor 23%, Architect 17% and the remaining 22% of respondents were from a Consultant firm. Fig. 2 shows the background of respondents.

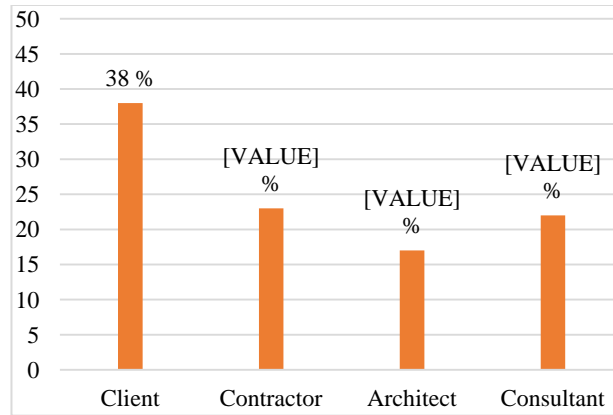


**Fig 2. Background of Respondents**

The Questionnaires were issued to professionals who hold positions in the organization such as: Senior Engineer, Architect, Project Manager and General Manager. A majority of respondents i.e. 55% had work experience of upto 7 years. 31% of respondents had work experience of upto 14 years. 6% of respondents fell into 15-20 years work experience category and 8% of respondents had work experience upwards of 21 years. Fig. 3 shows work experience of respondents.

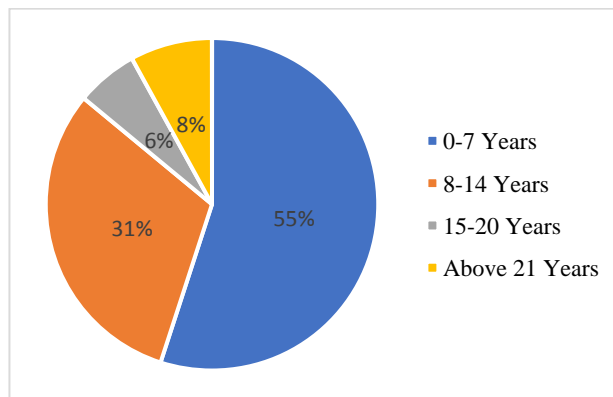


**Fig 3. Work Experience of Respondents**

The response from questionnaire was analyzed using Relative Importance Index (RII) method. The Relative Importance Index (RII) was computed using the formula given in Eq.1.

$$RII = \frac{\sum W}{A * N} = \frac{5n5 + 4n4 + 3n3 + 2n2 + 1n1}{5 * n} \quad \text{Eq. (1)}$$

W = weighting given to each factor by the respondent, ranging from 1 to 5, (n1= not effective, n2= less effective, n3= effective, n4= highly effective, n5= extremely effective). “A” is the highest weight (i.e. 5 in the study) and N is the total number of samples. The relative importance index ranges from 0 to 1. (Tam and Le, 2006). Lean techniques are then ranked on the basis of Relative Importance Index (RII). Table 2 shows the Relative Importance Index (RII) of Lean Techniques.

**Table 2. Relative Importance Index (RII) of Lean Techniques**

Lean Techniques	RII score	Rank
Last Planner System	0.72	1
Daily Huddle Meetings	0.644	2
Increased Visualization	0.634	3
Fail Safe for Quality	0.62	4
Kaizen	0.615	5
Just in Time	0.61	6
The 5 's	0.6	7
Poke Yoke	0.6	8
Concurrent Engineering	0.59	9
Value Stream Mapping	0.59	10
Total Quality Management	0.586	11
Integrated Project Delivery	0.58	12
Re- Engineering	0.57	13
Work Standardization	0.57	14
First Run Studies	0.56	15

The **Last Planner System** had the highest Relative Importance Index (RII) (**0.72**) (**1<sup>st</sup> Rank**) and was selected to be implemented on site.

**Phase IV- The Last Planner System**

One of the most effective ways to increase efficiency of the construction process is the Last Planner System. Mossman (2009) defined the last planner as a system for collaboratively managing the network of relationship and conversations required for program coordination and project delivery, by promoting conversations between trade foreman and site management at appropriate levels of detail before issue become critical. Last Planner System aims to shift the focus of control from the workers to the flow of work that links them together. Fig. 4 shows the components of the Last Planner System.

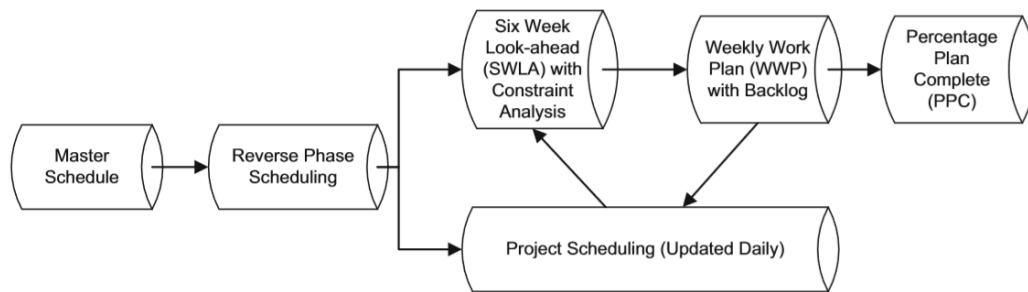


**Fig. 4 Schematic Representation of the Last Planner System (Source: Kovvuri et al. 2016)**

**Master Schedule**

The Master Plan is the complete project schedule, with milestones, that is usually produced for use in the bid package. It brings out duration of key activities in sequence. Phase Schedule is produced based on this Master schedule.

### Phase Schedule

Second stage of phase planning breaks down the master plan into major phases, each about 18 weeks. In phase schedule, detailing of work is done and trade wise goals are created, which are then monitored as milestones. It connects the master plan to the six-week look-ahead planning stage. The phase schedule is developed by a team consisting of all the last planners. Last Planners are the trade foreman and site supervisors who execute the work on site. It is closer to reality than the master schedule. Microsoft Project software was used to develop the phase schedule. Fig. 5 shows the phase schedule.

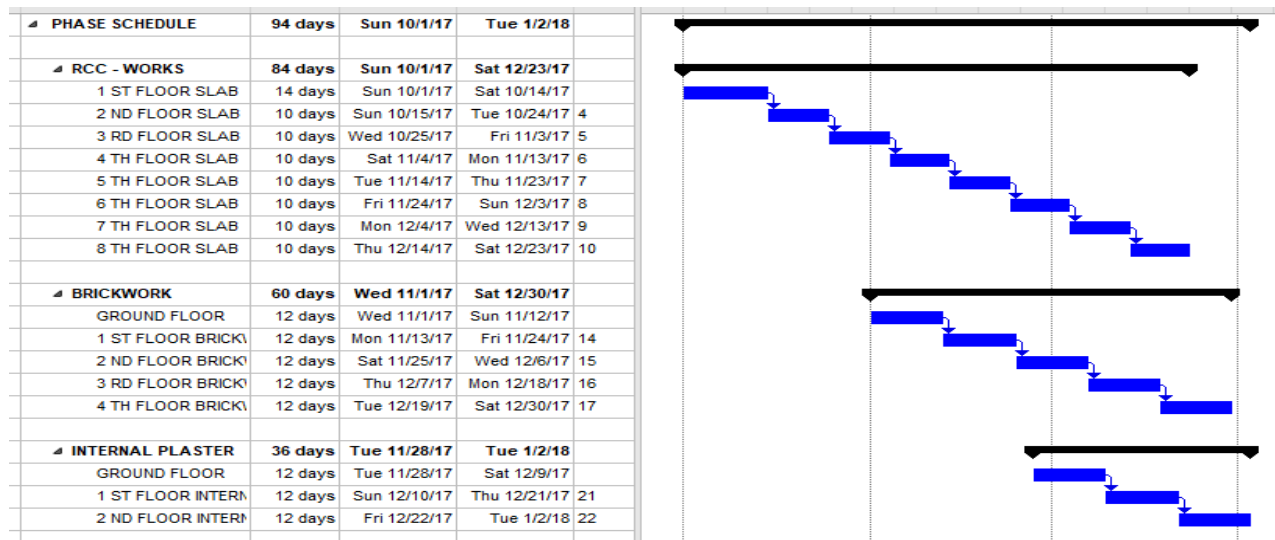


Fig. 5 Phase Schedule

### Six Week Look-ahead (SWLA)

Six Week Look-ahead connects the works to be undertaken on the site over the short term. The focus is shifted to making resources ready for the anticipated tasks, phasing out constraints for smoother workflow. Six Week Look-ahead is a tool to control workflow, acting as link between phase schedule and weekly work plans. The duration of look-ahead schedule is usually 6-week time frame. Constraint identification is done to make the tasks ready for execution ensuring that the necessary materials, machinery and information are available on time. The number of people involved in preparing these look-ahead plans should be as high as possible as a single person cannot identify all constraints in a construction project.

### Weekly Work Plan (WWP)

The look ahead planning trickles down to the fourth element of weekly work plan where last planners at site, who are usually the foremen or supervisors, promise to deliver work found achievable in the coming week. Tasks are entered into the weekly work plan only after resolving all the identified constraints. The key terms in the weekly work plan are 'Should', 'Can' and 'Will'. 'Should' indicates works to be done according to the look-ahead schedule. 'Can' indicates the work which can be achieved due to removal of various constraints. Upon considering all constraints, the works committed by last planners are then indicated by 'Will'.

### Percent Plan Complete (PPC)

The measurement metric of the Last Planner System is Percent Plan Complete (PPC). It is calculated as the number of activities that are completed as planned divided by the total number of planned activities. A note explaining the reasons justifies any work that had been planned but was not completed. Eq. (2) gives the P.P.C formula.

$$\text{Percent Plan Complete (P.P.C)} = \frac{\text{Number of Activities Completed}}{\text{Number of Activities Planned}} \quad \text{Eq. 2}$$

When the PPC is calculated, a re-programming of the services is made, indicating the services that had already been executed and those that had been planned but were not executed. It helps us to keep track of our project.

### CASE STUDY

The purpose of this work is to establish the suitability and benefits of the Last Planner System for the construction of low-cost housing. The belief that Indian construction projects and project teams are culturally different to the ones where lean principles have been successfully adopted had to be challenged. In this research a genuine implementation of the Last Planner System was conducted to answer some of these unanswered questions. It was decided to implement the Last Planner System on an affordable housing project. Many projects were short-listed for the implementation, project Goorishina was finally selected as it was found to be most suitable. It is an Affordable Housing Project by Prime Developers. Figure 6 shows layout plan of site.

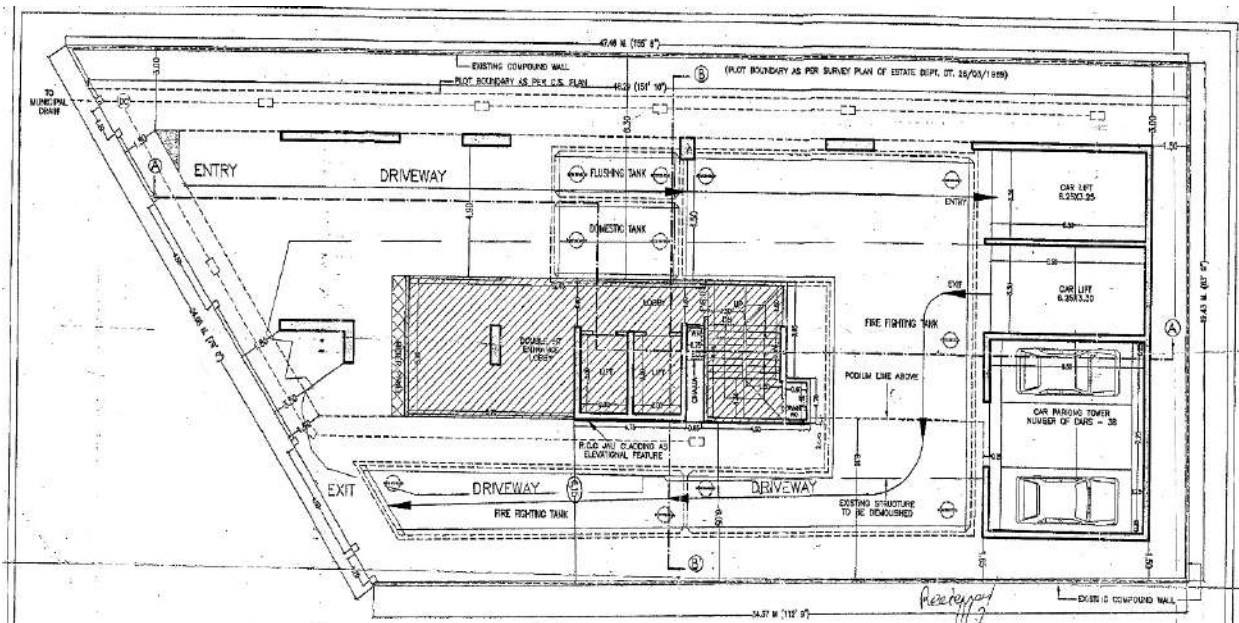


Fig. 6 Layout plan of site

Prior to the implementation of the Last Planner System the researcher calculated and analyzed PPC values for a period of ten weeks. Data from the project site was gathered and percentage of tasks delivered in a week to that planned for that given week was calculated.

The implementation of Last Planner System started when the researcher positioned himself on the site as part of project planning and monitoring team. The Master Schedule prepared for the project after identification of various milestones based on contract agreement at the starting of the project, itself became a key source for Last Planner System implementation. The Last Planner System was eventually implemented in close collaboration with the project team. The researcher remained embedded in the project team and conducted many formal and informal interactions to explain, learn and discuss issues surrounding the LPS implementation. Initially there were some

difficulties faced in implementing the Last Planner System. People were not aware of the concepts. They were used to the traditional process of construction. The Project Manager doubted whether his abilities were being questioned and showed little interest. The contractor took it as interference in his work. Such issues were tackled through convincing and educating.

Extensive data collection took place during the implementation phase. Look-ahead plans were prepared based on the current status and the activities to be executed during the next 6 weeks were broken down into sub-parts. Look-ahead plan was updated at the end of each week. Whenever an activity entered the last window of look-ahead plan it was broken down into sub-activities. Constraint analysis was carried out for the activities that entered into the last window of look-ahead plan. The planning team ensured the commitments using constraint analysis, prepared weekly plan and finally a check was made by the site in-charge. At the end of each week PPC values were calculated. The reasons for failure in activities committed was analyzed using daily progress reports and by taking feedback from the site engineers.

## RESULT

Before implementation of the last planner system, P.P.C was an average 54% only. Many reasons were observed on site, which can be attributed to such low P.P.C values. It was observed that there was lack of communication between different trades involved in the execution and planning. Foremen and labours complained that they were not involved in the planning process. Planning was done by planning engineers who were not fully aware of practical difficulties and local issues at the construction site. There were frequent quarrels and blame gaming among various teams of carpenters, fitters, labours, plumbers, electrical contractor, etc. There were frequent revision in drawings and a lot of rework. Waiting time for materials, equipments and drawings were quite high. There was lot of unnecessary movement of labours, materials and equipments on site. After implementation of the Last Planner System, efficiency of construction process started to improve. Figure 7 shows graphically, improvement in Percent Plan Complete (PPC) values after implementation of the Last Planner System.

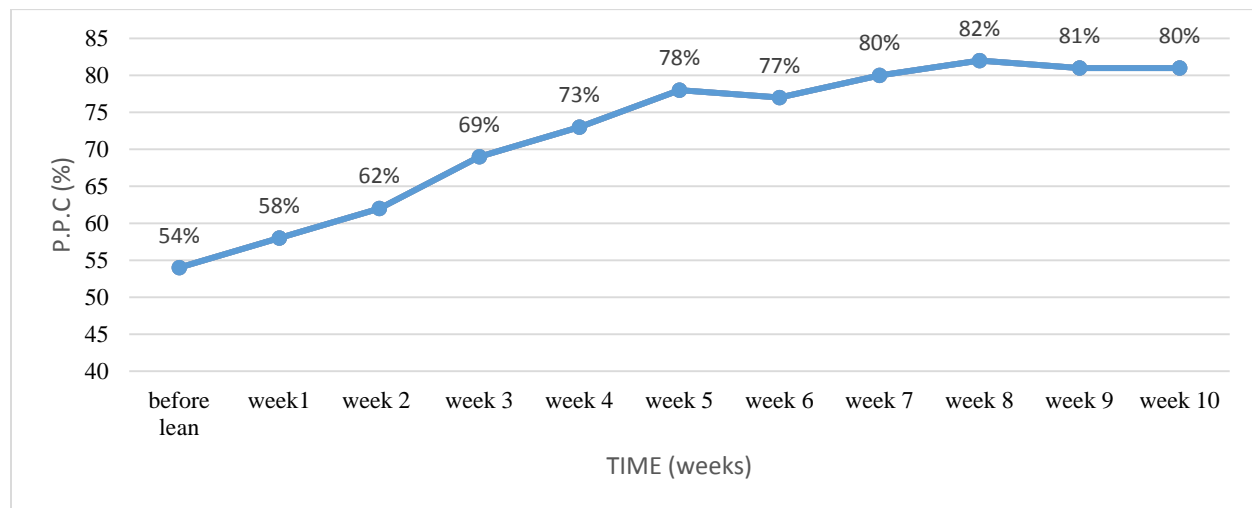


**Fig 7. Graphical Representation of P.P.C**

Percent Plan Complete (P.P.C) values started to increase, from 54% of PPC value before lean implementation, it increased to 58% in first week itself. From 58% it further increased to 62% in second week. It kept on increasing till an average 80% of P.P.C values was achieved by tenth week. It was observed that after implementation of the Last Planner System communication among different construction teams involved in project execution started to rise. A spirit of teamwork and camaraderie could be felt among the workers. There was less finger-pointing and blame-gaming among different trades involved in project execution. Quality of finished product was better than expected. There were less revision of drawings and therefore less reworks.

At 54% PPC values before Last Planner implementation, it would have taken 36 months to complete the project. After implementation of the Last Planner System, P.P.C values rose to an average 80%. At this pace the project would get completed in 25 months. That is 38% reduction in construction time. Figure 8 shows the time comparison.

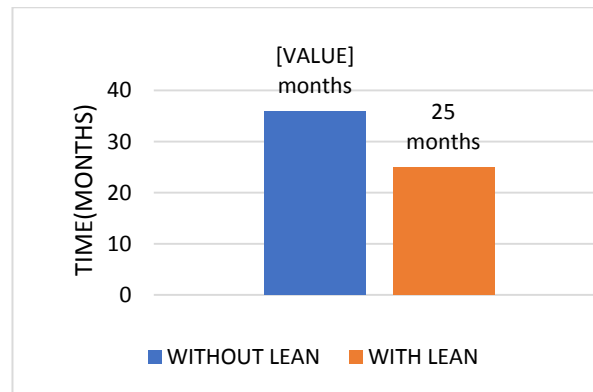


**Fig 8. Time Comparison**

It was observed that, after implementation of the Last Planner System there was substantial reduction of material waste produced on site. Wastage of steel decreased by 10%, cement by 13%, shuttering by 11%, besides other materials such as siporex block, sand, aggregates etc. Considering decrease in wastage of material and time, there will be cost savings of Rs 1.75 crores in construction cost. Earlier, estimated cost of construction was 18.91 crores. Now that has been reduced to Rs 17.15 crores. That is 12% reduction in construction cost of the project. Figure 9 shows cost comparison.

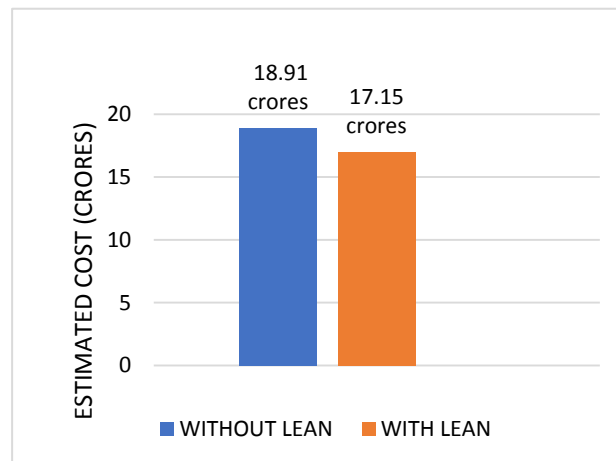


**Fig 9. Cost Comparison**

## CONCLUSION

This study identified and tested effectiveness of the Last Planner System, a lean construction tool in construction of an affordable housing project. Last Planner System carries along effective relationship which forms pillar of a stabilized project-based system that the tool promotes. Implementation of the new tool on an affordable housing project progressed through a learning curve which eventually resulted in generating value.

The tool proved to be successful in reducing wastage of materials, time and other resources. An organization involved in testing and implementing lean concepts in construction project management would benefit in terms of

reduced duration and cost savings. Better communication among different construction teams and a spirit of teamwork among workers was achieved from Last Planner System implementation. Initially some difficulties were faced in implementing Last Planner System, but that was tackled by convincing and discussing issues surrounding the Last Planner System implementation. Also, providing training and education to employees is a key to successfully gain benefits of Lean Construction tools. The Last Planner System was successfully integrated into the traditional construction process. This eliminates the belief that Lean Concepts are not suitable in the Indian Context. With increase in profit, it is expected that private developers would get attracted towards affordable housing segment and it would help in solving the problem of housing shortage. The study recommends that government should provide incentives to developers to build such projects.

## REFERENCES

- Ahuja Y., (2016), "Effective Utilization of Lean Management in Construction Industry", Intl Journal of Engineering and Innovative Technology (IJEIT) Volume 3, Issue 12, pp.29-33.
- Al-Saadi R., Abdou A. (2016). "Factors critical for the success of public-private partnerships in UAE infrastructure projects: experts' perception". International Journal of Construction Management, Volume 16, 2016 Issue 3, pp 234-248.
- Ballard G., (2008), " The Lean Project Delivery System: An Update", Journal of Construction Engineering and Management, Vol. 137, No.10, pp. 740-744.
- Bayfield R., and Roberts P., (2005). "Contract or Cooperation: Insights from beyond construction collaboration- The Honda experience". Lean Construction Journal, October 2005, Vol 2, Issue 3, pp 14-28.
- Beary P., (2005), "Bridging the Gaps – Towards a Comprehensive Understanding of Lean Construction", Proceedings of the 10th annual conference in the International Group for Lean Construction.
- Court F., P., Pasquire C. and Gibb A., (2009). "A Lean and agile construction system has a set of counter measures to improve health, safety and productivity in civil construction", Lean Construction Journal, pp 61-76.
- Chen K., Bing L., and Liu P, (2015), "Designing Affordable Housing towards sustainability standards", Conference: Housing- A Critical Perspective, Architecture MPS: Liverpool, Liverpool John Moores University, Liverpool: 08-09 April 2015.
- Fernandez S., (2009) "An Application of Poppers Method of conjectures and refutations to critique of emerging construction theories", Lean Construction Journal, pp 65-80.
- Gan X., Zuo J., Wu P., and Wen T., (2017) "How affordable housing becomes more sustainable? A stakeholder study" International Journal of Built Environment, volume 5, issue 7, pp 89-96.
- Gandhi S., (2012), "Economics of Affordable Housing in Indian Cities-the case of Mumbai". The Journal of Environment and Urbanization (Asia), Volume 2, Issue 5, pp 71-83.
- Gopalan K., and Venkataraman M., (2015) "Affordable housing: Policy and Practice in India", IIMB Management Review (2015), Science Direct, Volume 27, pp 129-140.
- Hosseini D., Nikakhtar K., Wong S., and Zavichi P.,(2017) "Application Of The New Production Philosophy To Construction", American Society of Civil Engineering. Page 414-420.
- Kovvuri P.R.R., Sawhney A., Ahuja R., Sreekumar A., (2016) "Efficient Project Delivery using Lean Principles- An Indian Case Study". Journal of Institute of Engineers India, Volume 1. pp 42-49.
- Lapinski A., and Horman M., J., (2005) "Lean Processes for Sustainable Project Delivery", Journal of construction engineering and management, American society for civil engineers, October 2005, Volume 1, pp 34-45.

- Lasselle L.J., (2012). "Affordable Housing in India: An inclusive approach to sheltering the bottom of the pyramid". *Journal of Sustainable Habitat*, 2012, Volume 3, Issue 8, pp 49-68.
- Mossman A., (2009), "Bridging the Gaps – Towards a Comprehensive Understanding of Lean Construction", *Proceedings of the 10th annual conference in the International Group for Lean Construction*.
- Nair D., Enserink B., Gopikuttan G., (2005) "A conceptual framework for sustainable- affordable housing for the rural poor in less developed economies", *World Sustainable Conference 2005, Tokyo, 27-29 September*
- Pastana A. and Gambatese M., (2016) "Implementation of Lean Tools on Safety in Construction Projects in Palestine", *Proceedings IGLC-22, Oslo, Norway*, pp 1205 – 1218.
- Ram P., and Needham B., (2016) "The provision of affordable housing in India: Are commercial developers interested?" *Habitat International, Science Direct, Volume 55*, pp 100-108.
- Reinbold A., (2016). "Benefits of Lean Construction for Affordable Housing". *International Master of Science in Construction and Real Estate Management. Volume 5*, pp 75-91.
- Salem O., Bjornfot Q., Anders A., and Erikshammar J. (2005), "Learning to see the Effects of Improved Workflow in Civil Engineering Projects", *Lean Construction Journal*, pp 35-48.
- Senaratne S., and Wijesiri D., (2008). "Lean Construction as a Strategic Option: Testing its Suitability and Acceptability in Sri Lanka". *Lean Construction Journal* 2008, pp 34-48.
- Sivam A., (2003) "Viewpoint Housing Supply in Delhi", *Institute of Social Research, Swinburne University of Technology, Melbourne, Australia. Elsevier, Volume 20*, pp 135-141.
- Sivam A., and Karupannan S., (2002), "Role of State and Market in Housing Delivery for low-income Groups in India", *Journal of Housing and Built Environment*, pp 69-88.
- Tam S., and Lee Y., (2006). "Evaluating structural equating models with unobservable variables and measurement error". *Journal of Marketing Research*, 48, 39-50. [9] Hair, F.J.Jr., Black, C.W
- Winston N., Monserrat P.E., (2007). "Sustainable Housing in the Urban Context: International Sustainable Development Indicator Sets and Housing". *Journal of Sustainable Housing and Management. Volume 11*, pp142-163.



## Minimizing Construction Material Waste by Modelling Order Quantity and On-Site Rejection Parameters

Shivendra Tiwari,<sup>1</sup> R. B. Magar <sup>2</sup> and Ashish S. Srivastava<sup>3</sup>

<sup>1</sup>PG Student, Department of Civil Engineering, Kalsekar Technical Campus, School of Engineering and Technology, New Panvel, Maharashtra, India. email: shivendra.tiwari68@gmail.com

<sup>2</sup>Professor and Head, Civil Engineering Department, Kalsekar Technical Campus, School of Engineering and Technology, New Panvel, Maharashtra, India, Corresponding Author

<sup>3</sup>Managing Director, Structech Consulting Engineers India Pvt. Ltd., Navi Mumbai and Ph.D. Research Scholar, Civil Engineering Department, Kalsekar Technical Campus, New Panvel, Maharashtra, India.

### ABSTRACT

Construction material wastages are one of the biggest problems associated with waste management in developing countries like India. The work aims to study the accordance, causes and degree of construction material resource wastage during the course of any type of construction project in India. To understand the Indian site scenario, a survey was conducted collecting experience base data related to twelve of the most common construction material wastages on Indian sites and their causes, ranking both materials and causes of wastage based on their frequency of occurrence and severity conditions on site. As the work aims at sustainable construction process, cost comparison was done to conclude for the costliest of top three ranked construction material wasted in large quantities. Based on cost comparison study, concrete being the costliest was adopted for further study to quantify the degree of wastages from a RMC plant production over a reasonable duration. The study revealed that an approximate of 10 - 12% of all concrete produced was either unused or rejected due to its poor quality. Correlation coefficients were obtained to justify the association of causes to the quantity of wastages observed during the study. Further using Simple Regression Analysis as a mathematical tool, models are developed for the prediction of concrete wastages with respect to the causes of the same, along with an equation to predict the overall wastages associated on daily basis. EOQ modelling is also done for the data of production as per sited demand to optimise the overall wastages of material in RMC industry.

**Keywords:** *Concrete waste; correlation analysis; material wastages; prediction modelling; resource optimization; regression analysis*

### INTRODUCTION

There are a few things certain in life such as death, transition and waste. Either of the three can't be avoided from happening as human produce waste in every form and everywhere even in outer space but, we can make our lives better with a proper management of these waste generated, Agarwal *et al.* (2015) & Tiwari *et al.* (2018). It is acknowledged that technological advances have impacted on the utilization of the resources and directly or indirectly it causes ozone depletion, deforestation, global warming, flooding etc., particularly in the developing nations. These factors are affecting the sustainability of the earth in terms of the resources ability to meet the need of current and future generations, Cartlidge (2004). As resources for construction industries are extracted from the nature and its miss use may result in non-sustainable development of our country. Hence, resource planning and management is one of the most important ingredient for competitiveness and profitability in today's construction industry which can be used to solve the above problems for a sustainable construction, Karaal and Nasr (1986).

The 11<sup>th</sup> & 12<sup>th</sup> five-year plan highlighted that, in terms of magnitude construction industry is second largest after agriculture and is growing at a very rapid pace with huge demands of people in search of better lifestyle and quality products. Which leads to increase in demand of various infrastructures to be constructed around the country, Shrivastava and Chini (2009). Let it be any type of construction project the material cost associated with it is nowhere less than 40-60% of total project cost which is a very high capital investment in any type of project,

Shrivastava and Chini (2009). When we talk about the wastage, estimated to be approximately 30-40% of the total quantity of materials at different stages of construction, Garba *et al.* (2016). Thus, this work was done to understand the degree & causes of material wastages at different stages during the course of construction with its prediction and to optimize them. A simple definition to waste can be loss of material during usage or decay of unused or unattended material on construction site or something that never gives a process of increase in value to the work of construction at any phase is termed as waste, Tiwari *et al.* (2018).

Different number of causes for material waste generation during construction is identified in different studies based on the area and country where study was conducted with the different ways of ranking. In Nigeria, a minimum of twenty-six (26) different causes of material wastage were identified in a study by Garba *et al.* (2016), and Ghanim (2014) studied sixty (60) causes of wastages out of a hundred (100) identified causes on construction sites in Jordan.

Feng *et al.* (1997) and Hegazy (1998) used Genetic algorithms as a technique for optimization, machine learning, automatic programming, transportation problems, adaptive control etc. for his resource optimization problems in his study. Hegazy (1999) did a significant amount of study on resource allocation and levelling. Which were solved mainly using heuristic procedures that cannot guarantee optimum solutions. Improvements were proposed to resource allocation and levelling heuristics and the Genetic Algorithm (GA) technique was used to search for near-optimum solution, considering both aspects simultaneously.

Optimizing resource utilization can lead to significant reduction in the duration and cost of repetitive construction projects such as highways, high-rise buildings and housing projects as concluded by Rayeset *al.* (2001), also developed model that utilize dynamic programming formulation and incorporates a scheduling algorithm and an interruption algorithm so as to automate the generation of interruptions during scheduling. Further in area of optimization Hegazy (2003) proposed optimization-based simulation models, which are integrated with commonly used project management software in which the bestowed approach determines the least cost and most productive amount of resources that achieve the highest benefit by cost ratio.

Cartlidge (2004) bestowed that sustainability is affected by such activities of resource wastages which also, puts a question for the availability of resources for the future generations concluding that we as engineers should find solutions for the optimum utilization and waste reduction techniques of the resources. Ellis and Kim (2005) solved case examples to illustrate the presentation and efficiency of the resource allocation model. As resource management is necessary in today's construction industry, Kandilet *al.* (2006) emphasis upon the automated system for the resource optimization using Spreadsheet software, database application and project planning software. Sadi and Al-Hejji (2006) and Ghanim (2014), performed an investigation in their study on time performance for different types of construction in Eastern Province of Saudi Arabia to test the causes of delay in construction projects. The type of data collection was in the form of field investigation conduction with Owners, Contractors and Consultants with a decent response rate to their survey.

Shrivastava and Chini (2009), not only studied about the construction waste production but also considered demolition waste production scenario in India as a considerable issue and challenge to suggest measures for minimization, along with its generation handling and disposal status on Indian sites keeping it with the aim of sustainability. Here author's study was an overview to Indian construction industry providing volumetric statistics of C&D waste generation along with suggestion of Indian government and construction practitioners about 3R's i.e. Reduce, Reuse and Recycle. Siu *et al.* (2013) uses regression techniques for addressing complicated prediction and classification problems with fundamental algorithms of "least square error" and "least mean square" in order to facilitate the prediction and classification of cycle times of construction operations in a viaduct bridge construction in which the installation was done by launching precast girders with a mobile gantry sitting on two piers. Author demonstrated input factors in connection with operations, logistics and resources using effectiveness of regression techniques in classifying and forecasting.

Ghanim (2014) studied the related reasons of material resource wastage accompanied by its magnitude on construction sites of Jordan. Author obtained the estimated magnitude of material wastage in percentage form along with probable causes for the same with the help of a questionnaire form-based survey. Survey was aimed to get responses from Client linked to construction industry, Contractors and Consultants and proposed causes on any

construction sites and concludes with the percentage of waste construction material identified in his study being from 15% to 21% on construction projects in Jordan along with his recommendations towards waste minimization.

Agarwal *et al.* (2015) linked population eruption, along with demand of cultivating life style of results in increasing demand of infrastructure for basic needs such as housing, transportation, business and education etc to be the main reasons for straining and extraction of limited resources avoiding the part of sustainability in construction industries around the world. Sonmez and Gürel (2016) opted for a new hybrid optimization method to achieve an improvement in optimal planning and scheduling of large-scale construction projects with multiple duration or resource execution modes and resource constraints which allows significant savings by optimum planning and scheduling of medium and large-scale construction projects with numerous duration or resource execution modes and resource constraints. Tiwari *et al.* (2018) reviewed that resource optimization is necessary at its sector because nature has enough for the need but never enough for greed. Espino *et al.* (2018) developed a methodology created on Multiple Regression Analysis (MRA) to assess flood risk in urban catchment areas by replacing storm water models which were replaced resulting in identifying parameters of runoff rates found in urban catchment area.

Concluding the above we can understand that multiple studies have been done to identify the causes of material wastages, magnitude of material wastages and further no more steps have been taken to minimize the material wastages along similar pattern of studies done by different authors previously. Multiple authors optimize the allocation and use of material using soft computing techniques, which can be difficult and tedious job for many construction practitioners. Hence this work aimed at minimizing construction material waste using simple techniques and tools which can be easily understood by different construction practitioners.

## **RESEARCH METHODOLOGY**

The design of this work refers to the plan, which was followed by the systematic study aimed at guiding the process of data collection and its analysis. This work consists of seven phases, as follows:

The initial phase of the study contained the study to identify the importance of this study, defining the problem statement, identifying aims and objectives of the study and developing plan of the study. In further stages of the study literature review including the study related to the causes of material wastage in Indian construction projects was done. Through the literature review forty-eight (48) direct and indirect causes of material wastages relatable to Indian construction site were identified of which twenty-four (24) directly relatable major causes were identified for the further study – poor strategy for waste minimization, ordering errors/limitations to order small quantities, quality constraints of material received, long duration of projects, leftover materials on site, shortage and lack of experienced labours, poor site conditions, wrong and shortage of materials, rework due to workers mistakes, damage caused by workers due to lack of experience, poor quality and non-availability of equipment, change in material prices, mistakes in quantity surveying and over-allowances, weather conditions, poor quality of materials, unnecessary material handling, intersection between various specialists, complicated designs, damage during transportation, theft and vandalism, poor contract documents, purchasing materials not complying with specifications, supply in loose form and frequent design changes.

### **Questionnaire Survey**

The third phase of the study consists of questionnaire design for the survey to be floated for gathering experienced based data from construction practitioners and industry personals including personal interviews along with the surveys. The questionnaire was designed in four parts for data collection. Part I of the questionnaire survey consisted simple questions for the response's personal details such as Name, Company, Post in the company, Experience in total, Responder being a client, contractor or a consultant and Whether he agrees for material wastage on his site?

Part II of the questionnaire consisted questions about material wastage of 12 most commonly used materials on Indian construction sites. In Part III, 24 most commonly found causes of material waste were selected for the questionnaire survey, questions in the survey, attached to each material contained a weightage meter (1 - waste up to 10%, 2 - waste between 10% to 20%, 3 - waste between 20% to 30%, 4 - waste between 30% to 40% and 5 - waste between 40% to 50%) for the responder to allot for that particular material wastage on their site based on the

percentage of material wastage. Based on the data gathered for the degree of material wastage on construction sites, a cumulative percentile average was calculated for each of the 12 commonly used materials.

Questions were made for each cause for material wastage contained two weightage meters one for frequency of occurrence (1 – rarely up to 5 – very frequent) and the other for severity of waste (1 – less severe to 5 – highly severe) for the responder to allot for that particular material wastage on his site. Part IV of the survey consisted questions asking for suggestions to improve the data collection method for the study.

Further in the work distribution of questionnaire and personal interviews from the construction practitioners and industry personals, this includes clients, consultants and contractors. The questionnaire was distributed online and was made available with personal meetings to seventy-one (71) individuals, as shown on Fig. 1 below:

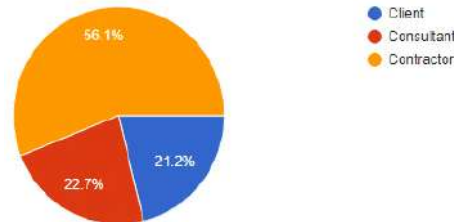


Fig. 1 Pi-chart showing responses from targeted responders

The above Fig. 1, illustrates that 56.1% of the responders were contractors highlighted in yellow portion being the highest of all, 22.7% were consultants highlighted in red portion of the pi-chart and 21.2% of rest were client out of all respondent as highlighted in blue portion. Similar is explained in the below Table. 1:

Table. 1 Response rate for questionnaire survey

Description	Consultants	Contractors	Clients	Total
Distributed	16	40	15	71
Respondents	15	37	14	66
Percentage of Response	93.75	92.5	93.3	93.2

Table. 1 show, the response rate for the questionnaire distributed to the construction practitioners having experience up to 30 years. Total of seventy-one (71) questionnaires were distributed to sixteen (16) consultants, forty (40) contractors and fifteen (15) clients. The total number of responses received was sixty-six (66). Giving a response rate of 93.2%. The data gathered from the responses of the survey itself cleared the major question raised before the start of this study, “If there is any wastage of construction materials on Indian site?” The results for the same are displayed in Fig.2 below:

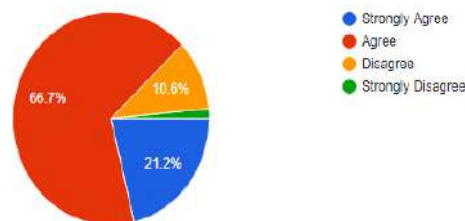


Fig. 2 Result showing presence of material waste in Indian construction industry

The above Fig. 2 shows the agreement of responders for material wastage on their sites in India. 21.2% of them strongly agreed and 66.7% agreed to material waste incurred, whereas, 10.6% disagreed for material wastage and approximately 2% of the responders strongly disagreed to material wastages on their construction sites.

### Descriptive and Frequency Statistical Analysis

Based on the data collected from the responders of the survey, a descriptive and frequency statistical analysis was done to get the three indices. All indices can be calculated as below:

Frequency Index: A formula is shown below which consist the rank component depending on the summation of the weightage allotted to one particular data depending upon its frequency of occurrence on site [Modified from Sadi (2006) and Ghanim (2014)].

$$\text{Frequency Index} = (\cong a (n/N)*100)/5 \quad \text{Eq. (1)}$$

In Eq. (1), 'a' is the constant expressing weightage given to each response (ranges from 1 for rarely up to 5 for always), 'n' is the frequency of the responses, and 'N' is total number of responses.

Severity index: Depends upon the severity of any particular event (how severely the event occurs), on basis of which the responder needs to allots a weightage to that particular event [Modified from Sadi (2006) and Ghanim (2014)].

$$\text{Severity Index} = (\cong a (n/N)*100)/5 \quad \text{Eq. (2)}$$

In Eq. (2), 'a' is the constant expressing weightage given to each response (ranges from 1 for less severe to 5 for highly severe), 'n' is the frequency of the responses, and 'N' is total number of responses.

In Eq. (3), Importance index: Based on the values of the above two indices the final values are obtained namely, Importance index which can be derived as below [Modified from Sadi (2006) and Ghanim (2014)]:

$$\text{Importance Index (IMP.I.) \%} = [(F.I.\% * S.I.\% )/100] \quad \text{Eq. (3)}$$

Where, 'F.I' and 'S.I' used as obtained from above Eq. (1) & Eq. (2).

### Cost Comparison

For the results achieved from the survey, top three materials being wasted were selected for a practical cost comparison, which was carried out to understand the costliest material. Further after the cost comparison work, data collection for the production as raw material or finished product along with its magnitude of waste was to be collected of the costliest material for further study.

Cost comparison was done between water, sand and concrete. Material cost for each material was compared based on per cubic meter unit. Upon market analysis in Mumbai region it was found that from water for construction purpose fluctuates somewhere between free of cost to ₹ 43.20 per cubic meter as per Water Charges Rules (2015-16) clause 1.5, point 21. Similarly, the sand in market varied from ₹ 353.35 – ₹400 per cubic meter as per DSR (2017). Whereas concrete being the costliest varied from ₹ 3000 for M10 to ₹ 7000 for M50 (Rates are as from RMC plant and may vary depending upon the ingredients and admixtures used in production process). This clears that, concrete is in need to be optimized in construction industry towards sustainability, as concrete is a mix of multiple raw materials as its ingredients are directly extracted from the nature.

### Correlation Analysis

A numerical measure, that means a statistical relationship between two variables with some correlation. The variables may be two columns of a given data set of observations made for one single individual, thing, or a process, which is often called a sample sets, or two components of a multivariate random variable with a known distribution. Correlation coefficient can be calculated by the below mentioned equation. The coefficient of correlation is denoted with 'r'.

The value of correlation will always stay between  $-1 \leq r \leq +1$ . As the value of 'r' moves above zero (0) towards '+1' it denotes that for every positive increase in one variable, there is a positive increase of a fixed proportion in the other which is directly proportional. Similarly, if 'r' moves below zero (0) towards '-1' means that for every positive increase in one variable, there is a negative drop of a fixed proportion in the other which denotes inversely

proportionality. When value of 'r' is equal to zero (0), that means for every increase, there isn't a positive or negative increase or decrease respectively. The value of 'r' can be calculated with the below mentioned Eq. (4) (NCBISD - National Centre for Biotechnology Information Search database).

$$r = \frac{\sum(XY) - \frac{(\sum X)(\sum Y)}{N}}{\sqrt{[\sum X^2 - \frac{(\sum X)^2}{N}][\sum Y^2 - \frac{(\sum Y)^2}{N}]}} \quad \text{Eq. (4)}$$

In the above Eq. (4), 'X' and 'Y' are the variables associated with the correlation requirements. A correlation analysis is carried out to understand the relationship between the daily production quantity of concrete in RMC plant with the daily waste incurred due to the causes of its wastage, namely (1) Ordering error/excess quantity production or limitation to order small quantity and (2) Rejection of transit mixer due to concrete quality issues. From the magnitude of correlation coefficients obtained it can be said using Table. 2, if the correlation formed is positive or a negative correlation.

Table. 2 Interpretation from degree of correlation (NCBISD).

Size of Correlation coefficient	Interpretation
0.90 to 1.00 (-0.90 to -1.00)	Very high positive (negative) correlation
0.70 to 0.90 (-0.70 to -0.90)	High positive (negative) correlation
0.50 to 0.70 (-0.50 to -0.70)	Moderate positive (negative) correlation
0.30 to 0.50 (-0.30 to -0.50)	Low positive (negative) correlation
0.00 to 0.30 (0.00 to -0.30)	Negligible correlation

The above Table. 2, can be utilized to interpret the meaning of correlations formed between production and waste incurred.

### Regression analysis

was used to make a model for prediction of concrete wastage due to the two main causes being: (1) Ordering error/excess quantity production or limitation to order small quantity and (2) Rejection of concrete due to its poor quality. The term regression arrived from genetics and was popularized by Sir Francis Galton during the late 19th century with his publication of Regression towards mediocrity in hereditary stature. It is a statistical tool for modelling in statistical analysis and includes different techniques for modelling and analyzing multiple variables, while it establishes relationship between a dependent variable and one or more independent variables or also known to be 'predictors'. More specifically, regression analysis helps one understand how the value of the dependent variable or 'criterion variable' changes when any one of the independent variables gets changed.

Regression analysis is used worldwide for predicting and forecasting purposes, while its use has overlapped with the field of machine learning techniques. However, this can lead to illusions or false relationships, so caution is advisable, correlation does not prove causation as stated by Armstrong (2012). In the study done for the prediction of concrete wastages three models were developed after finding the value of constants associated with the models, as in below Eq. (5):

$$(Y - \bar{y}) = byx(X - \bar{x}) \quad \text{Eq. (5)}$$

In the above Eq. (5), Y is the independent variable which in this study's case be the daily production quantity,  $\bar{y}$  is the mean of the daily production of concrete for a total of 'N = 455' days of data, byx can be derived from below mentioned standard Eq. (6), while X is the dependent variables being daily wastage incurred and  $\bar{x}$  is mean of total waste incurred for 455 days of production respectively.

$$b_{yx} = \frac{\sum XY - \frac{\sum X \sum Y}{N}}{\sum X^2 - \frac{(\sum Y)^2}{N}} \quad \text{Eq. (6)}$$

Where in above Eq. (6),  $b_{yx}$  is known as coefficient of regression of Y on X and N is the total number of values i.e. 455 as stated above. The model to be developed is a simple regression line equation which consists of two constants namely 'a' and 'b'. thus, the value for constant 'b' can be obtained from above equation 6 and value of constant 'a' can be obtained from below mentioned Eq. (7).

$$a = \bar{y} - b\bar{x} \quad \text{Eq. (7)}$$

Where in above Eq. (7), 'a' is the constant from the standard straight-line equation 8, mentioned below  $\bar{y}$  is the mean of the production and  $\bar{x}$  is the mean of wastage on daily basis.

$$y = a + b(x) \quad \text{Eq. (8)}$$

Where in the above Eq. (8), 'a' and 'b' are the constants of standard straight-line equation. Hence to develop models using regression analysis the constants 'a' and 'b' can be derived from above mentioned Eq. (6) and Eq. (7).

Developing a model

The study consists of developing a model for the prediction of waste that will be incurred from the data collected for daily production and wastage of 455 days. The model was developed using Data analysis tools add-in in Microsoft excel 2016. Data analysis tool pack can be used to develop complex models for statistical and engineering analysis, it works on provided data and parameters for each analysis to perform analysis and develop models and give results. The Final part of the study includes conclusions and recommendations based on the results obtained from the study and analysis.

EOQ modelling for daily Production of concrete

Further to optimize the reduce unnecessary wastages of concrete the total demand of the site for 455 days was divided into equal sections of 10 days each and Economic Order Quantity was obtained to identify the difference in the cost of waste incurred. This was done for a particular grade of concrete being M40 as it had higher degree of demand on site during the study period.

## RESULTS AND DISCUSSION

Findings from Cumulative Percentile Average analysis

Analysis done for the calculating degree of wastages and ranking based on those results from data collected by questionnaire survey and personal interviews. As shown in Table. 3 below, we can identify that, frequency statistical analysis revealed, on Indian construction sites the most wasted material (from rank one and below) are Water, Sand and Concrete.

Table.3 Results of the survey, showing percentages of wastage of materials.

Material	Percentages of wastage of materials					Average	Rank
	0-10%	11-20%	21-30%	31-40%	41-50%		
Water	19	12	16	12	7	21.72	1
Sand	19	17	21	9	0	18.39	2
Concrete	22	20	13	9	2	17.61	3
Bricks/Blocks	29	12	12	13	0	16.64	4
Mortar	31	9	14	12	0	16.33	5
Timber/Formwork	30	15	13	6	2	15.42	6
Floor furnishings/Ceramic tiles	31	18	9	6	2	14.66	7
Steel	32	16	11	6	1	14.35	8
Aggregate	32	17	11	5	1	14.05	9
Cement	35	14	13	4	0	13.11	10
Fuel	31	14	6	3	2	12.90	11
Pipes	34	22	7	2	1	12.21	12

In the above Table.3, it shows various frequencies scattered in different percentile range of material waste in. Sand, Bricks, Mortar and Cement show minimum wastage in 41-50% of waste range. Water, Sand and Concrete show the highest percentage magnitude of wastage among all responses. For further study a cost comparison of top three materials needs to be done in order to understand the costliest of them which needs immediate attention for waste minimization. The top three material wastes incurred from the above Table 3, are compared on their cost in Indian market scenario to move the experimental analysis ahead with concrete being the costliest among the top three.

Findings from Descriptive & Frequency Statistical analysis

Descriptive and frequency statistical analysis has been discussed and explained in methodology chapter of this study, which includes calculating frequency index for the causes of material waste by giving options to the individual to select a weightage from 1 – rarely up to 5 – very frequent for every cause or event identified during the study. Similar options were provided for severity of waste, 1 – less severe to 5 – highly severe for every cause or event identified during the study. The results from the survey data is tabulated in Table. 4 below:

Table.4 Ranked causes of resource wastages on construction sites.

Sr. No.	Cause of waste	FI	SI	II	Rank
1	Poor strategy for waste minimization	52.73	55.45	29.24	1
2	Ordering errors/Limitations to order small quantities	50.61	51.52	26.07	2
3	Quality constraints of material received	48.79	51.52	25.13	3
4	Frequent design and client's changes	47.27	49.39	23.35	4
5	Long project duration	45.45	47.27	21.49	5
6	Leftover material on site	45.15	46.97	21.21	6
7	Shortage and lack of experience of skilled workers	44.55	47.27	21.06	7
8	Poor site conditions	42.12	45.76	19.27	8
9	Wrong and lack of storage of materials	41.82	43.33	18.12	9
10	Rework due to workers mistakes	39.70	42.42	16.84	10
11	Damage caused by workers due to lack of experience	39.39	42.12	16.59	11
12	Poor quality and non-availability of equipment	37.27	40.91	15.25	12
13	Change in material prices	36.97	40.30	14.90	13
14	Mistakes in quantity surveying and over allowance	37.58	39.09	14.69	14
15	Weather conditions	35.15	39.09	13.74	15
16	Poor quality of materials	35.15	39.09	13.74	16
17	Unnecessary material handling	34.85	37.88	13.20	17
18	Interaction between various specialists	34.24	38.18	13.07	18
19	Complicated design	34.55	37.58	12.98	19
20	Damage during transportation	30.91	36.06	11.15	20
21	Theft and vandalism	30.61	35.15	10.76	21
22	Poor contract documents	29.09	35.45	10.31	22
23	Purchasing materials not complying with specifications	29.09	34.85	10.14	23
24	Supply in loose form	29.09	33.33	9.70	24

Table. 4 highlights that, Poor strategies for waste minimization, ordering errors, Limitations to order small quantities, Quality constraints for rejection of concrete and Long project duration are the major causes for material wastage of material on construction sites in India.

Correlation Coefficients Between waste incurred and production of concrete

Correlation coefficient analysis was done on the 455 numbers of data collected from the RMC plant in three sub categories:

Total quantity of daily concrete production (Y).

Total quantity of daily concrete produced/delivered in excess due to limitation of ordering small quantities (X1).

Total quantity of daily concrete rejected from client/site of construction for its poor quality (X2).

Total quantity of daily concrete waste incurred ( $X_3 = X_1 + X_2$ ).

The results obtained from the correlation analysis between the production and wastages incurred is as shown in below Table. 5.

Table.5 Correlation coefficients developed between Production and waste incurred

Sr. No.	Correlation between	Denotation	Correlation coefficient
1.	Production and waste incurred due to limitation of ordering small quantities/ordering error.	Y - X1	0.84
2.	Production and waste incurred due to rejection of concrete for its poor quality.	Y - X2	0.93
3.	Production and total wastage incurred.	Y - X3	0.92

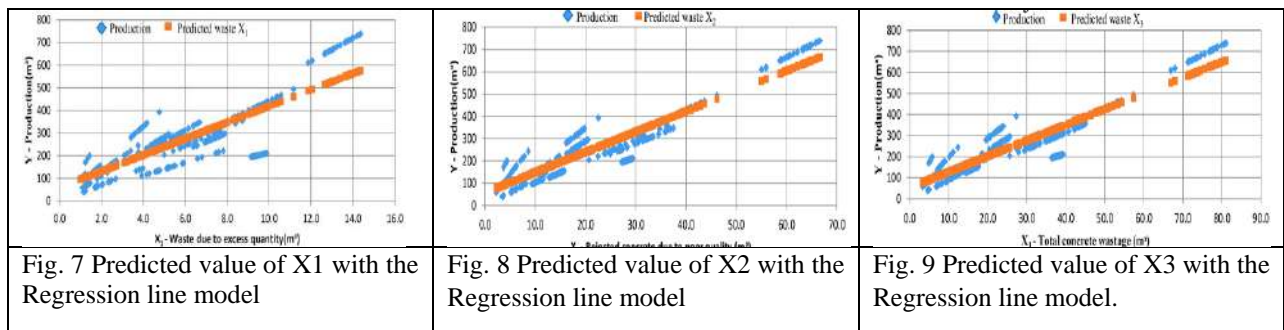
From Table.5, it can be summarized that the correlation between the daily production of concrete and waste incurred due to excess concrete production is 0.84 which comes out to be a high positive correlation, correlation between the daily production of concrete and waste incurred due to rejected concrete due to its poor quality is 0.93 which is a very high positive correlation and correlation between the daily production of concrete and total waste incurred is 0.92 which is also a very high positive correlation. Thus, it can be inferred from the above results that there is a very high positive correlation between the production and wastage of concrete on Indian sites which needs proper minimization.

Model developed for prediction of Concrete wastage

Regression analysis done using data analysis tool add-in in Microsoft excel 2016 bestowed the following results.

Regression Model between Y and X.

The analysis conducted was between the daily production quantity and waste incurred due to excess quantity of concrete production or limitation of ordering small quantities. Fig. 7, Fig. 8, and Fig. 9 plots the X1, X2 and X3 line fit plot respectively.



$$Y = 0.0196X_1 + 0.3112$$

Eq. (8)

$$Y = 0.0945X_2 - 2.6956$$

Eq. (9)

$$Y = 0.1141X_3 - 2.3844$$

Eq. (10)

Where for the developed Eq. (8), we get the values of constants 'a' and 'b' to be 0.3112 and 0.0196 respectively. From the above equation if we have the production values for the next day, the values of wastages X1 can be predicted easily. The analysis was conducted between the daily production quantity and waste incurred due to rejection of concrete due to its quality issues shown in Fig. 8. The Eq. (9) shows the prediction of daily waste incurred due to rejected concrete for its poor quality. Where for the developed Eq. (9), we get the values of constants

'a' and 'b' to be -2.6956 and 0.0945 respectively. From the above equation if we have the production values for the next day, the values of wastages X2 can be predicted easily.

The analysis also conducted between the daily production quantity and waste incurred due to rejection of concrete due to its quality issues shown in Fig. 9.

From the Fig. 9, the Eq. 10 has been developed, we get the values of constants 'a' and 'b' to be -2.3844 and 0.1141 respectively. From the above equation if we have the production values for the next day, the values of wastages X2 can be predicted easily. The line equation developed in Eq. (10), can be used by any of the three (client, contractor and consultant) parties to predict the degree of wastages that can happen during the next day of concrete production, transportation and placing, to be alert for the upcoming situation and be ready with the measure to optimize and minimize the wastage to some extent.

Results from EOQ modelling of the production

Economic Order Quantities were derived of daily production to fulfil each 10days demand of the site to keep the production and delivery in control. This practice will help to study & compare the difference in wastage incurred. EOQ was derived only for M40 grade of concrete as it was produced in huge quantities based on the demands of the site during the study period. Below mention Table states the difference in quantities of wastage of M40 grade concrete before and after the application of EOQ modelling.

Table. 6 Cost comparison of waste incurred before and after EOQ

Sr. No.	Description	Waste		Difference
		Before EOQ	After EOQ	
1.	Quantity (m <sup>3</sup> )	6384	1773	4611
2.	Cost (Rs.)	4,10,96,553.12	1,14,13,563.39	2,96,82,989.73

The above Table. 6 explains the obvious and a huge difference in quantity and cost of M40 grade concrete wastage of 4611m<sup>3</sup> valued at Rs. 2.97 crores approximately. Also, a correlation was derived between the new economic order quantity (denoted as p) and the difference in previous order quantities to the economic order quantity (denoted as q), which came out to be a strong downhill (negative linear relationship) at -0.945 (very high negative correlation). Regression analysis results between 'p' and 'q' are shown below Fig. 10 and EOQ prediction model.

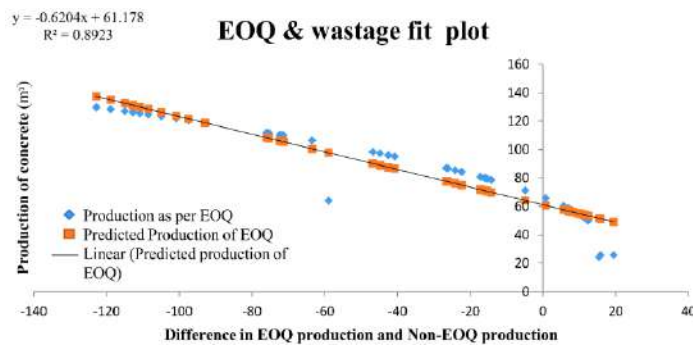


Figure. 10 Predicted Production as per EOQ

Figure.10 show the results of developed Eq. (10) as mentioned below, for the prediction EOQ Production of M40 concrete on daily basis.

$$Y = -0.6204X + 61.178 \quad \text{Eq. (11)}$$

Where for the developed Eq. (11), we get the values of constants 'a' and 'b' to be -2.6956 and 0.0945 respectively. From the above equation if we have the production values for the next day, the values of wastages X can be predicted too. The regression statistics for above Eq. (11) can be viewed as in below Table. 7.

Table. 7 Regression statistics for the developed Eq. (11).

Regression Statistics	
Multiple R	0.945
R Square	0.892
Adjusted R Square	0.889
Observations	46

The value of  $R^2$  signifies that linear model fits the set of observations by 89%, which is quite accurate for prediction purpose of wastages in RMC plant. The models developed in this study are subjected to only one particular RMC plant from where data was collected for the study purpose. Similar studies can be done to develop models for prediction of wastage associated to their pattern of production and wastage parameters.

## CONCLUSIONS

Different causes of material wastage and top materials being wasted were identified and ranked using experience-based data from the construction industry personals. Further a correlation was derived between them forming a highly positive relationship between the top material being wasted on site and its causes. Regression analysis was used to model the daily production quantities and on-site wastage parameters to obtain standard equations for prediction of concrete wastage. The models developed are subjected to work accurately only for the RMC plant from where data was collected during the course of this study. Similar models can be developed for different RMC plants as well using similar techniques. Wastages can be reduced by optimizing the work processes in construction industry and recycling of the unused materials where ever needed. In this study similar kind of practice was adopted for the minimization of concrete wastages associated with RMC and Client's part just by optimizing the daily order quantities. A simple and standard tool namely, EOQ (Economic order quantity) were derived for the daily production of RMC plant as per sites demand on daily basis. The differences in waste reduction in usual production quantity practice and as per EOQ practice were significant to say that the tools can be utilized to reduce huge degree of wastages diverting construction practices towards sustainability.

## REFERENCES

- Agarwal, R., Chaudhary, M. and Singh, J. (2015), "Waste Management Initiatives in India for Human Well Being", European Scientific Journal, /SPECIAL/edition ISSN: 1857 – 7881 (Print) e - ISSN 1857- 7431, pp. 105-127.
- Armstrong, J. S. (2012), "Illusions in Regression Analysis", International Journal of Forecasting, 28(3), pp. 1-11.
- Aravind, E. S. (2018), "Present Status of Waste Management in India and Recommendations", IIT Madras, ©2018 Built by - CivilDigital.com, Powered by WordPress.
- Cartlidge, D. (2004), Procurement of Built Assets, 1st Edition, U.K., Elsevier Butterworth- Heinemann.
- Ellis, R. D. and Kim, J. L. (2005), "Development of a Resource Scheduling Model Using Optimization", Construction Research Congress 2005.
- El-Rayes, K. and Moselhi, O. (2001), "Optimizing Resource Utilization for Repetitive Construction Projects", Journal of Construction Engineering and Management, 127(1), pp. 18-27.
- Esppino, D. J., Sillanpää, N., Doménech, I. A. and Hernandez, I. R. (2018), "Flood Risk Assessment in Urban Catchment Using Multiple Regression Analysis", Journal of Water Resource Planning and Management, 144(2), pp. 1-11.

Feng, C., Liu, L., and Burns, S. (1997), "Using Genetic Algorithm to Solve Construction Time-Cost Trade-off Problems." *Journal of Computing in Civil Engineering*, ASCE, 11(3), pp. 184-189.

Garba, A., Olaleye, Y. O. and Jibrin, N. S. (2016), "Material Resource Optimization for Sustainable Construction in Nigeria", *Journal of Engineering and Architecture*, 4(1), pp. 33-47.

Ghanim, A. B. (2014), "Study of Causes & Magnitude of Wastage of Material on Construction sites in Jordan", *Journal of Construction Engineering*, Volume (2014), pp. 1-6.

Government of India (2012), "12th five-year plan (2012-2017)", Planning Commission, Indian.

Hegazy, T. and El-Zamzamy, H. (1998), "Analogy-based Solution to Mark-up Estimation Problem.", *Journal of Computing in Civil Engineering*, © ASCE, 8(1), pp. 72-87.

Hegazy, T. (1999), "Optimization of Resource Allocation and Levelling Using Genetic Algorithm", *Journal of Construction Engineering and Management*, 125(3), pp. 167-175.

Hegazy, T. and Kassab, M. (2003), "Resource Optimization Using Combined Simulation and Genetic Algorithms", *Journal of Construction Engineering and Management*, 129(6), pp. 698-705.

Kandil, A. and El-Rayes, K. (2006), "MARCOS: Multi-objective Automated Construction Resource Optimization System", *Journal of Management in Engineering*, 22(3), pp. 126-134.

Sadi, A. A. and Sadiq Al-Hejji. (2006), "Causes of Delay in Large Construction Projects", *International Journal of Project Management*, 24(2006), pp. 349-357.

Shrivastava, S. and Chini, A. (2009), "Construction Material and C&D Waste in India", *Lifecycle Design of Buildings, System and Materials*, pp. 72-76, M.E. Rinker Sr., School of Building Construction, University of Florida, USA.

Siu, M. F., Ekyalimpa, R., Lu, M. and Abourizk, S. (2013), "Applying Regression Analysis to Predict and Classify Construction Cycle Time", *Journal of Computing in Civil Engineering*, ©ASCE, paper ID 1487824, pp. 669-676.

Sonmez, R. and Gürel, M. (2016), "Hybrid Optimization Method for Large-scale Multimode Resource-Constrained Project Scheduling Problem", *Journal of Management in Engineering*, ©ASCE, ISSN 0742-597X, pp. 1-10.

Tiwari, S., Magar, R. B. and Honnutagi, A. (2018), "Resource Optimization for Sustainable Construction: A State of Art", *International Advanced Research Journal in Science, Engineering and Technology*, 5(3), pp. 69-73.

Water Charges Rules and Sewerage & Waste Removal Rules, (2015), Hydraulic Engineer's Department and Chief Engineer (Sewerage Operation)'s Department, Brihanmumbai Mahanagarpalika, Maharashtra, India, pp. 8-10.



## Application of Multi Criteria Decision to Simulate Uncertainties in Construction Projects

Shweta Katrekar,<sup>1</sup> R. B. Magar,<sup>2</sup>  
G.B. Mahajan<sup>3</sup> and Yashvant S. Patil<sup>4</sup>

<sup>1</sup> #\*PG Student, Department of Civil Engineering, Kalsekar Technical Campus, School of Engineering and Technology, New Panvel, Maharashtra, India. email: [shwetakatrekar@gmail.com](mailto:shwetakatrekar@gmail.com)

<sup>2</sup> Professor and Head, Civil Engineering Department, Kalsekar Technical Campus, School of Engineering and Technology, New Panvel, Maharashtra, India. email: [rajendramagar69@gmail.com](mailto:rajendramagar69@gmail.com)

<sup>3</sup> Assistant Professor, Civil Engineering Department, Kalsekar Technical Campus, School of Engineering and Technology, New Panvel, Maharashtra, India. email: [gbmahajan73@yahoo.com](mailto:gbmahajan73@yahoo.com)

<sup>4</sup> Assistant Professor, Civil Engineering Department, S.S. Jondhle College of engineering and Technology, Asangaon, Maharashtra, India. email: [yashpatil2005@gmail.com](mailto:yashpatil2005@gmail.com)

### Abstract

Uncertainties are major cause for influencing the performance of a construction project. It can be generalized as the difference between the results and outcomes from usually expected values. The values can be considered to be Time, Quality and Economy of the project depending upon the project needs. In construction project management, the effects of unidentified risks and uncertainties obstruct the project time, quality and its economy. Thus upsets the project management and so its development. Identifying the uncertainty and quantitative analysis impacts the project performance and can notably enhance the exactness, validity and reliability of a project plan. This study describes a methodology to systemize, model, and diminish uncertainty. In essence, Multi criteria decision making model is developed. That is useful for analyzing uncertainties even with insufficient information or vague records. The work presents uncertainty assessment methodology based on Multi criteria decision making. An effective integrated project management tool to deal with subjective conclusion; that is used to configure large number of uncertainties. It included a questionnaire survey; based on the data obtained, the probability of factors causing uncertainties were quantified using importance index and multi criteria decision making. The results indicate that the major causes of uncertainties. The aim of this study is to propose a decision support tool to quantify the probability of uncertainties in construction projects by using Importance Index incorporated with multi criteria decision making. Using this theory an uncertainty assessment model was proposed. The model incorporated with experience of all 58 respondents using important index method along with multi criteria decision making (MCDM) technique giving the probability of major concerned factors of uncertainty as an output which will serve the purpose of this work.

**Keywords—** Multi criteria decision-making model (MCDM); Simulation; Uncertainties; Uncertainty assessment;

### INTRODUCTION

Uncertainty exists around us in the world which affects us directly or indirectly. The only way to avoid uncertainty is by assessing it, understanding it and try to take a preventive action to negate its impact. Any phenomena which cannot be predicted with certain degree of assurity due to insufficient or unreliable data is called uncertainty. Many construction projects face one of the biggest construction problems which is uncertainty caused by various project environments. It affects every part of the construction project in different ways throughout the project life cycle. In recent years, many contractors have expressed concern about the difficulty of overcoming the factors causing uncertainties, mainly because the contractor is not a position to determine the exact reason for the same in the construction processes. In previous years' scientists defines the ill-mannered planning approach towards construction process leads to uncertainties which integrates risk management, Smith (2003). Theoretically uncertainty can be defined as a situation involving ambiguous information, Brauers (1986). Initially when the causes and sources are identified then the required actions and measures to overcome and reducing the uncertain factors need to be analyzed. Solutions must be provided to explain the process of managing the risk and appropriate solution for management of the entire project life cycle, Snyder (2005). To ease the decision-making process to withstand uncertain circumstances, Del Cano and Cruz (2002).

In construction project management, it is the effect of risks and uncertainties on project time, quality and economy that is the subject of management and decision making. In dealing with risks and uncertainties management as challenges facing construction industry in developing countries in project management, the focus should be on:

- Identification of the various risks and uncertainties inherent in the project.
- Categorization and Quantification of risks and uncertainties in the project.
- Risk and uncertainty sensitivity analysis for the project.
- Project risks and uncertainties allocation and distributions to those with better capacity and mechanism to handle each categorization. Sharing the risks and uncertainties should be done only through terms and conditions of contract agreements.
- Project risks and uncertainties response and mitigation by the responsible people or parties to whom they were allocated and distributed.
- The fundamental bottom line of principles of management is that risks and uncertainties are not entirely negative but also holds significant opportunities that their proper management could be very much rewarding.

Well-organized, well-planned projects often simply fails for not being able to achieve the desired goal of quality, cost & time due to many uncertainties that prevail in the project. Project managers bear a solely responsible for resolving all kinds of uncertainties that prevail in the project. The client always expect their projects to run to plan and achieve predictable outcomes, time after time. But a manager's decisions are always constrained by the coincidence of time, cost and quality. Hence, there must be a better way to avoid the pitfalls created by the uncertainty, or make the organization in a position to handle the uncertainty in a much effective way than before. Brauers (1986) describes the reason of uncertainty and situations during the implementation of construction projects thorough description of steps for construction project risk management as the process of making informed construction project decisions.

Probabilistic methods assess the degree of compliance within various constraints, including duration, cost, and quality and their associated uncertainties. Independent processing is, therefore, required. The program evaluation and review technique (PERT) Malcolm et al. (1959) was a first step toward applying uncertainties to activity duration. Activities use the beta probability curve to calculate the most likely duration and variance. The project variance is the sum of the critical path activity variances. Martinez and Ioannou (1997) mentioned that despite the probabilistic aspect of PERT, activity duration was still optimistic. PERT is also unable to make a correlation between durations. In addition, errors may occur in cases of multiple peaks or discontinuous distributions.

Murray (1963), MacCrimmon and Ryavec (1964), and Grubbs (1962) have suggested alternatives to the PERT method. Different extensions emerged, taking cost and reliability into account. Other researchers, such as Halpin and Riggs (1992), Pritsker (1995), and Lu and AbouRizk (2000) suggested applying simulation to the PERT network. Daji and Reiar (1993) developed the back-forward uncertainty estimation (BFUE). This method introduces uncertainties to the duration of noncritical activities. To calculate the total duration of the project, this method considers the likelihood that any path will become critical. BFUE is based on the fact that noncritical paths may, during the work, becoming subcritical or critical depending on how the margins of activities are used. Practical decision-making difficulties are usually too complex and unintended to be considered through the scrutiny of a single criterion that will lead to the optimum decision. As per Zopounidis and Doumpos (2002) a more appealing approach would be the simultaneous attention of all applicable factors that are related to the problem, Multi criteria Decision Making (MCDM) composes an unconventional range of operations research that is allocated to the progress and execution of decision constructing and approaches to challenge complex decision struggles concerning multiple criteria objectives of inconsistent nature. Bennett (2003), the construction industry needs a distinct methodology due to the complexity of projects undertaken. The modified project life cycle should bring benefits to project management and its performance. Westland (2006), stress on the importance of time management is used to record actual time invested for execution of certain tasks. It also helps to allocate resources more effectually and control schedule of performing works, Han et al. (2007) proposed a value addition rate (VAR), a time-scaled metric to capture the activities that consume time or resources without increasing value.

Francis et al. (2013), highlights the limitation of these network-based scheduling techniques consider only a single action sequence. The chronographic model studied the dynamic time-scaled dependencies that allow continuous probabilistic simulations based on the internal variation of the production rate. The Construction projects which are complex in nature, uncertainty and risks in the same can develop from different sources. The evidence of the construction industry does not reasonably bonds when dealing with risks in projects.

Lmoussaoui and Jamouli (2016) proposed a new approach namely "Three-dimensional Risk Identification" based on the three parameters: Risk typology, project phases, and stakeholders in order to draw up an exhaustive list of risks

that may occur in different phases of a construction project. It presents a new approach based on MCDM for the prioritization of risks using the concept of weighted criticality. Its practical use has been tested on a real electrification project to identify the most critical risks.

It can be concluded from the literature review that difficulties in risk and uncertainties management were derived from a restricted outlook. Previous research on MCDM techniques in simulating uncertainties has been very limited, thus a vast scope to apply MCDM techniques to help estimate the probability of uncertainties in construction project. It is envisaged that the technique adopted may be very useful in analyzing factors causing uncertainties, in which significant decisions are influenced by many subjective factors. It enables various types of decision makers to overcome the uncertainties occurred during execution of project.

## RESEARCH METHODOLOGY

- A decision-making model will be developed to mitigate uncertainties in construction projects.
- Categorizing the factors as per the construction aspects of project cost, quality and time will be carried out.
- Probability index, impact index and importance index so as to quantify the uncertain factors or uncertainty in construction project will be estimated
- Multi criteria decision making technique in MATLAB will be applied on results obtained from importance index and impact index.

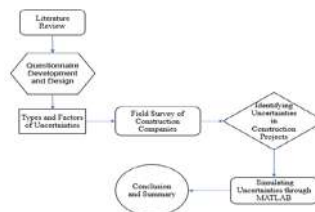


Fig. 1. Experimental programme

### Methodology

An online questionnaire was sent out as a follow up to the interviews. The aim was to focus on the general identified uncertainties, in order to put in a probability and impact matrix. Further investigation shows that there are top 15 factors causing uncertainty and affecting the projects in construction industry. The entire questionnaire survey as participated among contractors, consultants and clients of construction projects from various sectors as shown in Fig 2.

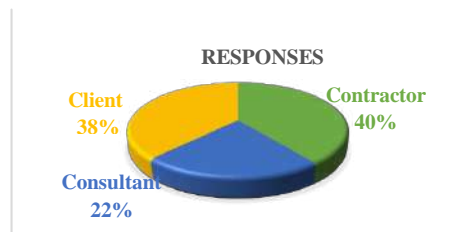


Fig. 2. Response chart

The Fig. 2 shows, 40% of contractors, 38% of clients and 22% of clients; which is why the research inclines more towards contractor's perspective. The research methodology adopted for this study comprised of literature review, email questioner, estimation of importance index, probability index and impact index and also validation of the same using multi criteria decision making in MATLAB.

### Evaluation of Importance Index

Importance Index (IMP INDEX) technique was adopted for this research; in this technique, for each cause/factor two questions were asked: What is the rate of occurrence for this cause? And what is the impact of this cause? Both rate of occurrence and impact were categorized on a five-point scale. Rate of occurrence is categorized as follows: very high, high, moderate, low, very low (on 5-1point scale) where, 5 is being the maximum as very high and 1 will minimum as very low. Probability index is used to rate causes of uncertainty based on rate of occurrence as identified by the participants.

$$\text{Probability Index (P.I.) (\%)} = \sum a (n/N) * 100/5 \quad \text{Eq. (1)}$$

Impact index: A formula is used to rate impact of cause on factors as indicated by the participants.

$$\text{Impact Index (I.I.) (\%)} = \sum a (n/N) * 100/5 \quad \text{Eq. (2)}$$

In above referred equation  $a$  is the constant expressing weighting given to each response (ranges from 1 for very low up to 5 for very high),  $n$  is the frequency of the responses, and  $N$  is total number of responses.

Each factor's importance index is calculated as a function of frequency, as follows [modified from Al-Hejji (2006) and Ghanim (2014)]:

$$\text{Importance Index (IMP.I.) (\%)} = [\text{P.I. (\%)} * \text{I.I. (\%)}] / 100 \quad \text{Eq. (3)}$$

The ranks of importance index made it is apparently cross-linkage of the relative importance of the factors as anticipated by the three groups of respondents (i.e. clients, consultants and contractors). Each individual cause's IMP.I. perceived by all respondents should be used to assess the general and overall ratings in order to give an overall picture of the causes of uncertainties in construction industry. Table. 1 shows the factors identified from the survey.

**Table. 1 Major Factors of Uncertainty**

Sr.no	Attributes	Particulars
1.	Cost	Planning
2.		Funding approval
3.		Cost estimation
4.		Budget controls
5.		Other technical
6.	Time	Planning
7.		Project management
8.		Scheduling
9.		Constructability
10.		Documentation
11.	Quality	Environmental
12.		Engineering
13.		Civil, Structural, Systems
14.		Construction management
15.		Legal matters

The importance index was further calculated from the factors causing uncertainties listed as per parameters of project cost, project time and project quality.

### ***Modeling and Simulation in Construction Projects***

Model and simulate dynamic system behavior with MATLAB, Simulink, and Simscape can be functioned in construction industry as well. Modeling is a mode to create a simulated representation of a real-world scheme that includes software and hardware. The software mechanisms of the model can be driven by mathematical associations, simulating the virtual representation under an extensive variety of conditions to see how it acts. Modeling and simulation are especially valuable for testing conditions that might be difficult to reproduce with hardware prototypes alone, especially in the early phase of the design process when hardware may not be available. Iterating between modeling and simulation can improve the quality of the system design early, thereby reducing the number of errors found later in the design process. Common representations for system models include block diagrams, schematics, and state charts.

Multi criteria decision making technique using MATLAB acquires coding to make the model run efficiently; the MATLAB coding involves following steps to be followed

1. Create a new Script file in the Editor
2. Copy paste these codes in the Script file
3. Create 3 Matrix namely X, W and Wcriteria
  - a) where X is the decision Matrix
  - b) W is the weights of the criteria
  - c) Wcriteria tells us that the criteria are beneficial or non-beneficial
4. Run the program.

## **RESULTS AND DISCUSSION**

### ***Probability Rate and Impact of Uncertain Factors***

Considering the ratings received from the participants the further calculations for probability index were thus intended. Each individual factor rate was summed up to examine the average rate of factors and probability index (P.I.) to identify the probability of factors causing uncertainties in respective construction project. Table. 2 highlights

the estimated probability index for uncertainties encountered.

**Table. 2 Probability Index**

Particulars	Rating	Average	Probability Index
Planning	178	3.068	0.613
Funding approval	173	2.982	0.596
Cost estimation	169	2.913	0.582
Budget controls	179	3.086	0.617
Other technical	154	2.655	0.531
Inventory Planning	190	3.275	0.655
Project management	197	3.396	0.679
Scheduling	195	3.362	0.672
Documentation	171	2.948	0.589
Environmental	172	2.965	0.593
Engineering	187	3.224	0.644
Civil, Structural Systems	195	3.362	0.672
Construction	182	3.137	0.627
Legal matters	164	2.827	0.565

Similarly, Impact index for each factor causing uncertainties in construction projects were estimated with due consideration of participant's rate of impact over the particular factors. These participants had individually rated the impact of the factors causing uncertainties for their projects as per their knowledge, judgement and experience. The following Table. 3 was hence functioned for estimating Impact Index (I.I.)

**Table. 3 Impact Index**

Particulars	Rating	Average	Impact Index
Planning	176	3.034	0.606
Funding approval	171	2.94	0.589
Cost estimation	167	2.879	0.575
Budget controls	177	3.051	0.610
Other technical	160	2.758	0.551
Inventory Planning	179	3.086	0.617
Project management	185	3.189	0.637
Scheduling	183	3.155	0.631
Constructability	190	3.275	0.655
Documentation	159	2.741	0.548
Environmental	176	3.034	0.606
Engineering	195	3.362	0.672
Civil, Structural, Systems	199	3.431	0.686
Construction management	189	3.258	0.651
Legal matters	165	2.844	0.568

From the below Table. 4, the factor Civil, Structural, Systems has maximum IMP.I. % i.e. 46.14 while the factor Other Technical possess least IMP.I. % as 29.30. This specifies that the factors encountered with maximum IMP.I. can be given attention on priority basis and its effects can be diminished during execution of construction projects. This will simplify the work of decision makers to decide the major factors affecting the project and thus immediately they can be taken into account so as to avoid the complex situations in near future and optimize their

outputs.

**Table. 4 Importance Index**

<b>Sr.no.</b>	<b>Particulars</b>	<b>P.I.</b>	<b>I.I</b>	<b>IMP. INDEX%</b>
1	Planning	0.61	0.61	37.25
2	Funding approval	0.60	0.59	35.18
3	Cost estimation	0.58	0.58	33.56
4	Budget controls	0.62	0.61	37.67
5	Other technical	0.53	0.55	29.30
6	Inventory Planning	0.66	0.62	40.44
7	Project management	0.68	0.64	43.34
8	Scheduling	0.67	0.63	42.43
9	Constructability	0.67	0.66	43.60
10	Documentation	0.59	0.55	32.33
11	Environmental	0.59	0.61	36.00
12	Engineering	0.64	0.67	43.36
13	Civil, Structural, Systems	0.67	0.69	46.14
14	Construction management	0.63	0.65	40.90
15	Legal matters	0.57	0.57	32.18

The Fig. 3 elaborates the important index % obtained from the statistical analysis that quantifies the uncertainties examined at project execution. It enables the project manager to model how events will unfold. Even a simple project has some or the other traits which dictates a sequence of events, estimates how long certain tasks will take and identifies the resources needed to accomplish the goals. More complex projects explicitly model many more key aspects of the project such as supply chain dependencies and benefits realization. As seen in the Fig. 3 the factor causing uncertainty in parameter civil, structural systems posses maximum percentile which determines the activities taking placing in this parameters are of greater concern and precautionary measures are to be taken so as to overcome the hurdels caused; whereas activities of other technical parameters doesnot requires much attention while execution. This approach takes a subjective view of probability as a measure of degree of belief in a hypothesis. Although it is a belief that this is a step in the right direction to represent epistemic uncertainty and still it is not satisfactory. Research into modern theories of uncertainty-based information, such as possibility theory, evidence theory, fuzzy set theory, and imprecise probability theory. However, these theories are not well developed when compared to probabilistic inference. In addition, none of these theories, except fuzzy set theory, has been applied to engineering analysis problems. The usefulness of the present framework results from two aspects, it formalizes and merges a broad range of activities conducted in complex system modeling and modern computational simulation.

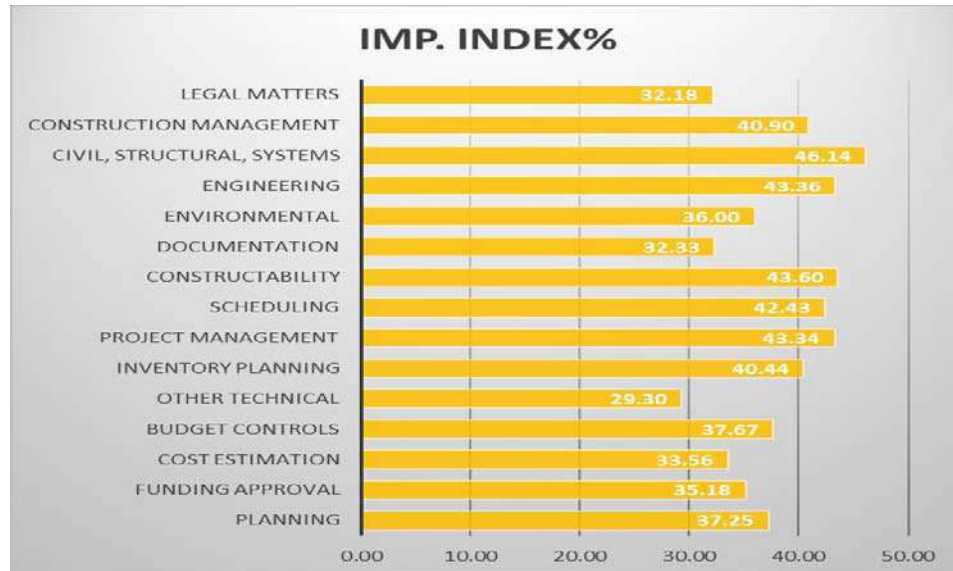


Fig. 3 Important Index

From Fig. 3 the decision makers can justify their decision to be taken for betterment of the construction project. The study of uncertainties will help decision makers to pinpoint the factors and its exact cause for which it was responsible.

**Decision making model**

Projects are naturally forward-looking, particularly when working under pressure. This makes it hard to reflect on the effectiveness of past decisions and quantify their success. Lessons can only be learnt by understanding how decisions have influenced events. This must be evaluated for their desirability which of the possible outcomes will achieve the protect objectives. In a rapidly changing and thus highly uncertain envly remnant may be the key to keep awkward situation under control. A good forecasting model must not only identify the project driven but properly understand its requirements as well. The research focuses on effective decision-making model to mitigate project uncertainties encountered during project life cycle. One such method is executed in the search by preparing decision matrix for analyzing the best suitable option for the alternatives based on the confronted criteria or factors. Each factor will have its own weightage which will enable the decision makers to identify the impact over factors. A decision-making process involves the following steps to be followed:

1. Identifying the objective/goal of the decision-making process
2. Selection of the Criteria/Parameters/Factors/Decider
3. Selection of the Alternatives
4. Selection of the weighing methods to represent importance
5. Method of Aggregation
6. Decision making based on the Aggregation results

Below Table. 5 shows decision matrix generated is to be filled by the decision makers to analyze the uncertainties examined at the time of construction project.

Table. 5 Decision matrix system

Criteria	Factor 1	Factor 2	Factor 3	Factor 4	Factor 5	Factor 6	Factor N
Alternative 1							
Alternative 2							
Alternative 3							
Alternative 4							
Alternative 5							
Alternative 6							
Alternative N							

Decision matrix assists to identify all the possible factors causing uncertainties as well as the probable alternatives to be performed to overcome the uncertainties. Thinking about the sequence of decision points helps to prioritize which areas of uncertainty to tackle first. With each step, these activities reveal more about what is known and unknown. Identifying 'failure states' also warns of particularly serious risks which deserve greater attention. Recognizing them as different aspects of an underlying root problem, which reduces the number of disorders left to deal with. If the right decision is made at the right time, the project proceeds to a desired state. A decision may even push the project into a failure state from which recovery is nearly impossible.

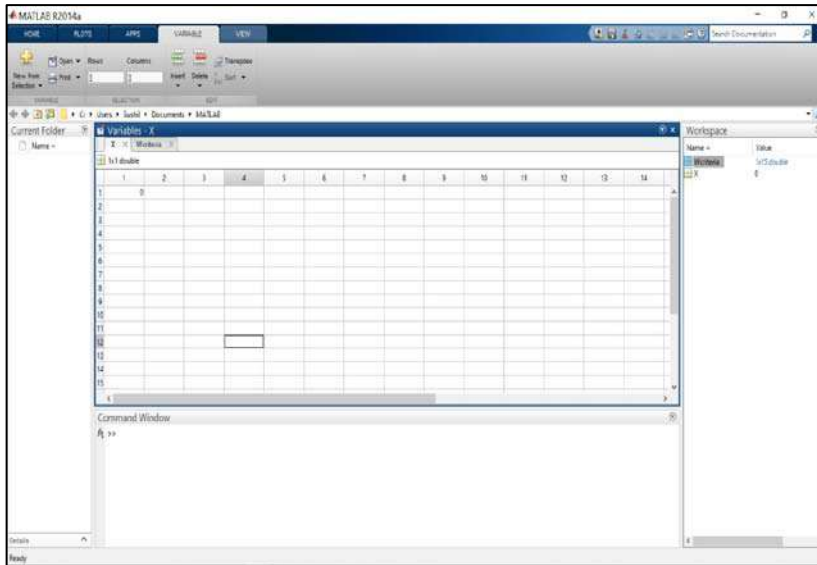


Fig. 4 Variable X

Fig. 4 shows successfully creating Variable X. It is developed in the MATLAB Program Software. Now similarly another variable is to be created and name it as 'W' likewise the variable letter must be in caps lock. The values assigned for this variable will be the weightages granted to each factor as per their impacts over the affecting factors of say uncertainties. This will categorise the factors as per their rates.

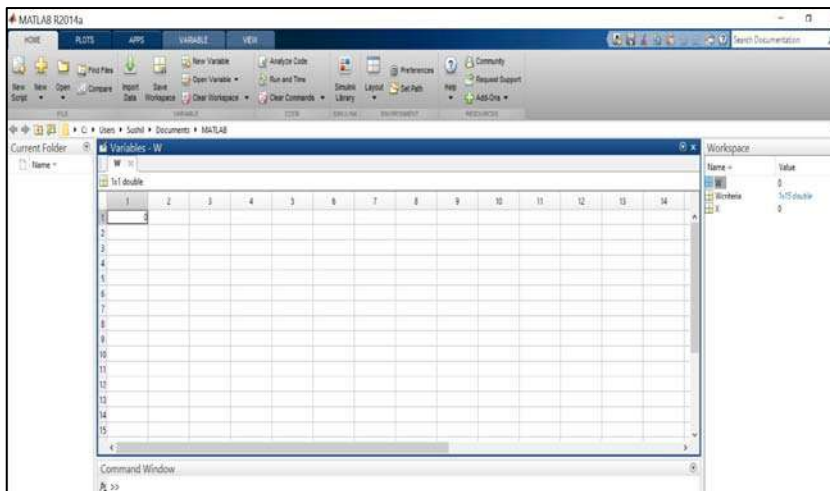


Fig. 5 Variable W

Fig. 5 Variable W consists of weights assigned for the factors rating as per their priorities and causes of concern for the project and project life cycle. These weights decide the rating of the factors that could probable impact over the success or failure of the event. The weights are to be filled up in the cell according to their ratings.

The high value factors are the ones which deliver maximum worry over lowest input. A large proportion of the result can be produced with a minority of effort. These are the quick wins. As a project manager struggles to understand what is happening within the project, there is a natural tendency to look for evidence to support predetermined ideas and reject what doesn't fit. However all evidence needs to be considered on its own terms. Reaching for the obvious explanation and thereby failing to consider viable alternatives can be avoided. Simple explanations are attractive but bring with them the risk of oversimplification. Measuring progress against the project plan can be self-deluding, particularly if the plan itself is based on considerable uncertainty and represents only what we would like to see happen.

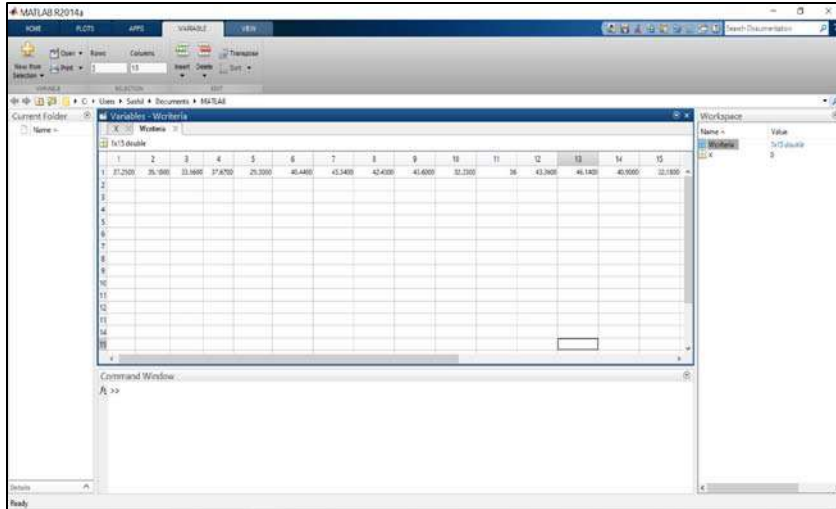


Fig. 6 W criteria

Now next it to create another variable and naming it as 'W criteria' in this as seen in Figure 6, the criteria are to be identified if they are beneficial or non-beneficial from the factors' perspectives. Beneficial criteria will have more weightage while non-beneficial. The criteria are assigned with values of IMP.I.% from Table. 4. Below Figure 8 is the illustration of how the W criteria will look alike when create in MATLAB

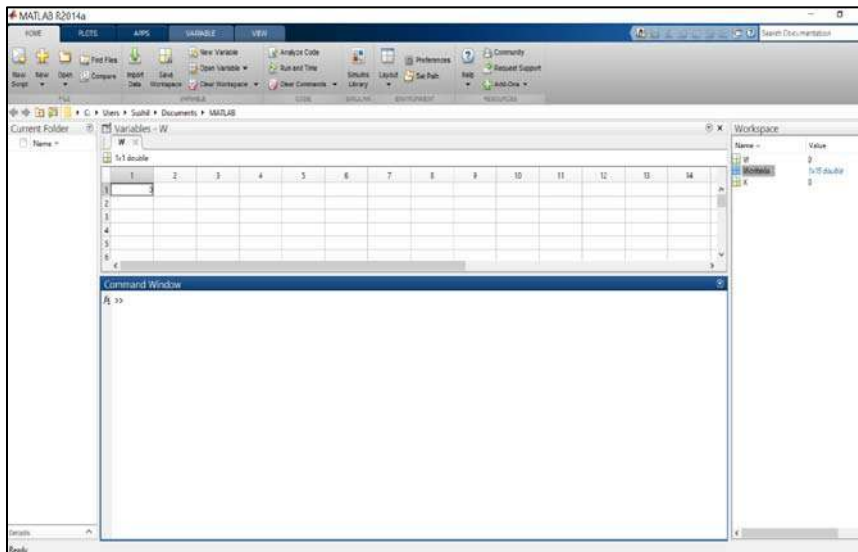


Fig. 7 Command window

The codes are set in command window to generate the model as shown in Fig. 7 illustrates the command window where the codes are to be designed. When the codes are entered the 'Enter' command is given which produce preference codes for the attributes of decision matrix. On basis of preference codes, the alternatives can be ranked with respect to the factors inclination.

The values of preference codes ultimately decide the ranks for the alternatives. The codes with highest ranks are the alternatives of lower fondness and the codes with lowest ranks can be higher preferences. A course of action is selected which will reduce the threat and evaluate a range of possibilities considering undesirable side-effects as well as the benefits.

### Codings

Codes for MATLAB interface

```
Xval=length(X(:,1));
for i=1:Xval
for j= 1:length(W)
if Wcriteria(1,j)== 0
Y(i,j)=min(X(:,j))/X(i,j);
else
Y(i,j)=X(i,j)/max(X(:,j));
end
end
end
```

```
end
for i=1:Xval
PWSM(i,1)=sum(Y(i,:).*W);
PWPM(i,1)=prod(Y(i,:).^W);
end
lamda=0.5
J=lamda*PWSM+(1-lamda)*PWPM;
Joint_generalized_criterion = num2str([J])
```

### ***Discussions***

The existing research in the domain of uncertainty engineering applies either numerical values of probability and impact, or worked with classical sharp jurisdiction of these values into certain sets for which many applications are not appropriate and did not correspond to the actual perception of cause. MCDM approach to modelling these processes minimizes these shortcomings. In MCDM technique using MATLAB, the model generated provides with preference codes which ranks the alternative with due consideration of their factors affecting optimization. The preference codes with higher value indicates the maximum affecting factors for that alternative. The preference codes with that of lower values indicates minimal affecting factors for alternatives. This procedure eases the decision makers to decide which alternatives are to be preferred and which alternative cannot be feasible; and further work over the factors which are obstructing the current situations optimization that remained unnoticed in initial stage of construction project. This technique nearly diminishes the factors causing uncertainty or any another aspect which tries to disturb the execution of construction project. Future research may look in more detail at uncertainty management processes, such as risk management planning, identification, measurement, prioritization, monitoring and control.

### **CONCLUSIONS**

There is always an uncertainty that prevails in the project which does not allow the decision maker to give an accurate data. So, the project manager needs to understand the exact source and root cause of the uncertainty, so that proper strategies can be employed to mitigate it. In this work various factors causing uncertainties in construction projects were identified from the experienced based data collected and literature review. These factors were analyzed by calculating probability causing uncertainties in construction projects by using Importance index method. Based on ranks obtained from the importance index the most important causes of uncertainty that affects execution of construction projects were identified. A MCDM model is developed using MATLAB software as a platform to simulate uncertainties. The developed model can be utilized by the construction practitioners like contractors, consultants and clients while critical decision making.

The model provides a probability distribution that allows the decision maker to select the project duration using the cumulative probability distribution based on the decision maker's risk aversion.

### **SUMMARY**

The entire study is about two main objectives:

- 1) Detecting and analyzing various factors and groups of factors causing uncertainties in construction projects based on their probabilities of impact calculated using importance index method.
- 2) To develop decision making model to determine actual uncertainty considering uncertain factors characterized by construction projects using Multi criteria decision making.

### **REFERENCES**

- Bennett, F.L., (2003). The Management of Construction: A Project Lifecycle Approach. Oxford: Butterworth Heinemann.
- Brauers, W.K. (1986) Essay Review Article: Risk, Uncertainty and Risk Analysis. Long Range Planning, Vol. 19, No. 6, pp.139-143.
- Chapman, C., Ward, S. (2002) Constructively simple estimating: a project management example, Journal of the Operational Research Society, Vol. 54, No. 10, pp. 10
- Daji, G., and Reiar, H. (1993). "Time uncertainty analysis in project networks with a new merge-event time-estimation technique." Int. J. Project Manage., 11(3), pp. 165–173.
- Del Cano, A. and Pilar de la Cruz, M. (2002) Integrated Methodology for Project Risk Management, Journal of Construction Engineering and Management, Vol. 128, No. 6, pp. 473-485.

- Francis, A., Bibai, J., and Miresco, E. T. (2013). "Simulation of scheduling logic using dynamic functions." *Manage. Procurement Law*, 166(3), pp. 145–158.
- Ghanim, A. B. (2014), "Study of Causes & Magnitude of Wastage of Material on Construction sites in Jordan", *Journal of Construction Engineering*, Volume (2014), pp. 1-6.
- Grubbs, F. F. (1962). "Attempts to validate certain PERT statistics." *Oper. Res.*, 10, pp. 912-915.
- Hafida Lmoussaoui and Hicham Jamouli "A decision support methodology for assessment of construction project risks", *International Journal of Applied Engineering Research* ISSN 0973-4562, 11(15), pp. 8743-8753
- Halpin, D., and Riggs, L. (1992). *Planning and analysis of construction operations*, Wiley, New York.
- Han, S., Lee, S., Golparvar-Fard, M., and Pe ña-Mora, F. (2007). "Modeling and representation of non-value adding activities due to errors and changes in design and construction projects." *Proc., 39th Winter Simulation Conf.*, S. G. Henderson, et al., eds., Institute of Electrical and Electronic Engineering, Piscataway, NJ, pp. 2082–2089.
- Lu, M., and AbouRizk, S. M. (2000). "Simplified CPM/PERT simulation model." *J. Constr. Eng. Manage.*, 10.1061/(ASCE)0733-9364(2000) 126(3), pp. 219–226.
- MacCrimmon, K. R., and Ryavec, C. A. (1964). "An analytical study of the PERT assumptions." *Oper. Res.*, 12(1), pp. 16–37.
- Malcolm, D. G., Roseboom, J. H., Clark, C. E., and Fazar, W. (1959). "Applications of a technique for research and development program evaluation." *Oper. Res.*, 7(5), pp. 646–669.
- Martinez, J. C., and Ioannou, P. G. (1997). "State-based probabilistic scheduling using STROBOSCOPE's CPM add-on." *Proc., Constructions Congress V*, S. D. Anderson, ed., ASCE, Reston, VA, pp. 438–445.
- Murray, J. E. (1963). "Consideration of PERT assumptions." *Eng. Manage.*, 10(3), pp. 94–99.
- Pritsker, A. B. (1995). *Introduction to simulation and SLAM II*, Wiley, New York, pp. 723–759.
- Sadi, A. A. and Sadiq Al-Hejji. (2006), "Causes of Delay in Large Construction Projects", *International Journal of Project Management*, 24(2006), pp. 349-357.
- Smith, N.J. (2003) *Appraisal, Risk and Uncertainty*. Thomas Telford Ltd., London, pp. 13-87.
- Snyder, L.V. (2005) *Facility location under uncertainty: A review*. In: Lehigh University Dept. of ISE Technical Report #04T-015 (accepted to publish in IIE Transactions).
- Westland J., (2006) "Project Management Life Cycle: A Complete Step-by-step Methodology for Initiating Planning Executing and Closing the Project", Kogan: Page Limited
- Zopounidis, C., and Doumpos, M.: 'Multicriteria Decision Aid Classification Methods' (New York, Springer, 2002).

## Evaluation of Worker Performance in Construction Project Using Six Sigma

Tanwar Saif,<sup>1</sup> R. B. Magar,<sup>2</sup> and Abdul Razak Honnutagi<sup>3</sup>

<sup>1</sup> PG Student, Department of Civil Engineering, Kalsekar Technical Campus, School of Engineering and Technology, New Panvel, Maharashtra, India. email: [saiftanwar@gmail.com](mailto:saiftanwar@gmail.com)

<sup>2</sup> Professor and Head, Civil Engineering Department, Kalsekar Technical Campus, School of Engineering and Technology, New Panvel, Maharashtra, India. email: [rajendramagar69@gmail.com](mailto:rajendramagar69@gmail.com), Corresponding Author

<sup>3</sup> Director, Civil Engineering Department, Kalsekar Technical Campus, School of Engineering and Technology, New Panvel, Maharashtra, India. email: [director.aiktc@gmail.com](mailto:director.aiktc@gmail.com)

### ABSTRACT

The main objective of this work is to evaluate worker performance index to improve construction productivity and practical solutions for construction performance improvement by applying the six-sigma technique. Construction productivity and performance improvement are vital focus areas in construction industry. Many researchers have experimented to improve project performance using various techniques such as lean principle, just in time, pull scheduling, and last planner. However, it is being observed that construction industry has witnessed a considerable decline in construction productivity in relations of both labour and organization subjects. Based on site observation, questionnaire survey, interviews and examining existing worker performance system. The finding shows that the managerial level and supervisors plays key role in improvement of worker performance. Worker performance index WPI is used to portion the worker presentation quantitatively for planning and execution phase of any construction process and worker productivity thereby improving overall performance through the evaluation of the performance in construction practices. Further Six-sigma technique is used to validate and advance the construction act and worker performance during construction execution phase. Managers and supervisors need to follow the management factors which is been recommended after the analyses done to advance the worker act and productivity of construction projects Thus, in this work, on basis of sigma level obtained, it can be concluded that WPI model proves to be successful for obtaining the suitable worker for a construction project with minimum defects with respect to their performance.

**Keywords—** *Worker Performance, Construction Productivity, Performance Management*

### INTRODUCTION

The success of every organization depends on its employee productivity and their performance. Workforce is the main component in the construction industry, which makes up 33-50% of the total project cost. (Hanna *et al*, 2001). Hence Improve overall efficiency construction industry. Construction industry today, is lacking a proper application of the performance management techniques. Due to lack of standard methods, every organization follows their own management factors to overcome or improve the worker productivity. This work Introduce the concept of employee performance measurement tools to increase productivity in construction. Worker performance is evaluated to overcome the low productivity of workers in construction projects while Six sigma helps to set acceptable value for worker performance index and maintain the same.

Al-Qudah (2014) suggested that analysis of appropriate human resource management (HRM) practices and confident worker behaviour as well as worker fulfilment, loyalty shall be done. The employees shall be considered as precious asset, which improves their self-confidence and loyalty which results in good quality and high performance.

Bernardin and Beatty (1984) defined record performance of the results of a particular business function, activity or behaviour for a certain period of time. Defining performance was considered a critical part of the performance management system, which performance standards that correspond to pre-designed levels of individual and organizational effectiveness. Borman (1991), Cardy and Dobbins (1994) and Heneman (1986) remarked that the S.M.A.R.T. (Specific, Measurable, Achievable, Realistic, Time bound) technique shall be used for performance evaluation of the employees by a fair, unbiased, and business-relevant basis. Cleveland *et al*. (1992) defined measurement of performance as a tool which reflects an employee's actual job performance levels in which accuracy should be the primary goal of appraisal system adopted. A fair performance appraisal system additionally helps the organisations to motivate employees. By providing financial incentives, it helps to motivate employees and makes them display an additional commitment within the organization and non-financial motivation can be achieved by only if further characters and responsibilities; it benefits the staff to own a good nationality behaviour that assistances them to give an additional input and extend their productivity (Kuppusamy, 2014).

The main purpose of an employee's performance measurement tool is to improve employee productivity by analyzing current performance levels. A Worker Performance Index (WPI) will help as a common assessment method construction management team (CMT) Additionally, select more details about the robot. The system collects system buyer collections systematically (Gannoruwa and Ruwanpura, 2008). Furthermore, Developing the method of benefit for free, will continue promptly or promptly and contribute as a better business, or an adjusting process of administration. (i.e. providing them training, replacing foreman etc.) This help builders get informed judgments about their workforce. By knowing the WPI of a certain worker, the CMT Is it possible to predict employee work before giving the site responsibility? A rating as well as expects to create a competitive environment for employees. This can also be used as a basis for salary, incentives, career advancement, and training program recommendations (Tumla, 2010). Despite many attempts, development of standard measuring scheme for productivity measurement (Park *et al.*, 2005 and Oglesby *et al.*, 1989). Rojas and Aramvareekul (2003) and Liberda *et al.* (2003) divided into human, management and external categories. The construction sector can have a greater impact on management. Pre-construction planning and business planning management and effective methods for influencing human categories Tumla (2010) used 16 performance evaluation factors for builders. These Factors, supervisors and the senior management. Factors, safety, quality, punctuality. There is no universal definition of employee job satisfaction that covers all views of specific job factors, individual characteristics and group relationships with co-workers at the same time. However, there are some definitions that are widely accepted like job satisfaction Performing and implementing accounting functions from their jobs (Huber, 2006).

Pheng and Hui (2004) stressed that strategies and concepts of Six Sigma shall be examined and applied to the construction industry to explore whether it can be beneficial to the organizations that implement it successfully. Sawant and Pataskar (2014) explained that, Six Sigma is a method of quality improvement implemented in manufacturing and other industries. Six-Sigma is a new construction industry. They describe the main theory, principles, methodology and various tools used by Six Sigma. Harry and Schroeder (2000); Pande *et al.* (2000) and Eckes (2001) highlight some key ideas can be drawn from the Six Sigma Roadmap. The steps to an ideal roadmap for establishing the Six Sigma system and launching improvements are to 1. Create and agree on strategic business objectives; 2. Identify key customers, core, key sub- and enabling processes, and owners of these processes; 3. Define customer requirements; 4. Measure current performance; 5. Prioritize, analyse, and implement improvements; and 6. Expand and integrate the Six Sigma system.

Pettijohn and D'Amico, (2001) showed that clear, concrete, and comprehensive feedback, compared to the estimated increased feedback, feedback, made it possible to more accurately assess the likelihood of success, ultimately contributing to fairness and productivity, allowing you to accurately assign past results.

Petri (1991) suggested a method of stimulating employees by effective motivation, which makes staff happier and committed to their jobs. There are different incentives and time unit policies which might conjointly function as motivators. Motivation is essential for work, because it gives satisfaction to workers at a site such as achievement, a sense of responsibility (Enshassi *et al.*, 2007). When employees are satisfied with their work, they will automatically commit themselves to their work. Making workers feel that they are citizens of the organization and consequently each one of these factors can facilitate them to increase their productivity (Kuppusamy, 2014).

Ahmed and Hussain (2010) reported that a better performance appraisal (PA) system integrated with better human resources practices will improve employee satisfaction and increase employee satisfaction and reduce the intentions of the craft to deliver efficiency in organizations. The above cited literature reviews the key elements of PM and summarizes the conceptual foundation of interlink between PM practices and job satisfaction, organizational commitment and individual behaviour, that affects the employee productivity. Performance management being the crux of HRM, many academics and practitioners believe that good sound quality results in a better level of job satisfaction, which ultimately improves organizational performance (Appelbaum *et al.*, 2000).

Zannah *et al.* (2017) revealed the five most significant causes of the performance of low-skilled workers in the Nigerian construction industry. These are: low wages, lack of adequate skill acquisition centers, lack of incentive schemes, vulnerability to health and safety services, and lack of standard pay scales for skilled workers. Therefore, there is a need to reduce the listed causes of low-skilled worker performance in order to improve their performance by various means in order to achieve successful delivery of construction projects. in the Nigerian Construction Industry. Poovitha *et al.* (2018) concluded that the most significant factors affecting performance management and appraisal are Performance Factors, Behavioural Factors, Grading System, Personal Effectiveness and Social Factors. Employees should perform on these factors to enhance performance which ultimately can help to get higher profits from the projects

Construction industry today, is lacking a proper application of the Quality management techniques. Though several techniques are developed by the researchers, their practical application, validation and reliability is still not properly documented. Worker performance management is the biggest challenge today in construction industry. Improper management may lead to low quality construction, over-budgeting, delay in construction work and so on. Hence, a proper method needs to be formulated in accordance to improve worker performance on site, such that the ultimate output of the project is achieved within the specified time and the planned cost, see Fig.1

## RESEARCH METHODOLOGY

- To develop management factor for evaluation of worker performance in construction projects.
- Grouping parameters according to the managerial level or supervisors' level.
- Application of WPI conceptual model based on management factors for evaluation of worker performance.
- Application of six-sigma on data obtained to improve worker performance.
- Assigning sigma level according to DPMO.

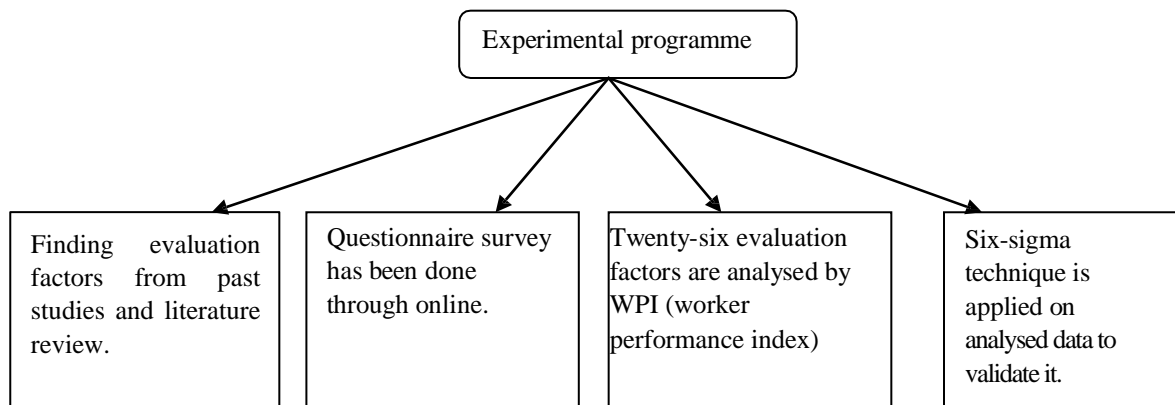


Fig. 1 Experimental programme

### Methodology

Initially it has the method and design used to conduct research. This is a quantity of data collected by a questionnaire. The technique for modeling and modeling was revised by customers, contractors, engineers and experts. There was a set of primary and secondary data. Primary data is collected from secondary data literature and query recordings. In addition, this chapter provides a variety of questions and answers to questions. The research selected for this study, serious literary analysis, mailing questionnaire, a conceptual model of WPI (worker performance index) and also to measure the performance of the same using six sigma technique.

### Evaluation of WPI

The same functions as the file types used for access also always work on the server. The base directory is the same as the language used. Note that this is the same as in your home directory. The folder folder name will be the same as the folder. By default, to change WPI settings, the main menu must reset the current password to the current one. Memory - This option controls the remote access server to control the menu key. (i.e. Likert), consequently, the factor is quantified. Controllability.

- Management Factors:** It evaluates employee records related to management procedures. It consists of employee attendance, punctuality and security records that are common to all employees. Factor score for management (FSMgmt) after the result, the subcomponent is total Likert values under that factor. shown in Table 1.

Table 1. Management Factors evaluation (Siriwardana, & Ruwanpura, 2012)

Sr no.	Management Factors (FSMgmt)
1	Attendance
2	Punctuality
3	Safety Record

$$FS_{Mgmt} = \sum(SC_{Mgmt1} + SC_{Mgmt2} + SC_{Mgmt3}) \quad \text{Eq. (1)}$$

- Supervisor's Assessment:** Immediate foreman to use their skills to evaluate each employee (ability to learn and

ability to work on own), Oral communication skills, team spirit and finally the overall recommendation of the employee supervisor. This assessment will provide feedback to the next supervisor who handles the employee's current performance. To minimize personal effects, reduce subjective considerations, and maintain fairness for all employees, immediate superiors must reassert the foreman's assessment. The criteria for assessing the supervisor must also be available to employees to ensure a fair and transparent assessment. In a similar process, factor score for Supervisors Assessment (FSSup) is obtained after totalling subcomponent Likert values under that factor shown in Table 2.

**Table 2. Supervisor's Assessment evaluation (Siriwardana, & Ruwanpura, 2012)**

Sr no.	Supervisor's Assessment (FSSup)
1	Attaining targets
2	Superiority of work
3	Arrogance and self-confidence
4	Management potential
5	Knowledge potential
6	Spoken communication skills
7	Line-up work
8	General approval

$$FS_{Sup} = \sum(SC_{Sup1} + SC_{Sup2} + \dots + SC_{Sup8}) \quad \text{Eq. (2)}$$

c) **Motivation Level Factors:** This evaluation is a change in the work Gannoruwa and Ruwanpura (2008). In Expectancy Theory, motivation is defined as a function of expectancy, instrumentality and valence. Expectancy (EP) - expectancy is a man who believes that he has led his labor to work. Instrumentality (PO) is the belief that better performance leads to more results or output. Valence (V) - Valence describes the strength with which workers appreciate the results or outputs of their personal performances. Factor score for motivation (FSMo) is calculated by the theory developed by Vroom (1964). Effort to Performance (EP) - Value is obtained by taking the average Likert value of the subcomponents under Effort to Performance category under Motivation Factor in Table 3.

**Table 3. Motivational Level Factor (modified from Hewage et al. 2011)**

Sr no.	Motivational Level Factors (FSMo)
1	<b>Effort to Performance (SAEp)</b>
1.1	Fairness in treating
1.2	Justice
1.3	Language styles
1.4	Sense of in-group
1.5	Accessibility of instruction
1.6	Assembly attachment
2	<b>Performance to Outcome (SAPo)</b>
2.1	Fairness (in reward setting)
2.2	Group construction
2.3	Gang work
2.4	Work performance link with outcome
2.5	Emotional strength of foremen
3	<b>Valence (SAv)</b>
3.1	Impartiality of reward (extrinsic and intrinsic)
3.2	Making extra money
3.3	Meaning of incentives
3.4	Performance according to outcome

Total score for Motivation Factors (FSMo) is given by,

$$FS_{mo} = \sum(SA_{Ep} + SA_{Po} + SA_v) \quad \text{Eq. (3)}$$

Worker Performance Index (WPI) is calculated by totaling all factor score values.

$$WPI = FS_{Mgmt} + FS_{Sup} + FS_{Mo} \quad \text{Eq. (4)}$$

**Validation using six sigma technique**

The next process is to validate the work of the worker performance index using Six Sigma Analysis. The worker performance is filtered from initial three filtration steps is termed as worker performance index. To verify and set a standard WPI for the workers to perform well, six sigma technique would be applied on his previous similar kind of performance. Defect measurement sheet would be generated in which the observed defects of the project would be marked. The defect also includes the time parameters. These defects would be quantified using six sigma equations and tables. Defect per Million Opportunity (DPMO) is calculated on the observed data collected, using Eq. 5(Han *et al.* 2008).

$$DPMO = \frac{(No.of Defects in data assessment sheet)}{No.of Opportunities of defects \times No.of Units} \times 1,000,000 \quad \text{Eq. (5)}$$

Based on DPMO, using sigma conversion as shown in Table 4, the sigma level is calculated for the workers.

**Table 4. Overview of Sigma Levels & DPMO (Chowdhury 2001)**

Yield	DPMO	Sigma Level
69.2	3,08,000	2
93.3	66,800	3
99.4	6,210	4
99.98	320	5
99.9997	3.4	6

On the Basis of Sigma Level attained by the worker, the worker performance would be verified using WPI. A relationship can be obtained between both the Performance Management Techniques using the Validation process.

**RESULTS AND DISCUSSION**

**Findings from WPI**

From 54 responses received, the worker performances were evaluated. On the basis of Likert scale, WPI was allotted to worker and as per Weighted Scale, relative weight was set for each worker. Thus, it can be stated as Higher the WPI Value of worker, higher will be the performance. The Average WPI of 54 workers according to evaluated factors is shown in Table 5.

**Table 5. Average WPI Of Workers**

Sr no.	Evaluation factors	Attributes	Average WPI of workers.
1	Management factor	Attendance	3.1
2		Punctuality	
3		Safety Record	
4	Supervisor’s Assessment evaluation	Attaining targets	3.3
5		Superiority of work	
6		Arrogance and self-confidence	
7		Management potential	
8		Knowledge potential	
9		Spoken communication skills	
10		Line-up work	
11		General recommendation	
A	Motivational Level Factors	<b>Effort to Performance (SAEp)</b>	3.3
12		Fairness in treating	
13		Justice	
14		Language styles	
15		Sense of in-group	
16		Accessibility of instruction	
17		Group attachment	
B		<b>Performance to Outcome (SAPo)</b>	
18		Fairness (in reward setting)	
19		Group construction	
20	Gang work		

21		Work performance link with outcome
22		Emotional strength of foremen
C		<b>Valence (SAv)</b>
23		Impartiality of reward (extrinsic and intrinsic)
24		Making more money
25		Meaning of incentives
26		Performance according to outcome

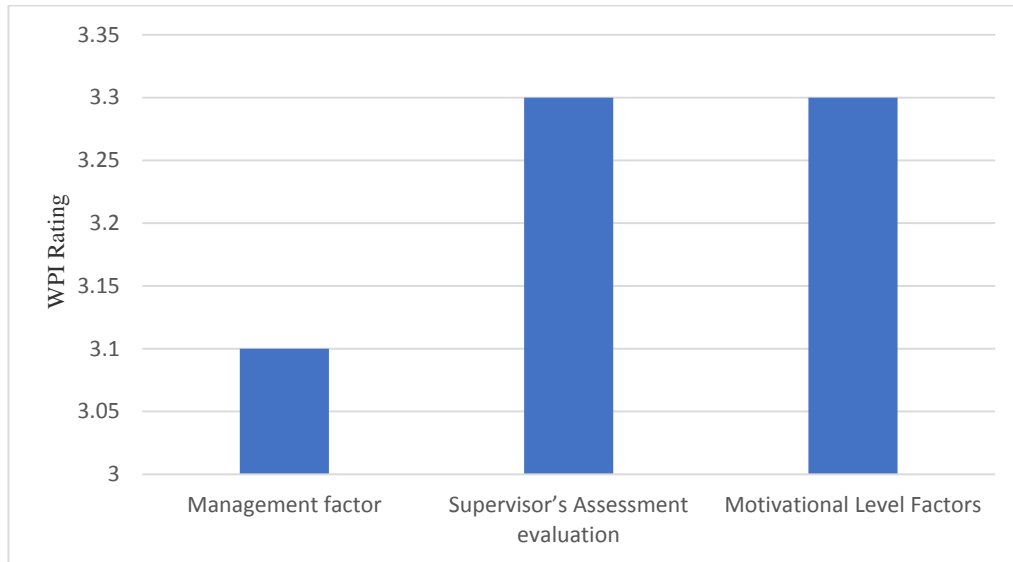


**Fig. 2 Average WPI of Workers.**

The success of every organization depends on its employee productivity and their performance. There was need to quantify the performance of the worker. Table 5 and Fig. 2, shows the average worker performance index of 54 workers where, WPI on the basis of management factors was 3.1 and that of supervisor's assessment factors and motivational level factors was 3.3 each.

**Findings from Six Sigma Model**

The defects in performance of workers was validated. The worker scored rating 1 and 2 on Likert scale was considered as defects, where 1 stands for very poor performance and 2 stands for poor performance. The observed defect measurements were converted to DPMO as shown in Table 6. The Sigma Level observed based on DPMO was 4.88. Since This fault calculation included a time-delayed parameter during the assessment, it was seen that the time of implementation of the project was completed within the stipulated time. Thus WPI is also capable of overcoming management issues in construction projects.

**Table 6. Sigma Level Calculation**

Sr no.	Evaluation factors	No. of Units Observed	Defects observed in Assessment Sheet	Opportunities	DPMO	Six-sigma
1	Management factor	Attendance	12	54	986.193	4.88
2		Punctuality	15	54		
3		Safety Record	15	54		
4	Supervisor's Assessment evaluation	Attaining targets	17	54		
5		Superiority of work	13	54		
6		Arrogance and self-confidence	15	54		

7	Motivational Level Factors	Management potential	16	54					
8		Knowledge potential	17	54					
9		Spoken communication skills	19	54					
10		Line-up work	14	54					
11		General recommendation	15	54					
<b>A</b>		<b>Effort to Performance (SAEp)</b>							
12		Fairness in treating	15	54					
13		Justice	14	54					
14		Language styles	17	54					
15		Sense of in-group	12	54					
16		Accessibility of instruction	16	54					
17		Group attachment	16	54					
<b>B</b>		<b>Performance to Outcome (SAPo)</b>							
18		Fairness (in reward setting)	14	54					
19		Group construction	14	54					
20		Gang work	14	54					
21		Work performance link with outcome	8	54					
22		Emotional strength of foremen	18	54					
<b>C</b>		<b>Valence (SAv)</b>		54					
23		Impartiality of reward (extrinsic and intrinsic)	15						
24		Making more money	13	54					
25		Meaning of incentives	11	54					
26		Performance according to outcome	15	54					
<b>Total</b>		<b>26</b>	<b>360</b>	<b>1404</b>					

Many studies have been conducted on WPI but yet no margin or minimum acceptable value of WPI was established. Thus there was need to implement six sigma technique to set a acceptable value of WPI. Table 6 shows the defects in the worker performance with respect to their opportunities factors and subcomponent of the factors. Using Eqn 5 DPMO was calculated as shown in Table. 6. Thus using the DPMO value & Table. 4 sigma level was obtained as 4.88. which indicates the WPI rating is not acceptable.

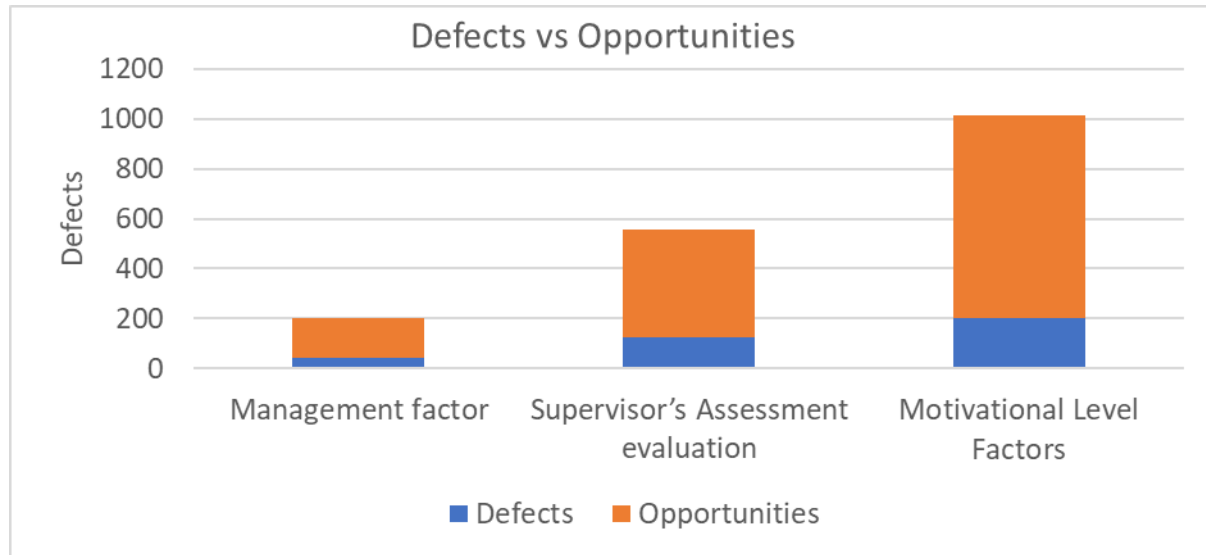


**Fig. 3 Defects vs Opportunities**

Fig. 3 shows the defects with respect to opportunities where, bar in blue denotes the defects from the total opportunities of their respected factors. It can be seen that from the management factor point of view, the workers are showing less defects, whereas, on the supervisor's assessment and motivational level front, the workers display very high defects. Hence, we can conclude that shows that these two factors affect the worker performance and construction performance and hence need to be strictly monitored.

## CONCLUSIONS

The situation of the workers is presented in this paper considering the administration, the evaluation of the supervisor and the level of motivation to evaluate the desertion of the workers. The proposed evaluation format of WPI is capable of generating data based on workers' performance indicators. Therefore, this information can be used to perform in-depth analyzes and to compare and contrast different categories of workers. The evaluative evaluation of the WPI concept in the identification of different structured groups was also considered. In addition, this concept can be extended to represent the performance levels of the group of workers. The authorities firmly believe that this method can be used to create a base for the production of workers with the results obtained. In addition to the planning, it is possible to analyze the monitoring of the individual trainees, as much as possible, at the end of identifying the critical situations at the same time and taking into account the corrective measures of the sea. The possible limits identified in this case included the opposition of the unions and the difficulties when large working groups were applied.

Six sigma results reveal that the performance of workers was unacceptable due to their low WPI. Thus, if a benchmark is set for comparing the number of defects assessed and number of opportunities to assess the defects, the WPI level of workers can be improved. Sigma level can also give acceptable WPI value of the worker performance for the future projects. Thus, in this research work, on basis of sigma level obtained, it can be concluded that WPI model proves to be successful for obtaining the suitable worker for a particular construction project with minimum defects with respect to performance.

## SUMMARY

The entire study is about improving worker productivity and performance in construction project in terms of quality, productivity, job satisfaction etc. This can be done by selecting the appropriate project consultant, such as project managers and supervisors. Studies show that workers are preferable to implementing the project to work at low wages, which often affects the schedule and quality of the schedule. In this way, this study examines the worker's performance by focusing on the selection of qualified employees by WPI model, so that the project execution can be carried out appropriately considering effective productivity and economic construction. Also, this study is accompanied with the validation of the WPI model by using Six Sigma Analysis. Thus, using Six Sigma analysis sigma level of the workers can be predicted, and on basis of this prediction the performance of workers can be

improved for the future projects. Using these techniques, a thorough analysis of workers' performances was done based on the Six-sigma assessment.

## REFERENCES

- Al-Qudah, H.M. et al (2014) 'The Effect of Human Resources Management Practices on Employee Performance'. International Journal of Scientific & Technology Research, 3(9).
- Bernardin, H. J. and Beatty, R. W. (1984) Performance Appraisal: Assessing Human Behaviour at Work. Boston: Kent Publishing Company.
- Borman, W. C. (1991) 'Job behavior, performance, and effectiveness'. In Dunnett, M. D. and Hough, L. M. (Eds.), Handbook of industrial & organizational psychology (2nd ed., 2:272-326). Palo Alto, CA: Consulting Psychologists Press, Inc.
- Cardy, R. L. and Dobbins, G. H. (1994) Performance Appraisal: Alternative Perspectives. Cincinnati, OH: South Western Publishing Company.
- Cleveland, J. Et al (1992) 'Analysing performance appraisal as goal-directed behaviour'. In Ferris, G. and Rowland, K. R. (Eds.), Research in personnel and human resources management. Greenwich: JAI Press.
- Heneman, R.L. (1986) 'The relationship between supervisory ratings and results-oriented measures of performance: A meta-analysis'. Personnel Psychology, 39:811-826.
- Gannoruwa, A., Ruwanpura, J.Y. (2008). "Development of an efficiency model for optimum construction productivity through effective supervision on worker performances". Proceedings of the CSCE Annual Conferences, Quebec City QC
- Tumla Shesta (2010) "Developing performance-based reward model for construction workers to improve construction productivity." M.Sc. Dissertation, Department of Civil Engineering, The University of Calgary at Alberta, Canada.
- Vroom, V. H. (1964). "Work and motivation". Wiley, New York.
- Park, H. S., Thomas, S. R., and Tucker, R. L. (2005), "Benchmarking of construction productivity", Journal of Construction Engineering and Management, 131(7), 772-778.
- Productivity Alberta (2011), "Productivity Builds". <http://www.productivityalberta.ca/articles/114/productivity-builds> (Nov. 2, 2011)
- O'Brien, K.E. (1985). "Improvement of on-site productivity". K.E. O'Brien and Associates Inc., Toronto, Ontario.
- Oglesby, C.H., Parker, H.W., and Howel, G.A. (1989). "Productivity improvement in construction". McGraw Hill, New York, NY.
- Rojas, M., and Aramvareekul, P. 2003. "Labor productivity drivers and opportunities in the construction industry." J. Manage. Eng., 192, 78–82. Statistics Canada (2011)., "Canada Year Book 2011- Chapter six Construction." <http://www.statcan.gc.ca/pub/11-402-x/2011000/pdf/constructioneng.pdf> (Nov. 2, 2011)
- Liberda, M., Ruwanpura, J., and Jergeas, G. (2003). "Construction productivity improvement: A study of human, management and external factors". Proceedings of the American Society for Civil Engineers, Construction Research Congress, Honolulu, Hawaii, USA.
- Pheng, L. S., & Hui, M. S. (2004). Implementing and Applying Six Sigma in Construction, (August), 482–489.
- Sawant, S.P., Pataskar, S.V. (2014), "Applying Six Sigma Principles in Construction Industry for Quality Improvement", ICAET.
- Pande, P. S., Neuman, R. P., and Cavanagh, R. R. ~2000. The Six Sigma way: How GE, Motorola and other top companies are honing their performance, McGraw-Hill, New York.
- The CIDB construction quality assessment system, Singapore. Eckes, G. ~2001. The Six Sigma revolution: How General Electric and others turned processes into profits, Wiley, New York.
- Harry, M., and Schroeder, R. ~2000. Six Sigma: The breakthrough management strategy revolutionizing the world's top corporations, Doubleday, New York.
- Pettijohn, C.E. et al (2001) 'Characteristics of performance appraisals and their impact on sales force satisfaction'. Human Resource Development Quarterly, 12(2): 127-146.
- Herbert, L. P. (1991) Motivation: Theory, Research and Applications (3rd. Ed.). Belmont, California: Wadsworth Inc.
- Enshassi, A.; Mohamed, S.; Abushaban, S. 2009. Factors affecting the performance of construction projects in the Gaza Strip, Journal of Civil Engineering and Management 15(3): 269–280.  
<http://dx.doi.org/10.3846/1392-3730.2009.15.269-280>
- India. N.S.D.C report (2009) 'Human resource and Skill requirement in the building and real estate services. New Delhi: National Skill Development Corporation Office.
- Huber, D. L. (2006). Leadership and Nursing Care Management (3rd ed.). Philadelphia: Elsevier Saunders.
- Deepa.E, and Kuppasamy.S. Impact of Performance Appraisal System on Job Satisfaction, Employee Engagement,

- Organizational Citizenship Behavior and Productivity Indian Journal of Applied Research, Vol.IV, Issue. II  
2014
- Ahmed, A., Hussain, I., Ahmed, S., & Akbar, M. F. (2010). Performance appraisals impact on attitudinal outcomes and organisational performance. *International Journal of Business and Management*, 5(10), 62-68.
- Appelbaum, E., Bailey, T., Berg, P., & Kalleberg, A.L. (2000). *Manufacturing advantage: Why high-performance work systems pay off*. London: ILR Press.
- Siriwardana, C. S. A., & Ruwanpura, J. Y. (2012). A conceptual model to develop a worker performance measurement tool to improve construction productivity. In *Construction Research Congress 2012: Construction Challenges in a Flat World, Proceedings of the 2012 Construction Research Congress*. <https://doi.org/10.1061/9780784412329.019>
- Hewage, K.N., Gannoruwa, A., and Ruwanpura, J.Y. (2011). "Current status of factors leading to team performance of on-site construction professionals in Alberta building construction projects." *Canadian Journal of Civil Engineering*, 38: 679–689
- Chowdhury, S. ~2001. *The power of Six Sigma: An inspiring tale of how Six Sigma is transforming the way we work*, Financial Times/Prentice- Hall, London.
- Zannah, A. A., Latiffi, A. A., Raji, A. U., Waziri, A. A., & Mohammed, U. (2017). Causes of Low-Skilled Workers' Performance in Construction Projects. *Path of Science*, 3(6), 4.1-4.15. <https://doi.org/10.22178/pos.23-7>
- R.Poovitha, D.Ambik, B.Lavanya. (2018). A REVIEW ON PERFORMANCE MANAGEMENT AND APPRAISAL IN, 1012–1015.

## A REVIEW ON THE IRREGULARITIES OF STRUCTURES

*Abdul Wahab Mobarez<sup>a</sup>, Babita Saini<sup>b</sup>*

Department of Civil Engineering, National Institute of Technology Kurukshetra, Haryana, India,  
 Email: [wahab.shamal0@gmail.com](mailto:wahab.shamal0@gmail.com)<sup>a</sup>, [babitasaini6@gmail.com](mailto:babitasaini6@gmail.com)<sup>b</sup> (Corresponding Author)

### ABSTRACT

Irregular structures (plan and elevation) are in demand due to functional purposes. These irregular structures are to be earthquake resistant; because, irregularities affect the seismic performance of the structures. Many research scholars have analyzed irregular buildings in elevation, plan and both elevation and plan, using different software. Few studies have been conducted on effect of shear walls, position of shear walls, holes in shear walls at various positions, bracing etc. on seismic behaviour of the irregular buildings. In the present paper a review of previous work done on irregular buildings and their seismic behaviour has been done in detail.

**KEYWORDS:** Irregular structures; seismic load; shear wall; bracing; analytical study.

### INTRODUCTION

Irregularity in building structures can be due to the irregular distribution in their stiffness, mass, strength and stiffness along with the building height. Most of the buildings are designed for wind and earthquake loads and when irregular buildings are constructed in high seismic zones or in high wind intensity zones, the analysis and design of these buildings become more complicated. Building irregularities are of different types in the structures depending on their location and scope. Table 1 shows the irregularity limits prescribed by IS 1893:2002, EC8:2004, UBC 97, NBCC 2005 and the horizontal and vertical irregularity limits as per IBC 2003, Turkish code 2007 and ASCE 7 – 05 are shown in Table 2.

**Table 1 Irregularity limits prescribed by various codes (Varadhrajan et al., 2012)**

Type of Irregularity	IBC 2003 [37]	TEC 2007 [71]	ASCE – 7.05 [5]
<b>Horizontal</b>			
a) Re-entrant corners	-	$R_i \leq 20\%$	$R_i \leq 15\%$
b) Torsional irregularity	-	$d_{max} \leq 1.2 d_{avg}$	$d_{max} \leq 1.2 d_{avg}$ $d_{max} \leq 1.4 d_{avg}$
c) Diaphragm Discontinuity	-	$O_a > 33\%$	$O_a > 50\%$ S > 50%
<b>Vertical</b>			
a) Mass	$M_i < 1.5 M_a$	-	$M_i < 1.5 M_a$
b) Stiffness	$S_i < 0.7S_{i+1}$ Or $S_i < 0.8 (S_{i+1} + S_{i+2} + S_{i+3})$	-	$S_i < 0.7S_{i+1}$ Or $S_i < 0.8 (S_{i+1} + S_{i+2} + S_{i+3})$
c) Soft Storey	$S_i < 0.7S_{i+1}$ Or $S_i < 0.8 (S_{i+1} + S_{i+2} + S_{i+3})$	$[\eta_{ki} = (\Delta_i / h_i) avr /$ $(\Delta_{i+1} / h_{i+1}) avr > 2.0$ or	$S_i < 0.7S_{i+1}$ Or $S_i < 0.8 (S_{i+1} + S_{i+2} + S_{i+3})$
d) Weak Storey	$S_i < S_{i+1}$	$[\eta_{ci} = (Ae)_i / < 0.80]$	$S_i < 0.6S_{i+1}$ Or $S_i < 0.7 (S_{i+1} + S_{i+2} + S_{i+3})$
e) Setback irregularity	$SB_i < 1.3 SB_a$	-	$SB_i < 1.3 SB_a$

**Table 2 Irregularity limits prescribed by various codes (Varadhrajan et al., 2012)**

Type of Irregularity	IBC 2003 [37]	TEC 2007 [71]	ASCE – 7.05 [5]
Horizontal			
a) Re-entrant corners	-	$R_i \leq 20\%$	$R_i \leq 15\%$
b) Torsional irregularity	-	$d_{max} \leq 1.2 d_{avg}$	$d_{max} \leq 1.2 d_{avg}$ $d_{max} \leq 1.4 d_{avg}$
c) Diaphragm Discontinuity	-	$O_a > 33\%$	$O_a > 50\%$ $S > 50\%$
Vertical			
a) Mass	$M_i < 1.5 M_a$	-	$M_i < 1.5 M_a$
b) Stiffness	$S_i < 0.7S_{i+1}$ Or $S_i < 0.8 (S_{i+1} + S_{i+2} + S_{i+3})$	-	$S_i < 0.7S_{i+1}$ Or $S_i < 0.8 (S_{i+1} + S_{i+2} + S_{i+3})$
c) Soft Storey	$S_i < 0.7S_{i+1}$ Or $S_i < 0.8 (S_{i+1} + S_{i+2} + S_{i+3})$	$[\eta_{ki} = (\Delta i / h_i) avr /$ $(\Delta i + 1 / h_i + 1) avr > 2.0$ or	$S_i < 0.7S_{i+1}$ Or $S_i < 0.8 (S_{i+1} + S_{i+2} + S_{i+3})$
d) Weak Storey	$S_i < S_{i+1}$	$[\eta_{ci} = (Ae)_i / < 0.80]$	$S_i < 0.6S_{i+1}$ Or $S_i < 0.7 (S_{i+1} + S_{i+2} + S_{i+3})$
e) Setback irregularity	$SB_i < 1.3 SB_a$	-	$SB_i < 1.3 SB_a$

Most of the irregularities are categorized into two types:

#### A-Vertical irregularities

- Mass irregularities
- Stiffness irregularities
- Strength irregularities
- Set back irregularities

#### B-Horizontal irregularities

- Asymmetrical plan –shapes
- Re –entrant corner
- Diaphragm discontinuity
- Mass discontinuity

A high –rise building is a tall building, as opposed to a low-rise building and is defined by its height. It can be used as the residential building, office building, or else other type of buildings like hotel, retail, or multiple purposes combined. A residential type high rise building is also termed as tower. block and maybe referred to as an “M.D.U.” (multiple dwelling unit). A high-rise building is also known as a sky scraper, mostly the material used for the structural system of high-rise building are reinforced concrete and steel. Most of the high-rise building have structural irregularities. The main aim of this paper is to provide the review of already published work on regular and irregular buildings designed for seismic load or wind load. Limits and criteria specified for the irregularities were defined by various codes of practice (IS 1893:1984, IS1893:2002 and ASCE 7:2005 etc.) and have been discussed briefly. Various types irregularities have been shown in figure 1(a, b, c).

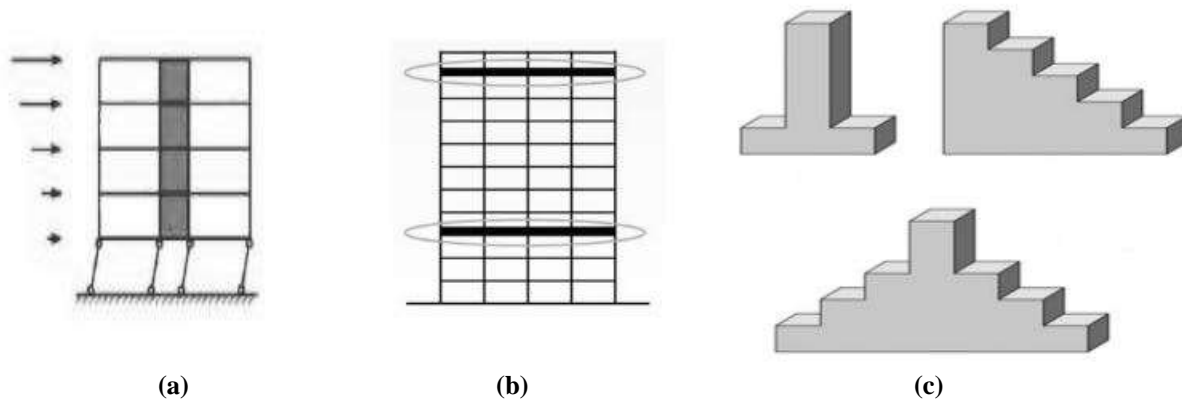


Fig. 1 (a) stiffness irregularity, (b) mass irregularity, (c) vertical geometric irregularity

### LITERATURE REVIEW

Patil et al. (2017) have done manual analysis of symmetric multi-storeyed buildings under earthquake loading. ETABS software was used for analysis which consider seismic coefficient method suggested by IS1893:2002. Analysis was done using 0.427 second of time period, 5% damping, zone 3, importance factor 1, response reduction factor 3, soil type 2 and live load  $3\text{kN/m}^2$ . From the result of manual and software analysis it was observed that both the analysis have same result; but, the base shear values were slightly higher in comparison to software analysis.

Alashker et al. (2015) analyzed real strength of structure using pushover analysis. A good tool for performing best design where the overall plan dimensions were taken as  $25\text{ m} \times 20\text{ m}$ ,  $20\text{ m} \times 16\text{ m}$ ,  $28.5\text{ m} \times 14\text{ m}$  and  $40\text{ m} \times 10\text{ m}$  with same area of  $400\text{ m}^2$ . Five storey building in which size of columns and beams were taken  $500\text{ mm} \times 300\text{ mm}$ . It has been reported that the total number of hinges increased by increasing plan aspect ratio.

Sarkar et al. (2010) have analysed 18 storey stepped building for irregularity, dynamic characteristics, weakness, strength and discontinuities in stiffness. The building was designed with equal bays; but, only step height and width were different. IS 1893:2002 and ASCE 7:2005 were used for the analysis of the stepped building. From the analysis the authors proposed partial formula for stepped building to determine the fundamental time period by modification of empirical formula which has been specified in code. It has also been shown that empirical formula for fundamental time period was a function of regularity index. Fig. 2 shows the vertical geometric irregularity according to (a) IS 1893:2002 and (b) ASCE 7:2005.

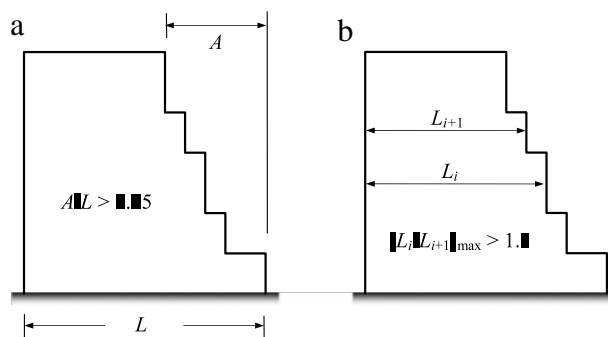


Fig. 2. Vertical geometric irregularity according to (a) IS 1893:2002 and (b) ASCE 7:2005.

Gokdemir et al. (2013) analyzed 3D 10 storey building frames using ETABS (2015). Size models were 35.5m and analyzed as per IS 1893:2002. One model was of regular plan and in the five models irregularity was introduced by varying plan shapes keeping area same. It has been reported that with the increase in number of modes, period of modes of vibration decreased and frequencies of modes increased. Fig 3 shows the regular and irregular building types, Fig 4 shows the failure of irregular structures and fig 5 shows Irregular building plans and recommendation.

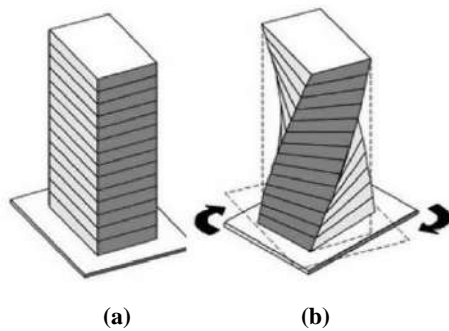


Fig. 3 (a) Regular building and (b) Irregular building



Fig. 4 Failure of irregular structures

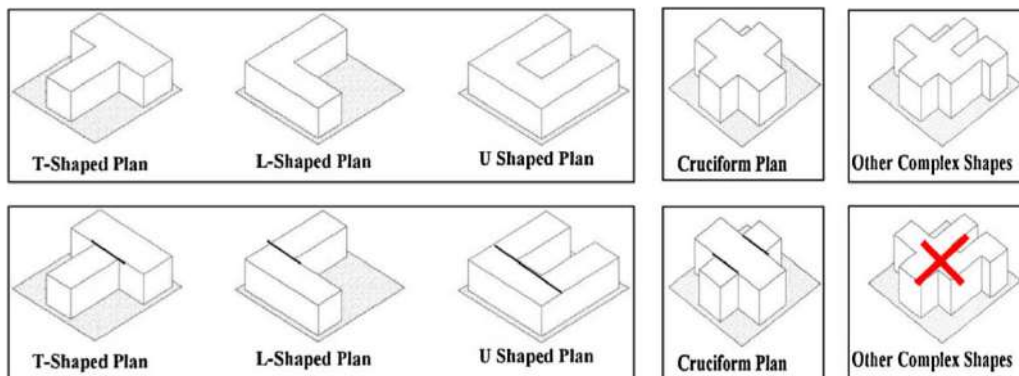


Fig. 5 Irregular building plans and recommendation

Khan and Dhamge (2016) have studied a G+10 residential building with swimming pool. IS 1893.1984 and STAAD PRO software was used for analysis, the mass irregularity was highlighted in the study. Maximum base shear, lateral displacements and storey drift was evaluated and axial force and bending moment were also calculated. A comparative study of mass irregularity in different floor levels was done, building was considered to be in different seismic zones. Plan dimension 12m×15m, height 3.5m, depth of foundation 3.5 m were taken in the study. It was reported that mass irregularity, joint displacement, base shear and story drift were essential for the study. It has been reported in the study that the maximum shear force was shown at first floor and minimum at top. According to IS 1893 (2002) limit of story drift was 14mm; but, it was found 14.726mm and 16.617mm.

Shah and Vyas (2017) analyzed G+14 building frames situated in zone-4, using IS 1893:2002. ETABS software was used for modeling and calculating parameter i.e. storey shear, storey drift and storey displacement. For comparative study of these parameters, three type of models with different irregularity i.e. horizontal irregularity, vertical irregularity and symmetric RC building with infill masonry walls were selected after analysis it was concluded that:

- ❖ due to symmetric infill masonry wall base shear was greater than other two cases.
- ❖ due to vertical irregularity, top story displacement was maximum as compare to infill wall structure
- ❖ Up to 10<sup>th</sup> storey level, storey drift was uniform but there was abrupt change occurred between 10 to 12<sup>th</sup> storey level due to vertical irregularity after that 12 to 15th storey again it is uniform.

Naveen and Chaya (2016) analyzed 10 storey RC frame building using ETABS 2015 software. Analysis has been done for both regular and irregular buildings using response spectrum method which was specified in IS 1893:2002.

Zone 5 was considered for location of 35.5m height of building. Six models were taken for comparative study in which one was regular building and others are irregular in nature. The comparative studies were done on the basis of storey drift, maximum storey displacement, storey stiffness and modes frequencies during earthquake. After analysis, it was observed that in irregular building structure:

- ❖ storey shear is higher than regular building structure.
- ❖ storey drift has maximum values as compared to regular building structure.
- ❖ frequencies were maximum.
- ❖ it was also observed that story drift increased up to 4<sup>th</sup> storey and after that it decreased up to 10<sup>th</sup> storey.
- ❖ frequency of modes increased with increase in number of modes.
- ❖ maximum storey drift decreased when number of storey increased.

Kumar and Singh (2018) analyzed the behavior of different irregularities in buildings. It was reported that the buildings which had eccentricity between center of mass and center of rigidity may face severe damage in comparison to buildings which have no eccentricity between these. For analyzing these buildings, the linear time history was used. (L), (C), and T shape nodes were used and modeled in ETABS software according to IS 1893 (P1) 2002. It was concluded that on comparing storey displacements, storey drift and maximum drift, the L shape and C shape building gave better results.

## CONCLUSIONS

In this study , it can be concluded that irregularity in a building structures is an important factor which affect many variables like base shear, storey drift, fundamental time period and so on.

- ❖ Period of modes of vibrations decrease by increasing the number of modes.
- ❖ Story shear is higher in irregular building structure than the regular building structure.
- ❖ Frequency of modes increases by increasing the number of modes.
- ❖ Storey drift varies with storey level and it has minimum values as compare to regular building structure.
- ❖ Storey shear increases with decreases in storey height.
- ❖ Storey maximum displacement is increases with increase in storey height.
- ❖ Top storey displacement is maximum for vertically irregular of structure and minimum for symmetric infill wall structure.

## REFERENCES

1. Alashker Yasser, Nazar Sohaib, Ismaiel Mohamed (2015) "Effects of Building Configuration on Seismic Performance of RC Buildings by Pushover Analysis, Open Journal of Civil Engineering", 2015, vol. 5, no. 2, 203-213
2. Gokdemir H., Ozbasaran H., Dogan M., Unluoglu E., Albayrak U. (2013) "Effect of torsional irregularity to structures during earthquakes" Engineering failure analysis, vol. 35, no. 15, (2013) pp. 713-717
3. Khan Pathan Irfan, Dhamge N. R. (2016) "Seismic analysis of multistoried RCC building due to for mass irregularity" International Journal of Engineering Development and Research, vol. 4, Is. 3, pp. 214-220
4. Kumar Gaurav, Singh V.K. (2018) "Effect of irregular configuration on seismic behaviour of RC Building", International Journal of Engineering research in Mechanical and Civil Engineering (IJERMCE), vol. 3, Is. 4, pp. 35-39.
5. Naveen. G.M, Chaya. S (2016)"Study on regular and irregular building structures during an Earthquake" International Journal of Latest Engineering Research and Applications (IJLERA), vol. 1, Is. 8, pp. 42-48.
6. Patil Rashmi S., Vidyadhar H.S. and Patil S. B. (2017) "Seismic analysis of multistoried building with and without vertical mass irregularity" World Journal of Engineering Research and Technology (WJERT) Vol. 3, 201, Issue 6, pp. 314-319
7. Sarkar Pradip, Prasad A. Meher, Menon Devdas (2010). "Vertical geometric irregularity in stepped building frames." Engineering Structures, Vol. 32, Is. 8, pp. 2175-2182,

8. Shah Kevin and Vyas Prutha (2017) "Effect of vertical geometric and mass irregularities in structure"  
*Proc. Int. conference on research and innovations in science, Engineering and Technology*, C. D. Modhera, G. J. Joshi, D.P Soni, Indrajit N. Patel, A. K. Verma, L. B. Zala, S. D. Dhiman, D. R. Bhatt, Jagdish M. Rathod, Bhargav C. Goradiya, Mehfuza S. Holia and Dharita K. Patel, eds. Vol. 1. 2017, pp. 87-92
9. INDIAN STANDARD COAD (IS 1893:2002)
10. Varadhragan S., Sehgal V. K. and Saini B. (2012) "Review of different structural irregularities in buildings" *Journal of structural engineering*, Vol. 39, No. 5, pp. 393-418



# Water Leakage Monitoring System in Building Using Internet of Things

Arya Vijayan<sup>1</sup> and Tejaswini D.Nalamutt<sup>2</sup>

<sup>1</sup>M.E Student , Department of Civil Engineering, Pillai HOC College of Engineering & Technology, Mumbai, India, aryavijayan@mes.ac.in

<sup>2</sup>Professor, Department of Civil Engineering, Pillai HOC College of Engineering & Technology, Mumbai, India, ntejaswini@mes.ac.in, Corresponding Author

## ABSTRACT

Water is one of the most valuable resources that is used globally. Many people across the globe lack access to clean consumable water, as only 3 % of fresh water is available for use. Urbanization and Industrialization are the main reasons for the water shortage. Apart from urbanization and industrialization, leakage in water distribution pipelines is the major concern for water shortage if not detected at early stage. Leakage can cause much damage to the building structures and it also leads to a huge loss of consumable water when supplied through water pipelines. In recent years, many studies have been conducted to develop an advance technology for better water management. As a result, a new automated technique, Internet of Things (IoT) is introduced that can connect the actual physical things to Internet. In this paper an attempt is made to illustrate IoT application through an implementation of water leakage detection and monitoring system. This paper emphasis on how sensor system can monitor, detect and locate the leakages in the pipeline system. This research also aims to develop a small scale prototype for real time water leakage alert system and to validate it through experimentation. An intelligent sensor network system consisting of flow sensors and a set of active sensor network platform is used to monitor and detect the leakage in pipelines. The flow sensors provided in the pipes gather the data related to discharge through pipelines. The data collected by sensors is processed by microcontroller- Arduino Uno. Finally, the processed data is monitored on internet using cloud computing.

**KEYWORDS:** —*Leak detection; flow sensor; Arduino uno; IoT; pipeline.*

## INTRODUCTION

Water is the most important, essential and limited natural resource responsible for life on earth (Wagan et al, 2013; Kulkarni, 2016). According to U.S Geological Survey Agency, around 97% of total water on the earth is found in oceans and only 3% is available as fresh water for use. Hence water is the basic need for all living things on earth. Water is used for various purposes such as drinking, washing, cooking, cleaning and many other things. It means around 150-250 gallons of water is used by a person daily for his household works (Hossain et al, 2015). In India, as a result of increase in population, more people are depending upon this limited resource and this is why it is extremely important to save & use the water carefully (Reddy et al, 2018; Singh et al, 2013). As per literature survey, more than 1.2 billion individuals lack access to clean consumable water worldwide (Hegde et al, 2016). Urbanisation and industrialisation is considered as the major reason for water shortage, but apart from these reasons, leakage in water pipelines are also major concern for water crisis. In Mumbai city, the leakage rate is reported around 70% because of pipeline leakages (). According to the Environmental Protection Agency, due to water leaks in infrastructures, around 1 trillion gallons of clean and treated water are lost annually. In addition to wastage of water, leaking pipes in buildings can cause some other problems like indoor flooding, wall deterioration, weakening of floor strength, reduction in water pressure in the pipeline etc. The building leakages are considered to be common but it is important to understand the causes and measures for prevention. The basic requirement of a building is to remain dry as far as possible. If this condition is not accomplished, the building may become unsafe from the structural point of view. Hence it is important to protect the premises from water damages by implementing water leakage monitoring system in early stages itself. Development of a proper water management system is considered as a complex and complicated due to the slower implementation of technology and aging infrastructure. In developed countries, high range acoustic devices are used to find sounds and vibrations developed in the pressurized pipes and thereby water leakage is detected while in developing countries, leakages are found only when it is visible

on the surface (Gopalakrishnan et al, 2017). As a result, wastage of considerable amount of water will be there. To avoid this condition, smart water leakage monitoring system connected with Internet of Things (IoT) can be introduced to the world by the advanced technology. Internet of things is a system, consists of linked devices, where the devices can be anything such as actuator, sensor, mobile phone etc. which can send and receive data over a communication channel (Mohammed et al, 2016). In 1998, Kevin Asthon invented the word “Internet of Things” into the world of technology (Santucci G, 2009). According to him, “IoT is about empowering the computers, so that they can see, hear and smell the world for themselves. The concept of IoT is considered as simple and powerful technique. The way how humans are using money transactions with the help of internet, the same way all the civil infrastructures and public service facilities such as buildings, bridges, traffic regulations, pollution, water supply etc. could be efficiently operated, monitored and controlled smartly using IoT (Praba, 2016). Figure 1 portrays the consents of IoT.

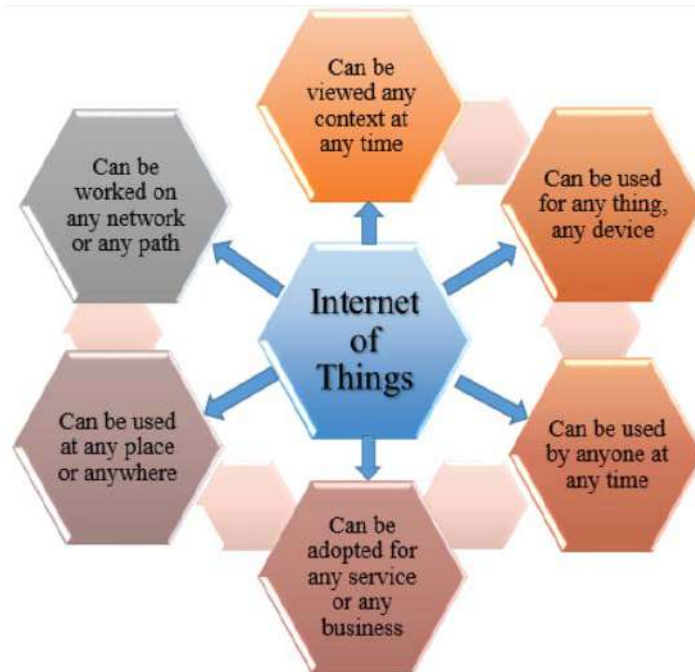


**Fig. 1 Consents of Internet of Things**

The extreme applications of Internet of things in day today real life can make the human life smart, safe and simple. IoT is having various applications in field of health care, agriculture, transportation, waste management, environment, buildings, bridges etc. Implementation of IoT in all these application zones reduces the human effort as well as increases the quality of life (Sethi, 2017). Figure 2 shows some of the important applications of IoT. This paper explains the real time water leakage monitoring system, which is one of the main applications of IoT. Various methods are available to detect and locate the water leaks in pipes, by connecting water monitoring system with IoT. Pressure measurements, flow measurements, vision based systems, acoustic measurements, fibre optic monitoring, ground penetrating radar based system etc. are some of the methods which are used for pipe monitoring. This study deals with flow measurement method using flow sensors integrated with micro controller to detect and locate the water leakage in pipelines.

Many researchers are carried out research on monitoring and detection of water leakages in pipelines. Reddy et al, 2018 have proposed a system which could detect the leakages, monitor and control the water supply through the pipelines. They placed the flow sensors in the water tank for continues information about the water level in the tank and accordingly the motor would function for automatic turn on and off. Flow sensors were placed in the pipelines to check out the water flow through the pipe. If any flow value changed in the pipe, then mechanically the motor will turn off and the supply stops for that pipe not to have more wastage of water and to deal with the flow of water. Saraswathi et al, 2018 have performed a study of the existing water pipeline to detect and monitor the leakage. They

developed a real-time prototype to detect the pipeline leakage and validate the developed prototype through experimentation. Mobile phone is configured as the alert sender of the system through which the user gets the information in the case of water leakage. They also designed a sensor system which can able to detect and control the level of water in a water tank. Sadeghioon et al, 2014 designed and developed a system to detect the water leakage in the water pipelines. They used FSR sensors to measure the pressure in the pipelines and temperature sensors are utilized to check the temperature around the pipes. They carried out laboratory as well as field test to validate the developed monitoring system.

In this paper, an intelligent system with flow sensors integrated with Arduino has been mentioned to find the leakage in pipelines. This method is meant to avoid the additional leak when water is flowing through the pipeline. This paper is arranged within the order of methodology that describes the operating of the proposed system, system design and the results that signify the efficient leakage detection in pipelines based on the proposed prototype.



**Fig 2: Application of Internet of Things**

## 1. METHODOLOGY

The aim of this paper is to develop an intelligent and smart system, which can perform the real time monitoring and detection of the water leakage in the pipelines in early stages itself. Figure 3 represents the major components of the proposed water leakage system. The system mainly consists of Arduino Uno, GSM, LCD, flow sensors and power supply.



**Fig. 3 Block diagram of water leakage monitoring system**

Water leakage monitoring system integrated with IoT is developed to save every single drop of water, which is wasted through pipeline leakages in building. The data that is used in this study is the rate of flow from sensors which is provided at the inlet and outlet section. Two water flow sensors are used to determine the inflow and outflow rate of water. In this study, YF- S201 is used as the water flow sensor which is having a working range of 1-30 L/min and water pressure  $\leq 2.0$  MPa. This sensor mainly consists of a rotor, plastic valve body and a hall effect sensor. When the water starts to flow through the sensors, the rotor rotates and the speed of that rotation (water) is directly proportional to the flow rate. Hall effect sensor generates pulse/signals for every rotation of rotor (Rahmat et al, 2017). The pulse generated by the hall effect sensors are send to the Arduino to analyse and display the flow rate. The flow sensors are connected by a 2 m pipe to measure the inflow and outflow through the pipe. Flow sensor consists of 3 wires; they are 5v power supply, pulse line and ground line. These are very easy to interface with Arduino, which makes the system smart. The signal line of flow sensor is connected with the digital pin 2 of Arduino where the power line and ground line of sensors are connected with the power line and ground line of Arduino. Figure 4 shows the YF-S201 flow sensor.



**Fig. 4 Flow Sensor**

A water pump is used to supply the water through the pipeline. When the system starts to work, water is allowed to flow through the pipeline which is connected with the inflow and outflow measurement sensors. Figure 5 shows the position of the water flow sensors in the pipeline. Initially, water flows through the inflow sensor and go out through the outflow sensor in the pipeline. The rate of inflow and outflow is sensed by the flow sensors connected to the pipe and have a diameter which is equal to the diameter of the sensors. The data obtained from the sensors are sent to the Arduino for processing while obtained results (inflow and outflow rate) are displayed on the LCD screen. Identification of the leakage in the pipes between the two sensors can be detected through difference in the inflow and outflow rate i.e., no difference between the inflow and outflow rate indicate no leakage while difference greater than 10L/min indicates the leakage

(Figure 6). When leakage get detected, Arduino will automatically activate the GSM to send alert messages to the registered mobile number and to the cloud system with the aid of a SIM card and external power supply. The flow diagram of the proposed system is described in Figure 7.



**Fig. 5 Position of Water Flow Sensors**

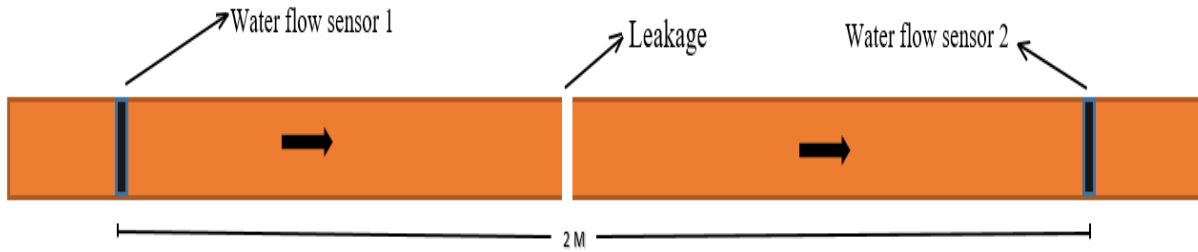


**Fig. 6 Leakage in Water Pipeline**

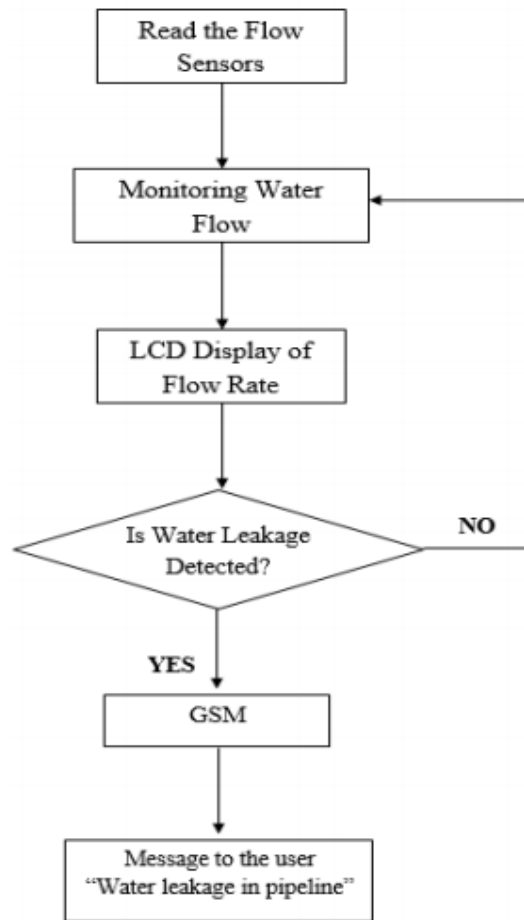


**Fig. 7 Flow chart of the water leakage monitoring**

## RESULT AND DISCUSSION

A prototype for real time monitoring of leakage in water pipeline was developed with the help of two serially connected flow rate sensors. The developed prototype is tested in various water flow conditions. Initially, the water flow is turned on and water is allowed to flow through the water pipelines. Both the sensors that are connected in the water pipeline gathered the data regarding rate of flow and analysed in the microcontroller periodically. By using algorithm for rate of flow calculation, the difference of inflow and outflow rate from the two consecutive sensors are found out. The difference obtained is compared and analysed with the threshold value by the micro controller to detect the leakage. Once the leakage is detected, notification regarding water leakage will be displayed on the LCD

screen as shown in Figure 8 and also at the same time it sends alert message to the user through sms and email for fixing the damaged pipeline system.



**Fig. 8 Leakage detection shown in LCD**

The graphs in Figure 9 and Figure 10 shows the data logged from two consecutive flow sensors in a given interval. Figure 9, shows the normal condition (no leakage) of water flow, where the rate of inflow and outflow are almost same. Initially there will be no water flow through the pipelines hence the flow rate is zero and when water is allowed to flow through the pipes, the flow rate increases which remains constant thereafter.

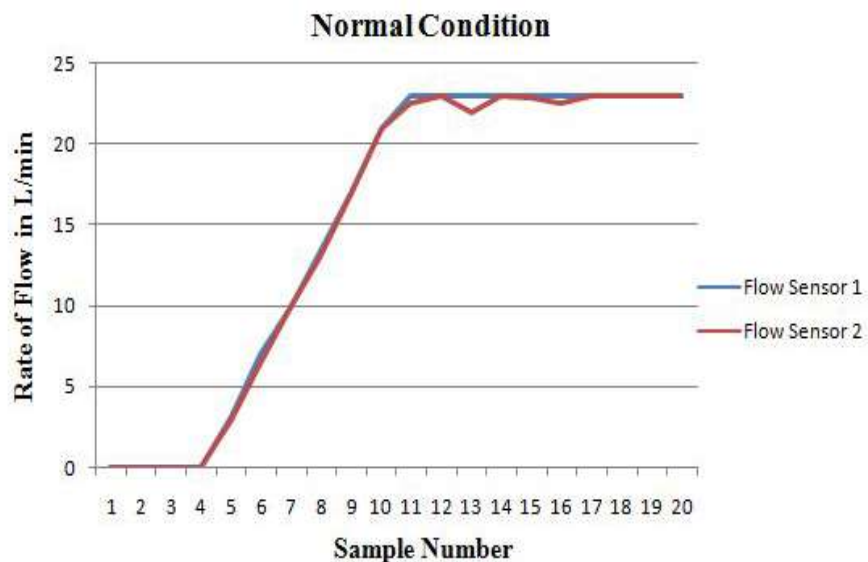


**Fig.9 Flow rate in no leakage condition**

Figure 10 shows the leakage condition in water pipeline. When there is a leakage in the pipe, the rate of inflow and outflow does not match with each other while if the difference in inflow and outflow rate is greater than the threshold value (10L/min), leakages is observed.

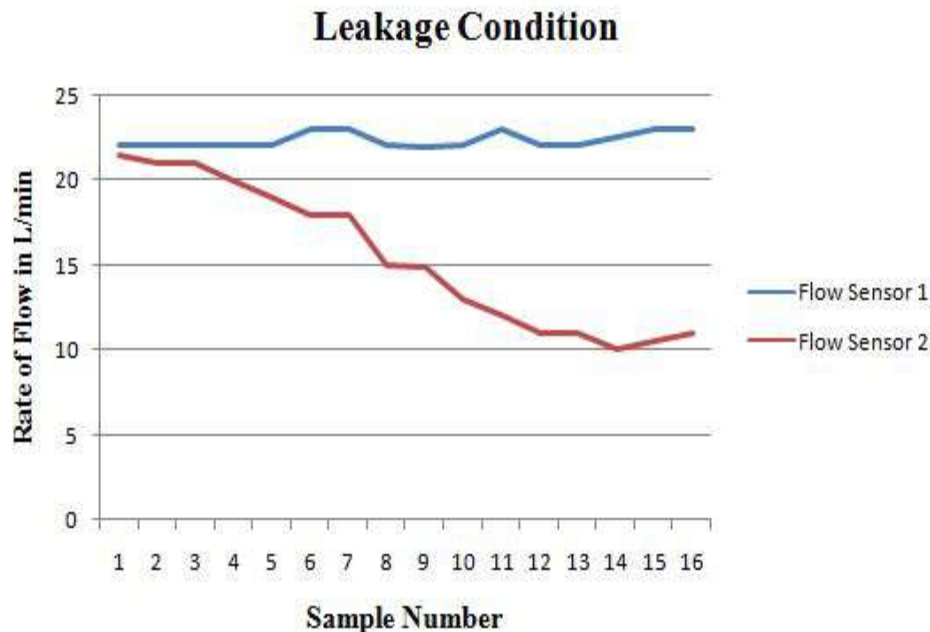


**Fig. 10 Rate of flow during leakage condition**

## CONCLUSION

It is essential to prevent leakages in the water pipelines as the amount of consumable water is only around 3% of the total available water on the earth. Normally a large amount of water is being wasted through leakages during the transmission of water using pipelines. Thus the proposed prototype with the modern technology and equipment helps to detect and monitor the leakage in water pipelines. The main advantage of this smart sensor network system is that, it has real time monitoring system with less interruption of user as well as the leakage detection system which rectifies in the early stage so that it reduces the intensity of damage.

A water flow measurement method using water flow sensors has been presented. This method permits easy and simple installation of the sensors in the pipes without disturbing networks of pipes. By using the technology Internet of Things, the flow of water through pipelines can be observed at anytime from anywhere. The monitoring and detection system may increase the initial cost, but in the long run it is cost effective as it reduces human power and maintenance cost.

## REFERENCES

- Gopalakrishnan P. Abhishek S.Ranjith R. Venkatesh R and Jai Suriya V (2017), “Smart pipeline water leakage detection system, International Journal Of Applied Engineering Research, Vol. 12, pp 5559 - 5564 .
- Hegde Adarsh, Gopi Kiran T S , Deepthi D ,T N Nagabhushany, S P Shiva Prakashy and Anand Raj S Ulley (2016), “Automated water flow control system”, National Conference on Product Design, July, pp. 1 – 9.
- Hossain Mohammad Zakir (2015) “Water: the most precious resource of our life”, Global Journal of Advanced Research, September, Vol. 2, Issue 9, pp 1436 – 1445.
- Kulkarni Pranita Vijaykumar and M. S. Joshi (2016), “An IOT based water supply monitoring and controlling system with theft identification”, International Journal of Innovative Research in Science, Engineering and Technology, September ,Vol. 5, Issue 9, pp 16152 - 16157 .

- Mohammed Shahanas.K and BagavathiSivakumar P (2016), “Framework for a smart water management system in the context of smart city initiatives in India”, proceeding of 2nd International Conference on Intelligent Computing,  
Communication & Convergence, 2016, pp 142 - 147.
- Praba A (2016), “IoT of Civil Infrastructures”, International Journal of Research in Advanced Technology, June, Vol. 1, Issue 6, pp. 6-9.
- Rahmat R F, Satria I S, Siregar B and Budiarto R (2017), “Water pipeline monitoring and leak detection using flow liquid meter sensor”, IAES International Conference on Electrical Engineering, Computer Science and Informatics, 2017, pp 1 -6 .
- Reddy Swetha, K.V.Chanakya, B.Eswari, Bhupati (2018), “Water leakage detection monitoring and controlling system using IOT”, International Journal of Engineering and Technology, pp 120 - 123.
- Sadeghioon Ali M, Nicole Metje, David N. Chapman and Carl J. Anthony (2014), “Smart Pipes: smart wireless sensor networks for leak detection in water pipelines”, journal Of Sensor and Actuator Networks, 2014, pp 64 - 78.
- Santucci Gerald (2009), “The Internet of Things: Between the Revolution of the Internet and the Metamorphosis of Objects”, Publication
- Saraswathi V, Rohit A, Sakthivel and Sandheep T J (2018), “Water leakage system using IoT”, International Journal of Innovative Research in Engineering & Management, Vol. 5, Issue 2, pp 67 - 69.
- Sethi Pallavi and Sarangi. R Smruti (2017), “Internet of Things: Architectures, Protocols, and Applications”, Journal of Electrical and Computer Engineering, Volume 2017, Article ID 9324035.
- Singh Omvir and Turkiya Sushila (2013), “A survey of household domestic water consumption patterns in rural semi-aridvillage, India”, GeoJournal-Spatially Integrated Social Sciences and Humanities, October, Vol. 5, pp 777 – 790.
- Wagan Farhan Hussain and Khoso Salim (2013), "Water shortage; its causes, impacts and remedial measures",Proceedings of 6<sup>th</sup> International Civil Engineering Congress, At Karachi, Pakistan, December.



## Silting and Scouring at Canal Confluence : A Review

Pradeep kumar<sup>1</sup>, Baldev setia<sup>2</sup>

<sup>1</sup>M.Tech student, Department of Civil Engineering, National Institute of Technology Kurukshetra, Haryana-136119, India, Email: [kumarpradeepbit@gmail.com](mailto:kumarpradeepbit@gmail.com)

<sup>2</sup>Professor, Department of Civil Engineering, National Institute of Technology, Kurukshetra, Haryana-136119, India, Email: [setia@nitkkr.ac.in](mailto:setia@nitkkr.ac.in), Corresponding Author

### Abstract:

Canal confluence are intermixing of streams with various stream includes and are general events beside the waterway. Canal confluences contain composite hydro-dynamics than far reaching streams because of various stream attributes of the two intermixing streams. Auxiliary dissemination creates because of intermixing of two streams which prompts bed disintegration. The disintegrated silt gets kept at various areas in the downstream of the intersection. Additionally, because of this water powered geometry of stream or channel gets changed at the conversion point. This occurs because of arrangement of high ebb and flow of streams at intersection which likewise dissolve the coating of the waterways and channels. Generally speaking in the momentum situation carelessness of channel and waterway stream prompts sparing misfortunes now and again of surges. Hence upkeep of waterways and administration of stream is a profound matter of concern. As the investigation of waterway stream design is perplexing, so broad lab/fields preliminaries have been done by different analysts and have indicated promising outcomes. Different investigations, for example, control of bed disintegration at 60° stream conjunction utilizing vanes and piles, trial investigation of coarse bed waterway juncture has been improved the situation application in fields. This paper delivers crafted by different examinations completed for answers for the issues of silting and scouring made at stream and canal. The present paper has been prepared in light of case study at the hand involving damage to the canal bed and banks at a canal confluence in Haryana.

**Keywords:** canal confluence; silting; scouring

### INTRODUCTION

Because of various stream qualities of two intermixing streams, there has been a composite hydro-dynamic than broad streams at channel conjunction. Stream and residue qualities are the depending factors for the cooperation of two streams. Canals confluence coming about into decimation of side dike at conjunction point. Based on these two canal, to be specific Western Yamuna channel (WYC) and Sutlej Yamuna Link (SYL) waterway in karnal region juncture at a point ( Fig.1and Fig.3). Because of various velocities and discharge of these two canal, there is an advancement of swirls at the conjunction area. Water now consistently assaults the side bank which creates scouring of that district and may prompt serious issue to structure in future ( Fig.2 and Fig.4).To conquer these issue some test work is should have been a done to get some suitable arrangement.

In present scenario water needs increases rapidly and level of ground water is decreasing day by day. So many of the state in our country depends on surface water like rivers, canals for farming ,drinking purposes etc. Therefore surface water has to be distributed through proper grid of rivers and canals. But for efficient working and uniform water distribution these rivers and canals has to be proper and well designed.

As the flow starts taking place so many problems starts generated like silting, scouring, bank erosion etc. These problems some time so serious which affect the structural performance, social and economic loss. To conquer these issue some strong foundation of test think about is needful for further application in fields issues.



**Fig.1** Two canal meets



**Fig.2** Destruction of banks of canal



**Fig.3** Damage due eddies



**Fig.4** Depletion of rip-rap of bank

Thusly this investigation center around utilization of exploratory examination for the welfare of fields issues at channel conjunction like silting ,scouring and bank disintegration and so forth. The schematic line diagram (Fig. 5) of waterway meeting at point appeared underneath which unmistakably makes the issues reasonable:

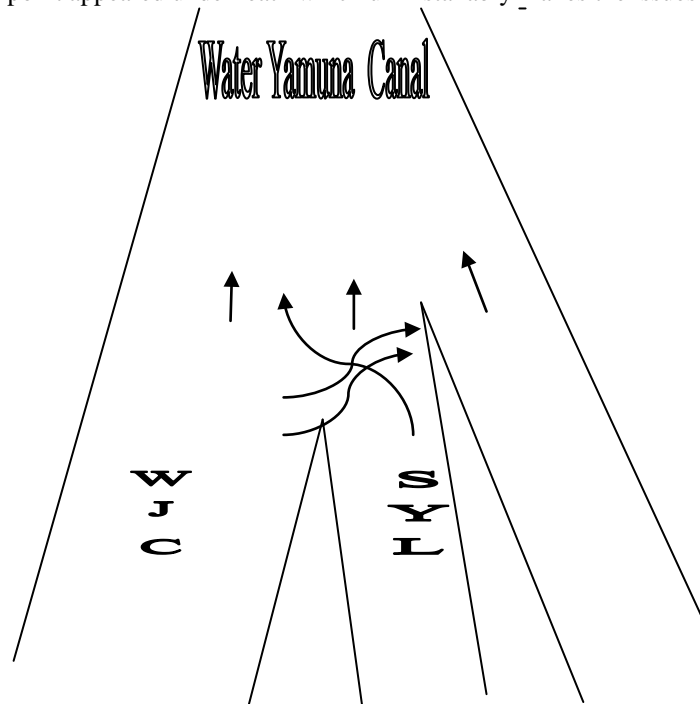


**Fig. 5** Schematic Diagram

On a concluding note, further research work is needed to be done in this direction whether we can use other alternative like spur, etc to reduce silting and scouring at confluence point.

### Theoretical Considerations

In canal confluence, vortices were created in at combining focuses might be because of various speeds or release of two

canals. In this way bank disintegration and scouring at juncture area can be broke down by applying energy condition to the control volume Fig. 6 demonstrates the definition portray of the converging of canals.

The energy condition for the control volume can be composed as:

$$P_2 - P_1 = \rho q_1 v_1 - \rho q_3 v_3 \sin\theta - \rho q_2 v_2$$

where  $P_1$  and  $P_2$  are the total pressure at section 1-1 and section 2-2 respectively,  $\rho$  is the mass density of water,

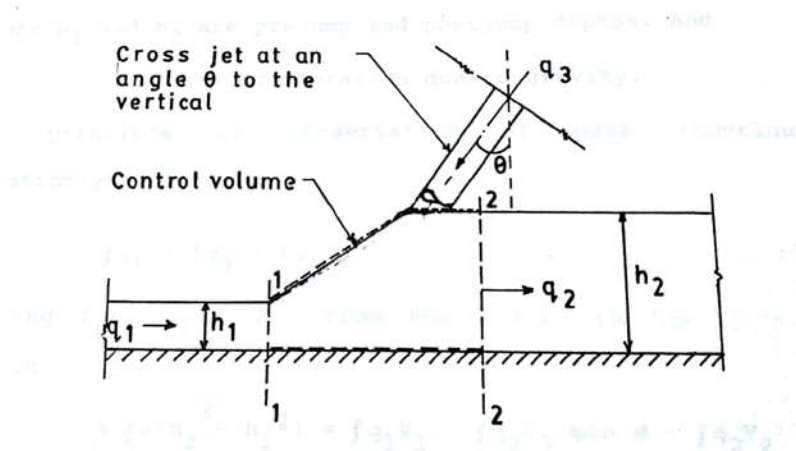


Fig. 6 Definition sketch

$q_1, q_2, q_3$ , are the discharge per unit width at section 1-1, section 2-2 and through the cross jet respectively.  
 $v_1, v_2, v_3$  are velocities of flow at section 1-1, section 2-2 respectively.

Energy Loss :

Energy loss confluence region can be evaluated by the difference between the total energy entering the system.

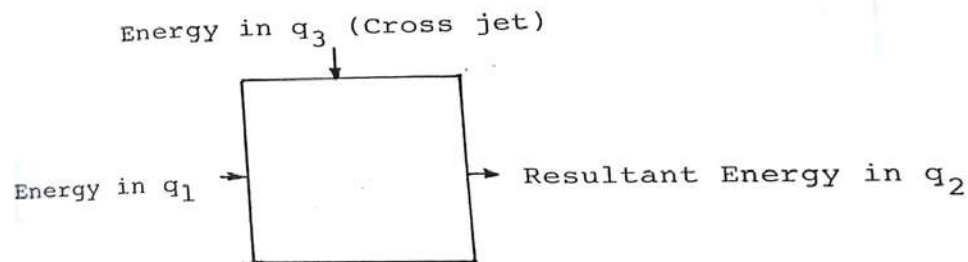


Fig. 7 Schematic diagram shows incoming and out going of energy

This can be analytically stated as :

$$\rho g q_2 E_L = \rho g q_1 E_1 + \rho g q_3 E_3$$

where  $E_1, E_2, E_3$  are the specific energies per unit width at section 1-1, section 2-2 and through the jet respectively and  $E_L$  is the energy loss per unit weight (shown in fig.7).

**Literature Review**

Different specialist gives their work to control silting and scouring at channel conjunction. Work of some analyst were exploratory model based which gives significant commitment for the application in fields.

**Ananth Wuppukondur, Venu Chandra(2017)**

Disfigured model with a non-uniform residue of mean molecule measure  $d_{50} = 0.28$  mm with an intersection point of  $60^\circ$  are utilized to play out the trials. The primary and sidelong streams at a juncture point of  $60^\circ$  and a test segment are appeared in Fig. 8. In the essential channel two diverse release proportions ( $Q_r =$  proportion of optional stream release to essential stream release) of 0.5 and 0.75 are utilized with a consistent stream profundity ( $H_m$ ) of 5 cm. Vanes of width  $0.3H_m$  (1.5 cm), thickness of 1 mm are put at  $15^\circ, 30^\circ$  and  $60^\circ$  vane edges as for principle stream. Circular Piers models of 8 and 12 mm breadth are additionally utilized. Two diverse separating of  $2H_m$  and  $3H_m$  (10 and 15 cm) between the vanes or piers are utilized to play out the investigations. The vanes or heaps were independently put in succession along the fundamental stream, 30 cm far from the internal bank disturbing the blending layer as appeared in Fig. 9. For  $Q_r = 0.5$  and 0.75 utilizing vanes, scour profundity decreases by 25% and 34%, individually.

**Table 1. Experimental data(Ananth Wuppukondur, Venu Chandra)**

S.No	$Q_m$	$Q_l$	$Q_r$	$V_m$	$F_m$	$V_l$	$F_l$	$V_d$	$F_d$
1	0.0067( $m^3/s$ )	0.0033	0.5	0.222(m/s)	0.317	0.133(m/s)	0.190	0.182(m/s)	0.260
2	0.0057( $m^3/s$ )	0.0043	0.75	0.185(m/s)	0.264	0.178(m/s)	0.250	0.182(m/s)	0.260

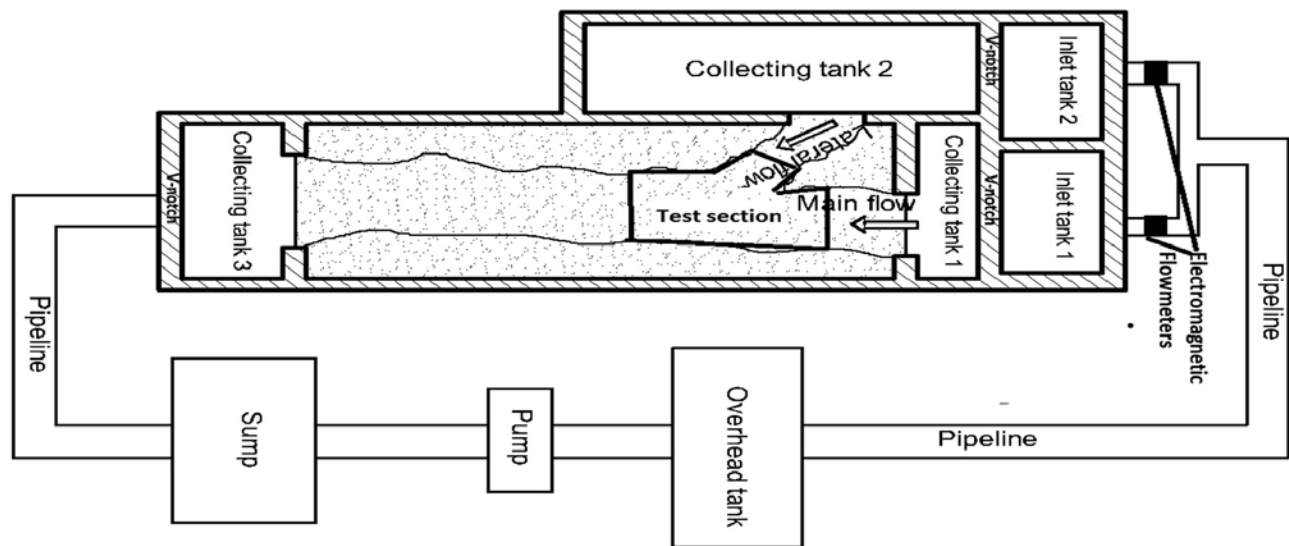


**Fig. 8 Setup of experiment**



**Fig.9** Orders of piles at the interflow

Velocities :

An Acoustic Doppler Velocimeter (ADV) with a recurrence of 25 Hz and precision of  $\pm 1$  mm/s was utilized to quantify the speeds at the conjunction locale. The test data is showed up in Table 1.

Limitations and use of ADV(Acoustic Doppler Velocimeter):

Limitation of ADV technique mainly due to a sample volume that is:

- greater than the smallest scales of motion in most turbulent flows and
- comparison to the distances from the bed is large where measurements of near are commonly required.

Besides, estimation of ADV can be fractional at separations from the bed that are outside the hypothetical and test measure of the Sample volume. The measure of obstruction between the informal lodging volume increments in extent which makes the signal to noise ratio(SNR) revealed by the instrument, so it give clients a bogus level of trust in results. Before information obtaining this point underscores the significance of directing sample volume mapping. ADV can precisely estimated mean speeds inside 1 cm of the bed (Daniel E. Dombroski and John P. Crimaldi,2007). When detailing disturbance insights, ADV clients should practice alert. Disturbance insights might be exact to as close as 1 cm from the bed for slower streams, anyway a similar level of precision may just be conceivable 3 to 4 cm from the bed for quicker streams. Additionally work is required in taking estimations in tempestuous streams with an unpleasant substrate which give a target assessment of ADV execution, as this will include extra unpredictability in adjusting the ADV and deciphering results.

Birjukova et al. (2014)

The target of this work is to add to such depiction at waterway juncture for reliable bed, where both essential and auxiliary channel beds have a similar rise. For that reason, an arrangement of investigations with settled bed under semi uniform methodology stream conditions was completed. The test office incorporated a 12 m long and 1 m wide primary channel, and a 4.5 m long and 0.15 m wide auxiliary channel. The conversion edge was  $70^\circ$  in order to speak to basic common conditions and the release proportion between releases in the auxiliary and in the essential channel was kept steady. An Acoustic Doppler Velocimeter (ADV) with a side-looking design was utilized to gauge the three parts of stream speed on a thick framework of estimating focuses, giving the precise portrayal of the mean stream and second-arrange speed minutes.

Mignot et al. (2013)

The present investigation went for estimating the qualities of two straightforward geometry three branch 90 subcritical intersection streams with solid inclinations of inflow speeds. The interface between the two inflows can be viewed as a quickened and bended blending layer that reaches out from the upstream district of the intersection towards the downstream branch. The investigation of such blending layer consequently requires an adjusted casing hub. Primary outcomes are: First the 2D Reynolds-Averaged-Navier– Stokes conditions are composed in the supposed Serret– Frenet neighborhood pivot framework dependent on ordinary and digressive nearby mean speed parts. This strategy ought to be utilized in any research center or field arrangement, particularly in locales where the point between the mean stream and the Cartesian casing pivot is huge. This empowers to all the more likely describe the blending layer and in this manner to survey the trade forms over the blending layer. Estimations uncover that the stream astute advancement of the convection speed, of the speed shortfall, of the greatest speed angle and of the blending layer width vary from the basic blending layer accessible in the writing. This specificity is by all accounts

an immediate outcome of the mind boggling parallel imprisonment identified with the side dividers and corners in the intersection. In channel junctures, the writing demonstrates that mind boggling geographies emphatically influence the stream highlights and the blending layer qualities.

Tong-huan et al. (2012)

Exploratory investigation were done on the developments of stream example and dregs transportation at a 90° open-channel intersection with various release proportions ( $q^*$ ) of the optional stream to the aggregate stream. The trial result demonstrated that the water surface profile at channel conjunction was impacted by auxiliary blending activity. Amid scouring tries different things with no advantageous silt, the movement of the bed stack was unpredictable and vacillated, while the bed stack release at first expanded and after that diminished monotonically. At the point when the water in the optional channel was clear, the biggest nearby scour showed up close to the shearing surface downstream of the intersection. The bed stack transport rate and the aggregate residue transport produced in time were recorded and broke down for various release proportions  $q^*$  for every situation. As indicated by the outcomes, the unmistakable qualities of a sharp-edged, channel juncture stream may be isolated into six primary zones. These test results are useful for the investigation and direction of reefs at an optional channel mouth.

Borghei and Sahebari (2010)

The scour designs at the intersection of two free bed channels were considered under clear-water conditions. The fundamental dimensionless factors are the edge between the two methodology stream branches, the release and width proportions of the tributary to the downstream channel branches, and the proportion of the mean downstream speed to the limit speed.

As per this work impacts of above parameters on scouring at channel intersection were talked about with unobtrusive exploratory setup. Consequently on more broad end these dependable variables for the scouring design, its area and the scour opening profundity should be considered under more nitty gritty examinations with an enhanced trial set-up. Further investigation of the stream designs including the portrayal of the bed shear pressure, violent motor vitality and unearthly examination is required.

### Interpretation

Ananth Wuppukondur, Venu Chandra(2017), Bed erosion leads by the composite hydrodynamics at canal confluence. According to his study using vanes, 25% and 34% reduction in scour depth for  $Q_r = 0.5$  and 0.75, respectively. Similarly, using pile models of 8 and 12 mm of circular shape, 25%, 38% and 27%, 43% reduction in scour depth for  $Q_r = 0.5$  and 0.75, respectively. There were reduction in scour depth, with an increase of vane angle and pile diameter, but increase of spacing leads to increased the scour depth. The measure of dissolved dregs lessened by 24% and 34% with vanes, for  $Q_r = 0.5$  and 0.75, individually. It is decreased by 28% and 39% with 12 mm heaps, individually.

O. Birjukova, S. Guillen, F. Alegria, A.H. Cardoso (2014), contribute his work for conversion edge was 70° in order to speak to regular characteristic situation and the release proportion among releases in the Primary and in the secondary waterway was set aside steady. Bed level of primary and secondary channel are same. It does not take considerations of difference in bed levels at confluence. Therefore further research needed in this direction.

### Conclusion

Reasonable number of research available. However the setup used seems to be on similar lines. Most of these works relate to the solutions through experimental modeling. Researches have obtained solution through the use of vanes, piles and a combination of these two. As per study of above researchers following points comes and these are follows:

- Piles have better execution over vanes in decreasing scour at the conjunction.
- Vanes and roundabout piles are used as scour improvement measures at a stream juncture. Neckline can be acquainted with the vanes or piles to decrease the local scour.

For the problem at hand , a solution through the use of rip-rap and preventive through modification in the longitudinal slope and use of appurtenances like vanes, piers etc will be explored. The study shall be preceded by theoretical consideration.

## References

- Ananth Wuppukondur, Venu Chandra (2017) Control of Bed Erosion at 60° River Confluence Using Vanes and Piles Int J Civ Eng DOI 10.1007/s40999-017-0147-1
- Birjukova O, Guillen S, Algeria F, Cardoso AH (2014) Three dimensional flow field at confluent fixed-bed open Channels. Proc River Flow, 1007-1014
- Borghesi S, Sahebari A (2010) Local scour at open-channel junctions. J Hydraul Res 48(4):538–542
- Baldev Setia, DVS Verma (1991) Hydraulic Jump Type Stilling Basin With Cross Jets Regional Engineering College
- BELL, JAMES H., and RABINDRA D. MEHTA. "Development of a two-stream mixing layer from tripped and untripped boundary layers", AIAA Journal, 1990.
- Best J, Reid I (1984) Separation zone at open-channel junctions. J Hydraul Eng 110(11):1588–1594
- Dombroski, Daniel E, and John P . Crimaldi.(2007) "The accuracy of acoustic Doppler velocimeter (ADV) measurement in turbulent boundary layer flows over a smooth bed", Limnology and Oceanography methods
- Liu et al (2012) Experimental study on flow pattern and sediment transportation at a 90° open-channel confluence. Int J Sediment Res 27(2):178–187
- Mignot E, Vinkovic I, Doppler D, Riviere N (2014) Mixing layer in open-channel junction flows. Environ Fluid Mech 14(5):1027–1041
- Pinto Coelho M (2015) Experimental determination of free surface levels at open-channel junctions. J Hydraul Res 53(3):394–399
- Rasool Ghobadian, Mahsa Basiri. "The effect of downstream curved edge on local scouring at 60 degree open channel junction using SSIIM1 model", Ain Shams Engineering Journal, 2016

## Interference of Bridge Piers on Local Scour: A Review

Anuj Kataria<sup>1</sup>, Baldev Setia<sup>2</sup>

<sup>1</sup>M.Tech, Department of Civil Engineering, National Institute of Technology, Kurukshetra; Haryana-136119, India; e-mail: anujkataria08@gmail.com

<sup>2</sup>Professor, Department of Civil Engineering, National Institute of Technology, Kurukshetra; Haryana-136119, India; e-mail: setia@nitkr.ac.in, Corresponding Author

### ABSTRACT

Scouring is a natural phenomenon which occurs due to removal of sediment particles from around the piers or abutment of a bridge due to flowing water. Scour at a single pier or group of piers is very complex phenomena, which affect the stability of a bridge structure. Local Scour around an individual bridge pier has been examined by a few specialists, however generally little work is available on scour around bridge piers, when they are located close to each other. In spite of broad work on an isolated pier, most of the bridges suffer damages due to local scour till today. It happens due to more intense difficulties due to the interaction of group of piers. The work planned to be conducted here in is concerned with wide investigational study of local scour around bridge piers placed in different patterns at varied pier spacing. The work which has been carried out by the various researchers on the interference of bridge piers on local scour located at varied spacing has some gap areas which are needed to be addressed. So it is needed to extend the same work by varying the piers spacing, piers size, pier, arrangements and of different median size ( $d_{50}$ ). In this paper, a detailed review of work on mutual interference of bridge piers on local scour located in close proximity with different arrangements is presented.

**Key word:** Local scour; bridge pier; open channel; interference; group of piers.

### INTRODUCTION

The removal of sediment from around the hydraulic structures (piers or abutments) located in a flowing water body is termed as local scour. Mostly bridge failure are caused by scouring around bridge piers and abutments, In a developing country like India failure of bridges pier is a serious issue as on the one hand it affects the developing economy and on the other hand it can result in damages to life and property. According to a study conducted by Brandimarte et al (2012), approximately 60 % of the bridge failures in the world take place due to scour and other hydraulic related issues. In an article, Huber (1991) stated that since 1950, more than 500 bridges had failed in USA and majority of the failures were due to scouring around bridge piers and abutments (Garde 1995).

In order to prevent the bridge piers from scouring the foundation of the piers must be deeper than the maximum possible depth of scour hole. Information of extreme depth of scour hole around a hydraulic structure is essential for safe and profitable design of bridge foundations. Calculation of Scour around a pier is a challenging problem for the hydraulic bridge engineers. Therefore, there is a need to develop some economical solution to the problem of scour and forms an issue for further research. Several researchers worked on the problem of scouring around hydraulic structure and advised some procedures. Numerous experimental studies have been conducted by several researchers i.e. Laursen and Toch (1956), Breusers et al. (1977), Melville (1997), Cardoso and Bettess (1999), Melville and Coleman (2000), for the calculation of scour depth around piers.

On the basic of mode of sediment movement in an open channel by flowing water, Chabert and Engeldinger (1956) categorized local scour into two groups, live bed scour and clear water scour. Clear water scour takes place when there is no movement of sediment into the scour hole. Furthermore, live bed scour happens when the scour opening is constantly bolstered with the residue by streaming water. It was seen that the most extreme clear water scour profundity around a scaffold dock is about 10% more prominent than the scour profundity computed for live bed. During the scouring mechanism around bridge pier, there are four components of flow field around a bridge pier. They are listed as: horseshoe vortex, down flow, bow wave, and wake vortices as shown in Fig. 1. The upcoming flow steadily become zero at the upstream face of the pier.

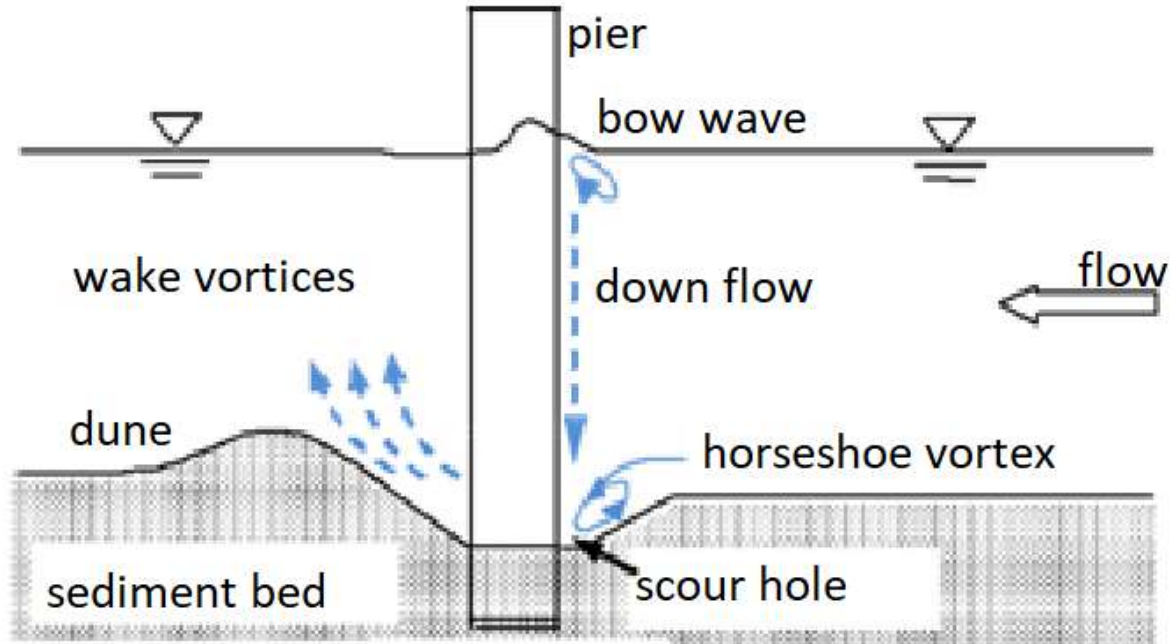


Fig.1 Scouring mechanism around bridge pier (Reference by ShivakumarKhaple et. al)

*The horseshoe vortex is developed due to the separation of flow that takes place at the up-stream face of the bridge pier and it moves by the sides of the pier (Raudkivi 1986). Due to which, a scour opening is built up around pier. A bow wave is created attributable to interference to the streaming water at the up-stream free surface neighboring to the pier and it rotates in opposite direction, if we compare it with horseshoe vortex. Owing to the opposite nature of motion, such wave does not play any role in the development of scour hole around the bridge pier.*

Time-based variation of scour depth around an individual bridge pier was widely studied by the many researchers (Yanmaz and Altinbilek 1991; Sumer et al. 1993; Dey 1999; Mia and Nago 2003; Oliveto and Hager 2005). And after the fully experimental procedure, it was observed that time require to reach the clear water scour depth was very long. It take a month or more to reach clear water scour depth. The presence of more than one pier may lead to the development and occurrence of a scour process around the bridge pier which is quite different from scour around single pier. On the basic of the several investigation carried out over the period of time many equations have been established for the calculation of depth of scour hole around the piers, however maximum equations have been developed for the single pier scour. As per above discussion it could be concluded that if a bridge pier is constructed as per the developed equations, it may leads to failure. In actual practice it may be happens that more than one piers placed close to each other due to which flow pattern around the bridge piers quite different from isolated piers. Which may leads to develop more or less scour around bridge pier, as per above discussion it can be observed that study of interference of bridge piers on local scour depth around the bridge piers is necessary and which is the topic of present study. It is needed to conduct numerous clear water scour experiments under steady uniform flow by considering the several piers pattern and equations are established for the calculation of depth of scour around group of bridge piers.

**LITERATURE REVIEW:** In this section various work done by researchers in previous time shown below.

**Work of previous researchers:**

Khaple et.al (2017): In this study 3 arrangements of pier were used i.e. (tandem, staggered and symmetrically staggered arrangements)

**Table: 1 Characteristics of sediments used in experiments (Khaple et. al, 2017)**

median size $d_{50}$ (mm)	Sp. Gravity(S)	$\sigma_g$	$\Phi$
0.960	2.65	1.21	$27^0$
1.80	2.65	1.18	$30^0$

In this experimental study two piers was used which are of different size. Diameter of piers were 60 mm and 82 mm. flow velocity is maintained as per  $U = 0.9U_c$ . critical shear velocity was used in this experimental work and the value of critical flow velocity calculated by using shields curves and then corresponds critical velocity was obtain by the equation given below, see Table 1.

**Two piers in tandem arrangements:**

$$\frac{U_c}{U_*} = 5.75 \log(h/k_c) + 6$$

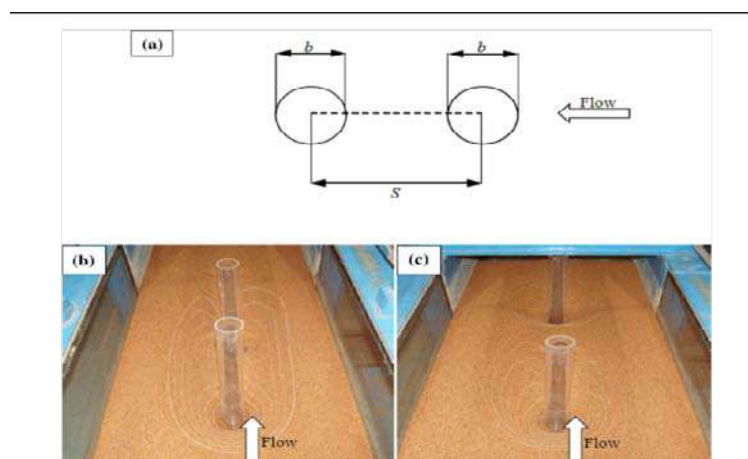


Fig. 2(a) shows two piers in tandem pattern, Fig. 2(b) and 2(c) shows the two piers in tandem pattern at relative spacing 4 and 10 respectively. (Shivakumar Khaple et. al)

Fig. 2, shows the pictures of experimental setup of two pier in tandem pattern. Two piers were inserted in bed of sediment along the mid- section for varying spacing  $S/b = 2, 2.5, 3, 4, 5, 6, 7, 8, 9, 10, 11,$  and  $12,$  as shown in fig 2(a). Front pier was fix at 8.50 m from inlet of channel and only the rear pier was moved.

He observed that, if spacing between two piers in tandem (piers along the direction of flow) arrangement is small, a combined elliptical scour hole was found. If spacing between two pier increases further, two separate elliptical shape scour hole at rear and front piers were found. It was observed after experimental procedure in this arrangement, scour depth at rear pier varies exactly from 0.8 to 0.870 times the depth of scour that was observed around individual pier. Hence, there is no additional criteria required for calculation of scour depth at rear pier. Minimum scour depth around rear pier in this arrangement was found at a relative pier spacing 8.0., which is reflected as the economical relative spacing for design purpose. Also observed that, scour depth around upstream pier in tandem and staggered pattern is nearly the same as that around the isolated pier.

**Two pier in staggered arrangement:**

In this pattern two similar piers of 60 mm diameter were used and fixed in the channel bed at a lateral spacing of  $L/b = 4$ , the stream wise relative spacing was varied from 2 to 10. Front pier is placed at a fix distance of 8.50 from the inlet of channel and only the rear pier is moved along the direction of flow (stream wise) stream wise at essential spacing and lateral off set spacing (width wise spacing).

It was found that depth of scour at up-stream pier was not dependent on lateral and stream wise spacing between two piers. However scour depth calculated around rear pier increase with increase in stream wise spacing. Depth of scour hole around rear pier at a lateral spacing (width wise spacing) of  $4b$  and stream wise spacing of  $2b$  was found to be equal that around the upstream pier.

**Three piers in staggered pattern:**

In this section of experiment 3 piers of 60 mm diameter was fixed in a sediment bed of size 1.80 mm. for 3 piers in this arrangement, scour hole depth around downstream pier for the stream wise relative spacing less than 8.0 and for small lateral relative spacing 2 was greater than that of individual pier. If radial relative spacing between rear and front piers increases, then the scour depth around rear piers increases. Scour depth around rear pier decreases, if width wise spacing between down-stream pier increases.

**Mubeen Beg and Salman Beg (2004):**

Width of flume was considered to be 75.6 cm and various flow parameters considered by Beg and Beg 2004 are as presented in Table 2.

**Table 2 .Various flow parameters used in this study (Reference by Beg et. al, (2004)**

Discharge Q (m <sup>3</sup> /sec)	Depth of flow Y <sub>0</sub> (cm)	Avg. flow velocity (m/s)	Flow Froude number F <sub>r</sub>	Pier Froude number F <sub>p</sub>	Partial Froude number F <sub>d</sub>	Flow Reynolds no. R <sub>e</sub>	Pier Reynolds no. R <sub>ep</sub>	Shear velocity U* (m/s)	Critical shear velocity U* <sub>c</sub>	Size of pier (m m)	Median size of sediments d <sub>50</sub> (mm)
41	14	.39	.33	.685	3.94	39551	12887	.053	.226	33.0	1.00

There are four arrangements used by the researcher as given below:

**Isolated pier:**

Various experiments were conducted by considering a pier model of diameter 33 mm and in that experimental study pier model was consider to be inserted at a distance 3.5 m from inlet. And these are the results obtained after experimental procedure. After experimental procedure it is observed scour depth calculated by Beg and Beg around an isolated pier is nearly match to scour depth calculated by Jain. Depth of scour hole as per Jain was 2.152.

**Piers in tandem arrangement:**

In tandem arrangement two piers model of same diameter (33 mm) were tested and these piers were placed in flume along the direction of flowing water with varying pier model spacing. And in this arrangement, up-stream pier model is located at a distance 350 cm from inlet of channel.

After seeing the above results of experimental procedure it is observed that when relative pier spacing = 0(both piers are in contact with each other), scour depth of upstream pier is very close to scour depth obtain for isolated pier and scour around the rear pier was nearly equal to 83.0 percent of scour around an individual pier. As per the results given by author, at relative pier spacing's between 0 and 2, width of scour hole with respect to diameter of pier is found to be 7.60. At spacing = 4.0, relative width of scour hole become 8.20. If spacing is further increase then relative scour hole width decrease up to the value of 6.70 at relative pier spacing 12.50. After that hole width is increases as the relative pier spacing increase and finally reached to 7.60 at relative pier spacing 25.0. Which is nearly equal to the width of scour hole at relative spacing = 0.

**Pier in lateral arrangement:**

It was observed after that at relative lateral pier spacing = 0 (both the piers touching to each other perpendicular to the stream flow of water), scour depth around both the piers were nearly equal to 2.110 times the single pier scour depth. At piers spacing's 1.0,2.0,3.0 and 4.0, the scour hole width around bridge pier were found to be 13.65,9.09,10.65 and 11.14 times the scour depth around the individual pier. As the relative spacing of pier just reach to the spacing value = 8, the width of scour hole is nearly equal to the scour depth around individual pier. And it is clearly observed when relative lateral pier spacing = 10, scour hole around bridge pier is free from interference effect of local scour. When lateral pier spacing reached to a value equal to 10 then the width of scour hole is free from interference effect of bridge pier.

**Piers in staggered arrangement:**

It can be concluded from the result that at  $\alpha = 45$  degree, the depth of scour around up-stream and down-stream pier are found to be equal to 1.140 & 1.230 times the depth of scour around isolated pier. At an angle of attack 7.5 degree and 15 degree, the scour depth at up-stream and down-stream piers were found to be almost 1.050 and 1.180 times the depth of scour hole around individual pier.

**Mubeen Beg and Salman Beg (2014)**

In this research paper researchers consider two unequal diameter piers with tandem arrangement and they performed series of experiments under steady uniform flow conditions by varied pier spacing and investigates the effect of mutual interference.

**Experimental program:**

In this study two piers models of different size are used and placed in tandem arrangement. Diameter of larger and smaller piers are 6.6 cm and 3.3 cm respectively. Larger and smaller piers are acting as front and smaller piers respectively. Such piers inserted perpendicularly in the sediment bed at varied relative piers spacing (0 to 90). Relative pier spacing means, spacing between two piers w.r.to diameter of pier. Fig 3 (a) and 3 (b) shows the arrangement of piers.

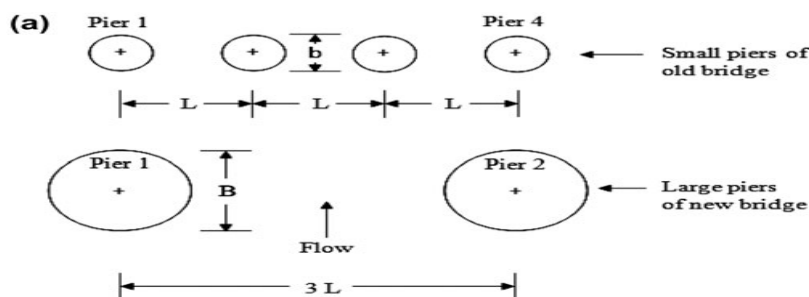


Figure 3(a). Newly and old bridge placed adjacent to each other (piers in tandem arrangement)

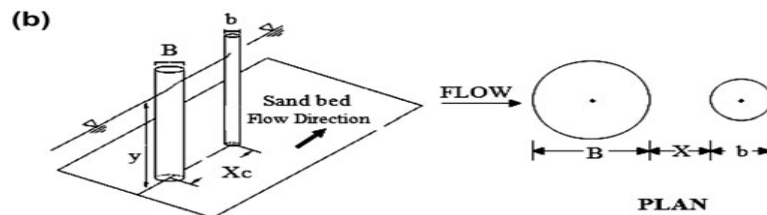


Figure 3(b). Two piers of different diameters in tandem arrangements (Reference by Beg et. al, 2014)

Properties of sediment used by Beg and Beg (2014) are as follows.

$$d_{84.1} = 1.030 \text{ mm}, d_{15.9} = .730 \text{ mm}, \sigma_g = 1.18 \text{ mm}, \text{Specific gravity } S = 2.650, \text{ angle of repose} = 32^\circ$$

**Depth of scour hole:**

After seeing the results of experiments conducted by Beg et. al (2014), it can be concluded that maximum scour depth around the front and rear pier are 1.860 and 1.350 times the scour hole depth around the rear pier at a relative spacing of 10 and 35 respectively. Scour depth around the downstream pier (33 mm) is minimum at relative spacing of 35. Fig. 4 shows the variation of relative scour depth with relative pier spacing.

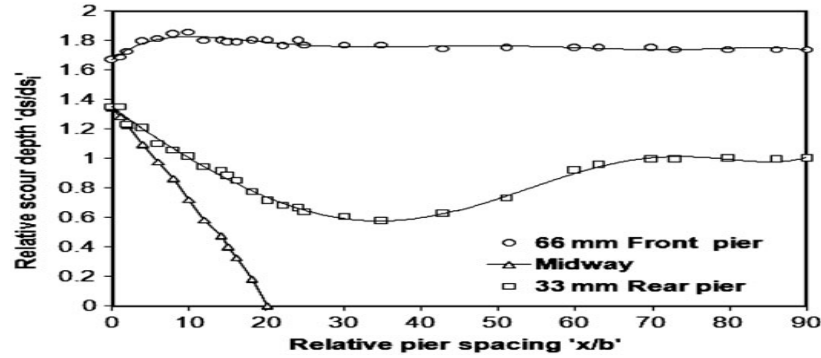


Fig. 4. Variation of relative scour depth with relative pier spacing (by Beg et. al)

**Length of scour holes:**

As per the results discussed by author, it can be observed that maximum length of scour hole at up-stream and down-stream face of thee up-stream pier comes out to be maximum at relative spacing 22 and 30 and minimum value of scour hole length at relative spacing 5 and 0 respectively. Similarly scour holes length around smaller pier (rear) at upstream and downstream face is minimum at relative spacing of 35.

Scour hole around smaller and bigger diameter piers start splitting from each other at relative spacing greater than 70.0.and get completely free from effect of mutual interference at relative spacing of 90. And finally it can be suggested that the down-stream pier (33 mm) should be located at relative spacing = 35.0 from front pier (66 mm) as the depth and length of scour hole is minimum at same spacing.

As per Beg and Beg (2017) for calculation of scour hole length it is need to plot the scour profile along the flow direction as shown in fig. 5(a), 5(b), 5(c). Fig 5(a) & 5(b) shows that the scour hole length of rear and front pier overlap to each other at relative pier spacing 1.0 to 14.0. Fig. 5(c) shows that when the relative pier spacing increase up to a value of 14.0, the bed level between both rear and front pier remains lower the level of un scoured bed. A common edge can be seen between both rear and front pier which splits the scour hole d/s of pier (66 mm) from the scour hole u/s of 3.3 cm diameter pier. The distance b/w the u/s face of rear pier and common brim provide the length of scour hole u/s of rear pier (3.3 cm). The distance b/w the d/s face of bigger diameter pier and common brim provide the scour hole length downstream of the bigger diameter pier.

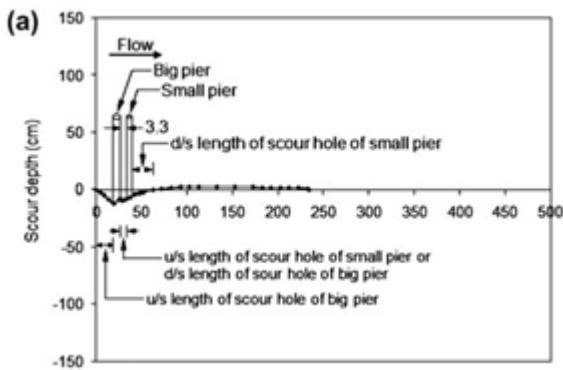


Fig. 5(a) profile of scour length along the flow direction At relative spacing = 1, (Beg and Beg, 2014)

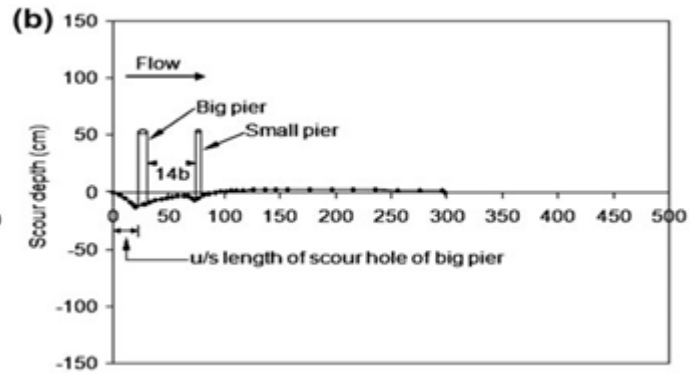


Fig. 5(b) profile of scour length at relative spacing of 14, (Beg and Beg, 2014)

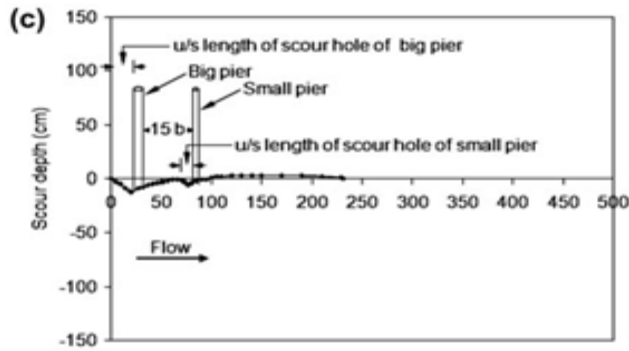


Fig. 5(c) profile of scour length hole along flow direction at relative pier spacing = 15

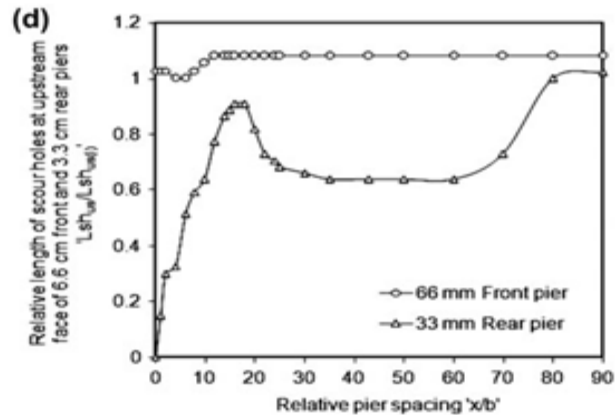


Fig. 5(d) variation of relative length of scour hole at the up-stream face of 6.6 cm and 3.3 cm rear piers (Beg and RPP 2014)

**B.MUBEEN: (three piers in staggered arrangement)**

In this paper author worked on pier models placed in staggered pattern in uniform coarse sand and various experiment was performed on clear water scour depth. Data about scour holes (length and width) are collected. After the experimental work it was found that maximum depth of scour hole around front and rear piers occur at  $x/b = 10$ . Most critical angle of attack ( $45^\circ$ ) was found at lateral pier spacing between two upstream piers  $Z_c/b = 9$  and downstream pier at stream-wise relative spacing of 10. Scour depth around the down-stream pier was found to be minimum at relative pier spacing of 40. Further increase relative spacing up to 65 and remains constant up-to stream wise spacing of 90. Hence it can be concluded that rear pier should be placed at relative spacing of 40. At this spacing scour around rear pier was found to be minimum.

**6. Conclusions:**

From the review of relevant literature on the subject of local scour around bridge elements, it is inferred that there is a significant body of literature available. However due to large number of bridges coming in close proximity. They may tends interfere with the flow modification of each other. . Most of the bridge failure takes place due to scouring around hydraulic structure and many research have been done by various researchers of Local Scour around individual pier, there is a lack of research work of local scour, when two or more piers are located close to each other .Hence it is need to extend the same work by varying pier spacing, pier arrangements, sediment size and flow conditions.

**7. References**

Beg.Mubeen, Beg S (2015) Scour hole characteristics of two unequal size bridge piers in tandem arrangement. *ISH J Hydraulic Eng.* 21(1):85–96. doi:10.1080/09715010.2014.963176  
 B.Mubeen (2015), “Mutual interference of bridge pier placed in staggered arrangement on local scour”, *Scour and Erosion – Cheng, Draper & an (Eds) 2015 Taylor & Francis Group, London, 978-1-138-02732-9.*  
 Beg mubeen, mutual interference of bridge pier on local scour, “Second International Conference on Scour and Erosion”, ICSE 2. 14.-17. November 2004 in Singapore.  
 Baker, C.J. (1981), “New Design equations for Scour around Bridge Piers” *J.of Hydraulic Division, ASCE*, Vol. 107, HY-4.  
 Breusers, H.N.C., Nicollet, G. and Shen, H.W. (1977). “Local scour around cylindrical piers.” *J.of Hydraulic Research*, Volume 15, No.3, page 211-252.7  
 Breusers, H.N.C, and Raudkivi, A. J. (1991), “Scouring” *2nd Hydraulic Structures Design Manual, I.A.H.R., A. A. Balkema/ Rotterdam – Netherlands.* Chabert, J and Engeldinger, P. (1956.) “Etude des Affouillement Autour des Piles De Ponts”.

- Lab Nat, d'Hydr.*, Chatou, France, October. Elliot, K.R. and Baker, C.J. (1978), "Effect of Pier spacing on scour around Bridge Piers", *J. of Hydraulic Division, ASCE*, Vol. 3.No.7, pp. - 1105-1109.
- Ettema, R. (1980), "Scour at Bridge Piers." Department of Civil Engineering, University of Auckland, New Zealand,  
*Report No. 216*, February.
- Hannah, C. R. (1978) "Scour at Piles Groups." University of Canterbury, New Zealand, Civil Cylindrical Engineering  
Research, *Report No.78* page 392.
- Hjorth, P. (1975), "Studies on the Nature of Local Scour", Department of Water Resources Eng., Lund Institute of Technology, *Bulletin Series A, No. 46*.
- Jain, S.C. (1981), "Maximum Clear Water Scour Around Circular Piers." *Journal of Hydraulic Division, Proc. ASCE*,  
Vol. 107, No.HY-5, May.
- Kothyari, U.C., Garde, R.J. and Ranga Raju, K.G. (1992a), "Temporal Variation of Scour around Circular Bridge Piers",  
*J.of Hydraulic Engineering, ASCE*, Vol. 118, No. 8, Aug., pp. 1091-1105.
- Kothyari, U.C., Garde, R.J. and Ranga Raju, K.G. (1992b), "Live-Bed Scour around Bridge Piers", *J.of Hydraulic Research, I.A.H.R.*, Vol. 30, No. 5, Aug., pp. 701-715.
- Laursen, E.M., and Toch, A. (1956), "Scour Around Bridge Piers and Abutments. 'Bulletin No.4, Iowa Highway Research Board.
- Melville, B.W. (1975), "Local Scour at Bridge Sites." University of Auckland, school of Engineering, Auckland, New Zealand, *Report No.117*.
- Melville, B.W. and A.J. Sutherland (1988), "Design Method for Local Scour at Bridge Piers", *J.of Hydraulic Engg. Proc. ASCE*, Vol. 14, No. 10, October.
- Melville, B.W. (1997), "Pier and Abutment Scour – Integrated Approach", *J. Hydraulic. Engg. ASCE*, Vol. 123, No 2,  
pp. 615-630
- Raudkivi, A.J. and Ettema, R. (1983), "Clear-Water Scour at Cylindrical Pier,"*J. of Hydraulic Engg., ASCE*, Vol.109,  
No.3. pp. 338-350.
- Shivakumar Khaple, Prashanth, Reddy Hanmaiahgari, Roberto Gaudio Subhasish Dey (2017) "Interference of an Upstream pier on local scour at downstream piers".
- Shen, H.W., Schneider, V.R. and Karaki, (1966), S.S. (1969), "Local Scour around Bridge Piers",*J. of Hydraulic Engg., Proc. ASCE*, Vol. 95, No. HY-6.



## FLOOD ESTIMATION AND MANAGEMENT STRATEGIES FOR RIVER YAMUNA USING GEOSPATIAL TECHNIQUES

*Munesh Kumar<sup>1</sup>, Baldev Setia<sup>2</sup>*

<sup>1</sup>M.Tech student, Department of Civil Engineering, National Institute of Technology, Kurukshetra,  
Haryana-136119, India, Email: muneshc.e100544@gmail.com

<sup>2</sup>Professor, Department of Civil Engineering, National Institute of Technology, Kurukshetra,  
Haryana-136119, India, Email: setia@nitkkr.ac.in, Corresponding Author

### ABSTRACT

During the last four decades, the hydrological characteristics of the Yamuna river basin have significantly changed. Due to the rapid urbanization in the basin, the runoff has considerably increased. Consequently, the flooding events are occurring more frequently and with higher magnitude. The High Flood Level (HFL) of 207.49 meters was recorded on Sept 6, 1978 after around 7 lakh cusecs (cubic feet per second) water was released in Yamuna on 3<sup>rd</sup> Sept 1978 at 04:00 hours from Tajewala barrage, that was decommissioned and replaced by Hathnikund barrage (located in Haryana) in early 1990s. The flood monitoring of River Yamuna began in 1963. The bank of Yamuna had witnessed flood in 1971, 1976, 1978, 1988, 1995, 1998, 2010 and 2013. It is almost a month after the Southwest monsoon arrived. By this time the river usually floods couples of times.

The Paper addresses various techniques for estimation of flood to alleviate the problems of riverine as well as flood in the cities located along the bank of the river. Four methods have been used namely California, Hazen, Weibul and Gumbel has been uses for the estimation of peak flood. Using the peak flood at various return-level safe width of the river has been computed.

**KEYWORDS:** Flood; estimation; Yamuna; frequency; Safe width; waterway

### INTRODUCTION

Cataclysmic events are a risk to human life and property. Floods are amongst the most repeated, widespread disastrous and frequent hazards of the world. A flood is an irregular ascent in the stream at which the runoff spillover its banks and immerses the connecting territory. It is always associated with loss of lives and properties if trained improperly. In this manner, surge moderation is an imperative part of legitimate waterway administration. A Flood recurrence examination is required to develop a technique for alleviating the surge chance with the productive administration of water assets. India is one of the most exceedingly awful surge influenced nations on the planet, likely next just to Bangladesh and records for one fifth of the worldwide demise tally because of floods (Mukesh Kumar 2017). Flood extent estimation for a specific territory is a vital piece of designing practices. Statistics and time series analysis plays a vital role in the calculation of peak flood discharge Underestimation of the design flood may lead to heavy economic, environmental and even loss of lives whereas the over estimation may lead to excessive expenditure on the proposed hydraulic structures. Therefore, optimum analyses are required while selecting the flood estimation method to avoid any loss. Hence, ideal investigations are required while choosing the flood estimation strategy to keep away from any misfortune.

River Yamuna is the longest and the second biggest tributary of the Ganga in northern India. Beginning from the Yamunotri Glacier at an elevation of 6,387 meters on the Banderpooch tops on the highest district of the Lower Himalaya in Uttarakhand, it voyages an aggregate length of 1,376 kilometers and has a drainage system of 366,223 square kilometers (141,399 sq. mi), 40.2% of the whole Ganges Basin. It crosses a few states Haryana; Uttar Pradesh and later Delhi. About 57 million individuals rely upon the Yamuna's waters. With a yearly stream of around 10,000 cubic billion meters and utilization of 4,400 cbm (of which water system establishes 96 percent), the waterway represents more than 70 percent of Delhi's water supplies. (Ref. Wikipedia). The course of the Yamuna River with its streams can be unmistakably found in Figure 1.

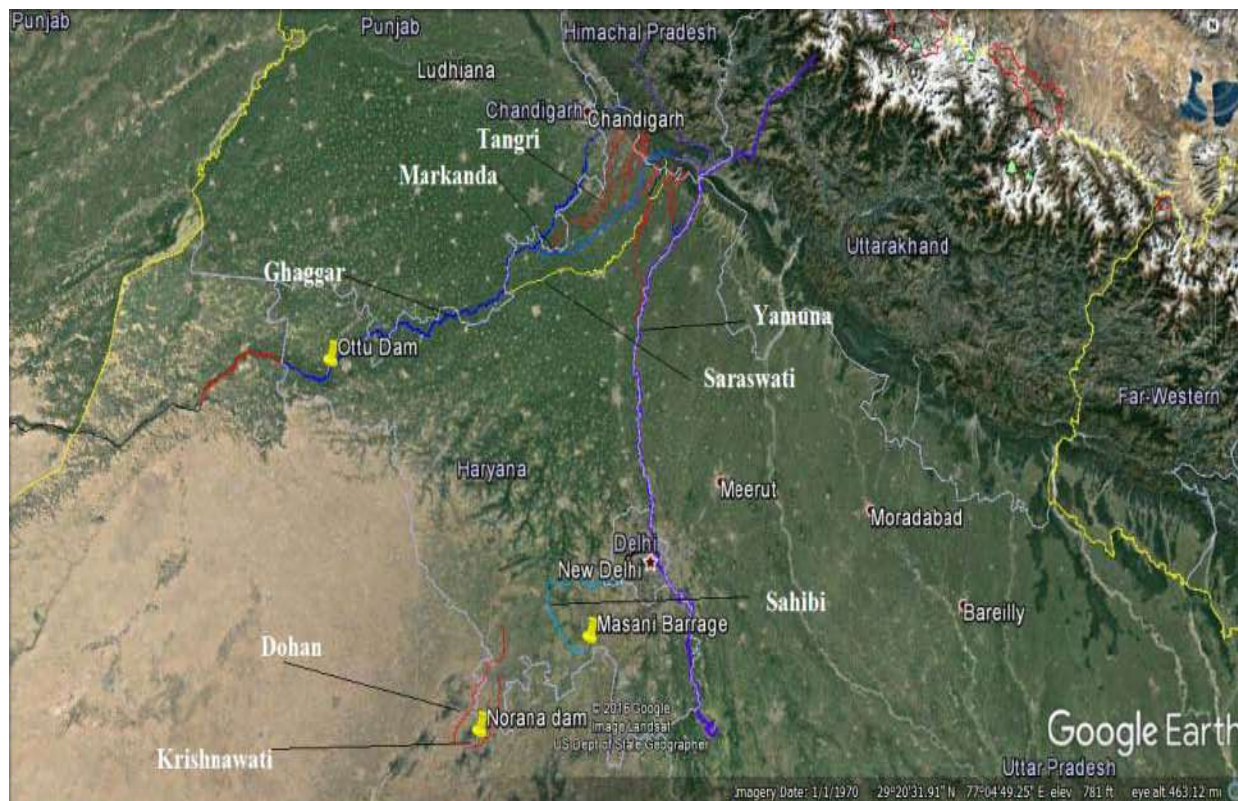


Figure 1: Course of river Yamuna from Yamunotri

### PROBLEM AND OBJECTIVE

River Yamuna being one of the old streams in the nation goes through most northern states including Haryana. In fact, it is the only perennial river that passes through the state of Haryana and contributes to the development of the state and thereby plays an important role. It is one of the major sources of irrigation system in Haryana. It works as a feeder for the canal system. Truly speaking, it is not inappropriate to state that river Yamuna is the lifeline of irrigation system in Haryana. It passes through many of the major cities of Haryana like Yamuna Nagar, Karnal, and Panipat and thereafter enters Delhi. The city of Delhi does not remain untouched in this regard though only for a few days every year.

Regardless of the above critical advantages of the stream Yamuna it has some major issues. Due to the recurring menace of floods in the river it threatens the life and property of the people residing in towns and villages near its banks. Extensive scale urbanization, decrease in dampness holding limit of soil, restriction of the conduit by development of dikes including some climatic components are the real patrons for increment in most extreme flood discharge. Due to increase in impermeable surface during urbanization increases the peak flow, decline the time of concentration and thus makes the area more flood prone (Wheater and Evans 2009). An investigation of Krellenberg et al. (2013) demonstrates that development of green space into the developed territories in Santiago, Chile made the region more slanted towards the flood. The rate of urbanization is relatively high in upper area of Yamuna that is only upstream of Delhi than district additionally up in the basin. The Bank of stream Yamuna has seen the fury of floods many a times that is in year 1971, 1976, 1988, 1995, 1998, 2010 and 2013. In the ongoing year on July 26, 2018 first surge of the flood was realized. Further with release of water it has increased themselves five times inside two days which was far away from expectation. Over the most recent couple of decades from 1963 to 2015, Yamuna has crossed threat level of 204.83 m at Old Railway Bridge Delhi 37 times. Thus it very important for a hydraulic engineer to be able to predict the design floods for safety, economy and environmental considerations.

Attempts of this paper are to study past yearly discharge information, estimate and extrapolate the design peak flood and to make comparable study for considerable number of strategies. From that point utilizing this peak design, safe width of the stream can be anticipated to protect the urban and provincial regions along the course of the waterway

## STUDY AREA

As the river Yamuna originates from the Yamunotri glacier nearly at an elevation of 6320 m above the mean sea level. It has total length of about 1376 km and a catchment area of 366000 sq. km at Allahabad (Mukesh Kumar 2017). After travelling through Himalayas many tributaries joins the Yamuna at Tajewala in Haryana. From here a headwork exists for eastern and western Yamuna canal. Further a new barrage named as Hathnikund barrage has been constructed nearly 3 km upstream at Tajewala barrage. River further passes through major cities like Yamuna nagar, Panipat, Sonipat etc. and then reaches to the national capital territory Delhi at Okhla barrage via Wazirabad barrage.

Area from Hathnikund barrage to okhla barrage is important for the assessment of vulnerability. The Hathnikund barrage situated in Haryana is nearly 200 km from the okhla barrage of NCT region. Forecast based on the recorded discharge at the Hathnikund barrage is important for the flood scenario. Travel time for flood water from Hathnikund barrage to Delhi varies between 32 to 72 hrs. (Kumar et al 2017), see Fig. 2.

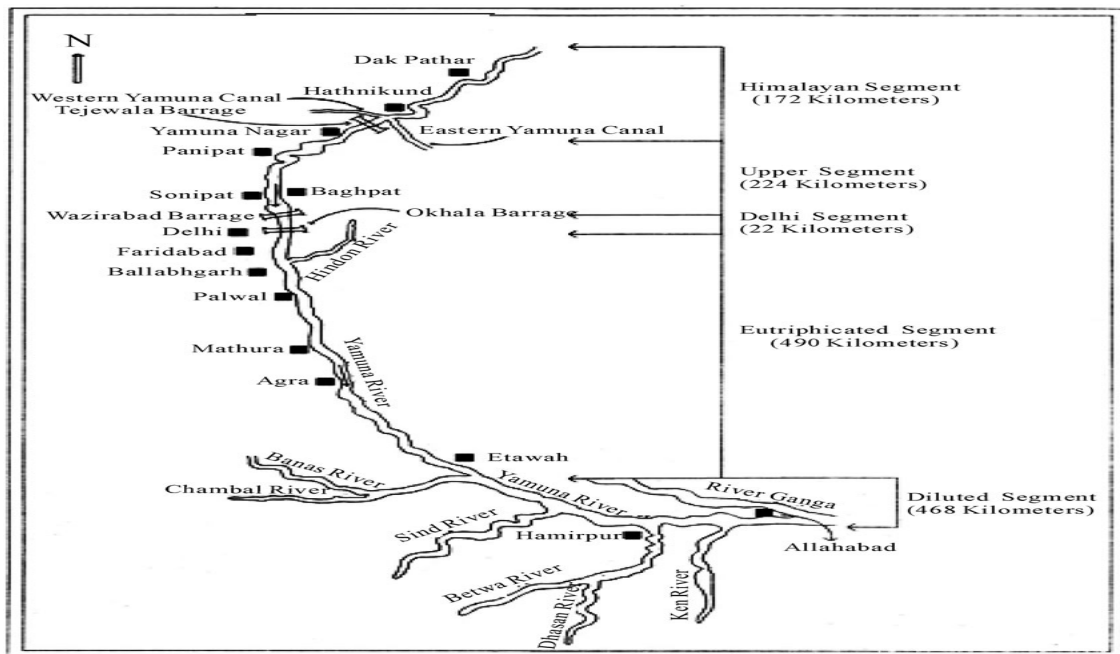


Figure 2: Different segment of river Yamuna (Journal of water resource & protection vol. 2 No. 5, 2010)

## METHODOLOGY AND DATA USED

Monsoon in district of Delhi and Haryana for the most part starts from 15 July and last till 15 October. Amid this season the respective irrigation department of Haryana and Delhi sets up control room for monitoring. The control room of particular zone keeps up the record of release discharge from Hathnikund barrage on the hourly premise. Release information of 32 years (1966 to 1997) has been utilized for the calculation of recurrence of flood. For the most part a base 30 years of information is considered as fundamental. This annual discharge data has been taken from river Yamuna at the older Tajewala barrage (decommissioned now and replaced by Hathnikund barrage).

Firstly the given set of data for 32 years from Tajewala has been arranged in descending order. Accordingly rank (m) has been assigned to each of these data. Using this value of rank (m) and total number of sample (N), probability of the event has been calculated using different formulas listed in Table 1. In the next step return period of the flood has been computed using Equation 1. Further using discharge data and calculated return period a graph has been plotted. For this plotted graph a best fit equation is selected according to the data trend. Utilizing this condition extrapolation for the surge at different return periods has been finished. In this manner calculation of recurrence of surge for different return interims 100 years, 500 years and 1000 years has been finished. At last utilizing Lacey's formulae, range of the protected width of the river related to the 100 year return period of flood has been computed.

$$T=1/P \quad \dots\text{Equation 1}$$

where **P**: probability of the event; **T**: recurrence interval or frequency of flood of certain magnitude. The following methods had been used for the computation of frequency of flood at T = 100 years, 500 years, and 1000 years.

**Graphical method**

These are the techniques utilized for calculation of surge recurrence by plotting the reasonable diagram among discharge and return period. From that point plotting the chart, it is relegated with best fit condition as indicated by pattern of Data. With this acquired condition for the given annual discharge information extrapolation for the arrival time of 100 years, 500 years and 1000 years has been completed. These techniques are presented in Table 1

**Table1. Plotting -Position Formulae**

Name of the method	Equation for P
California	$P= m/N$
Hazen	$P= (m-0.5)/N$
Weibull	$P= m/(N+1)$

Where m=order number of the event; N=total number of events in the data, P=probability of occurrence of event.

**Analytical method**

*Gumbel's distribution method:*

It is one of amongst most broadly used probability distribution function for extreme values in hydro-logic and meteorologic studies for prediction of flood peaks, most extreme breeze speed, and so on. In the recurrence investigations it is good to fit a probability distribution equation to the series of the flood information. The following equation has been given by the Gumbel for the practical use.

$$X_T = x + k \sigma \quad \dots\text{Equation 2.}$$

where  $X_T$  = required variate;  $x$  = mean of the data;  $\sigma$ =standard deviation;  $k$ =frequency factor expressed as:  
 $K= (Y_t - Y_n)/S_n; Y_t = -\ln(\ln(T/T-1))$

**RESULTS AND DISCUSSION**

The above graphical and analytical methods were used with annual discharge of 32 years to estimate the peak flood and are discussed below.

**California method:**

Firstly the given set of discharge for 32 years has been arranged in descending order. In like manner the rank (m) is allocated to each of this release. By utilizing this rank (m) and number of test information (N=32) return period has been figured by utilizing Table 1 along with Equation1. Utilizing return period (T) and given arrangement of discharge data, graph has been plotted as shown in Figure 3.

The best fit condition acquired for given arrangement of information is  $Q= 1269 \ln(T) + 2791.4$ . It has coefficient of determination ( $R^2$ ) estimation as 0.9175 which demonstrates a solid match to the information. From the equation, the flood for 100 year, 500 year and 1000 year return period were computed as 8635.36 cumecs, 10677.73 cumecs and 11557.34 cumecs respectively.

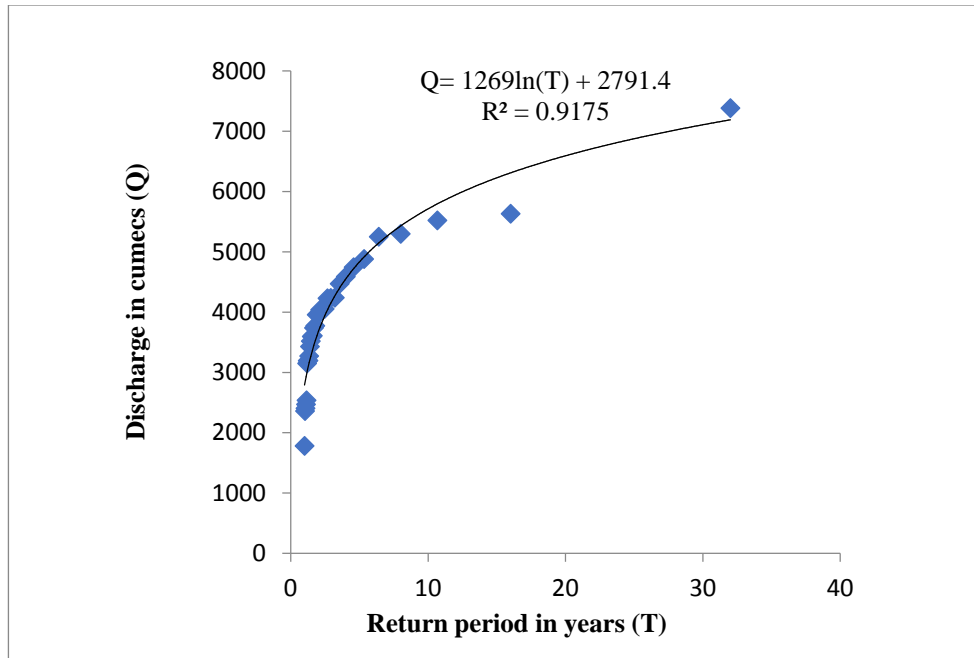


Figure 3: Discharge vs. Return period by California method

**Hazen's method:**

Likewise given information was arranged in descending order and when plotted with the Hazen's technique it gives  $Q = 1122.3 \ln(T) + 2845$ . It has  $R^2$  estimation of 0.9091 which shows a solid match to the information. From this obtained equation, the flood of 100 year, 500 year and 1000 year return period are 8013.3825 cumecs, 9819.65 cumecs and 10597.57 cumecs respectively were computed. The diagram with the relating condition can be seen unmistakably in Figure 4.

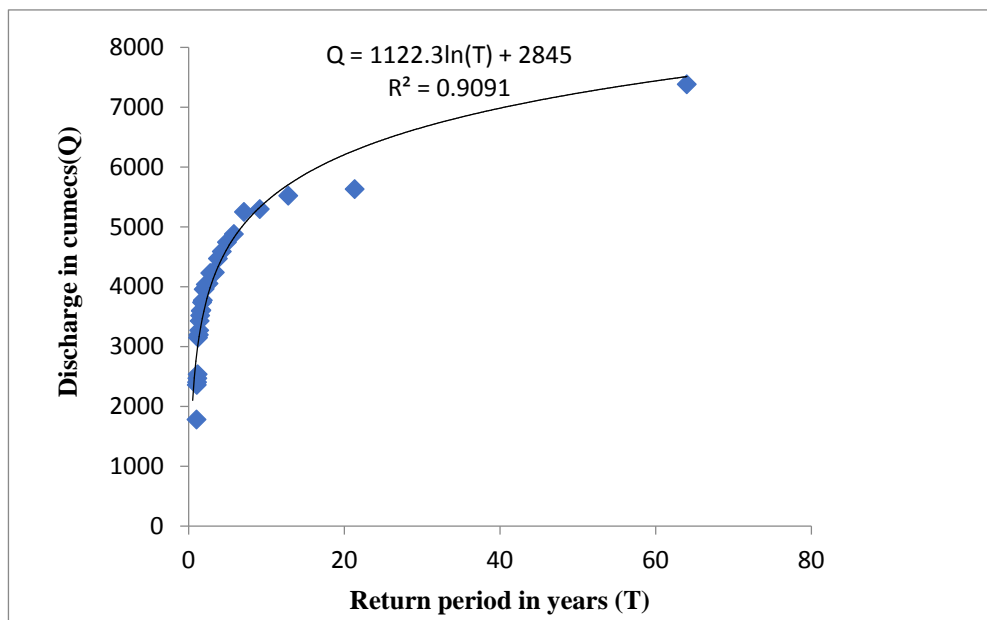


Figure 4: Discharge vs. Return period by Hazen

**Weibul's method:**

In like manner alternate techniques information is orchestrated and best fit condition by Weibul's strategy for the given 32 year data was observed to be  $Q = 1269 \ln(T) + 2752.4$ . It has a  $R^2$  estimation of 0.9175 which is little on the higher side than the past one and hence shows a solid match. The condition along with curve can be seen obviously in Figure 5. From the acquired condition, the design peak flood of 100 year, 500 year and 1000 year return period found to be 8596.36 cumecs, 10638.73 cumecs and 11518.34 cumecs respectively. This obtained condition along with given data can be clearly seen in Figure 5.

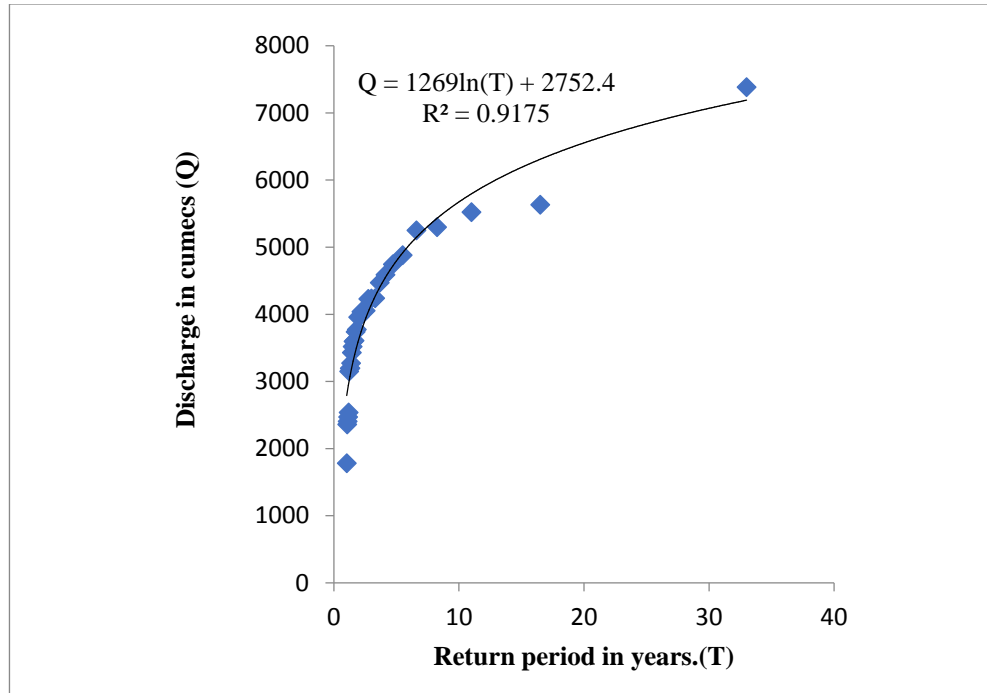


Figure 5: Discharge vs. Return period by Weibul's method

**Gumbel's distribution method:**

By utilizing the condition  $X_T = \mu + k\sigma$  estimation of peak flood for return period 100 years, 500 years, 1000 years has been registered using the following data:

Computed mean esteem ( $\mu$ ) = 3955.17;

Evaluated standard deviation ( $\sigma$ ) = 1133.90;

Processed estimation of  $K_{100}=3.137$ ;  $K_{500}= 4.39$ ;

Likewise for substantial interim  $Y_n = 0.577$  and  $S_n = 1.2825$ .

Utilizing these qualities with Equation 2, design flood has been computed. The design discharge return period of 100 years is 7512.30 cumecs; return period 500 years is 8940.93 cumecs and for return period 500 years is 8940.93 cumecs.

Aftereffects of four techniques for 100 years, 500 years, 1000 years flood are appeared in Table 2 and graphical examination in Figure 6. It was plainly seen that California technique extrapolates the pinnacle flood with higher size as contrast with different strategies.

**Table2. Acquired design flood at individual return period by different strategies**

Return period in (years)	Discharge in cumecs			
	California method	Hazen method	Weibul method	Gumbel's method
100	8635.36	8013.38	8596.36	7512.30
500	10677.73	9819.65	10638.74	8940.93
1000	11557.34	10597.57	11518.34	9556.64

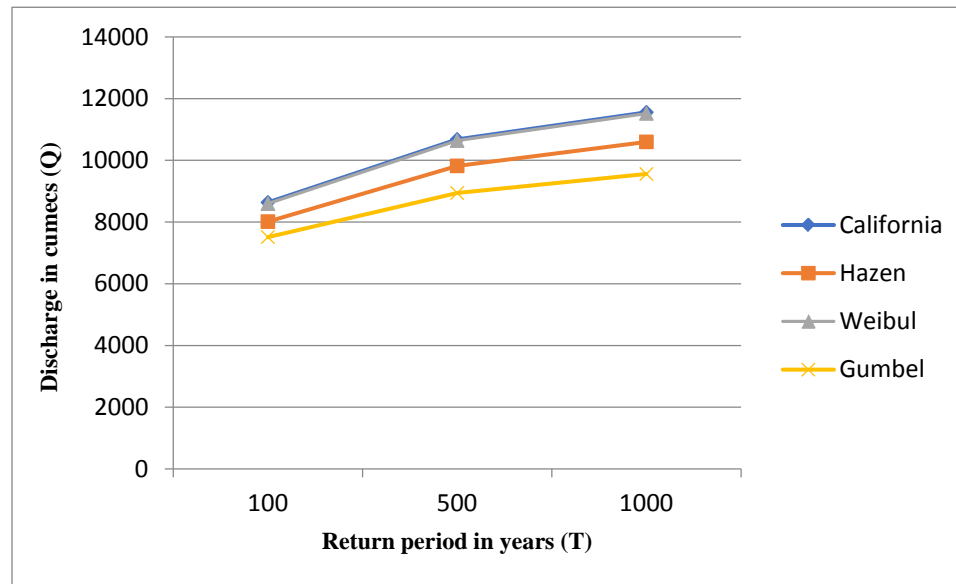


**Figure 6: Discharge vs. Return period by different strategies.**

**Safe width of the channel:**

By using Lacey’s formulae, safe waterway for the obtained peak flood has been computed as follows:

$$L \sim P = 4.75(Q)^{0.5}$$

where L= width of river; P= perimeter of cross section

In this case very wide channel has been assumed, thus depth has been neglected.

**Safe width corresponding to 100 years return period:**

- i) Considering the maximum obtained peak flood,  $Q_{max.} = 8635.36$  cumecs

$$L = 4.75(8635.36)^{0.5}$$

$$L = 442 \text{ m}$$

According to code of Town and Country Planning, Safe width of channel should be  $= 3*(442) = 1326 \text{ m}$

- ii) Considering the minimum obtained peak flood,  $Q_{min.} = 7512.3$  cumecs

$$L = 4.75(7512.30)^{0.5}$$

$$L = 412 \text{ m}$$

According to code of Town and Country Planning, Safe width of channel should be  $= 3*(412) = 1236 \text{ m}$

**CONCLUSION**

The occurrence of flood is a natural and an inevitable phenomenon. However, the frequency and magnitude of flood varies with the geological and hydrological characteristic of the basin. Reliable estimation of the flood discharge can help in mitigating the risk. The reliable estimates for the given data of 32 years have been done using the different methods which enhances the safety. The above study can be concluded as follows

- i) As per the study, peak flood discharge using California, Hazen, Weibul and Gumbel's method has been computed
- ii) Among the four appraisals California strategy gives maximum design flood. Similarly Gumbel's technique gives minimal estimation of peak discharge.
- iii) Safe width of River Yamuna for 100 year flood ought not to be less than 1236 m.

## REFERENCES

- Anil Kumar Mishra (2010), "A River about to Die: Yamuna" Journal of Water Resource and Protection Vol.2 No.5(2010), Article ID:1806,12 pages DOI:10.4236/jwarp.2010.25056
- Gawade , S., Pardeshi, K., and Sankhua, R.N. (2015). "Flood mapping of Yamuna river, Delhi, India. Global Journal of Multidisciplinary Studies", ISSN: - 2348-0459 www.gjms.co.in Volume-4, Issue-7 June 2015.
- Gurusamy, Senthil, and Jayaraman, G. (2012). "Flood inundation simulation in river basin using a shallow water model: application to river Yamuna, Delhi region." Int. J. Adv. Eng. Sci. Appl. Math., 4(4), 250–259.
- Krellenberg, K., Müller, A., Schwarz, A., Höfer, R., and Welz, J. (2013). "Flood and heat hazards in the Metropolitan Region of Santiago de Chile and the socio-economics of exposure." Appl. Geogr., Mar 31 38, 86–95.
- Khattak, M.S., Anwar, F., Saeed, T.U., and Sharif, M. (2016). "Floodplain mapping using HEC-RAS and ArcGIS: A case study of Kabul river." Arb J. Sc. Engg. (Springer), 41(4), 1375–1390.
- Kjeldsen TR, Smithers JC, Schulze RE (2002), "Regional flood frequency analysis in the KwaZulu-Natal province, South Africa" using the index flood method. J Hydrol 255:194–211
- Mukesh Kumar, Mohammed Sharif & Sirajuddin Ahmed (2017), "Flood risk management strategies for national capital territory of Delhi, India", ISH Journal of Hydraulic Engineering.
- Mukesh Kumar, Mohammed Sharif & Sirajuddin Ahmed (2018), "Flood estimation at Hathnikund Barrage, River Yamuna, India using the Peak-Over-Threshold method", ISH Journal of Hydraulic Engineering, Report (2015) on "How pollution kills the Yamuna River ", <https://sandrp.in/2015/04/13/blow-by-blow-how-pollution-kills-the-yamuna-river-a-field-trip-report/>
- Subramanya, K , "Engineering Hydrology", published by McGraw Hill education (India) private limited.
- WAPCOS.(1994), "Study on drainage system and flood control including water resources in National Capital Region", Water and Power Consultancy Services (India) Limited, May 1994.
- Wheater, H., and Evans, E. (2009). "Land use, water management and future flood risk." Land Use Policy. 26(26), S251–S264.



## A STUDY ON INNOVATION IN ACOUSTIC CONTROL OF BUILDING STRUCTURE THROUGH TEXTILE MATERIALS

*Sudhir Arora<sup>1</sup>, Akshay Choudhary<sup>2</sup>*

<sup>1</sup>Department of Civil Engineering, DAV University, Jalandhar – 144012

<sup>2</sup>e-mail: [akshaychdhr@gmail.com](mailto:akshaychdhr@gmail.com), Corresponding Author

### ABSTRACT

Sound is an impression of acoustic waves or sub-atomic exchange of motional vitality. Terrible, undesirable and irritating sound waves are commonly treated as Noise. This is an exceedingly abstract inclination. So it is hard to decide the dimension of acoustic control required while structuring a building or field. An assortment of ways are accessible to lessen commotion and they can be fundamentally assembled by latent and dynamic mediums. Inactive mediums diminish commotion by dispersing vitality and transforming it into warmth, while dynamic mediums require the use of outer vitality in the clamor lessening process. A noteworthy advancement can be found in the use of woven, non-woven and thwart films, purported Arch materials. Material films discover their applications as both inside and outside structures offering interdisciplinary difficulties for draftsmen, specialists, engineers, scientific experts, physicists, material originators and material researchers.

Materials are likewise utilized as sound safeguards, for instance, material inside parts of autos or covers in rooms that are utilized to retain sound vitality. Specialists have contemplated texture thickness to be the central point deciding sound assimilation, considerably more than texture weight or thickness. Sound ingestion expanded as texture thickness expanded to a specific point, appearing most noteworthy incentive at about 0.14 g/cm<sup>3</sup>. This paper expedites an outline structures acoustic issues in rooms or corridors worked out of material layers and the technique to quantify and break down NAC (Noise Absorbing Coefficient) or NRC (Noise Reduction coefficient).

### INTRODUCTION

Acoustic retention alludes to the procedure by which a material, structure, or item takes in sound vitality when sound waves are experienced, instead of mirroring the vitality. Some portion of the ingested vitality is changed into warmth and part is transmitted through the retaining body. The vitality changed into warmth is said to have been 'lost'. At the point when sound from an amplifier crashes into the dividers of a room some portion of the sound's vitality is reflected, part is transmitted, and part is retained into the dividers. Similarly as the acoustic vitality was transmitted through the air as weight differentials (or misshapenings), the acoustic vitality goes through the material which makes up the divider in a similar way [1]. Distortion causes mechanical misfortunes by means of transformation of part of the sound vitality into warmth, bringing about acoustic lessening, for the most part because of the divider's consistency. Comparative lessening components apply for the air and some other medium through which sound voyages. The portion of sound assimilated is administered by the acoustic impedances of the two media and is an element of recurrence and the occurrence point [1]. Size and shape can impact the sound wave's conduct in the event that they interface with its wavelength, offering ascend to wave marvels, for example, standing waves and diffraction [2, 3]. Acoustic ingestion is quite compelling in soundproofing. Soundproofing means to assimilate as much solid vitality (frequently specifically frequencies) as conceivable changing over it into warmth or transmitting it far from a specific area. As a rule, delicate, flexible, or permeable materials (like fabrics) fill in as great acoustic encasings - engrossing most solid, though thick, hard, impervious materials, (for example, metals) reflect most. How well a room retains sound is evaluated by the successful retention zone of the dividers, additionally named aggregate ingestion region. This is determined utilizing its measurements and the assimilation coefficients of the dividers [2]. The aggregate assimilation is communicated in Sabins and is helpful in, for example, deciding the resonance time of auditoria.

## Measurement of sound absorption

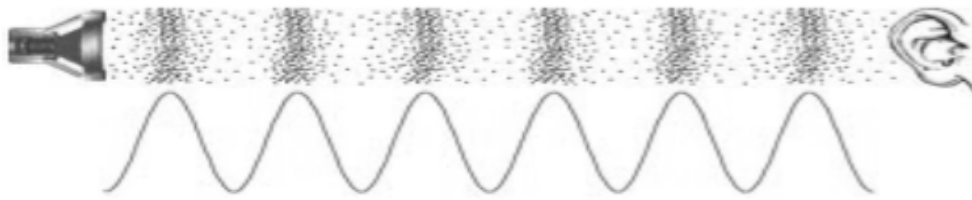


**Fig 1. Alternative patterns of dense and sparse particles**

Sound ingestion is a vitality change process. The motor vitality of the sound (air) is changed over to warm vitality when the sound strikes the cells or filaments. While diffused reflection parts the reflected sound wave in numerous ways. Diffusive surfaces are utilized to keep away from echoes and sound focuses particularly in rooms intended for music [1]. Sound wave achieves a surface of acoustic material amid its engendering in air and gets isolated into three segments: a reflected section, a transmitted part and a retained part (Figure 2). A beneficiary on indistinguishable side from the sound source can get both the occurrence and reflected sound waves. The capacity of the acoustic material to retain the occurrence sound wave can be assessed by looking at the sound power levels between the reflected sound wave and the episode sound wave. The assimilation coefficient  $\alpha$  is communicated as:

$$\alpha = \frac{\text{transmitted} + \text{absorbed energy}}{\text{total incident energy}}$$

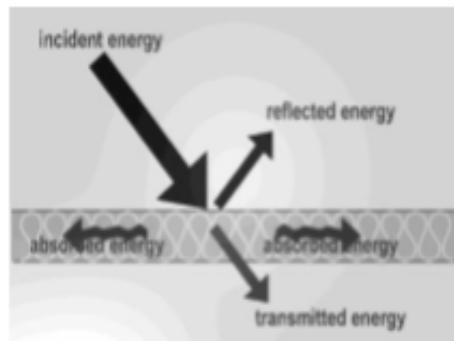


**Fig 2: Sound wave propagation**

Estimation procedures used to portray the sound absorptive properties of a material are reverberant field technique, impedance tube strategy and consistent state technique. Reverberant field technique is utilized to quantify the execution of a material presented to a haphazardly episode sound wave, which actually happens when the material is in diffusive field. Impedance tube technique utilizes plane sound waves that strike the material straight thus the sound retention coefficient is called typical frequency sound assimilation coefficient (NAC). Consistent state strategy (ASTM E336-71) is utilized to quantify the transmission coefficient of the materials. A third amplifier or even a second match of receiver can be put behind the test in a second impedance tube.

## Absorbent textile material

### Porous absorbers

Permeable safeguards are the most usually utilized engrossing materials, where thickness assumes a critical job in sound assimilation. These materials enable air to stream into clear structure where sound vitality is changed over to

warm vitality. Basic permeable safeguards incorporate cover, draperies, shower connected cellulose, circulated air through mortar and stringy mineral fleece/glass fiber. see Fig. 3.

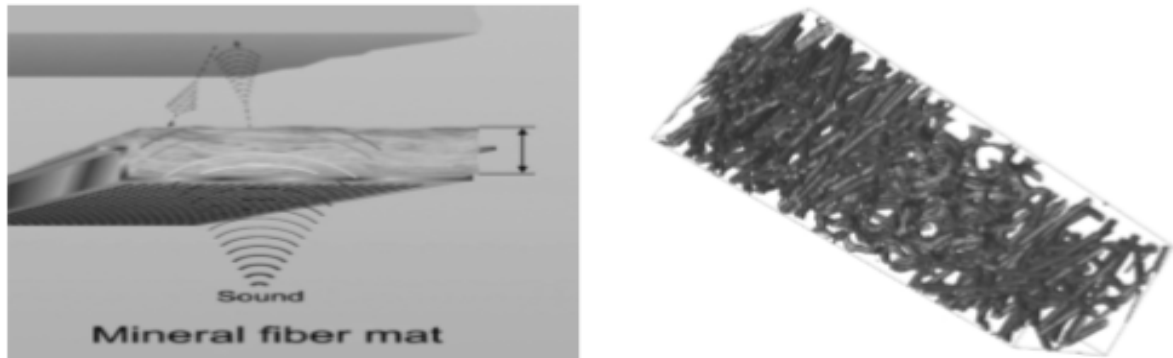


**Figure 3. Porous absorbers**

## Resonators

Full ingestion does not rely upon the properties of the material similarly concerning permeable assimilation. The assimilation is gotten by vitality misfortunes in a swaying framework. There are two fundamental sorts of resonators: Membrane and Cavity (Helmholtz) Resonators. Depression resonators as appeared in Figure 4, regularly act to ingest sound in a tight recurrence run. These resonators incorporate some punctured materials; e.g. HELMHOLTZ resonator. It has the state of a jug and the full recurrence is administered by the span of the opening, the length of neck and the volume of air caught in the chamber [4].

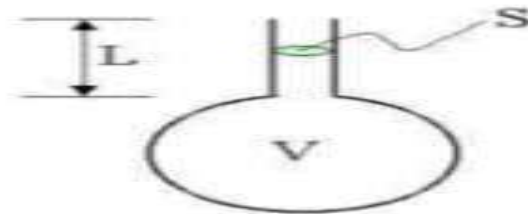


**Figure 4. Cavity resonator**

Board safeguards or film resonator is a thin, strong board at a separation from an inflexible divider with an encased air volume in the middle. Board safeguards are non-inflexible, non-permeable materials which are put over an airspace that vibrates in a flexural mode in light of sound weight applied by neighboring air particles. Basic board safeguards incorporate thin wood boards over casing, lightweight impenetrable roof and floors, coating and other vast surfaces fit for resounding because of sound.

## Factors that affect the sound absorption of textile material

### Fibre type

In an investigation on polyester, polypropylene, cotton and thick solid spongy material of various texture weight per unit territory, it was accounted for that polyester fiber textures indicate most elevated sound assimilation pursued by cotton fiber textures, polypropylene/cotton texture. Among empty polyester strands, strong polyester filaments and jute filaments, empty polyester fiber texture indicates most elevated sound ingestion, while strong polyester filaments demonstrate the least. Wide scope of fiber length, distance across, crease and spirally of fleece filaments empower it to retain sounds over a wide scope of frequencies.

### **Fibre size**

Thin filaments can move more effortlessly than thick strands on sound waves. An examination demonstrated that fine denier strands (1.5-6 dpf) perform preferable acoustically over coarse denier filaments. In the meantime smaller scale denier strands (<1 dpf) give a sensational increment in acoustical execution.

### **Fibre surface area and cross section**

Fiber surface region has coordinate relationship with sound ingestion. This is because of the reason that rubbing among filaments and air increments with expanded fiber surface territory. The sound ingestion in permeable material is because of the consistency of gaseous tension in the pores or the contact of pore dividers. In this way, solid ingestion increments with increment in explicit surface region of fiber. Among nonwoven textures produced using strands of various cross area, i.e. 4DG, trilobal, and round, 4DG fiber indicates most elevated sound protection, while round fiber textures demonstrate the least stable protection. 4DG filaments have profound forests and channels along their longitudinal pivot, which offer multiple times increasingly surface zone when contrasted with round strands. Tests delivered with high level of empty filaments likewise recorded the higher rates of sound.

### **Fibre type**

In an investigation on polyester, polypropylene, cotton and thick stable permeable material of various texture weight per unit zone, it was accounted for that polyester fiber textures indicate most astounding sound retention pursued by cotton fiber textures, polypropylene/cotton textures. Among empty polyester filaments, strong polyester strands and jute strands, empty polyester fiber texture demonstrates most astounding sound assimilation, while strong polyester strands demonstrate the least. Wide scope of fiber length, breadth, pleat and spirally of fleece filaments empower it to retain sounds over a wide scope of frequencies [5].

### **Air permeability**

A standout amongst the most essential characteristics that impact the sound retention qualities of a nonwoven material is the explicit stream obstruction per unit thickness. As a rule, when sound enters these materials, its abundancy is diminished by contact as the waves attempt to travel through the convoluted sections. In this way, the acoustic vitality is changed over into warmth vitality. The wind current obstruction per unit thickness is corresponding to the coefficient of shear consistency of the liquid (air) included and conversely relative to the square of the trademark pore size of the material. For a stringy material with a given porosity, stream obstruction per unit thickness is contrarily relative to the square of the fiber distance across. When all is said in done, with the expansion in recurrence, texture weight and the separation from the source, the degree of sound decrease increments while with the increment in air porousness, the degree of sound decrease by the material is diminished.

### **CONCLUSION**

Materials are additionally utilized as sound safeguards in structures, for instance, material inside parts of rooms or covers in rooms that are utilized to retain sound vitality. Material assumes an imperative job as an acoustic material in structures. By fluctuating the parameters of materials, vitality of the ingestion can be changed. As indicated by the writing, polyester fiber is viewed as best as an acoustic material for the structures. Denier scope of 1.5-6 dpf ought to be chosen for better retention of sound solid structures.

### **REFERENCES**

1. Arenas, J. P., & Crocker, M. J. (2010). Recent trends in porous sound-absorbing materials. *Sound & Vibration*, 12-17
2. Atwal, M. S., (1982). The Acoustic properties of textile fabrics. PhD Thesis, Leicester Polytechnic, Leicestero, England
3. Jayaraman, K. A. (2005). Acoustical absorptive properties of nonwovens, North Carolina University

4. Lee, Y., & Joo, C. (2003). Sound absorption properties of recycled polyester fibrous assembly absorbers. *Autex Research Journal*, 3, 78-84
5. Lou, C. W., Lin, J. H., & Su, K. H. (2005). Recycling Polyester and Polypropylene Nonwoven Selvages to Produce Functional Sound Absorption Composites. *Textile Res. J.*, 75, 390–394.
6. Teli M. D., Pal A., & Roy D. (2007). Efficacy of nonwoven materials as sound insulator. *IJFTR*, 32, 202-206
7. Thomann, M., & Jackson, S. (2009). The Acoustical Properties of Wool Carpet. *Historic Floor covering and Textile*.
8. Vallabh, S. R., Banks-Lee, P., & Seyam, A. F. (2010). New approach for determining tortuosity in fibrous porous media. *Journal of Engineered Fibers and Fabrics*, 5, 7-15
9. Acoustical Solutions Inc., (2011). PolyPhon Polyester Panels.
10. <http://www.acousticsblog.com/category/david-ingersoll> .



## Analysis of Spatial Distribution of Precipitation over Kabul River Basin

S. Sultani<sup>1</sup>, Arun Goel<sup>2</sup>

<sup>1</sup>M.Tech Student, Department of Civil Engineering, NIT Kurukshetra, Kurukshetra – 136123, Email: sham.sultanie@gmail.com, Corresponding Author

<sup>2</sup>Professor, Department of Civil Engineering, NIT Kurukshetra, Kurukshetra – 136123

### ABSTRACT

Rainfall is part of Hydrologic cycle, it has many spatial variability over the basin. The measure of precipitation received weekly, monthly, seasonally and yearly indicate distribution. Moreover, distribution of precipitation can be known by the length of droughts, wet spells and rainy days and is more vital as compared to the total rainfall.

About 25 years of civil war in Afghanistan (since late 1978) has caused environmental degradation and data as well as many climate stations have been demolished. Estimation of reliable precipitation distribution over Kabul River Basin which is highly mountainous at left flank ranging from 400 to 6000 meters above sea level is complicated. The Kabul River Basin is situated in upper east part of the country. The stream normally runs towards the east and later on join Indus River in Pakistan's northwest outskirts region. Despite the fact that it envelops only twelve of the region of Afghanistan it represents 35% of total population. The river basin includes the metropolitan region of Kabul, that is considered area of economic development in nation. Further it has an extensive portion of installed energy generation capacity.

The present work aims at dealing with the geo-statistical analysis of Kabul River basin and estimating the areas where precipitation occurs throughout the year, based on historical monthly data recorded in the stations. This data is from 1962-1978 and 2003-2015. The gap between the recorded data will be filled by using interpolation method.

**KEYWORDS:** *Rainfall; Kabul River Basin (KRB); Indus River.*

### INTRODUCTION

Afghanistan is considered as a land-locked nation. It is strategically situated on the intersection of three imperative regions: the Indian subcontinent toward the east, Central Asia toward the north side and the Middle East toward the west fig (1). The country is commanded by rise mountains and has been covered by a generally rich system of waterways.

It has five river basins namely, Amu Darya, Northern, Harirrod-Murghab, Helmand and Kabul river basin (Indus). As per G. M. K. Raphy Favre (2004), all major river basins are shown in fig (2) and Kabul river basin is being discussed in this article.



Fig. 1 Geographical map of Afghanistan with neighboring countries

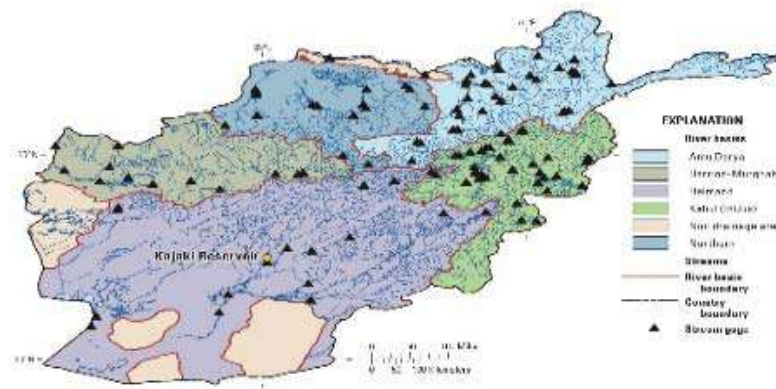


**Fig. 2 Major river basins of Afghanistan**

**ABOUT KABUL CITY**

Kabul is the capital of Afghanistan and one of the largest city regarding its population, and is located along the Kabul River. It has a population of around 4.6 million residents. Kabul city elevation of 1800 meters above sea level and makes is one of the highest cities in the world. There are 22 districts in Kabul with population representing diverse ethnic groups. The KRB is situated in eastern part of Afghanistan, in the vicinity of Pakistan border.

The Kabul stream has length of 435 miles (700 km), of which 350 miles i.e. about 80% are in Afghanistan. It starts from the Sanglakh Range 45 miles west of Kabul, it flows east past Kabul and Jalalabad city, north of the Khyber Pass into Pakistan, and past Peshawar; it joins the Indus waterway northwest of Islamabad. The Kabul waterway, is a standout amongst the most imperative streams in Afghanistan. The Kabul basin passes through nine areas of eastern Afghanistan: Kabul, Nangarhar, Wardak, Logar,, Kunar, Kapisa, Panjshir, Nuristan Laghman Parwan and a piece of Ghazni province.

The Primary catchments from the point of view of hydrology, atmosphere, and physiographic qualities, the Kabul River basin is partitioned in two noteworthy catchments. The upper basin comprises of two noteworthy sub-basins – the Panjshir sub-basin and the Logar-Upper Kabul sub-basin. The Lower Kabul sub-basin incorporates the watershed region from the intersection of the Panjshir and Upper Kabul waterways close to the beginning of the Naglu repository to the boundary of Pakistan. This part of the basin is presented in schematic form in figure 3.

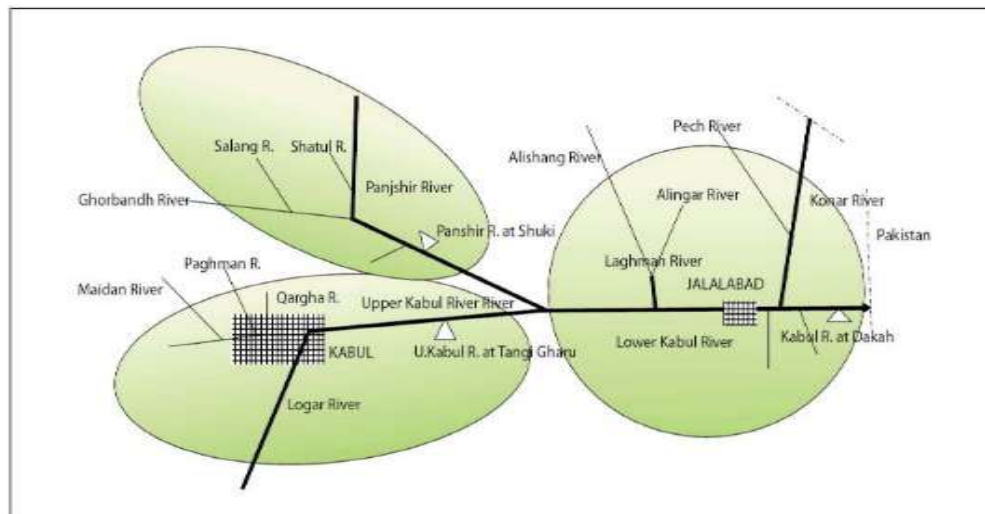


**Fig. 3 Schematic form of subdivision**

### **The Upper Kabul Subbasin:**

The Upper Kabul subbasin encompasses two catchments namely the Upper Kabul River and the Logar River, the first which, with three little streams, the Paghman, Qargha, and Maidan begins upstream of Kabul and moves from the focal point of the city; and the Logar River, which drains a sloping and dry catchment south of the city. The Logar catchment includes around 75 % of the drainage region of Logar-Kabul sub-basin over measuring zone at Tangi Gharu (figure 3). There is little yet imperative irrigated agribusiness around the Logar River. Additionally, there are various small hydropower stations on the smaller tributaries. However, the Kabul city is most important, which is the largest city of Afghanistan.

However, the Panjshir basin is situated towards the north side of the Logar-Upper Kabul sub-basin which is formed by the Panjshir River and has its major and minor branches such as the Shatul, Salang, and Ghorband streams as shown in figure 3. The upper piece of this catchment comprises of hills with high slopes in the Hindu Kush mountain area, which reach more than 6,000 m asl and generally remains covered by the snow all through the year. The southern segment of the watershed, specifically the right side portion of the Ghorband and Panjshir stream close to their conjunction, gets onto the expansive and tenderly inclining rich Shomali Plain which has got a portion of the noteworthy flooded regions in the sub-basin. Downstream of the conjunction with the Ghorband River and underneath the measuring station at Shukhi, the Panjshir River passes through a lofty, restricted chasm until the point where it joins the Upper Kabul River. Despite the fact that the drainage territory of the Panjshir River at Shukhi is comparatively shorter by around 84 % to the Upper Kabul River at Tangi Gharu, has got its normal yearly stream flow which is more than 6 times as substantial in the normal timing.

### **The Lower Kabul Subbasin:**

The Lower Kabul sub-basin is between the conjunction of the Upper Kabul streams and Panjshir waterway to the Pakistan boundary. It comprises of two substantial watersheds to left bank or toward the north of the primary stem of the waterway. These are (a) the Konar stream, which incorporates the Pech River and begins in Pakistan (b) the Laghman waterway, which incorporates the Alishang and Alinghar stream. There are a few little tributaries on the right bank, including the Surkhrud which is close to Jalalabad, which, having populace of 120,000(approx.), is considered as the main extensive city in the Lower Kabul sub-basin. The primary tributary of Kabul River flows eastbound from the conjunction with the Upper Kabul and Panjshir waterways through a tight chasm until its juncture with Laghman River, where valley gets wide. When primary tributary of the waterway proceeds eastbound, the valley augments into an expansive plain which involves the second biggest imperative rural zone in the Kabul River basin. Three dams & reservoirs are developed in the canyon for the generation of hydropower. The most minimal repository in this course, at Darunta, is upstream section of Jalalabad, and furthermore supplies water for irrigation, domestic and other needs of the region. Stream flow in the lower basin are received basically from the two huge, precipitous catchments, in particular, the Konar and the Laghman, whose higher snow and ice sheet covered regions achieve almost 6,500 m asl. Aside from the high rugged areas toward the north direction, the atmosphere of this lower locale is affected by southwest storm, with a couple of days every time of very low freezing temperatures.

### **Climate and Hydrology:**

The atmosphere is normally dry, typical of arid or semiarid type, having chilly winters and dry summers. The mountain regions of the upper east are sub-arctic with spell of cold and dry winters. In the mountains circumscribing Pakistan, an alternate periphery impact of the storm, by and large originating from the southeast, brings tropical air masses that manage the atmosphere among July and September. Time and again, these air masses advance into southern and focal Afghanistan, bringing rain and dampness. Atmosphere of Afghanistan as indicated by precipitation is classified as arid and semiarid.

According to Sidiqi et al. (2018), in central and northeast regions due to existence of high mountains precipitation is more but in western and southwest areas precipitation is less or no precipitation at all. The average annual precipitation in Afghanistan is 327mm and the average annual precipitation on Kabul river basin is 312mm where the majority of this precipitation occurs on northern region of basin. Over 30% of Kabul river basin is fed by glaciers and snow of Hindu-Kush and Paghman high mountains. The glacier starts melting in spring (Mar-May) due to increase in temperature degree and the melting process getting faster in summer as result an overall decrease in discharge therefore the basin remains with low discharge for the rest of the year. As shown below.

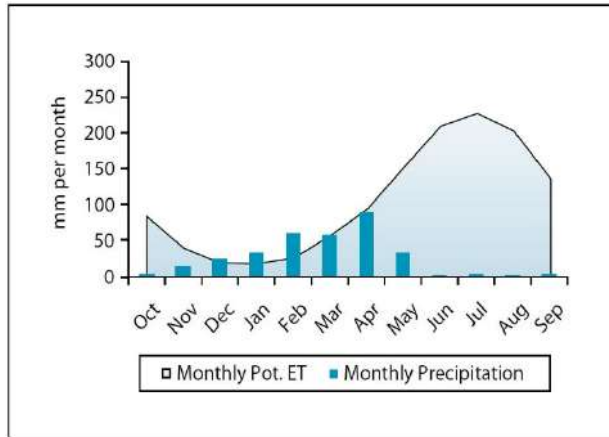


**Fig. 4 Monthly average precipitation over KRB**

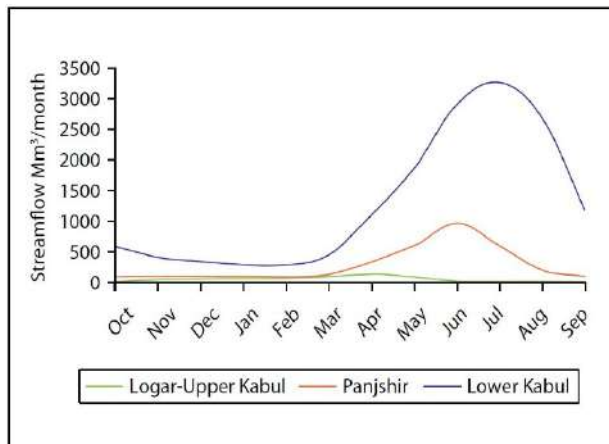


**Fig.5 Monthly average streamflow in KRB**

**ANALYSIS OF RAINFALL IN KRB**

Rainfall is an important part of hydrological system. This study is based on geo-statistical analysis for preparing accurate spatial analysis, estimation, forecasting and mapping of rainfall areas in KRB as there is lack of adequate gauging stations to cover all regions of the basin. Sarwar Qureshi (2002) has mentioned the historical rainfall data and

Stations with their locations are shown in Table 1 and Fig. 6.



**Fig.6: Stations location in KRB**

**Table 1: Gauging stations**

<b>ID</b>	<b>Station Name</b>	<b>Longitude</b>	<b>Latitude</b>
1	ASAD ABAD	71.15	34.86
2	ASMAR	71.33	35.02
3	BADAM BAGH	69.12	34.55
4	CHARIKAR	69.17	35.01
5	PANJSHIR	69.65	35.28
6	DARULAMAN	69.12	34.45
7	GUL KHANA	69.13	34.52
8	JABUL SIRAJ	69.25	35.13
9	JAGHATOO	68.38	33.82
10	JALALABAD	70.46	34.43
11	KABUL AIRPORT	69.21	34.55
12	KAPISA AGRI	69.33	35.2
13	KARIZMIR	69.05	34.63
14	KHOST	69.95	33.35
15	KOHESTAN	69.3	35.17
16	LAGHMAN	70.13	34.39
17	PAGHMAN	68.57	34.35
18	QARGHA	69.03	34.55
19	SAROBI	69.69	34.54
20	LOGAR	69.03	34.06
21	URGON	69.12	32.86

## CONCLUSIONS

The Kabul river is a prominent river in the country Afghanistan. Due to civil war of more than 25 years amidst Afghanistan, a shortfall of water related data is felt in Kabul river basin. This study incorporates the densely populated region of Afghanistan i.e. Kabul city. Therefore, it is expected to be vital for water supply and reconstruction purposes in the concerned portion of nation. Most of KRB area is covered by high mountains and the number of stations are very few which couldn't cover all the basin area. Therefore, the present work covered the analysis of rainfall over areas with no stations or away from the stations to analyze the areas with less or more precipitation over the basin and take decision for upcoming floods or drought accordingly. For the analysis of rainfall data kriging technique has been explained. Moreover, this method may also be used for Evaporation, Temperature, Humidity etc. For further work by using GIS, maps of the particular areas can be made which states more or less precipitated regions furthermore this method can be applied to other parts of the country which could be very useful for agriculture purpose.

## REFERENCES

- FAO (Food and Agriculture Organization of the United Nations) "Precipitation Database, CROPWAT," 1970 - 2000.
- USGS (United States Geological Survey) "AGROMET & NOAA," [Online]. Available: <<https://www.noaa.gov>>.
- G. M. K. Raphy Favre (2004), Watershed Atlas of Afghanistan, Kabul: FAO, AIMS, SDC.
- K. A. G. Murthy, "Geostatistical analysis for estimation of mean rainfalls in Andhra Pradesh, India," International Journal of Geology, pp. 37-51, 2007.
- Ahmad, M., & Wasiq, M. (2004). Water resource development in Northern Afghanistan and its implications for Amu Darya Basin (No. 36). World Bank Publications.
- R. Favre, R. and G.M. Kamal (2004), "Watershed Atlas of Afghanistan." Ministry of Irrigation, Water Resources and Environment Accessible at <[http://aizon.org/watershed\\_atlas.htm](http://aizon.org/watershed_atlas.htm)>.
- Report of climate change in Afghanistan by the World Food Programme (WFP), the United Nations Environment Programme (UNEP) and Afghanistan's National Environmental Protection Agency (NEPA).
- Sarwar Qureshi (2002), "Water Resources. Management in Afghanistan: The Issues and Options". WORKING PAPER 49, Pakistan Country Series No. 14. SM.
- G. R. Lashkaripour S. A. Hussaini, Water resource management in Kabul river basin, eastern Afghanistan, 18 September 2007.
- Scoping Strategic Options for Development of the Kabul River Basin, A multisectoral decision support system.
- Suliman Yousaf (2017) "KABUL RIVER AND PAK-AFGHAN RELATIONS", Central Asia Journal No. 80, Summer.
- Sayama, T., Ozawa, G., Kawakami, T., Nabesaka, S. and Fukami, K., 2012. Rainfall–runoff–inundation analysis of the 2010 Pakistan flood in the Kabul River basin. Hydrological Sciences Journal, 57 (2), 298–312.
- Matthew King and Benjamin Sturtewagen "Making the Most of Afghanistan's River Basins Opportunities for Regional Cooperation". February 2010.
- B. Alijani, J. O'Brien, B. Yarnal "Spatial analysis of precipitation intensity and concentration in Iran". 18 October 2007.
- Massouda Sidiqi, Sangam Shrestha and Sarawut Ninsawat "Projection of climate change scenarios in the Kabul River Basin, Afghanistan". CURRENT SCIENCE, VOL. 114, NO. 1310 6, 25 MARCH 2018.

## **A Review of Rainfall and Ground Water Level Trends of Kurukshetra, Haryana**

**Mridula Sharma<sup>1#</sup> and Arun Goel<sup>2\*</sup>**

<sup>1</sup>M.Tech Student, Department of Civil Engineering, National Institute of Technology, Kurukshetra, Haryana-136119;

e-mail: mridula0995@gmail.com

<sup>2</sup>Professor, Department of Civil Engineering, National Institute of Technology, Kurukshetra, Haryana-136119;

e-mail: drarun\_goel@yahoo.co.in, Corresponding Author

### **ABSTRACT**

This paper aims at synthesizing the literature, taking note of spatio-temporal variations in rainfall and ground water levels so that the response of groundwater systems to climatic stresses in the region can be understood. A single district, Kurukshetra in the Indian state of Haryana has been taken in order to avoid spatial heterogeneity of trends due to large area consideration. A sharp decline in ground water level and a mildly decreasing trend in precipitation of the region is observed, however, no clear increasing or decreasing precipitation pattern was observed on national-scale.

**KEYWORDS:** *Ground Water; Rainfall; Climate change; Trend.*

### **INTRODUCTION**

The Rainfall trends across the globe are altered due to change in the behaviour of hydrologic and climatic variables which are not invariantly spread throughout the region but have a distinctive localized pattern which along with hydro-geological parameters and land-use pattern have a profound impact on groundwater level and quality. This inter-relationship must be studied for better and sustainable planning of the resources. For such a study, smaller area consideration may prove to be more vital in terms of practical usability. Moreover, localized analyses are important for a country as vast as India since, one region may be undergoing floods while some other region may be facing drought – all veiled in a national-scale investigation and furthermore, without trend setting innovations for considering inter-basin transfer of water, regional shortages and abundances cause devastation harming the agricultural economy. Moreover, poor section of society is especially susceptible, being more dependent on local water, food supplies and other climate-sensitive resources.

Appreciable work has been done for both ground water level fluctuation and rainfall trends analysis and predictions separately but a combined study would be of greater vitality. Also, in order to avoid unclear trends and precise understanding, smaller study areas should be preferred. Therefore, in the present study Kurukshetra district of Haryana is being considered in terms of both rainfall and ground water level variability.

### **PAST STUDIES**

Goyal et al (2010) studied the changes in depth to water table below ground (bgl) in accordance with rainfall and groundwater development from 1987 to 2007 in agrarian district, Kaithal (adjoining Kurukshetra) of Haryana state

in India. It was noticed that profundity to subterranean water level in fresh water zones of the district (Kaithal, Pundri and Gulha blocks) declined in the range of 10 m to 23 m. However, In Kalayat and Rajaund i.e. saline water blocks, the levels were seen to sway in a comparatively limited scope of 4– 9 m. Also, it was stated that during 1997–2007, the rate of depletion was more compared to the preceding decade. This extreme deterioration of ground water resource was accredited to heedless extraction for irrigation purpose and reduction in precipitation since 1998. In order to manage resources sustainably, the study suggested changes in methods of irrigation and cropping pattern.

Tirkey et al (2012) analyzed groundwater level changes in accordance with precipitation considering, Palamu, a drought-stricken district in Jharkhand, India and concluded that however, there is ample precipitation in the south eastern area of the district where the water table is close to surface conditions during August, the average depth to water table below ground increases by the month of May because of the hard rock terrain present in the locale that disallows water to reach deep into the aquifer zones, and hence most of the water escapes in the form of runoff and some amount of it gets absorbed into the ground to sustain shallow aquifers. They therefore stated that these areas are more vulnerable to drought like conditions because of a consistent decline in the water level and suggested augmentation of subterranean water by making small water harvesting structures particularly at the places which are at elevation below 300m.

## STUDY AREA

Haryana, an inland state situated in north India between  $74^{\circ}28'$  and  $77^{\circ}36'$  E longitude and  $27^{\circ}39'$  to  $30^{\circ}35'$  N latitude covering a territory of 44,212 sq. km. The two major rivers that drain the land of Haryana are Ghaggar and Yamuna. Out of 22 districts of Haryana, Kurukshetra (as shown in Fig.1) is a holy district between East longitudes  $76^{\circ}26'27''$  and  $77^{\circ}07'57''$  and North latitudes  $29^{\circ}53'00''$  and  $30^{\circ}15'02''$ . Its eastern regions fall under the Upper Yamuna Basin and western regions fall under the Ghaggar basin. Major drainage in the area is provided by the river Markanda. Around 90% of geographical area of the district is cultivable and irrigation is done by both ground water and surface water. Also, the vital role of rainfall cannot be under-estimated. The meteorological conditions of Haryana are categorised as semiarid tropical to subtropical and yearly precipitation ranges from under 300 mm to more than 1000 mm, mean being 704 mm. Approximately, 75– 80% of the precipitation happens amid June and September. Significant harvests developed around there incorporate rice, wheat, mustard, maize, and certain fodder crops (Ground water information booklet, 2013).

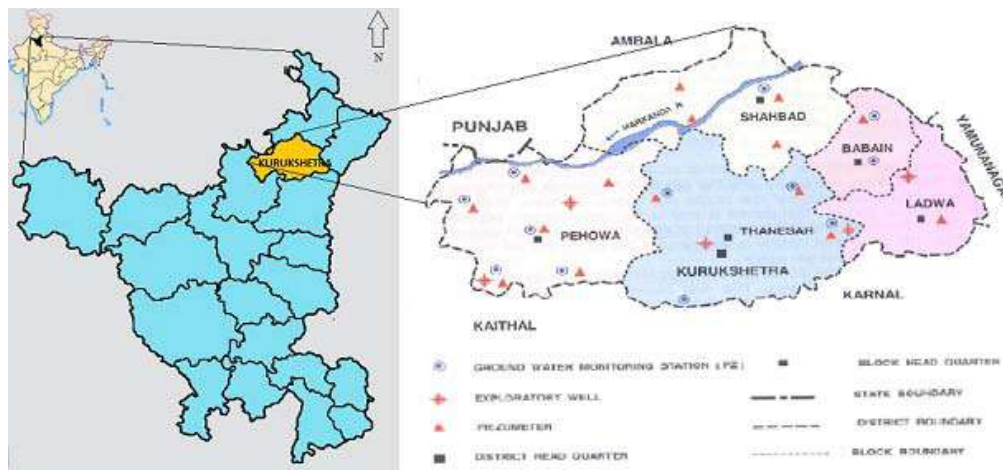


Fig. 1 Location of study area

## RAINFALL TRENDS

Mooley and Parthasarathy (1984) studied summer monsoon (June to September) precipitation of India for the time span between 1871 and 1978 and did not find any exact overall decreasing or increasing pattern in average annual rainfall across the country. This homogeneity in rainfall trends could be attributed to high variability over time and space [Lal M, 2001]. Krishnamurthy and Shukla (2000) investigated intra-seasonal and inter-annual variation in precipitation over India and stated that amid the dynamic stage, the rainfall was more than typical in central India whereas it was less than normal in northern and southern parts of India, however, this trend got altered in the break phase.

Sarker & Thapliyal (1988) studied rainfall variation in Ganga basin for hundred year data (1901-2000) and realized the need of some sub-basins' and districts' wise strategies in order to deal with the problems regarding the climate change.

Singh and Sontakke (2002) explored Climatic Fluctuations over the Indo-Gangetic Plains and derived that there has been a westbound move in precipitation exercises over the district and credited these spatial changes in precipitation exercises to a worldwide temperature alteration and related variations in the Indian summer rainstorm course and the general large-scale air movement that distributes heat on the surface of the earth.

Kothyari et al. (1997) reported declining precipitation incline over the Ganga basin, starting during the latter half of the 1960s. Bisht et al (2017) studied the trends across Indian river basins and observed that dominant part of the basin demonstrated a decrease in post-monsoonal precipitation amid 1971– 2015 for the vast majority of north India, which may prompt diminished yield creation hampering agrarian exercises. Additionally, Ganga basin was observed to be one of the most noticeably bad influenced basins because of decreased seasonal and yearly precipitation, aside from pre-storm. The catchment region of Yamuna adds up to 40.2% of the territory of Ganga Basin. Rai et al (2010) contemplated climatic parameters of Yamuna basin and noticed a general falling pattern in the yearly precipitation, monsoon precipitation, yearly rainy days and monsoon rainy days. Kumar et al (2010) examined month to month, seasonal and yearly patterns of precipitation utilizing month to month precipitation information of 135 years (1871– 2005) for 30 sub-divisions (sub-districts) in India and expressed that regarding level of mean per 100 years, Punjab and Haryana saw a huge escalating pattern in yearly precipitation. Krishan et al (2015) conducted the trend detection analysis of rainfall for 17 districts of Punjab including Patiala, Sangrur and Mansa which fall in ghaggar basin and indicated an increasing rainfall trends in annual, monsoon, pre-monsoon and post-monsoon seasons.

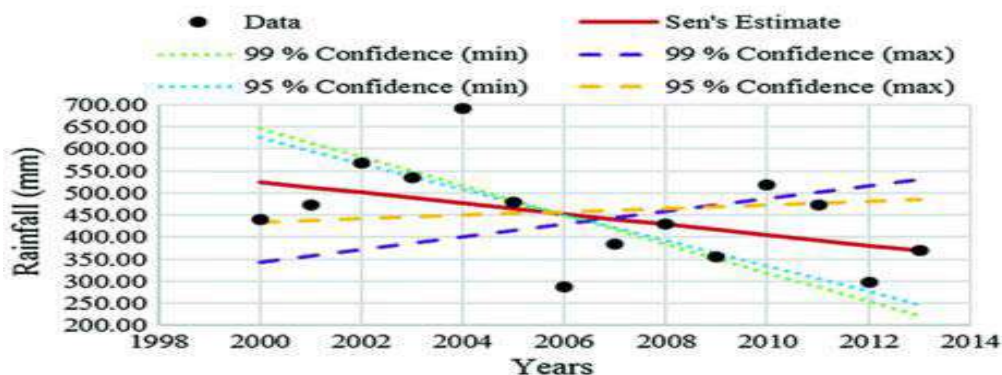


**Fig. 2** Rainfall trend in Kurukshetra district as noted by Soni and Singh (2017)

However, Kumar V. et al (2015) divided Haryana state into three zones and stated that the yearly typical precipitation value differed from 389.4 to 815.0 mm and noted an apparent diminishing pattern in precipitation from north east to south west Haryana. Also, as per, Rainfall Statistics of India-2016 (2017), both Haryana and Punjab remained in Deficient/ Large Deficient category of rainfall at least for three of the seasons as well as annually.

A local study conducted in Hisar district of Haryana showed a general increasing trend of 2.3mm/year and the seasonal pattern study uncovered a huge increment in precipitation amid pre-monsoon season but no major change during the post-monsoon period (Sharma et al, 2016). Similarly, in adjoining Fatehabad district also, in a study analyzing 113 years of rainfall trends, precipitation was found to increase for all seasons except winters. Also, it was noted that deficient and excess rainfall occurred with almost same frequency during study period (Rainfall Statistics of India – 2016).

In a study aimed at analysing Spatial and transient distribution of monthly precipitation in Haryana for the period 1970-2011, significant decrease in annual and monsoon rainfall was noticed at Thanesar (Kurukshetra). (Nain 2016)

Soni and Singh (2017) undertook a study to gauge the variation in climatic parameters of Kurukshetra district including rainfall, from 2000 to 2013 and observed a negative trend in rainfall with a rate of reduction of 12.00% as shown in Fig. 2.

### **DECLINING GROUND WATER LEVEL**

Rodell et al (2009) examined the perceptions from NASA's GRACE i.e. Gravity Recovery and Climate Experiment and observed that subterranean water was declining at a mean rate of  $4.0 \pm 1.0$  cm/year proportional stature of water ( $17.7 \pm 4.5$  km<sup>3</sup> yr<sup>-1</sup>) in the Indian states of Punjab, Haryana, Rajasthan and capital, Delhi and more than 109 km<sup>3</sup> of ground water vanished during August 2002 and October 2008, double the volume of India's biggest surface water repository, the Upper Wainganga in Madhya Pradesh. In spite of the fact that there were no extraordinary drifts in precipitation. Another examination combined satellite GRACE's information with hydrological models for excluding common variations and inferred that the area lost ground water at a rate of  $54 \pm 9$  km<sup>3</sup>/year during April, 2002 and June, 2008. It is expected to be the biggest rate of groundwater depletion in any approximately similar-sized locale of the world. Its plausible commitment to sea level ascent is probably comparable to that due to melting of Alaskan ice sheets. This pattern, if continued to sustain, will prompt a noteworthy water emergency in the area when this exhaustible asset gets depleted.

According to, Groundwater data booklet Kurukshetra (CGWB 2007), the groundwater development stage in Kurukshetra area was 166%. Examination of groundwater table profundity for past 24 years demonstrated a decreasing pattern in the locale at a rate fluctuating from 0.98 to 1.16 m/year (Tiwari, 2009).

As indicated by Groundwater scenario of India (2009– 10), amid the most recent 40 years, groundwater wells and tube wells have expanded multiple times, primarily in arid and semi-arid areas of the nation. In numerous blocks of Haryana, the ground water development stage is over 100% which demonstrates that the ground water extraction is more than recharge per year. (CGWB 2009)

Afterward, according to, Ground Water Information Booklet, Kurukshetra, (2013), the profundity of water level in the region ranges from 20.18 m to 32.64 m subterranean level in pre storm period and 21.80m to 34.41 m subterranean level amid post rainstorm period 2011. The profundity to water table map demonstrates that in huge parts of the area water table is over 30 m bgl and spreads in Ladwa, Babain, Shahabad blocks and portions of Thanesar block. The shallow ground water, in the profundity range of 20 to 25 m bgl spreads in south and west territories of the area covering Pehowa and Thanesar Blocks. It is likewise noticed that amid post monsoon period the region amid 20 m to 25m bgl gets diminished and the zone in which water table is 30 m bgl increases signifying stress on ground water resource to fulfil the agrarian interest amid both monsoon and non-monsoon period.

A general declination in water levels in the region is shown by net change in water levels varying from 1.14 m/yr to 1.71 m/yr amid the period 2000-2011. The highest rate of decrease in ground water level was noted in piezometer at Shahabad. It is additionally relevant to notice that the rate of declination was discovered to be much more than 1.0 m/yr. In the region, height of the water table lies in the range of 205 m to 240 m above mean sea level. General gradient of the ground water level is approximately 1.08 m/km. All inclusive, the flow of ground water is in the south- west direction.

Patle et al (2016) did mathematical modelling of declining ground water levels in Kurukshetra utilizing Auto Regressive Integrated Moving Average (ARIMA) model and expressed that the stochastic investigation of groundwater depths completed utilizing the most appropriate models ARIMA (2, 1, 1) and ARIMA (0, 1, 2) showed that by the year 2020, normal groundwater depths in the pre-monsoon and post-monsoon seasons in the locale are relied upon to decrease by 5.63 and 5.72 m respectively, over the base year 2010, if the groundwater extraction proceeds at a similar rate.

Afterwards, Singh et al (2017) conducted a GIS-based spatial and temporal analysis of groundwater level changes over Haryana in 2017 and observed the yearly normal decrease in groundwater in Haryana to be over 32cm/year, with strongest decline of 108.9cm/year in Kurukshetra District.

### CONCLUSION AND REMARKS

It is inferred from past studies that there is a clear and alarming declination in ground water levels in the region and although some decrease in local rainfall trends is also observed but decline in rainfall is not the only and prominent cause of such a sharp decline in ground water level. It is likely to be attributed to indiscriminate pumping of ground water for irrigation and other demands. Therefore, a need to explore rainfall vis-a-vis ground water trends in greater detail is felt since, such a study is expected to pave way for estimation of sustainable pumpage of ground water and play a vital role in accessing the scope of artificial groundwater recharge structures for mitigating the adverse impact of rainfall variability on groundwater.

### REFERENCES

- Anurag, Kumar A., Singh D., Singh R., Singh S. and Shekhar C.(2017). “Evaluating Rainfall Trends at Hisar (Haryana) in the Semi-arid Zone of North India.” *Annals of Arid Zone* 56 (3 & 4): 83-87.
- Bisht, D. S., Chatterjee, C., Raghuwanshi, N. S., & Sridhar, V. (2017). “Spatio-temporal trends of rainfall across Indian river basins.” *Theoretical and Applied Climatology*, 132(1-2), 419–436.
- CGWB (Central Ground water Board) (2007) *Groundwater information booklet Kurukshetra district, Haryana*. Ministry of Water Resources (MoWR), CGWB, Chandigarh.
- CGWB (Central Ground Water Board) (2009) *Groundwater scenario of India 2009–10*. MoWR, GoI, Faridabad.
- CGWB (Central Ground water Board) (2013) *Ground Water Information Booklet, Kurukshetra, Haryana*. Ministry of Water Resources.
- Goyal, S. K., Chaudhary, B. S., Singh, O., Sethi, G. K., & Thakur, P. K. (2010). “Variability analysis of groundwater levels - A GIS-based case study.” *Journal of the Indian Society of Remote Sensing*, 38(2), 355–364.
- IMD (India Meteorological Department) (2017). *Rainfall Statistics of India – 2016*. IMD, Ministry of Earth Sciences, Report no.: ESSO/IMD/HS/R. F. Report/01(2017)/23
- IPCC WG II. (Working Group II Contribution to the Intergovernmental Panel on Climate Change) (2007). “*Climate Change 2007: Impacts, Adaptation and Vulnerability*” Fourth Assessment Report, Summary for Policymakers.
- Kothiyari UC, Singh VP, Aravamuthan V (1997). “An investigation of changes in rainfall and temperature regimes of the Ganga Basin in India.” *Water Resour Manage* , 11: 17-34.
- Krishan G, Chandniha S. K, Lohani A. K. (2015). “Rainfall Trend Analysis of Punjab, India Using Statistical Non Parametric Test.” *Curr World Environ*, 10(3).
- Krishnamurthy V, Shukla J. (2000). “Intraseasonal and Interannual variability of rainfall over India.” *Journal of Climate* 13:4366–4377.
- Kumar, V., Jain, S. K. & Singh, Y.(2010).“Analysis of long-term rainfall trends in India.” *Hydrol. Sci. J.* 55(4), 484-496.
- Kumar, V., Niwas R. and Khichar, M.L. (2015). “Rainfall Zone and Its Trend Analysis in Haryana Using GIS.” *Journal of Agricultural Physics*. Vol. 15, No. 1, pp. 63-68.
- Lal M. (2001). “Climatic change—Implications for India’s water resource.” *J Indian Water Resour. Soc.*, 21, 101-119.

- Mooley, D. A. & Parthasarthy, B. (1984). “ Fluctuations of all India summer monsoon rainfall during 1871-1978.” *Climatic Change* 6, 287–301.
- Patle, G. T.; Singh, D. K.; Sarangi, A.(2016). “Modelling of declining groundwater depth in Kurukshetra district, Haryana, India.” *Current Science* (00113891), Vol. 111 Issue 4, 717-723.
- Rai, R.K., Upadhyay, A.R., & Ojha, C.S. (2010). “Temporal Variability of Climatic Parameters of Yamuna River Basin: Spatial Analysis of Persistence, Trend and Periodicity.” *The Open Hydrology Journal*, 4, 184-210.



## Investigating the Impact of Land Use and Land Cover Changes in Regions of Punjab: A Review

Smriti<sup>1</sup> Mahesh Patel<sup>2</sup>

<sup>1</sup>\*:#B. Tech. Student, Department of Civil Engineering, Dr B.R. Ambedkar National Institute of Technology, Jalandhar Punjab-144011; e-mail: [smritisaini71@gmail.com](mailto:smritisaini71@gmail.com)

<sup>2</sup> Assistant Professor, Department of Civil Engineering, Dr B.R. Ambedkar National Institute of Technology, Jalandhar Punjab-144011; e-mail: [patelm@nitj.ac.in](mailto:patelm@nitj.ac.in), Corresponding Author

### ABSTRACT

This work shows the dynamics of land use and land cover changes (LULCC) in various regions of Punjab. To understand these changes, several studies are investigated to understand the main cause and impact on social livelihoods, hydrological and biodiversity responses. It has been found that since past many centuries natural and human factors influenced the land use/cover. In the present study, more emphasis is given to pattern and trends and main drivers of LULCC in regions of Punjab. It has been found that built area is significantly increased from 1975 to 2010, resulting adverse impact on river morphology and hydrological responses. In addition to this, a substantial number of studies confirmed that the root driver for the LULCCs in the state was population growth among the six factors stated. Most of the LULCC is considered as a response of deforestation and increasing population, which has led to the conversion of closed forest area in most of settlements and barren land and also led to the fluctuation in the area occupied by water bodies. Consequently, this unceasing and unprecedented LULCC in Punjab has resulted in increased habitat and biodiversity loss, desertification, pollution risks and local climate alteration as well as other associated problem

**KEYWORDS:** *LULCC;; GIS; Remote Sensing; Patterns*

### INTRODUCTION

LULCC, acute environmental challenge for human being, plays a critical role in the appropriate management of the earth's surface, which is required to address the society (Mustard et al., 2004). Land is very important natural resource or perhaps it is viewed as the resource base instead of resource itself (Mather, 1986). Apart from that, LULCC are the greater determinants of overall ecological changes including extreme influence to social livelihoods (Olson et al., 2008). These changes are having the ability to influence the climatologically, hydrological and biodiversity responses. In addition to this, socio-economic development, population expansion, and pressures for land for agriculture are the main cause of LULCC (Lambin et al., 2003).

As almost all the basic necessities of humans such as food, clothing and shelter are dependent on land, so it leads to change in the utilization of the land. In general, land use signifies how a fragment of land is used, and it includes a sequence of operations performed by humans on land with an intension to procure benefits from the available land resources. Apart from that the other term is classified along with land use i.e. land cover. The land cover indicates the surface cover of earth and its corresponding subsurface, which includes the soil material, plants, and water (Prakasam, 2010). In addition to this, the term land cover implies the types of characteristics of the earth available (Lillesand and Kiefer, 2008). LULCC are the changes in the origin of the earth surface, which is influenced by the human activity since most ancient time in the biosphere (Turner II, 2001). Because of changes in land use and land cover there have been significant observational changes in river discharge morphology and discharge. As in urban areas, water cannot be infiltrated into ground due to surface of roads and infrastructure, which are made of impermeable material. Instead, it runs into drains and finally reaches into river. Then in rural areas, ploughing is done in such a way so as to direct

rainwater to rivers faster which increases discharge. One more factor is deforestation, due to which interception to rainwater decreases and it reaches the ground faster. Due to this the ground becomes saturated soon which thus results in increase in surface run-off. Change detection is analysed from the data of past years using supervised classification methods. Punjab has gone through dynamic LULCC since past many centuries due to significant transformation caused by natural and human factors. To understand these changes, many studies have been conducted however; there is still considerable uncertainty with regard to LULCC extent, trend and pattern in Punjab. The main aim of this article is to narratively synthesize and descriptively present the major findings of the studies conducted on LULCC in different regions in Punjab.

## STUDY AREA

The variations in LULC are studied in the regions of Punjab as shown in Figure 1, where red dots indicate the regions of investigation. These regions are Jalandhar, Punjab Siwaliks and further in that the LULCC of Rupnagar region is analysed. Jalandhar city is situated in northern Punjab in India between the latitude of 31° 19' 32" North and longitude of 75° 34' 45" East. It has an area of 102 km<sup>2</sup>. Jalandhar is coming under class 1 cities with a total population of 8,73,725. It is the 4<sup>th</sup> metropolitan city of the state of Punjab after Ludhiana, Amritsar and Gurdaspur. It stands at 56<sup>th</sup> position among Indian metropolitan cities. The city forms part of the Trans Indo Gangetic plain, topography is almost plain and the soil is very fertile in the area. It is surrounded by cultivating land from all positions. Maximum temperature varies from 19.4 degree Celsius in January up to 40 degree Celsius in May and June. The minimum temperature varies from 6.2 degree Celsius in January to 25 degree Celsius in May and June, correspondingly, winters are cold and summers are warm. The area received an average annual rainfall of about 569 mm. Maximum rainfall is received from the southwest monsoon. It is today going forth as a major hub for all economic activities in the country.



**Figure 1.** Location of study areas in terms of land use and land cover changes showing in red dots

From Figure 1, the region of Punjab Siwaliks can be defined, lying amongst rivers Sutlej and Ghaggar, situated in the Punjab, along Himachal Pradesh and Haryana boundary. The regions under these Siwaliks are Pathankot, Hoshiarpur, Rupnagar and Mohali. Punjab Siwaliks are the Himalayan hills ranges with their elevation ranging from 300 to 100 metres above the mean sea level and are formed as a result of Himalayan destruction. The geography of the region is hilly and as this has steep slopes which poses regions of arable agriculture. Siwalik region basically was covered with substantial dense jungles. However, the area under jungles is losing its amplitude since the last century. Currently, this region is under scrubs and small vegetation (Gosal, 2004). The ecology of this area is disturbed due to human invasions. Singh (2005) has found that since last five decades the region is undergoing severe environment and biodegradation

changes. The area is extended from 30°43'35''N latitude to 31°01'54''N latitude and 76°31'58' E longitude to 76°55'04''E longitude.

Rupnagar is located at 30.97°N ,76.53°E, which has an average elevation of 260 metres. The town is situated on bank of Sutlej River and Siwalik hill range spreads along the opposite bank of the river. Another region, Pathankot district, is a border district which lies at international border of Pakistan on its West. Pathankot, a densely populated city in the state of Punjab is ranked 9<sup>th</sup> after Ludhiana, Amritsar and Jalandhar, Patiala, Bhatinda, which lies on the geographical coordinates of 32° 17' 0" N, 75° 39' 0" E. Mohali is a city found in Punjab and it is situated at elevation 312 meters above sea level. This city has a population of 123,484 making it the 10<sup>th</sup> biggest city in Punjab.

### IMAGE CLASSIFICATION AND DATA INTERPRETATION

As study areas explained in the previous section are analysed by the researchers using image analysis and interpretation of data. Analysis for the region of Jalandhar is carried out by investigating the various features of land cover and land use images as shown in Figure 2, and Figure 3. It is clearly shown that built area is significantly increased from 1975 to 2010.

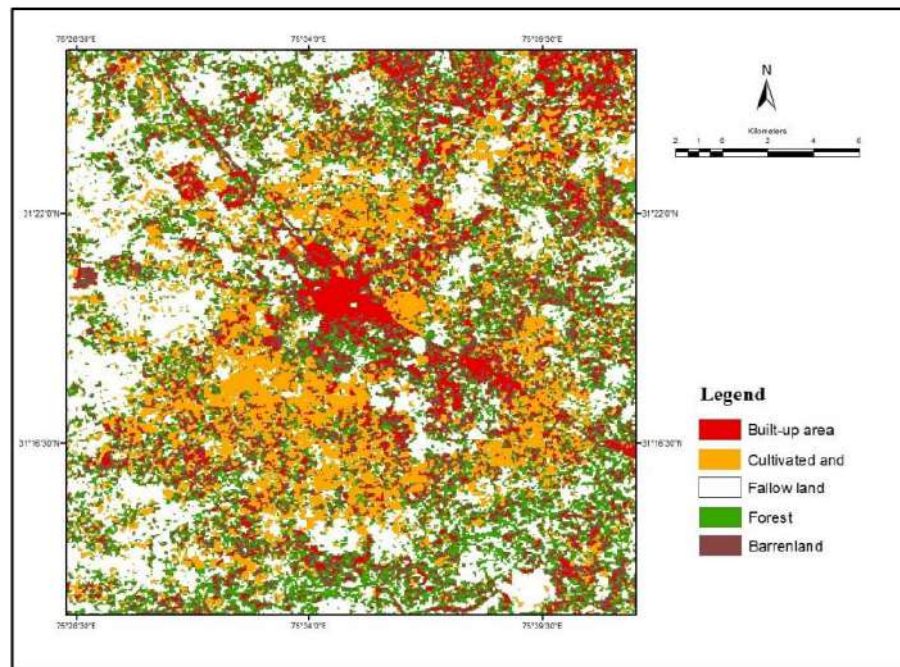


Figure 2. LULCC image of Jalandhar city in 1975 (Rani, 2014)

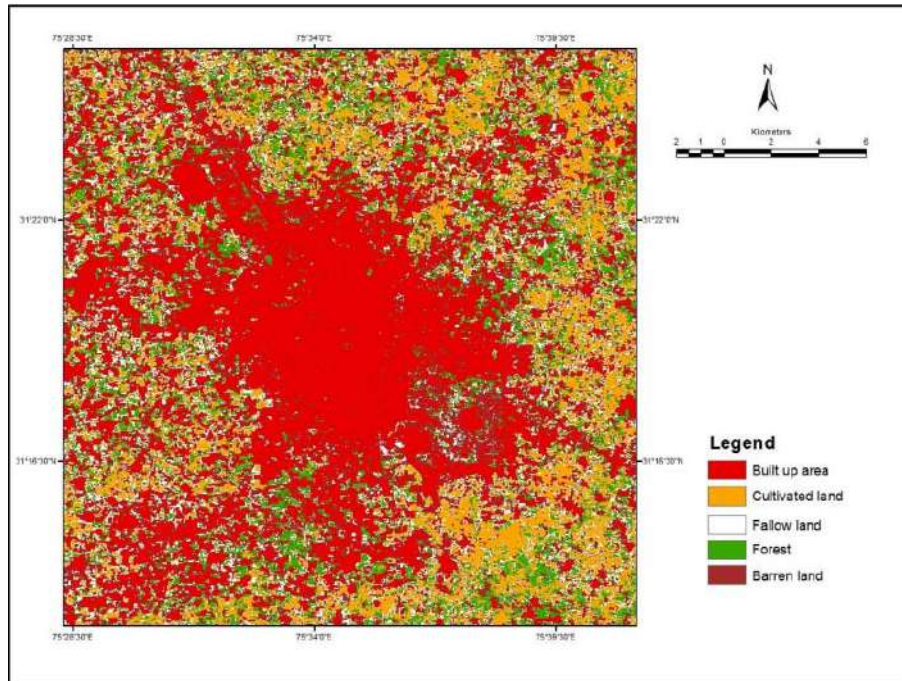


Figure 3. LULCC image of Jalandhar city in 2010 (Rani, 2014)

In addition to that Figure 4 indicates the detailed data interpretation of LULCC in the years of 1975, 1989, and 2010. From Figure 4, it can be observed that in 1975 agricultural land was dominant and built up area covered very minor area that mean less destruction of the land cover. Over the years, built up area were increased from 8% (1975) to 37% (2010) and agricultural land was decreased from 52% (1975) to 31% (2010), and forest cover was decreased from 22% (1975) to 18% (2010). Overall change revealed that built up area increased many folds in comparison to other classes. There are physical as well as socio-economic reasons behind these changes, resulting in urban expansion. Therefore, land use/land cover has changed drastically at the periphery of the city. As built up area has increased to 37% (2010) from 8% (1975). On the other hand agricultural land decreased to 31% (2010) from 52% (1975) so, urban expansion is considered the root cause behind it.

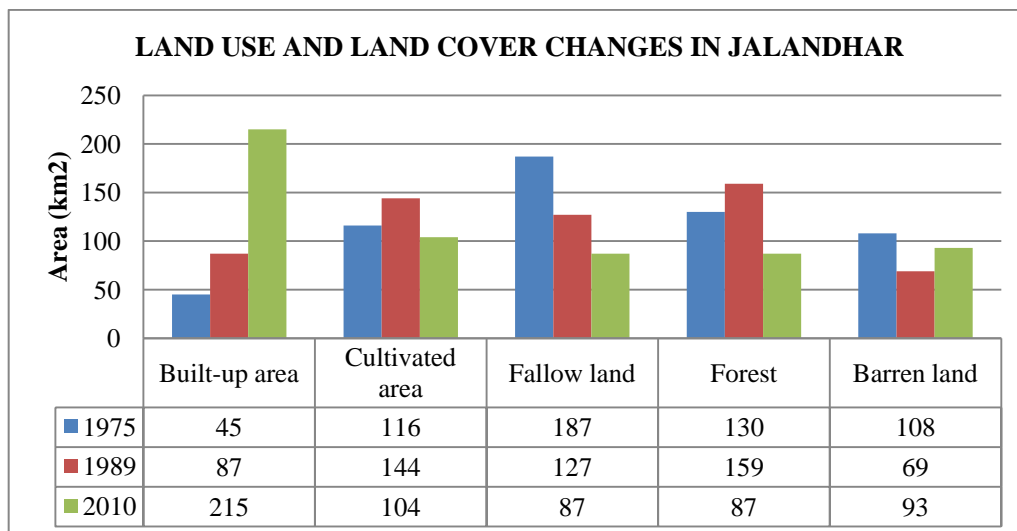


Figure 4. Comparison of the changes in land use and land cover over the years 1975, 1989, and 2010 (Rani, 2014)

The study further continued to another region of Punjab named Siwaliks that is belt extending from river Sutlej to Ghaggar as shown in Figure 5, where similar changes were found (Brar, 2013). By assessing the Figure 5, it has been

suggested that there has been an intense changes in the area occupied by closed forest, which has decreased by 69.92 km<sup>2</sup>. Also, there was an increase in area of barren forest (17.28 km<sup>2</sup>), agriculture (6.79 km<sup>2</sup>) and settlement area (6.17 km<sup>2</sup>).

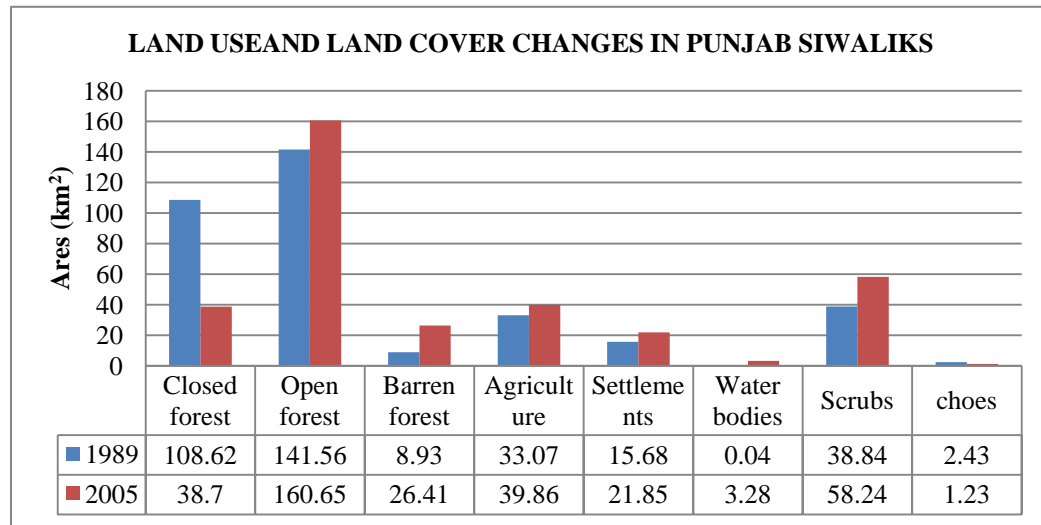


Figure 5. Relative comparison of LULCC in Punjab Siwaliks region in the years 1989 and 2005 (Brar, 2013)

Following that we can consider a portion of Punjab Siwaliks, Rupnagar for further analysis. Rupnagar district is supervised for its land cover in the year of 1989, 2000 and 2005 as shown in Figure 6. From Figure 6, it can be inferred that the change in spatial composition with reference to physiographic features to some extent. From 1989 to 2000, we can observe that there is an increase in number of settlements of about 60.4 km<sup>2</sup> and a decrease in cropland area of 89.61 km<sup>2</sup>. This decrease in cropland area maybe due to the result of increase in settlement and increase in fallow land, which can also be the cause of decrease under dense forest area by 118.83 km<sup>2</sup>. In addition to this, it has been noticed that an increase in salt affected land to 5.84 km<sup>2</sup>, which is due to overuse of fertilizers at the period of green revolution. Also, there is a significant decrease in water bodies by 3.9 km<sup>2</sup>.

Similarly, if we compare the classified data of 2000 and 2005, we can get a general view of trend in land change in Rupnagar district. Likewise, settlement area increased by around 33.12 km<sup>2</sup>, river area decreased around 3.9 km<sup>2</sup>, the crop land shows a decrease of 136.36 km<sup>2</sup>, and fallow land increased by 175.32 km<sup>2</sup> and so is the trend followed by land with scrubs, without scrubs and dense forest cover. If we take a holistic view of the available data and the inferred results, we can conclude by comparing the classified images of different year as it can be shown a declining trend from environmental point of view as there is a constant decrease in area under river, dense forest, and cropland while there is a drastic increase in settlement area.

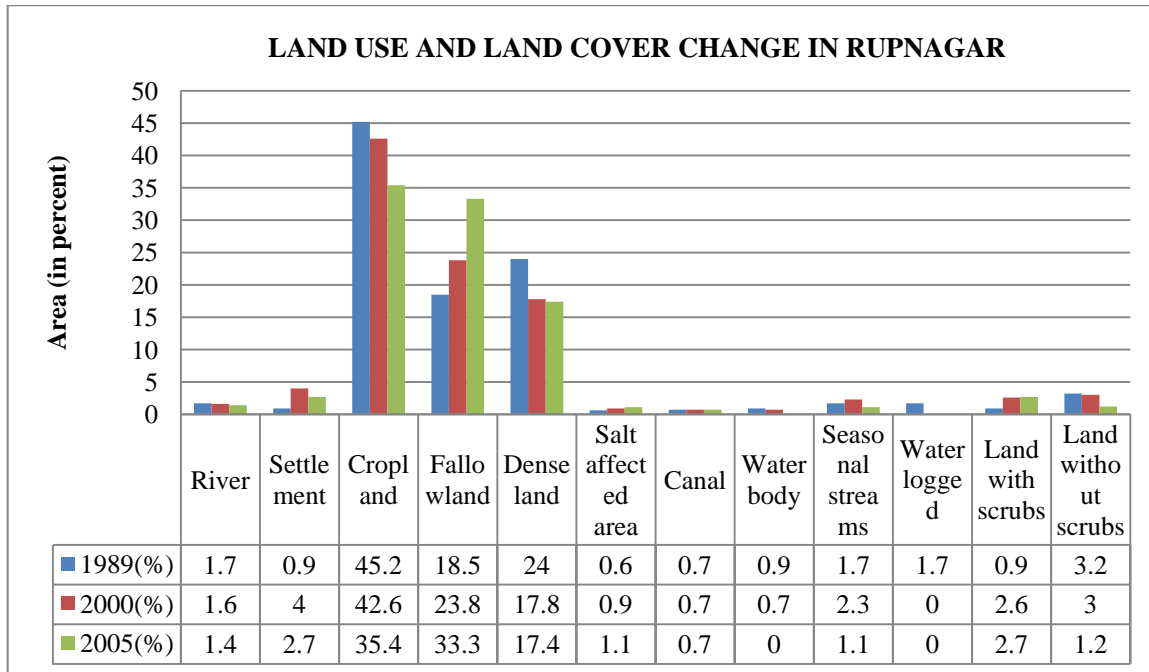


Figure 6. Changes in respective classes in the years 1989, 2000 and 2005 (Singh et al., 2010)

#### FACTORS AFFECTING THE CHANGE IN LAND COVER

The driving forces for LULCC can be classified into six parts: population; level of profusion; technological advancement; administrative economy; political organization of the region; and attitudes and values. Of these categories of driving forces, population produces the most controversy. However, it is one of the few variables for which worldwide data of reasonable accuracy are available, which provides a clear basis of statistical assessments of its role in various sorts of environmental change. At the regional scale, there are many studies that relate population growth and deforestation in developing countries in the tropics, although, their findings and methodologies have been questioned. Punjab is inhibited by a variety of population that has been subjected to constant changes due to migration people towards urban area. Although, the rate of population growth was steadily declining in year of 1960s, however, it has been grown rapidly (see Table 1) after serious majors have been taken by the government. Also, in the beginning of the second half of 20<sup>th</sup> century, it has maintained high fertility, resulted in significant growth and increase in the size of its population.

Table 1. Population growth, density and proportion of urban population (The World Bank)

Census year	1951	1961	1972	1981	1998	2003	2005
Population (in millions)	20.54	25.46	37.61	47.29	73.62	82.48	84.81
Density (person/km <sup>2</sup> )	100	124	183	230	358.5	402	413
Percentage of country's total population	60.9	59.4	57.6	56.1	55.6	55.5	55.3
Intercensal growth rate	-	2.18	3.40	2.74	2.63	2.3	1.9
Percentage of urban population	17.3	21.5	24.4	27.6	31.2	-	-
Growth rate of urban population	-	5.34	4.53	4.24	3.4	-	-

#### Conclusion

From all the study reviewed in this work show that LULCC is complex natural process. Also, LULCC involve heterogeneous components and interactions between them and hence it is difficult to model and figure out particular drivers for changes. However, understanding the main drivers of LULCC is important in formulation of policies and creating awareness to the people. Previous studies show that percentage of population growth is increasing, correspondingly, requirement of the house for each livelihood is increasing, and resulting built up area is increasing significantly. Thus, population growth has been referred as root cause for LULCC because population growth has increased the demand for food and associated expansion of agriculture. Specially, in the past periods, high yielding crop varieties and animal breeds, fertilizer and other inputs were not commonly available, and hence to meet high demand for food, expanding cropland was more practiced. Further, agriculture land is converted to non-agricultural land in order to support housing, irrigation, factories etc., which results into diversion of more and more fertile land of Punjab Also a prominent increase in barren land has been noticed, which is termed as desertification; that is degradation of land into arid area. This is mainly caused due to deforestation as it is quite visible from the data above where there is considerable decrease in forest area. This wood cutting leads to the erosion and oxidation of fertile soil. Therefore, density of natural vegetation is decreasing in this area, causing changes like increasing area under water bodies, agricultural land, and settlements are also found in a noticeable way. Another noteworthy change seen in land cover of Punjab is its increase in water bodies. This means the runoff of rivers has been increasing which can again be blamed on deforestation. This is because water won't seep into ground in urban areas due to impermeable surface and in rural areas (especially in hilly areas), because of deforestation interception to water decreases and it flows to rivers faster, thus leading to a growth in area under water bodies. In the last, research needs comprehensively on changes in river morphology due to LULCC and climate change, which can a future work of this study.

## REFERENCES

- Brar G. S. (2013). "Land Use and Land Cover Change with Remote Sensing and GIS: A Case Study of Punjab Siwaliks." *Int. J. Geomat. Geosc.*, 4(2), 296-304.
- Gosal G. S. (2004). "Physical Geography of the Punjab." *J. Punjab Studies*, 11(1), 19-37.
- Lambin, E., Geist, H., Lepers, E., (2003). "Dynamics of Land-Use and Land-Cover Change in Tropical Regions." *Annu. Rev. Environ. Resour.*, 28, 205–241.
- Lillesand T. M. and Kiefer R. W. (2008). "Remote Sensing and Image Interpretation." John Wiley and Sons, USA, 4th edition.
- Lambin, E., Geist, H., Lepers, E., (2003). "Dynamics of land-use and land-cover change in tropical regions." *Annu. Rev. Environ. Resour.* 28, 205–241.
- Mather P. M. (1986). "Review of: "Introductory Digital Image Processing: A Remote Sensing Perspective." *Int. J Remote Sens.*, 7(12), 1836-1838.
- Mather P. M. (2004). "Computer Processing of Remotely-Sensed Images: an Introduction, 3rd Edition." John Wiley and Sons Ltd, Chichester, England.
- The World Bank "Urban Population." (<https://data.worldbank.org/indicator/SP.URB.TOTL.IN.ZS>)
- Mustard J., DeFries R., Fisher T., Moran E. F. (2004). "Land Use and Land Cover Change Pathways and Impacts." Cochrane, M. A. (Ed.), Land Change Science: Observing, Monitoring, and Understanding Trajectories of Change on the Earth's Surface. Springer-Verlag, Dordrecht, the Netherlands.
- Olson J. M., Alagarwamy G., Andresen J. A., Campbell D. J., Davis A. Y., Ge J., Huebner M., Lofgren B. M., Lusch D. P., Moore N. J., Pijanowski B. C., Qi J., Thornton P. K., Torbick N. M., Wang J. (2008). "Integrating Diverse Methods to Understand Climate and Interactions in East Africa." *Geoforum*, 39, 898–911.
- Prakasam C. (2010). "Land Use And Land Cover Change Detection Through Remote Sensing Approach: A Case Study Of Kodaikanal Taluk, Tamilnadu." *Int. J. Geomat. Geosc.*, 1(2), 150-158.

Rani, S. (2014). "Monitoring Land Use/Land Cover Response to Urban Growth of The City of Jalandhar Using Remote Sensing Data." *Int. J. Advanc. Res.*, 2(6).

Singh C. K., Shastri S., Avtar R., Mukherjee S., Singh S. K. (2010). "Monitoring Change in Land Use and Land Cover in Rupnagar District of Punjab, India using Landsat and IRS LISS 3 satellite data." *Eco. Questions*, 13, 73-79.

Singh Y. (2005). "Operational Degradative Factors in Chandigarh Siwalik Hills, NW India." *Himalayan Ecology*, 13(1), 50-66.

Turner II B. L. (2001). "Land-Use and Land-Cover Change: Advances in 1.5 Decades of Sustained International Research." *Emergent, Sustainability Sci.*, 10, 269- 272.



## HUMAN INDUCED VIBRATIONS AND ITS EFFECTS ON STRUCTURE

Mudasir Nazeer,<sup>1</sup> H S Rai,<sup>2</sup> Jagbir Singh,<sup>3</sup> Kanish Kapoor<sup>4</sup>

<sup>1</sup>Research scholar, Department of Civil Engineering, Dr B R Ambedkar NIT Jalandhar, Punjab 144011, India,  
Email:Mudasir.ce.18@nitj.ac.in

<sup>2</sup>Professor, Department of Civil Engineering, Guru Nanak Dev Engineering College Ludhiana, Punjab 141006, India, Email:  
hardeep.raai@gmail.com

<sup>3</sup>Professor, Department of Civil Engineering, Guru Nanak Dev Engineering College Ludhiana, Punjab 141006, India, Email:  
jsdhillon26@gndec.ac.in

<sup>4</sup>Assistant Professor, Department of Civil Engineering, Dr B R Ambedkar NIT Jalandhar, Punjab 144011, India, Email:  
kapoor@nitj.ac.in, Corresponding Author

### ABSTRACT

Vibrations are the repetitive motions that cause the structural instability and unease to inhabitants. These vibrations of ground originated are transmitted through different layers of ground in the form of waves and mostly, waves of surface known as Rayleigh wave. Every structure is bound to vibrate if it possesses some elasticity in addition to its mass. The vibration effect depends upon the structural strength, structural behavior, material and dynamic properties in addition to intensity of undulations. Moreover with quick and fast industrial development besides land sacristies, industries are being set in the residential areas. And complaints regarding these vibrations arise at large and instead being solved by structural Engineers these are discussed at courtrooms. In this study structural vibrations related to forge hammer plants were studied and measured. Accelerations were taken in different directions around the heavy industrial plants with the help of sensor connected to instrument known as vib-scanner .it provides three values of accelerations viz, peak to peak ,zero to peak and Rms. Selection of instrument is also important, so we also discuss various issues related selection of instruments. Finally vibration reduction techniques (Gas cushion screen, Dampers, air mounts etc.) are discussed.

**KEYWORDS:** Acceleration (peak to peak, zero to peak, Rms), Vibration, Frequency, Accelerometer

### INTRODUCTION

The study of vibrations, mostly the seismic and blast induced vibrations are explored at large scale due to their dramatic effects and consequences on structure. The study of ground motions related to pile driving, hammer impact and traffic have not been explored to that extent as their magnitude is very less. Multistory gets its evolution from the existence and invention of lighter material, which is considered to material revolution. Limitations like very les inbuilt damping and minimum structure frequency made it less stable than old structures, made of stone and timber. Therefore with advancement in material and construction technology, structure becomes more prone to ground vibrations. There is not any accurate and criteria of permissible vibration, because it depends on large factors like structural behavior, structural

strength, material and dynamic properties etc. To make the effect of vibration under controlled rate, various techniques and methods like open trench method, gas cushion technique etc. are used. Among various methods used to minimize the ground motions, gas cushion technique is one of the fittest tool to be observed (Massarsch 2005). Sometimes human activities performed in various structures like fitness clubs, dance rooms, gymnasias floors etc. make conditions of vibration to such extent which sometimes become at alarming range and are unacceptable for safety (Allen and Pernica 1998). Resonance is the condition which is to take care of, as most of the floor vibrations are outcome of these resonance conditions, generally in case of light frame construction. Minimization of Vibration can also be done by providing extra stiffness to the floor structure; furthermore sometimes the problems can be simply addressed by providing damping or by isolating the equipment from direct contact. Moreover it is more important to make the proper position of any activity like aerobics or machinery on the proper floor. The aim and objective of this study is to study the problems of vibration related to forge hammers, thus we take different vibration response (acceleration) with different sensor mounted devices and to compare these calculated values with permissible values of Indian standards such that proper mitigation techniques are to be provided.

## **GROUND BORNE VIBRATIONS**

When a structural element deviates its original position for a definite interval of time is called vibration. Vibration is the property which can be gained by every element of universe having some mass and elasticity. Unwanted vibration can degrade the performance of the structure or it may cause fatigue of the structure. Thus it is advantageous to make decrement or minimize the effects of vibrational and consequential ill effects. Vibration isolators are mitigating devices, which isolates the source of vibration from the direct contact of structure. It is not possible to avoid vibrations totally in real but can be minimized to some good extent. These vibrations actually come from the two main reasons, rubbing contact and eccentricity. Many times these vibrations are used intentionally to perform a useful job. For example, we create vibration purposely in concrete compactors, rock drills and pile drivers. Vibrational waves in structures are also due to different rhythmic activities performed in or near the structure, like in stadiums, dance and health clubs, which are used for a large diversity of activities. Sometimes mismatching of the frequencies cause resonance, this is considered to be an alarming condition of vibration.

Waves produced by the action of construction works, airports, railway and road transport, explosions, etc. are known as man-made vibration. These vibrations are transmitted into the different layers of ground by different types of waves which travel in different pattern beneath the surface of ground. These waves are elastic in nature, which include surface waves, bulk longitudinal waves, Rayleigh waves and transverse waves, propagating into the ground through different depth and propagates with range of 1 - 200 Hz. These ground related vibrations are measured and defined in terms of velocity, acceleration or displacement of particle.

The different waves that transmit the energy from source to receiver are viz: Rayleigh (R) waves, shear (S) waves and Compression (P) waves. These waves radically form different patterns of motion in earth and rock particles while they travel from one part to other. Thus the effect of each wave is different and each deforms the structure in a different way. Body waves travel deep inside the earth and are predominately produced by Construction-related ground impacts. Their

path of propagation is outward in a spherical shape and overlap at a boundary of other layer (rock or soil). S and R waves are different in nature and are produced at point of crossing. Distant from the source of motion, all three waves arrive together and begin to separate as they are moving slowly from the P-wave and thus allow identification of waves. The speeds of these waves are also different, thus they can also be identified by its velocity of speed. Fastest is the P-wave, followed by the S, then the R-wave. The most dangerous wave is R wave which produce most disturbance along the surface of the ground, moreover P and S waves perish more rapidly than the R-wave. R-waves have large contributions, about 67 % of total energy, it is followed by S- waves which contributes 26% and then P-waves which contributes 7% (Sanayei et al. 2013).

### **SIGNIFICANCE OF EXPERIMENTAL WORK**

Industries are being set near the dwelling areas due to scarcity of land and population explosion. Moreover due to industrial revolution, business plants, factories, industries are being set more and more, which not only alter the climate conditions but also gain new challenges to structural and design engineers. Noise, vibration and air pollution are the main problems to concern.

Regarding the non-seismic vibrations, forge hammer vibration is the new challenge to rectify, which nowadays are more solved in courtrooms than by structural engineers. So need of the hour is to analyze these problems of hammer induced vibrations and provide design guidelines and remedial to avoid drastic effects of these strong ground motions.

### **EXPERIMENTAL PROGRAMME**

To study and analyze the effect of forge hammer induced vibrations, various sites are visited in industrial area of Ludhiana. Accelerations are measured with the help of vib-scanner in working and non-working conditions of hammer at different distances from the source of vibration. To achieve the objective of this work, eight different sites regarding the forge hammer vibrations are being selected. These selected sites are viz.

- a) Highway Industries Limited
- b) Deepak International Limited
- c) Panju Forging Enterprises
- d) Bharti Enterprises
- e) Kay Kay Steels
- f) Gupta Forging
- g) Safe Engineering
- h) SS Forging

### **INSTRUMENTATION**

In this study two types of instruments were used, one is the sensor fitted externally device known as vib scanner and other is the mobile fitted sensor. To access, identify and observe the problem of structure, ground vibrations are measured with variable instruments. Vibration response cannot be accessed by using a single type of instrument; a single instrument is not predictable to meet all the frequency and dynamic range requirements.

### Accelerometer

Device that measures acceleration or vibration of a structure or machine is called an accelerometer. While choosing a particular accelerometer following points should be kept in view.

- a) amplitude of vibration
- b) range of frequency
- c) temperature range of the equipment
- d) size of the sample
- e) Electromagnetic effects
- f) noise level

### Vibscanner

Vibscanner is a device which collects and interprets data like displacement, velocity and acceleration of vibration. Moreover measurement like shock pulse, temperature, rotational speed etc. are also monitored. It is clearly seen from Fig 1(b) that how to take the readings at the site.



Fig1(a) Vibscanner



Fig 1(b) Taking readings at the site

### Vib sensor 1.3.2

Vibration meter fitted in mobile phone as android application makes the device as simplest pocket vibrometer or accelerometer, with facilities like easy data collection and storage. Graphs of sine wave type and log data (when values are too small) are also generated.



Fig 2(a) Mobile fitted VibSensor

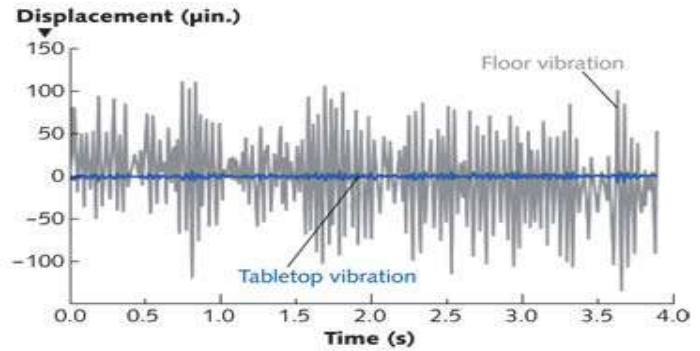


Fig 2 (b) Floor vibrations

## RESULT AND DISCUSSION

The results of acceleration that we obtain are tabulated below. The different values of acceleration Zero to Peak, Peak to Peak and RMS values are taken at each site. Vertical accelerations values of root mean square are only considered to make the comparison with the permissible IS values.

Frequency 10 – 100 Hz (Each case)

**Table 3 Highway Industries Limited (Acceleration)**

SITE	ZERO-PEAK m/s <sup>2</sup>	PEAK-PEAK m/s <sup>2</sup>	RMS m/s <sup>2</sup>
Non-working condition	0.512	1.021	0.212
Working condition At 2m	0.701	1.400	0.255
Working condition At 10m	0.631	1.241	0.211

**Table 4 Deepak International Limited (Acceleration)**

SITE	ZERO-PEAK m/s <sup>2</sup>	PEAK-PEAK m/s <sup>2</sup>	RMS m/s <sup>2</sup>
Non-working condition	0.501	1.001	0.211
Working condition At 2m	0.666	1.321	0.233
Working condition At 10m	0.612	1.221	0.222

**Table 5 Safe Engineering (Acceleration)**

SITE	ZERO-PEAK m/s <sup>2</sup>	PEAK-PEAK m/s <sup>2</sup>	RMS m/s <sup>2</sup>
Non-working condition Of hammer	0.502	1.001	0.200
Working condition At 2m	0.673	1.355	0.221
Working condition At 10m	0.644	1.282	0.213

**Table 6 Bharti Enterprises (Acceleration)**

SITE	ZERO-PEAK m/s <sup>2</sup>	PEAK-PEAK m/s <sup>2</sup>	RMS m/s <sup>2</sup>
Non-working condition	0.522	1.044	0.211
Working condition At 2m	1.431	2.852	0.251
Working condition At 10m	1.121	2.222	0.282

**Table 7 Android Device Readings (Fig 2 (a))**

DEVICE	SENSOR	RMS	RESONANCE
Redmi mobile V5.1.2	accelerometer, gyro, proximity	X(0.132)m/s <sup>2</sup> Y(0.122) Z(0.818)	X(9)Hz Y(15) Z(47)
Samsung V5 2.3 jellybin	accelerometer	X(0.333) Y(0.336) Z(1.131)	X(16) Y(21) Z(14)
Redmi V5.1	Accelerometer	X(0.111) y(0.073) Z(0.771)	X(8) Y(17) Z(42)
Samsung	Barometer, temp, humidity, accelerometer	X(0.131) Y(0.0571) Z(0.512)	X(9) Y(17) Z(46)

**Table 8 IS/ISO 4866: 2010**

SOURCE	FREQUENCY HZ	AMPLITUDE µm	VELOCITY mm/s	ACCELERATION m/s <sup>2</sup>
Traffic vibration Road, rail,	1 to 100	1 to 200	0.2 to 50	0.02 to 1
Blasting vibration	1 to 300	100 to 2500	0.2 to 100	0.02 to 50
Pile driving vibration Ground borne	1 to 100	10 to 50	0.2 to 50	0.02 to 2
Machinery outside vibration	1 to 100	10 to 1000	0.2 to 100	0.02 to 1
Machinery inside	1 to 300	1 to 100	0.2 to 30	0.02 to 1
Human activities	0.1 to 30	5 to 500	0.2 to 20	0.02 to 0.2
Earthquake	0.1 to 30	10 to 100000	0.2 to 400	0.02 to 20

Results show that acceleration values near the vicinity of 2 meters is more than the 10 meter spacing from the plant in working condition. The non-working condition measurements are mostly same at every distance. Further acceleration values are compared with the permissible values of IS/ISO 4866: 2010, and it was observed that these obtained values

with Vibscanner are in safe range but people comfort disturbance is the concern here which can be redressed by providing special shock absorber techniques. Further mobile phone fitted sensors are also used to make good comparison and to check the variability of results; Rms and Resonance values are taken but these sensors show different values, even device to device value differs because quality of the device and sensor were not similar.

### VIBRATION REDUCTION TECHNIQUES

Different types of techniques and methods are used to minimize the transmission ground motions and control the dangerous effects of vibrations either isolating the source (active isolation) or by protecting the receiver (passive isolation). Furthermore techniques used to reduce the effects of vibration like dampers, isolation screens etc. are discussed below.

#### Absorbing Damper

It acts as an energy absorber, works by squeezing itself to the tune and absorbs extra energy generated from the system. The common absorbing damper is viscous damper which is made of a cylinder surrounded by a piston and the head is divided in two chambers. It works on the principle of pressure difference, potential for flow is generated when relative motion is applied to the actuator and dissipation of energy takes place.

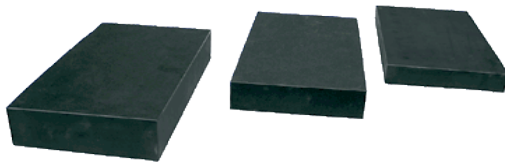


Fig 3(a) Common damper



Fig 3(b) damper over pier cap

#### Tuned Mass Damper (TMD) and Active Tuned Damper

It is a damper with mass-spring adjustment which can be tuned with the vibrations of structure. It actually acts as the shock absorber or vibration absorber. It dissipates the energy without disturbing the system thus acts as resistance of the system. Moreover some other dampers like Magneto-rheological which is fluid based damper and is one of the efficient damper used in dissipating the shock energy. These dampers actually add some stiffness to the system by setting frequency in accurate limits.



Fig 4(a) Tuned damper



Fig 4(b) Rheological damper

### Gas cushion isolation screen

This is the type of permanent isolation technique in which vertical wall like structure or barrier known as gas cushion is fitted inside the earth around the source of vibration. Having the advantage of low impedance, makes it permanent barrier to transfer the strong motions inside the earth. It is a thin wall flexible tube, inflates when air is blown inside and placed horizontally inside the trench. Furthermore, it is environmentally resistant to chemicals and acids thus provide good durability beneath the soil (Massarsch 2005).



Fig 5(a) Gas cushion screen



Fig 5(b) Gas cushion after installation

### CONCLUSION

In this present study attempt has been made to measure the vibration (acceleration) values around the heavy forge hammers installed in large industries. These measurements were obtained by Vibscanner which provides us three values (Zero to peak, peak to peak and Rms). On comparing the obtained values of acceleration with permissible standards, it was observed that not severe effects of these sites visited are seen but people annoyance and discomfort (shaking of windows and glass panes) was question to be discussed and here we discuss some techniques for mitigation of these effects of vibration. Among different techniques, gas cushion trench and open trench technique was quite beneficial to be used but gas cushion trench is more beneficial and aesthetically good than open trench method.

### REFERENCES

- Allen, D. E., and Pernica, G. (1998). "Control of Floor Vibration." *Engineering*, 133, 242–250.
- Bachmann, B. H. (1992). "Case studies of structures with man-induced vibrations." 118(3), 631–647.
- Brownjohn, J. M. W. (2005). "Lateral loading and response for a tall building in the non-seismic doldrums." *Engineering Structures*, 27(12 SPEC. ISS.), 1801–1812.
- Connolly, D. P., Kouroussis, G., Laghrouche, O., Ho, C. L., and Forde, M. C. (2014). "Benchmarking railway vibrations - Track, vehicle, ground and building effects." *Construction and Building Materials*, 92, 64–81.
- Department of Environment and Conservation NSW. (2006). "Assessing Vibration: a technical guideline." 35.
- Dijkmans, A., Ekblad, A., Smekal, A., Degrande, G., and Lombaert, G. (2013). "A sheet piling wall as a wave

barrier for train induced.” (June), 12–14.

Hao, H., Ang, T. C., and Shen, J. (2001). “Building vibration to traffic-induced ground motion.” *Building and Environment*, 36(3), 321–336.

Khandelwal, M., and Singh, T. N. (2007). “Evaluation of blast-induced ground vibration predictors.” *Soil Dynamics and Earthquake Engineering*, 27(2), 116–125.

Kisan, M., Sangathan, S., Nehru, J., and Pitroda, S. G. (2010). “IS/ISO 4866 : 2010.”

Massarsch, K. R. (1993). “Man-made vibrations and solutions.”

Massarsch, K. R. (2005). “Vibration Isolation Using Gas-filled Cushions.” *Soil Dynamics Symposium in Honor of Professor Richard D. Woods*, 1–20.

Popescu, T. D. (2010). “Analysis of traffic-induced vibrations by blind source separation with application in building monitoring.” *Mathematics and Computers in Simulation, International Association for Mathematics and Computers in Simulation (IMACS)*, 80(12), 2374–2385.

Sanayei, M., Maurya, P., and Moore, J. A. (2013). “Measurement of building foundation and ground-borne vibrations due to surface trains and subways.” *Engineering Structures, Elsevier Ltd*, 53, 102–111.

Thalheimer, E., Poling, J., Brinkerhoff, P., Herzog, T., York, N., and York, N. (2014). “A Simple , Effective Method for a ‘ Detailed ’ Building Vibration Analysis.” (August).



## CORROSION OF REINFORCED CONCRETE; A REVIEW

Abhinath B<sup>1\*</sup>, Davinder Singh<sup>2</sup>

<sup>1</sup>M.Tech Student, Dr B R Ambedkar National Institute of Technology Jalandhar, India; abhinath.bhuvanewaran@gmail.com

\*Corresponding Author

<sup>2</sup>Assistant Professor, Dr B R Ambedkar National Institute of Technology Jalandhar, India; singhdj@nitj.ac.in

### ABSTRACT

Failure of most of the concrete structures are mainly due to the corrosion of the reinforcement embedded in them. Durability of a structure is therefore depend on the corrosion resistance of the concrete used in it. Corrosion of reinforcement in concrete occur when it get exposed to chlorides or due to carbonation, which acidifies the concrete. This paper presents a review on the mechanism of reinforcement corrosion and various factors that influences the corrosion resistance of concrete such as composition of concrete, surrounding conditions which include temperature, relative humidity, extend of CO<sub>2</sub> exposure and extend of sulphate exposure, reinforcement cover and type of steel used.

**Keywords:** Corrosion; concrete; carbonation; chloride ingress.

### INTRODUCTION

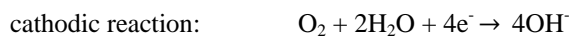
Corrosion of reinforcement in concrete significantly reduces the service life of structures. This has led to sever economic loss in the construction industry. Thus it is very important to study the factors influencing corrosion of reinforced concrete in order to save economic loss by designing corrosion resistant concrete rather than performing expensive repair of corroded structural reinforce concrete elements.

Concrete provides a passive alkaline layer that protects reinforcement from oxidation and electrochemical corrosion. Neville (1995) found that the protection of steel is reduced or made ineffective when the alkaline environment is destroyed by leaching with waste or partial neutralisation by chemical reaction between hydration products and CO<sub>2</sub> from the atmosphere. The passive layer is destroyed mainly due to carbonation and chloride attack. In order to prevent corrosion as well as to avoid spalling caused by the augmented volume of corrosion products, adequate cover for the reinforcement has to be provided. Permeability is the most important factor that increases the electric conductivity of concrete as well as it increases the availability of oxygen at the surface of the reinforcement, thereby enhancing corrosion of reinforcement in concrete. Permeability of concrete can be minimised by replacement of binder material with pozzolanic materials (fly ash, silica fume, blast furnace slag and coal bottom ash) which refines the pore size.

This paper presents a review on the mechanism of reinforcement corrosion and various factors that influences the corrosion resistance of concrete such as composition of concrete, surrounding conditions which include temperature, relative humidity, extend of CO<sub>2</sub> exposure and extend of sulphate exposure, reinforcement cover and type of steel used.

### CORROSION PROCESSES AND MECHANISMS

The corrosion of metals is an electrochemical process. For steel in concrete the following reactions occur:



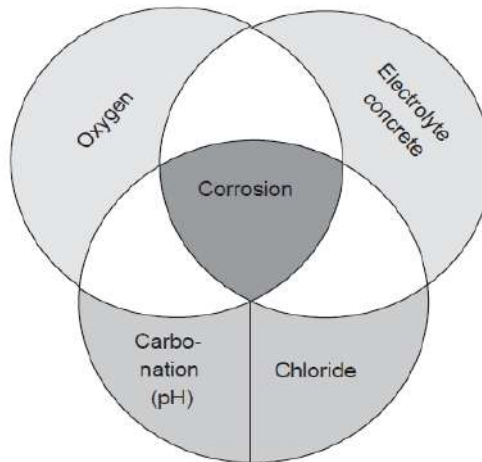
The following four conditions that must be fulfilled to start and maintain the corrosion process.

- i. An anodic reaction is possible. This is possible only if the passive layer of the steel bar breaks down and depassivation of the steel occurs due to carbonation resulting in lowering of pH of pore water or due to chloride ingress.
- ii. A cathodic reaction is possible. This is possible only if Oxygen as the driving force of the corrosion process is available at the interface of the reinforcement in a reasonable amount.

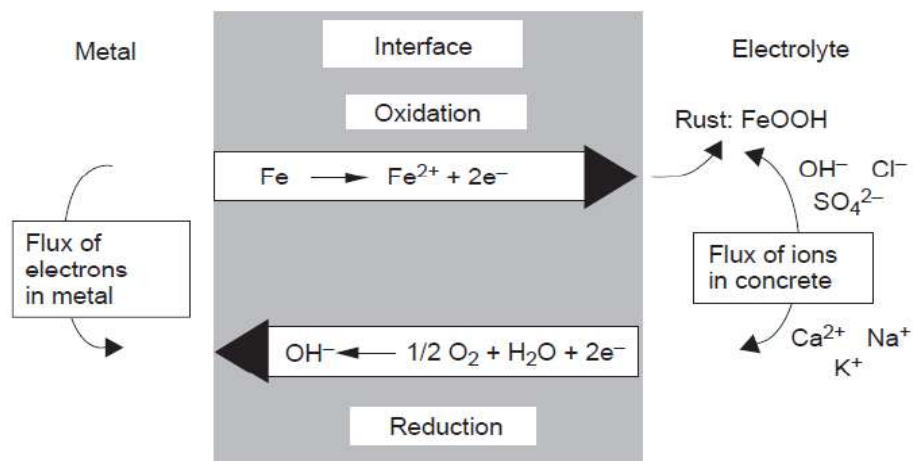
- iii. A flux of ions between the site of the anodic reaction and the site of the cathodic reaction is possible. This is possible only in the presence of a well conducting environment or electrolyte is available between the site of the anodic reaction and the site of the cathodic reaction.
- iv. A flux of electrons is possible. This is possible only if there is a metallic connection between the sites of anodic and cathodic reactions.

Fig. 1 below shows the necessary conditions for corrosion of steel in concrete (Hunkeler 1994). If any of these conditions are not satisfied, corrosion will not occur in reinforced concrete.

Fig. 2 below is the diagrammatic representation of corrosion as an electrochemical process (Hunkeler 1994).



**Fig. 1 Conditions for corrosion of steel in concrete (Hunkeler 1994).**



**Fig. 2 Corrosion as an electrochemical process (Hunkeler 1994).**

Corrosion initiation and propagation is highly influenced by the pH of the pore water, temperature, oxygen availability, moisture content and resistivity of concrete. Whereas the influence of chloride content in corrosion process is less. The corrosion mechanism occur in two different stages:

#### **Initiation stage**

During this period the passive layer that protects the reinforcement will be broken due to carbonation and chloride ingress. This stage consist of three processes namely:

**Transportation processes:** It refers to the transport of gases ( $O_2$ ,  $CO_2$ ), water and ions (chloride,  $Cl^{-}$ ) in concrete to the surface of the reinforcement through cracks and the pore system. The driving force for Diffusion of gases and ions is

provided by the concentration gradient and partial pressure difference; which occurs in pores filled with air or water. The driving force for Capillary suction of liquids is provided by the Surface tension and Contact angle; which occurs in pores filled with air. The driving force for Permeation of gases and liquids is provided by the Absolute pressure difference; which occurs in pores filled with air or water.

**Carbonation:** It is the reaction of atmospheric carbon dioxide ( $\text{CO}_2$ ) with the alkaline components of the cement paste (e.g.  $\text{NaOH}$ ,  $\text{KOH}$ ,  $\text{Ca(OH)}_2$  and calcium-silicate hydrates) leading to the reduction of pH value of the pore water. The reduction of pH is mainly due to the formation of  $\text{CO}_3^{2-}$  and  $\text{HCO}_3^-$  ions.

**Chloride ingress:** Tang (1997) found that the fastest ingress of chloride into concrete is caused by capillary suction of chloride-containing water (e.g. sea water, water with dissolved de-icing salts, chloride-containing floors, e.g. magnesia floors), which results in more or less deep chloride profiles. Chloride ingress is accelerated by alternate wetting and drying of concrete. The passive film of the steel is destroyed by chloride ingress enhancing its corrosion. It reduces the solubility of  $\text{Ca(OH)}_2$  thereby reducing pH of pore water. Due to the hygroscopic properties of salts present in concrete such as  $\text{CaCl}_2$ ,  $\text{NaCl}$ , it increases the moisture content. It also increases the electrical conductivity of the concrete.

The time period of the initiation stage depends upon factors like concrete quality, concrete cover, exposure conditions & sulphate content.

### **Propagation Stage**

At this stage corrosion rate starts to increase resulting in the depletion of reinforcement thereby leading to the deduction of its strength and accumulation of corrosion products such as rust. The time period of this stage is mainly governed by the electrolyte resistance influenced by temperature and moisture content and to a smaller part by electrochemical reaction resistances.

### **FACTORS INFLUENCING CORROSION RATE**

Corrosion rate influenced by several factors such as composition of concrete, surrounding conditions such as temperature, relative humidity, extend of  $\text{CO}_2$  exposure and extend of sulphate exposure, reinforcement cover and type of steel used.

#### **Influence of Concrete Composition**

The corrosion rate depends up on the electric conductivity of concrete. Higher the electric conductivity higher will be the corrosion rate as it enhances the electrochemical reaction. The electric conductivity of concrete depends upon the moisture content, permeability of the concrete as well as its moisture content. The pore structure and distribution has a major impact on electric resistivity of concrete as well as the easiness for ingress of depassivating media such as  $\text{CO}_2$  and chloride. Thus the concrete composition and properties of its constituents such as binder type, water–binder ratio, binder content, aggregate type, type and amount of admixtures have a major impact on the corrosion rate. The influence of these parameters can be determined by conducting carbonation resistance test, electric resistivity test or rapid chloride penetration test.

#### **Influence of binder type**

The mechanical properties of hardened concrete made up of ordinary Portland cement (OPC) is a result of the reaction between the  $\text{CaO}$  rich calcium silicate phases ( $\text{C}_2\text{S}$  and  $\text{C}_3\text{S}$ ) and water. The secondary hydration has the major role in pore size refinement of the concrete which reduces the permeability as well as the availability of free water in the pore structure of the concrete there by increasing corrosion resistance. This cannot be achieved by OPC alone. The addition of pozzolanic materials such as Fly ash (FA), Silica fume (SF), Ground granulated blast-furnace slag (GGBS) and Coal bottom ash (CBA) leads to secondary hydration which helps in pore refinement which in turn reduces permeability of concrete. Schiessl and Lay (2005) found that at an age of 28 days the resistivity of concrete produced with w/b-ratios from 0.40 to 0.60 is around 330–550 $\Omega\text{m}$  for slag cements, 380–410 $\Omega\text{m}$  for cement with silica fume, 70–220 $\Omega\text{m}$  for cements with fly ash in comparison with 40–114 $\Omega\text{m}$  for OPC. The hydration rate of FA is comparatively less than SF and GGBS during the early days. But on a longer span FA also gives high electric resistivity by secondary hydration. Hansson and Sørensen (1987) concluded that the fineness of cement has a great influence on chloride diffusion. As the fineness of binder increases, the chloride diffusion rate decreases. Studies conducted by Lawrence (1992) concluded that mortar made up of sulphate resistant Portland cement retains more than 82 to 94% compressive strength when

exposed to corrosive environment for an year, whereas mortar composed of PC and FA retained only 55 to 76% compressive strength for the same period of exposure.

### ***Influence of water-binder ratio***

As the water binder ratio increases the electric resistivity, carbonation resistance as well as the chloride penetration resistance reduces. This is mainly due to the presence of free water in the pores of concrete. More dry the concrete, more durable it is. But there should be enough water for the completion of secondary hydration, which is the most important factor determining the corrosion resistance of concrete.

### **Effect of aggregate type**

Concrete made up of denser aggregates such as granite is believed to show higher resistivity compared to those made with porous aggregates such as sandstones. Basheer et al. (2005) concluded that by maintaining a low average aggregate size in the mix can significantly reduce its air permeability. An increase in size and proportion of coarse aggregate in the mix increases its air permeability as well as increase in depth of carbonation. Study conducted by Yüksel et al. (2007) by partially replacing fine aggregate with GGBS and CBA observed a significant reduction in surface cracking as well as reduction in the loss of compressive strength due to freezing- thawing effect.

### **Influence of Temperature**

Hunkeler (2005) found that the corrosion rate almost becomes zero around temperature of -25°C to -45°C. As the temperature increases the corrosion rate also increases.

### **Influence of Curing period**

Test conducted by Parrott (1996) concluded that increase in curing time enhances corrosion resistance. But this can't be the same in all cases as curing time required varies from one mix to another depending upon its composition. His studies stated that reinforcement corrosion is more affected by the type of cement being used and the effect of curing period, cover to concrete or air permeability of exposed concrete have a small impact on corrosion rate.

### **Influence of Relative Humidity**

As the moisture increases the diffusion of oxygen becomes difficult. This is because the diffusion rate of oxygen into the pores filled with water is less compared to empty or air filled pores. The lack of oxygen at the surface of reinforcement reduces the rate of corrosion. But on the other side the increased moisture content increases the conductivity of the concrete which in turn increases corrosion rate. Concrete having a high water-binder ratio exposed to a highly humid atmosphere will show more conductivity than those having low water-binder ratio.

### **Influence of Chloride Content:**

As chloride ingress in the major reason for the depletion of reinforcement due to corrosion, its content has to be limited. Concrete having a total chloride content less than 0.2% by mass of cement is considered as having low corrosion risk, those having 0.4% by mass of cement have small corrosion risk and those having greater than 1.0% by mass of cement have high corrosion risk. Chloride content limits as recommended by some codes of practices, USA have 0.15% for chloride exposures and 0.30% for chloride free exposure, for UK it is 0.30% and for India it is 0.15%.

### **Influence Of Reinforcement Cover:**

The chances for carbonation and chloride ingress will reduce as the depth of reinforcement from the exposed surface increases. Thus the minimum cover to be provided for the reinforcement also depends to the exposure condition. Studies conducted by Arya and Ofori-Darko (1996) suggested that by increasing the depth cover to the reinforcement is the best way to limit corrosion frequency of intersecting cracking. Studies conducted by Scott and Alexander (2007) concluded that as the cover to the reinforcement increases from 20mm to 40mm the corrosion rate is significantly reduced in specimens made up all type binders ( PC, GGBS, FA and SF).

### **Influence Of Cracking:**

Concrete having cracked surface has more chances for corrosion than un-cracked ones. The presence of cracks makes chloride ingress much easier than un-cracked surface. Studies conducted by Otieno et al. (2010) found that for all 0.4mm and 0.7mm cracked specimens made up of different binders exceeded the active corrosion threshold whereas un-cracked specimens were still in passive corrosion state. Cracking has higher impact on corrosion rate of concrete made

up of OPC as compared to those replaced with SF, FA or Corex slag. It was also found that when a corroding RC structure is reloaded, the chances for reopening the self-healed cracks thereby increasing the width of the existing cracks leading to early failure of the structure. Andrade et al. (1993) found that the rate of bar cross-section loss in carbonation induced corrosion is more or less uniform, thus the service life of such corroding structural elements can be predicted with a better accuracy. But in the case of corrosion induced by chlorides, the corrosion rate cannot be predicted easily because there are chances for localized attacks that can penetrate in to much higher depths that may seriously affect the strength of the structural element. Studies conducted by Scott and Alexander (2007) concluded that during the initial curing period as well as for the end life, concrete made up of PC, GGBS, FA and SF have more corrosion rate as the crack width increases from .2mm to .7mm. As the crack width increases GGBS showed least corrosion rate for the end life due to secondary hydration leading to improvement of inter-facial transition zone and pore refinement.

## CONCLUSION

With the review on various factors influencing corrosion rate, it is evident that a durable concrete cannot be achieved by using OPC alone as binder material. The replacement of OPC with SF, FA and GGBS has enormously improved the corrosion resistance of concrete mix. More over pore size refinement due to the fineness of pozzolanic materials has led to the reduction of permeability of concrete. Concrete lower water-binder ratio have higher corrosion resistance than those having high water-binder ratio.

## REFERENCES

- Andrade, C., Alonso, C., and Molina, F. J. (1993). "Cover cracking as a function of bar corrosion: Part I-Experimental test." *Materials and structures*, 26(8), 453-464.
- Arya, C. and Ofori-Darko, F. K. (1996). "Influence of crack frequency on reinforcement corrosion in concrete." *Cement and Concrete Research*, 26(3), 345-353.
- Basheer, L., Basheer, P. A. M., and Long, A. E. (2005). "Influence of coarse aggregate on the permeation, durability and the microstructure characteristics of ordinary Portland cement concrete." *Construction and Building Materials*, 19(9), 682-690.
- Hansson, C. M., and Sørensen, B. (1987). "The influence of cement fineness on chloride diffusion and chloride binding in hardened cement paste." *Nordic concrete research*, (6), 57-72.
- Hunkeler, F. (1994). "Grundlagen der Korrosion und der potentialmessung bei Stahlbetonbauwerken, " EVED/ASB, Bericht VSS 510.
- Hunkeler, F. (2005). "Corrosion in reinforced concrete: processes and mechanisms." *Corrosion in reinforced concrete structures*, 1-45
- Lawrence, C. D. (1992). "The influence of binder type on sulfate resistance." *Cement and Concrete Research*, 22(6), 1047-1058.
- Neville, A. (1995). "Chloride attack of reinforced concrete: an overview." *Materials and Structures*, 28(2), 63.
- Otieno, M. B., Alexander, M. G., and Beushausen, H. D. (2010). "Corrosion in cracked and uncracked concrete–influence of crack width, concrete quality and crack reopening." *Magazine of Concrete Research*, 62(6), 393-404.
- Parrott, L. J. (1996). "Some effects of cement and curing upon carbonation and reinforcement corrosion in concrete." *Materials and Structures*, 29(3), 164.
- Schiessl, P., and Lay, S. (2005). "Influence of concrete composition." *Corrosion in reinforced concrete structures*, 91-134.
- Scott, A., and Alexander, M. G. (2007). "The influence of binder type, cracking and cover on corrosion rates of steel in chloride-contaminated concrete." *Magazine of Concrete Research*, 59(7), 495-505..
- Tang, L. (1997). "Chloride penetration profiles and diffusivity in concrete under different exposure conditions." Chalmers University of Technology. Publication P-97:3, Goteberg.
- Yüksel, İ., Bilir, T., & Özkan, Ö. (2007). "Durability of concrete incorporating non-ground blast furnace slag and bottom ash as fine aggregate." *Building and Environment*, 42(7), 2651-2659.



## AN OVERVIEW OF CONCRETE FILLED DOUBLE SKINNED TUBULAR COLUMNS

Aditya Kumar Tiwary<sup>1</sup>, Rajat Yadav<sup>2</sup>

<sup>1</sup>Civil Engineering Department, Chandigarh University, Mohali, [aditya.civil@cumail.in](mailto:aditya.civil@cumail.in), Corresponding Author

<sup>2</sup>Civil Engineering Department, Chandigarh University, Mohali, [je.suis.un.athee@gmail.com](mailto:je.suis.un.athee@gmail.com)

### ABSTRACT

The meteoric growth in light weight structures have open on doors to many revolutionary concepts and innovations. Studies have manifested that the lowered weight of the structures somehow help to fight the material cost with a better seismic performance. The hollow core structures aimed reducing the structural weight with an improved structural performance as well. The Concrete filled double steel tubes (CFDST's) can be taken as amalgamation of Hollow core columns and CFST's i.e. single skinned columns. The co-relation of CFST and Hollow core columns gave birth to Concrete filled double skinned tubular columns(CFDST) which can possess the advantages of both the concepts. A sedulous review of concrete filled double skinned columns is being conveyed through this article. The behavior of confined concrete as well as the confining inner and outer steel in the CFDST model and its overall structural behavior is being succinctly reviewed in this article and a simultaneous comparison of CFDST columns to solid concrete/ conventional columns is also being carried out where required.

**KEYWORDS:** Concrete filled double steel tubes, Composite Columns, Hollow core columns, Light weight structures

### INTRODUCTION

The system of confining concrete with outer steel tubes of defined thickness, termed out to be as concrete filled tube system (CFST's) and was majorly proposed for accelerating bridge construction. CFST's were aimed to reduce construction time with increased construction quality and safety. Moreover, with the use of these columns nominal traffic interference with increased seismic performance could be kept [Dawood et al. 2012]. CFST's have successfully showcased improved seismic, flexural and torsional behavior but on the other hand have faced several challenges as well. The centrally confined concrete took lesser amount of compression as compared to the steel per same cross sectional area. The torsional strength seemed to be ineffective of the centrally confined concrete. The concrete placed in the center added up a majority of weight making the system uneconomically heavy. Moreover, the concrete closer from the neutral axis proved to be ineffectual over its flexural strength. The possible downsides of CFST's gave rise to the concept of Concrete filled double skinned tubes(CFDST's), Which possessed collective advantages of hollow core columns and CFST's see Fig 1. This design confined the concrete between two hollow steel tubes of defined thickness which may or may not be of similar cross sections [Pagoulatou 2014].

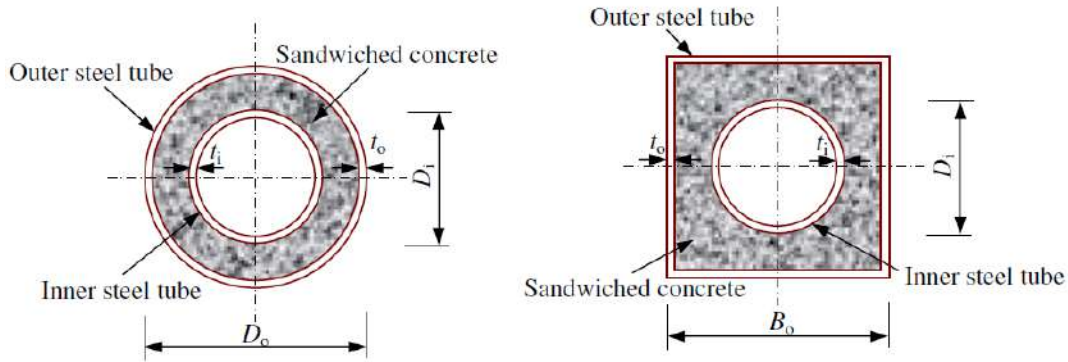


**Fig.1** Typical cross section on circular and square CFDST (Han et.al 2011)

The very core part of the CFST's were thought to be replaced or removed completely leaving a complete hollow section in the middle. The Concrete filled steel tubes(CFST's) became the very base for the further studies on CFDST's which were basically concocted to be used in submerged tube tunnels [Han et al. 2004]. Tests prove that the local buckling behavior of outer and inner steel was prevented/ resisted due to confined concrete. The confining tubes may also affect the mode of failure of concrete and bring down its behavior from being brittle to ductile [Zhao and Grzebieta 1999; Yang et al. 2004]. Through previous researches one can conclude that the increased confining pressure over concrete positively affects its strength and ductility performance [Watson et.al 1994; Paultre P 2001]. Owing to the removal of ineffectual core concrete, significant reduction in the self-weight could be achieved. The light weight of this system helps it in achieving better seismic performance and bring down the material cost as well making this a sustainable and environmentally friendly technology. Kang hai et. al [11] presented ultimate strength and composite modulus for CFDST's using energy theory and unified theory. They provided a core relation of steel ratio, Poisson's ratio of steel and horizontal deformation coefficient of concrete with axial stiffness.

$$E_O A = E_s A_{si} + E_s A_{so} + E_c A_c \quad (1)$$

$$\bar{E}_{so} = E_s - \frac{E_s v_s (D_o - t_o) (4v_c - v_s \alpha)}{8t_o \left( \frac{1-v_c}{K_E} - v_s \right)} \quad (4)$$

$$E_{ssc} A = \bar{E}_{si} A_{si} + \bar{E}_{so} A_{so} + \bar{E}_c A_c \quad (2)$$

$$\bar{E}_{si} = E_s + \frac{E_s v_s (D_i - t_i) (4v_c - v_s \alpha)}{8t_i \left( \frac{1-v_c}{K_E} - v_s \right)} \quad (3)$$

$$\bar{E}_c = E_c + \frac{E_c (4v_c - v_s \alpha)^2}{8(1-v_c - K_E v_s)} \quad (5)$$

In order to truly understand the CFDST members the common approach is, A separate analysis of the inner steel, outer steel and the confined concrete in between. Simple superposition method (equation 1) was used for estimating the composite column stiffness [Kang Hai et. al 2010]. The overall result could be modelled by combing the separate behaviors. They further calculated modified elastic modulus separately for each component using energy theory. The behavior of each component could be separately calculated and put down together for combined results. The combined stiffness of the composites can be presented using 2<sup>nd</sup> equation above derived with considering the confining effects. The value for modified elastic modulus of inner steel, outer steel and concrete can be calculated using equations 3,4 and 5 respectively. The effectiveness of confinement could be improved using external steel ring spaced up differently. The load carrying capacity can be influenced positively by decreasing the spacing between external steel ring confinement. The load carrying capacities was found to be improved for about 11.5% and 9.5% on average for CFDST's having hollowness ratios of 0.56 and 0.72 respectively [Ho et.al 2013].

## 2. MATERIAL PROPERTIES

**CONCRETE:** It is a composite brittle material used as a confined shell of definite thickness in CFDST's. concrete when under compressive forces tries to laterally deflect and brings the outer and inner steel tubes under lateral pressure. The distribution of stress can be easily visualized by fig.2 which showcases different components of the stub column under lateral stress. The confinement pressure through the outer and inner tubes can be defined using confinement coefficient as in equation 6 where  $A_s$  and  $A_c$  are areas of steel and concrete,  $f_s$  and  $f_{ck}$  are strength of steel and concrete [Kang Hai et. al 2010].

$$\xi_{SSC} = \frac{\sum A_s f_s}{A_c f_{ck}} \quad (6)$$

**STEEL:** The inner and outer steel tubes are the paramount of this composite augmentation. Generally, both the tubes are kept of similar properties but as the outer tube is the most exposed part for environmental corrosion hence a precise manipulation can be effectual for improving the structure life. The tubes are very much crucial for providing the confinement to the concrete shell also they are resistive and bolster in curtailing the spalled concrete during contact explosion. Generally, two grades of cold-worked steel is used Fe415 & Fe500 with characteristic yield strength ( $f_y$ ) of 415 N/mm<sup>2</sup> & 500 N/mm<sup>2</sup> respectively and with Elastic Modulus of 200000 N/mm<sup>2</sup>.

### CIRCUMSTANTIAL BEHAVIORS OF CFDST

The behavior of both CFDST's and CFST's is somewhat relative in nature. The CFDST's also help in speeding up the construction process and their outer steel skin helps as pre-form work. These section types similarly affect the quick finishing of undertaking as of CFST's. The real disappointment in regular sections have been coming through buckling. The bucking phenomenon in these kind of segments is imperative too. The genuine comprehension of the failure mechanism could be picked up by independently considering the conduct of infill concrete and the external and internal steel tubes. The concrete under compressive loading tries to displace laterally. This lateral displacement is confined by the inner and outer tubes leaving both of them under lateral pressure. The developed pressure thus tries to cause laterally

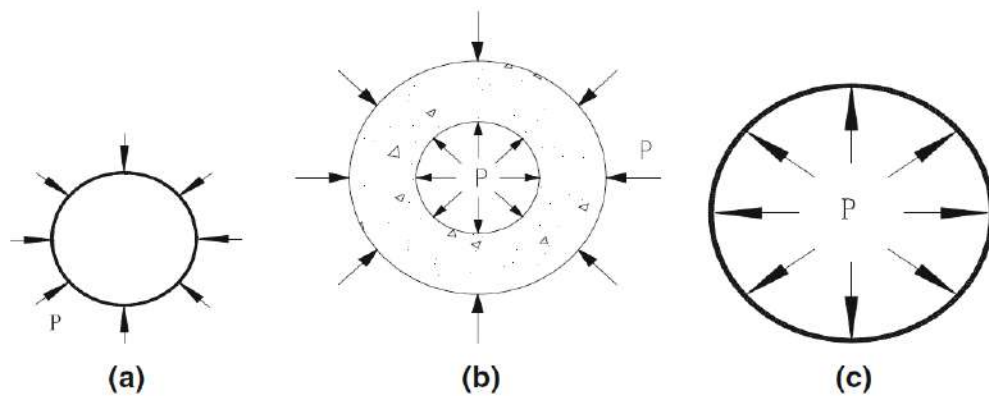


**Fig. 2** Stress model for various components of CFDST a) inner tube b) concrete shell c) outer tube [Kang Hai et. al 2010]

inward and outward deformation in the inner and outer steel tubes respectively. Essopjee et al. (2015) took a shot at the disappointments of concrete filled double skin tubes keeping in thought the length, diameter and the strength of the external cylinders. The fallout coordinated that the sections with least given length for example 1m, flopped because of

yielding of steel tube while in all the others large buckling was watched. Further they demonstrated that external buckling was the real reason for disappointment in external steel tubes though the internal steel tubes having bigger diameter to thickness proportion indicated internal buckling however those with smaller ratios observed no buckling additionally the increased specimen length caused a concurrent decline in compressive limits of CFDST's.

***Behavior under large deformation Axial & Cyclic loading [Xiao-Ling Zhao et al. 2010]***

The functioning of CFDST's under large deformation axial and cyclic loading is persuaded with the loading conditions and the diameter to thickness ratios. The columns having slenderness below 110mm were observed having multiple folds without any cracking. Whereas the columns with slenderness greater than 110mm showcased multiple folds with some sort of cracking. Further the study showed that the columns with slenderness less than 82mm wasn't affected with the cyclic loading on deformation front. However, the effect of cyclic loading tried to increase over columns with slenderness between 82mm-110mm. The effect was to be increased if the loads were to be applied late in the loading history. Columns with slenderness greater than 110mm were significantly affected with the cyclic loading applied at an early stage of total loading history. This is observed cause in columns with such greater slenderness the outer steel starts buckling at an early stage affecting the results severely [Zhao et.al 1999; Elchalakani et.al 2003, 2004, 2008].

The Table 1 lists down the results obtained by the X.L Zhao et. al in their studies. The table demonstrates a definitive load conveying limit of the CFDST's with 2 unique phases of presentation of cyclic stacking. One was at a beginning time when the load diminishes to 90% of the maximum load (Specimen name-90) and the second one comes late in the stacking history when the deformation achieves 60mm (example name-60). Further the Figures 3A and 3B demonstrates the failure modes of CFDST's. The figure 3A clarifies the failure of segments with slenderness ratio of around 82. For these sorts, various folds without splitting were watched. For these as well as for every one of the segments with slenderness ratio under 110, numerous folds without breaking was watched. Be that as it may, for the segments with slenderness ratio more prominent than or equivalent to 110, various folds with splitting was seen as appeared in the figure 3B.

**Table1.** Ultimate Capacity of CFDST Specimen by *Xiao-Ling Zhao et al. 2010*

Specimen label	D/t	$\lambda_e$	$P_{CFDST}$ (kN)
0111-90	19	35	1615
0111-60	19	35	1630
0211-90	24	40	N.A
0211-60	24	40	1487
0311-90	32	58	1264
0311-60	32	58	1279
0411-90	36	61	1115
0411-60	36	61	1114
0512-90	47	82	1695
0512-60	47	82	1681
0612-90	55	87	1629
0612-60	55	87	1580
0712-90	70	110	1394
0712-60	70	110	1404
0812-90	84	132	1317
0812-60	84	132	1336
0912-90	96	151	1317
0912-60	96	151	1320

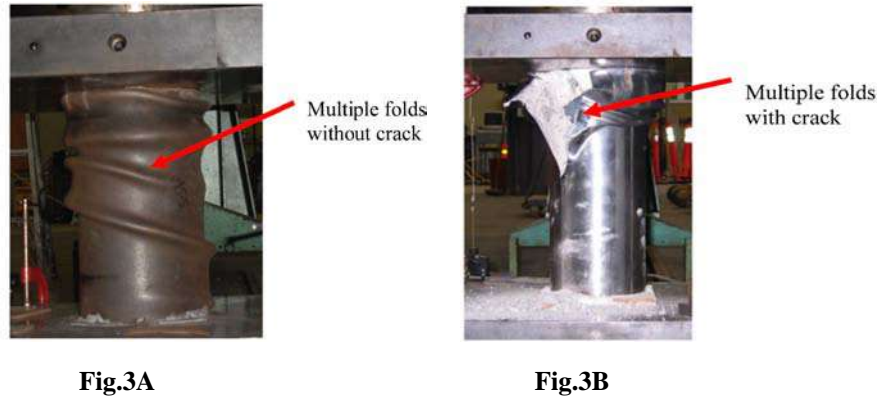


**Fig.3** Typical Failure Modes of CFDST's Under Cyclic Loading by *Xiao-Ling Zhao et al. 2010*

**Behavior under long term sustained loading [Lin-Hai Han et al. 2006]**

The CFDST's and the CFST's somewhat share lots of similarities under long term sustained loading behavior. The axial strain is observed to be increased significantly at preliminary stage and is most likely to attain 60% of the four months value within a month. After a span of approx. 100 days the axial strain was observed to be stabilized at a slower note. The point of outward buckling on the outer tube and inward buckling on the inner tube were found nearly on similar positions with a crushed confined concrete behavior at that point. A comparable conduct of CFDST's was concentrated with CFST's under long term sustained loading and had an exceptionally moderate impact on the Axial Strain Vs Deflection bend. Further examinations demonstrate that the load conveyed by the confined concrete will in general diminish for about 30.5% while an expansion of 31.2% of load on both the empty steel tubes internal just as external were watched.

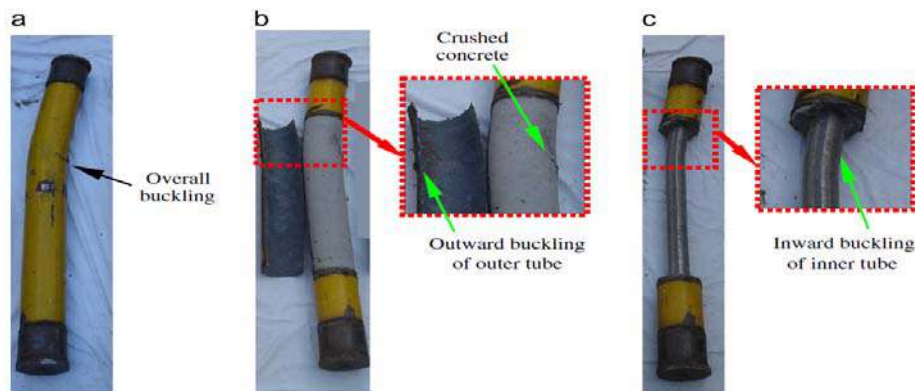


**Fig. 4** Typical Behavior of CFDST under Sustained Loading [Lin-Hai Han et al. 2010]

The long term sustained loading will in general create extra moment in the section reason for which it exhibits a decline in its ultimate strength with concurrent increment in lateral displacement. The regular conduct of the segments after the tests can be effectively made out from the figure 4. The individual conduct of the sandwiched concrete with internal and external steel can be comprehended through figure 5A.

The sustained loading over the column can be seen amid the stage from point A till point B. The extra moments produced in the test examples amid long term sustained loading will in general decline its ultimate load conveying limit (fig.5B). In any case, those moments aren't created during short term loading, prompting an increased ultimate strength.

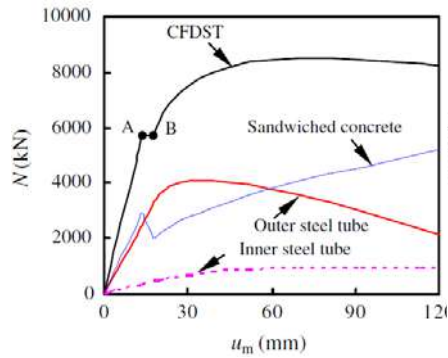


**Fig.5A**

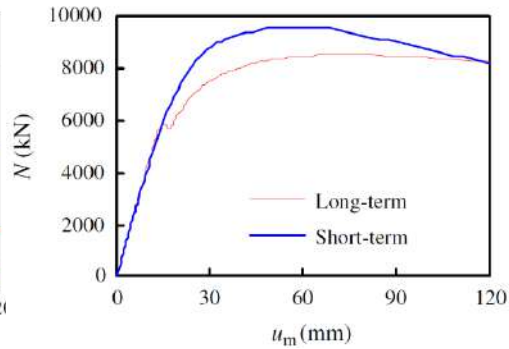


**Fig. 5B**

**Fig.5 A)** Behavior of the sandwiched concrete with internal and external steel

**B)** Ultimate load carrying capacities under long and short term loading

**Behavior against Corrosion [Wei Li et al. 2015]**

The Concrete filled double skinned tube structure when utilized in seaward zones are liable to consumption too. The impact of corrosion on these segments is almost certain equivalent to on different structures for example it diminishes its load carrying capacity. It was seen that the load carried by the internal steel tubes was not affected amid the corrosion time frame. The general decay was taken by the external cylinders bringing about the decline of its load carrying limit. Notwithstanding, setup with various conditions were made for the tests i.e. with uniform erosion (C), corrosion with sustained loading (PC), re-loading and sustained loading (PL) and under pre-loading, sustained loading with corrosion (PLC). a cozy relationship can be created between the strength of columns and the degree of corrosion utilizing the outcome information. With increment in the comparing corrosion levels an immediate strength decrease in the columns could be affirmed. In any case, one progressively significant perception which was made out from the tests was that the impact of consumption appeared to be autonomous from the combined loading. Fig.6 demonstrates the strength comparison information which helps in understanding the genuine conduct of the sections. The figure obviously characterizes that the segments with combined loadings LC-e, PLC-e are having same strength proportions as of the sections under uniform corrosion C-e. The change in the strength can be just seen through the rate change in corrosion levels which infers that the strength information is absolutely subject to the degree of corrosion applied independent of the combined loading effects. Till now no relationship could be made among corrosion and combined loading, see Table 2.

**Table.2** Results Under Corrosion, Pre-load and Sustained Load (Wie Li et.al. 2015)

Specimen Label	Outer tube thickness after corrosion (mm) Corrosion damage	Corrosion damage degree (%)	Measured ultimate Strength $N_{u,exp}$ (kN)
C-1	2.66	11.0	1443
C-2	2.63	12.0	1433
LC-1	2.36	21.1	1391
LC-2	2.33	22.1	1386
PL	2.99	N.A	1568
PLC	2.36	21.1	1349

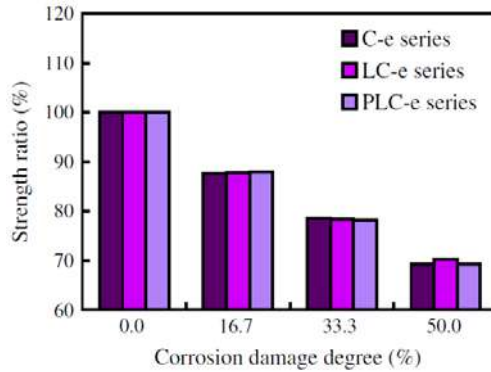


**Fig.6** Influence of Corrosion on Ultimate Strength

**Behavior under torsional loading (Sujith Anumolu et. al 2016)**

A rigorous analysis was done in order to unravel the response of CFDST columns under torsional loading. Different parameters of this composite column were tried to be linked with the obtained behavior.

The observation directed that the inner steel tube isn't much effective or influential towards the columns ultimate torsion. when the strength of the inner tube was allowed to increase correspondingly the ultimate torsion too increased but the ratio wasn't that high. Moreover, with the removal of the same the ultimate torsion came down than before. This somehow explained the moderate participation and importance of inner steel tubes within the scenario of ultimate torsion. Though the percentage change in ultimate torsion was seen to be much influenced with outer steel tubes (Fig.7A). The strength of concrete is also a less governing factor when discussing about the ultimate torsional strength. Even when the lateral stiffness is taken under consideration the concrete marks itself to be an extremely important element

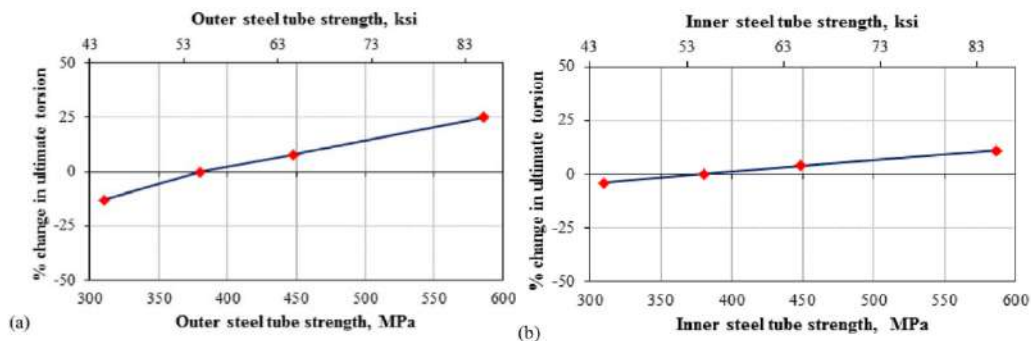


**Fig.7A**

**Fig.7B**

**Fig.7** Percentage change in ultimate torsion with varying strength of **A)** Outer steel tube **B)** Inner steel tube

Also, the increase in the concretes shell thickness can relatively decrease the steel tube dimensions in turn decreasing the ultimate torsional strength of the column. The Percentage change in ultimate torsion with varying strength of concrete can be seen through Fig. 8A. It notifies that the concrete may diminutively but do affected the ultimate torsional behavior. Further the increase in outer steel diameter to thickness ( $D/t_o$ ) ratio do plays an important part in the columns ultimate torsional strength. In totality it was observed that the behavior of the column under torsional loading is majorly dependent upon the outer steel tube.

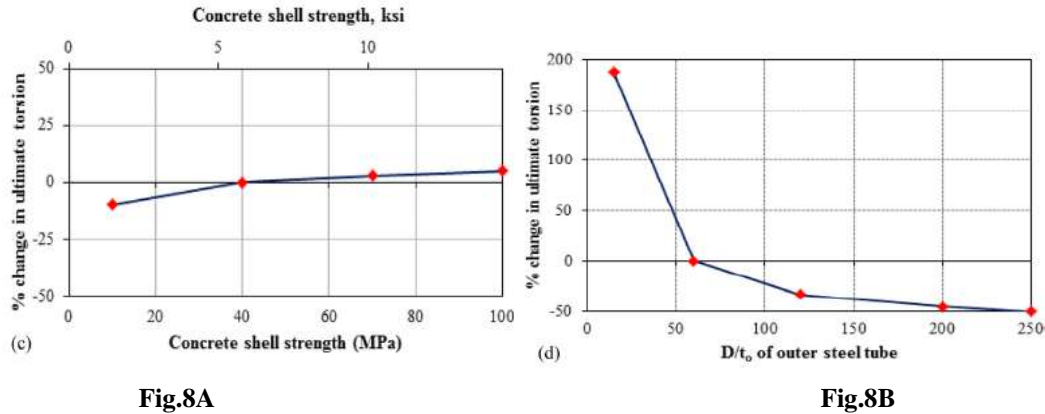


**Fig.8** Percentage change in ultimate torsion with varying **A**) Concrete shell strength **B**) Outer steel diameter to thickness (D/t<sub>o</sub>) ratio

**Behavior under Contact Explosion [Minghong Li et al. 2018]**

Some extreme amount of compressive power generation could be observed under the scenario of contact explosion. This phenomenon tends to produce large plastic strains in outer steel which when exceeding the fracture strain of steel can drive it against rupturing failure or cracking. The software simulation has showed that the major impact of contact explosion is on the areas directly under explosives (Fig.10). No further yielding in other parts of the inner or outer steel was observed. The studies further showcased that the one third of the front area was severely damaged, from the contact area of explosion compressive waves tend to produce after the explosion, these propagate throughout the material from the load source, these stress waves are the reason for other observed damages throughout the material. The generated compressive stresses can immediately cause concrete failure as they are then times higher than the compressive strength of concrete.

From all the elements of the composite column the behavior of concrete towards energy absorption was found to be outstanding. (Fig.9B). Approximately 80% of the energy imparted is being absorbed by the infilled concrete shell. Though some of the energy also gets absorbed through outer steel tubes but on the other hand inner steel tubes comes out to be least effective. In any case, the spalling of cement can be viably neutralized by the external steel tubes and an auxiliary harm through fast catapulted parts can be avoided. The harm caused on the internal and external steel tubes is to a noteworthy degree checked by the energy engrossing capacity of concrete under contact explosion.

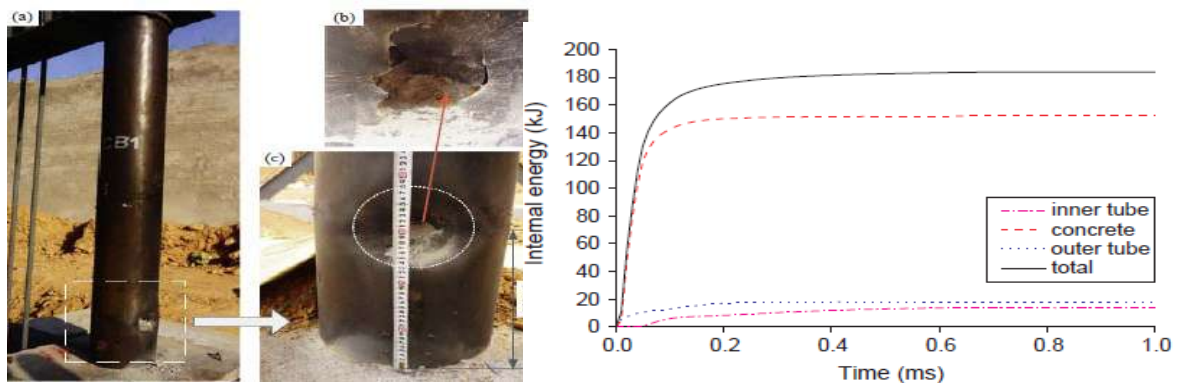


**Fig.9A**

**Fig.9B**

**Fig.9 A)** Area affected under Contact explosion

**B)** Energy absorption of composite column

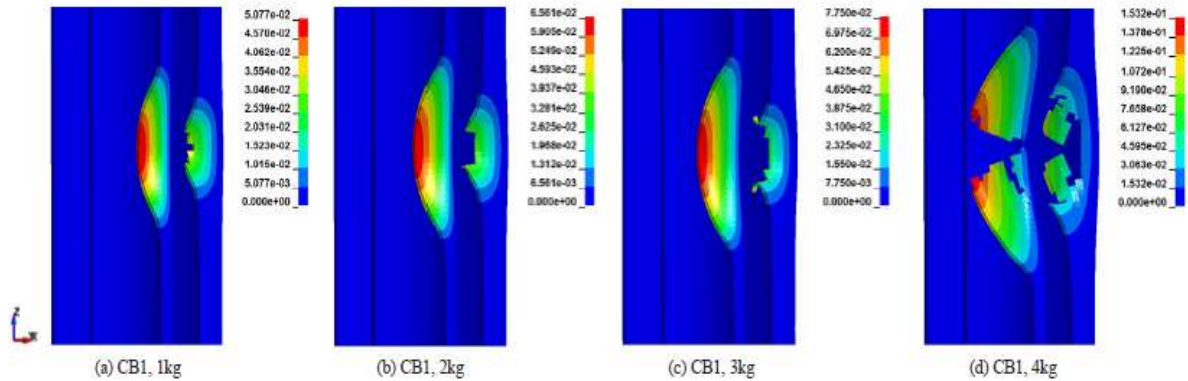


**Fig.10** Simulated Impact on CFDST's under contact explosion

## EXTERNAL STRENGTHENING TECHNIQUES

### *External Confinement using Steel rings [J. C.M. Ho et.al. 2013]*

The procedure of externally confining CFDST's with steel rings somehow tends to improve its mechanical properties like strength, stiffness and ductility. These properties are however much positively affected when the external rings get more closely spaced. The reason behind this might be the more continuous, uniform and greater confining pressure development due to the provision of external steel rings. Further it could be contemplated that the arrangement of the rings diminished the effective length of the external steel tube which specifically causes delay in buckling. The steel rings were seen to enhance the steel-concrete interface holding with a concurrent advancement of higher confinement pressure and restricted lateral deformation.

### *Strengthening using FRP sheets [Jun wang et.al. 2014]*

Strengthening structures using FRP was initiated in mid-1950's. since then it has been effectively used for rehabilitation of concrete structures. This system showcases a combined benefit of FRP, Hollow steel tubes and Hollow concrete shell hence confining CFDST with FRP sheets is an effective method of improving its strength. The failure in these types of jacketed columns starts with a sudden rupture of FRP jacketing followed by buckling of steel tubes. It was seen that the buckling of steel tubes could be delayed using FRP jacketing. Further a bilinear behavior in both load vs strain (specimen) & stress vs strain (concrete) curve were observed.

## CONCLUSION

- The accompanying investigation opened up portals for seeing further in detail system of concrete filled double skinned tubes. The audit shed lights on various practices of this subtle procedure with a point of evacuating this hypothetical idea from proposal and raising its utilization in continuous development. · A framework of concrete filled double skinned columns under axial compression, large deformation loading, corrosion, blast loading and torsional loading was deduced.
- It was recognizable that how successfully CFDST's could bear a portion of the above elements superior to anything the conventional columns and the concrete filled single skinned columns. Beforehand concrete filled single skinned columns were in more prominent logical consideration because of its enhanced flexural, seismic and torsional execution with a synchronous decrease in its development time attributable to the conduct of the external steel tube as pre-foam work.

- However, the concrete filled double skinned columns are a further adjustment of CFST's so as to neutralize the disadvantages of the last one. They will in general basically expel the inadequate center concrete and the heavy weight design, which was received utilizing an empty steel container of characterized thickness in the center. The mechanism of lateral displacement of concrete under axial compressive loading and the simultaneous confinement of the inner and outer steel tubes to the concrete shell could be obviously comprehended. The confining pressure from the internal and external cylinder advantageously affect the strength and performance of concrete.
- It was seen that the evacuation of the center concrete helped in lessening oneself load of the structure which thus spared the material and development time too. This decreased weight didn't just support up the structure monetarily yet in addition included to its seismic conduct, leaving a structurally, environmentally and financially sparkling idea driving.

## REFERENCES

- Bayrak O. and Sheikh S.A. (1998), "Confinement reinforcement design considerations for ductile HSC columns", *Journal of Structural Engineering, ASCE*, 124(9), 999-1010.
- Dawood, H., El Gawady, M., and Hewes, J. (2012). "Behavior of Segmental Precast Post-
- Elchalakani M, Zhao XL, Grzebieta RH. Concrete-filled steel tubes subjected to constant amplitude cyclic pure bending. *Eng Struct* 2004;26(14):2125\_35.
- Elchalakani M, Zhao XL, Grzebieta RH. Tests of cold-formed circular tubular braces under cyclic axial loading. *J Struct Eng, ASCE* 2003;129(2):507\_14.
- Elchalakani M, Zhao XL. Concrete-filled cold-formed circular steel tubes subjected to variable amplitude cyclic pure bending. *Eng Struct* 2008;30(2):287\_99.
- Essopjee, Y., Dundu, M., Performance of Concrete-Filled Double-Skin Circular Tubes in Compression, *Composite Structures* (2015).
- Essopjee, Y., Dundu, M., Performance of Concrete-Filled Double-Skin Circular Tubes in Compression, *Composite Structures* (2015).
- Han LH, Tao Z, Huang H, Zhao XL. Concrete-filled double skin (SHS outer and CHS inner) steel tubular beam columns. *Thin-Walled Structures* 2004;42(9):1329 55.
- Han, L.H., Tao, Z., Huang, H., Zhao, X.L.: Concrete-filled double skin (SHS outer and CHS inner) steel tubular beam-columns. *Thin Walled Struct.* 42(9), 1329–1355(2004).
- Ho J.C.M. and Pam H.J. (2003), "Inelastic design of low-axially loaded high-strength reinforced concrete columns", *Engineering Structures*, 25(8), 1083-1096.
- J. C.M. Ho; C. X. Dong (2013) *Thin-Walled Structures*, ISSN: 0263-8231, Vol: 75, Page: 18-29.
- Jun wang, ding zhou, " Mechanical behaviour of concrete filled double skin steel tubular (CFDST) stub columns confined by FRP under axial compression", *Steel and Composite*
- Kang Hai Tan • Yu Fen Zhang "Compressive stiffness and strength of concrete filled double skin (CHS inner & CHS outer) tubes" *Int J Mech Mater Des* (2010) 6:283–291.

Proceedings of National Conference: Advanced Structures, Materials And Methodology in Civil Engineering (ASMMCE – 2018), 03 - 04th November, 2018

PAPER CODE: C528

Lin-Hai Han et al. (2011) “Concrete-filled double skin steel tubular (CFDST) columns subjected to long-term sustained loading” *Thin-Walled Structures* 49 (2011) 1534–1543.

Lin-Hai-Han and Zhong Tao (2006), “Behavior of concrete filled double skinned rectangular steel tubular beam-columns” *Journal Of Construction Steel Research*, Volume 62, Issue 7, July 2006, Pages 631-646.

Minghong Li et al. “Experimental and numerical study on damage mechanism of CFDST bridge columns subjected to contact explosion” *Engineering Structures* 159 (2018) 265– 276.

Pagoulatou M, Sheehan T, Dai X and Lam D (2014) Finite element analysis on the capacity of circular concrete-filled double-skin steel tubular (CFDST) stub columns. *Engineering Structures*. 72: 102–112.

Paultre P., Legeron F. and Mongeau D. (2001), “Influence of concrete strength and transverse reinforcement yield strength on behavior of high-strength concrete columns”, *ACI Structural Journal*, 98(4), 490-501.

Sujith Anumolu et al. “Behavior of Hollow-Core Steel-Concrete-Steel Columns Subjected to Torsion Loading” *Journal of Bridge Engineering*. April 2016 DOI: 10.1061/(ASCE)BE.1943-5592.0000923.

“Tensioned Bridge Piers under Lateral Loads”, *ASCE Journal of Bridge Engineering*, Vol. 17, No. 5, pp. 735-746.

Watson S., Zahn F.A. and Park R. (1994), “Confining reinforcement for concrete columns”, *Journal of Structural Engineering*, ASCE, 120(6), 1799-1824.

Wei Li et al. “Behavior of CFDST stub columns under preload, sustained load and chloride corrosion” (2014) *Journal of Constructional Steel Research* 107 (2015) 12–23.

Wei, S., Mau, S.T., Vipulanandan, C., Mantrala, S.K.: Performance of new sandwich tube under axial loading: experiment. *J. Struct. Eng.* 121(12), 1806–1814 (1995).

Xiao-Ling Zhao et al. “CFDST stub columns subjected to large deformation axial loading” Volume 32, Issue 3, March 2010, Pages 692-703.

Yang, J.J., Xu, H.Y., Peng, G.J.: A study on the behavior of concrete-filled double skin steel tubular columns of octagon section under axial compression. *China Civil Eng. J.* 37(10), 33–38 (2004).

Zhao XL, Grzebieta RH, Elchalakani M. Tests of concrete-filled double skin CHS composite stub columns. *Steel and Composite Structures—An International Journal* 2002;2(2):129–42.

Zhao, X.L., Grzebieta, R.H.: Void-filled SHS beams subjected to large deformation cyclic bending. *J. Struct. Eng.* ASCE 125(9), 1020–1027 (1999).